WESTPRAC

TECHNICAL PAPERS

WESTPRAC IV 91

FOURTH WESTERN PACIFIC REGIONAL
ACOUSTICS CONFERENCE
BRISBANE AUSTRALIA

WESTPRAC IV 91

TECHNICAL PAPERS

WESTERN PACIFIC REGIONAL ACOUSTICS CONFERENCE IV
BRISBANE, 26-28 November, 1991

Co-sponsored by :

Queensland Department of Environment and Heritage
and
The Australian Acoustical Society

Host: **Griffith University**

(i)

WESTPRAC IV 91

WARBURTON FRANKI

Proudly representing

RION
Sound and Vibration
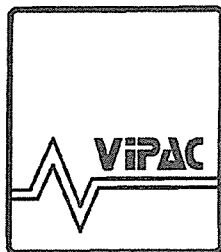
VIPAC Engineers and Scientists Ltd.are Australia's largest acoustic and vibration consultancy company.

WESTPRAC IV 91

FOREWORD

May we, on behalf of the Australian Acoustical Society and the Department of Environment and Heritage, welcome you to the 1991 Westprac Conference.

These pages contain the text of the 87 technical papers and four keynote addresses to be presented during the next three days.

We hope that the technical content and the discussion generated thereby will make a worthwhile contribution to the science and practice of acoustics and that the Conference itself will live up to the standard of excellence of previous Westprac Conferences.

We trust that your stay in Brisbane, both in the technical and the social sense, will be recalled with pleasure for many years to come.

The dedication, hard work and professionalism of the Organising Committee in bringing this event to fruition is acknowledged with thanks.

Stephen Samuels
President
Australian Acoustical Society

Graham Cleary
Director
Division of Environment

WESTPRAC IV 91

CONFERENCE ORGANISING COMMITTEE

Ron Rumble (Chairman)
Noela Eddington (Conference Convenor)
Lex Brown
Russ Brown
Graham Cleary
Robert Hooker
Greg Lee-Manwar
Nick Lindsay
Warren Middleton
Ross Palmer
Warren Renew

CLASSIFICATION OF SUBJECTS

STREAM 1.   ACOUSTICS RESEARCH AND DEVELOPMENT

1.1 ARCHITECTURAL ACOUSTICS

1.1a Auditorium Acoustics

1.1b Building Acoustics

1.1c Musical Acoustics

1.1d Treatments (absorption, transmission)

1.2 BIO ACOUSTICS

1.2a Biological - people

1.2c Communication - speech

1.2d Communication - hearing

1.3 SPECIALIST

1.3a Acoustic theory

1.3b Electroacoustics

1.3c Signal Processing

1.3d Ultrasonics

1.3e Underwater Acoustics

1.4 MEASUREMENT

1.4a Assessment

1.4b Instrumentation

1.4c Measurement techniques

1.4d Sound intensity

CLASSIFICATION OF SUBJECTS

STREAM 2. MANAGEMENT OF THE ACOUSTIC ENVIRONMENT

2.0 NOISE MANAGEMENT

2.1 Education

2.2 Environmental Planning

2.4 Economic Effects

2.8 Noise Abatement and Control

2.9 Effects of Noise

CONTENTS

KEYNOTE SPEAKERS

STREAM 1.   ACOUSTICS RESEARCH AND DEVELOPMENT

1.1 ARCHITECTURAL ACOUSTICS

1.1a Auditorium Acoustics

1.1b Building Acoustics

1.1c Musical Acoustics

1.1d Treatments (absorption, transmission)

1.2 BIO ACOUSTICS

1.2a Biological - people

1.2c Communication - speech

1.3e Underwater Acoustics

1.4 MEASUREMENT

1.4a Assessment

1.4b Instrumentation

1.4c Measurement techniques

1.4d Sound intensity

STREAM 2. MANAGEMENT OF THE ACOUSTIC ENVIRONMENT

2.0 NOISE MANAGEMENT

2.1 Education

2.2 Environmental Planning

2.4 Economic Effects

2.8 Noise Abatement and Control

2.9 Effects of Noise

COMMUNITY AND TRAFFIC NOISE

Wann Yu
Professor of Urban Planning and Transportation
Yonsei University, Seoul, Korea

ABSTRACT

As population grows and economic conditions improve the number of vehicles rise significantly. This and the fact that our living patterns become more complex and complicated has increased the traffic circulation, resulting in a higher level of traffic noise. On the other hand, people have become more conscious about noise problems. As the concern about noise rose, strict government control on noise have been laid out. The strict noise controls have highlighted the importance of the Ministry of Environment, however constructers and manufacturers consider the control as an obstacle. In order to reduce noise, this view on controlling community noise should change into one that considers it as an auxiliary for better living. The consideration of noise problems should be brought up at the beginning of planning cities and road networks. We also need to develop a noise reducing scheme that is dramatically different to hope for a more quiet society.

I. INTRODUCTION

People are more concerned about noise problems nowadays. The level of noise in our living environment increases as our living patterns become more complex and complicated. On the other hand, people become more sensitive about noise as their economic conditions improve. The greater their desire is for a more comfortable and better living environment, the more they are more annoyed by the level of noise which they had used to accept. Airplanes, trains, automobiles, industries, constructions, and other sources make more intensive noises and more frequently than in the past, these background noises are annoying people more than ever before.

Although noise is such a serious problem, the term "noise" does not have a definition which satisfies everyone. Noise and signal are considered as two different kinds of sound in the field of acoustics and electronics. Normally, uniform or random with a recognizable pattern distinguishes signal from noise. In psychology, noise is defined as man made sounds without meaning. Noise, in the field of behavioral science is considered unwanted sound by listeners. Thus, noise could be defined in terms of detector characteristics, information conveyed, or perceptual preference. Preference is a term explaining human response on sound as stimuli, but physical assessment of noise in this sense is not easy to make. A once desired sound may become an unwanted noise, and meaningless humming is

ıuman being that
ly a problem in
ic in developing
ı is often found.
ıat have a pile of
lega. ,   ction for a better
environment does ...   in a dynamically
transforming society. Newly ıı.....   ɔise problems which
have long existed in affluent societies. ıu. ..   ıuch more serious as
development without protection takes place at a rapid speeu. Yet the problem is
less recognized in newly developing countries where more damages are being made.
Complaints are often filed after people suffer excessively, not just
psychologically but medically and biologically. With economic development, their
complaints are becoming so acute that immediate action is required. Roof tiles,
for example, are cracked by airplane noise and vibration, and hearing losses are
reported after working in some leading industries. Developed countries have more
restricted control over the noise makers in their community as people are
sensitive about noise in their environment.

II. COMMUNITY NOISE

Noise is a problem for a large proportion of the urban population. The number
of urban dwellers affected is expected to increase in the future. This is a
result of continuing urbanization and increases in traffic flow. The proportion
of noise and vibration is significantly larger than any other categories among the
public complains filed at Ministry of Environment in Korea.

[FIGURE 1] COMPLAINS RELATED TO ENVIRONMENTAL POLLUTION
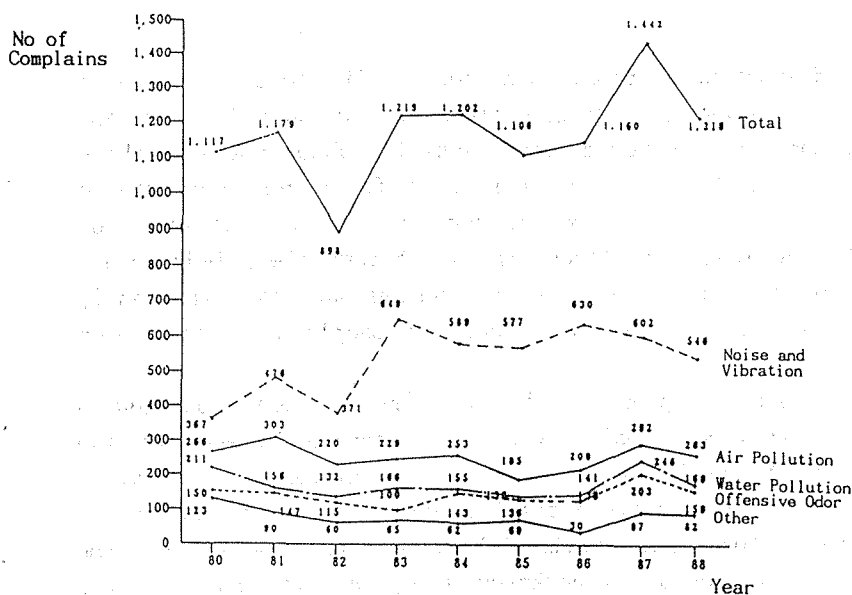
In America, 46 percent of urban population is bothered by noise. Among them 86
percent identified vehicle noise as a source. Another study shows that 25.3
percent of a nationwide environmental monitoring survey claimed vehicle noise as
the largest major neighborhood noise source. Noise from manufacturing industries

in urban areas is reported as another major urban noise source. This is because small and medium sized industries, acounting for 17 percent of the total of 24,810 industries recognized as noise creating industries in 1990 by Office of Environment in Korea, are located in mixed residential districts. Some of the machineries used by industries in mixed residential districts make the noise level over 90 dbs. Noise in residential communities is also caused by loudspeakers, construction works, repeated noises during night, and airplane noises. Clearly, noise level varies in different types of land use.

[TABLE 1] SOUND POWER LEVEL MADE BY MACHINERY

SOUND POWER(dB)	TYPE OF MACHINERY
90 and under	max. 5hp transmission, max. 20hp. plain lathe, max. 15hp hulling facility
90-95	max. 0.5 hp press, min. 20hp plain lathe, max. 0.5hp grinder, power sewing machine, min. 5hp automatic lathe, transmission
95-100	max. 5hp cutter, max. 4hp fan, min. 0.5hp tool lathe, power sewing machine, min. 20hp hulling facilities
100-105	min. 2hp press, min. 5hp cutter, max. 1hp textile machinery, 5-9hp fan, min. 500hp rolling machine, max. 150hp grain crusher, mill, compressor
105-110	printing machine, min. 2hp textile machinery, 10-40hp fan, min. 30hp stone crusher
110-115	electric generator, min. 50hp fan, min. 1,000hp rolling machine, min. 150hp grain crusher

The major reason that noise has become such a concern is obviously because of its effect on people. Human perception of noise is clearly related with the noise level. Table 2 shows how noise affects various human activities in daily life.

[TABLE 2] INFLUENCE OF NOISE

dB(A)

	dB(A)	OVERALL INFLUENCE	BIOLOGY	WORK EFFICIENCY	SCENE	
takeoff noise	110	hearing difficulties appear in 4 hours				110
jackhammer noise	100	hearing difficulties appear in 8-16 hours	change in electromyogram change in electrocardiogram	reduced typing speed		100
	90	earmuffs recomended	change in autonomic nerve & endocrine funtion	reduced work results, frequent mistakes		90
traffic noise	80		increase of energy metabolism	drop in understanding ability	SCENE	80
	70	takes time to adjust to noise		less concentration	workplace	70
typing noise	60	cannot ignore noise	sleeping disturbance (business district)		indoor sports arena	60
wind noise	50	feel noise	sleeping disturbance (residential district)	drop of calculating ability	large office, office located in a factory	50
livingroom noise	40	cannot feel any noise	change of brain waves	influence in writing & drawing	city housing, class classroom, hospital	40
	30	seem very silent feel isolated				30
park noise	20	no noise				20

dB(A)

		CONVERSATION	PERCEPTION	READING & THINKING	STANDARD NOISE LEVEL	
takeoff noise	110					110
Jackhammer noise	100					100
	90					90
traffic noise	80	coversation by phone impossible	very noisy	very disturbing		80
	70				industrial district (day), business district (day), industrial district (night)	70
typing noise	60	conversation possible within 1.3m	quite noisy	quite disturbing	mixed residential district(day), business district(night)	60
wind noise	50		noisy	little disturbing	residential district (day), mixed residential district (night)	50
livingroom noise	40			not disturbing	residential district (night)	40
	30					30
park noise	20					20

As more people are affected by community noise, strict government control on noise is expected. For example, Seoul Municipal Government set out the community noise control for loudspeakers, industrial noise, and construction noise recently as shown in Table 3. When any violation is found after August 10, 1991, Seoul Municipal Government will enforce the control by shortening working hours, prohibiting noise producing activities, and/or requiring noise barriers. Yet Seoul Municipal Government is facing many problems such as difficulty of community noise control due to ever increasing number of vehicles, speeding and honking of vehicles, wide spread of small urban industries, loudspeakers used by street venders, and the exessive construction cost of noise barriers to protect schools and hospitals ($350,000-$500,000/Km). Enforcing speed regulations to control noise, however, is not realistic. Prohibitting honking by moving vehicles is also difficult to enforce in a strict manner. Thus, controlling vehicle noise largely depends upon voluntary action by the unspecified citizen in short term basis. Acheiving a quiet community through urban land use and transportation planning is one of the long range strategies announced.

[TABLE 3] LIMITS OF COMMUNITY NOISE BY DISTRICTS(dB)

DISTRICTS	SOURCE OF NOISE		MORNING & EVENING 05-08,18-22	DAYTIME 08-18	NIGHTTIME 22-05
residential, park, within 50m from school or hospital	loudspeaker	outdoor	under 70	under 80	under 60
		indoor	under 50	under 55	under 45
	factory & workplace		under 50	under 55	under 45
	construction site		under 65	under 70	under 55
business, mixed industry	loudspeaker	outdoor	under 70	under 80	under 60
		indoor	under 60	under 65	under 55
	factory & workplace		under 60	under 65	under 55
	construction site		under 70	under 75	under 55

4

III. TRAFFIC NOISE

Along the major arterials in urban areas, vehicle noise level was recorded 75 to 82 dbs during daytime measured in LEQ. These noise levels are much higher than any standard for environment regardless of urban land use. Environmental standards for roadside in Korea for example are 65-55 dbs in all types of residential districts, 70-60 dbs in commercial and business districts, and 75-70 dbs in industrial districts during daytime-nighttime. Thus, outside noise should be reduced dramatically by building materials to meet the environmental standards. Noise levels decrease below 65 dbs as 10 to 50 meters away from the major arterials. Environmental standards for non-roadside areas are 50-40 dbs in residential districts, 55-45 dbs in mixed residential districts, 65-55 dbs in commercial and business districts, and 70-65 dbs in industrial districts in daytime-nighttime. Noise levels of residential districts in major cities in Korea in particular are higher than the standards set by Government.

[TABLE 4] NOISE LEVEL STANDARD BY LAND USE(dB)

LAND USE		NOISE LEVEL STANDARD	
		DAYTIME	NIGHTTIME
NON-ROADSIDE DISTRICT	RESIDENTIAL	50	40
	MIXED RESIDENTIAL	55	45
	COMMERCIAL	65	55
	INDUSTRIAL	70	65
ROADSIDE DISTRICT	RESIDENTIAL	65	55
	COMMERCIAL	70	60
	INDUSTRIAL	75	70

In residential districts in non-roadside, 109 points or 57 percent among 192 points surveyed during daytime and 88 points or 69 percent among 128 points during nighttime show the noise level being higher than the standards. In residential districts along roadsides, 88 points or 69 percent among 128 points during daytime and 98 points or 77 percent among 128 points during nighttime violate the neighborhood noise levels. Similar statistics are also reported in other countries.

IV. TREND OF COMMUNITY NOISE IN SEOUL

It is necessary to understand how and why community noise increases. As mentioned at the beginning, community noise tends to increase as our living pattern becomes more complex and complicated. Besides the fact that the noise level tends to increase, people become more aware of and sensititve about noise as economic conditions improve and as society becomes more affluent.
The increase in number of vehicles in Korea is marked significant during the past decade along with the increase in Gross National Products as shown in Table 5.

Statistics show that the number of vehicles has increased more significantly compared to that of population. The drop of increase rate in 1979 and 1980 may be explained by the political shakeup that occured during this period. The Korean economy has grown rapidly during the past few years. For its rapid growth Korea has depended largely on the international market rather than building a solid domestic market. Thus, the Korean economy has become very sensitive to the

[TABLE 5] INCREASE RATE OF POPULATION, GNP, NUMBER OF VEHICLES

YEAR	POP. (1000 p)	RATE (%)	GNP (100 M$)	RATE (%)	GNP/POP ($/P)	RATE (%)	NO. OF VEH (car)	RATE (%)	VEH/POP (car/1000P)	RATE (%)
1971	32883		95		289		144337		4.39	
1972	33505	1.89	107	12.63	319	7.96	150035	3.95	4.48	0.02
1973	34103	1.78	135	16.82	396	24.14	170714	13.72	5.01	0.11
1974	34692	1.73	188	39.26	542	36.86	183544	7.52	5.29	0.05
1975	35281	1.65	209	11.17	594	9.59	200521	9.25	5.68	0.07
1976	35849	1.61	287	37.32	803	35.19	226320	12.87	6.31	0.11
1977	36412	1.57	368	28.22	1012	26.03	282752	24.93	7.77	0.23
1978	36969	1.53	515	39.95	1396	37.94	384536	36.00	10.40	0.34
1979	37534	1.53	615	19.42	1644	17.77	494378	28.56	13.17	0.26
1980	38124	1.57	605	-1.63	1592	-3.16	527729	6.75	13.84	0.05
1981	38723	1.61	668	10.41	1734	8.92	571754	8.34	14.77	0.07
1982	39326	1.56	713	6.74	1824	5.19	646996	13.16	16.45	0.11
1983	39910	1.49	795	11.50	2002	9.76	785316	21.38	19.68	0.20
1984	40406	1.24	870	9.43	2158	9.59	948319	20.76	23.47	0.19
1985	40806	0.99	897	3.10	2194	1.67	1113430	17.41	27.29	0.16
1986	41184	0.93	1028	14.60	2505	14.18	1309434	17.60	31.79	0.16
1987	41575	0.95	1289	25.39	3110	24.15	1611375	23.06	38.76	0.22
1988	41975	0.96	1728	34.06	4127	32.70	2035448	26.32	48.49	0.25
1989	42380	0.96	2101	21.59	4968	19.19	2660212	30.69	62.77	0.29

international economy. The difference found in the vehicle increase rate may be explained by the fluctuation of the international economy. Though there are occasional drops the increase of vehicles has been constantly outnumbering the increase in population. Roads and other vehicle related facilities have not been able to keep up with this increase of vehicles.

[TABLE 6] POPULATION & DAILY TRIPS MADE IN SEOUL

YEAR	POPULA. (1000P)	RATE (%)	TOTAL TRIPS (1000 trips)	RATE (%)	TRIPS/POP. (trip/P)	RATE (%)
1971	5850	5.70	6276	10.9	1.14	
1972	6076	3.86	7048	4.8	1.16	1.75
1973	6290	3.52	7422	5.3	1.18	1.72
1974	6542	4.00	7850	5.8	1.20	1.69
1975	6889	5.30	8450	7.6	1.22	1.67
1976	7255	5.31	8959	6.0	1.24	1.64
1977	7525	3.72	9481	5.8	1.28	3.22
1978	7823	3.96	10600	11.8	1.41	10.16
1979	8114	3.72	12000	13.2	1.53	8.51
1980	8366	3.11	12600	5.0	1.56	1.96
1981	8676	3.70	13350	5.95	1.59	1.92
1982	8916	2.77	14629	9.58	1.69	6.29

As the Gross National Products passed $ 5,000 and as Korea became a developed country from a developing country, Korea experienced a strong trend of consumption. This brought an even greater increase of vehicles. Along with the policy to maintain travel costs comparatively low which the Korean government has been carrying out, the rise in number of vehicles has resulted in the increase of traffic circulation. This is one of the major factors of the increase of community noise. This could be found especially in major cities. Seoul, where one quarter of the national population inhabits in only 0.6 percent of the national land, shows an increase in number of trips made by each individual everyday.

Daily trip per person has steadily increased 1.70-1.90. The big jump in 1978-1979 and 1982 may be due to the change of counting methods or organizations, thus resulting in statistical discrepancies. The increase in number of daily trips of 6 major cities in Korea is shown in Table 7 below.

[TABLE 7] DAILY TRIPS MADE IN 6 MAJOR CITIES

	POPULATION (1000 P)		TOTAL TRIPS (1000 Trips)		VEHICLE NO. (cars)		TRIPS/PERSON (cars/P)	
	1981	1989	1981	1989	1981	1989	1981	1989
SEOUL	8676	10481	13350	19109	221644	991290	1.59	1.80
PUSAN	3250	3857	3253	6255	67053	234936	1.55	1.92
TAEGU	1838	2288	2353	3662	39251	131445	1.77	1.91
INCHUN	1142	1754	850	1529	20395	109369	1.24	1.68
KWANGJU	770	1613	1241	2356	13346	59597	1.71	2.21
TAEJEON	668	1613	747	1611	12391	71136	1.72	1.91

With an exeption of Inchun city, all other cities have larger daily trips per person than that of Seoul. Inchun city is adjacent to Seoul with the shared administrative boundaries and can be considered as a suburban area of Seoul. Thus, the lower rate of daily trips per person can be understood as a suburban phenomenon rather than an independent urban dwellers' behavior. Number of vehicle increases are outnumbering the population increase in all cities and the increases in daily trips per person is noticable in all cities. Clearly, this shows the change in travel pattern of urban dwellers in Korea.

Changes in noise levels according to land use in Seoul in 1984-1991 is shown in Figure 2-a,b,c,d. The noise levels shown here are the averages of an annual survey conducted at 8 to 12 different locations for each land use type.

[FIGURE 2-a,b,c,d] NOISE LEVELS OF SEOUL BY LAND USE TYPES
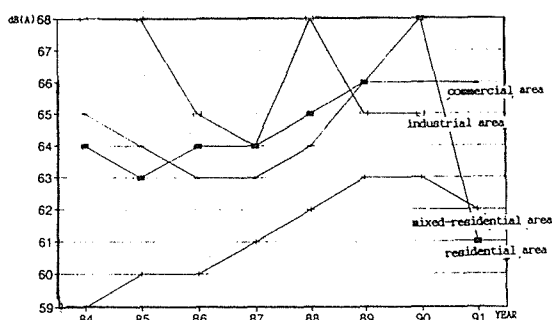
a: Seoul Daytime Non-Roadside
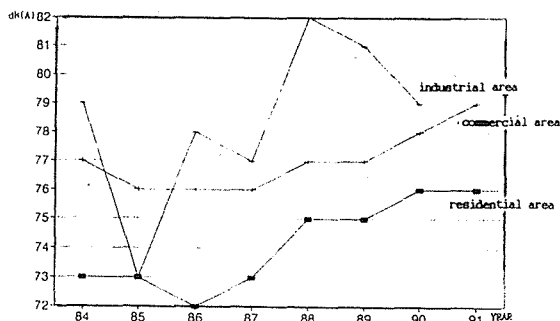
b: Seoul Daytime Roadside
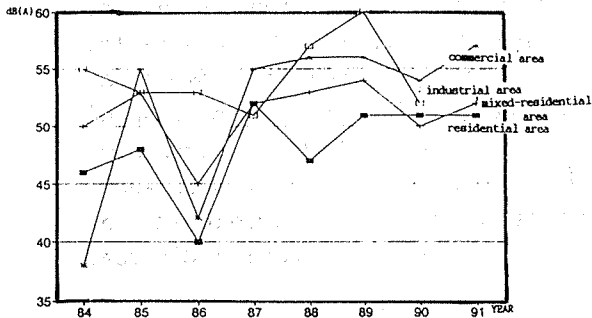
c: Seoul Nighttime Non-Roadside
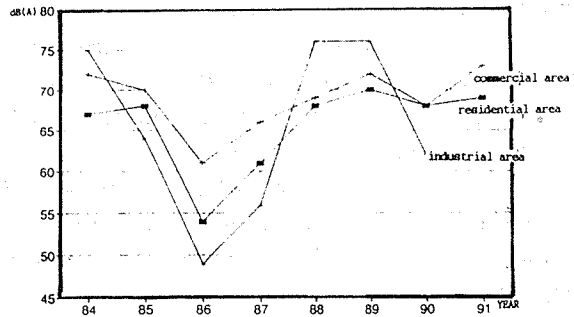
d: Seoul Nighttime Roadside

Noise levels in the industrial district should be considered an exception because the noise level differs dramatically in accordance with the condition the survey, which was taken at a given time each year, was conducted. Although noise standards have been strengthened, especially for vehicle operation and community noise sources, noise levels in residential and commercial districts have increased. Increases in noise levels during nighttime should be taken seriously, which is a result of extended rush hours and heavy traffic volume during the night. Noises according to land use types in all major cities except Kwangjoo have also increased since 1987 as shown in Figure 3. The drop of noise levels in Kwangjoo is yet to be identified.

[FIGURE 3] NOISE LEVELS IN 5 CITIES BY LAND USE TYPES(DAYTIME)
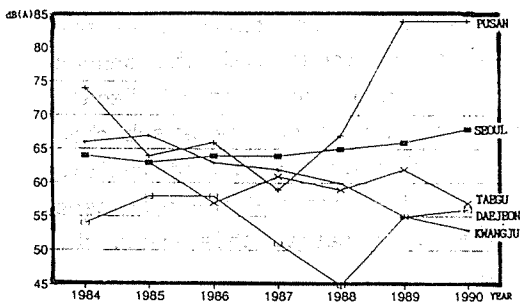
a: Non-Roadside
Residential District
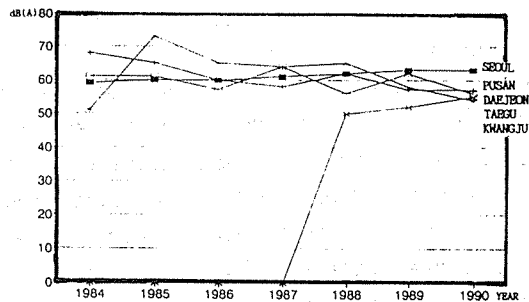
b: Non-Roadside
Mixed Residential District
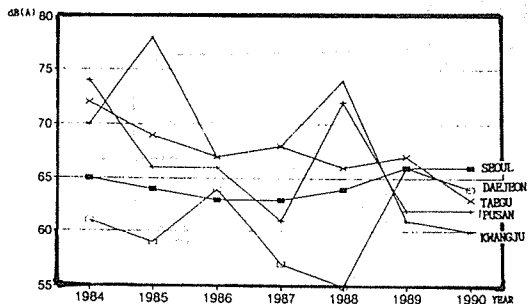
c: Non-Roadside
Business District
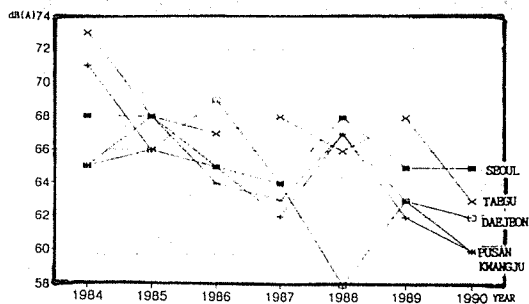
d: Non-Roadside
Industrial District

8
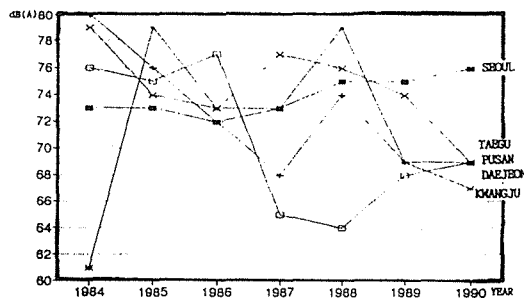
e: Non-Roadside
   Residential District
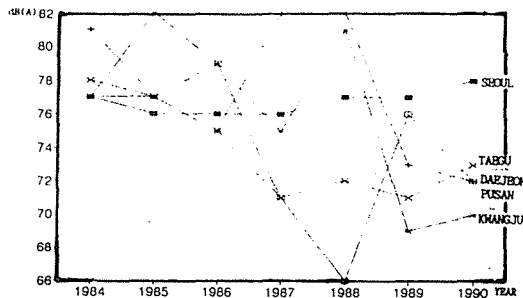
f: Non-Roadside
   Business District
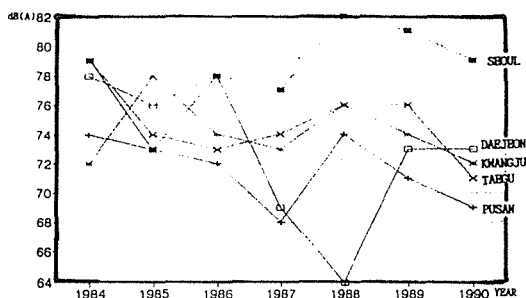
g: Non-Roadside
   Industrial District

V. NOISE REDUCTION FOR BETTER LIVING

Many different policies intending to reduce community noise have been suggested. These include strict regulations for automobile manufacturers, community noise sources, building acoustics, and constructing sound barriers for urbanized areas. Strict regulations for auto and truck driving, train and subway operations have been laied out. Relocation of residential areas and controlling aviation grounds have also been carried out. These are short and medium range tactics and strategies to control the noise already created. As a long range strategy, land use planning for a better living environment is mentioned frequently. However, it is difficult to even imagine that land use control could be effective for an already urbanized area. Land use control could be effective for building new towns which do not occur frequently. Even in a new town planning, the noise issue is not often considered seriously in the process of land use planning. Noise becomes only becomes a design factor at the final stage of designing. This is because the governmental organization is divided in such way that Ministry of Environment or an equivalent organization is considered only as a policy planning organization for society. In many cases, Ministry of Construction, Ministry of Commerce and Industry, Municipal Governments, or equivalent organizations consider organizations enforcing noise and other environment factors as obstacles to construction and manufacturing conveniences for better living. Unless the view on controlling community noise changes from considering it as an obstacle to considering it as an auxiliary for better living and the noise issue is brought up at the beginning of planning cities and road networks, the noise problem will become more serious. We should well be aware that some community noise could have long lasting psychological and biological effects

when human beings are over exposed to it, and that it could easily not be taken seriously until serious effects occur.

We need to develop a noise reducing scheme that is dramaticly different from policies that we are so accustomed to. Underground belt conveyors to transport daily conveniences, underground motor ways, improving telecommunication systems to reduce the need for travelling and agglomeration economies acheived by living in urban areas could be examples. Let us hope that the technology development will bring us a silent super sonic aircraft in the 21 century.

REFERENCE

Alexandre, A. et. al, Road Trffic Noise, Applied Science Publisher LTD 1975.
Brown, A.L. and Lam, K.C. "Urban Noise Surveys', Applied Acoutics, Vol. 20-1, pp. 23-39, 1987.
Chung, M.Y. & Yu, W.,"Evaluation of Expected Noise Impact of Industrial Development", Technical Papers of WESTPAC III 88, pp. 565-568.
Fidell, S., "Nationwide Urban Noise Survey", J. of Acoust. Soc. of Am., Vol 64, 1978.
Kim, H.C.,"An Impact Evaluation of Road Traffic Noise by Land Use Characteristics: Seoul Case", Technical Papers of WESTPAC III 88, pp. 561-564.
Kreisel, W.E. and Yu, W. "Motor Vehicles and Land Use Management in The Republic of Korea". Industry and Environment, Vol 6-2, 1983, pp. 15-18.
Maruyama, M., "Estimation of the Values of LEQ in Residential Areas", Proceedings of 2nd Japan-Korea Symposium on Acoustics, The Acoustical Society of Japan, 1983.
Ministry of Environment in Korea, "Noise Levels in Major Cities during the First Quarter of 1991 and Policy", undated press release.
Office of Environment in Japan, "Report of Automobile Traffic Noise", undated press release, 1988.
환경청, 서울시 전역에대한 소음실태조사 연구, 1981. (Office of Environment in Korea, A Study on the State of Noise Pollution in Seoul, 1981.)
Office of Environment, Korean Environmental Yearbook, 1989.
이 출재, 차 일환, "서울시 특정지역 교통소음의 고찰", 제 2회 일한음향학술발표회논문집, 1983, pp. 129-136.(Rhee, C.J. & Cha, I.W.,"A Discussion of Traffic Noise in Seoul", Proceedings of 2nd Japan-Korea Symposium on Acoustics, The Acoustical Society of Japan, 1983, pp.129-136)
Strumpf, D. and Strumpf, F.M. "The Prediction of a Neighbourhood from Traffic Noise due to a New Highway", Proceedings of Inter-noise 87, pp. 791-794.
Yu, W.,"Accuracy of Measurement for Assessing Human Response on Noise", Proceedings of Inter-Noise 87, pp.985-988
森田, "近隣騷音の 現狀と 規制狀況", 音響技術, Vol.10-35, 1981, pp. 1-5.(Morita, "Noise and Noise Control in Neighborhood," Acoustical Technology, Vol 10-35 1981 pp. 1-5)
한국건설기술연구원, 도로환경영평가 및 보전시설에 대한 조사, 최종보고서, 1988. (Korea Institute of Construciton and Technology, Noise Impact Assessment of Road Networks and Design Criteria for Traffic Noise Control Barriers, Final Report, 1988)
이광태 "소음과 주거환경," 주거용건물의 소음실태 및 저감대책에 관한 심포지움, 대한건축학회, 1991, pp.1-46. (Lee, K.T. "Noise and Residential Environment," Proceedings of Symposium on Noise and Noise Control of Dwellings, Korean Institute of Architects, 1991, pp.1-46.)

NOISE ABATEMENT IN DWELLINGS

Wang Jiqing
Institute of Acoustics
Tongji University
Shanghai, CHINA 200092

ABSTRACT

Lack of effective noise abatement has been cited as a major complaint by inhabitants of multi-unit dwellings for a long time. The number and power of acoustic sources in dwellings have grown tremendously thus stressing the need for noise abtement measures. In many countries, multi-unit dwellings are no longer built in the traditional way with thick and heavy floors and walls, but instead they are erected by modern prefab methods which usually involve reduced mass and thickness. As the demands of the general comfort of the inhabitant constantly grow, the desire for acoustic privacy increases, but economy stands diametrically opposed to these desires. Therefore, cheaper and simpler methods are always in demand to solve the noise problems, particularly for large scale dwelling constructions. All of these have led to increased emphasis on noise control in housing development and correspondingly a need for reliable technical information on this subject. The other interesting problems discussed in this paper are increased recognition of the importance of low frequency noise, demand for a short test method for sound insulation measurement in enforcement of building regulations, probability of using arithmetic average of the sound insulations at different frequencies (the method used half a century ago) instead of the current complicated grade curve method, etc..

1.0 INTRODUCTION

In many developing countries, new housing is always a long term undertaking. In China, the volume of housing accommodations needed is enormous; almost one hundred million m² of dwellings in urban areas are completed every year. And this volume will increase at a greater pace in the coming years. Newly built dwellings are expected to reach 50 million m² at the completion of the current 5-year plan (1991-1995) in the City of Shanghai alone. But our young building industry is facing many limitations that must be solved to meet the demands being placed upon it, when housing is still a major demand of the people whose main hope is merely to have a flat, even very small one. However as the demands for general comfort of inhabitants constantly grows and the desire for acoustic privacy increases, the economy nevertheless stands diametrically opposed to these desires. Therefore searching for a feasible compromise between a reasonable maximum of acceptable acoustical levels and the economic situation is a difficult goal, but one we must work toward.

Although the fundamental priciples of noise abatement in dwellings are well known to designers, in practice things are complicated by many other governing factors. For example, an effective noise control measure sometimes cannot be carried out in mass housing construction because the cost is too expensive or the process too complicated. Therefore, cheaper and simpler measures to solve the noise problems in dwellings are always in demand. As the current building trend is to use more and more light-weight structures, this problem becomes even more acute. All of these factors have led to an increased emphasis on noise abatement in housing development and correspondingly a need for reliable technical information on this subject.

2.0 OBSERVATIONS OF RESPONSE FROM SOCIAL SURVEY

Numerous studies on the reactions of people to environmental noise and the comparison of the results of a number of surveys of people's attitudes toward annoyance from aircraft and ground vehicle noise conducted in a number of western countries have appeared in much literature. The most comprehensive data have summarized in two well-known books by Schultz (1982) Community Noise Rating and Kryter (1985) The Effects of Noise on Man.

Here I will try to review the results of social surveys in China. The first survey of noise in dwellings in Shanghai[1] [2] was carried out almost three decades ago. There were 458 families interviewed in 1960 and 477 families in 1961 using different objectives for these two phases of the survey. At that time, people's living standards were, in general, considerably low. Complaints about noise were not the predominating one although the noise situation— noise existing inside the dwellings or intruding from outdoors, was severe. The biggest complaints from tenants initially were about the shortage of gas facilities, the need for larger space or another room, roof leakages, etc. But we also found that complaints about the noise from those dwellers with better accommodations became remarkable, even though the sound insulation between flats were the same as others or even a little better. It was obvious that noise problems in dwellings did exist but were just masked by other more urgent matters in some cases. Now in modern dwellings, inhabitants are more aware of the need for an undisturbed environment for listening, thinking, relaxation and sleep, and they desire more acoustic privacy.

A satisfactory acoustic environment was first defined (see Fig. 1) by studying the results of interviewing inhabitants in their homes, even though their opinions were somewhat arbitrary, corresponding with the noise levels measured at the same time in the rooms. A rank order scale was used for these evaluations, and a non-parametric

statistical method was used to analyze the results. Many other interesting results were also obtained from this detailed investigating survey.

In the early 1980s, a study of allowable noise level in indoor dwellings was carried out by Xiang[3]. The relationship between the responses of inhabitants from 93 families in Beijing and the noise levels, Leq, in daytime (15min.-sample noise in the period of 9-11 a.m. and 2-5 p.m.) is shown in Fig. 2(a). An Allowable noise level, Leq, of 45 dB(approximate 44.3 dB) was thus obtained, corresponding to the response of moderate quiet in the diagram. When this was compared with the response of inhabitants in other cities in China, a similar trend was found. This is shown in Fig. 2(b). These findings were used to outline a recommendation of maximum allowable noise levels in dwellings in Building Regulations[4] and were classified into three grades. Grade I for 40 dBA for more sensitive dwellers, Grade II for 45 dBA and Greade III for 50 dBA for low cost dwellings.

Recently Liu[5] conducted a survey of 905 families in Nanjing on the relationship between indoor noise levels, Leq, and the percentage of high annoyance during sleep, mental work(reading, writing and thinking) or rest and conversation, which are shown in fig. 3. Noise levels, Leq(16h) were measured during the daytime(6 a.m. to 10 p.m.) and Leq(8h) the nighttime (10 p.m. to 6 a.m.). 10% of high annoyance was assumed to be taken as the corresponding limit of permissible noise levels Leq; therefore the limits are: 35 dBA in night-time for sleep, 50 dBA (approximate 52 dBA in Fig. 3(b)) in day-time for mental work and 55 dBA (approximate 56 dBA in Fig. 3(c)) in day-time for rest and conversation (relaxation, conversation and musical appreciation).

Meanwhile, Zhen et al.[6] also reported a cumulative distribution of response of inhabitants to noise in dwellings(see Fig. 4), these authors suggested that the quality standard for noise was obtained from the noise levels which correspond to 30% in cumulative distributions for positive reaction. We can thus see in the diagram that the noise criteria for medium loudness and therefore for moderate annoyance would be considered as Leq57 dBA.

Interesting results were obtained in a comparative study between China and Japan[7] — survey on the noise environment of residences in urban areas. Reactions of inhabitants in the city of Beijing, China and in the city of Nagoya, Japan to noise environment are summarized in Fig. 5. A dramatic difference between reactions of inhabitants in these two cities was noted, although they had similar noise levels, Leq(24h) in Beijing was 1 dB higher than that in Nagoya. The percentage of positive reactions was much higher in Beijing (about 60%) compared with that in Nagoya (about 30%). But the relatioship between the loudness assessment of inhabitants and noise exposure levels, Leq, in residences showed considerable agreement in both cities (see Fig. 6).

Cross-cultural studies on noise problem have been carried out in Japan, Germany and UK since 1980[8], and in China since 1985, using a similar questionaire. The respondents in the first and second surveys in China were students and residents respectively[9] [10]. Among students, the results of surveys in different countries reflected the differences in social and cultural backgrounds, therefore, the Chinese results were more similar with Japenese results. The feelings of Chinese about neighborhood noise was intense. The attitude towards 'take care not to annoy neighbors by selfmade noise' was very critical. These results were also similar to Japenese results. 71% of the 387 residents interviewed about their living conditions complained mostly about noise problems. Fig. 7 shows the percentage of dwellers afraid to make noise by using domestic appliances and the percentage of dwellers annoyed by sounds heard from neighbors. The 'afriad rates' are much higher than the 'annoyed rates'.

3.0 MAXIMUM ACCEPTABLE NOISE LEVEL IN DWELLINGS

In many countries, surveys have been conducted on the effects of noise on various activities in everyday life. It can be seen from the results of these surveys[11] that 96% of the main noise sources annoying inhabitants were from outdoors. Therefore, in our country, outdoor noise, particularly from traffic, has its greatest effect on sleep, and to a slightly lesser degree on conversations in the home (including television, radio, telephone, etc.) followed by mental activity(reading, thinking).

Some studies have arrived at numerical relationships (rough approximations) between noise levels and the degree of effect on sleep, reading, thinking and relaxing, and particularly on speech communication.

Of course there are many other factors than noise that disturb sleep, such as age, occupation, characteristics of noise source, etc. But the limit of Leq(night-time) in general should be less than 40 dBA as no more than 10% of inhabitants were disturbed by noise[12] (see Fig. 8).

Studies of acceptable noise levels for listening to radio and television in dwellings indicate that for satisfactory listening by the average person the indoor Leq(1h) must not exceed 45 to 50 dBA, the lower level applying to steady noise. Of course, indoor noise levels that are 5dB lower are more comfortable and are desirable where possible. Thus acoustic consultants generally recommend that noise levels Leq (1h) not exceed 40 dBA, or at most 45 dBA in living room areas. For low cost dwellings, and also in year-round hot climate areas where residents keep their windows open, a limit of 50 dBA is acceptable.

By contrast, dwellings in colder climate areas may have higher acoustical requirements than in less confined situations. A recent paper[13] on noise complaints in Canadian residential condominiums analyzed why those owners complained when noise levels in their bedrooms were NC-30 or below. In one case, the lowest intrusive noise level was NC-26, but it might not seem so strange when you realize that the A-weighted background noise level was usually 10 dB below the noise level of the intrusion. In a sense, the background noise level plays the role of a reference level with which the noise under consideration is compared. Besides, the characteristics of the noise sources in those cases also exhibited sharp peaks or discontinuities in either the frequency or time domain. Therefore they increased the potential for annoyance.

4.0 LIMITATION ON THE USE OF DESCRIPTOR LEQ

Leq in decibels has been defined as the equivalent steady sound level to rate noises mainly for describing the onset and progression of permanent noise-induced hearing loss based on the energy or dosage principle. There is also considerable evidence to show that Leq applies to the prediction of annoyance in various community noise situations. But for inhabitants' activities indoors, this prediction would be less realistic. Fig. 9 shows two examples of noise doses received by individuals, husband and wife—office worker and home wife. Each noise dose, however, is a function of the recipient's life style. They have the same noise exposure during 7 p.m.-6 a.m. as they have a common daily life at home. Leq(24h)(without night-time penalty) of the office work husbant lived in suburban had a higher value than that of his wife by 8 dB. But the situation might not be so bad as this descriptor indicated. However, if the same value of Leq(24h) would be maintained at those higher levels at night, the situation would become very serious. Therefore a daily exposure diagram is very useful to examine the effects, but makes the assessment more complicated. Unfortunately few data concerning this matter are available at present.

14

5.0 ASSESSMENT BY GRADING CURVE METHOD

As the human perception of the loudness of noise depends upon its level and its frequency components, the amount of sound insulation required should at least equal the difference in noise spectra between the noisy room and the quiet one. Then if the noise penetrates to the quiet side it will not be heard or annoying. On the noisy side typical noises will be television, radio, voices, etc.; a NR-curve is usually used as acceptable criteria in the quiet room (see Fig. 10). The problem is the difficulty in making sure what levels and their spectra on both sides should be chosen for various situations in dwelling design.

Before WWII, Germany (1938) first proposed[14] an ideal sound insulation frequency curve for dwellings, which was equivalent to insulation provided by a 25 cm plastered brickwall measured in a laboratory. It was the most common party wall used at that time and its sound insulation was assumed to be sufficient for a dweller's acoustical privacy. This proposal was developed later and became known as the grading curve method for single number rating the sound insulation. ISO also recommended this method[15].

Sometime after WWII (1950s), Britian also proposed a grading curve (Grade I in their proposal), established on the basis of a wide survey and numerous in situ sound insulation measurements[16]. This grading curve was still based on the insulation provided by a 25 cm brickwall, but it did not agree very well with that proposed in Germany as seen from Fig. 11. This resulted in considerable confusion among the builders.

Fig. 12 shows some main rating methods used in Europe[17]. In Japan[18] [19], they use different reference curves (see Fig. 13) for sound insulation.

Moreover, with the changing trend towards prefabs, one might ask why the insulation provided by this brickwall should be a divine answer to the need for acoustic protection in dwellings. We have had a similar development for the requirements on impact sound insulation of a party floor, but there are much more complicated problem we should discuss in next section.

The correct shape of the grading curves were first studied with so-called 'wall filters' by Germany researchers[20]. They simulated the insulation curves of walls with electric filters and arranged a receiving room similar to a normal dwelling room. The observers listened to different complex sounds from loudspeakers, filtered through the 'wall' filters, and compared the loudness with a 1/3 octave band of random noise centered around 1000Hz. With this technique they demonstrated how different insulation curves influence the loudness of typical sounds in a receiving room. They found that quite different grading curves can be used as a basis for the insulation index without appreciably changing this objective measure compared with the subjective one based on loudness. Even the average figure seemed to follow the subjective measure surprisingly well. It seemed to be explained by the phenomena that two frequency ranges with good and bad insulation can compensate each other.

A comprehensive study on this subject with modern techniques has been conducted by Tachibana and his colleagues[21]. The source noises on the primary side of the walls were typical of indoor noise, M, and of rock music. The spectrum of the noise M was flat for the 250 to 1000 Hz bands, and fell off in the frequency bands both above and below. Simulated sound insulation charecteristics of 11 types of walls were chosen as shown in Fig. 14.

The hypothetical sound insulation properties were calculated from the assumed sound sources and the hypothetical transmitted sound from the experiment results. To arrange the all data, the following seven measures were used as assessment of sound insulation efficiencies of building walls: (1) D(ISO) , the measure prescribed in ISO 717/1, (2) STC, prescribed in ASTM E413, (3) D(JIS) , prescribed in JIS A1419, (4) MD, a similar measure as STC, but the reference curve of JIS A1419 is applied. (5) $\Delta L(125-4K)$, the arithmetic mean value of sound insulation effieciency (in dB) of octave bands from 125 Hz to 4 KHz, (6) $\Delta L(63-4K)$, similar value from 63 Hz to 4 KHz, and (7) ΔL_A, the level difference in A-weighted sound presure level. The results arranged by these measures are shown in Fig. 15(a) and (b). From this way of judging, we can see that the results arranged by $\Delta L(125-4\ K)$ and $\Delta L(63-4\ K)$ are most converged among the seven results in both figures. Here the arithmetic average of the sound insulation indices in octave bands is a good measure for the rating of sound insulation effi- ciencies of building walls.

6.0 ASSESSMEMT OF SOLID-BORNE INSULATION

Solid-borne noise usually orignates from impacts to the floor such as footsteps, moving of funiture (it is surprising how frequently the people upstairs move their funiture about), etc. It is a perfect nuisance to the inhabitants living below. There- fore, for the measurement of impact sound insulation, a standardized 'footstep' or 'tapping' machine[15] [22] has been used which has five hammers in line, each weighing 500 grams, and each falling freely 4cm at a total rate of 10 striking blows per second. The weighted normalized impact sound level $L'_{nT,w}$ referred to 0.5 second reverbe- ration time in the receiving room has been widely used as the single value for rating the floor (see Fig. 16(b)).

In the 1970s, when we prepared a Building Regulation proposal for impact insulation requirements for dwellings, a survey of dwellings with different floor constructions was conducted. These results, shown in Table 1, were the basis for that proposal i.e., $L'_{n,T,w} < 65dB$ for Grade I, and $< 75dB$ for Grade II. Since the economic situation at that time did not allow the use of a better impact sound insulation, we found some floor constructions with very poor impact sound insulation, $(L'_{n,T,w} > 85\ dB)$ which were totally unacceptable to the inhabitants. Since then, such types of floor cons- tructions are no longer being used and effective measures are being taken for improving the impact sound insulation. The Housing Administratoin Authority also drew a lesson from this that grave consequences would result if one put undue emphasis the weight of building element or economics and ignored comfort, acousti- cal privacy, etc. The living conditions in these dwellings were extremely bad, so bad in fact that many local authorities who had built dwellings with these types of floors were forced to modify them at heavy expense!

There is a wide range of opinion about the usefulness of the present tapping machine even though it has been the standard used by ISO in order to permit useful rank orde- ring of typical floor construction for footstep insulation. As footstep noise is felt to be one of the most important intruding noises in multi-unit dwellings, it has been well recognized that the impact force of the hammer machine is very different from the impact force of walking.

16

Table 1. Responses of in habitants to floor impact noise

	Types of R.C.Prefab Floor Construction	$L'_{n, T, w}$ dB	Percentage of the respondents		
			Acceptable	Moderate	Unacceptable
A	bare channel shape R.C. slab, bare R.C. large Panel	$\geqslant 85$	—	—	100%
B	bare 9-18cm hollow core R.C. slab	80-85	—	50%	50%
C	Same as B, with a suspended ceiling	< 75	10%	80%	10%
D	Same as B, with floor boards on battens	60-65	50%	50%	

For the measurement of the impact sound insulation it is not only necessary to imitate the special sound of walking, but the impact sound should represent different kinds of impact, for example, walking of women and men, playing and jumping of children, and moving of furniture. There is growing evidence, based on hundreds of North American tests, that ISO test results seriously disagree with the subjective evaluation of many floor/ceiling assemblies. Some questions have then been raised. For instance, what shape of criterion curve would represent the optimum improvement over the current curve for the standard hammer machine test? Should the frequency range on impact test be extended to lower frequencies, Which may be particularly important for joist floors? Should the tapping machine be modified or have a new exciting source instead of the current one? Therefore a sub-committee of the ISO Technical Committee 43 decided to form a study group in a 'New Hammer Source' in the late 1970s, but this group was disbanded after several years study without any encouraging results. So the ISO standard tapping machine is still being used, but one should keep in mind those deficiencies.

During the past two decades, some countries proposed new test methods, according to their individual considerations, such as in the USA, where two alternative test methods have been proposed, one a modified tapping machine (the middle hammer only was replaced with a hammer having a mass of 200 grams, two blows per second), and the other a 'standard' live walker. In Japan, where children jumping on tatami mats would be of major importance, they proposed using a heavyweight, soft impact source, or so called 'Bang Machine' method in addition to the ISO method to imitate such activity[23]. An ordinary automobile tire with a mass of about 7.3 Kg, tire pressure 1.5×10^5 Pa was used, with a free drop height of 80 cm, single blow for each measurement. Therefore they proposed a quite different criteria curve from one recommened by ISO for impact sound insulation assessment(see Fig. 13(b)).

7.0 IMPORTANCE OF LOWER FREQUENCIES

Significant recent developments have included the increasing recognition of the importance of low frequency noise as a component of room noise and community noise in general. The Room Criteria, or RC, curves represent on effort to recognize and quantify these components. The more recent revision of the noise criterion, or NCB, curves which include the 31.5 H_2 and 16 H_2 octave bands is a major step in extending a familiar and widely accepted form of criterion to include the often ignored low-frequency components of environmental noise.

Balanced Noise Criteria (NCB) (see Fig. 17) curves developed by Beranek[24] are based on the following considerations. Occupants of a space complain of imbalance in a noise spectrum using words like 'rumbly', 'hissy', 'annoying', etc. 'Rumble' is used here as a generic term meaning excessive noise in the octave bands with midfrequences below 1000 Hz. Excessive noise levels in the 31. 5 and 63 Hz bands may also cause perceptible vibrations or induced rattles in light-weight room partitions and ceiling systems, particularly in wood constructed buildings. It should also be noted that this can cause resonance of doors, windows or of furniture and wood floors and then produce rattling noises.

Fig. 18 shows an example[25] of a peak-hold frequency noise spectrum while the boiler was working. It is enough for sliding doors and windows (particular of Japanese style) to rattle. A-weighted sound pressure levels of rattling noise were 40-50 dB behind the doors.

It has been recognized that there is a need for additional low frequency limit for the living environmemt in the Dutch Noise Abatement Act, therefore Dutch Ministry of Environment and Housing (VROM) [26] has set a limit for the low frequency audio range based on experience of noise annoyance in the field (see Fig. 19).

Because we are improving our ability to measure and predict low-frequency noise, we are able to give more reliable sound transmission loss data for lower frequencies, say down to 63 Hz, in laboratory thereby allowing building designers to deal effectively with available noise data[27]. But we should note that because rooms in dwellings are small in size, it is still difficult to measure the sound levels in such low frequencies accurately in situ. We hope the 1990s will bring effective and valuable amendments to the standardized criteria and procedures which have gained acceptance in the 1980s.

8. 0 NEED A SHORT TEST METHOD FOR ENFORCING THE BUILDING REGULATION

In many countries, sound insulation requirements are included in building regulations, but only very few dwellings in Europe, and almost none in USA (1980) [28] and China have been tested to check the observance of building regulations. Therefore these regulations are not effectively enforced but remain a mere sheet document.

Field sound insulation measurements between dwellings on a broad scale is a very demanding job. For example, there are about 4-5 million m^2, or 80,000 to 100,000 dwelling units completed each year in the City of Shanghai alone. The amount of test work is enormous even if only a few percent of the newly completed dwellings are chosen test. Even minor mistakes during construction can spoil the best acoustical design, making insulation tests of newly completed buildings, therfore, an essential procedure to demonstrate compliance with the building regulations.

It was reported that the percentage of tested dwellings that fail to meet codes are very high, say 50 percent or even more in some European coutries[28]. This discouraging record of failure can be expected when no special incentives are offered to encourage the effective enforcement of noise control in dwellings. The only way to alleviate the current problem on inadequate sound insulation between dwellings is through the enforcement of building regulations. it is also widely accepted that the ISO 140 procedure and ISO 717 rating procedure are complicated, time consuming, expensive and require trained technical personnel. Therefore a simplified field test method of measuring sound insulation quickly and economically is needed.

18

The development of an ISO short test method[29] for the measurement of airborne sound insulation in buildings was started in 1982, and a Draft Proposal was finally approved in 1988. The method is based upon the determination of the difference of the 'A' weighted sound levels between adjacent rooms without regard to the paths of transmission. The criterion of validity for this short test was based on achieving a good correlation with the results obtained using the full ISO 140 procedure.

The short test method is basically intended for screening quality control of sound barriers in dwellings, so the current ISO Draft proposal would be sufficient for this purpose provided the experimental conditions are carefully controlled. Mainly it should include incidental pink noise, i.e., ideally the sound spectrum shape must be restricted as flat as possible.

One may argue that the test should be carried out in unoccupied room for several reasons: (1) The physical performance of the barrier describing the acoustical quality of the construction to be tested should avoid including furnishings in the receiving room; (2) A finished building should be checked for the acoustical requirements, before the permit for occupancy is signed; (3) Required remedial action against the construction company can be taken in case of failure; and (4) The acoustical conditions of the unoccupied receiving rooms may differ from each other but not as much as from furnished rooms.

For the above considerations, the absorption in the receiving room and thus the correction applied to the short test measurements can be discarded, therefore this short test method can be more simplified. The Japanese have already been doing this with their Standards, i.e., only sound pressure level difference measured[23]. The French regulations[30] which were modified in a similar way, state that A-weighted sound level in the receiving room must not exceed a given value when the source room is excited by a band limited pink noise. From the acoustical consultant's view, Yerges[31] states: 'A-weighted difference have served us well for many years. However, they do not yield diagnostic information. More importantly, they were really only stop-gap measures while we waited for computer controlled real time analysis equipment to become portable and affordable. That time has very nearly arrived. '

A new trend in single-number sound insulation rating focuses on the correlation between objective ratings and people reaction under different spectrum shape noise sources; therefore, the loudness and annoyance evaluation in the receiving room, weighting network procedure, extension of frequebcy ranges, etc., should be considered and re-examined. These problems also exist in the ISO 717 rating method. So it is a topic that need investigated more comprehensively.

Short tests of impact sound insulation seem to have received considerablly less interest than those of airborne sound insulation. So it seems that the only method is based on a frequency weighting and measurements of the overall level in the receiving room[32].

9.0 CONTROL OF INDOOR NOISE BY PLANNING

In multi-unit dwellings the stacking of identical units on sucessive floors one above the other so that kitchens are over kitchens and bathrooms are over bathrooms can aid considerably in noise control. These are not only noisy areas but frequently had hard surface floors which tend to increase the problem of impact sound insulation which is a souce of frequent complaints in existing dwellings. Such problems are costly to control by construction methods. The worst arrangement is to place noisy areas of one unit next to quiet areas of the neighboring unit, for example, kitchens next to neighbors' bedrooms, or a bedroom next to the elevator. In this case

even a 50 dB wall would probably be inadequate. Sometimes rooms are separated from adjacent noisy areas by buffer zones such as closets, stairways, halls and clothes closets, which are usually arranged to act as a sound barrier. If this is done, the 45 dB party wall may be adequate.

The plumbing fixtures serving kitchens and bathrooms are particularly troublesome sources of noise. The problem can be minimized by placing kitchens and bathrooms of adjacent units back-to-back and one above the other with the appliances in a wall away from the sensitive rooms. Methods of handling the special noise problems arising from mechanical and electrical appliances have been discussed elsewhere in many text books. It is particularly important in planning, however, to locate furnaces, pumps, compressors, fans and laundry equipment away from quiet areas such as bedrooms. In high-rise dwellings the location of elevators is a special problem since they may cause noise or vibration throughout the entire building. The above design principles may not be unfamiliar to the architect and dwelling designer, but they are usually ignored in their designing. Therefore they should always be reminded of them.

10.0 LIGHTWEIGHT CONSTRUCTION

The trend in modern industrial building today is the use of prefabs and field assembly for quick and economic construction; therefore lightweight building elements are essential. The other trend is using a dry process as much as possible. Hence panel-stud partitions are popular in residential buildings as they have the benefit of being lightweight, easy to install and quick to finish. But all of them have an adverse effect on sound insulation owind to their lightweight. How to improve the sound insulation of lightweight construction is a matter of primary importance.

We shall see, however, that the most pressing need is not for novel technical production methods or for magic new materials, but rather for the proper application of existing traditional methods of building construction.

10.1 Masonry Wall Solid clay brick has been widely used for thousands of years as the raw materials are readily available and the brick is easily produced. A 25 cm brick wall with both sides of plaster has long been recognized as a sufficient sound proofing barrier and has been taken as a standard for dwellings. But now clay is more treasured in high population districts and its use must be restricted. The Shanghai Municipal Government, for example, has issued a new regulation to encourage the use of lightweight wall material for construction and restrict the use of traditional solid clay brick to save energy and conserve land resources. This regulation has been enforced since May 1, 1991. A special charge (0.7 percent of the total investment of the project) is required if solid clay brick is used. The aim is to press the builders to use lightweight or hollow bricks or blocks for wall construction. You can see in the Table 2[33] as the weight decreases, their sound insulation performance is inevitably reduced. It is neither practical nor economical to further increase the mass and therefore the thickness of the wall. A more practical way is to add a thin resilent plate, separated bu an airspace, to the original, considerably heavier, partition. In order to prevent the buildup of resonances in the airspace between the wall and the skin and also to extract energy from the near field of the thin plate, the airspace is usually filled with a sound absorbing material.

This simple technique often permits the attainment of a considerable increase in sound insulation by very simple, cheap methods. This applies to new buildings as well as, in particular, to existing walls whose sound insulation had to be subsequently improved.

Table 2 Sound Insulation of Several Types of Wall and Floor Constructions[33]

| | Thickness (cm) | Weight (Kg/m³) | airborne sound | | Impact sound |
			average 100-4KHz	$D_{nT, w}$	$L'_{nT, w}$ (dB)
Load bearing wall: (both sides plastered)					
A. 22 cm solid clay brick	25	496	48	49	-
B. 22 cm air entraining silicate block	25	436	49	50	-
C. 14 cm ceramsite concrete panel	14	238	42	42	-
D. 14 cm vibrating brick slab	14	294	42	43	-
Non-load bearing wall:					
A. 9 cm hollow gypsum panel	9	50	28	39	-
B. 15 cm fly ash silicate block, both sides plastered	17	215	40	41	-
Floor:					
A. 16 cm, ellipse hocore conc. slab, with 3 cm cement screed	19	228	47	47	64
B. 16 cm, round hollow core conc. slab, with 3 cm cement screed	19	270	48	49	70
C. 16 cm, ellipse hocore ceramsite conc slab	18	178	38	38	78
D. 3 cm conc. panel with ribs and suspended ceiling	25	150	39	40	77

An example[33] of the effect of an additional layer of 2.5 cm wood-wool board attached to a 12 cm air entraining solicate block wall is shown in Fig. 20(a). The improvements ΔL and ΔR values of this construction are shown in Fig. 20(b). Owing to the nails, rigid point attachments, acting as sound bridges between two layers, the ΔR is significantly less than the ΔL. The improvement ΔR can be predicted with following expression:

$$\Delta R = -10 \log\left(\frac{f_0^4}{f^4} - n\sigma\frac{v_1^2}{v_2^2}\right) \text{, dB}$$

where f_0 is the resonance frequency of the attached layer, n is the number of bridges (nails), σ is the radiation coefficient, v_1 and v_2 are the velocities at the surface of the original wall and at the surface of the additional layer. Measured ΔL agrees well with the prediction.

The effects of different methods of attaching extra single layers of gypsum board to a concrete block wall were studied by Warrnock[27] recently. He concluded that lowering the mass-air-mass resonance frequency by increasing the thickness of wall-board or by increasing the depth of the air-space tends to increase the Sound Transmission Class (STC). Adding sound absorbing material to the cavity behind the gypsum wallboard lowers the resonance frequency, therefore improving the STC and sound insulation index at a low frequency. If the block itself is absorptive, the mass-air-mass resonance frequency may be lower than expected. Also, for a porous block, the effective depth of the airgap may be greater than the distance from the gypsum wallboard to the surface of the block. If this method is used as a remedial measure for an existing wall, care should be taken when the combination wall construction has a 50 dB or more sound insulation index. Because the flanking transmission will restrict the actual effectiveness in buildings, it is necessary to add extra layers to the flanking walls as well.

10.2 Panel-stud partitions These is some misunderstandings about panel-stud partitions spreading among builders and designers. They are usually cognizant of the benefit from double layers but ignore the harmful sound bridges caused by studs and rigid junctions at ceilings and floors. They often place insulating materials in between the cavity and ignore the mass or thickness of the cover plates.

It is well known that overall performance depends on the weight of the surface layers and the coupling through the air-space or through the studs, whichever is the more important. Usually the three factors are not independent, and it is difficult to present a simple analysis. Generally, increasing the mass of the surface layers reduces air-space transmission, but increasing their stiffness increases stud transmission; mineral wool in the space reduces air transmission; resilient connectors or separate studs (usually a staggered arrangement) reduces studs transmission. The overall performance may depend in a complicated way on each factor.

It is evident that the sound insulation of metal-stud partitions is higher than those made of wood by 5-7 dB on the average in similar panel constructions. Owing to the fact that U-shaped metal stud posses a resilient character. The sound insulation index R of a panel-metal-stud partition can be well predicted with following expression(Wang and Gu[34] [35]):

$$R = R_1 + R_2 - 20 \log K - 20 \log \frac{l}{sf_c} - 101 \ (dB)$$

$$(f > f_B, \ f < \frac{1}{2}f_c)$$

where R_1 and R_2 are values of the mass R for panel 1 and panel 2 respectively; K is the lateral equivalent stiffness per unit length of the metal stud; S is the surface area of the panel; l equals the total length of line connections; f_c is the critical frequency of panel 2 (panel facing the receiving room) at which the coincidence occured; and f_B is the bridge frequency. The results are shown in Fig. 21.

10.3 Floors The principles described for walls also apply to floors as far as airborne sound is concerned. As explained earlier the factors that determine airborne sound insulation are weight, stiffness, breaks in sound travel paths, and sound absorption within the space.

Transmission of impact sound through floors is an additional problem, which occurs when the floor vibrates due to direct mechanical contant. This noise is transmitted through the floor structure and radiates to the room below. This type of noise can lead to more complaints than airborne sounds.

22

The most effective method of reducing impact noise transmission is by the use of a soft floor covering such as a carpet and pad. Another method of control is to provide a floating floor surface. This can be done by separating the finished floor from the floor structure by means of a resilient layer such as fiberboard. Similarly the ceiling may be suspended by the use of resilient clips which partially isolate the ceiling from the floor structure.

Unfortunately the above measures are seldom used in mass-built dwellings in our country owing to economic problems, etc. We tried to design a less expensive floating floor that would reduce impact noise transmission years ago[36], but the complicated construction process prevented it from becoming popular. The quick development of the polyester industry has produced a less costly synthetic carpet, which may provide a better outlook to residents wishing to reduce annoying impact noise, even for those with poorly-constructed floors.

11.0 BUILDING FACADE

Results of a survey in Beijing(1986)[6] indicated that 96% of main noise sources annoying inhabitants in dwellings were from outdoors, and were mostly traffic noises. Therefore the noise reduction of the facade and facade elements are important for reducing the effects of the outdoor traffic noise on the indoor environment. But in the case of windows frequently opened for ventilation and cooling purposes, the noise reduction effects are very limited. There is little data available for the noise-reducing properties of facade constructions, with the exception of windows, for which most of the data has been obtained for fixed, unopenable sashes in laboratory.

There are two test methods, measurement with traffic noise and with loudspeaker noise, recommended in ISO 140/IV for field measurements of airborne sound trasmission of facade elements and facades. There is evidence[37] [38] that the real traffic noise source consistently gives lower noise reduction values than does loudspeaker radiated noise (see Fig. 22). This is thought to be related to the limited angles of incidence of the sound reaching the facade from the loudspeaker source; real traffic ranges from nearly grazing incidence to normal incidence as individual vehicles pass a building and it is well known that materials have a transmission loss at grazing incidence which will affect the overall results.

Facade with open windows may attenuate the traffic noise around 5 dBA and 10 dBA at most which depends on the window size, floor height, etc. Balcony and building recesses are alternatives for facade design, as they may affect some noise reduction. A series of field measurements[39] (see Fig. 23) were carried out to collect noise reduction data with road traffic as the main source for 14 rooms in two office buildings and 39 rooms in five apartments to determine the effects of a window closed or open, a balcony, floor height and an open area and room size. In the case of rooms with a balcony 1 meter deep with a closed parapet, the variations of noise reduction levels based on noise indices Lx and Leq have about 1 dBA to 3 dBA more than rooms without balconies. It is also obvious that a higher floor height has a more significant effect on noise reduction. A comparison between the noise reduction values of a window open and a window closed shows that the former is about 5 to 9 dBA less.

There was a new idea[40] [41] to design a building facade with perforated screens with unusual geometric design—thnadner screen (an amplitude gradient design) and splitter screen(a phase gradient design) (see fig. 24). The results obtained from scale model test indicated that these barriers as part of a courtyard can give protection ranging between -3 dBA and +8 dBA (at frequencies corresponding to a full scale range of 200 Hz to 4000 Hz) compared with that of a solid barrier of equal height. Such perforated screens as a modified acoustic grating could enable an architect to design a protective facade with respect to noise, which, at the same time, provides solar protection and ventilation.

A closed balcony can give maximum protection for the internal rooms, even in the case of open windows. Fig. 25 illustrates sample test results of closed balcony in field[42]. The closed balcony facade gives a noise reduction of 10 dB. Noise reduction of the partition with closed windows between the balcony and the bedroom is 30 dB. Therefore for the bed room a 40 dB protection against outdoor traffic noise can be achieved(see curve C in Fig. 25).

When dwellings (each flats has more than one room) are paralled to the road, the inhabitants need not spend all their time in rooms facing the noisy road. Then the rooms at the opposite side will be quiet and more satisfactory. This so-called 'escape room' is less annoying than those not paralled to road. An 'escape room' may have about 4 dB lower noise exposure[43] (see Fig. 25). Similar results were found in Japan and Vienna.

12.0 FLANKING TRANSMISSION

It is well known that the flanking sound transmission may seriously impair the sound insulation between flats in a multi-unit apartment building, because many measurements have shown that flanking elements transmit as much sound as or even more than partition. Therefore the effectiveness of sound insulation between flats not only depends on the insulating performance of the partition, but it also depends on the flanking transmission through structural elements common to the source and receiving rooms. The flanking transmission effect becomes more important when the sound insulation requirement between flats is high, and it may also differ in various buildings.

12.1 Fundamental Considerations

During the past decade, many detailed investigations on sound transmission between flats through partitions and flanking structures have been carried out. Fig. 27 shows an example[44] of a detailed measurement of the standardized sound level difference found in any of the building parts (partition floor and 4 flanking walls) between two living rooms separated by a floor. These levels, which were calculated from the velocity levels measured in situ, show clearly that the flanking out wall(facade) provides the poorest sound insulation and is mainly responsible for the transmission of sound. Therefore, to improve the sound insulation between flats, more data is needed on the sound insulation index for direct transmission of sound through the walls and floors and the velocity level differences across the junction, Dv. The literature gives many results of noise suppression testing in joints, most of which is referred to in laboratory tests of joint models. There is a relationship existing between velocity level difference across a junction and the transmission coefficient which can be defined as the ratio of incidence and transmitted power of the bending wall field at a junction. In practice, the transmission coefficient is essentially a function of the mass ratio of the coupled structure, i.e., the mass ratio of the partition and flanking elements. In most cases, the velocity level difference is practically independent of frequency. It is felt that field measurements are needed in order to quantify the vibration transmission through the structures, since the available theoretical work on that subject is insufficient or not suited for practical application. Values for Dv obtained in situ measurements have been published by several authors[45]. The values from Fasold-Sountag-Winkler are shown in Fig. 28.

Besides the mass ratio of the coupled structures, level difference Dv may also be increased by an insulating layer—elastic spacer between partition and flanking elements. For example, a layer of 3 mm bituminous felt may increase the Dv at the junction about 5 dB, and a layer of 10 mm cork may increase it 8 dB.

Some more complicated measures have been used to eliminate the flanking transmission path in sandwich facade wall elements[46]. The horizontal insulation of a 140 mm concrete partition wall was greatly reduced when slits were made in the facade panels with a saw, see Fig. 29. Special attention should be taken in these cases to insure that all the joints are sealed very carefully with a high quality never-hardening elastic compound.

However, all the above approaches may not be appropriate from the builder's view. For example, the elastic spacer makes the partition a free-satnding structure instead of a rigid joint at the junction and is not appropriate for a partition floor; the slitted facade panels are difficult to install, and this can lead to a water leakage problem.

12.2 Flanking Transmission To Rooms Without Common Partition

Either the airborne-sound or the solidborne-sound may be transmited to distant parts of the building through the flanking structure path, and therefore cause annoyance factors in rooms far apart from the source room. Also different flanking transmission effects may occur in different types of building construction.

In order to illustrate the severity of these flanking problems, some interesting sound insulation measurements between the source room and several surrounding rooms in dwellings with different construction types were carried out[47]. For solidborne sound, the impact sound levels L' measured in diagonal adjacent room corresponding to a reference value of 0.5 s reverberation time in the receiving room are shown in Fig. 30(a) when a standardized tapping machine was used in source room. The differences between the impact sound levels in the room under the source room (room C) and in the diagonal adjacent room (room D) (i.e., $\Delta L_1 = L'_C - L'_D$, dB) for the four construction types are shown in Fig. 30(b). Smaller differences ΔL_1 for the construction type(4) reveal the flanking transmission playing an important role in the impact sound transmission. This type of construction was the only one in which a suspended ceiling was used beneath the floor, so flanking becomes more important here than in the others. The differences between impact sound levels in room B (L'$_B$) and in room C (L'$_C$) were usually small and with negative values, as levels in both rooms were controlled by flanking transmission. The only exception that appeared here was in the case of (4), because the suspended ceiling reduced the radiation of sound to room D from the continuous structural floor of the source room.

Although measurement was carried out to include a whole dwelling[47]. For example, a map of the impact sound level distribution (at octave-band center frequency 1000 Hz and 2000 Hz) in many surrounding unoccupied rooms in two different construction types are shown in Fig. 31. The vertical attenuation (dB per story) and horizontal attenuation (dB per room) at far fields were thus obtained as a rough index for flanking transmission, which are shown in Table 3 and 4. A similar work had been done by Matsuda et al.[48], and one of their measurement results is shown in Fig. 32.

Table 3. Vertical attenuation in dwellings (dB/story)

Construction type	125 - 250 Hz		500 - 1000 Hz		2000 - 4000 Hz	
	Air-borne	solid-borne	Air-borne	Solid-borne	Air-borne	Solid-borne
Brick	-	5	-	5.5	-	9
Silicate Block	3	5	3.5	4.5	3	8
Ceramisite Conc. Panel	3	3.5	3	6	4	9
R.C. Skelton	-	6	-	7	-	8

25

Table 4. Horizontal attenuation in dwellings (dB/room)

Construction type	125 - 250 Hz		500 - 1000 Hz		2000 - 4000 Hz	
	Air-borne	solid-borne	Air-borne	Solid-borne	Air-borne	Solid-borne
Brick	4.5	2.5	4.5	4.5	7.5	8
Silicate Block	5	3	4.5	5	4	10
Ceramisite Conc. P.	4.5	3.5	4.5	5	4	7
R.C. Skelton	-	5	-	6.5	-	11.5

12.3 Prediction Of The Flanking Transmission

Calculations of the sound insulation between flats, flankong transmission being inc-
luded, are more useful to the building designer. Gerretsen[49] established a calcula-
tion model for the sound trasmission between flats by partitions and by flanking
structures, based on the application of classical theory, i.e., based on diffuse sound
fields and diffuse bending wave vibration fields. He developed a procedure by which
the sound insulation index between flats could be predicted from architectural draw-
ings and the materials to be used for a given building at the design stage. The neces-
sary input data was partly based on theory and partly on a large number of in situ
measurements.

The model for calculation of impact sound insulation was also deduced by Gerretsen[50],
following the same line of reasoning used in airborne sound insulation prediction. In
this approach, special attention was given to the admittance of floor constructions.
Measurements were carried out in order to collect data on this admittance for some
commonly used floors. These calculations showed a reasonable agreement with the mea-
sured values.

There was an another calculation method done with single numbers[44]. The wieghted
sound level difference $D_{n,T,w}$ (referred to 0.5 s reverberation time in the receiving
room, known as standardized level difference in ISO 140) can be calculated from

$$D_{n,T,w} = -10 \lg \left[10^{-D_{n,T,w,d}/10} + \sum_{i=1}^{n} 10^{-D_{n,T,w,r,i}/10} \right]$$

where $D_{n,T,w,d}$ is the weighted sound level difference given by the partition in dB,
$D_{n,T,w,r,i}$ is the weighted sound level difference given by the ith flanking element
in dB, and n is the number of flanking elements.

12.4 SEA Method

Statistical energy analysis (SEA) is the most suitable framework of analysis for stu-
dying flanking transmission and can be used not only for determinng the flanking tran-
smission between adjacent flats but transmission between any rooms over long distances
in a building. The SEA method makes use of the power flow between coupled systems,
describing the properties of the system using statistics. This method is used under
the assumption that the different flanking structures can be considered separately, the
interaction thus being negligible; and in fact the secondary power flows are indeed
negligible. Craik and Trancanamootoo[51] recognized that longitudinal and transverse

26

waves were assumed to be generated at the structural joints in addition to bending waves. Therefore it was assumed that coupling between all wave types took place at the joint. Each wave incident at the joint generates all wave types at all plates. Such a model is more complex than if only bending waves were being considered in the structure elements. But from the experimental results it was concluded by Craik that the omission of longitudinal and transverse waves should lead to large error in the predicted response at some distance from the source, although the errors were small close the source.

REFERENCES

1. WANG Jiqing et al., Noise survey of apartment houses in Urban Shanghai, Part. 1, Proc. of the 1960 Symposium of Shanghai Acoustics Group. Vol. 3, 21-35(1962)(in Chinese).

2. WANG Jiqing et al., Noise survey of apartment houses in Urban Shanghai, Part II, Proc. of the 2nd National Building Physics Conference, Beijing, 1962, 252-266(1965)(in Chinese).

3. XIANG Binnan, Study of allowable noise levels in dwellings in China. Proc. Inter-noise 87, Beijing, 1145-1148.

4. GBJ 118-88 Acoustical Design Regulations for Civil Buildings. Chapter 3, Residential Buildings (1988).

5. LIU Xiantu, Analysis of the acoustical environment of urban dwellings. Applied Acoustics 29(4)273-287 (1990).

6. ZHENG Darui et al., Study on environmental noise exposure of residence. Chinese Journal of Acoustics, (E), 8(3)243-253(1989).

7. Kazuhiro Kuns et al., Survey on noise environment of residence in urban area - Comparative study between China and Japan. Proc. Inter-noise 87, 871-874.

8. Seiichiro Namba et al., A cross-cultural study on noise problems. J. Acoust. Soc., Japan (E), 7(5)279-289 (1986).

9. ZHENG Darui et al., Cross-cultural study on a neighborhood noise problem results of students. Acta Acustica (C), 15(2)91-99(1990).

10. ZHENG Darui et al., Questionaire Survey on noise problems in apartment houses. Proc. Inter-noise 87, Beijing, China, 989-992.

11. ZHENG Darui et al., Study on environmental noise exposure of residence. Chinese Journal of Acoustics (E), 8(3)243-253(1989).

12. ZHENG Darui et al., Survey and analysis on sleep disturbance in Nagoya City. J. Acoust, Soc. Japan, (J), 40(11)730-735(1984).

13. WU Meiqin et al., Noise complaints in residential condominiums. Proc. NOISE-CON 90, Austin, Texas USA, 291-296.

14. DIN 4110. Technishe Bestimmungen fur die Zulassung neuer Bauweisen. Abschnitt D11. (Schallschutz) 1938.

15. ISO 717-1982. Rating of Sound Insulation in Buildings and of Building elememnts (1982).

16. P.G. Gray et al., Noise in three groups of flats with different floor insulations. National Building Studies. Research Paper No. 27. HMSO, London, 1958.

17. L.C. Fothergill, Sound insulation between dwellings. Applied Acoustics 24(4)321-334(1988).

18. JIS 1417 Field measurements of sound pressure level difference in buildings.

19. JIS 1419 Classification of airborne and impact sound insulation for buildings.

20. H.J. Rademache and G. Venzke, Die subjektive und objektive Bewertung des Schallschutzes von Trennwanden und-Decken, Acustica,9,409-416(1959).

21. H.Tachibana et al., Subjective assessment of indoor noises - Basic experiments with artificial sounds. Applied Acoustics, 31(1-3)173-184(1990).

22. ISO 140/I-VIII Building Acoustics - Measurements of sound insulation in buildings and of building elements (1978).

23. JIS 1418 Field measurements of impact sound transmission of floor in buildings.

24. L.L.Beranek, Balanced noise criterion curves, NCB, J. Acoust. Soc. Am., 86(2)650-664(1989).

25. H. Ochiai, M. Yamashita, Ratting of doors generated by low frequency sound in dwellings. Proc. Inter-noise 89, Newport Beach, USA, 843-846.

26. M.L.S. Vercammen, Setting limits for low frequency noise. J. Low Frequency Noise and Vibration, 8(4)105-109(1989).

27. A.C.C. Warnock, Sound transmission through some concrete block wall system. Proc. Inter-noise 90, Gothenborg, Sweden, 41-46.

28. T.J. Schultz, Noise Control for the 1980's: Building acoustics. Proc. Inter-noise 80, Miami USA, 65-84.

29. ISO DP 10052, 1989-01-17, Short test method for measurement of airborne sound insulation in buildings.

30. J.P. Vian, Comparison between European sound insulation rating methods for dwellings, Proc. 13th ICA, Yogoslavia 1989,81-84.

31. J.F. Yerges, The future of single number indices for assessing sound insulation as seen by the consultant. Proc. 13th ICA, Yogoslavia 1989,91-94.

32. J.Parmamen, Principles of constructing a short test method for impact sound insulation measurements. J.Sound & Vib. 128(2)181-194(1989).

33. WANG Jiqing, The progress made in the study of sound insulation in dwelling buildings. J.Tongji University (C), No.1,1979,1-19.

34. WANG Jiqing and Gu Qiangguo,Performance of sound TL of metal-stud light-weight panel partitions. Proc. Inter-noise 82, San Francisco, USA,475-478.

35. GU Qiangguo and WANG Jiqing, Effect of resilient connection of sound TL of metal-stud double panel partitions. Chinese Journal of Acoustics (E), 2(2)113-126(1983).

36. WANG Jiqing et al., Experiences on impact sound insulation of floors in dwelling buildings. Acta Acustica (C), 3(2)117-121(1966).

37. M.Burgess and A.Lawrence, Road trafic noise reduction of facades, measurement procedures and problems. Proc. Community Noise Conference, Toowooba, Australia 1986, 329-336.

38. A.Lawrence, Noise reduction on facades - more measurement results, Proc. 12th ICA, Toronto, Canada, 1986, E2-3.

39. H.C. Shih, Prediction of outdoor-indoor noise reduction by the configuration of building facade, Proc. Inter-noise 86, Cambridge, USA, 701-704.

40. L.S. Wirt, The control of diffracted sound by means of thnaders (shaped noise barriers), Acustica 42(2) 73-88(1979).

41. R.N.S. Hammad and B.M. Gibbs, The acoustics performance of builbing facades in hot climates: Part 1 - courtyards. Allpied Acoustics 16(2)121-137(1983).

42. E.Salzer, Stadtebaulicher Schallschutz. Bauverlag GmBH, Wiesbaden und Berlin(1982), p.89.

43. T.J. Shultz, Community Noise Rating, Apllied Science Publishers (2nd Edition) 1982, p.259.

44. J.Lang, Sound insulation in buildings - Requirements and the fulfillment. Proc. 29th Conference on Acoustics, High Tatra, Czechoslovakia, October 1990,144-150.

45. W.Fasold, E.Sonntag and Winkler, Bau- und Raumakstik, VEB, Verlag fur Bauwessen, Berlin 1986.

46. H.Elvhammar, M.Hansoson, Flanking transmission in sandwich facade wall elements. Proc. Inter-noise 90, Gotherburg,Sweden,79-82.

47. Wang Jiqing, Field sound insulation measurements in a concrete frame dwelling building with lightweight panel wall. Proc. 3rd National Building Physics Conference (C),1978,68-74.

48. Guri Matsuda et al., Propagation charateristics of solid-borne sound in building structures. J. Acouct. Soc.,Japan (J),35(11)609-615(1979).

49. E. Gerretsen, Calculation of the sound transmission between dwellings by partitions and flanking structures. Apllied Acoustics, 12(6)413-433(1979).

50. E.Gerretsen, Calculation of airborne and impact sound insulation between dwellings. Apllied Acoustics 19(4)245-264(1986).

51. R.J.M.Craik, A.Thancanamootoo, Flanking transmission through buildings. Proc. Inter-noise 90, Gotherburg, Sweden, 75-78.
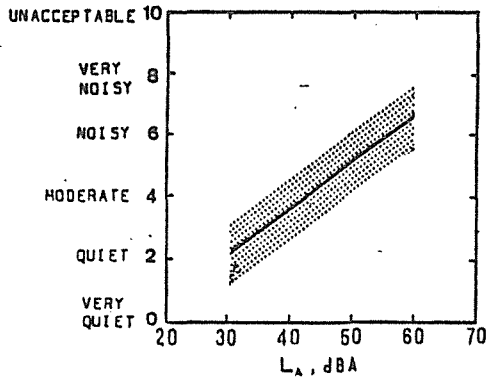
Fig.1 Relationship between responses of inhabitants and noise levels[1][2].
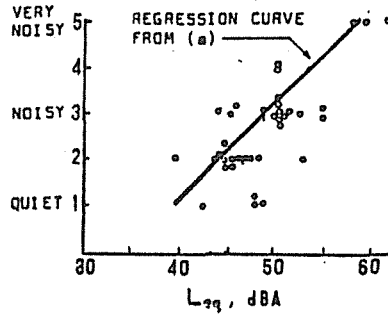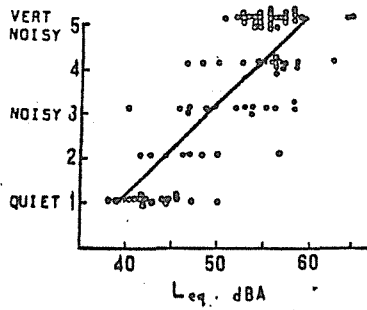
Fig.2 Relationship between responses of inhabitants and noise level Leq, (a) regression curve from responses in Beijing, (b) from other cities in China[3].
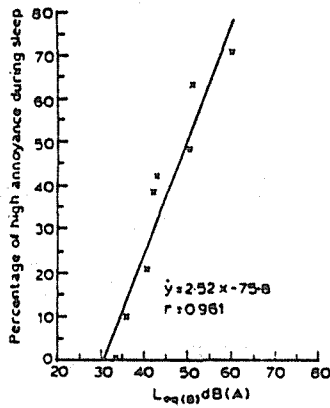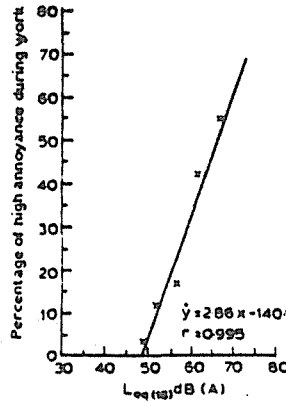
(a) Sleep   (b) Work   (c) Rest & conversation

$\dot{y}=2.52x-75.8$
$r=0.961$

$\dot{y}=2.86x-140.1$
$r=0.995$

$\dot{y}=1.498-75.13$
$r=0.92$
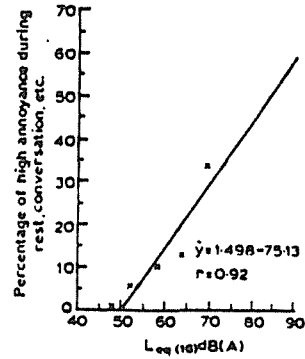
Fig.3 Relationship between pertange of people suffering a high degree of annoyance during (a)sleep, (b)work and (c)rest and conversation and the noise level[5].
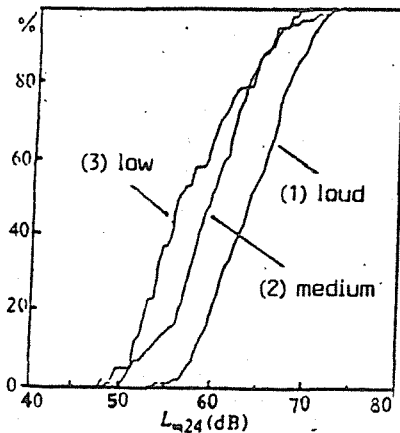
Fig.4 Cumulative probability distribution for different responses of loudness to noise in house[6].
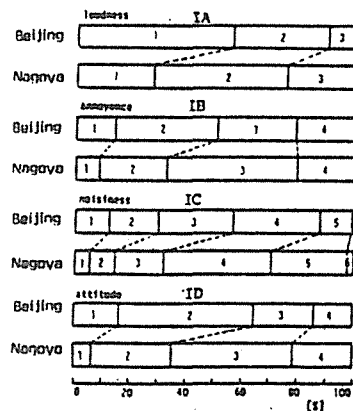
[A] How do you feel noise level around your residence ?
    Answer: (1) loud (2) medium (3) low

[B] Are you annoyed by it ?
    Answer: (1) very annoyed (2) annoyed
        (3) little annoyed (4) not annoyed

[C] Do you feel noisy around your residence ?
    Answer: (1) very noisy (2) pretty noisy (3) noisy
        (4) little noisy (5) quiet (6) very quiet

[D] How do you think about the noise ?
    Answer: (1) should be abated
        (2) desirable to be abated
        (3) pay no much attention
        (4) pay no attention

Fig.5 Reactions of inhabitants to noise environment, Beijing and Nagoya[7].

29
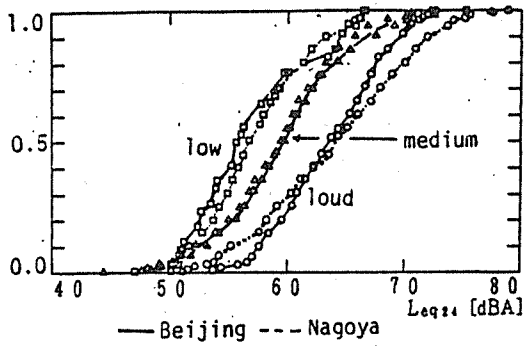
Fig.6 Cumulative distribution of Leq 24 for each group of reaction around residence on loudness of noise around residence[7].

SOUND SOURCE
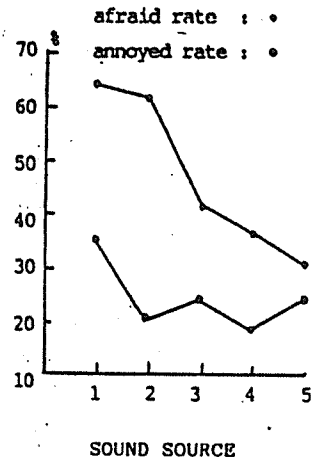
Fig.7 Comparison of afraid rate and annoyed rate [10]. 1.Stereo, 2.TV set, 3.Radio, 4.Sewing machine, 5.Washing machine.
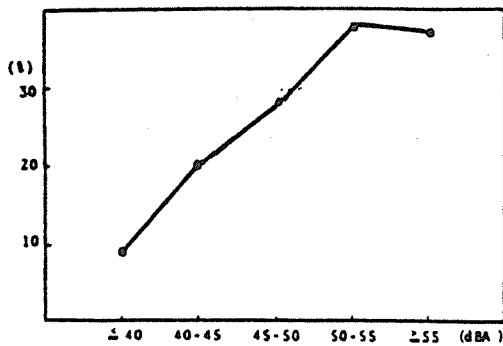
Fig.8 Relationship between Leq 1/6(1.5h) and percentage of sleep disturbance.
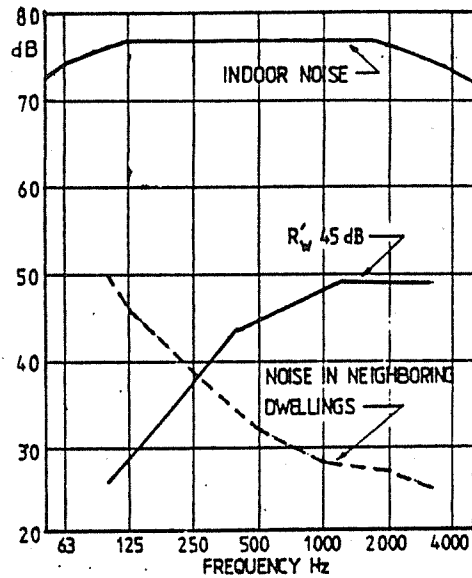
Fig.10 Noise penetrated into neighboring dwellings.
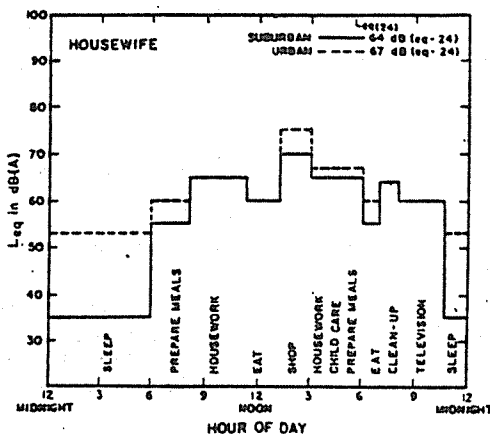
Fig.9 Typical daily noise exposure patterns of (a) an office worker and (b) his wife.

30
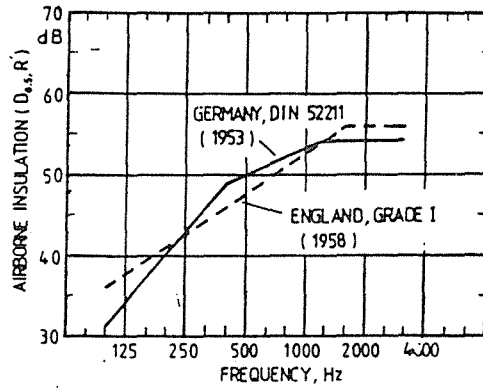
Fig.11 The Germany requirement and English Grade I
recommendation, both based on the brickwall
insulation do not coincide.
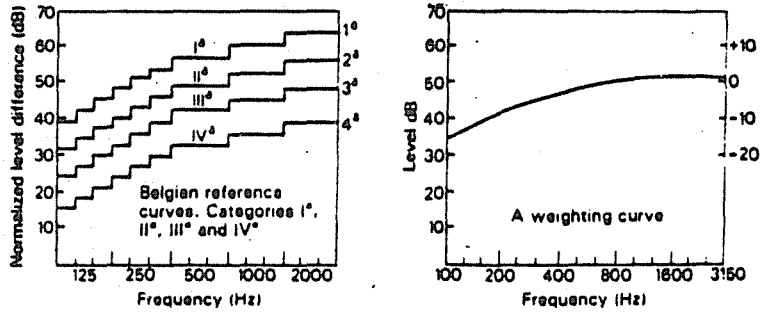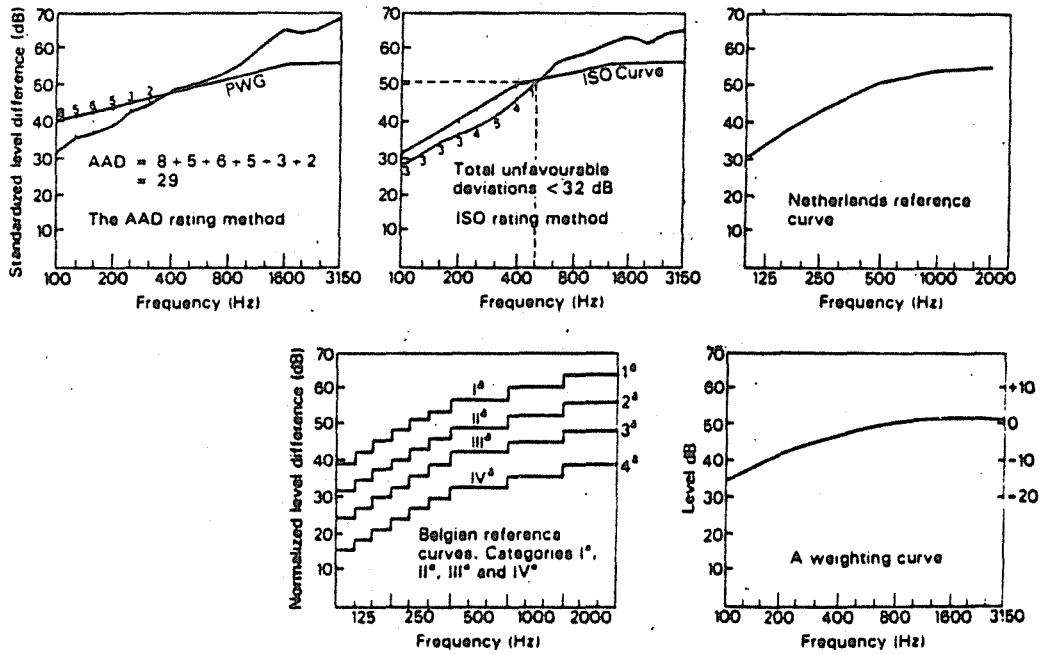
Fig.12 Main rating methods used in Europe[17].
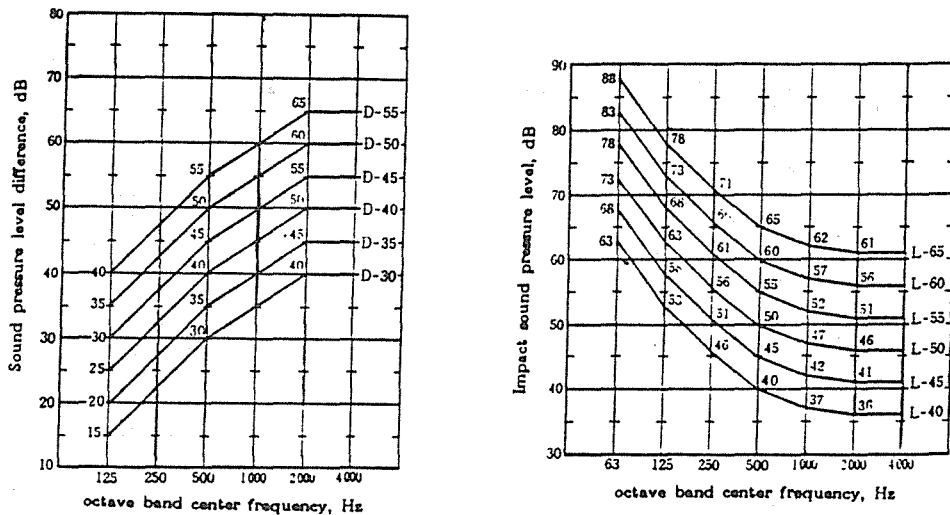
Fig.13 Japan standard(JIS 1419): Classification of air-borne and impact sound
insulation for builbings[19].

31
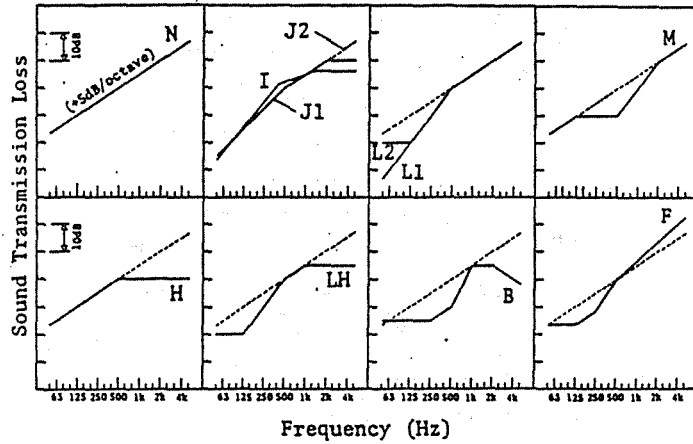
Fig.14 Sound TL spectra used in equal efficiency judgement test of fig.15[21].
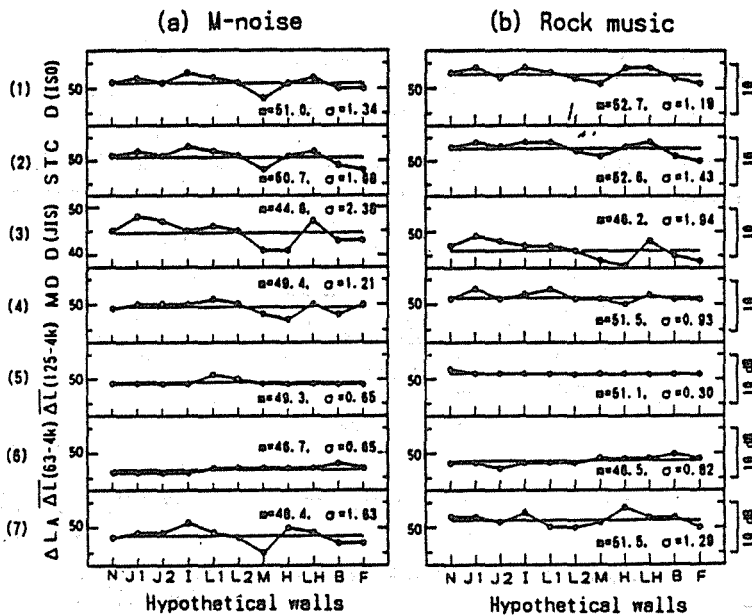
Fig.15 Comparison of sound insulation charecteristics judged equally efficient, evaluated by seven assessment measures (a)M-noise,(b)rock music[21].
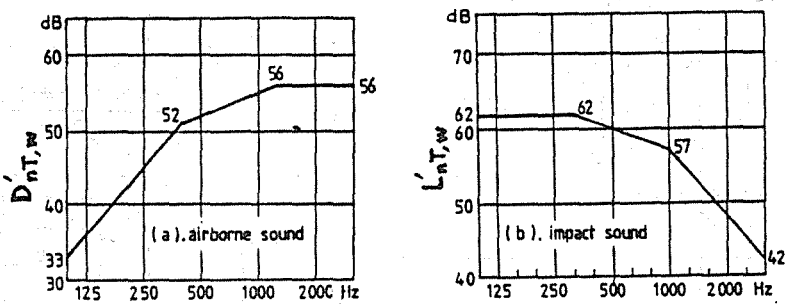
Fig.16 Reference curves for (a)airborne sound and (b)impact sound insulation in ISO 717[15].
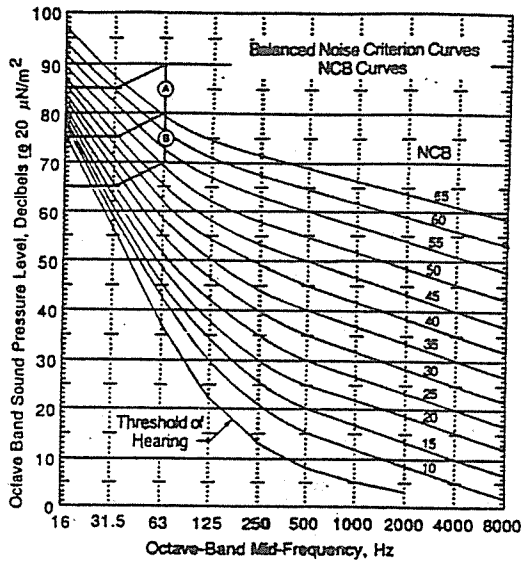
Fig.17 Balenced noise-criterion (NCB) curves for occupied rooms. Octave-band SPL of the magnitudes indicated in regions A and B may induce audible rattle or feelable vibration in lightweight partitions and ceiling constructions [24].
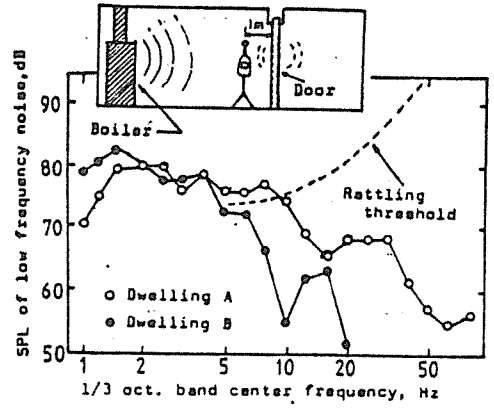
Fig.19 Spectra of low frequency noise by burning of a boiler[25].
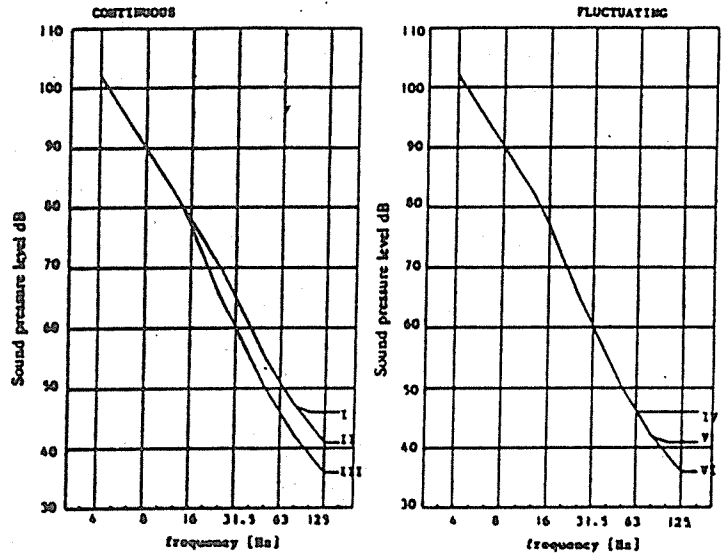
Fig.18 Low frequency noise limits for the living environment proposed by Dutch Ministry of Environment and Housing (VROM)[26].

CONTINUOUS NOISE	ADMISSIBLE dB(A) LEVEL (day-, evening- or nighttime)	FLUCTUATING NOISE
III	25	VI
II	30	V
I	35	IV
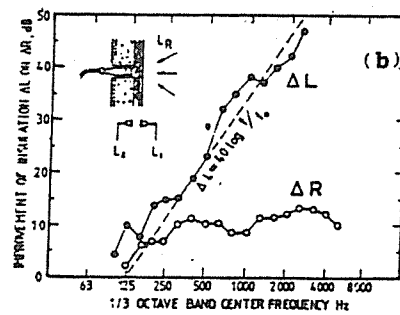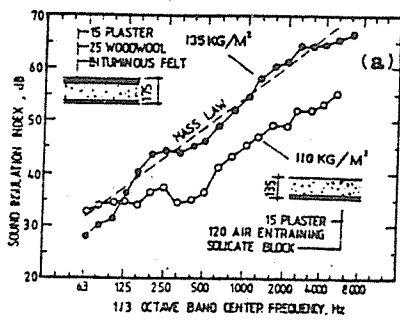
Fig.20 (a) Sound insulation indices R of an air-entraining solicate block wall before and after an additional layer being attached, (b) Sound insulation improvements measured between two rooms ΔR, and between two surfaces ΔL[33].
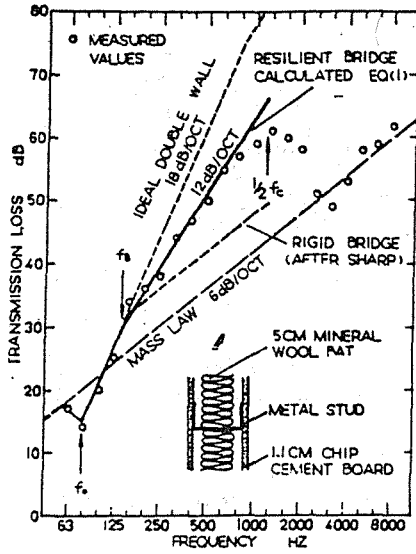
Fig.21 Measured values and predicted curve of the
TL of metal-stud partition[34][35].
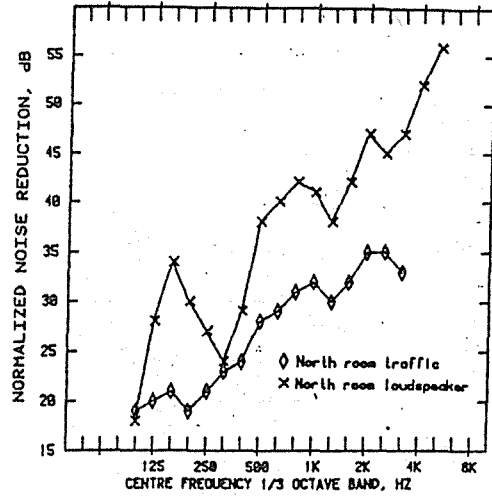
Fig.22 Comparison of results for facade attenuation
using londspeaker radiated noise and road
traffic noise as source[37].
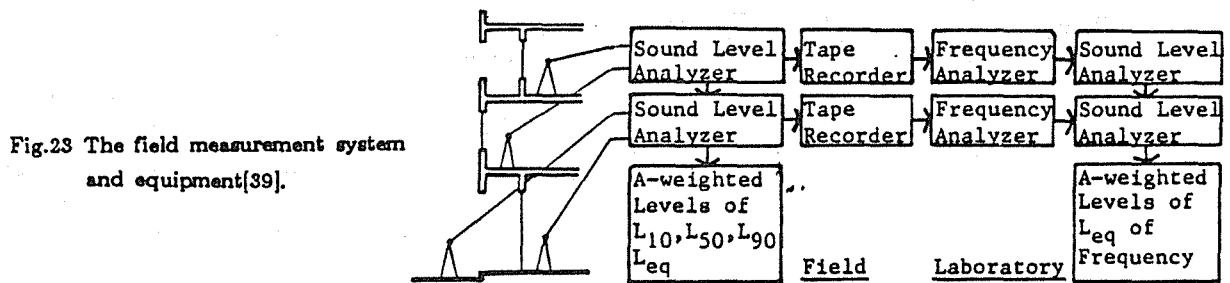
Fig.23 The field measurement system
and equipment[39].
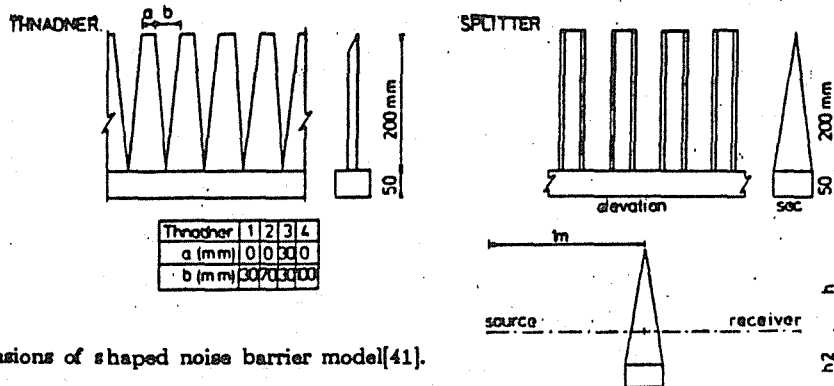
Fig.24 Dimensions of shaped noise barrier model[41].
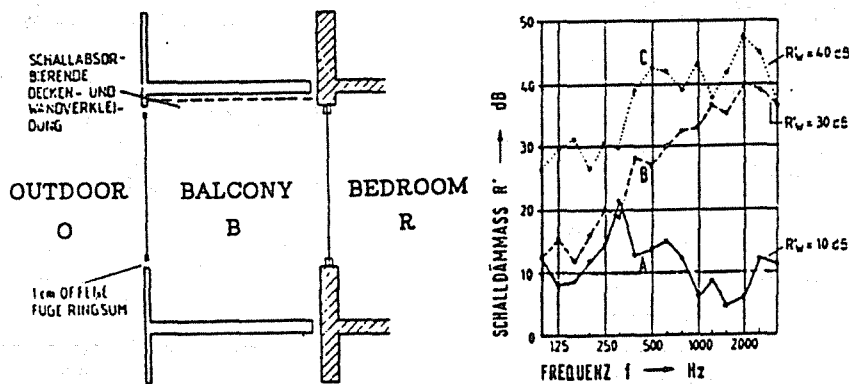
Fig.25 Using closed balcony (B) as a shelter of the bedroom (R) to protect the
outdoor noise[42]. Curve 1, measured between outdoor O and balcony B,
Curve 2 measyred between balcony B and bedroom R. Measured attenuation of
outdoor noise for bedroom(O-R) is shown in curve 3.

34
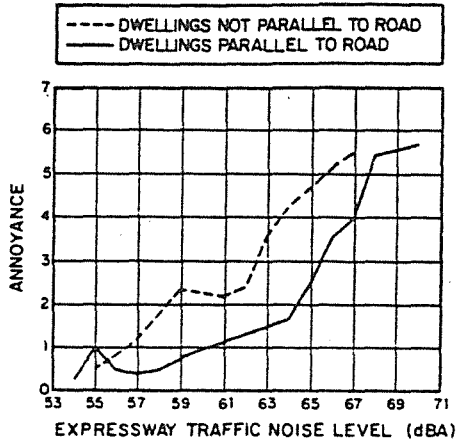
Fig.26 The "escape room" effect in the French social survey on expressway noise.
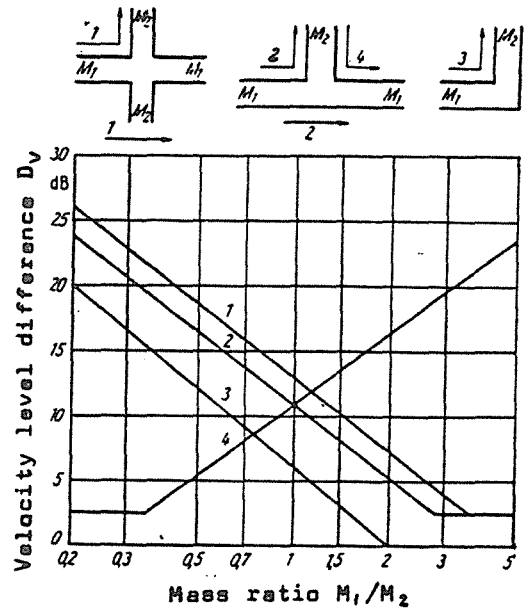
Fig.28 Level difference at a junction[45].

		D_{n,T_w} = 62 dB
-------	ceiling	
-------	outer wall	D_{n,T_w} = 54 dB
-------	outer wall with window	D_{n,T_w} = 58 dB
-------	partition 1	D_{n,T_w} = 62 dB
-------	partition 2	D_{n,T_w} = 62 dB
-------	floor	D_{n,T_w} = 75 dB
-------	sum of all building parts	D_{n,T_w} = 51 dB
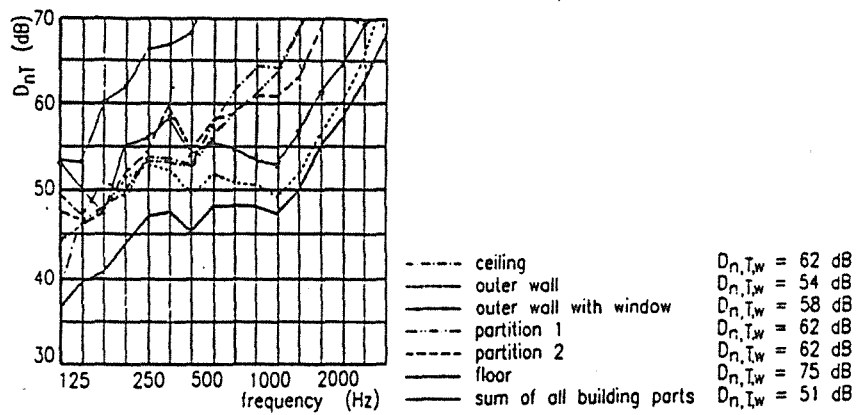
Fig.27 Sound level difference give by the single building parts (partition floor and flanking walls) as calculated from the measured velocity level[44].
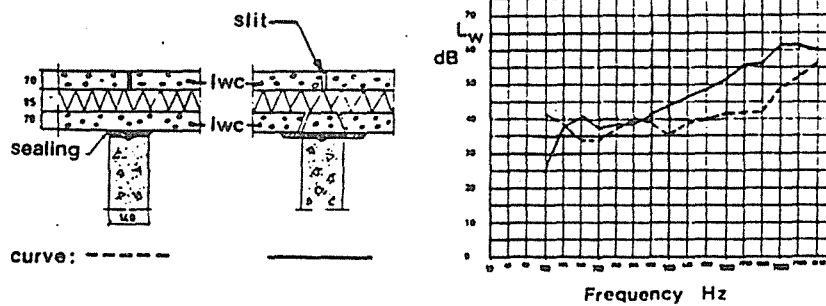
Fig.29. Horizontal flanking transmission in sandwich facade wall. Left: continous panels. Right: slitted panels.

35
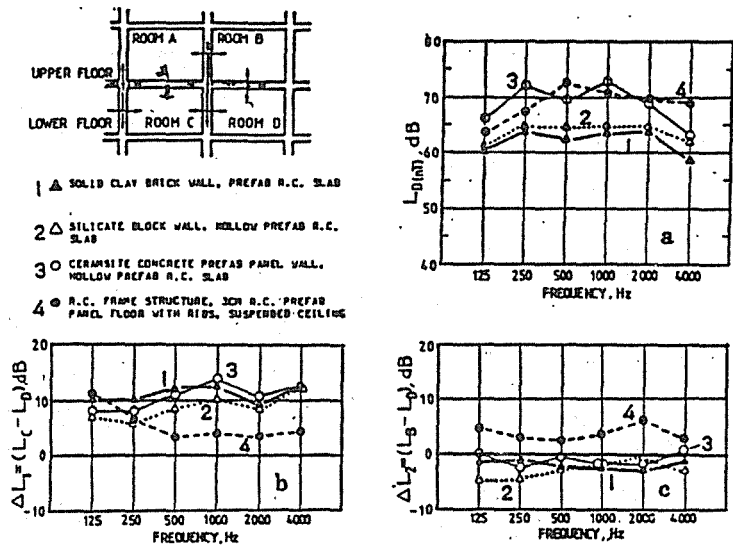
Fig.30 Flanking sound transmission between rooms without common wall and floor[47].
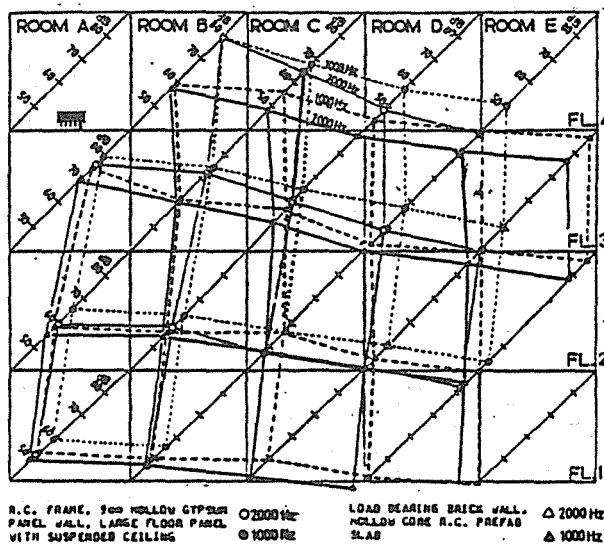
Fig.31 A pattern of the impact sound level distribution (at octave band center frequencies 1000 Hz and 2000Hz) in many surrounding rooms in two different construction type dwellings[47].
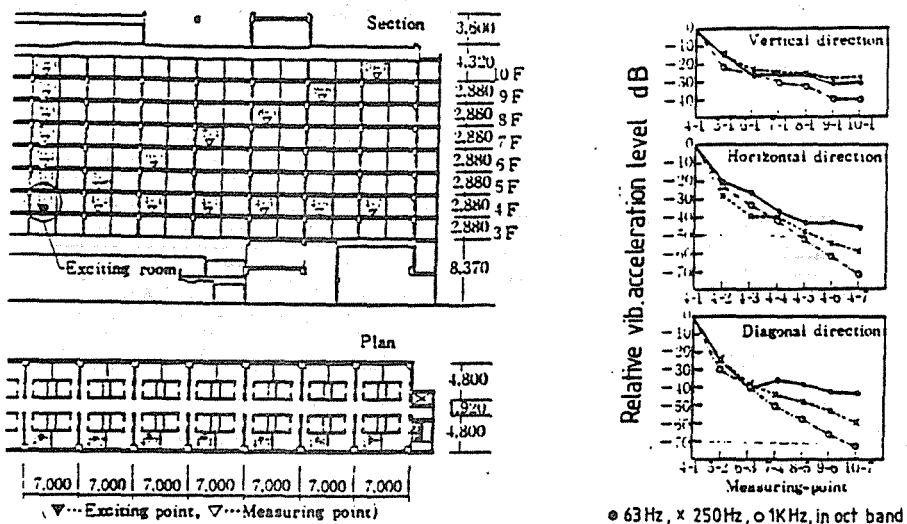
Fig.32 Propagation characteristics of solid-borne sound in a building[48].

36

IMPULSIVE NOISE

Toshio Sone
Research Institute of Electrical Communication, Tohoku University
2-1-1 Katahira, Aoba-ku, Sendai, 980 Japan

ABSTRACT   Impulsive noise has a high peak level of short duration, so that a different method from steady or slowly varying noise is required for its evaluation. Methods for evaluation and measurement of impulsive noise have been studied by many researchers from viewpoints of damage risk criteria, noise environment and others. This paper shortly reviews the researches on impulsive noise sources such as an elastic collision of solids, a rapid expansion of gas, footstep on the floor, and evaluation of impulsive noise from the points of its threshold, loudness and hearing damage induced by it. Then describes the results of the study on loudness of impulsive sounds including single and repeated bursts of simulated noise. A temporal summation model with a short rise time constant and a long decay time constant(the two-time-constants model) was combined with five existing frequency weightings and applied to various simulated noises and actual noises composed of impulsive and nonimpulsive components. It is shown that Zwicker's procedure for loudness calculation seems to be the best frequency weighting method among the five as far as the two-time-constants model is concerned.

1.0 INTRODUCTION

Since an impulsive sound has an extremely short duration and high peak level, it cannot be evaluated with the same measure as that for a steady noise. For example, it was reported that the A-weighted peak SPL of sound from an electric typewriter is about 20 dB higher than the A-weighted SPL measured with F detector-indicator characteristic and such difference is about 30 dB for a pneumatic nailing machine.

ISO 2204-1979 (Acoustics-Guide to International Standards on the measurement of airborne acoustical noise and evaluation of its effects on human beings) describes that an impulsive noise is a noise consisting of one or more bursts of sound energy each of a duration less than about 1 s. But this definition does not give a clear meaning. EEC Directive 79/117, on the other hand, gives a definite criterion from a practical point of view, i.e., the "impulsive" sound has a difference of 4 dB or more in the indication of sound level meter between " I " and " F " detector-indicator characteristics. According to this definition, noise burst with a duration of 500 ms or less is classified into an impulsive noise.

2.0 IMPULSIVE NOISE SOURCES

2.1 Impact noise caused by an elastic collision

In this class, noise from an impact forming machine, a drop hammer, a punch press etc. used in a factory, a pile hammer, a concrete breaker, an excavator etc. used at a construction site, and bell sound are included. Each of these sounds has its origin at a collision of solids, and fundamental considerations have been made by many researchers.

Akay[1] classified the stages of sound generation from colliding bodies into five: i.e. (1)air ejection from the space between two surfaces approaching each other, (2)rigid body radiation, (3)radiation due to rapid surface deformations, (4)pseudo-steady-state radiation referred to as "ringing," and (5)sound radiation due to material fracture. Which of these is the dominant source of impact noise generation depends upon the materials, the shapes of colliding bodies and the way of collision.

2.2 Impulsive noise due to a rapid expansion of gas

Impulsive sound generated by a gunshot was modeled by Coles[2] as an abrupt rise of pressure followed by its slow decay to negative pressure and recovery. Duration for positive pressure is called "A-duration" and CHABA provided the damage risk criteria for impact noise based on it. Another source of impulsive noise in the atmosphere is a sonic boom which is generated by the shock-wave pattern formed around an aircraft flying with a supersonic speed. These will be mentioned later.

2.3 Impulsive noise generated in buildings

Impulsive noise generated in buildings includes footstep noise, noise caused by children romping over a room and such like. They are sometimes the cause of complaint.

Method of measurement of floor impact noise is specified in ISO 140-1978 (Acoustics-Measurement of sound insulation in buildings and of building elements) and JIS A 1418-1978 (Method for field measurement of impact sound level of floors) for Japanese use. According to ISO 140, the measurement should be done using a tapping machine, while in JIS A 1418 two kinds of floor impact sound sources are specified; the lightweight source(a floor tapping machine) and the heavyweight source(usually a pneumatic tire for automobiles). The results of measurement (the single-number quantity of impact sound insulation rating in ISO and the average octave band sound pressure level in the receiving room in JIS) should be rated according to ISO 717/2-1982 (Acoustics-Rating

of sound insulation in buildings and of building elements) or JIS A 1419-1979 (Classification of air-borne and impact sound insulation for buildings).

3.0 EVALUATION OF IMPULSIVE NOISE

3.1 Threshold of impulsive sound

Threshold of short tone, short burst or pulsed tone has been studied for relatively long time. Garner[3] made an experiment on various durations of tone burst, and found that the threshold went up by 10 dB if the duration was shortened to one-tenth of the original burst, i.e. the threshold of short tone was decided by its acoustical energy. If the duration was less than about 10 ms, however, the tonal threshold did not rise so much as expected from the decrease of acoustical energy, and this was more conspicuous for 250 Hz tone than for 4 kHz tone. It is suggested, therefore, that the spread of spectrum contributes to the hearing threshold for a short tone.
Miller[4] made an experiment using noise burst with the duration from 22 ms to 1550 ms, and as the results he showed that the hearing threshold decreased by 10 dB for the increase of duration by ten times. Zwislocki *et al.*[5] carried out experiment using rectangular pulse, where the influence of the duration of pulse trains, the frequency of pulses, and the number of pulses on hearing threshold were investigated. They found, as the results, that the threshold depended on the spread of spectrum caused by the shortening of duration and a change in spectrum due to a change of repetition frequency as well as a change of sound energy.

3.2 Loudness of impulsive sound

In most studies on loudness of impulsive sound, tone bursts were used as stimuli. Duration of the burst, its repetition rate, and rise and decay time of the burst were changed, and their influence on loudness of tone bursts was investigated in those studies. The results show a tendency that within some extent of duration the level of a stimulus corresponding to the same loudness decreases 9–12 dB if the duration of burst increases tenfold. In other words, the loudness is nearly proportional to sound energy. The upper limit of tone burst under which this "energy rule" holds varies from 60 ms to 400 ms with the author. These critical durations for tone bursts are also related to the levels of stimuli.
As to the relation between loudness and the repetition rate of stimuli, experiments were reported by many authors. Stimuli adopted there were tone bursts, noise bursts, N-waves, exponentially decaying sounds etc., and the repetition rate was 1 to 100 pps. According to these experiments, to increase the repetition frequency ten times is equivalent to decreasing the level of stimuli by 10 dB(-10 dB/decade) for keeping the loudness unchanged as far as the duration is very short(about 1 ms). But for longer duration of an individual burst the level-repetition frequency ratio becomes smaller. Furthermore, it was shown that the repeated bursts gave the greater loudness than the steady sound which had the same sound energy as the bursts[6, 7]. As to the effect of rise time of a stimulus on loudness, it is reported that loudness increases as the rise time of a burst decreases, and noise bursts are more influenced by a change in rise time than tone bursts.

3.3 Hearing loss induced by the exposure to impact sounds

Hearing loss induced by the exposure to impulsive sounds is an acute problem to metal processing workers, shooters etc. The hazard of exposure to impulsive sound is said to be unable to estimate through its loudness.
Coles[2] divided the wave form of impact sounds into a single pulse represented by a gunshot sound and a reverberant wave which is usually seen in sound due to a collision. The names of "A-duration" and "B-duration" proposed by him have been used until today. He also proposed

the criterion for hearing conservation, and CHABA[8] proposed a damage-risk criterion in 1968 based on it. It shows the allowable limit of sound level of impulse noise, i.e. the limit within which NIPTS at the frequency of 3 kHz or above does not exceed 20 dB in 95% of people who are exposed 100 times a day to impulse noise, for twenty years. The line of peak pressure level vs. duration of impulse noise for the criterion decreases t the slope of -6.5 dB/decade up to the duration of 1.5 ms(A-duration) or to the duration of 200 ms(B-duration), and above them the criterion remains at the constant level of 152 dB(A-duration) or 138 dB(B-duration). EPA[9] modified the CHABA criterion on condition that NIPTS at 4 kHz does not exceed 5 dB in 90% of people, and the EPA criterion is lower by 12 dB than CHABA. The slope of -6.5 dB/decade in these criteria means that the increase in peak pressure level is allowed only by 6.5 dB for the decrease of duration to one-tenth, and it does not meet the energy rule. For the change in the number of exposure to impulse noise a day, -5 dB/decade(CHABA) and -10 dB/decade(EPA, >100) are adopted respectively.

In ISO 1999-1990(Acoustics-Determination of occupational noise exposure and estimation of noise-induced hearing impairment) the criterion is provided for working environment where noise exposure level for eight hours a day exceeds 85 dB.

3.4 Sonic boom

Sonic boom is generated by a supersonic flight of an airplane it is a kind of impulse noise, but is treated separately from general impulse noise, because its level is very high and it gives an influence on a wide area. Sonic boom has a relatively stable form(N-wave) differently from ordinary impulsive noise, so the definite methods of calculating its loudness have been proposed. Zepler[10] estimated the loudness of sonic boom from phon-weighted spectrum of N-wave. Johnson's method[11] uses Stevens' Mark VI after 1/3 octave band analysis of sonic boom. And ISO 2249-1973(Acoustics-Description and measurement of physical properties of sonic booms) describes the measurement of sonic boom. However, since sonic boom brings about house vibration because of its intensity, its influence cannot be estimated only by loudness.

3.5 Other investigations on impulsive noise evaluation

There have been various proposals as to how describe the specific feature of impulsive sounds. Detector-indicator characteristic " I " defined in IEC Pub.651-1979 (Sound level meters) is one of them, and with it the deviation of L_{Aeq} of impulsive sound after time-weighted by " I " from its true L_{Aeq} is used for describing the impulsivity of sound. Standard deviation and kurtosis of the distribution of short-term L_{Aeq} are also studied.

Furthermore, detailed analysis of impulsive sounds with Wigner distribution, Prony technique etc. is being studied. Other than studies mentioned here, there are many papers related to the evaluation of impulsive noise. Some of them treated perceived noisiness, pitch perception concerning impulsive sound, acoustic reflex, neural response to impulsive sound and so forth.

4.0 LOUDNESS EVALUATION OF IMPULSIVE NOISE

The research group including the author's laboratory carried out two stages of round robin test in Japan from 1981 to 1987 in order to establish a method for evaluating impulsive sound. Experiments on loudness of a single burst of impulsive sound were executed in the first stage round robin test[12]. Loudness and noisiness of repeated impulsive sound were investigated in the second stage[13]. As for a single burst of impulsive sound, its loudness corresponds well with the sound exposure level (the square-integrated value of sound pressure, L_{pE}) in our first stage.

Neither L_{Aeq} nor L_{pE}, however, evaluates the loudness of repeated impulsive sounds. According to our continued study, the loudness of repeated impulsive sound corresponds rather well with

the signal output through 2TC(two-time-constants) integrator which has a short rise constant of 100 ms and a long decay time constant of 5 s[14]. It is impossible to use this circuit alone, however, to assess the loudness of sounds having different frequency spectra because 2TC integrator acts only as a time-weighting circuit. If there is an appropriate frequency-weighting to be combined with 2TC integrator, the loudness of impulsive sounds with various frequency spectra may be evaluated. Thus, we looked for the best combination of time- and frequency-weightings based on the psychoacoustical experiments. As a result we propose a new method for this purpose, and apply it to 50 different noises including actual ones to examine its validity as a loudness descriptor for wide variety of noises.

4.1 Examination of the combination of time- and frequency-weightings

Some existing frequency-weighting functions are examined here in conjunction with our 2TC integrator for sound stimuli with several kinds of frequency spectra. First, we observed the effects of frequency spectra on the loudness of impulsive sounds. Second, we looked for the best combination of time- and frequency-weightings for evaluation of loudness of impulsive sounds.

PSE's(points of subjective equality) for loudness of impulsive sounds with several kinds of frequency spectrums were obtained. The temporal pattern of a pair of stimuli presented to subjects are shown in Fig.1. Subjects were asked to judge which burst of the pair was louder. Stimulus conditions used in the experiment are combinations of six kinds of carrier signals(pink noise, blue noise, - 9 dB/oct noise, complex signal composed of pink noise and 63 Hz tone with its harmonics up to the fifth, complex signal composed of pink noise and 1 kHz tone with its harmonics up to the fifth, and asymmetric rectangular waves), five kinds of repetition rate(single burst, 1, 3, 10 Hz bursts and steady sound), rise time of 1 ms, decay time of 100 ms and duration of 2 s. The comparison stimulus had a 200 ms steady duration with rise and decay time of 15 ms/20 dB, and its carrier signal was pink noise. Subjects were five young adults with normal hearing. Test stimuli were presented to a subject via headphones with peak level of 70 dBSPL. PSE's were estimated from the results of experiment by using the method of maximum likelihood[15]. In this study we applied 2TC integrator shown in Fig.2 which has the rise time constant of 100 ms and the decay time constant of 5 s [16]. This model was derived from our previous study in which the loudness of repeated impulsive sound with the repetition rate ranging from 0.2 to 30 Hz, and with the duration ranging from 1 to 50s was obtained. The model can supply the output which corresponds accurately to the loudness of repeated impulsive sound used in the experiment so long as the frequency spectrum of sound is fixed. As frequency-weighting functions to be combined with the model, we examined A-weighting, Mark VI[17], PL[18], Zwicker's loudness calculation procedure
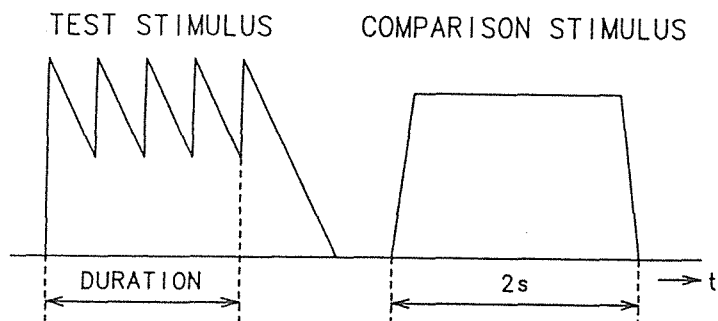
Fig.1 An example of time pattern of stimuli used in the experiment.

41

(LLZ)[19] and PNL[20].

A-weighting can easily be combined with 2TC integrator in the way that the A-weighted stimuli are fed into the model. The other four frequency- weighting methods, however, require the frequency analysis of the input signal. Thus, we examined possible methods of combining frequency analysis and temporal summation functions in the following four ways: (1)Frequency-weighting the band-pass outputs followed by an overall time weighting, (2)Time-weighting the band-pass filter outputs separately followed by frequency-weighting, (3)Frequency-weighting the results of short-term FFT analysis followed by an overall time-weighting, and (4)Time-weighting the frequency components of short-term FFT analysis separately followed by frequency-weighting.

The long decay time of 2TC integrator enables the integrator to hold the acoustical energy up to around 3 s. We think that the duration of 3 s corresponds to the boundary between the duration for which the judgment of loudness is subject to "perception" and that for which the judgment is subject to "memorization." If this assumption is valid, the function of 2TC integration model corresponds to a certain mechanism in a higher level of our auditory system and such a mechanism is expected to be located after a frequency-weighting mechanism. For this reason, we examined combination of (1) and (3) in further considerations.

Mark VI, PL, LLZ and PNL need the power spectrum in a free field as an input signal to the model. But we only have the information of the power spectrum at the entrance of auditory meatus because we present the stimuli through a headphone. Thus, the power spectrum at the entrance of auditory meatus was transformed into the power spectrum in a free field before the frequency-weighting was applied. We used a transfer function of the propagation path from the source to the entrance of auditory meatus averaged over a few subjects. As a result of preliminary consideration on the length of time window for frequency analysis in hearing, we obtained the power spectra at the interval of 0.64 ms for 1/3 octave filter, while adopted 5.12 ms duration of Hamming window for FFT analysis.

The outputs of the two methods, methods (1) and (3), were compared with subjective results. As a result, there were little differences between the band-pass filter(Method 1) and FFT analysis(Method 3). Anyway LLZ seems to be the best frequency-weighting among the five. According

$Rise \ Time \ Constant = C*(R1//R2)$
$Decay \ Time \ Constant = C*R2$
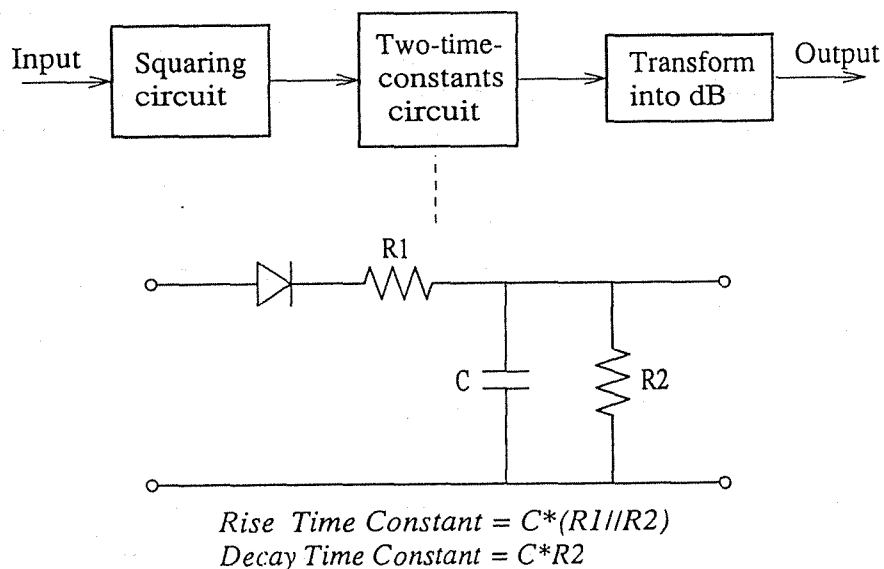
Fig.2 Block diagram of the 2TC (Two-Time-Constants) model and its equivalent circuit.

to this, we propose a new descriptor of loudness, $L_{\rm TF}$, which is calculated from the output of the system using the LLZ frequency-weighting function and 2TC integrator. $L_{\rm TF}(t)$ is a function of time, and is expressed by

$$L_{\rm TF}(t) \;=\; 10\log_{10}\{y(t)/y_0\}, \tag{1}$$

where y_0 represents the reference value corresponding to 0 dBSPL and $y(t)$ corresponds to an instantaneous sound pressure. Fig.3 shows the relation between PSE's for loudness and the maximum of $L_{\rm TF}$'s of stimuli obtained through Method 1 for LLZ. As seen from the figure, the new descriptor $L_{\rm TF}$ shows a good correspondence with PSE.

If the noise is rather long or has a fluctuating time envelope, the equivalent continuous loudness level $L_{\rm TFeq}$ defined by the following equation may be useful:

$$L_{\rm TFeq} \;=\; 10\log_{10}\left[\frac{1}{t_2 - t_1}\int_{t_1}^{t_2}\{y(\tau)/y_0\}d\tau\right], \tag{2}$$

where $t_2 - t_1$ is the observation time interval.
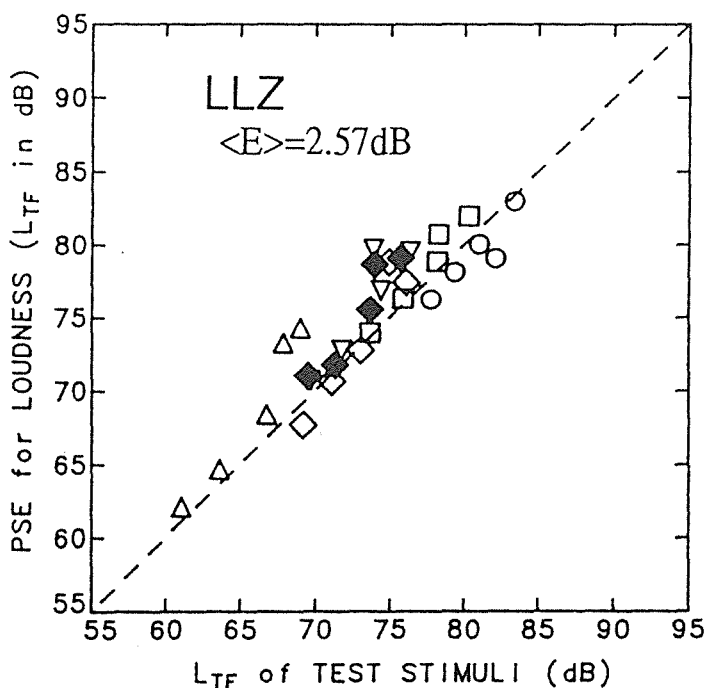
Fig.3 Relation between PSE for loudness of the simulated test stimuli and the maximum time- and frequency-weighted(LLZ) output of the model, $L_{\rm TF}$. $\langle E\rangle$ is an r.m.s. value of the difference in dB between PSE level and $L_{\rm TF}$ for all the conditiones tested.

4.2 Application of the proposed descriptor to actual noises

Actual impulsive noise sometimes has irregular peak levels and appearance intervals, and exists together with background noise. It is desirable, therefore, that a loudness descriptor is also applicable to such complex noises. As the repetition rate of a repeated impulsive sound changes from a very low value to a very high value, the sound continuously changes its nature from a series of isolated single burst to a steady sound. Under such circumstances, $L_{\rm TFeq}$ is expected to evaluate the loudness of not only impulsive noise but also of various complex noises. Thus, we applied the proposed method to 50 different noises including 42 actual noises(sounds from gun fire, fire bell, wooden panel being beaten, diesel pile hammer, typewriter, door knock, metronome, road traffic
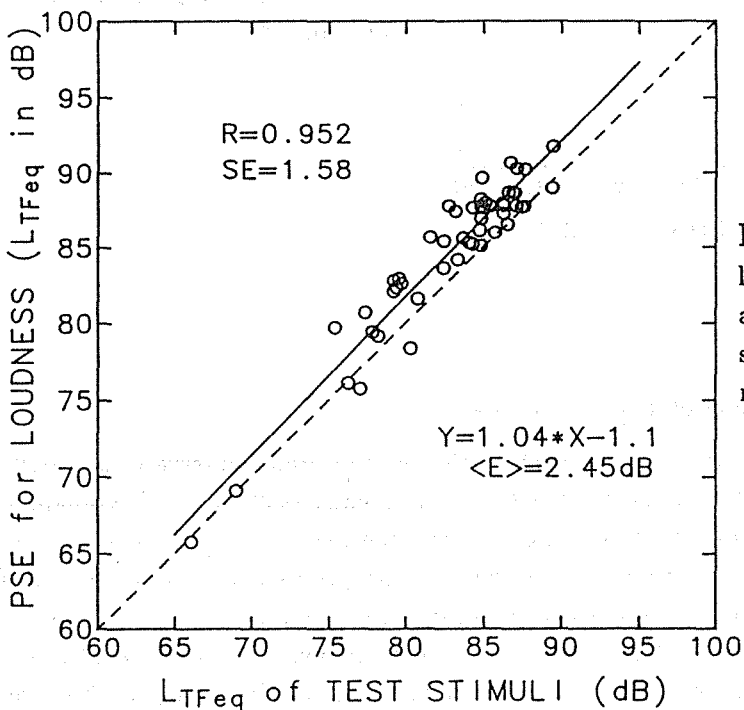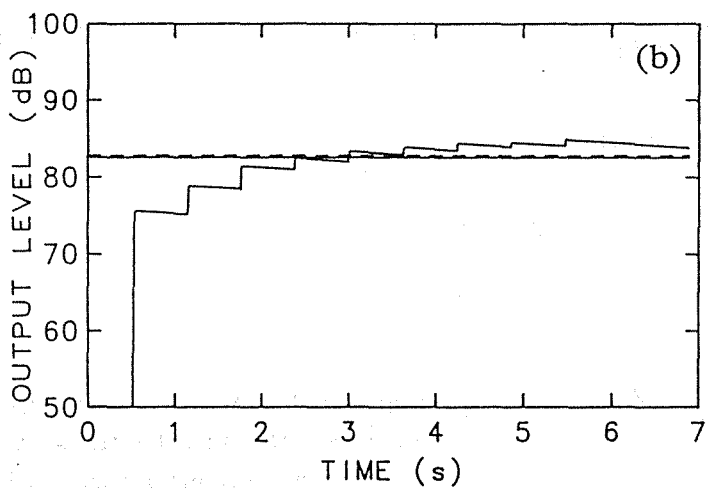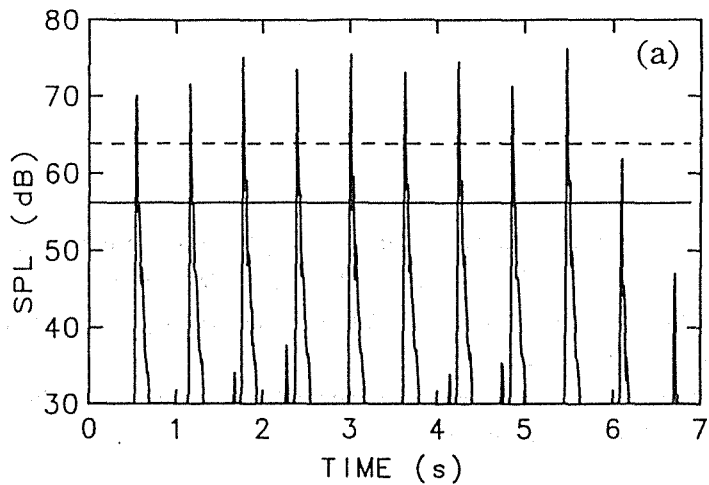
Fig.4 An example of evaluation of loudness for metronome sound in terms of L_{Aeq} and L_{TFeq}. (a)L_A with the time constant of 10 ms(time pattern), L_{Aeq} (horizontal solid line) and PSE in terms of L_{Aeq} (broken line), (b)proposed descriptor $L_{TF}(t)$ (step-like pattern), its equivalent continuous level LT-Feq(horizontal solid line) and PSE in terms of L_{TFeq} (broken line).

Fig.5 Relation between PSE for loudness of various complex noises and the output of the proposed descriptor L_{TFeq}. The solid line is a regression line.

and so forth) and 8 synthesized noises. Loudness of these 50 noises was subjectively evaluated to examine the applicability of the proposed method. The experimental procedure was similar to that stated in the above section. Most of the 50 noises used had impulsive components. The duration of the test stimuli was 7 s inclusive of a rising part and a decaying part. The comparison stimulus was the sound with a 4 s steady duration as well as a rising and a decaying part with 250 ms time constant. The carrier signal of the comparison stimulus was pink noise. The subjects were thirteen young adults including six males and seven females with normal hearing.

Fig.4 is an example of the experimental result for a metronome sound. This is a typical example of the impulsive noise with a relatively low repetition rate(1.6 Hz). Fig.4(a) shows the A-weighted SPL and L_{Aeq} (horisontal solid line) of the metronome sound. While the peaks of L_A is far larger than PSE level(broken line), L_{Aeq} is far less than PSE level. Fig.4(b) shows the result of evaluation by the proposed descriptor $L_{TF}(t)$ (solid curve) and L_{TFeq} (horizontal solid line). L_{TFeq} is nearly the same level with PSE for loudness. From these considerations, the new descriptor L_{TFeq} shows a good correspondence with subjective loudness not only for impulsive noise but also for slowly varying and steady noise. Fig.5 shows the relation between L_{TFeq} and PSE level for the fifty noises in terms of L_{TFeq}.

4.3 Discussion

New loudness descriptor L_{TF} well evaluates the loudness of a single and repeated bursts of impulsive sound. Although the combination of 2TC integrator and A- weighting is not always bad, Zwicker's procedure seems to be the best frequency-weighting for 2TC integrator.

2TC integrator used as a time-weighting for L_{TF} has the rise time constant of 100 ms and the decay time constant of 5 s. These constants were determined through our previous experiments using the artificial impulsive sounds with the duration from 1 to 50s and with the repetition rate from 0.2 to 30 Hz(including single burst). The range of the duration and the repetition rate is considered to be wide enough, since the maximum duration of 50s is much longer than the duration which is most easily perceived in a lump and the repeated impulsive sound with the repetition rate of 0.2 Hz is perceived as an isolated burst while that with the repetition rate of 30 Hz is perceived as steady sound. 2TC integration model, therefore, has a possibility to represent the loudness of not only repeated impulsive noise but also different kinds of time-varying noise. Actual noises, however, have too irregular peak levels and repetition rates as well as fluctuating background noise to use L_{TF} directly. Hence we proposed L_{TFeq}. As a result of its application to 42 actual noises, it might be an appropriate loudness descriptor for various complex noises.

Calculating procedure for L_{TF} and one for Zwicker's loudness meter are alike in appearance[21]. Zwicker's loudness meter used a non-linear(two kinds of time constants) integrator in order to evaluate the loudness of not only steady noise but also fluctuating noise. The time constants used in Zwicker's loudness meter, however, are far shorter than those of our model and their values are changed with input signal level. The two time constants integrator used in Zwicker's loudness meter does not aim at holding loudness sensation but compensating the effect of temporal masking. The difference in the aim between Zwicker's loudness meter and L_{TF} causes merits and demerits in loudness evaluation of some special noise. According to our previous study[16], it seems to be difficult to explain the increase in loudness for repeated impulsive sound with the low repetition rate from 0.3 to 3 Hz by using Zwicker's loudness meter because of its small time constants. On the other hand, L_{TF} cannot explain that the loudness of a sound with deep frequency-modulation is larger than that of a non-FM sound, because L_{TF} ignores the effect of lateral inhibition on loudness. In practical use, however, we are optimistic that the effect of deep FM in evaluating environmental noise is not so large.

References

[1] Akay A., A review of impact noise, J. Acoust. Soc. Am., 64(4), 977–987, (1978).

[2] Coles R.R.A., Hazardous exposure to impulsive noise, J. Acoust. Soc. Am., 43(2), 336–343, (1968).

[3] Garner W.A., The effect of frequency spectrum on temporal integration of energy in the ear, J. Acoust. Soc. Am., 19(5), 808–815, (1947).

[4] Miller G.A., The perception of short bursts of noise, J. Acoust. Soc. Am., 20(2), 160–170, (1948).

[5] Zwislocki J., Hellman R.P., Verrili R.P., Threshold of audibility for short pulses, J. Acoust. Soc. Am., 34(10), 1648–1652, (1962).

[6] Garner W.R., The loudness of repeated short tones, J. Acoust. Soc. Am., 20(4), 513–517, (1948).

[7] Garrett R.M., Determination of the loudness of repeated pulses of noise, J. Sound Vib., 2(1), 42–52, (1965).

[8] Kryter K.D., Ward W.D., Miller J.D., Eldredge D.H., Hazardous exposure to intermittent and steady-state noise, J. Acoust. Soc. Am., 39(3), 451–464, (1966).

[9] EPA Document 550/9-74-004, Information on levels of environmental noise requisite to protect public health and welfare with an adequate margin of safety, (1974).

[10] Zepler E.E., Harel J.R.P., The loudness of sonic booms and other impulsive sounds, J. Sound Vib., 2(3), 249–256, (1965).

[11] Johnson D.R., Robinson D.W., Procedure for calculating the loudness of sonic bangs, Acustica, 21(6), 307–318, (1969).

[12] Sone T., Suzuki Y., Kumagai M., Takahashi T., Loudness of a single burst of impact sound: Results of round robin tests in Japan (I), J. Acoust. Soc. Jpn.(E), 7(3), 173–182, (1986).

[13] Sone T., Izumi K., Kono S., Suzuki Y., Ogura Y., Kumagai M., Miura H., Kado H., Tachibana H., Hiramatsu K., Namba S., Kuwano S., Kitamura O., Sasaki M., Ebata M., Yano T., Loudness and noisiness of a repeated impact sound: Results of round robin tests in Japan(II), J. Acoust. Soc. Jpn.(E), 8(6), 249–261, (1987).

[14] Sone T., Ogura Y., Suzuki Y., Loudness evaluation of impulsive noise, INTER-NOISE 89 Proc., 821–826, (1989).

[15] Ogura Y., Suzuki Y., Sone T., On the errors in estimates when the method of maximum likelihood was applied to the result of psychoacoustical experiment obtained by the constant method, J. Acoust. Soc. Jpn., 45(6), 441–445, (1989). (in Japanese)

[16] Ogura Y. Suzuki Y., Sone T., A temporal integration model for loudness perception of repeated impulsive sounds, J. Acoust. Soc. Jpn.(E), 12(1), 1–11, (1991).

[17] Stevens S.S., Procedure for calculating loudness: Mark VI, J. Acoust. Soc. Am., 33(11), 1577–1585, (1961).

[18] Stevens S.S., Perceived level of noise by Mark VII and decibels(E), J. Acoust. Soc. Am., 51(2), 575–601, (1972).

[19] Zwicker E., Feldtkeller, Uber die Lautstarke von gleichformigen Gerauschen, Acustica, 5(5), 303–316, (1955).

[20] Kryter K.D., Pearsons K.S., Some effects of spectral content and duration on perceived noise level, J. Acoust. Soc. Am., 35(6), 866–883, (1963).

[21] Zwicker E., Daxer W., A portable loudness meter based on psychoacoustical models, INTER-NOISE 81 Proc., 869–872, (1981).

ADVANCES IN ACOUSTIC SIGNAL PROCESSING

Ma Yuanliang (Y.L.MA)
Institute of Acoustic Engineering
Northwestern Polytechnical University
Xi'an 710072, P.R.China

ABSTRACT Recent advances in Acoustic Signal Processing, particularly those topics which have important applications in underwater acoustics, noise control and ultrasonics are discussed. An overview on the development is given. Selected topics on Adaptive Processing, Beampattern Optimization and DSP beamforming, Artificial Neural Networks etc. are presented together with illustrative examples.

1. Introduction

Pushed by the evolution of information science and micro electronics, acoustic signal processing has advanced significantly during the past decade.

On the theoretical side, it seems that most important advances are made in the following aspects:

- Adaptive filtering
- Sensor array processing
- High resolution spectrum analysis
- Mathematical modelling of channels and systems
- AI / ANN and signal classification
- Active Sound Control
- Acoustic imaging and data transmission
- Generalized time—frequency distribution
- Matched field processing
- Inverse filtering. etc.

On the practical side, they are:

- Improvement of system development environment
- VLSI signal processing system (hardware)
- Software development
- Digital data acquisition
- High throughput real—time processing
- Display and Control
- System Integration etc.

These advances, of course, have strong influence on the development to the future both in research and application domains. A wide range of applications may benefit from the advances. To name the main ones, they are:

Underwater sound:

- Noise and interference cancellation
- Angular spectrum estimation
- Adaptive array processing
- Source localization
- Maneuval target tracking
- Target classification
- Fish detection
- Data transmission
- Remote sensing

Noise control:

- Noise source analysis
- Free—field noise attenuation
- Closed—room noise silencing
- Power flow measurement and analysis etc.

Ultrasonics:

- Medical instrumentation
- Non–destructive testing of materials
- Defect localization and classification
- Acoustic emission analysis
- Machinery fault diagnosis
- Well logging
- Leakage detection
- Security alarm
- Car avoidance
- Glasses or stick for the blind
- Robot vision etc.

The above list is by no means exhaustive, there are other aspects, e.g.speech and music applications in which acoustic signal processing also plays a very important role. In the following, some selected items will be presented in a brief but systematic way. The emphasis will be mainly put on the work conducted in the author's group. The emphasized topics are : Adaptive Processing, Beampattern Optimization and DSP beamforming, in addition to Artificial Neural Networks. Fandamental concepts and technical approaches will be made clear; Application examples are given, together with a reference index.

2. Adaptive Processing

Adaptive filtering and array processing theories and algorithms have been studied intensively. In recent years, it becomes popular to adopt adaptive methods in case of unknown or time–variant environment.

2.1. Adaptive wideband noise cancellation

Traditional Widrow type LMS algorithm and adaptive transversal filter can perform very well for line spectra as well as narrowband noise cancellation. In the author's group, an experimental modul implemented by TMS320C25 and 12–bit A / D converter can cancel single tone interference up to 50–60 dB. But, if the bandwidth increases, the cancellation ratio will normally come down. To the extreme end if the noise is wideband , especially coloured the cancellation ratio may drop to under 10dB, or the adaptive canceller completely fails to converge. Several approaches for overcoming the problem achieved limited success, for instance , increasing the length of adaptive transversal filter, or changing the filter into lattice structure together with some algorithm improvement etc. The underlying requirments for the coloured wideband noise cancellation problem are:

(1) The filtering structure should be capable of providing a sophisticated response for correcting any waveform distortion of the reference input in relation to the primary input.

(2) The algorithm employed should be insensitive to the eigenvalue distribution of the reference covariance matrix.

Two approaches have been found which can better satisfy the above requirements. One is the multiple subband canceller combined with normalized LMS algorithm with Recursive Power Estimation[1] . Another is the artificial neural network (ANN) based canceller[2] . Both of them can improve the cancellation ratio up to 30dB or more. Blockdiagram and re-

sult for the first approach are shown in Fig.1, while the ANN based approach is explained in section 4.1.
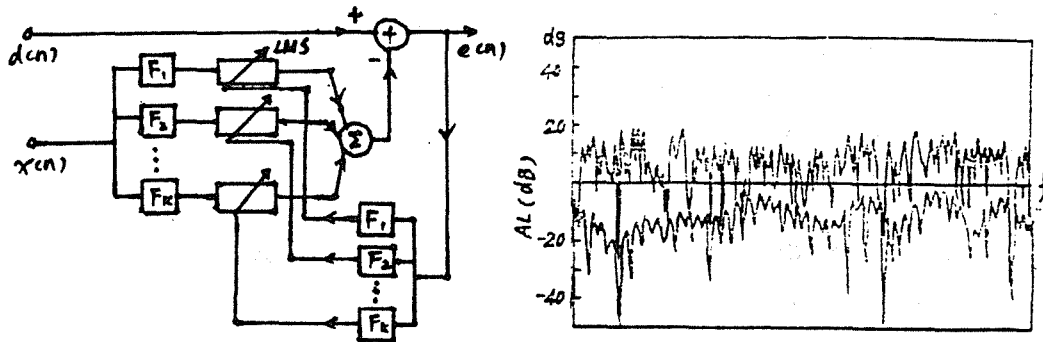
Fig.1 Adaptive Wideband Noise Canceller: blockdiagram and performance

2.2. Mainlobe Constrained Adaptive Array

Adaptive sensor arrays are useful in underwater environment, since the ambient noise field is normally nonwhite and variant. For this case an adaptive array can outperform a conventional phase—shift—and—summation beamformer, and particularly it can cancel strong plane wave interferences effectively. However, if there are several plane wave interferences and they are coherent with each other, an ordinary array may degrade considerably. Another problem an adaptive array may face is that it may cancel the wanted signal if the mainlobe direction is not precisely pointed on the signal direction. For the first problem a coherent signal—subspace transformation (CSST) scheme was proposed recently by Yang et al[3] . It introduces frequency domain smoothing and effectively decorrelates the interferences. And then the minimum variance adaptive array can work successfully. For the second problem our work will be presented in the following.

We also use a preadaptive transformation. It is called notch pattern transformation (NPT), through which spatial prefiltering is introduced before unconstrained noise cancellation as shown in Fig.2.
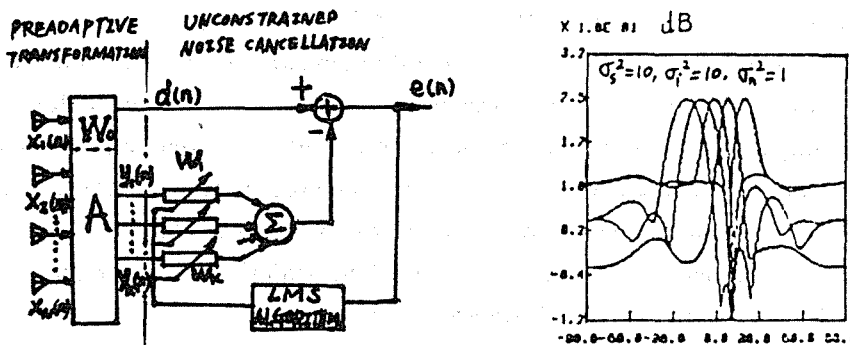
Fig.2 Mainlobe Constrained Adaptive Array: blockdiagram and beampatterns

The primary input of the following noise cancellation loop is provided by a conventional beamformer which forms a quiescent pattern. The reference inputs generated by the transformation possess notch patterns in which the notch region coincides with the mainlobe of the quiecent pattern. A detailed theoretical analysis and main computer simulation results are given in reference[4] . From that work, depending on the flatness of the notch bottom, first and second derivative constraint can be implemented conveniently. It is interesting that in combining with the wideband beamforming discussed in section 3.2, a wideband adaptive

50

array with mainlobe constraint can be implemented by simply using FIR filtering and unconstrained noise cancellation algorithms. Obviously, this makes adaptive arrays more feasible in underwater measurement applications.

2.3. Active Sound Control

Applying adaptive signal processing to noise control problems, we have adaptive active sound control. The basic idea is to add in one or a set of secondary sound sources in a noise field, which generate a sound field cancelling that generated by the original (primary) noise source. The secondary sources have to be controled by an adaptive processor since the primary source and sound transmission channel are normally time–variant.

The key elements for active sound control are sound field characterization and adaptive processor design. The adaptive processor may affect the system stability, convergence rate and noise cancelling ratio. In comparison with ordinary electronic cancelling systems, the adaptive processor for active sound control must solve additional problems, and hence is more difficult to design. The problems are ,

(1) Acoustic feedback from secondary sources to reference microphones
(2) Acoustic time delay and its variation produced by the sound transmission from secondary sources to error microphones
(3) Positioning of error microphones
(4) Complexity of modal distribution or directional pattern of the primary noise source
(5) Performance degradation for wideband case

The most distinctive factor concerns problem No.2. In the author's group, comparative study on four adaptive algorithms were conducted. They are filtered–x LMS algorithm, Intermittent LMS (ILMS) algorithm, filtered–x RLS algorithm, and Intermittent RLS (IRLS) algorithm[5][6][7]. The ILMS and IRLS algorithms are proposed by ourselves, which slow down the weight update to a time interval greater than or equal to the secondary–error time delay, while the processor utilizes the time interval for auxiliary (e.g. recursive covariance matrix inversion) calculations. It is observed that,

(1) For filtered–x algorithms, the time delay introduces additional error into the gradient estimate and hence may destroy the system stability, particularly if the delay is large and the adaptive factor is inadequately high.
(2) Convergence time of an adaptive sound control system is approximately $\triangle$ times greater than its electronic counterpart, where $\triangle$ is the time interval from secondary source to error microphone (when $\triangle > > 1$).
(3) Both ILMS and IRLS algorithms are more robust in comparison with the filtered–x algorithm and the noise reduction does not depend on $\triangle$, while IRLS improves convergence time and wideband performance simultaneously. Therfore the intermittent algorithms exibit great potential for further research and development.

Related results are shown in Fig.3.
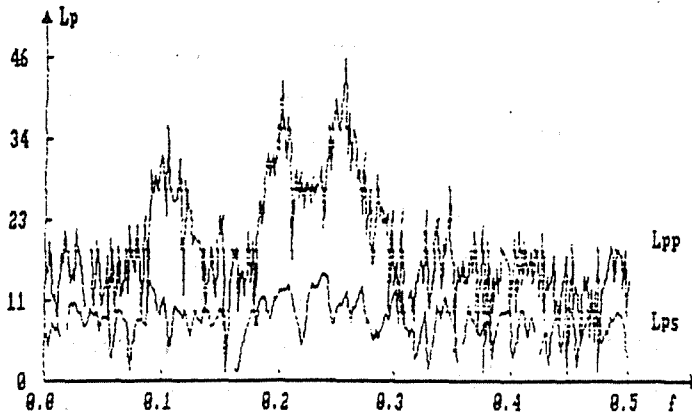
Fig.3 Active Sound Control: wideband result for the IRLS algorithm

3. Beampattern Optimization and DSP Beamforming

Conventional beampattern optimization is still very important not only due to its wide applicability for underwater sound, ultrasonics as well as noise control (beampattern synthesis of secondary sources) ,but also due to its potential for spatial domain tranformation in adaptive array processing as illustrated in section 2.2. As to DSP beamforming, thanks to the rapid development of DSP devices, digital processing approaches should be developed in parallel to take the resultant advantages.

3.1. Beampattern Optimization for Arbitrary Arrays

Suppose that the criterion for pattern optimization is chosen as follows: for a given look direction and mainlobe width, the optimal pattern minimizes the mean square of output when the array is exposed in a notch noise—field in which numerous independent noise sources of equal power are distributed uniformly over the expected sidelobe region. Additional assumptions are: the geometry of the array is given, and we are dealing with narrowband case.

From the above principle a mathematical model can be set up, and an optimal weighting vector can be solved out, which provides the optimal beam pattern expected.

From Fig.4, the output of the element No.i with element pattern $g_i(\theta_k)$ from the kth remote noise source of the notch noisefield is,

$$x_{ik}(t) = v_k(t)g_i(\theta_k)\exp(j(2\pi / \lambda)r_i\sin(a_i+\theta_k))$$

and the output of element No.i from all N noise sources is,

$$x_i(t) = \sum_{k=1}^{N} v_k(t)g_i(t)\exp(j(2\pi / \lambda)r_i\sin(a_i+\theta_k))$$

Using matrix notations, let

$$X = [x_1, x_2, \cdots\cdots\cdots, x_M]^T$$

$$C = [g_1(0)\exp((j2\pi / \lambda)r_1\sin a_1), \cdots, g_M(0)\exp((j2\pi / \lambda)r_M\sin a_M]^T$$

where M is the number of sensors, C is the signal vector in look direction ($\theta = 0$). According to optimal array processing principles, we can immediately solve out the optimal weighting vector in constraint of $W^TC = 1$ as follows

$$W_{OP} = R_{xx}^{-1}C^* / C^T R_{xx}^{-1} C^*$$

and then the optimal pattern will be

$$G(\theta) = W_{OP}^T C(\theta)$$
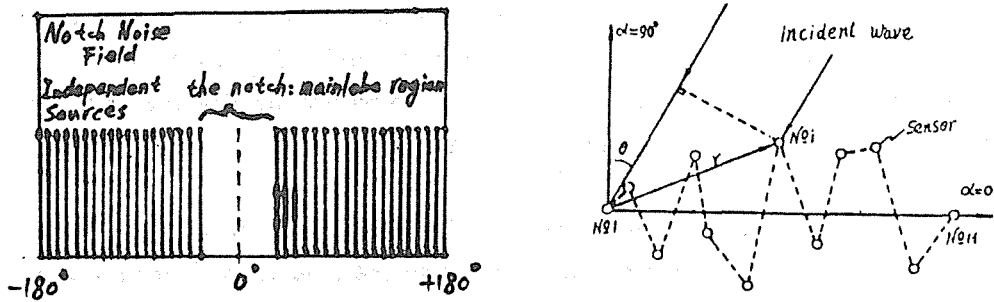
Fig.4 Optimization of Arbitrary Array: coordinate system and the notch noise field

It has been tested intensively by computer simulation that this method can achieve beam pattern optimization for array of arbitrary configuration[8][9][10]. Some results are shown in Fig.5. This method is also very useful for solving many practical problems in array design and applications, such as element failure in linear array resulting in a sparse array, inaccuracy of element position bringing up sidelobes, non—identical element pattern blocking array pattern optimization etc.
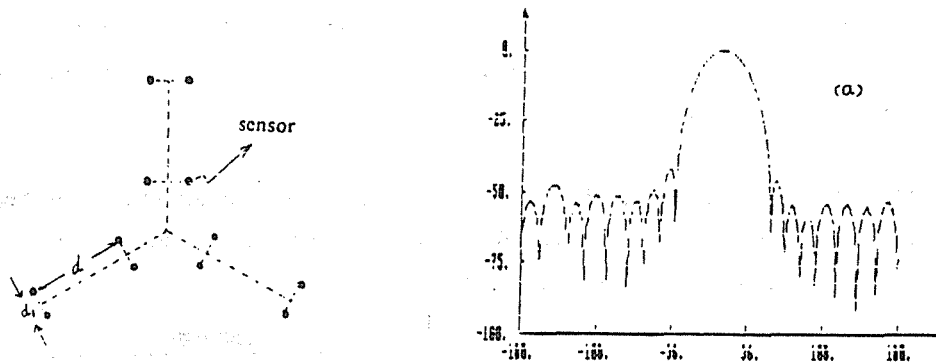
Fig.5 A 3—arm volumetric array and its optimized beampattern

3.2. DSP Micro—based Beamforming

Conventional beamforming in any case can be carried out by phase shift, amplitude weighting, time delay and summation, or a part of these processes. There is no problem on amplitude weighting and summation for any DSP microprocessors. The problem is how phase shift and time delay functions can be conveniently implemented.

It was found that for a narrow band centered at a given frequency, a constant phase—shift FIR filter can be designed successfully[11]. This was done by use of the adaptive modelling technique[12]. For example, a 4—tap FIR digital filter can provide arbitrary phase shift within 0.04 bandwidth centered at frequency 0.2 with maximum error less than 1 ° . The operation counts for it equals that for a complex multiplication.

For generating arbitrary time delay, we also proposed an easy—to—use FIR filtering scheme. It is a modification to Youn's method[13].

From Youn, it is proposed that a time delay digital filter should have an unit impulse response

$$h_d = Sinc(\omega(t-D)) \qquad |t| < \infty$$

In practice, if we have a FIR filter whose unit impulse response is a truncated version of the Sinc function, then it may approximate a time–delay filter with delay D. Unfortunately, the truncation may introduce a bias term into the time delay. To reduce the bias, the length of the FIR filter as well as related calculation load turns hign.

We modified the method by tolerating some amplitude distortion of the signal spectrum. In other words, instead of a flat amplitude response we permit the time delay filter to have a lowpass, highpass or bandpass response. In fact, this is more practical, particularly for the case of beamforming. In doing so, the time delay becomes almost unbiased and the length can be substantially shortened. The unit impulse response becomes

$$h_d'(t) = h_a(t) * Sinc(\omega(t-D))$$

where $h_a(t)$ is a window function which provides acceptable amplitude response together with a null phase response. It can be short and completely time–limited, thus $h_d'(t)$ is also a short and time– limiteddata sequence.

Typical results show that for one octave bandwidth, 4 taps are enough for generating time delay accurately with an error less than 1%. With 5 taps, it can generate a time delay to an accuracy up to 10^{-3} sampling interval[14] .

Combining the above techniques together, various beamforming applications have been tested successfully, as illustrated in Fig.6. A TMS320C25 DSP Micro based beamforming modul takes this approach and works very effectively[15] .
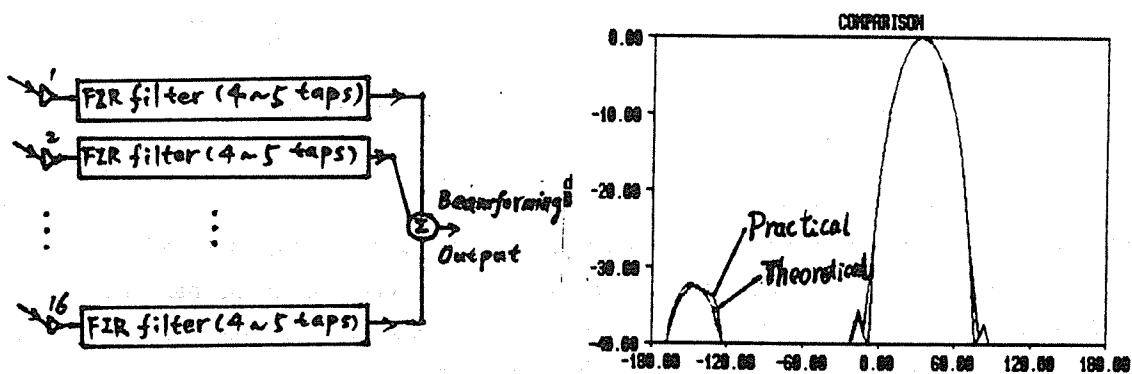
Fig.6 DSP Beamformer: blockdiagram and beampatterns for a 16–element volumetric array

4. Artificial Neural Network

Artificial Neural Network or Neural Computing appeared in late fifties and attracted much research interest until mid–1960s. After about 20 years of silence , it reappeared in mid–1980s and attracted much more interest not only in researach but also in development and applications.Since then, ANN reasearch has been springing up worldwide.

Distinctive features of ANN different from traditional signal and information processing approaches are: learning by examples, distributed and associative memory, abstraction and generalization ability, fault tolerance etc. Obviously, ANN is very suitable for acoustic signal processing and classification in various applications.

4.1. Wideband noise cancellation

Tan et al used a 2 layer back—propagation Network for wideband noise concellation[16]. It was shown that the canceller can outperfom its adaptive counterpart by 10–20 dB noise suppression. The reason for improvement lies in better modelling ability gained by hidden layer connections and nonlinear properties of the neuron function. The input signal plus noise and corresponding output are shown in Fig.7.
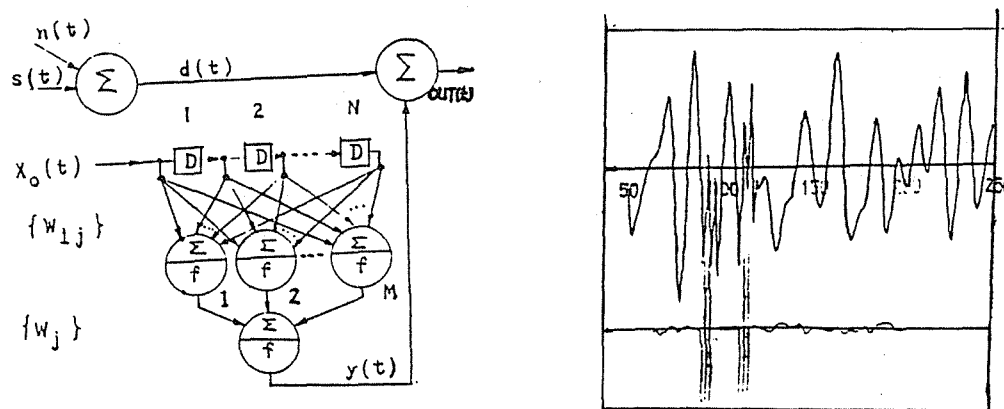
Fig.7 ANN Based Noise Canceller: blockdiagram and output signal

4.2. DOA Estimation by ANN

Ma et al proposed a ANN architecture, a Davies type pyramid net, for direction—of—arrival estimation of multiple correlated sources[17].

The network is especially ideal for separating 2 coherent and narrowband plane—wave sources. It provides very high resolution and an accuracy approaching C.R.bound of the related deterministic model. As an example,for a 4—element linear sensor array, when the input $SNR = 0,14,20,30dB$, the ANN can resolve 2 coherent sources within $1/3$, $1/5$, $1/10$, $1/20$ conventional beamwidth respectively. This is remarkable in comparision with other existing high resolution methods.

4.3. Signal Classification by ANN

Gorman, Sejnowski applied back—propagation network for sonar target classification[18]. It showed that the ANN performs comparably to the performance by the trained human operators and superior to a feature based nearest neighbor classifier. For non—destructive evaluation of materials, Chen[19] reported their experimental results in using neural networks.

In the author's group, a demonstrative software was set up and tested. The blockdiagram is shown in Fig.8a. A multiple–layer perceptron using back propagation training algorithm and sigmoid activation function is employed for feature extraction and mapping. Several Adalines are used for classification. The preprocessing could be a spectrum analyzer, if the input samples are assumed to be the power spectra. 8000 sample vectors represent 3 classes of signals in which half by half are used for training and testing respectively. Although the spectrum parameter varies in a wide range and additional noises are put in, the correct classification rate still keeps high[20] . It is interesting to note that the difference between class No.2 and No.3 is small and good result is still achieved, as shown in Fig.8b.
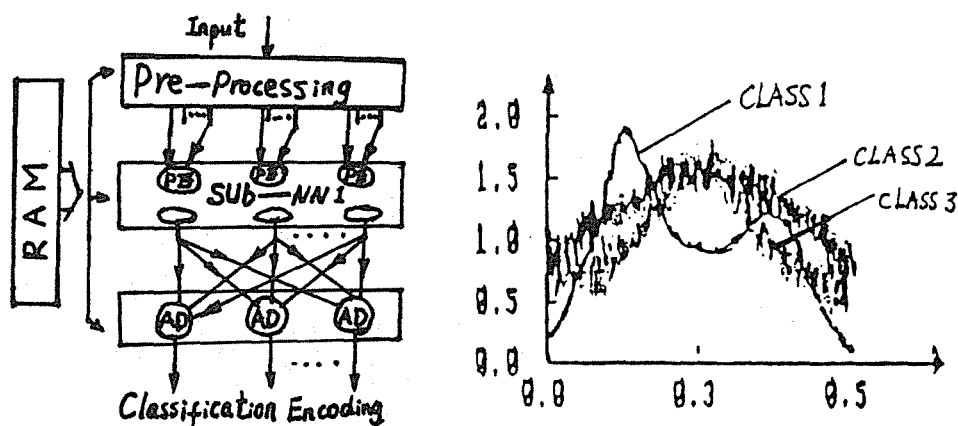
Fig.8 ANN Based Classifier: blockdiagram and recognized 3 different spectra

5. Concluding Remarks

Acoustic signal processing benefits from advances in both acoustic and signal processing disciplines. It is developing rapidly and exhibits bright future.

For oceanographic remote sensing and human living environment study, oceanic and inland oil exploration, material evaluation and testing, noise control and medical inspection etc., in a wide range of applications we find acoustic signal processing playing a more and more important role.

The advances achieved are significant while the remaining tasks are heavy but stimulating.

REFERENCES

[1] Chen, K.A., Sun, J.C., Ma,Y.L., "Adaptive Wideband Noise Cancellation", WESTPACⅢ, Proceedings pp665—668, 1988, Shanghai.

[2] C.X.Tan, Y.L.Ma, "Broadband Noise Cancellation Based on an Artificial Neural Network", Proc.of IAP / IMAC, 1990, Shanghai.

[3] J.F.Yang and M.Kaveh, "Digital Realization of the Real—Time Coherent Signal—Subspace Transformation for Array Signal Processing, Proc.of ICASSP88, PP2650—2653.

[4] Y.L.Ma, "A Distributed Approach for Mainlobe Constrained Adaptive Arrays", Advances in Signal Processing, Proc.of 1986 IEEE—ACADEMIA SINICA Workshop on ASSP, PP299—302.

[5] Chen.K.A., Y.L.Ma, "An Analysis of Performances for Adaptive Active Noise Controller", Submitted to Journal of Northwestern Polytechnical University.

[6] X.H.Shi, Y.L.Ma, J.C.Sun, "Adaptive Active Sound Control System Concerning with the Sound Propagation Delay", Submitted to Acta Acustica.

[7] K.A.Chen, Y.L.Ma, "An Intermittent Algorithm and Its Application to Adaptive Wideband Noise Control", Submitted to ICA 92, Beijing.

[8] Y.L.Ma, J.W.R.Griffiths, "Sidelobe Control for Arbitrary Array of Sensors", 4th International Conference on Digital Processing of Signals in Communications, Loughborough, 1984, IERE Publication No.62, pp.39—41.

[9] Y.M.Wang, Y.L.Ma, J.M.Liu, "Using Simulated Annealing to Estimate Parameters of Optimal Sensor Array", Proc. of China 1991 Int.conf. on Circuits and Systems, Shenzhen, China.

[10] Y.L.Ma, "Array Design and Processing Methods for Underwater Sound Measurement", Proc.of Int.Workshop on Marine Acoustics, China Ocean Press, 1990, pp.99—106.

[11] Y.W.Zhang, Y.L.Ma, "An Adaptive Modelling Approach for Generating Phase Shift", Submitted to IEEE Symposium on Industrial Electronics 1992.

[12] B.Widrow, S.D.Stearns, Adaptive Signal Processing, Prentice—Hall, Englewood Cliffs, NJ, 1985.

[13] D.H.Youn, N.Ahmed, G.C.Carter, "A Method for Generating a Class of Time—Delayed Signals", Proc.of ICASSP, 1981, PP.1257—1260.

[14] Y.L.Ma, "A Novel Approach for Generating Continuously Adjustable Digital Time—Delay", Memo. No.20, 1988, Institute of Acoustic Engineering, Northwestern Polytechnical University, Xi'an, China.

[15] Y.W.Zhang, et al, "A TMS320C25 Implemented Multi—Beamformer", Proc. of CCSP—91, 1991, China.

[16] C.X.Tan, Y.L.Ma, "An Artificial Neural Network Based Approach for Noise Control", Inter—Noise 91, Sydney.

[17] Y.L.Ma, C.X.Tan, "Training a Simplified Neural Network for High Resolution Direction Finding of Correlated Sources", Proc.of ISSPA90, pp.870—873, Gold Coast, Australia.

[18] R.P.Gorman, T.J.Sejnowski, "Learned Classification of Sonar Targets Using a Massively Paralell Network", IEEE Trans. on ASSP, Vol.36, No.7, July 1988, pp1135—1140.

[19] C.H.Chen, Signal Processing and Pattern Recognition in Non—Destructive Evaluation of Materials, ISSPA90, Tutorial C, Gold Coast, Australia.

[20] C.X.Tan, Y.L.Ma, "A Multi—Layer Mixed Neural Network for Spectrum Classification", Proc.of CCSP—91, 1991, China.

ACOUSTICAL CHARACTERIZATION OF A BAROQUE-STYLE ITALIAN THEATER BY VECTOR INTENSITY TECHNIQUE

E.Carletti,D.Stanzial,I.Vecchi
CEMOTER Institute – National Research Council of Italy
Via Canal Bianco, 28 – Ferrara – Italy

ABSTRACT

Results concerning acoustical measurements carried out in the Municipal Theater of Ferrara, built in 1790, are here presented.
Acoustical tests had to enlighten possible modifications of the acoustical coupling between the stage and the hall as a result of the original wooden stage replacement.
A detailed description of the acoustical field over the proscenium plane in terms of sound intensity measurements carried out before and after the restoration is presented. The acoustical response of the stage has been tested in terms of a sound power parameter k. Moreover a description of the acoustical field in the restored theater is obtained in terms of vector intensity maps over the proscenium plane.

1.0 INTRODUCTION

Recent restoration works of the Municipal Theater of Ferrara replaced the original wooden stage with a new one. The restoration project had to change the acoustic characteristics of the stage as little as possible; in this respect the wooden floor has been rebuilt following almost exactly the same structural layout as the original one, while the building structures were not touched.
An evaluation of the acoustic response of the stage before and after the restoration works was obtained by means of the following objective tests based on sound intensity measurements [E.Carletti]:
a) evaluation of the acoustic emission characteristics of the stage in terms of a sound power parameter k;
b) description of the acoustic energy flux through the coupling area between stage and hall in terms of sound intensity maps.

2.0 MEASURING EQUIPMENT

The hardware outline consisted of a 3360 B&K intensity analyzer equipped with a 1/2" microphone intensity probe. The combined use of 12 and 50 mm spacers guaranteed an accuracy of ±1 dB in 100-10k Hz frequency range. Measurements and subsequent experimental data elaborations were carried out by dedicated software packages.

3.0 SOUND POWER CHARACTERIZATION

A reference sound power source was placed at the center of the stage. The power emission in this environment was calculated from intensity measurements carried out over a 10 m ray hemisphere centered on the source. The basis of the hemisphere covered about 90% of the full stage surface. In this way the global power contribution of the stage in 100 - 10000 Hz was obtained as difference k between the measured sound power spectrum and the correspondent reference one.
The same test was repeated when the restoration works were finished.

3.1 Results

The k values obtained before and after the restoration works are shown in table 1.
Until 3150 Hz the difference between the correspondent k values before and after the restoration is within 0.5 dB. This shows that the stage replacement hasn't modified the acoustical response, the experimental error range being ± 1 dB.
For higher frequencies, the restored stage has a different

acoustical response. The sound spectrum is emphasized in 4-8 kHz frequency range while is roughly attenuated in the 10 kHz neighborhood.
This different response is attributable to different absorption properties of the new wood (different wood seasoning) respect to the original one.

TABLE 1

Freq.(Hz)	100	125	160	200	250	315	400	500	630
k(before)	3.1	3.2	3.2	3.4	3.9	4.2	4.3	3.0	4.7
k(after)	3.1	3.2	3.1	3.1	3.9	4.7	4.4	4.0	4.4

Freq.(kHz)	0.8	1.0	1.25	1.6	2.0	2.5	3.15	4.0	5.0
k(before)	4.1	3.5	2.7	1.0	1.9	2.8	3.7	3.3	1.4
k(after)	4.0	3.4	2.5	1.1	1.8	1.2	3.3	2.1	0.3

Freq.(kHz)	6.3	8.0	10
k(before)	1.7	1.0	0.3
k(after)	1.0	0.6	2.2

4.0 SOUND INTENSITY MAPS

In a theater the stage and the hall have different functions. Precisely stage "produces" sound while hall "receives" it. The description of the sound energy flux just through the vertical plane between these two environments gives an efficient characterization of their acoustic coupling [Y.Ando,L.Cremer].
In this respect the sound power reference source was placed in the middle of the stage and the normal component of the sound intensity vector was measured in an array of 6X10 points over the proscenium plane.
Dedicated software packages allowed to obtain iso-contour and three-dimensional intensity maps in 100-10000 Hz frequency range. The same tests were repeated after the restoration works.

4.1 Results

Fig.1 shows a three-dimensional view of 200 Hz sound intensity maps obtained before and after the restoration. In fig. 2 the correspondent 6300 Hz iso-contour maps, overlapped to the proscenium plane as seen from the hall, are displayed. Continuous lines represent sound energy flow coming from the stage toward the hall.

60

Until 800 Hz intensity maps before the restoration are smoother than the correspondent ones after the restoration. This behavior may be attributed to the different acoustic coupling between hall and stage due to the wooden floor replacement of the hall.
At higher frequencies the trend of correspondent maps is similar. This shows that in this frequency range the restoration didn't change the acoustic coupling.
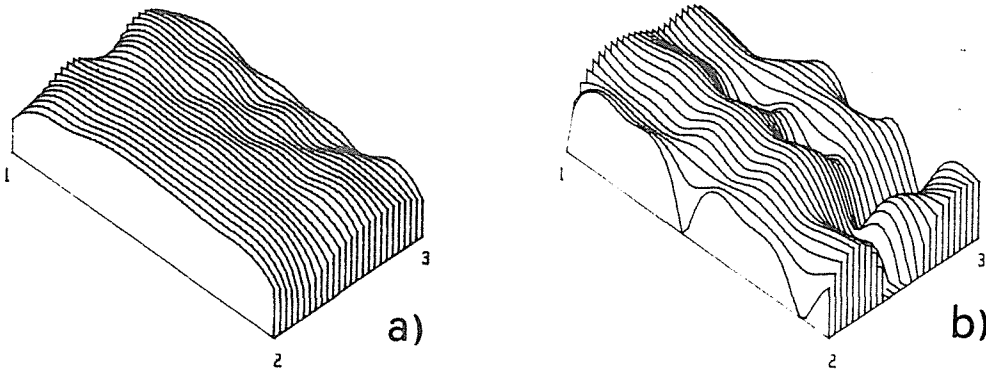
Fig.1 Three-dimensional view of 200 Hz sound intensity map obtained on the proscenium plane a) before and b) after the restoration works.
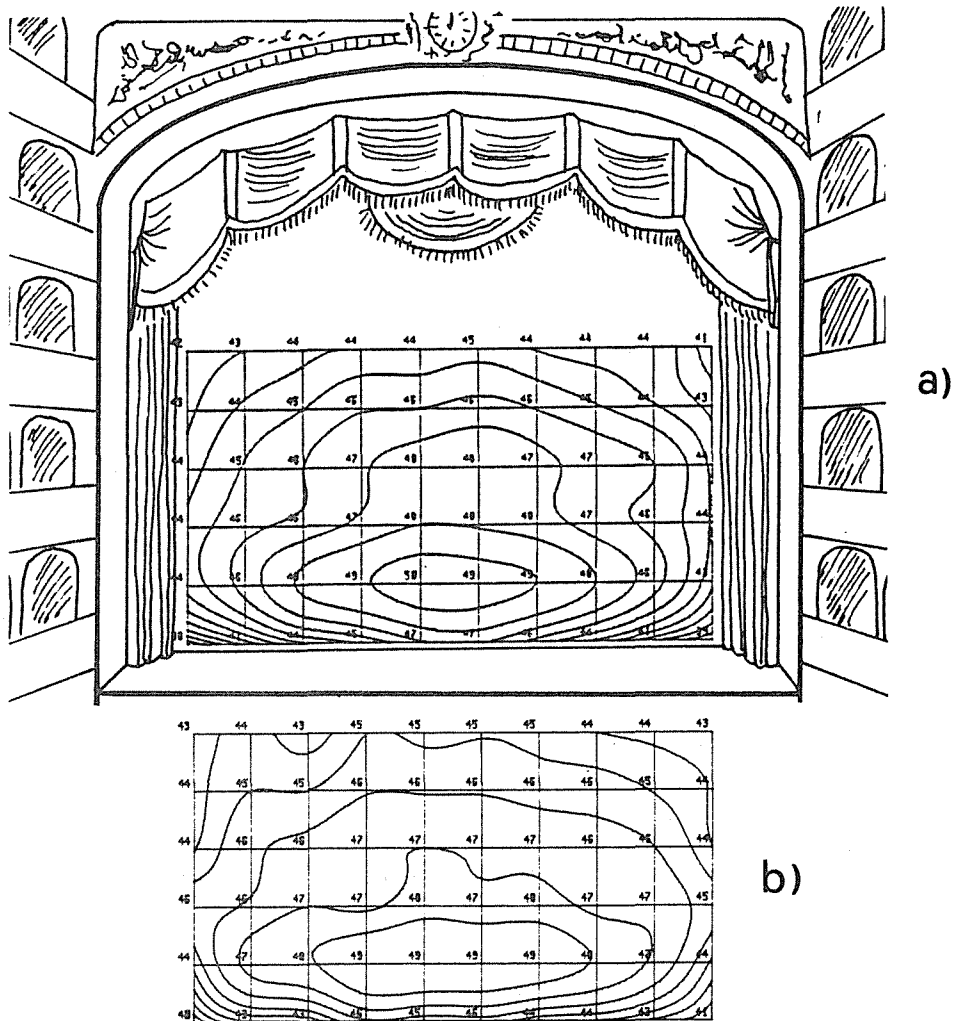
Fig.2 6300 Hz iso-contour maps a)before and b)after the restoration.

61

4.2 <u>Sound intensity vector measurements</u>

An additional description of the acoustic field in the restored theater was obtained in terms of vector intensity maps over the proscenium plane. This objective was reached by means of a six microphone intensity probe. In each point of the 6X10 grid the three intensity vector projections were measured serially by multiplexing the microphone signals in pairs.
Fig.3 a)and b) shows graphical views of vector sound intensity flux from the stage to the hall at 1600 Hz and 500 Hz (relevant frequencies for musicians).

a)

b)
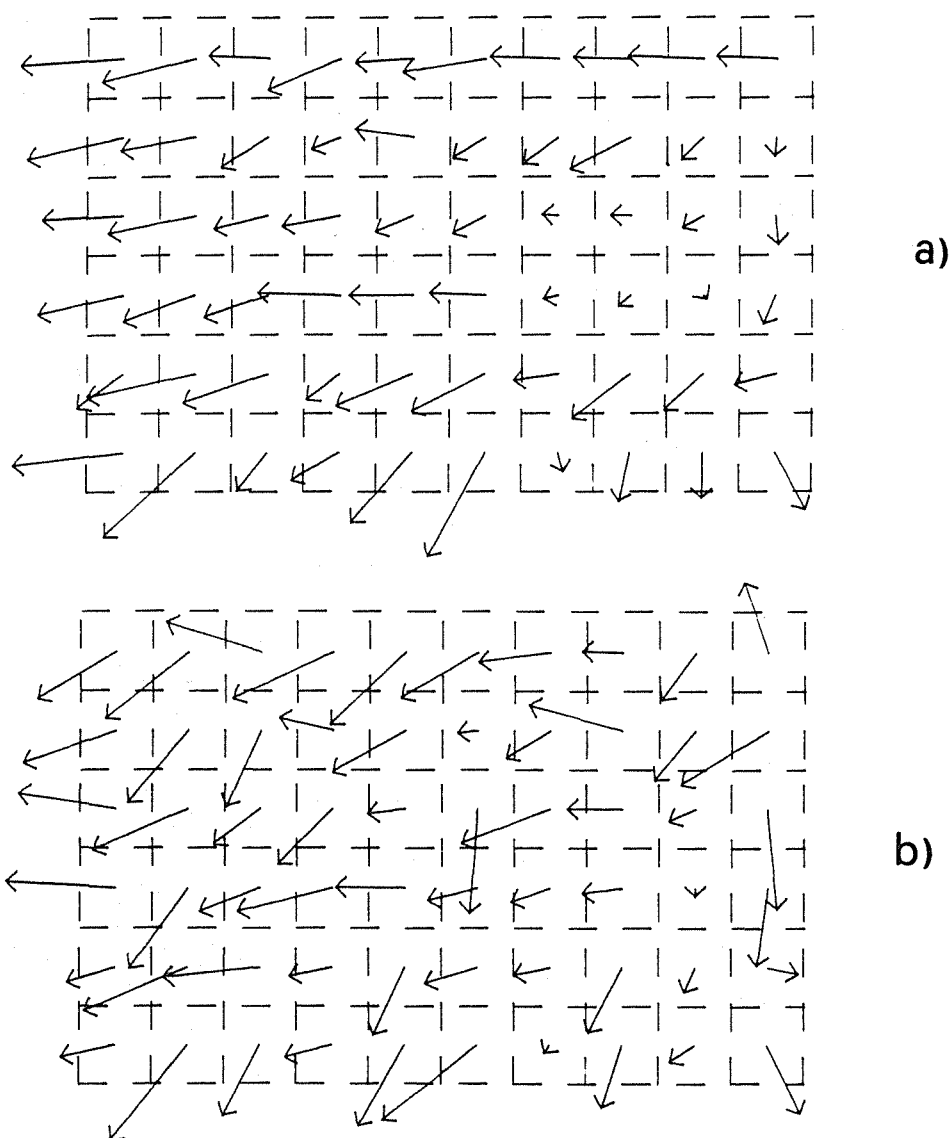
Fig.3 Graphical view of vector intensity flux from the stage at a) 1600 and b) 500 Hz frequencies.

5.0 CONCLUSION

Tests for evaluating the acoustical emission of the stage showed a different response of the restored stage as to

the original one only at high frequencies. This different behavior has been chiefly attributed to a different absorption coefficient of the replaced wood.
The description based on sound intensity maps over the proscenium plane gave a qualitative picture of the energy flux between hall and stage. The results showed that restoration works produced differences in the acoustic coupling between the two volumes only for frequencies below 800 Hz, while a similar coupling was preserved at higher frequencies.

6.0 REFERENCE

Y.Ando, Concert Hall Acoustics, Springer, Berlin 1985.

E.Carletti,A.Fuschini,D.Stanzial,I.Vecchi, Application of vector intensity techniques for the acoustical characterisation of a baroque-style italian theater, JASA, Supplement 1, Vol.86, Fall 1989.

L.Cremer, H.A.Muller, Principles and applications of room acoustics, Applied Science Pub., 1978.

SOUND REFLECTED FROM THE YINYIN PAGODA

CHEN TONG
INSTITUTE OF ACOUSTICS, CHINESE ACADEMY OF SCIENCES
CHINA

ABSTRACT

The mystery of the echo sound reflected from the Yinyin Pagoda at the Pujiu Temple is well-known in China. The echoes are heard like the sound of frog. This is due to the sound reflected from the wall and eaves of the Pagoda, especially the structure of eaves. The spectrum of echo sound has been analyzed in comparison with that of frog sound. The sound spectra of echoes reflected from the 3rd to 13th story are similar. The time intervals between adjoining echoes are around 10 ms. as the interval between sound pulses in frog sound. The reflection of sound from the wall and eaves has been studied by model experiment.

The Yinyin Pagoda is at the famous Pujiu Temple in Shanxi Province of China. The Pujiu Temple is constructed on a hill . It is a brick construction with square foundation. The Yinyin Pagoda has 13 stories and is 36.76 m high. The mystery of echo sound from the Pagoda is well known in China. The sketch of the Pagoda is shown in Fig. 1. Striking against the earth with a suitable stone at point A, the echo sound heard at a place beneath the Pagoda (point B) is like the sound of a frog.
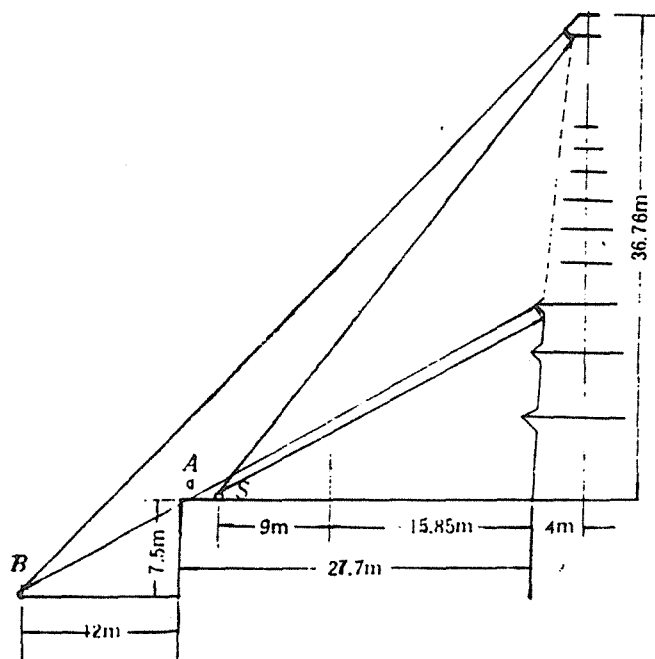
Fig 1. Sktech of the Pagoda

Reflection of Sound

Acoustical measurements have been carried out in place. After striking against the earth with stone at point S in Fig. 1, the sound pulses received at point B is shown in Fig. 2. The first pulse is the sound transmitted directly from the source at point S. Then, eleven echo sound pulses reflected from the Pagoda arrive at receiving point B. The first pulse arrives at 225 ms after the time of striking at point S. The last pulse arrives at 316 ms after striking.

From the arriving time of echo sound, the reflection of sound from the Pagoda can be determined. For the reflection of sound from the thirteenth story of the Pagoda, the sound path from the source (point S) to the receiving point B is estimated at 105 m from the sketch shown in Fig. 1. The temperature during measurement was about 10° C. The velocity of sound is taken as 336 m/s in the calculation of arriving time. The arriving time of the sound pulse reflected from the thirteenth story of the Pagoda is calculated as 313 ms. Hence, the last echo pulse arriving at the receiving point can be considered as the reflection of sound pulse from the thirteenth story of the Pagoda.

The sound path for the reflection from the third story is about 76 m and the calculated arriving time is 226 ms. The

65

first echo pulse arriving at the receiving point is due to
the reflection from the third story at the Pagoda.

Similarly, the reflection from which story of the Pagoda
for each echo arriving at the receiving point can be
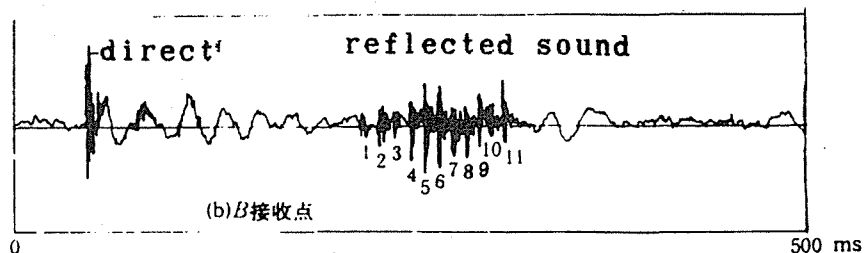
Fig 2. Sound pulses received at point B

determined. The results are listed as follows.

Echo sequence	Reflection from story	Arriving time (ms)	Time interval (ms)
1	3	225	
2	4	235	10
3	5	246	11
4	6	256	10
5	7	266	10
6	8	275	9
7	9	284	9
8	10	293	9
9	11	301	8
10	12	309	8
11	13	316	7

The echoes arriving at the receiving point are reflected
from the third to thirteenth story of the Pagoda. The
Echoes are reflected from the wall and eaves of the Pagoda.
The time intervals between adjoining echoes are mostly 9 -
10 ms. The reflection from the first and secend stories
cannot arrive at the receiving point.

Sound Spectrum

Frequency spectrum of sound received at point B was
analyzed by using sonograph, shown in Fig. 3. The first
line is the spectrum of direct sound arriving from the
source. The frequency range is mainly below 4 KHz. The
spectra of eleven pulses reflected from wall and eaves of
the Pagoda are labeled with sequence numbers. The energy of
echo sound is concentrated in the frequency range of 400 Hz
to 1700 Hz for all of the echo pulses. The reflection of
sound from the eaves is effective as the width of eaves is
larger than the wavelength of the incident sound. The width
of eaves is about one meter. It is impossible to have an
effective reflection at frequencies below 400 Hz. At high

66

frequencies, the sound is attenuated in air. Furthermore,
the high frequency sound is scattered by the edges of
bricks on eaves.
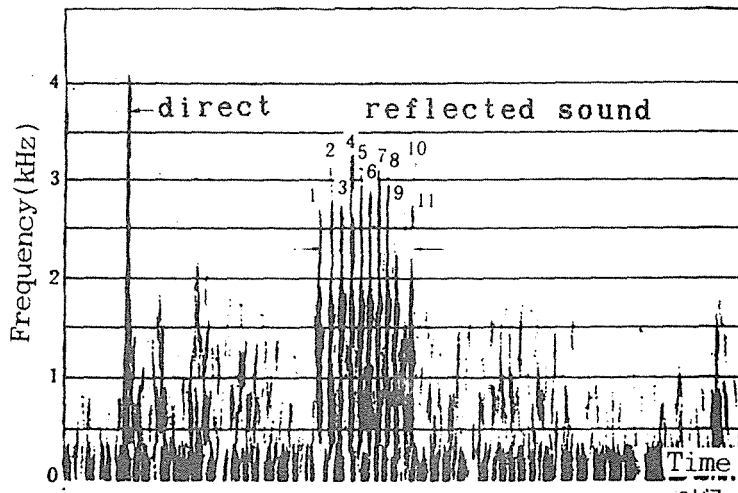
Fig 3. Sonogram of sound received at ponit B

Effect of Frog Sound

The echo sound received at some places beneath the Yinyin
Pagoda is a series of sound with time interval about 10 ms.
Under certain conditions this sound can be heard like the
sound of frog. Fig. 4 shows the sonogram of frog sound
recorded in nature. The frog sound consists of groups of
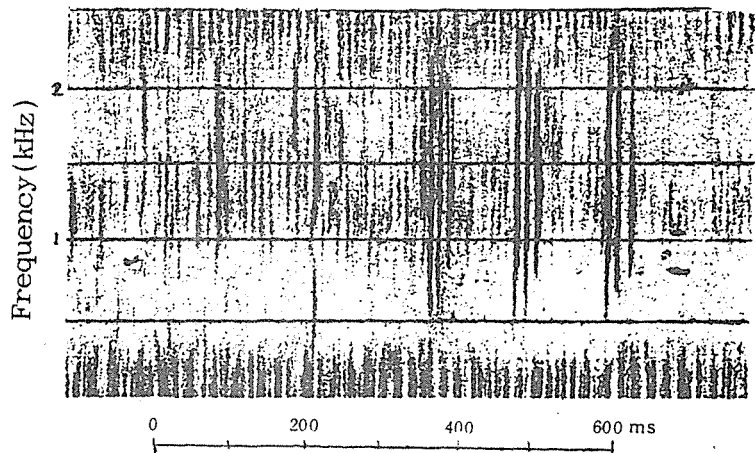
Fig 4. Sonogram of sound of frog in nature

sound pulses with time interval about 10 ms. The frequency
spectrum of each sound pulse is mainly in the range of 500
Hz to 2 KHz. The time and frequency characteristics of echo
sound received beneath the Yinyin Pagoda are quite similar

67

to those of the frog sound. This is the reason why the echo sound from the Yinyin Pagoda can be heard like the sound of frog. The main reasons are:

1. The frequency spectra of sound pulses reflected from different stories of the Yinyin Pagoda are similar in the frequency range from 400 Hz to 1700 Hz.

2. Frequency range of echo sound from the Yinyin Pagoda is similar to that of the sound pulse in frog sound.

3. The time interval between the adjoining echo sound pulses from the Yinyin Pagoda is around 10 ms, similar to that in the frog sound.

The positions of sound source and receiving point are important. For a suitable position of sound source, the conditions of sound reflections from the wall and eaves of the Pagoda must be almost the same for reflections from all the stories of the Pagoda to recieving point. This condition can be obtained only at receiving points beneath the Pagoda. Of course, the construction of eaves of the Yinyin Pagoda plays an important role in this phenomenon.

Model Experiment

The sound reflection from eaves and wall of the Yinyin Pagoda has been studied by model experiment. Half size model of eaves was made. The model of eaves was put on the ground of a semi-anechoic room. The ground of semi-anechoic
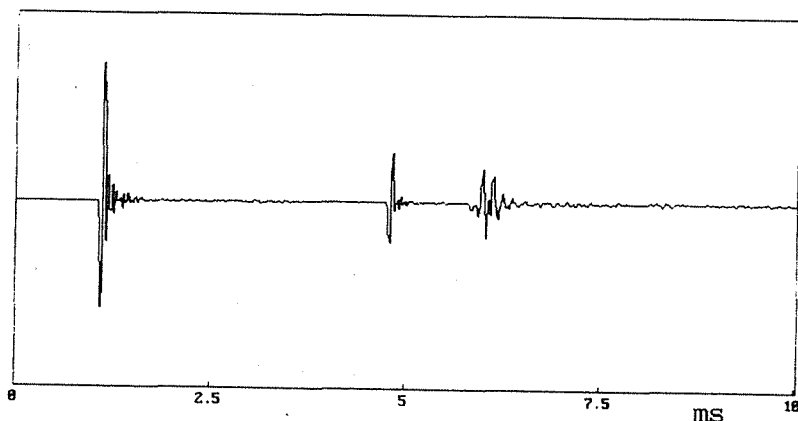
Fig 5. Sound pulses of model experiment

room simulates the wall of pagoda. The impulse sound source is an electric spark. The position of sound source is in the direction of real sound source with respect to the wall of the Pagoda. The measarements were carried out at different points around the eaves. Fig 5 shows a typical waveform received at a point within the angle between the inner surface of model and the ground of semi-anechoic room. The first pulse in the figure is the direct sound from the source to the receiving point. The second pulse is the sound reflected from the ground of semi-anechoic room. This sound does not present in the real case and is omitted in the analysis of measurement. The third pulse is the

68

sound reflected by the ground of semi-anechoic room and model of eaves. This is the needed sound to simulate the reflection of sound from the Yinyin Pagoda. The frequency response of the reflection is given by the ratio of sound spectrum of reflected sound to the spectrum of direct sound received at measuring point. An example is shown in Fig 6. More understanding of the reflection of sound from the Pagoda can be given from the model experiment.
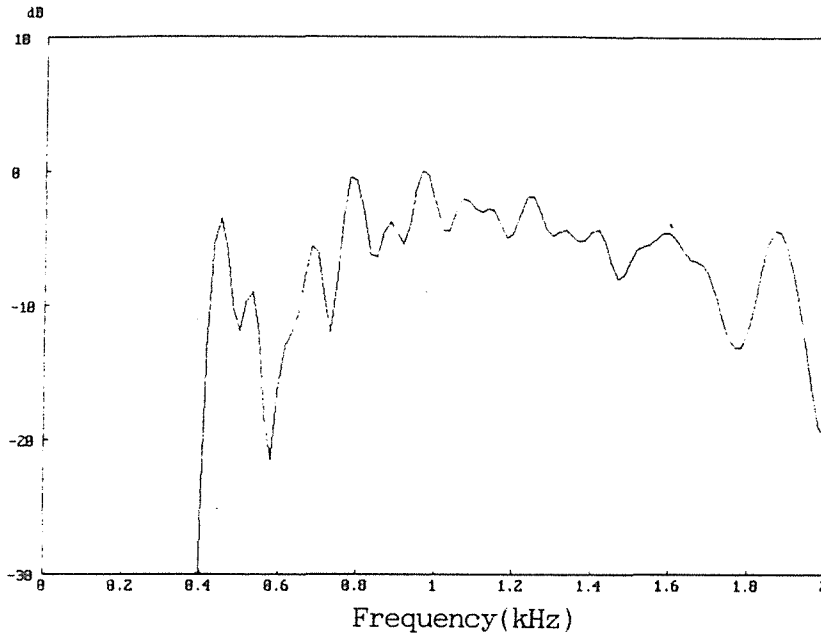
Fig 6. Sound spectrum of reflection

A STUDY ON THE ACOUSTICAL PROBLEM OF STEREO CINEMA

Chen Yanxun

Department of Architecture, Chongqing Institute of Architecture and Engineering, Chongqing, PO Box 630045, China

ABSTRACT

This paper presents methods and principles of acoustical design of stereo sound cinema from the viewpoint of psychological acoustics, electroacoustics and architectural acoustics. In this paper, acoustical design and measurement data are described in relation to the six channel Dolby stereo cinema.

1.0 INTRODUCTION

Since the 1920s, sound films have pushed the science of electroacoustical reproduction systems forward. During the last two decades, Hi-Fi electro-acoustical equipment has given conditions of wide frequency and high articulation, and has established a foundation for a true acoustical environment of a room. Dolby stereophonic equipment produces a standard condition in the acoustical quality in the studio or in the Dolby stereo cinema. Thus, audiences can listen to the same sound in any Dolby stereo cinema and in the studio. Acoustical principles and design requirements are presented below.

2.0 THE ACOUSTICAL PRINCIPLES OF THE STEREO CINEMA

2.1 The Directional Perceptions of Human Ears

The difference in intensity and the difference in time of arrival (phase) of the sound falling on two ears are involved in the perception of direction. Above 1 kHz the intensity effect dominates, because the ear nearer the source receives a greater intensity than the far ear and the 'sound shadow' (diffraction) caused by the head reduces the sound pressure on the far side. Below 1kHz the phase effect dominates. There are different diffractions for different frequencies, hence both ears in the sound field have differences in tone colour; the ear farther from the source hears less high frequency sound than the nearer ear.

There are about 4 degrees for differentiating the direction of the source in both ears. There is a maximum deviation of 6~7 metres around the sound source for differentiating the direction when the source is 100 metres away.

Boerger demonstrated in his investigations with Gauss-tones that the ear can simultaneously determine only two directions and then only when one signal lies in the frequency range below 1 kHz, and the other signal lies in the frequency range above 1.5 kHz.

It is assumed that the external part of the ear (i.e the pinna or auricle) acts to enhance the high-frequency sounds arriving from the front and to weaken those from the rear. The listener can therefore determine whether the sound comes from in front or behind. Blaurt measured with probe microphones at the entrances of the outer ears the level differences between sound waves incident from the front (ϕ - 0°) and from the rear (ϕ = 180°) Fig 1 shows the results. At low frequencies the head is small as compared with the wavelength and no differences can occur; but by 250 Hz the frontal sound predominates, whereas around 1 kHz the rear sound predominates. This alternation continues up to the highest frequencies.
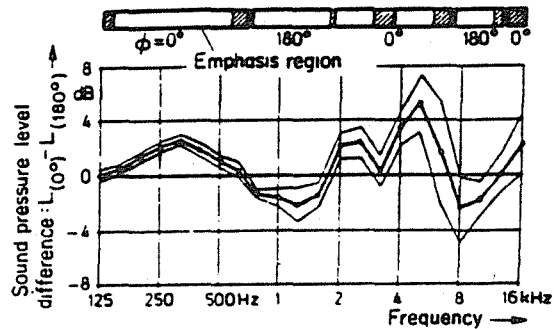
Fig 1. Sound pressure level difference at the eardrum between sound waves incident from the front (ϕ = 0°) and from the rear (ϕ = 180°), plotted against frequency.

If the person is seated in front of a single loudspeaker in an anechoic room and a one-third octave band noise is presented with a mid-frequeny that slowly progresses from low to high frequencies, he perceives the sound as arriving frontally until about 600 Hz. Then this impression gradually reverses, until at 1000 Hz the sound appears to arrive from behind, even though the test person is quite aware that the sound comes from the loudspeaker in front of him. At 2 kHz the impressions is again frontal; then the direction of incidence moves again, this time in a large arc over the head, toward the rear. The same directional impression occurs when the real sound is incident from above, from behind, or with the same phase from both sides.

There is no doubt, however, that localisation is easier for the listener if he is familiar with the signal. Plenge and Brunschen proved this by comparing the judgments of perceived directions (only five directions were used), as shown in Fig 2. There are very great differences in the percentage for the directional- impression of a known speaker and an unknown speaker.

If there are several loudspeakers distributed about a space, all operating in phase, then as we walk about from one loudspeaker to another we always perceive the nearest source to be the only source operating. The perceived location of the source is the incidence direction of the wave whose front arrives first. We called this phenomenon the 'law of the first wavefront'.
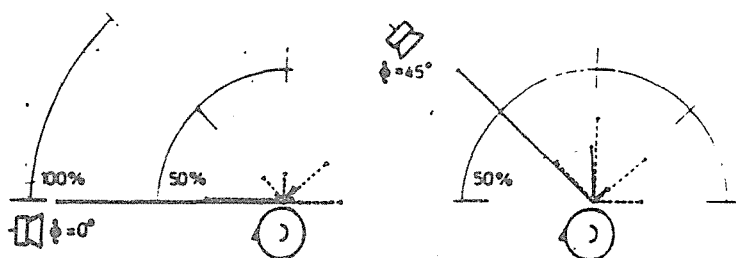
Fig 2. Relative frequencies of directional impression (restricted to five directions) for a known speaker (———) and for an unknown speaker (----).

It can be seen that the directional impression of both ears is a very complicated problem of psychological acoustics, and a simple conclusion can not be given yet.

2.2 Sound Processes of Electro-acoustical Coupling Rooms

It is different when we listen to the sound from inside a cinema and from inside a theatre. Inside a cinema the audience listen to a reproduced sound which is picked up by the microphone in the studio having a reverberation time T_1. The coupling between studio and cinema is a uni-directional electro-acoustical coupling. The reverberation process of reproduced sound is influenced by both studio and cinema and the energy density of sound does not decay according to the simple exponential law.

Equation (1) is an equilibrium equation for the sound energy in room 2 as shown in Fig 3:

$$V_2 \cdot \frac{dE_2}{dt} = -V_2\beta_2 E_2 + W_{A_2} \tag{1}$$

The radiation power of sound from the loudspeaker is

$$W_{A_2} = E_{02}V_2\beta_2 e^{-\beta_1 t} \tag{2}$$

where V_2 is the volume of room 2 (m^3), β_1 and β_2 are the decay rates of room 1 and room 2 respectively, and

$$\beta = \frac{cA}{4V} = \frac{c\bar{a}S}{4V} \tag{3}$$

E_{02} is the energy density of sound in room 2 without electro-acoustical coupling $(J.m^{-3})$, E_2 is the energy density of sound in room 2 with electro-acoustical coupling $(J.m^{-3})$, C is the velocity of sound (m/s), S is the total surface area of the room (m^2), $\bar{a}$ is the average Sabine sound absorption coefficient, A is the total Sabine sound absorption area (m^2) and $A = \bar{a} \cdot S$.

The solution of equation (1) is

$$E_2 = \frac{E_{02}}{\beta_2 - \beta_1}(\beta_2 e^{-\beta_1 t} - \beta_1 e^{-\beta_2 t}) \tag{4}$$

We can conclude from equation (4) that:

(a) The change of sound energy in the coupling room is restrained by the decay rate β_1, β_2

(b) the decay curve in room 2 is not a simple exponential curve

(c) the total decay is slower than that in either of the coupled rooms

(d) if the decay rate β_1 of the sound source room is very big, the decay process of the electro-acoustical system will be restrained by the decay rate β_2 in the cinema, and vice versa. When $\beta_1 \to oo$, eqn (4) becomes

$$E_2 = E_{02} e^{-\beta_2 t} \tag{5}$$

Under the condition of electro-acoustical coupling, the total reverberation time of the cinema T_r, can be approximately calculated by the following equation (6)

$$(T_r)^3 = (T_1)^3 + (T_2)^3 \tag{6}$$

Where T_1 is the reverberation time of the studio (s); T_2 is the reverberation time of the cinema (s). If $T_1 = T_2 = T$,
$T_r = 1.26T$ (s).
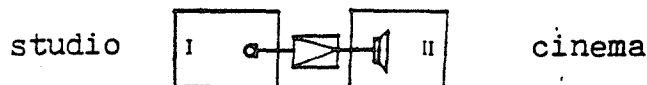
studio   ▢ cinema

Fig 3. Electro-acoustical coupling of studio and cinema.

2.3 The Location of the Sound Image for Stereo

The stereo system must produce the same effect as if the sound source were transferred into the auditorium of the cinema from the studio or sound source room. This lets the audience perceive the space impression of the sound source. In recent years the six channel Dolby stereo sound reproduction system has been established in some cinemas and in the wide screen cinema.

The locations of the sound image shows off the essential characteristics of stereo sound. These locations include;

(1) lateral locations,
(2) the width and mass impression for the sound image,
(3) the deepness location of the sound image,

The lateral location is called the width location or the angular location, because it is the most important factor showing the location impression. Today the stereo is called the width stereo. The lateral location shows the plane width region of stereo: the wider the region we perceived, the more the apparent stereo we got.

The ratio of the direct sound energy to the reverberation sound energy within the location of width is very important. There are accurate locations, if the direct sound energy is greater than the reverberation sound energy. There is also the drift of point image or the shaking of sound image if the reverberation sound energy is greater than the direct sound energy. If the ratio of reverberation sound energy to direct sound energy increases, the direction impression of the sound source will be blurred or will disappear.

The lateral location will also be influenced by the frequency characteristic of the sound source. The locations of the mid and high frequencies are easier than those of the low frequency sound; the sounds in the 1 ~ 3 kHz range are the more important for the location of the sound source.

The deepness location is determined by the time delay of the sound and the loudness, but a sound having a higher ratio of direct sound is also perceived to give the impression of far distance. For a given low sound level, the idea of deepness impression will appear unless some certain reverberation sound energy is produced at the same time.

The width of the sound image can distinguish the stereo impression of the source, such as a point source, line source, plane source or volume source. The mass impression response gives the quantity impression of some classification sources, and a stereo space impression of the width and the deepness.

3.0 THE ACOUSTICAL DESIGN PRINCIPLES OF THE MULTICHANNEL STEREO CINEMA

3.1 The Type of Plan and Elevation

The type of plan is limited by the technical characteristic of the loudspeaker and must adapt the plan type to the dire activity of the loudspeaker. The bi-radial horn loudspeaker JBL has the horizontal radiant angle of 90° to a frequency of 12000 Hz. The horn loudspeaker in E-VHP and HR systems also has horizontal and perpendicular emitting angles of
120° X 40°, 90° X 40°, 60° X 40°, 40° X 20° etc respectively.

The design of the plan and elevation should provide the widest complete sound coverage for the stereo cinema. The complete sound coverage is the essential condition for forming a stereo sound area. Fig 4 and Fig 5 show the sound coverage of a cinema with loudspeakers having emitting angles of 60° and 90°. In order that sound ray bundles of the loudspeakers are not reflected by the side walls, it is reasonable that the plan of a stereo cinema is a bell figure for the front 1/3 of the auditorium and a sector figure for the rear 2/3 of the auditorium.

complete
sound covege
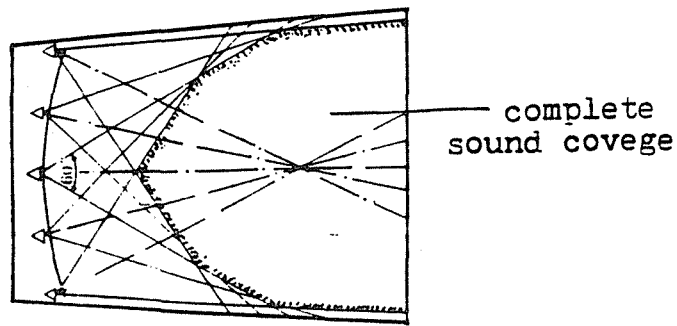
Fig 4.   Sound   coverage   of   stereo   cinema   with   loudspeakers
having radiation angle of 60°.

complete sound
coverage
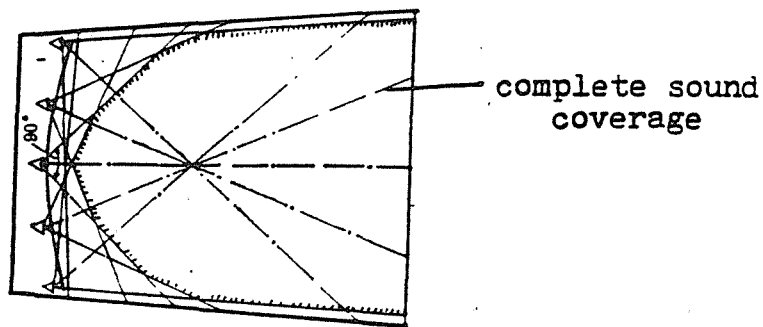
Fig 5. Sound coverage of stereo cinema with loudspeakers
having radiation angle of 90'.

The elevation of a stereo cinema with loudspeakers having a
perpendicular radiation angle of 40° should include the front
and rear seats in the complete sound coverage.   An example is
shown in Fig 6.   However, under normal conditions the balcony
seats of the stereo cinema are difficult to cover.
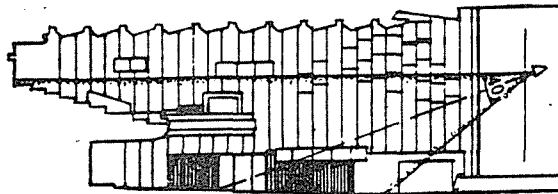
Fig 6.   The elevation of the Chongqing Shan Cheng six channel
Dolby stereo cinema in China.

76

3.2 The Reverberant Field in the Stereo Cinema

There is a reverberation time of 0.6 s in the majority of studios in a film processing factory. The reverberation time in the stereo cinema should be the same as in the studio. If the ratio of reverberation sound energy to direct sound energy increases, the direction sense of the sound will be blurred or will disappear.

Dolby system U.S.A. recommends use of T_{60} = 0.5 ~ 0.7 s for Stereo cinema; the recommended reverberation time in China for stereo cinema is 0.5 ~ 0.8 s. The author's idea is that the reverberation time should be shorter than 0.7 s for six channel stereo cinema in the sound frequency range 1 ~ 4 kHz. Otherwise the stereo sense will be blurred or will disappear. It is better that the reverberation time is shorter than 0.6 s in the range 1 ~ 4 kHz. In the 125 ~ 250 Hz low frequency range the reverberation time is a bit too long, and the stereo location will not be influenced.

The sound field should distribute well on the audience seats if the difference between max and min sound pressure levels is not higher than 6 dB (centre frequency 1 kHz oct, pink noise). The background noise level in the auditorium should be not higher than 35 dB (A), because the higher background noise level will break the stereo location.

4.0 THE CHONG QING SHAN-CHENG SIX CHANNEL DOLBY STEREO CINEMA IN CHINA

In 1988, the Chinese Chongqing Shan-cheng Wide Screen Cinema was reconstructed into a six channel Dolby stereo cinema. The plan of the cinema is a bell figure having a balcony. The total volume is 9270 m^3 (including stage volume), the volume of the auditorium is 7879 m^3, the total surface area of the room is 3078 m^2. The stalls have 872 seats, the balcony has 404 seats, and the seats are soft.

The reverberation time data are shown in TABLE 1.

TABLE 1. the reverberation time data (s)

frequency (Hz)	125	250	500	1k	2k	4k	note
T_{60} (empty)	0.75	0.67	0.61	0.61	0.61	0.62	measurement
T_{60} (filled)	0.89	0.64	0.65	0.65	0.58	0.58	calculation

The difference between the max and min sound pressure levels in the auditorium is 6 dB (83.77). The average sound level of the balcony seats is 79 dB (Lin) or 77 dB (A) and the average sound level in the stalls is 84 dB(Lin) or 82 dB(A). The average sound level in the balcony is 5 dB lower than the average sound level in the stalls, because the perpendicular radiation angle of the loudspeakers is too narrow.

When all air conditioning equipment in the room is operating, the background noise level in the auditorium is 48 dB(A). When only the film projector is operating, the background noise level is 39 dB(A).

Since the cinema has been in operation, the response of the audiences are that the stereophonic sense is outstanding, the speech sound is articulate and the music sound is sweet sounding. There is a balanced sense of tone, even though the reverberation time in the low frequency range is slightly long.

5.0 CONCLUSIONS

5.1 The sound problems of stereo cinema are the synthesis of architectural acoustics, electro-acoustics and psychological acoustics. Though the direction sense and location of sound image have been researched a large amount, the differences in results have been outstanding. In recent years the science of electro-acoustics has been advanced a great deal, but the unsymmetrical axial horn must be researched still further to satisfy further equilibrium sound field requirements.

5.2 The total reverberation time of cinemas under the condition of electro-acoustic coupling is calculated approximately by the following equation

$$T_r^2 = T_1^2 + T_2^2$$

where T_1 and T_2 are the reverberation times of the studio and cinema respectively.

5.3 The reverberation time should lie in the range 0.5 ~ 0.7 sec. Greater reverberation times will blur the location of sound images.

5.4 The present character of a loudspeaker can not contribute to the complete sound coverage for the stalls seats and balcony seats at the same time.

5.5 The absorption material should be distributed on the side wall, rear wall, front wall and rear ceiling for the stereo cinema.

REFERENCES

1. F A Everest, "Acoustic techniques for home and studio". TAB Book Inc. 1984. 78 ~ 79. 213 ~ 239.

2. M Rettinger, "Acoustic design and noise control". Chemical Publishing Co. 1977. 422 ~ 428.

3. John Eargle, "The academys new state-of-the-art loudspeaker system." SMPTE Journal. 1985.6. 667 ~ 675.

4. Lothar Cremer, "Principles and applications of room acoustics". Applied Science Publishers, 1982. 464 ~ 512.

5. Shen-hei, "Audio amplification technology "The Publishing House of Post and Telecommunications. China. 1982. 257 ~ 262 482 ~ 512.

STATISTICAL INVESTIGATION OF GEOMETRICAL PARAMETERS FOR THE ACOUSTIC DESIGN OF AUDITORIA

Chan H. Haan and Fergus R. Fricke
Department of Architectural and Design Science,
University of Sydney, NSW 2006, Australia

ABSTRACT

While methods of testing the acoustic design of an auditorium are quite sophisticated and successful, there is very little information available to help the designer at the conceptual design stage. As acoustic conditions in an auditorium are largely determined by geometrical parameters it should be possible to give guidance in these terms rather than in acoustical terms.

This paper reviews the usefulness and validity of the guidelines available to designers and looks at whether there are limits on the building form which must not be exceeded. As a result another approach to acoustical design is proposed which is based on a statistical analysis of the form of existing auditoria. It is possible that this type of approach could be used by designers to deal with other aspects of design as well.

1.0 INTRODUCTION

Over the past few decades the emphasis in research into acoustic design of auditoria has been on how audiences perceive the acoustics and on improving methods of assessing the acoustics once the basic design has been undertaken.

Before the 20th century, most acoustical design appears to have been based on precedent and guess work. In the first half of the 20th century reverberation time was the main acoustic criteria used for designing and assessing an auditorium. However, reverberation time could not explain the differences in the perception of the acoustics of auditoria. In the latter half of the 20th century, more complex criteria such as early decay time, spatial impression, lateral energy fraction and interaural coherence, have been used to explain perceived differences in auditoria. These new criteria may help to explain particular acoustical conditions but they are of little value in the early design stage because very detailed design data are required for their calculation. Also, there is still considerable uncertainty about the value of some of these criteria.

Many halls have actually been designed with minimal knowledge of acoustical theory. However, in most cases, the designers of these halls used information from other halls on which to base their designs. The acoustics of these halls is very variable but, in some cases, they are considered as models for current design of auditoria. The accumulated knowledge of the design of halls could be the best guidelines for better acoustic design: better than existing acoustical design techniques, at least at the conceptual design stage.

Beranek surveyed more than fifty halls and suggested quantified acoustic criteria for auditoria on the basis of the study. He developed a scale of acoustic quality for halls as well as assessing existing halls. Beranek's study, despite its limitations, is still used by many acousticians and consultants as a basis for auditorium design. During the 30 years since

Beranek's work almost no attempt has been made to develop new rules of thumb based on existing auditoria, and to re-evaluate data and design guides that are currently used, even though many new auditoria have been built using new styles and concepts.

What the designer needs in the initial stage of the design is basic information about the architectural form such as room volume, layout of audience seating and configurational shape of the auditorium. Later in the design process, the other methods including ray-tracing and model testing can only be used to refine and check the formulated designs. The present work is concerned with the early stages of the design process. The work presented here is essentially a re-evaluation of the rules of thumb that exist for the acoustic design of auditoria. These rules of thumb include the volume per seat, floor area per seat, the shape of the auditorium, the rake angle of the seating, and the maximum size of the auditorium and whether, in fact, there can be rules of thumb or combinations of these rules. Also, if these rules exist, which are the most important ? In order to answer questions such as this information must be obtained about existing halls and presented statistically. Most of the information presented refers to all halls, or subsets of them, eg. concert halls or drama halls. Only a very superficial attempt has been made to correlate the information about halls with how good the auditoria are acoustically.

2.0 AUDITORIUM PARAMETERS AND HALL CATEGORIES

The population for this statistical study could be all the existing and past auditoria which have been built but it is not possible to collect data of all halls and it is very difficult to obtain a random sample which is not biased as the information about the population is very limited eg. the number of halls in each country, the kind of architectural styles, the current major uses of the auditoria and changes to the halls are unknown in most cases. The statistical data of halls used in this study is from existing published information on auditoria in which data and scaled drawings are available. The sample, therefore, is unlikely to be random. The 325 halls used in the present study include halls in each of five use and type categories (see Table 2). The halls are in thirty five different countries and were built after 1750.

2.1 Investigated Auditorium Parameters

The shape of a room is hard to define numerically but, it can be approximately described by several variables such as the volume and the ratios between each of the three major dimensions of the room. For this study fourteen quantities were used to define the shape and acoustics of auditoria (without using acoustic measures directly). No acoustic parameters are included because, as indicated earlier, the purpose of this work is to try to provide size, shape and form information for designers which will be of use in the initial stage of the design when acoustical measures are not available. The physical attributes of each hall which were investigated are shown in Table 1.

Table 1. Physical attributes of auditoria which were investigated.

Auditorium Parameter	Abbr.	Unit	Auditorium Parameter	Abbr.	Unit
Room Volume	V	m^3	Seating Density	Sa/N	m^2/seat
Total Floor Area	St	m^2	Length to Width Ratio	L/W	
Audience Seating Area	Sa	m^2	Length to Height Ratio	L/H	
Number of Seats	N	seats	Width to Height Ratio	W/H	
Volume per Floor Area	V/St	m	Mean Rake Angle	MRA	degree
Volume per Seat	V/N	m^3/seat			

2.2 Category of Halls (Type & Use)

The halls used in this study were classified into 10 categories according to their major uses and the shape of the hall. Table 2 shows the categories of halls investigated in this study.

Five major types of halls were identified on the basis of their shape. Different types of halls were fashionable for auditoria (Forsyth) during certain periods, eg. rectangular shoe-box concert halls in the 19th century, horseshoe type halls for opera in the late 18th to 19th century and fan shaped halls for concert and multi-purpose auditoria after 1910. In the 20th century, more complex shapes have been developed to meet various requirements and conditions. The present classification was used for the purpose of explaining different acoustic treatments for each type of auditoria (Doelle). Among the hall types, 'geometric' means irregular designs which can't be classified as one of the other four types.

Two major classifications of halls, by use, have been made. If there is neither a separate stage house above the stage platform nor a proscenium wall, category A is used. The halls included in this category are concert halls and music recital halls which are usually used for musical performances (this category is now refered to as halls for music). If there is a stage house and a fixed proscenium, category B is used. Opera halls, drama theatres and multi-purpose halls are included in this category and classified separately depending on their main use.

Table 2. Numbers and categories of halls used in the study.

Use Category	A		B				
Auditorium Type / Use	Concert	Music-Recital	Opera	Drama	Multi - Purpose	Total Number	Percent (%)
Rectangular	40	8	0	16	18	82	25.2
Fan	18	2	6	21	18	65	20.0
Horse Shoe	9	1	16	5	8	39	12.0
Geometric	17	4	4	16	61	102	31.4
Arena	23	1	0	7	6	37	11.4
Total Number	107	16	26	65	111	325	100.0
Percentage(%)	33	5	8	20	34	100.0	

3.0 THE INTERRELATIONSHIP BETWEEN AUDITORIUM PARAMETERS

In order to explore the geometrical properties of halls and the relationships between parameters three types of analysis were undertaken; frequency distribution, linear regression and factor analysis. First of all, a factor analysis was carried out to determine the interrelationships between the room geometrical parameters. Through factor analysis, an overview of the importance of various auditorium parameters can be obtained.

Four factors were created which accounted for more than 90% of the total variance in the 'raw' data. The correlation coefficients for any two auditorium parameters can be plotted on any two factors in a four dimensional, rotated orthogonal factor space. Each parameter appears as a point in the figure, with coordinates equal to the correlation coefficients between that parameter and each factor respectively. Thus, all parameters with a high numeric value of the coordinates, along one dimension, are highly correlated to each other but not related to those parameters which have a high value on another dimension only.

Fig. 1 shows that the hall scale measures of V, St, Sa and N are highly correlated and therefore comprise the first dimension, whilst the volumetric ratio measures including V/St and V/N are also highly interrelated and form the second dimension. The parameters which do not come out with a high correlation along either of the first two dimensions can be seen to contribute to the third and fourth dimensions. In the same way, while the floor density measure, Sa/N, dominates factor three the ratios of linear dimensions ie. L/H, W/H comprise factor four. The two parameters which do not form any separate factor dimensions are MRA and L/W which are seen to be minor contributors to some factors eg MRA for factor four and L/W for factor three. This indicates that the mean rake angle and ratio of length to width does not critically affect the choice of other parameters.
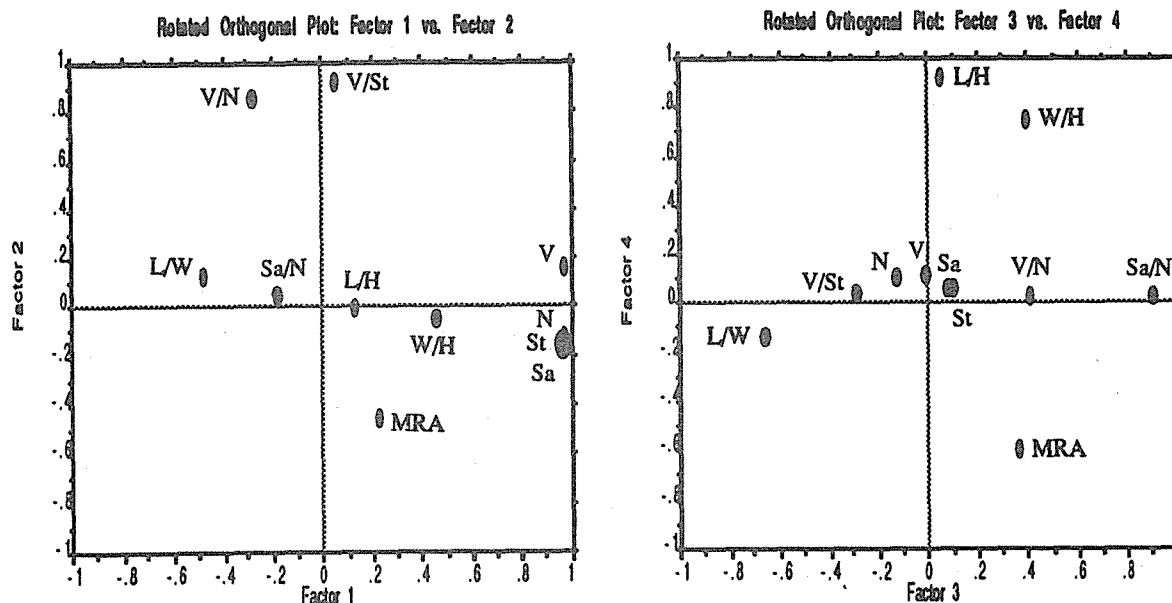
Fig. 1. The position of auditorium parameters in the first and second two dimensions and third and forthth dimensions of a four dimensional factor space.

Thus, the auditorium parameters mentioned above can be described by four different factors. It is interesting to see that the four factors also correspond to four subjectively different aspects : definite size of halls, ratio of volume to floor area and number of seats, floor density and dimensionless ratios of orthogonal linear dimensions. It is necessary to investigate data on at least one parameters in each factor group. In this paper, data on only three parameters are presented due to the limitation of pages ie. volume/seat, volume/floor area and total volume.

4.0 STATISTICAL DISTRIBUTIONS OF AUDITORIA DATA

4.1 Introduction

The assumption has been made that the halls reported in the literature, from which the present data were obtained, are reasonably good acoustically. If this assumption is correct and there is a large scatter in the data for any one variable, or between variables, then it is likely that there is no critical realtionship between these variables and a good acoustic. This means that either the rules of thumb are incomplete or the designer has considerable latitude in what he does. On the contrary, if there is little scatter in the data this is an indication that there are rules designers should follow. The data presented here also indicates that there are limits within which designers should normally operate.

Linear regression analyses were undertaken between each of the auditorium parameters. The results of the analyses are presented in scattergrams. In addition, the correlation coefficients of the regression lines are obtained. The r-squared value in each scattergram shows the degree of association between variables and level of reliability of the regression analysis. The equation, in the form of $y = a + bx$, relates the two variables is also given for the exact calculation of the y-value. The frequency distribution of some auditorium parameters were investigated and the results are presented in tables. An example of this analysis is given in Table 4.

4.2 Volume/Seat

Sabine showed that the reverberation time of an auditorium is directly proportional to the room volume and inversely proportional to the total absorption in the auditorium. As the

total absorption is largely dependent on the number of seats in the auditorium the reverberation time will be dependent on the volume/seat and so this is obviously an important characteristic and should be very useful in the early stages of a design.

Since Sabine's work, recommendations have been made for suitable reverberation times for each type of performance and hall. These translate into recommended values for hall volume and volume per seat for halls with different uses. Table 3 shows typical values of volume per seat for a number of different types of auditoria with different reverberation requirements. This data was obtained from Doelle , Bagenal and Knudsen.

Table 3. Recommended volumes per seat in auditoria. (m^3/seat)

Auditorium Type	Recommended volume/seat	
	optimum value	range
Concert Halls	7.8	6.2 - 10.8
Churches	7.2	5.1 - 9.1
Multi-purpose Halls	7.1	5.1 - 8.5
Opera Halls	5.7	4.5 - 7.4
Drama Theatres	5.0	-------
Cinema Theatres	3.5	2.8 - 5.1
Lecture Halls	3.1	2.3 - 4.3

Fig.2 shows a scattergram of hall volumes against volume/seat in concert halls and music recital halls . Although the correlation coefficient is quite low (r^2=0.212) it indicates that the volume per seat increases with the total volume of the hall.
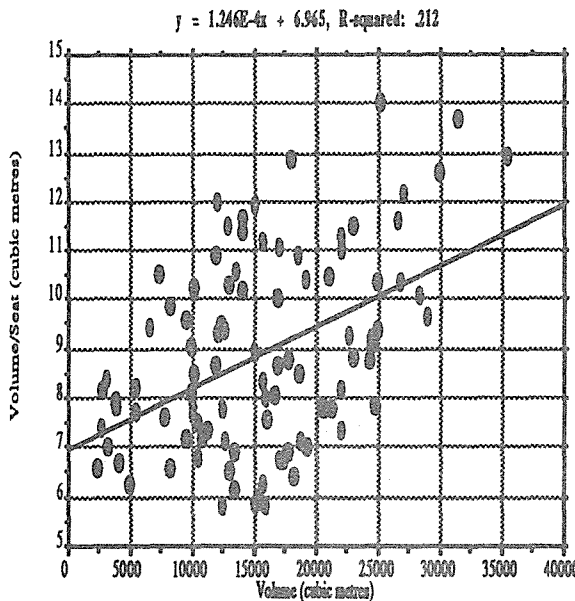
Fig. 2.Scattergram of vol/seat against volume in halls for music.
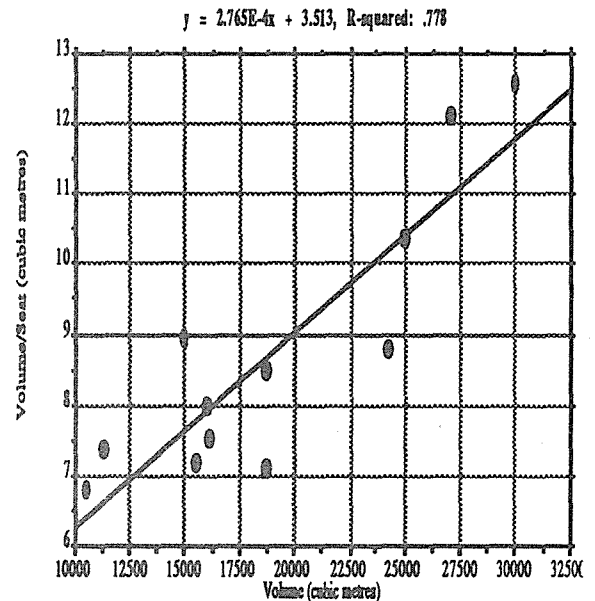
Fig. 3.Scattergram of vol/seat against volume in acoustically good concert halls.

The data on some concert halls, which have been recognized as acoustically good, are plotted in Fig.3. These halls are rectangular and non-rectangular halls in Europe and North America, built between 1870 and 1985. The halls used as "good" halls here are listed in the Appendix. The "good" halls were selected in a subjective way (opinions of musicians, critics and acousticians) and the selection cannot be justified at present. The correlation coefficient in this case is much higher (r^2=0.778). Comparing Figs. 2 & 3 shows that the regression for the "good" halls is steeper than the line in all halls for music. The corresponding volume/seat for a given volume in "good" halls is lower than the value in

halls for music within the volume range up to 22,500 m³. The volume/seat of "good" halls becomes higher when the volume is larger than 22,500 m³.

As a result of the investigations of the volume per seat value of halls Table 4 has been assembled.This table shows the mean and standard deviation values of volume/seat in different hall types. Two different values are given which represent the statistical results of volume/seat for all halls and for "good" halls. In the case of "good" drama halls no result is given as an insufficient number of halls were available.

Table 4. Statistical data on the volume/seat (m³/seat) in each type of hall.

Quality Rating	All Halls		Good Halls	
Auditoriun Type	Mean Value	Std. Dev.	Mean Value	Std. Dev.
Concert Halls	9.2	2.1	8.6	1.9
Multi-purpose Halls	7.8	2.4	7.7	1.2
Music Recital Halls	7.8	1.9	7.6	0.9
Opera Halls	6.4	1.3	5.6	1.2
Drama Theatres	6.0	1.5		

The results show that the good halls usually have lower mean volumes/seat and smaller standard deviations rather than "ordinary" halls. The order of the values in each halls is same as in Table 3 (eg the value is highest in concert halls and lowest in drama theatres). However, these values are significantly different to those given in Table 3. Consquently, it is possible that many halls have been built with larger volumes than the value obtained from the current rule of thumb. The values of volume per seat in most types of "good" halls are also larger than those from current rules except in the opera halls.

4.3 Volume/Floor Area

Audience absorption can be a significant factor in auditoria acoustics as it provides most of the absorption in a hall. Beranek postulated that the absorbing power of a seated audience, chorus and orchestra in a large hall increases in proportion to the floor area occupied by them and is nearly independent of the number of seated persons in that area. Beranek indicated that a volume/m² of seating floor area should be used as a design criterion. The floor area used here means the total floor area, including audience seating area of both stalls and balconies, the isle between the seat rows and around the seating and the stage area in the case of concert halls, or pit area in the case of opera halls.

Generally the volume/floor area increases with increasing volume. Comparing the correlation coefficients in scattergrams of volume against volume/floor area (r²=0.453) with that of volume against volume/seat (r²=0.212) higher correlations (and hence better rules of thumb) can be obtained if the volume/floor area rather than the volume/seat is used. These results appear to verify Beranek's conclusion.

Table 5 summarises the results of the investigation of the volume to floor area for each type of auditoria. The mean values and standard deviations are given for all halls and for "good" halls. In each case except opera halls, the "good" halls have a larger mean value and smaller standard deviation' than for the total population of halls used.

Table 5. Statistical values of volume to floor area (m) in the major types of the halls.

Quality Rating	All Halls		Good Halls	
Auditoriun Type	Mean Value	Std. Dev.	Mean Value	Std. Dev.
Concert Halls	11.8	2.4	12.2	2.0
Opera Halls	8.5	1.5	8.2	1.3
Multi-purpose Halls	10.2	2.4	10.6	1.4
Music Recital Halls	7.2	1.9	7.3	0.8
Drama Theatres	7.5	1.9		

4.4 Total Volume

At the initial design stage of an auditorium the determination of the volume is likely to be one of the most important design decisions. Designers have little information available to them on the appropriate size of halls except for the number of seats or the floor area which are determined at the schematic design stage. The data presented should be of help in this regard but it is worth looking, in more detail, at whether volumes are better based on floor area or the number of seats in the auditorium. Generally very high correlations coefficients are obtained when the total volume is related to factors such as floor area or number of seats (refer to Table 6). Thus, the results from these regression analyses could be used as more reliable design guides for auditoria.

The results of regression analyses of volumes as a function of floor area are shown in Table 6. The regression lines and their correlation coefficients are calculated for different hall types. The r-squared values are very high (about 0.8 or above). The volume in halls for music is larger than any other halls at certain value of floor area.

Table 6. Regression lines for volume based on the floor area for each hall use.

Quality Rating	All Halls		Good Halls	
Auditorium Type	Regression Line	r^2 value	Regression Line	r^2 value
Halls for Music	12.30 x St - 852	0.823	14.79 x St - 3234	0.903
Opera Halls	7.48 x St + 1309	0.831	8.36 x St - 284	0.824
Multipurpose Halls	10.53 x St - 402	0.828	10.71 x St + 561	0.863
Drama Theatres	8.50 x St - 217	0.854		

The scattergrams of some particular shaped halls were made when the volume is plotted as a function of floor area in both cases of all halls and "good" halls. The results of those regression analyses are assembled in Table 7. For some hall types no regression lines of good halls are given due to insufficient data. The correlation coefficients are very high (around 0.8 to 0.9).

Table 7. Regression lines for volume based on the floor area in various hall types.

Quality Rating	All Halls		Good Halls	
Auditorium Type	Regression Line	r^2 value	Regression Line	r^2 value
Rectangular Concert Halls	13.40 x St - 1117	0.865	14.65 x St - 2946	0.864
Fan Typed Concert Halls	13.44 x St - 3694	0.876		
Geometric Concert Halls	12.69 x St + 72	0.705	16.64 x St - 3934	0.886
Horseshoe Opera Halls	9.95 x St - 3679	0.863	10.01 x St - 3671	0.869

This analysis also showed the limits of the hall parameters. For example, in rectangular concert halls, the upper limit of volume is 25,000 m³ whereas the limit is extended to 45,000 m³ in fan type halls. The largest volume of a "good" concert halls is 40,000 m³ in most hall types except rectangular halls. Also, in horseshoe type halls, the volumes of "good" halls are not greater than 22,000 m³. These results indicate that the shape of the halls is also important for the determination of volume.

5.0 CONCLUSION AND DISCUSSION

The analyses carried out so far indicate that there is a reasonable basis for defining criteria which can be used in the early stages of an auditorium design. These rules of thumb do not require the calculation of any acoustical parameters and are based on the dimensions and shapes of halls. What the analysis also reveals is that the existing rules of thumb are not easy to substantiate on the basis of what exists. The present analysis would be much better

if only "good" halls were selected but the selection of "good" halls is difficult. Any hall which remains in use after some years is likely to be considered a good hall but an analysis based on this "antiquity factor" may not be of much value to today's designers. Other methods of determining "good" halls, eg. the Delphi technique, will be tried in future. It is likely that not all rules of thumb need be complied with. A study of the combinations of rules of thumb which give the highest correlation coefficients will be also be attempted as the next step in the present work.

Besides continuing with similar types of analyses to those presented in this paper it is also intended to look at alternative methods of expressing the geometry of auditoria. Two approaches are contemplated. One involves producing transforms which will allow a hall of any geometrical shape to be turned into the equivalent rectangular hall. The other involves a "spectral" approach. Auditoria are made up of solid objects (eg. walls) and these elements are in turn composed of smaller elements. The auditorium is also made up of a spectrum of element sizes. If an auditorium can be defined in this way and if the "spectrum" can be shown to correlate with the "goodness" of the hall then this approach will give much greater latitude to the designer than the approach taken in this paper. It will allow, if successful, much greater freedom for designers to explore what is possible. It will not, however, be a substitute for the ray-tracing programs and models used by acousticians.

REFERENCES

1. Bagenal, H., Alex Wood, Planning for Good Acoustics, Methuen, London, 1931.
2. Barron, M., Subjective Study of British Symphony Concert Halls, Acustica, 66, 1-14, (1988).
3. Beranek, Leo L., Music, Acoustics and Architecture, John Wiley & Sons., New York, 1962, 586pp.
4. Beranek, L. L., Audience and Seat Absorption in Large Halls, J.Acoust.Soc.Am., 32, 661-670, (1960).
5. Doelle, Leslie L., Environmental Acoustics, McGraw-Hill, New York, 1972, 48-121.
6. Forsyth, M., Auditoria-Designing for the performing arts, Mitchell,London, 1987,11-17.
7. Gade, A.C., Acoustical Survey of Eleven European Concert Halls, The Acoustics Laboratory Report 44, Technical University of Denmark, 1989, 130pp.
8. Knudsen, V.O., Acoustical Designing in Architecture, John Wiley & Sons, New York, 1950.
9. Sabine, W.C., Collected Papers on Acoustics, Harvard Univ. Press, Cambridge, 1927.

APPENDIX

List of acoustically good concert halls used in this study.

No. Name of hall	Tmid	Vol.	Seats	Year	Hall Type
1. Grosser Musikvereinssaal, Vienna	2.05	15000	1680	1870	Rectangular
2. Neues Gewandhaus, Leipzig	1.55	10600	1560	1886	Rectangular
3. Concertgebouw, Amsterdam	2.0	18700	2206	1887	Rectangular
4. St. Andrew's Hall, Glasgow	1.9	16100	2133	1887	Rectangular
5. Carnegie Hall, New York	1.7	24250	2760	1891	Horseshoe
6. Grosser Tonhallesaal, Zurich	1.6	11400	1546	1895	Rectangular
7. Symphony Hall, Boston	1.8	18740	2631	1900	Rectangular
8. Liederhalle Grosser Saal, Stuttgart	1.62	16000	2000	1956	Geometric
9. Neues Festspielhaus, Salzburg	1.5	15500	2158	1960	Modern Fan
10. Berliner Philharmonie Hall, Berlin	2.0	25000	2410	1963	Modern Arena
11. Concert Hall, Rotterdam	2.0	27070	2230	1966	Modern Arena
12. Gasteig Philharmonie, Munchen	2.1	30000	2387	1985	Geometric

A COMPUTER AIDED ACOUSTICAL DESIGN OF A MULTIPURPOSE HALL

Sang-Woo Lee
Dept. of Architectural Eng., Kyunggi Univ.
Seoul, Korea.

Won-Ryoung Choi
Dept. of Architectural & Planning,
Kwangju Highway Lines Inc.
Seoul, Korea.

Kyung-Hoi Lee
Dept. of Architectural Eng., Yonsei Univ.
Seoul, Korea.

ABSTRACT

Acoustical design process is an iterative trial and error process that relies on designer's knowledge and experience, and requires a considerable time in evaluating alternative design solutions. Accordingly, for the better design, computer applications are needed to save time and to abate errors in calculating sound pressure levels and reberveration times.

This study is aimed at developing a computer simulation program for the design and evaluation of acoustic performance in various auditorium design, and demonstrating an acoustical design of the multipurpose hall by the computer application, as a case study.

The computer simulation program developed in this study consists of one main program and seventeen subroutines. The program can be used as an initial design tool. Also, the program is capable of evaluating the current design under the appropriate design criteria and providing any necessary improvment. Usefulness and validity of the computer simulation program have been verified with the acoustical design of a multipurpose hall located in Kwangju city, Korea.

The result of this study shows that the computer simulation program can be used effectively not only as an useful design tool but also as a practical and convenient evaluation method of acoustic performance of existing auditoriums.

1.0 INTRODUCTION

Success or failure of auditorium design is almost determined by acoustic performance for music and speech. In acoustical design, the reflective surface of wall and ceiling for distributing the sound evenly to each seats, and the interior surface and finishings for securing the optimum reverberation time, are matters of prime importance. Therefore, acoustical design should be carried out at the preliminary stage of architectural design considering factors related to acoustic performance.

Generally, acoustical design process is iterative trial and error process that relies on designer's knowledge and experience, and requires considerable time in evaluating alternative design solution. Accordingly, for the better design, computer applications are needed to save time and to abate errors in calculating the sound pressure level and the reverberation times.

This study is aimed at developing a computer simulation program to evaluate acoustic performance in various auditorium designs, and to demonstrate acoustical design of a multipurpose hall by the computer application, with a case study.

2.0 PRINCIPLES OF ACOUSTICAL DESIGN

Principles generally considered in acoustical design are as follows:
- uniform distribution of sound pressure level over the seats by properly controlling the direct and reflected sound .
- maintainning the intelligibility and fullness of sound by securing optimum reverberation time.
- eliminating the acoustical defects at each seat such as long delays of reflections, eches, sound focusing, acoustic shadows, room resonance, etc.

- free from noise and vibration.

The reflecting surfaces of walls and the ceiling can be designed through ray - diagram method, assumming that the stage sound source is non - directive and the sound rays are subject to the same laws of light ray propagation. The shape, angle, location and size of each reflecting surface should be decided, in order that the sound pressure level at each seat affecting the direct sound and a few reflected components must be uniform.

The sound pressure level at each seat is given by the following equation:
$$SPL = PWL + 10 \ Log \ (1 \ / \ 4\pi \ r^2 \ )$$

SPL : sound pressure level at each seat(dB)
PWL : power level(dB)
r : distance from the source(m)

The location, angle, size of reflecting surfaces should be decided to reflect sound efficiently to the rear part of the audience on each floor.

The side walls of the auditorium must retain diffusible property to make the sound rich and absorbent property to maintain the optimum reverberation.

Generally, an excessive reverberation time lowers the speech intelligibility and the clarity of instrumental sound, while too short a reverberation time lower the liveliness of sound. Therefore, it is important to maintain a proper reverberation time which can enhance the speech intelligibility and convey various musical properties efficiently.

3.0 COMPUTER SIMULATION MODEL

This computer simulation model for the acoustical design of multi-purpose hall consists of a main program and 17 subroutines.

The repetitive calculation procedures by computer simulation are represented in Fig.1 and Fig.2, and the input data to be provided are listed in Table 1.

```
              ┌──────────────────────┐
              │    Data    input     │
              └──────────────────────┘
       ┌──────────────────────────────────┐
       │ Difference between the direct     │
       │ and the reflected Sound path      │
       └──────────────────────────────────┘

       ┌──────────────────────────────────┐      ┌──────────────────────────┐
       │ Sound pressure level by the direct│     │ Sound pressure level by the│
       │ sound (AS)                        │      │ reflected sound R1 (R1)   │
       └──────────────────────────────────┘      └──────────────────────────┘
       ┌──────────────────────────────────┐
       │ Sound pressure level difference   │
       │        (SPD = AS1 - R1)           │
       └──────────────────────────────────┘

       ┌──────────────────────────────────┐
       │ Composite correction value (DEL)  │
       └──────────────────────────────────┘
       ┌──────────────────────────────────┐
       │ Composite sound pressure level    │
       │        (ASL1 = AS + DEL)          │        ┌──────────────────────────┐
       └──────────────────────────────────┘        │ Sound pressure level by the│
                                                    │ reflected sound Rn (RN)   │
       ┌──────────────────────────────────┐        └──────────────────────────┘
       │ Sound pressure level difference   │
       │        (SPD = ASL1 - Rn)          │
       └──────────────────────────────────┘

       ┌──────────────────────────────────┐
       │ Composite correction value (DEL)  │
       └──────────────────────────────────┘

       ┌──────────────────────────────────┐
       │ Final composite sound pressure    │
       │ level (TASL = ASL1 + DEL)         │
       └──────────────────────────────────┘

   ┌───────────────────────┐  ┌───────────────────────┐
   │ Relative direct sound  │  │ Relative reflected sound│
   │ pressure level (DS)    │  │ pressure level (RS)    │
   └───────────────────────┘  └───────────────────────┘

       ┌──────────────────────────────────┐
       │ Final relative sound pressure     │
       │ level (Center seat of 1st row)    │
       └──────────────────────────────────┘

       ┌──────────────────────────────────┐
       │ Maintaining optimum sound pressure│
       │ level                             │
       └──────────────────────────────────┘
```

Fig. 1 Calculating Procedure for
Sound Pressure Level

Fig. 3 Plan of Main Hall

```
          ┌─────────────────────┐
          │    Data    input    │
          └─────────────────────┘
                    │
          ┌─────────────────────────────────┐
          │ Total absorption of finishing   │
          │ material (TM)                   │
          └─────────────────────────────────┘
                    │
          ┌─────────────────────────────────┐
          │ Air absorption (AL)             │
          └─────────────────────────────────┘
                    │
          ┌─────────────────────────────────┐
          │ Absorption of audience and seats│
          │ per occupied seat ratio (AUD)   │
          └─────────────────────────────────┘
                    │
          ┌─────────────────────────────────┐
          │ Total absorption per occupied seat│
          │ ratio (TA = TM + AL + AUD)      │
          └─────────────────────────────────┘
                    │
     ┌──────────────────────────┐  ┌──────────────────────────────────────┐
     │ Calculating reverberation time│ Calculating the ratio of absorbing  │
     │ (Equation of Eyring-Knudsen)  │ materialarea for maintaining optimum R.T│
     └──────────────────────────┘  └──────────────────────────────────────┘
                    │
          ┌─────────────────────────────────┐
          │ Maintaining optimum reverberation│
          │ time                            │
          └─────────────────────────────────┘
```
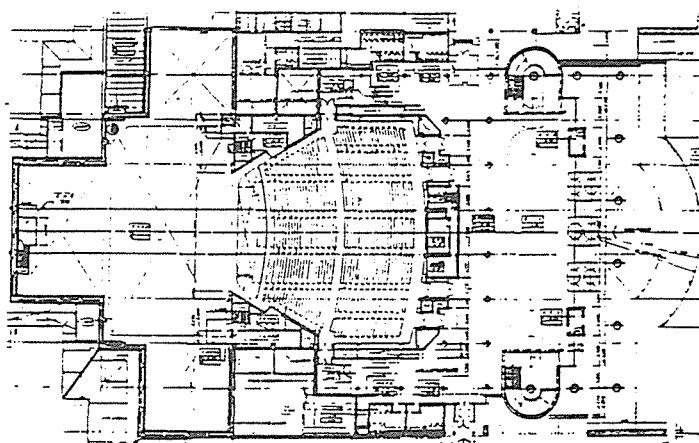
Fig. 2   Calculation Procedure of Reverberation Time

Table 1   Input Data for Computer Simulation

Item	Input Data
Relating Sound Pressure Level	Number of sound sources.
	Difference between the direct and initial reflected sound path.
	Number of direct sound and reflected sound paths.
	Number of seats.
	Number of rows of seats used in calculating sound pressure level considering side reflecting wall.
	Sound path.
Relating Reverberation Time	Number of interior finishing materials.
	The area of each material for maintaining preferred reverberation time.
	Occupied seat ratio required in maintaining optimum reverberation time.
	Optimum reverberation time.
	Indication of the sound absorption for maintaining preferred reverberation time.
	Occupied seat ratio.
	Volume.
	Indication of frequencies used in analysis.
	Indoor temperature.
	Finishing material area.
	Finishing material absorption.
	Occupied seats ratio.
	Absorptions of audience and seats.
	Air absorption.

4.0 COMPUTER APPLICATION AS A CASE STUDY

4.1 MAIN HALL SPECIFICATION

Main hall has a proscenium stage. The floor plan of the hall is a mixed type with the rectangular shaped rear part and the fan shaped front part approaching the proscenium. The cross section of the hall consists of the stepped floor on the ground level, and balcony structure on the first floor.
The architectural features of the auditorium are listed in the table 2.

Table 2. Architectural Design Criteria of Main Hall

Item			Content		
seat	hall	size(m) \ content	length(L)	width (W)	height(H)
		max.	37.5	37	17
		mean.	34	28.5	10
	maximum sound path	1st floor	32.9 M		
		2nd floor	40.5 M		
	volume (V)		14,623.95 M		
	surface area (S)		4,785.66 M		
	floor area	1st	1,059.2 M		
		2nd	400.4 M		
		total	1,459.6 M		
	seats	size	$1.0 \times 0.5 = 0.5$ M^2		
		number: 1st floor	1,258 seats		
		2nd floor	508 seats		
		movable	34 seats		
		total	1,800 seats		
	occupied area per seat(S/N)		0.81 M /seat		
	occupied volume per seat(V/N)		8.12 M /seat		
stage	size	part \ content	length(L)	width (W)	height(H)
		center	37.5 M	22.5 M	29.5 M
		side (2 part)	15 M	15 M	10.8 M
		rear	22.5 M	15 M	10.8 M
		Proscenium	---	20 M	9 M
	area		1,635.25 M2		

4.2 DESIGN OF REFLECTING SURFACE

In this plan, the locations of the sound sources on the stage and orchestra pit are selected in consideration of the use of the hall (multipurpose hall), and the reflecting surfaces are designed on the ceiling which are divided into five sections. The shapes and radiuses of curvature of the surfaces are shown in the Fig.4. The time lag between the direct sound and

reflected sound is controlled below 50ms(17M), to eliminate echoes. Besides, the cubic volume of the room is taken into account in order to project the light on the whole stage from lighting fixtures on the ceiling, and to get the proper reverberation effects.

The extent of traveling of the reflected sound travel on each surface is planned in such a way that the reflected sound by the surface R1, and R2 can reach over all of the seats on the ground and first floor, when the sound source is in the center of the forepart of the stage(S1), and the reflected sound by the surface R3 over the seats on the rear part of the first floor (behind the eighth row backward) and the entire floor, and there flected sound by the surfaces R4 and R5 over all the seats on the second floor.

Here, the sound pressure level for each row is chosen by the computer simulation according to the location, angle and size of the reflecting surfaces. Thus, the difference of the sound pressure levels between the first row of the first floor and the twenty - first row of the second floor due to the travel distance of the direct sound when the sound source is in the center of the forepart of the stage(S1),are reduced from 14dB to 8dB by the supplement of the reflected sounds, so that effective reflecting surfaces, which produce uniform sound pressure levels for all the rows of the seats, are designed.

The shape and size of the sound - diffuser on the wall is designed as a series of quadrangular - pyramid shapes(800mm X 1250mm X 300mm) in consideration of its diffusion effects and decoration, and they are made of 1.2mm thick brass - plates stuffed with plaster.

Radius of Curvature of R1 = 2,600 mm
Radius of Curvature of R2 = 2,600 mm
Radius of Curvature of R3 = 2,600 mm
Radius of Curvature of R4 = 8,000 mm
Radius of Curvatur of R5 = 14,400 mm
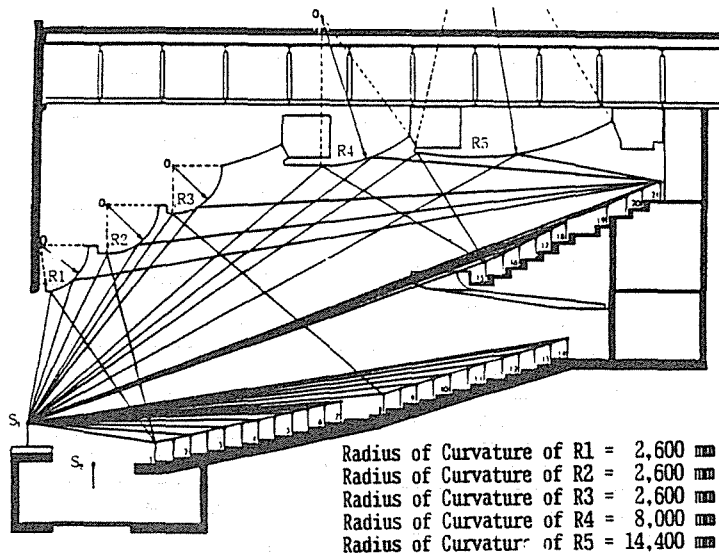
(Fig. 4) Distribution Range of Reflected Sound
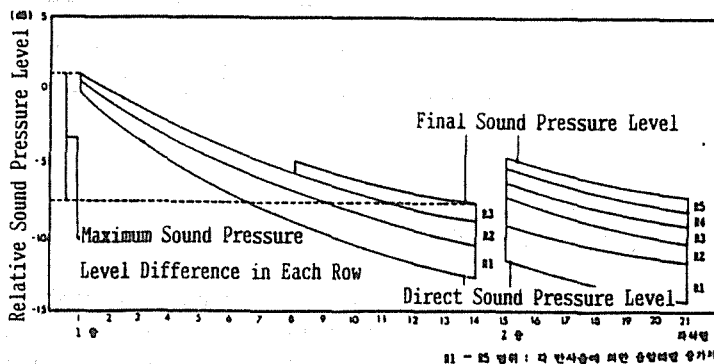
(Fig. 5) Distribution of Relative Sound Pressure Level in Each Row

92

Table 3   Indoor finishing Materials and Reverberation analysis.

Item			Materials	Area(m²)	125 Hz		500 Hz		2,000Hz	
					α	A	α	A	α	A
floor		aisle	heavy carpet	486.60	0.02	9.73	0.14	68.12	0.60	291.90
	seats	unoccupied	/	883.00	0.49	432.67	0.80	706.40	0.82	724.06
		100% occupied	/	883.00	0.60	529.80	0.88	777.04	0.93	821.19
		orchestra pit	wood panels	90.00	0.15	13.50	0.10	9.00	0.06	5.40
	total	unoccupied	/	1,459.60	/	455.90	/	783.52	/	1,021.42
		100% occupied	/	1,459.60	/	553.03	/	854.16	/	1,118.55
wall	front lateral wall	proscenium opening	/	180.00	0.30	54.00	0.40	72.00	0.50	90.00
		the lower part of front stage	wood panels	17.50	0.15	2.63	0.10	1.75	0.06	1.05
		sum	/	197.50	/	56.63	/	73.75	/	91.05
	middle and real lateral wall	front reflecting wall	marble	443.92	0.01	4.44	0.01	4.44	0.02	8.88
		middle sound absorbent wall	9mm wood veneer / GW25	229.86	0.40	91.94	0.15	34.48	0.10	22.99
		rear sound absorbent wall	acoustic wood panel	235.04	0.46	108.12	0.29	68.16	0.59	138.67
		door	leather on sponge	23.04	0.20	4.61	0.10	2.30	0.10	2.30
		window of lighting booth	heavy glass	20.40	0.18	3.67	0.04	0.82	0.04	0.82
		sum	/	952.26	/	212.28	/	110.20	/	173.68
	rear wall	sound absorbent wall	copenhagen rib / GW50	305.04	0.60	183.02	0.75	228.78	0.60	183.02
		door	leather on sponge	30.24	0.20	6.05	0.10	3.02	0.10	3.02
		window of control room	heavy glass	9.00	0.18	1.62	0.04	0.36	0.04	0.36
		sum	/	344.28	/	189.68	/	232.16	/	186.40
		total	/	1,494.04	/	458.60	/	416.11	/	451.11
ceiling		reflecting surface	G R C	1,152.58	0.01	11.53	0.02	23.05	0.02	23.05
		upper part of aisles	9mm wood veneer / GW25	168.12	0.40	67.25	0.15	25.22	0.10	16.81
	lighting booth	front surface	acoustical panel 6d-15P-5t / GW50. air space 80	53.42	0.32	17.09	0.62	33.12	0.48	25.64
		window	heavy glass	43.50	0.30	13.05	0.40	17.40	0.50	21.75
		lower part	9mm wood veneer / GW25	65.52	0.40	26.21	0.15	9.83	0.10	6.55
	balcony	lower part	12mm giupsum board	299.04	0.29	86.72	0.05	14.95	0.70	20.93
		front surface	acoustical panel 6d-15P-5t / GW50. air space 80	49.84	0.32	15.95	0.62	30.90	0.48	23.92
		total	/	1,832.02	/	237.80	/	154.47	/	138.65
air (m²)				14,623.95	/	/	/	/	0.007	102.37
total absorption		unoccupied		4,785.66	/	1,152.30	/	1,354.10	/	1,612.18
		100% occupied		4,785.66	/	1,249.43	/	1,424.74	/	1,708.31
reverberation time		unoccupied		/	/	1.78	/	1.47	/	1.13
		100% occupied		/	/	1.62	/	1.39	/	1.06

93

4.3 PLANNING OF REVERBERATION TIME

Main hall is a multipurpose auditorium for an opera, a lecture, a concert, a play, etc. Therefore, the range of the cubic volume of the room is between 9180 and 15300 M^3 (5.1 ~ 8.5 M^3 for each seat) as an indoor acoustical design standard of the auditorium, and an optimum reverberation time is about 1.4 sec (500 Hz, non - occupied) in consideration of the cubic volume of the room.

In this plan, the shapes and qualities of the interior finishing materials for each part of the room are chosen to maintain optimum reverberation time, taking into account the absorption and reflection characteristics and interior decoration. The reverberation time is determined by the computer simulation.

The reverberation time at several frequencies due to the interior finishing materials, are listed in Table 3.

5.0 CONCLUSION

This study suggests a solution for the acoustic design of a multipurpose hall by a computer simulation of the sound pressure level and reverberation time.

An architectural success of an auditorium for various public performance depends upon the quality of its indoor acoustical condition. A designer, thus, should keep an acoustical viewpoint, ranging from the schematic design stage to the evaluation stage after the construction.

The result of this study shows that the computer simulation program can be used effectively not only as an useful design tool which may allow to explore various alternative design solutions at early design stage, but also as a practical and convenient evaluation method of acoustic performance of existing auditoriums.

For the more effective acoustical design, a systematic and wide range of informations on the sound absorption and insulation properties of various architectural materials should be provided, along with computer simulation and evaluation.

REFERENCES

1. Kyung Hoi Lee, Architectural Environmental Science, Moon Eun Dang, Seoul, 1986.
2. Sang Woo Lee, An Evaluation of Acoustic Performance for Arts Center - Concert Hall, 1988.
3. Doelle, L. L., Environmental Acoustics, MaGraw-Hill Book Co., 1972.
4. Egan, M. D., Concepts in Architectural Acoustic, MaGraw-Hill Book Co., 1972.
5. Knudsen, V. O., Harris, C. M., Acoustical Designing Architecture, John Wiley Sons Inc., 1955.
6. More, J. E., Design for Good Acoustics and Noise Control, The Macmillan Press Ltd., 1987.

ODEON - A HYBRID COMPUTER MODEL FOR ROOM ACOUSTIC MODELLING

J.H. Rindel
The Acoustics Laboratory, Technical University of Denmark,
Building 352, DK-2800 Lyngby, Denmark

G.M. Naylor
The Acoustics Laboratory, Technical University of Denmark,
Building 352, DK-2800 Lyngby, Denmark

ABSTRACT

A room acoustic computer model for evaluation of rooms is
presented. Predictions of reverberation time, energy parame-
ters and reflectograms, with only modest calculation time,
are achieved with calculation methods which combine the best
features of both ray-tracing and image source methods.
Comparisons between measured and calculated data for the
Royal Festival Hall, London are presented. Most of the
calculated parameters show a systematic deviation from the
measured values, but the relative variation with position in
the hall is quite accurate. On the basis of the present
investigation some weak points of the model are discussed,
and possible future improvements are suggested.

1.0 INTRODUCTION

The computer model described here (named ODEON after the greco-roman enclosed music hall) is developed to form the basis of a system for creating binaural room simulations. From the calculated reflection sequences it is possible to derive objective room acoustical parameters, and this feature could be useful to consultants in room acoustical design if the results can be shown to agree with measured results in real rooms. The Royal Festival Hall in London has been chosen for a comparison between calculated and measured data.

2.0 THE COMPUTER MODEL

The model described here is based on ray tracing of a limited number of rays emitted from a source point. The reflections of the rays can be followed until any chosen time limit, and each reflection of the rays is treated geometrically as a basis for the construction (calculation) of an image source point. A detailed description of the computer model and its use is found in the manual (Naylor G.M.).

2.1 Generation of Early Reflections.

Early reflections are generated by calculation of image source points, which are checked for "visibility" and against duplication. The visibility check is performed by tracing the reflection path backwards from the receiver in the direction of the image source, the criteria being that the reflecting surfaces are met in the right order, i.e. the reverse of the order met by the ray that has generated the image source point. Reflections of low order are typically detected by
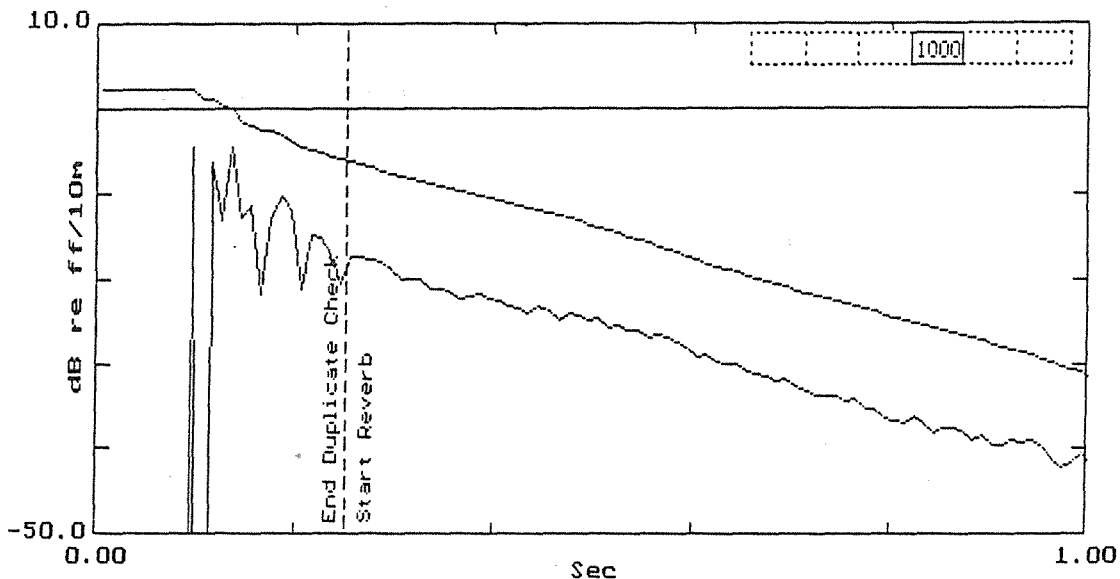
Fig.1. Example of calculated energy decay curve.

96

several sound rays, especially in case of large surfaces and
a large number of emitted sound rays. Therefore a check
against duplication is performed up to a certain order of
reflection. The energy of the reflections is calculated in
octave bands applying the absorption coefficients of the
surfaces met during the reflection path.

2.2 Generation of Reverberation Tail.
Higher order reflections are unlikely to duplicate because of
the increasing distance between the sound rays. Instead the
problem is a rapidly increasing number of image sources,
which are not discovered by the ray trace method. However,
the reflection density (number of generated image sources per
time unit) is very high, and the average density is a known
simple function of the number of rays and the mean free path
in the room. On the other hand, in a given volume the
expected average reflection density is also known, and it
increases with the second power of time. Thus, the rever-
beration tail of higher order reflections can be statistical-
ly approximated by applying a time-dependent correction
factor to the energy of the reflections generated in the
model, all reflections being accepted as representative for
the room. An example of a calculated energy-decay curve is
shown in Fig. 1. The transition from early reflections to
reverberation tail has here been set to 250 ms.

2.3 Fast Estimation of Reverberation Time.
A special method has been developed to give a very quick
estimate of the reverberation time from the decay curve for
the total sound energy in a room. From a source point a
relatively small number of rays are emitted in all direc-
tions, and after each reflection the total energy is reduced
in accordance with the absorption coefficient of the reflect-
ing surface.

3.0 MODELLING THE ROYAL FESTIVAL HALL

3.1 Geometrical Model.
The geometrical model is shown in Fig. 2. It contains 140
surfaces and 342 corner points. It is a rather rough model,
for instance the ceiling and the audience areas are repre-
sented by large, plane surfaces. On the side walls there are
many boxes, which have a front, a back and a bottom, but no
sides in the model.

3.2 Absorption of Surfaces.
One reason for choosing the Royal Festival Hall for this
investigation has been, that very good information is
available about materials and their absorption coefficients
(Parkin P.H. et al.). Values at 250 Hz and 1000 Hz have been
calculated by interpolation between the values at the
neighbouring octave bands, so all calculations could be made
in octave bands from 125 Hz to 4000 Hz.

The absorption data of the audience area (empty, upholstered chairs) has been taken from (Beranek L.L.). In the paper by (Parkin P.H. et al.) the data are given per seat in excess of the floor absorption, and this is no longer considered to be the best way to describe the absorption of an audience area.
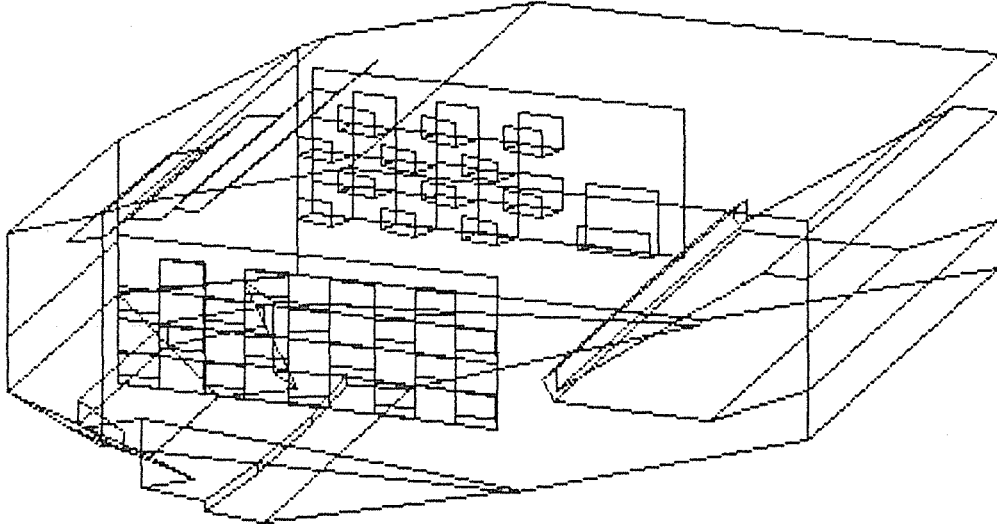
Fig.2. View of geometrical model of Royal Festival Hall.

3.3 Source and Receiver Positions.

Another reason for choosing the Royal Festival Hall has been, that detailed and up-to-date measured results have been published recently by our own laboratory (Gade A.C.). Two source positions on the orchestra podium (S1 and S3) were used in combination with five receiver positions (R1-R5), giving a total of ten source-receiver positions. The receiver positions R4 and R5 were on the balcony, the others on the main floor with R3 under the balcony overhang. In the computer model the positions have been chosen as close as possible to the positions used for the measurements. The height above floor level of the source and receiver was 1.0 m and 1.2 m, respectively.

3.4 Parameters Used in the Calculation.

Room volume:	$21950 \ m^3$
Temperature and Relative Humidity:	20 °C and 50 % RH
Number of Rays Requested (Used):	10000 (10037)
Duplicate Images Checked up to:	Order 6 or 250 ms
Statistical Reverberation Started at:	250 ms
Reflections Generated up to:	1200 ms
Number of Rays in Fast Estimation:	550

The calculation time for the present investigation was in total around 2 h 43 min on a 25 MHz 80386/387 PC. For each part of the calculation the respective times were:

Fast Estimated Rev. Time (Each of 2 Pos.):	1'05"
Ray Tracing (Each of 2 Pos.):	25'25"
Point Response (Each of 10 Pos.):	≈ 11'

4.0 RESULTS

4.1 Reverberation Time.

Calculated and measured reverberation times as a function of frequency are shown in Fig. 3. All situations are without audience. The fast estimated values are in relatively good agreement with the more detailed calculations averaged over ten positions. The measured values are somewhat diverging, however. The original old values (Parkin P.H. et al.) are higher, whereas the new values (Gade A.C.) are lower than the calculated ones. Possible explanations are either changes of some absorbing surfaces between the two measurements in 1951 and 1988, or a strong influence from the difference between the measuring methods.
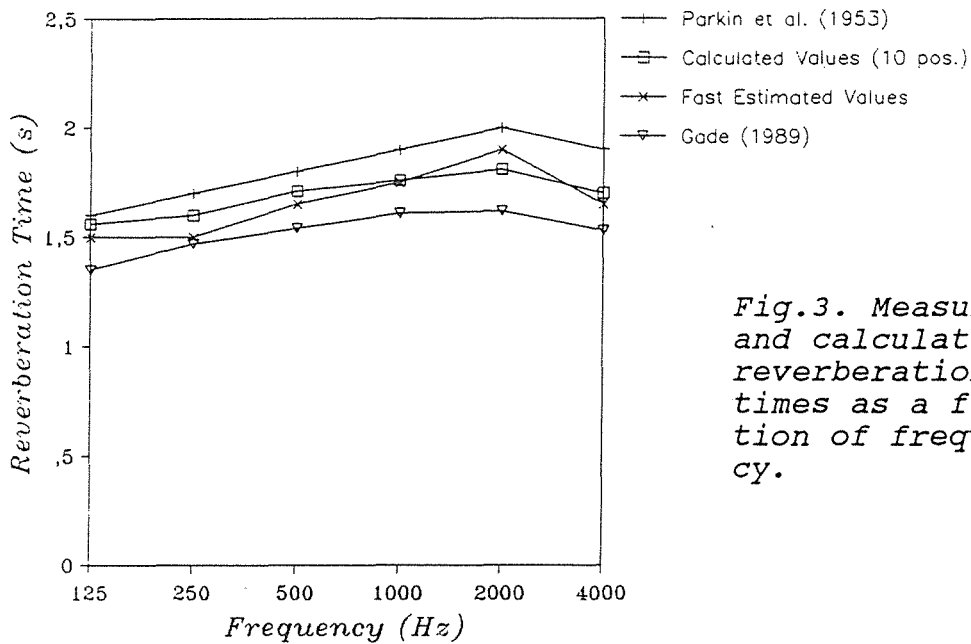
Fig.3. Measured and calculated reverberation times as a function of frequency.
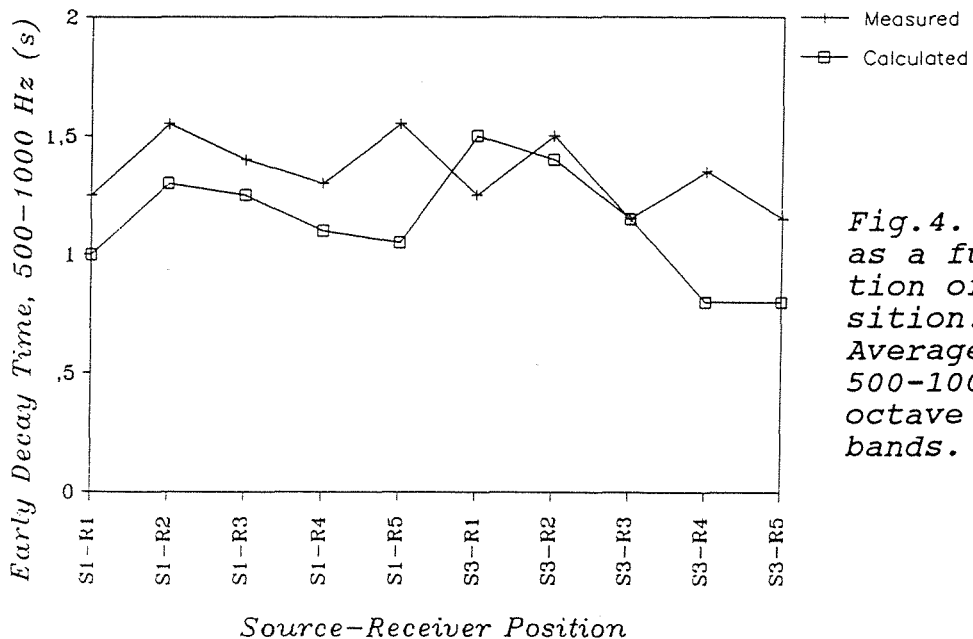
Fig.4. EDT as a function of position. Average of 500-1000 Hz octave bands.

4.2 Early Decay Time and Relative Sound Level.

Calculated and measured values of EDT averaged at 500 Hz and 1000 Hz are shown in Fig. 4 as a function of position. There is a tendency, that calculated values are lower than measured values, but the relative variation with position is more or less reproduced by the model, especially for source position S1. Fig. 5 is similar to Fig. 4, but for the relative sound level. The tendency is, that in remote positions the calculated values are too high, especially in positions R3 and R5 where attenuation of the direct sound due to propagation over seats are likely to influence the measuring results.
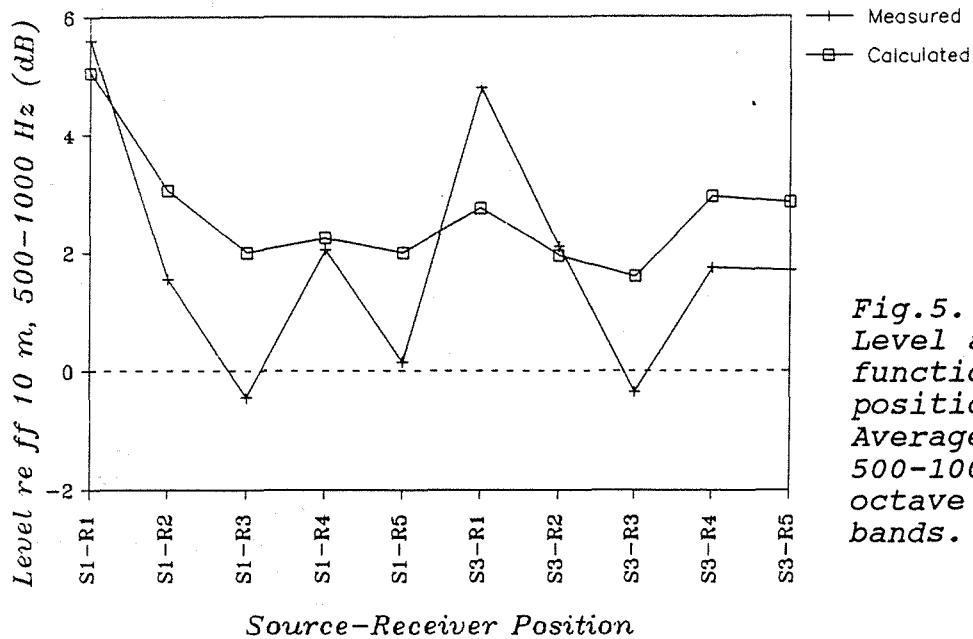
Fig.5.
Level as a function of position. Average of 500-1000 Hz octave bands.
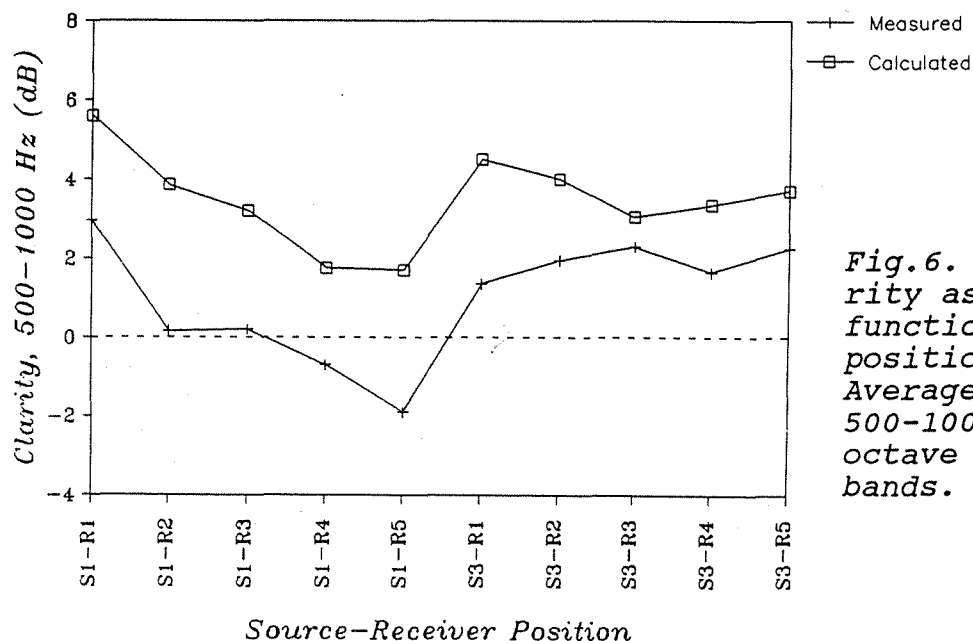
Fig.6. Clarity as a function of position. Average of 500-1000 Hz octave bands.
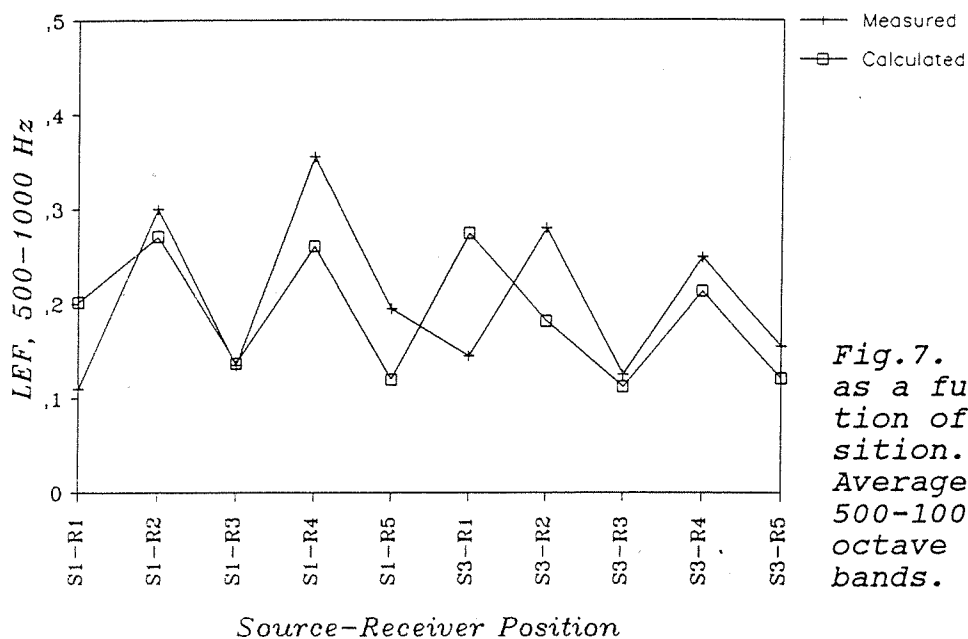
Fig.7. LEF as a function of position. Average of 500-1000 Hz octave bands.

Source-Receiver Position

4.3 Other Room Acoustic Parameters.

Measured and calculated results for the Clarity are shown in Fig. 6, and the relative variation with position is reproduced quite well by the model, however there is an offset pointing at too much early energy in the calculated impulse response. Results for the Lateral Energy fraction (LEF) are shown in Fig. 7, and for this parameter there is a close agreement between measurements and calculations.

5.0 DISCUSSION OF RESULTS

Deviations between measured and calculated results could be caused by several reasons, among which the following are listed:
- the geometrical model is too rough
- the absorption coefficients are not correct
- shortcomings in the calculation model

To the last point several shortcomings in the model can be mentioned:
- no diffusion
- no diffraction
- no angle dependence of reflection factors
- no phase relations in impulse response

It is not very likely that a further refinement of the geometrical model could eliminate the observed deviations, but on the other hand the surroundings close to the source positions are very important, so it might be possible to improve the results a little further compared to the present investigation. The absorption coefficients are always encumbered with uncertainty, especially for the audience area. Although not shown here, it has actually been tried to adjust the absorption of the audience areas to fit the measured reverberation times from 1988, but this did not improve the fit of the other parameters. This leaves the main

responsibility with the computer model itself. However, the possible influence of the lack of diffusion and diffraction cannot easily be evaluated.

A closer look at the results indicates, that most of the observed deviations can be explained from too high energy in the early part of the calculated impulse responses. It is not correct to add the energies of each reflection, instead they should be added as complex sound pressures with amplitude and phase. This would especially attenuate the direct sound and the early reflections from the walls, as these contributions are always followed closely by reflections in counterphase coming from the audience area. This leads to the hypothesis, that the computer model might be improved considerably if the reflections could be calculated in terms of sound pressure instead of energy, and if the surfaces could be characterized by their impedance or by an angle dependent pressure reflection factor. This is intended to be tried in the near future.

6.0 CONCLUSION

Measured and calculated room acoustic parameters in the Royal Festival Hall, London have been compared, and the variation with position is relatively well reproduced by the model. The calculated values of LEF are in very close agreement, whereas the values of EDT, Level, Centre Time and Clarity show systematic deviations. These might be caused by the present computer model's simplified energy addition of reflections and neglecting of the phase relations between reflections. This means that direct sound and early wall reflections are not attenuated as in the real hall. Still, with some caution and in the hands of trained acousticians, the present computer model can be a valuable tool in designing rooms.

REFERENCES

Naylor G., Odeon Room Acoustics Program, Version 1.0, User Manual, Publication No. 38, The Acoustics Laboratory, Technical University of Denmark, Lyngby, Denmark 1991.

Parkin P.H., Allen W.A., Purkis H.J., Scholes W.E., The Acoustics of the Royal Festival Hall, London, Acustica, 3, 1-21, (1953).

Beranek L.L., Music, Acoustics and Architecture, John Wiley, New York 1962. p.547.

Gade A.C., Acoustical Survey of Eleven European Concert Halls, Report No. 44, The Acoustics Laboratory, Technical University of Denmark, Lyngby, Denmark 1989.

THE DIFFERENCE THRESHOLD FOR REVERBERATION TIME AND SUBJECTIVE METHOD OF MEASURING REVERBERATION TIME

Chao Sun

Department of Mechanical Engineering,

The University of Queensland, QLD 4072, Australia.

Fergus Fricke

Department of Architectural and Design Science,

The University of Sydney, NSW 2006, Australia.

ABSTRACT

The just perceptible differences of reverberation times were measured. The dependences of the difference limen of reverberation time upon frequency and dynamic range were studied. Based on the results of difference limen tests, a subjective method of determining reverberation time by aurally comparing the sound decay in a room with standard electronically produced sound decays was investigated. For measuring reverberation times of less than 1.5 seconds, the results obtained by this method agree with those measured by the standard level recording method to within an accuracy of $\pm$ 0.2 second.

1.0 INTRODUCTION

Reverberation time is an important parameter and one of the most frequently measured quantities in room acoustics. Many attempts have been made at measuring reverberation time and improving the accuracy of these measurements.

Work presented in this article looks at the difference threshold for reverberation time and the possibility of judging reverberation time subjectively by means of electroacoustical apparatus.

The difference threshold for reverberation time was studied by H. P. Seraphim and the dependence of the difference threshold for reverberation time upon frequency was studied by G. Plenge. Seraphim's results show that for reverberation times between 0.6s. and 4.0 s. the relative difference limen is between 3% and 4%. An octave band of noise from 800Hz to 1600Hz, with a level difference of 30dB between the beginning and the end of the reverberant decay, was used in the tests. The difference threshold was defined as the value at which 75% of the test subjects could correctly identify the difference in two sound decays (W. N. Dember). A change of frequency and a reduction of the level difference to 20dB made little difference in the results. Plenge's results show that the difference threshold for decays with the first 200ms suppressed decrease for frequencies below 1000Hz. From the work of Seraphim and Plenge it can be seen that there is no need to measure differences of less than a tenth of a second for reverberation times between 1.5s. and 2.5s.. Another application of the above results, i.e. the possibility of judging reverberation time by comparing the sound decay in room with electroacoustically produced decay, can be explored.

Two experiments were carried out. The first was to determine the just noticeable differences in reverberation times and the dependence of this difference threshold upon frequency and sound level difference. The second experiment was to investigate the possibility of judging reverberation time by comparing the sound decay in room with the electroacoustically produced decays.

2.0 DIFFERENCE THRESHOLD OF REVERBERATION TIME

2.1 Just Noticeable Difference in Reverberation Times at 1kHz

An impulse of octave band limited white noise at 1kHz was fed into a reverberation processor (YAMAHA DSP-1) to produce reverberant decays of different rates. The reverberation times of the electronically produced sound decays can be varied from 0.3s. upwards, in steps of 0.1s..The experimenter selects the four to six sound decays to be presented, so that they cluster around the standard sound decay and each is paired with the standard decay. The sound decays were recorded on a tape via a tape recorder(SONY TC-510-2) and the subjects listened to tape through headphones in quiet rooms. Subjects

listened to pairs of decays and were required to judge which was the longer of the two. Each pair of sound decays had the same impulse length of 0.11s., the same level difference of 50dB and the same fine structure. Each pair of sound decays was presented twice in the same order, after which the subject was asked to make a judgement. 35 subjects with normal hearing ability, most of whom were young undergraduate and postgraduate students, were tested.

The difference threshold of reverberation times for octave band limited signals of 1kHz were calculated from the total judgements of 35 subjects and are presented in Table 2.1.1.

Table 2.1.1 The difference threshold of reverberation time at 1 kHz octave centre frequency

Reverberation Time (s)	0.5	0.7	0.8	1.0	2.0
Difference Threshold (s)	0.1	0.1	0.1	0.1	0.2

2.2 Difference Threshold of Reverberation Times At Different Frequencies

The difference threshold for a reverberation time of 0.8s.was tested for each octave band centre frequency from 125Hz to 4000Hz. The conventional psychometric method of measuring difference threshold was used. Three experienced subjects with normal hearing ability participated in the tests and each subject made 10 to 50 judgements for each pair of sound decays. For a comparatively large difference in reverberation times, in this case 0.2s and 0.3s, the subjects confidently made a judgement after listening to each pair of sound decays five times. For smaller differences in reverberation times, e.g. 0.1s., the subjects listened to the pair of sound decays repeatedly until they could make a judgement.

The difference threshold for a reverberation time of 0.8s, at octave band centre frequencies from 125Hz to 4kHz are shown in Table 2.2.1 The level difference between the beginning and the end of the sound decays for each octave band is also shown in Table 2.2.1.

The relative difference threshold increases at the lower frequencies of 125Hz and 250Hz which verified Plenge's results, even though Plenge used a different signal: reverberation signals with the first 200ms depressed.

Table 2.2.1 Difference Threshold and Level Difference For A Reverberation Time of 0.8s At Various Octave Centre Frequencies

Octave Frequency (Hz)	125	250	500	1K	2K	4K
Difference threshold (s)	0.1	0.1	<0.1	<0.1	<0.1	<0.1
Level Difference (dB)	46	50	56	61	65	66

2.3 Comparing Sound Decays with Different Level Differences

The purpose of this test was to investigate whether the subjects could judge the sound decays by their decaying rates rather than their time durations. Sound decays of different reverberation times and different level differences between beginning and end of the decays were given to the subjects for comparison. The subjects were to report which sound decayed faster.

The sound source was an impulse of band limited white noise at 1kHz. The reverberation time of the reference sound decay was 0.8s. and reverberation times of the other sound decays were 0.2s. and 0.1s. shorter or longer than the reference decay. The levels of the two sounds, at the beginning of the sound decays, were the same and the levels at the end of the decays were determined by a background noise signal which was adjustable. The background noise signal was also band limited white noise at 1kHz. The pulse length of the source signal was 0.1s. The level differences of each sound decay were 25dB, 35dB, 45dB and 55dB. After listening to each pair of sound decays the subject was to report which sound decayed faster. Uncertainty was excluded by repetitive listening until the subject could make a judgment. Two experienced subjects participated in the test.

A lower proportion of correct judgements was observed when the subjects were comparing two sound decays with 0.1s difference in reverberation time and the decay with the shorter reverberation time had much larger level difference than the other one. However the overall results show that the difference threshold for a reverberation time of 0.8s, at 1kHz, is still less than 0.1s for different level differences between the beginning and the end of the sound decays. So it can be concluded that, within the accuracy of our test, the subjects can judge the sound decays by their decaying rates rather than time durations.

3.0 SUBJECTIVE METHOD OF MEASURING REVERBERATION TIME

If individuals can identify the difference of 0.1s to 0.2s. in reverberation times between 0.6s. and 2.0s., reverberation time could possibly be measured by aurally comparing sound decays in the room with the electronically produced sound decays with known decay rates. Two experienced subjects took part in the experiment and reverberation times at octave band frequencies from 125Hz to 4kHz were judged for three enclosures. The three enclosures included a teaching lab, an office and a reverberant chamber. The reverberation times of the above enclosures were also measured as per Australian Standard 2460 - 1981, and the results were used for comparison with those obtained by the subjective method.

An impulse of octave band limited white noise was again used as the source signal and the length of the signal impulse was 0.1s. The sound decays in the room were recorded on a tape via Sony tape recorder. A Yamaha DSP-1 reverberation processor was used to provide electronically produced sound decays for the Teaching Laboratory and the office and A Yamaha REV7 reverberation processor was used for the Reverberant Room. The level differences of the sound decays which were produced by Yamaha DSP-1 at each octave band centre frequency are as shown in Table 2.2.1. The level differences, between the beginning and the end of the sound decays at each octave band centre frequency in these three rooms, are shown in Table 3.0.1. The beginning level of the electronically produced sound decays was adjusted to be the same as that of the sound decay in the room. The level at the end of the electronically produced sound decays was not adjusted to be the same as that of room sound decay, so the level difference between the beginning and the end of the electronically produced decays was not the same as that of the room sound decay. The fine structure of the electronically produced sound decays was adjusted to be as close as possible to that of the sound decay in the room by aurally comparing and estimating.

The electronically produced sound decays were input to the Sony tape recorder as source signal. The subjects listened to the electronically produced decays by selecting "source" and listened to the room sound decays on the tape. Four or five electronically produced decays with decay rates clustering around that of the room decay, were chosen and paired with the decay in the room. For each pair of sound decays, the subjects made judgments about whether the electronically produced decay was "faster" or "slower" than the sound decay in the room. The uncertainty was again excluded by listening to the pair repeatedly until a judgment could be made. The reverberation time of the electronically produced decay, which had the closest decay rate as the sound decay in the room, was taken.

3.1 The Teaching Laboratory

The Teaching Laboratory is located in Room 481, Wilkinson Building of Sydney University. Dimensions of the room are 10.6m x 14.0m x 3.0m. The floor is carpeted, two walls are brick faced and two other walls composed of glazing and brick. The

ceiling is concrete faced and furniture composed of desks, chairs and equipment. An omnidirectional loudspeaker was placed at the lecturing position and at a height of 1.4m. An artificial head with two microphones in the ears was placed on the desk at the centre of the room.

The subjects spent approximately five to ten minutes on assessing reverberation time in each octave band. The results are shown in Table 3.1.1, together with those measured by standard recording method.

3.2 The Office

The office is located in Room 478, Wilkinson Building of Sydney University. Dimensions of the room are 4.0m x 4.4m x 3.4m. The floor is carpeted, two walls are brick faced, one wall composed of wooden door and bricks, one wall composed of windows and bricks, and the ceiling is concrete. The furniture included wooden desks, books, papers and bookshelves against one wall. An omnidirectional loudspeaker was placed in the corner of the room, opposite to the door and at a height of 1.4m. The artificial head with microphones installed in the ears was placed on a desk in the centre of the room. The results are shown in Table 3.2.1, together with those measured by standard recording method.

3.3 The Reverberant Room

The reverberant room is located in the Acoustic Laboratory, Wilkinson Building of Sydney University. The dimensions are 5.2m x 6.4m x 4.0m. Twelve pieces of fibreglass boards (Area: 1.2 m^2 each) were distributed on the floor and against the walls. An omnidirectional microphone was placed in a corner of the room and at a height of 1.4m. The microphone was located in the centre of the room.

It was very difficult to simulate the sound decays in the reverberant room by altering the parameters of the Yamaha REV7 reverberation processor. The subjects found it hard to judge the reverberation times of the room for two reasons, first the sound decays in the room were too long and secondly, the electronically produced decays did not sound like the sound decays in the room. However, the subjects still estimated the reverberation times of the room. The results are shown in Table 3.3.1 together with those measured by standard recording method.

3.4 Discussion

The reverberation times which were obtained by the subjective method agreed with those measured by the standard method to within ±0.2s. for the Teaching Laboratory

and the office, where the reverberation times were less than 1.5s and a good simulation of the room reverberant decay was provided. A higher error was observed when judging reverberation times at lower frequencies, especially 125Hz. The subjects found that judging reverberation times at 125Hz was more difficult than that at higher frequencies. It is probably due to the lower hearing sensitivity and the smaller level differences between the beginning and the end of the sound decays at lower frequencies.

4.0 CONCLUSIONS

The difference threshold of reverberation times increases for longer reverberation times and for lower frequencies of 125Hz and 250Hz. The reverberation times of less than 1.5s could be judged subjectively within an accuracy of ± 0.2s by comparing the sound decay in the room with the electronically produced decays, providing the room reverberant decay is short, the sound decay in the room is relatively linear and the level difference between the beginning and the end of the room sound decay is more than 25 dB.

5.0 REFERENCES

Journals

Plenge G., Research on The Difference Limen of Reverberation Time as A Function of Frequency, Acoustica, 16, 269-278, (1965/1966).

Seraphim H. P., Research on The Difference Limen for Reverberation Time of Band Noise Pulses, Acoustica, 8, 280-284, (1958).

Books

Cremer L. and Muller H. A., Principles and Applications of Room Acoustics, (Volume 1), Applied Science Publishers, 1982, 503-509 and 413-435.

Dember W. N., The Psychology of Perception, Holt, Rinehart and Winston Inc., 1960, Chapter 2, "Threshold Measurement Techniques", 27-66.

Guilford J. P., Psychometric Methods, McGraw - Hill Book Company, New York, 1954, Chapter 6, "The Constant Method - Determination of a Difference Limen", 135-150.

Thesis

Sun C., Simplified Methods of Measuring Reverberation Time, Department of Architectural Science, University of Sydney, 1989

Table 3.0.1 Level differences (dB) between beginning and end of the sound decays in the three rooms at each octave band centre frequency

Octave Frequency (Hz)	125	250	500	1000	2000	4000
Teaching Lab	37	43	48	49	52	52
The Office	34	40	43	45	44	43
Reverberant Room	31	47	67	69	73	72

Table 3.1.1 Reverberation times (s) of Teaching Laboratory measured by the subjective method and the standard recording method

Octave Frequency (Hz)	125	250	500	1000	2000	4000
Subject 1	1.3	1.1	0.8	0.8	0.7	0.7
Subject 2	1.5	1.0	0.8	0.7	0.8	0.7
Standard Method	1.4	1.0	0.8	0.8	0.8	0.6

Table 3.2.1 Reverberation times (s) of the office, Room 478, measured by the subjective method and the standard recording method

Octave Frequency (Hz)	125	250	500	1000	2000	4000
Subject 1	0.6	0.6	0.5	0.5	0.5	0.5
Subject 2	1.0	0.7	0.6	0.6	0.6	0.5
Standard Method	0.8	0.7	0.6	0.6	0.6	0.6

Table 3.3.1 Reverberation times (s) of the reverberation room, measured by the subjective method and the standard recording method.

Octave Frequency (Hz)	125	250	500	1000	2000	4000
Subject 1	2.4	2.8	1.8	1.8	1.8	2.0
Subject 2	2.8	2.4	1.8	1.7	1.8	1.9
Standard Method	2.1	1.9	1.7	1.6	1.4	1.3

THE ACOUSTIC PERFORMANCE OF PLASTIC FOAM AND FIBROUS PREFORMED THERMAL PIPE INSULATIONS FOR SMALL DIAMETER PIPES

K. P. Byrne
School of Mechanical and Manufacturing Engineering
The University of New South Wales
Sydney
Australia

ABSTRACT

The paper presents the results of measurements which were made to determine the sound insertion losses produced by four different types of preformed thermal pipe insulations of Australian manufacture which are widely used to insulate small diameter pipes such as those used in building services. Usually, the primary reason for using these preformed thermal pipe insulations is to thermally insulate the pipes associated with refrigeration and airconditioning systems and to reduce the heat loss from hot water pipes. However, airborne sound directly radiated from small diameter pipes can be a problem and it is useful to know the sound insertion losses which these preformed thermal pipe insulations can produce. Sound intensity measurements have been used to determine the frequency dependent insertion losses produced by preformed thermal pipe insulations manufactured from four different materials in three typical thicknesses when applied to 25, 51 and 76 mm outside diameter copper pipes carrying turbulent water.

1.0 INTRODUCTION

It is sometimes necessary to attenuate the airborne sound radiated by small diameter (< 100 mm) pipes. An example of a situation where it may be necessary to do this is with water pipes in buildings. The usual way of attenuating the airborne sound radiated from pipes, particularly those used in process industries, is to lag the pipes with porous and impervious layers such as fibreglass blankets and metal cladding sheets. Although the relatively small diameter pipes used in buildings are often insulated for thermal purposes, the insulation is often not of the type used in process industries. Since a wide range of preformed thermal pipe insulations for small diameter pipes is available, it is obviously convenient to use these products for acoustical purposes if they have appropriate acoustical performance. These preformed thermal pipe insulations are commonly used for insulating hot water pipes in buildings and pipes associated with refrigeration and airconditioning systems.

Although there are a few publications in the readily accessible literature relating to the acoustic performance of pipe laggings, for example, the papers of Hale, Hale et al, Smith et al and Loney, these papers are concerned with the performance of laggings of the type used in process industries. There are, to the knowledge of the author, no published papers in the readily accessible literature relating to the acoustic performance of preformed thermal pipe insulations. The purpose of this paper is to present the results of measurements which were made to determine the sound insertion losses produced by four different types of widely used preformed thermal pipe insulations of Australian manufacture, when they are applied to small diameter pipes.

Frequently, noise problems associated with small diameter pipes arise because of rigid connections between these pipes and effective radiating elements such as walls which support them. However, it should be noted that this paper is specifically related to the problem of attenuating airborne sound directly radiated from small diameter pipes.

2.0 TEST PROGRAMME

The test programme involved measurements to determine the 1/3 octave band sound insertion losses produced by four different pipe insulation materials of three different wall thicknesses applied to three sizes of copper pipe.

2.1 Materials The preformed thermal pipe insulations used in the tests were of Australian manufacture and were made from four different materials. Similar preformed thermal pipe insulations are available in other countries. The materials used in the products which were tested are described below.

Material A was a flexible closed cell nitrile rubber vinyl blend which has a density of 85 to 105 kg/m^3 and a thermal conductivity of approximately 0.04 W/mK at 20°C.

113

Material B was a flexible closed cell polyethylene foam which has a nominal density of 55 kg/m³ and a thermal conductivity of 0.034 W/mK at 20°C.

Material C was a rigid closed cell expanded polystyrene foam which has a nominal density of 13.5 kg/m³ and a thermal conductivity of 0.038 W/mK at 20°C.

Material D was a rigid moulded glasswool. It has a nominal density of 85 kg/m³ and a thermal conductivity of 0.032 W/mK at 20°C.

2.2 Pipes Preformed thermal pipe insulations manufactured from each of the four materials described in the previous section were tested when applied to hard drawn copper pipes of outer diameters 25, 51 and 76 mm. The wall thickness of all pipes was 0.91 mm.

2.3 Insulation Thicknesses The materials described in Section 2.1 are used in Australia to produce preformed thermal pipe insulations in a range of thicknesses, depending upon the size of pipe to which they are applied. The flexible closed cell foam insulations are manufactured in nominal wall thicknesses of 10, 15 and 20 mm. The rigid closed cell polystyrene foam and glasswool pipe insulations are manufactured in a greater range of wall thicknesses than the flexible insulations and wall thicknesses of 25, 38 and 50 mm were selected for the tests.

Table I summarizes the combinations of material, pipe diameter and insulation thickness which were examined.

TABLE I
COMBINATIONS FOR TEST PROGRAMME

INSULATION MATERIAL	25 mm pipe			51 mm pipe			76 mm pipe		
	Insulation Wall Thickness (mm)			Insulation Wall Thickness (mm)			Insulation Wall Thickness (mm)		
A (Nitrile Rubber)	9	13	19	9	13	19		13	19
B (Polyethylene)	10	15	20	10	15	20		15	20
C (Polystyrene)	25	38	50	25	38	50	25	38	50
D (Glasswool)	25	38	50	25	38	50	25	38	50

3.0 TEST RIG

The basic method used to determine the insertion loss for a particular preformed thermal pipe insulation was to measure, in 1/3 octave bands, the average sound intensity level of the sound radiated from the pipe with and without the insulation fitted to it. If these

114

average sound intensity levels are denoted $L_{Iw}(f)$ and $L_{Iwo}(f)$, the 1/3 octave band insertion losses, $IL(f)$, are given by equation (1).

$$IL(f) = L_{Iwo}(f) - L_{Iw}(f) .$$ (1)

The essential features of the test rig used to make the sound intensity measurements can be seen in Figure 1.
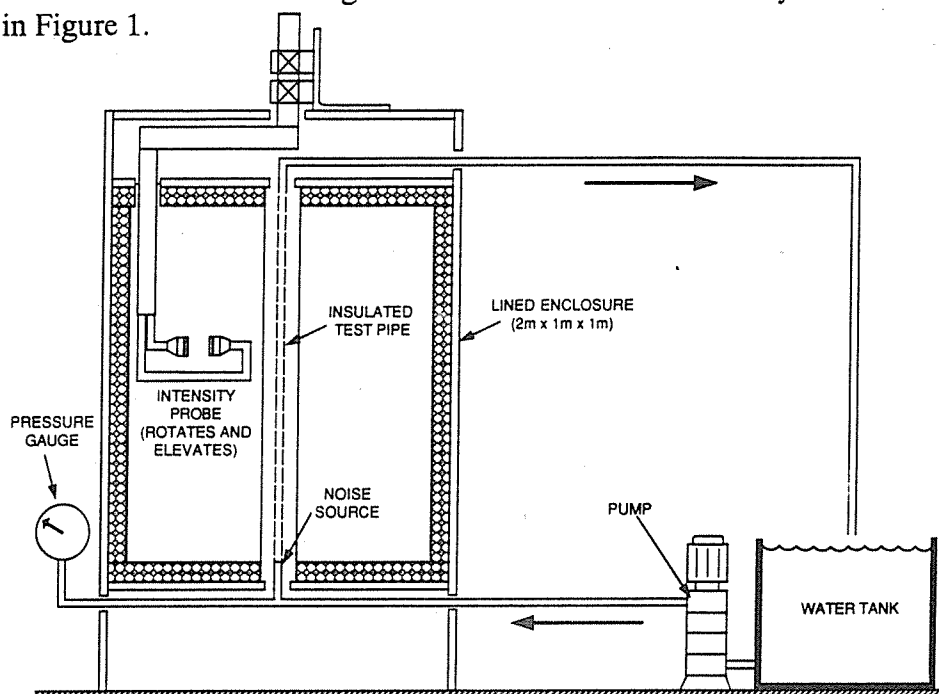
Figure 1. Arrangement of Test Rig

The pipes which were used in the tests were made to radiate realistic broad band sound by exciting them with turbulent internal water flow. The water flow was made highly turbulent by passing it through a multi-orifice fitting installed at the lower end of the test pipe. It can be seen from Figure 1 that the water was forced through the multi-orifice fitting and into the pipe by a multi-stage centrifugal pump. The pressure upstream of the fitting could be monitored by an accurate pressure gauge. The multi-orifice fitting was in fact the so-called "installation noise standard" described in ISO 3822/1 - 1983 'Acoustics - Laboratory test on noise emission from appliances and equipment used in water supply installations - Part I: Method of measurement'. The significant features of this "installation noise standard" are shown in Figure 2. The average sound intensity level of the sound radiated from the bare and insulated pipes was determined with a Bruel and Kjaer 2032 analyser. The recommendations given in the ISO Standard on sound power measurement ISO/DIS9614, were followed in making these measurements. The average sound intensity level was derived from 30
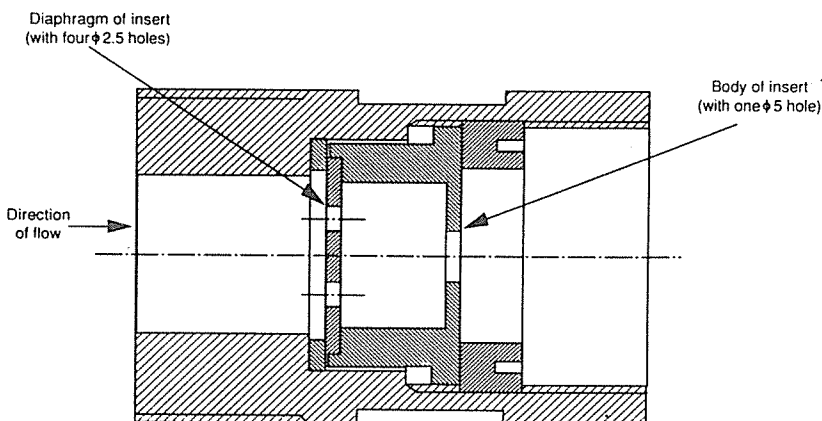
Figure 2. Details of Installation Noise Standard

115

individual sound intensity measurements made in a radial direction at 60° intervals in five equally spaced planes along the central 1000 mm section of the 2000 mm long insulated section of pipe which was contained in the lined enclosure. This lined enclosure, whose nominal internal dimensions were 2000 mm x 1000 mm x 1000 mm, was intended to facilitate the sound intensity measurements by attenuating both the ambient sound and the internal reverberant sound. The sound intensity probe was located 250 mm from the centre of the pipe.

4.0   AVERAGE SOUND INTENSITIES FOR THE BARE PIPES AND A TYPICAL INSULATED PIPE.

The average sound intensity levels of the sound radiated from the three bare pipes must be known, as shown by equation (1), so that the insertion losses produced by the various insulations can be determined. It is also necessary that the level of excitation of the pipe wall produced by the internal turbulent flow not be changed with and without the insulation on the pipe. It was assumed that if the pressure upstream of the orifice did not change, the level of excitation would not change. The three average bare–pipe sound intensity levels in 1/3 octave bands are shown in Figure 3. An indication of the quality of the sound intensity measurements is given by the sound pressure and sound intensity spectra shown in Figure 4 which are for the 13 mm nitrile (Material A) applied to the 51 mm pipe. The 1/3 octave band sound pressure levels are in dB re 2 x 10^{-5} Pa and the sound intensity levels are in dB re 10^{-12} watts/m².
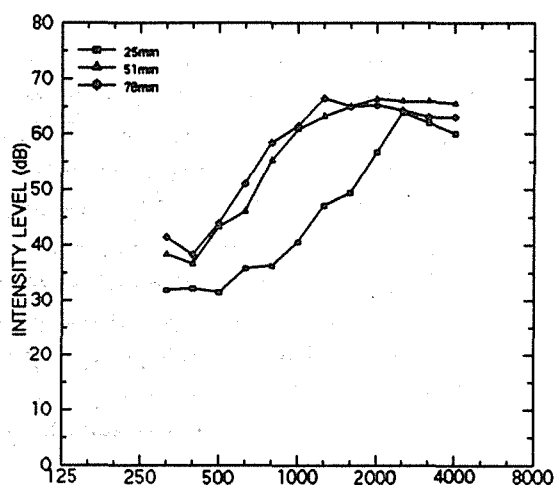
Figure 3. 1/3 Octave Band Average Bare–pipe Sound Intensity Levels
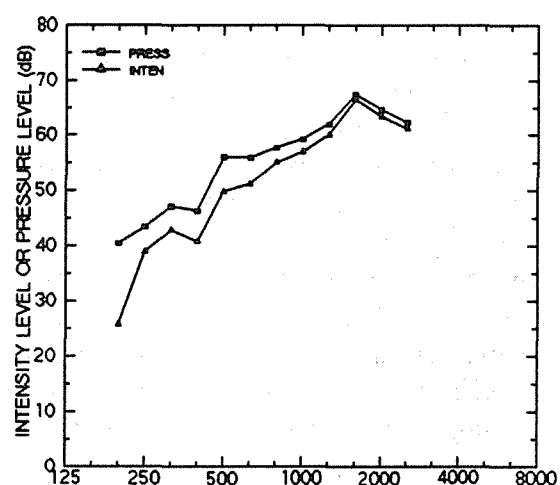
Figure 4. Typical 1/3 Octave Band Sound Pressure and Sound Intensity Spectra

5.0   RESULTS

The insertion losses produced by each of the combinations given in Table I are plotted in Figures 5 to 16.
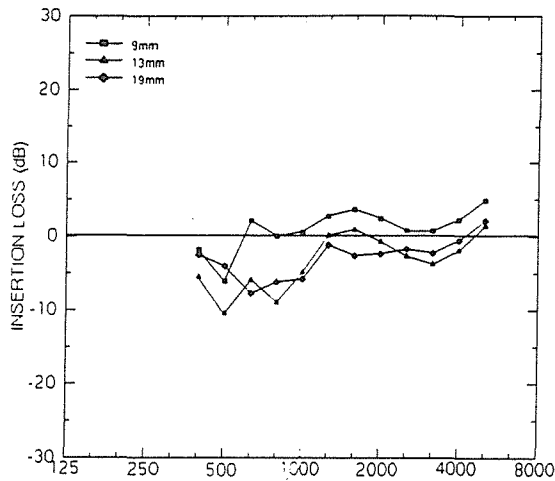
Figure 5. 1/3 Octave Band Insertion Losses for 9, 13 and 19 mm Wall Thickness Nitrile Rubber (Material A) Insulation with 25 mm Pipe.
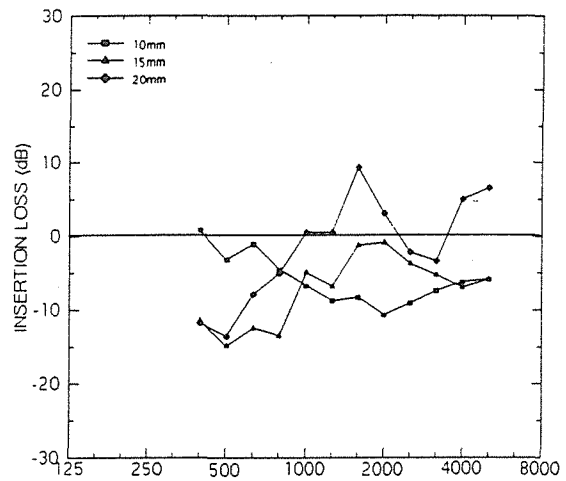
Figure 8. 1/3 Octave Band Insertion Losses for 10, 15 and 20 mm Wall Thickness Polyethylene (Material B) Insulation with 25 mm Pipe.
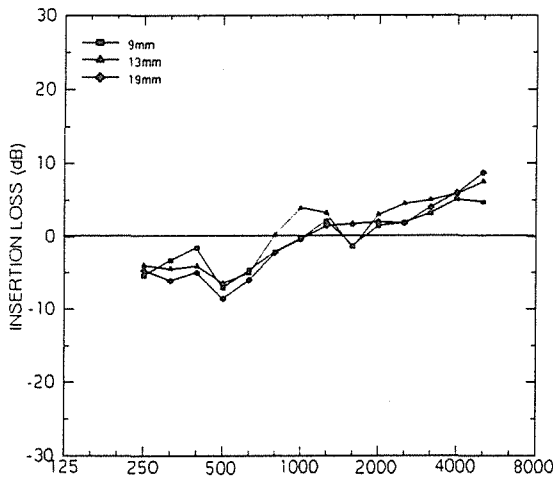
Figure 6. 1/3 Octave Band Insertion Losses for 9, 13 and 19 mm Wall Thickness Nitrile Rubber (Material A) Insulation with 51 mm Pipe.
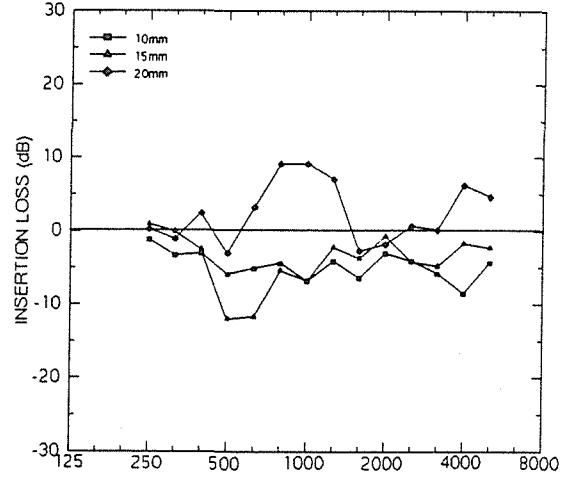
Figure 9. 1/3 Octave Band Insertion Losses for 10, 15 and 20 mm Wall Thickness Polyethylene (Material B) Insulation with 51 mm Pipe.
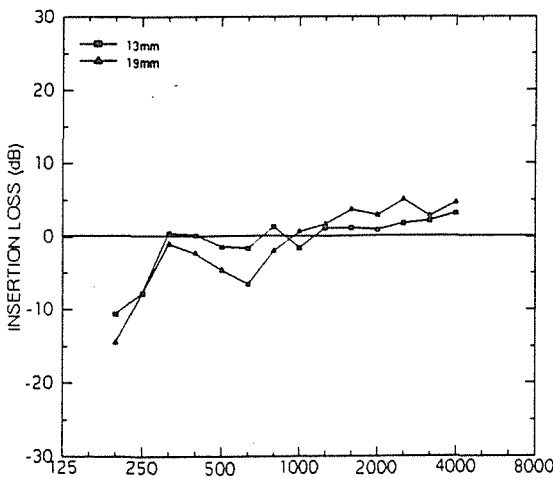
Figure 7. 1/3 Octave Band Insertion Losses for 13 and 19 mm Wall Thickness Nitrile Rubber (Material A) Insulation with 76 mm Pipe.
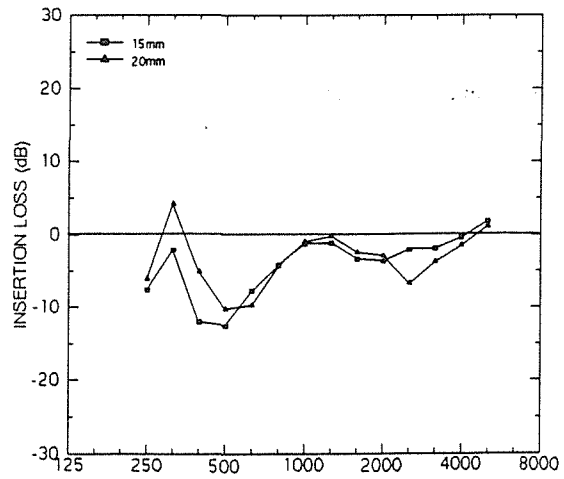
Figure 10. 1/3 Octave Band Insertion Losses for 15 and 20 mm Wall Thickness Polyethylene (Material B) Insulation with 76 mm Pipe.

117
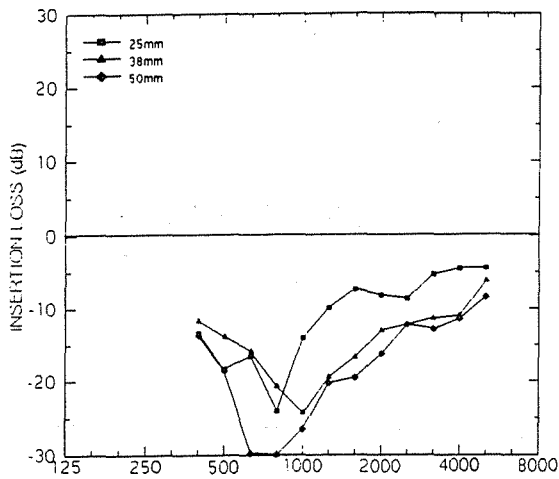
Figure 11. 1/3 Octave Band Insertion Losses for
25, 38 and 50 mm Wall Thickness Polystyrene
(Material C) Insulation with 25 mm Pipe.
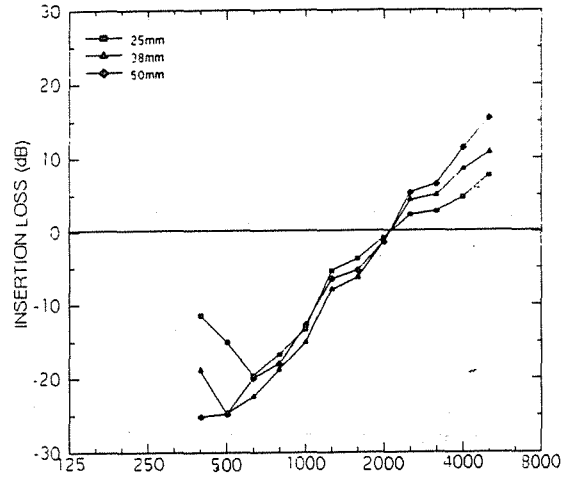
Figure 14. 1/3 Octave Band Insertion Losses for
25, 38 and 50 mm Wall Thickness Glasswool
(Material D) Insulation with 25 mm Pipe.
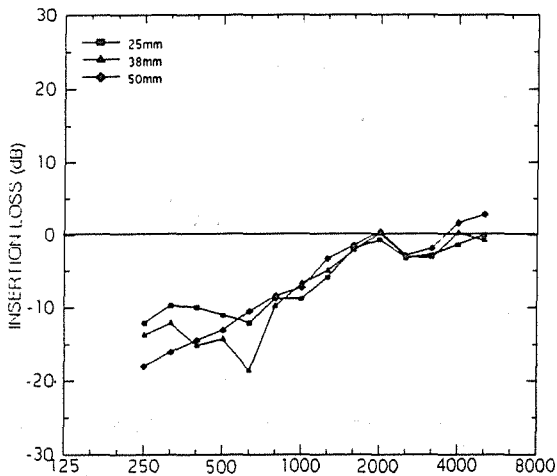
Figure 12. 1/3 Octave Band Insertion Losses for
25, 38 and 50 mm Wall Thickness Polystyrene
(Material C) Insulation with 51 mm Pipe.
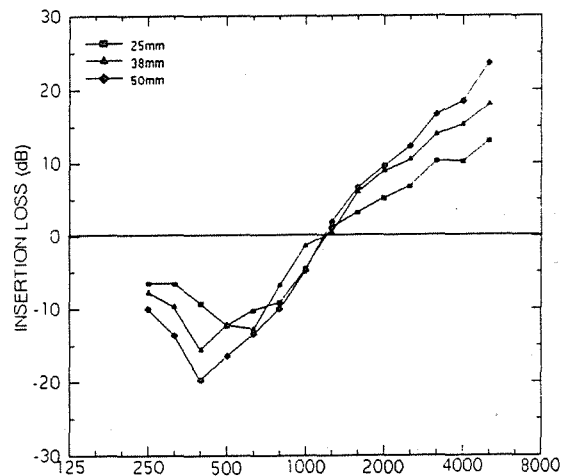
Figure 15. 1/3 Octave Band Insertion Losses for
25, 38 and 50 mm Wall Thickness Glasswool
(Material D) Insulation with 51 mm Pipe.
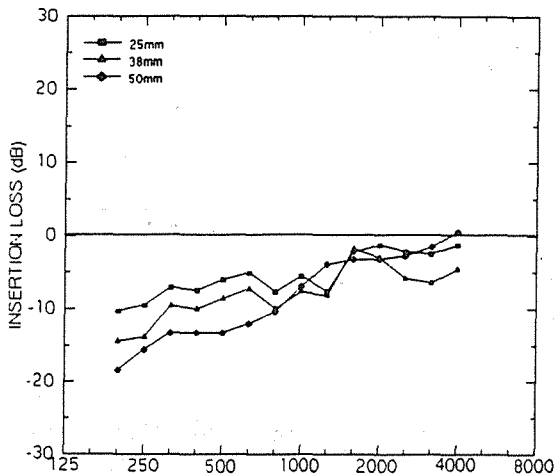
Figure 13. 1/3 Octave Band Insertion Losses for
25, 38 and 50 mm Wall Thickness Polystyrene
(Material C) Insulation with 76 mm Pipe.
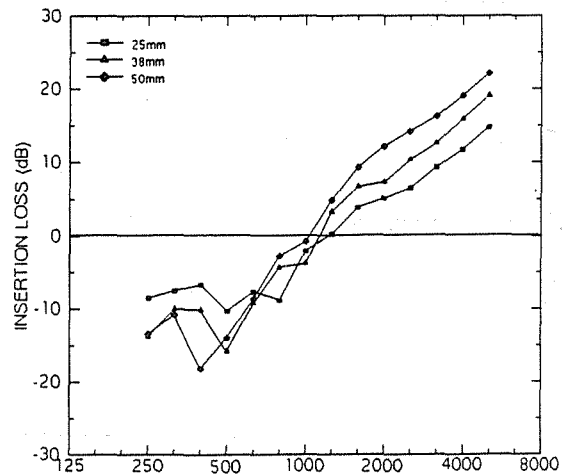
Figure 16. 1/3 Octave Band Insertion Losses for
25, 38 and 50 mm Wall Thickness Glasswool
(Material D) Insulation with 76 mm Pipe.

118

6.0 COMMENTS ON THE RESULTS

The most striking feature of the results plotted in Figures 5 to 16 is that the insertion losses are generally negative. Thus the fitting of these preformed thermal pipe insulations to pipes will generally increase the sound radiated by pipes. The fact that larger negative insertion losses are associated with smaller diameter pipes suggests, for the following reason, that this effect is associated with the preformed thermal pipe insulations being forced to vibrate because of their intimate contact with the vibrating pipe. Kuhn and Morfey have suggested that a significant component of the noise radiated from a pipe is associated with the bending vibrations of the pipe. It can be shown that, if a rigid cylinder of radius a is vibrating harmonically at a frequency of f Hz with a velocity amplitude of U_0 in a medium characterised by ρ , the density and c , the velocity of sound, the sound power per unit length radiated from the cylinder, W , is given by equation (2) if ka << 1 where k = 2π f/c.

$$W \approx \pi^2 (ka)^3 \rho c a U_0^2 . \tag{2}$$

It can be seen that W is proportional to the fourth power of the pipe diameter. Thus if 50 mm thick pipe insulation is applied to a 25 mm diameter pipe and the vibratory motion of the pipe is transmitted to the outer surface of the insulation without attenuation, it would be expected that the acoustic power radiated per unit length would increase by a factor 5^4 = 625 at low frequencies for which ka << 1. Obviously significant attenuation of the vibratory motion does occur with practical insulations. Otherwise these insulations would be less effective than they are.

It seems likely that the insertion losses produced by these preformed thermal pipe insulations could be improved greatly by arranging for an airspace to be present between the pipe and the insulation. A further increase in the insertion losses should be achieved by wrapping the insulations with a limp, massive impervious barrier.

7.0 REFERENCES

Hale, M. E., A Comparison of Several Theoretical Noise Abatement Prediction Methods for Pipe Lagging Systems, 96th Meeting of the Acoustical Society of America, Honolulu, Hawaii, 1978.

Hale, M. E. and Kugler B. A., The Acoustic Performance of Pipe Lagging Systems, ASME Winter Annual Meeting, Houston, Texas, 1975.

Loney, W., Insertion Loss Tests for Fibreglass Pipe Insulation, J. Acoust. Soc. Am., 76 (1), 150–157, 1984.

Kuhn, G.F. and Morfey, C.L., Transmission of Low–Frequency Internal Sound Through Pipe Walls, J.Sound and Vibration, 47, pp147–161, 1976.

Smith, T., Rae, J.M. and, Lawson, P., Pipe Lagging – An Effective Method of Noise Control?, Applied Acoustics, 13, 393–404, 1980.

SOUND INSULATION PERFORMANCE BETWEEN RESIDENTIAL UNITS AND NOISE REDUCTION METHODS IN APARTMENT BUILDINGS

Heung-sik Kim
Research Institute of Korea National Housing Corp
Seoul, Korea

Young-in Oh
Research Institute of Korea National Housing Corp
Seoul, Korea

Ha-geun Kim
Research Institute of Korea National Housing Corp
Seoul, Korea

ABSTRACT

In this paper, the performance of the sound insulation between residential units for apartments was surveyed and compared with the design criteria in Korea. The effects·related to the leaking and flanking of the sound were also investigated.

The Sound Insulation Performance depending on the materials and construction methods adopted was also studied in order to propose the wall system which satisfies the sound insulation criteria.

1.0 INTRODUCTION

Airborne sounds transmitted from residential units in apartments originate from TV, audio, video, piano and conversation, through the walls and windows. The Sound Insulation Performance (SIP) between residential units must be estimated based on the SIP of the walls and well as that of the windows Therefore, before the path and the degree of loss of the sound transmission are identified, the methods for the sound insulation have to be planned. In this paper, the SIP of the walls between adjacent units was surveyed for various structures and wall thicknesses. The effect of the flanking transmission, and design examples for noise reduction, were investigated as well.

2.0 SIP OF WALLS

Table 1 represents the sound insulation criterion for the walls between residential units in Korea. So the SIP of the wall measured in the laboratory has to be equal to this criterion.

Table 1   The sound insulation criteria for the walls between residential units

1/1 octave band freq(Hz)	125	500	1000	SIP
Difference in SPL (dB)	30	45	50	D-45

3.0 SURVEY OF THE SIP OF THE WALLS

3.1 OUTLINE OF PRESENT SURVEY

The Korea, walls between adjacent units in apartment buildings mainly consist of concrete structures, and their thickness are about 150 mm to 200 mm. In this paper, the difference in the SPL between adjacent units was measured in several ways. Figure 1 represents the model for surveying the SIP of various structures and wall thickness, and the effect of flanking transmission.

Measurement was carried out based on the Korean Standard KS F 2809. For the assessment of the SIP, measured values in the 1/1 octave band frequency were dotted in contour lines based on JIS 1419 related to "the classification of air-borne and the impact sound Insulation for buildings", and the estimated from the index determine on a 1 dB scale, not from the grade related to D which is determined on a 5 dB scale. In this paper, this index is termed the Sound Insulation Index (SII).
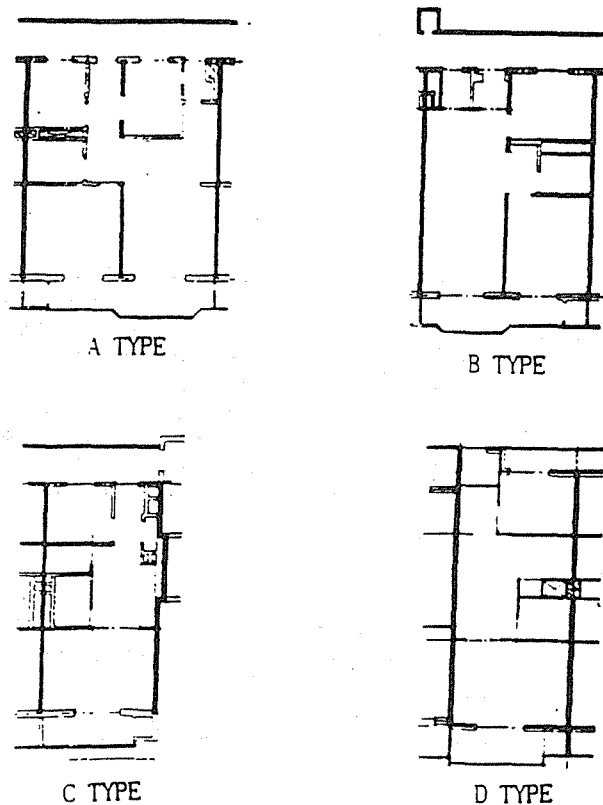
Fig. 1　The models for surveying the SIP

3.2 EFFECT OF WALL THICKNESS

The difference in SPL between adjacent units is 45 in the SII for 150 mm wall thickness, and 48 for 180-200 mm wall thickness. These values satisfy the SIP criteria in Korea (Sound Insulation Index: 45).

The SIP for 150 mm concrete wall is 45, while the Japanese Architectural Society suggests 48 for the SII. The main reason for the difference is that the sound is transmitted not only though the wall but also through the windows installed in exterior walls.

Table 1　The SIP of concrete walls between residential main rooms

The thickness of concrete wall	The SIP in 1/1 octave band (dB)						The SII measured in field	Model for survey	The SII measured in laboratory
	125	250	500	1000	2000	4000			
150mm	34	39	47	50**	56	60	45	A Type	48
180mm	34	42	48	53**	58	61	48	B Type	51
200mm	35	41**	50	54	58**	63	48	C Type	-

The symbol ** represents the frequency that determines the SII.

122

3.3 EFFECTS OF WALL STRUCTURE

The SIPs of walls for wall-slab and Precast Concrete (PC) structures were estimated. The wall-slab structure is one of the most popular systems in Korea, and recently the PC structure has been adopted due to the advantage given by the reduction of manpower. Those structures comprise the joints between floors and walls. The cracks in joints and thin walls may influence the SIP. The SIPs for the model structures were estimated in 10 places. Similar values of the SIP were observed between PC and wall-slab structures, although the walls of PC structures are thinner than those of wall-slab structures. They also satisfy the sound insulation criterion for walls in Korea.

Table 2 The SIPs of walls for wall-slab structure and PC structure

Wall structure	The SIP in 1/1 octave band (dB)						SIP measured in the feild	SIP measured in the laboratory
	125	250	500	1000	2000	4000		
Wall-slab 150MM	34	39	47	50	56	60	45	48
PC 120MM	34	38	46	52	59	65	45	-

3.4 EFFECTS OF FLANKING TRANSMISSION

Three cases are given below to examine the effects of the flanking transmission to the windows in the exterior walls. First, the storage partially intercepts the flanking transmission. Secondly, the partition partially intercepts it. Thirdly, there is no flanking transmission because the concrete walls between adjacent bathing units have no effect on the sound. Table 3 shows the results of the SIP for three cases. The SIP between adjacent bathing units is the same as that of the concrete wall itself. When the storage or partition partially intercepts the flanking transmission, the SIP of them are worse about 1-3 dB than those of the concrete walls measured in the laboratory. Table 4 represents how much the window effects on the SIP of the wall. The flanking transmission though the windows increases, when the window is opened in summer. The SII between residential units is 33 for the window opened, while it is 46 for the window closed.

Table 3 The SIPs by the effects of the flanking transmission

measurement condition	wall thickness			measurement condition
	150mm	180mm	200mm	
concrete wall in the Lab	48	51	-	Measured in the laboratory
Between bathes in A TYPE	48	-	-	No flanking transmission
Between main bedrooms in C TYPE	-	-	48	The lightweight panel intercepts the flanking trasmission in part
Between main bedrooms in D TYPE	47	48	50	The store house intercepts the flanking transmission partially

Table 4   The SIPs by the effects of flanking transmission of windows

Measurement condition	The SIP in 1/1 octave band						SII
	125	250	500	1000	2000	4000	
When the window is closed	31	38	47	52	60	63	46
When the window is opened	30	34	39	40	43	48	33

4.0 DESIGN EXAMPLES FOR THE SOUND INSULATION

4.1 SIP AT PREVIOUS SITUATION

If the compartments between adjacent residential areas have a problem related to the SIP, prior to designing of the sound insulation, the transmission path and loss should be fully investigated. Figure 2 represents one case that has a problem in the SIP. It is realized after examining the drawings that this problem was not caused by the poor quality of the concrete but by the aperture in the cement block that was adjacent to the concrete wall. The SIP of this wall was estimated and compared with the criteria in Korea.
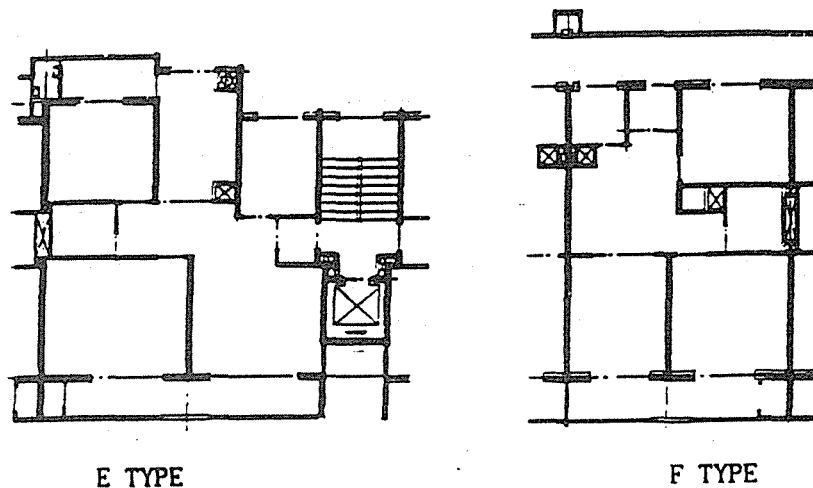
E TYPE   F TYPE

Figure 2   The case that has a flanking transmission path

The difference in SPL between main bed rooms of the E Type plan was about 35-40 in the SII, between baby bed rooms of the E type plan about 40-43, and between main bed rooms of the F Type plan about 41.
These SIPs are under the sound insulation criterion and it is considered that this poor performance is from the flanking transmission caused by the aperture.

Table 5 SIPs between units at the previous situation

Measurement Type	E TYPE		F TYPE	The SII of concrete wall measured in the laboratory
Measurement room	Main bed RM	Baby room	Main bed RM	
Concrete 150mm	-	40	-	48
Concrete 180mm	40	43	41	51
Concrete 200mm	35	41	-	-

4.2 SIP AFTER THE SOUND INSULATION DESIGN

In the previous section, it was concluded that the leak of sound was mainly due to the aperture in the cement block. So the glass wool and gypsum board were added on the cement block, as can be seen in Figure 3, to intercept the flanking transmission.
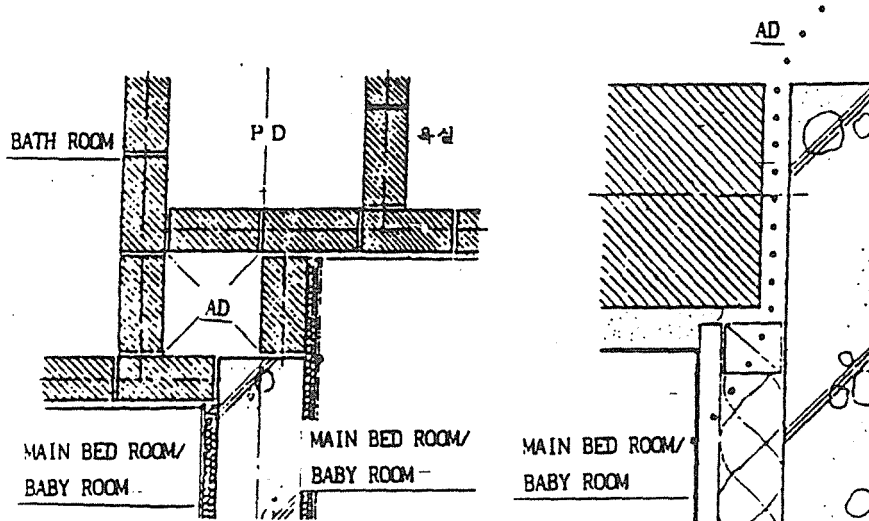
Figure 3   The method of sound insulation at the joints
of the concrete and the cement block

The difference in the SPL between adjacent units in the E and F Type plans after the glass wool and gypsum board were added was equivalent to 35-47 in the SII, as shown in Table 6. Some values of SIP are below the sound insulation criterion. This sound insulation design improves the SIP above the 250 Hz octave band frequency but the SIP falls off at 125 Hz, which is concerned with the resonant frequence domain (figure 4). The resonant frequency of this wall is 127 Hz and it is considered that the resonant frequency has an affect on the falling-off of the SIP.

If one frequency affects the SIP as in the above examples, the SIP of the wall needs to be estimated by various methods such as the SII or STC number.

Table 6 SIPs between units after the sound insulation Design

Measurement Type	E TYPE		F TYPE	The SII of concrete wall measured in the laboratory
Measurement room	Main bed RM	Baby room	Main bed RM	
concrete 150mm	-	40	-	48
concrete 180mm	45	42	44	51
concrete 200mm	47	35	-	-

□ at the previous situation
▓ after the sound insulation design
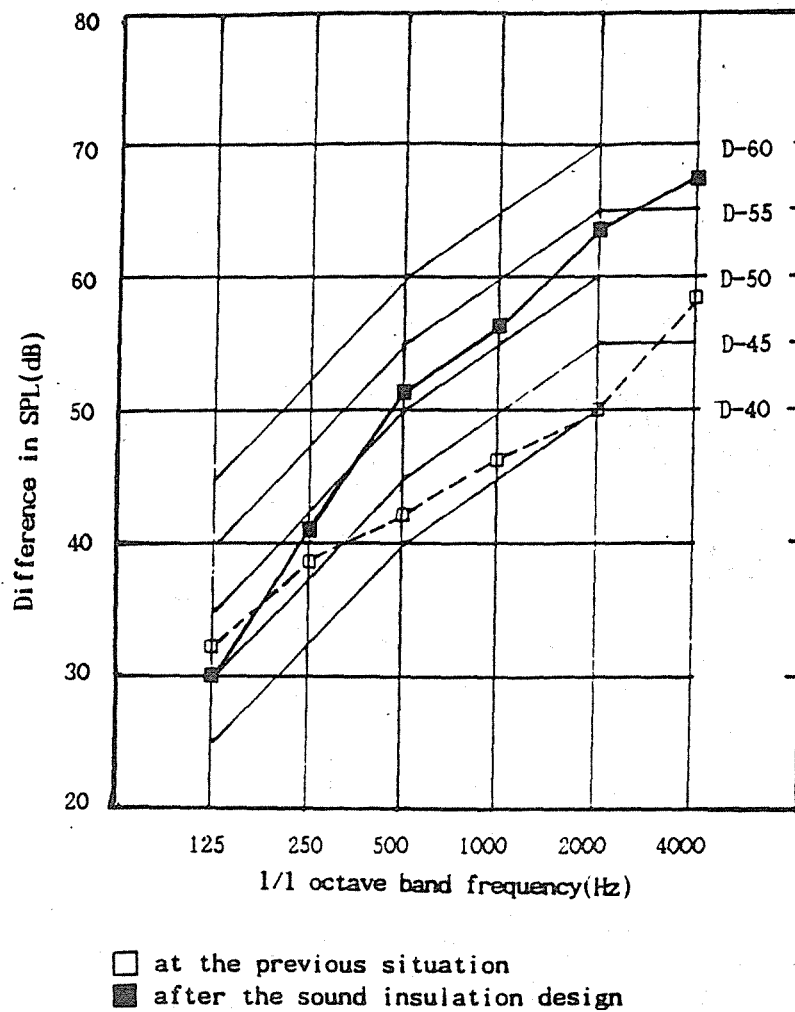
Figure 4 Difference in SPL after the sound insulation design

4.3 SIP OF CONCRETE WALLS

The SIPs of concrete walls in the A, B, C, D Type plans are shown in Table 7. The SIP of the concrete wall 150 mm thick is 45 in terms of the SII, for the 180 mm thick wall 48-49 SII, and for the 200 mm thick wall 48-51 SII. It is understood that the SIPs of concrete walls without any flanking transmission are above the sound insulation criterion in these results.

Table 7 Difference in SPL between adjacent units of concrete walls

Measurement Place	D TYPE	A ,B ,C TYPE	The laboratory
Concrete 150mm	45	45 (A TYPE)	48
Concrete 180mm	49	48 (B TYPE)	51
Concrete 200mm	51	48 (C TYPE)	-

5. CONCLUSION

The SIP between adjacent residential units in Korea is 45-50 in terms of the SII. There is no resulting problem to neighbours but some apartments have a problem because of not accounting for the sound insulation design.

No flanking transmission as well as no aperture is desirable to eliminate sound leaks. Especially, the cement block wall should not have an aperture even though it has a small area.

There are several sound transmission paths in apartments. So the methods for the assessment capable of evaluating the SIP between adjacent units in the field are required for the presentation of its performance in proper (one) index. Finally, the method for the assessment by the SII needs to be compared with that by the STC number.

REFERENCES

1. Korea National Housing Corp., The condition of indoor noises in apartments, 1979
2. Korea National Housing Corp., Noise criteria for improving the environments in residential areas, 1985
3. Korea National Housing Corp., Indoor noise criteria in apartment houses, 1986 ·
4. Korea National Housing Corp., Indoor noise reduction in apartment houses, 1988
5. Korea National Housing Corp., Impact noise criteria in apartment houses, 1990
6. KS F 2809, The method for measuring the difference in SPL in the field
7. Edward B. Magrab, Environmental Noise Control, John Wiley & Sons, 1975
8. Lyle F. Yerges, Sound, Noise, and Vibration Control, VNR, 1969
9. Malcolm J. Crocker, Noise and Noise Control Vol. 1, CRC, 1975

EXPERIENCES OF A BUILDING SERVICES ACOUSTIC ENGINEER

By **Ross H Palmer**
ACOUSTIC CONSULTANT
BE (Mech), MIEAust, RPEQ, M.Airah, MAAS, MNZAS.

P.O. Box 150 Mt Ommaney Brisbane 4074
Ph (07) 279 3745   Fax (07) 376 2360

ABSTRACT
This paper addresses common acoustic problems associated with high rise buildings.   Through the use of case studies various control methods are discussed.

The author concludes that the most common acoustic problems in high rise buildings arise from;
- inadequate vibration isolation
- fan instability
- regenerated noise
- location of fan coil units in ceiling voids
- poor location of major equipment external to the building

1.0 INTRODUCTION

I have encountered a number of "classical" building services acoustics problems in over twelve years as an acoustic engineer. These "classical" problems result from contravening or ignoring basic principles at the design stage. Problems result for the builder, contractor and tenant. Addressing these basic principles at the design stage by well qualified engineers could have ensured no extra costs would have been incurred and achieved a better result. In "classical" problems that escape detection at the design stage, significant modifications are often required with the final outcome not as good as it could have been.

Generally the problems fall into 5 categories;
- inadequate vibration isolation
- fan instability
- regenerated noise
- location of fan coil units
- environmental noise

2.0 VIBRATION ISOLATION

The structure of modern high rise buildings is considerably lighter than they were 25 years ago. Consequence that the building is better able to carry structure borne sound. This is clearly noticed in how the impact of a hammer on a concrete floor can be clearly audible 10 floors below. In a recent project the author was required to reduce a noise problem in a court building in which screw compressors had been installed directly above a judges office. Initially the noise was NC65 in the office with the noise clearly audible all the way down 10 floors to ground level. The chillers had been placed on a plinth that was isolated from the main slab with a layer of high density fibreglass, having an overall thickness of 300mm. The chillers had been mounted on 25mm TICO cork pads (see figure 1). Upon initial evaluation it was clear that the main problem was the vibrational energy entering the structure through the cork pads. These were changed to 75mm deflection spring mounts and the noise level dropped to NC40 (still 10 NC units above specification). A sound source was used to generate the same room sound pressure level as the compressors in the plant room (95dBA). This noise was not audible in the room below and showed that the problem was structure borne noise. At this stage all the condenser water pipework had spring hangers installed and the room noise level dropped to NC35. The final reduction was achieved by placing 35mm thick rubber pads under the spring mounts to achieve a level just above NC 30. Throughout this exercise it was clear that the problem was insufficient vibration isolation .
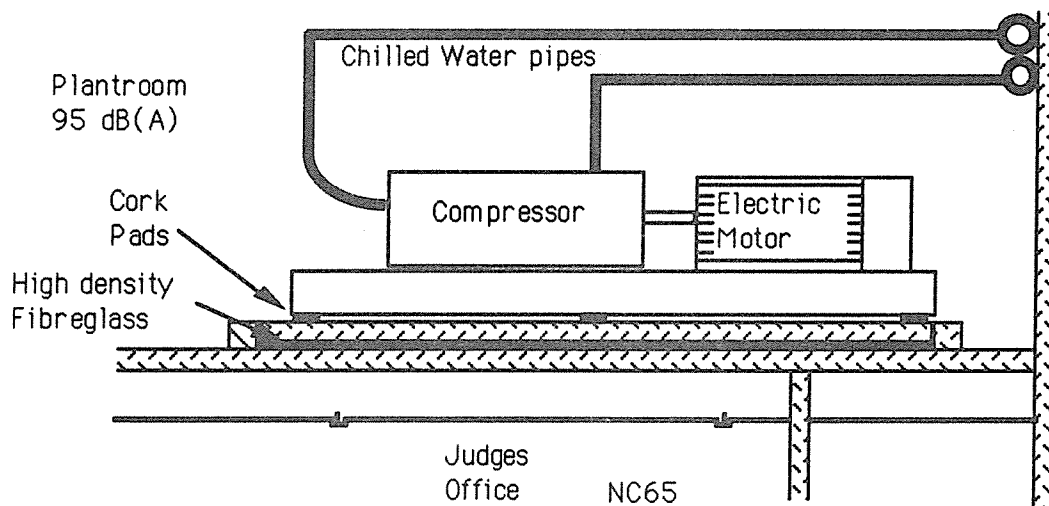
Figure 1: Compressor located above Judges office

Other problems experienced with insufficient vibration isolation relate to:
- ineffective vibration mounts on a toilet extract fan supported from the underside of guest room in a hotel
- 25mm spring mounts under a 650 kVA generator set located directly above a hotel executive suite. In this case the mounts were changed for air bags with the noise level in the room changing from 51dB(A) to close to 40dB(A) which was considered acceptable by all the parties involved.
- a generator set exhaust pipe anchored onto the under side of an office floor.
- refrigerant pipes mounted with out isolation off a floor slab and with the pipework in some instances touching the structural,wall penetrations. The consequence was that this energy travelled some 10m in the structure and radiated out in the hotel ball room at close to NR48, with a clearly distinctive tone.

129

2.1 FAN INSTABILITY

With the tendency in recent air conditioning systems to go to floor by floor air handling units there have been problems associated with noise from air conditioning plant rooms. This noise often breaks out of the ductwork and through the ceiling tiles (re figure 2).
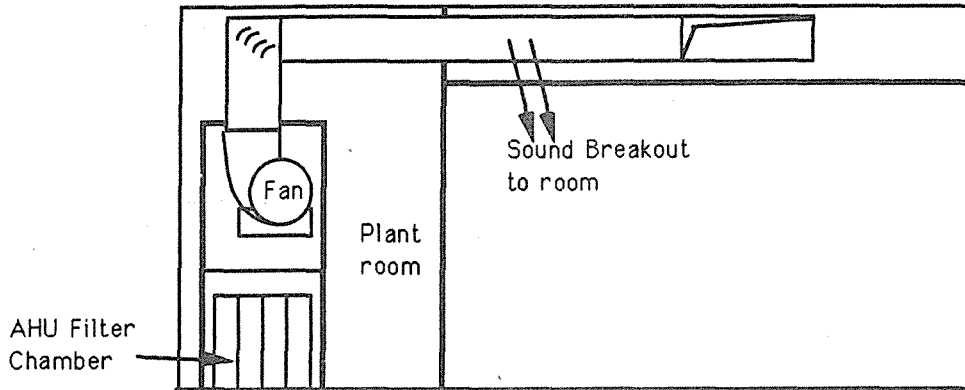
Figure 2: Breakout from AHU discharge Ducting

In some cases the noise is generated by the fan operating in an unstable point on its fan curve. Figure 3 shows a typical centrifugal fan curve.
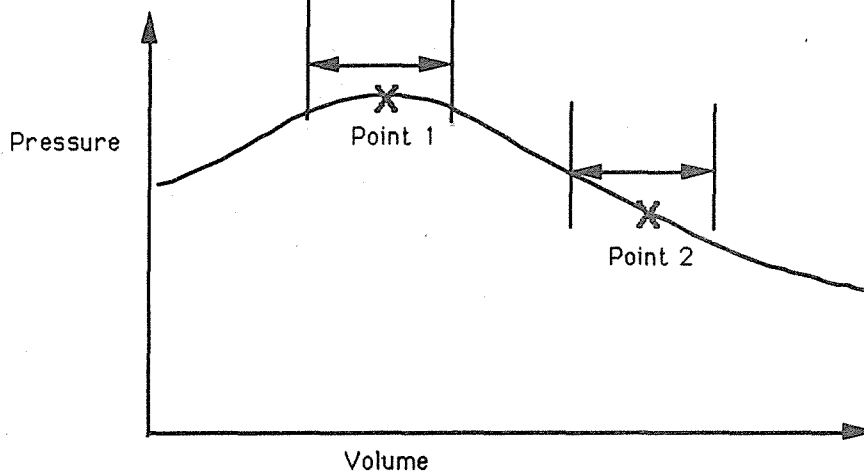
Figure 3 Fan curve showing two range of operations.
Positon 1 is not a suitable selection position.

If the fan were operating at point 2, it can be seen that under conditions of normal modulation of air volume from say a VAV box or duct damper, that the fan would operate up and down the fan curve. However at point 1 the fan has two points on the curve to oscillate from with the tendency to create instability within the fan. This is compounded by the fact that the fan as installed is in a very different configuration from that in which the test results were assessed and the fan curve derived. In practice due to turbulent discharge conditions a fan will tend to stall earlier than predicted by a standard fan curve. This argument also applies to the fan sound power levels which are determined by BS 484. Variations can in practice be at least 10dB above the test levels, particularly at low frequencies. These factors are very difficult to account for in practice and often a judgement based upon experience is required. In general the fan should be installed with at least 2 of the largest duct dimensions clear down the duct from the fan and the fan selected with as low a system resistance as possible. In one particular case in which this problem was encountered the fan was a 300mm diameter forward curved centrifugal fan operating at around 1000 rpm at 3200 l/s against a resistance of 600 Pa. Under this condition a noise level of close to NR38 was measured in the office space immediately outside the plant room. However at minimum air volume the duty change to around 1200 l/s against a resistance of 1100 Pa. Under this condition the noise level rose to around NR45 with a dominance of noise in the 31, 63 and 125 hz bands as shown in figure 4 below. The problem could have been solved by changing the method of modulating the air either by controlling the speed of the fan electrically or installing a by pas duct between the fan discharge and inlet. In this case for other reasons the fans were changed (all 38 of them !) for a larger fan running at a lower speed.
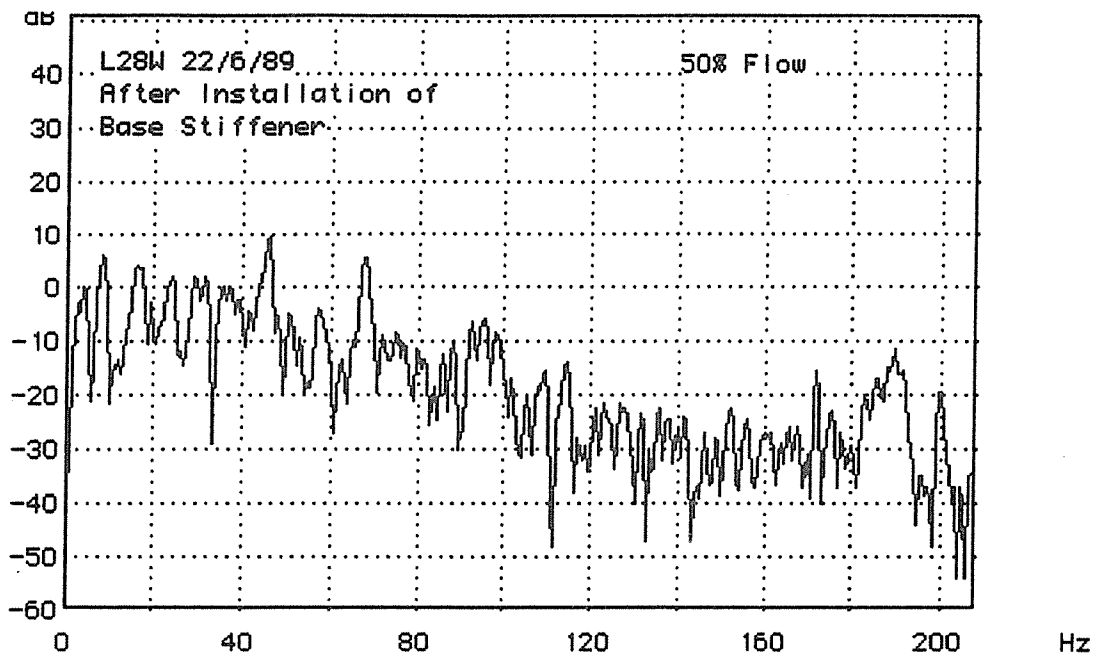
Figure 4 : FFT plot of dB / HZ for fan running at 50% flow .
Note 46 and 68 HZ peaks due to fan instability.

2.2 REGENERATED NOISE

This is often experienced in a number of forms. The most common is due to turbulent conditions at a diffuser or grille or say a return air grille. A commonly experienced condition is the installation dampers close to grills in noise sensitive areas, with the effect that if the damper is balanced to give more than say a 50Pa pressure drop, regenerated noise level in the room space will exceed NR35. A second condition is when ducts are sized to give high velocities with the consequence that turbulent airflow occurs and noise is generated at bends and duct branches. The solution with regenerated noise is to attempt to either reduce the system air volumes, increase the duct passage areas or reduce the duct turbulence. Regenerated noise problems can often occur in flexible acoustic ducting. This ducting enables air to be easily supplied in an insulated duct to various ceiling mounted diffusers. The problem with flexible ducting is that it can easily be set with sharp bends with the consequence that significant levels of noise can be regenerated. A recent case concerned an air-conditioning units ducting system in a high rise building. Because of architectural restraints the supply air registers were located off the side of the ducts and close to the fan discharge. In this case a level of NR50 was achieved instead of the design NR37 (re figure 5).
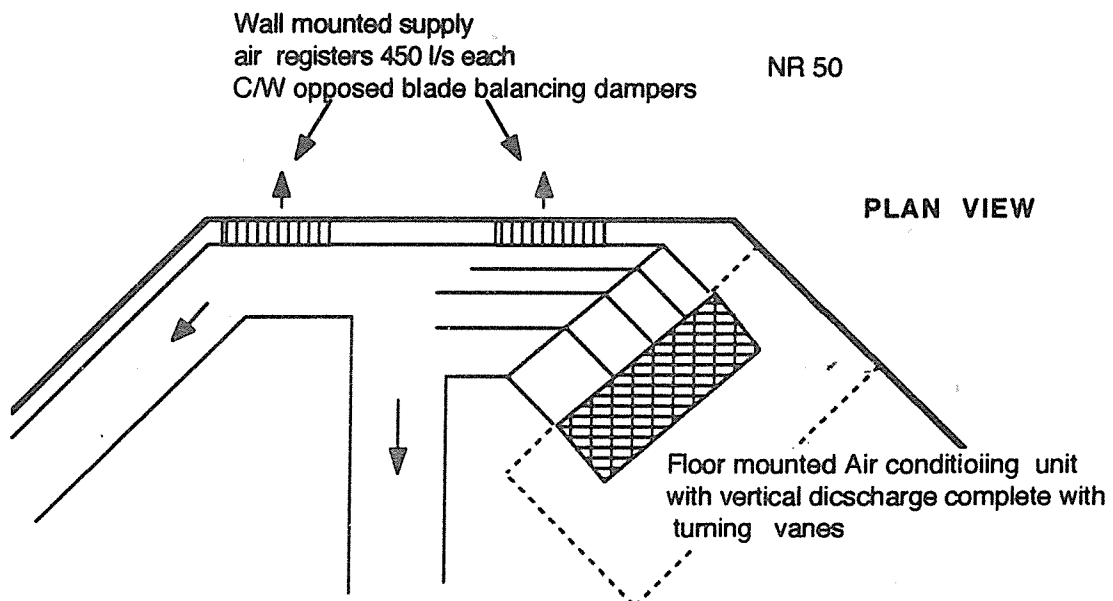
Figure 5 . Regenerated noise problem due to supply air registers too close to bends and taking directly off the side wall of the duct . All the ducts were lined internally with fibreglass

As with most acoustic problems regenerated noise is best solved at the design stage; at which time with the use of good standard practices the system can be appropriately sized (re ASHRAE Chap 53).

2.3 LOCATION OF FAN COIL UNITS IN CEILING VOIDS

With fan coil type air conditioning systems the major advantage is one of flexibility. The FCU can be located above the areas where the peak loads are to be relocated as tenancies change. They have the disadvantage that they can be noisy and with out careful consideration are likely to cause noise problems when above sensitive areas. Typically the noise can come from three locations (re figure 6):

- the return air side of the fan, particularly if a ducted system is used
- breakout from the case of the FCU
- breakout through the supply diffuser if the diffuser is close to the FCU.
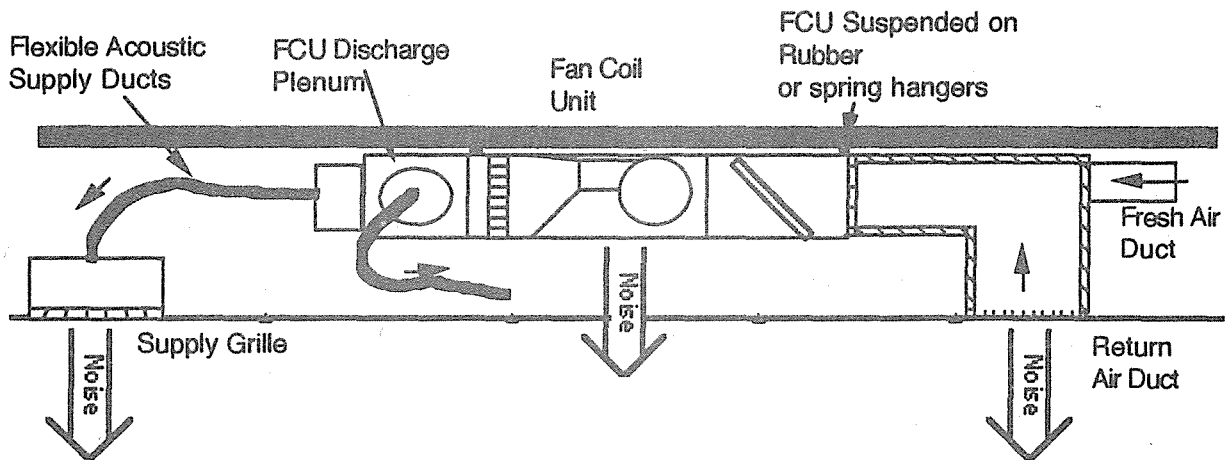
Figure 6: Fan Coil Unit above ceilig tiles
Noise Breakout

With FCU's around 800 L/s noise levels can be expected to be close to NR45 to 50 under the unit if a lightweight tile is used, the system has a ceiling void return and no special acoustic treatment considered. A ducted return can be expected to be close to NR50 to 55 if a short duct is used. From the authors experience FCU unit can usually be used successfully if the following is considered:

- selecting the fan at low static pressure
- increasing the mass of the ceiling tile
- placing 50mm fibreglass under the FCU to increase the ceiling absorption
- using "acoustic" flexible ducting
- selecting FCU with low sound power levels
- using a ceiling void return air system with the return air grills away from the FCU.
- vibration isolation for the FCU from the support slab and any ducting.

2.4 ENVIRONMENTAL NOISE

Frequently high rise buildings or retail developments are located near, or adjacent to noise sensitive areas. In these cases care must be taken that the services do not create excessive noise levels. Equipment such as car park extract fans, air cooled condensers, chillers, cooling towers, and pumps are all likely offenders. This problem has been experienced when an apartment air conditioning system cooling tower was located 5m from a residential boundary. In this case the tower was built within a 4m high fenced off area which served to effectively reduce the tower noise. However the pumps were forgotten resulting in noise levels of around 75dB(A) on the boundary. The problem was solved by building the pumps into an acoustic enclosure and installing a 2m high solid fence on the boundary.

3.0 CONCLUSION

By:
- the application of the basic principles of vibration isolation
- selecting fans and operating fans in a stable portion of their fan curve
- restricting duct and grille velocities to predefined values
- acoustically treating major plant located close to noise sensitive boundaries
- acoustically isolating hydraulic pipework above sensitive areas

the majority of the building services noise problems experience by the author could have been avoided.

Considerable cost could have been saved in the cases refereed to in this paper if sufficient detailed acoustic design had been carried out at the design stage.

THE PROPAGATION CHARACTERISTICS OF VIBRATION THROUGH BUILDING STRUCTURES

Nobuya Sakamoto, Kazutoshi Ishii
Environmental Survey Office Ltd., 4-1-29 Mita Minato-ku Tokyo 108 Japan

Tomotaka Hiramatsu, Heiichiro Ohkawa
Technical Research Center Taisei Corp., 344-1 Nasecho Totsuka-ku Yokohama 245 Japan

ABSTRACT

It is very difficult to estimate the propagation of vibration within complex structure buildings which is generated by machinery and equipments installed in the buildings or generated by trains runing along the nearby railway lines. In general, FEM technique has been adopted for the analysis of vibration propagation, but it seems to be inefficient due to time consumption and cost efficiency.
In order to acquire the propagation characteristics of vibration, we have carried out to the measurements of vibration in many buildings using the electro-dynamic shaker as a source of vibration.
The results show that the vibration propagation characteristics have a definite tendency on attenuation.

1, INTRODUCTION

There are a number of subway lines under the ground at the cities in Japan. The vibrations caused by these subway trains often travel into the nearby buildings. Furthermore, in recently-build buildings, structural frames become more and more light and thin, in order to reduce the weight and cost of construction.

These building constructions are more sensitive against the vibration generated by railway trains or machinery and equipments installed in buildings. For the prediction and vibration control of vibration or structure-borne noise in buildings, it is necessary to arrange the data banks on the vibration propagation characteristics in buildings. We have measured the propagation characteristics of vibration in these buildings using the electro-dynamic shaker as a source of vibration.

The measured values show that the attenuation of vibration energy with distance from excitation point has a definite tendency. That is, the attenuation of vibration energy through the building structures is represented by geometrical diffusion and internal dissipation in materials, just similar to the case of travelling waves in the infinitely homogeneous solid body.

In this paper, investigations into the propagation characteristics of vibration in two buildings, one of which extends in the horizontal direction and the is high in the vertical direction, are described.

2, MEASUREMENT

The outlines of two buildings are shown in Fig.1 and Fig.2. A-building has a three stories, reinforced concrete structure and B-building has 23 stories steel-framed reinforced concrete structure. Floor slabs in both buildings are excited by the method of a sine-sweep excitation using the electro-dynamic shaker and 1/3 octave-band acceleration levels are determined from the sweep-averaged acceleration that is synchronized with exciting force of the shaker by FFT analyzer.
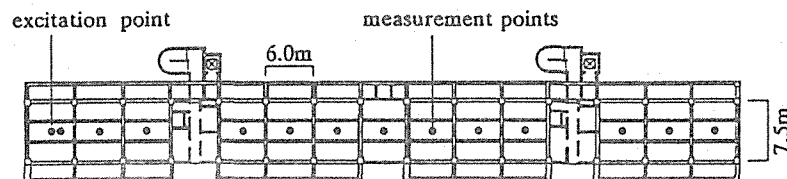
Fig.1 Position of an excitation point
and measurement points for A–building
(third floor plan)

3, PROPAGATION CHARACTERISTICS

Attenuations of vibration energy with distance from excitation point are shown in Fig.3 and Fig.4. These results show some common features. Firstly, attenuations of vibration energy is closely related to the distance from excitation point. Secondly, at high frequency regions, the

decrease in level per unit of distance is more than that for low frequency regions.

If the propagation of vibration energy through building structures is assumed to be similar to the traveling wave in the infinite solid body, amplitude of vibration at some distance from a vibration source can be represented by geometrical diffusion and internal viscous damping, as shown in the following equation;

$$u = u_s e^{-ar} r^{-n} \qquad (1)$$

where u is amplitude at distance r(m) from source and u_s the amplitude at the source.

α and n are internal damping factor and geometrical diffusion factor, respectively. Equation(1) is rewritten in terms of the distance from vibration source r_0 and r_i as follows.

$$\frac{u_i}{u_0} = e^{-\alpha(r_i - r_0)} \left(\frac{r_i}{r_0} \right)^{-n} \qquad (2)$$

where u_i/u_0 is the ratio of amplitudes at r_0 and r_i. Equation(2) becomes expressed by vibration acceleration level,

$$L_i = L_0 - N \log \left(\frac{r_i}{r_0} \right) - M(r_i - r_0) \qquad (3)$$

where L_i and L_0 are vibration acceleration levels at distance R_i and R_0, and $N = 10n$ and $M = \alpha \log e$ denote geometrical diffusion coefficient and internal viscous damping coefficient respectively. In case of A-building, by using the measured values and Eq.(3), M and N values are obtained by least square method and shown in Table.1(a) and curved lines in Fig.3.
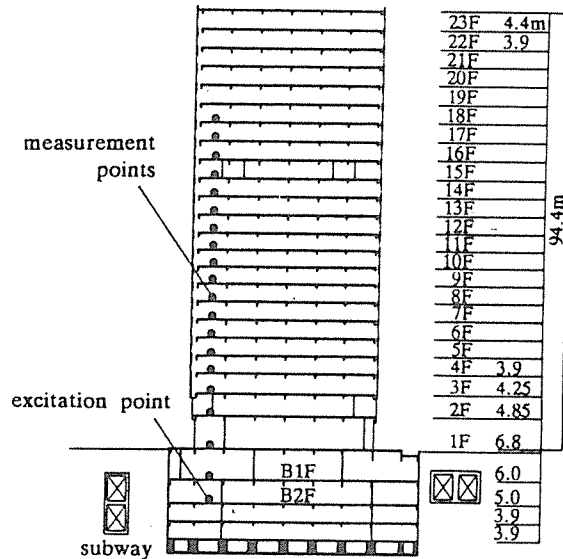
Fig.2 Position of an excitation point and measurement points for B-building (cross section)
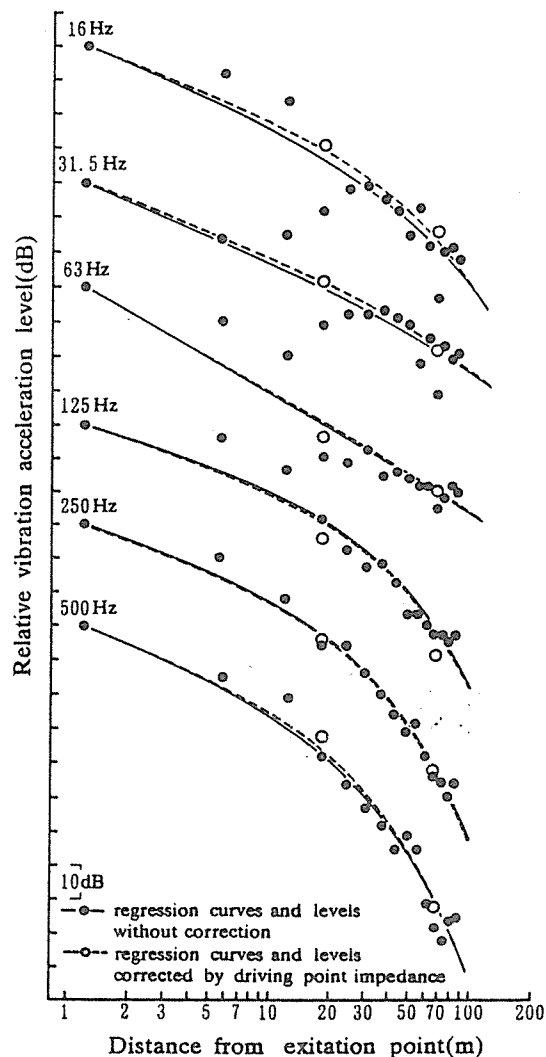
Fig.3 Attenuations of vibration in A-building and regression curves by method of least square

135

However, there are two core systems in this building. These sections of core systems have high impedance compared with other sections. The existence of these sections are not appropriate for assumption of Eq.(3). Accordingly, vibration level at core sections corrected by use of the difference of driving point impedance between core system floor and other sections floor. M and N values calculated from corrected measured values are shown in Table.1(b) and dotted lines in Fig.4. This results are somewhat small standard deviation of N value compared with Table.1(a). As shown in Table.1(b), N=21.4 (averaged value). If the geometrical diffusion in building constructions corresponds to the diffusion in the infinite solid bodies, theoretical value is N=20.

Fig.4 Attenuations of vibration in B—building and regression curves by method of least square

The experimentally obtained average N value may be seen to be in good agreement with the theoretical value. On the other hand, internal viscous damping coefficient M depends on the frequency as shown in Fig.5.

Table.1 Calculated N value for A—building.

Frequency(Hz)	16	20	25	31.5	40	50	63	80	100	125	160	200	250	315	400	500	Std—dev.	Ave.
(a) N	25.4	25.4	24.0	25.3	23.5	24.9	34.2	27.7	20.7	17.7	9.8	19.5	19.2	22.0	14.5	22.8	5.6	22.3
(b) N	21.8	22.0	22.3	23.0	21.4	23.8	33.0	26.2	20.7	18.9	10.5	21.0	19.6	22.0	14.5	21.7	4.8	21.4

The relation between M and α in Eq.(1), expressed in terms of frequency, is written as

$$M = \alpha \sqrt{f} \tag{4}$$

The measured value M is represented approximately by Eq.(4) and α may be nearly equal to 0.03. Cremer[2] gives decrease in level with distance for bending waves as

$$\Delta L_B = 4.34\pi \, \eta \, \Delta x / \lambda_B \tag{5}$$

By use of loss factor n(concrete, n=0.004~0.007) and thickness of 0.12m one can rewrite Eq.(5) in terms of frequency f as

$$\Delta L_B / \Delta x = 0.025 \sim 0.035 \sqrt{f} \tag{6}$$

From Eq.(6), the α value becomes 0.03 in case of the concrete materials. In the same way, in case of B-building, M and N values are obtained by least square method as shown in Table.2(a) and curved lines in Fig.2. The experimentally obtained N values are different from results of A-building. However, above 100Hz, the frequency characteristics of M are in good agreement with the calculated α values as shown in Fig.6.

These disagreement of N values may be caused by the difference in geometrical diffusion because of the fact that the excitation point is situated in the underground floor slab, and the attenuation of levels in vertical direction is larger than that in horizontal direction. At present, it is difficult to make clear the vibration propagation characteristics quantitatively in this case.
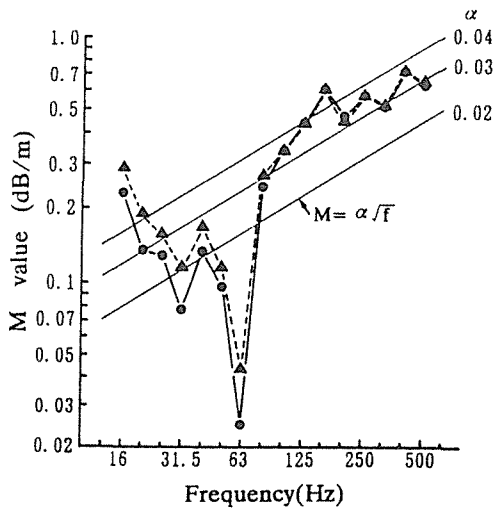
Fig.5 Calcurated M value for A—building
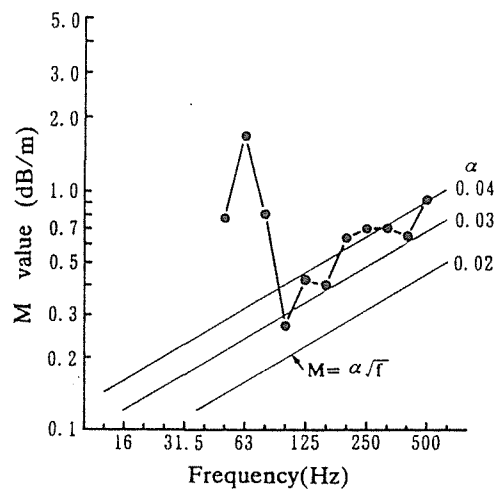
Fig.6 Calcurated M value for B—building

Table.2 Calculated N value for B—building.

Frequency(Hz)	16	20	25	31.5	40	50	63	80	100	125	160	200	250	315	400	500	Std—dev.	Ave.
N	-	-	-	-	-	-11.2	-41.4	-12.1	8.5	4.7	10.3	4.7	-6	7.6	8.9	4.3	15.45	-0.54

4, CONCLUSION

In case of a point excitation in buildings, the attenuation of vibration energy shows a definite tendency on attenuation. If the structure of buildings has continuous same sections like a geometrical uniform diffusion, it is possible to estimate the approximate attenuation of vibration levels. However, this attenuation of level is different from between vertical direction and horizontal direction.

5, REFERENCES

[1] Mastuda, "Propagation Characteristics of Sound in Building
    Structure." (in Japanese), INCE/JAPAN vol.14 No.1 1979.
[2]L.Cremer and M.Heckl, "Structure-Borne Sound.", Springer-Verlag 1973.
[3]Leo L.Beranek, "NOise and Vibration Control.", McGraw-Hill 1971.
[4]Ewing et al, "Elastic Waves in Layered Media.", McGraw-Hill 1957.

SOME EXPERIMENTS WITH PYEON-KYEONG;THE KOREAN TRADITIONAL PERCUSSIVE MUSICAL INSTRUMENT

J.H.Lee
Department of Electronics Engineering, Seoul National Univ.
Shinlim-dong, Gwanak-gu, Seoul 151, Korea

H.I.Kim
Department of Electronics Engineering, Seoul National Univ.
Shinlim-dong, Gwanak-gu, Seoul 151, Korea

Souguil Ann
Department of Electronics Engineering, Seoul National Univ.
Shinlim-dong, Gwanak-gu, Seoul 151, Korea

ABSTRACT

Time-varing spectrum analysis is performed on Pyeon-kyeong; one of the Korean traditional percussive musical instruments. The fundamental frequency of Pyeon-kyeong is important because it is used as a tuner when playing Dang-ak; a kind of Korean traditional musical forms. Therefore, the measurement of Pyeon-kyeong's fundamental gives the basis on the research of the entire Korean traditional music.

Pyeon-kyeong is composed of sixteen hard stones, usually made of jadite, each of which is shaped in the Korean letter " ㄱ ". Pyeon-kyeong is played by striking them with a mallet tipped with the horn of a cow.

In our experiment, time variant spectra of Hwang-jong-kyeong's tone corresponding to C5 of the piano , are computed and analyzed by using short time FFT with ten Pyeon-kyeongs manufactured in different periods. Also, the influence of the striking point upon the spectra is examined. Such results may be used to alter the mechanical structure of Pyeong-kyeong for the improvement of its timber and playing method.

139

1.0 INTRODUCTION

The research on the musical instrument by the analyzing the spectrum of its sound has been done by many scientists for a long time and considerable results have been reported. With those significant results, many studies on the development and the improvement of its form and sound have been accompanied, and they have contributed to the progress of musical instrument. Also, such theoretical studies has been applied to the western musical instruments from the early times. But the application of these analyses on the eastern musical instruments did not begin till several researchers had interests on the eastern musical instruments recently.

In the case of Korean traditianal musical instruments, there is little works done on analysis of the spectra of them. Therefore, a full-scale spectrum anslysis on the entire Korean traditional musical instruments is needed because it gives the basis to understand the Korean traditional music. To begin with, the study on Pyeon-kyeong has attracted more attention because it makes an important role in the Korean traditional musical form,"Dang-ak" - because its fundmental tone, "Hwang-jong-eum", is used as the reference when tuning the tone of other Korean traditional musical instruments.

2.0 THE PYEON-KYEONG

Generally, the Korean traditional music is classified by two parts; 'Hyang-ak' and 'Ah-ak'. As a kind of Ah-ak, 'Dang-ak' which was imported from China in earlydays makes an important role in the music played at the Royal Court. Pyeon-kyeong, the stone chimes, is the melodic instrument and has been used ever since it was imported from China during Koryo dynasty. Nowadays it is played in Confucian and royal ancestral shrine music. Pyeon-kyeong is important in Korean traditional music because

a)   b)
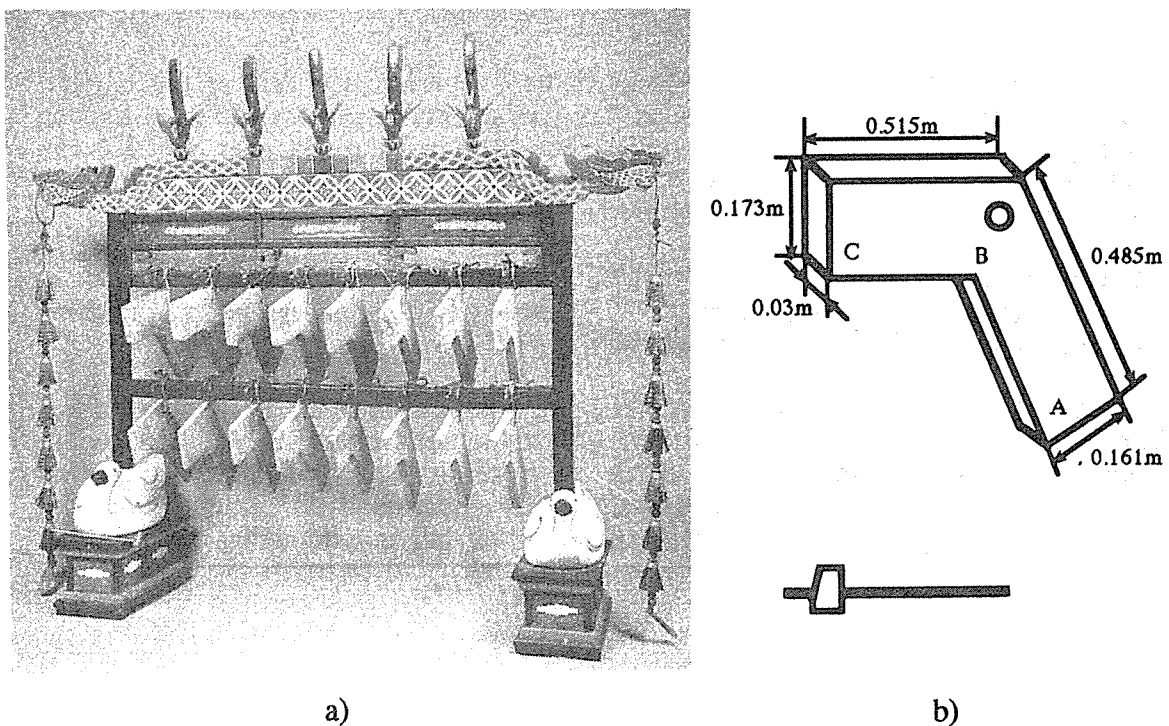
Fig. 1 a) The front view of Pyeon-kyeong.
b) The size of Kyeong, one of the sixteen bent stones which compose Pyeon- kyeong and a mallet.

the sound of Hwang-jong-kyeong is used as a tuner when playing Dang-ak. Pyeon-kyeong consists of a set of sixteen hard stones, usually made of jadite. Each of them is arranged by two upper and lower lines according to the order of tones as shown in fig 1(a). Each stone called 'Kyeong' is bent in the shape of the Korean letter "ㄱ ", or an inverted letter "L" also shown in fig. 1(b). The both arms of the bent stones have different sizes. Also, the ratio of the longer side to the shorter side of each stone, Kyeong, is different acording to the tone. For Hwang-jong-kyeong, the stone which produces the tone of 'Hwang-jong-eum', the longer side of it is long as one and a half times as the other side. Pyeon-kyeong is played by striking the lower end of the longer side of each stone with a mallet tipped with the horn. When munufacturing Pyeon-kyeong, if one of the Kyeongs produces too high tone over the correct one, the manufacturer makes its thickness thin by grinding it. If too low, he makes the longer arm shorter by grinding the end of it.

3.0 EXPERIMENTAL MEASUREMENTS

For ten kinds of Hwang-jong-kyeongs, the signals were analyzed by using the short-time Fourier transform(SFT) in order to decide the fundamental frequency as the reference when tuning the Korean traditional musical instrument and to understand the characteristic of Pyeon-kyeong including the influence of the different striking point on the spectrum.

The sounds were recorded by means of an AKG 414EB condenser microphone and a Teac X-2000 reel tape recoder in the recording room of the I.M.C.(Instructional Media Center) of Seoul National University. The reverberation time of the recording room was 0.2 seconds. The signal went from the microphone to the recorder and recorded on the digital audio tape, DENON DTR-100P. Each Hwang-jong-kyeong was set up with a microphone suspended 0.5m from the struck side of it in order to maintain a high signal-to-noise ratio, while at the same time minimizing other noise elements originating in the instrument itself. This microphone was on an axis perpendicular to the face of Hwnag-jong-kyeong. For the accuracy of the recording, the sound of the same Hwang-jong-kyeong was recorded three times by striking it the same number of times. The recorded signals were replayed and became the input to TMS320 digital signal processing board through the analog-digital converter and analyzed by using FFT. The signals were sampled at 40KHz and windowed by rectangular window of 2048 points (51.2ms). But, as usually at the transient period the frequency spectrum of Pyeon-kyeong is considerably complicated, so it is difficult to find the tone frequencies against the noise band because the meaningful partial frequencies are not dominant over the noise, sometimes. So we made time-frequency analysis by using SFT to determine the fundamental frequency and partial frequencies which last for a long time. Also, with those data obtained from the time-frequency analysis, the decay rates of the fundmental frequency and the partials were easily calculated. These data such as the fuandamental frequency and partials, sound pressure level, decay rates are important to synthesize the Pyeon-kyeong sounds.

Also, for one of several Hwang-jong-kyeongs, in order to know the influence of striking point on the spectra, we examined the three different kind of spectra with changing the striking points; the lower end of longer side(correct point), that of shorter side, and the connecting point of both sides which were named A,B, and C as shown in fig. 1 (b)

4.0 RESULTS AND DISCUSSION

Hwang-jong-kyeong's signal is very complicated at the beginning of the sound. As

Table 1. The frequencies of the partials.
    a) when striking the point A.
    b) when striking the point B.
    c) when striking the point C.

| [Hz] | PK#1 | PK#2 | PK#3 | PK#4 |
	avg	avg	avg	avg
1st Freq	527.30	537.10	532.20	537.10
2nd Freq	786.10	766.60	805.70	766.60
3rd Freq	1226.00	1255.00	1240.00	1255.00

(a)

| [Hz] | PK#1 | PK#2 | PK#3 | PK#4 |
	avg	avg	avg	avg
1st Freq	527.30	537.10	532.20	537.10
2nd Freq	786.10	766.60	805.70	766.60
3rd Freq	1226.00	1255.00	1240.00	1255.00

(b)

| [Hz] | PK#1 | PK#2 | PK#3 | PK#4 |
	avg	avg	avg	avg
1st Freq	527.30	537.10	532.20	537.10
2nd Freq	786.10	766.60	805.70	766.60
3rd Freq	1226.00	1255.00	1240.00	1255.00

(c)

time passed, the signal becomes approximately pure sine wave which determines the tone of Hwang-jong-kyeong. Table 1 shows the fundamental frequencies and the partial frequencies of four samples among ten Hwang-jong-kyeongs. Although they were made in different periods, their fundamental frequencies which represent the tone of each Hwang-jong-kyeong range from 527Hz to 537Hz. The average of the fuandamental frequency is 532.2Hz. Their second and the third partial frequencies also have the similar value to each other. Also, though striking the different points for the same Hwang-jong-kyeong, the fundamental frequency and the partial frequencies are the same. These frequencies contribute to the tone colour of the musical instrument. A half of average fundamental frequency is 266.1 Hz and this value corresponds to middle C of piano in western music. Actually that value makes a role of the reference when tuning other instruments in Dang-ak. Maybe the reason that the fundamental frequency of Hwang-jong-kyeong is set up at twice as high as that of the reference is to preserve Pyeon-kyeong for a long time against the fragility by making its width sufficiently thick.

However, not only for each different Hwang-jong-kyeong but also for the each different striking point of the samewhat Hwang-jong-kyeong, the decay rates are some different. Table 2 shows the results for several Hwang-jong-kyeongs. For the former case, the difference of the decay rates result from that of the damping loss between them. The difference of the damping loss may be caused by the difference of the time when they were manufactured. But, for the latter case, the difference of decay rates may be caused by the difference of the dominant modes. In other words, according to the striking points, which arm of the bented stone produces the modes more efficiently is determined. From the table 2, we can find the interesting phenomena. In the case of the fundamental frequency and the second overtone, the point A makes them last relatively longer than the point B or C. On the contrary, the first overtone lasts longer when the point C was striken. Although the precise structural analysis is required, the first and the third partials seem to be related to the longer arm of the Hwang-jong-

Table 2. The decay rates of the partials.
   a) when striking the point A.
   b) when striking the point B.
   c) when striking the point C.

| decay rate | PK#1 | PK#2 | PK#3 | PK#4 |
[dB/sec]	avg	avg	avg	avg
1st Freq	22.67	27.72	37.96	26.87
2nd Freq	67.76	42.46	47.13	41.70
3rd Freq	69.73	66.25	108.87	66.93

(a)

| decay rate | PK#1 | PK#2 | PK#3 | PK#4 |
[dB/sec]	avg	avg	avg	avg
1st Freq	23.59	26.28	37.22	25.93
2nd Freq	63.06	41.29	49.59	40.76
3rd Freq	69.92	65.84	101.41	52.72

(b)

| decay rate | PK#1 | PK#2 | PK#3 | PK#4 |
[dB/sec]	avg	avg	avg	avg
1st Freq	23.31	27.46	41.62	27.08
2nd Freq	44.62	37.17	55.72	40.68
3rd Freq	92.28	69.64	107.85	72.22

(c)

kyeong and the second partial to the shorter. Fig. 3 shows the rapid decay rate of the fundmental to other overtones when striking the shorter arm of Kyeong. It may be also corroborative of the above assumption. In addition to that, the ratio of the first partial to the second is almost same as that of the length of both arms, i.e. 1.5: 1. It makes us interested. These phenomena may give the clue to understand the acoustical structure of Pyeon-kyeong. Meanwhile, Fig.2 and fig. 3 represent how the change of the striking point gives the influence on the spectrum of Hwang-jong-kyeong. As shown in the spectrum, the peaks of the partial frequencies were observed as if the two kind of spectra overlaped together. From the results shown above, we could say that the vibration modes of Pyeon-kyeong are explained as those of two vibrating plates. One end of the one plate is attached to that of the other with an angle, where the joining point acts as a node. Also fig. 2 and fig. 3 shows that the sound of the point B or C is qualitively bad because the overtones last comparatively long time compared to the fundamental after considerable time passed. This phenomenum gives bad affection to the tone of Pyeon-kyeong.

5.0 CONCLUSION

The average value of the fundamental frequencies of ten Hwang-jong-kyeongs, which determine the tone of each Hwang-jong-kyeong was 532.2Hz. Hwang-jong-kyeong is the one of the sixteen bent stone of Pyeon-kyeong. A half value of it was 266.1Hz and this value is similar to that of middle C of piano. As other musical instruments are tuned to this value as a reference on playing Dang-ak, it is important to understand the Korean traditional music.

As well as the fundamental frequency, the overtones were similar between those Hwnag-

jong-kyeongs though the era when they were made was different each other. But the decay rates of them were different and it implies that the damping losses of them are different, which may be caused by the fact that they were manufactured in different periods.

When the striking points changed for the same Pyeon-kyeong's Hwang-jong-kyeong, the observed spectra showed different characteristic. This is caused by the change of the modes which are produced efficiently according to where the striking point is. From the spectra at the steady state and the time varying spectra of the sound, the sound produced when striking the lower end of the longer arm lasts long and its fundamental frequency remains strong compared with other overtones.

Finally, from the spectra of them, the vibrating modes of Pyeon-kyeong may be explained as thoes of two attatched plates which have the node at their joint point, although more analysis on the structure of Pyeon-kyeong is required.

REFERENCES

Lehman P.R., Harmonic Structure of the Tone of the Bassoon, Journal of the Acoustical Society of America, 36(9), 1649-1653, (1964).

Beauchamp J.W., Time-variant Spectra of Violin Tones, Journal of the Acustical Society of America, 56(3), 995-1004, (1973).

Weyer R.D., Time-Varying Amplitude-Frequency-Structures in the Attack Transients of Piano and Harpsichord Sounds-II, ACUSTICA, 36(4), 241-258, (1977).

Fletcher H., Bassett I.G., Some Experimental with the Bass Drum, Journal of the Acoustical Society of America, 64(6), 1570-1576, (1978).

Rossing T.D., Fletcher N.H., Nonlinear Vibrations in Plates and Gongs, Journal of the Acoustical Society of America, 73(1), (1983).

Feng S., Some acoustical measurements on the Chinese musical instrument P'i-P'a, Journal of the Acoustical Society of America, 75(2), (1984).

Kuntz H.L., Hixson E.L., Vibration Characteristics of the Two Buoy Bells, Journal of the Acoustical Society of America, 79(6), (1986).
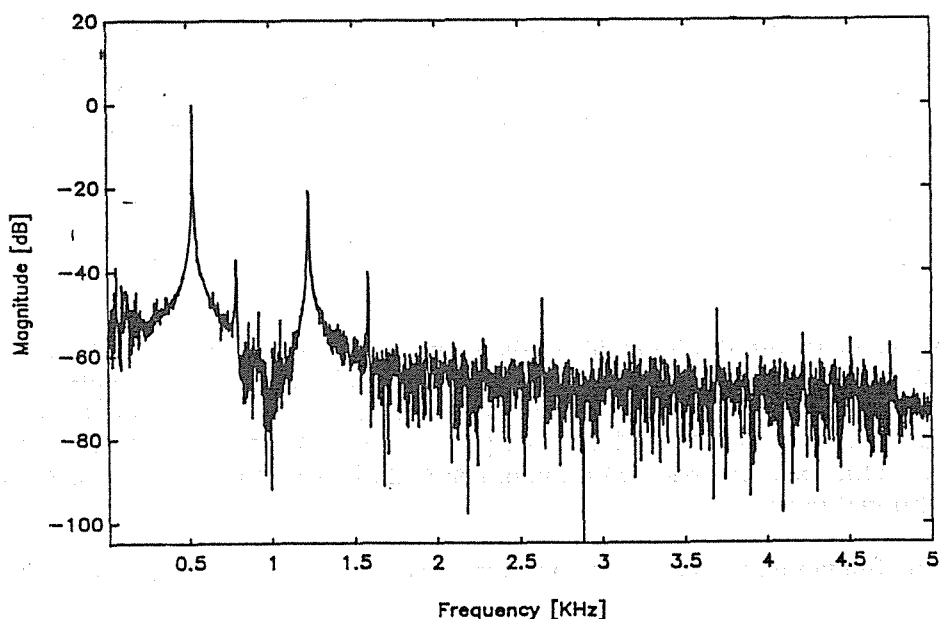
(a)
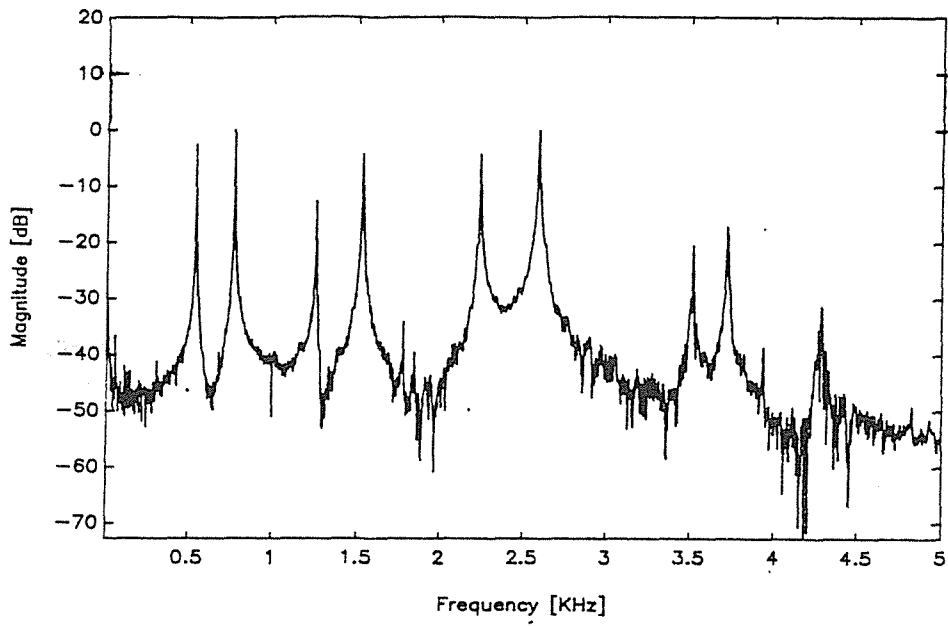
(b)
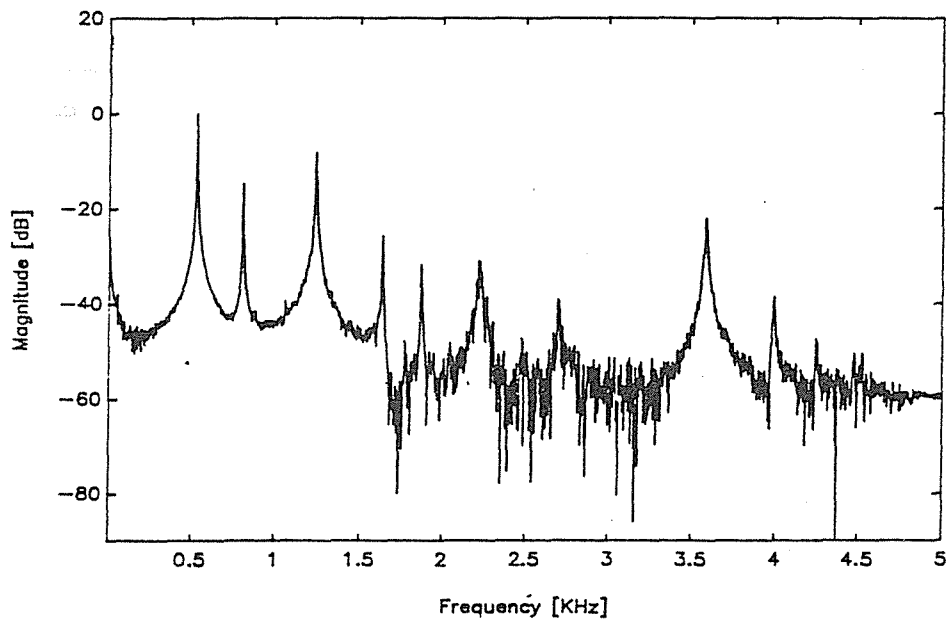
(c)

Fig. 2. The spectra of Hwang-jong-kyeong at steady state (0.5sec. after striking).
a) when striking the point A.
b) when striking the point B.
c) when striking the point C.

145

7 KHz

0   **3.0 sec.**

(a)

7 KHz

0   **3.0 sec.**

(b)

7 KHz

0   **3.0 sec.**

(c)
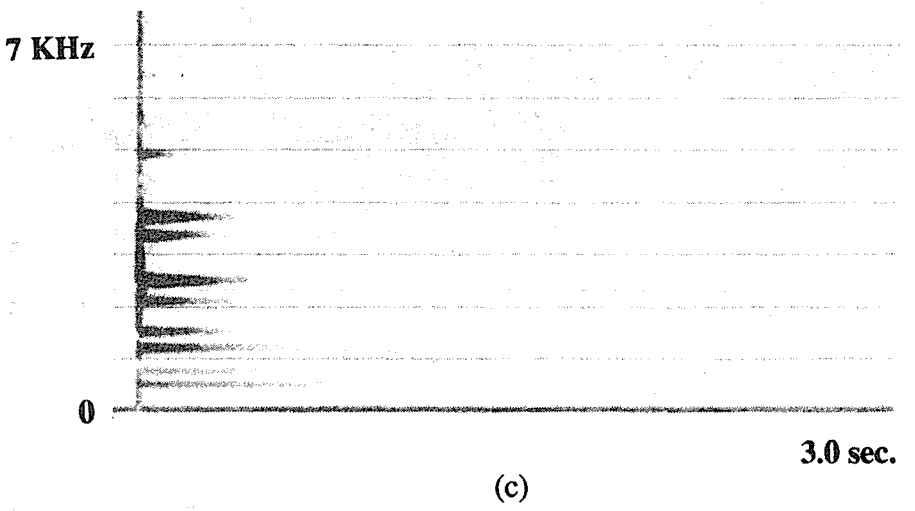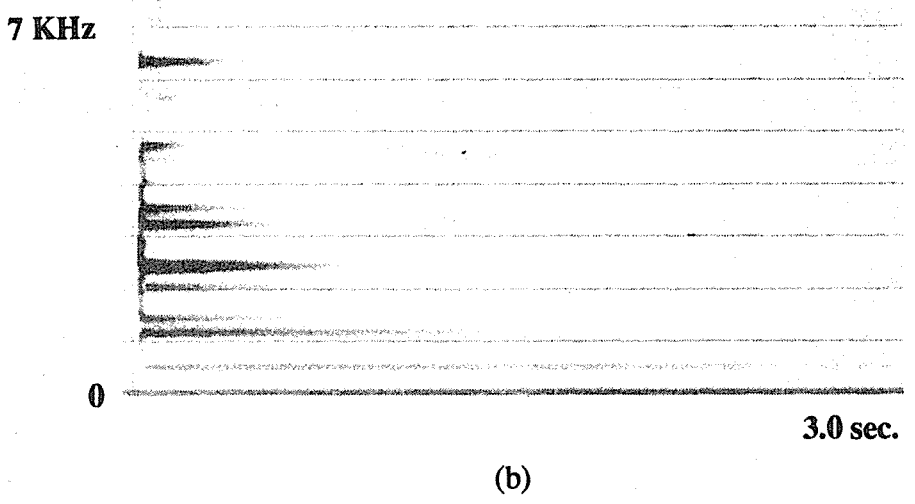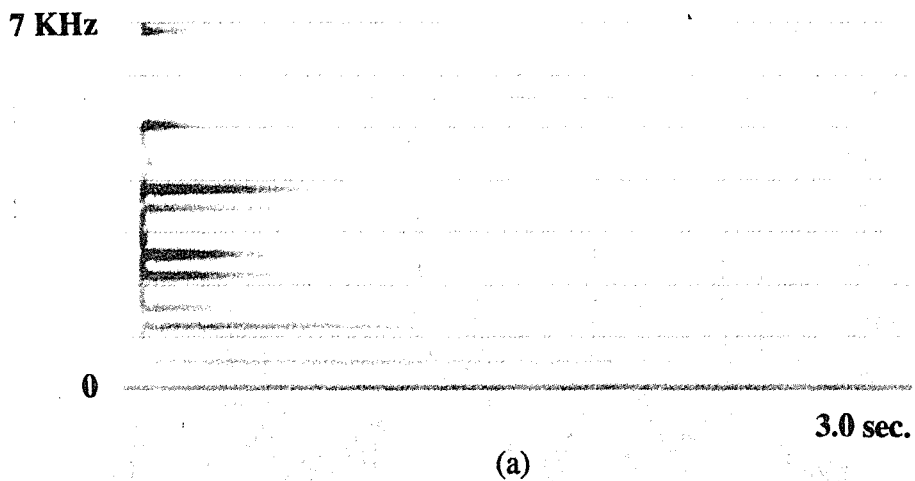
Fig. 3. Time variant spectra of Hwang-jong-kyeong.
　　 a) when striking the point A.
　　 b) when striking the point B.
　　 c) when striking the point C.

146

THE ACOUSTIC ABSORPTION OF SOME STAINLESS STEEL WIRE PACKINGS

C.A. Garson
Sugar Research Institute, Mackay

B.L. Manser
WBM Pty. Ltd., Brisbane

ABSTRACT

The performance of conventional, fibrous acoustic packings can be quickly degraded by the service environment in some applications. The acoustic absorption of two stainless steel wire products has been investigated with a view to their use as acoustic packing in steam exhaust silencers in raw sugar factories. The results obtained indicate that the stainless steel wire products should be effective packings for absorptive silencers. However, the amount of packing required to achieve an acceptable level of acoustic absorption is such that the cost of the stainless steel wire packing is much greater than that of conventional packings. This is considered likely to make silencers incorporating stainless steel wire packings uneconomic for routine applications such as steam exhaust silencers in sugar factories. There may be other applications in which the extended life of stainless steel wire packing would outweigh the greater initial cost.

1.0 INTRODUCTION

The process of making raw sugar from sugar cane involves squeezing and washing the juice from the fibrous part of the sugar cane plant and then concentrating the juice under vacuum until crystallisation can be induced under controlled conditions. The resultant sugar crystals are separated from the molasses in a centrifuge. After separation of the juice, the fibrous part of the sugar cane plant is used as fuel to produce high pressure steam for motive power. The low pressure exhaust steam from the steam turbines is used for process heating. The details of factory operation are such that the venting of low pressure steam to atmosphere is relatively frequent.

Absorptive silencers are used to control the noise from these steam vents. The packing normally used in these silencers is industrial fibreglass blanketing protected by a facing of perforated steel sheet, woven steel mesh and a layer of fibreglass tape. Experience indicates that this arrangement has an effective life of less than five years because of deterioration of the fibreglass packing.

2.0 SCOPE OF INVESTIGATION

The work presented in this paper involved an investigation into the feasibility of using stainless steel wool packings in the absorptive silencers fitted to steam vents in sugar factories. It was anticipated that the stainless steel would have an effective life considerably longer than that of fibreglass.

Specifically, the investigation sought to identify sources of stainless steel wools and quantify the acoustic performance of those products that might be suited for use as absorptive packing in steam silencers. A preliminary evaluation of cost effectiveness was also desired.

3.0 RESULTS AND DISCUSSION

Only two stainless steel wool products likely to be effective as packing materials were identified. Tests were conducted on samples of each of these stainless steel wool products and on a sample of fibreglass blanket for comparison. The three materials have been designated A, B and C in this paper. Details of the products were as follows:

Material A. This was a flexible fibreglass blanketing typical of the materials usually used by sugar factories to pack steam silencers. The material tested had a nominal, uncompressed thickness of 50 mm.

Material B. The form of this material was a continuous knitted sock of stainless steel wire. The wire from which this product was knitted was approximately rectangular in cross-section with dimensions of 0.4 mm x 0.1 mm.

Material C. This material was in the form of small, individual pads of entangled stainless steel wire. The wire from which these pads were formed was also approximately rectangular in cross-section but with dimensions of 0.4 mm x 0.05 mm.

To quantify the absorptive performance of the various materials, normal incidence absorption coefficients were determined. This was done by the Department of Mechanical Engineering, University of Queensland using impedance tube apparatus. The absorption

148

coefficients were measured at octave band centre frequencies
with 1/3 octave filtering for various arrangements of each of
the packing materials. A facing of perforated steel sheet (2 mm
thick sheet with 3 mm diameter holes at 5 mm staggered spacing),
woven stainless steel gauze (0.5 mm aperture, 0.28 mm diameter
wire) and a layer of fibreglass cloth tape (for the fibreglass
blanket only) was used in the tests. Where the test geometry
involved an air gap behind the packing, a similar facing was
used to restrain both sides of the packing. These facings are
typical of those used in actual silencers in sugar factories.

Two series of tests were carried out. These are described in
turn below.

3.1   Test 1.   Absorption coefficient tests were carried out on
the following arrangements in the first series of tests:

－   One layer of the fibreglass blanket (material A) compressed
     to a thickness of 40 mm (bulk density approximately
     60 kg/m^3).

－   Two layers of the fibreglass blanket (material A)
     compressed to a thickness of 80 mm (bulk density
     approximately 60 kg/m^3).

－   An 80 mm thickness of the knitted stainless steel product
     (material B) packed to bulk densities of 100 kg/m^3 (lightly
     compressed), 270 kg/m^3 (an intermediate bulk density) and
     330 kg/m^3 (approximately the highest bulk density that could
     be achieved when packed by hand).

－   An 80 mm thickness of the stainless steel pads (material C)
     packed to bulk densities of 260 kg/m^3 (lightly compressed)
     and 380 kg/m^3 (approximately the highest bulk density that
     could be achieved when packed by hand). The bulk density
     of these pads when unconstrained was greater than 100 kg/m^3
     so no test could be done close to that density.

The results obtained are shown in Figure 1. Several effects may
be noted from inspection of the figure:

－   As expected, the greater thickness of fibreglass blanket
     had a beneficial effect on sound absorption, particularly
     at the lower frequencies.

－   The high frequency absorption (8000 Hz) of all the
     materials was good. This was also expected since high
     frequency noise is relatively easy to absorb.

－   The performance of the stainless steel pads (material C)
     was clearly superior to that of the knitted stainless steel
     product (material B) at the mid frequencies. Since sound
     absorption at lower frequencies normally increases with
     increasing flow resistivity of the packing material, it is
     instructive to consider this response in terms of flow
     resistivity and the influence of fibre diameter (Beranek).
     The same flow resistivity could be achieved at lower bulk
     density if stainless steel wool comprising wires of smaller
     cross-section were available. This might impact greatly on
     the economic viability of using stainless steel wool
     packings.

－   The absorption of the stainless steel products generally
     improved with increasing bulk density. This is consistent
     with the expectation of a higher flow resistivity with
     increased bulk density.

149

A second set of tests was subsequently carried out as a result of the findings from Test 1.
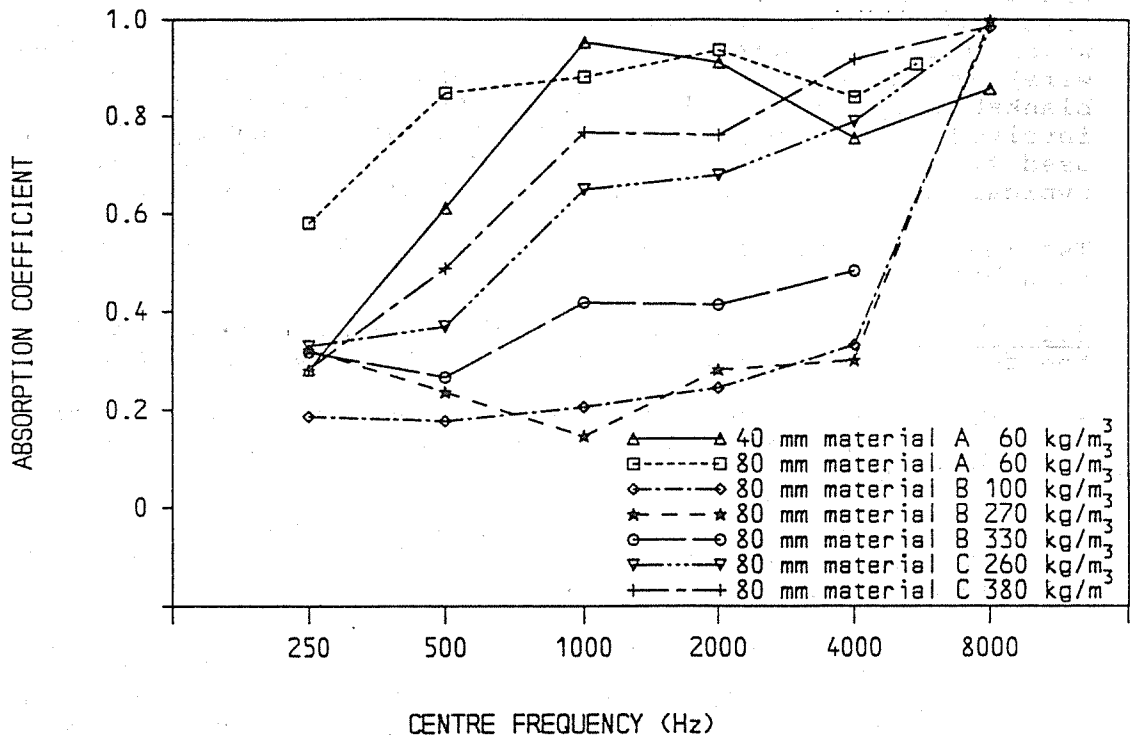
Figure 1.   Normal Incidence Absorption Coefficients of Various Packing Materials and Arrangements.

3.2   Test 2.   Only material C was evaluated in the second set of tests because it appeared the more promising of the two stainless steel wools.   Two physical arrangements of this material were evaluated at the bulk densities of 260 and 380 kg/m³.   The arrangements tested were as follows:

-   A 50 mm thickness of the material.   This was done to investigate the loss of performance with thickness of the layer of packing.

-   A 50 mm thickness of the material backed by a 30 mm air gap.   This was done to examine the significance of any improvement in absorption performance associated with introduction of the air gap.

The results from the second set of tests are presented in Figures 2 and 3 for the bulk densities of 260 and 380 kg/m³ respectively.   Results from the first series of tests for an 80 mm thickness of the fibreglass blanket (material A) and 80 mm of the stainless steel pads (material C) have been reproduced in Figures 2 and 3 for comparison.

Inspection of Figures 2 and 3 reveals the following features:

-   Reducing the thickness of the packing from 80 mm to 50 mm resulted in generally degraded performance.

-   Incorporation of a 30 mm air gap behind a 50 mm thickness of the packing increased the absorption performance below 2 000 Hz to a level almost as good as that achievable with 80 mm of the packing.

150
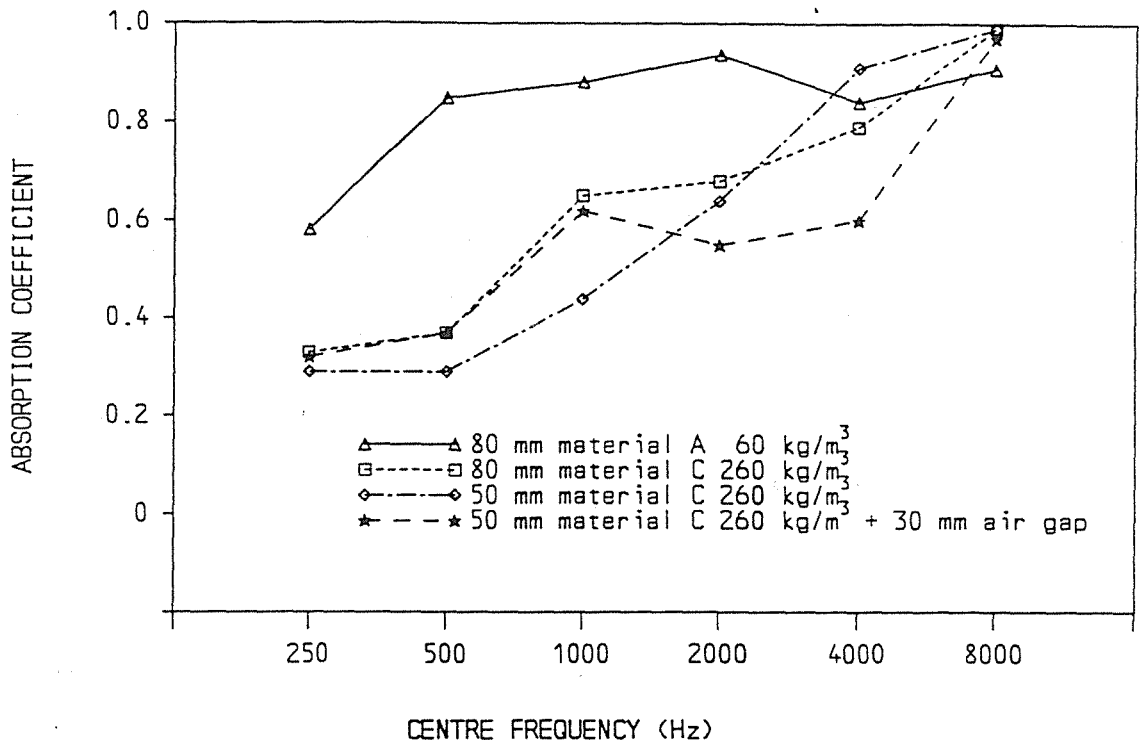
Figure 2. Comparison of Normal Incidence Absorption Coefficients for 80 mm of Material A and Various Arrangements of Material C Packed at a Bulk Density of 260 kg/m³.
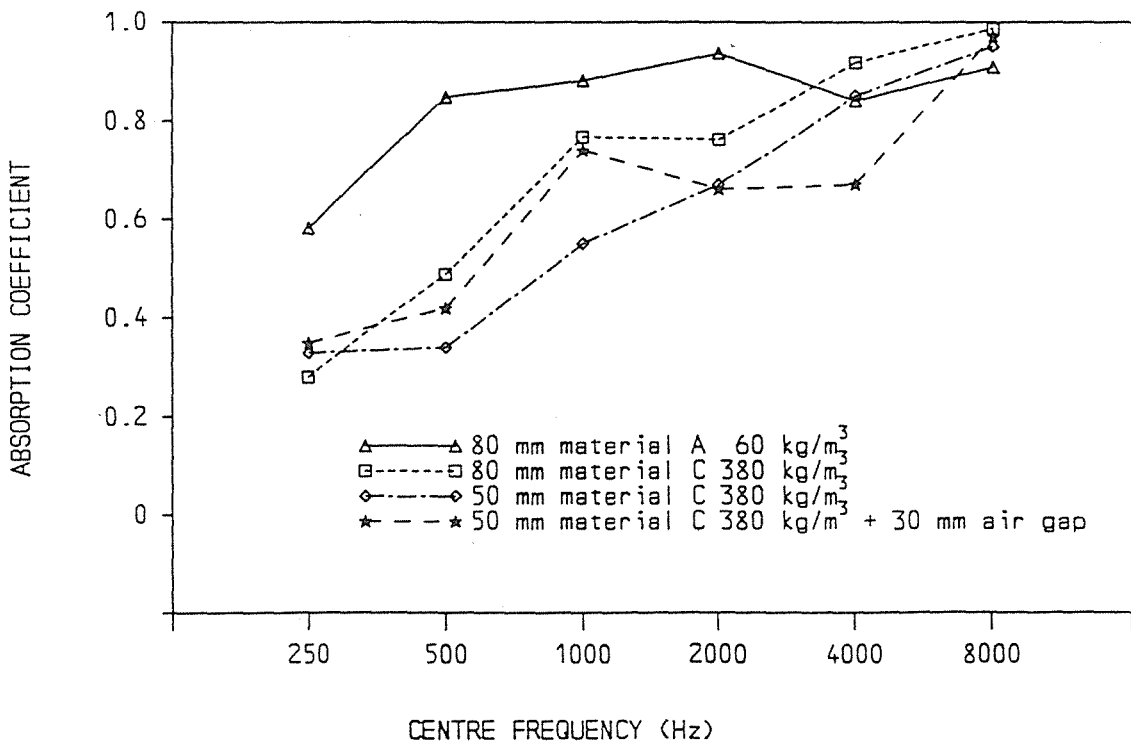
Figure 3. Comparison of Normal Incidence Absorption Coefficients for 80 mm of Material A and Various Arrangements of Material C Packed at a Bulk Density of 380 kg/m³.

Comparison of Figures 2 and 3 reveals that for material C, performance of the more tightly packed material was generally superior at the lower frequencies for all arrangements of the packing. However, the performance of material C did not approach that of 80 mm of the fibreglass blanket (material A) at the lowest frequency for any of the arrangements investigated.

3.3 Cost Comparison. For the purposes of the cost comparison, it was assumed that a 100 mm thickness of material C packed to a bulk density of 380 kg/m^3 would offer the same acoustic performance as 100 mm of fibreglass blanketing. A cash flow comparison of these two packings was performed for a silencer of 0.6 m internal diameter and 3 m length.

The life of a fibreglass packed silencer was assumed to be three years at which time it would require repacking. This was thought a conservative assumption with regard to justification of the use of stainless steel wool packing. It was further assumed that a silencer packed with stainless steel wool would require no maintenance at all during the period of interest. Estimates of the required rate of return, inflation and cost of repacking a silencer were also made.

On the basis of the assumptions made, the "break even" period for the silencer packed with stainless steel wool as opposed to the usual fibreglass blanket was calculated to be about 15 years.

4.0 CONCLUSION

The results obtained during this investigation indicate that a packing material of commercially available stainless steel wool can exhibit good sound absorption performance when an appropriate fibre size, packing thickness and bulk density are selected. Stainless steel wire products thus represent a real alternative to conventional fibreglass packings for applications in which fibreglass packings degrade rapidly.

It is envisaged that a packing material of stainless steel wool would suffer minimal degradation in a sugar factory steam exhaust silencer. Conventional fibreglass packing can have a life of only three years in this environment.

The material cost of the stainless steel packing has been found greater than that of fibreglass of equivalent absorption by a factor of about 20. A cash flow comparison has shown that stainless steel wire packing would most likely be considered uneconomic for routine silencer applications in sugar factories. However, there may be other industrial applications in which the extended life of a stainless steel wire packing does outweigh the greater initial cost.

ACKNOWLEDGEMENT

REFERENCE

Beranek L.L. (ed.), Noise and Vibration Control, McGraw-Hill Book Company, Sydney, 1971, 245-253.

SOUND ATTENUATION OF DUCTS   WITH V-WEDGE SOUND   ABSORBENT
MATERIALS

Rod Satory
Satory Acoustic Services
NEW ZEALAND

Wu Qunli
Satory Acoustic Services
NEW ZEALAND

ABSTRACT

There are a number of shortcomings in the usual design
for the normal sound absorption in ducted systems.   One
of the most disturbing aspects in the design of such
absorption systems   is the   limitations of   maximum
absorption in the length of the treatment. It is true
that this limitation no longer exists if there is a
velocity difference across the duct.

Our original redesign of a duct was to put all of the
absorption on one side of the duct which extended the
useful length of duct absorption in a relatively infinite
way. The other changes we were able to achieve with this
absorption on one side of the duct was to affect a much
less expensive   system   for an   absorption   design.
Practical designs can be affected that achieve absorption
for something like one tenth of the production cost of
the duct design.

Cost savings are to a significant extent affected by the
low cost mounting system but there are savings available
even though one of our designs that deal with erosion
problems and high velocity systems is used.

1.0 SOUND ATTENUATION OF DUCTS WITH V-WEDGE SOUND ABSORBENT MATERIALS

In an effort to treat sound absorption in ducts using the most economical method available the Authors have discovered that the treatment along one side of a round duct is very effective, inexpensive to mount and loses little in effectiveness with length. A formal test was conducted using British Standard 4718 as the test guide which confirmed the Empirical data from the field.

Amongst the variables checked using a standard V-Wedge of Polyurethane foam installed along one edge of the duct we varied the wedge for size, length and material. The duct was tried as a square duct, round duct, and different size of duct.
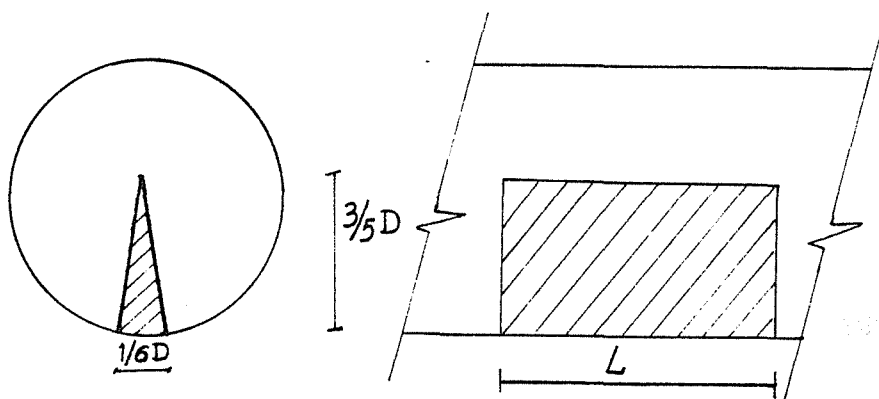
FIGURE 1:   Round duct with V-wedge
             sound absorbent material.

The V-wedge used for Sound attenuation is shown in Figure 1 covering 6.3 percent of the cross-sectional area of various diameter ducts. It is normally accepted that the sound attenuation levels increase with higher effective frequencies as the diameter of the duct decreases, (see Figure 2 on next page).

It is interesting to note that the sound attenuation is still very effective up to 8000 Hz.
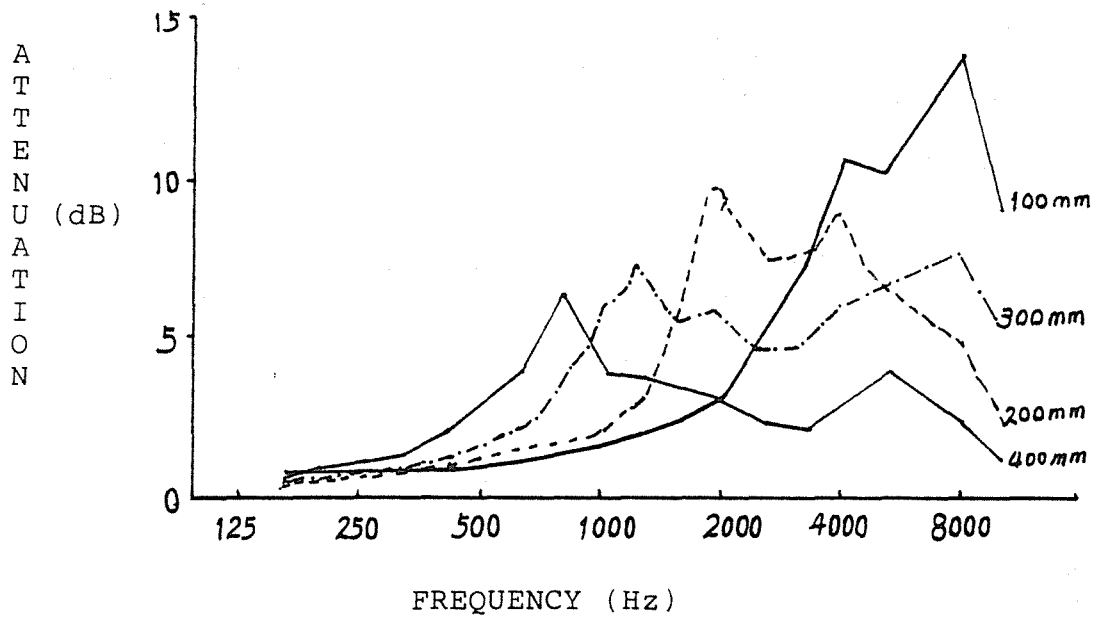
FIGURE 2. Effect of Duct Size on Sound Attenuation
(Duct diameter shown in mm above)

We get two peaks on each sound attenuation curve. The second peak can be greater than the first one and the effective frequency band of the attenuation is broad.
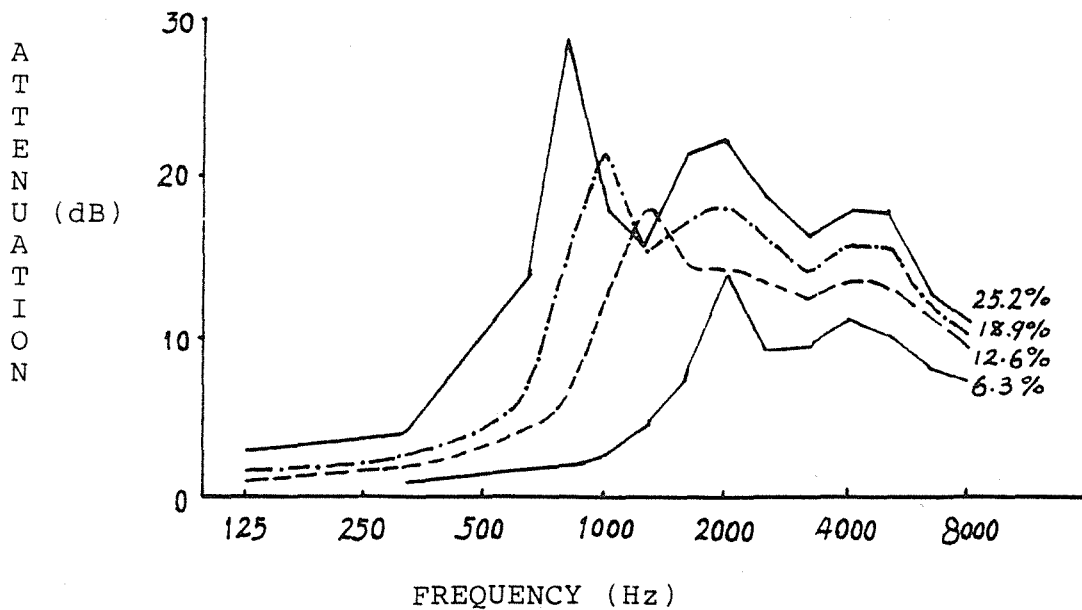
FIGURE 3: Percentage of Foam Varied
(200 mm diameter duct)

It is shown in Figure 3 that sound attenuation changes with the percentage of the cross-sectional area used for Sound Absorption. (S.A.)

As the percentage increases, the maximum attenuation
increases and the attenuation at low frequencies is
increased. There is 14 dB additional attenuation at 1250
Hz by simply adding a second (12.6% of the cross-section
area) V-wedge (Fig 2) and we get 16 dB additional
attenuation at 800 HZ by redoubling the size of the
V-wedge which is an effective way to achieve low
frequency attenuation.

Note the broad band attenuation curve between 1000 and
8000 Hz. Comparing these two treatments, the attenuation
curves shown in Figure 3 have narrow peaks at low
frequencies and the curves in Figure 4 have broad peaks
with more high frequency attenuation.
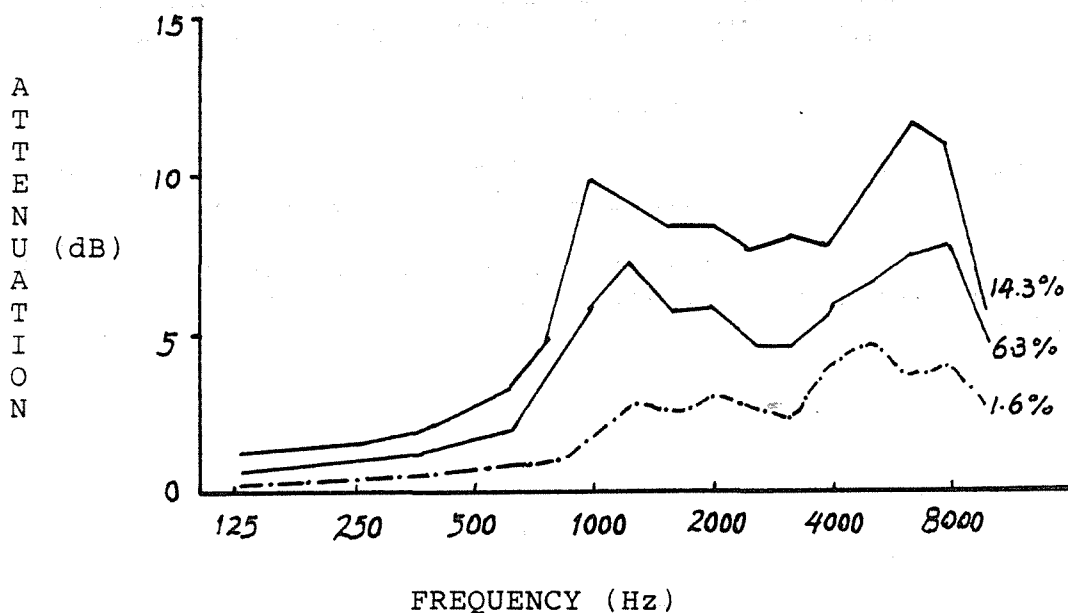
FIGURE 4:   Percentage of Foam Varied
            (300 mm diameter duct)

2.0 SOUND ATTENUATION OF VARIOUS DUCT LENGTHS

Previous data for rectangular lined ducts indicate that
as duct length increases, additional attenuation at low
frequencies can be achieved, while attenuation at high
frequency quickly reaches the condition where little
additional sound energy is absorbed. In the case of the
V-wedge duct system, data in Figure 5 (see next page)
indicates that the high frequency attenuation continues
to increase when increasing the length of the V-wedge
duct. The results show that we get 18 dB attenuation at
8000 Hz when using a 4 metre V-wedge in a 200 mm diameter
duct. As expected, the low frequency attenuation is
proportional to the length of the V-wedge duct.
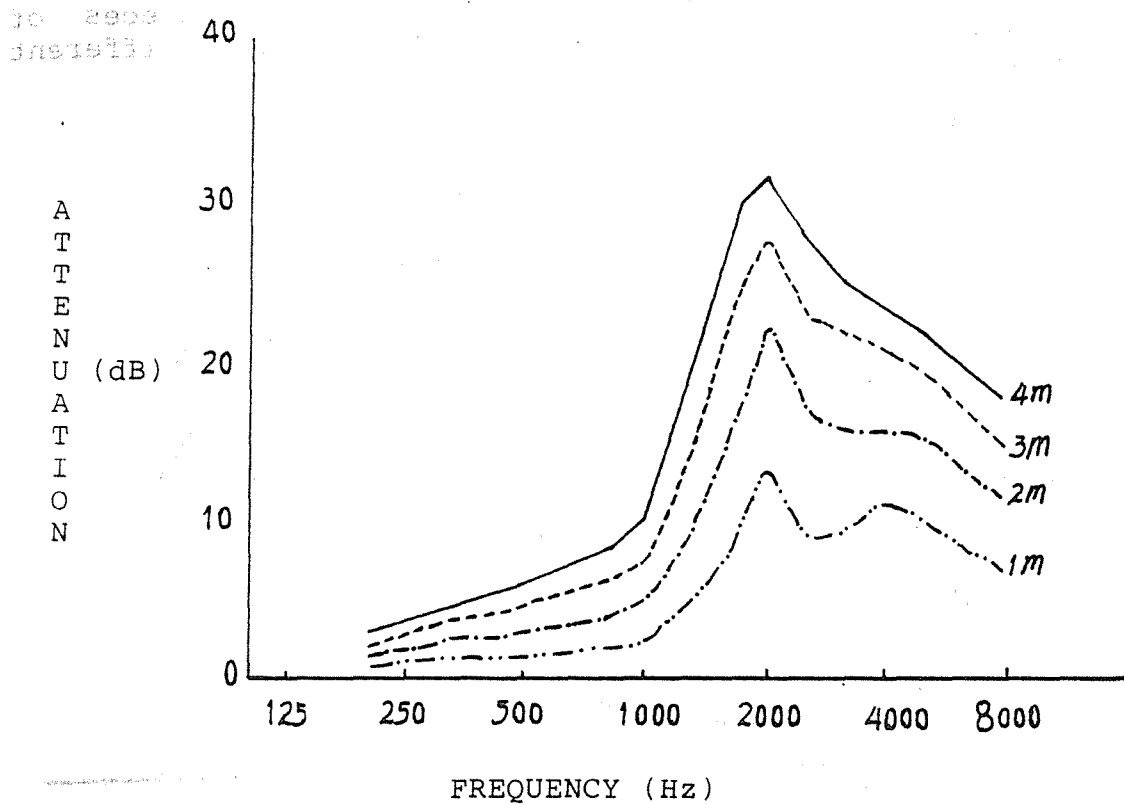
FIGURE 5: Foam Length Varied

3.0 COMPARISON OF SOUND ATTENUATION BETWEEN V-WEDGE DUCTS AND LINED DUCTS.

The question arises as to what advantages the V-wedge duct has when compared to the lined duct with an equal cross-sectional area using the same amount of sound absorbent material.

In an experimental comparison, a partly lined duct was made by lying the V-wedge against the interior duct wall, illustrated by Figure 6.
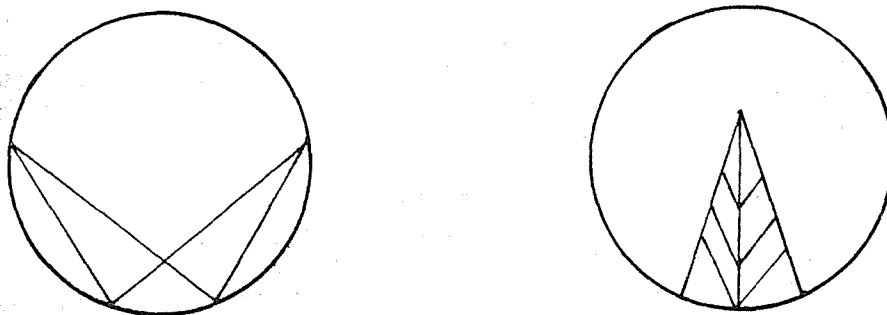
FIGURE 6: Foam position varied.

Figure 7 shows the sound attenuation of two pieces of
V-wedge in a 200 mm diameter duct with the two different
treatments.
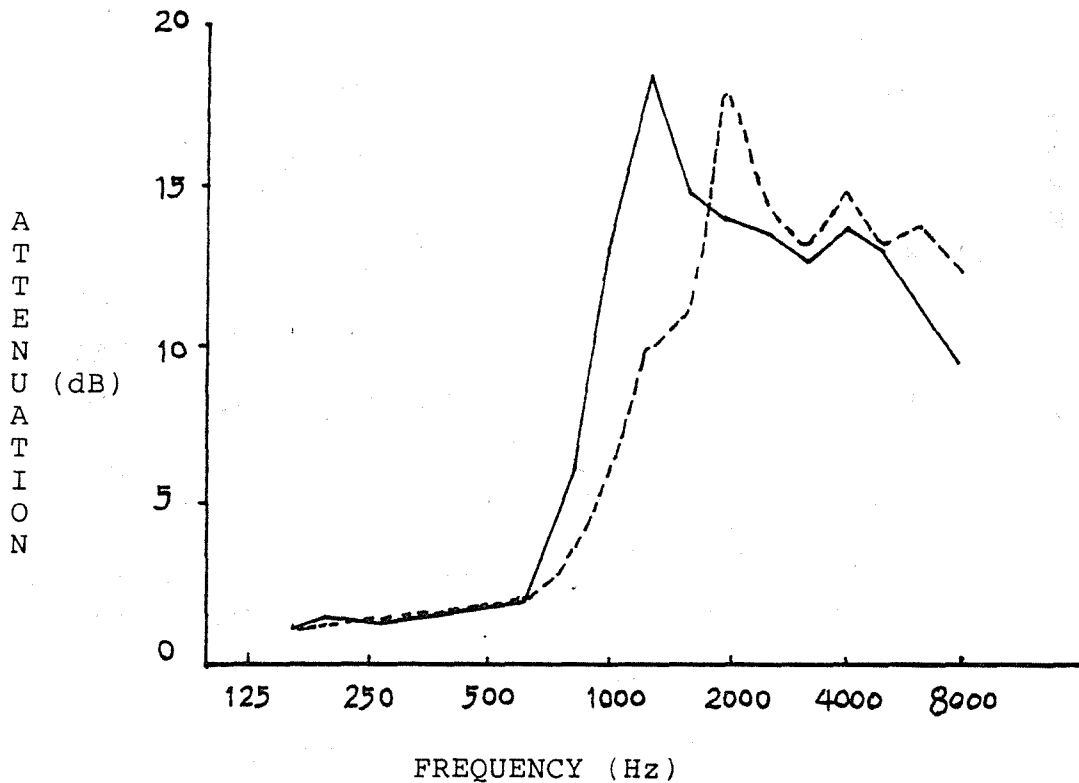
FIGURE 7: Foam position varied. See Fig 6.

The results show that the frequency of greatest
attenuation is higher when the V-wedges are against a
surface. When using V-wedge treatment on a round duct,
there was 7 dB additional attenuation at 1000 Hz and 8.5
dB at 1250 Hz. The data shows that more sound
attenuation can be achieved at low frequency by V-wedge
treatment than by lining the duct.

4.0 CONCLUSION

An experimental study was made of the sound attenuation
in a duct with V-wedge sound absorbent material. It is
found that the duct with the V-wedge material has the
following advantages compared to the lined duct with the
same amount of material:

1) More effective at low frequencies.
2) Better attenuation at high frequencies.
3) Much wider frequency band of sound attenuation.
4) Lower cost. (The V-wedge duct costs less than one
   tenth of the price of some commercial silencers).
5) Much less duct space used for SA materials.
6) Easier installation, and
7) Little loss of attenuation with length.

Summing up, the V-wedge treated duct is very effective on
sound attenuation and can be installed at a low cost.

ACKNOWLEDGEMENTS

REFERENCES

British Standard 4718

Methods of Test for Silencers for Air Distribution Systems
British Standard Institution, London. 1971

Books

Beranek L.L., Noise and Vibration Control, McGraw-Hill,
1971.

Sung-Hwan Ko, Sound Attenuation in Lined Rectangular Ducts
with Flow and Its application to the Reduction of Aircraft
Engine Noise. J. Acoust. Sco. Amer. 50. 1418. 1971.

Wassilieff C., Performance of Duct Acoustic Linings
Available in New Zealand. Trans. Vol. 12. No 2 Emch 73
1985.

White R. G., Noise and Vibration, Ellis Horwood, 1982.

AN UNUSUAL GRID SHAPED ABSORBING CEILING FOR A LARGE SPACE
---ACOUSTIC REFURBISHMENT TO CHANGE A GYMNASIUM WITH POOR
ACCUSTIC QUALITIES INTO A MULTI-PURPOSE AUDITORIUM WITH
EXCELLENT ACOUSTIC QUALITIES

Zhen KaiYuan

Department of Architecture, Southeast University,
Nanjing, People's Republic of China

Sun MingYuan

XuZhou Institute of Architectural Design,
XuZhou, People's Republic of China

ABSTRACT

A suspended-grid absorbing ceiling was installed in a gymnasium that was originally of poor acoustic quality. The ceiling resulted in reverberation times suitable for speech but was light enough to be borne by the structure. The natural lighting through the roof lights remained sufficient to illuminate the gymnasium in daytime. and the finish was light, reflective, and elegant.

Gymnasia in China are often used as multi-purpose auditoria, where, in addition to sporting activities, films, operas, and concerts take place. The gymnasium of Xu Zhou is the main hall of the city and is used for the full range of functions described. It was typical in that its large volume and the hard internal surfaces precluded good acoustics for speech and musical performance. In 1976, the authors of the paper were given the task of improving the acoustics by the introduction of additional absorption in such a way that the natural lighting remained adequate and the roof loading was not substantially increased.

The gymnasium is rectangular in plan, with a floor area of 51·8 m × 36·0 m (Fig. 1). The walls are of a height of 10·1 m, and the roof structure is a reinforced-concrete arch with an apex 16·4 m above floor level (Figs 2 and 3). The gymnasium can hold audiences of up to 3000 people, in which case the volume per person is 7·3 m³. The spectators' seating is formed from
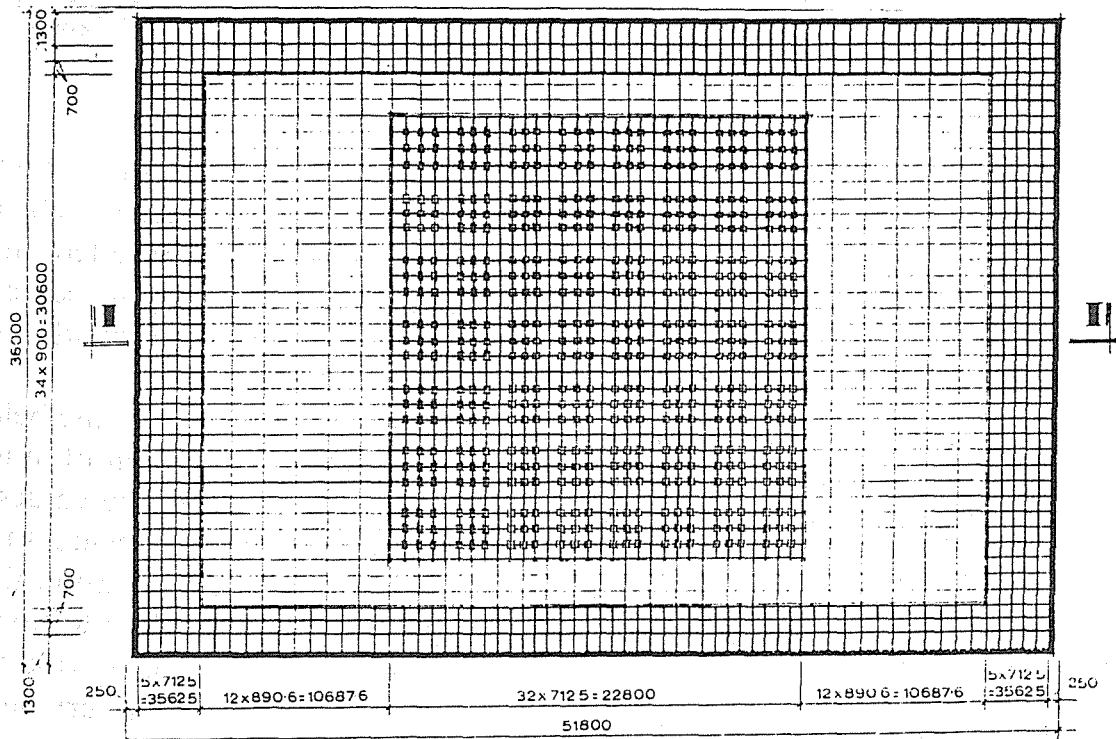
Fig. 1. Ceiling plan. (All dimensions in millimetres.)
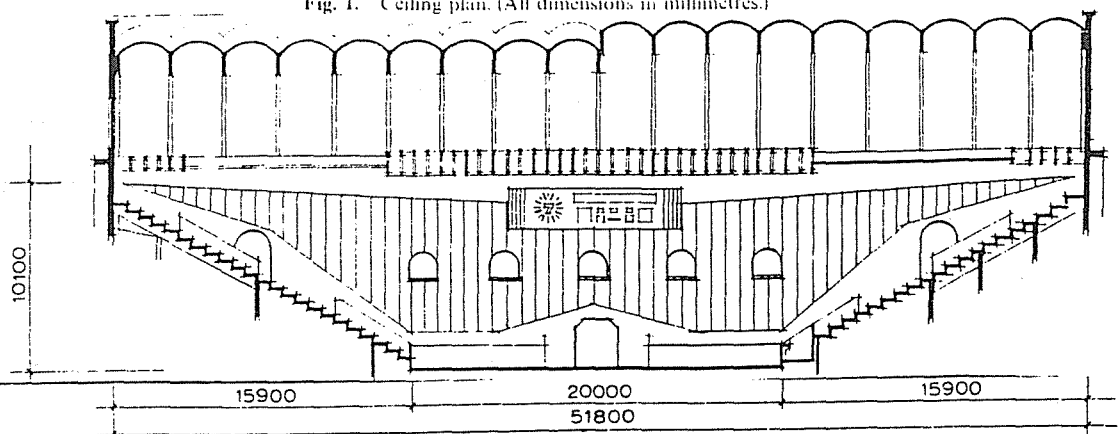
Fig. 2. Section I–I. (All dimensions in millimetres.)
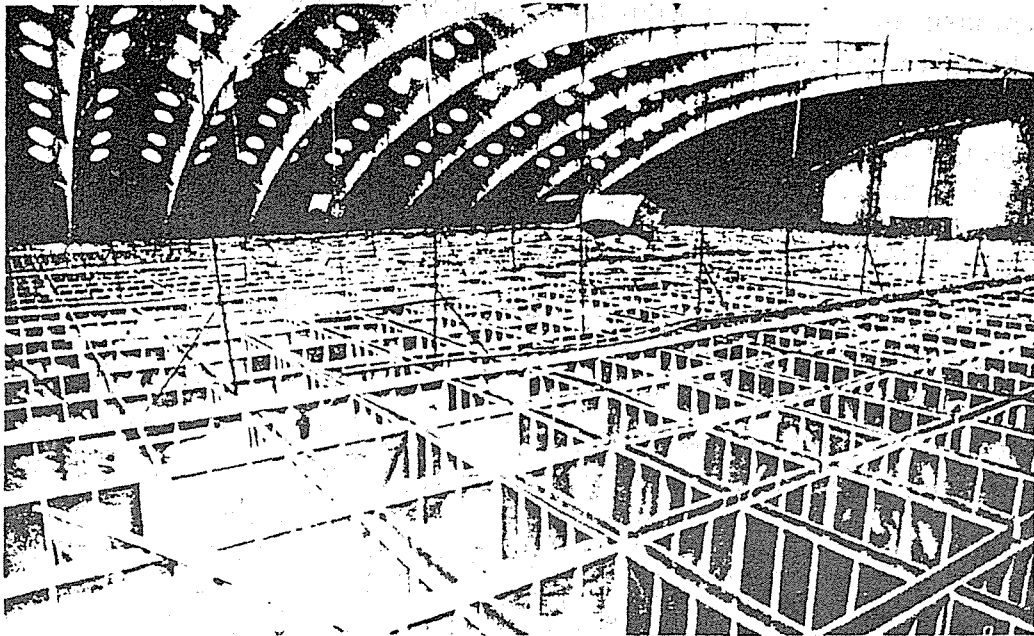
Fig. 3. The upper space of the ceiling with the original arched roof.

reinforced-concrete steps with no chairs or benches. The lighting is mainly natural from the side windows and through 320 roof lights, each of 500 mm diameter (Fig. 3). The large volume and hard surfaces resulted in a reverberation time that was too long, and activities involving speech and musical performance were limited. The reverberation times in seconds were measured and found to have the values given in Table 1.

Even when the gymnasium is fully occupied, a reverberation time below 2 kHz is too long for the perception of speech and the enjoyment of music. The percentage articulation index was also measured and yielded values of 50% for men's voices and 69% for women's voices. It was very evident that the sound quality could be improved by shortening the reverberation time. This was possible by the reduction of the effective volume or the addition of sound absorption or both. However, the authors were faced with two difficulties, since the original structure was not allowed to bear very heavy

TABLE 1
Reverberation Times

Octave						
Central frequency (Hz)	125	250	500	1 000	2 000	4 000
Reverberation time(s) (empty)	7·7	7·3	5·9	5·6	4·3	3·5
Reverberation time(s) (occupied)	4·5	4·5	3·0	2·6	2·1	1·6

162
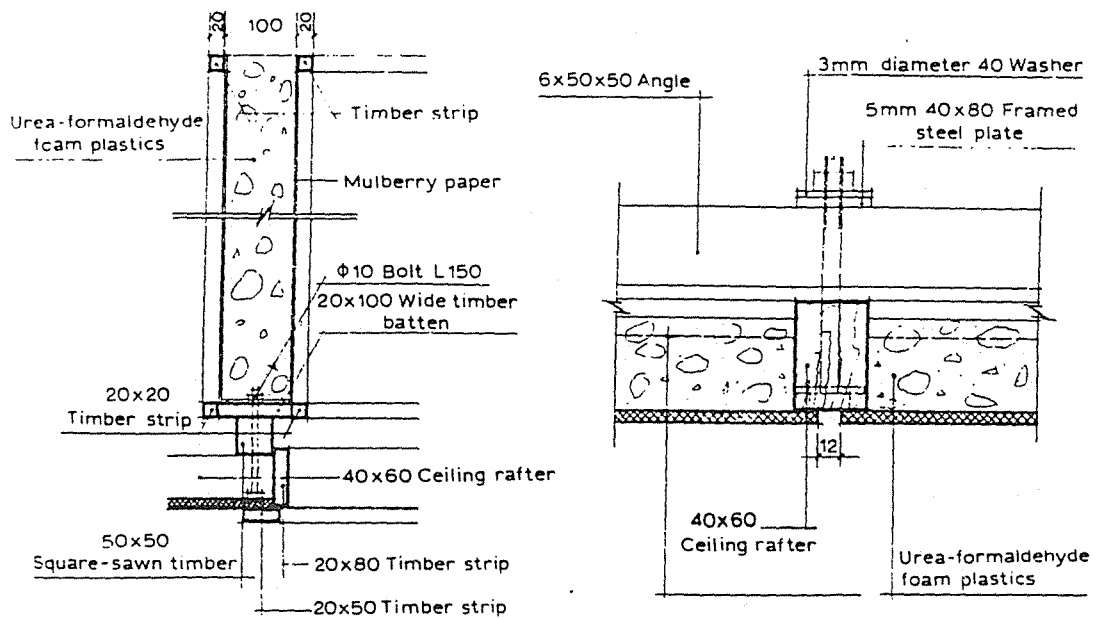
Fig. 4. The details of the ceiling construction. (All dimensions in millimetres.)

sound-absorption materials, and the daylight from the side windows and roof lights was not to be obstructed.

Four designs of absorbing ceilings were considered as follows.

(i) A large-area suspended ceiling, with a steel or timber frame and covered with 5-cm-thick glass-fibre board, was quickly rejected. This is a typical treatment for gymnasia in China but was not allowed here because of its weight and because it blocked the natural lighting through the roof.

(ii) Aluminium-coated corrugated sheeting inside the arched roof appeared to offer some advantages, including low weight, ease of installation, low cost, and good thermal insulation. It could also be perforated at the roof lights, and the silvering increased light reflectivity. However, it was not waterproof, and high humidity might eventually cause failure. The silvering easily tarnished and was not fireproof. The main disadvantage was that the volume of the gymnasium was not reduced significantly.

(iii) A step-shaped absorption ceiling, which reduced the volume to some extent, was also considered but again was rejected because of excessive weight.

(iv) A suspended-grid ceiling of timber strips with urea–formaldehyde foam plastics of density 12–15 kg/m³ was finally selected (Figs 2, 3, 4).

The frame forming the grid (Fig. 5) was suspended from the roof arch by cords (Fig. 3). The suspended ceilings were placed at both the central and

163
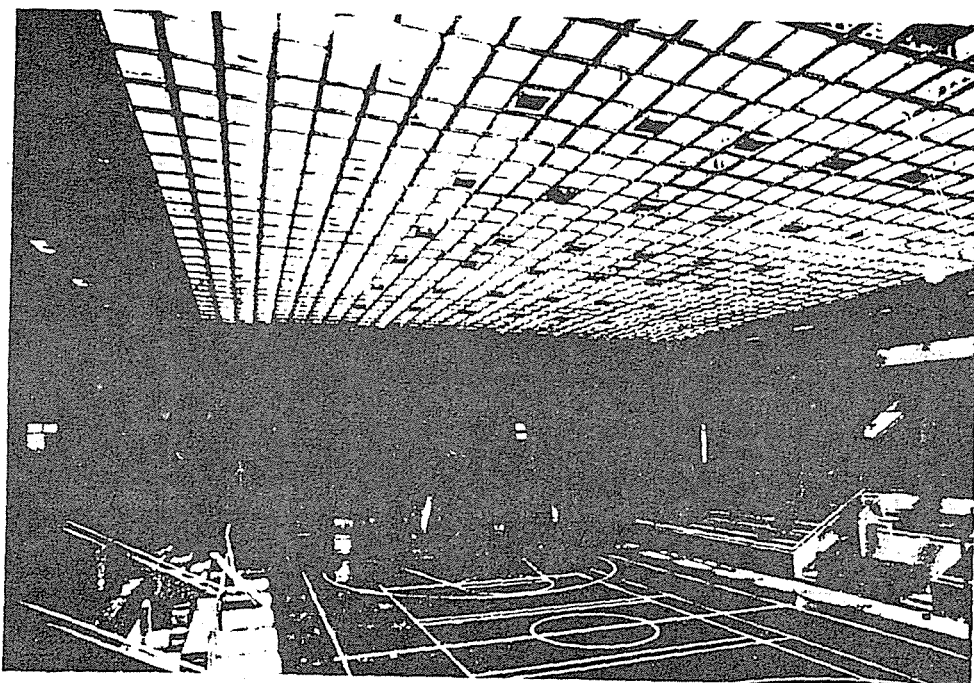
Fig. 5. The interior view of the gymnasium after re-forming.

TABLE 2

Reverberation Times

1 Octave						
Central frequency (Hz)	125	250	500	1 000	2 000	4 000
Reverberation time(s) (empty)	1·5	1·4	1·4	1·4	1·3	1·3
Reverberation time(s) (occupied)	1·0	1·0	1·0	0·9	0·9	0·8

the side parts of the gymnasium. The grid of the central part was of dimensions 900 mm × 715 mm with a height of 1 m, and that of the side part was of 715 mm × 600 mm, with a height of 0·5 m (Fig. 1). The rest of the ceiling was untreated.

The whole volume of the gymnasium could now be considered to be two coupled spaces, and the volume below the ceiling was reduced to about two-thirds of that of the original. In addition, the walls were treated with conventional absorbing material.

The measured reverberation times after installation were as given in Table 2. The percentage articulation index was again measured to give values of 87% for men and 89% for women. The client was very satisfied, and the level and range of activities allowed in the refurbished gymnasium increased.

A FIELD STUDY OF TRAFFIC NOISE & CARDIAC ARRHYTHMIA DURING SLEEP

Norman L. Carter
National Acoustic Laboratories, Chatswood, 2067. Australia

Stephen N Hunyor
Royal North Shore Hospital, St Leonards, 2065. Australia

ABSTRACT

There are reasons to suppose that exposure to traffic noise during sleep could increase the frequency of cardiac arrhythmias in susceptible people. We recorded physiological measures of sleep, and a single channel electrocardiograph, continuously overnight in 4 middle-aged and elderly males with cardiac arrhythmia, sleeping in their own homes. Recordings of the traffic noise in the bedroom, and outside the bedroom window, were made, and sleep stage, arrhythmia counts, and noise measurements in L_{Aeq}, L_{APeaK}, and L_{A1} were carried out for each 20-second interval of the night. Single indoor noise events exceeding 50 dBA peak were also identified. Noise levels were no greater in the same, or the two previous 20-second epochs, than they were in the epoch following those containing the arrhythmic (ectopic) heart beats. Chi-square tests of association between noise events exceeding 50 dBA and ectopic beats were also, in the main, non-significant. Those that were significant occurred predominantly when the subjects were in stage 4 sleep, and the association tested was between noise events, and ectopics occurring 20 seconds to one minute later.

1.0. INTRODUCTION

Previous studies have shown that noise induces a change in heart rate in people during sleep. The response consists of an increase, followed by a decrease, in heart rate (Johnson et. al., 1973; Muzet and Ehrhart, 1980, Kumar et. al., 1983; Vallet et. al., 1983). Several researchers have also reported a positive correlation between average minute-by-minute heart rate and noise level in people exposed to traffic noise while sleeping in their own homes (Kumar et. al., 1983; Greifahn and Gros, 1986). They also found that the response did not habituate, even after many years of exposure (Muzet and Ehrhart, 1980; Vallet et. al., 1983). Even when habituation occurred while the subject was awake, the response to the same noise reappeared during sleep (Johnson et. al., 1973).

The fact that the heart rate response to noise during sleep does not habituate suggests that noise may have an effect on health in the long term, even in otherwise normal people. On the other hand, the effect of noise during sleep on people who already have heart disease has not been studied. In people with cardiac arrhythmia (disturbances of heart rhythm due to abnormal sites of origin or conduction of the electrical activity in the heart which causes it to contract) an increase in heart rate due to quite mild psychological stress while awake is correlated with an increase in the frequency and severity of the arrhythmias (De Silva and Lown, 1978).

The most likely reason for the effects of noise on heart rate during sleep in normals, and the association of stress with cardiac arrhythmia in awake people is an increase in sympathetic tone. Direct evidence of this can be found in a report by Wellens (1972) that the noise of an alarm clock regularly led to self- limiting cardiac fibrillation (uncoordinated contractions) in a sleeping teenage girl. There was an abnormal substrate (the girl had a prolonged 'Q-T' interval in the electrocardiogram) but the fibrillatory response could be prevented by propranolol, a drug which suppresses sympathetic nervous activity.

The effect of noise on heart rate during sleep in normals, and the association of increased heart rate and arrhythmia with psychological stress in cardiac patients, both probably mediated by the sympathetic nervous system, suggested that noise could cause cardiac arrhythmias during sleep in susceptible people. If this were true then the consequences, in some cases, could be quite serious. Moreover, if the heart rate response to noise can habituate while the subject is awake, but reappear when he/she is asleep, then the same may apply to an arrhythmic response.

Nocturnal noise could also be linked to cardiac arrhythmia by way of sleep stage change. Some studies of arrhythmia during sleep have indicated that it is more common when sleep stage is changing (Otsuka et. al., 1982; Rosenblatt et. al., 1969; Smith et. al., 1972), and several researchers have shown that noise can cause sleep stage change without awakening (Jurriens, 1980; Vallet et. al., 1981), and increase the total number of sleep stage changes during the night. It is possible, therefore, that noise could lead to an increase in the frequency and/or severity of cardiac arrhythmias by way of more frequent changes in sleep stage.

In all modern cities very large numbers of people are subjected to environmental noise, mainly traffic noise, during sleeping hours. Also, cardiac arrhythmia is very common in the adult population (Glasser et. al., 1979; Fleg et. al., 1982). An effect of environmental noise on cardiac arrhythmia during sleep could, therefore, have widespread implications for patient management, community health and environmental planning.

The aim of the present study was to determine whether or not noise level during sleep was associated with a change in heart rhythm in people with cardiac arrhythmias. Sleep, noise and heart rate and rhythm were studied in people sleeping in their own homes. The passing traffic on a busy Sydney highway (Pennant Hills Road) was recorded on video tape, and the noise recorded throughout each night outside the dwelling and inside the bedroom. The subjects' sleep, ECG, respiration and blood oxygen saturation were monitored and recorded continuously throughout the night.

Subjects were studied on three nights each. The first night was used to accustom the subject to the test procedure. Ten subjects (aged 56 to 83 years) completed the study. Four of these had frequent arrhythmias during sleeping hours. Noise measurements and their relation to cardiac arrhythmia are reported for one night for each of these four subjects.

2.0. INSTRUMENTATION AND METHOD

2.1. Noise Recording and Analysis

A Bruel and Kjaer Type 4921 outdoor microphone system was placed between the house and the roadway such that the microphone was at the centre position of the bedroom window and one metre from it, in accordance with Australian Standard AS2702 (1974). The output of the microphone system was fed indoors to a high fidelity audio channel of a video recorder in a room adjacent to the bedroom.

The indoor microphone system used a Bruel and Kjaer half-inch condenser microphone type 4165 and Bruel and Kjaer Type 2204 sound level meter (SLM). The SLM and microphone were mounted on a tripod at the foot of the bed, at a height of 1.2 metres from the floor. The output of the SLM was fed to the second high fidelity audio channel of the video recorder. A Bruel and Kjaer pistonphone Type 4220 was used to calibrate the microphone/SLM system.

The noise recordings were analysed by replaying the tapes into a Metrosonics db 604 Sound Level Analyser, controlled by a PDP-11 computer. In each analysis the db 604 was manually programmed to analyse the noise, in one of two modes: Single Event or Multiple Interval mode. Separate analyses were also carried out for indoor and outdoor noise.

In Single Event mode the db 604 was instructed to log each noise event which exceeded 50 dBA (for the indoor noise channel) or 70 dBA (outdoor noise channel) for two seconds or more. For each of these noise events the db 604 stored the time of the event in seconds from Start (i.e. To), its duration above the 'threshold' value, in seconds, and its peak level (in dBA).

In Multiple Interval Mode the db 604 was programmed to log L_{Aeq}, L_{Amax}, L_{Apk}, L_{A90}, L_{A10}, and L_{A1} in each 20-second interval of the night. This too was carried out separately for indoor and outdoor noise channels.

2.2. Physiological Data

Sleep was monitored using standard methods. The electromyograph (EMG) was recorded from the submental (chin) muscles, the electrooculograph, (EOG), from one eye. The vertex EEG was duplicated because electrodes can be dislodged during the night (the subject was unattended). The signals were fed to a Teac SR-30 data recorder, and recorded overnight. Sleep stage and movement were hand scored in 20-second epochs, using the method of Rechtschaffen and Kales (1968).

The tape recorded ECG waveform from each night was replayed through the chart recorder to give a hard copy. This copy was hand 'scored' for arrhythmias, and the type of each arrhythmia and its onset time, in seconds from T_o, was entered into the computer.

2.3. Timing of Recordings For Subsequent Analysis

The reference time, 'Time Zero' (T_o) for all recorded signals was derived from the square wave calibration pulses generated by the Holter monitor at the outset of its recording, fed to the instrumentation recorder to provide a time reference for all of the physiological (EEG) DATA. It was also recorded on the normal audio channel of the video recorder to provide a time reference for the noise recordings and the video recording of the traffic.

3.0 RESULTS

3.1 Arrhythmias

Four subjects, aged 77, 60, 59 and 76, were found to have cardiac arrhythmias. The number of abnormal beats in each 20 second epoch of the night, regardless of type of arrhythmia, was derived. Three of the four subjects had only single ectopics. The remaining subject also had more complex arrhythmias.

3.2. The Relation of Noise to Cardiac Arrhythmia

3.2.1. Analyses Using Multiple interval Noise Data.

The association between the presence of ectopic beats in the 20-second epochs and the LAeq, LApk, and LA1 measures of noise level in these epochs was tested. The test assumed that if noise facilitates the appearance of ectopic beats then at least one of the two epochs preceding the ectopic-containing epoch, (designated ARH-2 and ARH-1) or that epoch itself (ARH), would have, on average, a higher noise level than the epoch following that containing the ectopic beat/s (epoch ARH + 1).

168

60 single factor analyses of variance were carried out, one for each combination of the three noise measures LAeq, LApk, and LA1, and each of the sleep stages 2, 3, 4, 3+4 (SWS), and stage REM, for each subject. None of the F values were significant at the .05 level of probability.

3.2.2. Analyses Using Single Event Noise Data

The foregoing analysis assumed that the likelihood of an arrhythmia is related to the average noise level, or to the highest instantaneous noise level encountered, in a given time interval. Alternatively, it could be assumed that only noise events exceeding some 'threshold' level would trigger arrhythmias, and that the frequency of arrhythmias in any interval would increase with the number of such noise events. To examine this possibility, the number of such noise events, and the number of ectopics, in every 20-second epoch of the night were tabulated, separately for (i) all night from lights out; (ii) all night from the commencement of the first period of stage 1 sleep; (iii) sleep stages 1+2; (iv) stage 4; (v) stages 3+4 (slow wave sleep or SWS); (vi) all stages of sleep except rapid eye movement sleep (REM), called non-REM (NREM) sleep; and (vii) rapid eye movement sleep (REM). Contingency tables were set up which had two or three categories of frequency of noise events exceeding 50 dBA for two seconds or more, and up to two or three categories of numbers of ectopics (e.g. 0; 1; >1). The number of categories in each case was such as to ensure adequate numbers in the individual cells of the contingency table.

None of the above Chi-Square tests were significant at the .05 level of probability in any subject/night. However, since the association tested was between noise events and ectopics, one possible reason for the finding was that some noise events occurred after the ectopic (though still in the same, 20-second, epoch). Again, there may have been a delay between the noise events and appearance of associated ectopic beats. To test these possibilities, an association between the number of noise events exceeding 50 dBA, and the number of ectopic one, and two, epochs later, was tested.

The analysis entailed the computation of an additional 14 Chi-squares for each subject (seven sleep 'stages' x two delays or 'lags'). The bulk of these Chi-squares were not significant. In one subject none was significant. The other subjects showed significant Ch-squares in Stage 4 sleep, with more ectopics than expected in epochs following noise events. One subject also showed more ectopics following noise events when the whole night, and the whole night after onset of stage one was analysed.

It may be that the likelihood of an ectopic following a noise event is greater for 'louder' noise events. Accordingly a further analysis was carried out in which, of the events above 50 dBA, only those with peak levels at, or above the median LApk were considered. The data were also subdivided as before according to sleep stage, and associations were sought between number of noise events in an epoch and number of ectopics in the same (unlagged), the next (lagged by one), and the following (lagged by two) epoch. Two of the subjects showed one significant Chi-square (p<0.05) each, again for 'lagged' analysis and sleep stage 4, with more ectopics following epochs with noise events than epochs without noise events.

In all of the above analyses each abnormal heart beat was treated as though it were an isolated event. In three of the four subjects this was, in fact, the case in that only single or isolated ectopics occurred. In one subject more complex arrhythmias such as sequences of abnormal or premature ventricular beats also occurred. For this subject additional analyses were carried out in which a numerical weighting was given to the more complex arrhythmias in arriving at an ectopic 'score' for each 20-second epoch. Chi-square tests were then carried out as before, in which an association was tested between the occurrence of noise events exceeding the median level (69 LApk) and ectopic score. These tests were repeated for each sleep stage, for ectopics in the same, and also for the two epochs following the epoch containing the noise event. None of these Chi-squares were significant at the 5% level.

4.0. DISCUSSION

The bulk of the above data show no temporal relationship between noise during sleep and the frequency of abnormal (ectopic) ventricular beats. On average, the noise level during, or up to one minute before, 20-second epochs containing ectopic beats, was not greater than it was during 20-second intervals after the ectopics occurred. A similar result was found when single noise events exceeding a predetermined threshold value were considered. In this case however, there may have been an association, in three of the four subjects, between these noise events and the appearance of ectopics 20-seconds to one minute later, when the subject was in stage 4 sleep. The effect was slight, however, and bearing in mind the large number of Chi-squares which were calculated, this result must be treated cautiously.

Again, the number of subjects we tested was very small. All were living active lives, and there was no way of determining whether any of them were unusually more, or less, susceptible to induced arrhythmias. Study of the possible effect of sleeping in a relatively noisy environment on the total number of ectopic beats overnight, by controlling the noise exposure on different nights, was not possible in the circumstances.

There are theoretical reasons for supposing that stage 4 sleep could be a vulnerable period for cardiac arrhythmias, but if there are effects they are more subtle than the present study was capable of revealing with any degree of clarity. We have commenced further studies in this area, which will be described elsewhere.

REFERENCES

Australian Standard 2702 - 1984. Acoustics - Methods for the Measurement of Road Traffic Noise Standards Association if Australia, Sydney, 1984.

De Silva, R.A., and Lown, B. Ventricular premature beats, stress, and sudden death. Psychosomatics 19, 649-661, (1978).

Fleg, J.L., and Kennedy, H.L. Cardiac arrhythmias in a healthy elderly population. Detection by 24-hour ambulatory electrocardiography. Chest 81, 302-307, (1982).

Glasser, S.P., Clark, P.I., and Applebaum, H.J. Occurrence of frequent complex arrhytrhmias detected by ambulatory monitoring. Findings in an apparently healthy asymptomatic elderly population. Chest 75, 565-568, (1979).

Griefahn, B., and Gros, E. Noise and sleep at home, a field study on primary and after effects. Journal of Sound and Vibration 105, 373-383, 1986).

Johnson, L.C., Townsend, R.E., and Naitoh, P. Prolonged exposure to noise as a sleep problem. Proceedings of the international Congress on Noise as a Public Health Problem, Dubrovnik, U.S. E.P.A. Report 550/9-73-008, 1973, 559-574.

Jurriens, A.A. Noise and sleep in the home: Effects on sleep stages. Sleep 1980. Fifth European Congress on Sleep Research Amsterdam. Karger, Basl, 1981, 217-220.

Kumar, A., Tulen, J.H.M., Hofman, W.F., Van Diest, R., and Jurriens, A.A. Does double glazing reduce traffic noise disturbance during sleep? Proceedings of the Fourth International Congress on Noise as a Public Health Problem, Turin. 1983, Vol. 2, 939-949.

Muzet, A., and Ehrhart, J. Habituation of heart rate and finger pulse amplitude to noise in sleep. Proceedings of the Third International Congress on Noise as a Public Health Problem. Freiburg. 1980, 401-404.

Muzet, A., Ehrhart, J., Eschenlauer, R., and Lienhard, M.P. Habituation and age differences of cardiovascular responses to noise during sleep. Sleep 1980. Fifth European Congress on Sleep Research. Amsterdam. Karger, Basil, 1981, 212-215.

Otsuka, K., Yanaga, T., Ichimaru, Y., and Seto, K. Sleep and night-time arrhythmias. Japan Heart Journal 23, 479-486, (1982).

Rechtschaffen, A., and Kales, A. (Eds.), A Manual of Standardised Terminology, Techniques and Scoring System for Sleep Stages of Human Subjects. BIS/BRI, UCLA, Los Angeles, 1968.

Rosenblatt, G., Zwilling, G., and Hartmann, E. Electrocardiographic changes during sleep in patients with cardiac abnormalities (abstr). Psychophysiology 6, 233, (1969).

Smith, R., Johnson, L., Rothfeld, D., Zir, L., and Tharp, B. Sleep and Cardiac arrhythmias. Archives of Internal Medicine 130, 751-, (1972).

Vallet, M., Gagneux, J.M., and Blanchet, V. Noise and sleep at home. Stage changes and arousals. Sleep 1980. Fifth International Conference on Sleep Research, Amsterdam. Karger, Basil, 1981, 220-224.

Vallet, M., Gagneux, J.M., Clairet, J.M., Laurens, J.F., and Letisserand, D. Heart rate reactivity to aircraft noise after a long term exposure. Proceedings of the Fourth International Congress on Noise as a Public Health Problem, Turin. 1983, 965-972.

Wellens, H.J.J., Vermeulen, A., and Durrer, D. Ventricular fibrillation occurring on arousal from sleep by auditory stimuli. <u>Circulation</u> 46, 661-665, (1972).

CARDIOVASCULAR PROCESSING OF NOISE AND HYPERTENSION

Barbara Griefahn
Institute for Work Physiology, Department 'Environmental
Physiology and Occupational Medicine', Ardeystr.67,
D-4600 Dortmund 1, Federal Republic of Germany

ABSTRACT

89 normal hearing hypertensive subjects (30-60 yrs) were expo-
sed to noise under controlled conditions in the laboratory.
Mood and cardiovascular responses were compared to those of
100 normal hearing and normotensive subjects of the same age.
A more detailed analysis was performed for a subgroup of 26
untreated hypertensives who were individually matched with 26
normotensive subjects.

48 noises, pink, traffic, and impulse noise were applied for
19 seconds and with equivalent sound pressure levels from 62
to 80dBA in 2 separate sessions. Mood was recorded in the
first, cardiovascular responses in the second session.

The only significant difference between normotensive and
hypertensive subjects was a smaller noise-induced vasocon-
striction in the latter group. This is explained by an in-
creased inertia of the blood vessels due to structural alte-
rations. There are some indications that this increased resi-
stance may be surpassed in hypertensives with a self-estimated
sensitivity to noise. If this is verified in extended studies
this group runs probably a higher risk to be impaired by envi-
ronmental noise.

1.0 Introduction

Noise causes numerous autonomic responses which are characteristic for stress (e.g. heart rate acceleration vasoconstriction, increased excretion of stress hormones).

Stress and thereby noise is assumed to contribute to the genesis of hypertension. The hypothetical pathogenic mechanism is as follows: noise increases the peripheral resistance and elevates the blood pressure. Longterm exposure causes smooth muscle hypertrophy of the blood vessels and thereby sustained hypertension. This is postulated e.g. by Andrén (1982), Neus et al. (1983), Singh et al. (1982) but denied by Borg (1981) und by Kornhuber & Lisson (1981).

Other authors suggest that hypertension is associated with a generally increased sympathetic reagibility. This, however, contradicts the consideration that the extent of acute vasoconstrictions must decrease due to structural alterations of the blood vessels, due to their increased rigidity and due to their smaller diameter (e.g. Korner, 1982).

2.0 Objectives

This study was designed to proof the following hypothesis: Hypertension is accompanied by a reduced elasticity and a smaller diameter of the blood vessels. Accordingly, noise-induced vascular responses (vasoconstrictions) must decrease while the cardiac responses (heart rates) are not expected to vary with the blood pressure.

3.0 Material and methods, experimental design

Subjects: 189 normal hearing subjects, 30 to 60 years of age, either resistant or sensitive to noise, took part in the experiments. 100 ss were normotensive and 89 were hypertensive (without severe longterm effects). The subjects were naive; they had never participated in noise experiments. Normal hearing was defined according to ISO 1999 and hypertension was assumed if the WHO-criteria for mild hypertension were fulfilled ($RR_{syst} > 140mmHg$ and/or $RR_{diast} > 90mmgHg$).

Experimental design: The subjects passed 2 sessions which were separated by half an hour. 48 distinct noises with durations of 19 seconds and consecutive intervals of 27 to 50 seconds were applied during each session.

Pink noise, traffic noise, and impulse noise with a repetition rate of 2 impulses per second (gunfire I) were presented with equivalent sound pressure levels of 62, 68, 74, and 80 dBA. The impulses were also applied with repetition rates of 1, 2, 4, and 8 per second and an equivalent sound pressure level of 71 dBA (gunfire II). Each noise was applied 3 times in a random order. During the 1st session the subjects assessed their mood during each single noise on 6 analoque scales. These data

were furtheron comprised to the variable called 'displeasure'. During the second session the physiologic variables heart rate and peripheral blood flow were recorded.

Statistics: The physiologic data were evaluated pulse by pulse and thereafter presented in 1-second intervals. The heart rates were standardized to a prestimulus rate of 60 beats per minute, the fingerpulse amplitude to 100%.

The t-test was calculated for dependent and for independent samples and the analysis of variance was completed. Differences are called 'significant' if the probability of errors does not exceed 1%.

As no differences existed between male and female subjects, the data of both sexes were combined.

The effects of self-estimated sensitivity to noise were analyzed, but whenever 2 samples are compared it was ensured that the ratios between sensitive and resistant subjects were the same in both groups.

4.0 Results

4.1 Hypertension vs normotension

Figure 1 presents the cardiovascular responses averaged over all trials regardless of the type of noise and of the equivalent sound pressure levels.
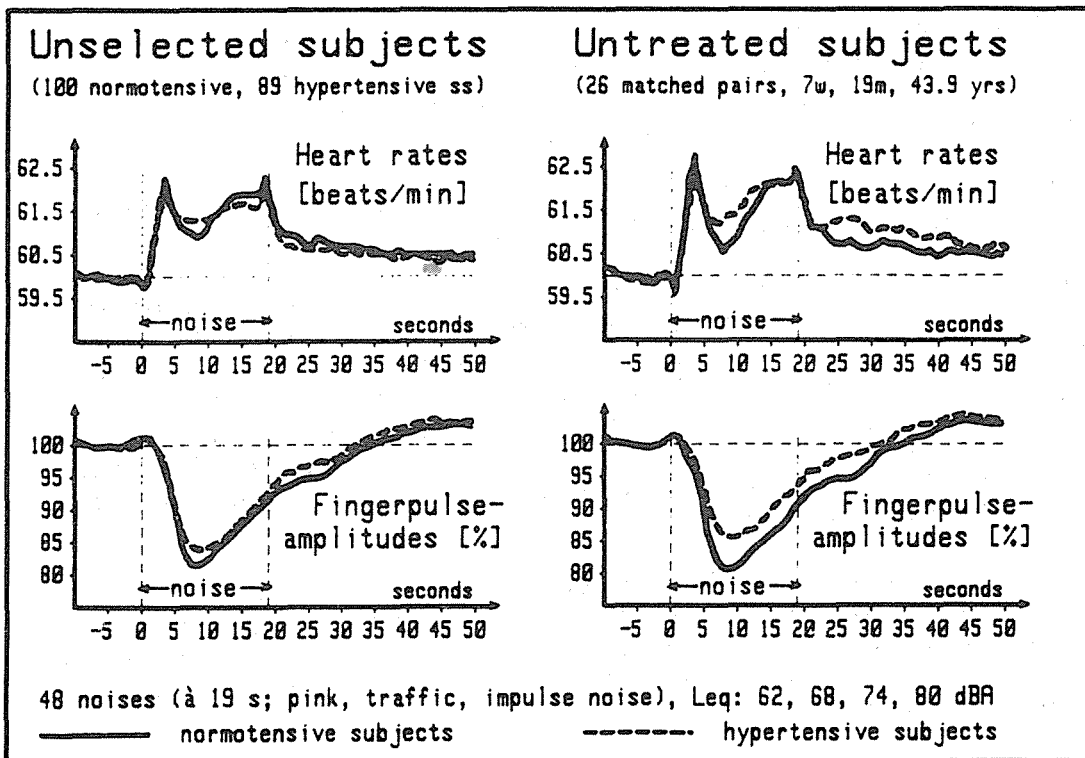
Figure 1

The **heart rates** accelerate shortly after noise onset and peak after 3-4 seconds. The consecutive minimum at 8-9 seconds is followed by a second, less steep acceleration, the second maximum is comparable to the first. Deceleration towards the baseline begins immediately after noise offset.

The responses of the hypertensive subjects vary less. Both maxima are below and the minimum is significantly above the appropriate data of the normotensive subjects.

Peripheral blood flow decreases 3 seconds after noise onset and the minimum occurs after 8-9 seconds. The consecutive gradual approach towards the baseline is finished 13 to 15 seconds after noise offset.

The vasoconstriction is less significant in hypertensive subjects from the 4th to the 10th second of noise exposure.

4.2 Untreated hypertensives vs matched normotensives

As two thirds of the hypertensives take remedies which interact with the cardiovascular system, the differences described are not unequivocally related to the blood pressure.

To determine the real effect of sustained hypertension the noise-induced responses of 26 untreated hypertensives were compared to those of 26 normotensives. The latter were individually matched to the hypertensives according to age, sex, and self-estimated sensitivity to noise.

Mood: Displeasure was the same in both 89 unselected hypertensives and 100 normotensives. But it became significantly less in untreated hypertonics compared to their normotensive controls (54.5:49.3, t=4.61, p<.1%, figure 2).

Cardiovascular responses: The response pattern is the same as observed for the total sample (figure 1, right part).

Heart rate: The smaller variation of the heart rate response observed in the untreated hypertensives is considerably more pronounced. The initial maximum is moderately but significantly below and the minimum is above the appropriate data of the normotensive subsample. The consecutive acceleration is the same in both subsets. This pattern explains the lack of a difference if the data are averaged over the period from the 3rd to the 18th second (figure 2).

Peripheral blood flow: The 26 untreated hypertensives reveal a significantly smaller vasoconstriction than their normotensive counterparts. The ascent of the return towards the baseline is less steep (0.66%/sec versus 0.75%/sec) indicating a relatively retarded recovery.
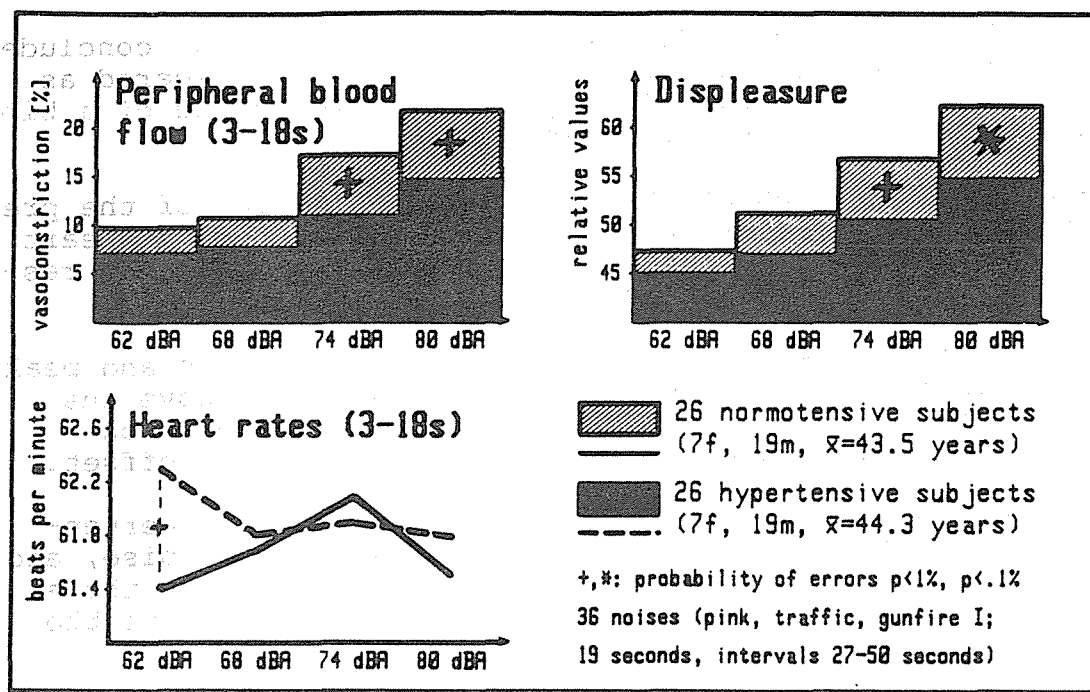
Figure 2

Equivalent sound pressure level: The analysis of variance reveals that displeasure and vasoconstriction increase significantly with the sound pressure levels in both groups. But, as the increase is less in the hypertensives, their responses are significantly smaller if the sound pressure levels exceed 68 dBA. On the contrary, heart rate accelerations are not systematically related to the noise intensity and the cardiac response is statistically different only at Leq = 62 dBA.

Sensitivity to noise and blood pressure: If the effects of noise are then related to blood pressure and to selfestimated sensitivity to noise, it becomes evident that the differences between the unselected hypertensives and normotensives base on the behavior of the resistant subjects. Sensitive subjects, however, reveal the same vasoconstriction regardless of their blood pressure though displeasure during noise exposure was significantly less in the hypertensive subsample.

5.0 Discussion

A characteristic cardiovascular response was observed in all subgroups. It consists of a moderate but significant heart rate acceleration and a pronounced vasoconstriction. The latter was observed by many authors (e.g. Jansen et al., 1981) and it indicates an elevated sympathetic tone.

Heart rate accelerations are generally regarded as a characteristic response to stress. But as it is a rather facultative

reaction (e.g. Andrén, 1982). Kryter and Poza (1980) conclude that vasoconstriction must not necessarily be considered as physiologically stressful. It may be a manifestation of a biological, reflexive protection mechanism.

This explanation, however, must be refused in view of the present results. The rather characteristic pattern of the heart rate response suggests that the effects of noise are not restricted to peripheral blood flow.

The heart rates accelerate shortly after noise onset and peak at 3-4 seconds. The consecutive minimum is still above the baseline and followed by a second increase. Deceleration towards the baseline begins immediately after noise offset.

This pattern was observed in normotensives and in hypertensives, it was evoked by pink, traffic, and impulse noise, and by any other sound pressure level. It is supported by those authors who performed a detailed analyses comparable to the analysis completed here.

The initial acceleration seems to be obligatary. It is also evoked by single acoustic impulses as well as by various traffic noise during awake or during sleep and it is probably caused by a transient, short latency inhibition of the vagal tone (Di Nisi, 1987; Griefahn, 1989; Muzet, 1985).

The second acceleration which follows the minimum after 8-10 seconds is probably caused by an elevated sympathetic tone or mediated by an increase of epinephrine (Eves & Gruzelier, 1984; Turpin & Siddle, 1978).

5.1 Untreated hypertension vs normotension

The following discussion is restricted to the subgroup of 26 untreated hypertensives and their appropriate normotensive counterparts.

Heart rates: The smaller variability of the heart rate responses of the hypertensives indicates a reduced flexibility of the cardiac function during elevated blood pressure.

The finding that the heart rate reactions are not systematically related to the equivalent sound pressure level is confirmed by other studies. It is rather characteristic that the cardiac function obeys the all-or-none law.

Peripheral blood flow: noise-induced vasoconstrictions were significantly smaller and the consecutive dilatation was relatively slower in hypertensives than in normotensives. Similar alterations were reported e.g. by Jansen et al. (1981) and by Singh et al. (1982). The reduced reactions are probably related to secondary structural alterations of the blood vessels. Smooth muscle hypertrophy and sclerotic processes attenuate

the elasticity of the blood vessels during sustained hypertension.

On the contrary other authors found particularly larger responses in subjects with newly detected mild hypertension and in subjects with a family history of hypertension (Jern et al., 1981). This is probably related to the fact that hypertension is accompanied by a hyperactivity of the sympathetic structures which probably becomes gradually less evident. When hypertension progresses the vascular responses decrease.

Another rather common assumption is that noise-induced vasoconstriction is influenced by mood. Though it is well known that noise evokes vegetative responses even in subjects who are not aware of the sound (e.g. during sleep, Griefahn, 1989), it is supposed that in case of concomitant emotions secondary vegetative alterations can superimpose the noise-related effects (Borg, 1981; Guski, 1980). This seems to be verified by the behavior of the hypertensives who are subjectively and physiologically less affected. The detailed analysis of 150 normotensive subjects (50 sensitive, 50 resistant, 50 indifferent), however, revealed that displeasure during noise was determined to a lesser degree by selfestimated sensitivity to noise.

The results of the cited papers and of the present study lead to the following hypothesis: long lasting noise exposure contributes to the genesis of hypertension in case of predisposing factors such as heredity which again increase the sympathetic reagibility. Repeated vasoconstrictions cause hypertrophic smooth muscles and thereby structural alterations of the blood vessels. This results in a smaller lumen and a reduced elasticity and finally in an attenuated vascular response and a slowing down of the consecutive recovery.

5.2 Sensitivity to noise

If resistant and sensitive subjects are considered separately, noise-induced heart rate accelerations are found to be independent from blood pressure in both these subgroups.

Displeasure during noise was different only in the sensitive subsamples and significantly less in the hypertensives. As discussed before this may influence the vascular response to a certain degree.

A detailed analysis revealed that sensitivity as recorded here is not specifically directed to noise but to a great variety of environmental stress.

As vasoconstriction was the same in sensitive subjects regardless of their blood pressure it may be assumed that the increased resistance, the reduced elasticity and the smaller diameter of the blood vessels of the hypertensive persons can perhaps be passed in particular situations.

The results indicate a relatively larger response in sensitive hypertensives. In view of the numerically very small differences (though significant) it is certainly premature to conclude that hypertensive people run a higher risk to be impaired by environmental noise in case of an additional personal sensitivity.

6 References

Andrén L, 1982: Cardiovascular effects of noise. Acta Med Scand 657:1-45

Borg E, 1981: Physiological and pathogenic effects of sound. Acta oto-laryngol (Suppl) 381:1-68

Di Nisi J, 1987: Modifications de la fréquence cardiaque et de la vasomotricité digitale provoquées par le bruit. Différences inter-individuelles au cours de la veille et du sommeil. Thèse, Université Louis Pasteur, Strasbourg 1987

Eves FF, Gruzelier JH, 1984: Individual differences in the cardiac response to high intensity auditory stimulation. Psychophysiology 21: 342-352

Griefahn B, Di Nisi J, 1989: Epidemiologic research on the effects of environmental noise on mood and cardiovascular functions. Interference with sensitivity to noise and blood pressure. CEC REF. EV4V 0055 UK(H)

Guski R, 1980: Über Zusammenhänge über Kreislauf- und Belästigungsreaktionen auf Straßenverkehrslärm in Wohngebieten. ZfL 27:126-132

Jansen G, Griefahn B, Gros E, Rehm S, 1981: Methodische Überlegungen zur Aussagefähigkeit der Fingerpulsamplitudenmessung im Rahmen der psychophysiologischen Diagnose von Lärmwirkungen. ZfL 28:95-104

Jern S, Sivertsson R, Hansson L, 1981: Possible relationship between psycho-emotional factors and hemodynamic patterns in the pathogenesis of mild blood pressure elevation. Clinical science 61:93s-95s

Korner PI, 1982: Circulatory regulation in hypertension. Br J clin Pharmac 13:95-105

Kornhuber HH, Lisson G, 1981: Bluthochdruck. Sind Industrie-Stressoren, Lärm oder Akkordarbeit wichtige Ursachen? DMW 106, 1733-1736

Kryter KD, Poza F, 1980: Effects of noise on some autonomic system activities. JASA 67, 2036-2044

Muzet A, 1985: Comparaison de la réactivité cardiovasculaire au bruit au cours de la veille et du sommeil. CEB/CNRS, Strasbourg. Comité Bruit et Vibrations. Convention no 82 243

Singh AP, Rai RM, Bhatia MR, Nayer HS, 1982: Effect of chronic and acute exposure to noise on physiological functions in man. Int Arch Occup Environ Health 540: 169-174

Turpin G, Siddel DAT, 1978: Cardiac and forearm plethymographic responses to high intensity auditory stimulation. Biological Psychology 6:267-281

ON THE CENTER PITCH ESTIMATION BY USING THE SPECTRUM LEAKAGE PHENOMENON FOR THE NOISE CORRUPTED SPEECH SIGNAL

Myungjin BAE
Dept. of Electronics Eng.,Hoseo Univ., Chungnam Korea, 337-850.

Ulje KIM
Dept. of Electronics Eng.,Hoseo Univ., Chungnam Korea, 337-850.

Misuk LEE
Dept. of Electronics Eng.,Hoseo Univ., Chungnam Korea, 337-850.

Souguil ANN
Dept. of Electronics Eng.,Seoul National Univ., Seoul Korea, 151-742.

ABSTRACT   Since the pitches of speech signals are characterized by a physical limitation of the coarticulation mechanism, a little deviations are observed with a center pitch in the pitch distribution. If the center pitches are used in the decision logic, the pitch detection algorithm will be not only simplified in procedure but also improved in accuracy.   In this paper, we proposed an algorithm that the center pitches are accurately detected by using the spectrum leakage phenomenon for the noise corrupted signals.

1.0 INTRODUCTION

In speech signal processing, if we can detect the pitches of speech signals, then the pitches can be used in the analysis of the vocal tract parameter without the influences of vocal cord. And they can be used to maintain the naturalness and intelligibility in speech synthesis. The pitch detection methods used until now are classfied into the time domain, the frequency domain, and the time-frequency hybrid domain method [1-3,7-12].

speech	periodicity	decision	
signals	accentation	logic	pitch
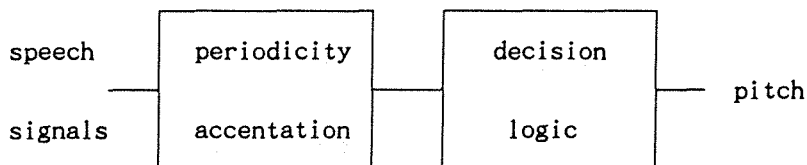
Fig.1-1. Typical processing for the pitch extration

Generally, the pitch is detected by the decision logic after periodic components were emphasized, as shown in Fig.1-1.

However, when the periodic components were accentuated in the pitch detection method, the components that present a wide band according to the age or sex can weakened rather than accentuated partially. In the pitch detection, the accuracy is decreased by errors that were generated in periodicity accentuation. And it is more difficult to detect when the speech signals are corrupted by background noise. So, the pitch detection that is strong in all cases is very difficult problem.

The pitch variation of speaker is limited by physical limitation of the coarticulation mechanism, and also it is varied by a mental security. Since the pitches have quasi-periodic property for a short time segment, it is not suddenly changed. The distribution of pitches that were detected for a short time have some deviations for the center pitch. We can use the property for pitch detection algorithim. If periodicity of speech signals was emphasized, and at the same time we used the center pitch that was detected in several frames, then the pitch detection became easy and more accurate. In this paper, we propose a new center pitch estimation algorithim that detects the center pitch using the spectrum leakage phenomenon.

2.0 THE LEAKAGE PHENOMENON OF SPEECH ENERGIES

Speech signals are classfied into voiced speech, unvoiced speech and silence by production sources. The unvoiced speech in the production models has not periodicity because its source is random noise. But, because the excitation source of voiced speech is a pseudo periodic sequence, the voiced waveforms are quasi-periodic. And since the energy of voiced speech is different from that of the unvoiced speech, the energy contour of speech signals can approximately indicate the variation of the phonemes.

For the window function $w(n)$, if a speech signal is $s(\cdot)$ and $A(n) = [s(n)^2]$, then the short time energy of speech signals, $E(n)$ is as follows:

$$E(n) = \sum_{k=\infty}^{\infty} A(k) \cdot w(n-k)$$
$$= A(n) * w(n) \tag{2-1}$$

In this case, if we apply the rectangular window with size N, then the frequency response is as follews:

$$E(e^{jwt}) = A(e^{jwt}) \cdot w(e^{jwt})$$

$$= A(e^{jwt}) \frac{\sin(\Omega NT/2)}{\sin(\Omega NT/2)} e^{jwT} N-1/2 \tag{2-2}$$

For Eq.(2-2), the short time energy calculated is equal to that of the speech

182

signal which passed through the low pass filter with cutoff frequency $f_c (= f_s/N,)$. Where f_s is the sampling frequency. At this time, if the low pass filter is ideal, then the frequency components above cutoff frequency is eliminated perfectly. However, for the retangular window as Eq. (2-2), the components above cutoff frequencies are remained by the side lobes of sinc function.

The spectrum of speech signal is a function of window length also, because the sampling period is fixed. For the spectrum of window function, the distance between main-lobe and side-lobe is varied by the size of N. At this time, if the bandwidth of main-lobe is shorter than the fundamental frequency, then the local peaks that we don't want will appear in the speech energy contour. On the other hand, if the band width is greater than the fundamental frequency, then smoothing phenomenon will happen, because variation characteristics of speech signal are not represented well.

The voiced spectrum is represented by the peaks and valleys of the harmonics. If the valleys and peaks of the spectrum of the window changes linearly, and at the same time, multiplied to the spectrum of voiced speech, then the peaks and valleys matched to each other, or not. For the former, the components above cutoff ferquency are added to the passband components. For the latter, the components above cutoff frequency are offseted each other. This is similiar to the leakage phenomenon of the window. When the window length is varied step by step, the energy contour that used the rectangular window function has the greatest variation. If the window length is accorded with the multiple pitches, the leakage phenomenon becomes minimum. The energy varied by the phenomenon is called as the leakage energy.

3.0 CENTER PITCH DETECTION USING THE LEAKAGE ENERGY

We assume that the leakage energy according to the window length is $E_l (\cdot)$. The speech energy obtained from n'th sample is ,

$$E_t (n) = E(n) + E_l (n). \qquad (3-1)$$

In order to measure the leakage, the rectangular window with the length N is applied to speech signal, and then the $E_t (n, N)$ are as follows:

$$E_t (n, N) = E(n, N) + E_l (n, N)$$
$$E_t (n-1, N) = E(n, N) + E_l (n-1, N)$$
$$\cdots\cdots\cdots\cdots$$
$$\cdots\cdots\cdots\cdots$$
$$E_t (n-N-1, N) = E(n, N) + E_l (n-N+1, N) \qquad (3-2)$$

Where the $E(n, N)$ is the energy in passband because it isn't influenced by delay time.

The maximum and minimum values of the energy according to the delay applied to the window are obtained as follows:

$$E_{max}(n,N) = Max[\ E_t(n,N),\ E_t(n-1,N),\cdots,E_t(n-N+1,N)]$$
$$E_{min}(n,N) = Min[\ E_t(n,N),\ E_t(n-1,N),\cdots,E_t(n-N+1,N)] \qquad (3-3)$$

Where the $E_{max}(n,N)$ and the $E_{min}(n,N)$ are the maximum and minimum energy of the function, respectively. If the variation of the leakage energy $E_l(n,N)$ has uniform distribution between the energies, the $E(n,N)$ without the leakage energy can be obtained as follows:

$$E(n,N) = [\ E_t(n,N) + E_t(n-1,N) + \cdots + E_t(n-N+1,N)] \qquad (3-4)$$

Then, we can approximately represent the Eq.(3-4) as,

$$E(n,N) = [\ E_{max}(n,N) + E_{min}(n,N)\ ] / 2 \qquad (3-5)$$

and then, the leakage energy as

$$E_l(n,N) = E_{max}(n,N) - E_{min}(n,N). \qquad (3-6)$$

The Fig.3-1 shows the maximum and the minimum values of Eq.(3-3) for speech signal /KAMSA HAMNIDA/. We can see that the maximum and the minimum values are varied with similar width, and thus that the assumption of Eq.(3-4) and (3-5) have been proved by them.

If one frame of speech signal is convolved with the window of the length N, then we can obtain the average leakage energy for each leakage energy. For the frame length M, the averge leakage energy $G_l(N)$ with the window length N is as follows:

a) Waveform /kamsa hamnida/

b) The maximum and minimum of speech energy

Fig.3-1. $E_{max}(\cdot)$ and $E_{min}(\cdot)$ contours

$$G_1(N) = \cfrac{1}{M-N+1} \sum_{n=0}^{M-N+1} E_1(n,N)$$

$$= \cfrac{1}{M-N+1} \sum_{n=0}^{M-N+1} [E_{max}(n,N) - E_{min}(n,N)] \qquad (3-7)$$
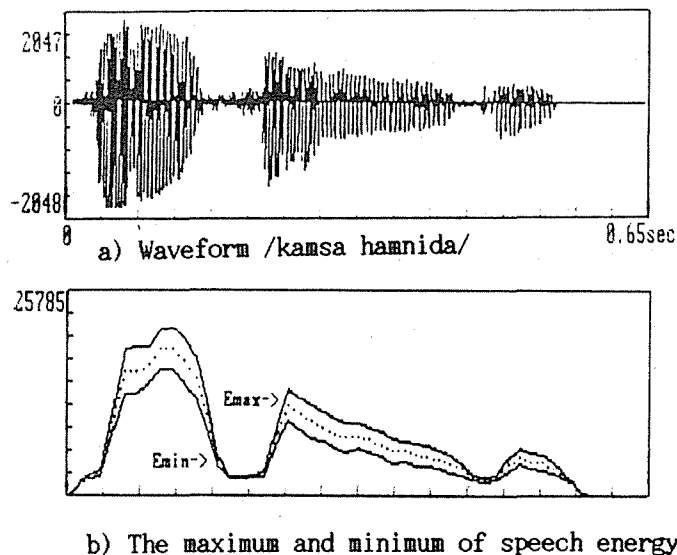
When the sampling frequency is 8KHz, the window length N is varied from 20 to 200 samples. Therefore, the frame length must be 400 samples at least. whenever the range of N was varied from 20 to 200, and at the same time, we obtained the contour of $G_1(N)$, then the contour should indicate the null points when the length is equal to the multiple pitches. Thus, we can say that the first null point is the dominant pitch.

a) speech wave form /SAM/

b) speech wave form /SA/ in /SAM/

c) The varation of averagy leakage
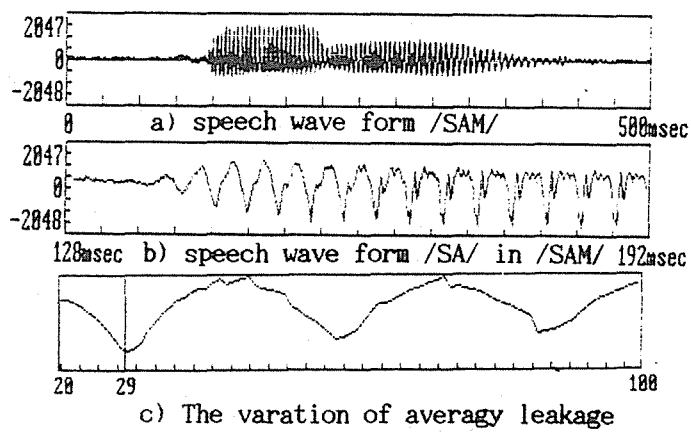
Fig.3-2. $G_1(\cdot)$ Contour for utterance /SA/ of /SAM/

The above assumption is proved by Fig. 3-2 that represents the result applied to the real speech and presents the contour of $G_1(N)$. The speech utterance used is /SA/ in /SAM/, and the speaker is a female of 26 years old. The frame length is 512 samples. From the Fig.3-2, the null points are indicated by the multiple pitches. And the shape of the null points shows a state of pitches on the frame. The Fig. 3-2 shows that the center pitch has 29-sample length. The length represents that the pitch is 3.625ms. Also, from the result, we can see that the algorithm can detect the center pitch well in the transition segment.

4.0 EXPERIMENTS AND RESULTS

The proposed algorithm has been implemented in IBM PC/AT with the 12-bit A/D converter. The sampling frequency was 8KHz. The following utterances were chosen.
Utterance 1) male speaker, 23 years old:
    / INSOONAE KOMAGA CHUNJAE SONYUNWL JOAHANDA /
Utterance 2) male speaker, 32 years old:
    / HOSEODAE JUNJAKONGHAKWA WMSUNGSINHO CHURITIM /

The experimental process is shown in Fig. 4-1. In analysis, the length of one frame is 256 samples and each adjacent frame is overlapped by 128 samples. And the rectangular window was used. We implemented to the Eq(3-3) for the range of N from 20 to 200 samples. Then we extracted the average leakage energy according to the range of the length variations. As result, we drawed the contour for the leakage energy detected. The minimum null points of the contour indicate the multiple pitches.
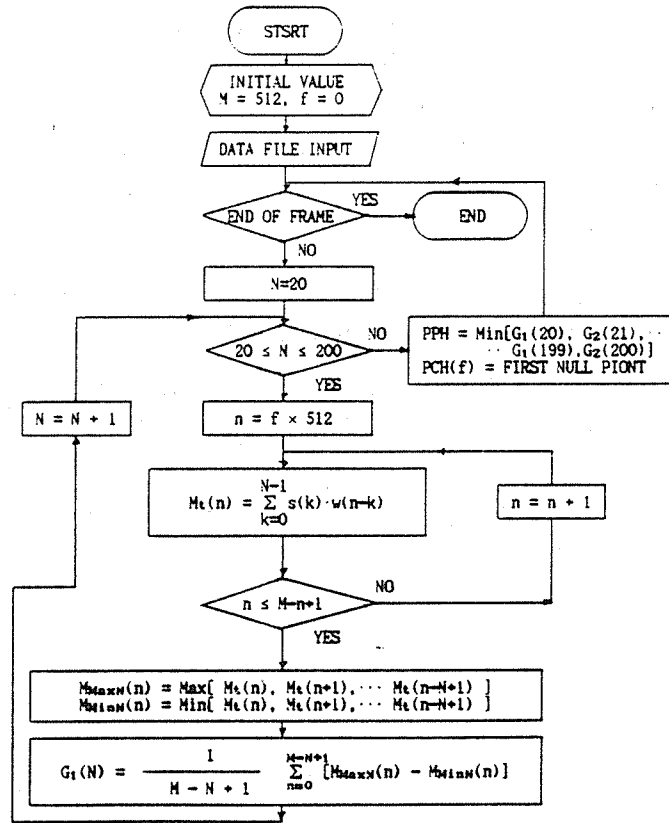
Fig. 4-1. Flow chart for computer simulation

In Fig. 4-2, Fig.a) shows speech waveform, Fig.b) shows the center pitches(line) that have been extracted in this paper and pitches(dashed line)
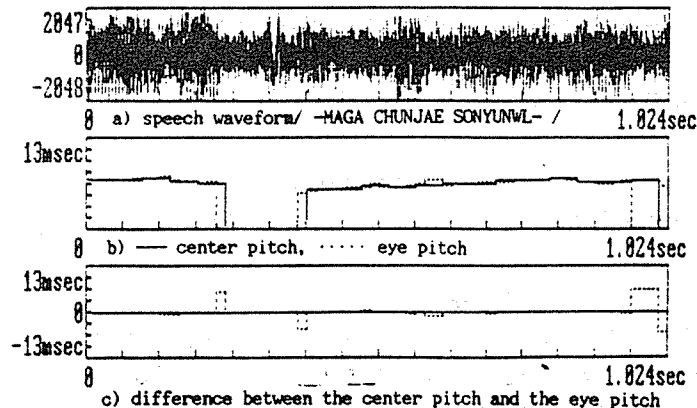
Fig. 4-2. Pitch contour for utterance(0dB Gaussian Noise)

186

that were checked by the eyes, and Fig.c) shows the difference between two pitches. We experimented again on the same utterance that was corrupted by 0-dB Gaussian noise.

From the results, the center pitches are different from the eye checked pitches in the end points of phonemes, because in this paper, we have used 512 samples as one frame length.

Gennernal pitch detection methods in time domain have difficulties to detect the pitches in transition segments. But, the proposed method in this paper can detect the pitches if speech signals have only the periodicity. And the proposed method is robust to noise corrupted speech, because it is involved the characteristic of low pass filter, and it can easily detect the averaged pitch in spite of some variation. Also, it can be used to decide the voiced and the unvoiced speech, because the unvoiced and silence have shorter pitches than 2.5ms.

5.0 CONCLUSIONS

The pitch of speech signal is not suddenly changed. The center pitch was detected by using the fundamental characteristics for all possible candidate pitches. The proposed method has used the rectangular window for the center pitch detection, because the rectangular window has the greater spectrum leakage than the other windows. At first ,in the time domain, the rectangular window was applied and then window length was varied step by step. At this time, the leakage energies are obtained. Here, the variation of the leakage energy is very serious, because the leakage phenomenon by the window can be added in the original energy according to the linear variation of the window length. The contour of the average leakage energy show the null point whenever the length of the window equal to the multiple pitches. Therefore, the first null point that the energy is minimum become the dominant pitch of the frame.

The proposed method is robust to noise corrupted speech, because it is involved the characteristic of low pass filter, and it can easily detect the averaged pitch in spite of some variation. Also, it can be used to decide the voiced and the unvoiced speech, because the unvoiced and silence have shorter pitches than 2.5ms.

REFERENCES

[1] Panos E. Papamichalis, Practical Approaches to Speech coding, Prentice-Hall inc., Englewood cliffs, N.J., 1887

[2] L.R. Rabiner. R. W. Schafer, Digital Processing of Speech Signals, Prentic-Hall inc., Englewood Cliffs, N.j., 1987

[3] Thomas W. parsons, Voice and Speech Processing, Mcgraw- Hill, 1987.

[4] Douglas O'Shaughnessy, Speech Communication, Addison Wesley, 1987.

[5] Nasir Ahmed, T. Natarajan, Discrete-Time signal and System, Prentice-Hall

inc, 1983.

[6] J. D. Markel, A. H. gray, Jr, <u>Linear Prediction of Speech</u>, Spinger-Verlag, 1980

[7] M. BAE, and S. ANN, <u>On Eliminating the Effects of Varying the Window Duration on Speech Energy Computation</u>, J., Acoust., Soc., Korea, Vol.9, No.2, 1990.

[8] M. BAE, and S. ANN, <u>Fundamental Frequency Estimation of Noise Currupted Speech Signal Using the Spectrum Comparison</u>, J., Acost., Korea, Vol.8, No.3, 1989.

[9] M. BAE, S. SHIN, S. ANN, <u>The Pitch Extraction of Voiced Speech by the Comparision Between the Orginal and Repeated Partial Wave Form</u>, J., Acoust.,Soc., Korea, Vol.7, No.5, 1988.

[10] M. BAE , S. ANN, <u>Inverse Rate Type Filterling for the Pitch Extraction</u>, J., Acoust., Soc., Korea, Vol.5, No.3, 1986.

[11] M. BAE, S. ANN, <u>The High Speed Pitch Extraction of Speech Signals Using the Area Comparison Method</u>, KIEE, Vol.22, NO.2, 1985.

[12] H. Duifhuis, L.f. Willems, and R. J. Sluyter, <u>Measurement of pitch in speech: An Implementation of Goldstain's theory of pitch perception</u>, J.,Acoust. Soc., Amer., vol. 71 pp.1568-1580, June. 1982.

CHINESE SPEECH RULE-SYNTHESIS SYSTEM

Hong NI
Department of language and communication, Institute of Acoustics, Academia Sinica
Beijing, 100080, P. R. China

Changli LI
Department of language and communication, Institute of Acoustics, Academia Sinica
Beijing, 100080, P. R. China

Fuyuan MO
Department of language and communication, Institute of Acoustics, Academia Sinica
Beijing, 100080, P. R. China

Jincheng SUN
Department of language and communication, Institute of Acoustics, Academia Sinica
Beijing, 100080, P. R. China

ABSTRACT

In this paper a Chinese speech synthesis by rules system has been described. In this system, there is a Chinese speech parameters database which generated by coding all 1281 Mandarin syllables based on multi-pulse LPC technique. Because one Chinese character pronunciation corresponding one syllable, when input Chinese text from keyboard of computer, the syllables speech parameters will be searched from the database. With decoding and then passing through a synthesis filter under control of rules, Chinese speech would be synthesized in real time with natural speech quality. This system has been realized in IBM-PC computer, with a DSP TMS320C25 acquisition/development board for real-time processing.

1.0 INTRODUCTION

In recent years, DSP, VLSI and AI develop speedily, this lay a good foundation for speech signal processing, and some text−to−speech system entry into social from laboratory.

It is the goal of this paper to research high quality Chinese text−to−speech system with new attainment of speech acoustics and DSP. The first step, researching high quality Chinese all−syllable speech database, all Chinese syllable can be synthesized by using feature parameters of the database, and it is easy to change its duration, intensity and tone by means of control the parameters. The next step is creating Chinese speech knowledge database, it includes Chinese syntax rules, grammar rules and other rules. According to the input text, the Chinese knowledge database can form pronunciation rules, and then the synthesis system can output fluent and natural Chinese speech. This realized really Chinese text to speech conversation.

2.0 THE FUNDAMENTAL PRINCIPLE AND ALGORITHM

2.1 Phonetic Units. Chinese language and Chinese characters have many features which are different from the European language. Each Chinese character pronunciation corresponds one syllable, although there are more than 10000 Chinese characters (words) in common use, considering with many characters have the same pronunciation in Chinese, there are 1281 difference pronunciation in Chinese. Chinese is tone language, each syllable has one tone of four. it is the best choice to use syllable as the synthesis basic unit. For text−to−speech system, of course, not only these syllables have correct articulatic pronunciation, but also, their pronunciation feature, e.g. stress, intonation, duration, lexical tone etc., can be controlled by rules.

2.2 Analysis−by−synthesis method· We selected syllables as the basic synthesis units, and used Multi−Pulse Linear Predication Coding (MPLPC) method as speech analysis and synthesis method, although MPLPC in major used in speech coding, but it may have good application in Chinese synthesis by rules.

The MPLPC algorithm use a group multi−pulse generation to instead of pitch pulse generation and white noise generation, and synthetic speech is produced with synthesis filter excited by the multi−pulse, pulses' location and amplitude are carried out by minimiz error between synthetic and original speech signal. The simplified pulse search algorithm is given as follows: pulse location n_i for the i−th pulse is determined by searching the maximum absolute value for g_i.

$$g_i = \frac{R_{hx}(n_i) - \sum_{k=1}^{i-1} g_k \times R_{hh}(|n_k - n_i|)}{R_{hh}(0)} \qquad 1 \leqslant n_i, n_k \leqslant N$$

Where N denoted the analysis frame length, $R_{hx}(n)$ is the crosscorrelation function between weighted speech and weighted impulse response, and R_{hh} is the autocorrelation function for the weighted impulse response.

2.3 Coding. A group of reflection coefficients and multi−pulse sequence have been gotten after doing MPLPC analysis to Chinese syllable speech signal, due to the parameters is too much to control them in synthesis by rules, it must be simplified.

After analysis, we find there are strongly periodical in vowel part (YunMu part) the multi−pulse sequence of all Chinese syllables can be divided three part after multi−pulse LPC analysis : (1) initial part which contains unvoiced consonant and transition between unvoiced and voiced sound. (2) middle part which contains a main vowel and it's a largest part of syllable, and (3) ending part which has no clear period as part (1). The K (PARCOR) coefficents and the location and amplitude of excitation pulses (multi−pulse) will be coded at bit rate of 9.6 Kb/s in part (1) and part (3). In part (2), there are a serial of period in which the K coefficients and excitation parameters change slowly and regularly from one period to others, and all periods can represented by using the K and excitation parameters of several period patterns. The K coefficients, the location and amplitude of exciting pulses and the pitch of periods pattern are coded and stored. All periods in part (2) can effectively be represented by interpolating period patterns. A syllable is synthesized by concatenating part (1), part (2) and represented part (2). In database, the average coding rate is about 1.6 K per syllable which duration is 330ms.

The example of this algorithm is shown in Fig. 1. (a) is a segment of original speech waveform. (b) is multi−pulse sequence of this speech. (c) is on period pattern of multi−pulse sequence. (d) is multi−pulse sequence used for synthesizing speech created by interpolation. (e) is the waveform of synthesizing speech.

(a)

(b)

(e)

(c)

(d)
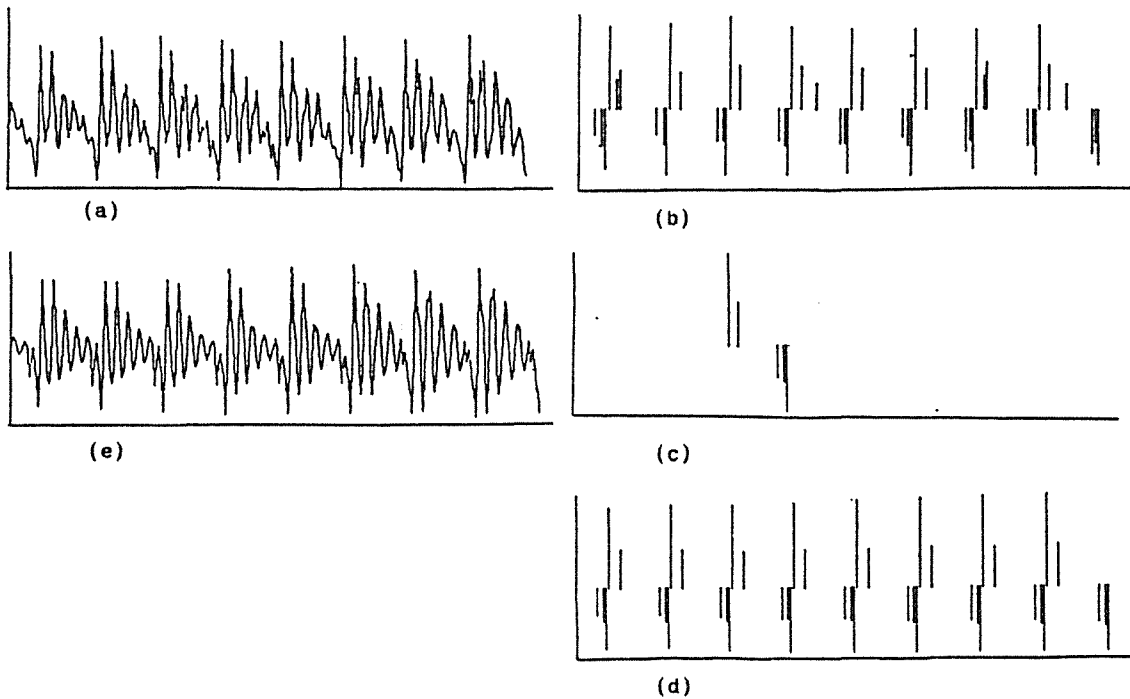
Fig. 1   (a) Original speech waveform
(b) Multi−pulse sequence of (a)
(c) A period pattern of multi−pulse sequence
(d) The multi−pulse sequence used for synthesizing speech
(e) The waveform of synthesis speech

3.0 THE SYSTEM REALIZATION

We devolped a Chinese all−syllable real−time analysis/synthesis system based on MPLPC method for a good research environment and devolpment tool of Chinese analysis and synthesis.

3.1 <u>Hardware.</u> The hardware of this system includes :

IBM−PC macrocomputer (XT, AT, 286, 386).

The programmable filter board (AF−2), it includes low−pass filter and speech reconstruction filter.

DSP TMS320C25−A high speed processing board.

TMS320C25−A high speed processing board can do ten millon multiplication/addition per second, (data word length is 16 bits, register and multiplier are 32 bits), it is a key part which ensures speech signal process in real time, the board has 32K byte program memory and 64K byte data memory, 12 bit A/D and 12 bit D/A converter, there is 8 bit PIO port, and DMA control circuit from PC macrocomputer to TMS320C25, this system combines high speed of digital signal processor and perfect opreating system of PC macrocomputer, with microphone, recorder and other equipment, it forms a speech processing system which function is powerful.

3.2 <u>Software</u> The software of this system includes :

Speech signal data collection and output, speech waveform edition and comparing, multi−pulse LPC analysis and synthesis, pitch detect, correct and edit speech synthesis parameters, sort and manage Chinese speech parameter database.

Due to the plentful hardware and software resources, the system not only is a good research environment and devolpment tool of Chinese speech analysis and synthesis, but also becomes a original version of Chinese text−to−speech conversion system.

Using the last speech analysis/synthesis system, we have done analysis and synthesis reasearch of Chinese all−syllable (1281 syllables), the original speech is from standard Chinese, the Chinese syllables are spoken by a man who speaks standard Chinese in recorder room, each syllable lasts about 300−400ms that is not allowed too short or too long. Then a 12 bit A/D converter is used to get the original data at sampling frequency of 10 KHz.

The procedure of analysis and synthesis have been done alternately, in the first, each syllable be analysised, get its feature parameters, then synthesis and restructe the syllable with the parameters. in synthesis procedure, correct the parameters by listening sound and comparing the original speech waveform with synthetic speech waveform, until the sound is satisfied. The parameters of 1281 syllables formed Chinese all syllable speech parameter database.

The system structure showed as Fig. 2.
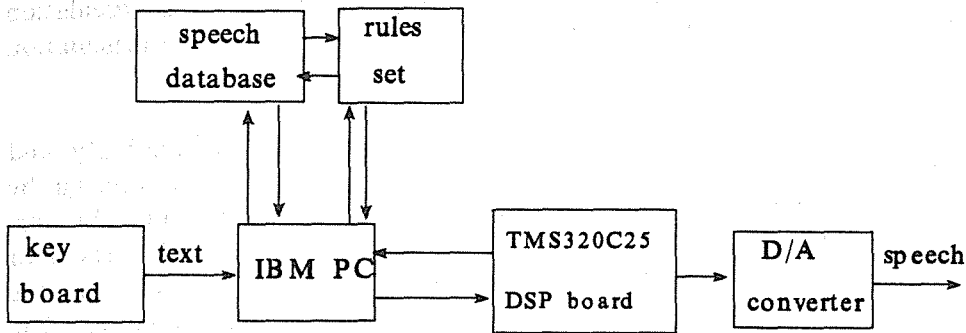
Fig. 2.　Block diagram of speech synthesis system.

Using this parameter database and synthesis software, we can synthesis all Chinese syllable real time with high articulation. Fig. 3 is a block diagram of synthesizing Chinese by rules. The text to speech rules select parameters of a syllable in the database and modify it by rules, which produce a serial multi—pulse sequences and vocal tract coefficients (K coefficients) for synthesizing a Chinese syllable.
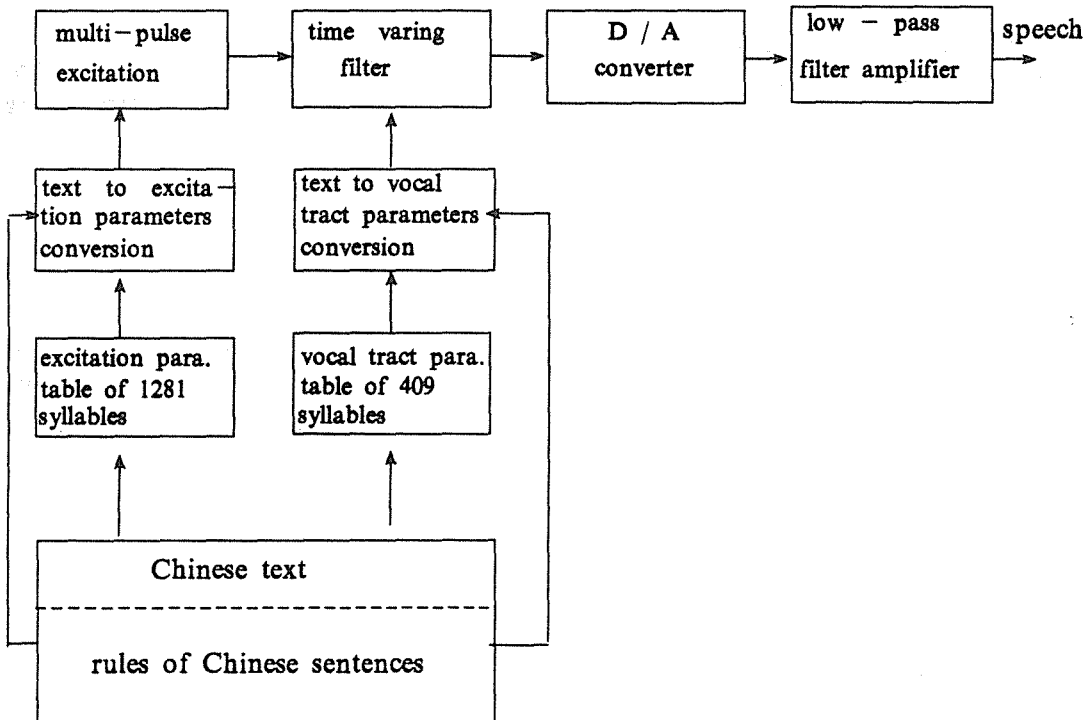
Fig. 3.　Block diagram of synthesis of Chinese by rules

4.0 EXPERIMENT

For appraising the quality of synthetic speech objectively, we have done a articulation test. The test troops contains ten members (five male and five female), the articulation result is 96.02 %.

Many Chinese text to speech systems are proposed in which high intelligibility and good naturalness are much hopeful. Our system is one of those systems andcan be used as a basic tool for studding speech analysis, synthesis and recognition. The normal Chinese character disk operating system of PC computer named CCDOS has been modified that ability of audio effect added when a Chinese character displayed on the monitor. Some sentences and short papers will be readied out from computer. The main purpose of this system is as a tool for studding text to speech, in which the rules of acoustics phonetics, phonetic linguistics and grammar including syllable juncture, pause juncture tone–sandhi tone model and so on, can easily be inserted and changed. The synthesizing speech output from a computer in real time and a large number of synthesizing speech will be judged for improving the quality of synthesis speech by modification of the rules. One of actual applications of this system in the near future is that can be used as a proff–read system of a computer the sound come out from this system simultaneously when the text displayed on the monitor.

5.0 CONCLUSION

Unrestricted Chinese sentences can be generated by the proposed Chinese synthesis by rules system in real time. The more tight rules set will be made in future research work.

6.0 ACKNOWLEDGEMENT

REFERENCES

Dennis H. Klatt "Review of text to speech system for English", J. Acoust. Soc. Am. 67, (3), 737–793, (1990)

Zhang Jialu "Acoustic parameters and phonological rules of a text–to–speech system for Chinese", ACTA ACUSTICA, vol. 13, no. 4, 113–120, (1990)

Lin—Shan Lee, et al. "The synthesis rules in a Chinese text—to—speech system", IEEE, Trans. ASSP, vol. 37, No.9, 1309—1320, (1989)

NI Hong, LI Changli and MO Fuyuan "Chinese all—syllable real—time synthesis system based on MPLPC technique", Proc. NCSICS, 92—95, (1989) (in Chinese)

MO Fuyuan, LI Changli, NI Hong "Chinese all—syllable real—time synthesis system", Proc. ICSP' 90, 369—372, (1990)

Atal, B.S. "High—quality speech at low bit rates: multi—pulse and stochastically excited linear predictive coders", Proc. ICASSP, 1681—1684, (1986)

Kazunori OZAWA and Takashi ARASEKI "Low Bit Rate Multi—pulse Speech Coder with Natural Speech Quality", Proc. ICASSP, 457—460, (1986)

Phoneme Recognition Using A Modified LVQ2 Method

Shozo Makino
Research Center for Applied Information Sciences, Tohoku University, Sendai, Japan.

Mitsuru Endo
Research Center for Applied Information Sciences, Tohoku University, Sendai, Japan.

Toshio Sone
Research Institute of Electrical Communication, Tohoku University, Sendai, Japan.

Ken'iti Kido
Chiba Institute of Technology, Narashino, Japan.

ABSTRACT This paper proposes a new phoneme recognition method based on the Learning Vector Quantization(LVQ2) algorithm. In the LVQ2 algorithm proposed by Kohonen, two reference vectors are modified at the same time if the first nearest class to an input vector is incorrect and the second nearest class to the input vector is correct. We propose a modified training algorithm for the LVQ2 method. In the modified LVQ2 algorithm, p reference vectors are modified at the same time if the correct class is within the N-th rank where N is set to some constant. Using this algorithm, the reference vectors of each phoneme are constructed from training samples. The likelihood matrix is computed using the reference vectors, where each row indicates the likelihood sequence of each phoneme and each column indicates the likelihoods of all phonemes for each 10-ms unit. The optimum phoneme sequence is computed from the likelihood matrix using the 2-level DP with duration constraints. The training based on the modified LVQ2 algorithm was carried out for speech samples in the 212 word vocabulary uttered by 7 male and 8 female speakers. The recognition experiment of 30 phonemes was carried out for speech samples in the 212 word vocabulary uttered by another 3 male and 2 female speakers. The phoneme recognition score was 89.1%. The phoneme recognition score obtained by the modified LVQ2 algorithm was higher than that obtained by the original LVQ2 algorithm. We applied this method to a multi-speaker-dependent phoneme recognition task for continuous speech uttered Bunsetsu by Bunsetsu. The training was carried out using 70 sentences uttered by two male speakers. The recognition experiment was carried out for another 226 sentences uttered by the same two speakers. The phoneme recognition score was 85.5% for the speech samples in continuous speech.

1.0 INTRODUCTION

The neural network approach is one of the very promising approaches to a phoneme recognition task. We have proposed a phoneme recognition method using the multi-layer perceptrons[1,2], which produced a hypothesis of a phoneme sequence. However, there is a problem in robustness for variations of duration within a phoneme because those systems used a phoneme reference pattern with average duration for each phoneme.

The Learning Vector Quantization(LVQ,LVQ2) methods were proposed by Kohonen et al.[3]. They showed that the LVQ2 was superior to the LVQ. However, in the LVQ2 method, two reference vectors are modified at the same time if the first nearest class to an input vector is incorrect and the second nearest class to the input vector is correct. If the given vector is recognized as the third rank, the modification is not occurred. McDermott et al.[4] developed a shift-tolerant phoneme recognition system based on the LVQ2 method. This system used multiple reference patterns with 70 ms of duration. Accordingly the system can deal with the variation of duration within a phoneme. However, this system did not make a hypothesis of a phoneme sequence but discriminated a phoneme from a given phoneme group for a given segment. Iwamida et al.[5] developed a LVQ-HMM phoneme recognition system. In this system, speech is at first transformed to a vector-code sequence using a code-book made by the LVQ2 method and then the discrete type of HMM is applied to the vector-code sequence. The phoneme recognition system also discriminated a phoneme from a given phoneme group for a given segment.

As described above, there still remain several problems in constructing a phoneme recognition system using the LVQ2 method as follows:

(1) No training algorithm if the rank of the given vector is greater than the second rank, and

(2) No segmentation and recognition method for continuous speech.

This paper describes a phoneme recognition system based on the Learning Vector Quantization algorithm and the 2-level DP[6]. The reference patterns are trained using the modified Learning Vector Quantization algorithms(MLVQ2) which we will propose in this paper. Each phoneme has multiple reference patterns with 70 ms of duration. Accordingly the system can also deal with the variation of duration within a phoneme. Next, we will investigate the optimum dimension to represent the reference patterns. Finally we will construct a phoneme recognition system by integrating the 2-level DP. The system produces a hypothesis of a phoneme sequence by taking into account phoneme duration constraints.

2.0 MODIFIED LEARNING VECTOR QUANTIZATION ALGORITHMS(MLVQ2)

The Learning Vector Quantization constructs non-linear boundary for classification using a training algorithm such as the perceptron learning. Kohonen et al.[3]proposed two versions(LVQ, LVQ2) of the Learning Vector Quantization. In the LVQ2 algorithm, the reference vector is modified when a given training vector x satisfies the following three conditions: 1)the nearest class to the given vector must be incorrect, 2) the next-nearest class to the given vector must be correct and 3)the training vector must fall inside a small, symmetric window defined around the midpoint of the incorrect reference vector and the correct reference vector.

In our preliminary phoneme recognition experiments using the LVQ2 algorithm, we found that the given training vector hardly contributed to the learning if the rank of the given vector was greater than the second rank.

We propose three modified training algorithms for the LVQ2 method. In the modified LVQ2(MLVQ2) algorithms, p reference vectors are modified at the same time if the correct class is within the N-th rank where N is set to some constant. The modified LVQ2 algorithms consists of the following 6 steps. In step 1, reference vectors are chosen using the K-Means clustering method from each class. In step 2, the nearest reference vector of each class to an input vector is selected. In step 3, the rank of the correct class is computed. When the rank of the correct class is n, we assume that the reference vector of the correct class is m_n. In step 4,

n is checked to see whether or not n falls in the range of $2 \leq n \leq N$. In step 5, the check is made to see whether or not the input vector falls within a small window, where the window is defined around the midpoint of m_1 and m_n. In step 6, the i-th reference vector is modified according to one of the following three versions of the modified LVQ2 algorithm.

MLVQ2.a[7] step 6:

$$[m_i]^{t+1} = [m_i - \alpha_n(t)(x - m_i)]^t \qquad (i=1, \cdots, n-1) \tag{1}$$

$$[m_n]^{t+1} = [m_n + \alpha_n(t)(x - m_n)]^t \tag{2}$$

MLVQ2.b step 6:

$$[m_{n-1}]^{t+1} = [m_{n-1} - \alpha_1(t)(x - m_{n-1})]^t \tag{3}$$

$$[m_n]^{t+1} = [m_n + \alpha_1(t)(x - m_n)]^t \tag{4}$$

MLVQ2.c step 6:

$$[m_i]^{t+1} = [m_i - \frac{\alpha_1(t)}{n-1}(x - m_i)]^t \qquad (i=1, \cdots, n-1) \tag{5}$$

$$[m_n]^{t+1} = [m_n + \alpha_1(t)(x - m_n)]^t \tag{6}$$

where, $\alpha_n(t)(0 < \alpha_n(t) \ll 1)$

$$\alpha_n(t) = \alpha_0 (1 - \frac{t}{T})^n \tag{7}$$

T = No. of iterations $\times$ No. of samples. $\alpha_0 = 0.02$

Figure 1 shows the examples of the three versions together with the LVQ3 proposed by E. McDermott[8]. In the MLVQ2.a, if the correct training vector is recognized as the n-th rank, the top $n-1$ reference vectors are moved away by α_n and the n-th reference vector is moved nearer by α_n. In the MLVQ2.b, the $n-1$-th reference vector is moved away by α_1 and the n-th reference vector is moved nearer by α_1. In the MLVQ2.c, the top $n-1$ reference vectors are moved away by $\alpha_1/(n-1)$ and the n-th reference vector is moved nearer by α_1. In the LVQ3 proposed by E. McDermott[9], the first reference vector is moved away by α and the n-th reference vector is moved nearer by α.
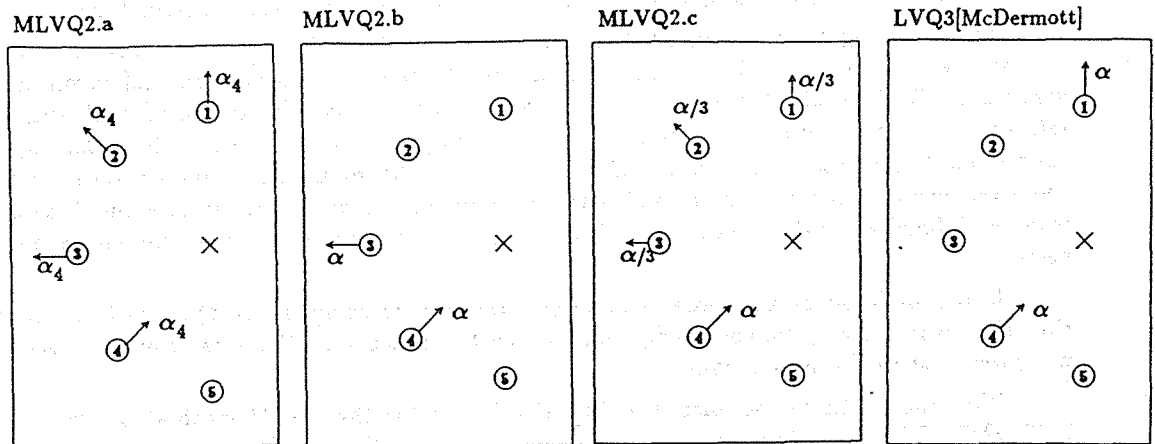
Numbers indicate ranks.

Figure 1 Examples of various LVQ algorithms (Rank of correct vector = 4)

3.0 COMPARISON AMONG THE VARIOUS LVQ ALGORITHMS

Recognition experiments were carried out for comparing the various LVQ algorithms. The recognition experiments were carried out for given phoneme segments: the beginning and final frames of each input phoneme are given. The trainings were carried out for phoneme samples in the 212 word vocabulary uttered by 7 male and 8 female speakers. The recognition experiments of 30 phonemes were carried out for phoneme samples in the 212 word vocabulary uttered by another 3 male and 2 female speakers.

Speech is analyzed by a 29 channel band-pass filter bank. The speech is represented by a sequence of logarithmic spectra with 10-ms frame shift.

The phoneme recognition system for the comparison is similar to the shift-tolerant model proposed by McDermott et al.[4]:

(1) 8 mel-cepstrum coefficients and 8 Δ mel-cepstrum coefficients are computed for every frame from the logarithmic spectrum. The value of each coefficient is normalized by the maximum magnitude of each coefficient. Each reference vector is represented by 112 coefficients(7 frames × 16 coefficients). Each class was assigned 15 reference vectors chosen by the K-Means clustering method.

(2) A 7-frame window is moved over the given phoneme segment and yields a 112(16x7) dimensional input vector every frame.

(3) In the training stage the various LVQ2 algorithms are applied to the input vector as described above.

(4) In the recognition stage we compute distances between the input vector and the nearest reference vector within each class.

(5) From this distance measure, each class was assigned an activation value a_w as follows:

$$a_w(c,t) = 1 - d(c,t) / \sum_i d(i,t) \tag{8}$$

where d, c and t are distance, class and time, respectively.

(6) The activation value of each frame is summed over the given phoneme segment.

(7) A class with the maximum activation value is regarded as a recognized output.
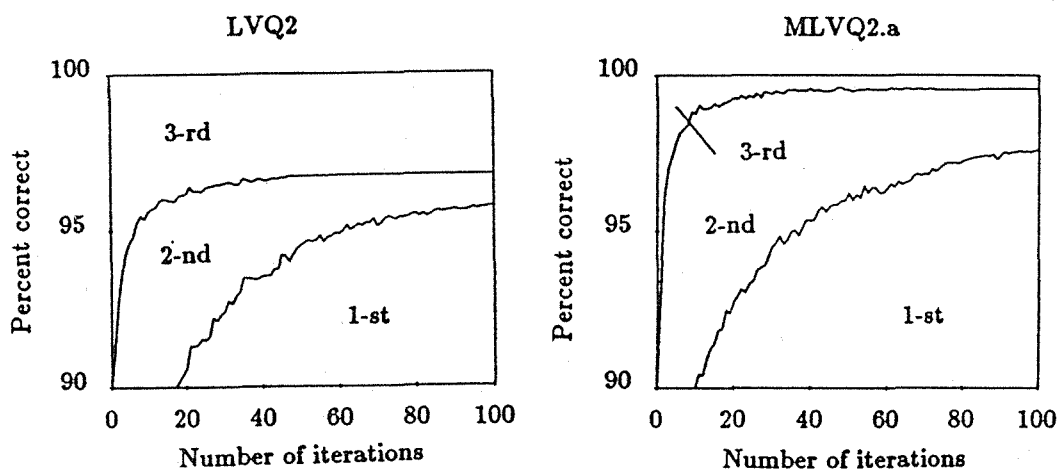
Figure 2 Relation between percent correct and number of iterations

Figure 2 shows the relation between recognition scores for /b/, /d/, /g/ consonants and number of iterations. In the LVQ2 method, the top-2 recognition score reached a plateau at small number of iterations and was lower compared to that obtained by the MLVQ2.a. That is, the Modified LVQ2 methods give a higher accumulated recognition scores because the

199

modification is carried out even if the rank of the given vector is greater than the second rank. Therefore, the recognition scores obtained by the MLVQ2 methods are higher than those obtained by the LVQ2 method.

Table 1 shows the phoneme recognition scores obtained by the various algorithms. The recognition scores obtained by the modified LVQ2 algorithms are higher by about 5% than those obtained by the LVQ2 algorithm. However, the MLVQ2.a gave a lower recognition score compared to the LVQ2 when the number of iteration increased and N was set to 30. In the MLVQ2.a algorithm, there remains a problem to define the value of N. The recognition scores obtained by the MLVQ2.b and MLVQ2.c increased as the number of iteration and N increased. Accordingly we will use the MLVQ2.b for phoneme recognition hereafter.

Table 1 Comparison among various LVQ algorithms
No. of iteration = 10

Algorithm	LVQ2	MLVQ2.a		MLVQ2.b	MLVQ2.c	LVQ3
N	(2)	10	30	(30)	(30)	(30)
Training set	82.4%	88.0	87.5	86.7	87.0	85.5
Test set	78.4	83.5	83.3	83.2	83.1	81.4

No. of iteration = 50

Algorithm	LVQ2	MLVQ2.a		MLVQ2.b	MLVQ2.c	LVQ3
N	(2)	5	30	(30)	(30)	(30)
Training set	86.4%	91.7	84.4	92.1	92.3	91.3
Test set	81.3	85.1	80.6	85.5	85.9	85.0

4.0 INVESTIGATION ON OPTIMUM DIMENSION OF REFERENCE VECTORS

In the experiments described above, we used the 112 dimensional vector computed from the 7-frame window, where each frame is represented by the 8 cepstrum coefficients and the 8 Δ cepstrum coefficients computed by the regression analysis over 5 frames. In this section, we will investigate the optimum dimension for representing a reference vector. We should investigate the following dimension:

(1)   Number(N_c) of the cepstrum coefficients computed in every frame

(2)   Number(N_d) of the Δ cepstrum coefficients computed in every frame

(3)   Number(N_s) of frames of the time span for computing Δ cepstrum

(4)   Number(N_w) of frames of the time window of the reference vector

We examined those variables described above by phoneme recognition experiments for /b/, /d/ and /g/ samples in the 212 word vocabulary uttered by 3 male and 2 female speakers, where the reference vector of each phoneme was constructed using speech samples uttered by another 7 male and 8 female speakers.

At first, N_w is set to 7 and then the optimum N_c and N_d are examined for N_s=3,5,7. Figure 3 shows the results for N_s=5. The combination of 8 cepstrum coefficients and 8 Δ cepstrum coefficients or 16 Δ cepstrum coefficients gave the best recognition scores for the test set. Next, in the case of using the parameters mentioned-above, the optimum N_s is examined. Figure 4 shows the results. The two kinds of parameters show the best recognition scores at N_s=5. There is no significant difference between the two kinds of parameters in the recognition scores. We will use 8 cepstrum coefficients and 8 Δ cepstrum coefficients obtained from 5-frame span hereafter. Under the conditions previously-described, we investigated on the optimum N_w. Figure 5 shows the results. The recognition scores were fluctuated. We will use 7 frames for N_w because the recognition score reached a plateau for the training set and relatively higher recognition score was obtained for the test set.

5.0 RECOGNITION OF PHONEMES IN SPOKEN WORDS

The recognition scores described in the previous section were obtained for given segments. It is necessary to carry out segmentation of speech for used as an acoustic processor in continuous speech recognition system. It is desirable to carry out simultaneously recognition and segmentation of phonemes. In this paper, we will use the 2-level DP for recognition and segmentation of phonemes in continuous speech. The phoneme recognition system is as follows:

(1) A 7-frame window is moved over an input speech and yields a 112(16x7) dimensional input vector every frame.

(2) The distances between the input vector and the nearest reference vector within each class are computed every frame.

(3) An optimum hypothesis for a phoneme sequence is made using the 2-level DP by taking into account phoneme duration constraints.

The following four kinds of constraints are examined for integrating to the 2-level DP.

(a) Minimum and maximum duration constraints of phoneme independent of the context.

N_c+N_d(Number of Coefficients)
$(N_s=3,\ N_w=7)$
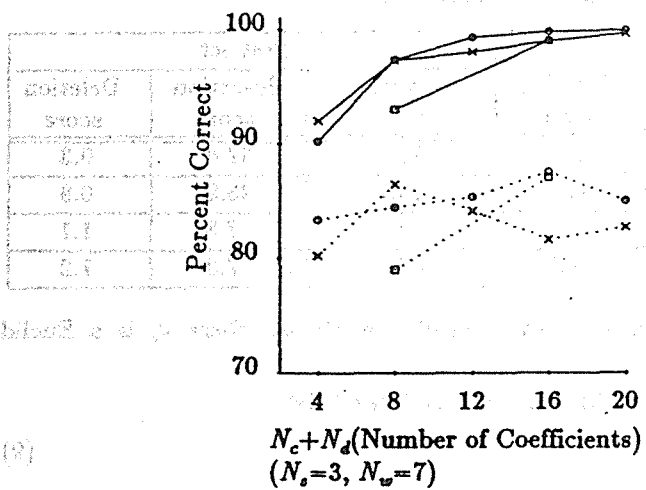
Figure 3 Effect of number of coefficients

N_s(Number of frames)
$(N_c+N_d = 16,\ N_w=7)$
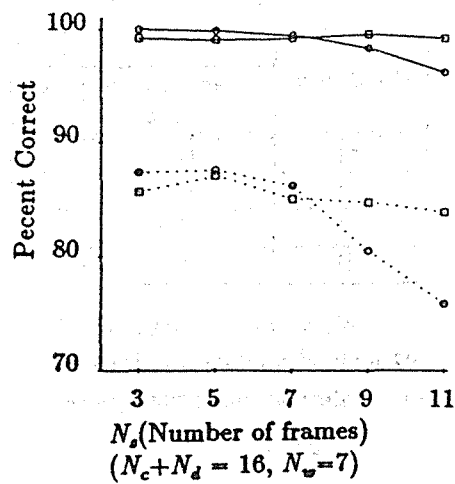
Figure 4 Effect of number of frames of time span for computing Δ cepstrum

N_w(Number of frames)
$(N_c=N_d=8,\ N_s=5)$
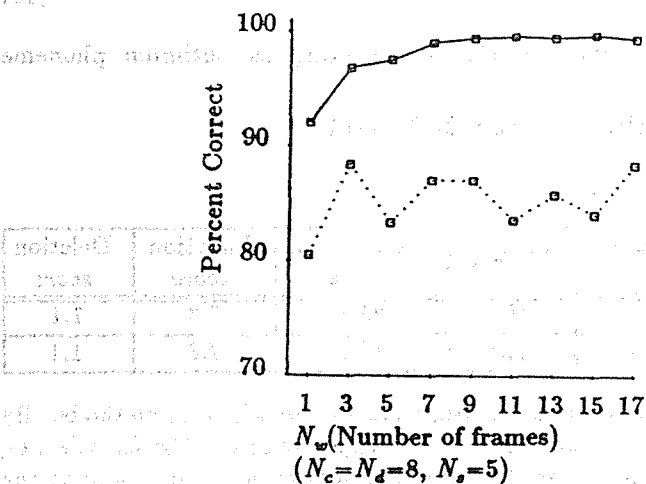
Figure 5 Effect of number of frames of time window of reference vector

——— Closed test
······ Open test

X   Cepstrum
O Δ cepstrum
□   Cepstrum+Δ cepstrum(1:1)

N_c: Number of coefficients of cepstrum
N_d: Number of coefficients of Δ cepstrum
N_s: Number of frames of time span
N_w: Number of frames of time window
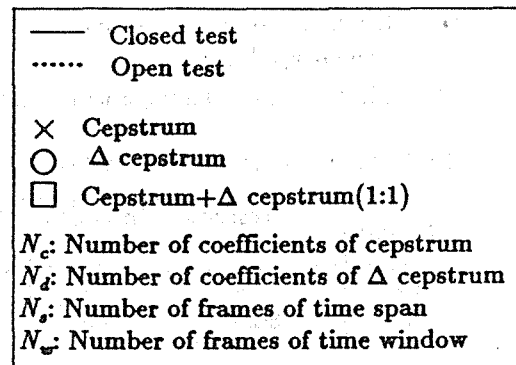
(b) (a)+phoneme connection constraints between successive two phonemes.

(c) Minimum duration constraints of phoneme dependent on the preceding phoneme, where the maximum duration constraints of phoneme is defined independent of the context.

(d) Minimum duration constraints of phoneme dependent on the preceding phoneme, where no constraints are used for the maximum duration constraints of phoneme.

The recognition experiments were carried out for evaluating the effectiveness of the duration constraints mentioned-above. The experimental conditions were the same as those described in the section 3.

Table 2 shows the recognition scores for the various constraints. As can been seen from the table 2, the minimum duration constraints of phoneme dependent on the preceding phoneme are very effective, on the contrary, the maximum duration constraints of phoneme are not necessary.

Table 2 Recognition scores for four kinds of duration constraints

Condition	Trainig set			Test set		
	Recognition score	Insertion score	Deletion score	Recognition score	Insertion score	Deletion score
(a)	96.2	38.2	0.2	91.1	57.6	0.3
(b)	95.8	13.2	0.3	89.7	23.9	0.8
(c)	95.4	3.7	0.6	89.1	7.3	1.1
(d)	95.3	3.7	0.7	89.1	7.3	1.2

Next we investigated the effectiveness of the following methods, where d_c is a Euclid distance of a phoneme class.

(a) Method using the square of the Euclid distance and the 2-level DP

$$d2 = d_c^2 \qquad (9)$$

(b) Method using the activation value and the 2-level DP

$$a_1 = 1 - d_c / \sum d_i \qquad (10)$$

(c) Method using the activation value and the DP for selecting an optimum phoneme sequence[9,10]

(d) Method using the logarithmic activation value and the 2-level DP

Table 3 Recognition scores for four kinds of methods

Method	Recognition score	Insertion score	Deletion score	Method	Recognition score	Insertion score	Deletion score
(a)	89.2	7.5	1.2	(b)	89.1	7.3	1.1
(c)	86.4	8.8	2.2	(d)	89.1	7.3	1.1

Table 3 shows recognition scores for the test set using the various kinds of methods. By comparing the method (b) to the method (c), the 2-level DP is superior to the DP for selecting an optimum phoneme sequence because the 2-level DP uses the information concerning to the phonemes with the rank ≥ 2. All distances or activation values gave similar performances.

6.0 RECOGNITION OF PHONEMES IN CONTINUOUS SPEECH

Recognition experiments were carried out for continuous speech uttered Bunsetsu by Bunsetsu. Each of two adult male uttered 148 sentences. The sentence speech were analyzed in the same fashion as described in the section 3. The additional training was carried out for

phoneme samples in 70 sentences uttered by the two male speakers, where the reference patterns of each phoneme obtained from the spoken words were used as the initial values. The recognition experiment of 30 phonemes was carried out for phoneme samples in the remaining 226 sentences uttered by the same two speakers. Table 4 shows relation between recognition scores and number of iteration in additional training. The recognition scores reached a plateau at ten iterations.

Table 4 Relation between recognition scores and number of iteration in additional training

Number of iteration in additional training	0	10	20	30	50
Recognition score	76.7%	85.5	85.9	86.3	86.3
Insertion score	10.3	6.9	7.0	6.5	6.2
Deletion score	4.0	4.0	4.0	4.0	4.1

7.0 CONCLUSION

We proposed a modified LVQ2 algorithm and showed its superiority to the original LVQ2 algorithm. We also showed that the 2-level DP using the Euclid distance obtained by the MLVQ2.b gave the best performance. The minimum duration of phoneme dependent on the preceding phoneme is the most effective constraint to achieve a high recognition score. In order to apply reference patterns obtained from spoken words to continuous speech, ten iterations in the additional training are sufficient for the adaptation.

REFERENCES

[1] S. Makino, T. Kawabata and K. Kido, "Recognition of Consonant Based on The Perceptron Model", Proc. of ICASSP-83, pp. 738-741(April, 1983)

[2] S. Moriai, S. Makino and K. Kido, "Phoneme Recognition in Continuous Speech Using Phoneme Discriminant Filters", Proc. of ICASSP-86, pp. 2251-2254(April, 1986)

[3] T. Kohonen, G. Barna and R. Chrisley, "Statistical Pattern Recognition with Neural Networks: Benchmarking Studies", IEEE Proc. of ICNN, Vol. 1, pp. 61-68(July, 1988)

[4] E. McDermott and S. Katagiri, "Shift-Invariant Phoneme Recognition Using Kohonen Networks", Proc. ASJ meeting, pp. 217-218(October, 1988)

[5] H. Iwamida, S. Katagiri, E. McDermott and Y. Tohkura, "A Hybrid Speech Recognition System Using HMMs with An LVQ-Trained Codebook", Proc. of ICASSP-90, pp. 489-492(April, 1990)

[6] H. Sakoe:"Two-Level DP-Matching -A Dynamic Programming Based Pattern Matching Algorithm for Connected Word Recognition-", IEEE Trans. Acoust. Speech and Signal Process., ASSP-27, 6, pp. 588-595(1979)

[7] M. Endo, S.Makino and K. Kido, "Phoneme Recognition Using A LVQ2 Method", Trans. IEICEJ, SP89-50 (September, 1989) (in Japanese)

[8] E. McDermott,"LVQ3 for Phoneme Recognition", Proc. ASJ meeting, pp.151-152(March, 1990)

[9] S. Moriai, S. Makino and K. Kido, "A Method for Selecting An Optimum Phoneme Sequence Using A Posteriori Probabilities of Phonemes", Journal of ASA supplement No. 1, PPP5 (November, 1988)

[10] S. Makino, A. Ito, M. Endo and K. Kido,"A Japanese Dictation System Based on Phoneme Recognition and A Dependency Grammar", Proc. of ICASSP-91, (May, 1991)

DESIGN, INSTALLATION AND TESTING OF A NEW PUBLIC ADDRESS SYSTEM FOR LANG PARK, BRISBANE.

Gray Pritchett
Vipac Engineers & Scientists Limited

Neil Packer
Creative Audio

ABSTRACT

Towards the end of 1990 the Lang Park Trust in Brisbane recognised the need for a new PA system for Queensland's Rugby League Headquarters - Lang Park.

The ground is used for football matches, union meetings and outdoor concerts. While a sound system for such a venue should not have to satisfy the requirements of a modern rock-band it must be able to make all announcements by the ground commentator or police at any football match or concert clearly audible and intelligible for safety reasons.

The existing system was generally inaudible at either end of the ground and barely audible in the newer stand on the eastern side of the ground, the Ron McAuliffe stand.

Vipac Engineers & Scientists Ltd. were appointed as acoustic consultants for the design of the new system and set the acoustic criteria that the new system had to meet. The electrical-electronic design was undertaken by Creative Audio.

A significant factor influencing success of the project was the multi-disciplinary approach to design. Historically, designs for similar projects have been developed in an isolated environment, usually either by acousticians or audio-electronics practitioners. Rarely has there been an adequate mix of practical and theoretical knowledge resulting in truly effective designs.

The new system was commissioned in February of 1991 and was found to be a vast improvement on the old system.

1.0 BACKGROUND

Towards the end of 1990 the Lang Park Trust in Brisbane recognised the need for a new PA system for Queensland's Rugby League Headquarters - Lang Park. With a maximum seating capacity of around 34000, Lang Park is second in size in Brisbane to only QE2 stadium at Mt Gravatt. The ground is used for football matches, union meetings and outdoor concerts. While a sound system for such a venue should not have to satisfy the requirements of a modern rock-band it must be able to make all announcements by the ground commentator or police at any football match or concert clearly audible and intelligible for safety reasons as stipulated in Australian Standard AS2220-1978 "Rules for Emergency Warning and Intercommunications Systems for Buildings."

2.0 EXISTING SYSTEM

The existing system was generally inaudible at either end of the ground and barely audible in the newer stand on the eastern side of the ground, the Ron McAuliffe stand. The only area that had a reasonable degree of audibility and intelligibility was the older western stand, the Frank Burke stand. The trust had received numerous complaints about inadequacies of the system and decided to upgrade.

To quantify the performance of the existing system, measurements of sound pressure level were taken during the 1990 Brisbane Rugby League Grand Final. A subjective assessment was also made of intelligibility. The sound pressure level of the PA system was measured on each of the four sides of the ground. Background noise level measurements were also taken at the same points.

Once the background noise levels had been measured it was possible to set the standards that the new system must achieve.

3.0 TENDER SPECIFICATION

A tender specification was written in October 1990. The tender was let December 1990. The specification set performance criteria as well as broad design requirements.

3.1 **Acoustic Performance Criteria.** The key acoustic performance criteria were -

1. Speech intelligibility - To be measured in accordance with Australian Standard AS2822-1985 "Acoustics - Method of assessing and predicting speech privacy and speech intelligibility".

2. Maximum Sound Pressure Level - Measurements of sound pressure level in specified areas of the ground and stands using a 800 Hz test tone.

3. Police Siren and Fire Siren - An emergency evacuation

siren and an "Attention" siren as specified by the Police must be clearly audible at all parts of the ground as must announcements from the police microphone.

3.2 **Design Requirements.** Development of the electrical-electronic design began with establishment of design criteria. These were determined in consultation with the client and through discussions between team members representing a range of disciplines applicable to the project. A significant factor influencing success of the project was the multi-disciplinary approach to design. Historically, designs for similar projects have been developed in an isolated environment, usually either by acousticians or audio-electronics practitioners. Rarely has there been an adequate mix of practical and theoretical knowledge resulting in truly effective designs.

3.2.1 **Design Criteria.** The design criteria were determined to be:

1. Transmission of intelligible speech to all seating areas of the stadium. Reproduced speech to be clearly audible and distinguishable above general ambient noise during Rugby League games, but not necessarily during the short, high peaks of ambient noise after goals are scored.

2. Transmission of band-limited light music programmes to all seating areas and wider band programme to one particular area (Frank Burke Stand).

3. The lowest cost system commensurate with all other criteria.

4. Low "spill" of sound to the immediate locale of the stadium.

5. A system to be easily operated by unskilled personnel, and requiring the lowest possible on-going upkeep cost.

6. A rugged and durable system, able to withstand the rigours of an outdoor public venue (i.e. vandal proof).

7. A system installed to professional quality norms, and where applicable, in compliance with Australian and International Standards.

8. A "zoned" system so that smaller audiences may be restricted to specific stadium seating.

3.2.2 **Design Parameters.** To meet the design criteria, certain critical design parameters were established.

1. Precise specification of electronic performance.

   If the criterion of a lowest cost system was to be met, performance of the system had to be contained within strict limits. Parameters which were strictly specified

206

included Bandwidth, Distortion (Total Harmonic), Signal-to-Noise Ratio, Crosstalk, Headroom, RF immunity, Overload performance, etc.

By way of illustration, two specific cases of strict specification and the accompanying rationale are provided below.

Bandwidth: Specified as 300Hz-7kHz +or- 3dB, for predominant use in reproducing high quality speech. (One area was specified as 100Hz-10kHz for improved light music reproduction).

The implications of reproducing wider band signals for speech use were considered to be unimportant in view of the additional cost of equipment required to handle the extremes of the audio spectra (particularly loudspeakers). The design called for the system bandwidth to be attenuated at 6dB per octave outside the limits.

Headroom: Headroom was specified variously throughout the system e.g.:

Mixer "Pre-Fader" Headroom: 35dB
Mixer Output Headroom: 16dB
Power Amplifier - loudspeaker: 6dB

Headroom was specified as the ratio of nominal operating level to the level at which harmonic distortion at the specified circuit point exceeds 3% in the band 300Hz to 7kHz.

2.   Loudspeaker Signal Transmission Technique

There are two basic methods of loudspeaker signal transmission:

a.   Low impedance - low voltage - high current, and
b.   High impedance - high voltage - low current.

Significant difficulties arose in the choice of a transmission technique for Lang Park. It was the desire of the client to have all of the amplification equipment in one or two locations for ease of serviceability, and for security reasons. As a result, some loudspeaker cables would be up to 300 metres long. Because of signal loss on cables, method "a" appeared to be out of the question. However, if the performance specifications were to be met, some of the loudspeakers would have to be run at levels approaching 100 watts.

A difficulty in using method "b" for such high power loudspeakers is that there are few, if any, manufacturers of quality, 100 watt line-to loudspeaker transformers.

Discussions with transformer manufacturers revealed that

the desired transformers could be manufactured with some difficulty and at relatively high cost. Comparisons were made of the cost of such transformers against the cost of very substantial loudspeaker cables required by method "a". Method "b" was chosen, as it appeared to have a slight edge in the area of cost, but also for consistency as it was the clear winner for the lower powered sections of the system.

3. Reliability and Fail Safe Performance.

System reliability was emphasised through specification of industrial installation techniques (buried cables, steel conduits, strained catenary cables, etc.) and through insistence on the use of high quality equipment and installation techniques.

A high degree of Fail Safe performance was designed into the system. Some techniques employed were:

- Redundant equipment (e.g. many lower powered amplifiers rather than few high powered amplifiers).
- Adjacent loudspeakers driven from different amplifiers.
- Re-chargeable battery powering of some equipment.
- Provision for later addition of uninterruptable power to the amplifier racks.
- Fire-proof cables in key areas.

4. Operational Simplicity

Emphasis was placed on the client's requirement to use the system without specialist operators. At every phase of design the question was asked "can this be operated simply?" The result is a system which, while inherently quite complex, can be operated by an unskilled announcer.

The emphases impacted on the design in several ways, some of which are listed below:

- Use of overload-proof microphones and pre-amplifiers.
- Use of microphones with frequency response independent of speaking position.
- Use of ambient noise dependent level controllers.
- Simple "Single-Switch" power - up on the whole system.
- All controls which affect system performance are locked away.

4.0 Testing of the System

Audibility and intelligibility are the two keys to a successful PA system. Testing for audibility involves measuring the maximum sound pressure level at receiver locations and is a relatively simple exercise involving only a sound level meter. Testing for intelligibility, however,

is a more involved process as intelligibility depends on the listener's hearing capabilities, the announcer's articulation and the content of the speech. AS2822-1985 "Acoustics - Methods of Assessing and Predicting Speech Privacy and Speech Intelligibility" sets out various means of predicting and assessing speech intelligibility. For this system, the subjective assessment method was used. A brief summary of this method, sometimes described as the Modified rhyme Test, is as follows.

The speech test material consists of 50 six-word sets of English monosyllabic words, arranged to form 50 related ensembles of six words each. Each ensemble is characterised by one vowel that is the nucleus of every word in it. All of the words in a given set of six start (or end) with the same consonantal phoneme or phoneme cluster and end (or start) with six different phonemic elements. An example set is shown below:

a swell
c yell
d smell
b sell
f tell
e well

The small letter superscripted before each word is used by the announcer to select which word in the set of six to read e.g. one announcer will read all the d words. A minimum of three people are needed to conduct the test, one acts as the announcer, one person monitors the announcer at 1m in front and the third person monitors the announcer at some point in the range of the PA system. It is possible to have more than one listener, each listener sitting at a different location.

The announcer reads the words in sentence form, e.g. "The first word is 'Swell.'" The listeners in the stadium then tick off from an identical list the word which most closely resembles what they think they heard. The listeners and speaker alternate until each person has announced once and listened at each listening position. At least one of the participants must be female. To determine if the system is satisfactory, the Articulation Index is calculated from the percentage of words that the listeners correctly understood and the graph shown in Figure 1. The level of speech communication obtained is determined from the Articulation Index and Figure 2.

The results of the Lang Park test on the new PA system showed it to be a "Good" system in most areas except for the upper area of the Ron McAuliffe stand which was "Fair".

REFERENCES

1. Australian Standard 2220-1978 - "Rules for emergency warning and intercommunications systems for buildings".

2. **Australian Standard 2822-1985 - "Acoustics - Method of assessing and predicting speech privacy and speech intelligibility".**
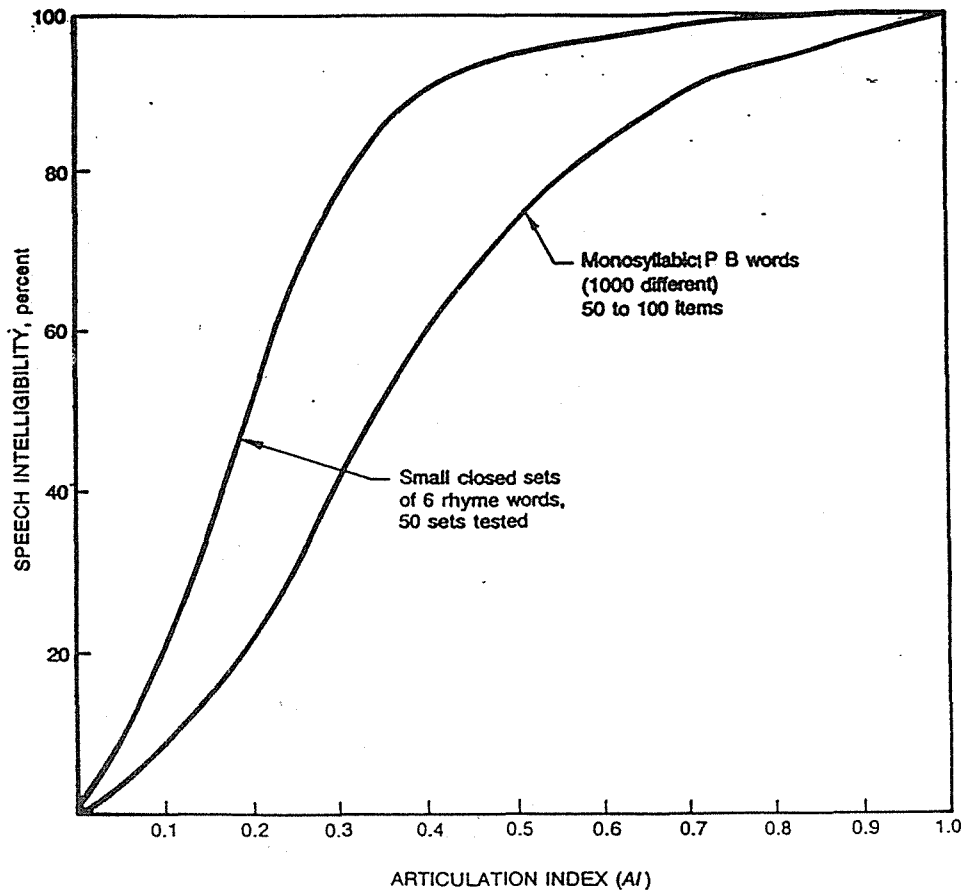
RELATIONSHIP BETWEEN ARTICULATION INDEX (*AI*) AND SPEECH INTELLIGIBILITY

FIGURE 1

RELATIONSHIP BETWEEN ARTICULATION INDEX, SPEECH
COMMUNICATION AND SPEECH PRIVACY

Articulation index (*AI*)	Speech communication	Speech privacy
0 0.05	None	Confidential
0.1		Normal
0.15 0.2		
0.25 0.3 0.35 0.4	Fair	Unsatisfactory
0.45 0.5 0.55 0.6	Good	
0.65 0.7 0.75 0.8 0.85 0.9 0.95 1.0	Excellent	None

FIGURE 2

IMPROVEMENT OF SPEECH DISCRIMINATION SCORE BY FILTERING TECHNIQUE IN SENSORINEURAL HEARING IMPAIRED

Kiyoshi YONEMOTO
National Rehabilitation Center for the Disabled
Japan

ABSTRACT   The purpose of this experiment is to investigate improvement of speech discrimination score by passing through filters for the sensorineural hearing impaired participants. In this paper, we measured Japanese speech discrimination score of the sensorineural hearing impaired participants by passing the monosyllable speech sound through two types of filter : "pitch frequency based comb filter (PC filter)" and "critical band based band pass filter (CB filter)". The coefficients of the PC filter were calculated from the fundamental frequency of the test material. The band widths of PC filters are 30, 50, 70, and 90 Hz, and the each filter is composed of 36 band BPF. The coefficients of the CB filter were calculated from the value of the critical band (Zwicker,1961). The band width of CB filters are 20, 40, 60, 80, and 90% of the corresponding critical band width, and the each filter is composed of 17 band BPF. From these experiments, we observed that only a participant improved speech discrimination score when the critical band filtered speech was used. However, all of the other participants' speech discrimination score, independent of their auditory function (hearing threshold level, frequency selectivity and temporal resolution) ability, were not improved at any condition of these two kinds of filtered speech sound.

1. INTRODUCTION

Although speech processing methods for hearing impaired people has been reported, reported results are not consistent. Some reports said that formant enhanced speech was one of speech processing methods useful for the hearing impaired subjects and suggest relationship between hearing threshold level and improvement of speech intelligibility score. Other reports did not support the usefulness of formant enhanced speech. We thought that these results were influenced by the other parameters of auditory function (Yonemoto, 1988).

We have measured Japanese speech discrimination score of the sensorineural hearing impaired participants using two types of processed speech sound : "formant-enhanced-speech" in which formant of vowels was enhanced and "consonant-shifted-speech" in which consonant part of VCV syllables was shifted toward the first vowel. We also measured frequency selectivity (the shape of the auditory filter) and temporal resolution (the ability of time gap detection) of the participants. These experiments suggested that the formant-enhanced-speech was effective for the participants who had poor frequency selectivity and the consonant-shifted-speech was useful for the participants who had low temporal resolution (Yonemoto, 1990).

In the present study, we investigated relationship between auditory function and improvement of speech discrimination score by the speech sound passed through 1) PC filter and 2) CB filter.

2. PARTICIPANTS

Three paid hearing-impaired listeners participated and six ears were measured. The hearing-impaired participants (aged 34-50 years) had cochlear origin sensorineural hearing loss, and their mean hearing threshold levels were in Table 1.

Frequency selectivity of the participants were measured to determine the shape of the auditory filter. We measured pure tone thresholds under various notched noise masking condition and estimated auditory filter shape by symmetric two parameter rounded-exponential model (Patterson, 1976). Furthermore, we estimated temporal resolution by measuring the thresholds of Gap-detection task (Fizgibborns, 1982). The value "p" indicates the sharpness of the auditory filter and the value "G" indicates the detected temporal gap threshold in Table 1.

Table 1 Mean hearing threshold level, value "p" (the sharpness of the auditory filter) and value "G" (the detected temporal gap threshold) for the participants.

Ps	Sex	Age		Mean HTL (dB HL)	p	G (ms)
A	F	3 2	R	8 1	14.7	6
			L	8 3	14.2	9
B	F	5 0	R	9 1	11.6	1 5
			L	1 1 9	9.3	2 5
C	F	3 8	R	8 1	6.4	2 3
			L	8 0	10.2	1 3

3. STIMULI

The speech signal to be presented was Japanese monosyllable male speech and was recorded on CD (TY-89, compact disk for evaluation of hearing aid fitting). The number of syllables was fifty, and presentation level was defined at subjects' most comfortable level. Test speech sound was produced by passing through the digital filter (IWATSU ISEL IS-201B) and presented by the earphone (TELEPHONICS TDH-49P/MX-41AR) monaurally (Fig 1).

PERSONAL COMPUTER
NEC PC-98XA

GP-IB

COMPACT DISC PLAYER
SONY CDP-333ESD

DIGITAL FILTER
IWATSU ISEL IS-201B

EARPHONE
TDH-49P/MX-41AR

POWER AMPLIFIER

ATTENUATOR
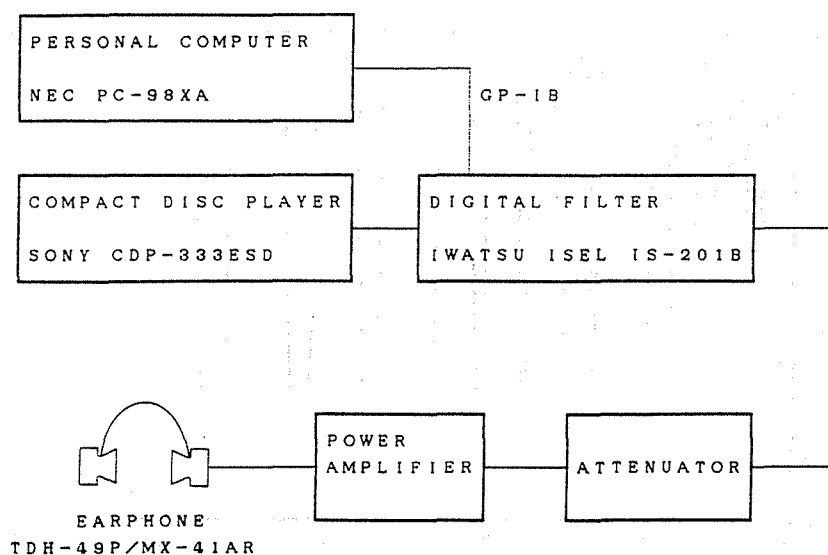
Fig.1 Block diagram of the measurement system.

4. PROCEDURE

The characteristics of the PC filter was defined by the fundamental frequency of the test speech signal and the coefficients of the digital filter were calculated with Kaiser-window method by the personal computer. This filter was constructed by 36 bands band pass filter, frequency interval of the center frequency of each BPF was
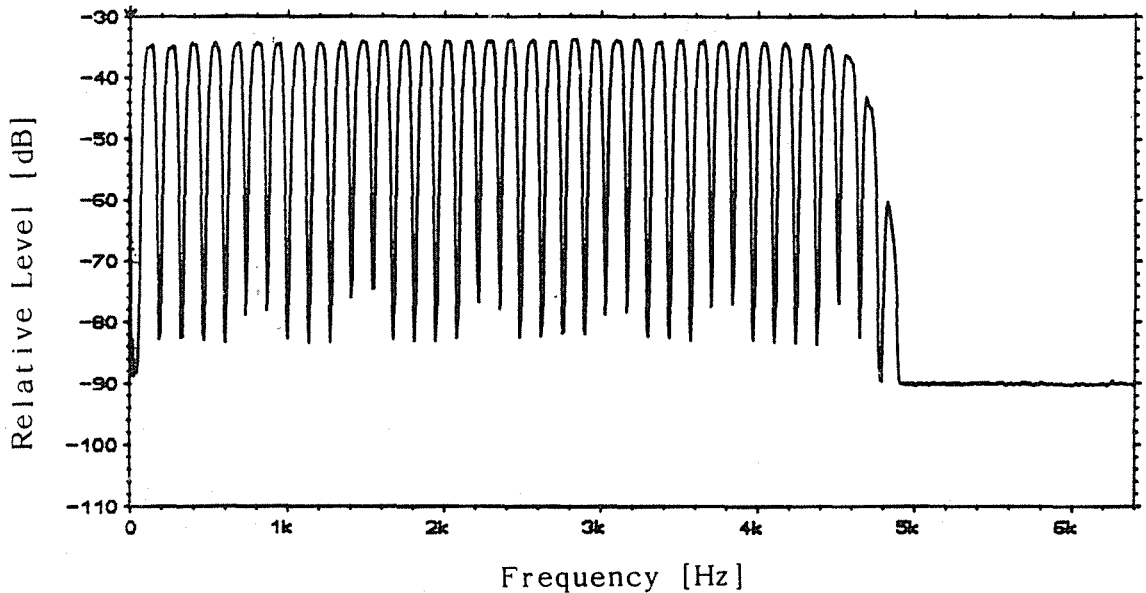
Fig.2 Frequency response of the PC filter. (band width : 70 Hz)
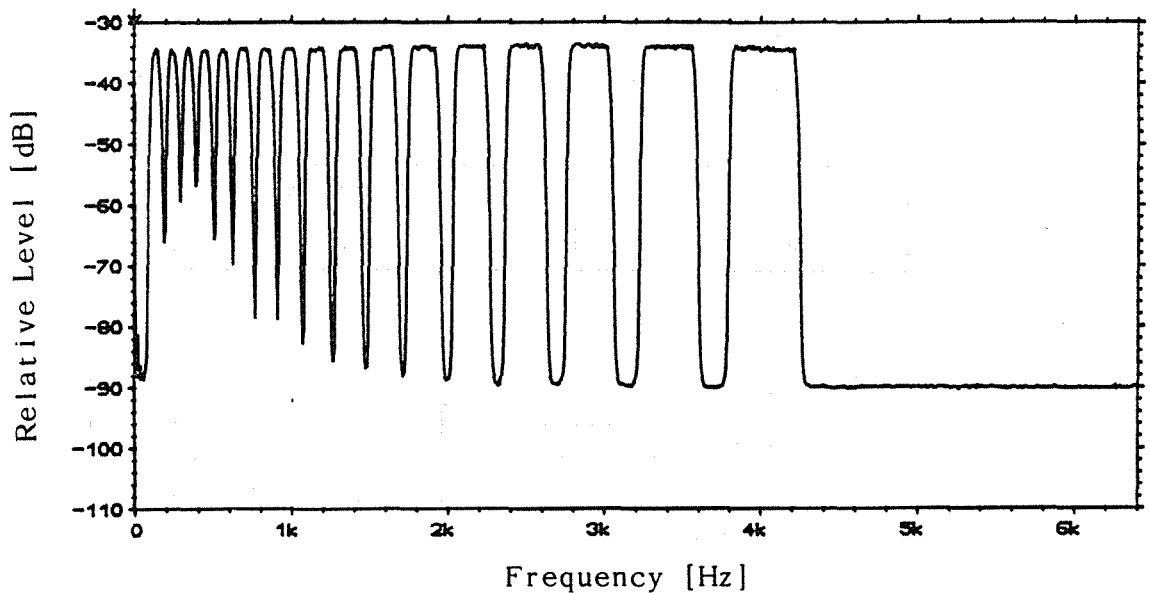
Fig.3 Frequency response of the CB filter. (band width : 60 %)

135 Hz and widths of each BPF were 30, 50, 70, 90 Hz. We measured speech discrimination score under passed speech through these four kinds of filter. One of the frequency responses was shown in figure 2.

The characteristics of the CB filter was defined by the value of the critical band (Zwicker, 1961), and the coefficients of the digital filter were calculated by Kizer-window method by the personal computer. This filter is constructed by 17 band BPF and band widths were 20, 40, 60, 80% of the corresponding critical band width. One of the frequency response was shown in figure 3.

5. RESULT

Each filtered speech discrimination score was shown in figures 4 to 9. Result of the PC filter was drawn by dashed line and CB filter was explained by solid line. In case of PC filter, the decrease of the speech discrimination with the decrease of band width was observed in all the participants' ear. In case of the CB filter, only one participant (figures 4 and 5) improved her score when band width was 80 and 90 %, but other participant' results did not show the useful improvement in speech discrimination score by this filtering method.
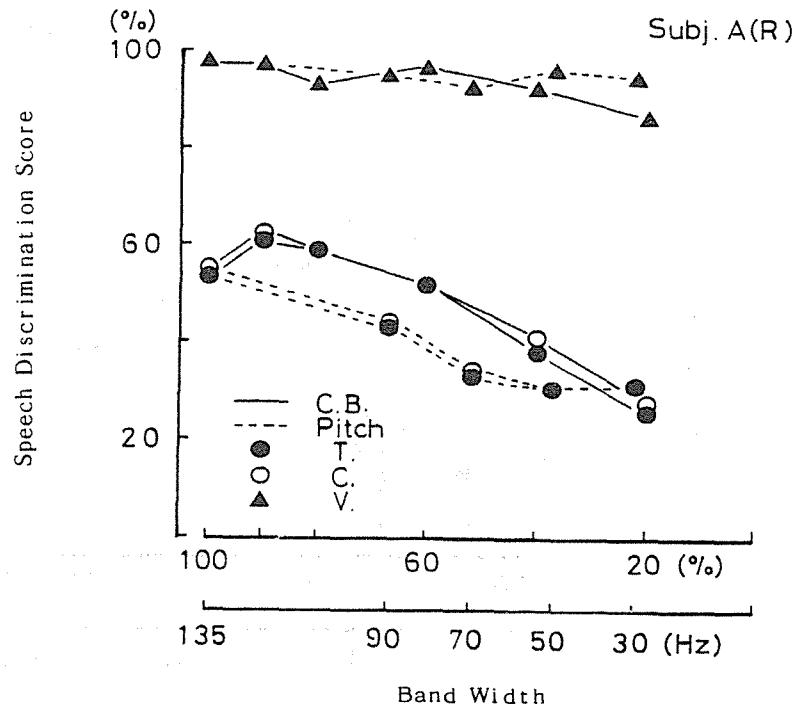
Fig.4 Each filtered Speech Discrimination score of participant A's right ear.
(C : consonant part, V : vowel part)
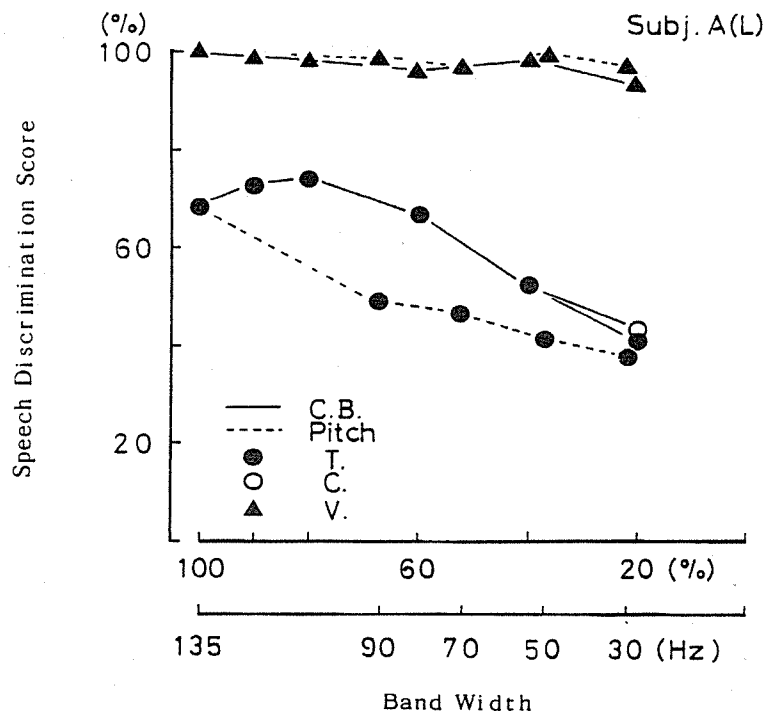
Fig.5 Each filtered Speech Discrimination score of
participant A's left ear.
(C : consonant part, V : vowel part)
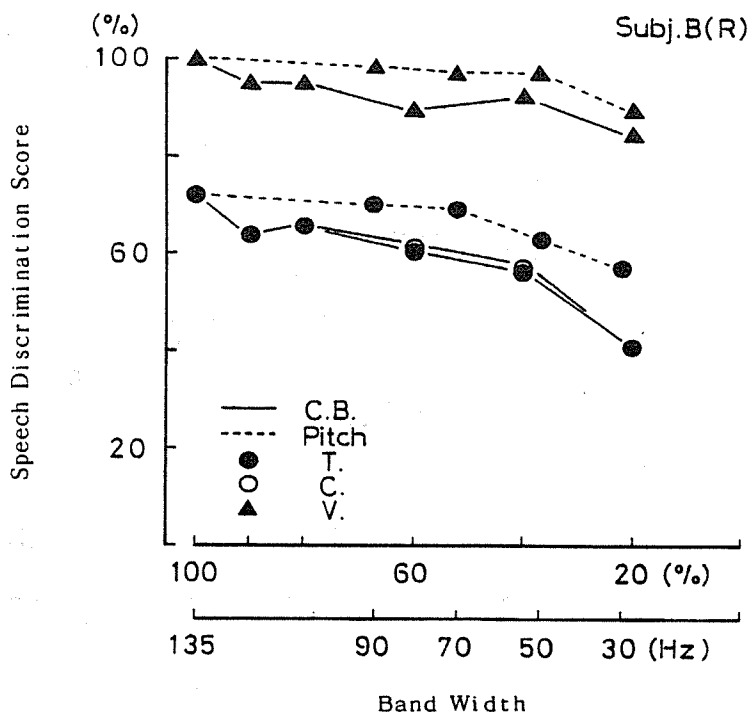
Fig.6 Each filtered Speech Discrimination score of
participant B's right ear.
(C : consonant part, V : vowel part)
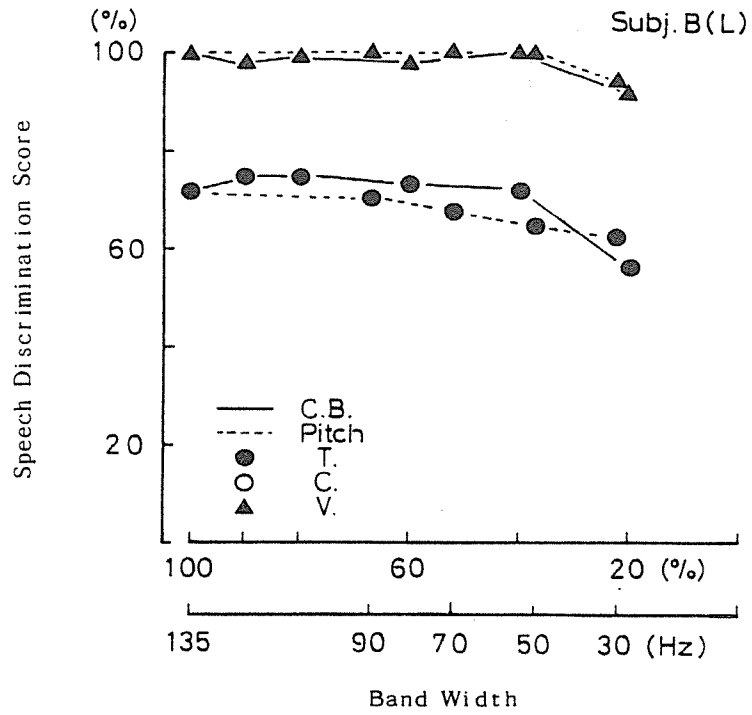
Fig.7 Each filtered Speech Discrimination score of
participant B's left ear.
(C : consonant part, V : vowel part)
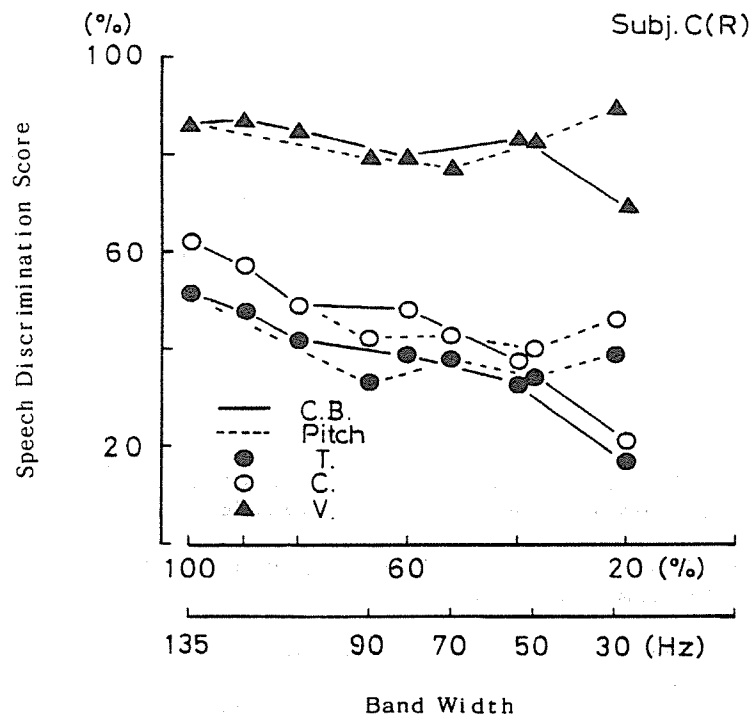
Fig.8 Each filtered Speech Discrimination score of
participant C's right ear.
(C : consonant part, V : vowel part)

217
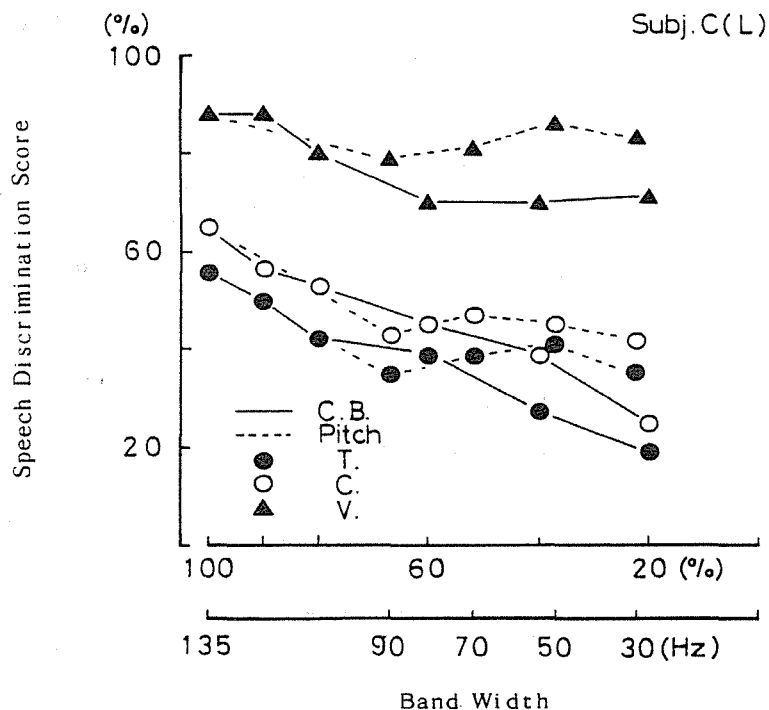
Fig.9 Each filtered Speech Discrimination score of
participant C's left ear.
(C : consonant part, V : vowel part)

6. CONCLUSION

We thought that wide shaped auditory filter mixes
spectrally closed frequency components and distorts
frequency information. Then, these speech processing might
be useful for the participants who had poor frequency
selectivity. But these result said that by the filtering
missed important speech information for hearing impaired
people.

REFERENCES

Fizgibbons P.J.,Wightman F.L.,Gap detection in normal and hearing-
impaired listeners,J.Acoust.Soc.Am.72,761-765,(1982).

Patterson R.D.,Auditory filter shapes derived with noise stimuli,
J.Acoust.Soc.Am.59,640-654,(1976).

Yonemoto K.,Kurauchi N.,Hamada H.,Miura T.,Relations between fre-
quency selectivity,temporal resolution,and speech intelligibility in
sensorineural hearing-impaired subjects,J.Acoust.Soc.Am.,S76,(1988).

Yonemoto K.,Kurauchi N.,Tauchi H.,Auditory function and effective
speech processing in sensorineural hearing impaired,"Proc.of XXth
International Congress of Audiology,42,(1990).

THE EFFECTIVENESS OF HEARING CONSERVATION METHODS AT INDOOR SHOOTING RANGES

Beno Groothoff
Environmental Directions
Australia

ABSTRACT

This paper considers a number of problems that can be experienced with measurements of gun noise at indoor shooting ranges and with hearing threshold levels. These problems consist mainly of incorrect measuring techniques and audiometric testing procedures, as well as the wearing of inappropriate hearing protection devices. The paper discusses common inaccuracies and means to overcome these. It also presents a method for evaluation of the effectiveness of hearing conservation methods through reliable measurements.

1.0 INTRODUCTION

Surveys undertaken on British infantry soldiers in 1965, 1969 and 1979 showed that slightly less than half had some degree of noise induced hearing loss and the proportion hardly changed despite the introduction of hearing protection in 1966. A survey in the US Army in the late 1970's told the same story. (Powell & Forrest 1988) The danger to hearing from small arms, such as rifles, machine guns and mortars has been amply demonstrated. (Burns 1973) Instructors in the use of firearms with armed forces, such as Army and Police, are likely to spend a considerable proportion of their working life at the shooting range. In doing so they would have a greater exposure to impulsive noise than, for instance, personnel shooting their training rounds. Instructors on indoor shooting ranges can be particularly disadvantaged due to the structure of these ranges which can cause reflections of the noise from the shots fired. These reflections, in actual fact, can increase the noise levels significantly.

This paper discusses briefly the most common problems associated with the measurement of gunshot noise and hearing levels. It also presents a method for the evaluation of hearing conservation methods at indoor shooting ranges through reliable measurements.

2.0 CHARACTERISTICS OF GUNSHOTS

2.1 Outdoors A single shot has two distinctive parts. The first part consists of the shockwave from the bullet as the muzzle velocity would be between approximately 600 and 1000 m/s depending on calibre and type of bullet. The bullet is therefore supersonic for several hundred metres after leaving the muzzle of the firearm.

The second part consists of the sound of the explosion in the firearm itself. This is illustrated in Figure 1 below representing the pressure wave form of a typical rifle shot at 4m distance. The time interval between start of the shot and the first passage through zero is 0.4 ms. The second large peak, at 3 ms, is caused by the sound of the explosion in the firearm.
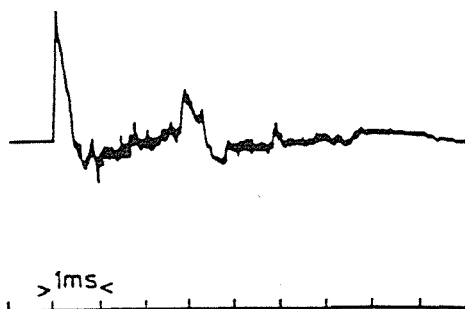
Figure 1
Pressure wave form of a typical rifle shot at 4m

The two components have different frequency characteristics and directionalities of which the shockwave is highly directional. These characteristics of a shot are such that the noise propagation is quite complex. (Smoorenburg 1979)

2.2 <u>Indoors</u> Indoor shooting ranges usually contain many reflecting surfaces. In such cases the pressure-time diagram forms a very complicated pattern as a result of the gun noise being reflected. The peak pressure direct from the source may well be much less than some of the reflections. This is illustrated in Figure 2 below which compares the first part of the pressure traces of a 5.56 mm rifle in an indoor range (a) 2 m to one side and (b) 2 m behind the muzzle. In (a) the sources of the different peaks are indicated, in (b) the direct pressure wave is much smaller than the following reverberant noise. (Note the different scales for the plots). (Powell & Forrest 1988)
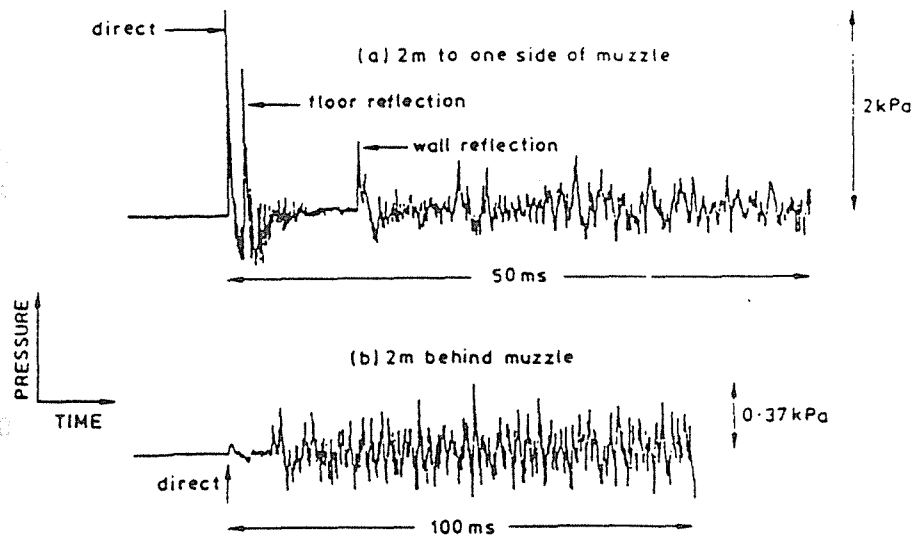
Figure 2
Pressure wave form of rifle shot on indoor range

3.0 NEED FOR HEARING CONSERVATION

The types of weapons and calibres used with armed forces such as Army and Police, as well as private security companies, fall typically in the range of the following calibres:- .22, 7.62mm, .38 and .357 magnum. The results of extensive practical tests of the shots fired with these weapons indicate noise levels in the range of 125 - 157 dB Peak Lin at the instructor's ear level when shots are being fired in close proximity, i.e. no more than 2.5 metres distance. These noise levels are capable of causing irreversible damage to the hearing mechanism in a relatively short period of exposure should adequate protection measures not be implemented and strictly adhered to.

4.0 FACTORS INFLUENCING THE RELIABILITY OF NOISE ASSESSMENTS

4.1 <u>Introduction</u> Special techniques are required when measuring impulse noise in order to be able to conduct reliable analysis of the noise and evaluation of its potential for the risk of hearing damage.

The difficulties encountered with impulse noise, according to Hassall and Zaveri (1979), stem mainly from the fact that they often contain high spectrum levels at low frequencies, are usually non-repetitive and are of very short duration.

Some of the more common equipment problems are discussed below.

4.2 Sound Level Meter A sound level meter. must be equipped for the measurement of peak sound pressure levels. Conventional sound level meters are quite unsuitable, the time over which they average to produce a r.m.s. answer is much longer than the duration of a typical weapon noise and therefore the pre- and post firing "silences" are included in the averaging and give an answer that is too low. Peak pressures and r.m.s. pressures are also no longer simply related, in fact, $P_{r.m.s.}$ cannot strictly be defined for a short duration impulse. (Powell and Forrest 1988)

4.3 Microphones It is of primary importance that the microphones and their pre-amplifiers function adequately at the pressures being measured. Free field type microphones may not possess this capacity. Suitable microphones are discussed in Chapter 6.0 Solutions to the Inadequacies.

4.4 Calibration Calibration procedures must be capable of covering the range of measurement. Calibration of all equipment should be checked "on site" before and after measurements.

4.5 Recording In the case of the use of an FM type tape recorder, care should be taken to avoid both over-recording, which will clip the peak, and under-recording, which will leave the signal buried in tape-recorder noise.

5.0 FACTORS INFLUENCING THE RELIABILITY OF AUDIOMETRIC TESTING

5.1 Introduction Factors which may affect the reliability of audiometric tests can be divided in avoidable and unavoidable sources. Some factors can be readily avoided through proper design and organisation of a testing program. Unavoidable sources are often inherent to the subject being tested.

5.2 Test Location Audiometry performed outside an acoustic laboratory, as is typically the case with industrial audiometry, will not necessarily provide totally accurate determinations of hearing level thresholds. (Hartley 1973) Thresholds measured under industrial conditions are generally 5 dB higher than would be under clinical conditions. (Dobie 1983) However, this is not necessarily a major disadvantage provided the discrepancy is consistent within the test program.

5.3 Background Noise Levels Many articles have been written of the need to perform audiometry only if the background noise level is within the recommended standard, or the test environment is sufficiently quiet. (Dobie 1985) Ideally a sound booth complying with the relevant standard should be used. Maximum acceptable background noise levels at specific frequencies are set out in Table 5.1 of Australian Standard 1269-1989 Hearing conservation.

5.4 Calibration The correct calibration of the audiometer forms an imperative element of accurate audiometry. Calibration therefore must be checked regularly. Depending on its use the calibration of the audiometer can consist of a daily function check and a monthly biological check apart from a yearly acoustical check by a suitable laboratory.

Calibration of the audiometer relates to both tone intensity and tone frequency and should be within the tolerance allowed by Standard ISO-389. This could mean, however, that through

recalibration of the audiometer small variations in tone intensity and/or tone frequency can be introduced even though the calibration settings are within the recommended standard at all times. (Woodford 1984)

5.5 Operator Variations between different operators can also lead to variability in the obtained data. However, this can be minimised by ensuring that a rigidly controlled technique is used. (Burns 1973) A method of minimising data variability due to operator error is to ensure that audiometry is only performed by a fully trained audiometrician or specially trained health professional, such as a trained nurse. (Dobie 1985)

5.6 Quiet Periods prior to Tests An accurate measurement of a subject's true pure tone hearing level threshold cannot be obtained if the subject is affected by a temporary shift in hearing level thresholds at the time of testing. (Burns 1973)

Australian Standard 1269-1989 Hearing conservation prescribes a period of quiet of not less than 16 hours prior to reference audiometry and a period of quiet of not less than seven hours for monitoring audiometry.

To avoid a temporary threshold shift in the subjects hearing level prior to audiometric testing, the subject's co-operation is required and the wearing of adequate hearing protection under strictly controlled conditions may be necessary.

5.7 Other Causes Apart from the above outlined major and largely avoidable causes of inaccuracies in audiometric data, many other factors can cause inaccurate data to be obtained. Factors which can cause an inability to respond accurately to pure tone stimuli can be;
- biological variations in the subject's thresholds and hearing loss either temporary or permanent in nature
- fatigue and/or disease
- inadequate instruction
- malingering
- incorrect earphone placement
- variations in headset pressure on the external ear
- improper stimulus presentation
- subject's improved performance through "learning"
- tinnitus
- variation of hearing protective devices worn by subjects.

6.0 SOLUTIONS TO THE INADEQUACIES

6.1 Noise Level Measurements To be able to successfully capture the short durations of impulse noise, modern sound level meters are equipped with the modes Peak and Impulse. In the Peak mode, with an integration time of approximately 20 μs, the highest level is measured that has been reached at any moment during the measuring period. In the Impulse mode an integration time of 35 ms is represented in accordance with I.E.C. 179.

A suitable sound level meter should be a Type 1 and be either a precision integrating or modular precision sound level meter. For the purpose of measuring weapon noise levels a specially adapted microphone should be fitted to the sound level meter. Suitable microphones are, for instance, the one eighth inch Bruel & Kjaer type 4138 and the half inch Bruel & Kjaer type 4147 microphones. The range of measurement should be suitable, either direct or through insertion in the circuit of an

attenuator, to measure the produced noise levels without overloading the system.

It would further be required to conduct a frequency analysis of the noise of some shots of the weapons used. A one to one or one third octave filter set could be used for this purpose in the field.

For the purpose of preserving the pressure time diagram of the impulse noise and/or frequency analysis, either a graphic level recorder or suitable tape recorder could be used. Suitable tape recorders are usually of the FM recording type in order not to lose some of the frequencies, particularly the higher, due to tape recorder noise. Of the non-FM type tape recorders a Nagra IV-S tape recorder will suffice.

Frequency analysis made from the recorded noise levels could incorporate a Real Time Analyzer, computer system and plotter.

Calibration of the equipment to manufacturer's specifications must be carried out prior to and immediately after the measurement period. Calibration and recalibration must comply with the requirements of Australian Standard 1259-1982, Sound Level Meters, for the particular type used.

6.2 Audiometric Testing A summary of all the available data comparing manual, self-recording and microprocessor controlled audiometers suggests that the self-recording audiometer generally provides a lower hearing level threshold at the frequencies typically tested in industrial audiometry. (Harris 1979, Neville 1989)

A review by Neville (1989) of the role of industrial audiometry and hearing conservation concludes that a microprocessor controlled audiometer has benefits over manually operated and self-recording audiometers.

These benefits include, amongst other things, standardised test procedure, avoidance of the problem of the operator being required to record positive and negative responses and assessing the validity of responses, (Harris 1980), and the fact that it can often be used as a manual type audiometer for the testing of subjects found difficult to test in the automatic mode. For this reason the use of two microprocessor controlled audiometers, to be used for the duration of the investigation, is recommended. Verbal advice from NAL suggests that audiometric testing be performed in abbreviated form only, i.e. at test frequencies of 1000, 2000, 4000 and 6000 Hz.

A comparison of manual and microprocessor controlled audiometers showed less inter-test difference in the case of the latter, but the mean difference for all frequencies was less than 1 dB and there was good correlation between individual results.

A period of 12 months as a minimum period is recommended for regular audiometric monitoring. Audiometric monitoring should be carried out before and after sessions. In order to be able to conduct the audiometric tests no more than two minutes after cessation of the exposure, backup range supervisors may be required to relieve the instructors allowing them to leave the range straight away for audiometric testing. In addition, a mobile test booth or stationary purpose built booth are required within a suitable distance from the range.

6.3 Test Space   Practical experience, such as obtained during previous investigations has shown that it is difficult to obtain a test room which has background levels sufficiently low to comply with the requirements of Australian Standard 1269-1989 and is near enough to the shooting range to enable personnel to be tested two minutes after cessation of their noise exposure, the latter being the main difficulty of the two.   Mobile sound booths generally do comply with these background levels and have the advantage that they can be positioned near the shooting range.

6.4   Test Frequencies   Australian Standard 1269-1989 prescribes different test frequencies for reference and monitoring audiometric testing.   These are:
-     reference testing; 500, 1000, 2000, 3000, 4000 and 6000 Hz
-     monitoring testing; 3000, 4000 and 6000 Hz.

The National Acoustic Laboratories (NAL) suggests that, for the purpose of detecting threshold shifts, testing at 1000, 2000, 4000 and 6000 Hz is sufficient.   Sinclair (1984) supports this view when he reports on studies performed by himself and by the Royal Air Force which, in 1970, introduced 3-frequency testing of both ears for reference and monitoring audiometry, without any pre-test preparation such as aural examination or avoiding noise exposure immediately prior to testing.   Test frequencies were 1000, 2000 and 4000 Hz.   It was found that, as a screening procedure for detecting significant hearing threshold loss before the onset of hearing disability, 3-frequency testing in each ear, without any preparation or aural examination, was an accurate and realistic alternative to 6 or 8-frequency testing. it was concluded that this procedure was effective in health and cost terms.

6.5   Hearing Protection Devices   It is recommended that instructors wear one type of HPD consistently throughout the investigation period whenever they are exposed to shooting noise.   Instructors should be re-trained in proper hearing protection practices.   These practices should be adhered to at all times where there is a likelihood of exposure to gun noise.

In addition, it would be necessary for instructors to become familiar with the requirement of testing for variations in threshold hearing levels within two minutes after cessation of the noise exposure and the reason for it.

7.0   RECOMMENDED METHOD

7.1   Noise Level Measurements   The conducting of noise level measurements of the noise that instructors are exposed to forms an integral part of any investigation.   In the case of impulsive type noise, such as weapon noise, it is even more important due to the potentially damaging effects of this type of noise.   It must therefore be measured correctly and hereto the following equipment is recommended to be used:

-     Precision Integrating or Modular Precision Sound Level Meter such as the Bruel & Kjaer Type 2231
-     Capacity of measuring noise levels up to at least 160 dB
-     Microphone adapted for this type of noise, e.g. the half inch Bruel & Kjaer Type 4147 microphone
-     One to one third octave filter set such as the Bruel & Kjaer Type 1625 Filter

225

- Recording system for either graphical or audio recording of the signals. Suitable tape recorders are of the FM recording type or the Nagra IV-s
- Calibration system capable of dealing with the measurement range.

7.2 Measurement Positions   It is recommended that noise level measurements be made in a sphere of max 30 cm from the subject's ears taking into account the directivity and sensitivity of the microphone as well as the direction of the noise approaching the ear. Measurements of the weapon noise levels should also be made at a set distance from the shooter so that noise level predictions can be made in case of signal overload at the subject's ear position.

7.3 Audiometric Testing   Audiometric testing, with a view to establishing if TTS is present after exposure to weapon noise, forms an important part of any investigation and must therefore be carried out under optimum conditions. To achieve these conditions it is recommended that:
- audiometric testing be made possible two minutes after cessation of exposure
- a mobile sound booth or purpose built sound booth near the indoor range be incorporated
- a micro processor controlled audiometer be used or, alternatively, a manually operated audiometer with a well-trained operator
- audiometric testing be performed before and after each session over a period of not less than 12 months per subject.
- instructors be educated and trained in the workings of the hearing mechanism, in particular the effects of impulse noise on it and the mechanism of recovery from noise exposure causing TTS to be at its maximum about two minutes after the cessation of the noise exposure, after which recovery continues in a more orderly fashion (Harris, 1979)
- an abbreviated audiometric test program be adopted for both ears, i.e. testing at 1000, 2000, 4000 and 6000 Hz only.

7.4 Hearing Protection Devices   In order to make the exposure to shooting noise as consistent as possible, it is recommended that a particular type of hearing protector, once chosen, be worn throughout the period of investigation whenever shooting sessions are held or exposure to shooting noise is likely.

The measured noise levels at the subject's ears and the known attenuation from the HPD can then be used to determine if the noise levels at the protected ears are sufficiently reduced. This can then be confirmed, or otherwise, through audiograms to establish if TTS is present or not.

BIBLIOGRAPHY

1.   Australian   Standard   1259-1982,   Sound   Level   Meters Standards Association of Australia, North Sydney

2.   Australian   Standard   1269-1989,   Hearing   Conservation Standards Association of Australia, North Sydney

3.   Burns, W., (1973) Noise and Man 2nd Edition, William Clowes & Sons Limited, London

4. Dobie, R.A., (1983) Reliability and Validity of Industrial Audiometry: Implications for Hearing Conservation Program Design Laryngoscope 1983, 93(7)

5. Dobie, R.A., (1985) Industrial Audiometry and the Otologist Laryngoscope 1985, 95(4)

6. Harris, C.M., (1979) Handbook Noise Control, 2nd Edition, McGraw-Hill Book Company, New York

7. Harris, DS.A. (1979) Microprocessor versus Selfrecording Audiometry in Industry, J. Aud. Res. 1979 a, 19

8. Harris, D.A., (1979) Microprocessor, self-recording and manual audiometry, J. Aud. Res. 1979 b 19

9. Harris, J.D. (1980) A Comparison of Computerised Audiometry by ANSI, Bekesy Fixed Frequency and Modified ISO Procedures in an Industrial Hearing Conservation Program. J. Aud. Res. 1980, 20

10. Hartley, B.P.R., Howell, R.W., Sinclair, A., Slattery, D.A.D., (1973) Subject Variability in Short Term Audiometric Recording Br. J. Ind. Med. 1973, 30

11. Hassall, J.R., Zaveri, K. (1979) Acoustic Noise Measurements Bruel & Kjaer, Denmark

12. Hodge, D.C., Garinther, G.R. (1970) Validation of the Single Impulse Correction Factor of the CHABA Impulse – Noise Damage – Risk Criterion Journal of Acoustical Society of America 48, 6 (part 2)

13. International Standard ISO 1999 – 1990, Acoustics – Determination of Occupational Noise Exposure and Estimation of Noise Induced Hearing Impairment 1990, Geneva, 1975

14. Neville, G.R., (1989) The role of industrial audiometry in the conservation of hearing, A review University of Qld.

15. Powell, R.F., Forrest, M.R., (1988) Noise in the Military Environment, Brassey's Defence Publishers, London

16. Smoorenburg, G.F. (1979) Voorlopige evaluatie van de geluidhinder van schiet inrichtingen Ministerie van Defensie rapport No BG-HR-10-01, The Hague June 1979

17. Woodford, C.M., The effect of calibration tolerance values on obtained audiometric threshold: A hearing conservation perspective. Am Ind Hyg Assoc Journal 1984 45, 2

OTHER SOURCES OF INFORMATION

1. Groothoff, B. (1990) Shooting noise, A research project into noise from various types of firearms on shooting ranges, Measurement techniques and Community Response, Environmental Directions Report, Brisbane February 1990

2. Groothoff, B. (1990) Noise Level Study Indoor Shooting Range at Police C.I.B. Building, Makerston Street, Brisbane, Environmental Directions Report, Brisbane March 1990

NOISE-INDUCED HEARING LOSS IN A POPULATION OF PUNJAB BUS DRIVERS

S.N.Gupta,
Department of ENT,
Dayanand Medical College,
Ludhiana-141 001 (India).

R.K.Dhir,
Department of ENT,
Dayanand Medical College,
Ludhiana-141 001 (India).

A.S.Bansal,
Department of Mechanical Engineering,
Punjab Agricultural University,
Ludhiana-141 004 (India).

ABSTRACT

Noise levels and their frequency spectra have been studied close to the ear of the bus drivers of many buses of Punjab Roadways. Hearing thresholds of 120 bus drivers were measured after excluding about 62 drivers having otological abnormalities or exposure to noise from fire arms during their previous army service. Noise-induced hearing loss (NIHL) or deterioration was found after substracting the hearing thresholds of unexposed normal ears from those of the affected ones. All the audiograms being convex downwards suggest that the sensitivity of hearing of subjects studied decreases with increase in frequency. Hearing impairment increases with duration of exposure and noise level. The audiograms also depict typical "dip" at 4 KHz in almost all the cases with a hearing loss upto 20dB.The deterioration in conversation frequency range of 0.5 to 2.0 KHz has also been observed. There is some indication of the right ears (facing the window) of the drivers having suffered more hearing loss at certain frequencies, as compared to the left ones. Most of the bus drivers have suffered varying degree of deafness over whole of the audiometric frequency range.

1.0 INTRODUCTION

Persons exposed to excessive noise slowly but inevitably

develop hearing loss. Noise-induced hearing loss(NIHL)
.can occur all of a sudden and in a rapid traumatic
manner only if the exposure is extremely severe.
Actually, the loss occurs at an inperceptibly slow rate
and without pain. Noise loud enough to produce temporary
threshold shift or a ringing in the ears often produce a
permanent hearing loss. The NIHL is the most prevalent irrev-
ersible diseas amongst the occupational diseases.

For conservation of hearing in and around the city of
Ludhiana studies have been initiated on noise surveys
(Bansal) and occupational hearing loss amongst industrial
and other workers (Gupta at el). A lot of literature is
available on the NIHL amongst the workers of industrially ·
advanced countries and in India also some work on the
hearing loss of industrial workers has been reported.
Although some studies on the hearing loss of automobile
drivers abroad have been reported (Michael et. al and
Dufresne et al) no such studies have been conducted so
far in India. This is mainly due to the lack of
consciousness and disregard of hearing hazard caused by
automobile noise. Buses and trucks generate a
considerable amount of noise which originates from
engines, air turbulence and frictional contact of
vehicles' tyres with the road. The drivers and their
employers need to be properly educated about the noise
hazards and the steps that are essential for noise
control and hearing conservation. However, no hearing
conservation programme will prove effective in the
absence of legislation enforcing the employer to
compensate for the hearing damage caused to the drivers
or operators exposed to excessive noise levels.

Most of the trucks in India, except the heavy duty ones,
are fitted with the same engines as those used in the
buses. Because of the load and traffic conditions trucks
move at low speed and noise levels recorded close to the
ears of the truck driver are rarely above 85 dB(A). Also,
as expected,Audiometric evaluation for hearing loss of a
group of truck drivers revealed no significant hearing
impairment. Noise levles measured inside the buses
varied from 85 to 94 dB(A),depending upon the speed and
condition of the buses. Studies on the noise levels of
the buses and the hearing loss suffered by the drivers
have been conducted and are presented here.

2.0 NOISE LEVEL MEASUREMENTS

Noise levels of about 20 buses of Punjab Roadways
(Ludhiana Depot) plying between Ludhiana and other cities
in Panjab State (India) were measured. The noise levels
were observed close to the ear of the operator while the
buses accelerated in different gears and finally when
they attained their normal cruising speed. Buses
selected were of two makes and some of these were almost
new and in very good condition. Some of the buses were
old and obviously their condition was not so good and the

condition of some old buses was really bad.

Noise levels were measured by using B & K Sound Level Meter No.2209 and by positioning the microphone close to the ear of the driver while the buses were on their routine journey and loaded to their full capacities. Besides measuring the dB(A) noise levels, octave band frequency analyses were also conducted by using B & K Octave Filter Set No.1613. Horns are extensively used by the drivers in India and their sound levels are significantly high. The imp. hold noise levels of horns in the vehicles varied from 110 to 112 dB(A). Frequent use of the horn further adversely affects the noise environment even inside the bus and thus adds to hearing impairment. Typical noise spectra of four different buses while operating at normal cruising speed (without the horn) are presented on Figure 1, while the information regarding these buses representing four different categories (I-New, II-old but in good condition, III-old and in bad condition and IV-the small bus for hill area, old but in good condition) is presented in Table 1. The dB(A) noise levels and the cruising speed of these buses at which the frequency analyses were carried out are also given in this table. The noise spectra of all these buses (Figure 1) indicate that the noise has maximum intensity at low frequency. It is expected to cause hearing loss not only in the low frequency range but also in the higher frequency range above 2 KHz. The dB(A) noise levels being above 85 dB(A), and exposure duration for the bus drivers is invariably 8 hours and above in a day, hearing loss to the bus drivers is expected to occur.
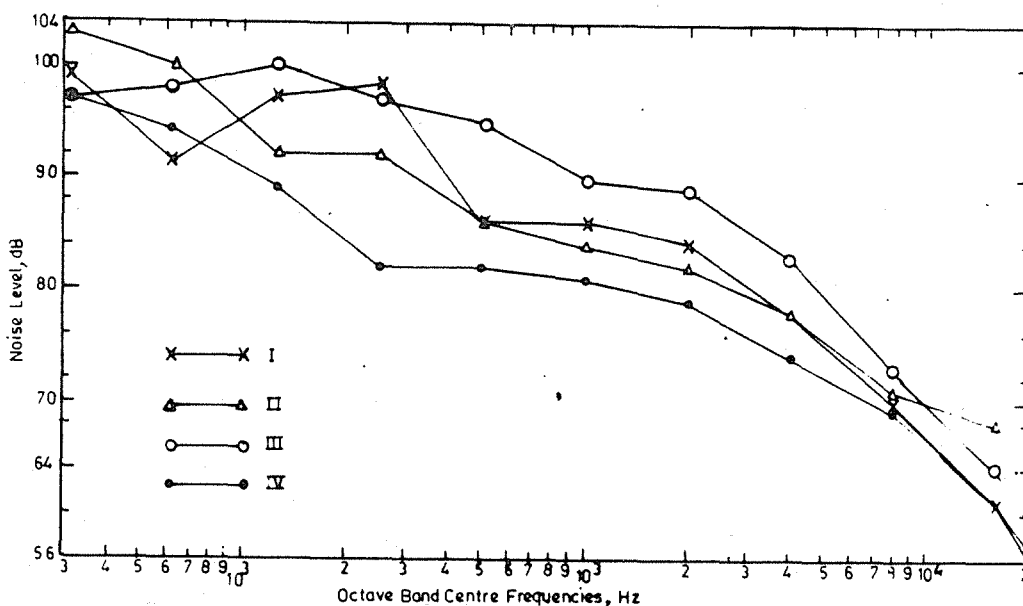
FIG.1 NOISE SPECTRA OF FOUR BUSES REPRESENTING DIFFERENT BUS CATAGORIES

Table 1:Information about buses representing four
       different categories.

Bus Cat.	Bus Regn. No.	Route:From Ludhiana to	Speed Km/hr	Noise level dB(A)	Bus Condition: New/old/good/ bad
I	Pb-12 8708	Amritsar	85	92.5	New,good
II	PBL 2863	Batala	75	92.0	Old,good
III	PBL 4269	Ahmedgarh	60	94.0	Old,bad
IV	PBL 2846	Kulu(Hill)	65	88.0	old,good

3.0 AUDIOMETRIC MEASUREMENTS

In this study 182 drivers were involved and they were
subjected to clinical examination. Before conducting
audiometric measurements, detailed information about
every driver was recorded regarding various otological
abnormalities and ex-servicemen with history of exposure
to blasts and fire-arms. Out of the total of 182 bus
drivers, 62 were excluded; which comprised of 36 ex-
servicemen, 12 with discharging ear, 10 diabetic and 4
hypertensive. For the measurement of the hearing
thresholds of the drivers Arphi Mark IV 700 Audiometer
was used. Its calibration was checked every day before
use, with the help of Autocal. A mobile sound proof
audiometric chamber was used to conduct the study. The
back ground noise inside the chamber was found to be
sufficiently below 30 dB at all the octava band centre
frequencies from 0.25 to 16 KHz. This conformed to the
accepted practice (American National Standards
Institute-1971). The standard procedure (Bienvenue and
Michael) was used to determine the threshold of hearing
of both ears of the subjects. The drivers were tested in
the morning after rest in order to exclude temporary
threshold shift. The bus drivers were grouped in five
years exposure duration of 1-5, 6-10, 11-15, 16-20, 21-
25 & 26-30 years; the corresponding number of exposed
drivers in these groups were 2,19, 21, 32,24 & 22,
respectively. The data regarding 1-5 year exposure
duration in which there were only two subjects has not
been included. The bus drivers were grouped according to
their age in five years age spans of 26-30, 31-35, 36-
40, years 41-45, 46-50 and 51-55 years, the
corresponding number of exposed drivers in these groups
were 14, 22,25, 20, 17 and 22, respectively. The mean
normal thresholds for these age groups were taken from a
separate study conducted earlier, which was based on the
threshold levels of normal ears of about 4150 local
subjects unexposed to excessive noise. These values are
given in Table 2. The deterioration due to noise was
calculated by subtracting these values from the mean
thresholds obtained in various age groups. For age upto
30 years the correction as against (30+to35 yrs)group

231

was applied.

Table 2:Average thresholds dB of normal ears at diff.Freqs.

Age groups (Years)	Frequency in KHz							
	0.25	0.5	1.0	2.0	3.0	4.0	6.0	8.0
30 ± 35	15.52	14.35	13.11	9.47	9.94	11.76	13.87	14.10
35 ± 40	16.90	14.58	14.67	10.21	11.88	14.67	16.46	18.01
40 ± 45	18.88	15.53	16.04	11.11	13.37	19.79	22.75	25.03
45 ± 50	19.31	16.73	17.22	11.99	14.44	20.71	24.81	26.83
50 ± 55	21.59	20.63	21.01	17.04	20.95	31.25	33.59	36.33
56 ± 60	22.78	21.10	21.97	19.19	24.81	33.59	39.37	41.92

4.0 DISCUSSION AND CONCLUSIONS

The mean pure tone threshold deterioration in drivers (Lt.ear & Rt. ear) of various groups of exposure duration are presented in Table 3. Variation of deterioration with frequency for drivers of different exposure groups (Lt.ear & Rt. ear) (6-10 yrs. to 26-30 yrs) are also presented in Figure 2. Exposure duration groups with less than 10 drivers have been neglected. The audiograms being convex downwards suggest that the sensitivity of hearing of subjects studied decreases with frequency, similar to that reported for white subjects (Gupta $_{at}$ el). In all cases the typical "dip" at 4 KHz is clearly depicted. The NIHL worsens with the increase in the length of exposure. Mean NIHL in Lt. and Rt. ear showed tendency to slightly higher deterioration of Rt. ear facing the open window. However, this has not been observed at all frequencies. The configuration of the audiograms show that the NIHL is a function of noise level, exposure duration and the frequency; with the aparent open dip at 4 KHz in all cases. This shows that almost all the drivers have suffered varying degrees of deafness.

Table 3: Mean pure tone threshold deterioration in drivers of various noise exposure groups at different frequencies (KHz)

Exposure (Years)	Ear	No. of Sub.	Mean deterioration audiogram							
			.25	.5	1	2	3	4	6	8
6-10	Lt.	19	0	-1	-2	-1	-2	-3	-6	-6
	Rt.	19	0	-1	-2	-1	-5	-8	-6	-6
11-15	Lt.	21	0	-1	-3	-2	-4	-11	-6	-8
	Rt.	21	0	-2	-1	-2	-4	-12	-10	-8
16-20	Lt.	32	-1	-3	-3	-5	-7	-12	-11	-10
	Rt.	32	0	-3	-1	-4	-8	-15	-11	-8
21-25	Lt.	24	-3	-5	-4	-5	-7	-13	-3	-1
	Rt.	24	-1	-2	-4	-2	-6	-16	-10	-4
26-30	Lt.	22	0	-3	-3	-2	-7	-16	-11	-5
	Rt.	22	0	-3	-2	-5	-8	-19	-14	-12
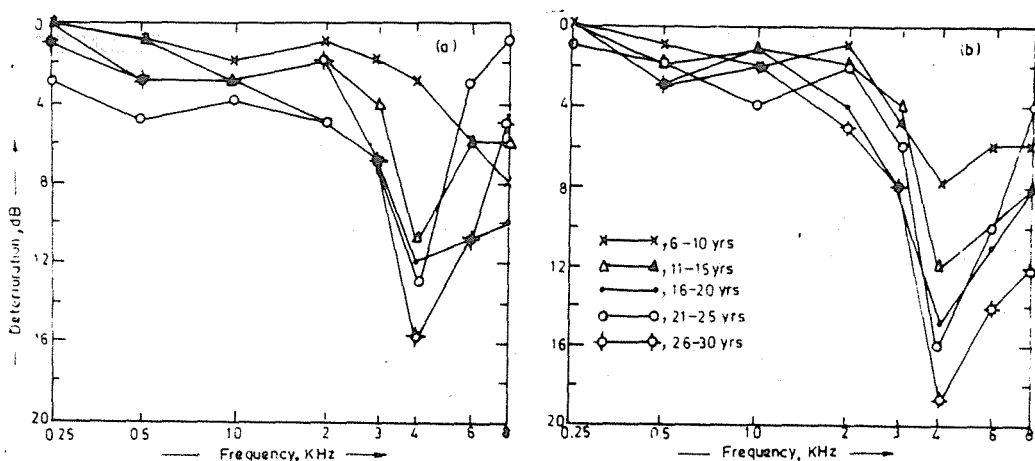
FIG 2 MEAN PURE TONE DETERIORATION AT DIFFERENT FREQUENCIES IN VARIOUS EXPOSURE DURATIONS IN THE (a) LEFT EAR AND (b) RIGHT EAR OF BUS DRIVERS

ACKNOWLEDGEMENT

REFERENCES

Bansal, A.S.Noise from agricultural machinery in India. Proceedings of 11th International Congress on Acoustics (11 ICA) held at Paris on July 19-27, 1983(5):267-270.

American National Standards Institute (1991). American Standard Criteria for background noise in Audiometer rooms,ANSI 301-1971.

Bienvenue, G.R. and P.L.Michael (1980). Permanent affects of noise exposure on results of a battery of hearing tests. Am.Ind. Hyg. Assoc.J.(41):535-541.

Gupta, S.N.Vipal Jain and A.S.Bansal (1988). Noise induced hearing loss in Ludhiana industrial workers. Proceedings of the 5th Int. Cong. on "Noise as public health problem" (Noise'88) held at Stockhom (Sweden) on Aug.21-25, 1988(2):91-97.

Michael, A., Nerbonne and Andrew, E. Accardi (1975). Noise-induced hearing loss in a truck driver population. The Journal of Auditory Research (15):119-122.

Dufresne, Ronald, M., Bnian, C. Alleyne, and Michael, R.Reesal(1988).Asymmetric hearing loss in truck driver. Ear and Hearing 9(1):41-42.

233

THE EFFECT OF THE FREQUENCY OF SOUND STIMULI ON THE PERCEPTION OF DURATION

J.Y.Jeon
Department of Architectural and Design Science
University of Sydney, NSW 2006, Australia

F.R.Fricke
Department of Architectural and Design Science
University of Sydney, NSW 2006, Australia

ABSTRACT

Three experiments were carried out to determine the just noticeable difference (JND) for the perception of sound duration and to find the effect of frequency on duration discrimination. This was done by undertaking pair comparisons and determining the JND for tone durations ranging from 50 to 800 msec. When one tone in a pair has a different frequency from the other (both tones were in the range 250 to 8000 Hz), it was found that duration discrimination was poorer for the tone with the lower frequency. For different frequency pairs subjects perceive the higher frequency to be longer in duration. The effect of frequency on duration discrimination is strong in cases where the pair of tones have a large frequency difference. However, when the higher tone frequency was above 4000 Hz, the effect of frequency difference on duration judgements with lower tones (from 250 to 4000 Hz) disappeared. The lower tones (262 to 1568 Hz) used in Experiment 2 were within the range of the frequency effect. The frequency effect was also studied in a musical context (Experiment 3) but it was concluded that rhythmic and 'interpretation' effects obscured the 'frequency' effects.

1.0 INTRODUCTION

Much research has been undertaken on the perception of frequency, intensity and direction of sounds. Although much work has been undertaken on factors affecting pitch and intensity perception, little work has been undertaken on the factors affecting duration perception. In particular there is a paucity of information on whether or not there is any effect of frequency difference on sound duration judgements, despite the obvious importance of such studies in the perception of music and the way we hear sounds.

Duration discrimination has long been of interest to psychologists. Many psychophysical studies have attempted to measure the sensory capability; the ability to respond differently to differing sensory inputs. Woodrow (1951) explained that duration discrimination was just under 10% in the range of intervals from 200 to 1,500 msec, and increased to 16%-20% as the standard interval increased beyond 2,000 msec. These results were confirmed by Small and Campbell (1962) for the range 40-400 msec, by Creelman (1962) for the range 100-1,000 msec, and by Abel (1972) for the range 50-500 msec. The 10% figure is essentially a constant Weber ratio for durations and intervals between about 200 and 2,000 msec.

In the preceding study of the frequency effect on duration judgements (Jeon and Fricke, 1991), it was found that the duration discrimination for a sequence of tones (Experiment 1) was similar to those obtained by previous workers (Abel, 1972; Creelman, 1962; Getty, 1975; Small and Campbell, 1962). The JND was nearly constant for intervals from 25 to 1600 msec, became larger for shorter intervals, and tended to get smaller for longer intervals up to 16 sec (Experiment 2). When the JNDs for tone pairs with different stimuli frequencies were compared with the JNDs of single tones (Experiment 3), it was found that duration discrimination was relatively poorer for the tone with the different frequency. This result may have been due to subject bias, but it has stimulated further research into other aspects of the effect of frequency on duration perception. How does the frequency effect duration discrimination in the frequency range from 250 to 8000 Hz? How do the pitch differences of two musical tones affect duration comparison? Does the frequency effect occur in music performance?

2.0 FREQUENCY DIFFERENCE EFFECT (EXPERIMENT 1)

2.1 Introduction
The study of auditory perception has been carried out with an overwhelming concern for the frequency and intensity discrimination. For frequency discrimination in particular we know, fairly well, the factors concerning the limits of discrimination with respect to the method of stimulus presentation, the dependence on intensity, the masking effect, and even the duration effect. However, we know very little about the effect of frequency on duration discrimination because this has received very little attention.

Subjects in the current experiment were presented with a pair of stimuli composed of high and low frequency pure tones. The subject's task was to discriminate differences in duration of the two tones and

ignore differences in the frequency of the tones. We were interested in how duration discrimination depended on the difference of tone frequencies in each pair of stimuli.

2.2 Experimental Method

There were two female subjects, both with normal audiograms. Subjects S.L. and N.J. had had 15 and 13 years of musical experience, respectively. N.J. had previously taken part in three other experiments on auditory duration assessments for a total of 20 hours. The subjects were paid for their services.

A Macintosh IIci computer controlled the experiments. The MacRecorder sound system with its application, SoundEdit™, enabled the recording, editing, playing and storing of sounds. The generated pure tone stimuli were saved in a range of file formats and presented by the other application, MacroMind Director. Stimuli were presented through a headphone.

The subjects were presented with a pair of stimuli composed of high and low frequency pure tones and asked to discriminate differences in duration of the two tones ignoring differences in the frequency of the tones. The data for the experiment were collected using a two-alternative forced-choice procedure (2AFC).

The subjects were tested individually in an anechoic room. Pairs of standard (S) and comparison (C) tones, where S was 50, 100, 200, 400 or 800 msec and the values of C/S were 1.04, 1.08, 1.12, 1.16, and 1.2 were presented. The interstimulus interval (ISI) for each pair of sounds was 1,040–1,600 msec while the time between pairs of sounds was fixed at 4 seconds.

The present experiment was designed to investigate the duration discrimination only when the lower frequency was the longer duration stimulus. Therefore, if S was 50 msec with 8000 Hz, C would be 50 (C/S=1.0) to 60 msec (C/S=1.2) with frequencies 250–8000 Hz. If S was 100 msec with 4000 Hz, C would be 100 (C/S=1.0) to 120 msec (C/S=1.2) with frequencies 250–4000 Hz, and so forth. In any given stimulus pair, C had equal or higher frequency with longer duration, while S had equal or lower frequency with fixed standard duration.

As equal amplitude tones would not sound equally loud (Handel, 1989), the subjects were given a control to adjust the amplitude of a second tone of different frequency to match the standard in loudness (the 8000 Hz sound was presented as a fixed standard). From the pre-test it was found that the relative amplitudes of the comparison stimuli (250, 500, 1000, 2000 and 4000 Hz) had different amplitudes (92, 64, 62, 58 and 56%, respectively) when the 8 kHz pure tone had a reference amplitude of 100%. The equal loudness settings of the standard and comparison stimuli, as determined in the pre-test, were fixed for the experiment.

In a session subjects listened to 600 pairs of sounds, i.e., 120 pairs each through 5 test sequences separated by 5 standard stimuli durations (50, 100, 200, 400 or 800 msec). The session was repeated 20 times in different sequence orders. Each sequence was presented by random sampling the 5 sequences. The order of the longer and shorter duration stimuli was equally distributed. Each subject completed the experiment in a period of approximately 3 weeks. The ability to discriminate the

duration was judged using 75 % correct scores. Responses of the subjects were recorded on answer sheets by the subjects themselves.

2.3 Results and Discussion

When the tone frequencies were the same, duration discrimination performance was described well by a simple model of duration discrimination. When the frequency was varied for the comparison tone of each sound pair, but fixed for the standard stimulus within a pair, duration discrimination performance was poorer than for equal frequencies. When the frequency difference between the two tones within a pair was large, performance was even worse.

The proportion of correct responses obtained in an investigation of frequency difference effects on duration judgements are shown in Fig. 1. They were obtained from two subjects as a function of duration increment rate, ΔT/T. The standard stimulus durations are from 50 to 800 msec and the standard stimulus frequencies are from 250 Hz to 8 kHz. As shown in Fig. 1, each subject has certain frequency ranges which are more important in duration discrimination than other frequencies, e.g. 1000 Hz vs. 250 Hz for N.J. and 2000 Hz vs. 250 Hz for S.L. The reason for this is unknown.

Both subjects showed the effect of frequency on duration judgements except for the 8000 Hz tone pairs. The effect of frequency on duration discrimination is strong in the case of a large frequency difference pair, however too high tone, like 8000 Hz, doesn't seem to have effect on duration judgements when comparisons are made with lower tones from 250 to 4000 Hz. Probably, it is because 8 kHz is outside the music and speech frequency range.
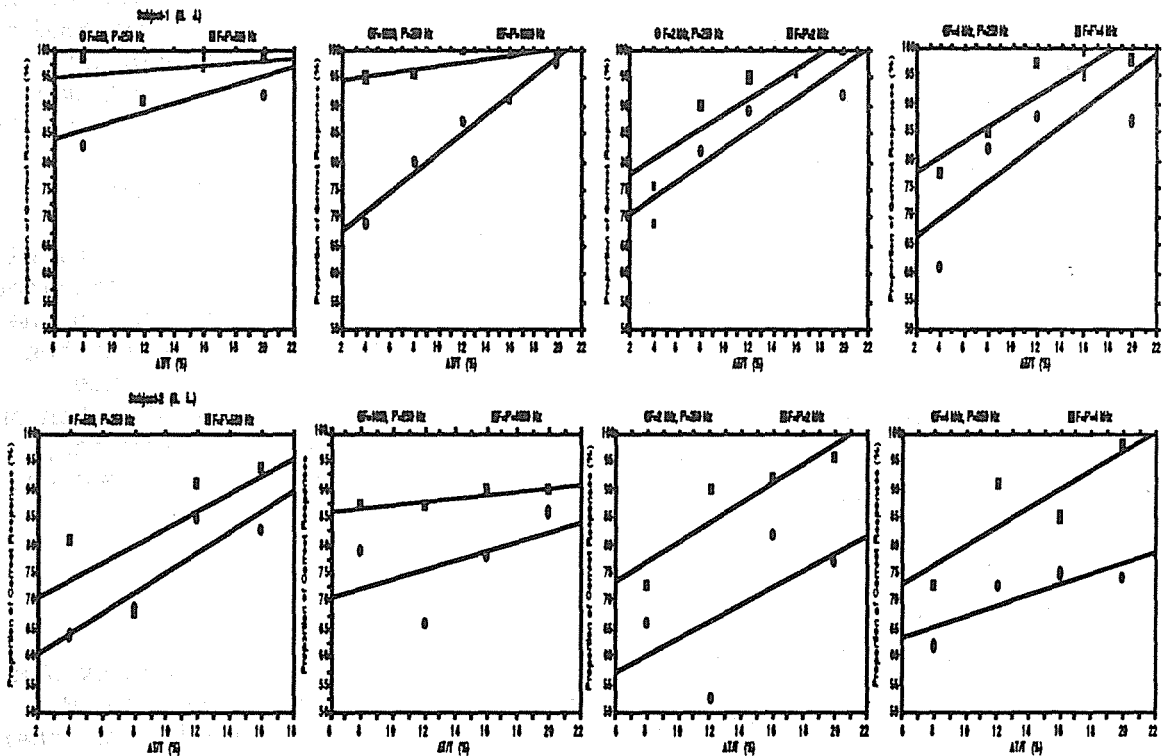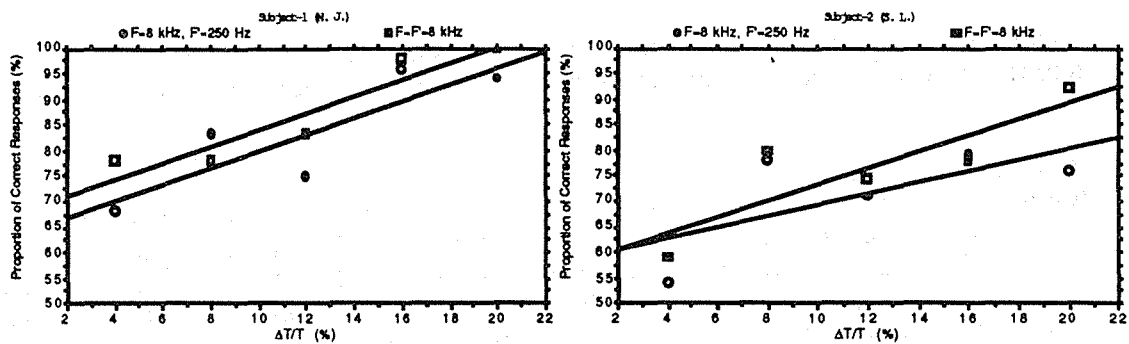
FIG. 1. The proportion of correct responses obtained in an investigation of frequency difference effects on duration judgements (for two subjects) as a function of duration increment, $\Delta T/T$. The standard stimulus durations are from 50 to 800 msec and the standard stimulus frequencies are from 250 Hz to 8 kHz. This figure shows that each subject has certain frequency ranges which are more important in duration discrimination than other frequencies.

3.0 DIFFERENT PITCH EFFECT ON DURATION DISCRIMINATION OF MUSICAL TONES (EXPERIMENT 2)

3.1 Introduction
A detectable change in frequency at normal listening levels can be as low as 0.5 Hz to 4 Hz for frequencies up to 3000 Hz. Above 6000 Hz, the ability to distinguish between two tones, on the basis of frequency, becomes very poor. Hirsh et al. (1990) observed that large pitch changes had a more disruptive effect on timing discrimination than did small ones. Above 6000 Hz the sense that tones have a musical pitch is rather weak and this may explain why the musical scale does not go above 4000-5000 Hz. This effect is due to physiological limitations (Handel, 1989) and is probably the reason why the two subjects, in the 8000 Hz case of the previous experiment, did not apparently respond to the frequency difference in the way they responded to 500-4000 Hz cases. As a consequence, the frequency range in this experiment was decreased and was confined to six musical tones over three octaves. The six musical tones were C4, G4, C5, G5, C6 and G6, which have frequencies, 262, 392, 523, 784, 1047 and 1568 Hz, respectively.

In this experiment subjects were also presented with a pair of stimuli composed of high and low frequency pure tones and asked to discriminate differences in duration of the two tones, ignoring differences in the frequency of the tones as in Experiment 1. However, the data for the experiment were collected using a three-alternative forced-choice procedure (3AFC) for more efficient measurement situations (Shelton and Scarrow, 1984). The subjects were required to select the sound they believed to be the longer or if they thought the duration of both the stimuli in the pair were the same they had this choice also (first/second/same).

3.2 Experimental Design
The two subjects from Experiment 1 (S.L. and N.J.) were joined by J.H., who had had 10 years of musical experience, and also joined by C.H., who was a nonmusician, but who had 10 hours of experience in two other experiments on auditory duration assessments.

The apparatus was the same as that used in the first experiment. The computer collected subject responses and stored·them in data files along with the stimulus and frequency difference for each trial.

The Experiment 1, in which subjects were asked to discriminate between long and short durations, was modified. Six musical notes were presented instead of the 250-8000 Hz pure tones of Experiment 1. Pairs of standard (S) and comparison (C) tones were presented, where S was 200 msec and the values of C/S were 1.03, 1.06, 1.09, 1.12, and 1.15. The interstimulus interval (ISI) for each pair of sounds was 1,770-1,800 msec the time. The subjects were supposed to spend the four second intervals, after each pair of sounds, for their judgements and the recording of these on their answer sheets.

So that both stimuli in a pair had equal loudness to meet the experimental planning, the subjects were given a control to match the loudness of the second tone to that of the first, as in Experiment 1. The amplitude of the highest tone in a comparison group was fixed as a reference and the amplitudes of the lower stimuli were compared. Each subject was asked to choose the sound pair which had the same loudness. From the pre-test it was found that the relative amplitudes of the comparison stimuli had different amplitudes. As a result of the pre-test, the equal loudness of the standard and comparison stimuli were fixed for the experiment, for each subject.

3.3 Results and Discussion
As shown in Fig. 2, when the pitch of the musical tone was fixed over trials, duration discrimination was described well by a simple model of duration discrimination. When the pitch was varied for the comparison tone of each pair, but fixed for the standard tone within a pair, duration discrimination was worse. As a result, it was found that the musical tones, C4, G4, C5, G5, C6 and G6, were within the range of the frequency effect revealed in the previous paper (Jeon and Fricke, 1991) and in Experiment 1. In case of N.J., who has absolute pitch, and has an average duration JND as small as 4.7% in the six musical tones, the frequency effect showed up in the first two C/Ss, 1.04 and 1.08 (100% correct responses for other C/S values).
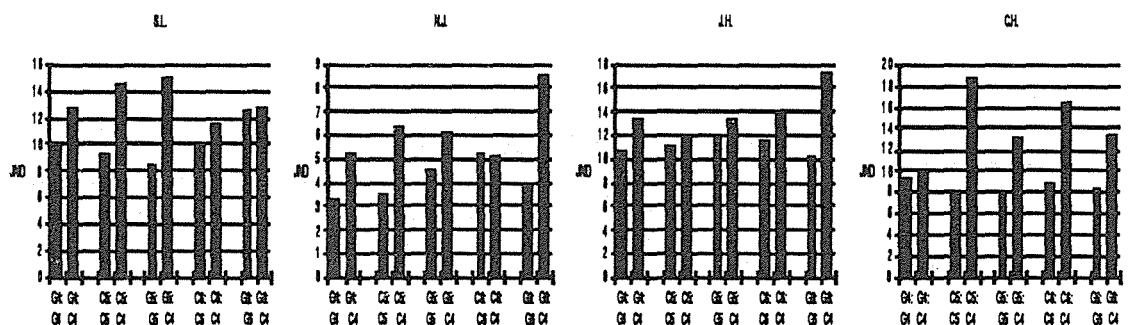
FIG. 2. Comparison of JNDs, of equal and different frequency tone pairs, obtained from the four subjects. The standard stimulus duration is 200 msec and the standard stimulus frequencies are from G4 to G6.

4.0 AN INVESTIGATION OF FREQUENCY EFFECT ON DURATION PERCEPTION IN MUSIC PERFORMANCES (EXPERIMENT 3)

4.1 Introduction

The present experiments were motivated by an interest in the applicability of temporal psychoacoustical data to the complex contexts of mixed sequences in music. In the previous two experiments, temporal discrimination was measured using two isolated signals to be compared in terms of duration difference. Is temporal discrimination comparable in cases where two such sounds are part of a music sequence?

A flute performance, `Mozart Flute Concerto No.1 in G, K.313' was chosen as model study. The flute produces individual waveforms which can be measured easily for each musical note. Of all orchestral instruments the flute produces sound closest to a pure tone and so is most easily compared to the results from previous experiments.

4.2 Experimental Design

The performances of five contemporary flutists were analysed and compared by measuring durations of their tone interpretations. The artists were Jean-Pierre Rampal, Hubert Barwahser, Claude Monteux, Neville Amadio and Egenia Zuckerman. Their recordings of `Flute Concerto No.1 in G, K.313 (Mozart)' were fed into the Macintosh IIci computer with the sound analyzing system. Three sets of equal rhythmic phrases (shown in Fig. 3) were selected from the concerto to compare the duration interpretation in a piece of music by each musician. The measurement of duration for each performance was compared in a pair of phrases with equal rhythms. The differences in duration were averaged for the five musicians to find any trend which depended on pitch.

FIG. 3. Three sets of equal rhythmic phrases from the Mozart Flute Concerto No.1 in G, K.313. They were selected to compare the duration interpretation in a piece of music by each musician.
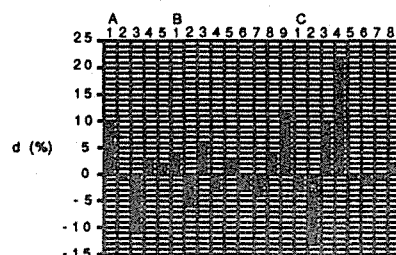
FIG. 4. Comparison of duration differences performed by the five flutists in three sets of equal rhythmical phrases. d is the difference in duration interpretation.

4.3 Results and Discussion

From the results shown in Fig. 4, the 6 pairs of notes (A1, A3, B9, C2, C3 and C4) are of particular interest because there are large differences in duration. The sound pairs of A3 and C2 are semiquavers where the musicians performed the lower tone with longer duration. The others (A1, B9, C3 and C4) are from semiquavers to crotchets where the musicians performed the higher tone with longer duration.

As Monahan and Hirsh (1990) point out, certain elements seem to be accented in rhythmic structures of the world of music. Accents may be generated by pitch changes or by longer temporal intervals. Overall the musicians played the higher notes longer than the lower notes, which is the reverse of what we would expect from Experiments 1 and 2, but this could be interpreted as the musicians trying to make the music less `mechanical'.

240

5.0 CONCLUSIONS

Three experiments were carried out to determine the just noticeable difference (JND) for the perception of sound duration and to find the effect of frequency on duration discrimination. Duration discrimination is worse when there are frequency differences. For different frequency pairs subjects perceive the higher frequency to be longer in duration. The effect of frequency on duration discrimination is strong in the case of a high frequency difference pairs, however too high a tone, like 8000 Hz, doesn't seem to have an effect on duration judgements when it is paired with lower tones, from 250 to 4000 Hz. The musical tones used in the experiment were within the range of the frequency effect. The frequency effect was searched for in a piece of music. Although no direct and continuing evidence for a frequency effect was found there is some evidence for the hypothesis that musicians overcompensate for frequency effects to make the music sound less mechanical.

REFERENCES

Abel S.M., Duration discrimination of noise and tone bursts, Journal of Acoustical Society of America, 51, 1219–1223, (1972).
Creelman C.D., Human discrimination of auditory duration, Journal of Acoustical Society of America, 34, 582–593, (1962).
Getty D.J., Discrimination of short temporal intervals: A comparison of two models, Perception & Psychophysics, 18, 1–8, (1975).
Handel S., Listening, MIT, Cambridge, MA, 1989, pp. 63–72.
Hirsh I.J., Monahan C.B., Grant K.W., Singh P.G., Studies in auditory timing: 1. Simple patterns, Perception & Psychophysics, 47, 215–226, (1990).
Jeon J.Y., Fricke F., The effects of stimulus frequency and intensity on the judgements of sound duration, Journal of Acoustical Society of America (to be published), (1991).
Monahan C.B., Hirsh I.J., Studies in auditory timing: 2. Rhythm patterns, Perception & Psychophysics, 47, 227–242, (1990).
Shelton B.R., Scarrow I., Two-alternative versus three-alternative procedures for threshold estimation, Perception & Psychophysics, 35, 385–392, (1984).
Woodrow H., The perception of time, in Handbook of Experimental Psychology, edited by S.S.Stevens, Wiley, New York, 1951, 1224–1236.

NEAR-FIELD BINAURAL REPRODUCTION SYSTEM FOR LISTENING TEST

Masayoshi Miura
AV Human Science Reserch Department
Corporate Research Laboratory
Sony Corporation,
1-7-4, Konan, Minato-ku, Tokyo, 108 Japan

ABSTRACT   In   the   Near-Field   Binaural   Reproduction
System (NBR-System),   special   small   loudspeakers   are   set
close   a   head   and   in   front   of   outer   ears.   As   might   be
suspected,   the   interaural   crosstalk   is   too   small.
Furthermore,   reflected   sound waves   from the   walls   are
relatively   small   compared to   the   direct   sound.   It   can be
considered   that   there   is   no effect   of   reflections.   An
anechoic   chamber   is   not necessary to   the NBR-System.   The
condition of listening room   for NBR-System is quiet only.
The   property of   loudspeaker for NBR-System   is close   to
flat,   however,   the NBR-System   must to be   eliminated the
duplication   of   the   inner   transfer   function(;due to   the
shape of   external ear   canal,   terminating   impedance,   and
so on)   in artificial-head   recording.   A spectral amplitude
of NBR-System is flat within   ± 3 dB between 100 Hz and 15
kHz.   The crosstalk signal   averages 20   dB below same side
signal between 100 Hz and 15 kHz. We use the NBR-System in
hearing-aid   fitting.   A   hearing-impaired   subject   can
estimate a hearing-aid in environment sounds reproduced by
NBR-System.

1.0 INTRODUCTION

Binaural recording by head and torso simulator(HATS) was originally intended for headphone listening. The headphone listening system has a merit that need not elimination of interaural crosstalk. However, the drawbacks of headphones are well known: unstable coupling to the ear, intracranial auditory image, and so on. For these reasons, binaural listening system by headphones has not been very successful.

The other side, difficult problems with true stereo reproduction by loudspeakers are interaural crosstalk and the influence of the walls and objects within the room. The acoustic property of each listening rooms is so different that crosstalk canceling and elimination of reflection waves are difficult. One of the ideal space for binaural reproduction by loudspeakers is an anechoic chamber. In 1963, Schroeder and Atal simulated original sound field by synthesizing the signals at the eardrums of a listener in an anechoic chamber. In their equalizing method, the symmetrical head-related transfer function(HRTFs) were used. In 1983, Hamada have reported orthostereophonic system, and their equalizing network can be applied to asymmetric condition of HRTFs.

We suggest a new binaural reproduction system, near field binaural reproduction system(NBR-System). This system is compact and need not an anechoic chamber.

2 CONSTRUCTION OF NBR-SYSTEM

2.1 Arrangement of loudspeakers

Figure 1 illustrates sound diffraction and crosstalk between two loudspeaker and HATS. $H_{LS}, H_{LO}, H_{RS}, H_{RO}$ are HRTFs from the input terminals of one loudspeaker(L or R) to the output terminals of same side microphone and other side microphone in the HATS's ears, respectively. Also each transfer function includes the loudspeakers.

In the NBR-System, special small loudspeakers are set close ahead and in front of outer ears. Figure 2 is an

example of loudspeakers arrangement. As is evident from figure 3, the crosstalk transfer functions H_{Lo} and H_{Ro} are too small. It can be considered that there is no effect of interaural crosstalk on sound image localization, therefore the NBR-System has not crosstalk canceling filters. Furthermore, reflected sound waves from the walls are relatively small compared to the direct sound.
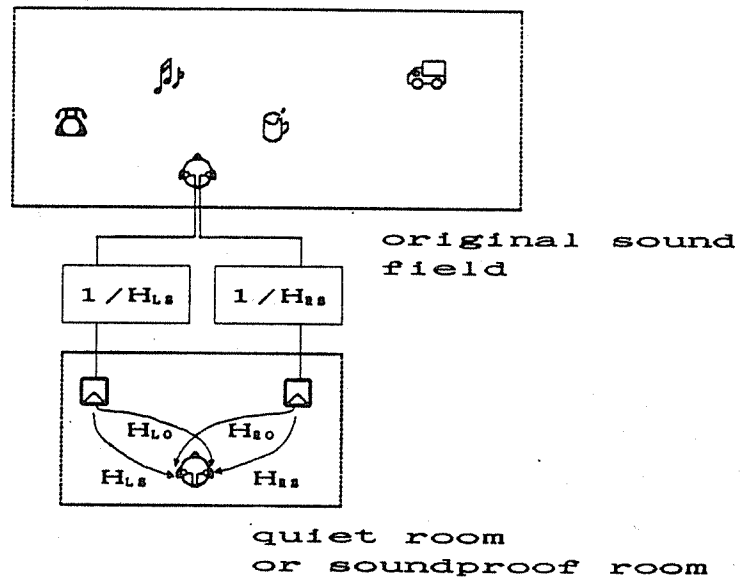
Fig. 1 Sound diffractions and crosstalks between two loudspeakers and a HATS.
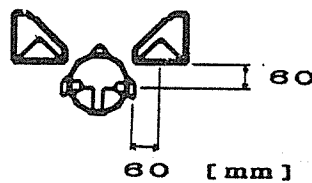
Fig. 2 Arrangement of the NBR-System loudspeakers.
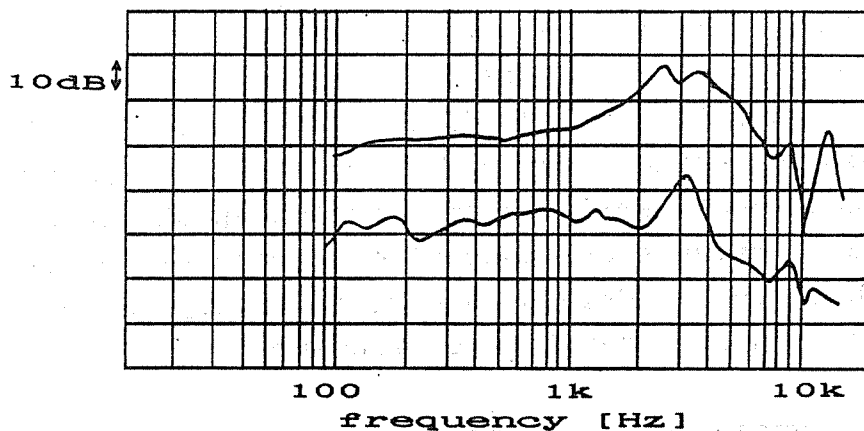
Fig. 3 Measured HLS and HLO.
Arrangement of loudspeakers is shown in figure 2.

It can be considered that there is no effect of reflections. The condition of listening room for NBR-System is quiet only.

2.2 Equalizing filters

In order to simulate original sound field at the eardrums of a listener, the NBR-System has equalizing filters. These filters are inverse filters of H_{LS} and H_{RS}. We use two channel FIR digital filter. The 16bits digital audio signals, provided by digital audio tape recorder at 48kHz sampling rate, are calculated 512 points convolution sum.

2.3 HATS

Conditions of HATS which is used for recording in binaural reproduction were discussed before. Ogura *et al.* demonstrated that the difference of the inner transfer function(due to the shape of external ear canal, terminating impedance etc.) between a HATS and listener did effect on the reproduced signals at the eardrum of the listener. We use Bruel & Kjaer 4128, 4158, 4159.

2.4 loudspeaker system

The property of loudspeaker for NBR-System is close to flat. And this loudspeaker is used close to ear, so that listeners need not large amplitude of loudspeaker, and small amplitude leads to low distortion. The loudspeaker system that is set close a head and in front of outer ear is quite unusual in shape since there is nothing to block listener's view. Figure 2 shows this fact. We can set a display system in front of listener if necessary, and the listener can be given listening test information.

3 EXPERIMENTAL INSPECTION

3.1 Procedure

In an ideal NBR-System, the transfer function from the input terminal of equalizing filter(L or R) to the output terminal of same side microphone in the HATS's ears is 1. In order to confirm experimentally physical performance of the NBR-System, white noise was fed left input terminal of equalizing filter and we measured output signals of HATS's

left ear microphone and right ear microphone.

3.2 Results

The results of physical performance test are shown in figure 4. The upper trace is the transfer function from left input terminal to the output terminal of right microphone in the HATS, and the lower trace is crosstalk signal. The left ear signal has a spectral amplitude which is flat within ± 3 dB between 100 Hz and 15 kHz. The right ear signal average 20 dB below the left ear signal between 100 Hz and 15 kHz. The result looks reassuring(i.e., the right ear signal is appreciably smaller than the left ear signal).

4 APPLICATION OF THE NBR-SYSTEM TO HEARING AID FITTING

After the hearing aid fitting, a hearing impaired subject often complains about environmental noise, for example, traffic noise, noise of doing the dishes, noise of turning over the newspaper. If he uses the NBR-System, he can estimate a hearing aid in reproduced environment sounds. Essentially, the NBR-System simulates original sound field inside ear canal entrance, but a sound field around outer ear is simulated enough. Figure 5 shows comparison HATS's microphone response in the original sound field with HATS's microphone response in the simulated sound field in

Fig.4 Results of physical performance test.
White noise was fed left input terminal of equalizing filter. The upper trace is the transfer function from left input terminal to output terminal of right microphone in the HATS. The lower trace is crosstalk signal, left input terminal to right ear microphone.

wearing a behind ear hearing aid. This result looks reassuring.

5 CONCLUSION

We develop a compact binaural reproduction system for listening test. The NBR-System needs only an area of 0.9m² . The room for listening test is not necessarily an anechoic chamber. The reproduction frequency range is between 100 Hz and 15 kHz within ± 3 dB. The maximum output sound pressure level measured with HATS B&K4128, is 120 dB. We use the NBR-System in hearing aid fitting. A hearing-impaired subject can estimate a hearing aid in environment sounds reproduced by NBR-System.

Fig.5 Comparision HATS's microphone response in the original sound field with HATS's microphone response in the simulated sound field in wearing a behind hearing aid.

REFERENCES

M. R. Schroeder and B. S. Atal, Computer simulation of sound transmission in room, IEEE Intern. Conv. Rec. 11, 150-155(1963)

H. Hamada, Construction of orthostereophonic system for the purposes of quasi-in situ recording and reproduction, J. Acoust. Soc. Jpn. 39, 337-348(1983)(in Japanese).

Y. Ogura, H. Hamada, N. Ikeshoji, T. Miura, On orthostereophonic system using S-DHM, Rep. JEEC. EA82-1, 1-8(1982)(in Japanese).

PERCEPTION OF TWO-TONE SIGNALS

Kenji Ozawa
Research Institute of Electrical Communication, Tohoku University
2-1-1 Katahira, Aoba-ku, Sendai, 980 Japan

Yoiti Suzuki
Research Institute of Electrical Communication, Tohoku University
2-1-1 Katahira, Aoba-ku, Sendai, 980 Japan

Toshio Sone
Research Institute of Electrical Communication, Tohoku University
2-1-1 Katahira, Aoba-ku, Sendai, 980 Japan

ABSTRACT   The effects of the phase difference between the components
of a two-tone signal on its perception were investigated in this study. First,
thresholds at frequencies twice that of the masker were measured as a function
of the phase of the maskee using the tone-on-tone masking technique. The
results were explained by the assumption of a vector summation of the mas-
kee and the aural harmonic caused by the masker. The effect of the phase
difference between the components of two-tone signals on their timbres was
then examined by applying the method of triadic comparison. The timbre
was perceived two-dimensionally with respect to the phase difference. These
results are considered to be incorporated in the idea of a "masked frequency
spectrum" which is assumed to describe the contribution of each component
of the sound to its timbre.

1.0 INTRODUCTION

It is well known that the perception of signals consisting of two components having a frequency ratio of exactly two is affected by the phase relation between the components. This monaural phase effect has been investigated by many researchers from various angles. In some of the studies, the perception of each component of the complex signal has been investigated separately. For example, it has been shown that when the lower frequency component is considered to be the masker, the threshold of the higher frequency component varies with its relative phase (Clack T.D. 1967a, 1967b, 1972, Nelson D.A. and Bilger R.C. 1974a, 1974b, Zwicker E.). At the same time, changes in loudness and pitch of the higher frequency component have also been found (Lamoré P.J.J. 1975, 1977a, 1977b, 1979). On the other hand, the perception of the complex signal as one unit has been investigated in other studies. The effect of the phase difference between the components on loudness, pitch, and timbre of the complex signal has also been widely investigated (Criag J.H. and Jeffress L.A., Hall J.L., Raiford C.A. and Schubert E.D.). It is natural to consider that the perception of a complex sound and that of the components are correlated with each other.

In this study, the threshold changes of the higher frequency component were measured as a function of its phase. Also, the effects of the phase on the timbre of complex signals were examined. Finally, the change in timbre was considered on the basis of the concept of a "masked frequency spectrum," taking measured threshold data into account.

2.0 EFFECT OF PHASE ON THRESHOLD OBSERVED IN TONE-ON-TONE MASKING

2.1 Method

Three subjects, two males and one female, 22 to 27 years of age, participated in the two experiments. They had no history of auditory problems, and the minimum audible pressure of each was checked using sweep-frequencies from 100 to 10,000 Hz with a Békésy type audiometer.

In one experiment, thresholds at frequencies (f_2) twice the masker frequencies (f_1) of 500 and 2000 Hz were measured using the tone-on-tone masking technique.

The threshold data were obtained as a function of the phase of the maskee in 30° steps from 0° through 360° by the method of limits. The level of the masker was fixed at 70 dBSPL (dB relative to 20 μPa). The masker was then presented periodically with a duration of 3.0 s and a pause of 2.5 s between sounds. The maskee had rise and decay times of 250 ms, each with the shape of a half-cycle of a cosine function. Total maskee duration was 1.5 s. The maskee was embedded in the masker with a delay of 1.5 s after its start. Four downward- and upward-sequences with the change in maskee levels at 2-dB steps were presented alternately, and the average of the last 6 judgments was employed as an experimental datum.

The stimuli were presented monaurally to the right ear of the subjects seated in a sound-proof chamber via headphone (YAMAHA YHD-3). The phase of the maskee was determined with an artificial ear (Brüel & Kjær 4153).

2.2 Results and Discussion

Figure 1 shows the thresholds as a function of the phase of the maskee. This monaural phase effect is sufficiently described by the assumption of a vector summation between the maskee and the aural harmonic which is the result of a nonlinear distortion of the masker (Clack T.D. 1972, Erdreich J. and Clack T.D., Schubert E.D.). The curves can be represented by the equation:

$$A_r^2 = A_e^2 + A_i^2 + 2 A_e A_i \cos\theta, \quad (1)$$

where A_e is the amplitude of the external tone (maskee), A_i is the amplitude of the internal tone (aural harmonic), θ is the phase difference between these two components, and A_r is the resultant amplitude. When the resultant of the summation attains an absolute threshold, the maskee become audible. The absolute threshold, A_i , and θ are estimated from the experimental data, i.e., A_e (Erdreich J. and Clack T.D.).

On the other hand, Nelson D.A. and Bilger R.C. (1974a) interpreted the effects of the phase on the threshold as being the result of temporal pattern discrimination at the neural stage. However, it can not be considered that the "phase lock" of discharges of cochlear fibers occurs in synchrony with the cycles of the stimulus waveform for the maskee frequency of 4000 Hz. Hence, the vector summation assumption seems to be a more reasonable explanation.
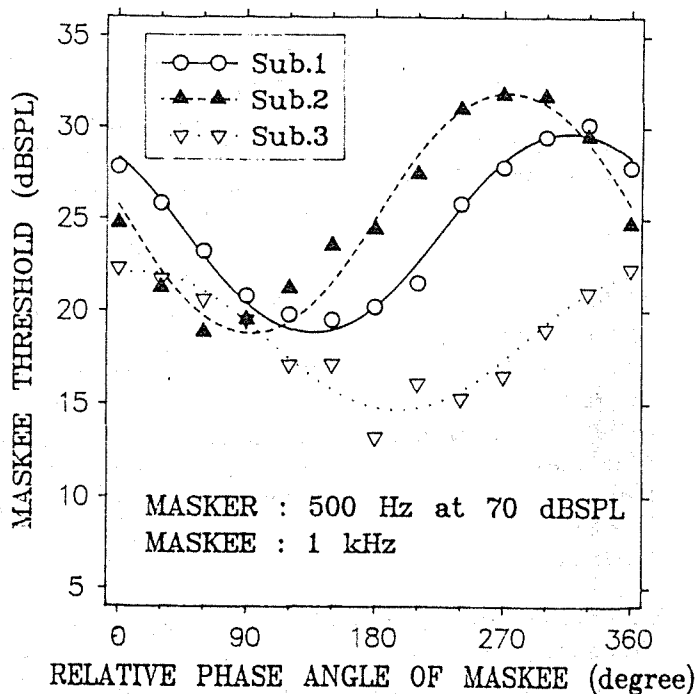
(a) Thresholds at 1000 Hz. The masker was 500 Hz at 70 dBSPL.
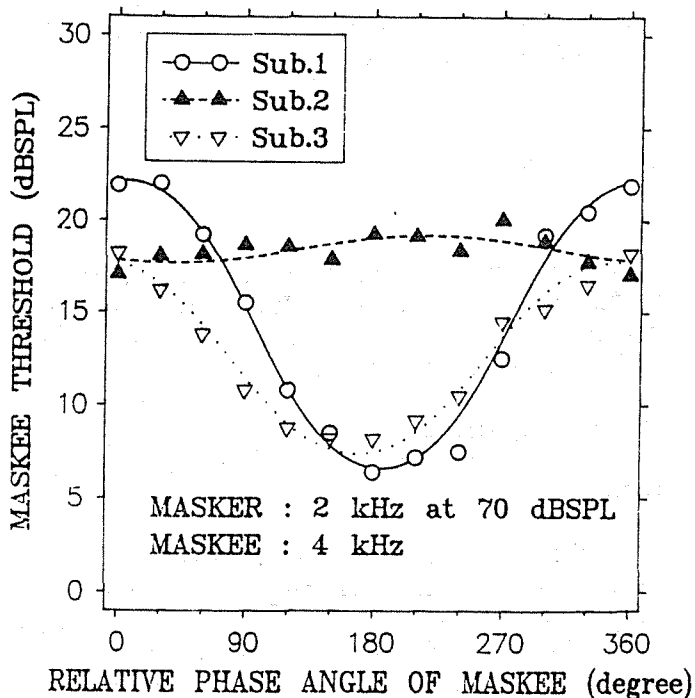
(b) Thresholds at 4000 Hz. The masker was 2000 Hz at 70 dBSPL.

Fig.1: Thresholds at frequencies twice that of the masker as a function of the phase of the maskee relative to that of the masker for three subjects. Curves represent the fit of Eq. (1).

250

3.0 EFFECT OF PHASE ON TIMBRE OF COMPLEX SIGNALS

3.1 Method

In this section, phase effect of the higher frequency component of the two-tone signal on its timbre was examined using the method of triadic comparison. The stimulus is given by the formula

$$f(t) = A_1 \sin(2\pi f_1 t) + A_2 \sin(2\pi f_2 t + \phi), \qquad (2)$$

where $f_2 = 2f_1$, and ϕ represents the phase difference determined with the artificial ear.

In the following experiments, two f_1 / f_2 pairs were used, i.e., 500/1000 Hz and 2000/4000 Hz pairs. The level of the lower frequency (f_1) component was fixed at 70 dBSPL. The higher frequency (f_2) component was presented at three levels (25, 35, and 45 dBSPL when f_1 is 500 Hz, and at 15, 25, and 35 dB when f_1 is 2000 Hz). The experiments were carried out separately for each frequency pair and each f_2 level. In each experiment, six different signals, with ϕ changing at 60° steps, were prepared.

Triads (A-B-C) were presented sequentially. Each stimulus had a duration of 1.5 s with 20 ms rise and decay times. Intervals of 0.5 s were inserted between stimuli. For each triad, the subjects judged which of A or C was closer to B in timbre. All possible triad combinations were presented eight times in random order.

The obtained judgments were transformed to dissimilarity matrices individually (Torgerson W.S.), which were used as inputs to Torgerson's multidimensional scaling program. Calculated results with the program show the relative location of the stimuli in Euclidian space.

3.2 Results and Discussion

Two indices of fitness, F and P, suggested that the stress was small enough even when a one-dimensional solution was employed for some of the dissimilarity matrices. However, a two-dimensional solution was employed, here, for all matrices to compare our results with Hall's.

Figures 2 and 3 show the stimulus spaces obtained as the results of computation for f_1 =500 Hz and f_1 =2000 Hz, respectively. All figures are drawn with the same criterion, i.e., with the JND (just noticeable difference) scale calculated by the method of Thirston's Case V. As Case V is a simplified method, it should be noted that JND in the figures is considered as an approximation.

First, the results for f_1 =500 Hz (Fig.2) will be discussed. For subject 1, when the level of the f_2 component was 45 dBSPL, the plot of the stimulus points formed an almost perfect circle with an angular distance of about 60° between adjacent points, in accordance with the results by Hall. However, when the level of the f_2 component was decreased to 25 dBSPL, the solution became one-dimensional. Minimum masking occurred at phase angles of 90° and 150° , while maximum masking occurred at 270° and 330° . Although Hall stated "if there is any one phase condition that is perceptually distinctive, then it is not revealed by the method of triadic comparisons," our results suggest that axis I is highly correlated with the audibility of the f_2 component, i.e., the

masked loudness of the component. Even if the level of the component was held constant, its masked loudness changed with the change in threshold due to its phase.

The variance of the points along axis I is interpreted by the loudness function of the masked tone, i.e., the f_2 component. When the level of the f_2 component was 25 dBSPL, the component was sometimes inaudible according to its phase angles, so the variance was rather small. When the level was raised to 35 dBSPL, the masked loudness of the component could be perceived for every phase angle, and the variance was found to increase. The variance was reduced in the case of 45 dBSPL, however, because the difference in the masked loudness of the component was reduced by recruitment.

On the other hand, the variance along axis II increases as the level of the f_2 component is raised. An increase in the f_2 component contributes to the difference in waveforms among the two-component signals. This suggests that axis II correlates with the difference in waveforms among the stimuli.

(a) Subject 1   (b) Subject 2   (c) Subject 3
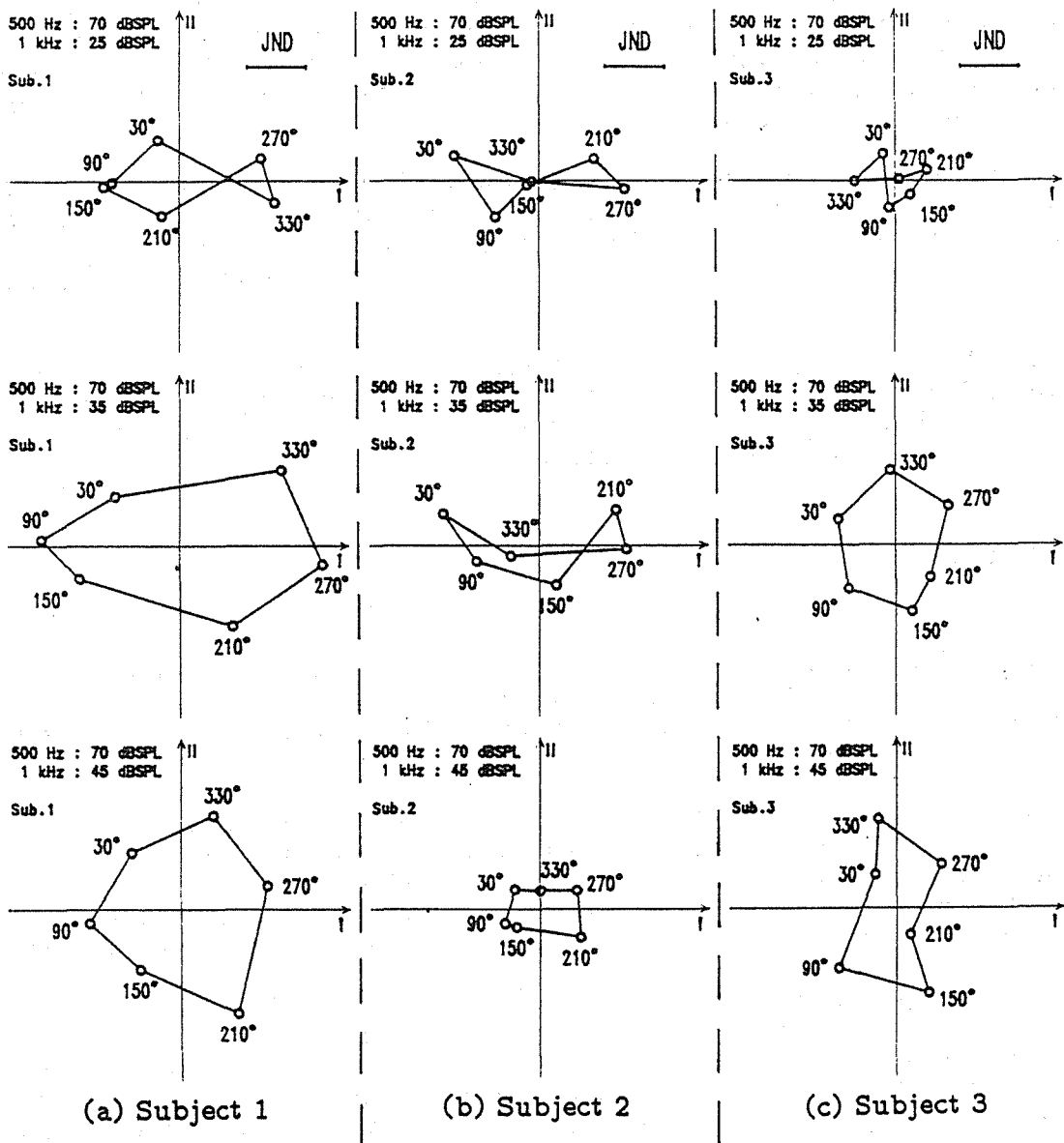
Fig.2: Individual locations of the two-tone signals in stimulus space based on subjective similarity. The frequency of the f_1 component of the signal was 500 Hz, and that of f_2 was 1000 Hz. The level of the f_1 component was 70 dB-SPL, while those of f_2 was 25, 35, and 45 dBSPL, respectively. The parameter is the phase angle of the f_2 component.

252

Regarding subject 2, the results showed features similar to those of subject 1.

As for subject 3, the significant feature is that the variance along axis I is small compared with those of the other subjects. This feature can be explained by the subject's own loudness function. This does not depend on the phase distinctly, since the phase effect on the threshold is relatively small as shown in Fig.1(a). However, reduction of the variance along axis II is also found as the level of the f_2 component is decreased.

With regards to f_1 =2000 Hz (Fig.3), for all subjects, the configurations of the stimulus points along axis I are similar to those shown in Fig.2. As to axis II, however, the stimulus points concentrate around the center irrespective of levels of the f_2 component. This reflects the fact that the "phase lock" of discharges of cochlear fibers does not occur simultaneously with the cycles of the stimulus waveform at the frequency.

(a) Subject 1   (b) Subject 2   (c) Subject 3
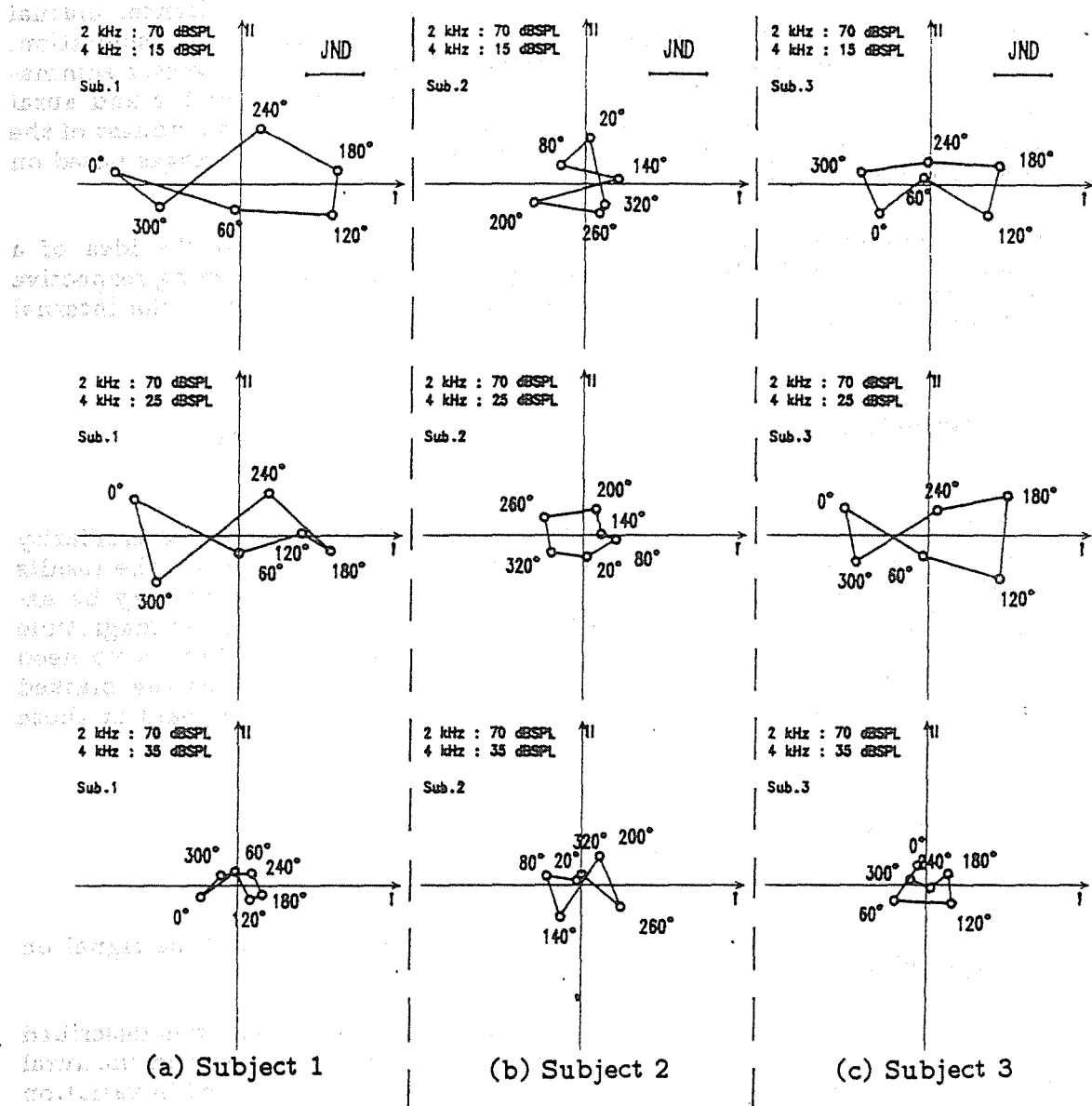
Fig.3: Individual locations of the two-tone signals in stimulus space based on subjective similarity. The frequency of the f_1 component of the signal was 2000 Hz, and that of f_2 was 4000 Hz. The level of the f_1 component was 70 dBSPL, while those of f_2 was 15, 25, and 35 dBSPL, respectively. The parameter is the phase angle of the f_2 component.

4.0 DISCUSSION

4.1 Masked Frequency Spectrum Concept

Some psychophysical experiments indicate that the perception of acoustical signal is strongly correlated with an "internal spectrum" rather than with its physical spectrum (Buunen T.J.F. *et al.*, Hirahara T). The internal spectrum of a complex signal consists of its "internal" components which are the output of signal processing in the auditory pathway. For steady complex sounds, the process has nonlinear functions such as critical band filtering, level adaptive filtering, lateral inhibition, internal masking, subjective tone generation and so forth.

In this paper, only two-tone complex signals were studied. Hence, mutual masking and subjective tone generation have to be taken into consideration. As the two components used have a frequency ratio of 1:2, the vector summation takes place between the higher frequency component and the 2nd aural harmonic caused by the lower frequency component. Thus, the loudness of the higher frequency component is reduced by masking, and also changes based on the vector summation as a function of its relative phase.

On the basis of the above discussion, the authors proposed the idea of a "masked frequency spectrum," consisting of the components having respective masked loudness, which is expected to be an approximation of the internal spectrum of the signal (Sone T. *et al.*).

4.2 Interpretation of The Results Based on The Present Concept

If the plot of the stimulus points form a circle, the subjective dissimilarity space corresponds with physical parameters (Hall J.L.). However, the results cannot directly be interpreted by any physical parameter. They may be explained by parameters of the masked frequency spectrum, i.e., the magnitude of the masked loudness and the phase of each component. There is no need to consider the phase of a high frequency component as far as the masked frequency spectrum is concerned, since the "phase lock" disappears at those frequencies.

5.0 CONCLUSION

The phase effects of the higher frequency component of a two-tone signal on its timbre were examined.

The variations of threshold in the higher frequency component was described by the assumption of a vector summation between the component and the aural harmonic caused by the lower frequency component. This resulted in variation of the masked loudness of the component. The timbres of two-tone signals were two-dimensionally perceived as a function of the relative phase of the component. One axis correlates with the masked loudness of the component, while the other correlates with the waveform of the signal.

The results are interpreted with the concept of the masked frequency spectrum.

[References]

Buunen T.J.F., Festen J.M., Bilsen F.A., and Brink G.van den, Phase effects in a three-component signal, J. Aoust. Soc. Am., 55(2), 297–303, (1974).

Clack T.D., Aural Harmonics: Preliminary Time-Intensity Relationships Using the Tone-on-Tone Masking Technique, J. Aoust. Soc. Am., 43(2), 283–288, (1967a).

Clack T.D., Aural Harmonics: The Masking of a 2000-Hz Tone by a Sufficient 1000-Hz Fundamental, J. Aoust. Soc. Am., 42(4), 751–758, (1967b).

Clack T.D., Erdreich J., and Knighton R.W., Aural Harmonics: The Monaural Phase Effects at 1500 Hz, 2000 Hz, and 2500 Hz Observed in Tone-on-Tone Masking When f_1 = 1000 Hz, J. Aoust. Soc. Am., 52(2), 536–541, (1972).

Craig J.H., Jeffress L.A., Effects of Phase on the Quality of a Two-component Tone, J. Aoust. Soc. Am., 34(11), 1752–1760, (1962).

Erdreich J., Clack T.D., An Algorithm for Analysis of Phase Effects: Application to Monaural Distortion Product Estimation, J. Aoust. Soc. Am., 52(4), 1124–1126, (1972).

Hall J.L., Monaural Phase Effects for Two-Tone signals, J. Aoust. Soc. Am., 51(6), 1882–1884, (1972).

Hirahara T., Internal speech spectrum representation by spatio-temporal masking pattern, J. Acoust. Soc. Jpn.(E), 12(2), 57-68, (1991).

Lamoré P.J.J., Perception of Two-Tone Octave Complexes, Acustica, 34, 1–14, (1975).

Lamoré P.J.J., Pitch and Masked Threshold in Octave Complexes in Relation to Interaction Phenomena in Two-Tone Stimuli in general, Acustica, 37, 249–257, (1977a).

Lamoré P.J.J., Investigation of Two-Tone Interaction in Octave Complexes with the Help of the Pulsation-Threshold Method, Acustica, 39, 7–15, (1977b).

Lamoré P.J.J., Phase Relations in an Internal Represention of Two-Tone Octave Complexes Acustica, 42, 296–301, (1979).

Nelson D.A., Bilger R.C., Pure-Tone Octave Masking in Normal-Hearing Listeners, J. Speech and Hearing Res., 17, 223–251, (1974).

Nelson D.A., Bilger R.C., Pure-Tone Octave Masking in Listeners with Sensorineural Hearing Loss, J. Speech and Hearing Res., 17, 252–269, (1974).

Raiford C.A., Schubert E.D., Recognition of Phase Changes in Octave Complexes, J. Aoust. Soc. Am., 50(2), 559–567, (1971).

Schubert E.D., On Estimating Aural Harmonics, J. Aoust. Soc. Am., 45(3), 790–791, (1969).

Sone T., Ozawa K., and Suzuki Y., A 'masked frequency spectrum' of a complex sound and its timbre, Proc. of Int. Cong. Acoust., 12(1), 415–418, (1989).

Torgerson, W.S., Theory and Methods of Scaling, John Wiery, New York, 1958.

Zwicker E., Influence of a Complex Masker's Time Structure on Masking, Acustica, 34, 138–146, (1976).

AIRCRAFT COCKPIT NOISE AND STUDENT PILOT HEARING

Yong-xiang Wu

Leader of the Group of Audition and Noise , Institute of
Aviation Medicine, Air Force , PLA of China

ABSTRACT   We measured the cockpit noise in the primary and
jet trainers and the basic hearing of the student pilots
before entering flying. We again measured their hearing at
the end of their first and second year of training. All the
cockpit noise levels were about 103 dB, except that of jet
trainer reached a level of 114 dB during zooming. the stud-
ent pilots' hearing did not alter significantly after two
years of flying. Their high frequency hearing loss did not
alter neither, even though some of them had original light
or even moderate degree of hearing loss before entering fly-
ing. So the physical standard concering the high frequency
hearing value in audiometery of student pilots, Air Force ,
PLA was relaxed..

1.0 INTRODUCTION

It had been proved by many scientists with the method of epidemiology, that the pilots' hearing injury, especially the high frequency hearing loss is serious (Tan z-w & Wu Y-x). But we have not yet found any report on the detailed direct relationship between the aircraft cockpit noise and the basic hearing of pilot. This paper just covers the study of this relationship. Firstly, we measured the cockpit noise in the primary and jet trainer and the basic hearing of pilots before entering flying. After they had flown for 1 or 2 years in these trainers, we again measured their hearing. Based on the data we investigated the actual relationship between cockpit noise and pilot hearing.

2.0 MATERIAL AND METHOD

2.1 Measuring the Cockpit Noise

The cockpit noise was measured by a precision sound levelmeter Model 2230 with its microphone sensor fixed in the front cockpit 15 cm away from the pilot's left ear at the ear level and a Demark made tape recorder Model 7005 mounted in the rear cockpit. The recording was maintained continuously during the whole flying. The data were processed by a Danish dual channel analyzer Type 2034. A IBM computer was used to treat, memorise and print these data.

2.2 Selecting the Student Pilots and the Contrast Group

A total number of 173 student pilots from the flight college of the Air Force were chosen as experiment group. They've passed the convention test of E.N.T.Department before entering the college. In order to eliminate the influence of age, 146 soldiers of the same age who do not expose to aircraft noise as the contrast group.

2.3 The Time and Method of Hearing Test

A Model OB77 audiometer was used to test the air conduction hearing by standard steps (Wang N-y). The test was made in a movable hearing test room in which the background noise was no more than 30 dB(A). The test frequency was from 125 Hz to 8000 Hz.

The first test was made in June-July '88, when the student pilots were still in class; the second test was made in 6-7 '89, when they had flown in primary trainer for a year; and the third time was in 6-7 '90, when they had flown in jet trainer for a year. Each year at the same time we also test the hearing of the contrast group.

3.0 RESULT

3.1 The Cockpit Noise Level of the Two Trainers

The noise levels of these two trainers in different flight conditions were shown in Table 1, and their frequency spectra were shown in Fig 1 and 2.

3.2 The Student Pilots' hearing Did Not Significantly Alter After 2 Years of Flying

Because of the elimination of the student pilots and the work change of the members in the

Table 1. trainer cockpit noise level(dB) during flying

type of trainer	flight condition			
	take off	cruising (1500m)	spiral	zooming dive
primary	104.6	103.4	104.5	104.7
jet		103.7	104.9	114.1 102.1
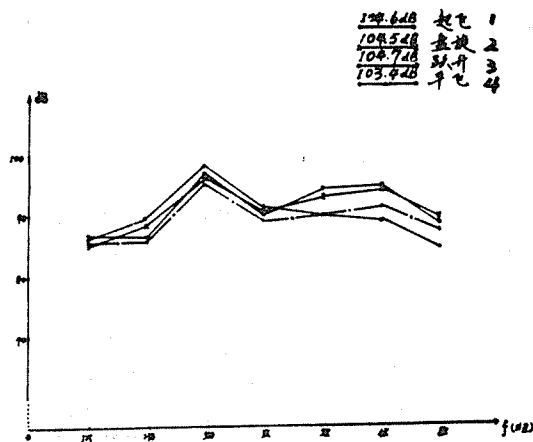
Fig 1 primary trainer cockpit
noise level during flying
note: 1--take off, 2--spiral
3--zooming, 4--cruising
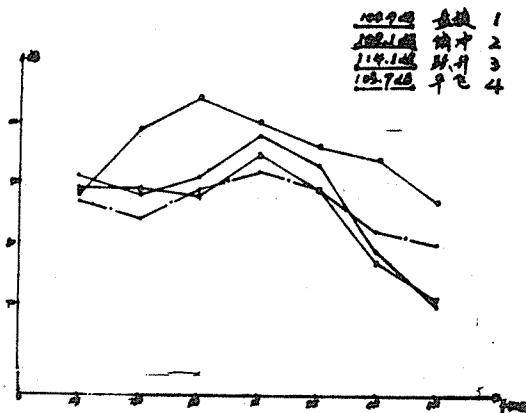
Fig 2 jet trainer cockpit
noise level during flying
note: 1--spiral, 2--dive
3--zooming, 4--cruising

contrast group, the numbers of the two groups were getting
less each year. As shown in Table 2 and 3, the hearing of
student pilots and contrast group did not significantly alter
in three years.

Table 2. 95th percentile(dB) of hearing among
the same group of student pilots

measured frequency (Hz)	1988 (N=173)	1989 (N=138)	1990 (N=93)
250	23.6	23.2	22.4
500	22.2	24.3	23.8
1000	19.1	19.4	19.1
2000	19.6	22.3	19.0
3000	23.5	27.8	25.8
4000	38.4	45.5	50.8
6000	51.7	56.4	55.9

note: 1988--the hearing before flying
      1989 & 1990--the hearing after 1 or 2 years
      of flying

Table 3. 95th percentile(dB) of hearing
among the contrast group

measured frequency (Hz)	1988 (N=146)	1989 (N=77)	1990 (N=39)
250	26.8	27.6	25.1
500	24.1	28.7	24.1
1000	19.8	22.3	20.3
2000	20.5	23.2	14.3
3000	26.7	24.5	25.3
4000	37.3	29.6	25.3
6000	48.7	50.8	33.4

3.3   <u>The Original High Frequency Hearing Loss of Student</u>
<u>pilots Did Not Get Worse</u>   The individual analyses of the
hearing of a student pilot, Mr Li, who had originally high
frequency hearing loss before entering flying, was shown in
Table 4. His hearing loss did not get worse after 2 years
of flying. As shown in Table 5 & 6, the average hearing level of 26 and 27 student pilots who had originally high freq-

Table 4. hearing levels(dB) of student pilot Mr Li

measured frequency (Hz)	left ear			right ear		
	1988	1989	1990	1988	1989	1990
250	5	5	5	5	10	10
500	5	0	5	10	10	10
1000	15	10	10	5	10	5
2000	20	20	20	5	5	10
3000	35	30	25	25	30	20
4000	50	60	50	50	45	50
6000	50	55	60	65	60	50
8000	50	40	20	35	35	40

Table 5. hearing average(dB) of 26 student pilots
with high frequency hearing loss

measured frequency (Hz)	left ear		right ear	
	1988	1989	1988	1989
3000	10.0	10.2	11.0	14.2
4000	13.8	14.6	13.9	14.6
6000	28.5	27.9	34.6	31.7

uency hearing loss also had no significant change after 1 or
2 years of flying (P<0.05). That is to say , the original
high frequency hearing loss did not worsen.

Table 6. hearing average(dB) of 27 student pilots
with high frequency hearing loss

measured frequency (Hz)	left ear			right ear		
	1988	1989	1990	1988	1989	1990
3000	12.2	12.5	12.2	14.1	15.2	14.1
4000	19.8	22.8	19.1	25.2	26.2	24.1
6000	35.4	37.2	35.4	41.5	37.6	39.4

4.0 DISCUSSION

4.1 To Determine the Cockpit Noise Correctly in Flying State

It is hard to determine the cockpit noise in flying state. We took the advantage of the two-crew cockpit trainer to fix the sound levelmeter in the front cockpit and the tape recorder in the rear cockpit, thus we could get the noise value of the whole flying course. As shown in Table 1, the noise values in all the trainers were about 103 dB, except that in the jet trainer during zooming reached to 114 dB. In the frequency spectra we could find that the level of primary trainer cockpit noise were all about the same from low to high frequency, except a little higher level was found at 500 Hz(See Fig 1.). It is a kind of mixed stable noise which may have relation to the characteristic of the propeller-driver aircraft. While the stable noise in one kind of jet trainer was mainly of low frequency(See Fig 2.), and those stable noise in several other kinds of jet planes that we had determined before were mainly of middle-high frequency.

4.2 It's a Fact That the Student Pilots' Hearing Did Not Significantly Alter after 2 Years of Flying

The values of cockpit noise of the two trainers were about 103 dB, and did not exceed the criteria limit of 108 dB(A) which was stipulated in the military standard of our country (Wu Y-x). On the other hand, the average amount of noise exposure computed according to the actual situation of total flying time and an average 30-minutes' flying per each flight time per day of the student pilot was also within the limit of the military standard for protecting hearing at home and abroad (Anonymous, Qian W-q & Britzford D). That is to say, the noise intensity and its effective time were under the permission of the standard, so it tallied with the fact that their hearing did not alter significantly.

As said before, many reports have proved that the high frequency hearing loss in pilot was serious. We know it for a fact and we belive it was because that the pilots fly the advanced jet aircraft or helicopter for too long in each flight. Naturely, the repeated hazardous exposure of the noise would give much more damage to the ear. Then their hearing loss might become serious day by day. However, based on the test of the basic hearing of 173 student pilots, we found that 53(30.6%) of them were of light degree high frequency hearing loss(See Table 5 & 6). From this fact we can say

that quite a few of serious high frequency hearing losser reported before were not attibuted to the aircraft noise . For example,among 166 fighter pilots we've reported(Wu Y-x) that the high frequency hearing losser was 53.6%. Although now we can not trace back their basic audiogram,at least we can say that some of their hearing loss were not caused by the aircraft noise. Then how could we find out the relationship between cockpit noise and pilot hearing? The only way is to take the basic audiogram before the begining of flight training and to have it followed up every year. Then we will get the sensible result.

4.3 Relaxing the High Frequency Hearing Value is Feasible When Recruiting Student Pilots Recently we have rechecked 2775 student pilots' hearing in eight different places. The results were calculated with 95th percentile (dB) of hearing It was about 40 dB at 4000 Hz and over 50 dB at 6000 Hz and about 30 dB at 8000 Hz. They had reached the light or even . moderate degree of high frequency hearing loss. Based on the natural distribute condition of our young students' hearing, we revised the hearing standard of the Air Force recruiting student pilots and stipulated the total hearing loss of two ears to be no more than 210 dB at the frequency of 4000,6000 and 8000 Hz. Will this relax influence the performance of pilot flying in the military unit ? As shown in Table 4-6 , the high frequency hearing loss did not get worse after two years of flying indicating that there was no effect on school flying. So we do think it would not inflenced the future pilot flying in the military unit too much. However the language hearing could only be influenced when the high frequency hearing loss moves into the language frequency, but as it was already proved by the service pilots that it is a very long process.

In the similar standard abroad , the hearing values of high frequency part tend to relax,too . For example, in medical examination and medical standards of USAF, the total hearing loss of two ears at 3000, 4000 and 6000 Hz is relaxed from 210 dB to 270 dB (Hill NS & Fitzpatrick DT). So based on the natural distribute condition of our young students' hearing and the reality of recruiting pilot stations, relaxing the hearing value of high frequency part properly is not only necessary, but also feasible.

5.0 REFERENCES

1. Anonymous, Outline Military Training of People Liberation Army of China, Volume 2(2), Air Force, PLA of China, Beijing, 1990, 123-125.
2. Britford D., Hazardous Noise Exposure,In: AF Regulation 161-35. Department of the Air Force, Washington,D.C.1982.
3. Fitzpatrick DT., An Analysis of Noise-Induced Hearing Loss in Army Helicopter Pilots, Aviat. Space Enviro. Med. 59(10),937-940,(1988).
4. Hill NS.,Medical Examination and Medical Standards, In: AF Regulation 160-43. Department of the Air Force, Washington, D.C. 1986.
5. Tan Z-w, etc., The hearing Analysis of 1057 Pilots, Flight Surgeon. (5), 6-8, (1985).
6. Qian W-q, etc., The military Standard of the People's Republic of China, Permissible Limit for Miltary Operation Noise, GJB Guo Jun Biao (military standards of the nation) 50-85, 1985.
7. Wang N-y, etc., The National Standard of the People's Republic of China, Acoustics-Pure Tone Air Conduction Threshold Audiometery-For Hearing Conservation Purposes, GB Guo Biao (national standards) 7583-87,1987.
8. Wu Y-x, etc., The Fighter Cockpit Noise and Pilot Hearing Journal of Troop Hygiene,5(4), 10-13,(1987).
9. Wu Y-x, etc., The Military Standard of the People's Republic of China, Fighter(Attacker) Cockpit Noise Limits. GJB Guo Jun Biao (military standard of the nation)565-88, 1988.

THE ARRANGEMENT OPTIMIZATION OF ERROR SENSORS FOR ADAPTIVE ACTIVE NOISE CONTROL WITHIN A RECTANGULAR ENCLOSURE

K.A.CHEN   Y.L.MA

P.O.Box 19, College of Marine Engineering
Northwestern Polytechnical University (NPU)
Xi'an, Shannxi 710072, P.R.China
TEL: (029) 53351—2618,   FAX: 0086+029 711959

ABSTRACT

It is of great importance for adaptive active noise control to achieve expected reduction of acoustic potential energy within an enclosed space. In this paper, effect of number and locations of error sensors (ES) is discussed, in order to keep the number of ES as few as possible.An interpolation method for error signal based on spatial sampling is presented, which has practical advanstage in case of primary source working at non—resonance frequencies , high modal density space and mutli—channel adaptive active sound control system.Finally, simulation results taking active control of a lightly damped rectangular enclosure for example are given.

1.0 INTRODUCTION

A great number of successful active control applications have already existed for many years, particularly for low–frequency noise in ducts [1]. Beacause of advances in VLSI and signal processing, more recently, active control of sound field in enclosed space has attracted special attention and some initial encouraging results for active control of propeller–induced cabin noise have been obtained[2].

Since primary source may come from structural radiation , sound tranmission or internal noise excitation and source parameters together with the transmission channel are time–variant, it is necessary for an adaptive system to track the variations and achieve optimum noise reduction. For an adaptive active control system the arrangement of error sensors have strong influence on complexity of practical installation and signal processing as well as attenuation level, in practice the sum of squared pressures received by a number of ES at discrete points is refered to as approximation of acoustic potential energy over space. Theoretically, an infinite number of ES are needed for optimum reduction, which is obviously impractical.

Thus, an interpolation method for error signal based on spatial sampling is presented in this paper, which can largely reduce the number of ES, particularly for primary source working at non–resonance frequencies, high modal density space and multi–channel adaptive active sound control system. Finally, simulation results taking active control of a lightly damped rectangular enclosure for example are given.

2.0 ADAPTIVE ACTIVE CONTROL OF ENCLOSED SOUND FIELD
2.1 PROBLEM DESCRIPTION

Suppose that the sound field to be discussed is steady and harmonic and can be expressed as sum of modal contributions with a time dependent factor $e^{i\omega t}$. The complex pressure of primary plus secondary sources at a given point r can be written as

$$p(r,\omega) = \sum_{n=0}^{N} \psi_n(r)a_n(\omega) = \psi^T a = \psi^T (a_p + Bq_s) \qquad (1)$$

where ψ , a_p are the Nth order vector of characteristic functions , and modal amplitude due to primary source only,and q_s is complex strength vector of secondary sources, whose elements are $\psi_n(r)$, $a_{pn}(\omega)$ and $q_{sm}(\omega)$ respectively. B is N × M matrix of modal excitation coefficients quantifying the excitation of the nth mode due to the mth secondary source, and its elements are $B_{nm}(\omega)$.

Nelson et al [2] introduced minimazation of total time–averaged acoustic potential energy as criterion of active sound control in enclosure, This quantity, E_p is proportional to the volume integrated mean square of acoustic pressure and is measurable.

$$E_p = (\frac{1}{4\rho c^2})\int p^2(r,\omega)dv = a_p^H a_p \qquad (2)$$

where ρ , c are the density and sound velocity of medium respectively, H denotes Hermitian transpose of a matrix.

According to unconstrained optimization theory, an unique set of secondary sources can be obtained [1]

$$q_{so} = -[B^H B]^{-1} B^H a_p \qquad (3)$$

this method is known as active minimazation of acoustic potential (AMAP) in enclosure.

2.2 IMPLEMENTATION AND PERFORMANCE

With regard to practical utlization of (3), a feasible approach is to monitor the amplitude of the error pressure fluctuation at a number of discrete sensor locations and adjust adaptively the strengths of secondary sources untill convergence.The system carrying out the above operation is so—called adaptive active sound control system.It is pointed out by passing that several adaptive algorithms such as filtered—x LMS[3]and intermittent RLS algorithm [6] have been developed for these systems.

The sum of squared pressures at r_l (l = 1, 2, ..., L) can be regarded as an approximation of the overall space acoustic potential energy,

$$J_p = \frac{V}{4\rho c^2} p^2(r, \omega) \tag{4}$$

It should be noted that driving the pressure to zero at a number of discrete locations may produce substaintial increase in the pressure amplitude at other locations.Therefore, an infinite number of ES are needed theoretically to achieve best possible overall reduction , which is obviously impractical, it is necessary to develope an alternative approach solving this problem.

For the sake of visualization of the study , Attenuation Level (AL) is defined as follows in which E_{pp} and E_{po} denote respectively acoustic potential energy due to primary source distribution only and primary and secondary sources distribution together.

$$AL = 10 lg\left(\frac{E_{pp}}{E_{po}}\right) \tag{5}$$

Theoretically, there are respcctively

$$E_{pp} = \frac{V}{4\rho c^2} a^H a_p$$

$$E_{po} = \frac{V}{4\rho c^2} [a_p^H a_p - a_p^H B[B^H B]^{-1} B^H a_p] \tag{6}$$

If the adaptive system contains L ES, then

$$E_{po} = \frac{V}{4\rho c^2} q_{sl}^H B^H B q_{sl} + q_{sl}^H B^H a_p + a_p^H B q_{sl} + a_p^H a_p \tag{7}$$

q_{sl} is the vector of optimum strengths of secondary sources , a detailed derivation can be found in reference [2].

3.0 INTERPOLATION OF ERROR SIGNAL

According to sampling theorem in time domain, for a limited—band temporal signal, if the sampling frequency f_s is greater or equal to at least twice the highest frequency (f_0), then x(t) can be represented as weighted sum of discrete sampled values of x(t), i.e.

$$x(t) = \sum_{k=-\infty}^{\infty} x(kT_s)\frac{sin(2\pi(t - kT_s))}{2\pi(t - kT_s)} \tag{8}$$

The rightmost term in above equation is a sampling function.In general there are many classes of sampling functions such as sinusoidal function, Laruerrel functions, and Legendre

polynomials[4].

Eq.(3) can be extended to cover spatial sampling [5]. For simplicity, a pure tone acoustic pressure p(r,t) is considered and it can be sampled at interval $(\triangle_x, \triangle_y, \triangle_z)$.

$$P(r,\omega) = \sum_{l=-\infty}^{\infty} \sum_{m=-\infty}^{\infty} \sum_{n=-\infty}^{\infty} f(x_l, y_m, z_n) S(l,m,n,x,y,z) \tag{9}$$

$$S(l,m,n,x,y,z) = \frac{sin\left(\dfrac{\pi x}{\triangle_x} - l\pi\right)}{\dfrac{\pi x}{\triangle_x} - l\pi} \frac{sin\left(\dfrac{\pi y}{\triangle_y} - m\pi\right)}{\dfrac{\pi y}{\triangle_y} - m\pi} \frac{sin\left(\dfrac{\pi z}{\triangle_z} - n\pi\right)}{\dfrac{\pi z}{\triangle_z} - n\pi} \tag{10}$$

where $\triangle_x$, $\triangle_y$, $\triangle_z$ are sampling interval along X, Y and Z respectively.
The spatial sampling formula is valid if

$$\triangle \leqslant \frac{\lambda_{min}}{2} \tag{11}$$

where $\triangle$ is one of $(\triangle_x, \triangle_y, \triangle_z)$, λ_{min} is the wavelength associated with the highest frequency.

Accordingly, pressure at some location which has not been picked up by a 'real' sensor can be interpolated by pressuers at other locations. Observed from eq.(1), spatial sampling of p(r, t) depends on characteristic function $\psi_n(r)$ only because $a_n(\omega)$ is a constant for a given instance. Taking one dimension standing wave which propagates along a finite long duct seated at two ends for example, one can interpolate pressure at any position from the pressures taking at 4n sampling points for the nth mode, the result seems quite satisfactory (in Fig.1).

4.0 ILLUSTRATION

Given a lightly damped, approximate 'two dimensional', rectangular enclosure whose dimensions are 2.264m × 1.132m × 0.186m. A damping ratio of 0.01 is assumed for all natural frequencies. For simplicity, only one primary point source at (2.2, 1.1, 0.12) and one secondary point source at (0.17, 0.9, 0.18) are considered.

$$a_{pn}(\omega) = \frac{\rho c^2}{V} \frac{\omega \psi_n(r_p) q_p(\omega)}{2\zeta_n \omega_n \omega - j(\omega_n^2 - \omega^2)} \tag{12}$$

$$B_{nm}(\omega) = \frac{\omega \psi_n(r_{sm})}{2\zeta_n \omega_n \omega - j(\omega_n^2 - \omega^2)} \tag{13}$$

$$\psi_n(r_{sm}) = \varepsilon_{n_1} \varepsilon_{n_2} \varepsilon_{n_3} cos\left(\frac{n_1 \pi x}{L_x}\right) cos\left(\frac{n_2 \pi y}{L_y}\right) cos\left(\frac{n_3 \pi z}{L_z}\right)$$

$$\varepsilon = \begin{cases} 1 & v = 0 \\ 2 & v > 0 \end{cases} \tag{14}$$

The operation frequencies are within the limits ranging from 10Hz to 300Hz, there are 8 main contributing modes whose natural frequencies and mode indexes are respectively

73.2Hz (1, 0, 0), 141.4Hz (0, 1, 0) (2, 0, 0), 163.7Hz (1, 1, 0), 207.0Hz (2, 1, 0)219.6Hz (3, 0, 0), 263.9Hz (3, 1, 0) and 293.6Hz (0, 2, 0).

In order to achieve AMAP adaptively, assume that 4 ES are placed in the same plane as the secondary source lays, located at (0.754, 0.377, 0.18), (0.754, 0.377, 0.18), (1.508 ,0.377, 0.18) and (1.508, 0.754, 0.18). For this case, AL is computed and shown in Fig.2 (curve B).In comparison with theoretical predicated value of AL(curve A in Fig.2), it shows that optimum AL can't be reached and inversely E_p is increased at some non–resonance frequencies, this is mainly because there are more modes significantly contributing to the pressure field at these frequencies and 4 ES is too few to approximate the overall space distribution of acoustic potential energy.

Acoustic pressures at 16 locations can be interpolated through pressures at positions of the 4 ES according to eq.(9), AL for this case agree well with the optimum value of AL.

In addition, 750 modes ($N_1 = 15$, $N_2 = 10$, $N_3 = 5$) are included for computing accurately the pressure amplitude at all frequencis up to 300Hz.

5.0   CONCLUSION

For an adaptive active sound control system in enclousure, one of the important parameter is number and locations of ES. Of course ES should be placed at points of maximum response for the major contributing modes and the number of ES should be as big as possible theoretically. However, in practice a great part of the error signals can be made by interporlating from limited 'real' error signals. The approach presented is of great advanstage for high density sound field and mutli–channel adaptive active sound control system.The price paid for this method is the computation burden which can be solved easier with the help of rapidly developing digital signal processors.

REFERENCES

[1] Leventhall, H.J., active Attenuators:Historical Review and Some Recent Developments, Inter–noise 80, 679–682.

[2] Bullmore, A.J., Nelson, P.A.Curtis, A.R.D., Elliott, S.J., the Active Minimization of Harmonic Enclosed Sound Fields, Part II: A computer Simulation, JSV(1987), 117(1), 15–33.

[3] Elloitt S.J., Nelson, P.A., Stothers, I.M., Boucher, C.C. In–Flight Experiments on the Active Control of Propeller–Induced Cabin Noise. JSV(1990), 140(2), 219–238.

[4] Oppenheim and Johonson, D.H., Discrete Representation of Signals, Proc.IEEE, Vol.60, No.6, June 1972, 681–691.

[5] Knight, W.C., Pridham, R.G. Kay, S.M., Digital Signal Processing for Sonar. Proc.IEEE, Vol.69, No.11, Nov.1981, 1451–1506.

[6] Chen, K.A., Ma, Y.L., Artifical Neural Network applied to Active Noise Control. submitted to ICA, Beijing, 1992.
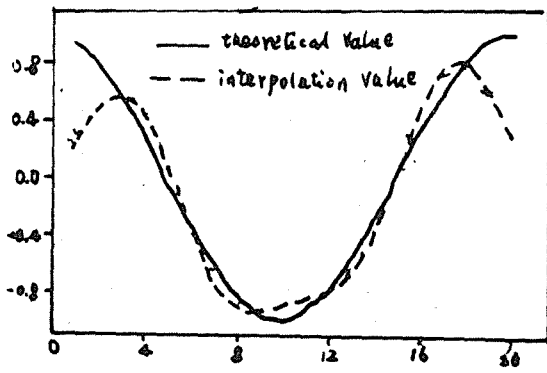
Fig.1   Pressures interpolation for one-dimension standing wave
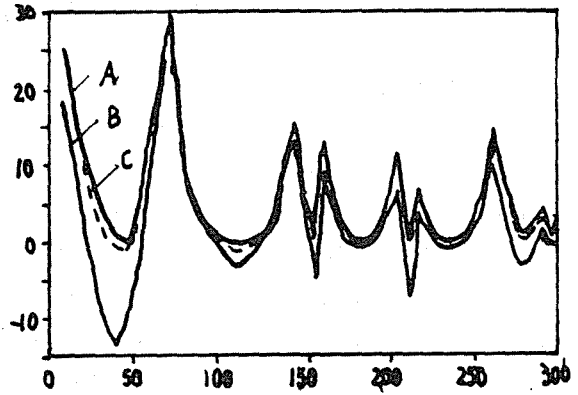
Fig.2   An improvement on AL by using interpolation
method for error signals

BARRIER ATTENUATION OF THE TRUNCATED WEDGE

C.G.Don
Department of Physics
Monash University, Melbourne, Victoria, Australia.

ABSTRACT

While exact expressions for the diffraction of sound from a point source by a thin semi-infinite sheet and a wedge have been available for many years, an exact solution for a truncated wedge has only recently become available. This solution, by I. Tolstoy, which assumes a harmonic line source, will be discussed. Problems arising when evaluating the theory will be indicated as well as limitations which occur at small barrier widths. Predictions will be compared with experimental measurements of the attenuation produced by truncated wedge barriers, with a width up to 0.5m. The acoustic impulse technique used to obtain these measurements over full sized barriers will also be described along with results from approximate expressions for wide barrier diffraction by Pierce and by Medwin. The phase information provided by the theories is evaluated by comparing predicted and measured waveshapes obtained behind the barrier.

1.0 INTRODUCTION

Barriers are an important architectural element for the reduction of noise. While exact theoretical models for the semi-infinite thin sheet and the wedge are available, including a formulation which permits speedier computation (Hadden and Pierce), real barriers have a finite width and rarely come to the sharp edge assumed by the wedge. A more realistic model for practical barriers is the truncated wedge, which reduces to a rectangular barrier when the exterior vertex angles are 270°. A semi-intuitive formula for the attenuation of a wide barrier is available (Pierce), while an impulse treatment can also be applied (Medwin). Both these methods are approximate, so the recently developed theory (Tolstoy) of an exact treatment for the truncated wedge provides a useful standard to compare predictions of other models, although Tolstoy's approach assumes a line rather than the point source of other models (Don).

2.0 OUTLINE OF TOLSTOY'S THEORY

Sound from a harmonic line source of angular frequency ω and wavenumber k, located at (r_s, θ_s) in Fig.1(a) diffracts over vertexes B' and B to the reception point at (r_r, θ_r). Some of the energy reaching vertex B will be backscattered to B'. Portion of this energy will then be re-diffracted back to B where partial backscattering will again occur. The resultant sound reaching the receiver is the sum of the main diffracted component and contributions from multiple scattering between effective line sources located at B and B'.

In general, the total field, Φ, produced at a point (r, θ) by a line source of strength A_n after diffraction by a vertex of angle θ_w, as shown in Fig.1(b), is given by

$$\Phi = \sum_{n=o}^{\infty} A_n \cos v_n \theta \, J_{v_n}(kr) \qquad (1)$$
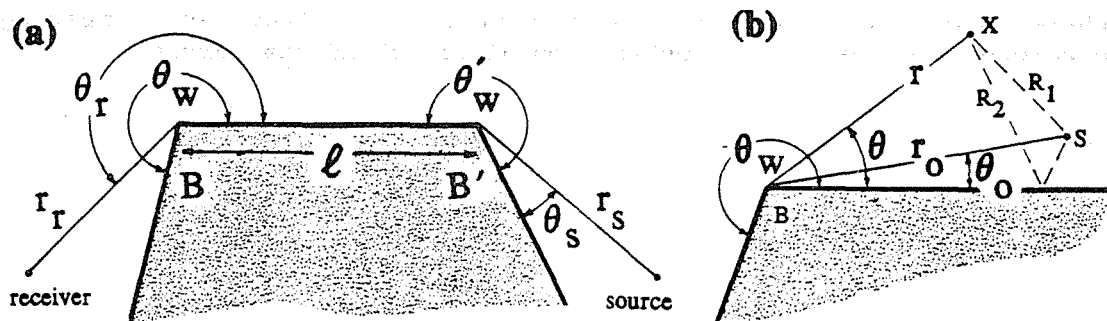
Fig.1: (a) Location of source and receiver relative to truncated wedge. (b) Geometry around a single vertex.

where $v_n = n \mu$ and $\mu = \pi/\theta$. For a source at (r_0, θ_0) and $r > r_0$,

$$A_n = 2\mu \, \varepsilon_n \, \mathcal{A} \, \cos v_n \theta_0 \, H_{v_n}(kr_0) / H_0(k\ell) \qquad (2)$$

where the Neumann factor $\varepsilon_n = 2$ except for $\varepsilon_0 = 1$ and the source amplitude $\mathcal{A}$ is defined at a distance ℓ from the source. The time dependence $e^{-i\omega t}$ has been omitted in all equations.

The diffracted component, Φ_D, can be determined by subtracting the direct and reflected components from the total field Φ. So, at point X in Fig.1(b),

$$\Phi_D = \Phi - \mathcal{A} \, [H_0(kR_1) + H_0(kR_2)] / H_0(k\ell).$$

When both S and X are on the wedge surface B - B' such that $\theta = \theta_0$ and $R_1 = R_2 = |r - r_0|$, then

$$= \mathcal{A} \, [2\mu \sum_{n=0}^{\infty} \varepsilon_n \, H_{v_n}(kr_0) \, J_{v_n}(kr) - 2 H_0(k|r - r_0|)] / H_0(k\ell) \qquad (3)$$

When calculating the field scattered back to a source from a vertex, ie. when $r \rightarrow r_0$, both the series and Hankel function in Eq.(3) become divergent, however, the singularities cancel leaving a convergent series, ξ. For a rectangular barrier, ξ is given by

$$\xi = 2i \sum_{m} \frac{e^{-i2m\pi/3}}{\sin(2m\pi/3)} \, J^2_{2m/3}(k\ell) + H_0(2k\ell) - iZ$$

$$+ \frac{i}{\pi} \ln\left(\frac{16}{27(k\ell)^2}\right) - \frac{2i\gamma}{\pi} - 1 \qquad (4)$$

where γ is Eulers constant and the factor Z is

$$Z = \frac{2}{\mu\pi} \sum_{m} \frac{1}{m} \, [J_{v_m}(k\ell) \, J_{-v_m}(k\ell) \, \Gamma_{(1+v_m)} \, \Gamma_{(1-v_m)} - 1]. \qquad (5)$$

The summation $\sum_{m}$ implies only nonintegral values of v_m are included.

Under this condition $\Phi_D = 2 \mu \, \xi \, \mathcal{A} / H_0(k\ell)$.

With primed quantities relating to vertex B' and assuming effective source strengths of b_n and b'_n located at the vertices the resulting fields at B and B' can be written as

$$\Phi_B = \Phi_S + \sum_{n=0}^{\infty} b'_n \, \cos v'_n \theta' \, J_{v'_n}(kr')$$

$$\Phi'_B = \overset{\circ}{\underset{n=o}{\Sigma}} b_n \cos v_n \theta J_{v_n}(kr) \tag{6}$$

where Φ_s represents the direct contribution from the source, ie. Eqs.(1) and (2) with $r_o = r_s$ and $\theta_o = \theta_s$. The field emanating from b'_n is the result of diffraction by B' of the effective field from B, which equals that coming from B minus that backscattered from B'. A similar statement applies to b_n. By using the above equations to obtain two sets of expressions which relate b_n and b'_n, the field at the receiver, Φ_r, can be expressed as

$$\Phi_r = \frac{\Phi_s \, [1-S]^{-1}}{2\mu H_o(k\ell)} \overset{\circ}{\underset{n=o}{\Sigma}} \varepsilon_n \cos v_n \theta_r H_{v_n}(kr_r) J_{v_n}(k\ell) \tag{7}$$

where $\qquad S = (1/4\mu\mu')^2 [\xi\xi'/H_o(k\ell)^2]. \tag{8}$

The quantity $[1-S]^{-1}$ is the multiple scattering correction to the simpler theory of double diffraction over the parallel vertices. Introducing $r_t = r_o + \ell + r_r$ as the distance from the source to receiver over the barrier, then the excess attenuation is given by

$$\text{Excess Attenuation} = 20 \log |(\Phi_r \, H_o(k\ell) / \, (\ell \, H_o(kr_t))| \, \text{dB}. \tag{9}$$

The barrier insertion loss can be calculated by adding $20 \log(r_t/d)$ to the excess attenuation, where d is the direct distance between source and barrier.

3.0 THE MULTIPLE SCATTERING FACTOR

For a rectangular barrier, $\theta_w = \theta'_w = 3\pi/2$ and $\xi = \xi'$. The summation of Bessel and Hankel functions required by Eqs.(4) and (5) are slow to converge at higher $k\ell$ values, as is indicated in Fig.2. In both cases, 300 terms have been used in the summations in Eq.(4). Using 50 terms in Eq.(5) gives reliable values only to $k\ell$ about 15. Even 255 terms does not produce convergence beyond $k\ell = 50$, which restricts the usefulness of the calculations at 1kHz to barriers about 3m wide. More terms were not used because the gamma functions in Eq.(5) exceeded the computer capacity. A noticeable deviation, labelled A, occurs around $k\ell = 21$. This is caused by a mismatch between the approximations used to calculate the Bessel and Hankel functions.

At higher $k\ell$ values there is a slow drift of $|1-S|^{-1}$ away from the mean of 1.0, which is caused by an upwards trend in the complex part of ξ. This arises from a small difference between iZ and the sum of the last two complex terms in Eq.(4), which is almost certainly due to incomplete summation of Z. It is tempting to suggest that for $k\ell > 50$ the terms should exactly cancel - thereby eliminating the drift at higher $k\ell$ values. If this drift is neglected, then above $k\ell \sim 15$, ξ

closely approximates to $0.47H_o(2k\ell)$ and the multiple scattering factor also has a damped oscillation depending on $2k\ell$. This can be interpreted as re-inforcement of the diffracted sound whenever the wavelength is a multiple of twice the barrier width.
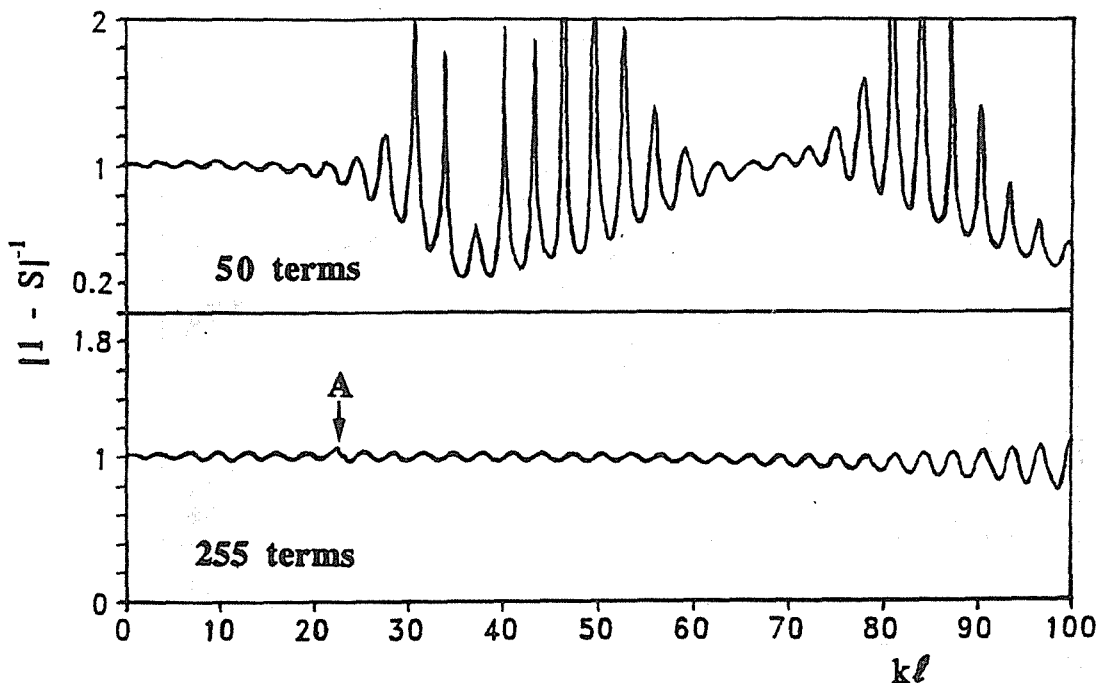
Fig. 2: Effect of increasing the number of terms in the calculation of multiple scattering correction factor.

Perhaps the most obvious feature of $|1-S|^{-1}$ is that it does not differ greatly from unity. To test its significance, predictions will be compared with measurements obtained using a rectangular barrier 0.45m wide.

4.0 EXPERIMENTAL RESULTS AND PREDICTIONS

The excess attenuation was measured by diffracting acoustic impulses around a barrier and comparing the diffracted waveshapes with those of pulses which had not experienced diffraction (Papadopoulos and Don). By Fourier analysing both waveforms and dividing the corresponding diffracted by the un-diffracted component, the excess attenuation was calculated over the frequency range 700Hz to 12kHz.

Fig.3(a) presents experimental excess attenuation data at reception angles of $\theta = 54^\circ$ and 83°, along with predictions of the Tolstoy theory when $|1-S|^{-1}$ is set to unity. The effect of introducing the multiple scattering factor is indicated in Fig.3(b). Overall the effect is slight, the increased attenuation at higher frequencies is largely caused by the drift in the complex part of ξ, as by 10kHz the barrier width makes $k\ell \sim 80$. A comparison of predictions from the

273

Pierce and the Medwin theory with those of Tolstoy shows the results generally agree within a dB, the Pierce approximation consistently over-predicting the attenuation.
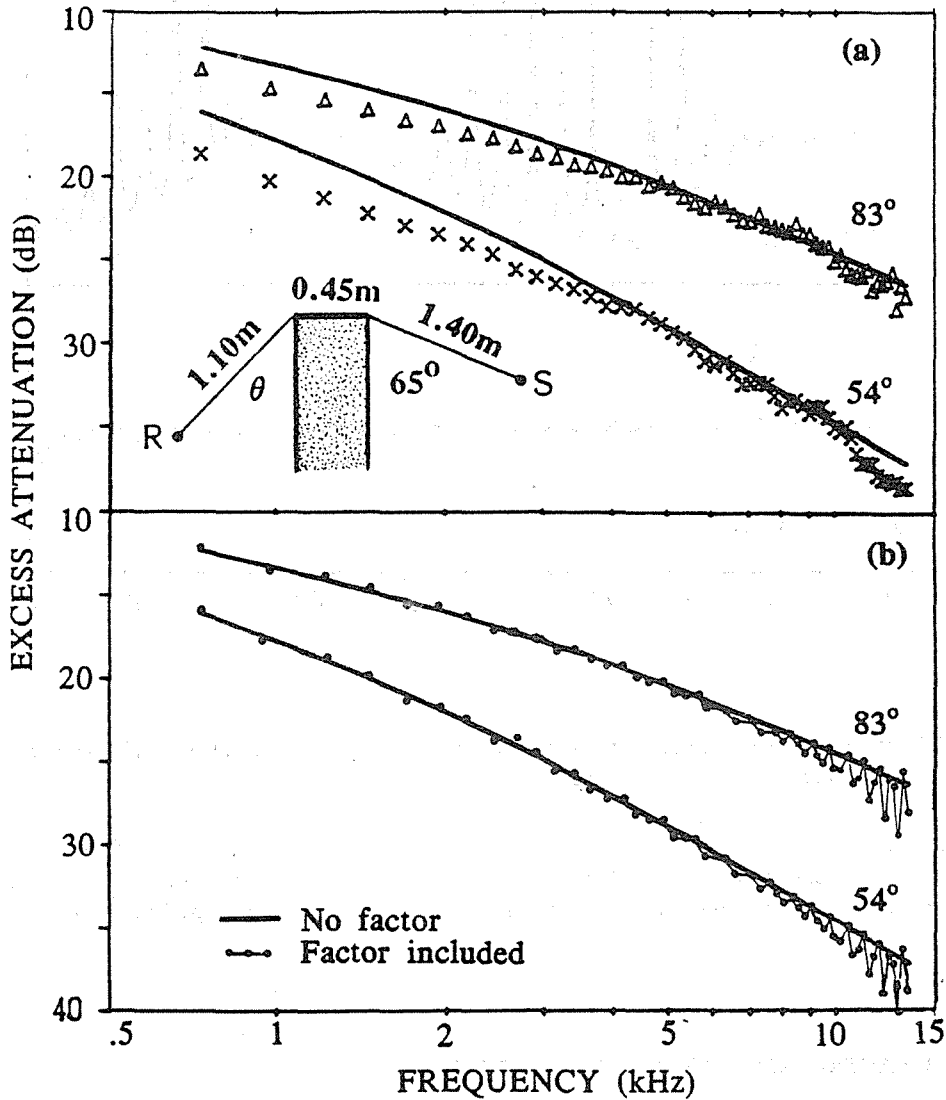
Fig.3: (a) Comparison of experimental results (symbols) with predictions of Tolstoy theory when $|1-S|^{-1}$ equals unity.
(b) Effect of including multiple scattering factor.

The predicted diffracted pulse waveform can be calculated by multiplying the theoretical diffraction factors by the appropriate frequency components in the direct pulse and then using an inverse transform. If the phase information is incorrectly included in the theoretical model then the shape of the resulting waveform does not agree with measurements . When this test is applied with factors deduced from the Tolstoy theory the waveforms are in good agreement.

An interesting verification of the principle behind Tolstoy's method occurs when the diffracted pulse shape behind the barrier is calculated with and without the multiple scattering parameter. The two waveforms are very similar, however, when they are magnified by, say 100, and the difference is plotted, a small peak occurs which is delayed from the main impulse by a time equal to that required for sound to traverse twice the barrier width.

Tolstoy's theory breaks down for thin barriers. If the thickness of the barrier is progressively reduced the predicted attenuations should tend towards the infinitely thin sheet - as given by the Hadden and Pierce prediction. However, the Tolstoy calculations diverge markedly at very small thicknesses. This limitation occurs because the $H_o(kl)$ term in the denominator of Eq.7 rapidly increases in magnitude as kl tends to zero, indicating it is inappropriate to model the vertex as a Hankel function at small distances.

5.0   CONCLUSION

To completely specify the attenuation of a wide barrier requires inclusion of the multiple scattering factor, however, this presents computational difficulties once $kl > 15$. In this range the summations involved in the calculation of ξ for a rectangular barrier can be approximated by a simple Hankel function of the form $H_o(2kl)$. In practice, the effect of the multiple scattering factor on the excess attenuation is very slight and can generally be ignored. Results from the Tolstoy theory agree with experimental data and with predictions based on either the Medwin or the Pierce approximations, although these assume a point rather than a line source. Because of its simplicity, the Pierce approximation is the more practical prediction technique.

REFERENCES

Don C.G., Application of a Hard Truncated Wedge Theory of Diffraction to Wide Barriers, J.Acoust. Soc. Am., (In Press).

Hadden W.J. and Pierce A.D., Sound diffraction around screens and wedges for arbitrary point source locations, J. Acoust. Soc. Am. 69, 1266-1276 (1981).

Medwin H., Childs E. and Jebsen G.M., Impulse studies of double diffraction: A discrete Huygens interpretation, J. Acoust. Soc. Am. 72, 1005-1013 (1982).

Papadopoulos A.I. and Don C.G., A study of barrier attenuation by using acoustic impulses, J. Acoust. Soc. Am (In Press).

Pierce A.D., Diffraction of sound around corners and over wide barriers, J. Acoust. Soc. Am. 55, 941-955 (1974).

Tolstoy I., Diffraction by a hard truncated wedge and a strip, IEEE J. Ocean. Eng., 14, 4-16 (1989).

Tolstoy I., Exact, explicit solutions for diffraction by hard sound barriers and seamounts, J. Acoust. Soc. Am., 85, 661-669 (1989).

UNUSUAL ACOUSTIC VIBRATION IN HEAT EXCHANGER AND STEAM GENERATOR TUBE BANKS POSSIBLY CAUSED BY FLUID-ACOUSTIC INSTABILITY

F. L. Eisinger and R. E. Sullivan
Foster Wheeler Energy Corporation
Clinton, New Jersey 08809-4000, U.S.A.

ABSTRACT

Flow channels of heat exchangers or steam generators containing tube arrays can be subject to acoustical vibration excited by flow of air, gas, or steam transversely across the tubes. Such vibration occurs when a flow disturbance inside the tube bank excites a strong acoustical (standing wave) mode of the channel. The acoustical modes typically excited are those which are related to the dimension perpendicular to both the fluid flow direction and the tube axes. Preventive measures taken in the design stage are typically directed against these commonly existing standing waves. Evidence is presented of the unusual occurence of standing waves which develop in the flow direction and in the tube axial direction. The causes for their development and methods of suppression are discussed.

1.0 INTRODUCTION

Acoustic waves can be excited by disturbances arising within the tube bundle but also away from the tube bundle in the ducting. Inside the tube bundle the excitation phenomena considered to be responsible for the development of acoustic vibration are primarily vortex shedding, but also turbulence, generated by crossflow. The effects of bends in the ducting, changes in cross section, turbulent swirling flow, and bluff bodies placed inside the duct are often the sources of acoustic vibration in the ducting away from the tube bundle.

Two types of acoustic modes are known to exist: Those which are bound to the tube bundle and decay in the adjoining ducting, and those which exist primarily in the ducting and decay within the tube bundle. Both of these modes, as shown by Parker (1978) and Blevins (1986), can be excited by acoustic disturbances within the tube bundle. As mentioned earlier, the duct modes can also be excited by disturbances within the duct proper.

The acoustic modes typically excited by crossflow in tubular heat exchanger or steam generator tube banks are the transverse modes (modes j = 1, 2, 3, ... in the y-direction) which are perpendicular to the direction of flow and tube axes. Longitudinal modes (i) in the flow direction (x), or transverse modes (k) in the direction of the tube axes (z) are rarely excited by crossflow and have not been reported in the literature. (The indices i j k give the number of acoustic waves in the flow (x), transverse (y), and tube axial (z) directions, respectively.)

In this paper we present evidence of unusual acoustic vibration in two cases: in one a tubular air heater, acoustic vibration occurred in the longitudinal (flow) direction, and in the second a steam generator economizer bank, acoustic vibration occurred in a direction transverse to flow, along the tubes.

2.0 THEORIES OF ACOUSTIC VIBRATION AND BRIEF REVIEW OF PUBLISHED WORK

The publications on acoustic vibration or resonances in tube banks typically assume that vibration due to crossflow will occur only in the j-modes, which are characterized by a fluctuating particle velocity in the y-direction (lift direction) which is perpendicular to the direction of flow and the tubes. Most of the experimental evidence, both laboratory and industrial does support this assumption.

Two principal sources causing acoustic vibration in tube bundles have been identified. They are:
(1) Vortex shedding
(2) Turbulence or turbulence-based instability

The vortex theory is well established and its validity very well documented experimentally. It is also widely used in design practice. According to this theory, the vortex shedding-induced fluctuating lift forces are perfectly capable of interacting with the particle velocities of the fluid column standing waves vibrating in the same direction. At resonance intense noise and vibration can be generated. Works of Baird (1954), Grotz and Arnold (1956), Putnam (1959), Chen (1968), Chen and Young (1974), Parker (1978), Eisinger (1980), Blevins (1986), Blevins and Bressler (1987), and Parker and Stoneman (1989) all support the vortex shedding theory of acoustic vibration.

The turbulence-based theory postulates a triggering mechanism initiating the acoustic vibration and sustaining it by the energy contained within the turbulent flow inside the tube bank. An instability-like phenomenon is postulated. Although there is some experimental evidence that such a mechanism might be at work in certain cases, no proof of such a mechanism has so far been offered. The following works fall to some degree in this category: Owen (1973), Funakawa and Umakoshi (1970), Fitzpatrick and Donaldson (1977), Fitzpatrick (1985, 1986), Rae and Murray (1987), Ziada et al (1988), Ziada and Oengoren (1991), and Oengoren and Ziada (1991).

A large body of experimental and theoretical evidence has accumulated over the years in the field of solid propellant rocket combustion where the effect of a superimposed acoustic field upon the turbulent flame combustion process has been studied. Pressure- and velocity-coupled instability mechanisms have been shown to exist, initiating strong acoustic vibration in the enclosed spaces of the combustion chamber. Since acoustic waves in the enclosed space of a combustion chamber are always present, at certain conditions the coupling mechanism can give rise to intense acoustic vibration. We mention only a few of the publications in this field: Culick (1966), Price and Dehority (1967), Culick (1970), Price (1979), Culick and Magiawala (1981), Ma et al (1990).

The instability mechanism of acoustic vibration in the combustion chamber seems to present supportive evidence for the turbulence-based theories of strong acoustic vibration in tube bundles. Although not proven yet, the interaction (coupling) of the acoustic waves always present inside a tube bundle (waves of different modes and magnitudes) with the turbulent flow field appears to be a plausible mechanism of excitation. It is this coupling mechanism which might have been responsible for the initiation of the unusual acoustic vibration described in the following paragraphs.

3.0 LONGITUDINAL ACOUSTIC VIBRATION IN A FULL SIZE TUBULAR AIR HEATER

3.1 <u>Experimentally Observed Acoustic Vibration</u>. The tubular air heater shown in Fig. 1 consists of two separate tube banks, bank 1 and bank 2. The tubes have an in-line arrangement and are supported by two tube sheets (at top and bottom), and by a tube support plate at mid-hight. The tubes are exposed to air flow on the outside and hot gas on the inside. The air enters the air heater at a right angle and as it makes a 90 degree turn enters bank 1 and bank 2 in crossflow. The heated air exits in a direction parallel to that of the inlet.
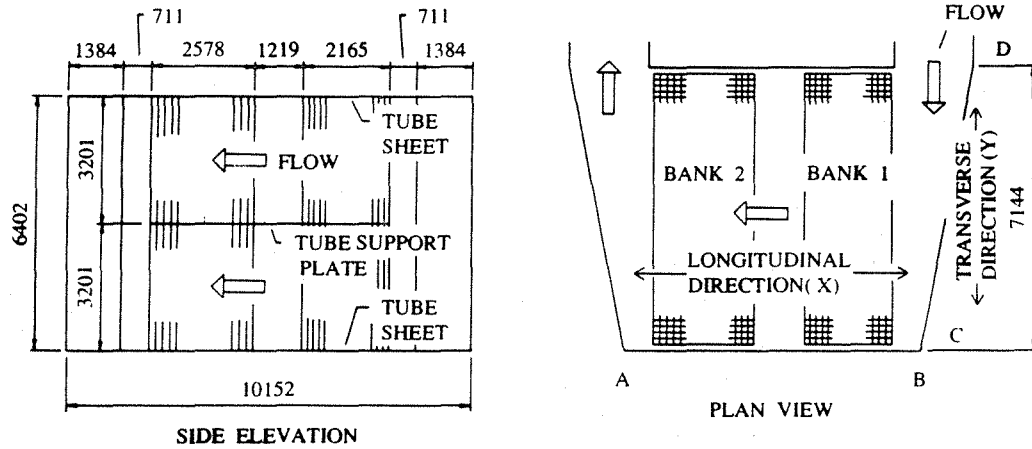
Fig. 1 Arrangement of tubular air heater

The air heater dimensions are given in Fig. 1. The geometry of the tube layout is given in Table 1. The air flow temperature increases as it passes through the air heater. Three flow conditions are specified, low (47%), medium (71%), and high (100%). The corresponding Helmholtz numbers $H_e = vS/c$ and Reynolds numbers $R_e = vD/v$ at the inlet and outlet of each bank are given in Table 1. Here v is the gap velocity, S is the Strouhal number, c is the effective speed of sound within the tube bank, D is the tube diameter, and v is the kinematic viscosity. The flow data were based on performance calculations of the air heater, correlated with control room data during operation.

Table 1: Air Heater Tube Bank Geometry and Flow Parameters

Bank No.	Tube O.D.	Side Spacing	Longit. Spacing	Air Flow					
				47%		71%		100%	
				$H_e \times 10^6$ In/Out	R_e In/Out	$H_e \times 10^6$ In/Out	R_e In/Out	$H_e \times 10^6$ In/Out	R_e In/Out
	mm	mm	mm	—	—	—	—	—	—
1	64	79	75	4,600/ 5,280	10,818/ 8,737	6,950/ 7,980	16,341/ 13,199	9,780/ 11,240	23,016/ 18,590
2	64	79	89	3,460/ 3,990	8,737/ 7,323	5,230/ 6,030	13,199/ 11,062	7,360/ 8,490	18,590/ 15,563

The air heater operated relatively quietly at low flows and became noisier at higher air flows. A particularly noisy vibratory condition developed when the air heater was exposed to the full load flow.

Fig. 2 shows plots of sound readings taken at a 1m distance from the casing in the longitudinal (AB) and transverse (CD) direction at the low, medium, and high flow conditions. The measurements were taken at an elevation just above the tube support plate using a Bruel and Kjaer (B&K) type 2230 precision integrating sound level meter in conjunction with a B&K type 2515 vibration analyzer. From these measurements, it can be seen that the acoustic environment around the air heater was relatively noisy. There was, however, no clearly developed standing wave pattern observed throughout the range of flow velocities, except at the high flow condition when suddenly an intense acoustic vibratory condition developed. This condition was characterized by a single frequency noise and a clearly defined standing wave. As shown in Fig. 2c, the standing wave was established *in the flow direction (x)* at a frequency of *75 Hz* in the third mode. There was some variation of the 68 Hz frequency sound in the transverse (y) and longitudinal (x) directions, however this did not represent a fully developed standing wave. A wave pattern in the longitudinal direction is already visible at the medium flow at the frequencies of 68 Hz and 52 Hz.

The presence of the longitudinal acoustic vibration was considered unusual and was treated with concern as the suppression of this type of vibration is more difficult then the typically occurring transverse acoustic wave in the y (lift) direction, which is easily treated by placing acoustic baffles within the tube bank in the direction of flow (Eisinger 1980).

3.2 Comparison of Predicted and Measured Acoustic Frequencies and Mode/Response Shapes. The air heater tube bank, including its untubed cavities, was modeled by finite elements using the effective speed of sound approach described by Parker (1978) and Blevins (1986). A two dimensional model representing the plan view of the air heater (with a dimension equal to unity in the vertical (z) direction) was constructed. The temperature gradient, both tube banks, and untubed cavities were included in this model. Acoustic natural frequencies and mode shapes were determined. The results are given in Table 2. The measured frequencies are also given in this table for comparison. The measured frequencies of 20 Hz, 41 Hz, 52 Hz, 68 Hz and 75 Hz compare well with those predicted. The measured response at 75 Hz (Fig. 2c) compares well with the predicted mode shape at 73.4 Hz with ijk = 3, 1, 0 in the longitudinal direction. The transverse component however appears distorted. The measured response at 68 Hz resembles to some degree the predicted one at 67.7 Hz, showing a not fully developed and somewhat distorted standing wave with ijk = 2, 2, 0.
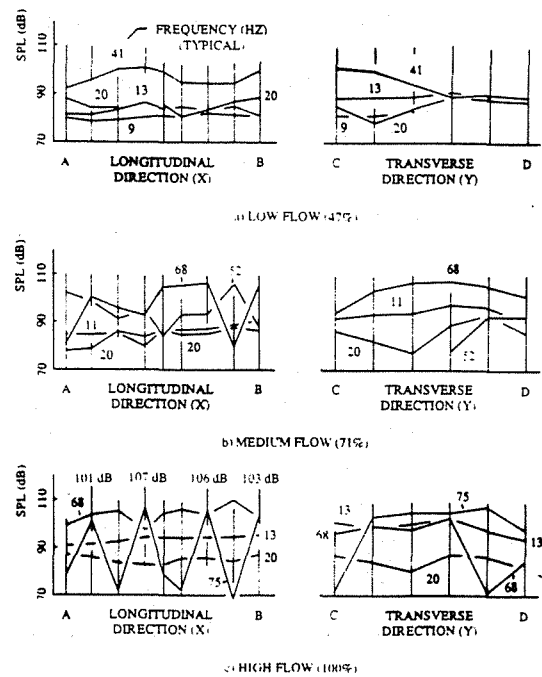
Fig. 2 Sound pressure levels at 3 air flow conditions measured around air heater at 1m distance from casing. (Measured at elevation just above tube support plate)

Table 2: Comparison Of Predicted and Measured Frequencies and Mode Shapes Within Air Heater Tube Banks

Predicted Frequency (Hz)	20.0	24.9	33.0	40.0	49.6	52.5	55.3	60.6	67.7	73.4	80.0
Predicted Mode i, j, k (Approximated)	1, 0, 0	0, 1, 0	1, 1, 0	2, 0, 0			1, 2, 0	3, 0, 0	2, 2, 0	3, 1, 0	0, 3, 0
Measured Frequency (Hz)	20			41		52			68	75	

3.3 Prediction of Intense Acoustic Vibration. At present there are no criteria for the prediction of flow-induced acoustic vibration in other than the j-modes. Nevertheless, we applied four of the existing criteria for in-line tube arrays to the 75 Hz vibratory condition, using the criteria of Chen and Young (1974), Ziada et al (1988), Fitzpatrick (1986), and Blevins (1990). The results are given in Table 3 and as can be seen, are mixed. Only the Blevins criterion, which is based purely on tube layout without consideration of flow conditions, predicts the acoustic vibration in both banks. The Chen and Young criterion predicts vibration only in one of the banks. The Ziada et al and the Fitzpatick criteria would not predict this acoustic vibration at all. More complete criteria for the onset of acoustic vibration clearly need to be developed.

Table 3: Prediction of Acoustic Vibration In Air Heater Tube Banks at Full Load (at Frequency of 75 Hz - Fig. 2c)

Strong Acoustic Vibration Predicted	Chen and Young (1974)	Ziada et al (1988)	Fitzpatrick (1986)	Blevins (1990)
Yes	Bank 2			Banks 1, 2 at 130 dB
No	Bank 1	Banks 1, 2	Banks 1, 2	

4.0 TRANSVERSE ACOUSTIC VIBRATION ALONG TUBE AXES IN STEAM GENERATOR ECONOMIZER BANKS

4.1 Experimental Results. The economizer tube banks are located at the bottom of a large steam generator with the tubes oriented from side-to-side of the unit. Bank 1 is located in the front, and bank 2 in the rear pass. Figure 3 shows the arrangement. There is one acoustic baffle located within each tube bank extending over the entire length of the banks from top to bottom. The economizer tubes are exposed to vertically oriented crossflow of hot gases leaving the steam generator heat recovery area tube banks. The tube banks above the economizer are perpendicular to the economizer tubes. There is an untubed cavity above the economizer banks with the lowest bank located 3200 mm above the economizer. An untubed discharge duct is located below. The tube layout is in-line with a constant side spacing and an alternating, narrow and wider longitudinal spacing. A division wall separates pass 1 from pass 2, making the flows through these passes relatively independent but regulated by dampers located 1575 mm below the banks.
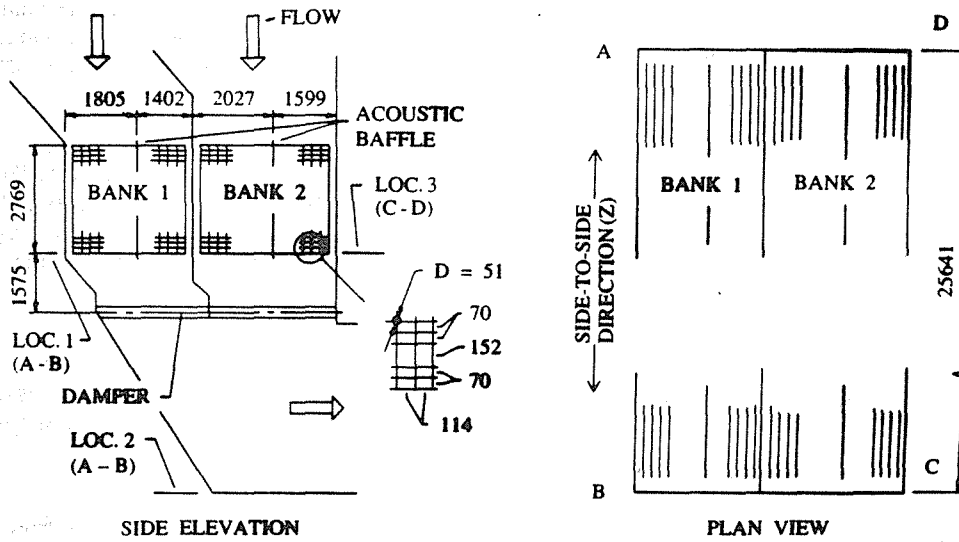
Fig. 3 Arrangement of economizer tube banks in lower portion of steam generator

The economizer tube banks developed strong acoustic vibration when exposed to full load gas flow. The parameters of the gas flow at the vibratory condition are given in Table 4. These were based on boiler performance calculations correlated with experimentally determined operating parameters.

Table 4: Economizer Tube Bank Geometry and Flow Parameters At Full Load

Bank No.	Tube O.D.	Side Spacing	Longit. Spacing	$H_e \times 10^6$ In/Out	R_e In/Out
	mm	mm	mm	—	—
1	51	114	70 152	4,530 - 6,540/ 4,170 - 6,030	9,198/ 10,302
2	51	114	70 152	6,410 - 9,260/ 6,080 - 8,790	14,669 15,798

During the noisy condition of the acoustic vibration, sound measurements were taken using the sound meter and vibration analyzer described in the preceding section. A complete sound survey was performed at several elevations all around the steam generator. There was no evidence of acoustic standing waves in any of the steam generators upper banks. The strong vibratory condition was confined to the economizer area giving the highest readings. Fig. 4 gives the results of the sound measurements taken at a 1 m distance from the boiler casing at locations 1 and 2 at the front, and at location 3 at the rear of the unit, in the side-to-side direction. The dominant frequency of the acoustic vibration was *42 Hz*. At location 1 a relatively mild wave developed (Fig. 4a), indicating that bank 1 was not experiencing
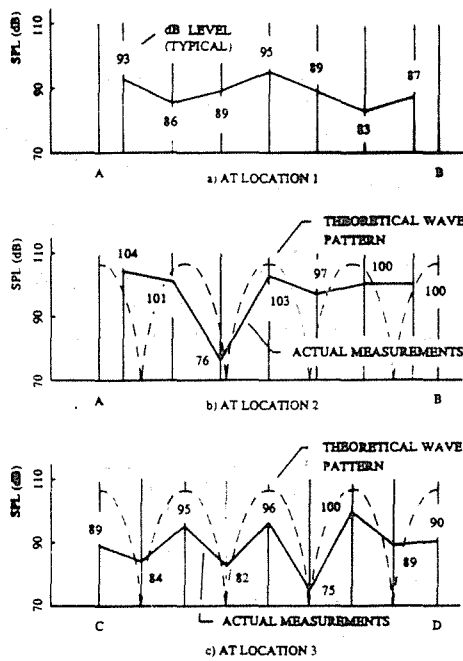
Fig. 4 Sound pressure levels at full load gas flow measured at 1m distance from economizer casing at 3 locations in side-to-side direction. All readings at dominant frequency of 42 Hz.

an intense noise condition at the 42 Hz frequency. The measurements at location 3 at the rear of the unit revealed a well developed 4th mode standing wave extending in the side-to-side direction, thus a *standing wave established along the tube axes (z)*, i = 0, j = 0, k = 4. The measured maximum sound pressure level (SPL) at the 42 Hz frequency was 99.7 dB. This corresponds to a SPL higher by about 20 - 25 dB on the inside, considering the sound transmission losses through the casing and insulation. At location 2 at the discharge duct, the measured sound levels were somewhat higher, with a maximum of 104.3 dB (Fig. 4b). The plot at this location is indicative of a wave similar to that at location 3 with a distortion. The relative difference between the strength of the waves at locations 3 and 2 can perhaps be partially attributed to the presence of tube supports, a total of four, located at about the points of the maximum acoustic velocity in the 4th mode standing wave. Although the area at these supports was 35% - 40% open, some effect on the acoustic amplitude could be expected.

The results show that the intense acoustic vibration developed primarily in bank 2 in the rear pass. The onset of this vibration was sudden, caused by slightly reducing the gas flow in pass 2 (and correspondingly increasing the flow in pass 1). By reversing this procedure, the vibratory condition could be abruptly stopped.

Acoustic vibration of this unusual type is again of concern to heat exchanger designers not only because it is difficult to predict but also because it is more difficult to suppress when it occurs.

4.2 Comparison of Predicted and Measured Parameters. Due to the presence of acoustic baffles which were designed to eliminate the typical j-mode acoustic vibration, no such vibration occurred. The gas columns within the tube banks extended 25.64 m from side-to-side along the tubes. Table 5 gives the predicted acoustic frequencies, modes 1 through 4 and the measured fourth mode (ijk = 0, 0, 4) frequency at 42 Hz. The comparison between the predicted and measured values is very good.

Table 5: Comparison Of Predicted and Measured Frequencies and Mode Shapes Within Economizer Tube Banks.

Predicted Freq. (Hz)	Bank 1	10.7	21.4	32.0	42.7
	Bank 2	10.3	20.6	30.9	41.3
Predicted Mode i, j, k (Approximated)		0, 0, 1	0, 0, 2	0, 0, 3	0, 0, 4
Measured Freq. (Hz)					42

4.3 Prediction of Strong Acoustic Vibration. As in the previous case of the air heater, we tested the existing prediction criteria for the development of intense acoustic vibration. Table 6 gives a summary of the results. It can be seen that Chen's and Young's, Ziada's et al, and Blevins' criteria would predict acoustic vibration in both banks. Fitzpatrick's criterion would not predict it in any of the banks. It should be mentioned that the positive prediction is primarily due to the presence of the larger longitudinal tube spacing. It is due to this spacing that the Blevins' criterion would predict a very strong vibration of up to 172 dB. This magnitude did not materialize. This case also points to the need for improved prediction methodology.

Table 6: Prediction of Acoustic Vibration In Economizer Tube Banks at Full Load (at Frequency of 42 Hz - Fig. 4c)

Strong Acoustic Vibration Predicted	Chen and Young (1974)	Ziada et al (1988)	Fitzpatrick (1986)	Blevins (1990)
Yes	Banks 1, 2	Banks 1, 2		Banks 1, 2 at 130-172 dB
No			Banks 1, 2	

5.0 MEANS OF ELIMINATING THE UNUSUAL ACOUSTIC VIBRATION

5.1 Suppression of i-Mode Acoustic Vibration. This mode of vibration is relatively difficult to suppress. We mention two types of structural modifications which might help.

(1) Increase acoustic damping, preferably by modifying the duct casing.

(2) Use overlapping single- or double-segmental baffles inserted inside the tube bank. A tortuous path of a single stream or a two stream flow, respectively, will be created and the acoustic frequencies increased. The negative effect is an increased pressure drop across the tube bank.

5.2 Suppression of k-Mode Acoustic Vibration. This acoustic mode is easier to suppress. Acoustic barriers in planes perpendicular to the tubes, parallel with the flow can be inserted to form porous baffles with as low an open area as possible. The number and location of these barriers depends on the mode(s) which need to be suppressed.

6.0 DISCUSSION OF RESULTS AND WORKING THEORY

The excitation mechanism for the unusual acoustic vibration which was experienced in full size heat exchangers is not fully understood at this time. If one postulated a vortex - excited system, one would find that at the vibration experienced, the maximum vortex shedding frequency was 30% below the 75 Hz vibration in the air heater, and a minimum of 47% above the 42 Hz frequency in the vibrating economizer bank using Fitzhugh's (1973) Strouhal numbers. These have been well correlated with experiments (Blevins and Bressler, 1987). Thus it appears that this vibration was not caused by the classical vortex shedding phenomenon. This may also be reflected to some degree in the existing acoustic vibration prediction criteria, the application of which gave mixed results.

Further, still within the vortex shedding theory, a shift of vortex shedding frequency in the tube bank by an acoustic field could occur. According to Blevins' study (Blevins 1985) on a single cylinder, an 8% shift required a 150 dB sound field. We would have needed a much greater shift and thus an even stronger sound field before the onset of the vibration. There was no evidence of this in the test data.

The prediction of acoustic frequencies and mode shapes was good considering the complexity of the arrangement of the heat exchangers. The theoretical mode shapes formed a good basis for the interpretation of the experimental data.

In cases like this one would explore all other possible sources which could be responsible for the onset of the acoustic conditions. We were not able to exclude the influence of many of the possible external sources, such as the effects of bends in the ducting, tube flexibility, and in the case of the economizer banks, the effect of the distant upper steam generator tube banks. It is conceivable that these effects may have played some role, both in contributing to the level of turbulence, and, perhaps in providing the stimulus for initiation of the acoustic vibration.

Considering all the available evidence, it would appear that the vibration experienced falls in the category of the coupling phenomena demonstrated to exist in enclosures with turbulent flow. Based on this theory, the underlying cause of this vibration would be the presence of turbulence in conjunction with vortex shedding -- a condition always present inside a tube bank. The superimposed acoustic waves of many different frequencies and amplitudes, also always present, would interact and couple with the turbulent flow field and at proper conditions initiate the acoustic vibration. Within this context, it appears, the mechanism which caused the unusual vibration in the tube banks was one of a *fluid-acoustic instability*.

7.0 SUMMARY AND CONCLUSIONS

Unusual acoustic vibration in heat exchanger tube banks which developed in full size operating units were described and evaluated using presently available methodology. The vibration did not meet the test of being excited by the traditional vortex shedding, or vortex shedding modified by an acoustical field. A *fluid-acoustic (coupling) mechanism* is put forward as the probable cause of the intense acoustic vibration experienced. Further studies of this theory are clearly needed.

ACKNOWLEDGEMENT

REFERENCES

Baird, R. C., Pulsation - Induced Vibration in Utility Steam Generation Units, Combustion, April 1954, 38-44.
Blevins, R. D., The Effect of Sound on Vortex Shedding From Cylinders, Journal of Fluid Mechanics, 161, 217-237, 1985.

Blevins, R. D., Acoustic Modes of Heat Exchanger Tube Bundles, Journal of Sound and Vibration, 109 (1), 19-31, 1986.

Blevins, R. D., and Bressler, M. M., Acoustic Resonance in the Heat Exchanger Tube Bundles - Part I: Physical Nature of the Phenomenon, Journal of Pressure Vessel Technology, Transactions of the ASME, Vol. 109, 275-281, 1987.

Blevins, R. D., and Bressler, M. M., Acoustic Resonance in the Heat Exchanger Tube Bundles - Part II: Prediction and Suppression of Resonance, Journal of Pressure Vessel Technology, Transactions of the ASME, Vol. 109, 282-299, 1987.

Blevins, R. D., Flow-Induced Vibration, Second Edition, Van Nostrand Reinhold Co., New York, 1990., 370-375.

Chen, Y. N., Flow Induced Vibration and Noise in Tube Bank Heat Exchangers Due to von Karman Streets, Journal of Engineering for Industry, Transactions of the ASME, February, 143-246, 1968.

Chen, Y. N., and Young, W. C., The Orbital Movement and the Damping of the Fluidelastic Vibration of Tube Banks Due to Vortex Formation, Part 3 - Damping Capability of Tube Bank Against Vortex - Excited Sonic Vibration in the Fluid Column, Journal of Engineering for Industry, Transactions of the ASME, 1072-1075, August, 1974.

Culick, F. E. C., Acoustic Oscillations in Solid Propellant Rocket Chambers, Austronautica Acta 12,2, 114-126, 1966.

Culick, F. E. C., Stability of Longitudinal Oscillations with Pressure and Velocity Coupling in a Solid Propellant Rocket, Combustion Science and Technology, Vol. 2, 179-201, 1970.

Culick, F. E. C., and Magiawala, K. R., Measurements of Energy Exchange Between Acoustic Fields and Non-Uniform Steady Flow Fields, Journal of Sound and Vibration, 75(4) 503-517, 1981.

Eisinger, F. L., Prevention and Cure of Flow-Induced Vibration Problems in Tubular Heat Exchangers, Journal of Pressure Vessel Technology, Transactions of the ASME, Vol. 102, 138-145, 1980.

Fitzhugh, J. S., Flow Induced Vibration in Heat Exchangers, Proceedings of UKAEA/NPL International Symposium on Vibration Problems in Industry, Keswick, April 1973, paper 427.

Fitzpatrick, J. A., and Donaldson, I. S., A Preliminary Study of Flow and Acoustic Phenomena in Tube Banks, Journal of Fluids Engineering, Transactions of the ASME, 681-686, December 1977.

Fitzpatrick, J. A., The prediction of Flow Induced Noise in Heat Exchanger Tube Arrays, Journal of Sound and Vibration, 99(3), 425-235, 1985.

Fitzpatrick, J. A., A Design Guide Proposal for Avoidance of Acoustic Resonance in In-Line Heat Exchangers, Journal of Vibration, Acoustics, Stress and Reliability in Design, Transactions of the ASME, Vol. 108, 296-300, 1986.

Funakawa, M., and Umakoshi, R., The Acoustic Resonance in a Tube Bank, Bulletin of the Japan Society of Mechanical Engineers, Vol. 13, No. 57, 348-355, 1970.

Grotz, B. J., and Arnold, F. R., Flow Induced Vibration in Heat Exchangers, Technical Report No. 31 Mech. Engineering Department, Stanford University, 1956.

Ma, Y., Van Moorhem, W. K., and Shorthill, R. W., An Innovative Method of Investigating the Role of Turbulence in the Velocity Coupling Phenomenon, Journal of Vibration and Acoustics, Transactions of the ASME, Vol. 112, 550-555, 1990.

Oengoren, A., and Ziada, S., Vorticity Shedding and Acoustic Resonance in an In-Line Tube Bundle, Part II - Acoustic Resonance, PVP - Vol. 206. Flow-Induced Vibration and Wear, The American Society of Mechanical Engineers, 135-145, 1991.

Owen, P. R., Buffeting Excitation of Boiler Tube Vibration, Journal of Mechanical Engineering Science, Vol. 7, No. 4, 431-439, 1973.

Parker, R., Acoustic Resonances in Passages Containing Banks of Heat Exchanger Tubes, Journal of Sound and Vibration, 57, (2), 245-260, 1978.

Parker, R., and Stoneman, S. A. T., The Excitation and Consequences of Acoustic Resonances in Enclosed Fluid Flow Around Solid Bodies, Proceedings, Institution of Mechanical Engineers, Vol. 203, C18187, 9-19, 1989.

Price, E. W., and Dehority, G. L., Velocity Coupled Axial Mode Combustion Instability in Solid Propellant Rocket Motors, Second ICRPG/AIAA Solid Propulsion Meeting, Anaheim, California, June, 1967.

Price, E. W., Velocity Coupling in Oscillatory Combustion of Solid Propellants, AIAA Journal, Vol. 17, 799-800, 1979.

Putnam, A. A., Flow Induced Noise in Heat Exchangers, Journal of Engineering for Power, Transactions of the ASME, Vol. 81, 417-422, 1959.

Rae, G. J., and Murray, B. G., Flow Induced Acoustic Resonances in Heat Exchangers, Proceedings International Conference on Flow Induced Vibrations Bowness-on-Windemere, Sponsored by BHRA, England, Paper E3, 221-231, 1987.

Ziada, S., Oengoren, A., and Buhlmann, E. T., On Acoustical Resonance in Tube Arrays, Part I - Experiments, International Symposium on Flow Induced Vibration and Noise, Vol. 3, Winter Annual Meeting, Chicago, Illinois, The American Society of Mechanical Engineers, 219-243, 1988.

Ziada, S., Oengoren, A., and Buhlmann, E. T., On Acoustical Resonance in Tube Arrays, Part II - Damping Criteria, International Symposium on Vibration and Noise, Vol. 3, Winter Annual Meeting, Chicago, Illinois, The American Society of Mechanical Engineers, 245-254, 1988.

Ziada, S., and Oengoren, A., Vorticity Shedding and Acoustic Resonance in and In-Line Tube Bundle. Part I: Vorticity Shedding, Proceedings of the Institution of Mechanical Engineers, Flow Induced Vibrations, 497-509, I Mech E, May 1991.

284

ACOUSTIC CHARACTERISTICS OF A FLANGED CIRCULAR PIPE USING THE FINITE ELEMENT APPROACH

Tsutomu Hiramatsu

Yoichi Ikeda

Department of Mechanical Engineering

Daido Institute of Technology

2-21,Daido-cho,Minami-ku

Nagoya,457,Japan

ABSTRACT

One numerical method in this study is a semi-analytical method. The interior domain of the pipe has many triangular elements from which may be obtained the propagation characteristics of the sound in the duct. The second domain is the semi-infinite field. The analytical modeling formulation such the pressure is given as Green's function in an axi-symmetrical field is used. These domains are combined with each other on an assumed boundary at the end of the flange. The other numerical method is applied for the exterior domain. That is, in the near-field of the outlet the isoparametric square finite elements are used, and for the far-field the hybrid-type infinite elements are used. To demonstrate these calculating methods, the exponential horn, conical horn, catenoidal horn and musical horn are used as the calculation models. This study shows that the hybrid techniques using combined finite and infinite elements are useful in predicting the sound pressure levels of the relatively near-field of the horn. The method of analytical modeling formulation is also useful in predicting the sound levels of the far-field and the direction patterns of these horns.

1. INTRODUCTION

A vast capability of up-to-date methodology and computer programs to deal with a very complex structure of noise source using the finite element approaches has been established [1-3]. In spite of the vast utility, the finite element methods are not easily accomplished a task for acoustic problems analyzing regions tending to infinity. In

order to overcome this draw-back, the finite elements are utilized for finite domain and the boundary elements are applied to infinite domain. This method gives accurate solution,, but results in an increased band width of system matrix [4]. Also, because of the interaction between all the nodes on the coupling boundary, computation time been required for the numerical integration is so much, then the advantage of this method will be often lost.

In this study, the first method for calculating to the pressure field in an infinite acoustic medium is the analytical modeling formulation obtained from the equation that governs the infinite domain and it is combined with the interior finite domain in which propagation characteristics has been obtained from the finite element approach [5-8]. The second method is the following procedure which is applied for the exterior domain of the pipe-outlet. That is, in the near-field of the outlet the isoparametric square finite elements with 20 nodes are used, and for the far-field the hybrid-type infinite elements are provided. These two domains combined with each other on an assumed boundary between the near-field and the far-field respectively. The above-mentioned methods applicable to acoustic radiation from circular pipes fitted with various typed flanges is presented.

2. BRIEF REVIEW OF THE APPROACH

Figure 1 shows the axi-sectional view of the pipe fitted with various typed flanges used in this study. The analyzed domain using finite element method of the near-field around the flanges is the area of 6 m x 6 m shown in Fig.1. Figure 2 shows the computational mesh systems for the finite domain of a conical flange. As shown in Fig.2, axi-sectional view, the interior region of the pipe contains acoustic sources sited on the left-side nodes of the finite element, and it is divided into 28 finite triangular elements for the axi-sectional plane. The domain between the open end of the horn and the assumed boundary is divided into 15 square elements, and the 16 hybrid-type elements are combined with these square elements on the interface boundary.[8] Figure 2 (b) shows the quarter cross-sectional view of the assumed boundary and mesh pattern of radiating sound. Each finite element is composed of a cubic iso-parametric element having 20 nodes, and each infinite element has 8 nodes.

Following discretized equation is obtained for numerical implementation into computer-usable form using finite element techniques.

$$
\begin{bmatrix} [F_{DD}] & [F_{DI}] & [F_{DB}] \\ [F_{ID}] & [F_{II}] & [F_{IB}] \\ [F_{BD}] & [F_{BI}] & [F_{BB}] \end{bmatrix} \begin{Bmatrix} P_D \\ P_I \\ P_B \end{Bmatrix} = \begin{Bmatrix} v_D \\ 0 \\ v_B \end{Bmatrix} \tag{1}
$$

hereupon,

$[F_{ij}] = [F_{ji}]$: the divided matrices of following equation

$$
F = [\frac{j}{\rho\omega} S - \frac{j\omega}{\rho c^2} M] \tag{2}
$$

where,

S : inertance matrix,   M : elastance matrix.

Subscripts;
  D: refers to driving force
  I: refers to the modes inside a finite domain
  B: the nodes on the interface boundary

P_i (i=D,I,B): pressure vectors
v_i (i=D,B): volume velocity vectors

$$v_D = j\omega u_D W \tag{3}$$

u_D: driving displacement, ω: angular frequency

W: distribution vector of driving displacement

On the other hand, relation between velocity and pressure on the interface boundary is as follows;

$$v_B = [S_{BB}]P_B \tag{4}$$

S_{BB}: radiation admittance on the boundary surface

As shown in Fig.3, the velocity potential in duct be given by the equation,

$$\Phi_{int}(r,z) = \sum_{m=1}^{\infty} (A_m e^{-jk_m z} + R_m e^{-jk_m z})W_m(r) \tag{5}$$

where,
      r: radius of duct

$$k_m^2 = k^2 - (\gamma_m/a)^2 \tag{6}$$

   k_m : wave number of m-th order in duct

   z :coordinate of axial direction

$$W_m(r) = \frac{J_0 (\gamma_m/a)r}{\sqrt{\pi}a J_0 (\gamma_m)} \tag{7}$$

In Eq.(5), the first term represents m-th Bessel traveling wave along the duct in the direction of increasing z towards the open end, and the second term represents the reflected wave on the open boundary.

   $J_\nu(.)$: 'ν'th-order Bessel function,
   γ_m: positive solution of $J_1(\gamma_m)=0$,
   a: representative radius of open boundary

The exterior velocity potential is given as follows, using the Green's function in an axi-symmetrical field.

$$\Phi_{ext}(x) = \frac{1}{2\pi}\int_{S'} \frac{v_z(x')}{(x-x')} e^{-jk|x-x'|} dS' \tag{8}$$

The particle velocity on the S'-surface is obtained as,

$$v_z(x') = - \frac{\partial \Phi_{ext}(x')}{\partial z'} \tag{9}$$

Compatibility conditions for combination between the interior and exterior fields are,

$$\Phi_{int} = \Phi_{ext}, \qquad -\frac{\partial \Phi_{int}}{\partial z} = -\frac{\partial \Phi_{ext}}{\partial z} \qquad (10)$$

Then we obtain the following relations:

$$\{A\} + \{R\} = [E](\{A\} - \{R\})$$

$$\{A\} = \{A_1 A_2 \cdots A_M\}, \qquad \{R\} = \{R_1 R_2 \cdots R_M\} \qquad (11)$$

where,

[E] : stationary wave ratio.

Now, we introduce the following relation,

$$Z = [E - I]^{-1}[E + I] \qquad (12)$$

I : unit matrix, Q : displacement distribution on the open boundary.

Then, $$A = ZR \qquad (13)$$

$$v_B = jQK[A - R] \qquad (14)$$

$$R = 2\pi \ell_e \int_{-1}^{1} rq[w_1(r), w_2(r), \cdots, w_M(r)]d\zeta_2 \qquad (15)$$

where, $K = [k_i]$ $(i=1,2,\cdots,M)$

As shown in Fig.4, the outlet element, the interpolation function vector be written by ζ_i co-ordinates

$$Q = \{\zeta_1^2 - \zeta_1\zeta_2, \ 4\zeta_1\zeta_2, \ \zeta_2^2 - \zeta_1\zeta_2\}$$

Then, the radiation admittance on S'surface is thus derived,

$$S_{BB} = \frac{1}{\omega\rho} QK[Z - I][Z + I]^{-1}Q^T$$

The following discretized equation is consequently obtained,

$$\begin{bmatrix} [F_{DD}] & [F_{DI}] & [F_{DB}] \\ [F_{ID}] & [F_{II}] & [F_{IB}] \\ [F_{BD}] & [F_{BI}] & [F_{BB}-S_{BB}] \end{bmatrix} \begin{bmatrix} P_D \\ P_I \\ P_B \end{bmatrix} = \begin{bmatrix} v_D \\ 0 \\ 0 \end{bmatrix} \qquad (16)$$

Next, the directional characteristics of sound field for the semi-infinite domain is finally obtained as following relations using the foregoing A and R. The pressure in the far field is given by,

$$p(\mathbf{x}) = \frac{j\omega\rho}{2\pi|\mathbf{x}|} e^{-jkL} \pi a^2 \sum_{m=1}^{M} jk_m (A_m - R_m) \frac{1}{\sqrt{\pi} a J_0(\gamma_m)} \frac{2ka \cdot \sin\theta J_0(\gamma_m) J_1(ka \cdot \sin\theta)}{(ka \cdot \sin\theta)^2 - \gamma_m^2}$$

$$(17)$$

The normalized pressure is written as,

$$p_{norm} = |p_{norm}| e^{j\phi(\omega)} = \frac{p(L,\theta)}{p'} \qquad (18)$$

where,
$$p' = \frac{j\omega\rho}{2\pi L} e^{-jkL}\pi a^2 v, \qquad L = |\mathbf{x}| \tag{19}$$

$\pi a^2 v$: volume velocity.

3. COMPUTATIONAL RESULTS

Figure 5 shows the sound pressure distribution at near-field of the outlet of the pipe with conical horn, which is calculated by using the hybrid-type finite and infinite element methods as shown at top the foregoing section. Figure 5 (a) shows the bird'eye view or three dimensional plot at 100 Hz, and also Fig. 5 (b) shows the equi-pressure contour plots of the same one.

In Fig.5 (b), each contour line separates with only 2 dB, so the fine structure of the near-field is obtained. Figures 6 (a),(b),(c),(d) and (e) show the calculated frequency characteristics of the normalized driving impedances of the straight pipe, conical, exponential, catenoidal (musical) horns respectively using Eq(16). In these figures, R and X denote the admittance and reactance respectively. In Fig.6(a), the resonance frequencies appeared explicitly, but in the other Figures 6(b)-(e), these frequencies are not so clearly.

Figure 7 shows the calculated frequency characteristic of the far field sound pressure ratio of each horn, which is obtained by calculating of Eq.(18); the rato: the analytical modeling formulation /the equivalent point source method. From this Figure, the normalized pressure levels, that is, each pressure level obtained from the exact calculating formula Eq.(17) is in excess of nearly 10 dB from the result from the equivalent point source approximation.

Figure 8 shows the calculated beam patterns in the far-field using Eq.(17) for the flanged pipes, whose frequencies are from 0.1 to 0.5 kHz. Figure 8 (a) for the straight pipe is almost half-circle, and from (b) to (d), conical, exponential and catenoidal horns respectively, are well similar with each other. Figure 8 (e), parabolic horn (musical horn) shows complicated pattern for each frequency.

4. CONCLUSIONS

In this paper, two different finite element techniques are applied in order to approach the noise field of flanged pipes. From these studies, we understand it can be seen that the hybrid techniques using the combined finite and infinite element is a useful method of prediction for the near-field sound pressure levels around the pipe outlet and the method of combination between FEM and analytical modeling formula is also useful for prediction of the far-field sound pressure levels and the beam patterns for the flanged pipes.

REFERENCES

(1) J.T.Hunt, M.R.Knittel and D.Barach: Finite element approach to acoustic radiation from elastic structures, J.Acoust.Soc.Am., 55,pp.269-280(1974).

(2) A.Craggs: An acoustic finite element approach for studying boundary flexibility and sound transmission between irregular enclosures, J.Sound and Vib.,30,3,pp.343-357(1973).

(3) P.P.Silvester, D.A.Lowther, C.J.Carpenter and E.A.Wyatt: Exterior finite elements for 2-dimensional field problems with open boundaries, Proc.IEEE, 124,12,pp.1267-1270(1977).

(4) W.L.Meyer, B.A.Bell, B.T.Zinn and M.P.Stallybrass: Boundary integral solution of three dimensional acoustic radiation problems, J.Sound and Vib.,59,2,pp.245-262(1978).

(5) Y.Kagawa, T.Yamabuchi and A.Mori: Finite element simulation of an axi-symmetric acoustic transmission system with a sound absorbing wall, J.Sound and Vib.,53,3,pp.357-374(1977).

(6) G.Jeng and A.Wexler: Iso-parametric finite element, variational solution of integral equations for three-dimensional fields, Int. J. Num. Mech. Engg, 11,pp.1455-1471(1977).

(7) K.Moriya: Two-node hybrid infinite element for the analysis of steady-state wave problems, Theoretical and Applied Mechanics, Proc.of 31th Japan National Congress for Applied Mechanics,31,pp.49-61(1981).

(8) T.Hiramatsu, Y.Komura, M.Shintani and H.Genno: Prediction of acoustic field perturbed by a cylindrical tank using finite element approach, J. Acoust. Soc. Jpn. (E), 11,pp.11-18(1990).
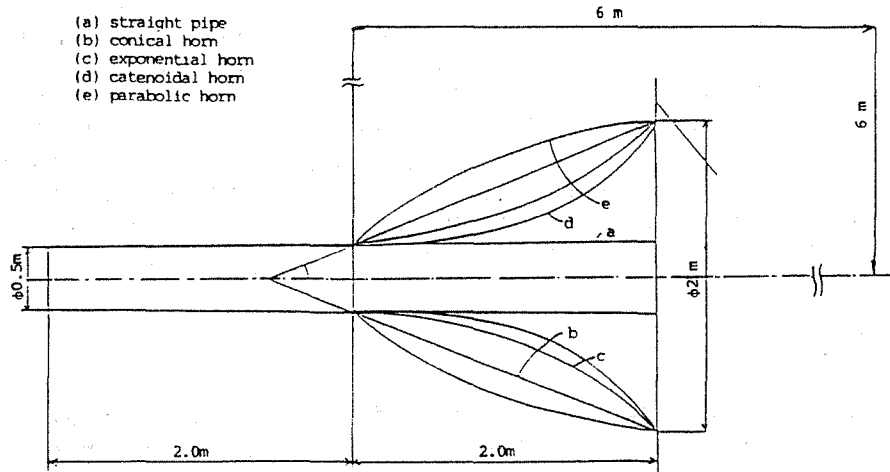
Fig.1 Axi-sectionl view of the pipes with various typed flanges and thier analyzed domain

(a) axi-sectional view

(b) cross-sectional view

Fig.2 Computationl mesh system by FEM

semi-infinite field

internal field

S'surface

external field
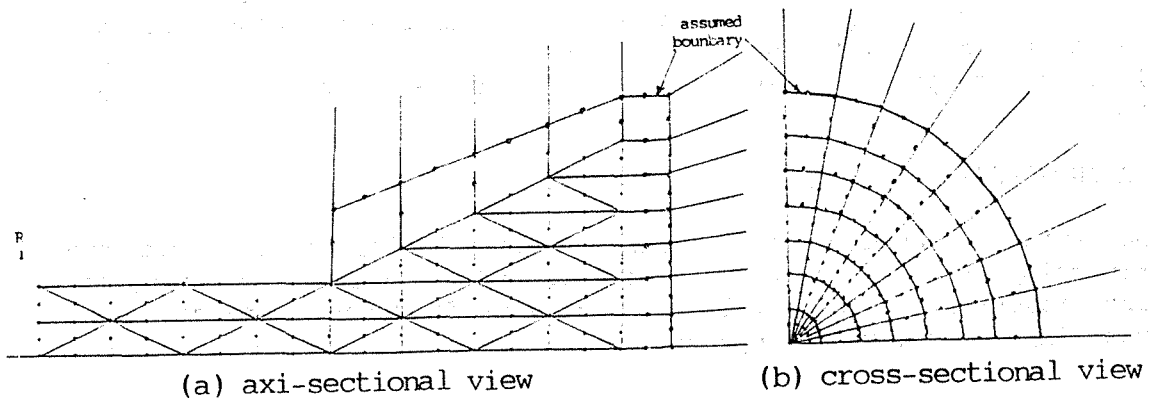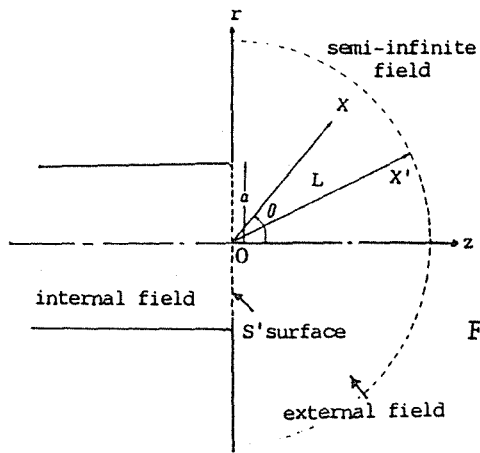
Fig.3 Connection system at outlet
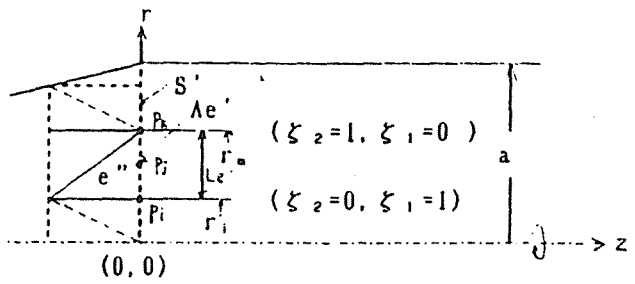
Fig.4 Outlet elements and local coodinate

$(\zeta_2=1, \zeta_1=0)$

$(\zeta_2=0, \zeta_1=1)$

(0,0)

(a) Equi-pressure contour plots

(b) Three dimensional plot

Fig.5 Sound pressure distribution at near-field

(a) straight pipe

(a) straight pipe

(b) conical horn

Fig.6 Frequency characteristics of the driving impedance (i)

(b) conical horn

Fig.8 Beam patterns in the far-field (i)

291
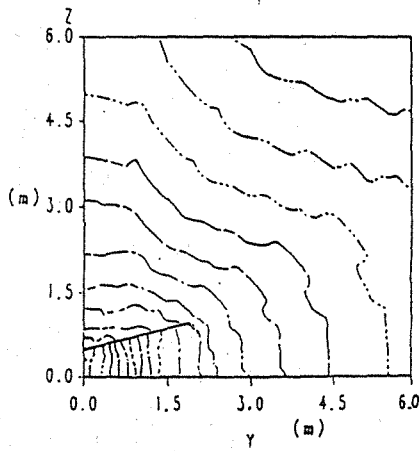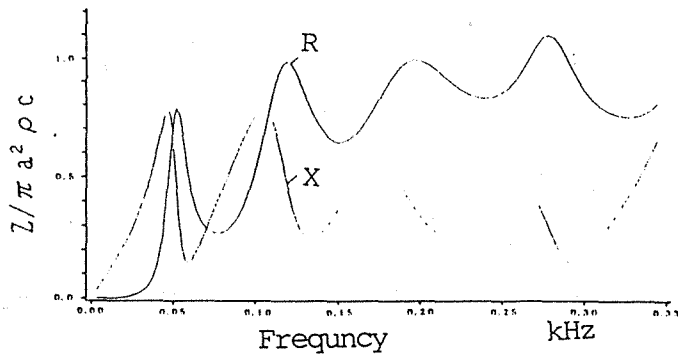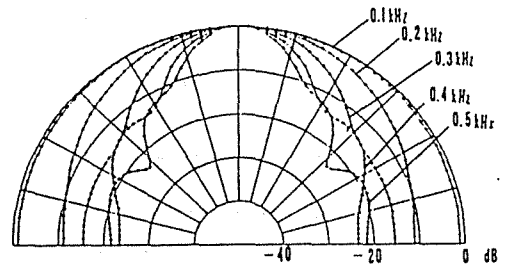
(c) exponential horn

(c) exponential horn
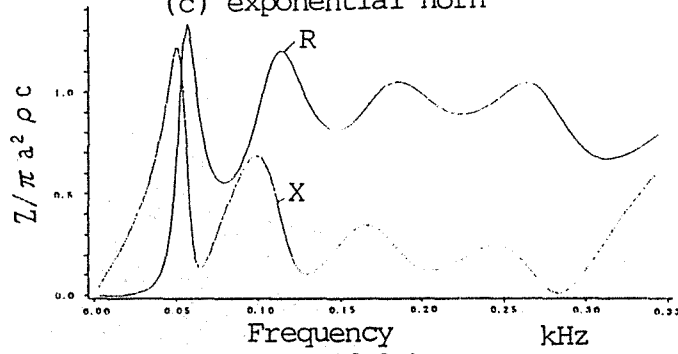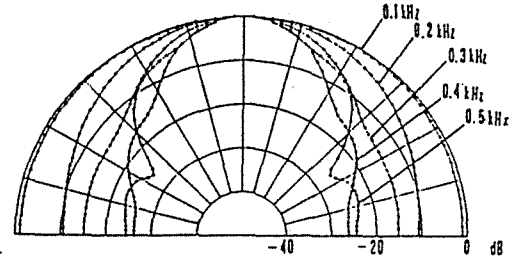
(d) catenoidal horn

(d) catenoidal horn
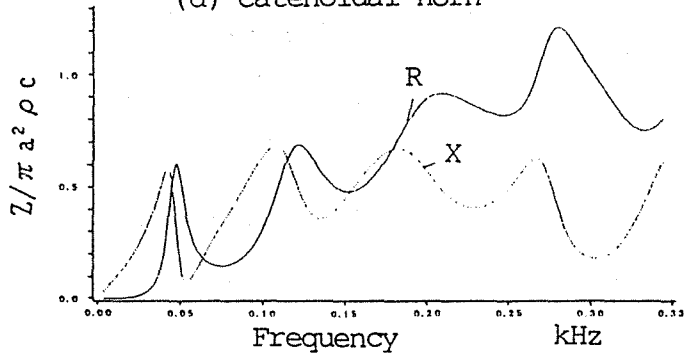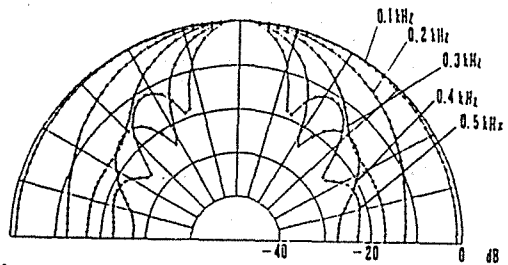
(e) parabolic horn

(e) parabolic horn

Fig.6 Frequency characteristics of
the driving impedance (ii)

Fig.8 Beam patterns in
the far-field (ii)

a:straight pipe
b:conical horn
c:exponential horn
d:catenoidal horn
e:parabolic horn
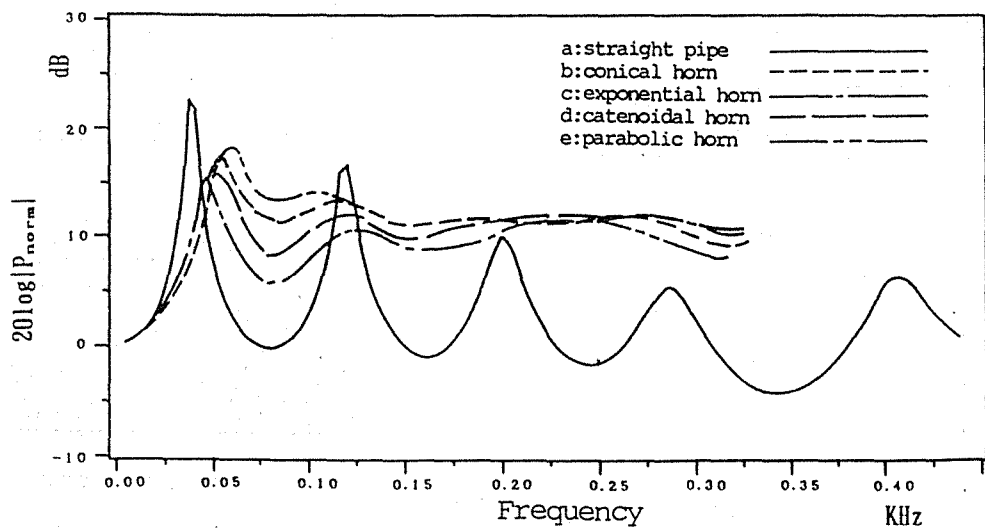
Fig.7. Sound pressure ratio of each horn calculated using Eq.(18)
(analytical modeling formulation/equivalent point source method)

AN EMPIRICAL PREDICTIVE MODEL FOR CALCULATING THE BREAK-OUT TRANSMISSION LOSS OF CIRCULAR AND FLAT-OVAL SHEET STEEL DUCTS

Bruce Manser
Member of the Institution of Engineers Australia
Member of the Australian Acoustical Society (Queensland Division)

ABSTRACT

An estimation procedure for calculating the break-out transmission loss of flat sided steel ductwork was originally developed by Cummings (1985) and this procedure forms the basis of the current ASHRAE (1987) recommended procedure. However, no such procedure exists for circular ducts, pending further theoretical and experimental investigation of the mechanisms which affect the break-out behaviour.

In this paper it is shown that the break-out TL results presented by ASHRAE (1987) and Cummings (1985) for specific circular duct sizes can be normalised in such a way as to produce a fair approximation to the overall narrow band behaviour for a wider range of duct sizes, and on an octave-band basis the predictions are more than adequate for normal acoustic design purposes.

The ASHRAE (1987) predictive method for rectangular ducts and that developed here for circular ducts can be combined to yield predictions for flat-oval ducts at all frequencies of interest. The predictions compare favourably with the limited data reported in ASHRAE (1987).

293

1.0   INTRODUCTION

While predictive schemes offering a fair degree of reliability exist for calculating attenuation due to noise propagation internally along ductwork, methods for predicting noise break-out from ducts are far less reliable. To some extent, the problem lies in the representation of the manner of noise transfer from within the duct to the surrounding void (usually a ceiling space for most critical situations) and then into an occupied space. Frequently, noise break-out is at its worst immediately outside plantrooms where sound attenuators have not been fitted to the ductwork and light-weight ceilings have been employed. The high noise levels internal to the duct cause the duct walls to radiate into the ceiling space, and because of the low insertion loss of light-weight ceilings the resultant noise levels in the occupied room below the ceiling may be excessive. Most problems tend to be at low frequency, typically at 125 Hz when rectangular ductwork is used. Break-out from circular ducts at low frequency is usually less severe than for rectangular ductwork.

Figure 1 illustrates typical comparative performances for a square and round duct of similar dimensions. Clearly, these different characteristics can be used to greatest advantage if the various performances can be predicted with satisfactory accuracy. Cummings (1985) and ASHRAE (1987) present reliable schemes for predicting the break-out transmission loss of rectangular ductwork, but methods for determining the break-out transmission loss of circular ducts are very limited, with apparently wide variations being observed in measured performances of ducts varying only slightly in diameter or wall thickness.

In this paper, a generalized scheme is presented which permits a reasonable engineering estimate to be made for the break-out transmission loss of circular steel ducts. By combining this with the ASHRAE (1987) method for rectangular ducts, a procedure is described which can be used for predicting the break-out transmission loss of flat-oval steel ducts.

2.0   DEFINITIONS

2.1   DEFINITION OF BREAK-OUT TRANSMISSION LOSS

The definition adopted for all duct types is that used in ASHRAE (1987), namely:

$$TL_{out} = 10 \log_{10} \left(\frac{W_i}{A_i} \cdot \frac{A_0}{W_o} \right)$$

Expressed in more familiar notation, this equation becomes:

$$TL_{out} = PWL_i - PWL_o + 10 \log_{10} \left(\frac{A_o}{A_i} \right)$$

where W_i is the incident sound power within the duct.

W_o is the break-out power radiated from the duct walls.

PWL_i is $10 \log_{10} (W_i)$

PWL_o is $10 \log_{10} (W_o)$

A_i is the cross-sectional area of the duct.

A_o is the exposed surface area of duct walls (typically calculated as: duct perimeter x duct length)

It must be remembered that the value of TL_{out} to be used in the calculation of break-out power must have been determined so as to conform with the definition. Values of TL determined from room-to-room transmission loss tests are not directly useable without modification.

2.2   DEFINITION OF RING FREQUENCY

The ring frequency (f_r) corresponds to the frequency when one bending wavelength fits around the circumference of the duct. It can be calculated using the following equation:

$$f_r = C_L'/(\pi D) \approx 1709/D \text{ for steel duct sheeting}$$

where D = duct diameter (metres)

C_L' = longitudinal velocity of propagation in the duct wall (m/s)

$$= \left[\frac{E}{\rho(1 - v^2)} \right]^{0.5}$$

$\approx$ 5370 m/s for steel duct sheeting

E = Young's Modulus (N/m^2)

$\approx$ 206 x 10^9 N/m^2 for steel

ρ = density of duct wall material (kg/m^3)

$\approx$ 7850 kg/m^3 for steel duct sheeting

v = Poisson's ratio ($\approx$ 0.3)

2.3   DEFINITION OF CRITICAL OR COINCIDENCE FREQUENCY

The coincidence frequency (f_c) is that frequency for which the wavelength of the acoustic mode propagating through the air within the duct coincides with the bending wavelength of the duct wall sheeting. The coincidence frequency can be calculated using the following equation:

$$f_c = C^2/(1.8 t C_L') \approx 12.39/t \text{ for steel duct sheeting}$$

where C = speed of sound (m/s)

= 346 m/s for air at 25°C

t = duct wall thickness (metres)

C_L' = longitudinal velocity of propagation in the duct wall (m/s)

$\approx$ 5370 m/s for steel duct sheeting

2.4   DEFINITION OF CUT-OFF FREQUENCY FOR PLANE WAVE MODE PROPAGATION

The cut-off frequency is defined for the purposes of this paper, as the frequency at which 0.586 x wavelength for the sound propagating within the duct fits across the diameter of the duct. Above this frequency it is possible for non-plane wave propagation to occur such that higher order structural modes of the duct wall are readily excited by the higher order acoustic modes within the duct. Thus, the cut-off frequency can be expressed as:

$$f_{cut\text{-}off} = 0.586\,C/D \approx 203/D \text{ for air at } 25^{0}C$$

where   C   =   speed of sound (m/s)
        =   346 m/s for air at 25°C
    D   =   duct diameter (metres)

2.5   DEFINITION OF LIMITING FREQUENCIES FOR UPPER PLATEAU

The upper limiting frequency (f_u) is defined as the frequency at which one quarter of a wavelength for the sound propagating within the duct fits across the diameter of the duct. The lower limiting frequency (f_1) is equal to half the upper limiting frequency.

The relevant equations are:

$$f_u = 0.25 \ C/D$$
$$f_1 = 0.125 \ C/D$$

3.0   PREDICTION SCHEME FOR CIRCULAR STEEL DUCTS

3.1   DESCRIPTION OF CHARACTERISTIC ZONES

Figure 2 shows a typical break-out transmission loss representation for a circular duct. Various zones can be identified where it is possible to generalize the behaviour of the range of test results presented in ASHRAE (1987) and Cummings (1985) for steel ducts. Figure 3 shows the data from ASHRAE (1987) presented in a normalised format from which an approximate prediction scheme can be deduced.

The explanations given are specifically for steel ducts although the normalization process has included a correction for materials of different density. Great care should be taken in interpreting the trends noted for steel ducts where alternative materials are being considered. It is possible that low frequency trends attributed to positioning with respect to the upper plateau limiting frequencies may be related to other factors which are not directly identifiable from the test data on steel ducts alone. Also, significant changes in wave propagation speeds may occur for other materials where the ratio of density to Young's modulus is greatly different from that of steel.

The zones used for the purposes of developing a generalized prediction scheme are as follows:

Zone A - At a frequency corresponding to the ring frequency of the circular duct, the break-out TL reaches a minimum of about $22 + 20 \log_{10} (\rho/\rho_s)$ dB. The duct wall density is 'ρ' while 'ρ_s' is the reference density of steel. The frequency range where break-out TL is directly affected by the ring frequency is approximately equal to a one-half octave on either side of the ring frequency.

Zone B - This zone is characterized by a series of modal resonances excited by frequencies within the duct corresponding to higher order acoustic modes (i.e. above the plane wave mode). This zone extends from about half an octave below the ring frequency down to the cut-off frequency. It is possible to define a lower plateau level which represents the lower bound of the resonant troughs. The break-out TL (dB) corresponding to this lower plateau level can be expressed as $84 + 20 \log_{10} (t/D) + 20 \log_{10} (\rho/\rho_s)$ where 't' is the duct wall thickness and 'D' is the duct diameter, both in consistent units. The duct wall density is 'ρ' while 'ρ_s' is the reference density of steel.

Zone C - For frequencies below the cut-off frequency, the break-out TL increases from the lower plateau level toward a higher plateau level. The values characteristic of the higher plateau level are achieved once the frequency falls to the upper limiting frequency defined in Section 2.5.

Zone D - A fairly well defined plateau in the break-out TL characteristic exists over a frequency range from the upper limiting frequency (f_u) to half this frequency.

The break-out TL level (dB) of this upper plateau is typically $106 + 20 \log_{10} (t/D) + 20 \log_{10} (\rho/\rho_s)$ where 't' is the duct wall thickness and 'D' is the duct diameter, both in consistent units. The duct wall density is 'ρ' while 'ρ_s' is the reference density of steel. Ideal circular duct theory for plane wave mode propagation does not predict the presence of a plateau and it is suggested by Cummings (1985) that the behaviour is influenced by deviations from circularity. This makes noise radiation via "bending" type modes much easier than via a "breathing" type mode.

Zone E - At frequencies below about half the upper limiting frequency, the break-out TL tends to fall with reducing frequency from the characteristic TL plateau level.

The precise TL behaviour in Zone E is characterized by a number of structural mode resonances which are not well understood. Cummings (1985) has developed a theory based on mode - coupling behaviour which gives a fair description of observed data. This zone is normally at the lower end of the frequency range of interest so that some greater uncertainty in predicting behaviour within this zone is tolerable. Consequently, representing the break-out TL as falling at a rate of 6 dB per octave for frequencies below the lower limiting frequency (f_l) is adequate for estimation purposes.

Zone F - At very low frequencies, the break-out TL tends to increase back toward a value similar to the upper plateau level, as the frequency decreases. This zone normally includes frequencies below the region of interest.

Zone G - Above the ring frequency, the break-out TL can be expected to rise back toward the mass law type behaviour for rectangular ductwork, less about 5 dB. The rate of rise is typically 15 dB per octave. However, for thicker plates, the coincidence or critical frequency may

limit the performance at higher frequencies of interest. Well above the coincidence frequency, the break-out TL behaviour can be expected to approach that for rectangular ductwork less about 10 dB.

3.2 PREDICTION SCHEME

With reference to Figure 2, the prediction scheme is as follows:

(a) Calculate the ring frequency (f_r) as per Section 2.2 and assign a minimum TL of $22 + 20 \log_{10} (\rho/\rho_s)$ dB at this frequency (Zone A). The duct wall density is 'ρ' while 'ρ_s' is the reference density for steel.

(b) Calculate the height of the lower plateau as $84 + 20 \log_{10} (t/D) + 20 \log_{10} (\rho/\rho_s)$ (Zone B).

(c) Join the $22 + 20 \log_{10} (\rho/\rho_s)$ dB point at the ring frequency to a point on the lower plateau at a frequency of $f_r/\sqrt{2}$.

(d) Calculate the cut-off frequency as per Section 2.4 and extend the lower plateau from $f_r/\sqrt{2}$ to this frequency (Zone B).

(e) Calculate the height of the upper plateau as $106 + 20 \log_{10} (t/D) + 20 \log_{10} (\rho/\rho_s)$ (Zone D).

(f) Calculate the limiting frequencies for the upper plateau as per Section 2.5 and plot the upper plateau between these frequencies (Zone D).

(g) Join the point on the upper plateau at f_u to the point on the lower plateau at $f_{cut-off}$ (Zone C).

(h) For frequencies below f_1, draw a line falling at 6 dB per octave from the point on the upper plateau at f_1.

(i) For frequencies well above the ring frequency, draw a line corresponding to mass law behaviour for rectangular ductwork less 5 dB. The basic equation is: TL $= 20 \log_{10} (q\ f) - 50$.

This equation can be represented on the normalized plot (Figure 3) as:

$$TL - 20 \log_{10}(t/D) - 20 \log_{10} (\rho/\rho_s) = 20 \log_{10}\left[(\rho t) \times (\rho_s/\rho) \times (D/t) \times (f/f_r) \times f_r\right] - 50$$

$$\approx 92.6 + 20\log_{10} (f/f_r) \quad for\ steel\ ducting$$

where q is surface weight of ducting (kg/m^2)
f is frequency (Hz)
f_r is ring frequency (Hz)
ρ is density of ducting (kg/m^3)
ρ_s is density of steel (kg/m^3)
t is duct wall thickness (metres)
D is duct diameter (metres)

298

(j)   Draw a line from the $22 + 20 \log_{10} (\rho/\rho_s)$ dB minimum at the ring frequency at a slope of 15 dB per octave until it meets the line drawn in (i) above. This now completes the predicted curve of TL except for corrections for coincidence effects.

(k)   The effect of coincidence is now determined as a set of corrections to be subtracted off the curve developed so far. The corrections are produced on a separate plot (Figure 4). Firstly, draw a line corresponding to the break-out TL for rectangular ductwork at higher frequencies, namely:

$$TL = 20 \log_{10} (qf) - 45$$

Calculate the coincidence frequency as per Section 2.3. For steel ducting, assign a value of 35 dB at this frequency and a value of 40 dB at frequencies of 1.765x, 0.567x and 0.182x coincidence frequency (f_c). At 0.321x coincidence frequency (f_c), assign a TL of 43 dB for steel ducting. Sketch in a sinusoidal variation between these 4 points.

Now draw a line at 5 dB below the TL line for rectangular ductwork for frequencies above 21.79x f_c. Join the 40 dB point at 1.765x f_c to the point on the line at 21.79x f_c.

The deviations of the curve so produced from the straight line for rectangular ductwork represent the corrections which must be applied for the coincidence effect. These deviations are valid for both rectangular and circular steel ducts. For materials other than steel, the various frequency ratios and TL's at those frequency ratios used in the construction will vary. Scaling the TL value according to $20 \log (\rho/\rho_s)$ while keeping the frequency ratios the same will be approximately correct for other materials such as aluminium.

The corrections should now be subtracted off the results determined at the end of (j) above.

(l)   The final curve produced at the end of (k) above represents a fairly conservative estimate of the narrow band TL behaviour for a circular duct. For octave band predictions, it is more representative to produce typical octave band TL's from this curve by determining individual values off the curve at one ninth octave band frequencies and combining in accordance with the following equation:

$$TL_{O/B} = - 10 \log_{10} \left[\left(\sum_{i=1}^{9} 10^{-TL_i/10} \right) / 9 \right]$$

299

where

TL_i is the transmission loss taken from the curve at the i th one ninth octave band frequency.

For a duct of length 'L', the individual $TL_{O/B}$'s should be limited so as to be greater than: $TL_{min} = 10 \log_{10}(4L/D)$.

4.0   PREDICTION SCHEME FOR FLAT-OVAL DUCTS (AS DEPICTED IN FIGURE 5)

4.1   BREAK-OUT TL FOR FLAT SIDES

For the flat sides of the ductwork having width 'w' equal to 'a-b' the ASHRAE (1987) method is used with minor modifications. The method can be summarised as follows:

Below a frequency of less than 2 C/b ('C' is speed of sound in air in m/s; and 'b' is effectively the depth of the duct between the flat plates in metres), the break-out TL for the flat plates of width 'w' is calculated as:

$$TL = 10 \log_{10} [fq^2/w] - 13$$

Above the frequency given by 2 C/b, the breakout TL is calculated as:

$$TL = 20 \log_{10} [qf] - 45$$

Corrections for coincidence effects should be made in accordance with Section 3.2 (k)and octave band TL's should be calculated generally as described in Section 3.2 (1). However, for a duct of length 'L', the break-out TL should be limited so as to be greater than:

$$TL_{min} = 10 \log_{10} [2L \, w/ (wb)]$$

4.2   BREAK-OUT TL FOR CURVED SIDES

The break-out TL for the curved sides is calculated as described in Section 3.0 as if the two curved sides made up a full circular duct.

4.3   OVERALL BREAK-OUT TL FOR FLAT-OVAL DUCTS

By considering the power flows within each sectional area of the duct and the radiating surface areas of the flat and curved sides, the break-out TL for the entire duct is then calculated as follows:

$$TL_{overall} = -10 \log_{10} \left[\frac{10^{-TL_{rect}/10}}{(1 + \pi b/(2w))} + \frac{10^{-TL_{circ}/10}}{(1 + 2w/(\pi b))} \right]$$

Figure 6 shows a typical result for a 600mm x 300 mm sheet steel duct with 0.7 mm wall thickness.

5.0 CONCLUSIONS

The predictive scheme developed for circular ducts is seen from Figure 3 to offer fairly conservative but realistic estimates of TL by means of a straightforward procedure akin to that developed by Cummings (1985) for rectangular ductwork. A simple means for correcting TL's for coincidence effects has also been presented and this can be applied to both circular and rectangular ductwork. A procedure has also been developed for predicting TL's of flat-oval ducting across the full frequency range of interest. The predictions closely match ASHRAE (1987) data at frequencies where these are given.

6.0 REFERENCES

ASHRAE, 1987 ASHRAE Handbook -HVAC Systems and Applications, Chapter 52, pp 52.18 - 52.23.

Cummings A., Acoustic Noise Transmission through Duct Walls, ASHRAE TRANSACTIONS 1985, V91, Pt.2.
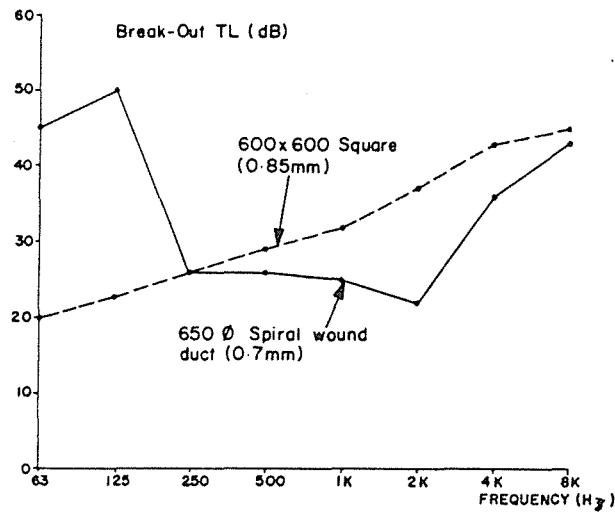
COMPARATIVE O/B BREAK-OUT
TL FOR CIRCULAR AND SQUARE DUCTS   Fig 1
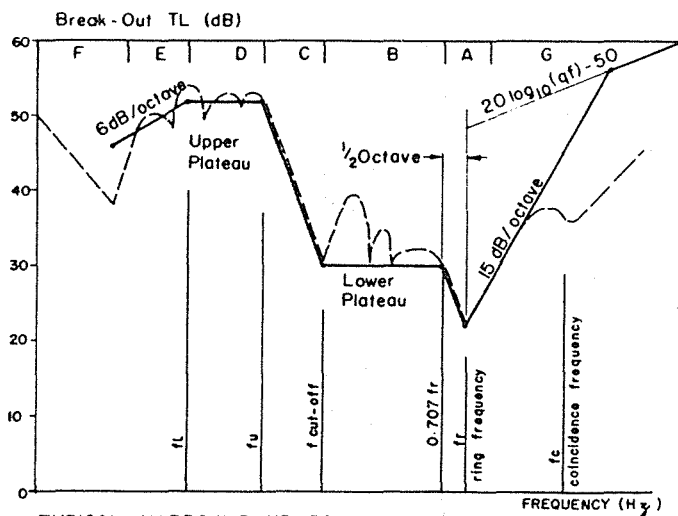
TYPICAL NARROW BAND BREAK-OUT TL FOR
CIRCULAR DUCT WITH PREDICTIVE APPROXIMATION   Fig 2
OVERLAID FOR REGIONS EXCLUDING COINCIDENCE

Normalized Break-Out TL
$TL - 20\log_{10}(t/D) - 20\log_{10}(P/P_s)$

High frequency limit=
$92.6 + 20\log_{10}(f/fr)$

NORMALIZED FREQUENCY
$10\log_{10}(f/fr)$
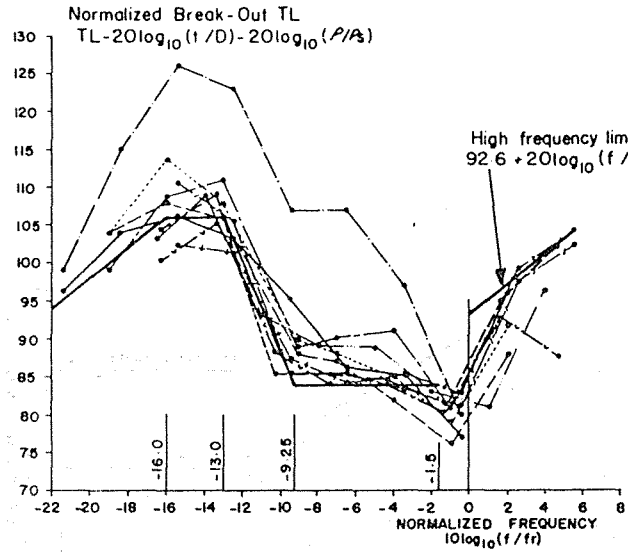
TL DATA FROM ASHRAE (1987) FOR
CIRCULAR DUCTS NORMALIZED AND COMPARED   Fig 3
WITH PREDICTIVE APPROXIMATION

Break-Out TL (dB)

$20\log_{10}(qf) - 45$

10 dB/octave

5 dB

40

43

40

35

0.182 x fc

0.321 x fc

0.567 x fc

fc

1.765 x fc

21.79 x fc

FREQUENCY (Hz)
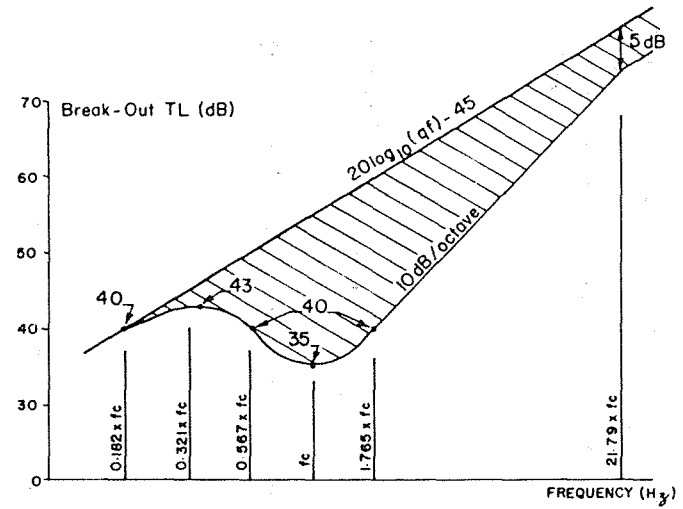
CORRECTIONS DUE TO COINCIDENCE TO BE
SUBTRACTED FROM Fig 2 PREDICTIVE   Fig 4
APPROXIMATION

Major Axis 'a'

Flat Plate Width 'w'

Minor Axis 'b'
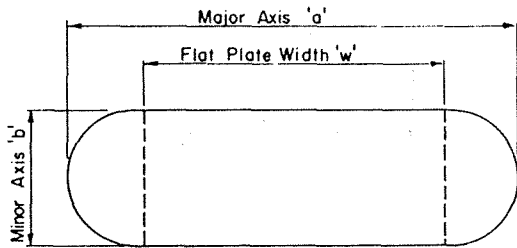
TYPICAL GEOMETRY FOR A
FLAT-OVAL DUCT   Fig 5

Break-Out TL (dB)

FREQUENCY (Hz)
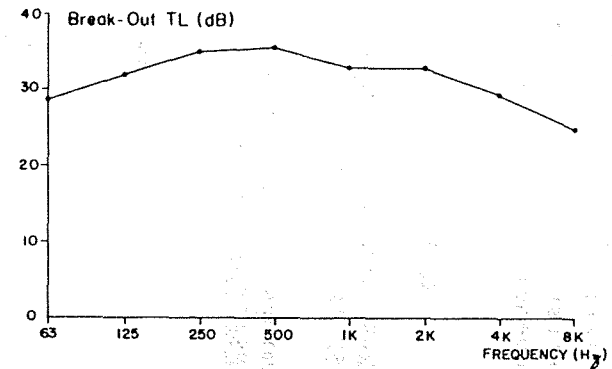
TYPICAL CALCULATED O/B BREAK-OUT
TL FOR 600mm x 300mm FLAT-OVAL   Fig 6
DUCT (0.7mm THICK STEEL WALL)

A PRACTICAL METHOD FOR CALCULATING ACOUSTICAL DIFFRACTION BY A WIDE BARRIER

K.Takagi
Department of Environmental and Sanitary Engineering, Faculty of Engineering, Kyoto University, Kyoto City, Japan.

M.Matsubara
Ultimate Disposal Devision Water Quality Control Dep. Public Works Reserch Institute.

K.Hiramatsu
Department of Environmental and Sanitary Engineering, Faculty of Engineering, Kyoto University, Kyoto City, Japan.

ABSTRACT   A simple and practical method for calculating noise reduction by a wide barrier is proposed by the present authors.

In this method the noise reduction ΔL in dB is given $\Delta L = \Delta L_1 + \Delta L_2 - 5$, where ΔL_1 is the reduction due to the facing corner of the wode barrier and ΔL_2 is the reduction due to the other side corner of the barrier. Various noise reductions calculated by the present method were compared with the previously obtained experimental data. The calculations were also carrie out based on the method proposed by Maekawa and Kurze.

It was found out that the fit between the calculated value and the observed data were satisfactory when we use the present method.

1.0 INTRODUCTION

Several methods have been proposed for calculating acoustical diffraction due to a wide barrier(Fujiwara K. et al., Kawai T., Kurze U. J., Maekawa Z.(a), Maekawa Z.(b), Pierce A. D.). Some methods, based on precise theories, give good fit to experimental data, but are rather complicated and inconvenient from practical point of view. Among the remaining methods, there are two simple practical methods. One is the method by Maekawa Z.(b) who proposed to determine an equivalent height of an assumed thin barrier. The other is by Kurze U. J. who proposed to calculate the double diffraction at two corners.

In this paper, another method based on Kirchhoff's approximation theory is proposed and the results of calculations following the above three methods were compared with experimental data presented by previous investigators. (Maekawa Z.(a),Fujiwara K. et al.).

2.0 METHOD OF CALCULATION

2.1 Method by Maekawa

One method was proposed. by Maekawa Z.(b) in his early attempt at this problem. As is shown in Fig.1, a wide barrier is assumed to be a thin barrier having a height determined by the intercept of two tangents of the wide barrier running from the source and receiver. This method is also used widely from practical view points, although theoretically it does not seem sufficient.

2.2 Method by Kurze

The other method is described in the report by Kurze U. J. The reduction , ΔL in dB is given by the following formula

$$\Delta L = \Delta L_X + \Delta L_Y - 5 + 20\log_{10}L/d \tag{1}$$

The value, ΔL_X ,in dB is the reduction by a thin barrier XX' in Fig.2, where the source and receiver are S and P'. Similarly ΔL_Y is determined by a thin barrier YY' where S' and P are the source and receiver. L is the sum of r_1 , w and r_2 , and d is the direct distance from S to P. In calculating ΔL_X and ΔL_Y , Maekawa's Chart is used. Although the limitation of this method is not clear, it is easily recognized that the value ΔL does not coincide with the value obtained from a single thin barrier, when the width w tends to zero.

2.3 Method by Present Authors

The present authors would like to propose the following method to obtain the reduction ΔL in dB by a wide barrier.

$$\Delta L = \Delta L_X + \Delta L_Y - 5 \tag{2}$$

In equation (3), the value, ΔL_X , in dB is the reduction by a thin barrier XX' in Fig.3, where the source and receiver are S and Y. ΔL_Y is the reduction in dB determined by a thin barrier YY' where the source and receiver are S and P.

ΔL_X is obtained from Maekawa's chart by calculating $\delta_x = r_1 + w - r_3$ ($N_x = 2\delta_x/\lambda$) and ΔL_Y is obtained similarly by calculating $\delta_y = r_3 + r_2 - d$ ($N_y = 2\delta_y/\lambda$), where r_1 = SX, w = XY, r_2 = YP, r_3 = SY and d = SP in Fig.3. It is important to take notice of the fact that in calculating the effects of thin barrier X' , only the part of XX" should be taken into considerations.

Therefore the value of reduction in dB due to thin barrier X" X' must be reduced from ΔL_X. The necessity of this way of calculation can be easily understood when one considers the case where the width w tends towards zero. The constant -5 in eqn(3) is introduced for this reason.
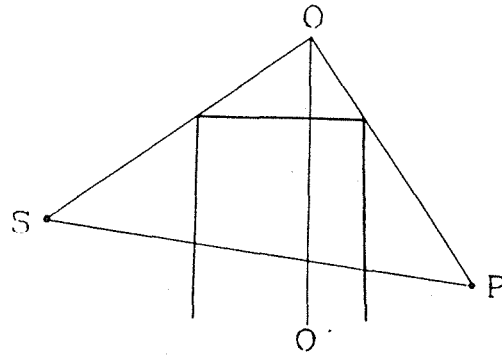
Fig.1 Approximation of a wide barrier to a thin barrier by Maekawa.
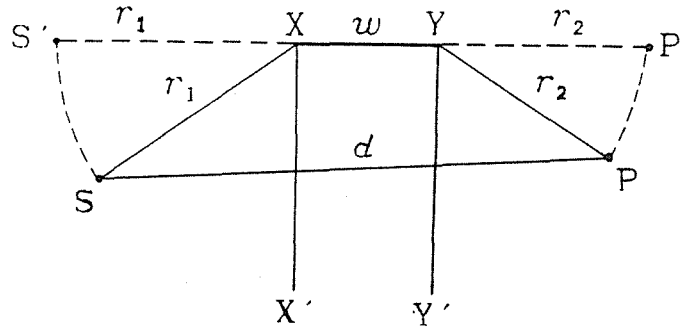
Fig.2 Method of calculating double diffraction for a wide barrier by Kurze. S is a source, P is a receiver and w is the width of a barrier.
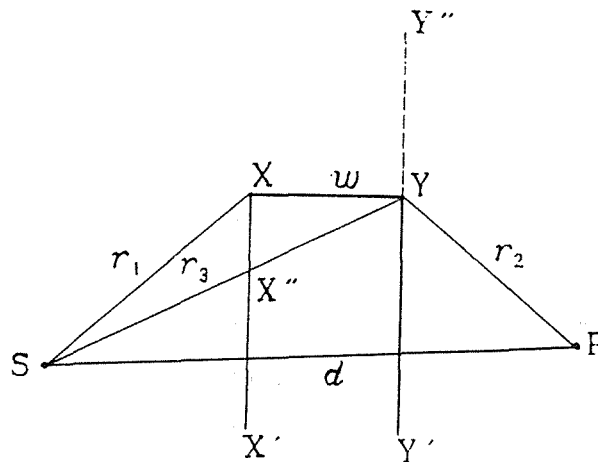
Fig.3 Method of calculating noise reduction of a wide barrier by the present authors. Diffraction due to a thin barrier XX' and YY' are considered.

3.0 EXPERIMENTAL DATA BY PREVIOUS INVESTEGATORS

In order to compare the calculated values from these three methods with the values of experimental results, data from model experiments carried out by Maekawa Z.(a), and Fujiwara et al. using a wide barrier were adopted. Fig.4 shows the outline of the experiment by Maekawa Z.(a). θ_1 was determined equal to θ_2, and two cases were adopted: $\theta_1 = \theta_2 = 22.5°$ and $\theta_1 = \theta_2 = 45°$. The distance OS was kept constant at 100cm and OP was changed from 10 to 150cm. Two different values of width w were chosen; 1.5cm and 12cm. The frequencies of sound used were 5, 10, 20, and 40kHz. The absorption due to air was taken into consideration by the present authors and the correction was made following the method shown by ANSI.

Fig.5 shows the outline of geometry of experimental conditions by Fujiwara et al. The width of thick barrier is 30cm. The distance from source to source side barrier is 50 cm, and two cases of θ were adopted; $\theta = 110°$ and $\theta = 135°$. In each case, l is taken so as to be 10, 20, 30, 50, 100, 130, 150, and 200cm. One third octave band noise whose center frequencies are 4, 8, and 16kHz are used.
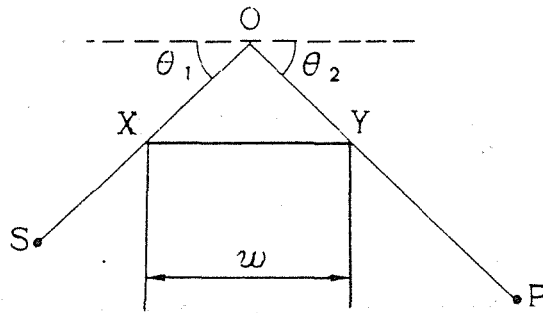
Fig.4　Outline of the experiment with a wide barrier carried out by Maekawa.
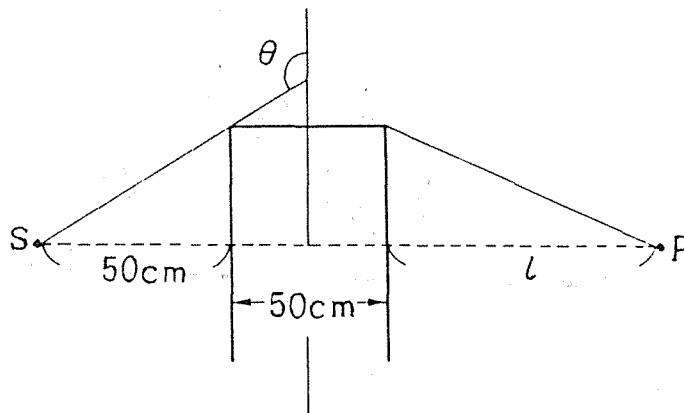
Fig.5　Geometry of experimental condition carried out by Fujiwara et al.

4.0 RESULT

In Figs. 6-8, the correspondence between the calculated values and the observed data from Maekawa Z.(a) are shown. In these figures, (a) is the case where w is 1.5cm and (b) is the case where w is 12cm. Fig.6 indicates that the method proposed by Maekawa gives smaller reductoin values than the experimental data. Fig.7 shows that the correspondence between calculated values and observed data are fairly good when width w is 12cm, while the correspondence is not satisfactory when width w is 1.5cm. So far as the present data are concerned, the fit seems best, as shown in Fig.8, when we use the method determined by eqn(3).

In Figs.9-11, the correspondence between the calculated values and the observed data from Fujiwara et al. are shown. Compared with Figs.6-8, fit is not so good. However, fit is best when one uses the present authors' method.

Theoretically, this method tends to overestimate the noise reduction by a wide barrier when we calculate ΔL_X and ΔL_Y without using Maekawa's Chart. On the other hand it is well known that the line showing noise reduction in Maekawa's Chart is drawn about 3-5 dB below the various experimental data. The combined effect of overstimation and underestimation may result in the good fit.

(a)   (b)
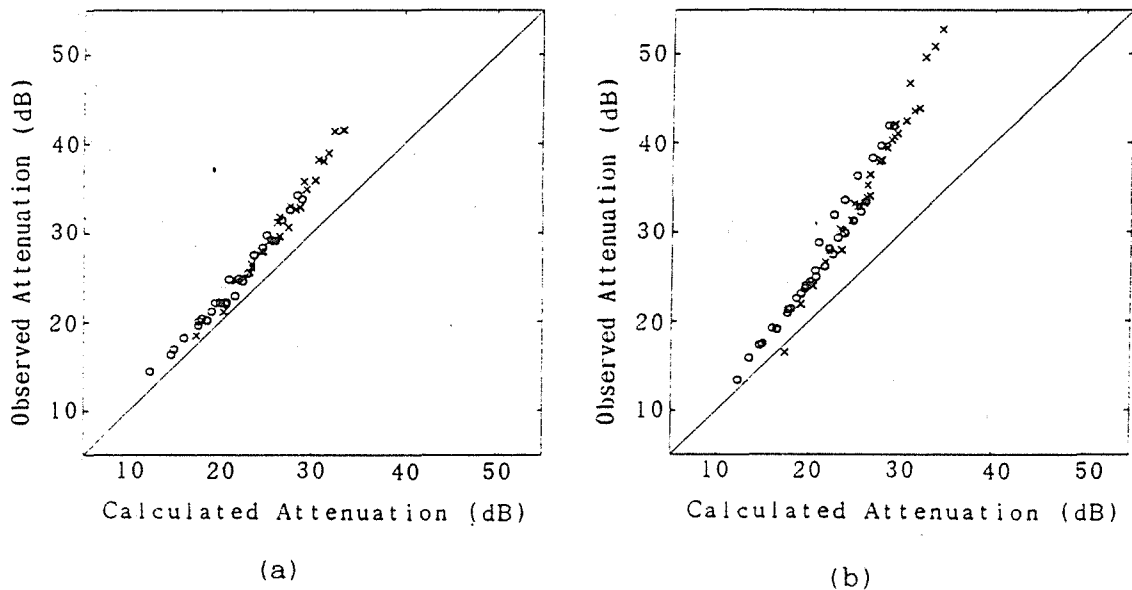
Fig.6   Comparison of noise reduction by a wide barrier between calculated and measured data. Calculation is carried out by Maekawa's method.(a)w =1.5cm, (b)w =12cm. Open circles are the data for θ =45° and crosses are for θ =90° .

307
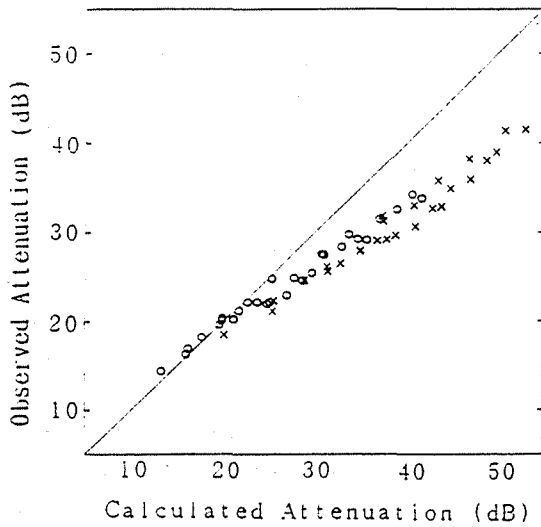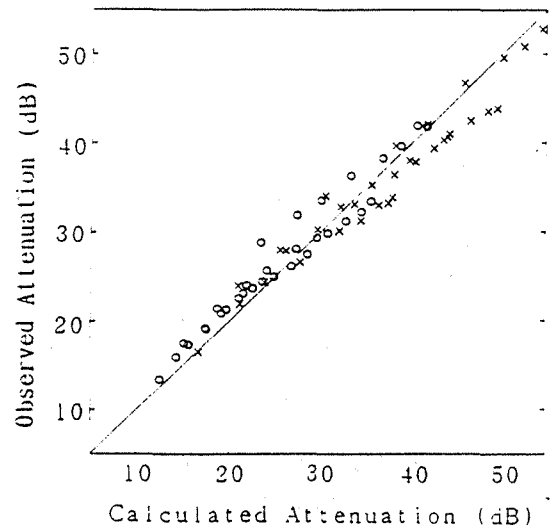
Fig.7 Comparison of noise reduction by a wide barrier between calculated and observed data. Calculation is carried out by Kurze's method. (a)w =1.5cm, (b)w =12cm. Open circles are the data for θ =45° and crosses are for θ =90° .
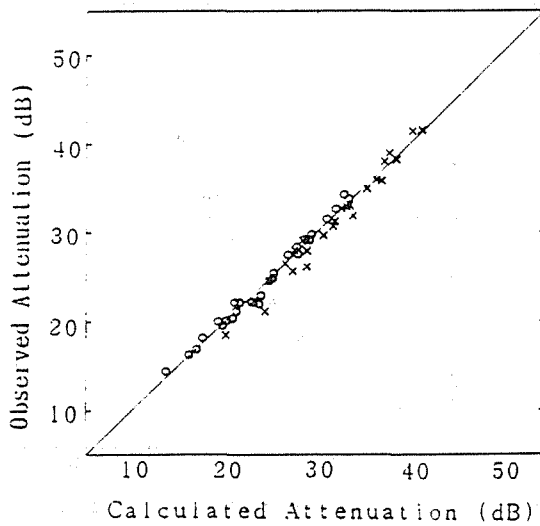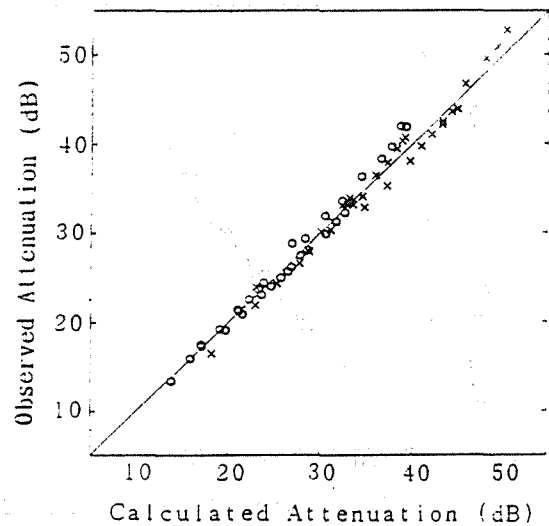
Fig.8 Comparison of noise reduction by a wide barrier between calculated and observed data. Calculation is carried out by the present authors' method. (a)w =1.5cm (b)w =12cm. Open circles are the data for θ =45° and crosses are for θ =90° .
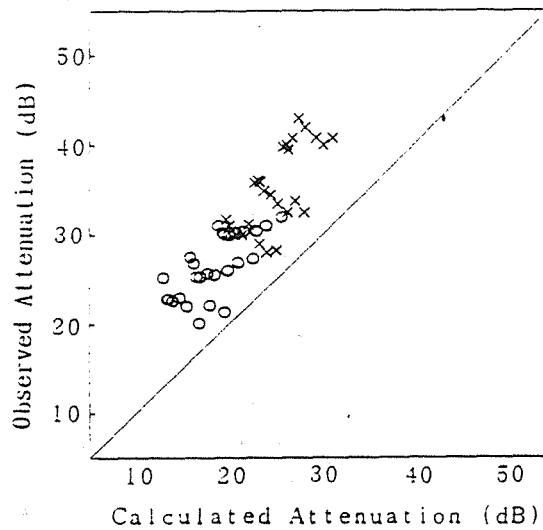
Fig.9   Comparison of noise reduction by a wide barrier between calculated and observed data. Calculation is carried out by Maekawa's method. Open circles are the data for θ =110° and croses are for 135° .
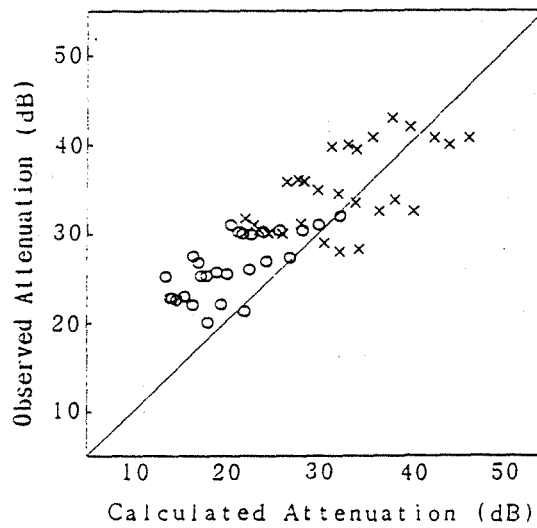
Fig.10   Comparison of noise reduction by a wide barrier between calculated and observed data. Calculation is carried out by.Kurze. Open circles are the data for θ =110° and croses are for 135° .
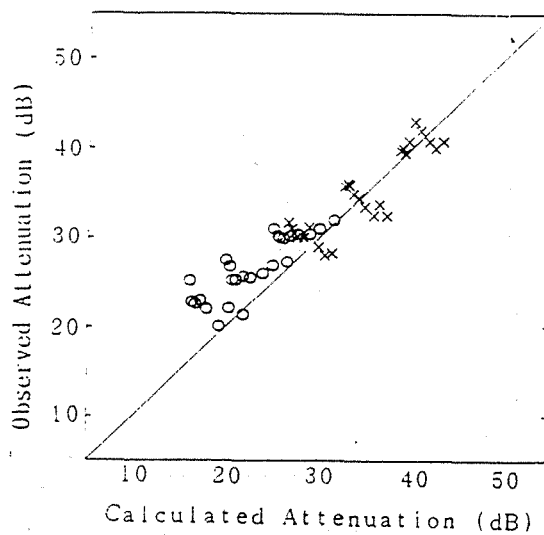
Fig.11 Comparison of noise reduction by a wide barrier between calculated and observed data. Calculation is carried out by present authors. Open circles are the data for θ =110° and croses are for 135° .

REFERENCES

ANSI, Method for the Calculation of the Absorption of Sound by the Atmosphere, ANSI SI 26, (1978).

Fujiwara K. et al., Noise Reduction by a Thick Barrier, *Journal of the Acoustical Society of Japan*,31(12)725-729(1975).

Kawai T., Sound Diffraction by a Many-Sided Barrier or Pillar, *Journal of Sound & Vibration*,79 229-42(1981).

Kurze U. J., Noise Reduction by Barriers, *Journal of the Acoustical Society of America*,55(3)504-18(1974).

Maekawa Z.(a), Theoretical Analysis on Data from Experiment of Acoustical Diffraction by a Barrier, *Trans. AIJ*, 68(6)153-8(1961)(in Japanese).

Maekawa Z.(b), Noise Reduction by Screen,*Applied Acoustics*,1(3)157-73(1968).

Pierce A. D., Diffraction of Sound Around Corners and Over Wide Barrier, *Journal of the Acoustical Society of America*, 22(5)941-55(1974).

SELECTION OF ERROR SENSOR LOCATION IN THREE-DIMENSION SPACE ACTIVE SOUND CONTROL

Chong Wang

Iustitute of acoustical Engineering,Northwestern Polytechnical University,Xi' an,China

Jincai Sun

Iustitute of acoustical Engineering,Northwestern Polytechnical University,Xi' an,China

ABSTRACT

For an adaptive active attenuation system,the error sensor can be regarded as a monitor. The adaptive system adjusts the complex strengths of secondary sources continuously in order to keep the sound pressure at the postiton of error sensor minimum. In priciple,if a global reduction is needed in space,a large number of error sensors distributed in space are needed. But this is unpracticable because much more error sensors may cause many questions. So it is important that how to obtain the best possible effects by using limited error sensors,that is how to selecting the best places of error sensors. This paper deals with an adaptive active control system and a acoustic system of which the secondary source is point source. The selection of error sensor postiton is discussed and it is found that error sensor should be put in the direction that the directivity of optimal sound field is minimum. In experiments,two secordary sources are used and a global reduction is obtained by using only one error sensor.

1.0 INTRODUCTION

In recent years,techniques of active sound control in three-dimension space have been developed rapidly. In the theory of active sound control,a method for calculating the optimal complex strengths of secondary sources has been developed by minimizing the sound power output of the acoustic system[1]. In the application of active control,adaptive techniques have been widely used. It provides a effective manner for practical use of active sound control in three-dimension space[2].

The principle of adaptive active control is that the adaptive systems receive the signal of the primary source,then send the output signal adaptively filtered to secondary sources,and meanwhile error signal which is received by error sensor located in space is fed back to the systems, the systems can adjust the complex strengths of secondary sources in order to keep the sound pressure at the error sensor position minimum. Up to now,it has been successfully used in active control of cabin noise[3],active control of sound radiation from vibrating plate[4],active control of power flow in structures[5],etc. But the developments of adaptive active techniques and theory of the active sound control are independent. That means that there is not any relations between the sound reduction obtained by adaptive system and predicted by theory. On the one hand,it makes the thoretical prediction meaningless,on the other hand the sound reduction obtained by adaptive system in general is not maximun. Therefore,it is important to find a bridge between them. That is to use adaptive system to obtain the maximun sound reduction which is predicted by theory.

In this paper,The best sound attenuation obtained by using adaptive system in free field is discussed. An attempt to find a relation between two approaches by selecting the number and positions of the error sensors has been made. Two typical cases are discussed and corresponding experiments are carried out.

2.0 THEORY

Fig. 1 shows the principle of adaptive active control of sound. The active control is realized by minimizing the sound pressues at the error sensor position. When a lot of error sensors are used,the realizing criterion of active control is to minimize the sum of mean square of sound pressures at all error sensors positions. Thus in free field, if the secondary sources are put near the primary source,and a lot of error sensors are put in all the directions around the primary and secondary sources,a"global"sound reduction can be obtained. It can be proved that the reduction is just the maximum reduction predicted by theory[1]. But in practice this is unpracticable,because much more error sensors will make system complex and increase the amount of computation so that the processing of real time is affected. Actually in most cases,putting so many error sensors are not allowed. It is concerned that if there is any possible to use limited error sensors to obtain the maximun sound reduction. It should be noticed that although adaptive system minimizes the sound pressure at the error sensor position,there is no reason to say that the sound reduction in space is maximun. Therefore,some "specific points"or"specific directions"in the field should be found, which represent the sound reduction property of the

space. When the sound reduction effects at the points or in the directions are the best, the effects in the space must be the best. In order to discuss the possibility of this approach, two typical cases are chosen. Assume that the primary and secondary sources are all point monopole sources.

2.1 Single Secondary Source

The sound field produced by monopole primary source is:

$$p_p = \frac{k\rho_0 c_0}{4\pi r_p} Q_p e^{j(\omega t - k r_p + \frac{\pi}{2})}$$

and the sound field of secondary source is

$$p_s = \frac{k\rho_0 c_0}{4\pi r_s} Q_s e^{j(\omega t - k r_s + \frac{\pi}{2} + \psi)}$$

where ψ is the phase angle of secondary source's complex strength relative to that of primary source. For simplicity, the phase angle of primary source's complex strength is assumed to be zero. In this case, the total sound field in the space is given by,

$$p = p_p + p_s = \frac{e^{j(\omega t - k r + \frac{\pi}{2})}}{4\pi r_p} \cdot k\rho_0 c_0 [Q_p e^{-j\frac{kd}{2}\cos\theta} + Q_s e^{j\frac{kd}{2}\cos\theta}] \qquad (1)$$

where d is the distance between two sources, θ is shown in Fig. 2a. Considered that adaptive system minimizes the mean square of error signal, the mean square of sound pressure can be obtained from equation (1).

$$p_s^2 = \frac{1}{2}p \cdot p^* = (\frac{k\rho_0 c_0}{4\pi r_p})^2 [Q_p^2 + Q_s^2 + 2Q_p Q_s \cos(kd\cos\theta + \psi)] \qquad (2)$$

Assume that one error sensor is put in the direction $\theta = \theta_0$, and the mean square of sound pressure at the error sensor is $\frac{k\rho_0 c_0}{4\pi r_p}\varepsilon$, so that

$$Q_p^2 + Q_s^2 + 2Q_p Q_s \cos(kd\cos\theta_0 + \psi) = \varepsilon^2 \qquad (3)$$

This equation can be reduced to

$$\begin{cases} Q_s = -Q_p \cos(kd\cos\theta_0 - \psi) \\ \varepsilon = Q_p \sin(kd\cos\theta_0 - \psi) \end{cases} \qquad (4)$$

Equation (4) shows that if Q_p, ε are known, $Q_s e^{j\psi}$ can be uniquely determined. That is for single secondary source only one error sensor should be used, and the complex strength of secondary source is

$$Q_s = -Q_p \cos(\arcsin\frac{\varepsilon}{Q_p}) e^{-j(kd\cos\theta_0 - \arcsin\frac{\varepsilon}{Q_p})} \qquad (5)$$

Substituting equation (5) into equation (1)

$$p = \frac{k\rho_0 c_0}{4\pi r_p} Q_p \cdot \sqrt{\alpha^2 + 1 - 2\alpha\cos(kd\cos - \psi)} e^{j(\omega t - k r_p + \psi)} \qquad (6)$$

where $\alpha = \cos(\arcsin\varepsilon/Q_p)$, $\psi = kd\cos\theta_0 - \arcsin\varepsilon/Q_p$. The total sound power output of the acoustic system is

$$\frac{W_0}{W_p} = 1 + \alpha^2 - 2\alpha\text{sinc}kd \cdot \cos(kd\cos\theta_0 - \arcsin\varepsilon/Q_p) \qquad (7)$$

where $W_p = \frac{K^2\rho_0 C_0 Q_p^2}{8\pi}$ is the sound power output of primary source. It is found when $kd\cos\theta_0 = \arcsin\varepsilon/Q_p$, that is $\theta_0 = \arccos((\arcsin\varepsilon/Q_p)/kd)$ the sound reduction of acoustic system is maximum,

$$\frac{W_0}{W_p} = 1 + \alpha^2 - 2\alpha\text{sinc}kd \qquad (8)$$

and also when $\varepsilon/Q_p = \sqrt{1 - \text{sinc}^2 kd}$, $Q_s = -Q_p\text{sinc}kd$

313

$$\frac{W_0}{W_p} = 1 - \text{sinc}^2 kd \tag{9}$$

This equation is just the maximun sound reduction which also can be obtained by Nelson's theory[1]. So it is possible to use only one error sensor to obtain the best attenuation effect for single secondary source if the error sensor is put in the direction $\theta = \theta_0$, and the error signal is adjusted so as to satisfy $\varepsilon = Q_p \cdot \sqrt{1 - \text{sinc}^2 kd}$.

Fig. 1 Principle of adaptive active control of sound
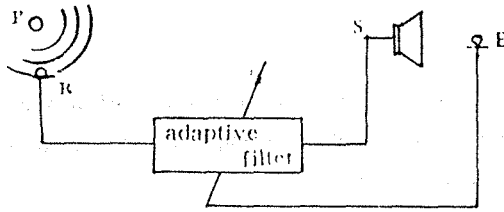
● primary source Q_p
■ secondary source Q_s
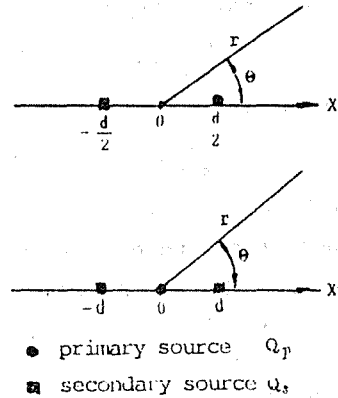
Fig. 2 Sources arrangement

2. 2 Two Secondary Sources

Assumed two secondary sources are put near the primary source symmetrically, the distance from primary to secondary source is d, and the complex strengths of two secondary sources are $Q_{s1}e^{j\psi_1}$ $Q_{s2}e^{j\psi_2}$ respectively. the total soound pressure in the space is

$$p = p_p + p_{s1} + p_{s2} = \frac{k\rho_0 c_0}{4\pi} \left[\frac{Q_p}{r_p} e^{j(\omega t - kr_p)} + \frac{Q_{s1}}{r_{s1}} e^{j(\omega t - kr_{s1} + \psi_1)} + \frac{Q_{s2}}{r_{s2}} e^{j(\omega t - kr_{s2} + \psi_2)} \right] \tag{10}$$

The mean square of sound pressure is

$$p_r^2 = \frac{1}{2} p \cdot p^* = (\frac{k\rho_0 c_0}{4\pi r_p})^2 [Q_p^2 + Q_{s1}^2 + Q_{s2}^2 + 2Q_{s1}Q_{s2}\cos(2kd\cos\theta - \psi_1 + \psi_2) + 2Q_pQ_{s1}\cos(kd\cos\theta - \psi_1) + 2Q_pQ_{s2}\cos(kd\cos\theta + \psi_2)] \tag{11}$$

Here two error sensors are needed at least. Assume that two error sensors are put in the direction $\theta = \theta_1, \theta = \theta_2$ and the mean square of sound pressure at the error sensors are $\frac{k\rho_0 c_0}{4\pi r_p}\varepsilon_1, \frac{k\rho_0 c_0}{4\pi r_p}\varepsilon_2$ respectively.

$$\begin{cases} Q_p^2 + Q_{s1}^2 + Q_{s2}^2 + 2Q_{s1}Q_{s2}\cos(2kd\cos\theta_1 - \psi_1 + \psi_2) + 2Q_pQ_{s1}\cos(kd\cos\theta_1 - \psi_1) \\ \qquad + 2Q_pQ_{s2}\cos(kd\cos\theta_1 + \psi_2) = \varepsilon_1^2 \\ Q_p^2 + Q_{s1}^2 + Q_{s2}^2 + 2Q_{s1}Q_{s2}\cos(2kd\cos\theta_2 - \psi_1 + \psi_2) + 2Q_pQ_{s1}\cos(kd\cos\theta_2 - \psi_1) \\ \qquad + 2Q_pQ_{s2}\cos(kd\cos\theta_2 + \psi_2) = \varepsilon_2^2 \end{cases} \tag{12}$$

Considered that adaptive system minimizes the sum of $\varepsilon_1^2 + \varepsilon_2^2$, when the system is stable, there must be $\varepsilon_1^2 = \varepsilon_2^2$. Subtracting above two equations.

$$Q_{s1}Q_{s2}[\cos(2kd\cos\theta_1 - \psi_1 + \psi_2) - \cos(2kd\cos\theta_2 - \psi_1 + \psi_2)] + Q_pQ_{s1}[\cos(kd\cos\theta_1 - \psi_1) - \cos(kd\cos\theta_2 - \psi_1)] + Q_pQ_{s2}[\cos(kd\cos\theta_1 + \psi_2) - \cos(kd\cos\theta_2 + \psi_2)] = 0 \tag{13}$$

It is found that when $\cos\theta_1 = \cos\theta_2$, the left side of equation (13) equals to zero constantly. It indicats that the two equations are correlative. As a result it is impossible to uniquely determine the complex strengths of two secondary sources. Therefore if two error sensors are used, θ_1, θ_2

314

should satisfy $\theta_1 \neq -\theta_2$ and $\theta_1 \neq \theta_2$. Equations (12) can be reduced to

$$\begin{cases} Q_p = -Q_{s1}\cos(kd\cos\theta_1 - \psi_1) - Q_{s2}\cos(kd\cos\theta_1 + \psi_2) \\ Q_p = -Q_{s1}\cos(kd\cos\theta_2 - \psi_1) - Q_{s2}\cos(kd\cos\theta_2 + \psi_2) \\ \varepsilon_1 = Q_{s1}\cos(kd\cos\theta_1 - \psi_1) - Q_{s2}\sin(kd\cos\theta_2 + \psi_2) \\ \varepsilon_1 = Q_{s1}\sin(kd\cos\theta_2 - \psi_1) - Q_{s2}\sin(kd\cos\theta_2 + \psi_2) \end{cases} \qquad (14)$$

From equations (14), $Q_{s1}e^{j\psi_1}$, $Q_{s2}e^{j\psi_2}$ can be obtained. Because of the symmetry of the position of secondary sources with respect to the primary source, the position of error sensors should be symmetrical. Assume $\theta_2 = \pi - \theta_1$, then

$$\psi_1 = \psi_2 = \text{arctg}\,\varepsilon/Q_p \qquad (15)$$

$$Q_{s1} = Q_{s2} = -Q_p \cdot \frac{\sqrt{1 + (\varepsilon/Q_p)^2}}{2\cos(kd\cos\theta_1)} \qquad (16)$$

Substituting equations (15), (16) into (10),

$$p = \frac{k\rho_0 c_0}{4\pi r_p} Q_p \cdot \sqrt{1 + 2\beta^2 \cdot [1 + \cos(2kd\cos\theta)] - 4\beta\cos(kd\cos\theta)\cos\psi_1} \cdot e^{j(\omega t - kr_p + \zeta)} \qquad (17)$$

where $\beta = \sqrt{1 + (\varepsilon/Q_p)^2}/2\cos(kd\cos\theta_1)$, $\psi_1 = \text{arctg}\,\varepsilon/Q_p$. The total sound power output is

$$\frac{W_0}{W_p} = 1 + 2\beta^2(1 + \text{sinc}2kd) - 4\beta\cos\psi_1\text{sinc}kd \qquad (18)$$

It can be proved that when $\beta = \cos\psi_1\text{sinc}kd/(1 + \text{sinc}2kd)$, that is $\theta_1 = \arccos\left(\frac{1}{kd}\arccos\frac{1 + \text{sinc}2kd}{2\cos^2\psi_1 \cdot \text{sinc}kd}\right)$, the sound reduction is maximun,

$$\frac{W_0}{W_p} = 1 - \frac{2\text{sinc}^2kd}{[1 + (\varepsilon/Q_p)^2](1 + \text{sinc}2kd)} \qquad (19)$$

and also when $\varepsilon \to 0$, $\frac{W_0}{W_p} \to 1 - \frac{2\text{sinc}^2kd}{1 + \text{sinc}2kd}$ (20)

Epuation (20) is just the maximun sound reduction which can be predicted by theory[1]. It means that for two secondary sources, two error sensors are needed and the maximun sound reduction can be obtained if two error sensors are put in the directions θ_1 and $\pi - \theta_1$, respectively.

3. 0 DISCUSSION

In previous discussions, the relations between sound power output and positions of error sensors for two cases are deduced. For further discussion, numerical computations are carried out. Fig. 3 shows the results calculated by equation (8). It is shown that for any values of kd, there exists an optimal value of ε/Q_p which is corresponding to maximun sound reduction. When kd is small, the range of optimal value of ε/Q_p is wide. When kd is large, the effect of optimal value on the sound reduction is obvious. Fig. 4 shows the optimal directions of error sensor versus the values of kd and ε/Q_p. It can be seen that the optimal direction exists only when $\arcsin \varepsilon/Q_p <$ kd, and this optimal direction is not $\theta_0 = \frac{\pi}{2}$ which is generally regarded as. The values of kd is different, so is the optimal direction. It should be paid attention that equation (8) is valid only when the optimal direction exists. In practice, one should find the optimal value of ε/Q_p in Fig. 3 according to value of kd, and then according to values of kd, ε/Q_p, find out the optimal direction. It can be proved that optimal values of ε/Q_p always satisfy $\arcsin \varepsilon/Q_p < $kd. It means that for a given value of kd, there exist a optimal value of ε/Q_p and a optimal direction.
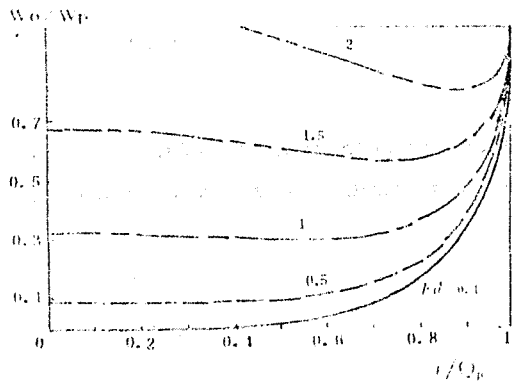
Fig. 3. Sound attenuation versus ε/Q_p
One secondary Source
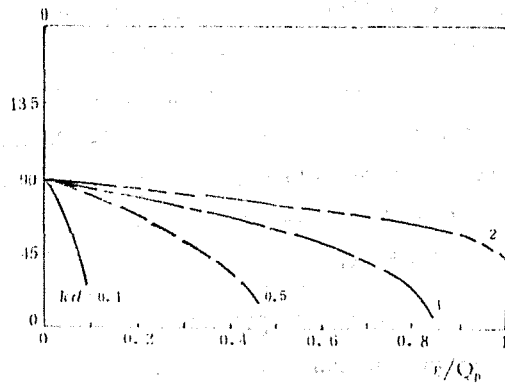
Fig. 4 Optimal direction versus ε/Q_p and kd:
One secondary Source

Fig. 5 shows the results of equation (19). For any values of kd, when ε/Q_p tends to zero, the attenuation tends to the greatest. Fig. 6 shows the optimal direction θ_1 versus ε/Q_p and kd. It can be seen that the optimal direction exists only when $\arccos \dfrac{1+\text{sinc}2kd}{2\cos^2\psi_1 \cdot \text{sinc}kd} < kd$. Because the optimal value of ε/Q_p is zero, then the optimal direction is $\theta_1 = \arccos(\dfrac{1}{kd}\arccos\dfrac{1+\text{sinc}2kd}{2\text{sinc}kd})$. when kd is small, then $\theta_1 \approx 60°$. In this case, the two optimal directions in which the error sensors should be put are $60°$ and $120°$.

The optimal directions have been discussed when the sound reduction is maximun. It also can be proved that these optimal directions are just the directions which the directivity of the optimal sound field are minimun. In practice, we can firstly calculate the complex strengths of secondary sources by using optimal theory, such as Nelson's theory, then obtain the optimal sound field, put the error sensors in the directions in which the directivity is minimun. However it should be noticed that the number of error sensors must be equal to that of secondary sources at least, and if there are more than one minimum directions in the optimal sound field, error sensors should be put in the directions which are uncorrelated each other, for instance, the directions of θ_1, $\pi-\theta_1$ are uncorrelated and those of θ_1, $-\theta_1$ are correlated.
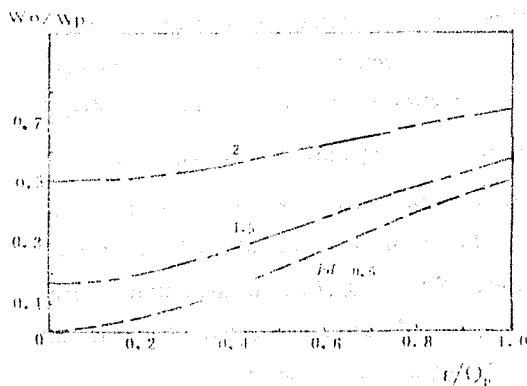
Fig. 5. Sound attenuation versus ε/Q_p:
Two secondary sources
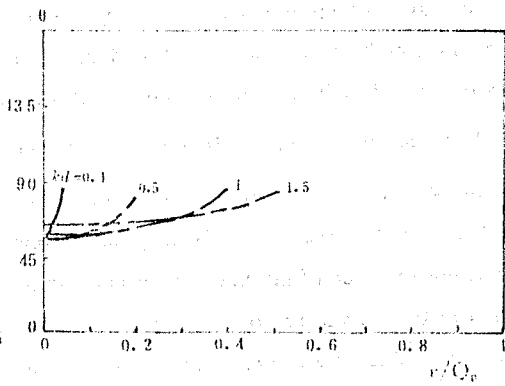
Fig 6. Optimal direction versus ε/Q_p and kd:
Two secondary Sources

4. 0 EXPERIMENT

The experiments are carried out in a semi-anechoic room. the primary source is a 6 inch loud-speaker installed in a box. The secondary sources are the same as the primary one. The adaptive system is the "NPU-307 adaptive active control device" which is manufactured by the Institute of Acoustical Engineering of Northwestern Polytechnical University. Fig. 7 shows the sound pressures in space using only one secondary source and one error sensor. Fig. 8 shows the sound pressures in space using two secondary sources. Considered that the primary source is symmetric, according to equations (15) and (16) , the two secondary sources are fed by same signal. In this case only one error sensor was used and put in the direction $\theta_1 = 60°$. In the experiments the optimal value of t/Q_p was obtained by adjusting the knob of the amplifier of error signal input on the device. It can be seen the effects are satisfied.
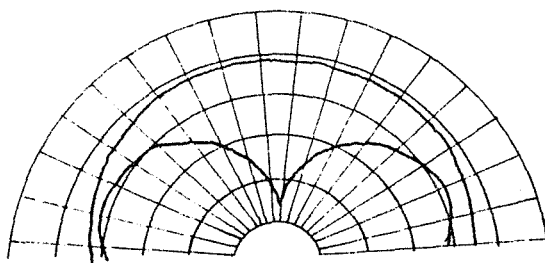
Fig. 7 Sound pressures in space using one
secondary source ; PSL-device off ;
RSL-device on
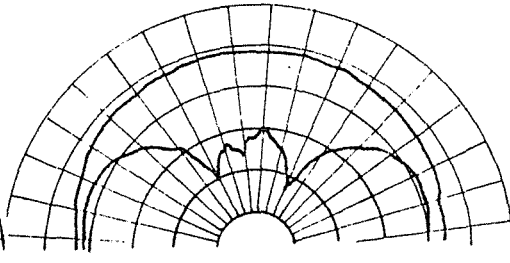
Fig. 8 Sound pressures in space using two
secondarysources ; PSL-device off ;
RSL-device on

5. 0 CONCLUSION

In this paper, the selection of the positions of error sensors to get the best attenuation effect is discussed. The theoretical and experimental resusts show that this method is practicable. Though the conclusions are obtained from two simple cases, it is thought that the techniques also suit for other cases.

References

1. P. A. Nelson, etc, "The Minimum Power Output of Free Field Point Sources and the Active control of Sound"J. S. V, 116(3), 1987

2. K. A. Chen, etc, "Adaptve Wideband Noise Cancellation"WESTPAC Ⅱ 1988, Shanghai, china.

3. A. J. Builiuore, etc. "Theoretical Studies of the Active Control of Propeller-induced Cabin Noise", J. S. V, 140 (2), 1990

4. C. Deffayet, etc. "Active control of Low-frequency Harmonic Sound Radiated by a Finite Panel". J. A. S. A. 84(6), 1988

5. R. white, etc"Experiments on Active Control of Flexural Wave Power". J. S. V, Vol112(1), 1987 〗

AN IMPROVEMENT OF THE FREQUENCY RESPONSE OF THE HORN LOUDSPEAKER SYSTEM

Sejin Doo
Department of Electronics Engineering, Seoul National University
San 56-1 Shillimdong, Kwanakku, Seoul, 151-742 Korea

Koengmo Sung
Department of Electronics Engineering, Seoul National University
San 56-1 Shillimdong, Kwanakku, Seoul, 151-742 Korea

ABSTRACT

Horn loudspeaker systems are highly efficient in converting electrical energy into acoustical one and therefore frequently used for the public address system. However, the acoustical impedance looking out of the diaphragm of the horn driver shows relatively high fluctuation especially at low frequency range due to reflections of sound between the throat and the mouth of the horn, and this results in the fluctuation of sound pressure level also.

In order to cope with this disadvantage of the horn loudspeaker system, we have placed the partitions having different dimensions with each other near the mouth of the horn in order to lower down the Q of the horn resonance and thus to flatten the impedance curve. For the purpose of analysis, wave propagation phenomena within the horn are analyzed and numerical calculations are performed. Coupling of the throat impedance with electrical impedances of the horn driver and the amplifier is analyzed and the resulting power output is calculated. The results show that partitioning a horn with different dimensions improves the frequency response of the horn loudspeaker system.

1.0 INTRODUCTION

Among several types of loudspeaker systems, horn loudspeakers are best in converting electrical energy into acoustical one and therefore are widely used for public address. However, as there exists cut-off frequency owing to the flare rate of the horn, the lower limit a horn loudspeaker can reproduce is above the cut-off frequency (Olson, H. F.). In addition, the impedance curve looking out of the diaphragm shows relatively large ripples especially in the lower frequency range, which are caused by the reflections of sound between the throat and the mouth of the horn loudspeaker.

Since the ripple in the impedance curve results in the same kind of fluctuation in the frequency response curve of the horn loudspeaker, it is desired to alleviate the ripple characteristics.

2.0 MULTI-LENGTH PARTITIONED HORN

In a horn loudspeaker, the diaphragm is coupled to the air via a horn. The horn magnifies the effective size of radiating surface as the wave travels along the horn, and thus relatively small diaphragm can be used. If the horn were infinitely long the wave excited by the diaphragm would spread out outwards only so that there will be no reflection coming back to the diaphragm. However, the length of the practical horn is to be finite and there must be reflection at the boundary of the mouth. The reflection continues back and forth along the horn and if the frequency of the wave coming out of the diaphragm corresponds to the inverse of the reflection period then the strength of the wave inside becomes greater and vice versa. These phenomena result in resonance characteristics of the finite horn.

The resonance of the finite horn gives characteristic 'colouration' to the timbre it produces and it is not desirable in view of the fact that the horn loudspeaker is used only to reproduce and not to modify the sound of the sources.

In order to lower down the amplitude of the ripples in the impedance curve, we designed a horn as shown in Fig.1. Inside the horn near its mouth is partitioned into several sections whose dimensions are different each other. We call it here the 'multi-length partitioned partitioned (MLP) horn'. Inner ends of the partitions can be lengthened down to the throat of the horn if required.
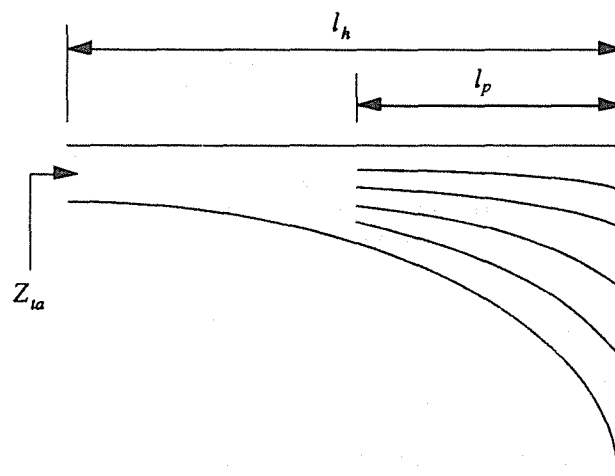
Fig.1 Multi-dimensionally partitioned horn

3.0 THEORY

As the large area near the mouth of the horn is partitioned into several sections isolated each other, the wavefront traveling along each section can be considered more planar than if it were traveling along the whole area of the horn. Therefore it is reasonable to approximate the pressure at the mouth of each section as that caused by the plane piston. Then we can replace the radiation impedance of each section to that of the plane piston.

In order to calculate the complex velocity at the mouth of each partitioned horn, we solve the horn equation with respect to velocity potential $\phi(x, t)$

$$\frac{\partial^2 \phi}{\partial t^2} - c_0^2 \frac{d}{dx}(\ln S)\frac{\partial \phi}{\partial x} = c_0^2 \frac{\partial^2 \phi}{\partial x^2} \qquad (1)$$

where c_0 is the sound speed and S the cross-sectional area of the horn. For the monochromatic wave propagating in an exponential horn $S(x) = S(0)e^{2mx}$, $\phi(x, t)$ is given by (Temkin, S.)

$$\phi(x,t) = A\exp[-mx + i(\sqrt{k^2 - m^2}x - \omega t)] + B\exp[-mx - i(\sqrt{k^2 - m^2}x + \omega t)] \qquad (2)$$

where A and B are constants determined by the boundary conditions and $i = \sqrt{-1}$. Using the relations $u = \frac{\partial \phi}{\partial x}$ and $p = -\rho_0 \frac{\partial \phi}{\partial t}$, we can equate at the mouth the radiation impedance Z_r and $S(l)(p/u)_{x=l}$:

$$\frac{i\rho_0\omega[A\exp(-ml + i\sqrt{k^2 - m^2}l) + B\exp(-ml - i\sqrt{k^2 - m^2}l)]}{A(-m + i\sqrt{k^2 - m^2})\exp(-ml + i\sqrt{k^2 - m^2}l) + B(-m - i\sqrt{k^2 - m^2})\exp(-ml - i\sqrt{k^2 - m^2}l)} = \frac{Z_r}{S(l)} \qquad (3)$$

The acoustical impedance at the throat is likewise given by

$$z(0) = \frac{i\rho_0\omega(A + B)}{S(0)[A(-m + i\sqrt{k^2 - m^2}) + B(-m - i\sqrt{k^2 - m^2})]} \qquad (4)$$

From the equation (3) and (4), A and B which are functions of frequency and in general complex can be evaluated and then z(0) can be calculated as a function of frequency. In the case of the partitioned horn, total acoustical impedance at the throat is considered to be a parallel connection of the impedances of sub-horns. When the horn is partially partitioned, i. e., when the horn is not partitioned down to the throat, another boundary condition is added at the position where the partition is ended and the impedance at the throat can be likewise calculated.

On the other hand, the input impedance looking out of the throat is coupled to the electrical impedance of the loudspeaker unit. Therefore the particle velocity at the throat is influenced by both of these impedances. If we let the acoustical impedance of the horn looking out of the throat to be R+jX obtained above, the particle velocity at the throat is given by

$$u(0) = \frac{C}{R_a + R + i(X + \omega m_a - \frac{1}{\omega C_a})} \qquad (5)$$

where C is a constant determined by the characteristics of the loudspeaker unit and the amplifier, and R_a, m_a, and C_a are the acoustical resistance, mass, and compliance of the loudspeaker unit respectively. Power output from the loudspeaker unit is simply the constant multiple of the product of $|u(0)|^2$ and $Re[z(0)]$.

4.0 SIMULATIONS AND RESULTS

First, we have calculated the acoustical impedance at the throat for a fully partitioned horn. The horn is partitioned into five sub-horns and their lengths are 55.0, 58.4, 62.1, 65.9, 70.0 cm respectively. Five sub-horns have the same cut-off frequency, 170 Hz. Absorption by the air is neglected but the attenuation at the inner walls of the horn is taken into consideration. As a rough value for the attenuation constant α within the horn, $\alpha = 0.05$ nepers/cm was used irrespective of frequency in calculating both the impedance at the throat and the power output (Munjal., M. L.).

A partially partitioned horn as shown in Fig.1 was also simulated. It has the same length as that of the fully partitioned horn, but the difference is that it has the non-partitioned portion near the throat. Length of that portion is 20 cm and therefore the shortest sub-horn is 35cm long and so on.

The resulting acoustical impedance curves are shown in Fig.2 and Fig.3 respectively. For comparison, the curve for the conventional multicellar horn, whose length is 65cm, is overlayed. It can be seen that the ripples of the impedance curves of MLP horn are alleviated in both cases, especially in higher frequency range. The fully partitioned horn shows improved characteristics in almost the whole frequency range of interest, whereas the partially partitioned horn has the comparable peaks as the multicellar horn at 250 Hz and 500 Hz.
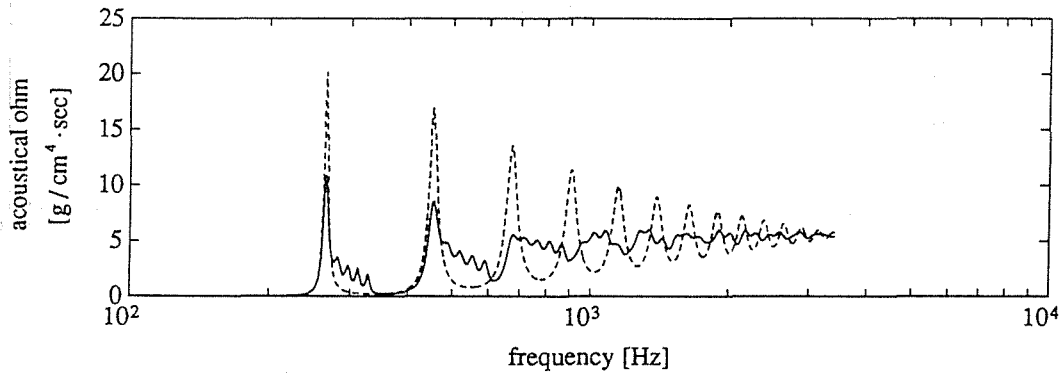
Fig.2 Real part of the acoustical impedance looking out of the throat
of a fully partitioned horn.
(solid line : fully partitioned horn, dashed line : multicellar horn)
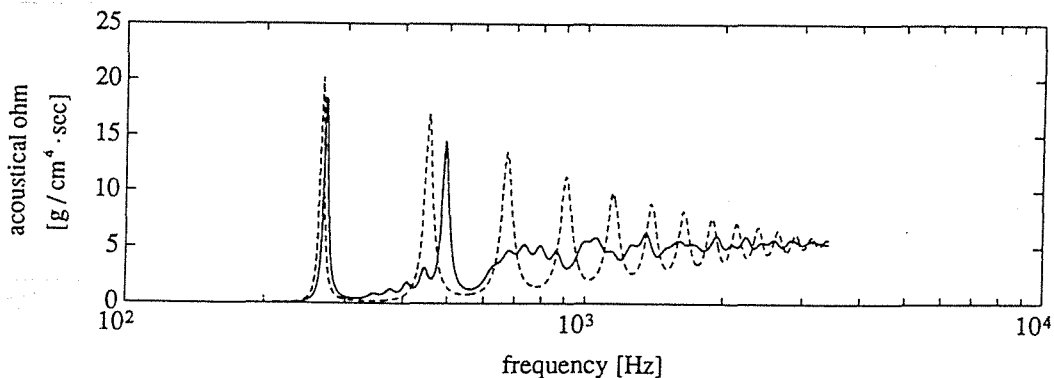
Fig.3 Real part of the acoustical impedance looking out of the throat
of a partially partitioned horn.
(solid line : partially partitioned horn, dashed line : multicellar horn)

321

The power output from the loudspeaker unit is also calculated. Mass, compliance, and resistance for a specific tweeter, whose resonance frequency is 1 kHz, radius 2.5 cm and Q=1.0, are measured and they are 0.79g, $3.2 \times 10^{-9} \sec^2/g$, and 5.0×10^3 cgs mechanical ohm respectively. Power output when this tweeter is used as a driver unit of the MLP horn is shown in Fig.4 and Fig.5.

As the impedance of the driver unit is coupled to the throat impedance, power output shows somewhat different characteristics compared to the throat impedances shown in Fig.2 and Fig.3: it is lower in both low and high frequency range and the improvement of the frequency response is prominent even in the frequency where peaks existed in the impedance curve. Comparing Fig.3 and Fig.4, we can say that the dip at about 300 Hz of the fully partitioned horn is flattened whereas it is not much flattened in the case of the partially partitioned horn.

Frequency response of the power output is in general improved by multi-dimensionally partitioning the horn but it is difficult to assert which method of partitioning is more effective in improving the frequency response of the horn loudspeaker system.
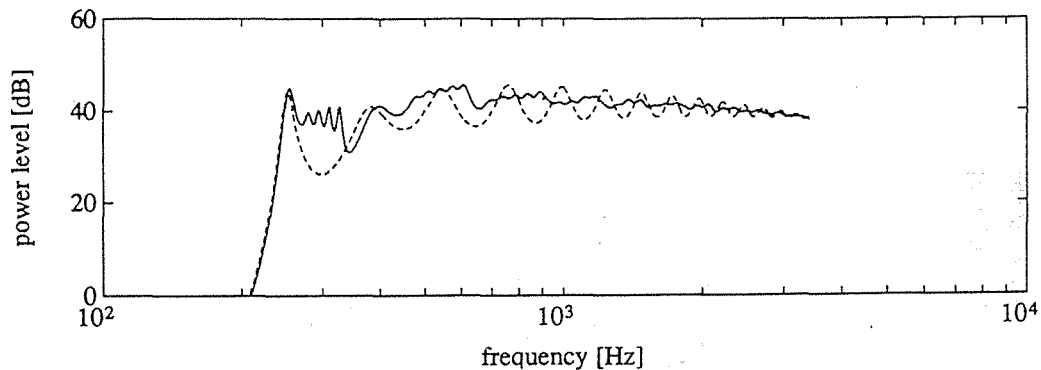
Fig.4 Power output level at the throat of the fully partitioned horn.
(solid line : fully partitioned horn, dashed line : multicellar horn)
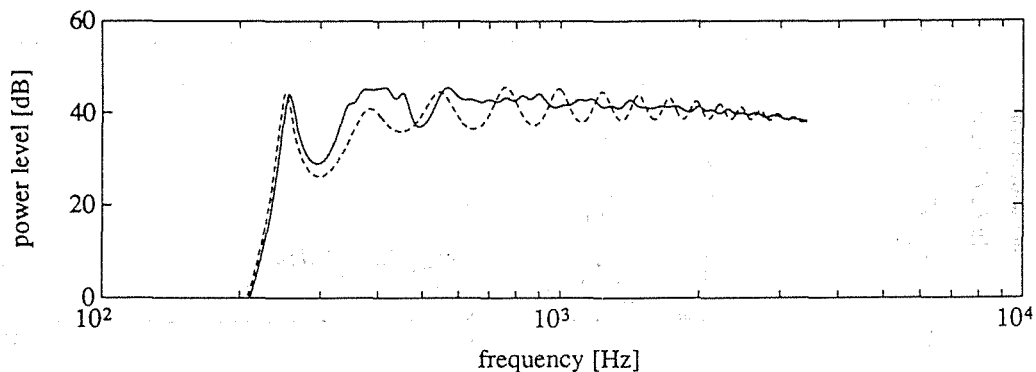
Fig.5 Power output level at the throat of the partially partitioned horn.
(solid line : partially partitioned horn, dashed line : multicellar horn)

322

5.0 CONCLUDING REMARKS

In order to lower down the ripple characteristics of the impedance curve looking out of the throat of a horn loudspeaker, we have proposed a partitioned horn, whose large area near its mouth is divided into several sections each of which having different length. The impedance plot calculated and the resulting power output shows that the ripple is alleviated when the horn is multi-length partitioned into several sections.

So far in this study, we have investigated only the input acoustical impedance of the partitioned horn looking out of its throat and the frequency response of the power output. On the other hand, as the particle velocities when the sound wave is output out of the mouths of the multi-length partitioned horns may differ in phase and amplitude, it is necessary that this phenomenon be studied and thereafter the sound output be calculated. Such an investigation is the theme of further study of the horn loudspeaker.

REFERENCES

Beranek, L. L., Acoustics, McGraw-Hill, N.Y., 1954, 268~284.
Kinsler, L. E., Fundamentals of Acoustics 3rd ed., John Wiley & Sons, N.Y., 1982, 200~210.
Munjal, M. L., Acoustics of Ducts and Mufflers, John Wiley & Sons, N.Y., 1987, 241~244.
Olson, H. F., Elements of Acoustical Engineering 2nd ed., D. Van Nostrand Company, N.Y., 1947, 98~109.
Temkin, S., Elements of Acoustics, John Wiley & Sons, N.Y., 1981, 164~171.

APPLICATION OF HIGHER-ORDER SPECTRA TO THE ANALYSIS OF UNDERWATER ACOUSTIC DATA

G. J. Frazer
Centre for Signal Processing Research, School of Electrical and Electronic Systems Engineering,
Queensland University of Technology, AUSTRALIA

P. J. O'Shea
Centre for Signal Processing Research, School of Electrical and Electronic Systems Engineering,
Queensland University of Technology, AUSTRALIA

B. Boashash
Centre for Signal Processing Research, School of Electrical and Electronic Systems Engineering,
Queensland University of Technology, AUSTRALIA

ABSTRACT

In this paper we briefly review the topics of stationary signal analysis, time-varying signal
analysis, higher-order spectral analysis and introduce time-varying higher-order spectral analysis.
We demonstrate the application of some of these techniques, including the power spectrum, the
spectrogram, the Wigner-Ville time-frequency distribution, the bispectrum, the time-varying
bispectrum and Gerr's third order Wigner distribution, to some underwater acoustic data and
demonstrate the merit of including higher-order spectral information when signaturing
underwater acoustic sources.

1 Introduction

Underwater signals, both biological and manmade, are often characterised by their acoustic emissions. Analysis in both the time domain and the frequency domain has been a standard approach for signals of this type[1]. More recently, it has been recognised that the time and frequency analysis of signals should be viewed jointly[1] and practical time-frequency analysis tools have been developed and applied to underwater acoustic signals[1][2]. The analysis methods mentioned use either the time series data directly, as in time domain analysis, or second moment information such as the power spectrum, the autocorrelation or the time-frequency distribution, for a frequency or time-frequency domain approach. The analysis tools mentioned thus far do not make use of signaturing features introduced by non-Gaussian signals and non-linearities inherent in the underwater source or introduced by the propagation medium.

A supplementary technique for analysing underwater acoustic data is to consider higher order cumulant sequences for the data and their corresponding spectra[6] [9]. The most well known of these spectra are the bispectrum and the trispectrum[10], which are the third and fourth order spectra associated, respectively, with the third and fourth order cumulant sequences. With the bispectrum and the trispectrum, non-Gaussianity and non-linearities inherent in the data can be identified and used to augment the signature of the acoustic source derived using the more traditional techniques referred to earlier. However, existing higher-order spectral analysis techniques assume that the signal is stationary and that the ergodic property can be used to produce consistent estimates of the bispectrum or trispectrum. Often the signal to be analysed is not stationary and attempts have been made to define a time-varying higher-order spectra [7] [12] [3] [11]. Many analysis methods in current use are optimal for Gaussian and linear models but are suboptimal when the problem is one of analysing non-stationary, non-linear and non-Gaussian signals. Time-varying higher-order spectra are one approach for problems of this type.

2 Signal Analysis: A Review of Recent Developments

We now review some methods for the signal analysis techniques which we applied to underwater acoustic data. We assume that the signal $\{x(t); t \in R\}$ is a random process which can be fully described by a joint probability density function (pdf), $p(x)$. This pdf is unknown.

2.1 Stationary Signal Analysis

If we impose the restriction that the pdf of the process, $x(t)$, is not changing with time, then for analysing the signal, one often uses the power spectrum of the process defined as;

$$S(f) = \int_{-\infty}^{\infty} \mathbf{E}\{x(t)x(t+\tau)\}e^{-j2\pi f\tau} d\tau \qquad (1)$$

Where $R_x(\tau) = E\{x(t)x(t+\tau)\}$ is the autocorrelation of $x(t)$, and dependent only on the lag variable τ. The power spectrum $S(f)$, is the Fourier transform of the autocorrelation of $x(t)$. Power spectral analysis reveals the presence of any periodicities in the signal, some of which may not have been obvious in the time domain. Problems of estimating the power spectra have been considered for many years. If a priori information is available about the signal then very high performance power spectral estimators can be devised[8].

2.2 Time-Varying Signal Analysis

The assumption of stationarity is very often not valid. When the signal is nonstationary, i.e. $R_x(t, \tau) = \mathbf{E}\{x(t)x(t+\tau)\}$, the power spectrum becomes "smeared" and much of the important information contained in the signal is lost. For this reason, the notion of a time-frequency distribution has arisen[1]. This type of distribution attempts to localise the energy, or energy density, in time and frequency. A class of time-frequency distributions defined below has proven very useful.

$$\rho_z(t, f) = \int_{-\infty}^{\infty} \int_{-\infty}^{\infty} \int_{-\infty}^{\infty} e^{j2\pi v(u-t)}g(v,\tau)z(u+\frac{\tau}{2})z^*(u-\frac{\tau}{2})e^{-j2\pi f\tau} dv du d\tau \qquad (2)$$

where $z(u)$ is the analytic signal derived from $x(n)$, and the function $g(v,\tau)$ determines the particular time-frequency distribution. A more general class of time-frequency distributions which is optimal for any time-frequency distribution has recently been proposed in [4] and [5].

Two well known members of this class are the Wigner-Ville distribution, where $g(v,\tau) = 1$, and the spectrogram, where $g(v,\tau)$ is given by $g(v,\tau) = \Pi_{2\Delta}(\tau)\frac{\sin\pi(\Delta-|\tau|)v}{\pi v}$. The actual formulation of the Wigner-Ville distribution is;

$$W(t,f) = \int_{-\infty}^{\infty} z(t+\frac{\tau}{2})z^*(t-\frac{\tau}{2})e^{-j2\pi f\tau}d\tau \tag{3}$$

with the spectrogram being;

$$S(t,f) = \left| \int_{t-\Delta/2}^{t+\Delta/2} x(t)e^{-j2\pi fu}du \right|^2 \tag{4}$$

The power spectrum and the time-frequency distribution present second moment properties of the signal. Signals with joint pdf other than multivariate Gaussian contain more information than can be analysed using second moment tools.

2.3 Higher-Order Spectral Analysis

Consider now, a series expansion of the pdf[9]. The second characteristic function, or cumulant generating function, of a random variable, X, with probability density function, $p(x)$, is defined as;

$$\Psi(f) = \ln E\left\{e^{-j2\pi fx}\right\} \tag{5}$$

It can be expanded in a power series for $e^{-j2\pi fx}$, giving;

$$\Psi(f) = \ln\left\{\int_{-\infty}^{\infty} e^{-j2\pi fx}p(x)dx\right\} = c_1\frac{(-j2\pi f)^1}{1!} + \ldots + c_r\frac{(-j2\pi f)^r}{r!} + \ldots \tag{6}$$

where c_r are a set of descriptive constants for the distribution, called the cumulants.

For a sequence of real random variables, $\{x_1, x_2, \ldots, x_n\}$, the joint r^{th} order cumulants are defined to be;

$$c_{k_1,k_2,\ldots,k_n} = (-j)^r \frac{\partial^r \ln \Phi(f_1, f_2, \ldots, f_n)}{\partial f_1^{k_1} \ldots f_n^{k_n}}\Bigg|_{f_1=f_2=\ldots=f_n=0} \tag{7}$$

where $r = k_1 + k_2 + \ldots + k_n$ and $\Phi(f_1, f_2, \ldots, f_n)$ is the joint first characteristic function given by;

$$\Phi(f_1, f_2, \ldots, f_n) = E\left\{e^{-j2\pi(f_1x_1+\ldots+f_nx_n)}\right\} \tag{8}$$

Recall that the power spectrum is the Fourier transform of the second moment sequence of the signal. Likewise, a class of spectra can be defined from the higher cumulant sequences. For zero mean random variables the moment and cumulant sequences are identical for orders one, two and three. For higher orders, however, they are not the same. Two useful higher-order spectra are the bispectrum and the trispectrum which are the Fourier transforms of $c_3(\tau_1, \tau_2)$ and $c_4(\tau_1, \tau_2, \tau_3)$, the third and fourth order cumulant sequences, respectively. Higher-order spectra based on cumulant sequences have the desirable property that for a symmetric pdf, the bispectrum and higher-order spectra are identically zero. In addition, the cumulant of the sum of two random variables is the sum of the cumulants of each random variable. For zero mean signals we use the bispectral definition derived from the moment sequence;

$$B(f_1, f_2) = \int_{-\infty}^{\infty}\int_{-\infty}^{\infty} E\{x(t)x(t+\tau_1)x(t+\tau_2)\}e^{-j2\pi(f_1\tau_1+f_2\tau_2)}d\tau_1 d\tau_2 \tag{9}$$

Clearly, the bispectrum and other higher-order spectra present extra information to that contained in the power spectrum, since they use additional terms from the series expansion of the pdf of the process. Naturally the series expansion of the pdf may itself be time-varying. In this case the definitions of higher-order spectra presented so far will smear the spectra and information will be lost.

2.4 Time-Varying Higher-Order Spectral Analysis

There is currently no single unified approach to the analysis of time-varying higher-order spectra. Several extentions to time-varying second moment analysis methods have been proposed [7] [11] [5]. Thatcher and Amin extended the third moment stationary bispectrum, introducing the "running bispectrum" [12] with what is a generalisation of the spectrogram. We now call this the time-varying bispectrum. There are no reported applications of these methods to real data and no reports of how the distributions are best interpreted.

The definition for the time-varying bispectrum is a generalisation of the definition of the spectrogram.

$$B(t, f_1, f_2) = \int_{t-\Delta/2}^{t+\Delta/2} \int_{t-\Delta/2}^{t+\Delta/2} x(t)x(t+u_1)x(t+u_2)e^{-j2\pi f_1 u_1 - j2\pi f_2 u_2}du_1 du_2 \tag{10}$$

Gerr introduced the third-order Wigner distribution, which he called the Wigner bispectrum. He derived it from the Wigner distribution by retaining the lag centering property of the Wigner-Ville distribution and requiring that if the signal is third order stationary then the expectation of the new definition is the same as the traditional bispectrum. His Wigner bispectrum, for a signal $x(t)$, is;

$$\begin{aligned} W_x(t, f_1, f_2) = \int_{-\infty}^{\infty} \int_{-\infty}^{\infty} & x(t - \tfrac{2}{3}u_1 - \tfrac{1}{3}u_2)x(t + \tfrac{1}{3}u_1 - \tfrac{1}{3}u_2) \\ & .x(t + \tfrac{1}{3}u_1 + \tfrac{2}{3}u_2)e^{-j2\pi(f_1+f_2)u_1 - j2\pi f_2 u_2}du_1 du_2 \end{aligned} \tag{11}$$

Swami generalised the Wigner bispectrum by retaining the same conditions as Gerr but allowing a wider class of centered lags.

Boashash and O'Shea derived a class of higher-order spectra by recognising that the bilinear product in the Wigner-Ville distribution is the first order central finite difference phase estimator. They selected higher order phase estimators and derived the appropriate distributions. Interestingly, they select a subspace of the higher-order distribution and show it to be the optimal time-frequency distribution for signals with polynomial phase law. Their distribution is of the form;

$$\rho_{z_s}^g(t, f) = \int \int \int \phi(\nu, \tau) K_{z_s}^g(\lambda, \tau)e^{j2\pi\nu(\lambda-t)}d\nu d\lambda e^{-j2\pi f\tau}d\tau \tag{12}$$

where;

$$K_{z_s}^g(t, \tau) = \prod_{k=1}^{q/2} [z_s(t + c_k\tau)]^{b_k}[z_s^*(t + c_{-k}\tau)]^{-b-k} \tag{13}$$

and $\phi(\nu, \tau)$ is the 2D smoothing function, and the limits on the integral are from $-\infty$ to $+\infty$. The conventional WVD may be recovered from the generalised one by setting $q = 2$, $b_{-1} = -1$, $b_0 = 0$, $b_1 = 1$, $c_{-1} = -1/2$, $c_0 = 0$, $c_1 = 1/2$. They define time-varying higher-order spectra by taking the expected value of (12).

3 Analysis of Underwater Acoustic Data

The data analysed in this paper are digitised recordings of underwater acoustic emissions of whales. The sample plots in this section show a segment of the signal data analysed, the power spectrum of the signal, the spectrogram, the Wigner-Ville distribution, the bispectrum, the mean of the magnitude of the time-varying bispectrum normalised by the signal power in each frame, 1 slice of the time-varying bispectrum and 1 slice of Gerr's Wigner bisectrum.

4 Interpretation

It is difficult to determine much from the time domain plot, (see figure 1) other than that it looks like noise but varies in amplitude over time. The power spectrum (see figure 2) indicates a concentration of energy around the frequency range $\frac{1}{10}\frac{f_s}{f_s}, \frac{1}{5}\frac{f_s}{f_s}$. It is not clear from the power spectrum whether there is any relationship between the frequency components visible. Indeed, the power spectrum plot shows little other than the frequency extent of the signal. For example, are all frequencies present all the time, or do they begin and end at different times, and if so, when?

The Wigner-Ville distribution (WVD) (see figure 4) shows clearly a dominant spectral line starting at about $\frac{1}{3}t_f$ and increasing from approximately $\frac{1}{10}f_s$ to approximately $\frac{1}{4}f_s$ where it remains before terminating at about $\frac{4}{5}t_f$. Additional lower level signal energy is also visible, some of which will be artifacts introduced by the unsmoothed bilinear term in the definition of the WVD. Nevertheless, this distribution shows considerably more information than either the time signal plot or the power spectrum and clearly indicates the signal is non-stationary.

The spectrogram (see figure 3) is a smoothed version of the WVD. While it removes the artifacts visible in the WVD, it also smoothes useful signal information and blurs the beginning and end of the signal transients. It shows the dominant time-varying frequencies well. Once again, this distribution is a substantial improvement on the signal plot and the power spectrum.

The bispectrum, as defined, assumes stationarity in the same manner as the power spectrum. Consequently the bispectral plot shown (see figure 5) is the average, or smeared, bispectrum over the complete signal. The critical features visible (all 12 regions of symmetry are shown) are the major peak at approximately $(\frac{1}{10}f_s, \frac{1}{5}f_s)$, indicating phase coupling between these frequencies and the minor peak at approximately $(\frac{1}{5}f_s, \frac{1}{5}f_s)$ which indicates the generation of harmonics. Most definitely the signal should be considered to be generated by some non-linear process, and this knowledge may help detection, analysis, classification and interpretation of signals of this type. Note that this information is not available from any of the previous plots.

The normalised power time-varying bispectrum (see figure 6) shows the mean of the magnitude of the time-varying bispectrum, for successive frames, normalised by the power in the frame of signal for which the bispectrum has been calculated. This gives an indication as to the presence of non-Gaussian and non-linear behaviour throughout the duration of the signal.

The single time slice of the time-varying bispectrum (see figure 7) indicates harmonic behaviour but does not indicate phase coupling which can only be detected when multiple realisations of the process are available.

The single time-slice of Gerr's Wigner bispectrum (see figure 8) is difficult to interpret and no conclusion is drawn from it.

5 Conclusion

Conventional signal analysis procedures do not utilise all the information available in many practical signal analysis problems. It has been demonstrated that the use of higher-order spectral analysis improves time, frequency and time-frequency analysis methods and provides the analyst with important additional information.

6 Acknowledgements

References

[1] B. Boashash. Time-frequency signal analysis. In S. Haykin, editor, *Advances in Spectral Estimation and Array Processing*, volume 1 of 2, chapter 9, pages 418–517. Prentice Hall, Englewood Cliffs, New Jersey, 1990.

[2] B. Boashash. *Methods and Applications of Time-Frequency Signal Analysis*. Longman Cheshire, Melbourne, Australia, 1991. ISBN No. 582 86873 4.

[3] B. Boashash and P. J. O'Shea. Time-varying higher order spectra. In *Proceedings of 9th Kobe International Conference on Electronics and Information Sciences*, Kobe, Japan, June 1991.

[4] B. Boashash and P. J. O'Shea. Time-varying higher order spectra. In Constantinides and Cappelini, editors, *Proceedings of Digital Signal Processing Conference*, Florence, Italy, September 1991.

[5] B. Boashash and P. J. O'Shea. Time-varying higher order spectra. In Franklin T. Luk, editor, *Advanced Signal Processing Algorithms, Architectures and Implementations*, San Diego, USA, July 1991. Proceedings of SPIE.

[6] D. Brillinger. An introduction to polyspectra. *Ann. Math. Stat.*, 36:1351–1374, 1965.

[7] .N. L. Gerr. Introducing a third order Wigner distribution. *Proceedings of the IEEE*, 76:290–292, March 1988.

[8] S. M. Kay. *Modern Spectral Estimation: Theory and Application*. Prentice Hall, Englewood Cliffs, New Jersey, USA, 1987.

[9] J. M. Mendel. Tutorial on higher-order statistics (spectra) in signal processing and system theory: Theoretical results and some applications. *Proceedings of the IEEE*, 79(3):278–305, March 1991.

[10] C. L. Nikias and M. R. Raghuveer. Bispectrum estimation: A digital signal processing framework. *Proceedings of the IEEE*, 75(7):869–891, July 1987.

[11] A. Swami. Third-order Wigner distributions: Definitions and Properties. In *Proceedings of the IEEE International Conference on Acoustics, Speech and Signal Processing*, Toronto, Canada, April 1991.

[12] J. D. Thatcher and M. G. Amin. The running bispectrum. In *Proceedings of the Workshop on Higher-order Spectral Analysis*, pages 36–40, Vail, Colorado, USA, June 1989.

WHALE DATA
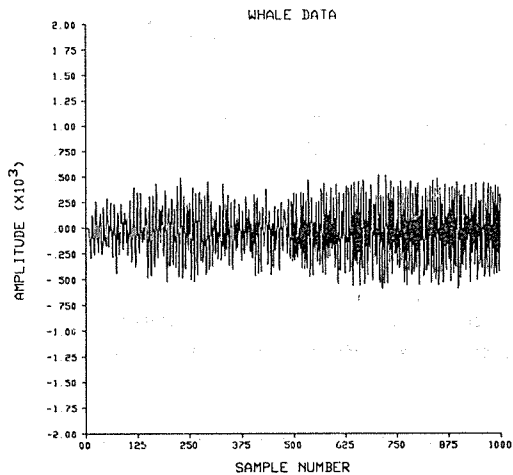
Figure 1: 1024 samples from the underwater acoustic signal data
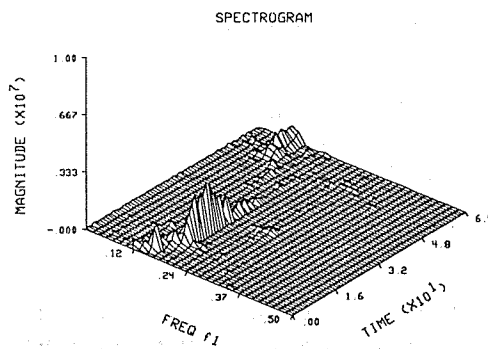
SPECTROGRAM

Figure 3: Spectrogram of the underwater acoustic data.

WHALE DATA POWER SPECTRUM
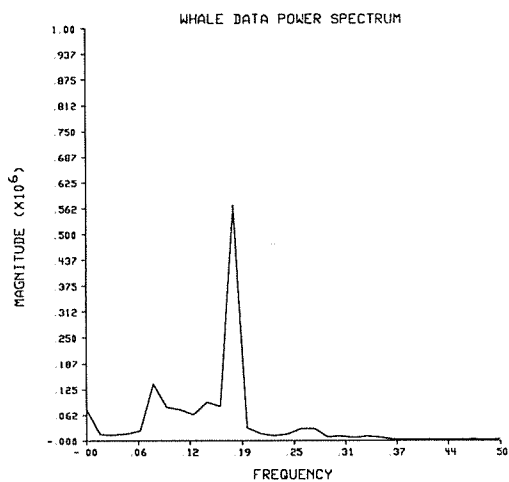
Figure 2: Power spectrum of the underwater acoustic data.

WIGNER-VILLE DISTRIBUTION
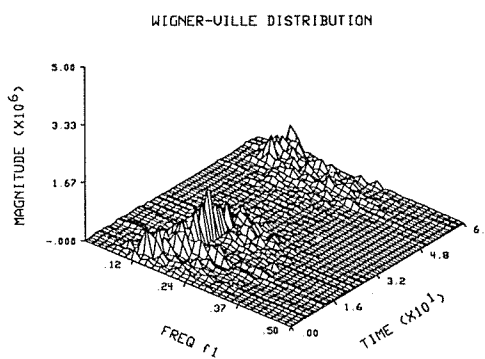
Figure 4: Wigner-Ville distribution of the underwater acoustic data.
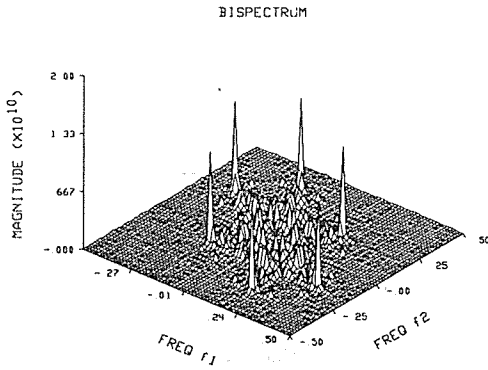
Figure 5: Bispectrum of the underwater acoustic data. (Note, all 12 symmetry regions are shown)
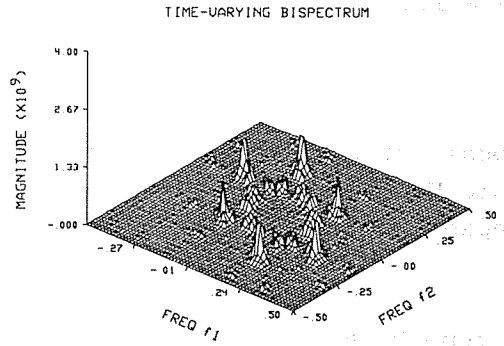
Figure 7: 1 time slice of a time-varying bispectrum of the underwater acoustic data. (Note, all 12 symmetry regions are shown)

NORMALISED POWER TVB MEAN MAGNITUDE

GERR'S WIGNER BISPECTRUM
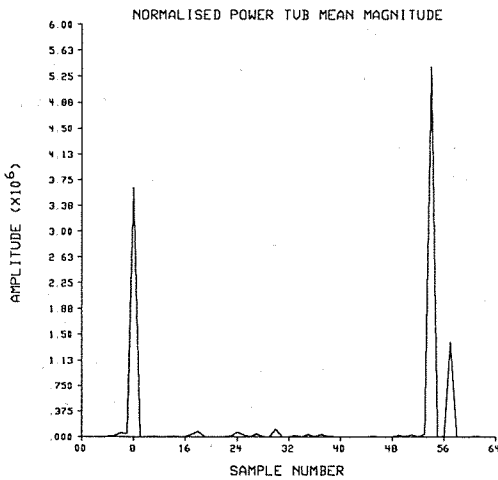
Figure 6: Normalised power time-varying bispectrum mean for the underwater acoustic data.
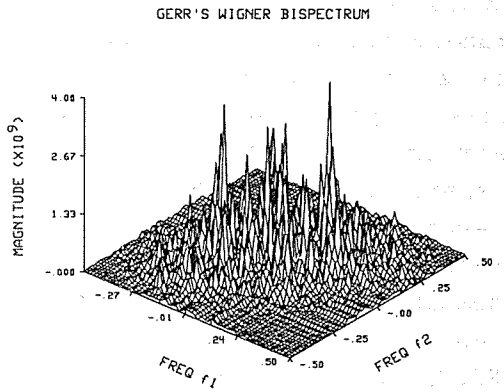
Figure 8: 1 time slice of Gerr's third order Wigner distribution of the underwater acoustic data.

A STOCHASTIC EVALUATION FOR THE FLUCTUATION PROBABILITY FORM
OF ENVIRONMENTAL NOISE AND VIBRATION BASED ON THE Z-TRANSFORM
TECHNIQUE

Yoshifumi Fujita
Kure National College of Technology, 2-2-11 Aga-Minami, Kure, 737
Japan

Mitsuo Ohta
Faculty of Engineering, Kinki University, 1 Takaya-Umenobe, Higashi-   ·
Hiroshima, 729-17 Japan

ABSTRACT

Needless to say, the whole probability distribution is necessary to
evaluate fluctuation characteristic of the environmental stationary
random noise and vibration. In this paper, based on the positive use
of z-transform, we propose a new trial of expressing the discrete
level type probability distribution. Here, it is characterized by the
agreement between the theoretically derived expression and the
experimentally observed expression for the statistical moments with
several type lower order and the positive use of z-transform
technique. Then, by transforming this z-domain expression to s-
domain one, the Laplace transform of the probability density function
can be obtained and its inversion can be numerically calculated by
FILT, which is one of methods for the numerical inversion of Laplace
transformation. The cumulative probability distribution is given as a
step response of the linear system of which the transfer function is
described by the Laplace transform of the probability density
function. In addition, by the convolution theorem, the compound
distribution of the sum of two independent random processes can be
easily obtained. Finally, by applying the proposed method to the
actually observed noise, the effectiveness of theoretically derived
cumulative probability curve has been experimentally confirmed too.

1.0 INTRODUCTION

The environmental random noise and vibration in our daily life shows very often a local stationarity with non-Gaussian type probability characteristic. Needless to say, owing to this non-Gaussian property, the use of only mean and variance is not sufficient to evaluate the fluctuation of the noise and vibration, and it is necessary to find a whole probability distribution. Up to now, several methods to obtain the probability distribution were proposed. In this paper,by paying attention to the similarity between the cumulative distribution function(abr. cdf) and a step response of the linear system which can generally approximate a general type transfer function of the first order as suggested by Ziegler & Nichols, we propose a new method of artificially finding an equivalent sampled data control system model matched to various type of cdf curve appearing in the actual environmental noise and vibration. More concretely,by employing some z-transform of the impulse response , the frequency distribution of discrete level is first determined reasonably based on the equivalence of the statistical moment information which is stable and commonly latent in the fluctuating data. The probability density function(abr. pdf) can be obtained by the relationship transforming the pulse transfer function to the transfer function which is derived by approximating the step response of the continuous linear system with the broken line constructed of line segments connecting points plotted for the step response of the discrete linear system. The numerical inversion of the Laplace transform is performed easily by means of FILT(Hosono T.). The cdf is given as a step response of the system described by the Laplace transform of the above pdf. In addition, the compound distribution curve for a sum of two or more random variables can be easily calculated as a response of two or more serial linear systems by using the convolution theorem of the Laplace transform.
Finally, the proposed method is applied to the actually observed traffic noise and music(i.e.,Karaoke) sound and then its effectiveness is experimentally confirmed.

2.0 THEORETICAL CONSIDERATION

In order to evaluate the environmental random noise and vibration fluctuating widely and stationarily with a non-Gaussian type probability distribution form, first let us consider the problem of determining its whole probability distribution form. Based on the similarity between the cdf curve and a step response of the linear system, we can find out the system simulating the step response to the pdf curve(Ziegler J.B. and Nichols N.B). Now, let us attempt to obtain an approximate discrete level system of the original continuous level system in a sampled-hold style. The random variable takes only discrete level values 0,1,2,..... Let us distinguish the following two cases. One is the case where the decreasing slope of

frequency distribution curve as X tends to infinity is smaller than the one as X tends to negative infinity and the other is the reverse case.

First, let us consider the former case. By dividing the overall level range of the random variable X into subintervals of width h and letting x_0 be the level value of middle point of 0-th$(i=0)$ subinterval. Let us define the random variable I and its discrete level type probability as follows:

$$I=[Y], \quad Y=\frac{X-x_0}{h} , \tag{1}$$

$$p_i=\text{Prob.}\{I=i\}, i=0,1,2,\ldots \quad , \tag{2}$$

$$q_i=\text{Prob.}\{I\leq i\}=\sum_{j=0}^{i} p_j , \tag{3}$$

where the notation [Y] means to get the integer closest Y. The present problem becomes to determine the probability p_i by using the moment statistics of Y. In order to solve this problem, let us introduce the z-transformation P(z) of $\{p_i\}$ $(i=0,1,2,\ldots)$ expressed as follows (Takahashi Y.):

$$P(z)=p_0+p_1z^{-1}+p_2z^{-2}+ \quad +p_mz^{-m}+p_mrz^{-m-1}+p_mr^2z^{-m-2}+$$

$$=p_0+p_1z^{-1}+ \quad +p_{m-1}z^{-(m-1)}+p_m \frac{z^{-m}}{1-rz^{-1}} \tag{4}$$

Here, it must be noticed that the present z-transform is newly defined only for a level axis differing from the original definition of z-transform at a time axis. By the definition of z-transform and its expectation, the following relationship can be derived:

$$P(1)=1 , \quad (-1)^k(z(\quad z(z \, P'(z))' \quad)')'|_{z=1} = \left\langle I^k \right\rangle , \tag{5}$$

where ' and <> denote the differentiation with respect to z and the average operation respectively. By substituting Eq. (4) into Eq. (5) and by letting theoretically derived statistical moments be equivalent to the actually observed statistical moments of Y and taking a value of m adequately, the simultaneous equations with respect to $p_0, p_1, \ldots, p_m, r$ are obtained, especially by taking m=3,4 and 5 and putting from k=1 to k=m in Eq. (5), we have the following simultaneous equations :

(i) case with m=3:

$$p_0 + p_1 + p_2 + \frac{p_3}{1-r} = 1 ,$$

$$p_1 + 2p_2 + \frac{p_3}{(1-r)^2} + \frac{2p_3}{1-r} = \langle Y\rangle ,$$

$$p_1 + 4p_2 + \frac{2p_3}{(1-r)^3} + \frac{3p_3}{(1-r)^2} + \frac{4p_3}{1-r} = \langle Y^2 \rangle \quad ,$$

$$p_1 + 8p_2 + \frac{5p_3}{(1-r)^4} + \frac{6p_3}{(1-r)^3} + \frac{7p_3}{(1-r)^2} + \frac{8p_3}{1-r} = \langle Y^3 \rangle \quad ,$$

$$p_1 + 16p_2 + \frac{24p_3}{(1-r)^5} + \frac{12p_3}{(1-r)^4} + \frac{14p_3}{(1-r)^3} + \frac{15p_3}{(1-r)^2} + \frac{16p_3}{1-r} = \langle Y^4 \rangle \quad .$$

$$\left. \right\} (6)$$

(ii) case with m=4:

$$p_0 + p_1 + p_2 + p_3 + \frac{p_4}{1-r} = 1 \quad ,$$

$$p_1 + 2p_2 + 3p_3 + \frac{p_4}{(1-r)^2} + \frac{3p_4}{1-r} = \langle Y \rangle \quad ,$$

$$p_1 + 4p_2 + 9p_3 + \frac{2p_4}{(1-r)^3} + \frac{5p_4}{(1-r)^2} + \frac{9p_4}{1-r} = \langle Y^2 \rangle \quad ,$$

$$p_1 + 8p_2 + 27p_3 + \frac{6p_4}{(1-r)^4} + \frac{12p_4}{(1-r)^3} + \frac{19p_4}{(1-r)^2} + \frac{27p_4}{1-r} = \langle Y^3 \rangle \quad ,$$

$$p_1 + 16p_2 + 81p_3 + \frac{24p_4}{(1-r)^5} + \frac{36p_4}{(1-r)^4} + \frac{50p_4}{(1-r)^3} + \frac{65p_4}{(1-r)^2}$$
$$+ \frac{81p_4}{1-r} = \langle Y^4 \rangle \quad ,$$

$$p_1 + 32p_2 + 243p_3 + \frac{120p_4}{(1-r)^6} + \frac{120p_4}{(1-r)^5} + \frac{150p_4}{(1-r)^4} + \frac{180p_4}{(1-r)^3}$$
$$+ \frac{211p_4}{(1-r)^2} + \frac{243p_4}{1-r} = \langle Y^5 \rangle \quad .$$

$$\left. \right\} (7)$$

(iii) case with m=5:

$$p_0 + p_1 + p_2 + p_3 + p_4 + \frac{p_5}{1-r} = 1 \quad ,$$

$$p_1 + 2p_2 + 3p_3 + 4p_4 + \frac{p_5}{(1-r)^2} + \frac{4p_5}{1-r} = \langle Y \rangle \quad ,$$

$$p_1 + 4p_2 + 9p_3 + 16p_4 + \frac{2p_5}{(1-r)^3} + \frac{7p_5}{(1-r)^2} + \frac{16p_5}{1-r} = \langle Y^2 \rangle \quad ,$$

$$p_1 + 8p_2 + 27p_3 + 64p_4 + \frac{6p_5}{(1-r)^4} + \frac{18p_5}{(1-r)^3} + \frac{37p_5}{(1-r)^2} + \frac{64p_5}{1-r} = \langle Y^3 \rangle ,$$

$$p_1 + 32p_2 + 243p_3 + 1024p_4 + \frac{120p_5}{(1-r)^6} + \frac{240p_5}{(1-r)^5} + \frac{390p_5}{(1-r)^4}$$
$$+ \frac{570p_5}{(1-r)^3} + \frac{781p_5}{(1-r)^2} + \frac{1024p_5}{1-r} = \langle Y^5 \rangle \quad ,$$

$$p_1 + 64p_2 + 729p_3 + 4096p_4 + \frac{720p_5}{(1-r)^7} + \frac{1080p_5}{(1-r)^6} + \frac{1560p_5}{(1-r)^5}$$
$$+ \frac{2100p_5}{(1-r)^4} + \frac{2702p_5}{(1-r)^3} + \frac{3367p_5}{(1-r)^2} + \frac{4096p_5}{1-r} = \langle Y^6 \rangle \quad .$$

$$\left. \right\} (8)$$

For the latter case, Eqs. (1) and (2) should be replaced to

$$I=[Y] \, , \, Y=\frac{x_0-X}{h} \tag{9}$$

and

$$p_i=1-\text{Prob.}\{I=i\} \, . \tag{10}$$

For the purpose of obtaining the probability distribution of the original random variable, the z-transform P(z) of the discrete level type distribution obtained by employing the above procedure should be changed to the Laplace transform P(s) of the continuous level type probability which is considered as an approximation of the original probability distribution. The following well known property (Sigemasa T.) in the control system theory is adopted to convert the discrete level system to the continuous level system. Now, let us assume that the pulse transfer function of the discrete level system is described as follows:

$$G_p(z) = \frac{b_0+b_1 z^{-1}+b_2 z^{-2}+}{1+a_1 z^{-1}+a_2 z^{-2}+a_3 z^{-3}+} \quad . \tag{11}$$

By approximating the step response of the original continuous level system with broken lines consisting of line segments derived by the points plotted for the step response values of the corresponding discrete level system, the transfer function of the original continuous system is given as

$$G(s) = \frac{e^{\tau s}-1}{\tau s} G_p(e^{\tau s}) \, , \tag{12}$$

where τ is the sampling time. By expanding both the denominator and the numerator of Eq. (12) into power series with respect to s and rewriting it in the form of the numerator 1, we obtain

$$G(s) = \frac{1}{G_0 + G_1 s + G_2 s^2 +} \, , \tag{13}$$

where

$$\left.\begin{array}{l} A_0=1+\displaystyle\sum_{i=1}^{\infty} a_i \, , \quad B_0=\displaystyle\sum_{i=0}^{\infty} b_i \, , \\[2mm] A_k = (-1)^k \frac{\tau^k}{k!} \displaystyle\sum_{i=1}^{\infty} i^k a_i \, , \\[2mm] B_k = (-1)^k \frac{\tau^k}{k!} \displaystyle\sum_{i=1}^{\infty} i^k b_i \, , \end{array}\right\} \tag{14}$$

$$H_0 = A_0 \; / \; B_0 \; , \quad H_k = (A_k \cdot \sum_{i=0}^{k-1} H_i B_{k-i})/B_0 \; , \tag{15}$$

$$G_0 = H_0 \; , \quad G_k = H_k - \sum_{j=2}^{k+1} \frac{\tau^{j-1}}{j \; !} \, G_{k+1-j} \qquad \cdot \tag{16}$$

Therefore, the objective Laplace transform $P(s)$ can be obtained by substituting $P(z)$ into $Gp(z)$ and setting $\tau=1$. The cumulative probability function curve is given as a unit step response of the system described by the transfer function $P(s)$ and is calculated by means of FILT(Fast Inversion of Laplace Transform), which is one of useful methods to perform the inverse Laplace transformation numerically(Hosono T.).

3.0 EXPERIMENTAL CONSIDERATION

The proposed method is applied to the actually measured traffic noise and the music(i.e.,Karaoke) sound. First, we consider measurements of 500 points sampled at every 0.5 second intervals of the traffic noise measured in Hiroshima City. Because there are more rapidly decreasing observation data downward to the lower range than upward to the upper range, Eqs. (1) and (2) are employed. By taking $x_0=43$(dB),$h=3$(dB), we have the following statistical moments:

$\langle Y \rangle = 3.52966, \langle Y^2 \rangle = 13.80654, \langle Y^3 \rangle = 58.56751, \langle Y^4 \rangle = 265.50292,$

$\langle Y^5 \rangle = 1273.24850, \langle Y^6 \rangle = 6413.168903.$

Based on substituting these moments into Eq. (8) and solving it, we find an available solution such as

$p_0 = -0.00414178, p_1 = 0.0498108, p_2 = 0.100316, p_3 = 0.414088,$

$p_4 = 0.203078, p_5 = 0.202336, r = 0.145719.$

By converting $P(z)$ by using Eqs. (13),(14),(15) and (16) we have the following Laplace transform of the estimated pdf :

$$P(s) = \frac{1}{0.999996 + 3.029663 \, s + 3.873767 \, s^2 + 2.5197618 \, s^3 + 0.66155736 \, s^4} \; .$$

The theoretical cdf is given as a unit step response of the system described by this Laplace transform and is easily calculated by means of FILT. Figure 1 shows the results. Here, the theoretically derived cdf is expressed by a solid line and experimentally sampled values of the frequency distribution are expressed by dotted points. We can see the good agreement between the theoretical curve and experimental values.

Next, we examine the music sound (i.e.,Karaoke noise), which is five hundred data of Karaoke music sampled at every 0.5 second intervals Since this distribution has more gentle slope downward to the lower range of level than upward to the upper range, Eqs. (9) and (10) should be used, instead of Eqs. (1) and (2). By taking $x_0=78$(dB) and $h=2$(dB), the statistical moments with the n-th order (n=1,2,...,6) can be concretely calculated as follows:

$\langle Y \rangle = 3.2897 \; , \langle Y^2 \rangle = 12.598325 \; , \langle Y^3 \rangle = 55.30345 \; , \langle Y^4 \rangle = 278.97154,$

$\langle Y^5 \rangle = 1637.78455$, $\langle Y^6 \rangle = 11306.91231$.

By substituting these moments into Eq. (8) and solving it, the following solution can be reasonably chosen as:

$p_0 = 0.0002098, p_1 = 0.047395, p_2 = 0.288364, p_3 = 0.190906,$

$p_4 = 0.359535, p_5 = 0.064399, r = 0.433062.$

By utilizing Eqs. (13) ,(14),(15) and (16), we have

$$P(s) = \frac{1}{0.999999 + 2.789699\, s + 2.9614477\, s^2 + 1.3867435\, s^3}$$

Thus, we have obtained the result shown in Fig.2.
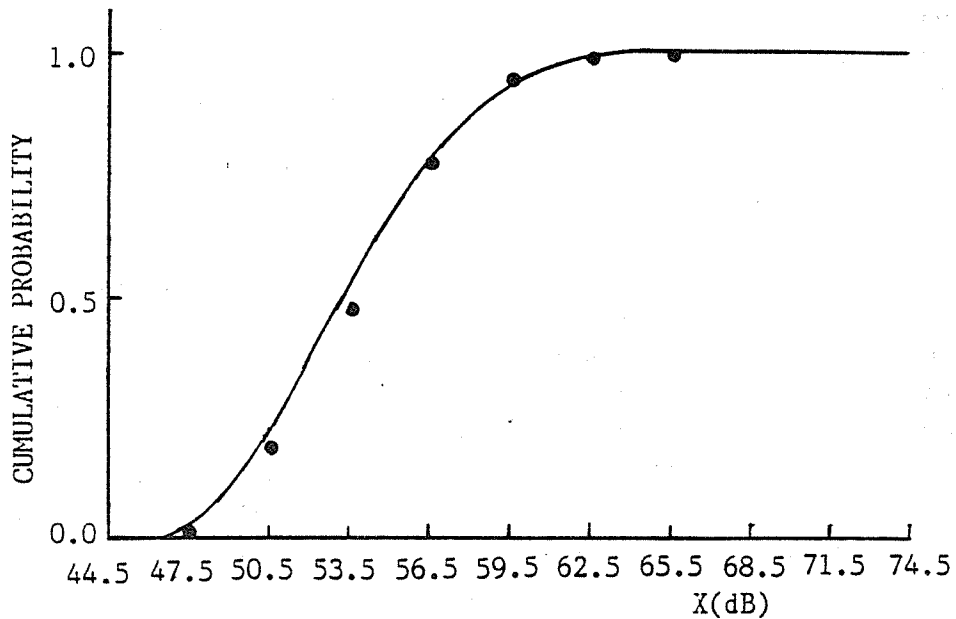
Fig.1 A comparison between the theoretically calculated cdf curve and experimentally sampled values for the traffic noise.
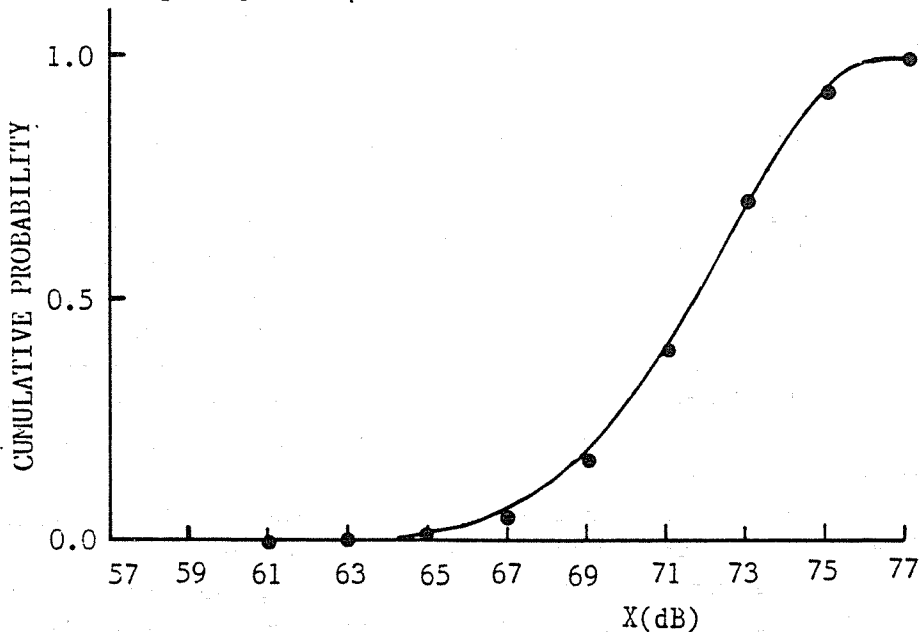
Fig.2 A comparison between the theoretically calculated cdf curve and experimentally sampled values for the music sound(i.e.,Karaoke noise).

The theoretically calculated curve agrees well with experimentally sampled values. In addition, we have attempted to use Eqs.(1) and (2). Then, the overshooting style has been occurred especially in the upper level range.

We have concluded from the experimental results that it is necessary to choose a suitable width of subinterval in order to get an available solution of Eqs. (6),(7) and (8).

4.0 CONCLUSION

For the purpose of estimating the whole probability distribution for the evaluation of the environmental random noise and vibration fluctuating widely and irregularly, a new method has been proposed that the z-transform of the discrete level type probability distribution described by some rational type pulse transfer function expression is determined by letting its statistical moments be equivalent to the statistical moments of the actually observed original data. Furthermore, the z-transform of the discrete level type probability distribution is converted into the form of an equivalent Laplace transform, which is an approximation of the objective pdf, and the corresponding cdf is calculated easily as the step response by using FILT. The proposed method has the advantage of obtaining the probability expression convenient to calculate the compound probability distribution for a sum of two independent random variables. The proposed method has been applied to the actual traffic noise and music sound and it is proved that only employing lower order statistical moments until 5-th or 6-th order is sufficient to estimate a whole probability distribution curve.

REFERENCES

Journals

Hosono T.,Numerical Inversion of Laplace Transform and Some Application to Wave Optics,Radio Science, 16(6),1015,(1981).
Takahasi Y.,Tomizuka M.,Auslender D.M.,Discrete Time Control of Industrial Processes(Finite Time Settling Control Algorithm for Single-Loop Digital Controller),Trans. ASME Journal of Dynamic Systems,Measurement and Control,97(4),354-361, (1975).
Ziegler J.G. and Nichols N.B., Optimum Setting for Automatic Controllers, ASME Trans.,64,759,(1942).

Reports

Sigemasa T.,A New Trial of Converting a Pulse Transfer Function to s-Domain Expression of Low Frequency Characteristics , 20-th SICE Symposium,SICE,19-20 ,(1981).

AN. IDENTIFICATION METHOD FOR THE ACOUSTIC SYSTEMS BASED ON THE HIERARCHICAL
ORTHOGONAL PROJECTION THEOREM AND ITS APPLICATIONS TO THE REVERVERATION TIME
MEASUREMENT

Kazutatsu HATAKEYAMA
Faculty of Engineering, Hiroshima University, Higashi-Hiroshima, Japan.

Mitsuo OHTA
Faculty of Engineering, Kinki University, Higashi-Hiroshima, Japan.

ABSTRACT

 *In this paper, the problem of evaluating the non-stationary acoustic systems
under random background noise of arbitrary distribution type is considered from
the statistical viewpoint. The transient wave forms of stochastic systems are
strongly depend on the initial state as well as the random input and the
background noise of arbitrary distribution type. For removing the effects of
background noise and the errors generated by assuming artificially the initial
values of transient stochastic systems, the orthogonal projection theorem is
introduced as the fundamental rule in the estimation. Thus, by generalizing
the theorem into a new form matched to the actual complexity of various
transient wave forms, a dynamical method of identifying the unknown parameters
of the acoustic systems together with estimating the present and the initial
states has been proposed in the orthogonally expanded series form whose
expansion coefficients reflect various mutual correlations among the present,
initial states and the observation hierarchically. Finally, the validity of
the theoretical method has experimentally confirmed by applying it to the
actual problems of identifying the reverberation characteristics of a room
under random background noise.*

1.0 INTRODUCTION

In general, for designing effectively
the sound systems such as the sound
insulation walls and others, it it
fundamentally important to evaluate
the acoustic characteristics of the
system in the actual measurement
situations. Nevertheless, when
measuring the environmental acoustic
data, the observations show usually
the arbitrarily fluctuating distri-
bution forms apart from the Gaussian
probability functions due to the
diversified statistical causes, the
existence of random background noise
and the complexity of the physical
mechanisms. Then, the statistical
methodologies should be inevitably
introduced for obtaining the correct
parameters of the environmental
acoustic system. One of such
methodologies is the method by Kalman
[Kalman, R.E., & Bucy, R.S.] in the
field of linear filtering and predic-
tion theory.

But the actual phenomena do not
satisfy the idealized situations
which were introduced to derive the
methodologies. For overcoming the
restrictions in the Kalman's method,
various methodologies of generalizing
it had been proposed up to now [Ohta,
M. et al. 1976, 1984]. The non-
linear filters proposed by us [Ohta,
M. et al. 1984] in the orthogonally
expanded expression was shown to give
the reasonable estimates for the non-
Gaussian acoustic systems by utiliz-
ing not only the linear but also the
nonlinear correlation infomations of
phenomena hierarchically.

But the transient acoustic phenomena
such as the reverberation process of
a room strongly depend on the initial
state of the system as well as the
random fluctuations of input and the
background noise. The value of
initial state is not konwn a priori.
It is also difficult to detect the
initial state owing to the existence
of random background noise of arbit-
rary distribution type. By assuming
the initial state, the recursive
estimation algorithms had been deriv-
ed up to now. Then, even if the
estimates of unknown states for the
acoustic systems could be recursively
decided at each time stages in the
systematical forms, the value of
their initial conditions should
always be given artificially. Thus,
the estimated values inevitably
contains a kind of errors due to the
artificially decided boundary
conditions of the filters. For
improving the accuracy of the
estimates more, we should establish
some methodology of determining the
true initial state together with
estimating the unknown state and the
parameters of the systems.

In this paper, from such viewpoint, a
new tirial of identifying the unknown
acoustic parameters together with
estimating the transient wave forms
and the initial states of the non-
stationary acoustic system is pro-
posed by introducing the well-known
orthogonal projection theorem.

More concretely, for improving the
accuracy of the estimates, the
augumented general stochastic model
is introduced by adopting the initial
conditions and the parameters as the
new state variables. Then, in order
to evaluate the effects of noise on
the estimates of augumented state
variable, we firstly pay our atten-
tion to the orthogonal projection
theorem as the fundamental rule in
the estimation. By generalizing the
orthogonal projection theorem into a

new form matched to the hierarchical evaluation of actual complexity of various wave forms and introducing the orthogonally expanded expression of the conditional probability function, a unified estimation algorithm has been established in the series expansion form. Each expansion coefficient in the algorithm reflects successively various statistical informations among the parameters, the present, past states and the observation.

In a special case when considering the Gaussian linear systems, the proposed algorithm for estimating the mean and variance of the unknown state coincides with the well-known algorithm of Kalman's filtering theory.

Finally, the effectiveness of the proposed theory has been experimentally confirmed by applying it to the reverberation time measurement under random background noise. By utilizing the linear and nonlinear correlations in the algorithm, the proposed method is experimentally proved to give more superior estimates than the conventional methods.

2.0 THEORETICAL CONSIDERATIONS

2.1 Formulation of the Stochastic Acoustic Systems
The signals of the environmental acoustic systems are originally generated as the fluctuations of the air and measured on an energy scale, which show the typical non-Gaussian statistical properties. Then, based on the additive property of energy quantities and their physical mechanisms, the acoustic signal x_k and its noisy observation y_k could be formulated with use of the following general system and observation equations :

$$x_{k+1} = F_k(x_k, u_k; \theta), \qquad (1)$$

$$y_k = G_k(x_k, v_k), \qquad (2)$$

where u_k denotes the transient input, whose non-stationary statistics can be give a priori. θ is the parameter vector characterizing the system function $F_k(\cdot)$. $F_k(\cdot)$ and $G_k(\cdot)$ are a priori known analytic functions. When considering the decibel data, an observation mechanism of logarithmic type should be expressed in Eq.(2). The background noise v_k on an energy scale is usually generated from the other sources and shows the statistical independency with the objective signal x_k.

For the transient phenomena, x_k is strongly depend on its initial value x_0. The initial state x_0 is usually decided artificially from the outside of the system and not known in the actual measurement situation. Then, when identifying the unknown systems, the errors due to the artificially chosen boundary condition of filters should be removed as well as minimizing the effects of background noise.

For identifying the time-invariant parameter θ accurately, it is necessary to estimate the time-varying transient wave form x_k and its initial state x_0 simultaneously. Then, the system equations on θ and x_0 should be foumulated :

$$X_{1k+1} = X_{1k}(\equiv x_0), \qquad (3)$$

$$X_{2k+1} = X_{2k}(\equiv \theta), \qquad (4)$$

$$X_{3k+1}(\equiv x_{k+1}) = F_k(X_{3k}, u_k; X_{1k}, X_{2k}), \qquad (5)$$

$$y_k = G_k(X_{3k}, v_k), \qquad (6)$$

where $\mathbf{x}_k(\equiv [X_{1k}, X_{2k}, X_{3k}]^\tau)$ is the augmented state variable at a time

342

stage k. By introducing the stochastic model with the augumented state variable, the errors due to the artificially chosen initial state could be minimized together with removing the effects of the background noise on the estimates.

2.2 The Nonlinear Siganl Processing Method Based on the Orthogonal Projection Theorem

In the actual situation of measuring the transient fluctuations of environmental acoustic signals, the objective signals show the non-stationary and non-Gaussian properties owing to the diversified statistical causes of fluctuations. Also, their observations can be given under the strong contamination by undesirable random background noise.

From the information theoretical viewpoint in evaluating the non-Gaussian phenomana, the linear and nonlinear correlation between the unknown state and the noisy observations should be detected and utilized as much as possible for obtaining the reasonable estimate. Here, for evaluating the individual effects of the noise and the artificial boundary conditions for filters, we will paying our attention to the least squares type error criterion function J conditioned by the past and present observation sequence $Y_k (\equiv \{y_1, y_2, \cdots, y_k\})$:

$$J = <(x_k - \hat{x}_k)^2 | Y_k>. \qquad (7)$$

As is well-known, the optimal estimate $\hat{x}_k$ which minimizes the conditioned error criterion J in Eq.(7) can be given as the conditioned mean value: $\hat{x}_k = <x_k | Y_k>$, without depending the probability distribution forms of random process. That

is, the optimal estimate can be given as the projected value of X_k onto the observation space so as to minimize the estimation error J.

Then, by rewriting the expectation operation $<\cdot | Y_k>$, the necessary and sufficient condition for the optimal estimate $\hat{x}_k$ could be proved that $\hat{x}_k$ should satisfy the following orthogonal projection theorem :

$$<(x_k - \hat{x}_k)y_k | Y_{k-1}> = (x_k - \hat{x}_k, y_k) = 0. \qquad (8)$$

Under the assumption of Gaussian and linear properties for the phenomena, $\hat{x}_k$ can be calculated with the linear function of the innovation process ν_k $(= y_k - <y_k | Y_{k-1}>)$. Nevertheless, the innovation process can not always exist explicitely for arbitrary non-Gaussian processes.

When considering the non-Gaussian signal, we should sometimes evaluate not only the mean and the variance but also the higher order statistics of x_k. Based on the Weierstrass's interpolation theorem, the arbitrary statistics can be expressed by the expected value of a polynomial function. Then, firstly by approximating the arbitrary statistics on x_k with use of a polynominal function $f(x_k)$ of order N, we would estimate $\hat{f}(x_k) (= <f(x_k) | Y_k>)$ by evaluating newly the statistical independency of the estimation error $f(x_k) - \hat{f}(x_k)$ in the same way as Eq.(8).

Next, for grasping the statistical independency of estimation error for the non-Gaussian processes, we will focus on the fact that the optimal estimate can be given by evaluating the orthogonality in Eq.(8) with use of the linear correlation between the estimation error $x_k - \hat{x}_k$ and the observation y_k. The estimation

problem under consideration is how to separate the observation space $\{y_k\}$ into the two sub-spaces independent and dependent with the estimation error $f(x_k)-\hat{f}(x_k)$.

Then, the following new expression of the orthogonal projection theorem can be finally obtained by generalizing Eq. (8) :

$$(f(x_k)-\hat{f}(x_k),\ \xi_k)=0,$$

for arbitrary observation $\xi_k \in \{y_k\}$

$$(9)$$

where $\hat{f}(x_k)$ denotes the optimal estimate of $f(x_k)$, and ξ_k means the arbitrary element in the observation space $\{y_k\}$ composed with the possible observation y_k. The optimal estimate $\hat{f}(x_k)$ can be determined with use of the correlations between the estimation error and the arbitrary element in observation space so that the error is orthogonal to the observation space.

The arbitrary statistics of possible observation y_k can be uniformly evaluated a priori with use of the conditional probability function $P(y_k|Y_{k-1})$. So the evaluation of the correlations with ξ_k in Eq. (9) could be reduced to the correlations with the arbitrary function $g(y_k)$ in the observation space characterized by $P(y_k|Y_{k-1})$. For expressing the correlations in Eq. (9) between the estimation error and the arbitrary function $g(y_k)$ in the unified form, it is a good plan to expand $P(y_k|Y_{k-1})$ hierarchically by introducing the fundamental probabiblity function $P_0(y_k|Y_{k-1})$ and its associated orthogonal polynomials $\{\phi_m(\cdot)\}$. From the viewpoint of rapid convergence and steadiness, the fundamental probablility function $P_0(y_k|Y_{k-1})$ should be selected to describe the dominant probability portion of y_k or

as a fundamental probability function in the analysis :

$$P(y_k|Y_{k-1})=P_0(y_k|Y_{k-1})\sum_{m=0}^{\infty}\alpha_m\psi_m(y_k),$$

$$(10)$$

$$\alpha_m=<\phi_m(y_k)|Y_{k-1}>$$

$$=<\phi_m(G_k(x_k,v_k))|Y_{k-1}>,\quad (11)$$

where the differences of the phenomena from the fundamental probability function are reflected hierarchically in each expansion coefficient α_m.

Under the assumption of completeness of Eq. (10), the observation space can be spanned by the orthogonal function $\{\phi_m(y_k)\}$. Then, the arbitrary polymonial function $g(y_k)$ in the observation space can be expressed as follows :

$$g(y_k)=\sum_{m=0}^{M}\beta_m\ \phi_m(y_k),\quad (12)$$

where the coefficient β_m is an arbitrary parameter with arbitrary order M intorduced for expressing the arbitrary element in the observation space.

Then, by substituting Eq. (12) into Eq. (9) and cosidering the arbitrariness of β_m, the generalized orthogonal projection theorem can be expressed as follows :

$$(f(x_k)-\hat{f}(x_k),\phi_m(y_k))=0.$$

for $m=0,1,2,\cdots$. $\quad (13)$

That is, by introducing the orthogonal series expression for the conditional probability function, the statistical independency of estimation error with arbitrary observation could be evaluated hierarchically by using the conditional correlations with the orthogonal polynomianls of arbitrary order.

344

Also, by considering the fact that the estimate $\hat{f}(x_k)$ is an element in the observation space $\{y_k\}$, the estimate $\hat{f}(x_k)$ under considerarion can be expressed with use of these orthogonal functions :

$$\hat{f}(x_k) = \sum_{m=0}^{N} \kappa_m \psi_m(y_k), \qquad (14)$$

where the coefficient κ_m should be determined so that $\hat{f}(x_k)$ satisfy the concrete expression of the generalized orthogonal projection theorem in Eq. (13). By substituting Eq. (14) into Eq. (13), the coefficient κ_m can be determined by solving the simultaneous linear equations of Eq. (13).

When applying Eq. (13) to the actual data, we should consider the reliability of experimental observations. Then, the following practical algorithm of deciding the coefficients κ_m could be derived by omitting the higher order statistical terms over certain N-th order :

$$[\kappa_0, \kappa_1, \cdots, \kappa_{N-1}]^T = [a_{ij}]^{-1}[b_{ij}], (15)$$

where $[a_{ij}]$ and $[b_i]$ are a $N \times N$ dimensional matrix whose (i,j) element is a_{ij} and a N-dimensional vector with the i-th element b_i $(1 \leq i, j \leq N)$:

$$a_{ij} \equiv (\psi_{i-1}(y_k), \psi_{j-1}(y_k))$$

$$= \sum_{m=0}^{N} \alpha_m I_{i-1,j-1,m}, \qquad (16)$$

$$b_i \equiv (f(x_k), \psi_{i-1}(y_k))$$

$$= <f(x_k)\psi_{i-1}(y)|Y_{k-1}>$$

$$= <f(x_k)\psi_{i-1}(G_k(x_k,v_k))|Y_{k-1}>, \qquad (17)$$

where $I_{ijm} \equiv \int \psi_i(y_k) \cdot \psi_j(y_k) \cdot \psi_m(y_k) \cdot P_0(y_k|Y_{k-1})y_k$. Finally, the estimation algorithm (Eq. (14)) could be decided at each time stage k.

Then, by combining Eqs. (14) and (15) with the prediction algorithm for arbitrary polynomial fucntion $f(x_{k+1})$:

$$<f(x_{k+1})|Y_k> = <f(F_k(x_k,u_k))|Y_k>, \qquad (18)$$

the recursive algorithm of identifying the acoustic system together with estimating the present and initial states of non-Gaussian type can be finally realized.

In a simplified special case when the process has the linearity with Gaussian variables and known initial state, the proposed algorithms for estimating the mean and variance could be shown to coincide with the well-known algorithms by Kalman.

2.3 Derivation of the Practical Algorithm for the Non-Gaussian Acoustic systems

By adopting the conditional probability function $P(y_k|Y_{k-1})$ as the artificial probability function $P_0(y_k|Y_{k-1})$ in Eq. (13), the concrete expression of proposed estimation algorithm in Eqs. (13) and (14) can be realized as follows :

$$\hat{f}(x_k) = <f(x_k)|Y_{k-1}> + \sum_{m=1}^{N} \kappa_m \psi_m(y_k), \qquad (19)$$

where $\kappa_m = <f(x_k)\psi_{m-1}(G_k(x_k,v_k))|Y_{k-1}> = \int f(x_k)\psi_{m-1}(G_k(x_k,v_k))P(x_k|Y_{k-1})P(v_k)dx_k dv_k$. Here, the conditional probability function $P(y_k|Y_{k-1})$ and its associated orthogonal polynomial $\psi_m(y_k)$ can be calculated by introducing the statistical Hermite series probability expression and the Schmit's orthogonalization technique as follows :

$$P(y_k|Y_{k-1}) = N(y_k;y^*_k, \Omega_k)\sum_{n=0}^{N} \gamma_n$$

$$\cdot H_n((y_k-y^*_k)/\Omega_k^{1/2}), \qquad (20)$$

$$y^*_k = <y_k|Y_{k-1}>$$

$$= \langle F_K(X_{3K}, u_K; X_{2K}) | Y_{K-1} \rangle, \quad (21)$$

$$\Omega_K = \langle (y_K - y^*_K)^2 | Y_{K-1} \rangle$$
$$= \langle (F_K(X_{3K}, u_K; X_{2K}) - y^*_K)^2 | Y_{K-1} \rangle, \quad (22)$$

$$\gamma_n = \langle H_n((y_K - y^*_K)/\Omega_K^{''2}) | Y_{K-1} \rangle / n!$$
$$= \langle H_n((F_K(X_{3K}, u_K; X_{2K}) - y^*_K)/\Omega_K^{''2}) | Y_{K-1} \rangle / n!, \quad (23)$$

$$\psi_m(y_K) = \sum_{n=0}^{m} \lambda_{mn} H_n((y_K - y^*_K)/\Omega_K^{''2}), \quad (24)$$

where λ_{mn} ($n=0,1,\cdots,m$) denotes the Schmit's orthogonalization coefficient. Then, by using the predicted mutual correlation statistics $\langle X_{1K}^i X_{2K}^j X_{3K}^r | Y_{K-1} \rangle$ on the multi-dimensional state variable $\mathbf{x}_K$ and the a priori known statistics on v_K, the estimation algorithm can be realized. (Other concrete expressions are omitted owing to the page-limitation).

3.0 Experimental Considerations

For confirming the validity and the effectiveness of the proposed computer aided algorithm, the actual problem of measuring the reverberation process and the reverberatin time under the contamination of random background noise is considered.

Based on the discrete expression of Sabine's reverberation equation and the additivity of energy quantities, the following system and observation equations can be formulated for the initial state x_0 of averaged energy in a room and the reverberation parameter F :

$$X_{1K+1} = X_{1K} (\equiv x_0), \quad (25)$$

$$X_{2K+1} = X_{2K} (\equiv F = \exp\{-13.8\Delta/T\}), (26)$$

$$y_K = X_{1K} \cdot \{F_{2K}\}^K + v_K, \quad (27)$$

where y_K denotes the discrete noisy observation at a time k and T

denotes the unknown reverberation time (Δ: sampling interval).

Figure 1 shows the schematic drawing of experimental arrangement. The white noise is used as the background noise in measuring the reverberation time T (250 Hz, Δ=0.1 s).

In Figs. 2 and 3, the estimated results by proposed algorithm are shown in several cases of adopting various values of initial estimates of x_0 and F. As the results by Kalman filter give the biased esties, the proposed mehtod gives the reasonable estimates of x_0 and T. Then, the validity of our method could be partly confirmed.
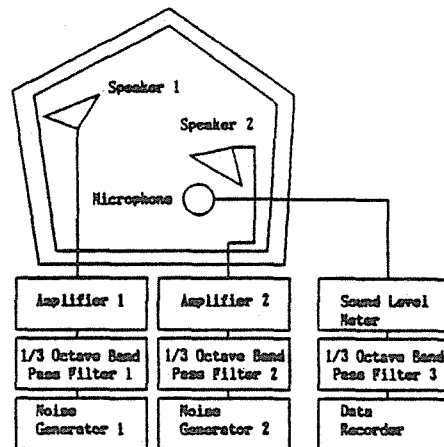
Fig.1 Schematic drawing of experimental arrangement.

4.0 Conclusions

This paper describes a new attempt at dynamical estimation for transient acoustic systems under random background noise.

By generalizing the orthogonal projection theorem, a recursive state estimation algorithm for the non-

Gaussian process was proposed with the algorithm of estimating the initial state of the system. Finally, the validity of the method is experimentally confirmed.

But the research is at an early stage of study. So there remain many future problems such as : how to truncate the higher order terms in the algorithm by considering the reliability of observed data in the actual measurement situation, or how to derive the more simplified algorithm based on the proposed method.

Fig.3 A comparison between theoretically estimated reverberation curves and experimentally observed points. The observed data contaminated by random background noise are marked as (O)(250 Hz) and true values of reverberation process x_k are marked as (●). Theoretical curves are lined as (—) by our method and as (----) by Kalman's method ($F_0=0.6$).
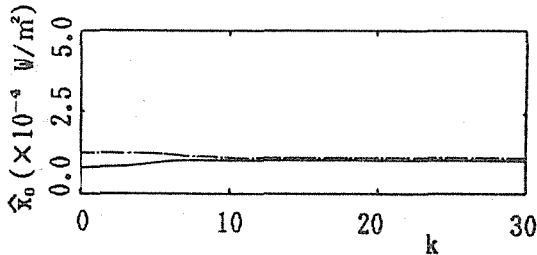
a) Estimated results of x_0.
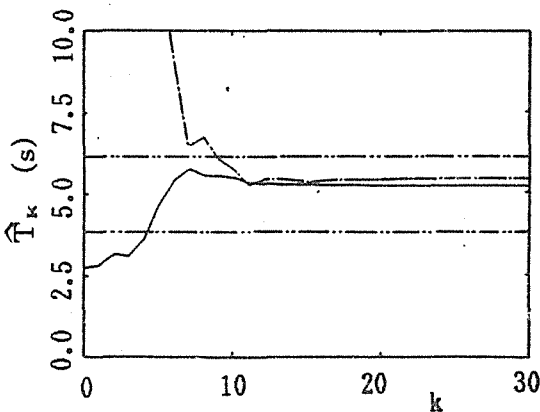
b) Estimated results of T.

Fig.2 Estimated results of initial state x_0 of reverberation process and reverberation time T of a room. The theoretical estimates are lined as (— :x_0 =79 dB, $F_0=0.6$, —·—·—:x_0=81 dB, $F_0=0.9$) by proposed method under background noise (250 Hz). The tolerance ranges of T are lined as (—··—··—).

Reference
Kalman, R.E., and Bucy, R.S. : New Results in Linear Filtering and Prediction Theory, J. Basic Engineering, Ser.D, Vol.83, 1961, pp.95.

Ohta, M., et al. : General State Estimation Algorithm for Quantized Noisy Systems from a System-Theoretical Viewpoint with Special Reference to Room Acoustics, J. Sound and Vibration, 94 (1984) pp.573.

Ohta, M., et al. : Some Unified Methods in Multivariable Linear Filtering and Prediction Problems by use of the Expansion Form of Bayes' Theorem, Proc. 26th Japan National Congress for Applied Mechanics, 26 (1976) pp.383.

347

THE STUDY OF MULTISTAGE SHOCK RESPONSE SPECTRUM

Pang Jian   Shen Rongying   Yan Jikuan

Institute Vibration, Shock and Noise Research
Shanghai Jiao Tong University
Shanghai, 200030, China

ABSTRACT

Due to advantage of Shock Response Spectrum (SRS) analysis, such as able to describe quantitatively and able to reproduce shock environment in laboratory, this method is widely used. However, the study is mainly concentrated on single-stage isolation system. In this paper SRS analysis to multistage isolation system is developed and some formulae are derived. Take a two-stage isolation system as an example, SRS diagrams are given out. The technology of simulation is used to verify SRS analysis. The results show that SRS analysis is in compliance with simulation calculation, and it can be used to guide shock isolation of multistage isolation system.

1. INTRODUCTION

SRS analysis has been widely used in shock isolation problems. So far the application of SRS analysis has been limited to single-stage isolation system. To a single-stage isolation system, in which SRS only depends on shock pulse shape that is a function of frequency. A multistage shock isolation is much more complex than a single-stage one. SRS of multistage isolation system depends not only on shock pulse shape but also has relation with the construction parameters of isolation system. A certain shock pulse doesn't result in certain SRS. However, to a fixed multistage isolation system in which stiffness and mass are defined, SRS can be obtained.

2. THEORETICAL MODEL

Mechanical model of multistage isolation system is shown in figure 1. The system is subjected to base shock pulse. Assumptions are as followings: (1) Only vertical pulse excitation is considered. (2) All mass are rigid bodies. (3) Damping is neglected. (4) All springs are linear.

The motion equation of the system can be written as

$$\mathbf{M}\ddot{X} + \mathbf{K}X = -\mathbf{M}\ddot{Z} \tag{1}$$

where

M, K — Mass and stiffness matrix of system respectively.

$X, \ddot{X}$ — displacement and acceleration of mass relative to base respectively.

$\ddot{Z}$ — acceleration of base shock.

3. SHOCK RESPONSE SPECTRUM ANALYSIS

3.1. SRS of single-stage isolation system

A single-stage mass spring system is shown in figure 2. Absolute acceleration SRS is expressed as follows

$$A(\tau/T) = max(\frac{\ddot{y}(t)}{\ddot{z}_0}) \tag{2}$$

where

τ — shock pulse time.

T — natural period.

$\ddot{y}$ — absolute acceleration of mass.

$\ddot{z}_0$ — maximum acceleration of base shock.

Relative displacement SRS is given as

$$R(\tau/T) = max(\frac{x(t)}{z_0}) \tag{3}$$

where z_0 — maximum displacement of base shock pulse.

SRS is divided into initial SRS and residue SRS. Initial SRS is defined when maximum response appears within shock pulse time, and residue SRS is defined when maximum response appears after shock pulse.

3.2. SRS analysis of multistage isolation system

If Φ is the modal matrix for non-damped system, i.e., $\Phi^T M \Phi = diag(m_i)$, $\Phi^T K \Phi = diag(k_i)$, $G = -\Phi^T M$ and $X = \Phi q$, the motion equation of multistage isolation system can be decoupled and has the following form

$$diag(m_i)\ddot{q}_i + diag(k_i)q_i = \ddot{z}_i \tag{4}$$

where $\ddot{z}_i = \sum_{j=1}^n G_{ij}\ddot{Z}$.

As a result, the original coupled equations excited by $\ddot{Z}$ have been transformed to uncoupled equations excited by $\ddot{z}_i$. The transient response solution is obtained in closed form in terms of $\ddot{z}_i$. Then the resulting values of q_i, $\dot{q}_i$ and $\ddot{q}_i$ are transferred back to the original coordinates. Therefore, SRS of multistage isolation system can be obtained by means of SRS of single-stage isolation system.

3.2.1 Relative displacement SRS of multistage isolation system

Relative displacement SRS of ith mass is

$$R_i = max(\frac{x_i}{z_0}) \qquad (5)$$

in which $x_i = \sum_{j=1}^{n}(\phi_{ij}q_j)$. Assume that all $q_j(j = 1, 2, ..., n)$ have same phase, thus

$$max(x_i) = \sum_{j=1}^{n}[\phi_{ij}R\frac{z_0}{M_i}\sum_{j=1}^{n}G_{ij}] \qquad (6)$$

Desired SRS is obtained

$$R_i = \frac{max(x_i)}{z_0} = \frac{R}{M_i}\sum_{j=1}^{n}[\phi_{ij}\sum_{j=1}^{n}G_{ij}] \qquad (7)$$

3.2.2 Absolute acceleration SRS of multistage isolation system

Absolute acceleration SRS of ith mass is

$$A_i = max(\frac{\ddot{y}_i}{\ddot{z}_0}) \qquad (8)$$

where

$\ddot{y}_i = \sum_{j=1}^{n}\phi_{ij}\ddot{p}_i - \sum_{j=1}^{n}\phi_{ij}\ddot{z}_i + \ddot{z}$.

$\ddot{p}_i$ — absolute acceleration response of ith mass of uncoupled system.
Therefore

$$A_i = \frac{(A-1)}{M_i}\sum_{j=1}^{n}[\phi_{ij}\sum_{j=1}^{n}G_{ij}] + 1 \qquad (9)$$

Equation (7) and (9) give out the predicted relative displacement and absolute acceleration SRS respectively.

4. EXAMPLE AND ANALYSIS

. Take a two-stage isolation system as an example, see figure 3, in which: $k1 = 56000kg/cm$, $k2 = 53100kg/cm$, $m1 = 29.5kg/cm$ and $m2 = 31.0kg/cm$. Half-sine pulse is adapted as shock pulse excitation.

Figure 4–6 display relative displacement, initial acceleration and residue acceleration SRS respectively.

The displacement between two masses $(x_1 - x_2)$ and displacement between the lower mass and the base are considered in engineering. Figure 4 shows that $(x_1 - x_2)$ is much smaller than x_2. Therefore, x_2 is the major factor to cause system damage, which should be controlled seriously.

Figure 5 shows that the acceleration of the upper mass is smaller than that of the lower mass within isolation region $(\tau/T << 1)$ whereas the acceleration of upper mass is lager than that of lower mass within amplification region. In engineering, shock pulse time is very short that usually in several milliseconds,

and the natural period of isolation system (T) is always rather long, and τ/T is small enough so that the shock response is in isolation region. When the system is subjected to shock pulse, shock effect on the upper mass is smaller than that on the lower mass and also is smaller than that of a single-stage isolation system. Generally, the upper mass is a machine or an equipment, therefore an effective shock isolation is obtained by means of two-stage isolation system.

Figure 6 gives out the residue acceleration SRS that also shows the same results with the initial acceleration SRS within isolation region, but the acceleration of the upper mass is larger than that of lower mass when τ/T is at a medium region.

The simulation initial acceleration SRS is shown in figure 7 that is in compliance with theoretical SRS in trend and magnitude satisfactorily.

5. CONCLUSIONS

From above investigation some conclusions can be drawn

1. SRS analysis is a useful and convenient method to analyze shock response of multistage isolation system. For a given shock excitation, the resulting relative displacement and absolute acceleration of every stage can be obtained from the shock spectrum diagram.

2. Simulation calculation shows that the above multistage SRS analysis is available.

6. REFERENCES

[1] F.C.Nelson, The response spectrum method of solution for displacement excitation. The Shock and Vibration Bulletin, May, 1981

[2] J.E.Ruzicka, Passive shock isolation, Part II. J.S.V. September, 1970.

[3] C.Mansuso, F.Saclchi, Main propulsion diesel generator sets with acoustics and double resilient mounting for low noise application. Shipboard Acoustics Proceeding, 1986, The Netherland.

[4] C.M.Harris and C.E.Crede, Shock and vibration handbook. McGraw-Hill, 1976.
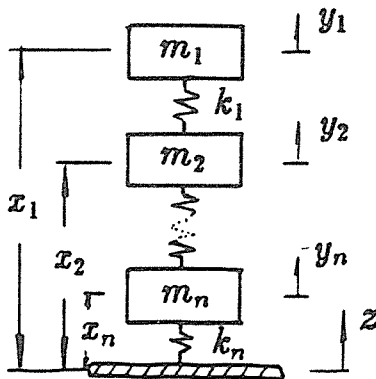
Figure 1: Multistage isolation system
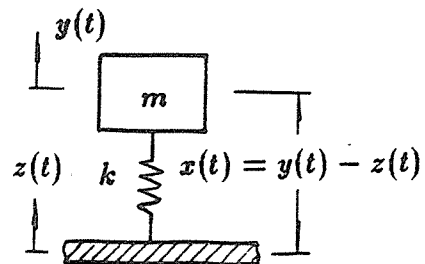
Figure 2: Single stage isolation system
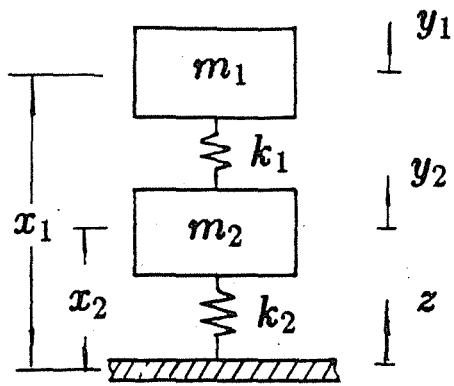
Figure 3: Double stage isolation system
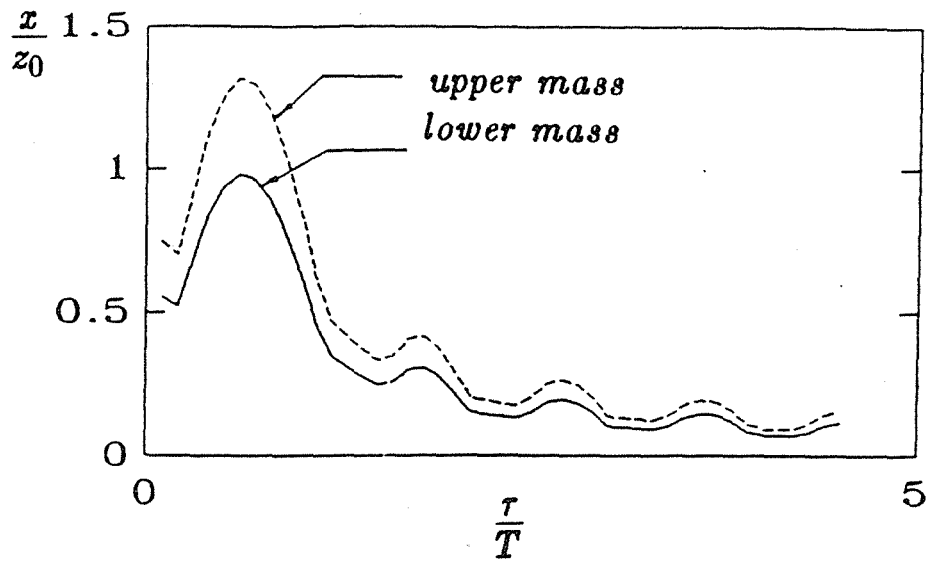
Figure 4: Relative displacement shock response spectrum
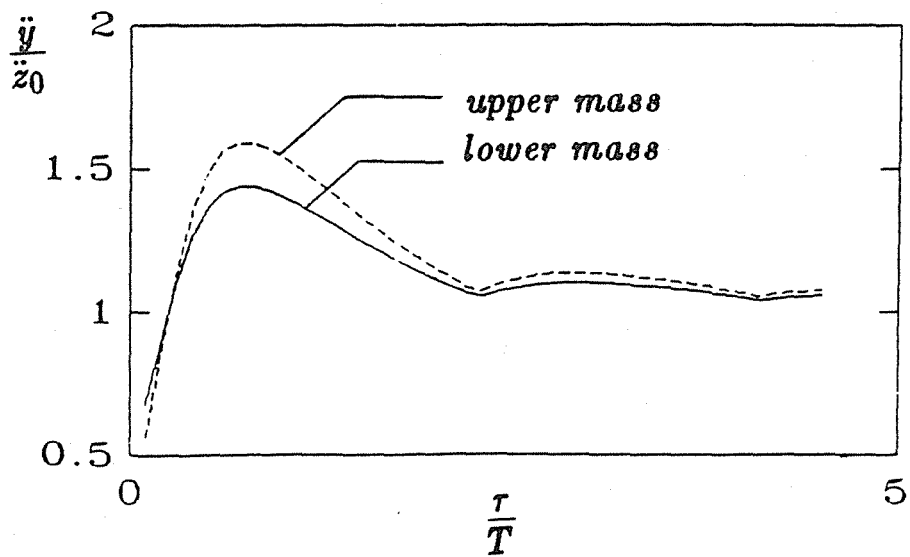
Figure 5: Initial acceleration shock response spectrum
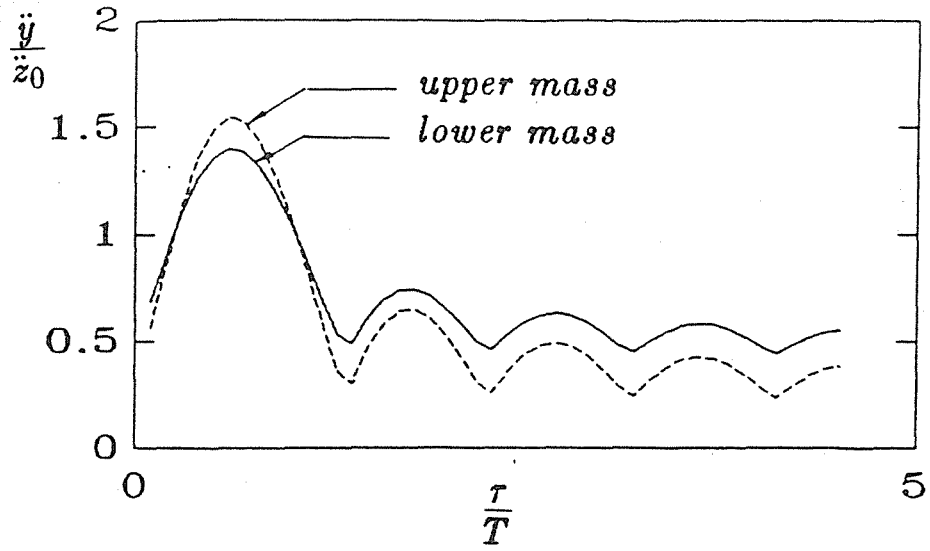
Figure 6: Residue acceleration shock response spectrum
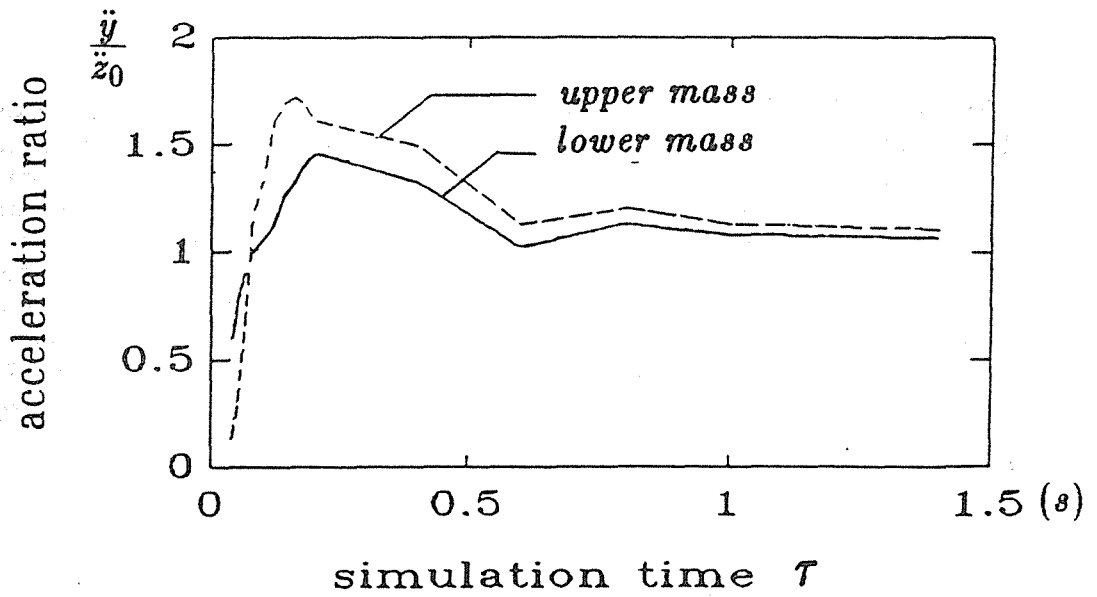
Figure 7: Simulation initial acceleration shock response spectrum

NON-STATIONARY CHARACTERISTICS OF NOISE AND BEARING VIBRATION OF HYDRAULIC TURBINE AT A TRANSITIONAL STAGE OF ROTATION

Yoshiaki Takakuwa
Faculty of engineering, Hiroshima Denki Institute of Technology
Japan

Mitsuo Ohta
Faculty of engineering, Kinki University
Japan

Hideo Minamihara
Faculty of engineering, Hiroshima Denki Institute of Technology
Japan

Masafumi Nishimura
Faculty of engineering, Hiroshima Denki Institute of Technology
Japan

ABSTRACT This paper describes the basic trial of detecting the malfunction of hydraulic turbine and journal bearing of the hydropower station at the early stage in the beginning of the operation by the use of fundamental information of noise and vibration as the basic state information on the turbine. The background of this study is based on the actual situation of hydropower station. In general, though the trouble of hydraulic turbine scarcely occurs, once some trouble arise, there is the danger to develop rapidly into the grave failure such as the damage of journal bearing. Further, it is pointed out that the malfunction of hydraulic turbine rather occurs at the stage of transitional rotation after the operation start than at the steady state. In spite of this indication, because of the difficulty of monitoring the turbine which is installed in the violent water stream, and also because of the difficulty of analyzing the non-stationary characteristics of noise and vibration, almost no practical method detecting the malfunction of the turbine during the transitional stage is actually used.
In this paper, first, the non-stationary characteristics of noise and bearing vibration are considered in relation to the speed rise of hydraulic turbine after the rotation start. Next, the continuous FFT analyses on noise and vibration are discussed. From these results, the non-stationary characteristics of noise and vibration at normal state after starting the operation are estimated to be stable, even though the transitional phenomena are extremely non-stationary, and their characteristics are clearly shown in closed relation to the transitional rise of turbine rotation introducing a simple model of turbine generator. Finally, a practical method monitoring the turbine state and a clue to detect the malfunction of the turbine at the transitional stage in the beginning of operation start are proposed.

1.0 INTRODUCTION

In general, the failures owing to the hydraulic turbine are not so frequent at the hydropower station. However, when a grave machinery failure such as the damage of journal bearing arises, it is sometimes originated from the troubles of hydraulic turbine. In addition, some of the small hydropower stations are operated by the remote control as the unmanned station for economization. Needless to say, the remote control operation system must properly based on the telemetering and monitoring systems which provides the method of malfunction detection. Therefore, the monitor and the detection of malfunction of the turbine is one of the most important problem to operate the turbine generator safely. Nevertheless, as is well-known, the direct state sensing of turbine, which is installed in a runner housing with the violent water stream while operation, is quite difficult. Consequently, it is the real situation that a periodical inspection or a routine checkup of the turbine by skilled workers is indispensable especially in the remote controlled station to avoid unexpected accident. From these facts, the method how to monitor the turbine and the journal bearing effectively is still not established and left to study as one of the important problems.

Concerning the detection of mechanical malfunction of turbine generator for the steady state, the following methods are well-known; (a) detection of the abnormal temperature rise of bearing metal and lubricating oil, (b) detection of the abnormal level of acoustic noise and vibration and/or their FFT spectrums, (c) evaluation of the statistical information on journal displacement and/or the prediction error using the AR model (Ogino T. *et al.*) and (d) the AE techniques (Sato I. *et al.*). On the other hand, it is pointed out that the accident of turbine generator occurs rather at the stage of transitional rotation after the operation start than at the steady state of rated operation (Hosoya Y. *et al.*). However, almost no methods is practically used for the non-stationary stage of turbine from the operation start to the rated speed, excepting few methods monitoring the temperature rise. In this respect, it is strongly required to study the effective method detecting the malfunction of turbine or journal bearing at an early stage of transitional rotation after the operation start.

Under the background above, this paper describe a basic study about the non-stationary characteristics of noise and journal vibration of the hydraulic turbine, focusing the transient stage after the operation start. The results show a clue to establish the method detecting the malfunction of turbine and journal bearing at an early stage. There is much left to study about the confirmation of the clue to the malfunction detection of actual failure.

2.0 THEORETICAL BACKGROUND

2.1 Observation of Noise and Vibration In this study, the noise and vibration are focused as the basic state information on the hydraulic turbine and the journal bearing. First, let us consider the difference of the physical characteristics between the noise and the vibration by citing a simple model of well-known circular plane surface sound source. Now, let $\dot{Z}_r$ be the radiation impedance of this sound source, then the impedance can be expressed by the following well-known equation:

$$\dot{Z}_r\left(= \frac{\dot{F}}{V_0}\right) = \pi a^2 \rho_0 c \left[\left\{ 1 - \frac{J_1(2ka)}{ka} \right\} + \frac{S_1(2ka)}{ka} \right] = R_r + jX_r , \qquad (1)$$

$$R_r \equiv \pi a^2 \rho_0 c \left[1 - \frac{J_1(2ka)}{ka} \right] , \qquad X_r \equiv \pi a^2 \rho_0 c \frac{S_1(2ka)}{ka} , \qquad (2)$$

where $\dot{F}$ is the reactive force of air, $\dot{V}$ is the vibration velocity of surface source, a is the radius of source, ρ_0 is the density of air, c is the sound velocity, $k(= \omega/c, \omega$: angular frequency) is the phase constant, $J_1(2ka)$ is the Bessel function of 1st kind and order 1 and $S_1(2ka)$ is the Struve function of order 1. It is well-known that the following approximations are easily found for the low $(ka < 1)$ and high $(ka > 5)$ frequency regions:

$$R_r \simeq \frac{\pi\rho_0 c}{2c^2}a^4\omega^2, \qquad X_r \simeq \frac{8\rho_0}{3}a^3\omega \qquad (ka < 1), \qquad (3)$$

$$R_r \simeq \pi\rho_0 ca^2, \qquad X_r \simeq 0 \qquad (ka > 5). \qquad (4)$$

The hydraulic turbine generator is, of course, not so simple, but the basic relation between the noise and the vibration can be considered by the model. These equations show that the information on a sound noise is not always directly related to a vibrating body, but is transmitted by the air reflecting its physical characteristics and is also related to the surface area of the body. On the contrary, the information on an acceleration vibration of the object is directly related to the force applied to one. Noticing this fact, it is expected that another important information on the turbine and the journal bearing will be obtained if the difference between the noise and the vibration observed at the same time is carefully analyzed.

2.2 Input Torque and Acceleration of Rotation   Next, the rotation speed is also focused as another basic state information on the hydraulic turbine and the journal bearing. Because, the non-stationary stage of turbine generator, which has the large moment of inertia, is characterized by the speed and the acceleration of rotation. Now, let us consider the equation of a simple model of rotational motion of the turbine generator, then the input torque T is easily expressed as the following well-known equation:

$$T = J\frac{d\omega}{dt} + B\omega + L, \qquad (5)$$

where J is the moment of inertia,, B is the coefficient of viscosity, L is the load torque, ω is an angular velocity and t is a time. When the no load torque and constant input torque are assumed during some accelerating period after the operation start, the viscosity coefficient B and the input torque can be estimated by the following relation:

$$\frac{d\omega}{dt} = -\frac{B}{J}\omega + \frac{T}{J}, \qquad (6)$$

where the moment of inertia J is previously known, and the speed ω and the acceleration $d\omega/dt$ are measured experimentally. Hereupon, if there exist some components of noise and the vibration that are directly proportional to the input toque, they can be analyzed by using equation (5) comparing the actually observed speed characteristics. That is, if it is the case, the non-stationary characteristics of noise and vibration become more clearly related to the rotation speed.

3.0 EXPERIMENTAL METHOD

In order to examine the fundamental characteristics of acoustic noise and bearing vibration of the hydraulic turbine generator at the beginning of the operation start, the experiments have been made on a turbine generator at a hydropower station where two turbine generator of the same type (the vertical shaft single runner single discharge spiral Francis turbine generator) were installed. During the experiments, the background noise and vibration were negligibly small, though another turbine generator had been operated constantly at the rated power. Fig. 1 shows the schematic drawing of the turbine generator and the experimental arrangement.

3.1 Turbine Generator The ratings of a generator are: 12,000 kVA, 600 rpm, 12 poles and 60 Hz. The weight and the fly-wheel effect of a rotor are: 37,800 kg and 66,000 Kg-sq. m. The number of vanes are: 18 runner vanes and 20 guide vanes. The whole weight of rotating body is supported by a thrust bearing and the radial weight of the journal is supported by three guide bearings as shown in the figure.

3.2 Arrangement of Pickups There were some restrictions and difficulty in setting the pickups from the reason that the experimental machine was actually working as a peak load generator. The arrangement of pickups is also shown schematically in the figure. A microphone was located at about 1 m high from the floor over the turbine housing. An acceleration vibration pickup was attached on a guide bearing over the housing. A light pickup of photocell-type, which is used to detect the initiation of rotation and to measure the rotation speed, is located near by the light reflection tapes on and around the turbine journal. Two displacement pickups of eddy current-type were used to measure the radial vibration of journal on a rectangular coordinate.

3.3 Measurement and Analyses The noise, the acceleration vibration, the rotation speed and the displacement vibration of journal have been continuously recorded by a data recorder during the transient stage of the operation from 0 to rated speed after the operation start. Further, the electrical output power of the generator have been recorded according to the necessity. The analyses have been made by a personal computer with A/D converter reproducing the recorded data.
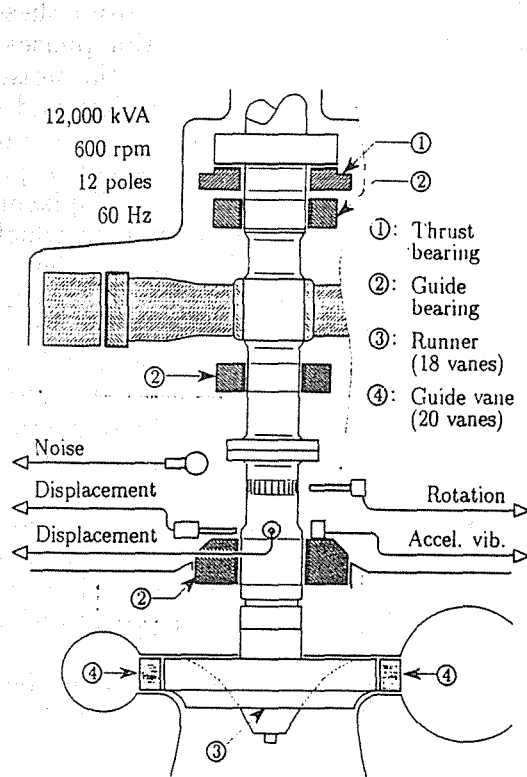
Fig. 1 Schematic drawing of a hydraulic turbine generator and the arrangement of pickups for noise, vibration and rotation.
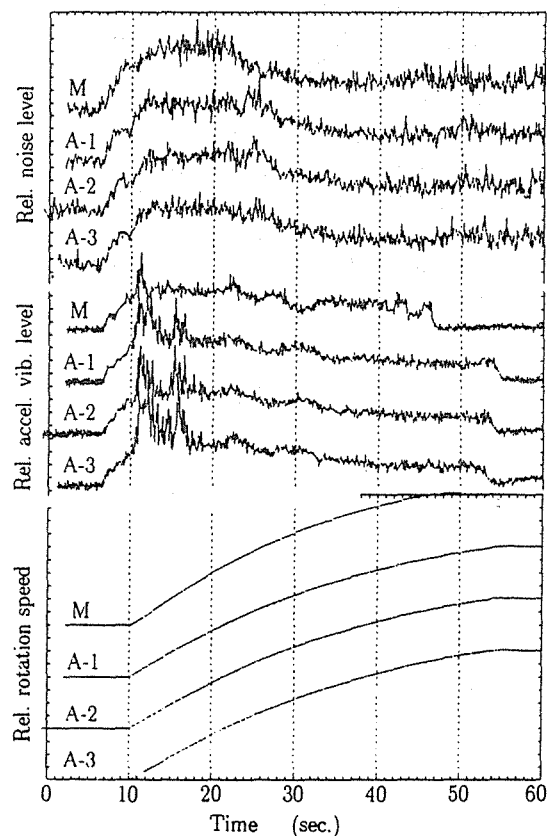
Fig. 2 Comparisons of non-stationary characteristics by two different starting method: (M) is by the manual start, and (A-1) to (A-3) are by the automatic start.

4.0 EXPERIMENTAL DISCUSSIONS

4.1 General Characteristics In the beginning, the measurement has been made for several times of operation start in order to evaluate the stability of information on the noise and the acceleration vibration. Figure 2 shows the observed results comparing two different starting methods and three cases by the same method: the method (M) is a manual start by the operators but three cases (A-1,2,3) are automatically started by the same method using a sequence controller. The noise, the vibration and the rotation speed of turbine observed at each operation are shown comparing with another operation in the upper, middle and lower part of the figure respectively. The relative value of noise and the vibration are plotted in rms at every 0.1 sec. by the A/D converted data sampled with 5 kHz, and the rotation speed at the same time is plotted in rpm.

It can be seen from the figure that the aspects of the traces (A-1), (A-2) and (A-3) are almost the same, that are all the cases when the turbine is automatically started by the same sequence. On the contrary, it can be seen that the aspect of the traces (M) is clearly different form the other aspects of the traces (A-1,2,3). Here, the discussions on the difference between two aspects obtained by two different starting methods are considered to have an important meaning. Nevertheless, the object of our present study is to find some methods detecting the malfunction of the turbine when it is started by the automatic controller. Therefore, let us focus the traces (A-1,2,3).

Now, the transient phenomena of the turbine state can read out from these figures. In the followings, they are discussed by dividing into six major phases with the time. *Phase 1)* 6 to 10 sec.: Before the beginning of rotation, the noise and acceleration vibration show the rapid increase but the journal show slow and small fluctuation. *Phase 2)* 10 to 14 sec.: Just after the rotation start, the noise and the vibration increase more. The journal first seems rolling until the aspect of journal loci changes at 13 sec. through the other observation of the journal displacement. The first peak of the acceleration vibration appears in this duration, in which the journal turns only 4 revolutions. *Phase 3)* 14 to 23 sec.: After above, the second peak of the acceleration vibration appears. The noise is large but comparatively constant, and the vibration show the same aspect excepting the second peak. *Phase 4)* 23 to 28 sec.: The peak of the noise appears in this duration, though the vibration rather show a slight decrease. *Phase 5)* 28 to 54 sec.: During this time, it is difficult to point out the clear features. Both the noise and the acceleration vibration show small change. This time corresponds to the duration that the turbine speed shows moderate increase toward the rating speed. *Phase 6)* After 54 sec.: After the rotation speed reaches to the rating speed at about 54 seconds, the acceleration vibration rapidly decreases to some constant level, but it is not so evident as for the noise. After this time, the noise and the vibration are almost stationary during the regulation of the speed until the time when the generator begins to be loaded.

These phases mentioned above are estimated to be stable even though the phenomena are extremely non-stationary, if the turbine and the journal bearing are at the normal state, whenever the turbine is started by the same sequence. Considering this fact, the evaluation of these phases will be a clue to establish a method detecting the malfunction of turbine or journal bearing at the transitional stage.

4.2 Frequency Analyses In order to clarify the difference of features between the noise and the acceleration vibration from another view point, the frequency analyses are made on the same data of (A-1) as a representative example. Fig. 3 shows the results of the continuous FFT analysis for over 30 seconds (2 sec. of time scale is deviated from Fig.2). Now, let us extract only the evident features from the

figure corresponding to the previous phases. *Phase 1)* 4 to 8 sec.: The frequency components of about 500 Hz appear in the both spectrums of noise and acceleration vibration at 5 sec., and the component of about 900 Hz appears at 7 sec. only in the acceleration spectrum. *Phase 2)* 8 to 12 sec.: The component of 900 Hz also appears in the noise after the rotation start. Moie evident feature is seen only in the acceleration, that is the frequency component of about 1.5 kHz shows the abrupt increase and decrease. *Phase 3)* 12 to 21 sec.: At about 13 sec., both spectrums once decrees for a while. After this, the 1.5 kHz component of the acceleration spectrum again shows the clear peak. *Phase 4)* 21 to 26 sec.: The intense power spectrum of about 1.0 kHz appears in the noise, though it is rather small in the acceleration vibration. It is difficult to discuss further detailed characteristics on Fig. 3.

Fig. 4. shows the characteristics of power components of four frequency bands of both noise and acceleration vibration. Each power component of frequency band is composed of the FFT spectrums of Fig. 3 that are continuously analyzed at every 0.2 sec. From the figure, the transitional feature of each power component is clearly shown in the different type of changing form with time, separated from each other. Now, let us consider only the frequency bands of B3 and B4, that show the evident difference between the noise and the acceleration. As shown in the theoretical background equations from (1) to (4), the information on acceleration vibration is directly related to the force applied to the journal bearing, but the information on noise is related to the surface area of vibrating body.

Sampling freq. : 5 kHz
LPF cutoff freq. : 2 kHz
Data length : 1024 points
Window : Hamming
Spectrum Scale : Linear
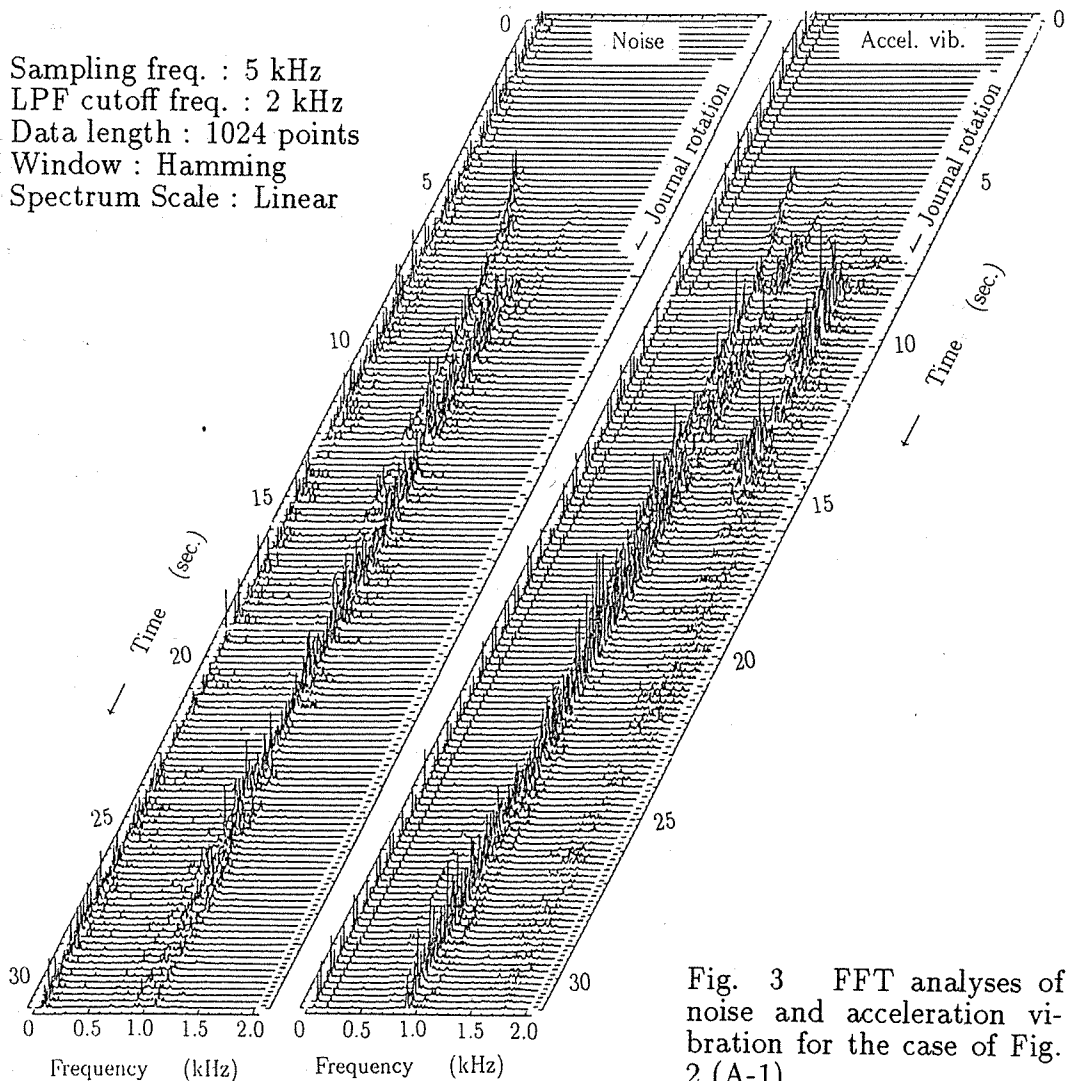
Fig. 3　FFT analyses of noise and acceleration vibration for the case of Fig. 2 (A-1).

Therefore, the area that originate the noise and the vibration by some factors can be estimated by comparing the difference of two power components of the same bands of noise and vibration. For example, the following estimations are reasonably derived: First, the increasing part of the band B3 of the noise, which is not so evident in the acceleration, is propagated from the turbine casing having the large surface area, and is caused by the water flow. Next, the evident peaks of the band B4 of only the acceleration is caused by the partial and small area of journal bearing caused by the frictional force.

4.3 Relation with Speed Rise

From the experimental results above, the information on noise and vibration become more clearly related to the transitional stage after starting the operation of hydraulic turbine. Further, if there exist some power components of frequency bands that are directly proportional to the input toque, it becomes more easily to monitor the state of turbine and journal bearing by separating them from other band components. First, the coefficient of viscosity B which is a parameter of rotational motion

a) Noise

b) Acceleration vibration

Fig. 4 Transitional characteristics of power components of frequency bands with the frequency ranges of B1:5-508, B2:508- 859, B3:859-1172 and B4:1172-1192 in Hz.

is estimated according to equation (4), using the Speed-Acceleration characteristics obtained by the actually observed Speed-Time characteristics. Here, B is actually not a constant value and its effect is comparatively small at the stage of speed acceleration, but it is worthy to know the approximate value. Next, by using the parameter and equation (3), the relations between the power components of frequency bands and the characteristics of the speed rise of the turbine are examined. Figure 5 shows the relation between the components and the speed rising curve. The results show the strong relation between the rotation speed and the acceleration vibration of which spectrum bands are B-1 and B-3.

4.4 A Monitoring Method for Automatic Start

From the analytical results above, the transitional non-stationary characteristics of noise and acceleration vibrations are clarified. The stability of them are experimentally examined in Fig. 2 for the same starting operations. Therefore, a simple and practical method monitoring the turbine and the journal bearing, which reflects their state more directly than the customary method based on the temperature measurement, can be considered and proposed as follows : (1) First, the noise and the acceleration vibration must be measured after dividing into some adequate frequency bands in addition to the turbine speed, that are the basic information and are easy to obtain, even the turbine generator is actually working. (2) Next, the characteristics of them must be compared, noticing the difference between the noise and the vibration. Further, the frequency band component which has the strong relation to the rotation speed must be examined in distinction from the others. (3) Then, if there happen the failure such as the chipping off of the bane blade or the damage of the bearing metal, the
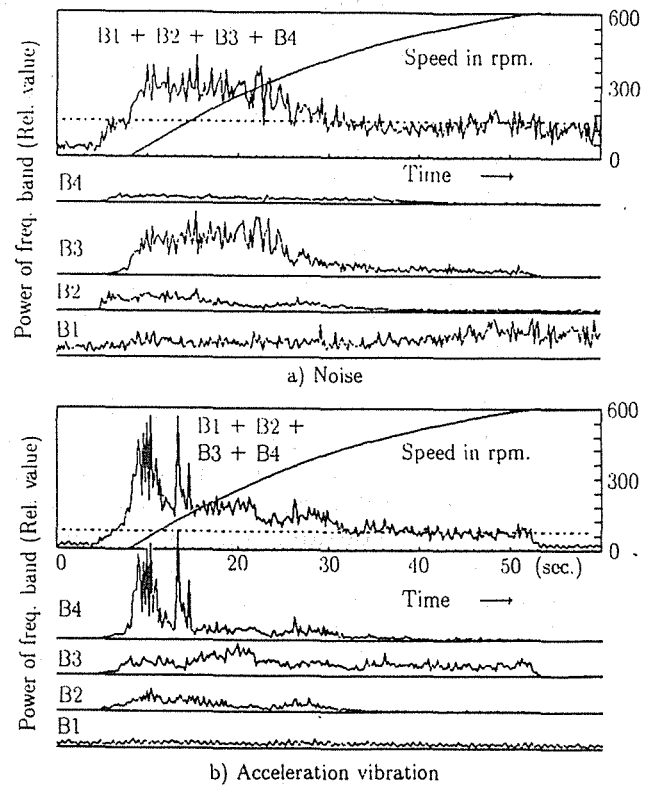
a) Noise

b) Acceleration vibration
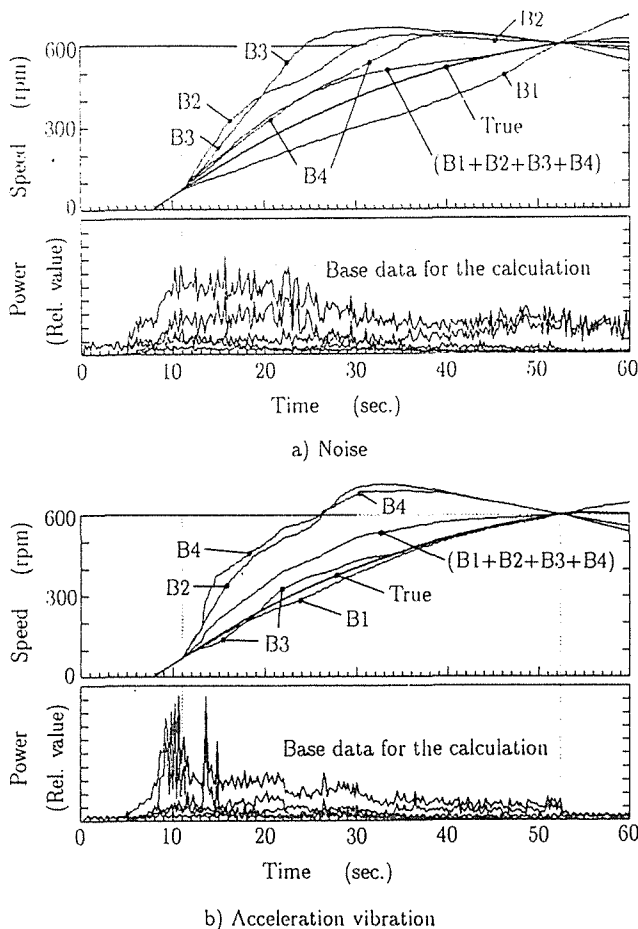
Fig. 5 Calculated results of speed rising characteristics assuming that the power components of frequency bands are directly proportional to the input torque.

malfunction will be detected by comparing the difference of these aspects with the normal phases.

Here, concerning the customary method based on the temperature rise, there exist a problem that the abnormal change appears late after the occurrence of failure because of the large time constant. Further, concerning to another customary method based on the noise or the vibration, it is used for the non-stationary starting duration as the warning monitor if the over all level exceeds the limited value or not. Of course, the FFT methods are used rarely, but the method noticing the difference between noise and vibration proposed in this study does not seem to be reported until now.

5.0 CONCLUSION

First, it has been experimentally shown that the non-stationary characteristics of noise and acceleration vibration at the transitional stage of hydraulic turbine after starting the rotation are considerably stable, if the turbine is automatically started by the same sequence. On this basis, the FFT analyses are made as a representative example of the noise and the vibration. In order to clarify the aspects of them, the FFT results are divided into four frequency bands and shown with the speed rise curve at the same time. From the above results, by considering the difference of physical characteristics between noise and vibration, the capability of estimating the turbine phenomena has been discussed. Finally, a practical method monitoring the turbine for the transitional stage after the rotation start has been proposed. There remain many problems to confirm the effectiveness of the method.

REFERENCES

Hosoya Y. et al., J. IEE Japan, 108, 9, pp. 893-898 (1988) (in Japanese).

Ogino T. et al., Systems and Control, 24, 11, pp. 710-718 (1980) (in Japanese).

Sato. I. et al., Rotating Machinery Diagnosis with Acoustic Emission Techniques, Journal of Acoustic Emission, 2, 1/2, pp. 1-10 (1983).

ERRORS ANALYSIS OF ADAPTIVE NOTCH FILTERS FOR CANCELLING ENGINE NOISE

Xu Maolian
Institute of Naval Medicine, Shanghai, China

ABSTRACT

It is not economical or efficient to cancel engine noise by using acoustic board, sound insulation or active acoustic noise cancelling when we only need to send speech signal out in engine noise environment. In this case, we use adaptive notch filters (ANF) to reduce noise as the spectra of engine noise, in most cases, are line spectra.

In this paper, the transfer function of ANF is deduced and errors of A/D, D/A as well as Doppler frequency deviation errors are also discussed. The analyses show us that the error variance, when using a 8bit A/D converter, is nearly as large as that when using a 12bit A/D converter because of adaptive algorithm. It is also smaller for the effect of D/A. But it is even larger for Doppler frequency deviation. So we get the conclusion that the errors may be mainly caused by the effect of Doppler frequency deviation. The cancelling results show that the period noise can be attenuated by 40dB to 60dB in the range 20-600Hz.

1.0 INTRODUCTION

It was very successful to cancel single frequency signal with adaptive notch filter (B. Widrow). For engine noise, ANF may be used to reduce the noise. In this paper, we mainly deal with the errors of ANF. The following assumptions and restrictions, for convienence, will be used.
(1) The convergence time of ANF is large.
(2) The errors which will be discussed are in the range of the notch band of ANF.
(3) The input signal is a random stationary process.

2.0 THE SYSTEM OF ANF

The principle diagram of ANF is shown in Fig.1 where the input

$$x(t) = \sum_{i=1}^{L} A_i \operatorname{Sin}(\omega_i t + \varphi_i) + s(t)$$

$$r_{si}(jT_s) = C\operatorname{Sin}(\omega_i jT_s)$$

$$r_{ci}(jT_s) = C\operatorname{Cos}(\omega_i jT_s)$$

$$r_{sL}(jT_s) = C\operatorname{Sin}(\omega_L jT_s)$$

$$r_{cL}(jT_s) = C\operatorname{Cos}(\omega_L jT_s)$$
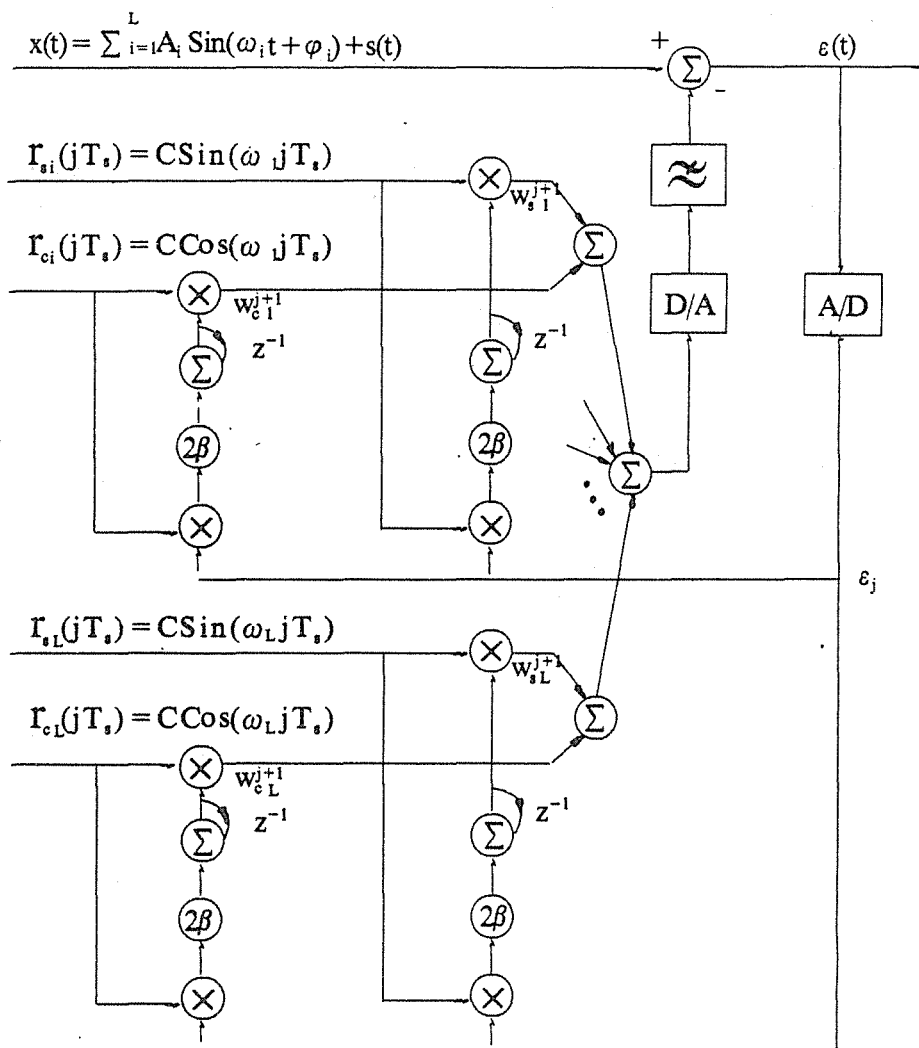
Fig.1. Principle Diagram of ANF

signal is x(t), the reference signals are r_{si} and r_{ci} (i=1,2,...,L) and the error is $\varepsilon(t)$. it is composed by

363

several adaptive notch filters. The transfer function $H(S)_M$ of modified adaptive notch filters (MANF) in complex domain is established as follows [2].

$$H(S)_M = \frac{1}{1 + \beta C^2 \sum\limits_{i=1}^{L} \dfrac{(S Cos\delta_k - \omega_k Sin\delta_k)}{S^2 + \omega_k^2}} \qquad (2.1)$$

where δ_k is nearly zero in this case of Fig.1. So that the transfer function $H(S)$ of ANF is derived as

$$H(S) = \frac{1}{1 + \gamma \sum\limits_{i=1}^{L} \dfrac{S}{S^2 + \omega_k^2}} \qquad (2.2)$$

where γ is the system adjusting parameter which controls the convergence time and such as

$$\gamma = \beta C^2 \qquad (2.3)$$

Equation (2.2) shows us that if there is noise with frequency f_i (i=1,2,...,L), then $|H(j\omega)|$ will be zero and consequently the noise is cancelled.

3.0 THE ERRORS ANALYSIS

3.1 <u>The roundoff errors</u> According to Fig. 1, the equation of the system with the equivalent value α_i of roundoff errors is written as

$$\varepsilon(t) = x(t) - 2\gamma \sum\limits_{i=1}^{L} \{Sin\omega_i t \int_0^t [\varepsilon(t) Sin\omega_i(t) + \alpha_i] \, dt$$
$$+ Cos\omega_i(t) \int_0^t [\varepsilon(t) Cos\omega_i t + \alpha_i] \, dt\} \qquad (3.1)$$

From the above equation, the error variance within i-th notch band (i=1,2,...,L) is deduced as the following equation when the system is stable.

$$\sigma_i^2 = 4\alpha_i^2 \qquad i=1 \ 2 \ \dots \ L \qquad (3.2)$$

3.2 <u>The A/D Quantinization errors</u> In this section, we assume
(1) The A/D is a b+1 bit (b+1>>1) converter.
(2) The mean value of quantinization errors is zero, which are random errors with the uniform probability distribution.
(3) The other parts are ideal except for the A/D converter.
(4) The maximum Amplitude of s(t) is larger than q (q=2^{-b}).

The errors in notch bands are then nearly zero. Now let us

explain it. Assume that there are components of the errors with the frequency f_i ($i=1,2,...,L$). then the following equation satisfies

$$\varepsilon(t) = \sum_{i=1}^{L} \delta_i Sin(\omega_i + \phi_i) + s(t) \qquad (3.3)$$

where δ_i ($i=1,2,...,L$) is not all zero by the assumption.

And the signal after A/D is

$$\varepsilon_j = \varepsilon(t)\,|_{t=jT_s} + \Delta_j \qquad (3.4)$$

where Δ_j is a random error.

The mean value of the above equation is such that

$$E[\varepsilon_j] = E[\varepsilon(t)\,|_{t=jT_s} + \Delta_j]$$

$$= E[s(jT_s)] + \sum_{i=1}^{L} \delta_i Sin(\omega_i jT_s + \phi_i) + E[\Delta_j] \qquad (3.5)$$

We can see, from the equation (3.5) and Fig. 1, that weights w_{si} and w_{ci} ($i=1,2,...,L$) will be adjusted to reduse the error because the correlation values between the reference signal and the errors are not equal to zero. δ_i ($i=1,2,...,L$) will be zero when the weights are stable after a long time.

3.3 The D/A Quantinization Errors The following assumptions are given the same as in 3.2.
(1) The D/A is a b+1 bit converter.
(2) The other parts are ideal except for the D/A converter.

From the assumptions above, it is not difficult to get the error variance as

$$\sigma_i^2 = \sum_{k=1}^{L} \frac{2qF_s}{3\pi^2} \left(1 - Cos\frac{2\pi f_i}{F_s}\right) \left(\frac{\frac{Sin\pi f_s}{F_s}}{f_k}\right)^2 \Delta f \qquad (3.6)$$

$$(i = 1\ 2\ ....\ L)$$

where Δf is the band width of measuring instrument.

3.4 THE ERRORS OF EFFECT OF DOPPLER FREQUENCY DEVIATION In the real environment, the frequency of the noise is not stable, for example, caused by the varity of rotational speed of engine. We assume that i=1, for convenience, and if the increment of frequency is δ, then it is easily obtained from equation (2.2).

$$H[j2\pi(f_1+\delta)] = \frac{1}{1 + j\dfrac{\gamma(f_1+\delta)}{2\pi[f_1^2 - (f_1+\delta)^2]}} \qquad (3.7)$$

or

$$|H[j2\pi(f_1+\delta)]| \approx \frac{1}{\sqrt{1+(\frac{\gamma}{4\pi\delta})^2}} \tag{3.8}$$

For example, if f_1=100Hz, δ=0.001, then the amount of attenuating capability of ANF can be reached by -54dB only.

4.0 THE EXPERIMENTAL RESULTS

In these experiments, every band width of ANF is 1Hz, Δf=10Hz, L=9, F_s=2570Hz, α_i=39mv (i=1,2,...L) and f_i=65Hz, 81Hz, 114Hz, 130Hz, 146Hz, 162Hz, 179Hz, 195Hz.

1) The roundoff errors

From equation (3.2) the theoretical result is
$$\sigma_i = 78mv \tag{4.1}$$

and the experimental result is given by
$$\sigma_{ei} = 79mv \tag{4.2}$$

2) The A/D converter errors

In these experiments, 8bit and 12bit A/D converters are used respectively. The theoretical result σ is
$$\sigma = 0 \ mv \tag{4.3}$$

and the experimental results, when using 8bit and 12bit A/D converter, are nearly the same value which is
$$\sigma_e = 2 \ mv \tag{4.4}$$

Noting: The background noise in these experiments is approximately equal to 2 mv.

3) The D/A converter errors

In this experiment, the value of q is 256 and the theoretical result σ and the experimental result σ_e are given as follows:
$$\sigma = 14.4mv \tag{4.5}$$

and
$$\sigma_e = 10-25mv \tag{4.6}$$

4) The cancelling results

In this experiment, the acoustic noise with frequency f_i

(i=1,2, ...,14) is received by microphone and is taken as the input signal x(t) in Fig. 1. The power of component of ε(t) within the range of the i-th band of ANF is then measured and its results are given in Table 1. In addtion, the cancelling results of MANF [2] are also written in Table 1 for comparison.

Table 1. The results of cancelling

Frequency f_i (Hz)	40	80	120	160	200
Before Cancelling (dB)	86	87	86	100	98
After Cancelling (ANF) (dB)	41	41	39	37	37
After Cancelling (MANF) (dB)	43	43	40	39	37

240	280	320	360	400	440	480	520	560
90	90	91	91	92	93	78	85	87
36	35	34	33	32	31	30	29	29
36	35	34	34	33	33	33	33	33

5.0 CONCLUSIONS

From the experiments, we can see, the experimental results are approximate to the results of theory. The results of A/D errors show us that the error variance, when using a 8bit A/D converter, is nearly as large as that when using a 12bit A/D converter. So we can use 8bit A/D instead of 12bit A/D, for economy, to design the ANF system.

The cancelling results show that attenuating capability of ANF is nearly the same as that of MANF. The reasons are that firstly there is some background noise. And secondly their noise sources are the same and the attenuating capability may be mainly decided by the effect of Doppler frequency deviation which affects the frequencies of the source and is the cause of the results of both systems.

The implementation of ANF is simpler than that of MANF and the system can be used to attenuate the period noise on digital computer and analogous circuits. Then the good cancelling capability will be reached.

REFERENCES

[1]   B.Widrow el, Adaptive Noise Cancelling: Principle and Application, Proceedings of the IEEE, Vol. 63, NO.12, 1698-1716, 1975.

[2]   Xu Maolian, Xiang Dawei, The Analysis and Application of Modified Adaptive Notch Filters for Acoustic Noise Cancelling, WESTPA III, Vol. 1, 417-420, 1988.

ADAPTIVE-DELTA-MODULATION SYSTEM WITH PRE-GIVEN DELTAS AND COMPENSATING ERRORS

Xu Maolian
Institute of Naval Medicine, Shanghai, China

Li Zhien
Institute of Naval Medicine, Shanghai, China

ABSTRACT

A new adaptive-delta-modulation type with pre-given deltas (ADMPD) and compensating errors is introduced. The pre-given deltas are selected for various kinds of the speech by a least square error criterion. The errors between the input signal and estimated signal are correlated with the encoding datas. The signal-to-noise rate (SNR) will be increased as we compensate the errors according to the correlation property.

In this paper, except for the errors analysis, we also present the system of speech synthesizer with a single-chip micro-controller. The system can be used for the speech machine, which needs to be changed frequently and requires natural and clear voice.

1.0 INTRODUCTION

In recent years, machine speech has been used in many fields, such as computer-controlling speech instruction of the airport, etc. Delta modulation (DM) or adaptive delta modulation (ADM) may be used in these cases and has been discussed (N.S.Jayant, C.V. Chakravathy). In this paper, ADMPD is introduced. We will mainly deal with optimization of DM and ADM methods with various kinds of their parameters. From the analyses, the ADMPD system is set out.

The fidelity criterion used to define optimum performance is that of minimum square error or noise power.

2.0 THEORY

2.1 The Algorithm

We will first of all discuss DM and ADM coding. Assume s(t) represents the input speech signal, x_n the sampled signal. Their relation satisfies

$$x_n = s(T_s) \tag{2.1}$$

where T_s is the cycle of sample. If the frequency is F_s then $T_s = 1/F_s$.

And denote, at time-instant i, the estimated signal, encoding data and increment by x_n^o, b_n and D_n respectively. The following equations are established:

$$b_n = \begin{cases} 1 & x_n > x_n^0 \\ -1 & x_n \leq x_n^o \end{cases} \tag{2.2}$$

$$x_{n+1}^o = \begin{cases} x_n^o + D_n & b_n = 1 \\ x_n^o - D_n & b_n = -1 \end{cases} \tag{2.3}$$

$$D_n = \Delta \tag{2.4}$$

or

$$D_n = D_{n-1} M^{b_n b_{n-1}} \tag{2.5}$$

where Δ is a constant and M is such that

$$1 < M < 2 \tag{2.6}$$

Equations (2.2), (2.3) and (2.4) represent DM method, and

equations (2.2), (2.3) and (2.5) represent ADM method.
Equation (2.5) shows that the step size of ADM is
exponentially increased. Thence its amount of companding
capability is improved comparing with DM method. But the
SNR is not as good as the latter one. The reasons are that
the increments of speech signal do not increase
exponentially and the maximum step size is much larger
than the maximum increment of the signal. If we select the
proper deltas, we will either improve the companding
capability or increase the SNR. This method is called
ADMPD, and its increment D_n, in some part of speech, is
satisfied with the following equations:

$$C_n = \begin{cases} C_{n-1}+1 & b_n=1 \\ C_{n-1}-1 & b_n=-1 \end{cases} \qquad (2.7)$$

$$D_n = F_i(C_n) \qquad (2.8)$$

where F_i is funtion of the i-th group of deltas, and i
satisfies

$$\varepsilon_n = X_n - X_n^o \qquad (2.9)$$

$$N_i = \sum \varepsilon_n^{o2} \qquad (2.10)$$

and

$$N_i = Min \qquad N_i \in [N_1 \quad N_2 \quad \ldots \quad N_L] \qquad (2.11)$$

where ε_n is the error at time-instant n. ε_n^o is the output
of low pass filter with the cut-off frequency f_a when the
input is ε_n, and N_i (i=1, 2, ..., L) is the error power
when the i-th group of deltas are selected.

ADMPD method is described as follows: The proper group of
deltas are selected according to the certain amplitude and
frequency of speech by the minimized mean square error in
order to increase the SNR and improve companding
capability.

2.2 The Analyses of SNR In this section, we will, for the
convenience of systems analysis and design, derive the SNR
approximately instead of strict derivation. Assume
(1) The input signal is sine wave and that is

$$X_n = A_m Sin(2\pi f_c T_s) \qquad (2.12)$$

(2) The errors are independent each other and its autocorrela-tion function can be written as

$$E[\varepsilon_k \varepsilon_j] = \begin{cases} \sigma^2 & k=j \\ 0 & k \ne j \end{cases} \quad . \qquad (2.13)$$

(3) ε_n is a random error with the uniform probability distribution in the range $[-p, p]$ and p is the largest equivalent error.

1) DM coding

Define

$$p = \gamma \Delta = F(f_c \quad A_m \quad F_s) \Delta \qquad (2.14)$$

where γ is the equivalent parameter, and is given as the following equation from the computer simulation:

$$\gamma = \sqrt{\frac{\Delta F_s}{3 \pi f_c A_m}} \qquad \frac{2 \pi f_c A_m}{F_s} \le \delta \le \frac{6 \pi f_c A_m}{F_s} \qquad (2.15)$$

From the assumptions, the error power N^2 and the signal power S^2 are derived as

$$N^2 = \frac{f_a p^2}{3 F_s} \qquad (2.16)$$

$$S^2 = \frac{A_m^2}{2} \qquad (2.17)$$

and ensuing SNR is then the following:

$$\left(\frac{S}{N}\right)^2 = \frac{3 A_m F_s}{f_a p^2} \qquad (2.18)$$

and the maximum SNR is

$$\left(\frac{S}{N}\right)^2 = \frac{3 A_{max} F_s}{f_a p^2} \qquad (2.19)$$

where A_{max} is the largest amplitude of signal when Δ is decided and it is easy to be obtained as

$$A_{max} = \frac{F_s \Delta}{2\pi f_c} \qquad (2.20)$$

2) ADM coding

As the step size in ADM method increases exponentially, the largest error will excess to the optimized one of DM. Here the relation among f_c, F_s, A_m and M will be discussed when the maximum SNR is reached. And the SNR equation will not be discussed.

If the slope increments of signal become larger, then the optimized M is needed to increase and is approximately written as the following

$$\frac{2\pi f_c A_m}{F_s} = \alpha M_{opt} \beta \qquad (2.21)$$

that is

$$M_{opt} = 10^{\frac{lg \frac{2\pi f_c A_m}{\alpha F_s}}{\beta}} \qquad (2.22)$$

where α is the factor and β is the equvalent exponential factor. We get that $\alpha=0.48$, and $\beta=10.4$ by computer simulation.

3) ADMPD coding

As discussed above, the SNR will varies with M for the certain signal in ADM system. The maximum SNR is about that of optimized DM system. In ADMPD system, the SNR is as same as that of optimized DM system because the deltas are selected properly, and is written as

$$(\frac{S}{N})^2 = \frac{3A_m^2 F_s}{2 f_a P^2} \qquad (2.23)$$

3.0 ADMPD WITH COMPENSATING ERRORS

In ADMPD system, the largest step size had better not excess the optimized Δ of DM in order to reduce overshoot-noise. In this case, there is obviously correlation between the errors and encoding datas.

Therefore the errors can be reduced after they are compensated according to correlation property. The following is, for convenience, a simple compensating equation.

$$Y_{n-1} = \begin{cases} Y_{n-1} + b_{n-1} D_{n-1} & b_{n-2} = b_{n-1} = b_n \\ Y_{n-1} & other \end{cases} \qquad (3.1)$$

4.0 THE EXPERIMENTAL RESULTS

In these experiments, the cut-off frequency f_a is 3kHz, the sample frequency 20kHz and the signal frequency 800Hz (the reason which we select 800Hz is that the main components of speech are in the range 700Hz to 800H). that is

$$X_n = 129.34 Sin(\frac{1600\pi n}{20000}) \qquad (4.1)$$

Let

$$(\frac{S}{N}) dB = 20 log(\frac{S}{N}) \qquad (4.2)$$

1) DM coding

The experimental and theoretical results which are calculated by equations (2.18), (2.14), (2.15) and (4.2) are given in Table 1.

TABLE 1. THE RELATIONS BETWEEN THE SNR (dB) AND Δ

Δ	96	64	57	51	44	38	32
THEORY RESULTS	12.8	14.7	15.3	15.7	16.3	17	17.7
EXPERIMENTAL RESULTS	11.8	14.7	15.2	15.6	16.2	16.8	17.6

2) ADM coding

The experimental and theoretical results which are calculated by equation (2.22) are given in Table 2.

TABLE 2. THE RELATIONS BETWEEN M_{opt} AND A_m

A_m	32.33	64.67	129.34	258.68
THEORY RESULTS OF M_{opt}	1.3	1.4	1.5	1.58
EXPERIMENTAL RESULTS OF M_{opt}	1.3	1.4	1.55	1.6

3) ADMPD Coding

According to equation (2.23), the theory result is calculated as

$$\frac{S}{N} = 17.7\,dB \qquad (4.3)$$

We select a group of deltas as 2, 4, 8, 14, 20, 26, 31, 35, 37. Then the result of experiment is obtained as

$$\frac{S}{N} = 17.9\,dB \qquad (4.4)$$

4) ADMPD with Compensating Errors

The experimental result is

$$\frac{S}{N} = 20.8\,dB \qquad (4.5)$$

5.0 SPEECH PROCESSOR WITH A SINGLE-CHIP MICROCONTROLLER

In the encoding of ADMPD system, we use a digital signal processor TMS32010 to deal with the speech signal. As to the decoding part, a slice of P8031 is used as CPU for implementation. Fig.1 and Fig.2 illustrate its principle block diagram and its circuit chip respectively.
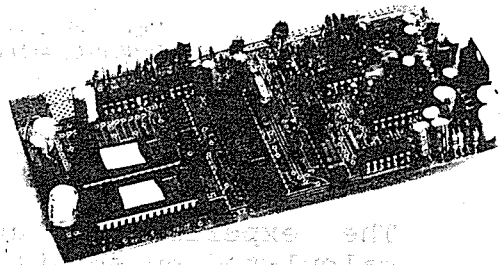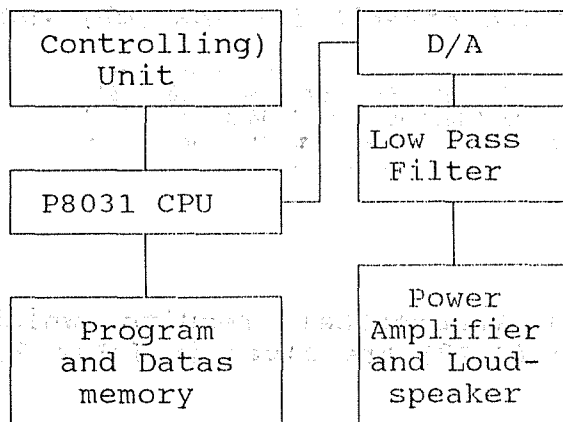
Fig.1. Principle Block Diagram of Decoding Part of ADMPD

Fig.2. Photograph of the Circuit Chip of the Decoding Part

From the above discussion, to implement the ADMPD system, in real time, is difficult. But if we rectify the differentiated input signal s'(t) and make the direct

current add to x_n. Then in encoding process, the direct current is detected with the low pass filter, and the group of deltas are properly selected according to the direct current. The system with this method is a quasi-ADMPD system. The function of the system is near to that of ADMPD.

6.0 CONCLUSIONS

The SNR performance and optimization of DM, ADM and ADMPD with compensating errors have been presented. From the analyses and from those of computer simulation, the following findings are made.

(1)   The SNR peformance of ADMPD with compensating errors remains higher than that of DM or ADM.

(2)   The companding improvement offered by ADMPD appears to be as same as that of ADM and much better than that of DM.

(3)   The overshoot-noise is reduced in ADMPD system comparing with that in ADM system.

REFERENCES

[1]   N.S. Jayant, A First-Order Markov Model for Under-standing Delta Modulation Noise Spectra, IEEE Trans, COM-26, 1316-1318, 1978.

[2]   C.V. Chakravathy, M.N. Faruqui, Two Loop Adaptive Delta Modulation Systems, IEEE Trans. COM-22, 1710-1713, 1974.

COMPARISONS OF DETECTION PERFORMANCES BETWEEN FS-PDMP SYSTEM AND TYPICAL
SIGNAL DETECTORS

Shuying Zhang
Shanghai Acoustics Laboratory, Academia Sinica
456 Xiao-Mu-Qiao Rd., Shanghai, P.R.China (200032)

Yong Sun
Shanghai Acoustics Laboratory, Academia Sinica
456 Xiao-Mu-Qiao Rd., Shanghai, P.R.China (200032)

ABSTRACT

A signal detection system composed of a Frequency-Stepping signal
generator and a corresponding Post-Detection-Matched-Processor has been de-
veloped for active sonar detection. Essentially this system(called FS-PDMP
system) is a tone-correlation detector because the detection performance of
the system is entirely determined by the tone(i.e. the mode of frequency
variation) of a FS signal. The characteristic function and the Receiver's
Operation Characteristic curves of the system have been derived. Through
comparisons, the differences of detection performances in time and Doppler
resolutions, detectable input signal to noise ratio and ROC curves between
the FS-PDMP system and other typical signal detectors, such as the well
known Matched-Filter and the Energy-Detector have been evaluated.

1.0 INTRODUCTION

It is known that because of the phase fluctuation, the multipath interference or the dispersive effect associated with sound transmission in complicated underwater channels, the well-known Matched-Filter often cannot be effectively used in the active sonar detection. Also, the simple Energy-Detector is usually unsatisfied because of bed resolutions both in time and Doppler. Therefore, the alternative approach to performing the pulse compression for a long emitting signal, i.e. the FS-PDMP system, has been developed through a series of theoretical and experimental studies (Zhang S.).

In the FS-PDMP system, the Frequency-Stepping signal source can flexibly generate a long signal with an arbitrary FS mode by arranging a set of digit-codes, and the Post-Detection-Matched-processor can be automatically matched with the corresponding FS mode to execute the tone correlation for the FS signal. In this paper a theoretical analysis of the FS-PDMP system and some comparisons of detection performances between this system and other typical signal detectors have been made briefly.

2.0 THEORETICAL ANALYSIS OF THE FS-PDMP SYSTEM

Fig. 1 is the principle diagram of a PDMP. An FS signal passes through a pre-filter and a set of parallel channels in succession. Every channel consists of a narrow-band filter plus an envelope-detector. Through a set of switches controlled by the FS signal source, the output of the channel that corre sponds to the frequency of the n-th unit in a given FS mode is connected to the input terminal of a matched delay-line which provides the input signal with a time-delay of $(N-n-1)\tau$. After the outputs of N channels are added in the delay-line and smoothed by a low-pass filter, the total detect ion response is supplied.
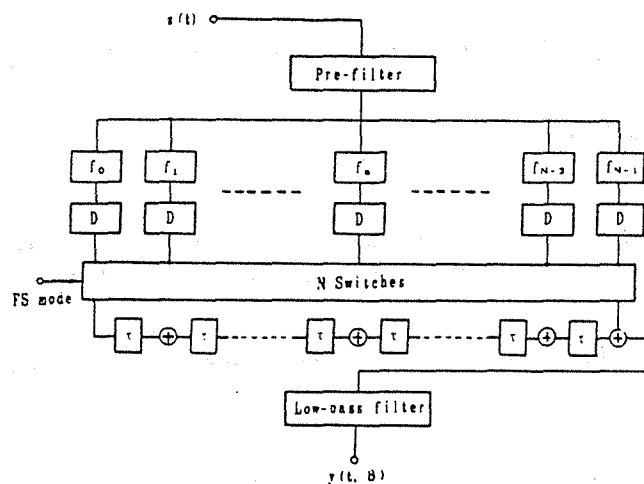
Fig. 1   The principle diagram of a Post-Detected-Matching-Processor

2.1 **Characteristic function** Suppose that the pulse-response function of the n-th narrow-band filter is

$$h_n(t) = \frac{1}{\tau}\text{rect}\left(\frac{t}{\tau}\right)\exp(j2\pi f_n t)$$

(1)

and that the FS signal satisfies the narrow-band condition, so a received signal with doppler frequency can be written as

$$s(t) = \exp(j2\pi\beta t) \cdot \sum_{m=0}^{N-1} \text{rect}\left(\frac{t-m\tau}{\tau}\right) \exp\{j2\pi f_m(t-m\tau) + j\varphi_m\}$$

(2)

where τ is the duration of each unit, and f_n, φ_n are the frequency and the initial phase of the n-th unit respectively, rect(x) is the well-known rectangular function. It is obvious that as the N frequencies $\{f_n\}$ are arbitrarity arranged, a variety of FS modes can be designed. If s(t) enters the n-th filter, the output of the filter will be determined by

$$e_n(t, \beta) = \int_{-\infty}^{+\infty} h_n(t-\xi) s(\xi) d\xi$$

$$= \exp(j2\pi f_n t) \cdot \sum_{m=0}^{N-1} \text{rect}\left[\frac{t-(m\mp1/2)\tau}{\tau}\right] (1\pm\frac{t-m\tau}{\tau}) \text{ sinc}$$

$$\{(f_m+\beta-f_n)[\tau\pm(t-m\tau)]\}\exp\{j\pi(t-m\tau)(f_m+\beta-f_n)+j\varphi_m\}$$

(3)

For the sake of simplicity, the envelope of $e_n(t, \beta)$ can be considered to be a constant within $(m-1/2)\tau < t < (m+1/2)\tau$. So, by making $t=m\tau$ the output of the envelope-detector behind the n-th filter is

$$\tilde{e}_n(t, \beta) = \sum_{m=0}^{N-1} \text{rect}\left(\frac{t-m\tau}{\tau}\right) |\text{sinc}[(f_m+\beta-f_n)\tau]|,$$

$$n=0, 1, \ldots\ldots, N-1$$

(4)

Each $\tilde{e}_n(t, \beta)$ is correspondingly delayed by a time of $(N-n-1)\tau$, then the outputs of N delay-lines are added and normalized, and the original point of time is shifted to $(N-1)\tau$. As a result, a total output of PDMP is derived as

$$y(t, \beta) = \frac{1}{N}\sum_{n=0}^{N-1} \tilde{e}_n(t+n\tau, \beta)$$

$$= \frac{1}{N} \cdot \sum_{m=-(N-1)}^{+(N-1)} \text{rect}\left(\frac{t-m\tau}{\tau}\right) \cdot \sum_{n=0}^{N-1} R(m+n) |\text{sinc}[(f_{m+n}+\beta-f_n)\tau]|$$

(5)

and $R(X) = \begin{cases} 1, & 0 < X < N-1 \\ 0, & X=\text{other values} \end{cases}$

(6)

Clearly, $y(t, \beta)$ is the characteristic funtion determining the detection performance of the FS-PDMP system. Several typical cases are as follows:

2.1.1 t=0 and $\beta\neq0$ This case corresponds to m=0 in Eq. (5), therefore

$$y(0, \beta) = |\text{sinc}(\beta\tau)|$$

(7)

Let $|y(0, \beta_{d1})| < 0.7$, the Doppler-resolution is defined as

$$\beta_{d1} = \pm0.44/\tau$$

(8)

2.1.2 $\beta=0$ and $t\neq0$. Assume that the frequencies of N units are arbitrarily arranged, but their values are different from each other, and that within a given frequency band, $f_0-(f_0+W)$, the difference between any two frequencies is the integer times of W/N. Therfore, only when m=0, is the $y(t, \beta)$ of value and equal to

$$y(t, 0) = rect(t/\tau)$$

(9)

and the time-resolution is

$$\tau_{d1} = \pm\tau/2$$

(10)

2.1.3 y(t, β) of typical FS signals.

a) Single FS, f_n=constant.

$$y(t, \beta) = rect\left(\frac{t-m\tau}{\tau}\right)\left(1-\frac{|m|}{N}\right)|sinc(\beta\tau)|$$

(11)

b) Progressively increasing FS, $f_n = f_0 + n/\tau$.

$$y(t, \beta) = rect\left(\frac{t-m\tau}{\tau}\right)\left(1-\frac{|m|}{N}\right)|sinc(m+\beta\tau)|$$

(12)

In Eqs. (11) and (12), m=0, ±1,..., ±(N-1).

c) Random FS. Assume that N frequencies in the FS modes are different

from each other, and that the diffrence between any two frequencies satisfies $|f_{n1}-f_{n2}| = n/\tau$, n=1, 2, ...N-1. Then

$$y(t, \beta) \approx rect(t/\tau)|sinc(\beta\tau)|$$

(13)

In Fig. 2, the main response regions of the above three y(t, β) have been indicated: y_m is the value of y(t, β) at the centre of each response unit corresponding to m=0, ±1, ... ±(N-1) and the boundary values of these units are defined as 0.7 y_m.

(a) Single FS   (b) Progressively increasing FS   (c) Random FS
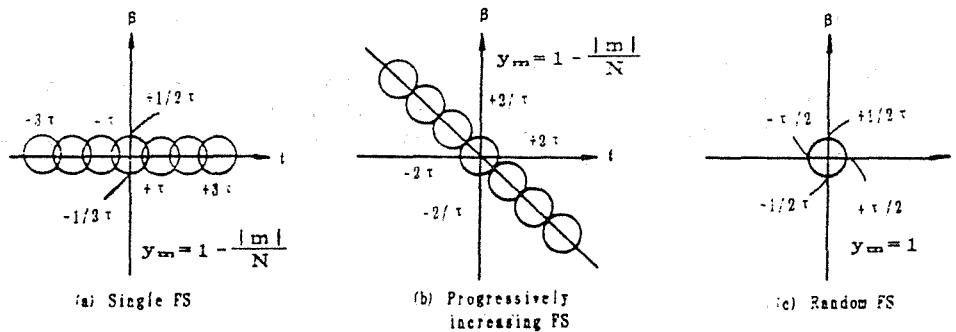
Fig. 2 The main response regions of three typical y(t, β) functions

2.2 Detectable signal to noise ratio (SNR)

It is known that the probability density of the envelope of a sine signal plus a narrow-band Gaussian noise is a Rician function (Whalen A. D.)

$$p(z) = \frac{z}{\sigma^2}\exp\left(-\frac{z^2+A^2}{2\sigma^2}\right)I_0\left(\frac{Az}{\sigma^2}\right)$$

(14)

where A is the amplitude of the sine signal, σ^2 is the variance of the narrow-band noise, and $I_0(x)$ is the modified Bessel function of zero order. The input signal to noise ratio (SNR) of an envelope-detector is defined as $\gamma = A^2/2\sigma^2$. When $\gamma < 1$, the mean and variance of z is

$$\langle z\rangle = \sqrt{\frac{\pi}{2}} \cdot \sigma \left(1+\frac{\gamma}{2}\right), \quad (\langle z^2\rangle - \langle z\rangle^2)_{\gamma=0} = (2-\pi/2)\sigma^2$$

$$(15)$$

Suppose that the output noises of N narrow-band filters are independent of each other, and that the output SNRs of these filters are equal, therefore after the outputs of N envelope-detectors are delayed respectively and added together, the total mean is the sum of the means of N outputs and the total variance is the sum of the variances of N outputs. When $N \gg 1$, according to the 'central limit theorem', the output noise of PDMP satisfies the Gaussian distribution and the output SNR of PDMP is defined as

$$(SNR)_o = \frac{[N(\langle z\rangle - \langle z\rangle_{\gamma=0})]^2}{N(\langle z^2\rangle - \langle z\rangle^2)_{\gamma=0}} = \frac{\pi N \gamma^2}{4(4-\pi)}$$

$$(16)$$

Assume the pass-band of the pre-filter in PDMP is W. Then $\gamma = \tau W (SNR)_{11}$, where $(SNR)_{11}$ is the input SNR of N narrow-band filters. Substituting γ into Eq. (16), the detectable SNR of an FS-PDMP system can be estimated

$$10 \lg(SNR)_{11} > 5 \lg d + 0.3 + 5 \lg N - 10 \lg(TW) \quad dB,$$

$$(17)$$

where $T = N\tau$ is the length of an FS signal and $d = (SNR)_o$ is the detection index defined at the end of a PDMP. For both Progressively increasing FS and Random FS, $W = (N-1)/\tau$, i.e. $TW = N(N-1) \approx N^2$, hence the equation

$$10 \lg(SNR)_{11} > 5 \lg d + 0.3 - 15 \lg N = 5 \lg d + 0.3 - 7.5 \lg(TW) \quad dB$$

$$(18)$$

2.3 <u>Receiver operating characteristics (ROC)</u> For the convenience of computation, the envelope-detector in Fig. 1 is assumed as a quadratic detector. Thus, the normalized statistic appears at the output of the system is

$$y = \sum_{n=0}^{N-1} q_n^2 / \sigma^2$$

$$(19)$$

where $\sigma^2 = N_o \tau / 4$, and $N_o/2$ is the power spectral density of white noise at the input of the system. Obviously q_n^2 is the squared envelop of a sine wave plus a narrow-band noise, and so y is noncentrally X^2 distributed with 2N degrees of freedom (Whalen A. D)

$$p_1(y) = \frac{1}{2} \left(\frac{y}{\lambda}\right)^{(N-1)/2} \cdot \exp\left(-\frac{y}{2}-\frac{\lambda}{2}\right) I_{N-1}[(y\lambda)^{1/2}]$$

$$(20)$$

where the noncentral parameter is equal to

$$\lambda = NA^2 \tau^2 / 4\sigma^2 = 2E/N_o$$

$$(21)$$

and $E = NA^2\tau/2$ is the energy of a FS signal with N units. $I_{N-1}(X)$ is the modified Bessel function of the first kind and order N-1. With no signal present, y has a central X^2 distribution with 2N degrees of freedom.

$$p_0(y) = \frac{(y/2)^{N-1}}{2\Gamma(N)} \cdot \exp(-y/2)$$

$$(22)$$

Where $\Gamma(N)$ is the well-known Γ function.

Let detection threshold be y_T, the false-alarm probability of the system is

$$P_{f_a} = \int_{y_T}^{\infty} p_0 (y) \, dy = 1 - P (N, \, y_T/2)$$

<div align="right">(23)</div>

and $P (a, b)$ is the incomplete Gamma function,

$$P (a, b) = \frac{1}{\Gamma (a)} \int_0^b e^{-t} \cdot t^{a-1} dt$$

<div align="right">(24)</div>

The probability of detection is

$$P_d = \int_{y_T}^{\infty} p_1 (y) \, dy = Q_N (\frac{\lambda}{2}, \frac{y_T}{2})$$

<div align="right">(25)</div>

and $Q (c, d)$ is the generalized Marcum Q-function

$$Q_N (c, d) = \int_d^{\infty} (\frac{Z}{C})^{(N-1)/2} \cdot \exp (-Z-C) \cdot I_{N-1} [2 (CZ)^{1/2}] \, dZ$$

<div align="right">(26)</div>

By using the particular series expansions of P and Q (Abramowitz M.) a large amount of ROC curves of FS-PDMP system have been computed in linear and probabilitic coordinates respectively. Fig. 3 shows three sets of ROC curves corresponding to N=4, 8, 16 respectively.

3.0 DETECTION PERFORMANCES OF TYPICAL SIGNAL DETECTORS

The typical signal detectors for active sonar detetion are the Matched Filter (i.e. cross-correlator) and Energy-Detector respectively. The first one (MF) is the optimum receiver for the case of an exactly known signal in a background of white noise, however, the second one (ED) is the optimum reriever for the case of a completely unknown signal in a background of Gaussian noise (Urick R. J.). For comparisons, some parameters determining the detector performances of MF and FD are summarized as follows.

3.1 <u>Matched filter</u>   The characteristic function of the MF is the well known Woodwards ambigurity function.

$$X (\tau, \beta) = \int_{-\infty}^{\infty} S^* (t) S (t+\tau) \exp (-j2\pi\beta t) \, dt$$

<div align="right">(27)</div>

where arterisk denotes complex conjugat.
Therefore the time and Doppler resolution are determined by

$$|X (\tau_{d3}, 0)| = 0.7 \quad \text{and} \quad |X (0, \beta_{d3})| = 0.7$$

<div align="right">(28)</div>

respectively. In the case where s (t) is a frequency (or phase) modulated signal with a rectangular envelope,

$$\tau_{d3} = \pm 0.44/W \quad \text{and} \quad \beta_{d3} = \pm 0.44/T$$

<div align="right">(29)</div>

Where W and T are the spectrum width and pulse duration of the signal respectively. The detection index defined at the end of a MF is $d = 2TW (SNR)_{i2}$, hence

$$10 \lg (SNR)_{i2} = 10 \lg d - 3 - 10 \lg (TW) \quad dB$$

<div align="right">(30)</div>

The ROC curves of MF can be defined by the false alarm probability

$$P_{f_a}= \int_{y_T}^{\infty} (\pi N_0 E)^{-1/2} \exp[-y^2/(N_0 E)] \, dy = Q(\beta)$$

(31)

and the probability of detection

$$P_d= \int_{y_T}^{\infty} (\pi N_0 E)^{-1/2} \exp[-(y-E)^2/(N_0 E)] \, dy = Q[\beta - (\frac{2E}{N_0})^{1/2}]$$

(32)

where $\beta = y_T (2/N_0 E)^{1/2}$ and the definitions of y_T, N_0 and E are the same as those in section 2.3. $Q(x)$ can be expanded as a series for computation.

$$Q(x) = \frac{1}{2} - \frac{\exp(-x^2/2)}{(2\pi)^{1/2}} (x + \frac{x^3}{3} + \frac{x^5}{3\times5} + \frac{x^7}{3\times5\times7} + \cdots)$$

(33)

3.2 <u>Energy detection</u> An energy detector is composed of a quadratic detector, a prefilter with a pass-band W and a post-integrator with a integral time equal to the signal length T. Therefore no Doppler resolution can be defined and the time resolution is determined by

$$\tau_{ds} = \pm 0.5T$$

(34)

For the convenience of making comparison, suppose $W=N/\tau$ and $T=N\tau$ (see section 2.2). Because the post-integrator is used for accumulating a certain amount (i.e. $TW=N^2$) independant signal samples, the normalized statistic appearing at the output of ED has a noncentral χ^2 distribution with $2N^2$ degrees of freedom. Therefore the ROC curves of ED are also computed by Eq. (23) and (25), but N should be replaced by N^2. Correspondingly the detection index defined at the end of a ED is $d=TW(SNR)^2_{is}$. Hence

$$10 \lg (SNR)_{is} = 5 \lg d - 5 \lg (TW)$$

(35)

Fig. 4 gives three sets of ROC curves corresponding to MF, ED and FS-PDMP (N=8) respectively.

DETECTION PERFORMANCE OF FS-PDMP SYSTEM
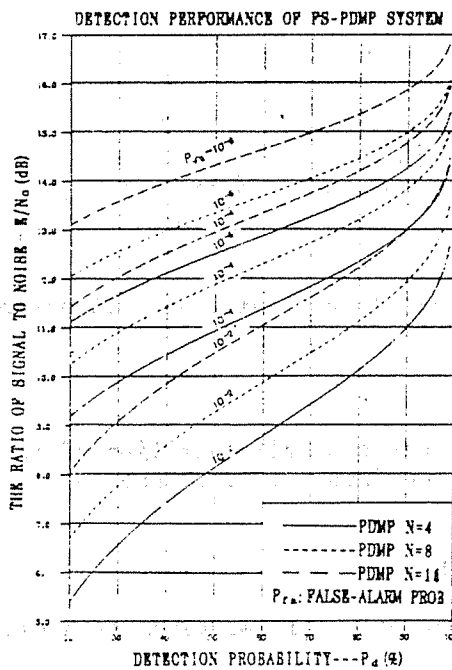
Fig. 3 ROC Curves of PDMP (N=4, 8, 16)

COMPARISON OF PDMP RECEIVER (N=8) TO COHERENT RECEIVER & ENERGY RECEIVER
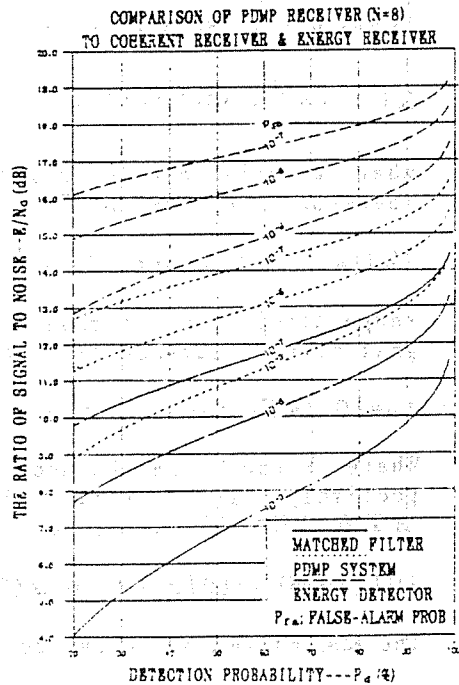
Fig. 4 ROC curves of MF, ED, and FS-PDMP (N=8)

4.0 CONCLUSION

Based on the above analyses, the differences of detection performances between FS-PDMP, MF, and ED cab be evaluated as follows:

4.1 <u>Resolution</u> Either time or Doppler resolutions of FS-PDMP is inferior to that of MF by a factor of N ($\tau_{d1}=N\tau_{d2}$, $\beta_{d1}=N\beta_{d2}$). However the resolution of ED is more inferior ($\tau_{d3}=N\tau_{d2}$ and no Doppler resolution).

4.2 <u>Detectable SNR</u> Usually a signal in noise can be rather reliably detected if the detection index $d=4$. Therefore the difference of the detectable input SNR between PDMP and MF, or ED and PDMP is equal to $2.5\lg(TW)$ dB (e.g. 4.5 dB when $TW=N^2=64$).

4.3 <u>ROC curves</u> According to Fig. 4, corresponding to a given P_d and P_{fa}, the needed value of E/N_0 for FS-PDMP is greater than that for MF, but smaller than that for ED, and almost equal to the average of the latter two.

To conclude, theoritically the detection performance of FS-PDMP is superior to that of ED, but inferior to that of MF. However, owing to the fact that the characteristic function $y(t, \beta)$ of FS-PDMP is independent of the phases of FS signal, practically this system can be more effectively used for active sonar detection under complicated sound transmission conditions.

REFERENCES

1. Zhang S., "Research on Frequency Stepping Signal", Acta Acustica, 7(5), 90-301, (1982) (in Chinese).
2. Zhang S., "A Study of FS-PDMP System", Chinese Journal of Acoustics, 5(3), 205-213, (1986).
3. Whalen A.D., Detection of Signal in Noise, Academic Press Inc., Chap. 4, 1971.
4. Abramowitz M. and Stegun I.A., Handbook of Mathematical Function, Nat. Bur. of Std. Appl, Math. Ser. 55(1966) August.
5. Urick R.J., Principle of Underwater Sound, McGraw-Hill Inc., Chap. 12, 1975.

A METHOD FOR HIGH RATE TRANSMISSION OF ACOUSTIC DATA THROUGH COAXIAL CABLE

J.W.Zhao   W.Ding   Q.P.Tu   P.Xin
P.O.Box 19
College of Marine Engineering,
Northwestern Polytechnical University (NPU)
Xi'an, Shannxi 710072, P.R.China

ABSTRACT

This paper presents a method which can be used to realiz the time-sharing two-way transmission of high rate acoustic data and command data between an underwater data acquisition module and a remote control and processing centre. Through inserting pulse-modulated carrier wave in time-domain to guide frequency,this method has successfully solved the problem of local-carrier restoration from intermittent signal, and so makes it easy to coherently demodulate the intermittent 2PSK signal with low bit-error-rate. An experimental system has been made. Its transmission rate is 3-6Mbps, transmission distance is 500-1000m and bit-error-rate is lower than 10^{-6}. In this system different kinds of signals, such as acoustic data, power pulses, command data and DC current can be two-way transmitted simultaneously through only a single-lead coaxial cable. Such a system is especially suitable for ocean acoustic telemetry, deep-ocean acoustic data acquisition, underwater robots and sonars which need high rate data transmission.

1.0 INTRODUCTION

In ocean acoustic telemetry, deep-ocean acoustic data acquisition and some of other underwater explorations, it is often needed to transmitt multiple channel sensor data to a remote contral and processing centre with high rate,and, at the same time, to send cotrol commands, DC current and power pulses downwards to the underwater data acquisition modules. When strict confinement to the sizes and weights of transmission cables exists, using a single-lead coaxial cable is superior to using a multiple-lead cable. In other words, if the effective diameter and weight of the transmission cable is constant, the transmission distance by use of a single-lead coaxial cable will be several times as large as that with a multiple-lead cable.This advantage will grow with the number of the sensor channels.

On the other hand, it is a difficult technical problem to realize the high rate two-way transmission with low bit-error-rate through only a single-lead coaxialcable. The reason will be simply described in the next section.

This paper proposes a method which we call Guiding Frequency by Inserting Pulse-Modulated Carrier Wave in Time-Domain, or Time-Domain Frquency-Guiding.It has been used in an experimental transmission system and proved a successful method for solving the problem mentioned in the last paragragh.

2.0 METHOD OF TIME-DOMAIN FREQUENCY-GUIDING

2PSK (2 Phase Shift Keying) modulation has high anticlutter ability and has found wide applications. Because of the absence of carrier component,the restoration of local-carrier becomes the heart of the matter in the coherent demodulation of 2PSK signals.When we use only a single-lead coaxial cable as media in a time-sharing two-way transmission system, the demodulator at the receiver end will get an intermittent input. There is always a non-input interval between any two adjacent segments of input 2PSK signal.This will make trouble to the working of PLL (Phase-Locked Loop).At the beginning points of each input segment,the restored local-carrier often has not the required frequency,or shows a phase ambiguousness. This will affect the bit synchronization and make bit-error-rate significantly rise.

To overcome the above difficulty, the Time—Domain Freqnency — Guiding method is proposed in this paper. It can remove the phase ambiguousness without affecting the high anticlutter ability of 2PSK modulation.

The principal points of this method can be simply described as follows.(1) At the transmitter end, a narrow pulse filled up with carrier wave is inserted at the beginning point of each 2PSK signal segment which will be sent out. We call this pulse frequency—guiding signal. This signal will be used in receiver for local—carrier restoration. The relationships among 2PSK signal segments, frequency—guiding signal and the compound transmitting signal are shown in Fig.1.
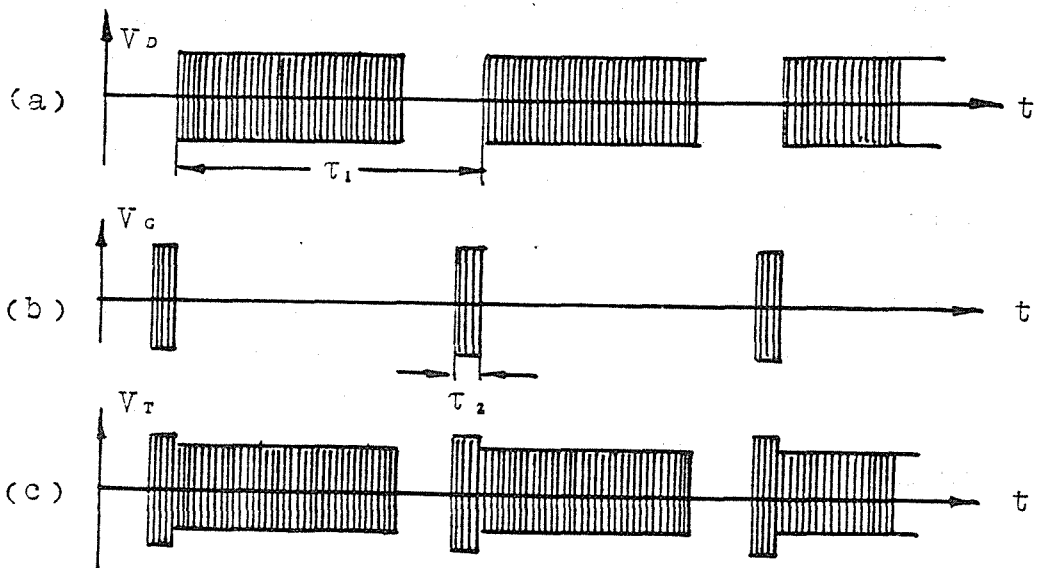
Fig.1.   (a) 2PSK signal segments;(b) frequency—guiding signal;

(c) compound transmitting signal.

(2) At the receiver end, when frequency—guiding signal is present, PLL turns into holding—state. In this state the control voltage of VCO (Voltage—Controled Oscillator) keeps constant, and so the output frequency and phase do not change.The construction and working principle is shown in Fig.2.

The PLL consists of a PD (Phase Detector), a S / H (Sample / Holding circuit) and a VCO.τ_1 is the repetition period of the frequency—guiding signal, and equals the period of 2PSK signal segments.τ_2 is the width of each frequency—guiding pulse, which should be a little more than the catching—time of the PLL.τ_3 is the width of the S / H control pulse which should be equal to or less than τ_2. The S / H control pulse is sent out by some other circuit when fre-

quency—guiding signal is present.
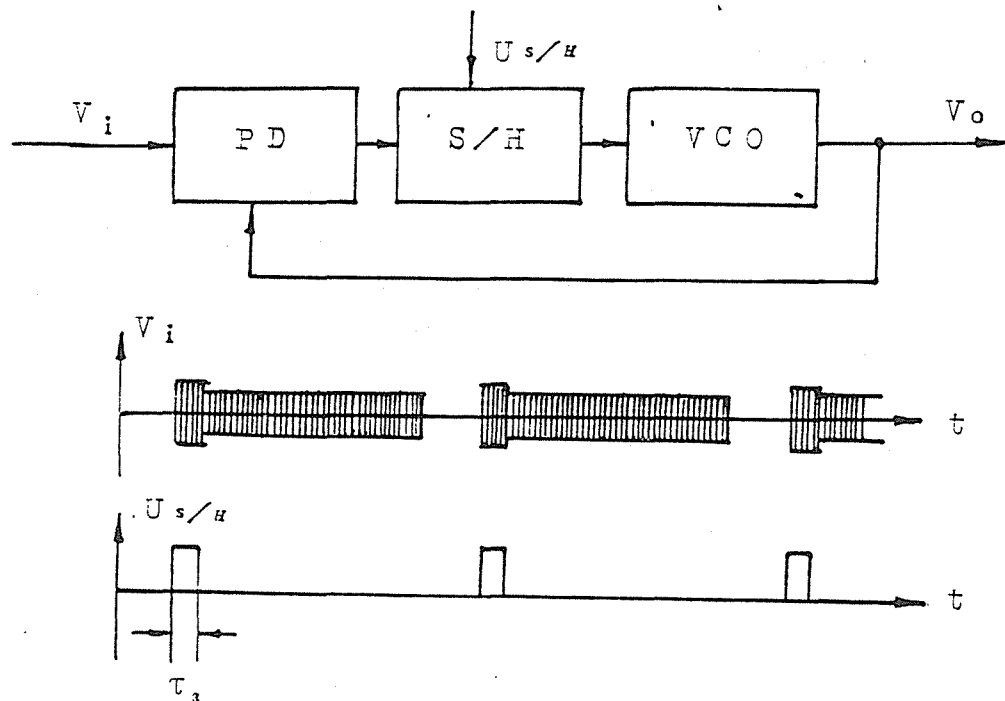
Fig.2.   The construction and working principle of the PLL

The difference between such a PLL and a normal PLL is that a S / H is interposed between the PD and VCO of the former. This S / H plays the role of a switch in the loop. When a frequency—guiding pulse arrives, the S / H control pulse makes the switch shut, then the PLL turns into tracking—state and the output of the VCO will be forced to the required frequency and phase. As soon as the frequency—guiding pulse disappears, the switch is immediately opened, and the oscillation frequency and phase of VCO keeps unchanged.

Applying such a method to the local—carrier restoration of intermittent 2PSK signal we can remove the phase ambiguousness throughly.

There are two ways to get the S / H control pulses. If the inserted frequency—guiding signal is of a higher peak—peak value than 2PSK signal, we can get the desired pulses through clamping and envelope—detection at the receiver end. But to do so will increase the complicatedness of the transmitter hardware. The second way does not need high peak—peak value frequency—guiding pulses. It utilizes the intermittence of the received signal to flip—flop a circuit to yield a pulse at the arrival of each 2PSK signal segment. We have chosen this way in our experimental system.

3.0 EXPERIMENTAL SYSTEM

Through properly selecting PD, VCO and S / H, we can construct a local—carrier restoration circuit which is able to work at high frequencies. But generally, acoustic data is of a relative low sampling rate. It is also reasonable to think that the data transmission rate is lower than 6Mbps. So the required carrier frequency should be lower than 24MHz. In such a condition, the carrier—restoration circuit can be realized with an IC chip TA7193 and a little number of digital IC chip. TA7193 is originally designed for color TV sets. It contains many functional circuits such as amplifiers, AGC, PD, VOC, S / H and multipliers. We use only one chip of TA7193 to finish the coherent demodulation of intermittent 2PSK signal. This makes the hardware of the receiver very simple, reliable and cheap.

The transmission rate of our experimental system reachs 6Mbps, transmission distance reachs 1000m, and the bit—error—rate is lower than 10^{-6}. The number of sensor channels is 25. If we use a multiple—lead cable instead of a single—lead coaxial cable to transmitt the same amount of data, the diameter of the cable will become 5 times larger.

Through interposing simple frequency—division networks at the two ends of the single—lead coaxial cab e, different kinds of signals, such as acoustic data, command data, low frequency power pulses and DC current can be two—way transmitted simultaneously. Such a system is especially suitable for ocean acoustic telemetry, deep—ocean acoustic data acquisition, underwater robots and sonars which need high rate data transmission.

4.0 CONCLUSION

If strict confinement to the sizes and weights of data transmission system exists,we may use a single—lead coaxial cable as media, select 2PSK as modulation, and insert frequency—guiding signal in time—domain to realize the coherent demodulation. This has proved to be an effective method to realize the two—way high rate transmission of multiple—channel acoustic data. This method has several advantages such as long transmission distance, low bit—error—rate, and small size

of cable. In addition, it can two—way transmitt different kinds of signals simultaneously

REFERENCES

Journals

Lindsey W.C. and Chie C.M., A Survey of Digital Phase—Locked Loop,Prec. IEEE Vol. 69, No.4 pp. 410–451, April 1981.

Books

Best, Roland E., "Phase—Locked Loops Theory, Design and Applications" Mc GRAW—HILL, 1984.

MORRIS D.J.,"Communication for Command and Control Systems", Printed in Great Britainbg A. Wheaton,1983.

PC-BASED ULTRASONIC POWER MEASUREMENT IN MILLIWATT RANGE

Cheol Ho Hwang, Moon Jae Jho, Sang Joon Suh, Hee Joon Eun

Acoustics & Vibration Laboratory
Korea Standards Research Institute
Taedok, Korea

ABSTRACT

A PC-based ultrasonic power measurement system in milliwatt range is constructed. The ultrasonic power can be determined by measuring the radiation pressure applied on a target using a PC and a self-compensating microbalance.

The accuracy of measurements strongly depends on the acoustic properties of the targets. Hence a high performance reflecting and an absorbing target are developed based on the acoustic radiation theory. Measurements are carried out under the control of PC.

In order to check the feasibility of the system, the ultrasonic power for the two targets is measured. Also the measurement errors due to the system and the reproducibility of the measurements are examined. The relative error between the two targets is proved to be less than 4%. For the ultrasonic power range larger than 10mW the standard deviation for repeated measurements is less than 2%.

1. INTRODUCTION

Currently with the increasing use of medical ultrasonics there is a need for accurate acoustic power measurements. A number of methods to measure the power output from ultrasonic transducers have been developed. These are the measurement of the radiation force on an appropriate target in the sound field(Herry), the scanning of the ultrasonic field using a calibrated hydrophone(Herman), the method of the light diffraction(Haran), and the calorimetric methods(Zieniuk).

The major advantage of radiation force measurement method is that the total radiated power can be obtained without integrating the field data over the cross section of the radiated sound beam irrespective of field restrictions. In addition the measuring devices are rather easy to handle and to calibrate.

In this study, a perfect absorbing and a perfect reflecting target were developed and the measuring system that could be used for ultrasonic power measurements in the milliwatt range was constructed by using those targets and microbalance. And the measurement system is automated by using PC.

2. Principles of measurements and system construction

If ultrasonic wave is applied on the boundary surface between two media and thus the difference between energy densities on both sides of the surface exists, force is applied to the surface in the direction that energy densities decrease. This force per unit area is called the radiation pressure. If ultrasonic wave is perfectly absorbed or perfectly reflected, ultrasonic power W can be expressed by the following equations(Gooberman):

For a perfectly absorbing target (R=0):

$$W = P_{rad} \cdot S \cdot c = F_{rad} \cdot c \tag{1-a}$$

For a perfectly reflecting target (R=1):

$$W = P_{rad} \cdot S \cdot c/2 = F_{rad} \cdot c/2 \tag{1-b}$$

where P_{rad} is the radiation pressure , F_{rad} is the time-averaged force applied on the boundary surface, S is the cross-sectional area of the beam from the ultrasonic transducer, c is the velocity of sound in the fluid and R is the reflection coefficient.

Fig.1 shows the instrumentation setup which is used in this study to measure the ultrasonic power. As can be seen in Fig.1, the ultrasonic transducer was positioned at the bottom of the vessel to radiate the ultrasonic power vertically upwards. And the target is suspended from one arm of the electrobalance by a thin wire. When the transducer is activated, the sound beam emitted from the transducer is intercepted by a target and then the target is deflected momentarily from equilibrium. By using this deflection the mechanical force acting upon it is measured . This force is equal to the mass changes multiplied by the acceleration of free fall, g=9.81m/sec^2. And thus the ultrasonic power can be obtained by using

equation (1-a). The ultrasonic power is as follows for the perfect absorbing target.

$$W = F_{rad} \cdot c = m \cdot g \cdot c, \qquad (2)$$

where m is the mass changes due to the radiation pressure.

The measurement method for the perfect reflecting target is identical with the case for the perfect absorbing target except for the fact that an absorbing lining of the measuring vessel is necessary to prevent the multiple echoes between the target and the transducer as shown in Fig.1.
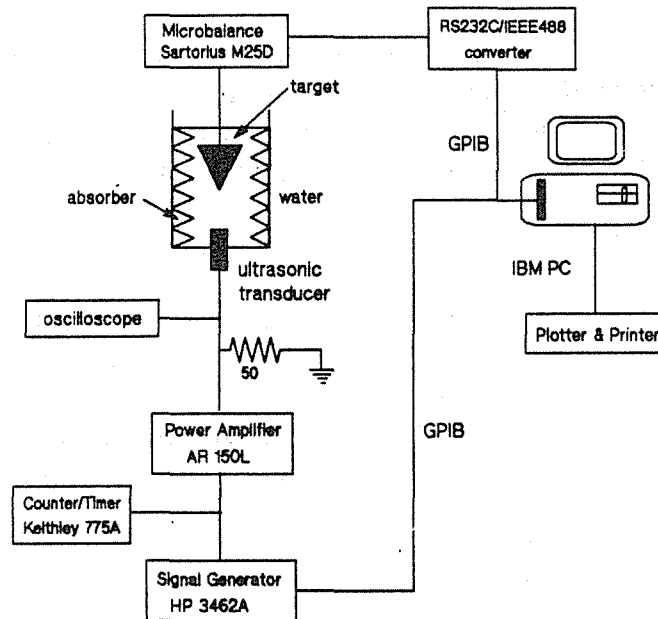
Fig.1. Experimental setup of the ultrasonic power measurement system.

If the angle between the normal to the reflecting surface and the propagating direction of the ultrasonic wave is θ, the target is subject to the vertical force $F = 2F_{rad} \cos^2 \theta$. From this we can obtain the ultrasonic power as follows if the target is a perfect reflector.

$$W = F \cdot c / (2\cos^2 \theta) = mgc / (2\cos^2 \theta) \qquad (3)$$

Equation (3) is reduced to Equation (2) for θ of 45° .
The most important thing in the instrumentation setup is to design good targets since the measurement accuracy depends on the acoustic properties of the targets used. Fig.2 shows the structure of the reflecting target made in this study. The cone-shaped reflecting target is made of high-impact polystyrene plastic foam and is coated by a 10 μm-thick nickel layer produced by electroplating to enhance the characteristics of acoustic reflection on the surface. The target is 60 mm in diameter, 7mm in thickness and 45° in θ. Fig.3 shows the section of the wedge type absorbing target made of natural rubber. To eliminate the effects due to the

392

changes in compressibility and density of the rubber and to enhance the absorbing properties, glass powder of 0.1mm in diameter is compounded in the ratio as show in the figure.
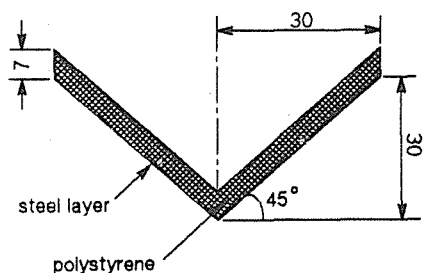
Fig. 2. Cone-typed reflecting target.   Fig. 3. Wedge-typed absorbing target.
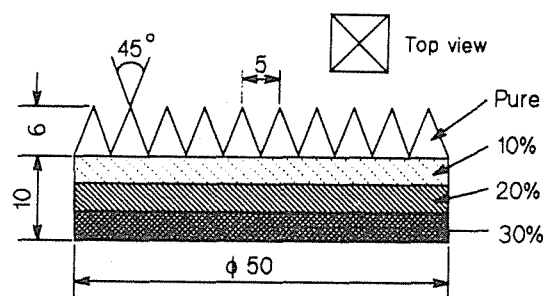
Distilled water is used in order to reduce cavitation on the faces of the transducer or target. A water vessel and an electrobalance are located on the vibration isolation table to reduce the error caused by the environmental vibration. The water vessel is placed inside an acryl box to prevent the effect of unexpected air flow.

Measurements are performed under the control of PC. Readings of the electrobalance are automatically stored in the PC and the true ultrasonic power is determined by the least square approximation and extrapolation to compensate for the transient response of the balance.

3. Performance evaluation

The measurement of radiation pressure is based upon the assumption that the target absorbs or reflects ultrasonic waves perfectly. Hence the acoustic properties of the target have to be made to fit one of these ideal characteristics and its properties must be verified by careful experiments. But in reality, it is almost impossible to confirm the precise acoustical properties of the targets due to the relatively large measurement errors in detecting the acoustic characteristics. This paper compares the test results between the reflecting and the absorbing target.

As shown in Fig. 4 (a), the mass measured by the absorbing target increases slowly with time after a 1MHz sinusoidal signal is applied to the ultrasonic transducer. This is due to the volume increase of the target which results from thermal expansion. Ultrasonic power can be determined from this mass change by equation (2). In case of absorbing target shown in Fig. 4 (a), the average of mass change is 13.2mg, which is equivalent to 200mW ultrasonic power. The difference in power measurements between a reflecting and an absorbing target is 7mW, which is less than 4% of relative error. This error is caused by the measurement and imperfect acoustic characteristics of targets. Even though the targets used in this study do not satisfy the desired acoustic properties perfectly, the experimental results show that the systematic error of measurement is less than 3%, which includes the

error caused by imperfect acoustic properties of the targets and the calibration error of the electronic microbalance.
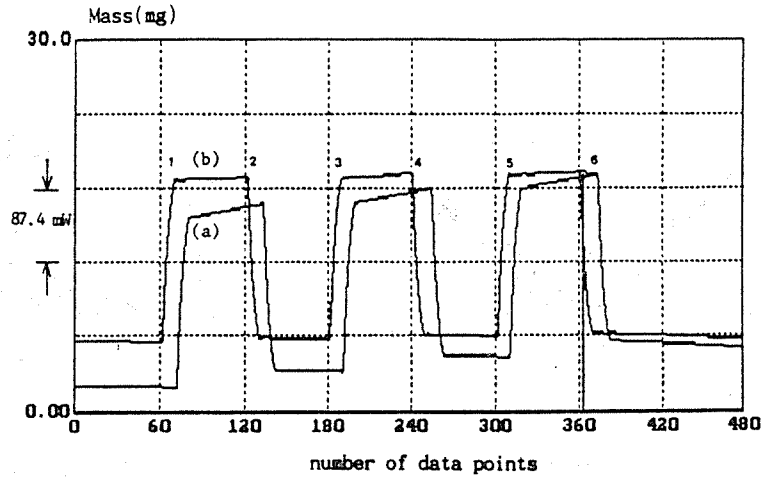
Fig. 4. Electro-balance output curves measured with two different targets
(a) absorbing target   (b) reflecting target.

The measuring range of the microbalance is from 1μg to 100mg which corresponds to the ultrasonic power between 15μW and 1.5W. But the environment of the measurement system varies with time due to the external vibration, air flow, temperature or atmospheric pressure change, causing measurement error.

Power of about 0.75mW is generated and tested in order to check the performance of measurement for the submicrowatt power range. The result is presented in Fig.5. The curves in this figure show very irregular form. Theoretically all the mass must increase with time due to the thermal expansion effect mentioned above. The curve No. 1 in which the output power decreases with time, can be explained by the environmental change of the measurement system which is much larger than the effect of thermal expansion. The highest power level of the six curves from No.1 to No.6 is 0.81mW. On the other hand, for the curve No.3, 0.71mW. The average ultrasonic power level is about 0.75mW and the relative standard deviation is 4.4%.
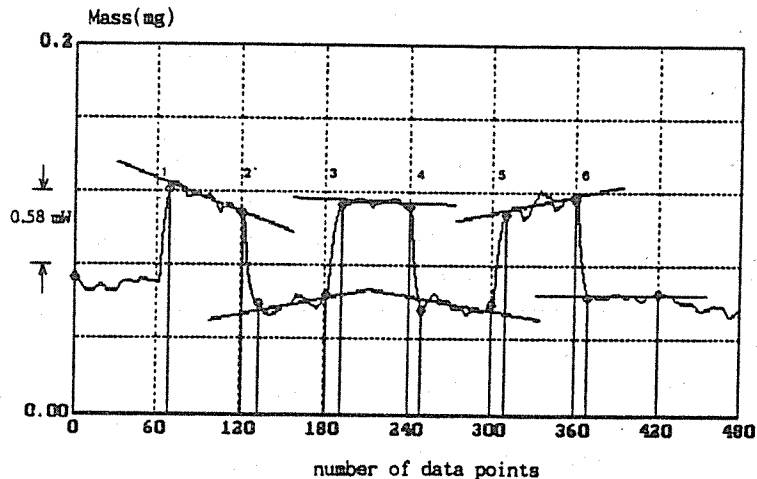
Fig. 5. Output curve of electro-balance from 0.75mW ultrasonic power.

The reproducibility of measurement system with absorbing target is examined by the following four experiments:

(1) Measurement of mass reading when preset voltage for the ultrasonic transducer is recoverd after turning off the system for at least a few minutes,

(2) Comparison of the mass readings before and after mechanical shock(i.e. after a few minutes from the shock in an arbitrary ultrasonic field),

(3) Measurement of ultrasonic power change for varing temperature,

(4) Measurement of mass reading for the target repositioned to its original place after removal.

Above experiments are repeated five times each and the results show the standard deviations of 2.14%, 1.87% and 1.68% for the case, 1mW, 10mW, 100mW, respectively. The main error sources might be classified as mechanical and electrical ones. The mechanical error sources may include the buoyance change of the target caused by external environmental change and the adhesive force change caused by imperfect wetting of the transducer and the target.

4. CONCLUSION

The results of experiments can be summarized as follows:

1) The results of ultrasonic power measurement with two different types of targets agree with each other very well with the relative error less than 4%.

2) When the ultrasonic power level goes down to 0.75mW, the relative error is 13.4%. In order to achieve high accuracy for the low level power less than 1mW, the measuring system has to be isolated from external vibrations and target has to be small enough to gurantee the minimized thermal, mechanical and noise effects.

3) The test of reproducibility produced 2% standard deviation. The major sources for this error might be the inaccuracy of electronic equipments in reproducing same voltage level and the buoyancy change of the target due to the varing experimental environment.

There might be many other error sources not mentioned in this study and we are going to try to spend more time in the furture research for this area. We believe that the identification of error sources would be very helpful to the development and maintenance of more accurate measurement systems. Our future work, in which applications of other measurement techniques and comparisons of results will be carried out, might be a solution for this problem.

REFERENCE

1. Gooberman, G.L., Ultrasonics, Hart Publishing company, New York, 45-47(1968).

2. Herry, M.J., Experimental studies on acoustic radiation pressure, J.Acoust.Soc. Am., 27.891(1955).

3. Herman, B.A., Harris, G.R.,Calibration of miniature ultrasonic receivers using a planar scanning technique, J.Acoust.Soc,Am., 57, 1436(1982).

4. Haran, M.E., Stewart, H.F., Comparison of an acousto-optic and a radiation force method of measuring ultrasonic power, J.Acoust,Soc.Am., 57.1436(1975).

5. Kossff, G., Balance Technique for the measurement of very low ultrasonic power outputs, J.Acoust.Soc.Am., 38, 880-881.

6. Zieniuk, J. Chivers, R.C., Measurement of ultrasonic exposure with a radiation force and thermal methods, Ultrasonic, 14,161(1976).

A STATISTICAL STUDY ON THE SPECKLE IMAGE IN ULTRASONIC IMAGING

Shigeharu MIYATA
Faculty of Engineering, Kinki University
5-1-3, Hiro-Koshingai,Kure-city,Hiroshima,737-01 Japan

Mitsuo OHTA
Faculty of Engineering, Kinki University
1, Umenobe, Takaya,Higashi-Hiroshima city, Hiroshima,729-17 Japan

Osamu NAGANO
Faculty of Engineering, Kinki University
5-1-3, Hiro-Koshingai,Kure-city,Hiroshima,737-01 Japan

ABSTRACT

In the ultrasound diagnosis field, an analysis of speckle image texture in ultrasound B-scans is one of the important researches using stochastic signal processing method.In this paper, it is focused on finding out theoretically the probability density function of the speckle image texture for the intensity. First, the occurrence mechanism of speckle image texture is treated by introducing the functional model for the actual ultrasound diagnosis equipment system. As a result , a unified probability density function expression has been explicitly proposed and it has been clarified that the present expression agrees with the well-known Rayleigh and Rician probability density functions as two special cases. Then, the legitimacy and the effectiveness of proposed stochastic analysis method has been experimentally confirmed by applying it to the speckle pattern of clinical B-scan image actually utilized for diagnostic purpose.

1.INTRODUCTION

As is well-known, in the ultrasound diagnosis, the investigation of image texture in the ultrasound B-scan is one of the important areas using a stochastic signal processing method. Ultrasonic measurements are potentially very useful to examine the structure of soft tissues since one feature of diffuse and local disease process of many organs, e.g., liver and spleen, is any destruction of the normal tissue architecture. But, when analyzing the ultrasound scattered by tissue, one is faced with an usually unknown geometry in the body, an unknown propagation path through overlying tissue, etc.. So, ultrasonic measurements don't yet seem to be completely understood because of a fairly complicated physical factors, such as absorption, reflection, scattering of pulsed ultrasonic pressure waves from a tissue medium , and the electrically detecting apparatus for displaying backscattered or echo pulses. The image texture, or speckle, results from an interaction between the ultrasonic pulses transmitted into the body and the structures of the tissues. In general, there are two standpoints for analyzing the image texture. One is that the texture in the image of soft tissue is observed only as irregular or undesirable noise. Several investigators on ultrasound B-scanning studying the character of ultrasound speckle only as the random noise by using a stochastic analysis method

[1,2,4,7,8]. On the other hand, another one is that the texture of the ultrasound B-scan image is associated with the microstructure of soft tissue as some regular signal and accordingly is fairly useful as a basis for diagnosis[3,5,6].

Our viewpoint is based on the latter one since the reflection and the absorption of ultrasound wave are originally caused by the variation of acoustic impedance of a tissue medium, even if the correspondence between an image texture and a tissue texture greatly depends on the scatter's size and spatial distribution of the scatters within the pulse length of incident pulse. So, it seems to be possible to abstract some information on the objective structure if a skillful stochastic signal processing method of the image texture can be found.

The stochastic researches(e.g.,probability density expressions) on a speckle pattern were discussed by many researchers in connection with the tissue characterization. Concretely, for the case of diffusely scattering material with many fine particles, a Rayleigh probability density function for the magnitude was already derived[1]. However, it is inevitable to consider the statistical properties of ultrasound speckle for the general case of clinical image that tissue can be modeled as a lot of uniformly distributed small scatters. That is, in the case when the soft tissue has some microstructure, we have to try to find more unified probability density expressions for the speckle due to the randomly distributed particles with a specular reflection. For this case, the probability density function for the intensity was expressed as a Rician probability density function[3]. Almost all of these previous studies treated only a typical case without a specular component, or were limited to a simple case when the signal is limited in a sufficiently narrow frequency band.

From the above point of view, this paper is focused on finding out theoretically how the probability density function of the image texture for the intensity is affected by the frequency bandwidth of the incident pulse, time constant of the square law detector and the existence of a specular component. First, the occurrence mechanism of speckle image texture is treated by introducing the functional model for the actual ultrasound diagnosis equipment system. As a result , a unified probability density function expression for the speckle pattern has been proposed explicitly from the theoretical viewpoint by use of a characteristic function method of probability and it has been clarified that the proposed unified expression agrees with the well-known Rayleigh and Rician probability density functions(abbr. pdf) as two typically special cases. Especially, the asymptotic property from Rayleigh probability density function to Rician probability density function has been hierarchically discussed in an individually independent form based on the orthonormal expansion expression with increasing a intensity of coherent specular component. Then, the legitimacy and the effectiveness of proposed stochastic analysis method has been experimentally confirmed by applying it to the speckle pattern of clinical B-scan image actually utilized for the diagnostic purpose.

2. Theoretical Consideration

2.1 Ultrasound Imaging System

It is widely known that individual elements of the speckle pattern do not necessarily represent individually physical scattering elements, but the speckle pattern is indeed influenced by the actually functional structure being scanned. Furthermore, the ultrasound pulsed echo is an envelope detected as an image. So, when the problem of image texture(or speckle pattern) is discussed, the influence of the operation of a measuring system upon the resultant image texture should be first considered. In this section, we consider theoretically how the distribution of the image texture for the intensity is affected by a frequency bandwidth of the incident pulse, a time constant of the detector and the existence of the coherently reflected wave components especially in comparing with Rayleigh and Rician distribution in the case of narrow frequency bandwidth. The block diagram of actual ultrasonic diagnosis equipment system is shown in Fig.1. The echoes

from a point reflector at the focus on the central axis arrive simultaneously after crossing the surface of active transducer elements by introducing appropriate electronically controlled swept time delays. Then, the signals are compressed to video display levels by a logarithmic amplifier, detected by the detector and summed for final display. The signal rectified after passing through this logarithmic amplifier is mathematically expressed as even function. Furthermore, by expanding this function in the form of Taylor series expansion, this signal can be expressed as sum of even power series. However, supposed that the higher frequency components are cut off owing to the cascaded low pass filter or are greatly attenuated than the second order power component, the intensity corresponding to the brightness displayed can be regarded as being functionally equivalent to the output intensity via mean squaring detector as shown in Fig.2. Consequently, by putting aside its detailed signal transformation in the individual part of the actual ultrasonic equipment system, for catching a central mode of signal transformation which can be held through a whole process, it is sufficient to pay our attention to mainly the mean squaring detector in the imaging process. Accordingly, the pdf expression of the speckle pattern obtained by the equivalently standardized measurement system model of imaging process as shown in Fig.3 is considered.

2.2 Model Expression for Ultrasound Imaging

In an ultrasound B-scan image, the pulsed incident ultrasound pressure wave f(t) with a frequency bandwidth W is observed as an intensity image texture resulting from an interaction between the structures of tissues and the coherent ultrasonic pulses transmitted into the body, after passing through the square law detector with an averaging time T in Fig.3. Of course, the ultrasound pressure wave f(t) consists of a signal component S(t) from the regular tissue with specularity and a random noise component(i.e., speckle) N(t) from the irregular tissue with diffusely scattering particles, after absorption and reflection caused by the regular and irregular variation of acoustic impedance. Of course, differing from the signal component, this random component N(t) shows an undetermined property as a sum of infinite elemental echo components from an ensemble body of scattering particle with random phase and random amplitude caused by various type reflection and absorption from the irregular change of acoustic impedance based on the diffusely scattering tissues. Thus, the observed ultrasound intensity after passing through the square law detector in a B-scan image can be explicitly expressed as follows:

$$E=\frac{1}{T}\int_0^T f^2(t)dt = \frac{1}{T}\int_0^T \{S(t)+N(t)\}^2 dt. \tag{1}$$

Supposed that f(t) is repeated with a constant period T, f(t) can be expanded in the following Fourier series :

$$f(t)=N(t)+S(t) \cong \sum_{n=1}^{N} \{(a_n+c_n)\cos(\frac{2\pi}{T})nt+(b_n+s_n)\sin(\frac{2\pi}{T})nt\}, \tag{2}$$
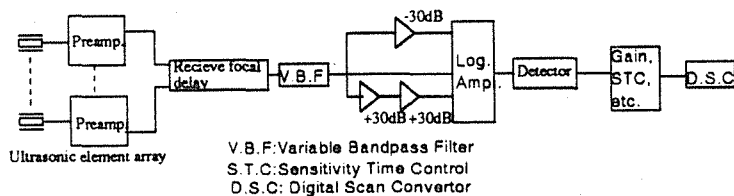
Fig.1 The block diagram of the actual ultrasonic diagnostic equipment system
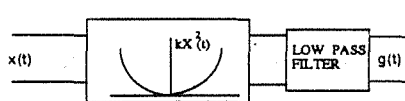
Fig.2 The standardized equipment model for the actual ultrasonic diagnosis equipment system where a signal component:
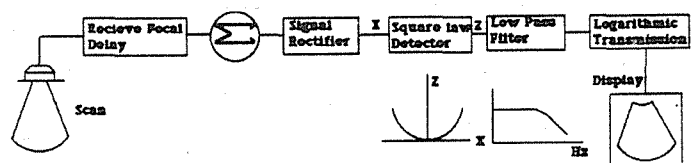
Fig.3 Measurement system model

$$S(t)=\sum_{n=1}^{N}\{c_n\cos(\frac{2\pi}{T})nt+s_n\sin(\frac{2\pi}{T})nt\} \tag{3}$$

with a power:

$$E_s=\frac{1}{T}\int_{0}^{T}S^2(t)dt = \sum_{n=1}^{N}(c_n^2+s_n^2)/2 . \tag{4}$$

Here, Fourier coefficients a_n's and b_n's are all statistically independent of each other and are Gaussianly distributed with mean value of zero.

When $f(t)$ has an arbitrary frequency bandwidth $W=f_0\cdot(N_2-N_1)$ $(f_0=1/T)$ of ideal rectangular type , the mean intensity expression can be obtained by use of a complete relation of Parseval equation as follows:

$$E(\equiv R^2)=\frac{1}{T}\int_{0}^{T}f^2(t)dt\cong\sum_{n=N_1}^{N_2}\{(a_n+c_n)^2+(b_n+s_n)^2\}/2=\sum_{n=1}^{N}X_n^2 \tag{5}$$

with

$$X_n=(a_n+c_n)/\sqrt{2}, \quad (b_n+s_n)/\sqrt{2} , \tag{6}$$

where R shows an effective value of intensity fluctuation.

Following Shannon's sampling theorem in the frequency domain, when the Fourier transformation $F(f)(\equiv\int_{0}^{T}f(t)e^{-j2\pi ft}dt)$ is sampled at every Nyquist cointerval $1/T$, the number of sampling necessary to determine $f(t)$ is given as

$$N=\frac{2W}{1/T}+1\cong2TW(\text{for large T and/or W}). \tag{7}$$

Here, the dimension N is related to the degree of freedom of the intensity fluctuation.

2.3 Probability Density Expression for Random Process with a Regular Component for Infinite Numbers of Scatters

The present problem is : what is the probability density distribution of the observed ultrasound intensity $E(\equiv R^2)$ for the Gaussian ransom process $f(t)$ in the presence of a regular signal component $S(t)$ under Eq.(5)? If the random ultrasonic pressure wave $N(t)$ is originally a white noise, the statistical property of randomness is reflected in each of a_k and b_k, and it follows an independent Gaussian distribution with mean value of zero and constant variance. In the case of considering the random process with a regular component $S(t)$, each component $X_n(n=1,2,...,2TW)$ is given by Eq.(6)($X_n=(a_n+c_n)/\sqrt{2}$ or $(b_n+s_n)/\sqrt{2})$, which is a scalor sum of each components for incoherent and coherent ultrasound waves. So, each of X_n has the following statistical properties as (mean value)

$$\mu_n(\equiv<X_n>)=c_n/\sqrt{2}, \quad s_n/\sqrt{2} \qquad (\forall n) , \tag{8.a}$$

(variance)

$$\sigma_0^2(\equiv<(X_n-\mu_n)^2>)=<a_n^2>/2, \quad <b_n^2>/2 \qquad (\forall n) , \tag{8.b}$$

where $< >$ denotes an ensemble average. Accordingly, a joint probability density function of X_i's can be expressed in the form of N products of one dimensional Gaussian distribution owing to the statistically independent property among X_i's as follows:

$$P(X_1,X_2,\cdots,X_N)=\prod_{n=1}^{N}P(X_n)=\prod_{n=1}^{N}N(X_n;\mu_n,\sigma_0^2) \tag{9}$$

with

$$N(X_n; \mu_n, \sigma_0{}^2) = \frac{1}{\sqrt{2\pi}\,\sigma_0} \exp\{-\frac{(X_n-\mu_n)^2}{2\sigma_0^2}\}. \tag{10}$$

Now, in order to reflect hierarchically and explicitly the effect of each coherent component μ_n, $P(X_n)$ is reduced in advance as follows:

$$P(X_n)=N(X_n;\, 0,\sigma_0{}^2) \sum_{j=0}^{\infty} \frac{\mu_n{}^j}{j!\sigma_0{}^2} H_j(\frac{X_n}{\sigma_0}). \tag{11}$$

Then, substituting Eq.(11) into Eq.(9), a joint probability density function can be rewritten as

$$P(X_1,X_2,\cdots,X_N)=\prod_{n=1}^{N} N(X_n;\, 0,\sigma_0{}^2) \sum_{j=0}^{\infty} \frac{\mu_n{}^j}{j!\sigma_0{}^2} H_j(\frac{X_n}{\sigma_0}). \tag{12}$$

It is more convenient to start with a characteristic function (or moment generating function) to derive the probability density function of intensity E based on Eq.(12). The characteristic function of E becomes through the original definition by letting $\theta=jt(j=\sqrt{-1})$ as

$$M_E(\theta)=\int_0^{\infty} e^{\theta E}P(E)dE= \int_{-\infty}^{\infty} \cdots \int_{-\infty}^{\infty} \exp\{\theta\sum_{n=1}^{N}X_n{}^2\}\cdot P(X_1,X_2,\cdots,X_N)dX_1 dX_2\cdots dX_N$$

$$=\prod_{n=1}^{N} [\int_{-\infty}^{\infty} \exp\{\theta X_n{}^2\}\cdot P(X_n)dX_n] =\prod_{n=1}^{N} [\sum_{j_n=0}^{\infty} \frac{\mu_n{}^{j_n}}{j_n!\sigma_0{}^{j_n}}I_{j_n}], \tag{13}$$

where

$$I_{j_n}= \int_{-\infty}^{\infty} \exp\{\theta X_n{}^2\}\cdot N(X_n;0,\sigma_0{}^2)H_{j_n}(\frac{X_n}{\sigma_0})dX_n = \frac{1}{\sqrt{\pi}} \frac{(4\sigma_0^2\theta)^{j_n/2}}{(1-2\sigma_0^2\theta)^{(j_n+1)/2}} \Gamma\left(\frac{j_n+1}{2}\right). \tag{14}$$

Under substitution:

$$j_n=2k_n,\ m=N/2,\ s=2\sigma_0^2, \tag{15}$$

the characteristic function of E can be consequently expressed after some troublesome calculations as follows:

$$M_E(\theta)=\prod_{n=1}^{N} \left\{ \sum_{k_n=0}^{\infty} \frac{2^{k_n}\mu_n{}^{2k_n}}{(2k_n)!\, s^{k_n}} \frac{1}{\sqrt{\pi}}\cdot \frac{(2s\theta)^{k_n}}{(1-s\theta)^{k_n+1/2}} \Gamma\left(k_n+\frac{1}{2}\right)\right\}$$

$$=\sum_{k=0}^{\infty} \sum_{k_1+k_2+\cdots+k_N=k} \prod_{n=1}^{N} \frac{2^{k_n}\mu_n{}^{2k_n}}{(2k_n)!\, s^{k_n}} \frac{1}{\sqrt{\pi}} \frac{(2s\theta)^{k_n}}{(1-s\theta)^{k_n+(1/2)}} \Gamma\left(k_n+\frac{1}{2}\right)$$

$$=\sum_{k=0}^{\infty} \sum_{k_1+k_2+\cdots+k_N=k} \frac{1}{(1-s\theta)^m} \left(\frac{s\theta}{1-s\theta}\right)^k \frac{\mu_1{}^{2k_1}\cdots\mu_N{}^{2k_N}}{s^k} \prod_{n=1}^{N} \frac{2^{2k_n}}{(2k_n)!\sqrt{\pi}}\Gamma\left(k_n+\frac{1}{2}\right) \tag{16}$$

Using the well-known property of Gamma function:

$$\Gamma\left(n+\frac{1}{2}\right)=(2n)!\sqrt{\pi}/(2^{2n}n!) \tag{17}$$

and the following relation :

$$B\equiv\sum_{n=1}^{N}\mu_n{}^2 , \tag{18}$$

we can finally obtain the characteristic function of P(E) as follows:

$$M_E(\theta)(=\int_0^\infty e^{\theta E} P(E)dE)=\frac{1}{(1-s\theta)^m}\sum_{k=0}^\infty \left(\frac{s\theta}{1-s\theta}\right)^k \left(\frac{B}{s}\right)^k \frac{1}{k!}\frac{1}{(1-s\theta)^m}\exp\left\{\frac{B}{s}\frac{s\theta}{1-s\theta}\right\},\quad (19)$$

where s,B and m denote an average intensity of one frequency component of random component N(t), an average intensity of signal(or specular) component S(t) and a half of dimension(TW), respectively. In principle, the probability density function of E can be obtained from the above characteristic function of P(E) using the inverse Fourier transformation of $M_E(\theta)$ supported by Levy's inverse lemma. But, the different way of transformation will be now adopted in order to reflect hierarchically and explicitly the effect of coherent(or specular) component S(t)(intensity is B). The characteristic function of P(E) in Eq.(19) can be expanded in the Taylor's expansion type as

$$M_E(\theta)=\frac{1}{(1-s\theta)^m}\sum_{n=0}^\infty \frac{1}{n!}\left(\frac{s\theta}{1-s\theta}\right)^n \left(\frac{B}{s}\right)^n.\quad (20)$$

If a well-known Carson integral is used under substitution $p=1-s\theta$, $a=m-1$, $z=\frac{E}{s}$, as follows:

$$\frac{1}{n!}\frac{1}{p^{n+\alpha+1}}(p-1)^n=\int_0^\infty e^{-pz}\frac{z^a}{\Gamma(n+\alpha+1)}L_n^{(\alpha)}(z)dz,\quad (21)$$

comparing Eq.(20) with Eq.(21), the following probability density function of Laguerre series expansion type is directly derived as

$$P(E)=\frac{1}{\Gamma(m)s^m}E^{m-1}e^{-(E/s)}\left\{1+\sum_{n=1}^\infty (-1)^n\left(\frac{B}{s}\right)^n \frac{\Gamma(m)}{\Gamma(m+n)}L_n^{(m-1)}\left(\frac{E}{s}\right)\right\}\quad (E>0),$$
$$=0\qquad\qquad\qquad (E\le 0).\quad (22)$$

The cumulative distribution function(abbr. cdf) expression is calculated as follows:

$$Q(E)\equiv\int_0^E P(E)dE=\int_0^E p_\Gamma(E;s,m)dE +p_\Gamma(E;s,m)\sum_{n=1}^\infty(-1)^n\left(\frac{B}{s}\right)^n\cdot\frac{\Gamma(m)}{\Gamma(m+n)}\frac{E}{n}L_{n-1}^{(m)}\left(\frac{E}{s}\right),\quad (23)$$

where

$$p_\Gamma(E;s,m)=\frac{E^{m-1}}{\Gamma(m)s^m}e^{-E/s}.\quad (24)$$

Equation (22) is the expression with Gamma distribution as first term and reflects hierarchically the effect of intensity B in any expansion coefficients. In the case with m=1 in Eq.(22), it can be verified that Eq.(22) agrees completely with a Rician distribution as a whole. Thus, Eq.(22) shows hierarchically the asymptotic property from Rayleigh pdf to Rician pdf with increasing a magnitude of coherent(or specular) component. Furthermore, in a special case when there is no specular reflection and a frequency bandwidth of f(t) is comparatively narrow, that is, m=1, Eq.(22) can be reduced to a well-known Rayleigh distribution .

3.Experimental Consideration

In the preceding section, we have derived theoretically the expression of probability density function on the ultrasound intensity E in the presence of a specular signal component. In this section, we have confirmed the effectiveness of the above theory from the experimental viewpoint by applying it to the speckle pattern of clinical B-scan image actually utilized for diagnostic purpose. We have obtained experimental data by using a microdensitometer to scan film transparency images of ultrasound B-scans. The stepped gray scale included in the film image was calibrated in terms of decibel, which was set on the basis of the most gray scale corresponding to the weakest ultrasound echo magnitude.

Then, the speckle fluctuations in terms of photographic density was converted to fluctuation in ultrasound echo intensity.

Figure 4 shows a comparison between a Laguerre series expansion type distribution(see Eq.(22)) and an experimentally sampled values for cumulative distribution. This results shows that the curve of Laguerre series expansion type distribution moves towards the experimentally sampled values with successive addition of the higher expansion terms. The curve of Laguerre series expansion type distribution almost converges with n=15.

In order to discuss superiority or inferiority among Rayleigh distribution , Rician distribution, Gamma distribution and Eq.(22) , first, their distribution parameters have to be previously estimated. A parameter m(=N/2) is directly obtained as m=TW from its definition by using an nominal bandwidth W with a center frequency 3.5MHz of input ultrasound pulse used and a time constant of T of square law detector. In this experiment, an estimate m=2 has been first obtained, and the other parameters have been estimated by use of method of moment as follows:

A) for Rayleigh distribution(m=1) : $2\sigma_0^2=<E>$, B) for Rician distribution(m=1) $B=<E>^2-$

$<(E-<E>)^2>$, $2\sigma_0^2=(<E>-B)$, C) Laguerre series expansion type distribution(Eq.(22)):

$B=<E>^2-<(E-<E>)^2>$,$2\sigma_0^2(=s)=(<E>-B)/m)$, D)for Gamma type distribution(Eq.(24)) :

$2\sigma_0^2(=s)= <E>/m$.

Figure 5 shows a comparison between experimentally sampled values and theoretically evaluated curves for the cumulative probability distribution. It is obvious that Rayleigh distribution, Rician distribution and Gamma distribution don't fit the experimental distribution at all. This reason seems to be as follows. Rayleigh distribution taking only sufficiently narrow frequency bandwidth into account and Gamma distribution taking frequency bandwidth W and a time constant T into account corresponds originally to a
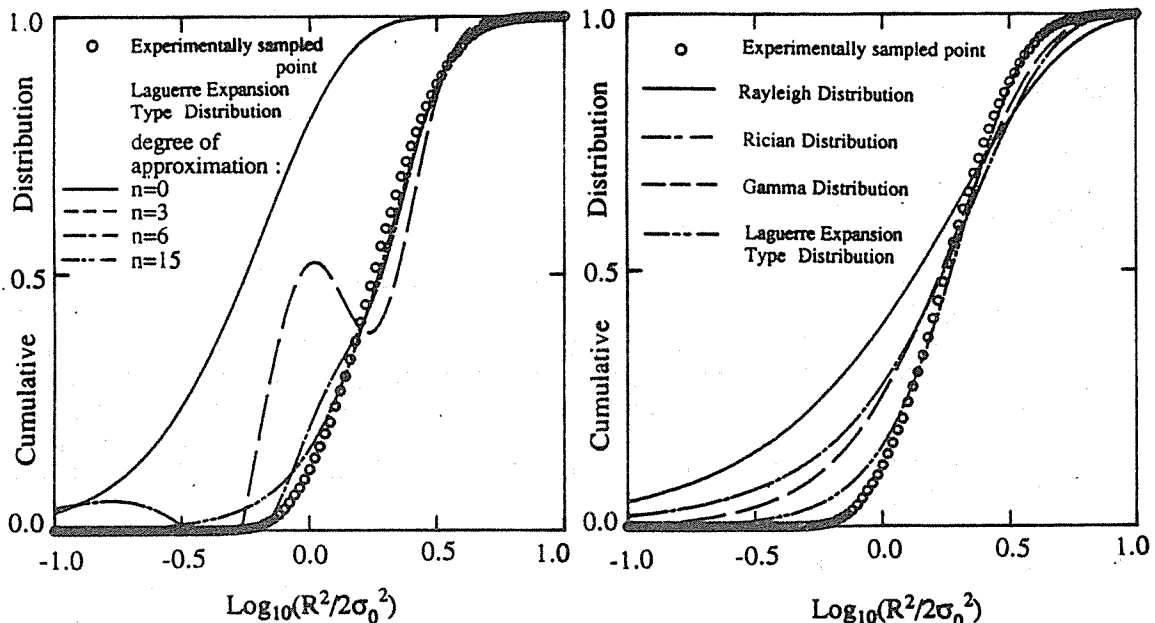
Fig.4 A comparison between the proposed Laguerre expansion type distribution (Eq.(22)) shown with the successive numbers ,n, of each expansion term.

Fig.5 A comparison between theoretically evaluated curves and experimentally sampled points for cumulative distribution for speckle pattern of B-mode image.

special case of pure diffuse scattering, often to a fully developed speckle pattern. Rician distribution results from the combination of a strong specular component and weak random components, but the input signal is assumed to have a sufficiently narrow

frequency bandwidth. On the other hand, with regard to the proposed Laguerre series expansion type distribution, the fitness is quite better than the other three type distribution expressions. This reason is that the effect of equipment and physical parameters, that is, a frequency bandwidth of input ultrasound pulse, a time constant of square law detector and the presence of specular scattering are explicitly reflected as distribution parameters.

4.Conclusion

In this paper, we have studied theoretically how the probability density function of the speckle image texture can be given in the more actual case with presence of a specular component with the perfect correlation among the scattered waves. Here, the occurrence mechanism of speckle image texture has been treated by introducing the functional model for the actual ultrasound diagnosis equipment system. From the above point of view, the unified probability density function for the intensity fluctuation of resultant waves of incoherent ultrasound random waves and specular type coherent ultrasound waves, after passing a square law detector, has been derived from the theoretical viewpoint by use of a characteristic function method of probability. It has been found that the present theory completely agrees with the well-known Rayleigh and Rician distribution expressions as two typically special cases.

The main part of present research has been first focused on a new establishment of unified stochastic theory since it is at an early stage of study. So, there remain many kinds of problems on i)detecting some meaningful information for abnormal tissue buried under the speckle pattern, in connection with stochastic image processing, ii)finding the quantitative evaluation method for the studying tissue characterization , iii) taking the effect of frequency dependent attenuation character into account, iv) finding the method to detect only the effective signal by using not only the above static type imaging processing but also the dynamic type digital filter, and so on.

Acknowledgment

References

1)Christoph B.Burckhardt :Speckle in Ultrasound B Mode Scans,IEEE Trans. on Sonics and Ultrasonics, Vol.Su-25, No.1(1978),1-6.
2)John G. Abbott and F.L. Thurstone:Acoustic Speckle;Theory and Experimental Analysis,Ultrasonic Imaging, Vol.1(1979),303-324.
3)Joynt LF:A Stochastic Approach to Ultrasonic Tissue Characterization, Ph.D. thesis, Stanford University, also published as Tech. Report No.G557-4(1979).
4)Dennis L Parker: Analysis of B-scan Speckle Reduction by Resolution Limited Filtering, Ultrasonic Imaging, Vol.4(1982),108-125.
5)S.W.Smith and R.F.Wagner: Ultrasound Speckle Size and Lesion Signal to Noise Ratio; Verification of Theory, Ultrasonic Imaging, Vol.6(1984),174-180.
6)J.M.Thijssen and B.J.Oosterveld: Speckle and Texture in Echography;Artifact or Information, Ultrasonic Symposium(1986),803-809.
7)Robert F.Wagner,Michael F. Insana and Stephen W. Smith:Fundamental Correlation Lenghths of Coherrent Speckle in Medical Ultrasonic Images,IEEE Trans. on Ultrasonics,Ferroelectrics and Frequency Control, Vol.35, No.1(1988),34-44.
8)Levin Nock and Gregg E. Trahey: Phase Aberration Correction in Medical Ultrasound Using Speckle Brightness as a Quality Factor, J.Acoust. Soc. Am. Vol.85,No.5(1989),1819-1833.

NARROW BAND ULTRASONIC DETECTOR FOR LEAKAGE INSPECTION

Shao Zhi-Chang
Institute of Acoustics, TongJi University,
1239 Siping Road, Shanghai, 200092, China.

ABSTRACT

Leaks through the orifice in all kinds of pressure system usually create broad band noise covered the frequencies from 20 to 100 kHz. Thus the conventional ultrasonic detectors must have several kHz receiving bandwidth at about the 40 kHz centre frequency in order to avoid missing in checking leaks. But when the interference noise is high the leakages can not be detected properly by such detector.

A new design with a narrow band receiving technique is presented in the paper. The experiment results have shown if the receiving band is reached to ± 150 Hz, the leak still can be well detected but the random interference noise be greatly reduced. It has been verified by inspecting the overhead telephone cables passing through the trees with rustle noise by the swaying of leaves. Owing to its high receiving sensitivity ($\leq$ 0.3 nbar at $\geq$ S/N 6 db) it can be worked with many advantages in any kinds of leakage testing, such as a 0.1 mm diameter hole with 0.1 kg/cm^2 of pressure can be detected at 2.5 to 3.0 meters away. This detector does not need any low noise components and special transducers, so that it is more suitable for manufacture. Besides, it can also be applied in other weak signal detection and localization such as inspecting the white ants etc.

1.0 INTRODUCTION

Leaks in all kinds of pressure system and sealed system can be non-destructively detected by the ultrasonic detector. It has been used in chemical industry, telephone communication, food industry and construction work, etc.

Conventional ultrasonic detector must have a wide receiving bandwidth which covers a main range of the leak noise frequencies in order to miss few leaks in practice, if any. But it can be easily effected by the environmental interference noise. Sometimes while the interference noise is serious the leakage can't be detected properly.

A new ultrasonic detector with a narrow band receiving technique is presented in the paper. It not only notices the main range of the leak noise frequencies but also mainly considers the variation of the leak noise intensity on its frequency range. The testing results have shown if the receiving bandwidth of the detector reaches to +/- 150 Hz at the 40 KHz center frequency, the random intermittent interference noise can be reduced a lot but the leak noise still be well recognized in practice.

2.0 PRINCIPLE OF LEAK DETECTING

Fig.1 schematically explains the principle of leak detecting as the gas or liquid passes through the orifice in all sorts of pressure system. It causes the turbulent flow to produce ultrasonic noise, usually the subsonic speed jet noise, which covers a broad band spectrum from 20 KHz to 100 KHz, one of which is shown in Fig.2. It has
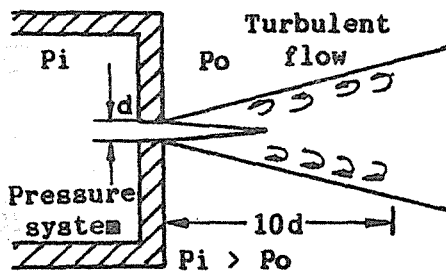
Fig.1. Schematic diagram of producing leak noise in pressure systems.
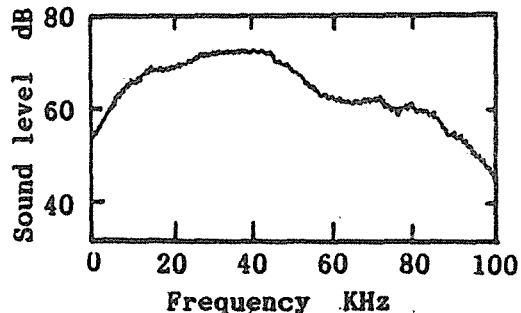
Fig.2. Schematic ultrasonic spectrum of typical gas leak.

following features. The leak ultrasonic spectrum shows a noticeable peak frequency and it can be estimated by the following formula.

$$f = k \, v/d \qquad\qquad [\text{Hz}] \qquad (1.1)$$

Where f is the peak frequency; v is the flow speed on the leak nozzle, m/s ; d is the diameter of the leak orifice, m ; and k is the constant, which depends on Reynolds number (usually, k = 0.2). For example, v = 200 m/s, d = 0.1 mm, that f = 40 KHz. The flow speed v is direct proportion to the square root of the pressure difference of the pressure system (Pi - Po). Its leak transmit sound power level Lw can also be approximately estimated by the formula below when it belongs to subsonic speed jet noise.

$$Lw = - 45 + 10 \lg S + 80 \lg v \qquad [\ dB\ ] \qquad (\ 1.2\ )$$

Where the S is the area of the leak orifice, which is considered as a circular jet nozzle, ㎜ ; v is also the flow speed of the leak, ㎜/s. Its error between the calculating value and the experiment measurement value is within +/- 5 dB. For above example its Lw is: Lw = 84 dB. The sound power W of the leak noise is a eight-power relationship with its flow velocity v when the Mach number (M = v/c) is less than 2. That is, if the flow speed v is doubled, its sound power W will gain 256 times or its sound power level Lw will gain 24 dB. On the other hand these hind of leak spectra are similar to each other and the different value of theirs octave sound level is less than 10 dB within 6 octaves range. Finally, this sort of ultrasonic noise has obvious directivity. It also depends on the Mach number.

Thus leaks in pressure system can produce continuous, stationary ultrasonic noise signals and its transmit sound power or sound power level is concerned with its flow speed. It can be, therefore, pinpointed by finding those leak ultrasonic noise signals.

If it is an unpressured sealed system, a ultrasonic generator is placed inside the system in which it transmits the same ultrasonic frequency as the ultrasonic detector. The ultrasonic wave can be escaped or penetrated through the leak orifice to outside of the sealed system and be picked up by the ultrasonic detector shown in Fig.3. The ultrasound transmission coefficient of a standard leak orifice is shown in Fig.4, and we can see at the 40 KHz to 50 KHz the transmission coefficient is relatively small. Using this technique leaks as small as 0.02 ㎜ thickness of the standard orifice with 20 ㎜ length can be easily detected.
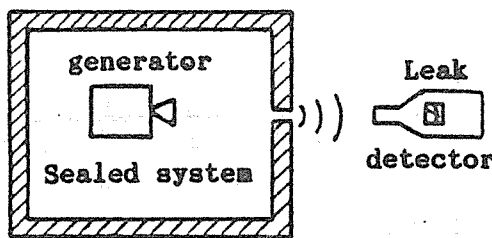
Fig.3. Schematic diagram of leak detecting of unpressurize systems.
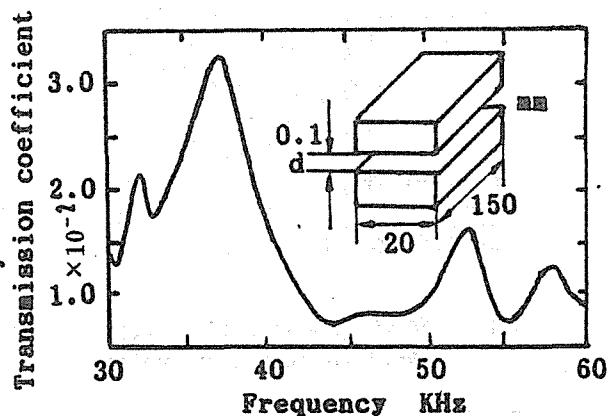
Fig.4. Correlation between transmission coefficient and frequency for a orifice.

3.0 ULTRASONIC LEAK DETECTOR

The block diagram of a typical ultrasonic leak detector is shown in Fig.5. It can be worked by the battery and operated by one hand. Its receiving transducer usually uses piezo electric crystals which convent the ultrasonic waves into electrical signals. From the transducer the small output signal voltage passes to the preamplifier then to
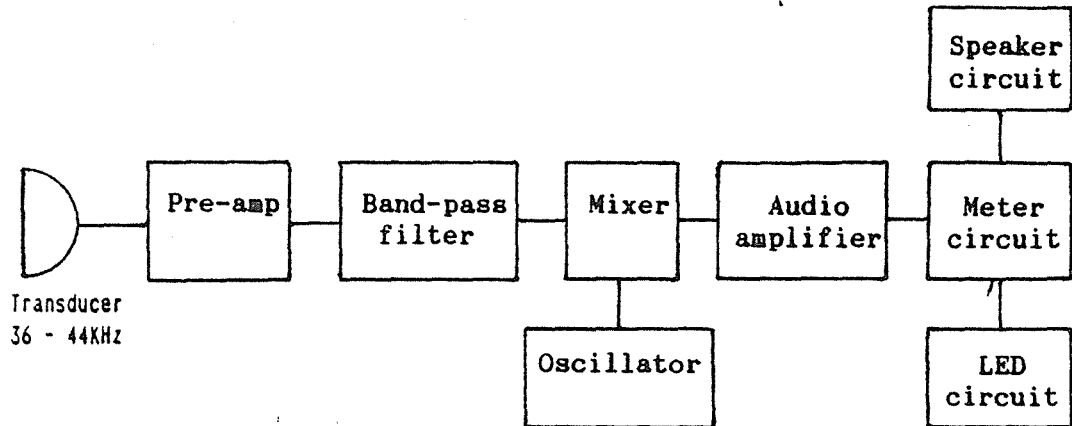
Fig.5. Simplified block diagram of typical ultrasonic leak detector.

the band-pass filter stage to limit the other interference noise and reaches to about 1μV resolving power limit. And then the amplified signal will be heterodyned in the mixer stage with a 40KHz local oscillator and generated a beat frequency turned into the audible range. This can then be amplified further in the audio amplifier stage to provide a suitable signal voltage for some indicator units such as the built-in loudspeaker (or output to headphone), LED or Meter indicator to displays the relative leak noise signal intensity. These audio frequency signals have distinct characteristics which allow the user to identify the different leak source.

The bandwidth of the detector depends on the frequency range of the ultrasonic spectrum of the typical leaks which contain a noticeable component at around 40 KHz so that conventional ultrasonic detector and its transducer have a bandwidth +/- 4 KHz at 40 KHz center frequency (some detectors even have +/- 12 KHz) in order to avoid missing leaks in practice. In this case the detector has to be a special low noise stage in preamplifier to allow detection of small or distant leaks that just above the noise level of the amplification circuits, and its transducer also must be specially designed to fit its bandwidth. Thus it is difficult and expensive for this kind of detector to design as well as manufacture. But the most important thing is that this kind of bandwidth is still too wide to avoid the environmental interference noise in some sites.

4.0 NARROW BAND ULTRASONIC DETECTOR

Could we use more narrow receiving band to limit the interference noise and obtain the same leak detecting effect ? From the leak noise spectrum, which is shown in Fig. 1, we also can see the variation of the leak noise intensity over the whole range is little. So only a small part of the leak noise frequencies can be detected , the leakage will still be pinpointed out in practice. In different leak sits the amplitude differences of their spectra in certain frequency, such as 40 KHz, are little about 10 dB to 14 dB. If the receiving sensitivity of the detector can be raised that dB value by the narrow band technique, the inspecting of the leaks also don't be missed. When the bandwidth of the detector reaches to +/- 150 Hz, just about 1 / 25 bandwidth of the conventional detector, it can get as 14 dB (5 times

407

) high sensitivity as conventional detector in the same ratio of signal to noise. That is the narrow band detector can still obtain the same effect in leak detecting.

When the environmental interference noise is intermittent, the narrow band detector can greatly reduce that noise and obtain more advanced leak detecting effect. It can be explained by the Fig.6 and Fig.7.
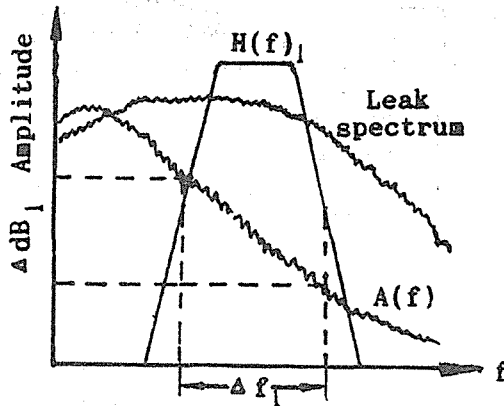
Fig.6. The interference noise output of the conventional band mode.
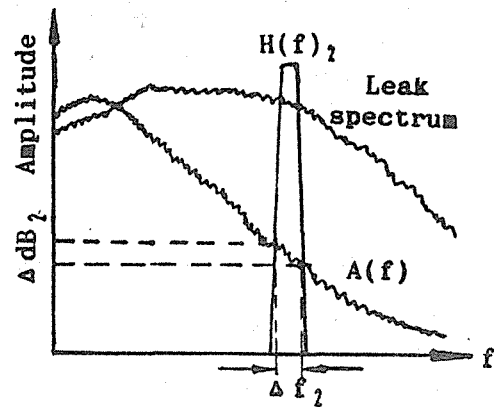
Fig.7. The interference noise output of the narrow band mode.

In Fig.6 and Fig.7 the $H(f)1$ and $H(f)2$ is the frequency response function of the band-pass filter of the detector (the filter amplitude characteristic), $A(f)$ is the spectrum of the input interference noise signal and $\Delta dB1$ and $\Delta dB2$ is the output amplitude of the interference noise with the filter. Because the output frequency spectrum of the detector is $B(f) = H(f) \cdot A(f)$ and the filter amplitude characteristic is $H(f)2 << H(f)1$, the output amplitude $\Delta dB2$ is more less than $\Delta dB1$. So the narrow band detector can greatly avoid the environmental interference noise. It can be designed out by using a solid narrow band-pass filter instead of normal band-pass filter stage which is shown in Fig.5. The sound receiving sensitivity of the narrow band detector can reaches to about 0.3 nbar, that is the input voltage sensitivity is about $0.2\mu V$ ($S/N \geqslant 6$ dB) without any specially low noise components.

5.0 CONCLUSION

We compare the experiment results with the narrow band detector and normal leak detector for inspecting the leakage of the overhead cables, which contain dry air to prevent moisture from entering , at the ground aiming the overhead cable. When the cable passes through the street trees, and the rustle interference noise, which is produced by the wind to sway the leaves, sometimes is serious, that the normal leak detector can't find out the leakage, but the narrow band detector still can do it well. Besides in order to test the inspecting effect of the narrow band detector a 0.1 mm diameter hole leakage with 0.1 kg/cm^2 of pressure can be detected at 2.5-3.0 meters away. Thus it shows the leak detecting sensitivity of the narrow band detector is as the same as the normal leak detector. This kind of detector can fit any normal transducers and needn't use any specially low noise components so that it is more suitable for manufacture and make the detector more cheaply.

6.0 REFERENCES

1. M. I. Dawes., Ultrasound Detectors, Ultrasonics5,(1), 1-7,(1967).

2. Hisaji Shimizu, etc., Study on Small Sound Waves due to Gas Leaks, High Pressure Container,Vol.(18), No.11, 1-5,(1981).

3. Hisaji Shimizu, etc., Gas Sonic, Pipe & Installation (10), 29-32, (1984).

ANALYSIS FOR THE TRANSIENT SOUND FIELD OF ULTRASONIC TRANSDUCER BY TLM METHOD

G Zhang* and C Wykes
Department of Manufacturing Engineering and Operations Management, Nottingham University, Nottingham NG7 2RD, England

*This research is currently carring out in the Ultrasonics Group, Department of Manufacturing Engineering and Operations Management, Nottingham University where the author is a PhD student from P. R. China.

ABSTRACT

The Transmission Line Matrix(TLM) method is used to simulate the sound field produced by ultrasonic transducer. It has the advantage of modelling both of physical process of transient wave propagation and wave characteristics in the near field of transducer. Numerical calculations for a few typical transducers have been made in order to test the accuracy of TLM method and to demonstrate its use. These results show that there is a good agreement with the analysis method.

As a time-domain numerical method, it is proved that the TLM method is a potential tool for industrial and medical ultrasonics engineers.

1.0 INTRODUCTION

Transmission line matrix(TLM) modelling has become well established since its introduction in 1972[1], first as a technique for the investigation of electromagnetic wave propagation and later for other electronic and electrical problems. More recently, it has been applied to diffusion and heat propagation problems.

The application of TLM to acoustics has been more limited, and it has been used very little for the modelling of the transient sound filed of ultrasonic transducer. The paper presented here is a part of author's research work whose aim is to expand TLM application area into modelling of transient near field of variety of ultrasonic transducers for both of industrial and medical usages.

2.0 TLM METHOD

TLM is a method which physically models wave propagation. It is thus ideally suited to simulating the passage of sound through a medium. The medium through which the waves propagate is modelled as a cartesian mesh of transmission lines. The electrical behaviour of such a network is well described and will not be repeated here for simplicity.

2.1 Numerical Treatment.
An exact numerical solution is then provided for the waves travelling on the transmission lines. This solution is designed to be easily implemented on a computer. When applying the technique to acoustics, the properties dealt with are velocity and either displacement or pressure.

Concentrate our attentions into 2-D TLM method and consider a sound-impulse delta function of unit magnitude introduced into terminal 1 ($_0V^i_1 = 1$) of the basic matrix element shown in figure 1(a). The magnitude of the pressure impulse at the junction is 1/2. Pressure impulse ($_1V^r_n$, n = 1,2,3 and 4) of 1/2 will be launched into lines 2, 3 and 4, while a reflected pulse of -1/2 appears on line 1, as shown below in figure 1(b).
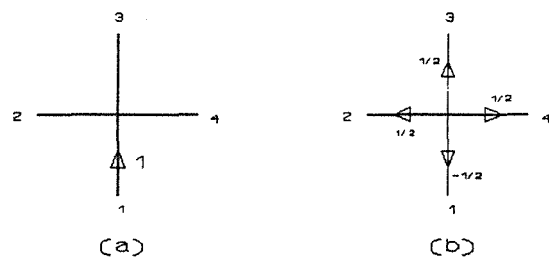
Figure 1

These four impulse then become the incident pulses on the adjacent nodes in the network, and process is repeated. Briefly, there are main two parts of the process, one is known as scattering given in the equation below,

$$_{k+1}V^r_n = \{ _kV^i_1 + _kV^i_2 + _kV^i_3 + _kV^i_4 \} / 2 - _kV^r_n \qquad (1)$$

and another is known as connection given as follows

$$_{k+1}V^i_1(z, x) = _{k+1}V^r_3(z, x-1)$$

$$_{k+1}V^i_2(z, x) = _{k+1}V^r_4(z-1, x)$$

$$_{k+1}V^i_3(z, x) = _{k+1}V^r_1(z, x+1)$$

$$_{k+1}V^i_4(z, x) = _{k+1}V^r_2(z+1, x) \qquad (2)$$

Here k is the number of iterations.

With the repeated operation of equations (1) and (2), sound-impulses will traverse the TLM mesh.

2.2 Modelling of Transducers. Transducers are modelled quite simply in TLM. Transmitters are simulated by injecting a series of appropriate impulses into the nodes corresponding to the transmitter geometry.

3.0 RESULTS

In order to test the accuracy of our TLM program, a few typical 2-D models which have been solved theoretically were set up.

3.1 The Plane Strip Aperture on Infinite baffle. The theoretical solution for the model in figure 2(a) could be found under cw assumption as follows

Axial Distribution of pressure

$$|P_{axis}(z)| = \sqrt{2}P_0 [C^2(\frac{a}{\sqrt{2\lambda z}}) + S^2(\frac{a}{\sqrt{2\lambda z}})]^{\frac{1}{2}} \qquad (3)$$

Lateral Distribution of pressure

$$|P(x', z)| = \qquad (4)$$

$$\frac{P_0 z}{\sqrt{2(x'^2+z^2)}} ([C(\frac{a+2x'}{\sqrt{2\lambda z}}) + C(\frac{a-2x'}{\sqrt{2\lambda z}})]^2 + [S(\frac{a+2x'}{\sqrt{2\lambda z}}) + S(\frac{a-2x'}{\sqrt{2\lambda z}})]^2)^{\frac{1}{2}}$$

Here, $C(\cdot)$ and $S(\cdot)$ are the Fresnel integals, λ the wavelength and D is the maximum linear dimension of the aperture.

In the testing, the parameters are a = 14.25 mm, f = 500 kHz, λ = 0.686 mm and TLM mesh space/wavelength, i.e. $\Delta l/\lambda \approx 0.073$ which should be less than 0.1 according to TLM method. The results are shown in figures 2(b) - (d).

Keep in mind that the equations (3) and (4) is just suitable on the condition

$$z/a \geq 1.19 \quad \text{i.e.} \quad z \geq 17 \text{ mm}$$

Analysis indicate that the maximum relative errors is less than 5.5%.

(a)

(b) Axial Distribution

(c) Latarl Distrburion Z = 50 mm

(d) Latral Distribution Z = 60 mm
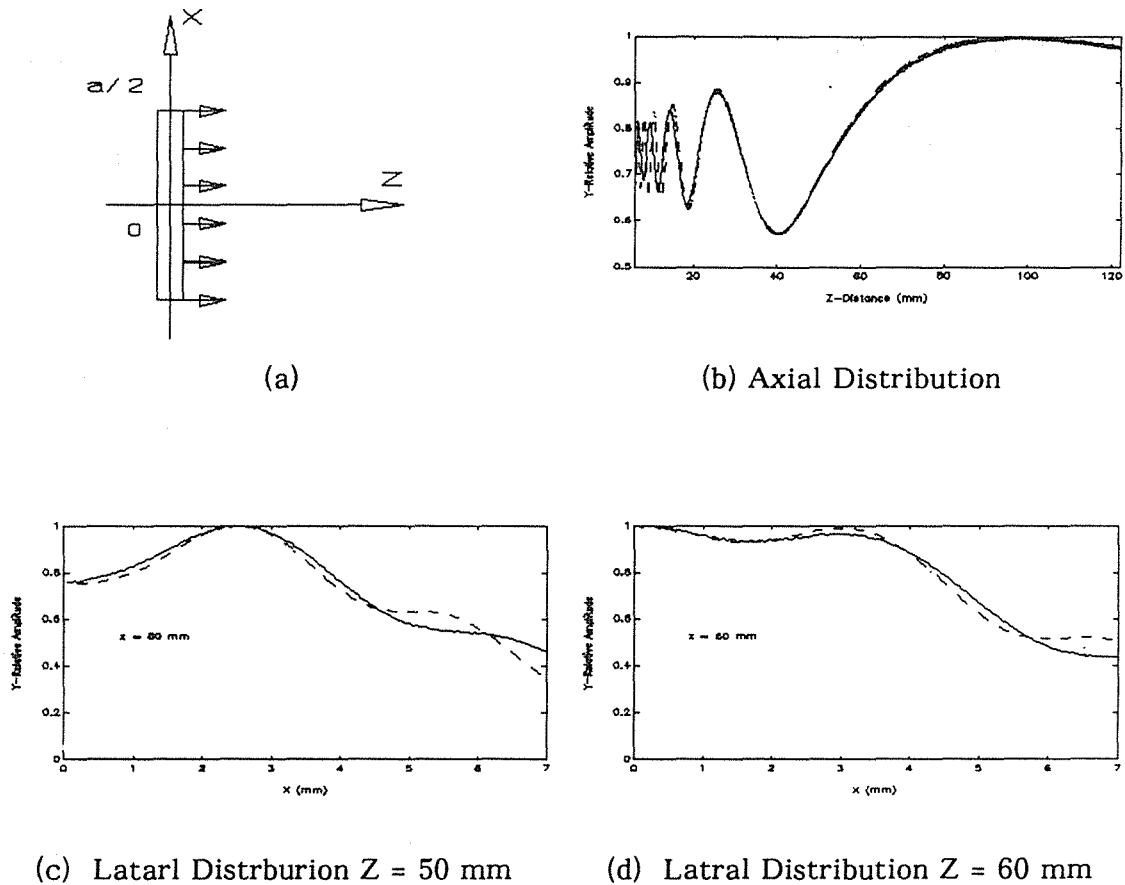
a = 14.25 mm   f = 500 kHz
--- Theoretical Values   — TLM Values

Figure 2

413

3.2 The Strip Aperture on Cylindrical Baffle.
The theoretical solution in serial form could be obtained for the configuration as shown in figure 3,

$$P(r,\varphi) = A \sum_{m=0}^{\infty} \epsilon_m \frac{\sin m\varphi_0}{m\varphi_0} \frac{H_m^{(2)}(kr)}{\dfrac{dH_m^{(2)}(ka)}{d(ka)}} \cos m(\varphi - \varphi_\mu)$$

$$\epsilon_m = \begin{bmatrix} 1 & m=0 \\ 2 & m\neq 0 \end{bmatrix};\qquad\qquad (5)$$

Here, $H_m^{(2)}(\cdot)$ is the second type Hankel function and a the radius of cylinder. The parameters are given as a = 2.2 mm, f = 500 kHz, λ = 0.686 mm and $\Delta l / \lambda$ = 0.04. Two different φ_0 are tested, i.e. φ_0 = 5.5° and φ_0 = 29° respectively.
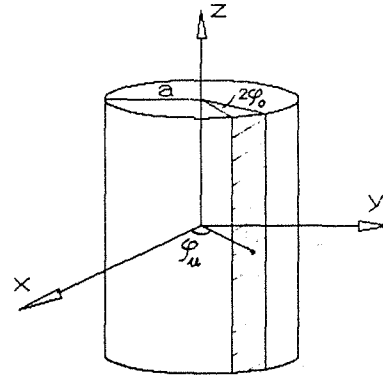
Figure 3

The contour plots of the near fields are shown in figure 4 ((a) for φ_0 = 5.5° and (b) φ_0 = 29°) obtained by 10log $| P / P_{max} |$ with contour levels at 0,-1,-2,..,-20 dB.
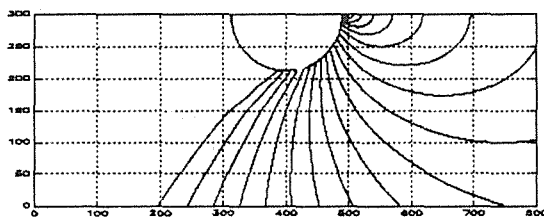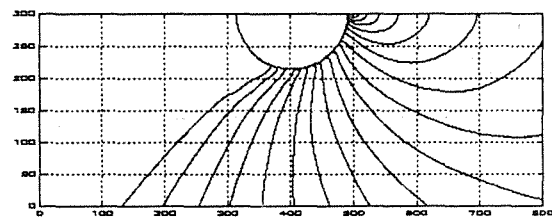
Theoretical Solution   TLM Numerical Solution

Figure 4(a) φ_0 = 5.5°
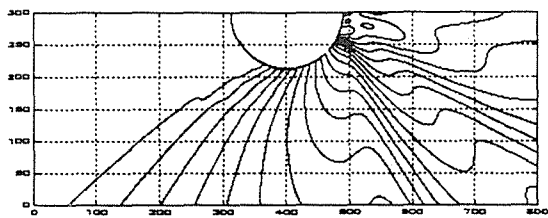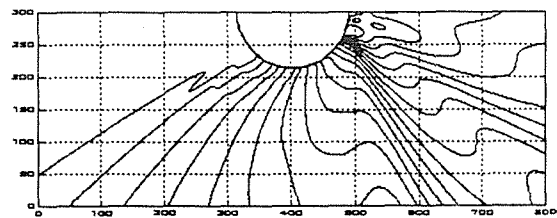
Theoretical Solution   TLM Numerical Solution

Figure 4(b) $\varphi_0 = 29^\circ$

Figure 5 and Figure 6 are the results at a serial output points.
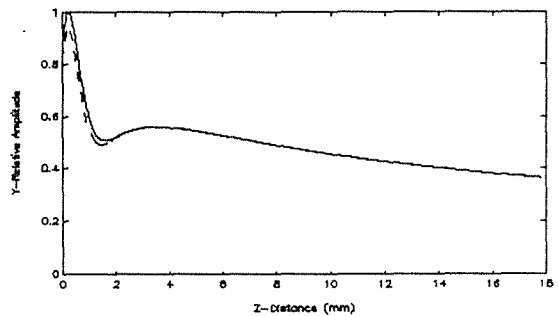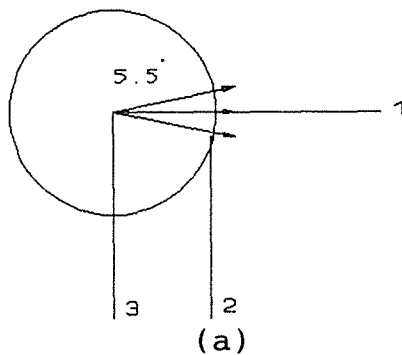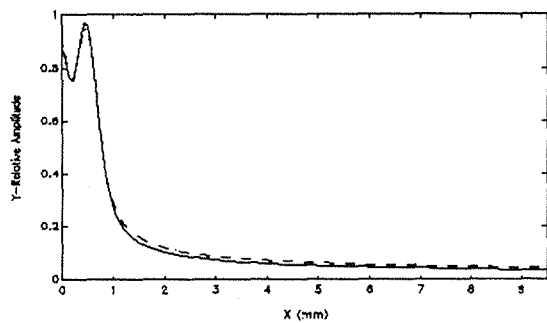
(a)   (b)   Axial Distribute 1
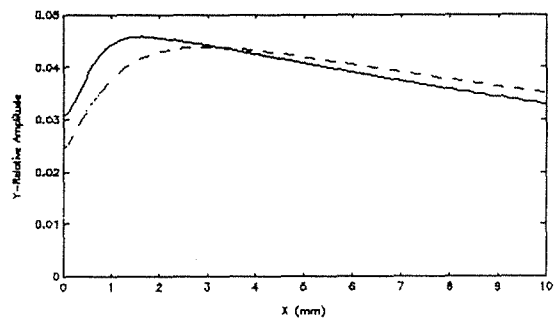
(c)   Latral Distribute 2   (d)   Latral Distribute 3

a = 2.2 mm $\varphi_0 = 5.5^\circ$ f=500 kHz
--- Theoretical Values   —— TLM Values

Figure 5

(a)

(b) Axial Distribute 1

(c) Latral Distribute 2

(d) Latral Distribute 3
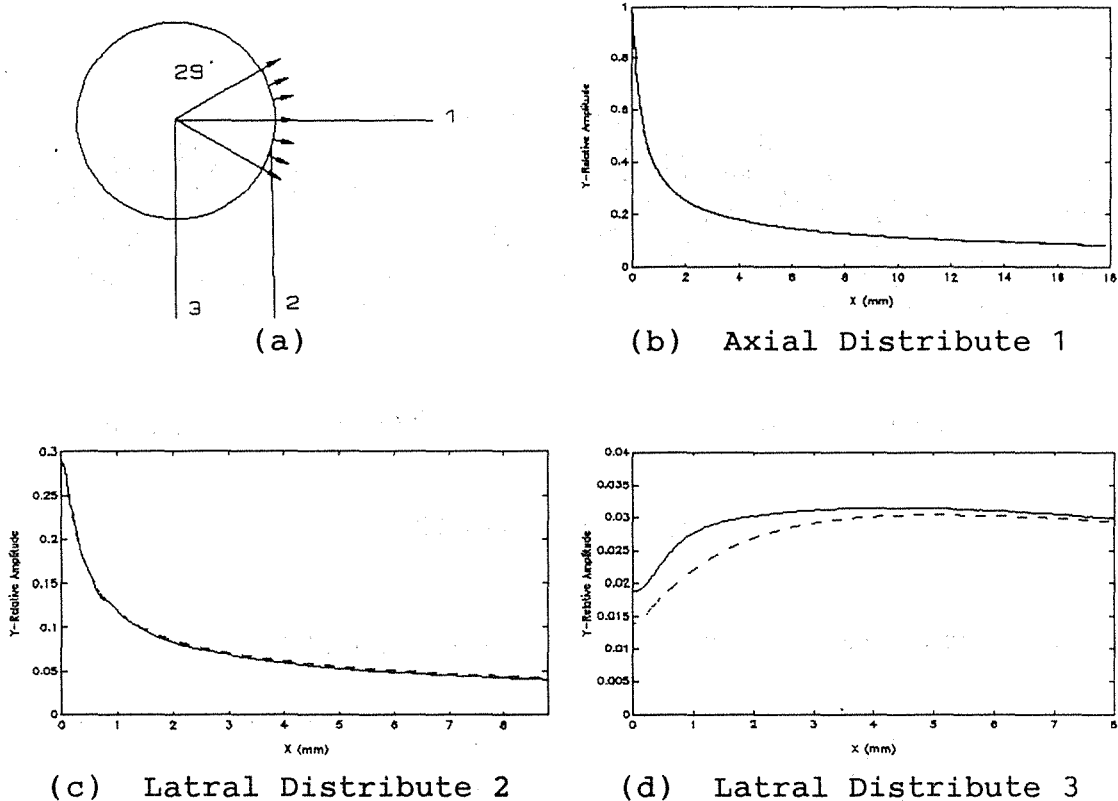
a = 2.2 mm $\varphi_0 = 29^\circ$ f=500 kHz
--- Theoretical Values   — TLM Values

Figure 6

The results indicate that in the most area the maximum relative errors could be under 5.5%, but in the sound shadow these could be up to 10% which might be caused by numerical erros.

4.0 CONCLUSIONS

The results have shown that the TLM method may be used to provide a numerical solution in the time domain for the transient near field of ultrasonic transducers. In addition, the TLM has a distinct advantage in terms of the simplicity and easy of implementation and expansion to 3-D, complex geometries and inhomogeneous medium problems, which make it to be a potential tool for industrial and medical ultrasonics engineers.

REFERENCES

Johns, P.B., Beurle, R.L., "Numerical Solution of 2-dimensional Scattering Problems Using a Transmission-Line Matrix", Proc. IEE,118, (9), 1203-1208 (1971)

Pomeroy, S.C., "Ultrasonic Phased Arrays for Robotics Modelling and Experimental Implementation", PhD Thesis, Nottingham University, (1989)

RECENT DEVELOPMENT OF UNDERWATER ACOUSTICS IN CHINA

GUAN Dinghua

Institute of Acoustics, Academia Sinica, Beijing, China

ABSTRACT

In this paper a brief introduction of development of under-
water acoustics in China was given. Great emphasis is given
to the research of influence of sea bottom on propagation of
sound in shallow water. Optimum frequency for shallow water
in connection with some of our experiments was discussed.
Remote sensing of sea bed sediments was developed by Chinese
acousticians and has good application. For simplification of
calculation, theory of average sound field was developed. In
our theory the difficulty of divergence was overcome by the
use of a generalized phase-integral approximation. Experi-
ments on long range reverberation were conducted in shallow
water. By a new theory the coefficients of backscattering
of very small grazing angles were extracted . Some experi-
ments on mode filtering in water tank and at sea were shown.
High frequency internal wave and its influence on fluctua-
tion of sound was discussed. Transformation of rays and
modes was discussed.

417

1.0 INTRODUCTION

The coasts of China are bounded by very wide continental shelf with shallow water. So great emphasis was paid on research of propagation of sound in shallow water by Chinese acousticians. In shallow water area sea bottom and temperature profile in water column play important role in propagation of sound. the aim of this paper is to review some of the most significant results achieved in China recently.

2.0 OPTIMUM FREQUENCY FOR SHALLOW WATER.

Sound propagation loss in shallow water depends on attenuation in sea water and in sea bed sediments In the case of isovelocity profile in high frequency range the propagation loss is mainly due to volumn attenuation in the water column and scattering loss at the rough boundaries and increases with increasing frequency. As frequency decreases loss due to these two mechanisms decreases monotonously, and more part of energy propagates in sea bottom, so attenuation loss in the sediments becomes the dominant loss mechanism. If the sea bed attenuation (in dB/m) decreases linearly with frequency, effect on propagation of sound in shallow water is an increasing of overall propagation loss as frequency decreases. These two mechanisms cause the existence of the so-called optimum frequency. (Jensen F.B. and Kuperman W.A.) conducted a numerical simulation study along with a comparison of theoretical and experimental results. They found that the optimum frequency was strongly dependent on water depth, had some dependence on the sound speed profile but was only weakly dependent upon bottom type. (Gershfeld D.A.) established analytical relationship between environmental parameters and optimum frequency. But it seems to us that optimum frequency does not always exist. Sea going measurements of propagation loss in several shallow water area off the Chinese coast have been conducted. We have never observed any apparent optimum frequency. Either there is no optimum frequency in these area, or the optimum frequency is much lower than predicted by the existing theories. Several possible explanation can be suggested for these phenomena.

3.0 REMOTE SENSING OF SEA BED SEDIMENTS

Several methods of remote sensing of sea-bed sediment by normally incident sound pulses and by propagation data were developed by us. To extract information of surficial sea-bed sediment in small localized area relatively high frequency acoustic signals were used(Meng J.S. and Guan D.H.). Using normally incident sound pulses and measuring "tails" of reflected signals can give some estimation of attenuation of sound in sea-bed sediments. These waveforms can also be used for classification of sediments with rather high classification rates(Meng J.S. and Guan D.H.). Zhou Zhiyu et al developed a method of estimation of thickness and porosity of the surface sediment layer by explosive pulses(Zhou Z.Y.).

For prediction of propagation loss in shallow water it is necessary to know the averaged parameter of sea-bed sediments. As to simplify calculation for small grazing angles

linear relationship between bottom reflection loss and grazing angle has been widely used by many authors and many calculation conducted by our scientists was based on this assumption. Among them, vertical coherence method(Zhou Z.H.), suggest by Zhou gives the expression for vertical correlation coefficient between two hydrophones in homogeneous layer, from which bottom reflection loss at small grazing angles can be found easily. For a linear negative gradient sound speed profile the exponential decay of sound waves can be used for extraction of bottom reflection loss (Zhou J.X.). Spatial filtering(Lo E.C.) of normal modes can give the bottom reflection loss through amplitude ratio of higher modes to first mode. Dispersion analysis and attenuation of the first mode can be used to calculate sea-bottom sound velocity and attenuation.

Based on averaged sound field theory inverse method for calculating the bottom loss and scattering coefficient of sea bottom are proposed. For isovelocity water it is proved(Guan D.H.) that the angular dependence of bottom loss can be analytically transformed from transmission loss curves.

4.0 AVERAGE SOUND FIELD

The sound field in shallow water usually consists of a great number of rays or modes and forms a complicated interference structure in space which often could not be observed or does not coincide with calculated one. In order to simplify calculation many authors studied the average field in shallow water.

In a paper (Brekhovskikh L.M.) began to investigate the transmission loss in homogeneous shallow water by using the normal mode theory. He obtained the well known 3/2 power law. Later on some authors (Smith P.W., Brekhovskikh L.M.) studied the average field in inhomogeneous shallow water, and got the integral expression of the average intensity by use of ray and normal mode method respectively. However, their integral expressions possess the property of divergence, that is, the average intensity becomes infinity when the receiver depth equals to the source depth. Chinese acoustician (Zhang R.H.) suggested smooth averaged field method by use of a generalized phase-integral approximation to overcome this difficulty.

Average sound field method is widely used to calculate propagation loss, noise field and reverberation and always gives good result. Especially simple and clear result can be achieved for isovelocity cases and in the cases, where bottom loss can be expressed as linearly dependent to grazing angle at small grazing angles. Small personnel computer can be used for prediction of averaged sound field instead of large computer, when normal-mode program is used.

5.0 LONG RANGE REVERBERATION

Reverberation in the sea is formed mainly from scattering from sea surface and sea bed. The basic theoretical frame of reverberation in deep water has been established quite well

for a long time. The backscattering strength of the sea bed
has also been reported by a number of investigators. In deep
water, the path from source to bottom and back to receiver
are simple, and the grazing angle of incident sound and
sound scattered back from the bottom is readily determined
from the ray diagram. In shallow water, however, the matter
is not so simple. The problem is that the mutipath transmis-
sion in shallow wave guide and multi-angle scattering at the
bottom must be taken into account. Long range reverberation
can be calculated by angular power spectrum (averaged flux)
method(Zhou J.X.). By using this model the reverberation
derived backscattering strength for frequency band of 0.8-
4.0 KHz and grazing angle of 2 -10 was achieved. These data
well join the data from deep sea measurement.

6.0 MODE FILTERING

When sound propagates in shallow water over long distance
there are only several modes which decide characteristics of
sound field. Recently mode filtering becomes an important
approach for research of multipath field in shallow water.
Some experiments were conducted in model tanks(Wang Y.) and
others at sea. In these experiments vertical array of recei-
vers and eigenfunction weighting network are used. From
output of weighting eigenfunction network signals of several
modes can be separated. These experiments show that fluctua-
tion of each normal mode is much less than that of total
field. We can see that the fluctuation of total field is
mainly due to interference of modes(Clay C.S.). Sea bottom
parameters such as bottom loss at different grazing angles
can be extracted from sea experiments of mode filtering.

7.0 INFLUENCE OF INTERNAL WAVES ON TRANSMISSION OF SOUND

Internal waves exist when density of sea water varies with
depth. Internal waves have horizontal scales of 100m to 10
km, with vertical scale of 1 to 100m. Time scales go from 1
minute to 15 hours. The characteristics of internal waves
depend on vertical density profile of sea water. In shallow
water many interesting phenomena in propagation of sound are
induced by internal waves. Study of internal waves and
fluctuation of sound was conducted in shallow water of
Yellow Sea for many years(Wang D.Z.). In this region in
summer time there is very strong and sharp thermocline,
where the temperature change in vertical distance of several
meters is as large as 10 C. Vaisala frequency of this region
is 1 1/min. the highest reported.

Several chains of thermisters were fixed in the sea for
measurement of internal waves. Analyses of results show that
the internal wave spectrum decreases with increasing fre-
quency as -2.5 power of frequency. This spectrum lies
between -2 power curve of G-M spectrum and -3 power curve of
Brekhovskikh's spectrum. In vertical direction internal
waves have multimode structure. The propagation direction of
internal waves is toward the shore. In its activity there
are relatively active period and relatively passive periods.

Internal waves are one of the reasons which cause fluc-
tuation of sound. Measurements in shallow water show that

the active and passive periods of fluctuation of sound
signals coincides with that of internal waves. Phase fluc-
tuation of sound occurs mainly in the period of fading of
sound signals. Spectrum of sound phase fluctuation decreases
with increasing frequency in the power of -2 to -3, similar
to that of internal wave intensity spectrum. Spectrum of
amplitude fluctuation of sound decreases with increasing
frequency in the power of -1 to -1.5. In the frequency band
between 1 and 12 minutes there are peaks of amplitude fluc-
tuation. In the active period of internal waves amplitude
fluctuation up to 20 dB at very low frequency has been
observed. Such kind of strong fluctuation would give serious
interference on the work of underwater sound systems.

8.0 ABNORMAL ATTENUATION OF SOUND

At some region of shallow water in Yellow Sea in the summer
time there are very strong and sharp thermocline and inter-
nal waves and abnormal attenuation of sound propagation loss
at frequency range between 300 Hz and 1200 Hz had been
observed. In order to explain such a strange phenomenon,
Zhou et al made continuous observation over a four year
period at August at same area and have found that there are
very large deviations in frequency response of sound trans-
mission loss for different directions and time. For seven
different directions we get different transmission loss
frequency response curves, between them there is 30 dB
deviation at some frequencies. At the experiment site the
sea bed is flat. The sediments along different tracks are
similar and we didn't find any evidence of fish shoal. The
real cause of this abnormal phenomenon is not clear yet.
Since it always occurs at summer time when there are sharp
thermocline and internal waves, quite possible, this pheno-
menon may be caused by moving internal wave pakets.

9.0 MODES AND RAYS

In the theoretical studies of wave propagation, there are
two well known representations of the field, mainly mode
representation and ray representation. Each representation
has advantages and disadvantages in different cases. Each
member of each representation possesses a different degree
of information concentration for describing the field. The
different representations of the same field must have some
interrelations. Some "ray" effects of the modes were studies
by Tolstoy and Weston. Recently the "ray" effects produced
by the constructive intererence of adjacent modes were inve-
stigated by Tindle and Guthrie. The Poisson summation formu-
la for modes and images for homogeneous plane layer with
perfectly reflecting boundaries was proved by Pekeris. The
Poisson summation formula for the asymptotic representations
of modes and rays was established by Batorsky and Felsen. By
introducing the general function of the mode and the genera-
lized ray, a strict Fourier transformation between rays and
modes was proved (Gao T.F.) in the case when the branch-cut
does not appear. And in a later paper(Gao T.F.) the effect
of the branch-cut on the transformation between modes and
rays was discussed.

REFERENCES

Brekhovskikh L.M., Waves in Layered Media, Academic Press, 1980.

Brekhovskikh L.M., Fundamental of Ocean Acoustics. Springer Verlag, New York, 1984.

Clay C.S., Wang Y.Y. and Shang E.C., J. Acoust. Soc. Am. 77(2), 424-428 (1985).

Gao T.F. and Shang E.C., J. Sound Vib. 80(1), 105-115(1982).

Gao T.F. and Shang E.C., J. Acoust. Soc. Am. 73(5), 1551-1555(1983).

Guan D.H., Acta Oceanologica Sinica, 1(1), 52-57 (1979).

Jensen F.B., Kuperman W.A., J. Acoust. Soc. Am. 73(3), 813-819 (1983).

Lo E.C. et al, J. Acoust. Soc. Am. 74(6), 1833-1836 (1983).

Meng J.S., Guan D.H., Acta Oceanologica Sinica 1(1), 48-53 (1982).

Meng J.S., Guan D.H., Acta Oceanlogica Sinica 4(4), 503-509 (1985).

Smith P.W., J. Acoust. Soc. Am. 55(44), 1197-1204 (1974)

Wang D.Z. et al, Acta Acustica, 3(3), 209-217 (1981).

Wang Y. et al, Acta Acustica 2(1), 78, (1980).

Zhang R.H., Acta Oceanologica Sinica, 3(6), 535-545 (1981).

Zhou J.X., Acta Acustica 4(1), 34-43 (1979).

Zhou J.X., Acta Acustica 5(2), 86-99 (1980).

Zhou J.X., Guan D.H., Shang E.C., Luo E.S. Chinese J. Acoust. 1(1), 54-63 (1982).

Zhou Z.Y., Meng J.S., Marine Geotechnology 7(3), 211-219 (1988).

CALIBRATION OF A LARGE PASSIVE SHIPBOARD SONAR ARRAY USING A BOTTOM
MOUNTED ACOUSTIC BEACON

Jan P. Holland
Penn State University
APPLIED RESEARCH LABORATORY
P. O. Box 30
State College, PA 16804

ABSTRACT

        A technique has been developed for the Naval Air
Development Center that can be used to calibrate shipboard
hydrophones. The technique can utilize an acoustic transmission
reflected off the ocean bottom or pulses from an acoustic beacon
located near the ocean bottom as a calibration source. This paper
describes the derivation of the technique as well as an example of
the use of acoustic signals to calibrate a 144 element shipboard
passive array. Also shown are examples of the calibration
accuracies as a function of the portion of the acoustic pulse
utilized for the calibration for both SASS acoustic returns and the
bottom mounted acoustic beacon.

1.0 INTRODUCTION

This paper describes a technique that was developed for the Naval Air Development Center, Warminster, PA, that can be used to calculate the receive hydrophone sensitivity and relative phase characteristics for individual hydrophones mounted in a large shipboard passive array operating at sea. Initially, the technique was designed to use a bottom mounted acoustic beacon pulse for a rough system check-out for the SONARRAY Sonar System (SASS) installations on new construction ships. The acoustic beacon was not ready for deployment when some SASS bottom return data became available, so the bottom return data received at the sonar were used to determine the accuracy that could be obtained without the acoustic beacon. Later, when acoustic beacon data became available, the technique was used again to calibrate the 144 element receiving array on the USNS Maury. The results of both analyses are reported here along with some guide lines that can be used to obtain the most accurate calibration results.

2.0 SASS SYSTEM AND ACOUSTIC BEACON DESCRIPTION

SASS is a bottom profiling system and has a receiving array that is mounted athwartships about 60 m aft of the bow and is approximately 9.1 m in length. The receive hydrophone array consists of 144 line hydrophones that are 52 cm long and are spaced 1/2 wavelength apart on centers. The receive array is covered by a streamlined dome fairing. The active transmitting array is approximately 9.1 m in length and is mounted along the center line of the ship about 1 meter astern of the SASS receiving array. The transmitting array is used to generate a fan beam athwartships.

SASS is a digital system that can obtain quadrature data samples simultaneously for all 144 hydrophones for 1000 sample times utilizing SASS's 3 ms sample rate. One SASS ping, or three 100 millisecond acoustic beacon pulses with a 1 second repetition rate could be stored and saved for later analysis. The SASS system operates at a frequency of 12 kHz and was using a receive system bandwidth of approximately 150 Hz. The acoustic beacon was located off the Florida coast in approximately 4755 meters of water and its source transducer was located approximately 9.1 meters above the bottom.

3.0 CORRECTIONS TO THE ACOUSTIC DATA

The technique described here corrects the receive signal out of each receive hydrophone for the wavefront curvature, ship's roll, and steering angle of the receive array at the time the pulse is received. After the individual hydrophone pulse data has been corrected for these effects, the hydrophone signal is then used to determine the response of each individual hydrophone in the receive array. In general, the absolute hydrophone sensitivity can be determined if a calibrated omni-directional hydrophone is located inside the sonar dome. SASS has two omni-directional calibrated hydrophones that are located outboard of the SASS array inside the SASS dome. Therefore, this type of calibration can include the effect of the baffle material, etc. in the sonar dome on the hydrophone receive sensitivity.

The phase correction from hydrophone to hydrophone for ship's roll and steering angle to the acoustic beacon at the time of reception

of the acoustic pulse can be calculated by:

$$\Phi_{error} = 180 \times sine\ (\theta_{steer} - \theta_{roll}).$$

where

Φ_{error}, θ_{steer}, and θ_{roll} are in degrees.

The steering angle correction must be used if data fairly far into the acoustic bottom return pulse are used or data from the acoustic beacon are used. Also a bottom slope correction must be included for the active SASS pulse case.

The second type of phase correction accounts for the wavefront curvature of the acoustic bottom reflected wave or the beacon pulse received at the hydrophone array, and can be calculated from the simple equation:

$$\phi_{error} = \frac{360}{\lambda}\left\{\sqrt{\left[\frac{(N-1)}{2}\lambda + \frac{\lambda}{4}\right]^2 + \frac{D^2}{cos^2(\theta_{steer})}} - \frac{D}{cos\ (\theta_{steer})}\right\}$$

where
  λ is the wavelength in meters, D is the water depth in meters (twice the water depth for the SASS pulse), and θ_{steer} is the steering angle in degrees from the array to the beacon on the bottom (relative to vertical). N varies from 1 to 72 and corresponds to port or starboard hydrophone No. 1 to 72 (hydrophone No. 1 is located at a distance of $\lambda/4$ from the center line of the ship and hydrophone No. 72 is outboard). This phase correction is symmetric about the centerline of the array and is assumed to be minimum for the center elements (port and starboard hydrophone No. 1) and maximum for port and starboard element No. 72 for computational ease. The phase error is added to the steering and roll angle corrections to calculate an equivalent constant phase wavefront at the SASS hydrophone array face. Wavefront curvature corrections are small for deep water, for example, an acoustic beacon depth of 5000 meters gives a hydrophone phase correction of approximately 6° maximum across the face of the array.

4.0 ACOUSTIC BEACON DATA ANALYSIS

The stored data from the acoustic beacon were obtained by quadrature sampling the preamp output for SASS, so the data includes all variations in the system electronics as well as variations due to the hydrophone response, sonar dome effects, etc.

The magnitude of the data recorded on Starboard Hydrophone No. 72 (outboard array element) as a function of sample number is shown in Figure 1. Three acoustic beacon pulses can be seen with amplitudes of about 86 dB, since the total time window is three seconds. The noise level at this time was about a magnitude of 55 dB, so the signal-to-noise ratio was about 30 dB for the data sets. Only two valid sets of data (called data set 2 and 3) like the one shown in Figure 1 were available for analysis, and each contained three beacon pulses. The beacon was located within 2.7° of directly under the receiving array and the maximum ships roll was about three fourths of a degree. The first data samples were located on the leading edges of the acoustic pulses, the second samples were located near the leading edges of the pulses, and the third set of samples analyzed for each ping were located near the ends of the

pulses. The first two sample times were picked to try and avoid any multipath problems from signals reflected off the ocean bottom. The sample times near the ends of the pulses were examined to see if the calibration accuracy was dependent on the position of the data samples in the pulse.
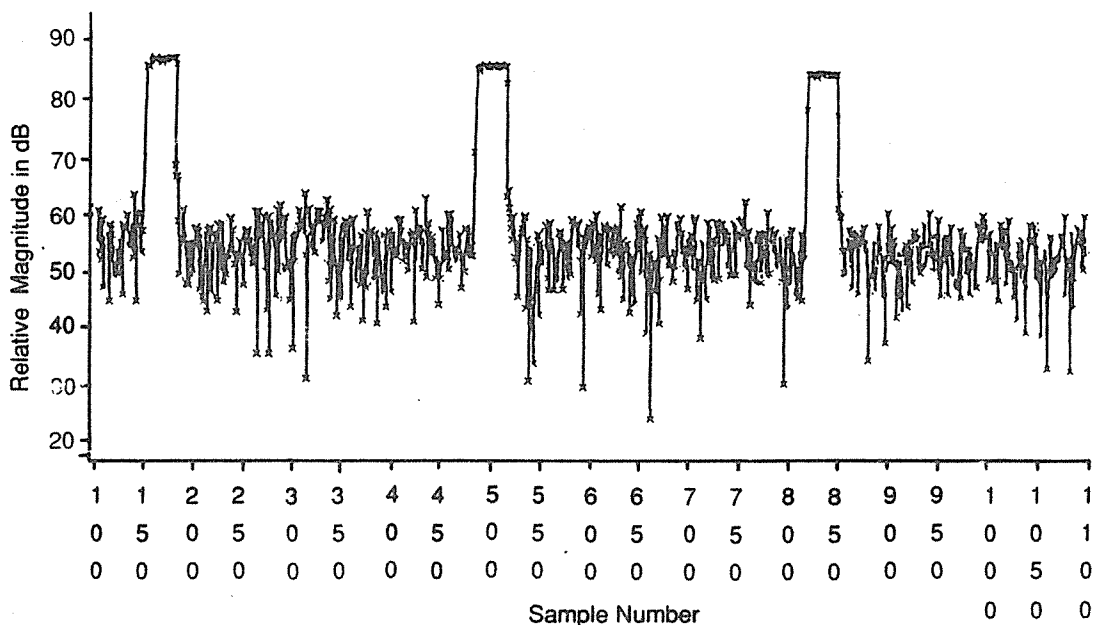
Figure 1. Acoustic Beacon Output on Starboard Hydrophone No. 72 (Data Set 2) as a Function of Sample Number

A typical plot of the hydrophone magnitude and phase angle versus receive hydrophone number (position in the array) for an acoustic beacon pulse is shown in Figure 2 for sample number 480 from data set three. The roll angle was 0.41° and the steering angle to the acoustic beacon was -0.8° at the time sample 480 was taken as shown in Table I. Similar plots were run for the other six pings examined from the acoustic beacon data. The standard deviation of the magnitude and the phase across all 144 hydrophones as a function of sample number for these six pulses are shown in Table I.
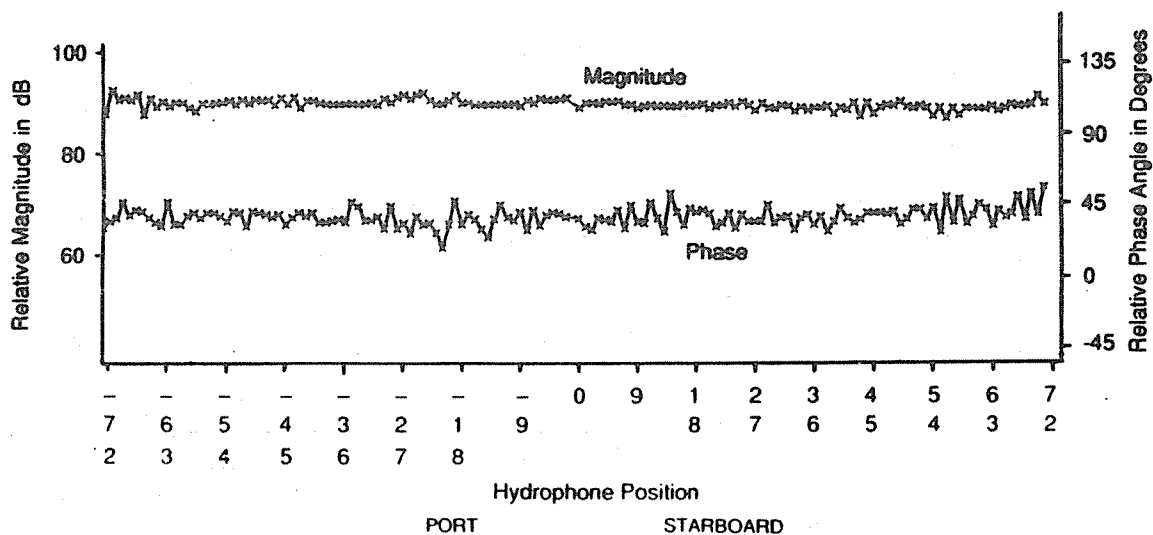
Figure 2. Acoustic Beacon Output Magnitude and Phase as a Function of Array Position for Sample No. 480 Data Set 3

426

The data from data set number 3 gave the best results with a
standard deviation on the order of three fourths .of a dB in
magnitude and a phase standard deviation of about 5°. The phase
correction ($\theta_{steer} - \theta_{roll}$) was smaller for data set 3 than it was for
data set 2. Whether or not this is the reason for the lower
standard deviations for data set 3 cannot be positively determined
without additional data. It should be noted that these standard
deviations include all the variations in acoustic propagation from
the beacon to the sonar dome, variations in the transmission
characteristics through the sonar dome, variations in the transducer
characteristics, i.e., sensitivity and phase, as well as variations
in the system electronics through the preamps and the analog to
digital converter in the SASS system.

TABLE I. MAGNITUDE AND PHASE STANDARD DEVIATIONS

Data Set 2

Sample Number	Pulse Number	Magnitude dB	Phase Degrees	Steering Angle Degrees	Roll Angle Degrees
149	1	1.33	10.5	2.04	0.07
159	1	1.33	10.7	2.04	0.07
179	1	1.36	11.1	2.04	0.08
482	2	1.87	9.6	2.335	0.20
491	2	1.37	9.7	2.330	0.20
512	2	1.37	10.1	2.330	0.21
817	3	1.35	9.8	2.67	0.37
823	3	1.35	10.1	2.68	0.38
847	3	1.73	12.6	2.68	0.39

Data Set 3

Sample Number	Pulse Number	Magnitude dB	Phase Degrees	Steering Angle Degrees	Roll Angle Degrees
137	4	0.83	4.8	-0.812	0.41
146	4	0.76	5.6	-0.802	0.41
167	4	0.82	5.7	-0.800	0.41
470**	5	2.40	48.5	-0.817	0.41
480	5	0.79	5.3	-0.802	0.41
500	5	0.77	5.5	-0.80	0.41
804	6	0.77	5.1	-0.730	0.44
818*	6	0.75	5.4	-0.718	0.45
834	6	0.77	6.2	-0.73	0.45

* Data Overloaded
** Noise ahead of the pulse

The computed magnitude and phase standard deviations appeared to be
relatively constant along the pulse indicating no interference from
bottom or surface reflections.

The hydrophone channel magnitudes were not adjusted to obtain the
hydrophone receive sensitivities because data were not collected on
either of the two omni-directional hydrophones located in the sonar
dome. The hydrophone channel gains and phase characteristics can be
obtained by using a SASS system calibration signal that can be
injected at the hydrophone outputs. Had this data been acquired,
actual hydrophone receive sensitivities and phase characteristics
could have beer. calculated.

5.0 SASS ACOUSTIC PING ANALYSIS

Two SASS active pings obtained in 2140 meters of water off the Florida coast were available for analysis, these were SASS ping 12 and ping 13. Ping 12 was selected for analysis and is shown in Figure 3. The SASS digital record contained 1000 time samples or a three second time window for all 144 hydrophones. The acoustic bottom return starts at sample number 977 and reaches a maximum by sample number 984. The amplitude across all 144 hydrophones for sample number 984 is shown at the top of Figure 4.
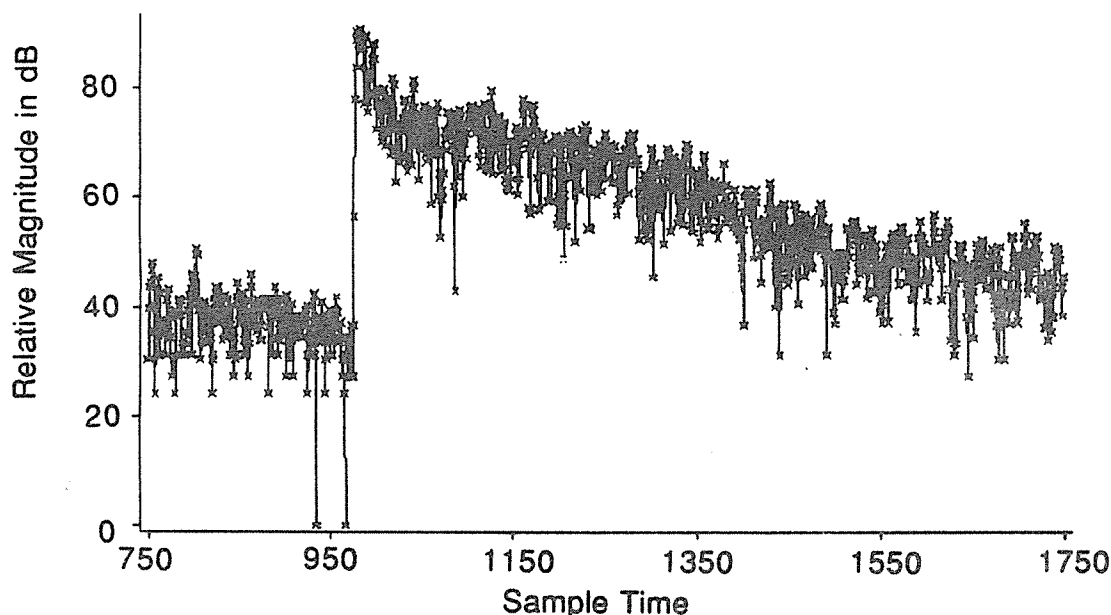
Figure 3. Time History for SASS Ping 12. (Port Hydrophone No. 36)

The cyclic amplitude variations for sample number 984 were probably caused by constructive and destructive interference of the returns from different areas illuminated on the ocean bottom by the 7 ms SASS pulse.

The only time that a single spot is illuminated on the bottom is at the very leading edge of the acoustic pulse when the surface of the ocean bottom nearest the hydrophone array is illuminated. Therefore, it was decided to examine the magnitude and phase characteristics for samples approaching the leading edge of the pulse. The cyclic nature of the hydrophone output magnitude became less and less predominant as the leading edge of the pulse was approached. At sample number 977 (the leading edge of the pulse), the magnitude was almost constant and showed only a part of a cycle of variation as shown at the bottom of Figure 4. The lower magnitudes observed near the starboard end of the hydrophone array may be caused by the fact that the ship roll or a bottom slope induced a time delay in each of the simultaneous bottom reflected data samples so that the acoustic bottom return is actually sampled at slightly different points along the leading edge of the pulse (the pulse rise time was about two samples or six milliseconds). No information on the bottom slope or type was available for the SASS ping 12 data.

The standard deviation of the 144 hydrophone outputs decreased from 6.7 dB to 4.1 dB as the sample number decreased from 984 to 977 as

428

shown in Table II. The lower standard deviation of 1.8 dB for
sample number 980 was caused by clipping in some of the data at that
time. Part of the standard deviation is due to the fact that the
transducer channel responses were not identical prior to
installation in SASS. Previous free field hydrophone calibrations
have shown a standard deviation of 0.4 dB and 3 degrees in
hydrophone receive sensitivity magnitude and phase respectively.
Also, the leading edge data becomes more susceptible to noise
contamination because the magnitude is lowest at the leading edge of
the pulse.
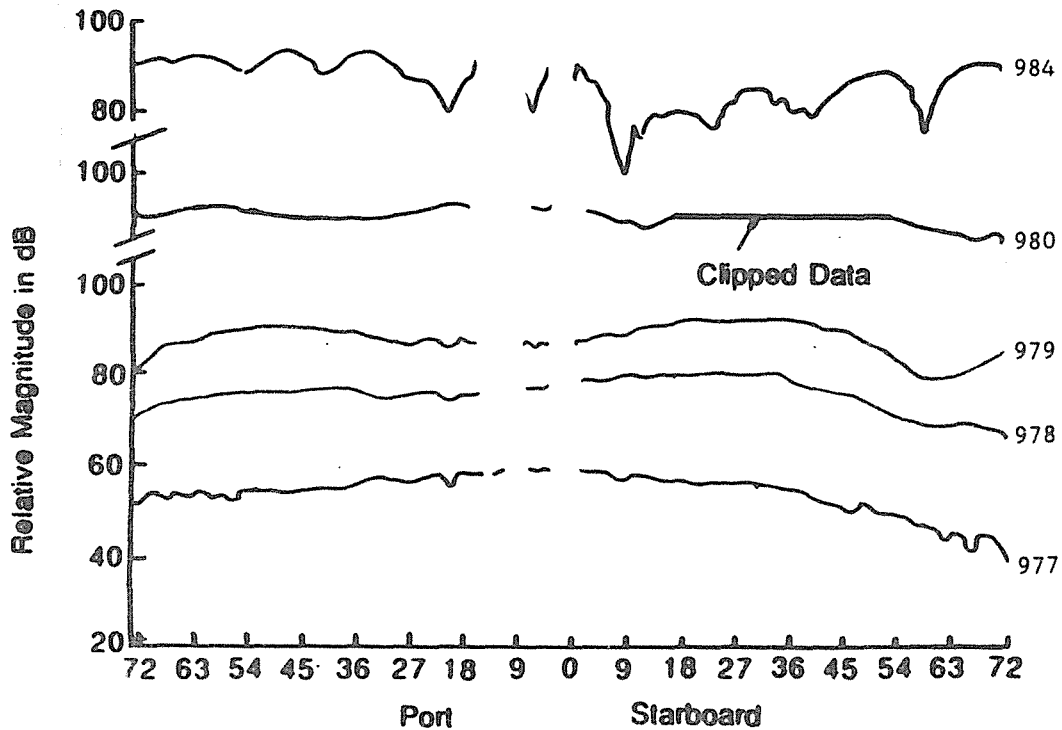
Figure 4.   SASS Hydrophone/Preamp Output Magnitude for Ping 12 as a
            Function of Hydrophone and Sample Number

The cyclic hydrophone phase angle for sample number 984 shown at the
top of Figure 5 is indicative of some degree of roll, steering
angle, or bottom slope since there are approximately five 0 to 360
degree phase transitions or a phase shift of about 1800 degrees
across the array. This would correspond to a combined roll plus
bottom slope plus steering angle of about 4 degrees, i.e., 5 λ
across a 72 λ array. The variability in the phase improved as the
leading edge of the pulse was approached as shown at the bottom of
Figure 5. The phase variation across the array for sample number
977 is very small. Note that there is some error in the ships roll
correction or a bottom slope as evidenced by the slight slope in the
phase angle as a function of hydrophone position. The standard
deviation of the hydrophone phase data is shown at the right side of
Table II and is a minimum of 13 degrees at the leading edge of the
pulse, i.e., sample number 977 and increases as samples further into
the acoustic bottom return are examined (57 degrees at sample time
980). If the residual slope of the phase across the hydrophone
array had been compensated for by doing a least squares fit to the
data and subtracting out the residual slope, the standard deviation
would be less than the 13 degrees shown (such an error could be
introduced by a roll angle error or bottom slope of about 0.1
degree).

429

TABLE II

SASS HYDROPHONE/PREAMP MEAN AND STANDARD DEVIATION DATA
AS A FUNCTION OF SAMPLE NUMBER FOR PING 12

Sample Number	Magnitude in dB		Relative Phase Angle in Degrees	
	Mean	Standard Deviation	Mean	Standard Deviation
776*	37.0	6.0	40.4	97.9
777	54.0	4.1	-86.4	13.4
778	77.8	3.5	-77.5	24.9
779	87.8	3.8	-52.7	39.1
780	91.5	1.8**	-9.6	57.4
784	85.5	6.7	***	***

   * Noise ahead of pulse
  ** Some data clipped
 *** Influenced by steering angle so not meaningful
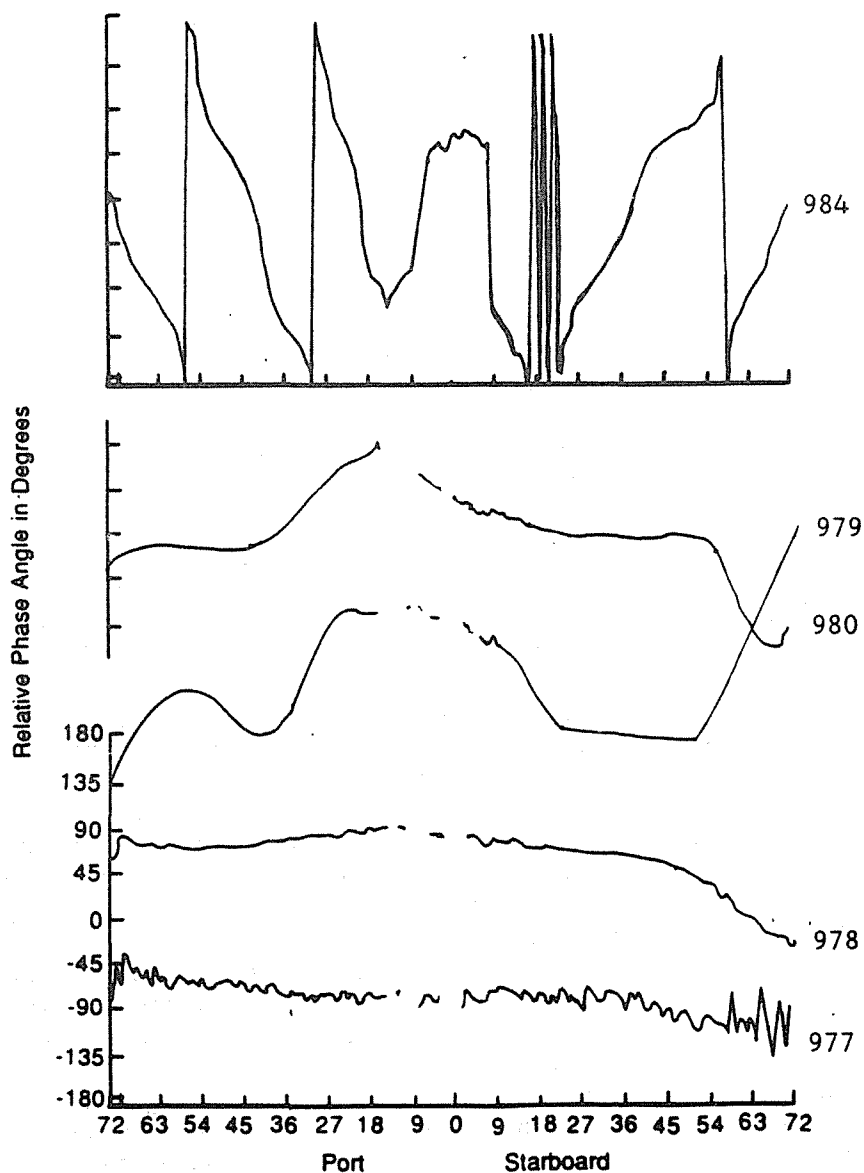
Figure 5. SASS Hydrophone/Preamp Output Phase for Ping 12 as a Function of Hydrophone and Sample Number

The best calibration data obtained for the ping 12 data gives a magnitude standard deviation of 4 dB and a phase standard deviation of 13 degrees. This includes the free field hydrophone calibration variability of 0.4 dB and 3 degrees for the magnitude and phase standard deviations respectively. When using this type of a calibration, leading edge pulse data for a flat non-sloping bottom measured in a low sea state (no ship roll) should produce the best results. Averaging data over many pings should also help reduce the magnitude and phase variance. Since only 2 pings were available for analysis, the potential gain due to averaging could not be determined.

6.0 CONCLUSIONS

A receive hydrophone calibration technique has been developed that is suitable for use for large passive shipboard arrays. Results of tests with a bottom mounted acoustic beacon as an acoustic source have produced data with a magnitude standard deviation of 0.75 dB and a phase standard deviation of about 5° for the 144 hydrophones calibrated based on the data from 3 beacon pulses (the free field hydrophone sensitivity variability was 0.4 dB and 3 degrees). These variations also include propagation anomalies, sonar dome effects, preamp, and analog to digital converter anomalies. The calibration accuracy is not dependent on the position of the data sample in the pulse for the acoustic beacon data.

Some variability in calibration accuracy was noted for the different times/data sets examined. It appeared that the data set with the smallest steering minus roll angle gave the best test results.

The best results of tests utilizing a single SASS acoustic bottom return as a calibration source have produced data with a magnitude standard deviation of 4 dB and a phase standard deviation of 13 degrees. Data from the leading edge of the acoustic pulse yields the best calibration accuracy. The best conditions for calibrating the array when using a SASS active ping are a non-sloping flat bottom and low sea-states so that minimum ship roll will result. Averaging data from many pings should reduce the variance when using SASS pulses for calibration.

IN SITU MEASUREMENTS OF ACOUSTIC CHARACTERISTICS OF MARINE SEDIMENTS BY AN OPEN ACOUSTIC-TUBE METHOD

Masao Kimura
Faculty of Marine Science and Technology, Tokai University
Japan

Michitaka Inui
NTT Corporation
Japan

Hiroshi Shimizu
Aomori University
Japan

ABSTRACT

The determination of the acoustic properties of marine sediments is important in the field of underwater acoustics. We previously proposed a new method of determining the sound velocity and the attenuation constant of sediments, by measuring the resonant characteristics of a piezoelectric transducer which is placed at the top-end of an acoustic tube vertically inserted into the sediment. In the present paper, we describe in situ measuring system for an open acoustic-tube method, and show the measured results. The length of the acoustic-tube is about half wave length. We devise and fabricate a small-sized transducer with low resonant frequency, that is, bimorph type piston transducer. Its resonant frequency is 3.2kHz. We use pulse response method for measuring the admittance of the transducer. The results show that the measured values of the sound velocity relatively agrees with the measured values of sediment samples at 90kHz by pulse transmitting method, and the measured values of the attenuation constant also relatively agrees with the modified values at 3.5kHz from the measured values at 90kHz.

1.0 INTRODUCTION

Determination of the acoustic properties of marine sediment is important in the field of underwater acoustics. We previously proposed a new method of determining the sound velocity and the attenuation constant of sediments by measuring the resonant frequency and the motional admittance at resonance of a piezoelectric transducer placed at the top end of an acoustic-tube inserted vertically into the sediment (Kimura M. and Shimizu H.,1986,1989). And we showed the usefullness of the method by laboratory experiments (Kimura M. and Shimizu H.,1989,1990).

The present paper describes a measuring system developed to apply this method to in situ measurements, and the experimental results.

2.0 PRINCIPLE AND PROCEDURE OF MEASUREMENT

As shown in Fig.1(a), a cylindrical tube, whose inner radius is a, is inserted into a sediment so that the radiation surface of a piezoelectric transducer placed at the top-end of the tube touches the sediment. Assuming that the plane sound wave travels in the tube, the equivalent circuit of this system is given approximately as shown in Fig.2. In this circuit,

L, C, R, C_θ	: equivalent circuit parameters of the transducer in the vicinity of the resonant frequency,
$Z_{\theta t}$	: acoustic characteristic impedance of the sediment in the tube,
$\gamma_t (= \alpha_t + jk_t)$	: propagation constant of the sediment in the tube,
α_t	: attenuation constant of the sediment in the tube,
k_t $(= \omega/c_t)$	: phase constant of the sediment in the tube,
c_t	: sound velocity in the tube,
l	: length of the sediment in the tube,
Z_r $(= R_r + jX_r)$	: radiation impedance viewed from the tube-end,
Z_a	: acoustic load impedance of the transducer,
Y_m	: motional admittance of the transducer.

In order to obtain sufficiently accurate measurements, the following experimental conditions have to be satisfied: (1) $k_t a = 0.2 \sim 0.5$, (2) $\omega_T \doteqdot \omega_\theta$ (ω_T: resonant angular frequency of the loaded transducer, $\omega_\theta = 1/\sqrt{LC}$), and (3) $\alpha_t l < 0.1$. Considering these conditions, the acoustic load impedance Z_a is approximately expressed as

$$Z_a = Z_{\theta t} \frac{2(\alpha_t l + p)}{1 + \cos\{2(k_t l + q)\}} + jZ_{\theta t} \frac{\sin\{2(k_t l + q)\}}{1 + \cos\{2(k_t l + q)\}}, \quad (1)$$

where,

$$p = \frac{1}{2} \log_e \left\{ \frac{\sqrt{1 - 2(R_{r\theta}{}^2 - X_{r\theta}{}^2) + (R_{r\theta}{}^2 + X_{r\theta}{}^2)^2}}{(1 - R_{r\theta})^2 + X_{r\theta}{}^2} \right\}, \quad (2)$$

$$q = \frac{1}{2} \tan^{-1} \left(\frac{2X_{r\theta}}{1 - R_{r\theta}{}^2 - X_{r\theta}{}^2} \right), \quad (3)$$

$R_{r\theta} = R_r/Z_{\theta t}$, and $X_{r\theta} = X_r/Z_{\theta t}$.

At $\omega = \omega_T$, the imaginary part of $1/Y_m$ is equal to zero, that is

$$RQ \left(\frac{\omega_T}{\omega_\theta} - \frac{\omega_\theta}{\omega_T} \right) + Z_{\theta t} \frac{\sin \{2(k_{tT}L + q)\}}{1 + \cos \{2(k_{tT}l + q)\}} = 0 , \tag{4}$$

where, $k_{tT} = \omega_T/c_t$, Q is the quality factor of the unloaded transducer. The real part of $1/Y_m$ at $\omega = \omega_T$ is equal to the resonant resistance R_T of the loaded transducer, that is,

$$R + Z_{\theta t} \frac{2(\alpha_t L + p)}{1 + \cos \{2(k_{tT}l + q)\}} = R_T . \tag{5}$$

By numerically solving Eq.(4) using the measured values of ω_θ, ω_T, R, Q, and $Z_{\theta t}$, the value of $k_{tT}L + q$ can be obtained. From this value and q calculated substituting the measured values of R_r, X_r, and $Z_{\theta t}$ into Eq.(3), the sound velocity in the tube c_t, can be obtained as

$$c_t = \frac{\omega_T}{k_{tT}} . \tag{6}$$

To obtain the sound velocity in free space c, from the decreased velocity in the tube c_t, we use Kuhl's equation (Kuhl V.W.,1953).

The attenuation constant in the tube α_t, can be expressed from Eq.(5) as

$$\alpha_t = \frac{1}{l} [\{1 + \cos(2(k_{tT}l + q))\} \frac{R_T - R}{2Z_{\theta t}} - p] . \tag{7}$$

By substituting k_{tT} and the measured values of R, R_t, $Z_{\theta t}$, p, q into Eq.(7), α_t can be obtained.

The radiation impedance $Z_r (= R_r + jX_r)$ and the acoustic characteristic impedance Z_θ can be obtained by measuring the acoustic load impedance of the transducer settled as shown in Fig.1(b), at the fundamental resonant frequency and at such a high frequency as to satisfy the condition of $k_t a > 3$, respectively.

3.0 TRANSDUCER AND AN OPEN ACOUSTIC-TUBE

In order to make in situ measurements at a low frequency below several kHz, a small-sized transducer with a low resonant frequency was needed. We therefore devised and fabricated a bimorph type piston transducer which met these requirements, as shown in Fig.3. In this transducer, an additional mass was joined to the center of a bimorph type transducer, and an end surface of an additional mass almost vibrated like a piston. The diameter of radiation surface was 40 mm. This transducer was fixed with a stainless steel tube, whose thickness

and inner diameter were 8 mm and 41 mm, respectively. Unloaded resonant frequency of this transducer was about 3.2kHz. The acoustic tube was also a stainless steel tube of the same thickness and inner diameter, and its length was about a half wave length. The end of the tube was tapered with an angle of 15 degrees to be inserted easily into sediment. Acoustic tube are shown in Fig.4. Fig.4(a) is correspond to Fig.1(a), and Fig.4(b) to Fig.1(b). From now on, we call the former long tube, and the latter short tube.

4.0 PULSE RESPONSE METHOD (Kimura M.,1989)
      Fig.5(a) shows the principle of pulse response method for measuring resonant characteristics of transducer. In Fig.5(a), pulse voltage v(t) applied to the electric termi al of transducer and motional current $i_m(t)$ flowing into transducer were sampled respectively, then each discrete spectrum V(k), $I_m(k)$ (k=1,2,---,N,N: sampling number in FFT) were obtained. Next, the ratio of each spectrum $|I_m(k)|$ / $|V(k)|$, that is, the absolute values of motional admittance were obtained. As these values were discrete values shown in Fig.5(b), we could not obtain the exact resonant frequency f_0, resonant resistanse R, and quality factor $Q(=f_0/(f_2-f_1))$. So first we obtained a smooth curve passed near these data points by least squares approximation method. Next, from this curve, we could get the exact values of these paremeters.

      Input and output waveforms and their asmplitude spectra of unloaded bimorph type piston transducer are shown in Fig.6. Input waveform to the transducer was AC pulse with one period, its pulth width was 260 μs. The motional admittance of the transducer was detected by the differential method using current probe. Sampling interval used in FFT was 40 μs, and sampling number was 4096.

5.0 IN SITU MEASUREMENTS
      In situ measurements were done at Shimizu port (its depth is 15~20 m) using small vessel of Tokai University from October to December 1990. Size of the measuring frame for acoustic-tube was 0.7m(length), 0.7(width), 0.3m(hight). And two acoustic-tubes (long tube and short tube) and piezoelectric transducer for measuring acoustic characteristics were installed in the lower part of the frame. The measuring frame was taken down to the sea bottom by a wire. Then long tube protruded from the frame was inserted into the sediment. Vibrating surfaces of transducers in the long tube, short tube, and piezoelectirc transducer touched the sediment. Signal cable of transducer was taken down along the wire. Besides, to investigate the inserted condition of the tube, we installed VTR set in the frame. We got the sediment sample using Smith McIntyre bottom sampler at the same location. We show measured values of density, porosity, and mean diameter in Table 1.

      To investigate the usefullness of an open acoustic-tube method,

we first measured sound velocity in sea water. We show the
experimental results in Table 2. In Table 2, c is the measured value
at about 2m upper the sea bottom. And c_M is the calculated value
using Medwin's equation (Medwin H.,1975) from the measured values of
temperature, salinity and depth. The results show that the measured
values of the sound velocity almost agrees with the calculated values.
Measured values of sound velocity and attenuation constant of
sediments are shown in Table 3 and Table 4, respsctively. In Table 3,
c_{90} is the value of sound velocity obtained at 90kHz by pulse
transmitting method. The results show that the measured values of the
sound velocity relatively agrees with the measured values at 90kHz.
In Table 4, α_{90} is the value obtained at 90kHz by pulse transmitting
method. And $\alpha_{3.5}$ is the modified values at 3.5kHz obtained from the
measured values at 90kHz, assuming that the attenuation constant of
marine sediment is proportional to 0.7 power of frequency(Kimura M.
et al.,1990). α also relatively agrees with $\alpha_{3.5}$.

6.0 CONCLUSION
    We describe a measuring system developed to apply an open
acoutic-tube method to in situ measurements of acoustic properties of
marine sediments, and show the experimental results at Shimizu port.

    From now, we will make many in situ experiments, and accumulate
those data.

REFERENCES
Kimura M. and Shimizu H., A Method for Measuring Acoustic Properties
of Marine Sediments, Proc.12th ICA,H1-1,Toronto,(1986).

Kimura M. and Shimizu H., A New Method of Simply Measuring Acoustic
Properties for Marine Sediments and its Basic Experiments, Jounal of
Acoustical Society of Japan,45,274-281(1989) [in Japanese] .

Kimura M. and Shimizu H., A Method for In Situ Maesurement of Sound
Velocity and Attenuation Constant of Marine Sediments, Proc.13th ICA,
13C-3,Belgrade,(1989).

Kimura M., Study on Fast Mesurements in an Open Acoustic Tube Method,
Journal of Marine Acoustics Society of Japan,16,211-218(1989) [in
Japanese] .

Kimura M. and Shimizu H., An Open Acoustic-Tube Method for Measuring
sound Velocity and Attenuation Constant of Marine Sediments, Japanese
Jounal of Physics Supplment,29-1,206-208(1990).

Kimura M.,Watanabe T. and Nishimura M., Sound Velocity and Attenuation
Constant of Marine Sediment Model with Particle Size Distribution,
Read at the Spring Meeting of the Acoustical Society of Japan, 783-784
(1990) [in Japanese] .

Kuhl V.W., Die Eigenschaften wasselgefüllter Rohre für Winderstands
-und Schallgeschwindigkeitsmessungen,: Acustica,3,111-123(1953).

Medwin H., Speed in Water, a Simple Equation for Realistic Parameters,
Journal of Acoustical Society of America,58,1318-1319(1975).
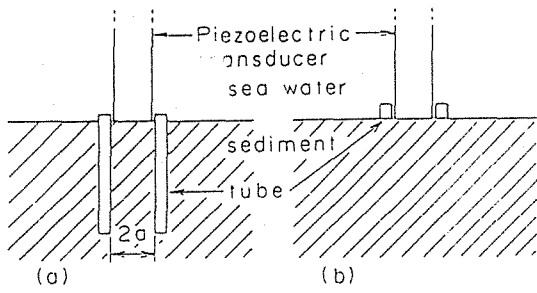
Fig.1 Configuration for measuring (a)sound velocity and attenuation constant, (b)radiation impedance and acoustic characteristic impedance.
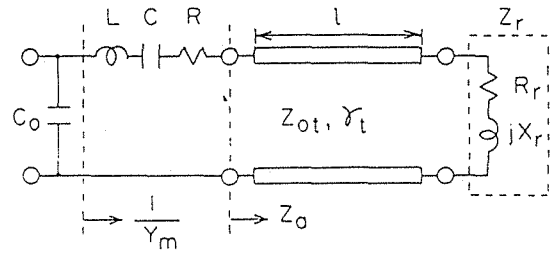
Fig.2 Equivalent circuit of the system.
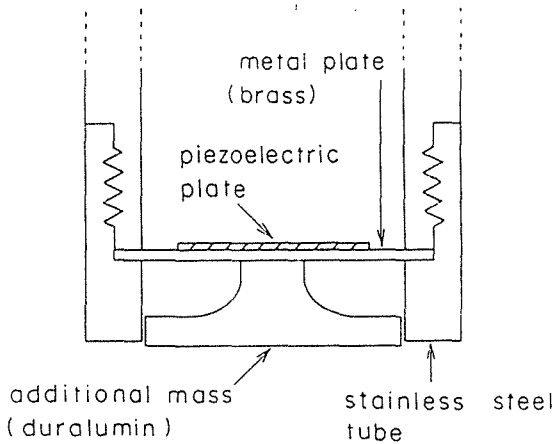
Fig.3 Bimorph type piston transducer.
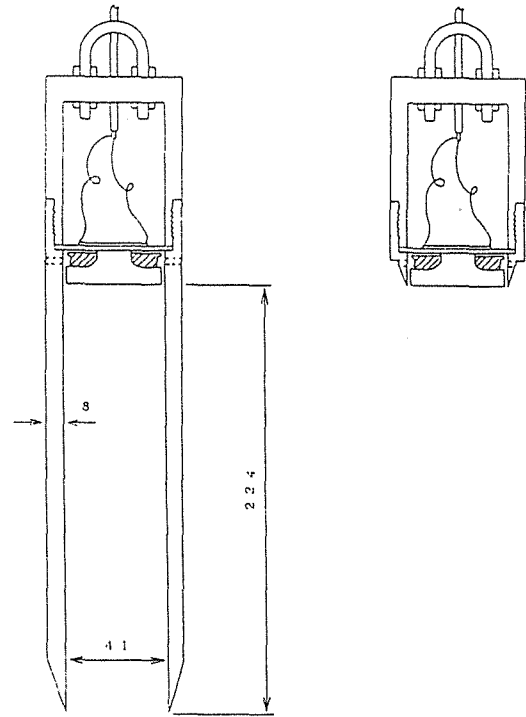
(a) long tube   (b) short tube

Fig.4 Open acoustic-tubes.

$$|Y_m(k)| = \frac{|I_m(k)|}{|V(k)|} \quad , \quad k = 1,2,\cdots\cdots,N$$

(a)

(b)
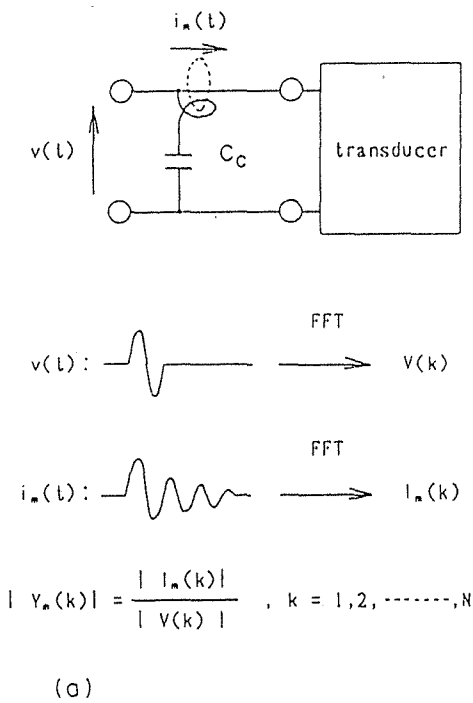
Fig.5 Principle of pulse response method.

438
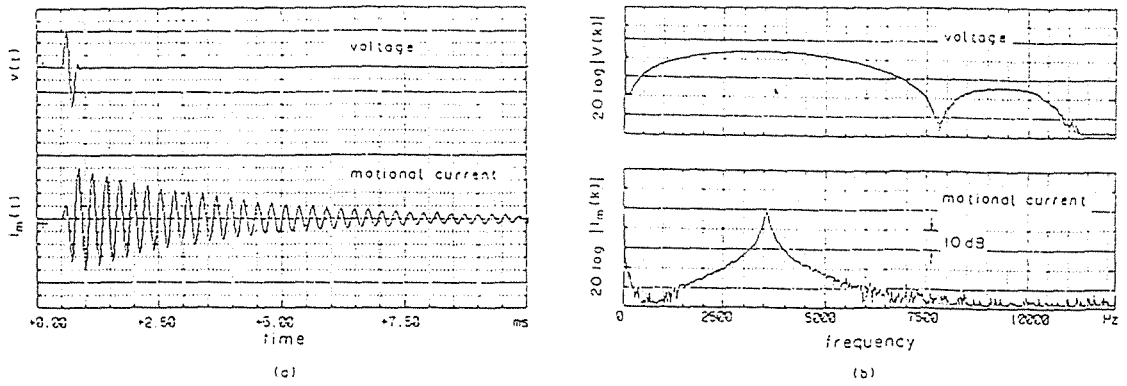
Fig.6 Waveforms(a) and amplitude spectra (b) of bimorph type
piston transducer.

Table 1 Measured values of density,
porosity and mean diameter.

month	day	St.No.	ρ (kg/m³)	β	d_m (μm)
10	25	1	1.68×10³	0.60	77
		2	1.71	0.59	83
		3	1.71	0.58	91
	26	1	1.68	0.59	83
11	24	1	1.70	0.61	76
	26	1	1.66	0.65	75
		2	1.62	0.68	77
12	13	1	1.66	0.62	74
		2	1.68	0.62	76
		3	1.66	0.59	81

Table 2 Measured values of sound
velocities for sea water.

month	day	St.No.	c(m/s)	c_M(m/s)
10	25	1	1550	1530
		2	1540	1530
		3	1540	1530
	26	1	1540	1530
11	24	1	1510	1520
	26	1	1500	1520
		2	1500	1520
12	13	1	1520	1510
		2	1510	1510
		3	1510	1510

Table 3 Measured values of sound
velocities for marine sediments.

month	day	St.No.	c(m/s)	c_{90}(m/s)
10	25	1	1590	1620
		2	1630	1650
		3	1640	1650
	26	1	1640	1620
11	24	1	1580	1600
	26	1	1620	1600
		2	1620	1630
12	13	1	1620	1620
		2	1620	1620
		3	1630	1620

Table 4 Measured values of attenuation
constants for marine sediment.

month	day	St.No.	α (dB/m)	α_{90} (dB/m)	$\alpha_{3.5}$ (dB/m)
10	25	1	4.8	39	4.0
		2	3.2	32	3.3
		3	2.9	33	3.4
	26	1	3.6	40	4.1
11	24	1	4.4	41	4.2
	26	1	3.8	38	3.9
		2	3.8	32	3.3
12	13	1	3.9	41	4.2
		2	3.6	39	4.0
		3	3.5	30	3.1

AMBIENT-NOISE MEASUREMENTS IN THE SHALLOW WATER OF THE KOREA STRAIT

Jungyul Na
Department of Earth and Marine Sciences, Hanyang University.
Ansan, Kyunggi-do, KOREA 425-791

Moonsub Jurng
Agency for Defense Development, BOX 18, Chinhae, Kyung Nam,
KOREA 645-600

ABSTRACT

The noise levels measured at two different depths in shallow water where the
ship traffic noise are prevalent show a higher level on the lower depth at
frequencies less than 100 Hz. The seasonal change in noise level depends on the
propagation condition. The spectra shape is very close to the one previously
reported by Urick(1986) for the area of high shipping density.

1.0 INTRODUCTION

The sources of shallow-water noise are known to be highly variable in time since the noise background is a mixture of shipping noise, wind noise and biological noise(Urick,1986). In particular, if the measurement site is located close to busy harbors the dominant noise source will be ship traffic so that greater variability and higher noise levels can be expected(Perrone and King,1975). However, only a rough indication has been given of the levels at offshore coastal locations where the ship traffic noise is prevalent. It has been assumed that locally generated noise such as a nearby ship traffic does not show depth effect on the noise level in shallow water except low frequency shipping noise originating at a distance(Ross,1976).

On the other hand, if the water mass undergoes seasonal change that results in a different sound velocity profile, propagation condition may affect the depth dependence of the noise level(Piggott,1964).

In order to verify the depth dependence of noise levels and to identify the causes, the noise measurements were made at a fixed site which is about 15 miles offshore in the Korea Strait. The noise samples were taken hourly for 30 minutes over 48 hours in every other month.

Two omni-directional hydrophones located at 10m and 70m depth respectively were moored from the ship at 100m depth of water. Wind and current speeds were also observed over the same period. The number of ships within the area of 12 mile radius was recorded from the ship's radar.

2.0 DATA SELECTION

Among the data set collected every other month over one year period, data from the months of May and November were selected since they represented typical propagation conditions in terms of the sound velocity profile. Also, they reflect the period of stable wind speed and about the same number of ships within the area of 12 mile radius.

Fig.1 shows the temperature profiles across the strait which were taken at the time of the noise measurement. Station F1 is located very close to the busy harbor and the measurement site is close to the station F3. In May the water was rather weakly stratified compared to the one of November in which a strong thermocline was formed at two different depths, one near the bottom and another near the surface. Propagation effects due to these temperature profiles will be discussed later. In order to minimize the tidal effect that includes a strong
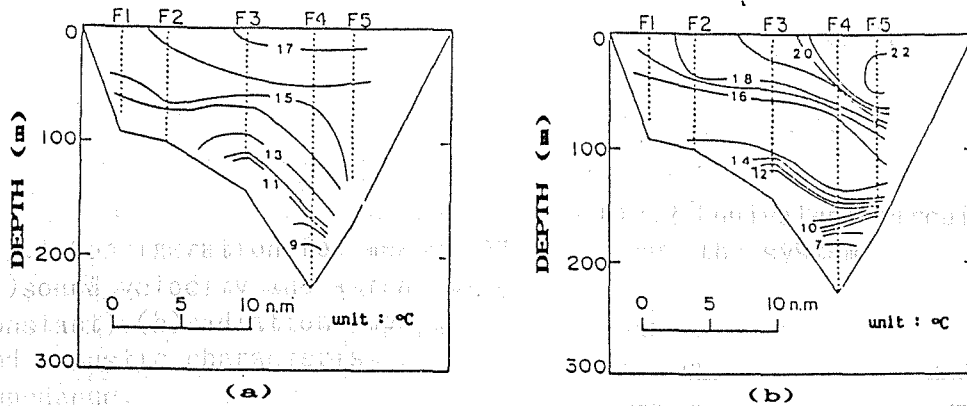
Fig.1. Vertical temperature distributions across the Strait in May(a) and November(b).

tidal current of speed of 1 knot, the time of observation was selected around 1600 hour(local time) which was very close to the high tide. The number of ships was also considered at the same time to have similar background noise. The average number of ships during the period of measurement turned out to be about five.

3.0 AMBIENT-NOISE SPECTRA
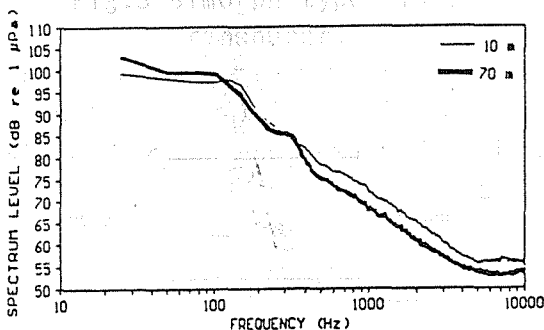
Fig.2. Representative ambient-noise spectra in May for the indicated hydrophone depths (1-Hz frequency resolution, 30-min integration time).
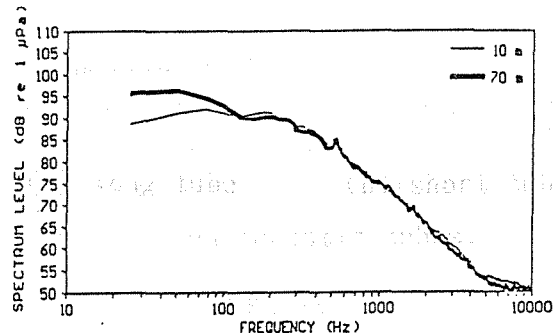
Fig.3. Representative ambient-noise spectra in November for the indicated hydrophone depths(1-Hz frequency resolution, 30-min integration time).

Fig.2-3 show the ambient-noise spectra averaged over 30-min period at two different depths (10 and 70 meters) for May and November in 25 Hz-10 kHz band.

From both figures it is clearly seen that at frequencies less than 100 Hz the noise-levels measured by the 70m-hydrophone are dominant over the noise-levels at 10m- hydrophone. At frequencies greater than 100 Hz, the noise-levels at 10m-hydrophone are higher than those measured at 70m except at the tonal frequencies. The average wind speed for both May and November was 4-knot over its entire observed period, therefore locally generated wind noise

did not contribute much to explain the difference. The difference in noise-levels exists between May and November for the upper and the lower hydrophones. In May the levels are higher at frequencies less than 200 Hz but they become lower than November for frequencies between 200 Hz and 5 kHz. The slope of the spectrum at frequencies greater than 200 Hz appears to be independent of depth and season and averages -7dB/octave.
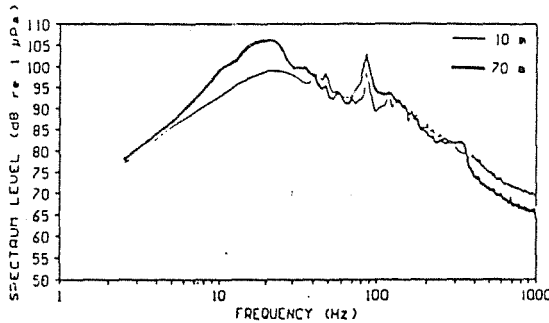
Fig.4. Ambient-noise spectra in May for the indicated hydrophone depths for lower frequencies (2.5-1000 Hz, 1-Hz frequency resolution and 30-min integration time).
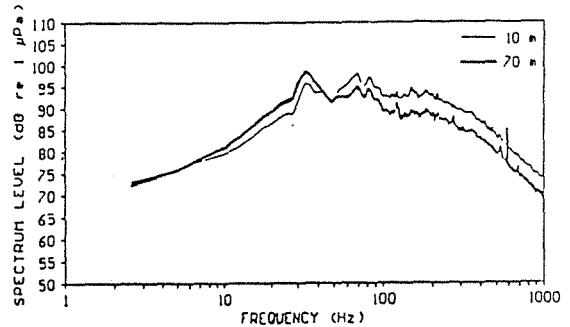
Fig.5. Ambient-noise spectra in November for the indicated hydrophone depths for lower frequencies (2.5-1000 Hz, 1-Hz frequency resolution and 30-min integration time).

Since the dominant noise sources are ship traffic, spectrum levels for frequency band of 2.5 - 1000 Hz are shown in Figs 4-5. The tonal components clearly indicate that the spectrum levels are dominated by the local ship-traffic noise that gives the maximum of the spectra a more peaked appearance near 20 - 30 Hz band. This type of spectrum was presented as an idealized ambient noise spectrum (Urick,1986) due to shipping and present spectrum corresponds to the case of heavy shipping. The most unusual aspect of ship traffic noise in this area is that the noise levels at the lower hydrophone always exceed the levels of upper hydrophone. For two different size of ships, 50 ton fishing vessel and 20000 ton cargo ship, the radiated noise spectra(Fig. 6-7) also show the higher levels at the lower hydrophone with the maxima at 20 Hz indicating that the effects of ship size on the spectrum level are not significant at all.
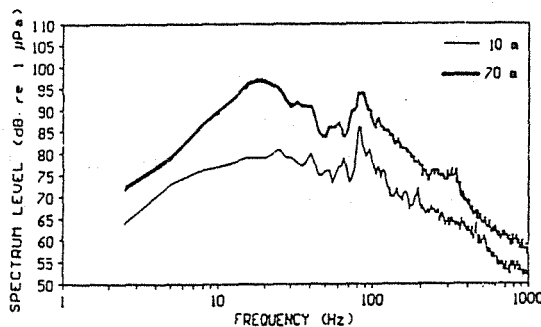
Fig.6. Radiated noise spectra for 20000ton cargo ship measured at 2mile range for the indicated hydrophone depths(1-Hz frequency resolution, 1-min integration time).
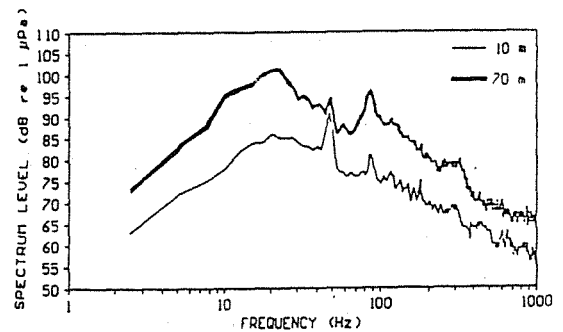
Fig.7. Radiated noise spectra for 50ton fishing vessel at 2-mile range for the indicated hydrophone depths (1-Hz frequency resolution and 1-min integration time).

It is interesting to note that when the ship is located at short range the depth variation of spectrum levels are different from the figures 4-5 at frequencies greater than 50 Hz. The difference implies that high frequency noise which is greater than 50 Hz may be influenced by range and bottom absorption while propagation.
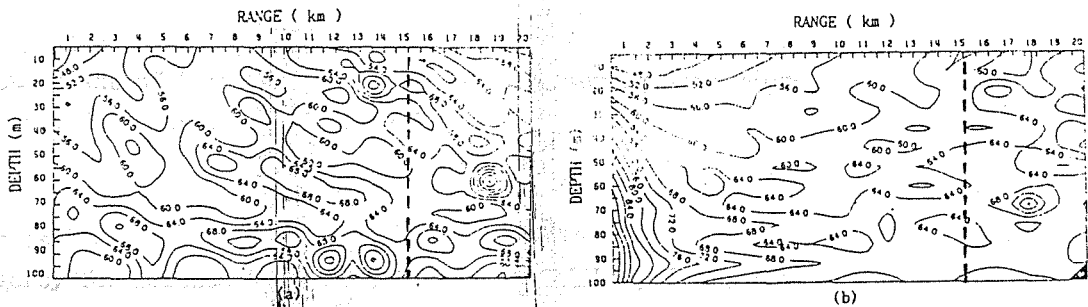
Fig.8. Range-depth distribution of the propagation loss in May for two frequencies, 50Hz(a) and 300Hz(b), for source at 7m. The dotted line indicates the position of hydrophone.
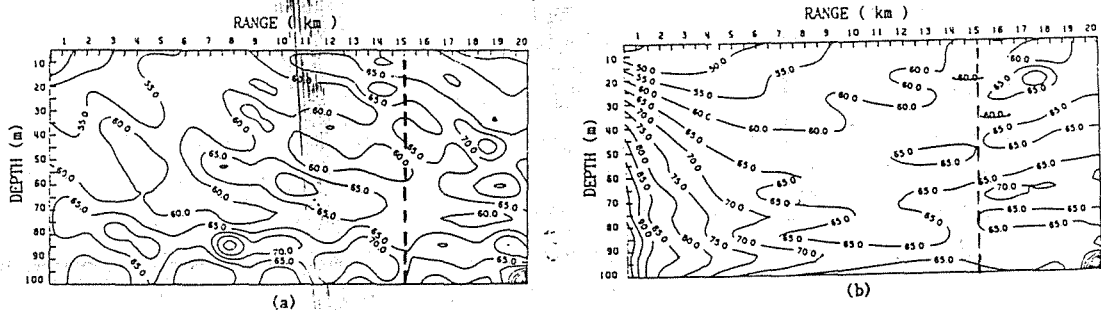
Fig.9. Range-depth distribution of the propagation loss in November for two frequencies, 50Hz(a) and 300Hz(b), for source at 7m. The dotted line indicates the position of hydrophone.

Fig.8-9 present the propagation loss calculated based on the observed sound velocity profiles for 50 Hz and 300 Hz using IFD(Lee and McDaniel,1988).

The sources are assumed to be located at zero range which is shallow coastal area and the hydrophones are located around 15 km – range at which the propagation loss of 50 Hz at the lower hydrophone depth appears to be equal or less than that of upper one. However, it is quite clear for 300 Hz in that the propagation loss is greater at the lower depth. This explains the differences in levels presented in the figs 2-3.

As seen in Fig.8-9 the propagation condition seems to affect the depth dependence in such a way that a negative gradient in the sound velocity profiles causes the sound wave refracted and interacted with bottom. Presence of the thermocline in November actually increases the grazing angles at the bottom causing more propagation loss near the bottom(Fig. 9(b)). Also the shift of maximum spectrum level toward lower frequency in May(Fig.4-5) is suggested as a result of different propagation condition. However, the cutoff frequency, which

is between 9-10 Hz does not seem to influence the spectral changes.
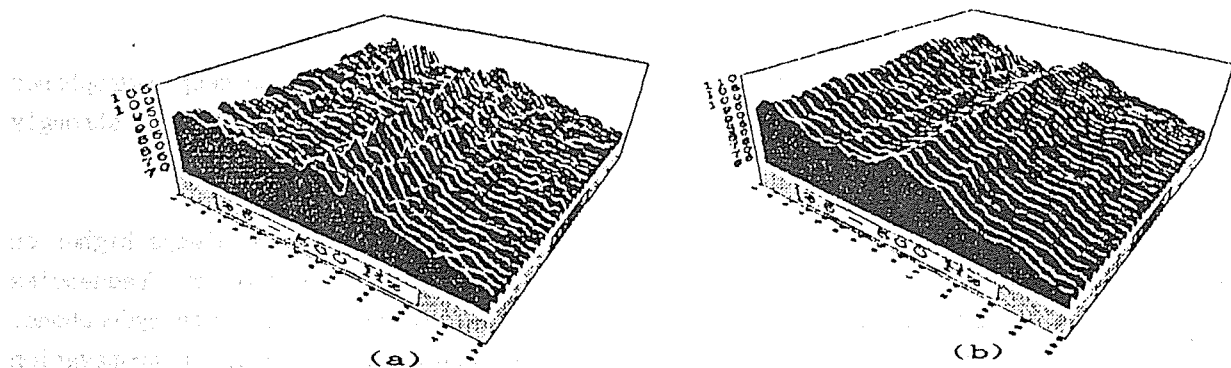
Fig.10. Time variations of ambient-noise spectra for 14-frequencies
(tonals) in May for 10m(a) and 70m(b) hydrophone depths.
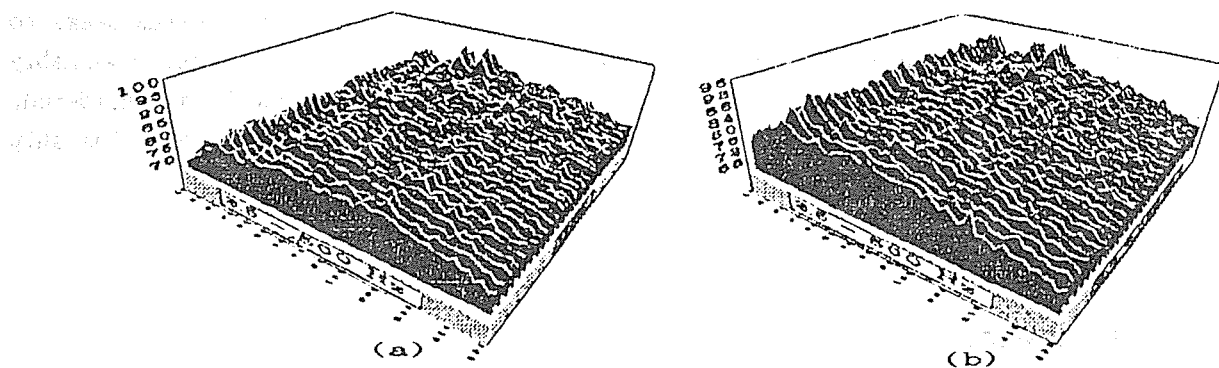
Fig.11. Time variations of ambient-noise spectra for 14-frequencies
(tonals) in November for 10m(a) and 70m(b) hydrophone depths

The time variability of ship traffic noise has been known to be dependent on the number of tones, or lines, occuring in the bandwidth of the analyzer. For 14-lines, or 14 frequencies, one-minute averaged spectrum has been plotted over 30-min period(Fig.10-11). The spectra levels of 14-lines seem to be quite steady especially on the lower hydrophone in May, but in November it fluctuates very much over the same period of time. As presented before(Fig.6-7) the spectra shape is independent of ship size and the number of ships observed is same during the period of measurement in May and November.

Therefore, this variability may be due to the difference in tonal frequencies as well as the horizontal directionality of noise sources that has not been measured. The propagation condition or different propagation path of noise is another factor that could influence the variability.

4.0 SUMMARY

It has been shown that the noise levels measured by shallow and deep hydrophones in shallow water where the ship traffic noise is prevalent are strongly depth-dependent at frequencies less than 100 Hz.

The depth dependency of noise level is such that the levels are always higher on the deeper hydrophone. Seasonal changes in noise level show that at frequencies greater than 200 Hz it becomes significantly pronounced at the lower hydrophone. The depth variation of noise levels has been explained in terms of propagation conditions.

It was also shown that the spectra shape is very close to the one presented by Urick(1986) for high shipping density. The time variability of spectrum seems to be dependent upon the directionality of noise sources and it was remarkably steady in May. Tides, wind and long-term variability have not been considered, however, it may not change the average spectra shape that is caused by the ship traffic noise.

REFERENCES

Urick, R. J., Ambient Noise in the Sea, Peninsula Publishing, 1986.

Perrone, A. J. and L. A. King, Analysis Technique for Classifying Wind and Ship-Generated Noise Characteristics, JASA 58, 1186, 1975.

Ross, D., Mechanics of Underwater Noise, Pergamon Press, New York, 1976.

Piggott, C. L., Ambient Sea Noise at Low Frequencies in Shallow Water of the Scotian Shelf, JASA 36, 2152, 1964.

Lee, D. and McDaniel, S. T., Ocean Acoustic Propagation Finite Difference Methods, Pergamon Press, New York, 1988.

Reflection, refraction, transmission and radiation of acoustic waves by a T junction in piecewise-continuous plate construction

Bernd Wendlandt

Department of Defence, Materials Research Laboratory, DSTO,
P.O. Box 50, Ascot Vale, Victoria 3032, Australia

ABSTRACT

A finite element numerical model is presented which simulates vibrations in and around structural discontinuities in visco-elastic materials excited by a sinusoidal pressure wave or pulse generated by noisy machinery. Vibration mode transfer processes at corners of a T shaped structural element are investigated and as an example of the versatility of the technique, an example of radiation of sound from such a structure into water loading the T is presented.

2 INTRODUCTION

A primitive finite difference model is developed which is able to simulate the vibration and acoustic response of an inhomogeneous,piecewise continuous, visco-elastic material structure to an incident pressure wave. The model simulates a limited degree of macroscopic distortion, up to thirty percent strain, and traces the passage of a pressure or vibration pulse, or sinusoidal wave, through a multilayer, structural T intersection. The T may be loaded with a fluid. A typical cross-section of the structural T intersection modelled is shown in Figure 1. The model simulates the conversion of dilatational waves into flexural and shear waves at the corners of the T intersection and the sound radiated by such a T intersection into the surrounding fluid . A detailed understanding of these wave conversion processes is important for the design of sound absorbing structures and understanding underwater radiation properties of ship structures.

3 MODEL

The propagation of a pressure or stress wave through a compressible medium is described by the laws of conservation of mass and momentum and the equation of state which relates the pressure or stress in the medium to the strain and its material properties [2]. The behavior of a relatively weakly-perturbed system can be solved by numerical methods using the Lagrangian technique [3]. This technique is particularly suited to calculations where discontinuities in physical properties occur.

3.1 Conservation of Mass

The law of conservation of mass for a compressible medium can be expressed in mathematical form in a frame of reference which moves with the fluid, the Lagrangian frame, and is

$$\frac{d\rho}{dt} = -\rho \nabla \cdot \vec{v} \tag{1}$$

where ρ is the mass density and $\vec{v}$ is the local velocity of the fluid. The discrete numerical representation of the Lagrangian approach defines cells of material whose corners, and hence boundaries, move with the local fluid velocity. The present study considers three dimensional (x, y, z) space to examine details of shear and normal stresses in the three orthogonal directions. In this system the indices i, j, k indicate cell position counters in the x, y and z directions respectively. Considering

,for example, motion in the x direction, the position of a cell corner at time $t + \delta t$, x_{ijk}^{n+1} is related to its previous position x_{ijk}^{n} by

$$x_{ijk}^{n+1} = x_{ijk}^{n} + v_{x_{ijk}}^{n+\frac{1}{2}} \delta t \tag{2}$$

where the superscript n indicates a particular instant of time via the relationship $t = n\delta t$, and the velocity variation over the interval δt is represented by an average. Corresponding expressions can be derived for the y and z coordinates of the cell corner.

In the time interval $n-1$ to n, the density variation of the cell designated ijk which is bounded by the corner indices ijk, $i+1jk$, $i+1j+1k$, $i+1j+1k+1$, $ij+1k$, $ij+1k+1$, $ijk+1$, $i+1jk+1$, is using a vector cross product notation, given by

$$\rho_{ijk}^{n} = \rho_{ijk}^{n-1} \frac{\{ \mid \vec{c} \cdot (\vec{a} \times \vec{b}) \mid + \mid \vec{f} \cdot (\vec{d} \times \vec{e}) \mid \}^{n-1}}{\{ \mid \vec{c} \cdot (\vec{a} \times \vec{b}) \mid + \mid \vec{f} \cdot (\vec{d} \times \vec{e}) \mid \}^{n}} \tag{3}$$

where $\vec{a}, \vec{b}, \vec{c}, \vec{d}, \vec{e}$ and $\vec{f}$ are the vectors of the side of the cell shown in Figure 3, and where for example $\vec{a}$ is the vector linking $x, y, z \mid_{ijk}$ and $x, y, z \mid_{i+1jk}$.

3.2 Conservation of Momentum and Equation of State

T he law of conservation of momentum may be expressed [4] in terms of stresses σ_{ij} and velocity components v_i along the axes of cartesian coordinates in tensor notation [5] as

$$\rho \frac{dv_i}{dt} = \frac{\partial \sigma_{ij}}{\partial x_j} \tag{4}$$

The velocities of the cell corners, derived from Equation 4 may be expressed in the discrete form of Equation 2 where the spatial derivatives of the stresses are averaged over the centers of neighbouring cells and the density at the corners are also obtained from the average density of the cells adjacent to the cell corner under consideration.

These are for $v_{i_{ijk}}$

$$v_{i_{ijk}}^{n+1/2} = v_{i_{ijk}}^{n-1/2} + \frac{2\delta t}{\sum_{l=i-1}^{i} \sum_{m=j-1}^{j} \sum_{o=k-1}^{k} \rho_{lmo}^{n}} \sum_{(over neighbouring cell centers)} \frac{\sigma_{ij_{imo}}^{n} - \sigma_{ij_{i-1mo}}^{n}}{X_{i_{imo}}^{n} - X_{i_{i-1mo}}^{n}} \tag{5}$$

Where the summation signs for the tensors may be omitted under the summation convention for tensors [11]. The $X_{i_{ijk}}^{n}$ is the the position tensor component of the center of the cell designated ijk at the time increment n. The above system of equations is complemented by the equation of state of the material, which links the strain ϵ experienced by the fluid to the stresses imposed on it. The strain tensor is related to the displacements in the first order non-linear approximation, the Green-Lagrangian strain tensor [6], by

$$\epsilon_{ij} = (u_{i,j} + u_{j,i} + u_{k,i}u_{k,j})/2 \tag{6}$$

where $u_{i,j}$ represents differentiation of tensor u_i with respect to the displacement tensor x_j. Incorporation of this non-linear strain into Equation 8 enables the Hookean-Kelvin stress-strain constitutive equation to accurately model material responses for strain values up to 30%, and enables the present model to simulate the propagation of non-destructive shock through inhomegeneous structures.

The direct and symmetric strains at the cell centers of the numerical scheme used here are related to the displacements at the cell corners by

$$\epsilon_{ij_{ijk}}^{n} = \frac{1}{8} \sum_{over unit cell corners} \frac{u_{i_{i+1mo}}^{n} - u_{i_{imo}}^{n}}{x_{i_{i+1mo}}^{n} - x_{i_{imo}}^{n}} + \frac{1}{2} \left(\frac{u_{k_{i+1mo}}^{n} - u_{k_{imo}}^{n}}{x_{i_{i+1mo}}^{n} - x_{i_{imo}}^{n}} \right) \left(\frac{u_{k_{i+1mo}}^{n} - u_{k_{imo}}^{n}}{x_{j_{i+1mo}}^{n} - x_{j_{imo}}^{n}} \right) \tag{7}$$

where the displacement $u_{i_{ijk}}^{n} = x_{ijk}^{n} - x_{ijk}^{0}$. The displacements at all cell corners are calculated by integrating the velocities at the corners via Equation 2.

The equation of state can be written for an orthogonal coordinate system as [5],

$$\sigma_{ij} = \lambda \epsilon_{mm} \delta_{ij} + 2\mu \epsilon_{ij} \tag{8}$$

The parameter $\epsilon_{mm}\delta_{ij}$ represents the sum of the orthogonal strains; λ and μ are known as Lamé's constants and μ is also called the modulus of rigidity and measures the resistance of the substance

to distortions. These constants are related to Young's modulus E and Poisson's ratio ν by $\lambda = \frac{\nu E}{(1+\nu)(1-2\nu)}$ and $\mu = \frac{E}{2(1+\nu)}$.

The simplest general linear relationship between a change in stress and associated strain which gives a representation of the elastic behaviour of many materials, including metals , under normal conditions of temperature and pressures, and also describes damping of vibrations by internal friction can be written in tensor notation as

$$\sigma_{ij} + t_0 \frac{\partial \sigma_{ij}}{\partial t} = \lambda \left(1 + t_1 \frac{\partial}{\partial t}\right) \epsilon_{mn} \delta_{ij} + 2\mu \left(1 + t_2 \frac{\partial}{\partial t}\right) \epsilon_{ij} \tag{9}$$

where t_0, t_1 and t_2 are characteristic relaxation times of the material and describe the complex nature of the elastic moduli in the time domain used commonly in steady state impedance formulations .

The internal friction causes a phase delay in the transmission of steady sinusoidal signals through the material which can be expressed as a loss-tangent, $\tan \delta$, which is related to the relaxation times and the frequency ω of the signal by $\tan \delta_\lambda = \frac{\omega(t_1 - t_0)}{1 + \omega^{-2} t_1 t_0}$ and $\tan \delta_\mu = \frac{\omega(t_2 - t_0)}{1 + \omega^2 t_2 t_0}$.

The angle δ measures the lag of strain behind stress and is known as the loss angle of the material and provides a measure of the internal damping of stress waves [4] . The magnitudes of t_0, t_1 and t_2 of materials commonly used in acoustic structures vary with frequency and no simple formular exists which relates the loss tangent to the the frequency and the characteristic times. Such materials can also readily be characterized by the simpler Kelvin-Voigt model [4],where the relaxation times t_1 and t_2 in Equation 9 are a function of frequency and $t_0 = 0$.

The above system of equations provide a complete description of the response of a material to an acoustical or vibrational excitation.

3.3   Spectral Analysis

The interpretation of simulation of structural vibrations with the model of Equation 1 to Equation 9 may be facilitated by examining the corresponding wave equations and their spectral relations. The wave equations describing the propagation of vibrations through materials which are characterized by the constitutive law ,or equation of state, Equation 9 can be expressed for dilatation, Θ, and torsion, Ψ, as

$$\rho \frac{\partial^2 \Theta}{\partial t^2} = \nabla^2 (\lambda^* + <\mu^*>) \hat{\Theta} + <\mu^*> \nabla^2 \hat{\Theta} + Q_\theta \tag{10}$$

and

$$\rho \frac{\partial^2 \Psi}{\partial t^2} = (\nabla \cdot \mu^* \nabla) \hat{\Psi} + Q_\psi \tag{11}$$

where $\hat{\Theta} = \Theta + \nabla \Theta \cdot \delta \vec{x}$ and $\hat{\Psi} = \Psi + \nabla \Psi \cdot \delta \vec{x}$ and result from the linearized form of the Green-Lagrangian strain. The term $\delta \vec{x}$ is an increment of the position vector of the spatial location (x, y, z). In this approximation, the density ρ at position (x, y, z) and time t is related to the initial, unperturbed density from the law of conservation of mass by $\rho \approx \rho_0 (1 - \Theta + \Theta^2)$, to second order in Θ. The $<\mu^*>$ represents the average value of μ^* over a small volume of computational cell and can be justified by the integral form of the divergence theorem. The terms Q_θ and Q_ψ link the dilatational waves and torsional waves at structural and material inhomogeneities and can be expressed as

$$Q_\theta = [\nabla <\mu^*>] \cdot \nabla \hat{\Theta} - \frac{\nabla \rho}{\rho} \cdot \left[\nabla(\lambda^* + <\mu^*>)\hat{\Theta} + <\mu^*> (\nabla \hat{\Theta} + \nabla \times \hat{\Psi})\right] \tag{12}$$

and

$$Q_\psi = \frac{\nabla \rho}{\rho} \times \left[\nabla(\lambda^* + \mu^*)\hat{\Theta} + <\mu^*> \nabla \hat{\Theta} + \mu^* \nabla \times \hat{\Psi}\right] \tag{13}$$

The spectral analysis may be carried readily if the oscillating part of the Θ and Ψ is represented in complex notation by $exp\imath(\vec{k} \cdot \vec{x} - \omega t)$, where k is the wavenumber and ω is the angular frequency of the wave motion.

In this notation, the spectrum form of Equation 10 and Equation 11 may be written as the quadratic expression $ak^2 - \imath bk - c = 0$. The spectrum relation for the wavenumber is then in terms of material properties and angular frequency is given by

$$k(\omega) = \pm \frac{\sqrt{4ac + b^2}}{2a} + \imath \frac{b}{2a} \tag{14}$$

The coefficients for the spectrum form of the wave equation for the dilatational wave ,Equation 10, are given by

$$a_\theta = \lambda_\omega + 2 < \mu >_\omega \; +(2\nabla \left[\lambda_\omega + < \mu >_\omega\right] + \nabla < \mu >_\omega - \frac{\nabla \rho}{\rho})\hat{k} \cdot \delta\vec{x} \qquad (15)$$

and

$$b_\theta = \left[2\nabla\left(\lambda_\omega + < \mu >_\omega\right) + \nabla < \mu >_\omega - (\lambda_\omega + 2 < \mu >_\omega)\frac{\nabla \rho}{\rho}\right] \cdot \hat{k}+ \qquad (16)$$

$$\left[\nabla^2(\lambda_\omega + < \mu >_\omega) - \frac{\nabla \rho}{\rho} \cdot \nabla(\lambda_\omega + < \mu >_\omega)\right] \qquad (17)$$

and

$$c_\theta = \rho\omega^2 + \nabla^2(\lambda_\omega + < \mu >_\omega) - \frac{\nabla \rho}{\rho} \cdot \nabla(\lambda_\omega + < \mu >_\omega) \qquad (18)$$

where $\hat{k}$ denotes unit vector of $\vec{k}$.

The coefficients of the spectrum form of the torsion wave equation are similarly given by

$$a_\psi = \mu_\omega \qquad (19)$$

and

$$b_\psi = \left[\hat{\vec{x}} \cdot \nabla \mu_\omega - \mu_\omega \hat{\vec{x}} \cdot \frac{\nabla \rho}{\rho}\right] \hat{k} \cdot \hat{\vec{x}} \qquad (20)$$

and

$$c_\psi = \rho\omega^2 \qquad (21)$$

Here the Lamé operators have converted in frequency space to the complex parameters $\lambda_\omega = \lambda(1 + \imath\omega \left[\beta_\sigma - \beta_\lambda\right])$ and $\mu_\omega = \mu(1 + \imath\omega \left[\beta_\sigma - \beta_\mu\right])$.

Inspection of the exponential presentation of the dilatation and torsion waves shows that the waves are travelling waves when $\vec{k}$ is real and are progressively dampened with distance from their point of generation as $\exp - \vec{\kappa} \cdot \vec{x}$ when *veck* is complex and $\vec{\kappa}$ represents the imaginary component of $\vec{k}$. Equation 14 has at least one complex root for $\vec{k}$ when material properties are inhomogeneous and $b \neq 0$ even when plastic and viscoelastic effects are negligible. Thus travelling waves are may be dampened when they are scattered in inhomogeneous materials or interact with surfaces of a structure. Torsional waves in rods have their $b_\psi = 0$ and are propagated without damping as is of course observed experimentally. Discontinuities in a structure may act as re-radiators of dampened waves and transform dampened waves into travelling waves. Waves whose frequencies and direction of propagation relative to material interfaces make $b^2 \gg 4ac$ are completely dampened and do not propagate.

4   CALCULATIONS/RESULTS

The model above was programmed to simulate the acoustic and vibrational response of a T shaped structure.

A typical unit cell of computation, centered on a T junction is shown in Figure 1 by dashes. The simulation was set up to consider two cases, a: the acoustic structure was assumed to be a repetition of the unit cells extending to infinity in the y and z direction as indicated in Figure 1, or b: the T junction was assumed to be in an infinite plate. The infinite plate boundaries are simulated in the model by introducing absorbing boundary conditions at the edges of the unit cell . Tests indicated that the amplitudes of displacements computed were accurate to within half of one percent. This figure was considered good for the spatial grid used and the complexity of the calculations involved [10].

The sinusoidal excitation was inserted through the velocity term of Equation 5 into the unit cell of computation at the left hand edge and the spatially decaying nature of the wave generated is shown in Figure 2. The reflections of the dilatational component from the upper and lower surface of the structure form, in accordance with Equation 14, an evanescent and a travelling wave and the overall wave decays with distance from the source. The travelling wave refracts into the T as shown in Figure 3. The change in the acoustic impedance of the structure at the junction of the T causes a small wave to be reflected which is visible in the small hump in the envelope shown in Figure 2. The transmitted wave is shown in Figure 4. The versatility of the model is illustrated by the computation of the transmission of a vibration generated in the stem of a T section into water loading the upper part of the T, see Figure 5.

5 CONCLUSION

A numerical model has been developed which is able to compute the transmission, reflection and refraction of a vibrational wave across a T shaped structure and the transmission of a vibration into water loading the T.

References

[1] Snowdon,J.C.(1968) *Vibration and Shock in Damped Mechanical Systems*,Wiley,New York.

[2] Sommerfeld,A.(1964).*Mechanics of Deformable Bodies*, Academic Press, New York.

[3] Potter,D.P.(1973) *Computational Physics*,Wiley,New York.

[4] Jaeger,J.C.,(1956). *Elasticity,Fracture and Flow*,Methuen, London.

[5] Jeffrey,H.and Jeffrey,B.S.,(1962)*Mathematical Physics*, University Press, Cambridge.

[6] Dunham, R.S.,(1989)Report ANA-89-0081, ANATECH Research Corp., USA.

[7] Hildebrand,F.B.(1962)*Advanced Calculus for Applications*, Prentice Hall,New York.

[8] Scharnhorst,K.P,Madigosky,W.M. and Balizer,E.(1985)*Scattering Coefficients and the Absorption Edge of Longitudinal Coherent Sound Waves in Selected Inhomogeneous Materials*,Report NSWC TR 85-196.

[9] Jaeger,J.C.(1981),*An Introduction to Applied Mathematics*, Clarendon Press, Oxford.

[10] Brown,D.L.,(1984),*A note on the Numerical Solution of the Wave Equation with Piecewise Smooth Coefficients*,Mathematics of Computation, Vol.42,No. 166, April 1984, pp 369-391.

[11] Spiegel,M F.,(1959) *Vector Analysis*,Schaum,New York.

[12] Kolsky,H.(1953)*Stress Waves in Solids*, Clarendon Press, Oxford.

[13] Madigosky,W.,(1988),private communications.
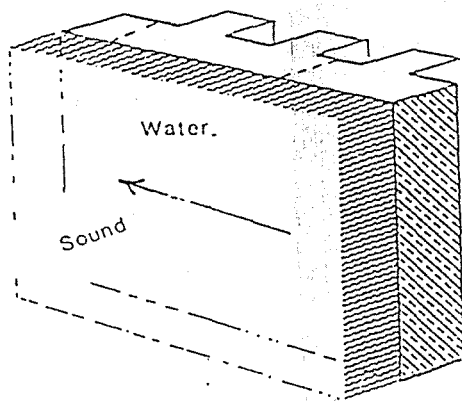
Figure 1: Section of T structure modelled.
Unit cell is shown · · ·.
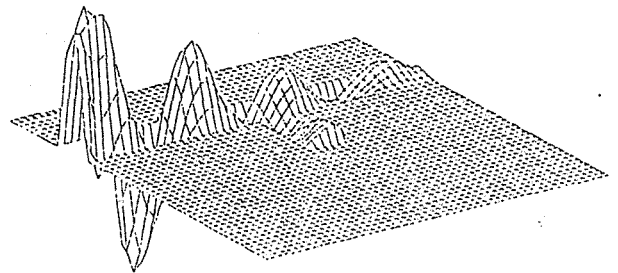
Figure 2: Evanescant and travelling wave
generated on left edge of T structure shown
and launched in x direction shown.
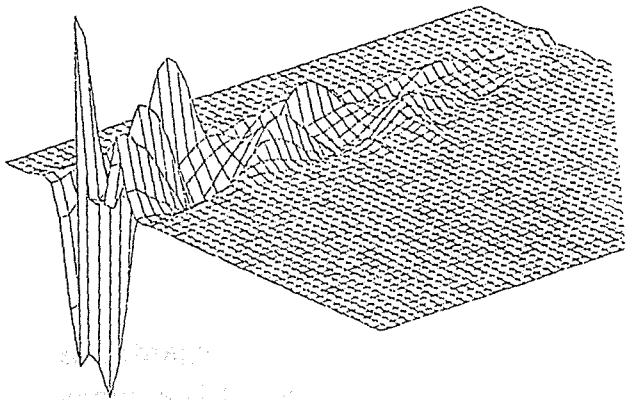
Figure 3: The y axis component of wave refrating into stem of T
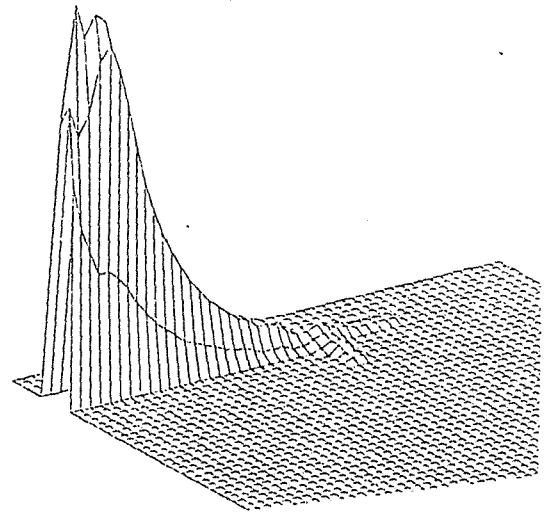
Figure 4: Envelope of evanescant and travelling wave interacting with T intersection of structure
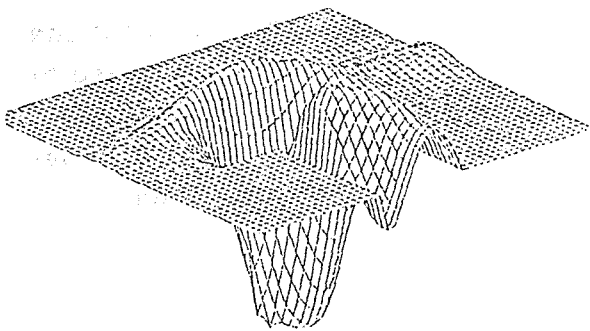
Figure 5: Radiation of wave which is generated in stem of T and travelling in direction of $-y$ into water loading loading the T

THE RADIUS LENGTH ESTIMATION OF UNDERWATER TARGETS

Yiqin Xie,Jianguo Huang and Xiaodong Yu

College of Marine Engineering
Northwestern Polytechnical University
Xian 710072, P.R.China

ABSTRACT In target recognition the length of targets is usually regarded as an ideally basic characteristic which is used in classificator design.The principle and method for the radius length estimation of underwater targets are described in this paper. Firstly the mathematical model of underwater target echo is formulated and the reflection coefficient seqence is solved by deconvolution. Based on these the radius length of targets is estimated. Then these estimation methods of target radius length are discussed.The better one of them is adaptive least square lattice(LSL) deconvolution.It can be used to find the maximum duration between the peaks of target weight sequence and then to estimate the target radius length. Finally some computer simulation results are given, which show the effectiveness for the proposed methods.

1. INTRODUCTION

Target recognition techniques widely used in the areas of industry and many sciences.The extraction of futures is the key to solve recognition problems.Although a few of methods are presented,the procedures of them related with the applications. It is necessary to determine the efficient tutuers and its extraction methods according to the characteristics of practical problems.Target length is an obvious physical futuer and the estimation of it is able to give an important hint to target recognition in many cases[3].

The samples to be recognized are a waveform or a set of waveforms in many practical problems. These waveforms of target echoes or target radiation signals contain the target information. For example, the electrocardiogram waveforms include the information which tells us that the function of patient hart is normal or not.The extended waveforms of target echoes contain the information of target radious length . Because the measured data are very long, the transformation or compression is needed to obtain the essential futures. Optimal classificator can basically process a variety of original waveforms and compliment the target recognition.Optimal detector is used to extract the target future before the classificator because it is useful to make the recognition easier[4][5].

For actual underwater targets, their scatter characteristics are described by many scatter elements or some strong discrete regions(i.e. bright—points) which are random distributed in the distances and directions[6].The delay between the waveforms of two bright points includes the information of target length.The target weight function or the target weight sequence is used to represent the random model of bright—points for the target scatter characteristics.Then target weight sequence can be founded by using adaptive lattice filter, high— resolution direction—of—arrival(DOA) estimation,and so on [7][8][9].Based on these the estimation of target radius length or efficient target reflection length can be obtained.If more futures of target weight sequence are further extracted and future vectors to be classified which are the input of a designed target classificator are formed, target classification and recognition can be well conducted according to a decision rule.

2. TARGET ECHO

The echo in the observation place is a 'random function. It is related to many undeterministic factors.What will be discussed below is the simplified description of the echo characteristics.

2.1 THE RANDOM BRIGHT—POINT MODEL OF TARGET SCATTER

Rayleigh formulated the scatter strength of a small unresonance ball as

$$T = \frac{I_s}{I_i}\bigg|_{r=1} = a^2(ka)^4[\frac{l-1}{3l} - (\frac{g-1}{2g+1})cos\theta]^2 \tag{1}$$

where I_s is scatter wave strength,I_i is incident wave strenth and a is the radius of ball.k equals $2\pi/\lambda$ which is the wavenumber of sound in medium.l represents the elasticity ratio between the ball and medium and g is to be the density ratio of the ball to medium.θ denotes the angle between incident wave and scatter wave. For the static and hard ball in consideration of l> >1 and g> >1,Eg.(1) becomes

$$T = a^2(ka)^4[\frac{1}{3} - \frac{1}{2}cos\theta]^2 \tag{2}$$

For backward scattering,$\theta = \pi$.Then target strength in dB is given by

$$TS = 10lg[(1082)\frac{a^6}{\lambda^4}] \tag{3}$$

Eq.(2) shows that the scatter processes possess the geometric mirror reflection property when ka> >1. The greater ka is, the stronger the backward scattering will be.From Eq.(3) , TS increases along with the increasment of a/λ.Due to the complexity of real target construction and the variation of target posture the target backward scattering is regarded as the reflection of the random distributed bright—point model.

2.2 TARGET ECHO MODEL

The targets and channels are referred to a linear time—variant filter.Assume that the weight function of two—way transmission channel is $h_1(t) * h_2(t)$,which represents the target weight function of target reflection characteristics h(t).The impulse response of emission signal f(t) which passed through two—way transmission channel is called sub—wave s(t).So

$$s(t) = f(t) * h_1(t) * h_2(t).$$

Then the echo processes are

$$r(t) = s(t) * h(t) \tag{4}$$

In discrete form

$$r(k) = \sum_{i=1}^{L} s(k-i)h(i) \tag{5}$$

Eg.(5) means that r(k) is the summation of s(k) which delays in i (i= 1,2,···,L) units and then weighted by the target weight sequence h(i) . It can also be described as that the echo in measured place is composed of L element echoes reflected from different points. h(i) is a random process in which the high amplitudes represent the target bright—points.

For the convenience of discussion, suppose that h(t) is the multiplication of stationary Gaussian process g(t) and bright— point weight function w(t),

$$h(t) = g(t)w(t) \tag{6}$$

where w(t) is a random distributed finite impulse sequence.

In computer simulation we assume that w(t) is the finite impulse sequence which probability distribution function is known. The typical weight function is show in Fig.1.Three peaks A,B,C are corresponding to the three bright-points.The amplitude value of the peak represents the strength of the bright-point and the width of the peak represents the range of the bright-point area.The maximum duration among the peaks can be used to estimate the radius length of target. The position of bright-points is determined by the delay of bright-point echo to the emission signal.Deleting the effect of channals for convariance and considering noise interference N(t) and reverberation interference R(t) , Eg. (6) becomes

$$r(t) = f(t) * g(t)w(t) + N(t) + R(t) \qquad (7)$$

Based on this the simulation of target echo can be conducted.

3.0 ESTIMATION OF TARGET RADIUS LENGTH

The echoes contain the information of underwater targets. The useful information extracted from them can be used to target detection,direction finding and classification. Some methods to estimate the target radius length are discussed below.

3.1 THE WIDTH OF OBSERVED ECHOES

The key to determine the width of observed echoes is to correctly find the beginning and terminal of the echo waveforms.When noise and signal with noise all are Gaussian distributed ,one method to determine the echo width is given as follows:Firstly to select the data window length M to make the window contain all possible echo data and M is greater than the maximum width of echoes.Then to determine the beginning index n_b and terminal index n_a of echo which maximize [3]

$$SNR = \frac{\frac{1}{I}\sum_{k=n_b}^{n_a} |r_k| - \frac{1}{M-I}\sum_{k} |r_k|}{\sqrt{\frac{1}{M-I}\sum_{k}(|r_k| - \frac{1}{M-I}\sum_{k}|r_k|)^2}} \qquad (8)$$

where $\{r_k\}$is the sample sequence within the data window M and variable I $= n_a - n_b + 1$ which is regarded as the echo length. $\sum_{k}$ represents the summation of data within the data window except assumed echo data .The range of summation is M−I. We change n_b and n_a in succession and then compute $\sum_{k=n_b}^{n_a} (\cdot)$ in which all possible combination of data within the data window should be included.When $n_a - n_b + 1$ is less than the width of emission pulse τ the computation will be stopped.Based on the estimation $\hat{I}$which maximizes SNR.we can find the target radius length

$$L = \frac{1}{2}(\hat{I} - \tau)c \qquad (9)$$

where c is velocity of sound.This method needs to compute the mean and variance for a great number of data combinations and to compare all the redults.So the compu-

tation is vary large. In addition it is also required to determine the time when the echo appears and the possible maximum width of echo delay.

3.2 FOURIER TRANFORM

Assume that emission signal f(t) is a short pulse.The weight sequence $h_0(i)(i = 1,2,\cdots ,N)$,which represents the reflection of N target bright-points,is an approximate constant.We can emit another long pulse with the carrier frequency f_1 which is used to measure the carrier frequency f_2 of echo.Doppler coefficient $D = \dfrac{f_2}{f_1}$.If SNR is high the reflection wave of moving target for the short pulse f(t) is given by

$$r(t) = \sum_{i=1}^{N} h_0(i) f(Dt - \tau_i) \tag{10}$$

where τ_i is the delay of emission signal caused by the ith reflection point.The Fourier transform of r(t) becomes

$$R(w) = \int_{-\infty}^{\infty} \sum_{i=1}^{N} h_0(i) f(Dt - \tau_i) exp(-j\omega t) dt$$

$$= F'(\omega) \sum_{i=1}^{N} h_0(i) exp(-j\omega \frac{\tau_i}{D}) \tag{11}$$

where $F'(\omega) = (1 / D)F(\omega / D)$,which is the Fourier transform of f(Dt).

When $R(\omega)$ is divided by the spectrum of emission wave f(Dt) in which time index t is scaled by D,we write

$$H(\omega) = \frac{R(\omega)}{F'(\omega)} = \sum_{i=1}^{N} h_0(i) exp(-j\omega \frac{\tau_i}{D}) \tag{12}$$

Then the inverse Fourier transform of $H(\omega)$ is

$$h(t) = \frac{1}{2\pi} \int_{-\infty}^{\infty} \sum_{i=1}^{N} h_0(i) exp(-j\omega \frac{\tau_i}{D}) exp(j\omega t) d\omega$$

$$= \sum_{i=1}^{N} h_0(i) \delta(t - \frac{\tau_i}{D}) \tag{13}$$

Clearly,h(t) is the compressed discrete impulse sequence of target bright-points.That the maximum duration between the peaks of sequence multiplicates D is just the delay of reflection wave, from which the estimation of target radius length can be found.

For the static targets,or the targets which radius velocity relative to the length estimator is approximately zero,D = 1. Simulation results show that the performance of this method is deteriorated in low SNR.

3.3 ADAPTIVE LEAST SQUARE LATTICE(LSL) DECONVOLUTION

Using lattice filter theory the recursive algorithm of one step linear prediction error filter is

$$f_0(k) = b_0(k) = r(k) \tag{14a}$$

458

$$f_m(k) = f_{m-1}(k) + k_m b_{m-1}(k-1) \qquad (14b)$$

$$b_m(k) = b_{m-1}(k-1) + k_m f_{m-1}(k) \qquad (14c)$$

$$k_m = \frac{\sum_k b_{m-1}(k-1) f_{m-1}(k)}{\sqrt{\sum_k b_{m-1}^2(k-1) \cdot \sum_k f_{m-1}^2(k)}} \qquad (14d)$$

where r(k) is the input. $f_m(k)$ denotes the mth order one step forward linear prediction error,which is the least square estimation of target weight sequence h(k) when the emission wave s(k) is minimum phase.$b_m(k)$is the m th order one step backward linear prediction error and k_m denotes the partial correlation coefficient.Recursive algorithm (14) for one step linear prediction error lattice filter is illustrated in Fig.2. When r(k) is the input signal, we can find $f_m(k)$, i.e. target weight sequence estimation $\hat{h}(k)$, successfully both in order and in time.Prediction error output $f_m(k)$ corresponds to filtering the reflection wave r(k) by using the inverse filter factors.It means that r(k) is the result of deconvolution.

In Eq.(14) equally weighting the error sequence summarized and moving the weight sequence,we can adaptively estimate the parameters k_m of lattice filter successively.Assume that the weight function is w(k),then k_m is the function of time,denoted by $k_m(k)$,

$$k_m(k) = -\frac{\sum_j w(k-j) b_{m-1}(j-1) f_{m-1}(j)}{\sqrt{\sum_j w(k-j) b_m^2(j-1) \sum_j w(k-j) f_{m-1}^2(j)}} \qquad (15)$$

In solving $f_m(k)$ and $b_m(k)$ we suppose that the (m− 1) th order forward and backward prediction error sequences have been found as

$f_{m-1}(k)$, $b_{m-1}(k)$, $k = 1,2,\cdots,m$

When m = 1, it is zero order and $f_0(k) = b_0(k) = r(k)$.

In order to reduce the sampling rate we need to demodulate the reflection wave r(t) and then use the complex envelop. Hence the modulus of complex $f_m(k)$ is the target weight sequence estimation $\hat{h}(k)$. According to the maximum time delay between the peaks of $\hat{h}(k)$,we can find the estimation of the target radius length

$$L_1 = L\cos\alpha = \Delta t \cdot c / 2$$

where L is the target geometry length and α is the angle between the target course and the observation direction.The other futures, such as the number of bright−points,also can obtained from $\hat{h}(k)$.

Adaptive LSL deconvolution algorithm has the property of simple computation,fast convergence and stable performance. The simulation results to estimate the target weight function are shown in Fig. 3 to Fig.8.$|\hat{h}(k)|$represent respectively the bi− bright− point and the tri−bright−point target weight functions in Fig.3 and Fig. 6, where the duration between the bright−points is 4ms for the previous one as well as 4ms and 3ms(maximum duration 7ms) for the last one. The corresponding target echoes r(t) are shown in Fig.4 and Fig.7,where the widthes of emission signals are

repectively 10ms and 5ms.the SNR's of echoes are 16dB and 19 dB.The carrier fre-quencies are all 2KHz.in Fig. 5 and Fig. 8 the estimated results $|\hat{h}(k)|$ for the related $|\tilde{h}(t)|$ are given.the duration of two bright—points is 4ms in Fig.5 and the durations among three bright—points are 2ms and 5ms(maximum duration 7ms) in Fig.8. The order of adaptive lattice filter is selected to be 3 ~ 10 and the length of moving win-dow to be 30 ~ 50 because the simulation results are more stable in this region.

4.0 CONCLUTIONS

In many cases the target backward scattering can be regarded as the reflecting of ran-dom distributed bright—point model.So we can treat the target interface as the set of some discrete points in distances and directions.Target radius length is changed with the variation of observation angle for the target radius length estimator. The maximum duration between the peaks of target weight sequence is solved by the adaptive LSL deconvolution and then the target radius length can be obtained.To extract the more futures of target weight sequence will be helpful to the target recognition and classi-fication.

REFERENCES

[1] Devijver,P.A.,and Kittler,J.,Pattern Recognition: A Statistical Approach,Prentice—Hall,1982

[2] Liddell,I.G.,Pattern Recognition, Proc. NATO ASI on Signal processing,1972,P.715

[3] Leif Bjørnø(ed.),Underwater Acoustics and Signal Processing, D.Reidel Publishing Company,1981,pp.567—570

[4] Merier,L.,Target Classification and Hypothesis Testing, Aspect of Signal Processing NATO ASI, 1976, p.257

[5] Chestnut.P.,A Sonar Target Recognition Experiment, J. Acoust. Soc. Am., Vol.66, No.1, 1979, pp.140—147

[6] Ol'shevskii,v.v., Statistical Methods in Sonar, Consultant Bureau , Plenum Pub., 1978.(Chapter 5)

[7] Friedlander,B., Lattice Filter for Adaptive Processing, Proc.of IEEE, Vol.70, No.8, 1982, pp.829—867

[8] Haykin,S.et al., Array Signal Processing, Prentice—Hall, Englewood Cliffs, 1985.(Chapter 4)

[9] Alexander,S.T., Adaptive Signal 'Processing: Theory and Applications, Springer—Verlag, New York, 1986(Chapter 10).
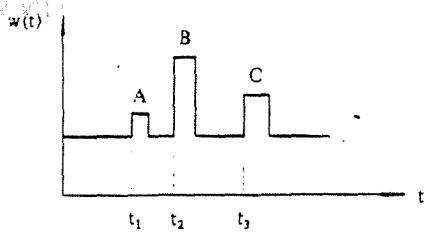
Fig.1 The scheme of tri-bright-point
weight function
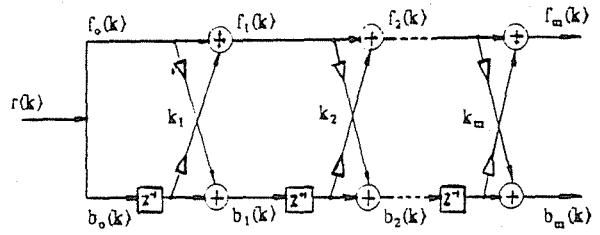
Fig.2 The lattice network of one step linear
prediction error filter
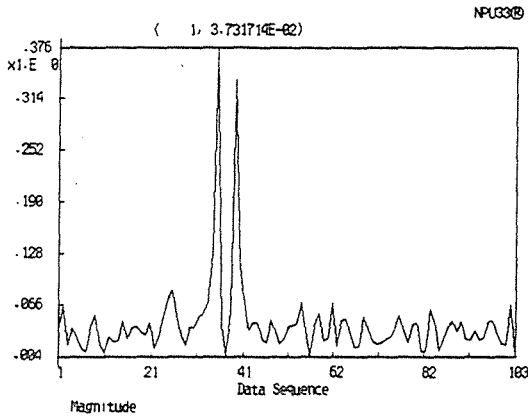
Fig.3 Bi-bright-point target weight function
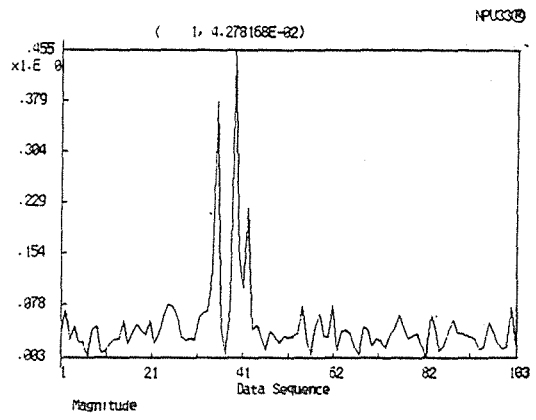
Fig.6 Tri-bright-point weight function to be estimated
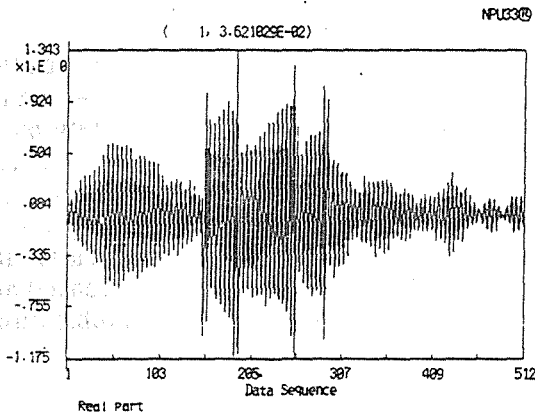
Fig.4 The target echo obtained from Fig.3
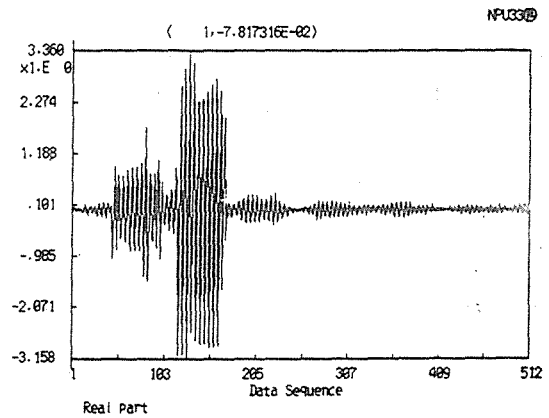
Fig.7 The target echo obtained from Fig.6
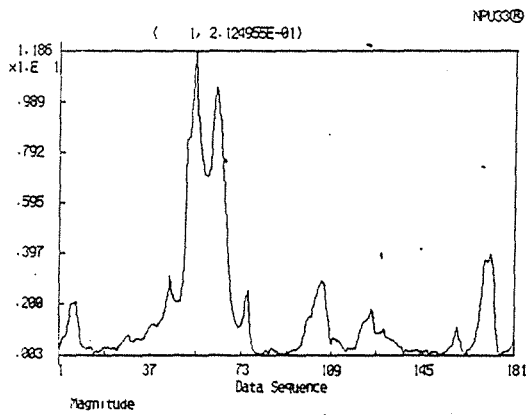
Fig.5 Estimated results for Fig.3 using the data of Fig.4
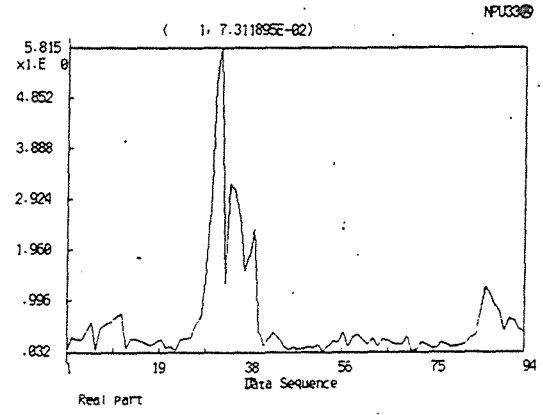
Fig.8 Estimated results for Fig.6 using the data of Fig.7

461

ACOUSTIC BACKSCATTERING FROM A CYLINDRICAL BUBBLE CLOUD IN WATER

S.W. Yoon and K.J. Park
Department of Physics
Sung Kyun Kwan University
Suwon 440-746
Republic of Korea

L.A. Crum and R.A. Roy
National Center for Physical Acoustics
The University of Mississippi
University, MS 38677
U.S.A.

ABSTRACT

Acoustic backscattering from a cylindrical bubble cloud in water was studied experimentally. For theoretical analysis a general scattering theory was used, in which the bubble cloud was modeled as a lumped element scatterer characterized completely by its geometry and void fraction. When the void fraction was less than 1% and the incident frequency was greater than individual bubble resonance frequencies, the experimental results show that the acoustic backscattering from a bubble cloud depends mainly on the void fraction rather than the individual bubble sizes. It was also theoretically and experimentally observed that the overall acoustic backscattering levels were increased and the scattering peak moved to lower frequencies when the void fraction of the bubble cloud was raised.

1.0 INTRODUCTION

In the ocean bubble clouds can be generated by various processes of hydrodynamic interactions between air and water and be formed in the upper layers down to tens of meters by Langmuir circulation, turbulence and other mechanisms [Thorpe (1984)]. This kind of bubble cloud is observed theoretically and experimentally to be a likely mechanism to generate ambient noise below 1 kHz in the ocean [Lu et al. (1990) and Yoon et al.(1991)]. If such a bubble cloud is a good noise source, it might also serve as a strong scatterer of sound in water. Recently a theoretical study of the acoustical scattering cross-section of spherical bubble clouds [d'Agostino and Brennen (1988)] was presented; however, there is little experimental data on the scattering from bubble clouds that is available to compare with these and other theoretical studies. It is the purpose of the present paper to present experimental observation and compare it with the classical scattering theory assuming a bubble cloud as a lumped element scatterer which can be characterized completely by its geometry and void fraction.

2.0 EXPERIMENTAL PROCEDURE

To understand the experimental results of acoustic scattering from bubble clouds, we must know more clearly the physical parameters of the bubble clouds themselves. We discovered that it was not easy to produce bubble "puffs" with a constant void fraction. It was too difficult to initiate or to terminate the bubble production quickly enough to generate reproducible geometrical shapes. To avoid these difficulties, we made bubble-filled columns which had a constant flux of air flow. The void fractions of bubble columns and the sizes of individual bubbles can be precisely controlled by an in-flux of air into a number of nozzles at the bottom of a tank of water. These bubble columns have made it possible to understand more precisely the physical parameters of these columns as acoustic scatterers.

2.1 Apparatus

The experimental geometry is shown in Fig. 1. To generate the bubble column, a cylindrical bubble maker was designed which consisted of forty-nine nozzles as shown in the inset of Fig. 1. The individual nozzles are connected by separate tubings with a manifold to an air-supply system to provide the same air pressure at each nozzle. To eliminate any other mechanical noise sources, compressed air was used as the air supply system. Details about the bubble maker are described in Yoon's paper [Yoon et al. (1991)].

2.2 Data Acquisition

A sound projector (NRL:USRD Type F-33) was driven with a power amplifier in the frequency range of 11 kHz to 50 kHz. The tone bursts of 250 μs width were fed to the power amplifier (ENI 1040 L) by a function generator (HP 3314 A) with the repetition rate of 1s to avoid possible interference with the reflection from the walls of the water tank. A hydrophone (B&K 8103) with a charge amplifier (B&K 2635) was installed at the center of the projector to receive echo signals from scatterers at a distance of 1.5 m from the

projector. The bubble columns were generated. These measurements were carried out in a water tank with dimensions of 2.1 m x 2.1 m x 1.8 m.
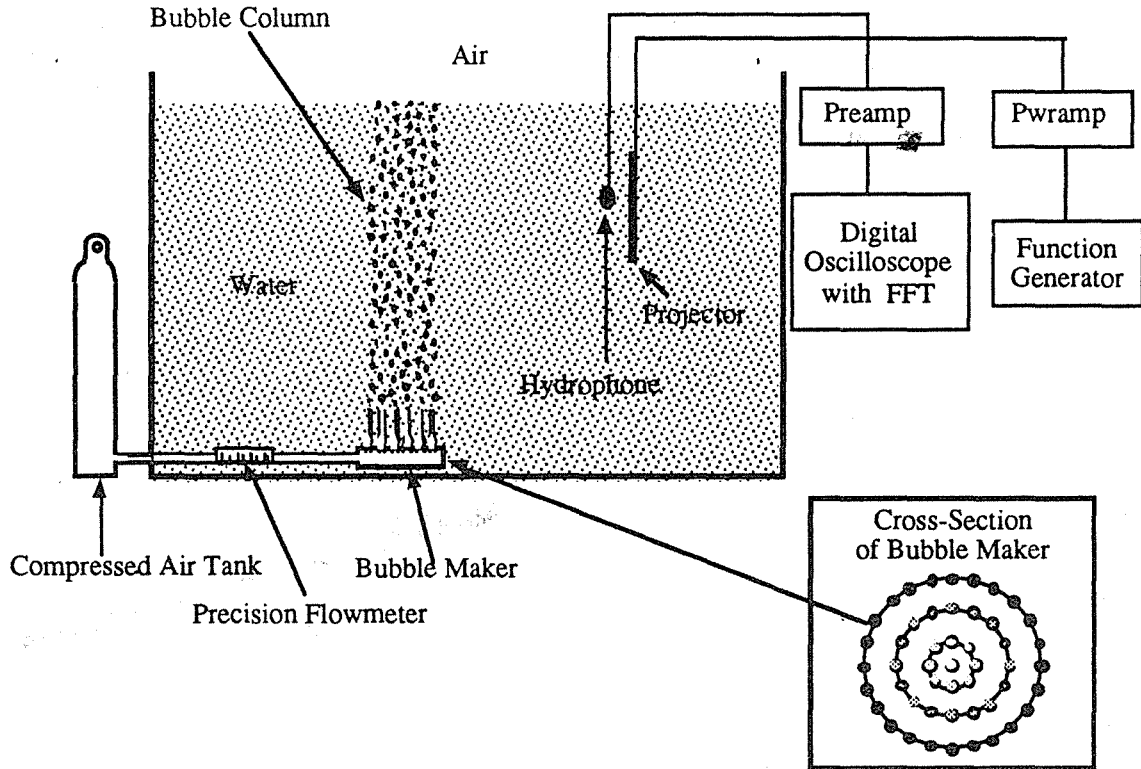
Fig. 1. Diagram of experimental apparatus.

3.0 THEORY

The classical scattering theory is well established and described in detail in Flax et al. (1981) and only a final formula for a back-scattered pressure field will be given here for an infinite plane wave incident on a solid elastic cylinder of radius a and density ρ_g whose axis coincides with the z axis:

$$p_{sc}\left(r, \phi = \pi\right) = P_o \, e^{ikr} \left(\frac{2}{i\pi kr}\right)^{\frac{1}{2}} \sum_{n=o}^{\infty} \varepsilon_n (-1)^n R_n \, (kr) , \qquad (1)$$

where P_o is the incident pressure amplitude, k is the wave number, ε_n is the Neumann factor ($\varepsilon_n = 1$ for n = 0 and $\varepsilon_n = 2$ for n > 0) and R_n (kr) is a function of kr which can be determined by the boundary conditions of the scatterer. As the argument of the function R_n, the wave number k depends on the sound speed in the medium of the scatterer and the ambient fluid. A quantity called the far-field form function f_∞ is defined to give a nondimensional representation of the back-scattered pressure

$$f_\infty(r, \phi = \pi) = \left(\frac{2}{i\pi kr}\right)^{\frac{1}{2}} \sum_{n=0}^{\infty} \varepsilon_n (-1)^n R_n (kr) \quad , \qquad (2)$$

In general, the above form function describes the steady-state back-scattered pressure amplitude from an elastic cylinder.

Treating a bubble column as a lumped element scatterer such as an elastic cylinder we can calculate the form function with the appropriate physical parameters such as density and sound speed of bubble column [Commander and Prosperetti (1988)]:

$$\rho_m = (1 - \beta) \rho_w + \beta \rho_a \quad , \qquad (3)$$

$$c_m = c_w / [1 + 4\pi c_w Nb / (\omega_0^2 - \omega^2 + 2i\delta\omega)] \quad , \qquad (4)$$

where the subscripts m, w and a represent the quantities in the bubbly mixture, water and air bubble, respectively. ρ is density, β is the void fraction of the bubble column, c is the sound speed, N is the number of bubbles per unit volume of the bubble column, b is the individual bubble radius, ω_0 is the angular resonance frequency of an individual bubble, ω is the incident angular frequency and δ is the damping constant of the bubbly mixture. If we also consider the incident frequency to be much higher than the resonance frequency of individual bubbles, the sound speed in the bubble column can be approximated by that in the ambient fluid, *i.e.*, water. According to these assumptions, the bubble column will have very similar acoustic impedance to that of water and thus be acoustically transparent. However, from the results of our experimental studies, the sound speed given above could not explain our data. For theoretical calculation of the form function we introduced the sound speeds by the ad hoc values.

4.0 RESULTS AND DISCUSSIONS

To measure the dependence of the backscattering amplitude on the void fraction, we varied the void fractions by three different ways. First, by changing the numbers of opened nozzles in the bubble maker as shown in Fig. 2, and by keeping the same sizes of individual bubbles and the same shapes of bubble columns, we were able to vary the void fractions of the bubble columns. The effective radius of the bubble column was measured to be 0.15 m and the individual bubble radius to be 2.4 mm, both measurements obtained from photographs. Figure 3 shows the dependence of the backscattering amplitude from the bubble column on the nondimensional ka of the bubble column for three different void fractions.
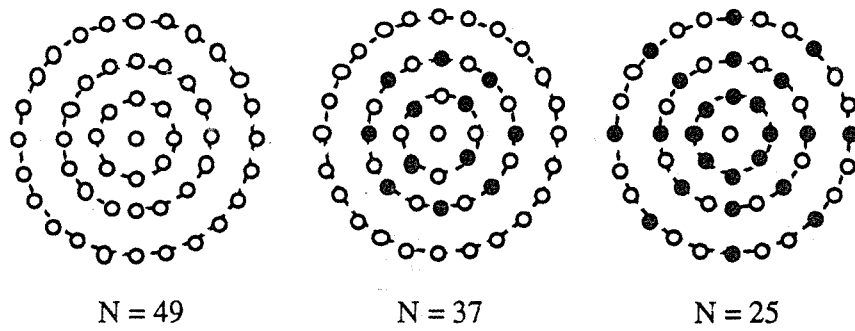
Fig. 2. Cross-section of cylinder bubble maker. N is the number of opened nozzle. The open and closed circles represent the opened and closed nozzles respectively.
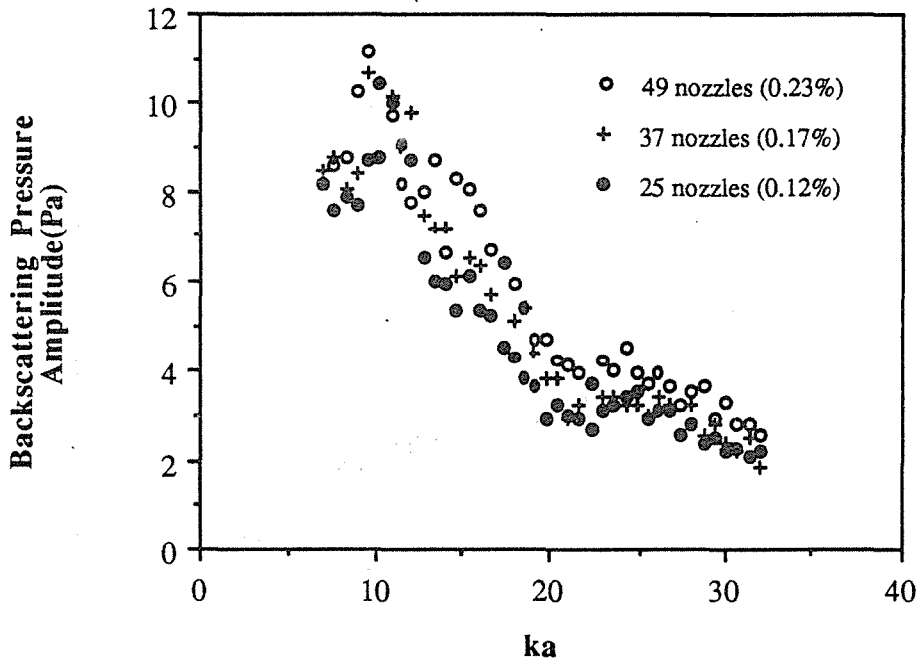
Fig. 3. Backscattering pressure amplitude vs. nondimensional bubble column ka. The void fraction is varied with the number of the opened nozzles in the larger bubble maker. Shown on the figure are the void fractions observed for the same flow rate per each nozzle (i.e., constant individual bubble size).

466
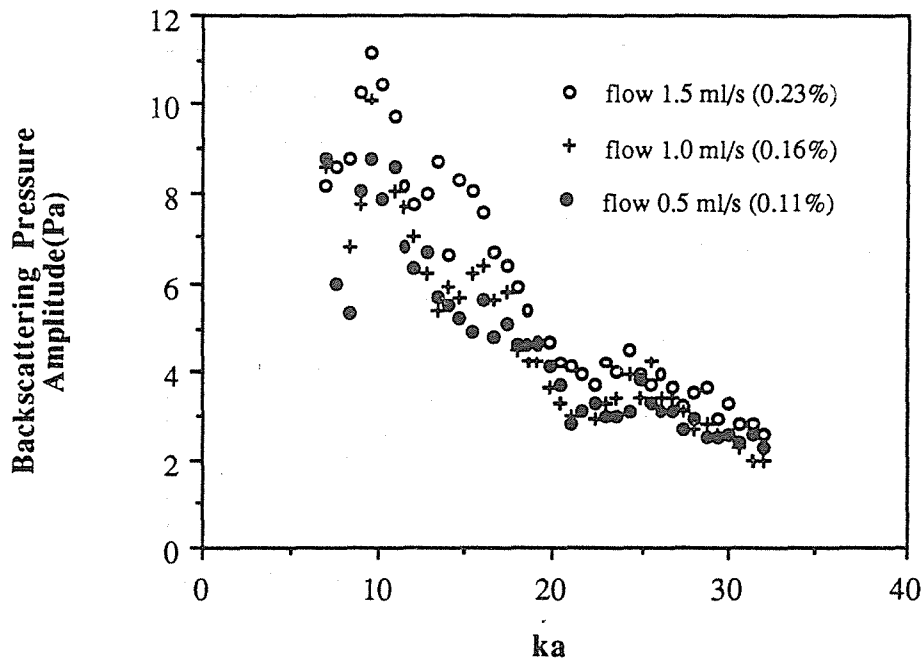
Fig. 4. Backscattering pressure amplitude vs. nondimensional bubble column ka. The void fraction is varied with changing the flow rate per each nozzle (*i.e.*, varying individual bubble size).

In the second case, we varied the void fractions by changing the air in-flow rate, which also changed the individual bubble sizes. In this case, we kept the same number of the opened nozzles of the bubble maker as in the previous case. The various flow rates gave the individual bubble radii of 2.4 mm, 2.0 mm or 1.6 mm for void fractions of 0.23%, 0.16% and 0.11%, respectively. The measured backscattering amplitudes are also shown in Fig. 4. as a function of the nondimensional radius.

Both Fig. 3 and Fig. 4 show the measured backscattering amplitudes from the bubble columns that have different void fractions and different individual bubble sizes. The nondimensional bubble column radii ka are given as $7.0 \leq ka \leq 31.9$ for the projecting frequency range, 11 kHz $\leq f \leq 50$ kHz. The peak backscattering amplitudes occurred at ka $\simeq 10$, which is at almost half of the individual bubble resonance kb $\simeq 20$. Both Figs. 3 and 4 show very similar trends of the dependence of the backscattering amplitude on ka even though in the second case (Fig. 4), there are different individual bubble sizes as well as different void fractions. The relatively small amplitude peaks were also observed at ka $\simeq 25$ for both cases. There are some variations of the peak locations but we could not see any big variations of those in Fig. 4 even when we changed the individual bubble sizes of the bubble columns. As expected we observed that the higher the void fraction, the stronger the backscattering amplitude.
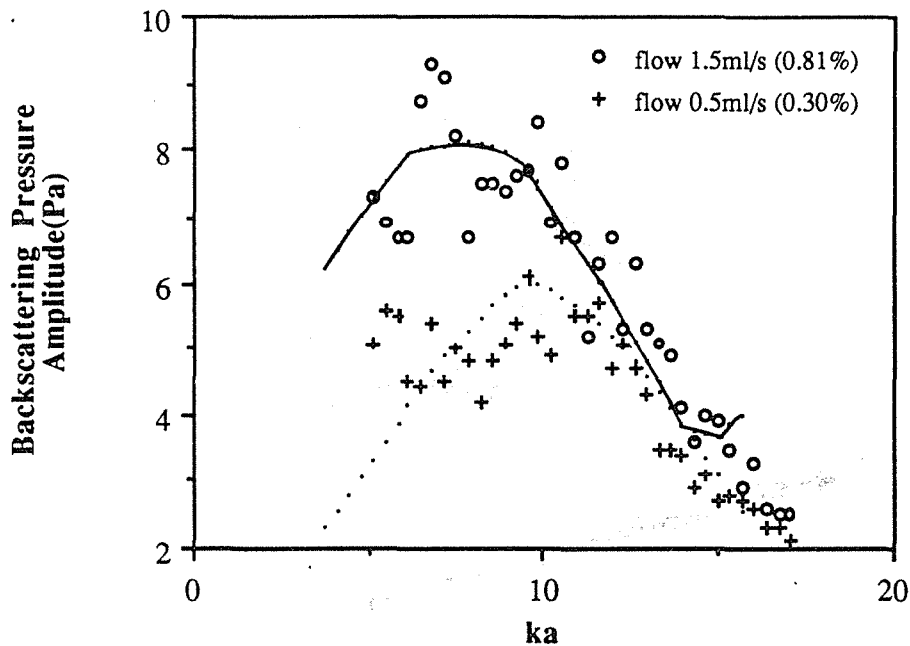
Fig. 5. Backscattering pressure amplitude vs. nondimensional bubble column ka. Each curve represents the theoretical prediction based on the classical scattering theory with c_m = 1200 m/s for solid line and c_m = 1250 m/s for dotted line.

To obtain more variation in the void fraction, we performed the same experiments as before with the smaller radius of the bubble column as the scatterer. The effective radius of the bubble column was now changed to 0.08 m. The measured scattering results are shown in Fig 5. The higher void fraction column was made of 2.4 mm-radius bubbles and the lower one of 1.6 mm-radius bubbles. The void fractions are 0.81% and 0.30%, respectively. In Fig. 5 the solid line is the backscattering amplitude theoretically computed with the sound speed c_m = 1200 m/s of the bubbly mixture for the void fraction β = 0.81% and the dashed line with c_m = 1250 m/s for β = 0.30%. Both theoretical curves give reasonable agreement with measured data. By raising the void fraction the peak of the backscattering amplitude moved to the lower frequency region and the amplitude levels were increased.

5.0 CONCLUSION

By performing a relatively simple experiment, we have been able to understand some details about the bubble cloud acting as an acoustic scatterer in water. As anticipated, we

observed that the backscattering amplitude from the bubble column increased as the void fraction was raised. Effects due to the variations of individual bubble sizes were not dominant in our observation. The theoretical results for the backscattering amplitude based on the assumption of the bubble cloud as a lumped element scatterer gave reasonable agreement with the experimental data. The peaks of the backscattering amplitudes moved to the lower frequency region by raising the void fraction of the bubble cloud.

ACKNOWLEDGMENTS

REFERENCES

Commander K.W., Prosperetti A., "Linear pressure waves in bubbly liquids: Comparison between theory and experiments," *J. Acoust. Soc. Am.* **85**, 732-746 (1989).

d'Agostino L., Brennen C., "Acoustical absorption and scattering cross sections of spherical bubble clouds," *J. Acoust. Soc. Am.* **84**, 2126-2134 (1988).

Flax L., Gaunaurd G.C., Überal H.,"Theory of Resonance Scattering" in *Physical Acoustics Volume XV*, edited by W.P. Mason and R.N. Thurston, Academic Press, New York, 1981, 191-294.

Lu N.Q., Prosperetti A., Yoon S.W., "Underwater noise emissions from bubble clouds", *IEEE J. Ocean. Eng.* **15**, 275-281 (1990).

Thorpe S.A., "The effect of Langmuir circulation on the distribution of submerged bubbles caused by breaking wind waves," *J. Fluid Mech.* **142**, 151-170 (1984).

Yoon S.W., Crum L.A., Prosperetti A., Lu N.Q., "An investigation of the collective oscillations of a bubble cloud," *J. Acoust. Soc. Am.* **89**, 700-706 (1991).

A RAY-MODE THEORY OF SURFACE

-GENERATED NOISE IN THE SEA

Zhang Renhe   **Zhu Baixian**   **Wu Guoqing**

State Key Laboratory of Acoustics, Institute of Acoustics, Academia Sinica,Beijing 100080,P.R.China

Summary

A theoretical model of ambient sea noise including surface sources and stratified ocean is discussed .The noise sources are assumed to be statistically independent directional acoustic sources situated on the surface,and the effects of ocean environment on ambient noise are studied.The normal-mode theory of surface-generated noise is developed,and the normal-mode formula of the directional density function suitable for small grazing angles is analytically continued to be consistent with the ray formula suitable for great grazing angles.The unified formulae to calculate the intensities,spatial correlation and vertical directivity of ambient noise are presented.

I.INTRODUCTION

Interaction of wind and sea-surface is one of the main causes inducing the ambient sea noise.The wind-dominated noise in shallow water often shows substantial defferences in spectrum level under the same windspeed and sea-state conditions,these differences may be caused by different environmental parameters such as sound-speed profile,water depth and bottom properties. The main purpose of this paper is to study the dependence of surface-generated noise on ocean enviroment .A theoretical model made up of surface acoustic sources and stratified ocean is studied,the normal-mode theory of surface-generated noise is developed and the formulae of intensities,spatial corrtelation and vertical directivity are obtained.

II.MODEL OF SURFACE-GENERATED NOISE AND RAY THEORETI-CAL FORMULAE

The model geometry is shown in Fig.1.

We assume that

1.Statisitically independent directional acoustic sources are uniformly distributed on the surface,and each source has the down-ward single-sided directivity as follows[1]

$$D(\alpha, \psi) = \begin{cases} 0 & \alpha < 0 \\ E\gamma(\alpha) & \alpha > 0 \end{cases} \tag{1}$$

where α is the grazing angle and $\gamma(\frac{\pi}{2}) = 1$. Assume that the average number of sources per unit area is N, then $\sigma = N < E^2 >$ is the source intensity at vertical direction emitted by unit area.

2.The ocean is assumed to be a stratified medium ,the surface and bottom reflection coefficients are $- V_s$ and $V_b e^{-i\varphi}$, respectively.
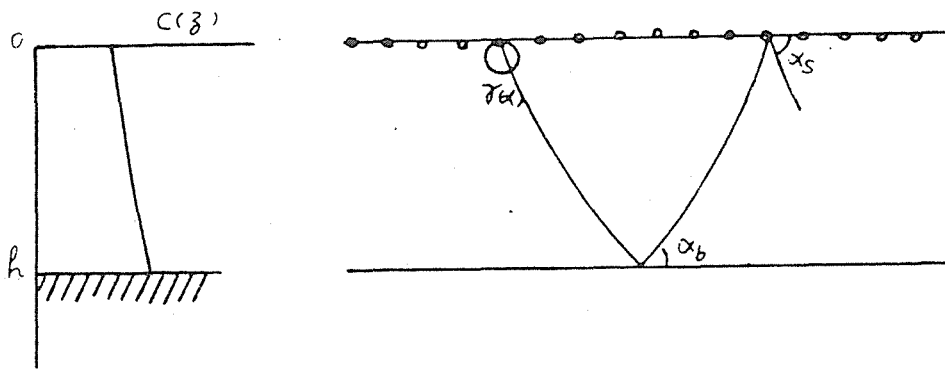
Fig.1   MODEL OF SURFACE-GENERATED NOISE

The acoustic flux diagram of surface-generated noise is shown in Fig.2. According to the ray theory,the acoustic flux emitted from $A_1, A_3, A_5,\dots$arrives at the receiver at grazing angle $(-\alpha)$,while that from $A_2, A_4,\dots$arrivies at the receiver at grazing angle α .Taking account of bending of ray and surface and bottom reflection losses,the directional density function Nr(α,z) of ambient noise can be get[2-4]:

$$N_r(\alpha,z) = \begin{cases} \dfrac{\sigma\gamma^2(\alpha_s)exp(-2aL_1)}{[1 - V^2exp(-2aL)]sin\alpha_s} & \alpha < 0 \\[4mm] \dfrac{\sigma\gamma^2(\alpha_s)exp(-2aL_2)V_b^2}{[1 - V^2exp(-2aL)]sin\alpha_s} & \alpha > 0 \end{cases} \tag{2}$$

where $V = V_s V_b$, a is the absorption coefficient in seawater.

When the frequency is lower and the grazing angle α is great enough ,one has

$$2aL < < 1 \qquad (3)$$

In this case ,Equation (2) can be simplified as

$$N_r(\alpha,z) = \begin{cases} \dfrac{\sigma\gamma^2(\alpha_s)}{(1-V^2)\sin\alpha_s} & \alpha < 0 \\[4mm] \dfrac{\sigma\gamma^2(\alpha_s)V_b^2}{(1-V^2)\sin\alpha_s} & \alpha > 0 \end{cases} \qquad (4)$$

The physical meaning of Inequality (3) is that the sound absorption in one cycle of ray is very small.
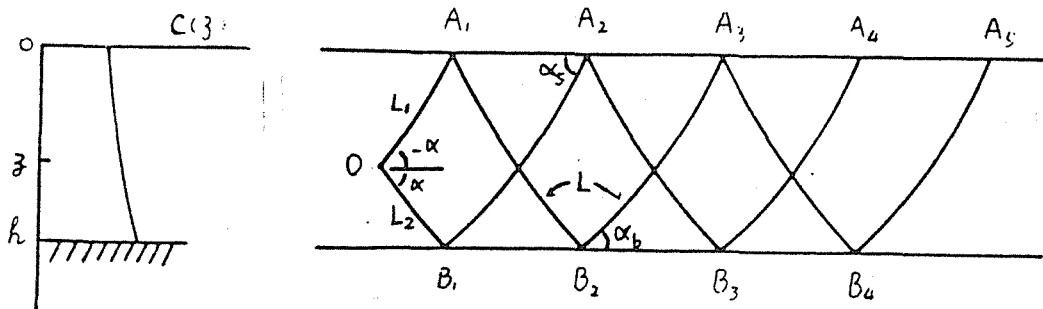
Fig,2   Acoustic flux diagram of surface-generated noise

III.NORMAL-MODE FIELD OF SINGLE NOISE SOURCE

As shown in Fig.3, a directional source O_i is situated on the surface, the re-ceivers A and B are at depths z and (z+d), respectively. If $\dfrac{\rho}{r} < < 1$,then one has

$$\overline{DO_i} \cong r - \rho\sin\theta \qquad (5)$$
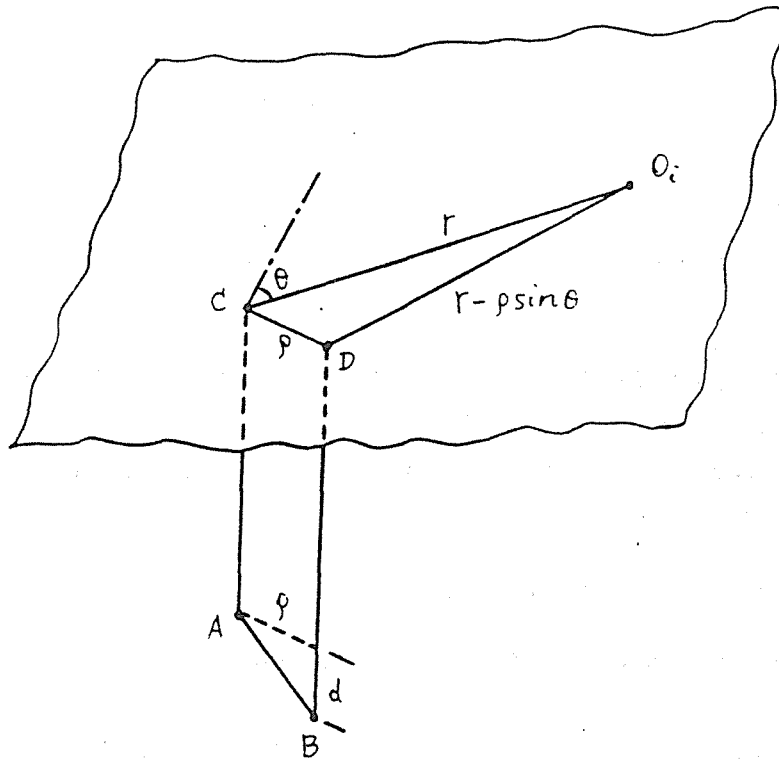
Fig.3 Geometric relationship between source and receivers

According to the normal–mode theory of a directional radiator[1], the acoustic pressures at points A and B emitted by the source O_i respectively are

$$P_i(A) = E\sqrt{\frac{8\pi}{r}}\, e^{i\frac{3\pi}{4}} \sum_l \frac{1}{S_l}\sqrt{\frac{\mu_l}{V_s}}\, q_l(0)q_l(z)\gamma(\alpha_s')sin\left(\int_0^z \sqrt{k^2(y) - v_l^2}\, dy\right.$$

$$\left. - \frac{i}{2}\ln V_s\right)exp[-(\beta_l + \alpha)r + i\mu_l r] \tag{6}$$

$$P_i(B) = E\sqrt{\frac{8\pi}{r}}\, e^{i\frac{3\pi}{4}} \sum_l \frac{1}{S_l}\sqrt{\frac{\mu_l}{V_s}}\, q_l(0)q_l(z+d)\gamma(\alpha_s')$$

$$* sin\left(\int_0^{z+d} \sqrt{k^2(y) - v_l^2}\, dy - \frac{i}{2}\ln V_s\right)$$

$$* exp[-(\beta_l + \alpha)(r - \rho sin\theta) + i\mu_l(r - \rho sin\theta)] \tag{7}$$

Taking the smooth–average over range and depth simularly to Ref.[5],and then taking the ensemble–average ,the correlation function can be obtained as follows:

$$< \overline{P_{i}(A)P_{i}^{*}(B)} > \; = \frac{4\pi < E^{2} >}{r} \sum_{i} \frac{\mu_{i}}{S_{i}^{2}V_{z}} q_{i}^{2}(0)q_{i}^{2}(z)\gamma^{2}(\alpha_{z}^{'})$$

$$cos(d\sqrt{k^{2}(z) - \mu_{i}^{2}} - iln V_{b})exp[- 2(\beta_{i} + \alpha)r + i\mu_{i}\rho sin\theta)] \qquad (8)$$

where the bar and triangular brackets denote the smooth−average and ensemble−average,respectively.

IV.INTENSITY ,SPATIAL CORRELATION AND DIRECTIONAL DEN-SITY FUNCTION OF AMBIENT NOISE

The total acoustic pressures at points A and B are the superposition of those from all sources ,i.e.

$$P(A) = \sum_{i} P_{i}(A) \qquad\qquad P(B) = \sum_{i} P_{i}(B) \qquad\qquad (9)$$

As the sources are statistically independent , one has

$$< \overline{P(A)P^{*}(B)} > \; = \sum_{i} < \overline{P_{i}(A)P_{i}^{*}(B)} > \; = N\int < \overline{P_{i}(A)P_{i}^{*}(B)} > ds \qquad (10)$$

where $ds = rdrd\theta$ is the area element on the surface. Instituting Eq.(8)into Eq.(10)and completing the integration, then one yields

$$< \overline{P(A)P^{*}(B)} > \; = 8\pi^{2}\sigma\sum_{i} \mu_{i}q_{i}^{2}(0)q_{i}^{2}(z)\gamma^{2}(\alpha_{z}^{'})cos(d\sqrt{k^{2}(z) - \mu_{i}^{2}}$$

$$- iln V_{b})J_{o}(\mu_{i}\rho) / V_{z}(\beta_{i} + \alpha)S_{i}^{2} \qquad (11)$$

where J_{o} is the zero orderBessel function .

Since the terms of series (11) vary slowly with l, the summation can be approximated by the corresponding integration. Let $\mu_{i} = k(z)cos\alpha$,Equation (11) can be transformed as the integral with respect to α :

$$< \overline{P(A)P^{*}(B)} >$$

$$= 2\pi\sigma\int^{\pi/2} \frac{cos\alpha sin\alpha\gamma^{2}(\alpha_{z})J_{o}(k\rho cos\alpha)cos(kdsin\alpha - iln V_{b})}{V_{z}[B + \alpha S(\alpha)][D(0) + sin^{2}\alpha_{z}]^{\frac{1}{2}}[D(z) + sin^{2}\alpha]^{\frac{1}{2}}} d\alpha \qquad (12)$$

where $\alpha_{z} = arcos(\frac{kcos\alpha}{k(0)})$, $B = - ln V_{z}V_{b}$, $D(z) = 0.875|\frac{2}{\omega}\frac{dc}{dz}|^{\frac{2}{3}}$.

we discuss the properties of ambient noise from Eq.(12).

1.Directional density function (DDF)

By using the following equality

$$cos(kdsin\alpha - iln V_b) = \frac{1}{2}[V_b e^{ikdsin\alpha} + \frac{1}{V_b}e^{-ikdsin\alpha}] \tag{13}$$

Equation(12) can be written as

$$< \overline{P(A)P^*(B)} > = \int_{-\pi/2}^{\pi/2} 2\pi cos\alpha N(\alpha,z)J_o(kp cos\alpha)e^{ikdsin\alpha}d\alpha \tag{14}$$

where

$$N(\alpha,z) = \begin{cases} \dfrac{\sigma sin(-\alpha)\gamma^2(\alpha_s)}{2V[B + \alpha S(\alpha)][D(0) + sin^2\alpha_s]^{\frac{1}{2}}[D(z) + sin^2\alpha]^{\frac{1}{2}}} & \alpha < 0 \\[4mm] \dfrac{\sigma sin\alpha \gamma^2(\alpha_s)V_b^2}{2V[B + \alpha S(\alpha)][D(0) + sin^2\alpha_s]^{\frac{1}{2}}[D(z) + sin^2\alpha]^{\frac{1}{2}}} & \alpha > 0 \end{cases} \tag{15}$$

Equation (14) denotes the relationship between the spatial correlation and directional density function ,in which $N(\alpha,z)$ is just the directional density function deduced by the normal−mode theory.

2.Spatial correlation coefficient $\Gamma(d,\rho;z)$

one get

$$\Gamma(d,\rho;z) = \frac{\displaystyle\int_{-\pi/2}^{\pi/2} cosN(\alpha,z)J_o(kp cos\alpha)e^{ikp sin\alpha}d\alpha}{\displaystyle\int_{-\pi/2}^{\pi/2} cos\alpha N(\alpha,z)d\alpha} \tag{16}$$

3.Intensity of ambient noise

Let $d = \rho = 0$, one gets the intensity $I(z)$

$$I(z) = \pi\sigma\int_0^{\frac{\pi}{2}} \frac{(1 + V_b^2)cos\alpha sin\alpha \gamma^2(\alpha_s)d\alpha}{V[B + aS(\alpha)][D(0) + sin^2\alpha_s]^{\frac{1}{2}}[D(z) + sin^2\alpha]^{\frac{1}{2}}} \tag{17}$$

V. CONNECTION BETWEEN THE NORMAL-MODE AND RAY FORMULAE

The ray formula (1) of DDF is suitable for great grazing-angles, while the normal-mode one is suitable for small grazing angles in general, How do they connect? This is a interesting problem.

When the grazing angle is great enough, the modified terms $D(0)$ and $D(z)$ in Eq.(15) can be neglected. In addition ,if the frequency is lower enough, for great grazing angles one has

$$aS(\alpha) < \, < B(\alpha) \tag{18}$$

In this case, Equation(15) can be simplified as

$$N(\alpha,z) \cong \begin{cases} \dfrac{\sigma\gamma^2(\alpha_s)}{2V(-\ln V)\sin\alpha_s} & \alpha < 0 \\[3mm] \dfrac{\sigma\gamma^2(\alpha_s)V_b^2}{2V(-\ln V)\sin\alpha_s} & \alpha > 0 \end{cases} \tag{19}$$

The physical meaning of Inequality (18) is that the absorption coefficient is much less than the attenuation coefficient $\beta = \dfrac{B}{S}$ of normal mode.

The ratio of two directional density functions is

$$\delta = \frac{N}{N_r} = \frac{V^2 - 1}{2V\ln V} \tag{20}$$

The ratio δ versus V is listed in Table 1.

Table 1. Ratio δ versus V

V	0.9	0.8	0.7	0.6	0.5	0.4	0.3
δ	1.0019	1.0083	1.0213	1.0441	1.0820	1.1459	1.2597
$10\log\delta$,dB	0.0080	0.0359	0.0916	0.187	0.342	0.592	1.003

We can see from Table 1 that for great grazing angles both formulae of DDF are consistent well.

REFERENCES

[1] R.Zhang and B.Zhu J.Sound Vib, 119, 207(1987).

[2] R.N.Hamson, J.Acoust.Soc.Am.,78,1702(1985).

[3] R.J.Talham,J.Acoust.Soc.Am.,36,1541(1964).

[4] R.M.Kennedy and T.K.Szlyk, J.Acoust.Soc.Am.,86,1920(1989).

[5] R.Zhang and Q,Wang, J.Acoust.Soc.Am., 87, 633 (1990)

NOISINESS OF IMPULSIVE NOISE
IN BACKGROUND NOISE

Masanao Ebata
Department of Electrical Engineering and Computer Science,
Kumamoto University, 2-39-1 Kurokami, Kumamoto 860 Japan
Phone : +81-96-344-2111 (Ext.3622), Fax : +81-96-345-1553

Hiromitsu Miyazono
Department of Mechanical and Electrical Engineering,
Yatsushiro National College of Technology, 2627
Hirayamashin'machi, Yatsushiro 866 Japan
Phone : +81-965-35-1611 (Ext.228), Fax : +81-965-33-0616

Tsuyoshi Usagawa
Department of Electrical Engineering and Computer Science,
Kumamoto University, 2-39-1 Kurokami, Kumamoto 860 Japan
Phone : +81-96-344-2111 (Ext.3623), Fax : +81-96-345-1553

ABSTRACT

There are many studies of rating noise, but the method has
not been established yet. Especially in the rating of
impulsive noise, there are some problems even though an
evaluation based on energy level is effective to some
extent. In this study, the noisiness of impulsive sound is
measured when background noise is presented at various
levels and various band widths. The results are follows;
(1) the noisiness decreases as the increase of background
noise level, (2) the noisiness decreases as the increase
of band width of background noise. The former phenomenon
can be explained by the difference in the energy level of
the impulsive noise and the background noise. However, the
latter one is not expected from the evaluation based on
the energy level. To derive more accurate rating, two
methods are discussed: one is based on NOY and the other
based on a background correction which is similar to a
loudness rating.

1.0 INTRODUCTION

Although many studies have been published on noise rating, the method of evaluation is still one of the major topics. The rating of impulsive noise is thought to depend on not only its time pattern but also background noise. In this study, we measure the noisiness of impulsive noise in background noise. In the experiment, we investigate the effect of band width of background noise on noisiness of impulsive noise and the effects of spectrum characteristics of impulsive noise within background noise.

2.0 EXPERIMENT 1:
EFFECTS OF BAND WIDTH OF BACKGROUND NOISE

2.1 Method

Figure 1 shows the schematic diagram of apparatus in this experiment. A pair of stimuli, test stimulus including background noise and comparison stimulus, is presented to a subject through headphone in acoustically insulated room. The test stimulus is impulsive noise. The subjects are asked to judge which stimulus in a pair is more noisy. The PSE (points of subjective equality) of the impulsive sound is estimated on noisiness. In this procedure, PSE is defined as sound pressure level of comparison stimulus which is judged as noisy as test one. Figure 2 shows the time pattern of the stimulus. The carrier of the test and comparison stimuli are sinusoidal wave (1kHz). The rise and decay time are 3 and 100 ms respectively for 20 dB change in level.

Fig. 1
Schematic diagram of apparatus

Fig. 2 Time pattern of stimuli

The steady durations of impulsive noise are 100, 30 and 0 ms and the peak level is 85 dB. The comparison stimulus is a steady sound lasting 200 ms and rise time and decay time are 5 ms for 20 dB change in level. The level is one of nine levels which differ by a step of 2.5 dB based on preparatory experiment. The background noise is a band noise. The band widths are one third octave, one octave and two octave and the center frequency is 1 kHz. The band noise are presented at the test stimulus at 50 to 70 dB. The order of stimuli is randomized. The subjects are twenty-five male students with normal hearing ability.
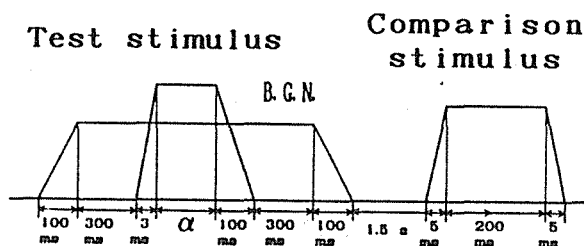
2.2 Results

Figure 3 shows the relationship between background noise
level and PSE i.e. SPL of comparison stimulus which is
judged as noisy as test stimulus. Dashed line is PSE
without background noise. The symbols of ● , ▲ and ■
indicate the results of 100, 30, 0 ms steady duration of
impulsive noise, respectively. As is obvious from figure
3, the noisiness of the impulsive sound decreases as
background noise increases and steady duration of
impulsive noise is shorter. These results indicate that
the decrease of noisiness is due to masking effect of
background noise on impulsive noise. Consequently, it is
no significant difference among three band widths. In
loudness, masking effect to sinusoidal stimulus from band
noise depends on band width. However, the decreasing of
the noisiness has an influence on not band width but the
simple level of background. When the steady duration of
impulsive noise is 0 ms, the noisiness decreases as the
increase of band width of background noise.
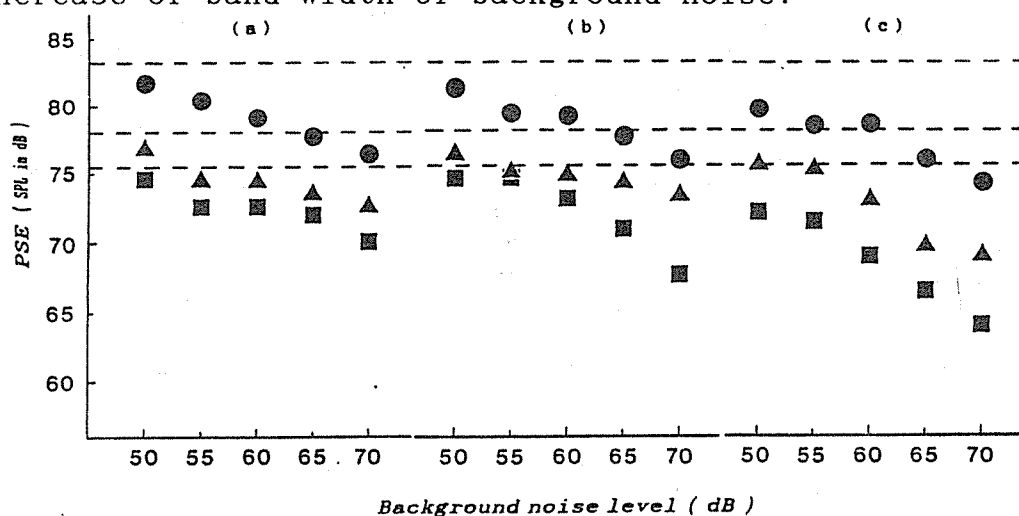
Fig. 3 Relationship between background noise level and PSE
Background noise (a):1/3 octave, (b):1 octave, (c):2 octave
Steady duration of impulsive noise ● :100 ms, ▲ :30 ms, ■ :0 ms
------: Without background noise

3.0 EXPERIMENT 2:
EFFECTS OF SPECTRUM CHARACTERISTICS OF IMPULSIVE NOISE

3.1 Method

In second experiment, the method of successive
categories is adopted. After the impulsive noise including
background one is presented to subjects through
headphone, they were required to judge the
noisiness of the impulsive sound using seven
categories from 7 (Extreme noisy) to 1 (Not at all).
There are no definition for the categories except 1 and
7. They are left to the judgment for the subjects.
Figure 4 shows the time pattern of the stimulus. The
carrier of the impulsive noise is three kinds of broad

band noise. The spectrum char-
acteristics of impulsive noise
are -6 dB per octave, -3 dB
per octave (pink noise) and 0
dB per octave (white noise).
Thus, the rise and decay time
are 3 and 100 ms for 20 dB
change in level, respectively.
The steady duration of impul-
sive noise are 100,30, 0 ms
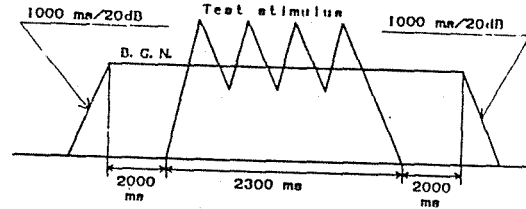
Fig. 4 Time pattern of stimuli

and the repetition rate is 3 and 10 times per second. The
peak level of impulsive noise is ranged from 55 to 75 dB
by a step of 5 dB. The background noise is a pink noise
and steady sound lasting about 7 s and rise time and decay
time are 1 s for 20 dB change in level. The background
noise are presented at period of the impulsive noise at
50 to 70 dB. and at less than 30 dB(no presentation of
background noise). The order of stimuli is randomized.
The subjects are six male and female students and they
have normal hearing ability.

3.3 Results

A part of results are shown in figure 5. This figure
shows the relationship between background noise level and
noisiness as a function of peak level. The symbols of ● ,
▲ , × , ■ , ▼ indicate the noisiness of the average of
the all subjects to judged to 55, 60, 65, 70, 75 dB of
peak level of impulsive noise. In higher peak level of
impulsive noise, the noisiness is the same as background
noise level changes. However, in lower level, it is
obvious that the noisiness decreases as background noise
level increases.
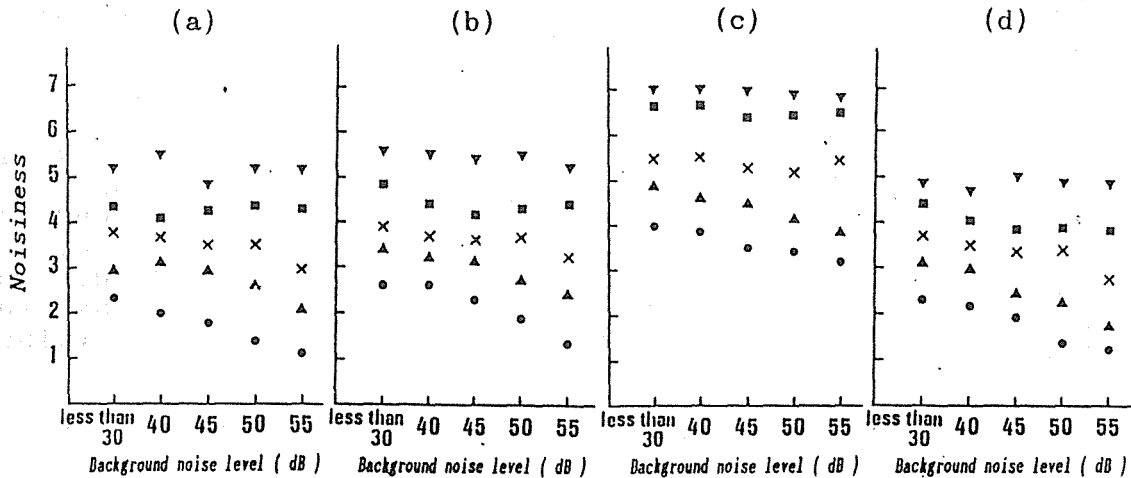
Fig.5 Noisness category score, plotted as a function of background
noise level.
(a): -6 dB/oct, 10 times/sec, (b): -3 dB/oct, 3 times/sec,
(c): -3 dB/oct, 10 times/sec, (d): 0 dB/oct, 3 times/sec

4.0 DISCUSSION
ESTIMATION OF NOISINESS OF IMPULSIVE NOISE IN BACKGROUND NOISE

4.1 Revised Lpn method [1]

In order to estimate noisiness of impulsive noise in background noise, the revised Lpn is proposed in this paper. The revised Lpn is derived as follows. In the first step, the frequency analysis of impulsive noise and background noise is made with one-third octave band filters. The noisiness (noy) is obtained in each band. In the second step, the noy in each band is derived by subtracting the noy of background noise from the noy of impulsive noise in each band. If it is negative, it is defined as zero. In the third step, the noisiness is calculated by Eq.(1).

$$\text{Noisiness} = \text{Nmax} + 0.15(\Sigma n - \text{Nmax}) \qquad (1)$$

where Σn is noys summed in all bands and Nmax is the maximum number of noys in any one band. And the revised Lpn is represented by Eq(2).

$$\text{Lpn} = 10\log_2(\text{Noisiness}) + 40 \qquad (2)$$

4.2 Loudness function method

According to Lochner et.al.[2], the masked loudness Sm of pure tone is

$$\text{Sm} = k(\ I^{\alpha} - I^{\alpha}_{thr}\ ) \qquad (3)$$

where I_t is an intensity of pure tone, I_{thr} is an intensity at threshold and k and α are constants. In order to apply this formulas to noisiness, the formulas is modified as follows

$$\text{Noisiness} = 10\log_{10}(\ \int I^{\alpha}dt - \int I_0^{\alpha}\ dt) + k \qquad (4)$$

where I is an intensity level of impulsive noise, I_0 is intensity level of background noise and both k and α are constant. The noisiness of impulsive noise can be estimated by Eq(4). In this study, the exponent α is 0.23 to minimized the difference between the result and the estimated value. The value of k is defined as the difference between the estimated value and the obtained PSE.

4.3 Estimation of noisiness using by two methods

Using two methods, noisiness of impulsive noise in background noise is estimated for a part of data obtained in experiment 1. Figure 6 shows the relation between the increased PSE based on background noise and background noise level. In this figure, solid and dashed line represent estimated values of revised Lpn and loudness function method, respectively. When the background noise is not presented, the estimated value and the noisiness

482

are adjusted to zero in vertical scale. As the results, there is not noticeable difference between two estimated values which are shown in figure 6.
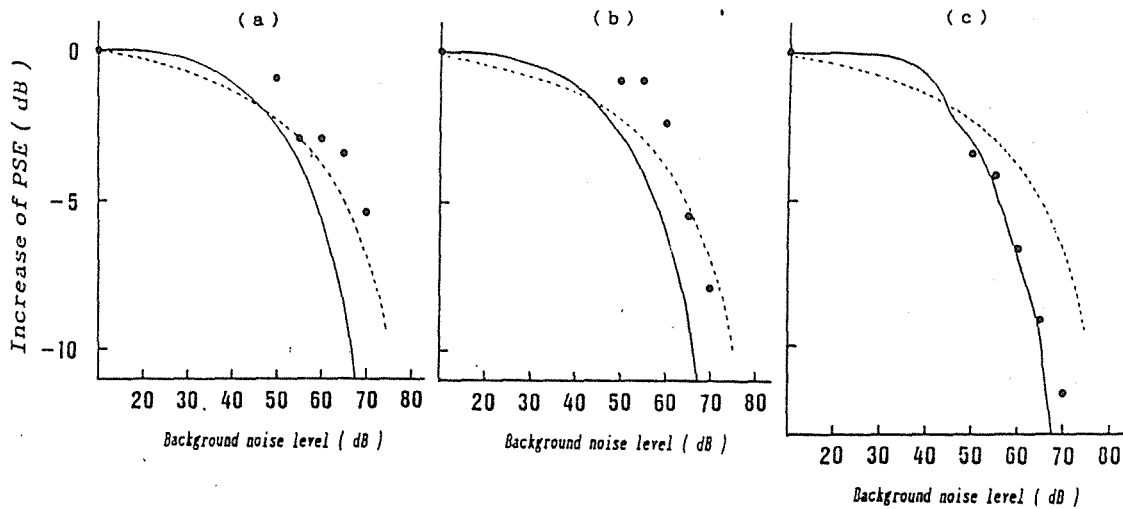
Fig. 6 Increase of PSE, plotted as a function of background noise level, and estimated results.
Steady duration of impulsive noise is 0 ms.
● :Experimental result,
Solid line: Revised Lpn, Dashed line: Loudness function method,

5.0 CONCLUSION

In this study, we measure the noisiness of impulsive noise in background noise. The results shows that the noisiness decreases as the increase of background noise level, and the noisiness dose not change or decreases as the increase of band width of background noise. However, when the peak level of impulsive noise is higher, the noisiness cannot be affected by background noise. In order to estimate the decreases of the noisiness by background, two methods are discussed. As a results, both methods give better estimation compared with conventional rating methods

REFERENCE

1) Kryter, K.D. and Pearsons, K.S. "Some Effect of Spectral Content and Duration on Perceived Noise Level" J.A.S.A. 35, 866(1963)
2) Lochner.J.P.A and Burger.J.F." Form of the loudness function in the presence masking noise " J.A.S.A. 33, 1705(1961)

THE EFFECT OF TIME CONSTANT OF AVERAGED SQUARING CIRCUIT ON THE STOCHASTIC RESPONSE FLUCTUATION OF THE SOUND LEVEL METER

M. Ohta
Faculty of Engineering, Kinki University,
Takaya, Higashi-Hiroshima 729-17, Japan

E. Uchino
Faculty of Computer Science and Systems Engineering,
Kyushu Institute of Technology,
Kawatsu, Iizuka 820, Japan

ABSTRACT In this paper, the effect of a time constant of averaged squaring circuit in the sound level meter on the output fluctuation pattern of signal is discussed from theoretical and experimental viewpoints. First, a fluctuation index by which the stochastic characteristics of fluctuation of signal can be evaluated quantitatively is newly proposed, and then the relationship between a time constant, τ, of exponential type averaging and a time constant, T, of linear type averaging is discussed based on this fluctuation index. In conclusion, the well-known experience law, which is simply stated that when $T \cong 2\tau$, the stochastic characteristics of the output fluctuation patterns coming out of the respective measuring instruments with exponential and linear type averaging circuits become approximately equal so far as up to the second order moments are concerned, has been obtained theoretically and experimentally.

1.0 INTRODUCTION

As is well-known, noise problems, e.g., community noise, road traffic noise, aircraft noise, machinery noise, construction noise, etc., are very important problems in the modern society. These noises are usually measured and/or recorded by a sound level meter and/or a level recorder for noise environment assessment. These measuring instruments have their own specific time constants. That is, the sound pressure signal is averaged by the RC circuit with a specific time constant after passing through the squaring circuit in order to simulate approximately the characteristics of man's hearing response to the time fluctuation pattern of sound.

For example, as for a sound level meter, exponential type averaging is carried out, which gives more weight to the recent sample points than to the previous ones (Hassall J.R. and Zaveri K.). Needless to say, it has a time constant of 0.125(sec) for "fast" mode and 1(sec) for "slow" mode. On the other hand, the mean operation of squared signal is defined mathematically in another way by idealized linear type averaging, where an equal weight is given at all time points within its averaging time period. It is observed that the output fluctuation pattern through the averaging operation of exponential type differs fairly from the one through the linear type averaging operation. That is, the statistical characteristics of the output fluctuation are affected by what kind of averaging operation is used. Therefore, in order to evaluate precisely the real fluctuation of sound, the internal averaging mechanism of measuring instrument should be positively taken into due consideration.

The change of a time constant of measuring instrument inevitably causes the change of the output fluctuation pattern. In this paper, the mutual relationship between the time constants of exponential type averaging and linear type averaging is discussed analytically. First, a new concept of fluctuation index of the n-th order based on the n-th higher order moment is defined to consider the statistical characteristics of the fluctuation pattern of signal. Main concern here is to derive the mutual relationship between a time constant, τ, of exponential type averaging and an averaging time period, T, of linear type averaging when each output fluctuation pattern has the same fluctuation index. If it is evaluated by the fluctuation index of the second order, $T \cong 2\tau$ is resulted analytically. This is consistent with the well-known experience law, which shows the legitimacy of the present theory. The effectiveness of the theory has also been confirmed by applying it to the actual room acoustics data.

2.0 THEORETICAL CONSIDERATIONS

2.1 *Formulation of the Problem* Consider the following two input-output systems illustrated in Figs.1 and 2.

Input   Output

$x(t)$ → [Squaring Circuit] → [RC Integrator] → $A(t)$
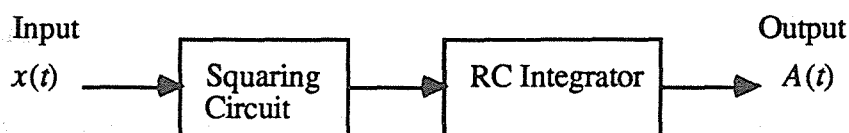
Fig.1. Exponential type averaging of squared signal.

Input   Output

$x(t)$ → [Squaring Circuit] → [Ideal Integrator] → $B_T(t)$
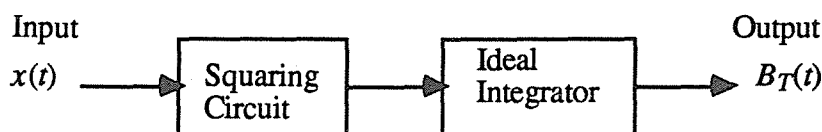
Fig.2. Linear type averaging of squared signal.

Figure 1 shows the block diagram of the averaging mechanism of the actual sound level meter, and Fig.2 shows the block diagram of the ideal one. The respective outputs are described by:

$$A(t)=\int_0^\infty x^2(t\text{-}v)f(v)dv, \qquad f(v)=\frac{1}{\tau}e^{-v/\tau} \tag{1}$$

and

$$B_T(t)=\frac{1}{T}\int_0^T x^2(t\text{-}v)dv, \tag{2}$$

where $x(t)$ is an input sound pressure, τ is a time constant of instrument, T is an averaging time period of an ideal integrator, and $A(t)$ and $B_T(t)$ are energy-valued outputs. Now, let define a new concept of fluctuation index of the n-th order for signal $E(t)$ by:

$$\alpha_n \equiv \frac{\langle (E(t)\text{-}\langle E(t)\rangle)^n\rangle}{\langle E(t)\rangle^n}, \tag{3}$$

where $\langle * \rangle$ means an ensemble averaging of $*$. The auto-correlation coefficient of sound pressure, $x(t)$, reflecting the correlation characteristics of fluctuation pattern is defined usually by:

$$C(s)\equiv\frac{\langle x(t)x(t+s)\rangle}{\langle x^2(t)\rangle}. \tag{4}$$

Next, by assuming the ergodic process (Maybeck P.S.), an ensemble-averaging can be replaced by a time-averaging, and thus Eqs.(3) and (4) become as:

$$\alpha_n \equiv \frac{\overline{(E(t)\text{-}\overline{E(t)})^n}}{\overline{E(t)}^n}, \tag{5}$$

$$C(s)\equiv\frac{\overline{x(t)x(t+s)}}{\overline{x^2(t)}}, \tag{6}$$

where $\overline{*}$ means a time-averaging of $*$.

The problem here is to find a relationship between τ and T when each fluctuation of $A(t)$ and $B_T(t)$ has the same fluctuation index defined by Eq.(3).

2.2 Fluctuation Index for the Output, A(t), Exponentially Averaged

Under the assumption of stationary process, the first order moment of $A(t)$ coming out of the circuit with exponential type averaging is given by:

$$\overline{A(t)}=\int_0^\infty \overline{x^2(t\text{-}v)}f(v)dv=\overline{x^2(t)}\int_0^\infty f(v)dv=\overline{x^2(t)}, \tag{7}$$

and the second order moment is given by:

$$\overline{A^2(t)} = \int_0^\infty \int_0^\infty \overline{x^2(t-v_1)x^2(t-v_2)}f(v_1)f(v_2)dv_1dv_2. \tag{8}$$

It can be shown for a stationary Gaussian signal, $x(t)$, that:

$$\overline{x^2(t-v_1)x^2(t-v_2)} - \overline{x^2(t)}^2 = 2\overline{x^2(t)}^2 C^2(s), \tag{9}$$

where $C(s)$ is the auto-correlation coefficient of $x(t)$ defined by Eq.(4) with $s=v_1-v_2$. Now, here we consider the fluctuation index of the second order, α_2, of Eq.(5). The concrete expression of α_2 for $A(t)$ is realized as follows by substituting Eqs.(7), (8), and (9) into the definition of Eq.(5):

$$\alpha_2 = \frac{\overline{(A(t)-\overline{A(t)})^2}}{\overline{A(t)}^2} = \frac{\overline{A^2(t)} - \overline{A(t)}^2}{\overline{A(t)}^2} = 2\int_0^\infty \int_0^\infty C^2(s)f(v_1)f(v_2)dv_1dv_2. \tag{10}$$

Further considering $s=v_1-v_2$, Eq.(10) can be rewritten as follows:

$$\alpha_2 = 2\int_0^\infty \int_{-\infty}^{v_1} C^2(s)f(v_1)f(v_1-s)dsdv_1. \tag{11}$$

Now, let τ_0 be the time constant of the input signal, $x(t)$. Here, we assume the following conditions:

$$\text{(i)} \ \tau \gg \tau_0, \quad \text{(ii)} \ C(s)=0 \ \text{when} \ |s| > \delta \gg \tau_0. \tag{12}$$

Then, it can be said that the attenuation of $f(t)$ is slow under the condition of $\tau \gg \tau_0$ when s is small, and thus $f(v_1-s)$ can be approximated well by $f(v_1)$. Then, Eq.(11) becomes as:

$$\alpha_2 = 2\int_0^\infty f^2(v_1)\int_{-\infty}^{v_1} C^2(s)dsdv_1. \tag{13}$$

Next, by considering $C(s)=0$ when $|s| > \delta$ and $\delta \ll \infty$, one obtains:

$$\int_0^\infty f^2(v_1)\int_{-\infty}^{v_1} C^2(s)dsdv_1 \cong \int_0^\infty f^2(v_1)dv_1\int_{-\delta}^{\delta} C^2(s)ds. \tag{14}$$

Then, replacing the integral interval of s: $-\delta \to \delta$ by s: $-\infty \to \infty$ (because $C(s)=0$ when $|s| > \delta$), one obtains the final expression of α_2 as:

$$\alpha_2 = 2 \int_0^\infty f^2(v_1)dv_1 \int_{-\infty}^\infty C^2(s)ds = \frac{2}{\tau} \int_0^\infty C^2(s)ds. \qquad (15)$$

Here, we have used the relation, $C(s)=C(-s)$.

2.3 Fluctuation Index for the Output, $B_T(t)$, Linearly Averaged   The
first and the second order moments of $B_T(t)$ in Fig.2 are given by:

$$\overline{B_T(t)} = \frac{1}{T} \int_0^T \overline{x^2(t-v)}dv = \overline{x^2(t)} \frac{1}{T} \int_0^T dv = \overline{x^2(t)} \qquad (16)$$

$$\overline{B_T^2(t)} = \frac{1}{T^2} \int_0^T \int_0^T \overline{x^2(t-v_1)x^2(t-v_2)}dv_1 dv_2. \qquad (17)$$

In the same way as we derived Eq.(11), the fluctuation index of the second order , α_2', for $B_T(t)$ becomes:

$$\alpha_2' = \frac{\overline{B_T^2(t)} - \overline{B_T(t)}^2}{\overline{B_T(t)}^2} = \frac{\frac{1}{T^2} \int_0^T \int_0^T \left\{ \overline{x^2(t-v_1)x^2(t-v_2)} - \overline{x^2(t)}^2 \right\}dv_1 dv_2}{\overline{x^2(t)}^2}$$

$$= \frac{2}{T^2} \int_0^T \int_{-v_1}^{T-v_1} C^2(s)ds dv_1. \qquad (18)$$

Now, here we also assume the similar condition as Eq.(12) as follows:

$$\text{(i) } T \gg \tau_0, \text{ (ii) } C(s)=0 \text{ when } |s| > \delta \gg \tau_0. \qquad (19)$$

If $T \gg \delta$ then we have:

$$\int_0^T \int_{-v_1}^{T-v_1} C^2(s)ds dv_1 \cong \int_0^T dv_1 \int_{-\delta}^\delta C^2(s)ds. \qquad (20)$$

Thus, Eq.(18) becomes as follows:

$$\alpha_2' = \frac{2}{T^2} \int_0^T dv_1 \int_{-\delta}^\delta C^2(s)ds. \qquad (21)$$

Next, replacing the integral interval of s: $-\delta \to \delta$ by s: $-\infty \to \infty$, one obtains the final expression of α_2' as:

$$\alpha_2' = \frac{2}{T^2} \int_0^T dv_1 \int_{-\infty}^{\infty} C^2(s)ds = \frac{4}{T} \int_0^{\infty} C^2(s)ds. \tag{22}$$

2.4 Relationship between Two Type Time Constants In consideration of the equivalency of the fluctuation index of the second order between $A(t)$ and $B_T(t)$, the following relation concerning time constant can be easily obtained by putting $\alpha_2 = \alpha_2'$:

$$T = 2\tau. \tag{23}$$

As for the higher order fluctuation indices than the second order, they are calculated as follows, e.g., for $n=3$ and 4:

$$\alpha_3 = \frac{8}{3\tau^2} \int_{-\infty}^{\infty} \int_{-\infty}^{\infty} C(s_1)C(s_2)C(s_2-s_1)ds_1ds_2 \tag{24}$$

$$\alpha_4 = \frac{12}{\tau^2} \left(\int_0^{\infty} C^2(s)ds \right)^2 + \frac{12}{\tau^3} \int_{-\infty}^{\infty} \int_{-\infty}^{\infty} \int_{-\infty}^{\infty} C(s_1)C(s_2)C(s_3-s_2)C(s_3-s_1)ds_1ds_2ds_3 \tag{25}$$

and

$$\alpha_3' = \frac{8}{T^2} \int_{-\infty}^{\infty} \int_{-\infty}^{\infty} C(s_1)C(s_2)C(s_2-s_1)ds_1ds_2 \tag{26}$$

$$\alpha_4' = \frac{48}{T^2} \left(\int_0^{\infty} C^2(s)ds \right)^2 + \frac{48}{T^3} \int_{-\infty}^{\infty} \int_{-\infty}^{\infty} \int_{-\infty}^{\infty} C(s_1)C(s_2)C(s_3-s_2)C(s_3-s_1)ds_1ds_2ds_3. \tag{27}$$

Page limitations preclude an inclusion of their detailed calculation processes. Now, by putting $\alpha_3 = \alpha_3'$ and $\alpha_4 = \alpha_4'$, one obtains the following new relationship between τ and T:

$$T = \sqrt{3}\,\tau \tag{28}$$

and

$$\sqrt[3]{4}\,\tau \leq T \leq 2\tau. \tag{29}$$

3.0 EXPERIMENTAL CONSIDERATIONS

In order to confirm the effectiveness of the present theory, it has been applied to several types of the actual input-output sound data, and their fluctuation indices have been

Table I.

Fluctuation index $\left(\sqrt[n]{\alpha_n}, \sqrt[n]{\alpha_n'}\right)$ for a classic music (Slow Mode; $\tau=1.064(\text{sec})$).

Averaging Operation	Time Constant	Fluctuation Index		
		n=2	n=3	n=4
Exponential Type	τ	0.4978	0.5327	0.7601
Linear Type	2τ	0.5076	0.5028	0.7173
	$\sqrt{3}\,\tau$	0.5236	0.5307	0.7520
	$\sqrt[3]{4}\,\tau$	0.5330	0.5480	0.7740

Table II.

Fluctuation index $\left(\sqrt[n]{\alpha_n}, \sqrt[n]{\alpha_n'}\right)$ for a classic music (Fast Mode; $\tau=0.125(\text{sec})$).

Averaging Operation	Time Constant	Fluctuation Index		
		n=2	n=3	n=4
Exponential Type	τ	0.7029	1.084	1.694
Linear Type	2τ	0.7382	1.066	1.589
	$\sqrt{3}\,\tau$	0.7600	1.119	1.685
	$\sqrt[3]{4}\,\tau$	0.7732	1.153	1.749

Table III.

Fluctuation index $\left(\sqrt[n]{\alpha_n}, \sqrt[n]{\alpha_n'}\right)$ for a traffic noise (Slow Mode; $\tau=1.064(\text{sec})$).

Averaging Operation	Time Constant	Fluctuation Index		
		n=2	n=3	n=4
Exponential Type	τ	0.4318	0.3731	0.5845
Linear Type	2τ	0.4551	0.3197	0.5668
	$\sqrt{3}\,\tau$	0.4693	0.3585	0.5949
	$\sqrt[3]{4}\,\tau$	0.4782	0.3824	0.6138

Table IV.

Fluctuation index $\left(\sqrt[n]{\overline{\alpha_n}}, \sqrt[n]{\alpha'_n}\right)$ for a traffic noise (Fast Mode; $\tau=0.125(\text{sec})$).

Averaging Operation	Time Constant	Fluctuation Index		
		n=2	n=3	n=4
Exponential Type	τ	0.5786	0.6891	0.9479
Linear Type	2τ	0.6274	0.7081	0.9773
	$\sqrt{3}\tau$	0.6418	0.7322	1.007
	$\sqrt[3]{4}\tau$	0.6509	0.7479	1.028

calculated. Concretely, for example, a classic music or a traffic noise recorded on a data recorder in advance is played in the reverberation room. The diffused sound of the input signal has been measured by a sound level meter. These measurement sound data have been converted to energy-scaled data, and then the fluctuation indices of $n=2,3$, and 4 have been calculated for these energy-scaled data. The results are shown in Tables I-IV. It is observed that these results are well consistent with the theory.

4.0 CONCLUSIONS

In this paper, in order to evaluate the stochastic characteristics of the fluctuation pattern of signal, a new concept of fluctuation index has been first proposed. Then, the mutual relationship between two types of time constants of the measuring instruments has been discussed theoretically based on this fluctuation index. The effectiveness of the present theory has been confirmed experimentally too by applying it to the actual sound data.

ACKNOWLEDGMENT

REFERENCES

Hassall J.R. and Zaveri K., *Acoustic Noise Measurements*, Brüel & Kjær, Nærum, 1979.
Maybeck P.S., *Stochastic Models, Estimation, and Control Volume 1*, Academic Press, New York, 1979.
Acoustic Measurements According to ISO Standards and Recommendations, Brüel & Kjær, Nærum.

The Sydney & Brisbane Noise Terminals

A. D. Wallis (1) & R. W. Krug (2)

1.   Cirrus Research Ltd. Acoustic House, Hunmanby UK.

2.   Cirrus Research Inc. Wauwatosa, Wisconsin, USA.

1 Introduction

In 1989, the decision was taken by the Civil Aviation Authority of Australia, to upgrade the noise monitoring system at Kingsford Smith International Airport in Sydney and install a noise monitor in Brisbane.

The system was to interface with the existing secondary radars to generate flight track information to correlate with the noise data and provide a database for the noise data as well as the complaints from the public. Additionally, staff at Canberra must be able to run the system remotely and data from the host computer had to be available at various locations other

than the individual airports.

The system chosen was the Cirrus Adacel CA1000 which not only fulfilled all the tender technical requirements, the only system offered which did this, but also could provide recognition of the aircraft events even when radar data was not available. The NMT used in the CA1000 is a linear development of the Short Leq technique described elsewhere by Wallis and Holding and while new code had to be written for the UNIX operating system and some modifications made to the radar software, the techniques used follow closely the original work on data storage.

New noise monitoring terminals, already under development under a United Kingdom Small Firms Merit Award for Research and Technology (SMART) grant were able to be used, almost unmodified, for this application. These new terminals, Cirrus Research type CRL 243 were specified to operate for 7 days, storing raw Short Leq data every second, with storage for 7000 recognised aircraft plus a large number of environmental data sets which could be taken at various intervals from 5 minutes up to 24 hours. The most important feature however of the new terminals is that they were designed to be configured 'on the fly' by the operator to carry out far more functions than any one installation would need. Thus, the same terminals used for this application can also be used elsewhere, for example at small feeder airports, without having to be modified for this use. It would only be the external program which would have to be modified.

2 The System overview

As 'new technology' was to be the keynote of the system, the whole system is geared round a host computer, which takes data from either a communications computer or the terminals themselves. Data is also available from the radar which gives the flight number from the decoded 'Squawk' or IFF transmission from the aircraft with its positional information as in fig.1

The system can operate with as many Noise monitoring terminals (NMT) desired, but common sense would seem to suggest that no-one would use more than 50 or so. However, one manufacturer makes much play of the

fact his system can handle 99 terminals, so a limit was set of 100 NMT per system. While this may seem a ridiculous number, commercial pressure force such decisions. At Sydney, the initial installation was 8 heads, with 4 at Brisbane, these numbers being typical of the smaller International airport installation.

The communications processor handles all the communication with the NMT, the radar and any weather station connected, although at both Brisbane and Sydney the weather option was not needed. The weather data normally available in the system includes:-
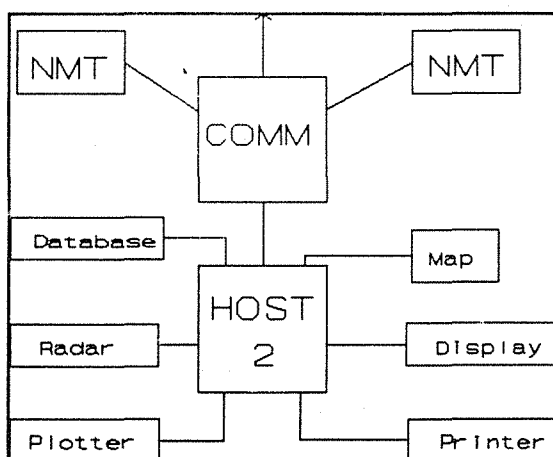
Figure 1 System outline

Wind Direction and Speed
Humidity
Air and Ground temperature
Precipitation
Radiation
Atmospheric pressure

These functions mean that not only can the aircraft noise levels be recognised and measured, but they can also be correlated with the weather data to carry out propagation prediction or other related tasks.

Each NMT can operate via 'dial up' lines or dedicated 'tie' lines, the only operating difference being in the real time functions available. At Sydney and Brisbane, permanent tie lines are used and each NMT sends each 1 second Leq value as it is calculated, for use with a real time map display located wherever the CAA might wish; as well as on the host computer screen. The 1 second Short Leq data can also be used for back-up storage on the hosts hard disk. Additionally, each NMT can be switched to allow the remote operator to hear the actual noise of the 'event' to ensure that it is an aircraft that is being recognized and not some other unrelated event. The audio system also means that there is telephone connection between the NMT and the host computer to allow voice communication for fault finding

etc.

3 The NMT.

The design of the NMT follows closely the Short Leq system described by Wallis and Luquet. The NMT has a dynamic span of over 110 dB and thus there is no auto-ranging required with the corresponding loss of data. The raw data, which is generated by totally analogue means, is acquired as 1/16th second Short Leq elements, which are used in several ways.

The 62.5 mS data is fed to an 'S' converter previously described by Krug which generates the 'S' or slow response as given by an exponential sound level meter to IEC 651 type 1 accuracy. This is done to allow the Ln series to be calculated as many people prefer this to be computed from the 'S' response rather than the more logical raw Short Leq data. The original Short Leq element was 1/8th Second to match the 'F' response, but changing to 1/16th second gives the 'S' response well inside the tolerances of IEC 651 type 1 rather than right on the tolerance limit. Naturally, the 1/8th second data can be provided by concatenation if required.

The raw 16th second data also feeds the recognition algorithm, which in the Sydney and Brisbane units is a fairly simple dual threshold and guard algorithm described by Stollery. Normally the NMT has provision for much more complex recognition parameters, but it was felt that as radar data was available and the new algorithms were untried, that simplicity should be the keynote. In the event, the simple approach allowed the whole system to be assembled in Australia, installed and commissioned well inside the allotted schedule.

All recognised aircraft events are stored in an 'event' store which can hold up to 7000 events with the following typical parameters.

Time,
Max level,
SEL
Leq,

Threshold data, Duration

The time is used not only to time stamp the event, but to allow the host to use this as a pointer to the raw data in memory so that any suspect recognition can be recovered from the NMT at any time in the next 7 days. After this, unless data has been transferred to the host, the data is automatically overwritten.
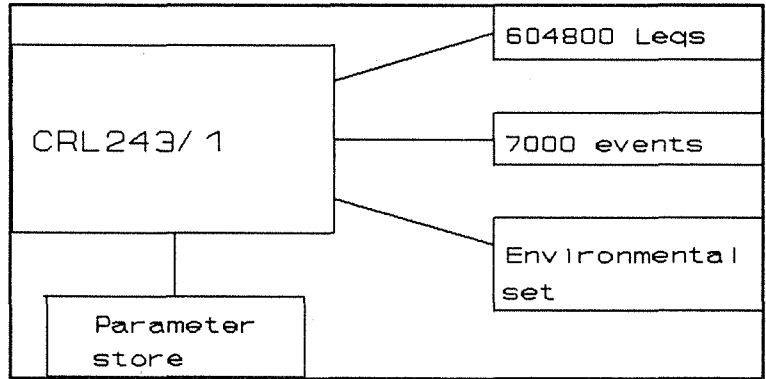
Figure 2 NMT storage

All stores in the unit are automatically overwritten when full, but with 7000 events stored, there is little danger of losing valuable information. As an aside, the storage capacity of the Sydney and Brisbane systems is the minimum available on the system. For other sites, the memory capacity can be increased by four times allowing 28,000 events and 1 month of 1 s time history data with suitable environmental storage for the site. These memory sizes, while being today considered large will probably be seen as ridiculously small in a very short time. At ICA in 1983 when a 44k memory was proposed for such use by Cirrus Research, it was ridiculed as 'overkill'; how strange this seems today, only 8 years later.

4 New features

While the NMT described has greater storage capacity than any previous device, this in itself is a simple engineering progression, not meriting special attention. However, it is in the more unusual features that the new NMT shows how technology has advanced. The main new feature of the NMT is the ability to store its own configuration in an EEPROM. This device, a none-volatile storage medium, can be written
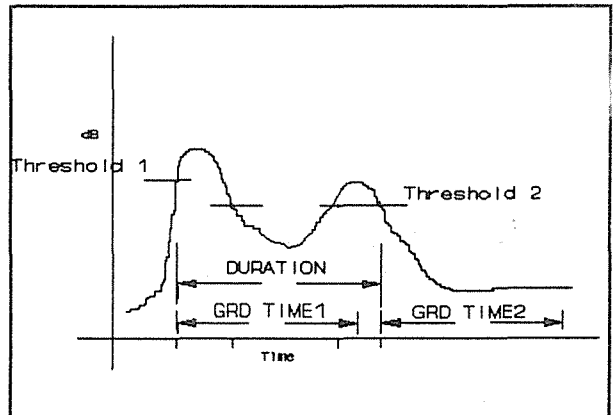
Figure 3 Event detection parameters

to in-situ and re-programmed with a different set of data. The device is truly none-volatile in that it does not lose its data even with no power applied, thus there is no need for back-up batteries to keep the data. This technique, first described by Krug for use in a dosimeter is ideal for such applications.

In the CRL 243, the EEPROM is used to store data which change the measurement function. Typically, various templates, algorithms and functions are sent to the unit from the host and these can change the total measurement set. For example, the environmental data stored has typically 10 parameters. These can be almost any metrics as desired by the user. For example, the user may require the following as his environmental block.

Block start time
L1,
L10,
L50,
L90,
L99,
Lmax,
Leq,
Time of Max

At some other time, totally different parameters may be needed. This data is sent to the NMT from the host and these parameters will remain until changed again by the operator. In the same way, the calibration routine, the event recognition parameters, the mode of transmission and many other obvious parameters can be selected by the user and sent to the NMT.

In the present systems, the parameters of recognition are shown in fig 3 and while very simple, provide a very good 'hit rate' of recognised events. While these are the only parameters used today, the system can be re-configured to have many more template parameters simply by changing the system ROM, a two minute field operation. It is to be expected that as experience is gained with the system, the users will request different types of template and these can be provided with little problem.

5 Raw Data

Many publications have detailed the ability of Short Leq devices to present acoustic data in a form not available before computerization and the new NMT can send standard Short Leq data in the form already established.

Fig 4 shows a plot from the suite Acoustic Editor, downloaded from an NMT at Sydney airport during installation, using the pointer in the event data. Such plots can be automatically sent from the NMT to the host so that even checking on the NMT recognition performance can be done automatically.
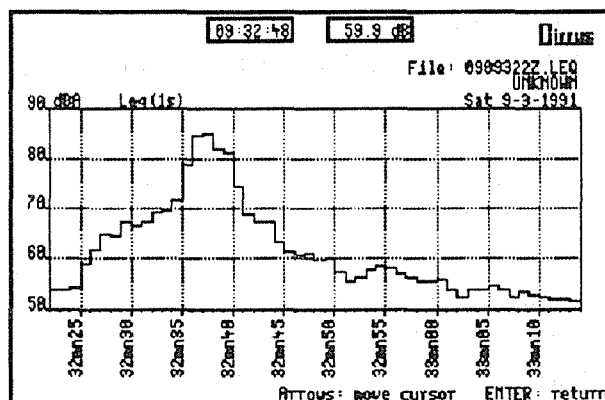
Figure 4   An Aircraft event

The simple DOS program normally provided at feeder airports indeed does this automatically and transparently to the operator.

6 Data provided.

The data-base of the new system is particularly impressive. Using as its engine the Informix system, it can give correlation of the noise in many ways and provide automatic reports for use by the CAA. Complaints on noise from the public are handled automatically, the complainants post code being used to generate automatic letters reporting on the probable noise which caused the complaint.

Individual aircraft can be identified by type and by carrier and the system can list noise infringements by these fields. Additionally, any flight track, noise level or other statistical data can be recalled for one year from the computers hard disk, but indefinitely using the data stored on the back-up tape. Thus, data can be taken from the store and used for future research into the complex relationships between noise and other functions. Indeed the data storage aspect of the system allows any event to be recalled at any time in the future. Thus if a penalty system is imposed, the airline operator can be provided with the raw data in the form of time histories matched to the radar

data giving the movement information.

7 Summary

Using Short Leq technology a system has been designed that can provide noise data well in excess of the older systems currently installed at many airports, many on main frame computers.

Based on simple 80386 desk-top computer, the very inexpensive noise monitoring system installed at these two airports has given a noise measurement capability almost un-imaginable a decade ago.

The data base incorporated gives automatic outputs to allow the system to generate reports in almost any format desired, yet gives a security level far in excess of other contemporary designs.

While the system was foreshadowed in early work on Short Leq its realization required intense cooperation between the two companies involved in the system design.

References

Krug R. W.   'Dosimeter interfacing using the DP37 interface'
Proceedings Internoise   1986 Boston, USA   pp 1351 -1356

Stollery C. P   'Aircraft event recognition algorithms implemented in a simple microprocessor'
To be published Proceedings Internoise 1991 Sydney, Australia

Wallis A.D. & Holding J.M   . 'A method of generating Short Leq'.
Proceedings Internoise 1984 Honolulu,   USA   pp 1039-1042

Wallis A.D. & Luquet P.J   'Computer Acquisition of large data sets'
Proceedings Internoise 1987 Beijing, China   pp 1423-1426

ACOUSTIC AND VIBRATIONAL RESEARCH TECHNIQUES ON HYDRAULIC COMPONENTS

E.Carletti, G.Miccoli, I.Vecchi
Earth-Moving Machinery and Off-Road Vehicle Institute -
CEMOTER - National Research Council of Italy
via Canal Bianco, 28 - 44044 Cassana (Ferrara) - Italy

ABSTRACT

The application of acoustic and vibrational research techniques to external gear pumps is explained, our attention being focused on:
a) sound power level, sound pressure, sound intensity and structural vibration measurements that allow a description of acoustic and vibrational fields due to complex sources both in space and time;
b) pump fluidborne noise and internal flow losses evaluation with a test procedure based on the use of the anechoic system and the measurement of the source characteristic impedance;
c) assessment of pump actual operating features, i.e. internal pressure distribution, as input data to finite element model computation of casing stress distribution and consequent structural modifications.
The sensitivity of these techniques has been considered for a noise optimisation procedure and the achievement of the best trade-off between acoustic and functional performances.

1.0 INTRODUCTION

The main causes of gear pump noise emission can be summarized as tangential and radial tooth deflections, oil and air jets occurring during the engagement cycle.

The above events produce noise at the gear meshing frequency. Moreover, when the gear itself acts as an acoustical radiator, the radiation from gear arises. The amount of this radiated noise depends on the relationship between the excitation frequencies and the gear wheel natural frequencies.

In summary, pressure fluctuations and cavitation effects generate fluidborne noise; eccentricity or imbalance of rotating parts, as well as vibrations of structural parts, generate structureborne noise; and structural vibrations interact with the surrounding air causing airpressure fluctuations, i.e. airborne noise.

These three forms of noise are correlated by the dynamic characteristics of the system and the acoustic coupling between vibrating surfaces and surrounding medium.

In the paper a gear pump case study is presented. The airborne noise and the pump fluidborne noise are primarily considered owing to their leading positions.

2.0 PUMP AIRBORNE NOISE EVALUATION

Noise influence of the following design parameters was evaluated to "optimize" noise emission of a 9 tooth gear pump:
1) type of gear set (the same geometry and tooth number, but different material and treatments);
2) type of bearing blocks.

Considering standard configuration and varying the two parameters above, noise pump emission was determined at different values of discharge pressure, by the following intensity based analysis:
1) sound power calculation;
2) near field sound pressure and intensity measurements around the pump casing;
3) vibration measurements.

2.1 Procedures

The basic instrumentation consisted of a B&K 3360 analyzer equipped with 1/4" and 1/2" microphone intensity probes and 4393 delta shear piezoelectric accelerometer (for vibration tests). An H&P computer, running dedicated software packages, supervised measurements and subsequent data processing.

As the influence of gear set type on sound emission is concerned, detailed results are reported in the reference paper (Carletti E.).

After having equipped the pump with the "optimal" gear set, the comparison between two couples of improved bearing blocks a and b, specifically designed to limit fluid pressure transients at gear meshing, was carried out.

* Sound power – Sound power level was derived from intensity measurements on a suitable surface enclosing the pump. Contributions of all intensity components normal to the surface were merged into the overall sound power spectrum.

Bearing block b showed average sound pressure level 3 dB lower than the corresponding bearing block a. This datum, giving only a global evaluation of noise emission, is necessary to check whether acoustic performances lie within specified limits, but is completely insufficient to understand the origin of acoustic phenomena generation.

* Intensity maps – Near field normal intensity values were measured on an equally spaced point grid of a plane parallel to each face of the pump. In order to concentrate on effects due to the pump only, all frequencies related to the drive shaft dynamics were excluded during data processing. The same procedure was repeated for sound pressure measurements, while vibration data were carried out by stud mounting the accelerometer to the pump casing upper face.

Fig.1 compares the casing velocity maps with near field sound pressure and intensity maps, obtained on a surface parallel to the pump upper face at 200 Hz frequency and 100 bar working pressure.

The analogy between pressure level distribution and vibration pattern confirms the good fitting of structural vibratory behaviour of a surface with wave phenomenon

Fig.1 – Maps at 200 Hz. S=suction, D=discharge

near the surface itself. The effect of the increasing of the high pressure region along the gear enclosure is represented with an erratic velocity distribution of maxima and minima for the a couple of bearing blocks. An acoustical energy "sink" appears at the supply region for case b, being intensity, pressure and casing velocity values always lower for this couple of bearing blocks.

* Gating spectra – Intensity spectra were recorded for thirty adjacent windows along the shaft revolution, each spectrum being the acoustical contri-

Fig.2 – Gated spectra within 200-8000 Hz frequency range.

bution corresponding to a different portion of revolution. For each pump configuration and discharge pressure,the intensity probe was placed over the middle of the pump upper face at a distance such as the global emission from all the surfaces of the pump could be collected. A fixed optical probe, facing the shaft, controlled the analyzer averaging process at different points of the gear revolution. The same procedure was applied for casing velocity measurements (Fig.2).

Levels at meshing frequency (220 Hz) and first harmonic are dominant. For set b these levels are relatively constant throughout the cycle, while for set a strong discontinuities can be observed either in intensity or vibration levels, both at the same angular position.

3.0 PUMP FLUIDBORNE NOISE EVALUATION

A test procedure, based on the use of the anechoic system, allows the assessment of pump source flow and equivalent source impedance. These are two fundamental complex quantities for pump noise potential evaluation, their product determining the pressure ripple along the circuit and so the main vibration source on components and connecting pipelines.

The test method characterizes entirely a pump as to its hydraulic noise. As a matter of fact, it provides the knowledge of the pump flow ripple at entry to delivery line, i.e. the pump fluidborne noise, and that of the pump internal flow losses, making the impedance a pump noise evaluation parameter.

3.1 Procedures

The reflectionless delivery line was made by a variable capacity with an adjustable diaphragm at its entrance (Fig.3). Both impedance and source flow were derived from measurements of ripples occurring when two different diameter pipes act as independent impedance values at the pump outlet port.

Fig.3 - Schematic diagram of the experimental set-up.

The harmonic analysis of pressure ripples was carried out with a digital frequency response analyzer while the complex data reduction was performed on a mainframe computer to obtain the source impedance and the flow ripple.

The reliability of the test procedure has been proved at various operating conditions on 11 gear pumps, different as displacement and gear tooth number (Miccoli G.).

Verified, moreover, the sensitivity of the method to source impedance and pump flow ripple variations for different geometry pump components, the fluidborne noise optimi-

sation of the gear pump has been carried out, adopting the relief grooves size as design parameter. Fig.4 shows the drawing of both A and B bearing blocks, being the distance d between the edge of the suction relief grooves and the symmetry axis of the bearing block A 0.8 mm shorter.

The classic plane wave transmission equation, describing the form of the complex standing wave in the circuit and the pressure ripple at any point, can be considerably simplified if the circuit is so arranged that the pump is discharging into an acoustically reflectionless delivery line and the pressure ripple is measured close to the pump outlet. Once the pump internal impedance and its ideal flow have been determined, such an anechoic system provides a useful means of knowing the pump flow ripple at entry to delivery line and the pump internal flow losses, simply by pressure ripple measurements (Fielding D.).

Fig.4 - Bearing blocks drawing.

The circuit reflectionless condition, main parameter for the accuracy of the results, was obtained adjusting the diaphragm with regard to the loading pressure and comparing the waveforms of the pressure signal at three different points of the delivery line (Fig.3), so making the value of the termination impedance and that of the pipe the same.

A typical behavior of the source impedance (Fig.5) is very close to the theoretical one (Edge K.A.), showing an anti-resonance between 1 kHz and 2 kHz, meshing frequency being about 220 Hz, with a phase change from -90° to positive values. Pump ideal flow ripple (Fig.6) turns out from the sum, magnitude and phase, of the actual flow ripple and the internal flow losses.

Fig.5 - Source impedance Zs
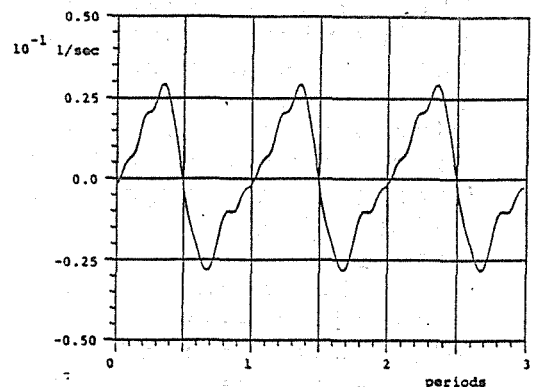
Fig.6 - Ideal flow ripple Qs

A comparison (Fig.7) among the hydraulic noise characteristics for the pump with different couples of relief grooves shows that bearing blocks A increase the pump leakage flow Q_l, without necessarily lowering the actual flow ripple Q_e, measure of the pump fluidborne noise. The difference between the behaviors of the pump ideal flow rate Q_s is due to the fact that they depend on both Q_e and Q_l and also on their phase opposition, better for relief grooves B.
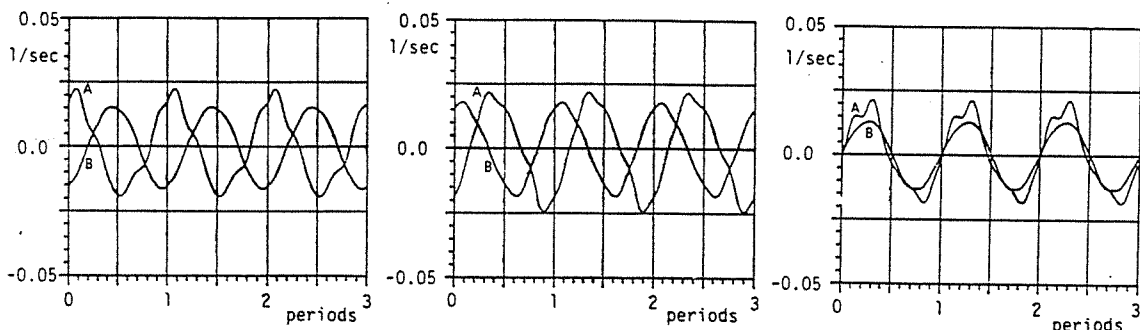
Fig.7 - Bearing block Ql, Qe, Qs flow ripples comparison.

Moreover, experimental data confirmed impedance mean-
ing, a greater source value vs. harmonics pointing out a
lower pump leakage flow. A value of airborne noise 3 dB(A)
lower for grooves B, at test loading pressure, emphasized
result accuracy.

4.0 PUMP STRUCTURAL ANALYSES

Both experimental and theoretical techniques have been used
to obtain a detailed description of the cyclic loads and
forces acting on the stationary pump casing and rotating
gears. Their knowledge, together with that of the overall
dynamic equilibrium conditions, are prerequisite for the de-
velopment of a general structural analysis of the external
gear pump.
    An experimental procedure with relevant computation
steps has been carried out to describe the pump internal
pressure behavior and the consequent gear load distribution.
    A comprehensive representation of the pump casing
stresses has been obtained with a 2-D finite element analy-
sis, comparing the response to some reference pressure dis-
tributions with that for actual pump operating characteris-
tics (Miccoli G.).

4.1 Procedures

A set of experimental data about the gear pump internal
pressure history has been recorded with a piezoelectric
transducer fixed inside the driving gear shaft and communi-
cating with a tooth vane. That solution provides a knowledge
of the pressure distribution not only on the casing inner
surface but also inside the meshing zone and trapped volume.
In such a way, the analysis of pressure loads on gears is
exhaustive and a precise calculation of radial resultants on
these possible.
    For all different operating conditions, the pump had a
pipe with anechoic termination as external load, such as
that described above. The use of a reflectionless system is
due to the fact that the analysis of the pump operating fea-
tures must be carried out without introducing the effect of
any external unwanted influences on the measured quantities.
    Fig.8 shows a typical behavior of the pump internal
pressure ripple corresponding to a gear shaft revolution. In

505

a vane between contiguous teeth, during fluid transfer from suction to delivery port, the pressure rises quickly from zero to delivery value. Fluid compression phenomenon for the trapped volume is represented with the maximum pressure peak corresponding to the two gear meshing angular positions. The following pressure drop occurs when trapped volume opens to suction.

The above actual pump operating features as input data allow the computation of radial load resultants on the gears.

Fig.9 is an example of the final output of the computer program on purpose worked out.

For the 2-D finite element analysis, the ANSYS code has been used. The non-linear contact between pump structure and bearing blocks has been simulated by means of a shaped rigid surface on the inner inlet side of the casing or with a finite element model of the bearing blocks, using 2-D interface elements. This second kind of solution gives a geometric configuration close as much as possible to the real one and allows to follow the deformation of the contacting surfaces.

Among the main results, the good analogy between very local stress concentration points, suggesting the possibility of fatigue crack propagation lines, and the actual fatigue failures of this type on some strain aged pumps.

Moreover, the radial resultant on the gear shaft, corresponding in our model to the reactions at the traslational constraints on the bearing block, is in very good agreement with that directly computed from the experimental results, when taking into account the absence of contact force between meshing teeth. Fig.10 represents the pump stress behavior using the real pressure distribution from experimental data and the finite element model

Fig.8 - Pump pressure time history. Loading pressure: 50 bar.
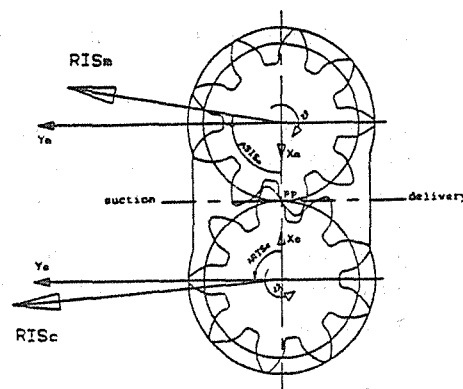
Fig.9 - Resultant forces on the gear shafts and angles. RISc,ARISc:driven gear. RISm, ARISm:driving gear.
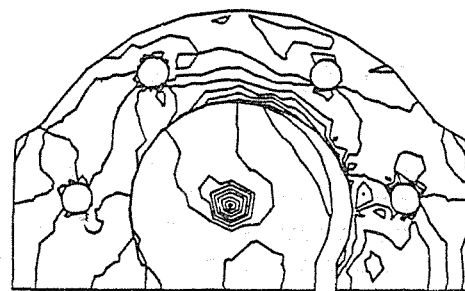
Fig.10 - Equivalent Von Mises stress distribution Real pressure with bearing block FE model. Nine equally spaced contour lines.

of the bearing blocks. The error in both angle and magnitude evaluation is maintained within a few percent.

5.0 CONCLUSIONS

Complementing the usual single title of merit (sound power) with multiple titles (intensity maps, gating spectra and vibration measurements) gives effective and precise ways of evaluating each design parameters in terms of minimum noise emission.

The test method for assessing fluidborne noise, being very sensitive to pump structural modifications, proved to be the basic tool for a noise optimisation procedure and the achievement of the best trade-off between acoustic and functional performances.

Numeric simulation in order to evaluate the component quality at design stage together with experimental procedure allowed the computation of pump casing stress distribution, starting from pump internal pressure actual behavior, with consequent possibility of structural modifications.

REFERENCES

Carletti E., Vecchi I., Acoustic Control of External Gear Pumps by Intensity Measuring Techniques, Noise Control Engineering Journal, 35(2), 53-59, (1990).

Miccoli G., Bragion A., Gear Pump Fluidborne Noise by Source Flow and Impedance Evaluation, Noise-Con 88, 487-492, West Lafayette, Indiana, 1988.

Fielding D., Taylor R., Martin M., Foster K., Notes on the Selection of a Standard Delivery Condition for the Theoretical Prediction and Experimental Measurement of Pressure Ripple, 5th Int. Fluid Power Symposium, Paper F1, Durham, England, 1978.

Edge K.A., Johnston D.N., A New Method for Evaluating the Fluidborne Noise Characteristics of Positive Displacement Pumps, 7th Int. Fluid Power Symposium, 253-260, Bath, England, 1986.

Miccoli G., Paoluzzi R., Computer Aided Analysis of the Gear Pump Casing, 3rd Bath Int. Fluid Power Workshop, Bath, England, 1990.

REAL-WORLD ATTENUATION OF HEARING PROTECTORS

David Eden
Principal, Eden Dynamics Pty Ltd.

Ray Piesse
Acoustic Consultant, Eden Dynamics Pty Ltd

ABSTRACT

The performance of personal hearing protectors, earmuffs and earplugs, appears to be much less in the field than laboratory test results indicate. In this paper, overseas laboratory data is compared with Australian laboratory data. It is seen that the Australian laboratory data is closer to the "real-world" performance than test figures obtained in USA laboratories. The different test methodologies explain some of the differences. The Australian Standard 1269 "Hearing Conservation" should give slightly better performances than the results obtained if protectors were tested in accordance with Australian Standard 1270 "Hearing Protection Devices".

Differences expressed as Sound Level Conversion or SLC_{80} values between "real-world" and laboratory performances of hearing protectors are set out. The "real-world" performance for earplugs is estimated to be up to 9 dB less than the laboratory SLC_{80} when tested in accordance with AS 1270. The "real-world" performance of earmuffs is likely to be 6 dB less than the performance obtained in laboratory tests to AS 1270.

The effectiveness of hearing protectors is decreased when they are not worn all the time. A table showing the performance of a protector when it is not worn all the time is included.

508

1.0 INTRODUCTION

The attenuation of hearing protectors, when measured in Australian laboratories in accordance with Australian practice, can be achieved in the workplace provided there is an effective hearing conservation program in place that implements all the requirements of AS 1269 "Acoustics – Hearing Conservation." In other situations, common in the real-world, the attenuation of earmuffs and earplugs will be reduced and therefore the hearing protection will not be as effective.

2.0 EXPERIMENTAL EVIDENCE

There are a number of reports which show that the effective attenuation of hearing protectors as worn in the workplace, or their real-world performance, is significantly less than estimated by laboratory measurements. These reports which included data from 50 different industrial plants and 1551 hearing protector users, were summarised by E H Berger of E.A.R Division, Cabot Corporation USA and the results published in a report entitled "Using the NRR to Estimate the Real-World Performance of Hearing Protectors" in Sound & Vibration, January 1983. The differences between the USA laboratory and real-world measurements of attenuation of earmuffs and the most commonly used types of earplugs taken from this report and presented as SLC_{80} values are given in the following Table 1.

TABLE 1 – DIFFERENCES BETWEEN USA LABORATORY AND REAL-WORLD ATTENUATIONS OF HEARING PROTECTORS

PROTECTOR TYPE	LABORATORY ATTENUATION SLC_{80}	REAL-WORLD ATTENUATION SLC_{80}	DIFFERENCE
Earmuffs (209 subjects)	30	17	13
Foam Earplugs (280 subjects)	34	14	20
Pre-fabricated Earplugs (217 subjects)	27	6	21

The results for the real-world attenuation of hearing protectors given in Table 1 are apparently representative of the performances obtained in the workplaces where hearing conservation programs have been poorly implemented and supported although there is a suggestion that the results may be biased towards over-estimating typical real-world performance.

It has been known for some time that laboratory hearing protector tests carried out in the USA where Berger's work was done showed higher attenuation than those obtained in Australia where the results were thought to be closer to real-world performance. The difference is thought to be due to the different procedures employed in fitting the devices during the test of acoustic performance. In the USA it has been the practice to carefully fit, train and motivate subjects for the testing procedure whereas in Australia after the correct size of device is chosen for each subject, the subject is then asked to fit the protector in the presence of broad band noise in accordance with the manufacturers' instructions.

In an attempt to simulate what Berger describes as "achievable" use i.e. "that which can be obtained by a typical wearer who makes a conscientious effort to properly use the device in a manner consistent with a reasonable degree of comfort", he carried out measurements on earmuffs which were fitted by the subjects after they had read the manufacturers' instructions (called "Laboratory - Subject Fit"). The results of those tests which are taken from his paper "Can Real-World Hearing Protector Attenuation be Estimated Using Laboratory Data" published in Sound and Vibration December 1988, are shown in the following Table 2.

TABLE 2 - COMPARISON OF LABORATORY AND REAL-WORLD HEARING PROTECTOR ATTENUATION

PERFORMANCE MEASUREMENT	ATTENUATION SLC_{80}
Typical Laboratory (USA)	27
Laboratory-Subject fit (USA)	23
Real-world	17

No real-world data were available for the earmuffs tested in the typical laboratory and subject fit studies used to obtain the data given in Table 2. The results of these studies were therefore compared by Berger with the average real-world attenuation of many earmuff types given in Table 1. As Berger states in his paper "the difference between makes is usually smaller than the within device standard deviation across real-world users", the real-world data therefore "provide a useful (but certainly not conclusive) basis for comparison ...".

Since the fitting procedures employed in the subject fit tests carried out by Berger are similar to (but not the same as) those specified in Australian Standard 1270-1988 "Acoustics - Hearing Protectors" it is likely the tests carried out by the National Acoustic Laboratories (NAL) to the Australian Standard gave comparable results.

The data given in Table 2 therefore suggests that there is a possibility that the SLC_{80} value of the real-world performance of earmuffs in poorly defined hearing conservation programs is 6 dB less than the data published by NAL in Australia. The NAL performances can be regarded as achievable in a hearing conservation program conducted as described in Australian Standard 1269-1989 "Acoustics - Hearing Conservation". As pointed out above, the difference is not conclusive but tends to be supported by a difference of 6 dB between the average of the SLC_{80} values of all ear-muffs given in the sixth edition of "Attenuation of Hearing Protectors" published by NAL which is 23 dB and the real-world attenuation given by Berger.

It is also useful to note that the SLC_{80} values for earmuffs on which the real-world data was obtained (presented in Table 1) is greater than the value presented in Table 2 for the typical laboratory results. This suggests that the real-world performance reported by Berger has probably not been influenced by the use of a preponderance of poor performing earmuffs.

3.0 THE E.A.R. EARPLUG

In his report, Berger also examined the real-world performance of the E.A.R earplug as a particular brand of foam earplug and provides the results of these surveys. The SLC_{80} value was calculated for the best result of the three surveys and was found to be 13 dB.

The laboratory SLC_{80} value given in the NAL report for the hearing protector is 22 dB giving a difference between Australian laboratory test and real-world attenuation of 9 dB.

4.0 PERFORMANCE DECREASES WHEN NOT WORN ALL THE TIME

The above estimates of the difference between real-world and laboratory tests do not take into account "breaks" in wearing hearing protectors while being exposed to excessive noise. The effect of this has been calculated in terms of effective SLC_{80} values and is shown in Table 3. The method used for the calculations is based on the SLC_{80} definition. It is that calculation and rounding to whole decibels which gives the trivial 1 dB error (4 dB rather than 3 dB) for protectors worn 50% of the time.

TABLE 3 - EFFECT OF NOT WEARING HEARING PROTECTION FOR PART OF THE TIME EXPOSED TO NOISE

TIME NOT WORN	1%	5%	10%	50%
Nominal SLC_{80}	Effective SLC_{80}			
6	6	6	5	3
10	10	9	8	3
15	14	11	10	4
20	17	13	10	4
25	20	14	11	4
30	21	14	11	4

5.0 APPLICABILITY OF SLC_{80} VALUES

It should be noted that low values of SLC_{80} may often approach the C-A value for many noises where C and A are the noise levels in dB(C) and dB(A) respectively. In these cases the estimated in-ear noise levels are higher than they should be and more accurate results should be obtained by using octave band sound levels. Nevertheless the small figures have been included in Table 3 to indicate the significance of time corrections.

SLC_{80} values should not be used in calculations of in-ear noise levels in cases where the value is close to the C-A value. Care should be taken where SLC_{80} - (C-A) is less than 5 dB since this leads to estimated in-ear noise levels which are higher than they should be. The SLC_{80} calculation method can not be used where SLC_{80} - (C-A) is negative. In these cases, the in-ear noise levels should be calculated using octave band sound pressure levels.

6.0 FACTORS AFFECTING REAL-WORLD PERFORMANCE

The factors which affect the real-world performance of hearing protectors are best summarised in a book entitled "Noise and Hearing Conservation" Fourth Edition, published in 1986 by the American Industrial Hygiene Association. The summary is quoted as follows:

1) Comfort - This is ignored in laboratory tests but is crucial in the real-world.
2) Utilisation - Due to poor comfort, poor motivation or poor training, earplugs may be incorrectly inserted and earmuffs may be improperly adjusted.
3) Fit - Fitting and sizing of earplugs must be carefully accomplished for each ear. If they are not, performance will be degraded.
4) Compatibility - Since not all HPD's [Hearing Protection Devices] are equally suited for all ear canal and head shapes, the proper device must be matched to each user.

5) Readjustment - Since HPD's can work loose or be jarred out of position, employees must be advised of the need for readjustment.

6) Deterioration - No HPD's are permanent or maintenance-free. They must be inspected at least twice yearly, and replaced or repaired as necessary.

7) Abuse - Employees often modify HPD's to improve comfort at the expense of protection. This must be avoided.

8) Removal - When devices become uncomfortable they are often removed to give the ears a "break". This can dramatically reduce the effective protection ...".

If a company has implemented a hearing protection program in accordance with AS 1269-1989 then it could be expected that the factors listed above will have been largely eliminated and individual wearers of hearing protection are likely to be receiving the estimated protection.

However, where a hearing protection program is not fully supported by management and has not been well defined, workers have not been educated or motivated, hearing protectors have not been appropriately selected and fitted and their wearing not adequately supervised, it can be expected that people will receive less than the protection estimated using Australian laboratory data.

It should be noted that there is an advantage in implementing a program in accordance with AS 1269. AS 1269 has a more stringent requirement for fitting protectors than the test method specified in AS 1270-1988 "Acoustics - Hearing Protectors". There is possibly a small margin of safety for workers fitting their protectors using AS 1269 who may be getting greater attenuation from their protectors than estimated from laboratory data.

7.0 CONCLUSION

Where the hearing protection program recommended in Australian Standard "Hearing Conservation" 1269 has not been implemented in full, the attenuation received from hearing protectors is more likely to be shifted towards the "real-world" performance shown in the lowest line of Table 2 for the times hearing protectors are worn.

A full implementation of AS1269 is the best way of protecting the hearing of people exposed to noise. If all the requirements of AS1269 are not met, then the performance of ear muffs and earplugs used in calculations to ensure people will not lose their hearing should be the real-world performance. Even these low figures have to be shifted lower when the hearing protectors are not worn all the time they should be.

AN IMPULSE RESPONSE ESTIMATION METHOD

ONLY BY AVERAGING

Ken'iti Kido and Toru Yamazaki

Chiba Institute of Technology
Tsudanuma 2-17-1, Narashino 275, JAPAN

ABSTRACT

This paper describes a new method of the estimation of impulse response
of a sound transmission path from a sound source to an observing point. The
estimation of the impulse response is important for the design of an FIR
filter used in active noise suppression systems or other acoustic systems in
electro acoustics, architectural acoustics and acoustical measurements. Up to
the present, many sophisticated estimation methods have been proposed and
used, that is, the method using an impulse, the cross spectral method using
noise as the source signal, the method using adaptive filter algorithm or the
linear predictive algorithm with an assumption where the transmission path is
composed of an autoregressive system.
     The method introduced in this paper does not need complicated
computation and is very simple in principle. The new method is explained
using the principle of convolution.
     The principle and the estimation method will be described in the first
place and some results obtained by the computer simulations and the
experiments will be shown.
     The result obtained by the new method is not affected by the property of
circular convolution as the well known cross spectral method and the method
uses most of the sampled data effectively. But, the source signal should be
random in amplitude or in pulse interval. Finally, it is discussed what is
obtained if a sequence correlated each other is used as the source signal.

1.0 INTRODUCTION

When both the input and the output signals of a transfer system can be observed, the transfer function and the impulse response of the system is usually estimated by use of the cross spectral method. The estimated transfer function is the ratio of the cross spectrum of input and output signal to the power spectrum of input signal in the method. And the impulse response is the inverse Fourier transform of the transfer function. A number of computations of Discrete Fourier Transform (DFT) are necessary for the estimation of transfer function. A special treatment is also required to avoid the errors due to circular convolution which is one of the peculiar property of the DFT.

Now, it may not be a big problem by use of the Fast Fourier Transform (FFT) algorithm[Cooley, 1965] that a number of computations of DFT are necessary. And the method to avoid the error due to circular convolution has already been established[Kim, 1986]. But, the estimation method proposed in this paper is considered to be worthy of notice because of the way of thinking.

This paper describes first the principle of the method for the estimation of impulse response only by averaging in accordance with the explanation of convolution. Next some investigations on the method based on the results of computer simulation are presented. And the other computer simulation is shown in which the input signal is a convolution of a random sequence and an impulse response. What is obtained in such a case is also described.
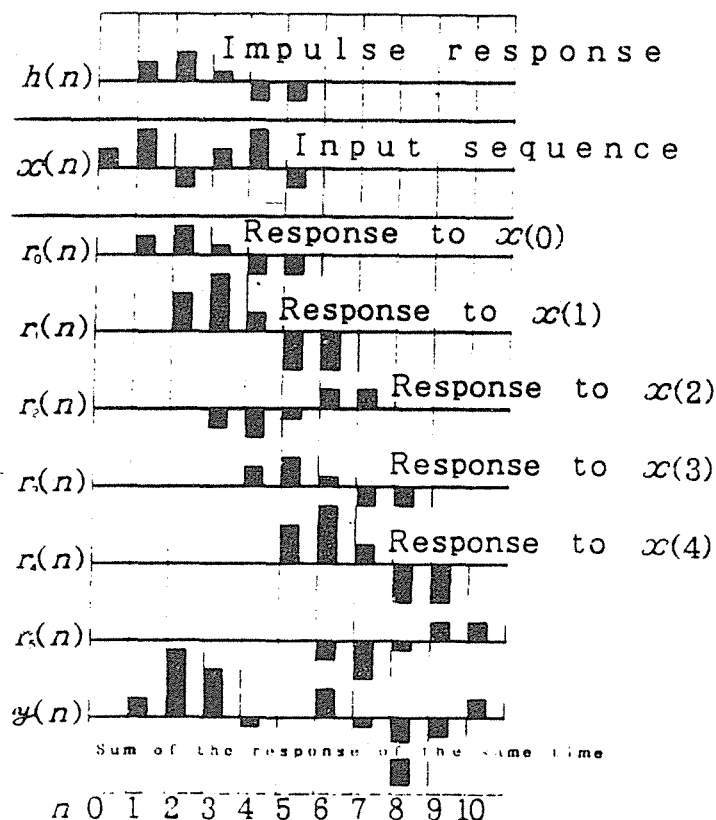
Fig. 1   Schematic explanation of convolution

515

2.0 PRINCIPLE OF THE METHOD

The response $y(n)$ of a system whose impulse response is $h(n)$ $(n=0,1,2,\cdots$: discrete time) to a input signal $x(n)$ is expressed by the following equation as the convolution of $x(n)$ and $h(n)$[4].

$$y(n)=\sum_{p=0}^{P} x(p)h(n-p)=\sum_{p=0}^{P} x(n-p)h(p) \tag{1}$$

Figure 1 shows the relation between the input sequence $x(n)$, the impulse response $h(n)$ and the output sequence $y(n)$. The input signal is expressed as the sequence of pulses which are the sampled values of the signal. The response to each sampled pulse of input signal is similar to the impulse response and the amplitude is proportional to the value of input pulse. The responses to every sampled pulse of input sequence $x(n)$ are illustrated as $r(n)$ in the figure. The instantaneous value of output signal at each sampling time is the sum of the responses along the longitudinal line indicating the same sampling time. It may be clear from this explanation that the output sequence contains the responses of each input pulse shifting one by one. Therefore, it may be considered that the impulse response is obtained by averaging the output sequence after normalized by the corresponding input pulse.

The output sequence contains not only the response to an input pulse of corresponding time but also the response to the input pulses of the other time. Therefore, the input samples of the other time should have random positive and negative value so that the averaged value approaches zero by increasing the number of averagings.

Next, the above described will be investigated using equations.

Using the second term of the right hand side of Eq.(1), $y(n),y(n+1),y(n+2)$, $\cdots$ are written down as follows:

$$y(n) =x(n)h(0)+x(n-1)h(1)+x(n-2)h(2)+\cdots+x(n-p)h(p)+\cdots+x(n-P)h(P)$$
$$y(n+1)=x(n+1)h(0)+x(n)h(1)+x(n-1)h(2)+\cdots+x(n+1-p)h(p)+\cdots+x(n+1-P)h(P)$$
$$y(n+2)=x(n+2)h(0)+x(n+1)h(1)+x(n)h(2)+\cdots+x(n+2-p)h(p)+\cdots+x(n+2-P)h(P) \tag{2}$$

$$y(n+p)=x(n+p)h(0)+x(n+p-1)h(1)+x(n+p-2)h(2)+\cdots+x(n+p-p)h(p)+\cdots+x(n+p-P)h(P)$$

The value of $y(n+p)$ in this equation divided by $x(n)$ which is the value of input sample before p discrete time is expressed as the following:

$$\frac{y(n+p)}{x(n)} = \frac{x(n+p)}{x(n)} h(0)+ \frac{x(n+p-1)}{x(n)}h(1)+\cdots+\frac{x(n+p-p)}{x(n)}h(p)+\cdots \tag{3}$$

In the right hand side, the coefficient of $h(p)$, $x(n+p-p)/x(n)$ is 1 and the other coefficients $x(n+p-i)/x(n)$; $p\neq i$ of $h(i)$ take positive and negative random values. Therefore, the coefficients of $h(p)$ for $p\neq i$ should approach to zero at the limit of $N\rightarrow\infty$ when the mean value of $y(n+p)/x(n)$ is taken changing the value of n, where n is the number of data used for the averaging. If the above discussion is correct, $h(p)$ is obtained only by averaging. But, the term $y(n+p)/x(n)$ should not be used in the averaging process if the absolute value of $x(n)$ is less than a finite value to prevent the use of too big a value of $y(n+p)/x(n)$. The averaged result is written as the following:

$$\frac{1}{N}\sum_{n}^{N} \frac{y(n+p)}{x(n)} = C_0 h(0) + C_1 h(1) + C_2 h(2) +\cdots+ C_p h(p)+\cdots \tag{4}$$

$$= \sum_i C_i h(i) \tag{4'}$$

where,

$$C_i = \begin{cases} \dfrac{1}{N} \sum_n^N \dfrac{x(n+p-i)}{x(n)} & : i \neq p \tag{5-1} \\[2ex] 1 & : i = p \tag{5-2} \end{cases}$$

Equation (5-1) adopts only the case where $|x(n)|$ exceeds a finite value larger than zero. And the coefficient C_i approaches to zero increasing N when $i \neq p$, under the condition that the mean value of the random sequence $x(n)$ is zero. And the next equation holds good.

$$h(p) = \lim_{N \to \infty} \frac{1}{N} \sum_j^N \frac{y(n+p)}{x(n)} \tag{6}$$

The numberof divisions by(n) carried out in the computation of this equation is NP for a impulse response of length P. The number is much smaller than that of multiplication in the cross spectral method, but it is still a considerable number.

The number ofdivisionscan be made zero using a binary sequence of random interval, because there is no requirement in the distribution function of the source signal $x(n)$ excepting for that the mean value should be zero. Using such the source signal, the above equation (7) is rewritten as follows:

$$h(p) = \lim_{N \to \infty} \frac{1}{N} \sum_n^N \mathrm{sgn}\{x(n)\} y(n+p) \tag{8}$$

The discussion in the preceding is rather intuitive and the method is confirmed by a computer simulation.

First, the impulse response is estimated by the method described here using a random sequence as the input to a single resonance transmission system. The output sequence for this simulation is directly computed as the convolution of input sequence and the impulse response of the system.

Figure 2 (a) shows the input sequence which is the computer generated uniform random sequence, (b) the output sequence which is the convolution of the input (a) and the impulse response of the system shown in Fig. 3 (a).

The impulse response estimated by the sequence shown in Fig.2 (a) and (b) is shown in Fig.3 (c). The agreement is indicated by the overlapped figure of Fig.3 (b) and the difference between the real impulse response and the estimated one shown in (d).

Figure 2 (c) shows a binary sequence made from a random sequence of (a) using the signs of successive pulses in the sequence. The convolution of the sequence (c) and the impulse response used for making sequence (b) from (a) is shown in Fig.2 (d). Figure 3 (e) shows the result of estimation from the sequences of Fig.2 (c) and (d). The difference between the estimated one and the true impulse response is very small as shown in Fig.3 (f).

3.0 NORMALIZATION ONLY BY SIGN

According to the preceding description, the output sequence normalized by the corresponding input sample is the sum of the impulse response whose magnitude is proportional to the input sample and the noise due to the other input samples, and the impulse response can be estimated reducing the noise from the output sequence by averaging. From this argument, it is considered that the sign of the input sample can be used instead of the value of the input sample. The polarity and the magnitude of the response to the input sample buried in the output signal depends on the sign and the magnitude of

SOURCE WAVE W1: NR= 777 TOTAL LENGTH= 6000

(a)

R1 = RESPONSE TO W1

(b)

SOURCE WAVE W2

(c)

R2 = RESPONSE TO W2

(d)
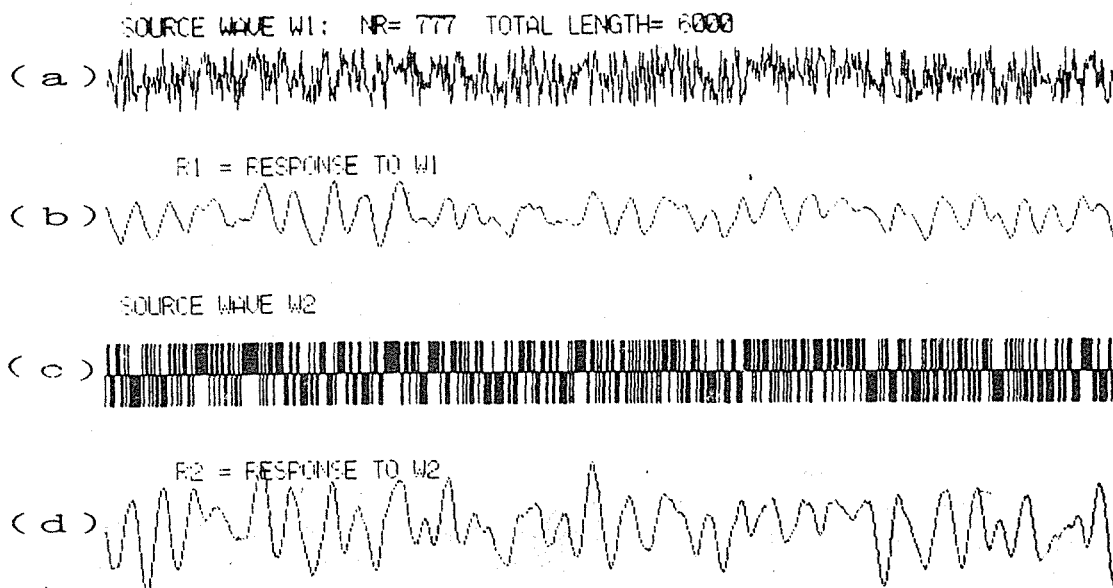
Fig. 2 Examples of input and output sequences of the system used in the computer simulation of the estimation of impulse response
(a) random input sequence
(b) response of the system to input (a)
(c) impulse sequence of random interval
(d) response of the system to input (c)

(a) TRUE IMPULSE RESPONSE

(b) IMPULSE RESPONSES OVERLAPED

(c) ESTIMATED FROM RANDOM NOISE
H1= 5861

(d) ESTIMATION ERROR
ERROR COEF. E1= .131983

(e) ESTIMATED FROM IMPULSE TRAIN
K2= 5961

(f) ESTIMATION ERROR
ERROR COEF. E2= .135229
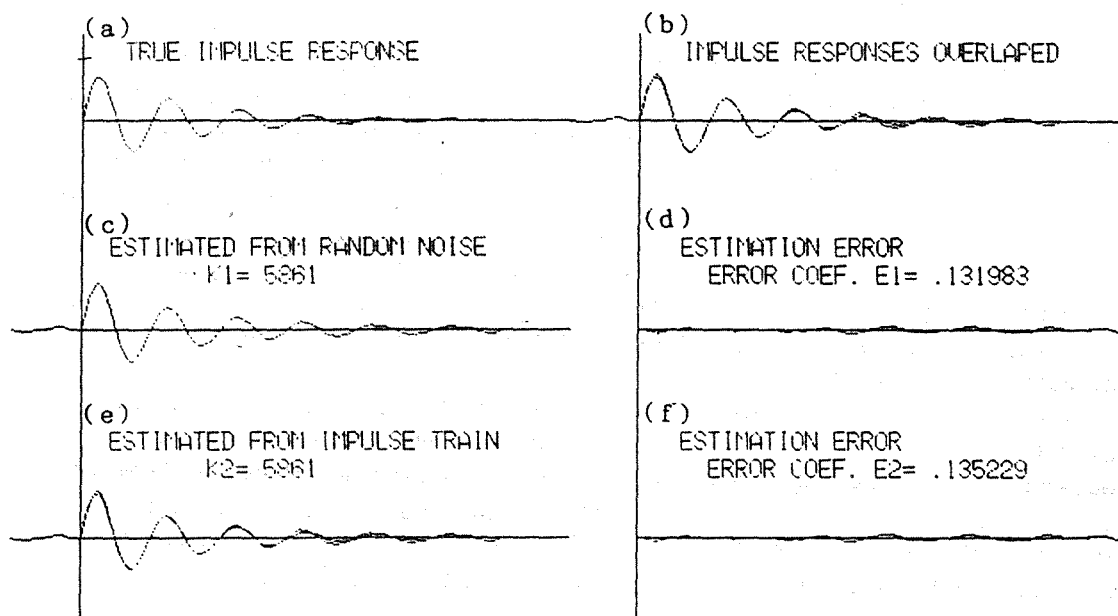
Fig. 3 Impulse response of a system, estimated impulse responses and the estimation errors
(a) impulse response $h(n)$
(b) overlap of the exact impulse response and estimated ones
(c) impulse response estimated by Fig. 2 (a) and (b)
(d) estimation error of (c)
(e) impulse response estimated by Fig. 2 (c) and (d)
(f) estimation error of (e)

impulse responses buried in the output sequence becomes the same as that of the response to the positive input pulse. Therefore, the resultant wave form from which the noise is eliminated by averaging should be similar to the impulse response.

From the above considerations, the following equation to estimate $h(p)$ is deviced:

$$h(p) = \lim_{N \to \infty} \frac{1}{N|x(n)|} \sum_{n}^{N} \text{sgn}\{x(n-p)\}y(n) \tag{9}$$

This equation is the same as that to compute the cross correlation using the sign of random signal. Therefore, it can be said that the method described here coincides with the method of estimating the impulse response using the cross correlation of input and output signals using random noise as the input.

The normalization of Eq. (6) is not necessary in this method and the same result is obtained only by the averaging after modifying the sign of $y(n)$ by the sign of $x(n-p)$. The computation quantity can be much reduced.

Figure 4 shows the result of computer simulation for the confirmation of the validity of this method. In this figure, (a) shows the impulse response, (b) the overlap of the real and the estimated impulse responses, (c) the impulse response estimated by the method in this chapter using only the sign of $x(n)$ and (d) the estimation error. The validity of the method using only the sign of input sequence is shown here.

4.0 CASE OF COLORED INPUT SIGNAL

The impulse response is not exactly estimated when a colored signal is used for the input sequence. The obtained result in such the case is explained as follows.

Let $u(n)$ be the random sequence, $g(n)$ the impulse response of a filter with which the colored input signal $x(n)$ is made from $u(n)$. That is, the input signal $x(n)$ is expressed as follows:

$$x(n) = u(n) * g(n) \tag{10}$$

The output signal or the system is the convolution of $x(n)$ and $h(n)$, and the following relation holds.

$$y(n) = x(n)*h(n) = u(n)*g(n)*h(n) = u(n)*\{g(n)*h(n)\} \tag{11}$$

The result obtained by the same method as described in the preceding chapter should be $g(n)*h(n)$ in this case if the sign of $x(n)$ is similar to that of $u(n)$. In the previous method, the sign of the output signal should be normalized by the sign of $u(n)$ to obtain $g(n)*h(n)$, but the sign of output signal is normalized by that of $x(n)=u(n)*g(n)$ in this case as $u(n)$ can not be observed. When $g(n)$ is a simple function such as two points moving average, the sign of $x(n)$ will not much differ from that of $u(n)$ and the obtained result will be proportional to $g(n)*h(n)$, but when $g(n)$ is a complicated wave, the sign of $x(n)$ differs much from that of $u(n)$ and $g(n)*h(n)$ will be eliminated in the same way as the response to the other input samples.

The validity of the discussion is confirmed by a computer simulation. Figure 4 (e) and (f) show the results in a case where $g(n)$ is two points moving average: $g(n)=1$ for $g(n)=0,1$ else $g(n)=0$.

Figure 5 shows the results of another case where the impulse response is a sum of decaying sine waves and $g(n)=(\sin(3.14*n/4) : n=0$ to 4 else $g(n)=0$.

(a) TRUE IMPULSE RESPONSE

(b) IMPULSE RESPONSES OVERLAPED

(c) ESTIMATED FROM RANDOM NOISE
K1= 4961

(d) ESTIMATION ERROR FOR $h(n)$
ERROR COEF. E1= .325944

(e) ESTIMATED WAVE FORM USING
COLORED INPUT $u(n)*g(n)$
K2= 4961

(f) DIFFERENCE BETWEEN
ESTIMATED AND $g(n)*h(n)$
ERROR COEF. E2= .127254
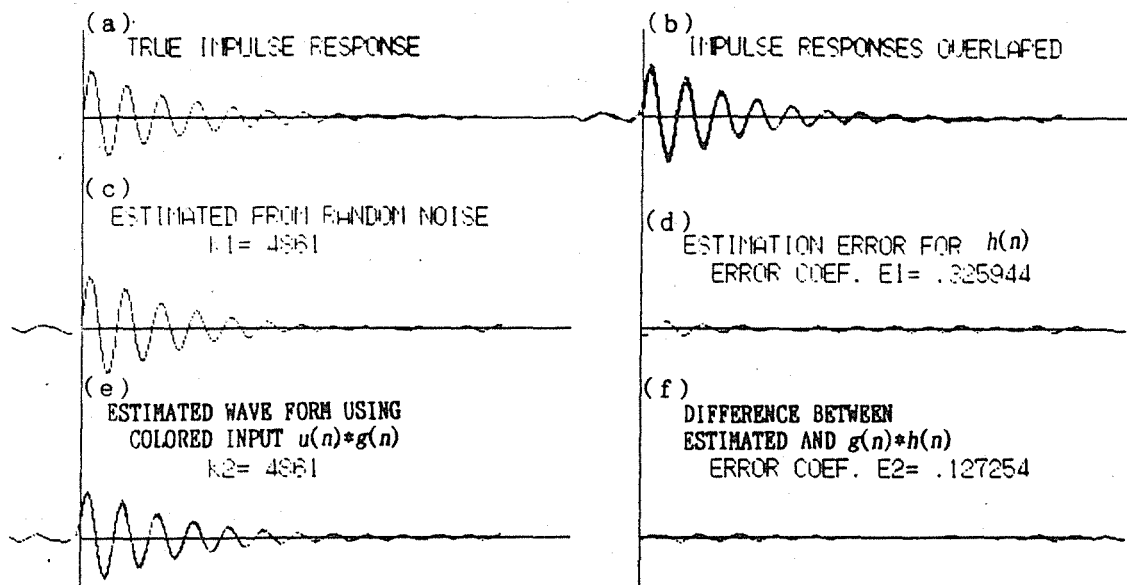
Fig. 4 Results of impulse response estimation by a random and colored input sequence and the response to them.
(a) impulse response $h(n)$
(b) overlap of the exact impulse response and estimated ones
(c) impulse response estimated by random input $u(n)$ and the response to $u(n)$
(d) estimation error of (c)
(e) wave form estimated by colored input $u(n)*g(n)$ and the response to it, where $g(n)=1$ for $n=0,1$ else $g(n)=0$.
(f) difference between estimated wave form and $g(n)*h(n)$

(a) TRUE IMPULSE RESPONSE

(b) IMPULSE RESPONSES OVERLAPED

(c) ESTIMATED FROM RANDOM NOISE
K1= 5961

(d) ESTIMATION ERROR FOR $h(n)$
ERROR COEF. E1= .0845465

(e) ESTIMATED WAVE FORM USING
COLORED INPUT $u(n)*g(n)$
K2= 5961

(f) DIFFERENCE BETWEEN
ESTIMATED AND $g(n)*h(n)$
ERROR COEF. E2= .296009
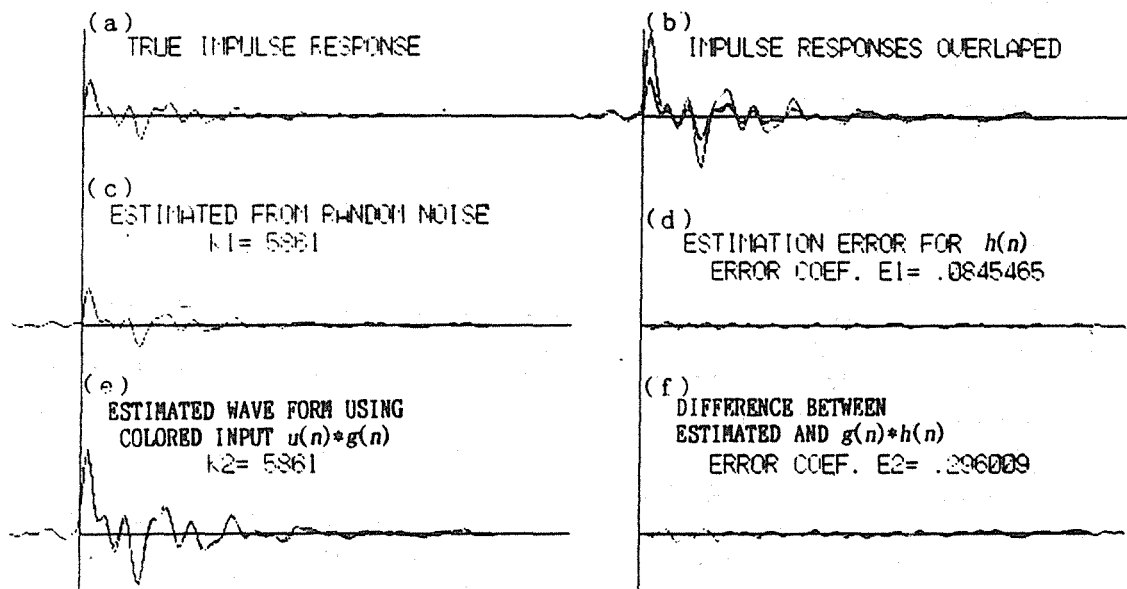
Fig. 5 Results of impulse response estimation by a random and colored input sequence and the response to them.
(a) impulse response $h(n)$
(b) overlap of the exact impulse response and estimated ones
(c) impulse response estimated by random input $u(n)$ and the response to $u(n)$
(d) estimation error of (c)
(e) impulse response estimated by colored input $u(n)*g(n)$ and its response, where $g(n)=(\sin(3.14*n/4))^2$ for n=0 to 4 else $g(n)=0$.
(f) difference between estimated impulse response and $g(n)*h(n)$

5.0 CONCLUSION

This paper proposes a new method of consideration to estimate a system by use of the input and the output signal, where no multiplication is necessary. The computation quantity is much less in this method than in the conventional cross spectral method. But, the input signal of this method should be random in amplitude or in the interval of successive pulses and the mean value of the input sequence should be zero.

According to the investigation, the following are made clear:

(1) the impulse response of a system is estimated by making the average of the values of output sequence normalized by the samples of input sequence shifting one by one.

(2) the input sequence should be random in the amplitude or in the interval of the successive samples and the mean value should be zero to obtain impulse response by the method in (1).

(3) using the constant amplitude positive and negative pulses of random interval as the input sequence, the impulse response is obtained without division by the input sequence.

(4) in the case of random input sequence, normalization by the input sequence can be changed to the normalization by the sign of the samples of input sequence, and the number of divisions can be much decreased.

(5) when the input sequence is the convolution of a random sequence $u(n)$ and an impulse response $g(n)$, the obtained result by the same method is the convolution of $g(n)$ and the impulse response of the system $h(n)$. But $g(n)$ should be a simple function not to eliminate $g(n)\ h(n)$ by the averaging.

Those results are confirmed by computer simulations.

References:
[1] Cooley,J.W. and Turkey,J.W. "An Algorithm for the Machine Calculation of Complex Fourier Series, Math. of Computer; 19,90 pp.297-301 (1965)
[2] Kim,C.D. Abe,M. and Kido,K. "Investigations on the method for the estimation of impulse response using a rectangular pulse," J.Acoust.Soc.Jpn.(E) Vol.7, No.5 pp.239-247 (1986)

NOISE LEVEL DISTRIBUTIONS IN ENVIRONMENTAL ACOUSTICS

Michel Maurin

Institut National de Recherche sur les Transports et leur
Sécurité, Laboratoire Energie Nuisances, INRETS-LEN
Case 24, 69 675, BRON Cedex, France

ABSTRACT.

In environmental studies noise levels are naturally fluctuating
and lead to statistical processing, often a basic
assumption is made to their normality behaviour.
As equivalent noise level $Leq_{\Delta t}$ is given by $10 \log(\Delta \int V / \Delta t)$
with $V = \int p^2 / p_0^2$ a theoretical framework for Leq may intro-
duce V as a positive PSII (process with stationary and inde-
pendent increments), characteristic functionsof which are
known and rather simple to work with.
This model has many advantages. Here it is shown how, for
positive PSII of second order, V increments distribution
tends to a normal law with vanishing variance as time of
integration Δt increases.   An   associated asymptotic log-
normal property yields convergence of noise equivalent levels
$Leq_{\Delta t}$ distribution to a normal distribution. With it normality
status becomes clearer.

1.0 INTRODUCTION.

The idea that road traffic noise levels are normal (gaussian) is rather ancient in literature, and probably its repeated presence has rendered more obscure the origin and nature of this property ; in some cases it had been considered as an hypothesis or postulate (Bastide). Anyway this is an extreme position because there is also an opposite behaviour (no mention of normality). Here we open a discussion on this topic and propose a specific model for noise equivalent level Leq in order to cast a new light on it.

2.0 A SLIGHT REVIEW FOR ROAD NOISE LEVELS AND NORMALITY.

The assumption of normal fluctuations for road noise levels is found in many papers with different degrees of belief. For instance it is found in Beranek (1971) under a minor formulation "If the probability distribution of the instantaneous A levels is reasonably Gaussian, …", but he says also "that many traffic noise situations are not Gaussian".

At the same time the hypothesis is more precisely involved in order to set up relationship $\widehat{Leq} = \bar{L} + 0,115 \ S_L^2$ or $L_{50} + 0,115 \ S_L^2$, $\bar{L}$ and S_L^2 are usual statistics of observed noise levels L_i and the result an overall Leq estimator for the whole period of acoustic investigation (Aubrée Auzou Rapin). This is a classic formula coming from an identity between moments of normal and log-normal distributions (Johnson Kotz); $\bar{L}$ and L_{50} are two estimators for mean(L_i), the first more efficient than L_{50}. It appeared in a D.R. Johnson note (1969) as mentioned by Robinson, and has been frequently repeated (Liénard, Migneron).

As Beranek did, acoustical papers by others took up again the assertion (Bishop, Fisk), and with no doubt its influence occurred in the Robinson NPL with a $2,56 \ \sigma_L$ quantity inspired by $(L_{10} - L_{90})$ expression in TNI.

Conversely Kurze and several Japanese authors have been unaware of this assumption (roughly for the same time), and

developed   more or less intricate statistical techniques in
order to describe noise level distributions around roads and
motorways (for instance Otha Mitani). This renders more
remarkable a recent proposal into which normal distribution
is used as a technical first order term in a statistic series
expansion (Otha Nakasako). So Gaussian assumption has a long
past behind it in road traffic noise, and few people remained
unconcerned about it.

3.0 THE PSII MODEL FOR ACOUSTIC ENERGY.

Here is a new framework for noise levels based upon the
definition of noise equivalent level itself.

3.1 A model. Truly $Leq_{\Delta t} = 10 \log\{1/\Delta t \int p^2(t)/p_0^2 \, dt\}$

integrated from t to t+Δt, where p(t) is the instantaneous
acoustic pressure and $p_0 = 2 \times 10^{-5}$ Pascal. So if we call $V = p^2(t)/p_0^2$ an "acoutic power" (Bastide), Leq is defined by the
increments $\Delta(\int V)$ of the "acoustic energy" $\int p^2(t)/p_0^2 \, dt$ and
this remark leads us to consider energy $\int p^2/p_0^2 \, dt$ as a time
process defined by the way of its increments, (or with suita-
bly filtered p_A^2, … and related energy). Here the classical
logarithm in acoustics may be considered as a mere transform
variable between observed noise levels on time intervals [t_i
$t_i + \Delta t_i$] and the related average increments for V.

When noise levels are relatively stable, for instance during
day hours, the model is completed by taking increments on
separate time intervals of same duration Δt stationary. Among
such processes the most curious and disquieting are the time
homogeneous processes with independent increments, also cal-
led processes with stationary and independent increments
PSII. They have been quite described by Lévy then by Khint-
chine and are closely related to infinitely divisible distri-
butions (Feller).

What is important is that for general PSII X_t, one knows comple-
tely the characteristic function of X_t. Moreover characteris-
tic function for positive PSII (because it is logarithm) is simple
to handle with a Lévy measure $d\Pi(u)$ on R^+ (Bouleau), their

general form is given by $\Phi_{X_t}(z) = \exp\{t \int_0^{+\infty} (e^{iuz} - 1)\, d\Pi(u)\}$

under the condition that integral $\int_0^{+\infty} \inf(1,u)\, d\Pi(u)$ is finite.

Furthermore we consider positive PSII of second order, namely Lévy measure for which $E_0 = \int_0^{+\infty} d\Pi(u)$, $E_1 = \int_0^{+\infty} u\, d\Pi(u)$ and $E_2 = \int_0^{+\infty} u^2\, d\Pi(u)$ are finite ; note E_0 and E_2 finite is a

sufficient conditions for E_1 to be finite, and more generally that when they are finite, E_n $n \geq 1$ $d\Pi(u)$-moments are respective cumulants of same order for X_t distribution divided by t. Within such framework for $V \equiv X_t$ one gets mean($\Delta \!\!\int V$) = $E_1 \Delta t$ and variance($\Delta\!\!\int V$) = $E_2 \Delta t$ (Bastide) and we showed how normality assumption is useless because statistical estimation for Leq is quite the same with or without it (Maurin).

3.2 An asymptotic property. A positive PSII of the second order for acoustic energy V yields a more accurate result.
Lemma : If E_0 and E_2 are finite, average increment distribution of X_t/t converges in distribution to the normal law $\mathcal{N}(E_1, E_2/t)$ when $t \rightarrow +\infty$.

Proof : characteristic function for X_t/t variable is $\Phi_{X_t/t}(z)$ = $\exp\{t \int_0^{+\infty} (e^{iuz/t} - 1)\, d\Pi(u)\}$ and it can be written

$\exp\{t \int_0^{+\infty} e^{iuz/t}\, d\Pi(u) - t E_0\}$ with $t \int_0^{+\infty} e^{iuz/t}\, d\Pi(u) = t E_0 + iz E_1$

$- z^2/2t\, E_2 + o(1/t)$. So $\text{Log}(\Phi_{X_t/t}(z))$ converges uniformly in z to $iz E_1 - z^2/2t\, E_2$ as t increases, namely the logarithm of the characteristic function of the normal distribution of mean E_1 and variance E_2/t.   ◆

Examples :
- measure $d\Pi(u) = u^{-3/2}\, du$ which yields a one sided stable process (Bouleau) does not agree because neither E_0 or E_1 are finite ;

- gamma measures $d\Pi(u) = \lambda^a\, e^{-\lambda u}\, u^{a-1}/\Gamma_{(a)}\, du$ with a and λ positive parameters agrees, $E_0 = 1$, $E_1 = a/\lambda$, $E_2 = a(a+1)/\lambda^2$.

3.3 Application to noise levels.

Lemma is an extension of central limit theorem to time processes, it shows that the distribution of $10^{Leq_{\Delta t}/10}$ tends to be asymptotically Gaussian as Δt increases. However we noted environmental acousticians are preferably concerned by the Gaussian behaviour of $Leq_{\Delta t}$. This final point is resolved thanks to a statistical property related to normal and log-normal laws, namely if $Y = Log\ X$ is a normal random variable with a vanishing variance σ_y^2, X is a log-normal variable which converges in law to a normal variable with a positive mean m_x and a vanishing variance $\sigma_x^2 = m_x^2\ (exp(\sigma_y^2) - 1)$ (Johnson Kotz).

In our case $c\ Leq_{\Delta t} = Log(\Delta \int V/\Delta t)$, $c = 1/10\ Log10 \# 0,23$; consequently asymptotic normal variable $\Delta \int V/\Delta t$ with positive mean E_1 becomes also an asymptotic log-normal variable and so $c\ Leq_{\Delta t}$ converges to a normal variable as Δt increases. The two moments of the asymptotic normal distribution for $c\ Leq_{\Delta t}$ are :

variance$(c\ Leq_{\Delta t}) = Log(1 + E_2/(t\ E_1^2))$,

mean$(c\ Leq_{\Delta t}) = Log\ E_1 - 1/2\ variance(c\ Leq_{\Delta t})$.

What is important in acoustic assessment is an estimator for $10\ log\ E_1$ (Bastide, Maurin), this is made using the relationship: $10\ log\ E_1 = 1/c\ Log\ E_1 = mean(Leq_{\Delta t}) + c/2\ variance(Leq_{\Delta t})$. Here the independence property included in PSII gives us an other result, i.e. the independence of measures $Leq_{\Delta t i} = L_i$ and the usual estimators $\overline{L}$ and S_L^2. For mean(L_i) and variance(L_i), one gets again $\widehat{Leq} = \overline{L} + 0,115\ S_L^2$ as an unbiased estimator for Leq.

4.0 CONCLUSION.

The logical status of normality for noise levels is quite clear within the PSII framework for acoustic energy $V = \int p^2(t)/p_0^2\ dt$; Gaussian behaviour is an asymptotic consequence of the model as the measurement's duration increases.

This first result goes together with the foregoing considerations about the model itself. The Leq definition is a true

invitation to consider energy model in terms of its incre-
ments ; in particular PSII are quite known, they render
possible and easy the discussion because of independence and
stationarity. This model is essential in the clarification,
and today's sound level meters that both integrate acoustic
power on successive time intervals (say energy increments)
and store them into micro-information memories fail in with
it.

REFERENCES.

Aubrée D., Auzou S., Rapin JM., Etude de la gène due au trafic automo-
bile urbain, CSTB, *Annexe n° 3 Sites de mesure et méthodologie*, juin
1971, 166-212.

Bastide J.C., Estimation et mesure du niveau acoustique continu équiva-
lent, *Revue de Statistique Appliquée*, vol XXXVI n° 3, 5-14, (1988).

Beranek L.L., *Criteria for noise and vibration in communities, buil-
dings and vehicles*, in Beranek, *Noise and Vibration Control*, Mc Graw
Hill, 1971, 554-603.

Bishop D.E., *Noise surveys ; community noise*, in Harris C.M., *Handbook
of noise control*, Mc Graw Hill, 1979, chap. 35, 35-14.

Bouleau N., *Processus stochastiques et applications*, Hermann, 1988,
151-179.

Feller W., *An introduction to probability theory and its applications*,
J. Wiley vol 2, 1971, 554-565.

Fisk D.J., Statistical sampling in community noise measurement, *Journal
of Sound and Vibration*, vol 30 n° 2, 221-236, (1973).

Johnson N.L., Kotz S., *Continuous univariate distributions - 1*, J.
Wiley, 1970, 112-131.

Kurze U.J., Statistics of road traffic noise, *Journal of Sound and
Vibration*, vol 18 n° 2, 171-195, (1971).

Lienard P., *Décibels et indices de bruit*, Masson, 1978, 28-30.

Maurin M., A propos d'une hypothèse gaussienne en Acoustique, *1er
Congrès Français d'Acoustique*, Lyon, C2-1990, vol II, 729-732.

Migneron J.G., *Acoustique urbaine*, Masson, Presses de l'Université
Laval-Québec, 1980, 67-75.

Otha M., Mitani Y., A prediction method for road traffic noise genera-
ted from arbitrary non Poisson type traffic flow based on an approach
equivalent to that for a standard Poisson type traffic flow, *Journal
of Sound and Vibration*, vol 118 n° 1, 11-21, (1987).

Otha M., Nakasako " , An evaluation theory for a mixed model stochastic
system and its application to non stationary road, *Acustica*, vol 71
n° 2, 121-126, (1990).

Robinson D.W., Towards a unified system of noise assessment, *Journal of
Sound and Vibration*, vol 14, n° 3, 279-298, (1971).

CHARACTERISATION OF DELAMINATION IN GFRP COMPOSITES UNDER COMPRESSION LOADING USING ACOUSTIC EMISSION TECHNIQUES.

TENG C. M.
Affiliation : Nanyang Technological University
SINGAPORE

LIM M. K
Affiliation : Nanyang Technological University
SINGAPORE

CHAI G. B.
Affiliation : Nanyang Technological University
SINGAPORE

ABSTRACT

Acoustic Emission is a non-destructive testing technique which offers practical means for detecting the onset of damage and damage progression in fiber reinforced composites. Many efforts have been made to monitor the damage process by tensile failure but few on the effect of compressive failures.

Uni-directional 6-ply GFRP specimens were fabricated by the hand-lay up method in the laboratory and artificial delamination were placed at different ply so as to correlate the specimen AE signal counts with failure mechanisms such as matrix cracking, fiber-matrix interfacial cracking and fiber breakages in the GFRP composite specimens.

This paper is concerned with the investigation of compressive failure by buckling of glass-fiber reinforced (GFRP) composites using acoustic emission technique. The AE results that were obtained were correlated with the load-displacement curve and also verify visually for the translucent GFRP specimens in this case.

1.0 INTRODUCTION

Delamination is a commonly observed failure mode in laminated composite materials between composite layers and is the fundamental issue in the evaluation of laminated composite structures for durability and damage tolerance. This is even more so after the parts had entered service, where they will be exposed to a variety of operational use and also misuse. Acoustic emission (AE) was used by the following authors to assess the behaviour of the specimens to study its behaviour under different loading conditions as a function of time.

Awerbuch and Eckles [1] monitored the AE during quasi-static loading of a variety of cross-ply graphite/epoxy laminates with different stacking sequences and containing different ratios of ply thickness to correlate the AE results with the actual failure processes for the different laminates. The results obtained indicate that the stacking sequence strongly affects the event intensities, e.g. event amplitude, energy, duration, rise-time and counts. The ringdown counts analysis results which were applicable in this paper indicated that AE initiates at a lower load level in laminates with fibers normal to the loading direction than with fibers parallel to the loading direction.

Benzeggagh, Prel and De Charentenay [2] monitored the AE count rate of Mode I delamination on Double-Cantilever Beam (DCB) glass-epoxy with artificial defects and show that damages initiating at the artificial crack were detected by AE without any crack opening. The various fracture mechanism were explained using the crack tip strain profile. In relation to this paper, a change in the shape of the strain curves were observed by them as coinciding with strong AE signals which accompanies crack opening and which were also confirmed by visual observation. Works on GFRP and CFRP specimens [3] were carried out prior to this work. In another paper on Mode I delamination test, De Charentenay *et al.* [4] show that monitoring acoustic emission allows the initiation fracture energy, that is characteristic of material bonding to be determined.

In this paper experimental results of AE counts and strain readings of compressive failures by buckling were collected and different failure stages were identified. The source of signals was narrowed down to a single source - using artificial defects to constrain delamination growth between predetermined layers.

2.0 EXPERIMENTAL PROCEDURE AND SPECIMENS

2.1 Instrumentation system

The instrumentation setup shown in Figure 1 for the experiments were:

- Nicolet 310 digital oscilloscope for recording the AE time signals
- Tokyo Sokki TDS-301 strain datalogger for recording the strain values.
- B & K Type 2635 Charge amplifier
- Dunegan Model S9204 piezoelectric sensors
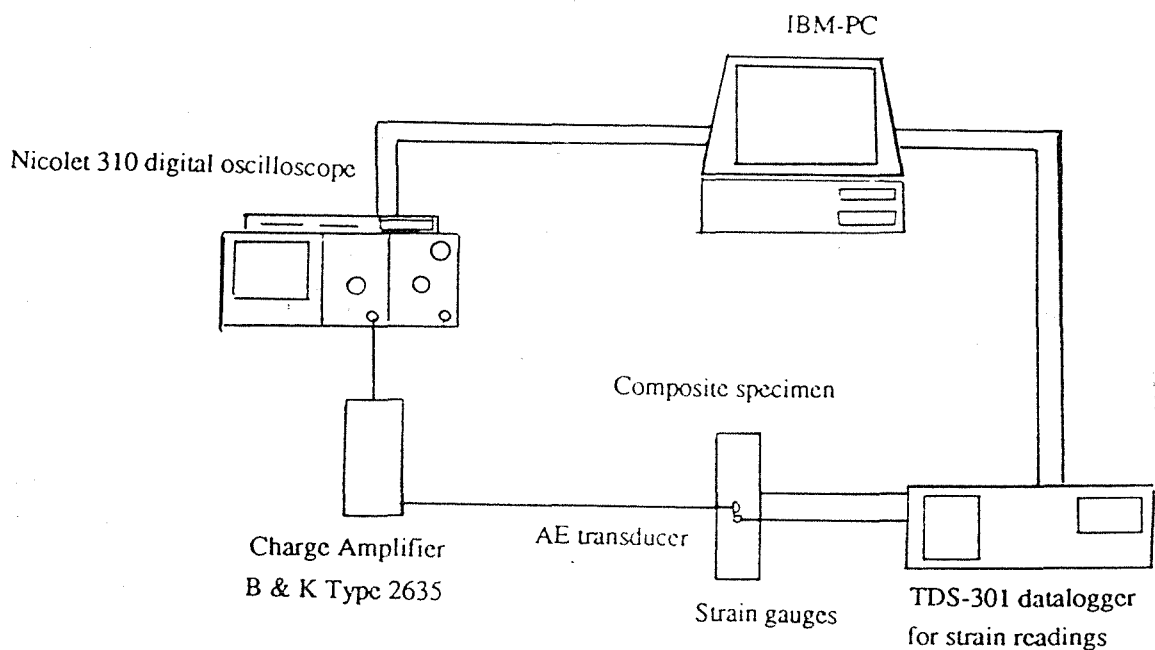
Figure 1 : Instrumentation setup for the compressive (buckling) test.

2.2 Test specimens

Experiments were conducted on 6-plys, hand-lay unidirectional glass-fiber reinforced polyester (GFRP) composite specimens with artificial delamination initiator of thickness 0.125 mm and length 60 mm, to study the crack propagation at the desired interface. The delamination insert was placed in the middle of the gauge length (150 mm) and through the width. Strain gauges placed back-to-back (strain 1 and 2) at the mid-section of the delaminated region, provides a detailed picture of the specimen contour under load. Every test specimen were strain-gauged back-to-back to measure uniaxial and bending strains. To monitor possible delamination growth, markings were added on the white-painted edge of the specimen. The specimen dimensions are shown in Figure 2. Clamped-ends of at least 15 mm length were allowed for at each end.
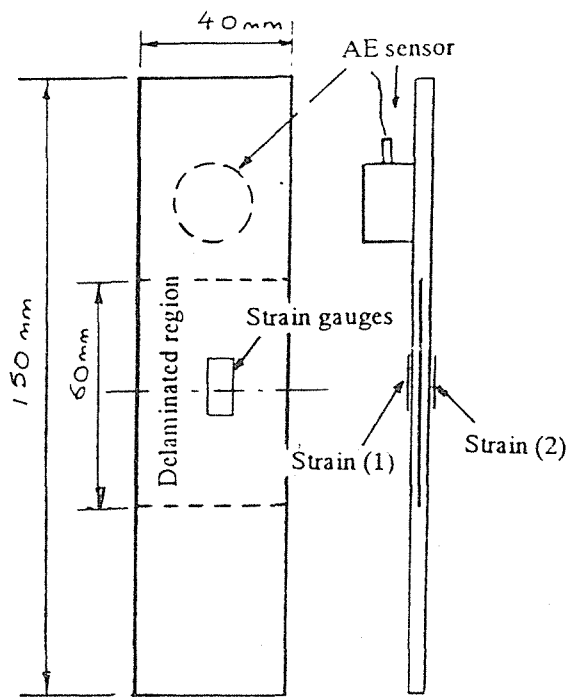
Figure 2 : Specimen details.   Figure 3 : Testing jig.
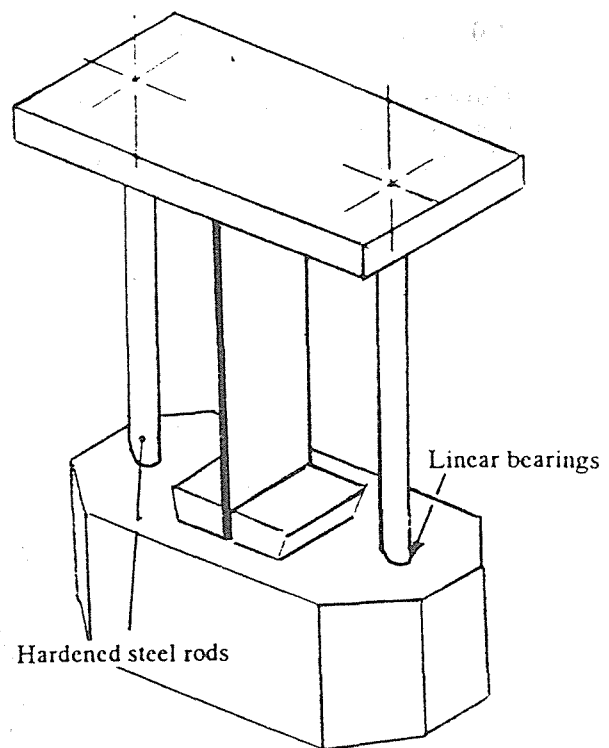
2.3   Test fixtures

The test jig was rigidly designed such that there would be no bending load induced on the specimen throughout the test. Varying specimen thickness up to a maximum of 10 mm can be tested with this jig. Figure 3 shows the design and layout of the test jig used.

2.4   Loading and procedures

The tests were carried out on an Instron machine (Model 1195A) with the crosshead speed set at 0.5 mm/min. Acoustic emission (AE) signals from the AE sensor were first amplified and then filtered before it was stored in the Nicolet 310 digital storage oscilloscope for further processing.

Intermittent loading was carried out in order to store the AE time signals into the Nicolet 310 oscilloscope as the whole test is longer than the oscilloscope scan time. Prior to the conducting the test, an AE time signal was recorded to determine the threshold level setting. The level of threshold was set to remove background and electrical noise. Rubber pads was used to isolate the AE sensors from the mechanical noise of the Instron machine hydraulics to provide an acoustic mismatch at the loading area. Slippage at the grips which causes friction noise were avoided by using serrated grips.

Monitoring of the crack opening was by estimation of the white-painted markings along the edge of the specimens. An IBM-PC based BASIC program was written to control the start and stop of the test and also to process the AE time signals to obtain the AE counts and correlating the AE counts with the strain readings. No continuous data collection was possible at this stage of the experiment.

3.0 DISCUSSION ON EXPERIMENTAL RESULTS

Curves of load-displacement, load-acoustic emission counts and strain-acoustic emission counts were plotted for each test. An interpretation of the strain curves and the load curve obtained is shown in Figure 4 and 5.
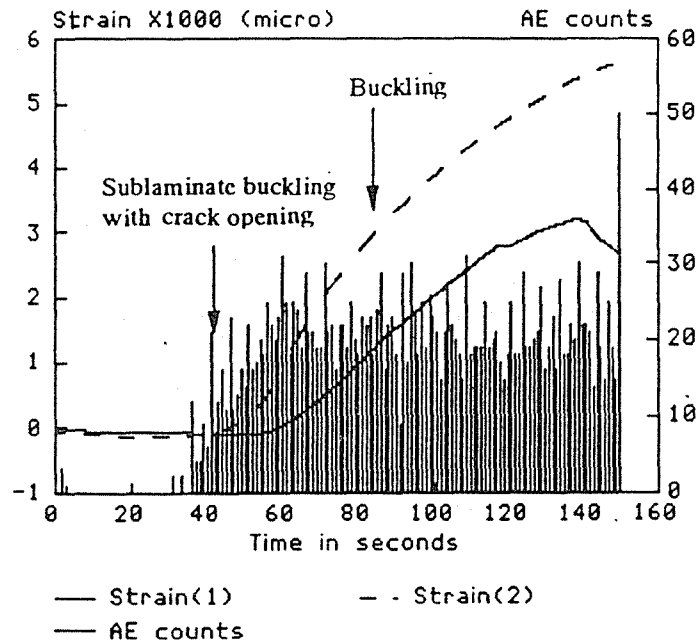
Figure 4: Strain-AE curve for delamination at the 1- and 2-ply. Delamination growth is about 2mm at the upper delaminated region only.
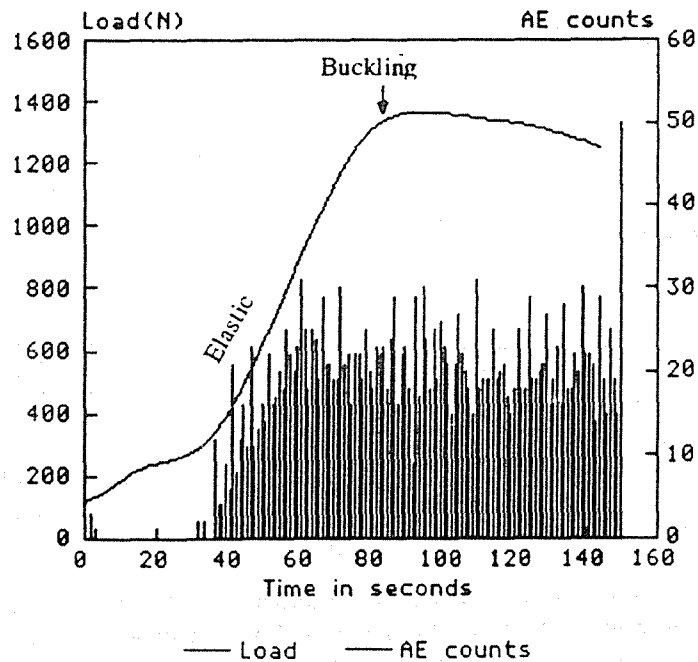
Figure 5: Load-AE curve for delamination at the 1- and 2-ply.

532

Case 1 - Delamination between 1st and 2nd ply.

In Figure 4 and 5 AE signals were detected close to the start of the test indicating the damage initiation. The initial linear portion of the load-time curve which is quite linear and is due to the opening of the delamination defect. The curve became non-linear when the crack extends. The compressive strains in Figure 4 moves into the tensile region as the load increases and the point where the signs of the strain reversed coincides with a slight drop in the load curve indicating that the sublaminate had buckled with crack opening. In this case it occurred before reaching the buckling load. Subsequently, the load continue to rise indicating that there were no crack extension. Finally, crack extension occurred soon after the specimen had buckled and is indicated by an increase in AE activity.

Case 2 - Delamination between 2nd and 3rd ply.

In Figure 6 and 7 for a delamination between the 2- and 3-ply, the reversal of sign of the strain (1) and (2) coincides with the buckling load, in this case with no crack opening at this point. The buckling of the sublaminate occurred after the specimen had buckled · (Figure 6). Crack extension was observed here with increases in AE and also a change in direction of the load curve. The crack front was elliptical with more rapid extension along the edges than the central portion.
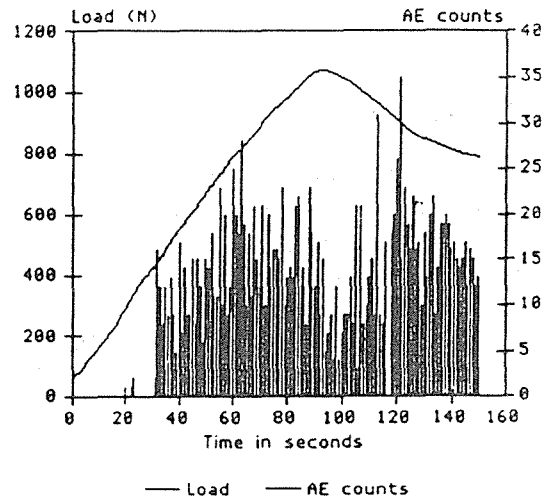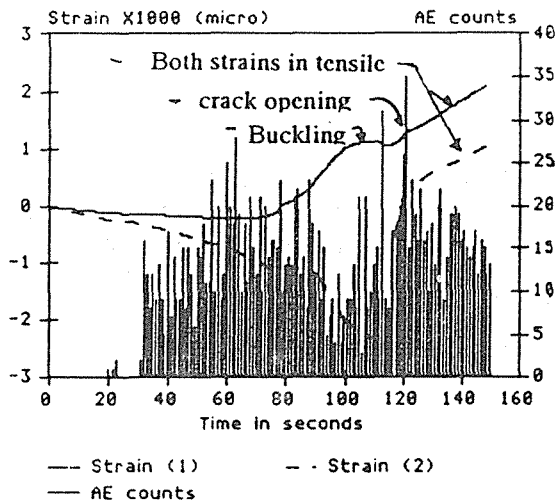
Figure 6: Strain-AE curve for delamination at the 2- and 3-ply. Crack growth to 8mm at the edge and 2mm at the centre.

Figure 7: Load-AE curve for delamination at the 2- and 3-ply.

Case 3 - Delamination between the 3rd and 4th ply

In Figure 8 and 9 for a delamination between the 3- and 4-ply. The sublaminate buckled with crack opening before the buckling load. Towards the later stages the crack extension stops and the whole specimen buckled accompanied by an increase in AE activity. A further crack extension occurs after reaching the buckling load, with the strain curves showing a sign reversal. A parallel crack front was observed and as the test proceeds no further crack growth was observed.
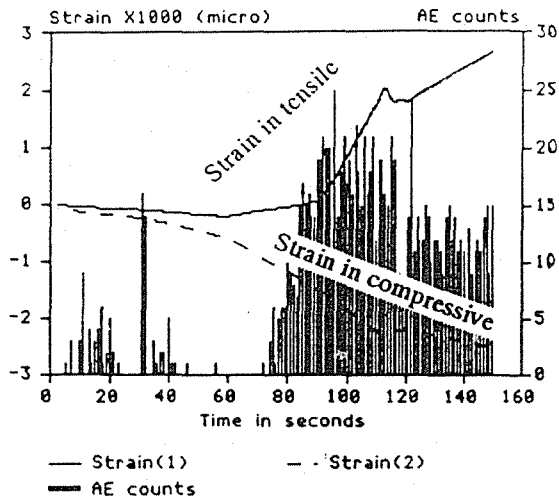
Figure 8: Strain-AE curve for delamination at the 3- and 4-ply. Crack growth to 2mm with slight opening of the crack region.
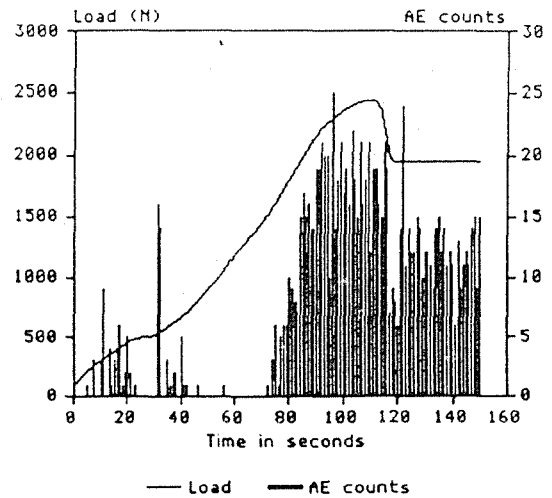
Figure 9: Load-AE curve for delamination at the 3- and 4-ply.

General comments

In all the 3 cases discussed above, the AE signals were present during the load hold due to reasons explained in section 2.4 of the paper. This emission tapers off and finally dies off. The amplitude of this "relaxation" emission is more prominent after a crack had extended. A possible reason was that the crack is still unstable and takes a while to reach an equilibrium state. Therefore, it is possible that some important emission were not recorded due the Nicolet recordings as was observed in Case 2 where an increase in AE activity was expected at the strain peaks.

CONCLUSION

The postbuckling shape of the specimen is different for different geometric configurations and depends on the location of the delamination point on the specimen. In all the crack growth observed, the delamination grow towards one end - the upper delaminated region and could be due to lack of perfect symmetry of the test fixture.

An increased in acoustic emission activity was observed during a reversal of strain signs accompanying a crack opening and also during a crack extension. It might be possible to quantify the energy of this signal with the fracture energy and this work is in continuing.

The use of the technique of acoustic emission to detect the onset of delamination and crack extension is viable. However, much work still needs to be carried out to obtain a quantifiable results as to the extent of the crack - its length and its propagation direction and correlating them with the acoustic emission energy.

REFERENCES

Journals.

1. Awerbuch, J., And Eckles, W.F., "Detection of Failure progression in Cross-ply Graphite/Epoxy through Acoustic Emission", Proceedings of the International Symposium on Composite Materials and Structures, Beijing, China June 10-13, 1986, pp. 889-898.

2. Benzeggagh, M., Prel, Y., And de Charentenay, F.X., "Experimental analysis of Mode I delamination testing", Proceedings of the Fifth International Conference on Composite Materials (ICCM-V), San Diego, California, July 29-30, August 1, 1985, pp. 127-139.

3. De Charentenay,F.X., And Benzeggagh, M.,"Fracture Mechanics of Mode I Delamination in Composite Materials," Advances in Composite Materials, Proceedings of the Third International Conference on Composite Materials, Paris 26-29, August 1980, Vol. 1, Bunsell, A.R. Et Al (eds), pp. 186-197.

4. De Charentenay, F.X., Harry, J.M., Prel, Y.J., and Benzeggagh, M.L., "Characterising the Effect of Delamination Defect by Mode I Delamination Test," Effect of Defects in Composite Materials, ASTM STP 836, American Society for Testing and Materials, 1984, pp. 84-103.

5. O'Brien, T.K., "Characterisation of Delamination Onset and Growth in a Composite Laminate," Damage in Composite Materials, ASTM STP 775, K.L. Reifsnider (ed.), American Society for Testing and Materials, 1982, pp. 140-167.

A SOUND INTENSITY BASED MEASURING FACILITY
FOR SOUND POWER AND SOUND TRANSMISSION LOSS

Richard W. Guy
Centre for Building Studies
Concordia University
CANADA

Junping Li
Centre for Building Studies
Concordia University
CANADA

ABSTRACT

A small hemi-anechoic chamber was constructed to facilitate sound power measurements by the point to point intensity technique and ISO draft standard 9614 was followed to validate a test procedure and qualify results.

The facility, which also forms part of a sound transmission loss suite, is described and simple schemes are presented for the validation and calibration of the intensity measurement system. Results are presented which suggest that a criterion and some field indicators of ISO 9614 require modification and that the minimum specified measurement distance of 0.5 metres could be reduced.

1.0   THE TEST FACILITY

The test facility is shown diagrammatically in Figure 1, and consists of a vibration isolated hemi-anechoic chamber lined with acoustic wedges on five of its sides, the floor being surface sealed concrete. The chamber can be the reception room to a reverberant source room for sound transmission loss measurements, or isolated for sound power measurements as in the present case. The hemi-anechoic chamber provides optimal measurement conditions by way of minimizing extraneous noises and room effects; it also allows the prospect of floor mounted source directivity evaluation, should that be necessary.

The Bruel & Kjear Sound Intensity Analyzing System Type 3360 is employed and arrangements have been made to semi automate measurements by way of software controlled probe placement and test sequencing (Guy, R.). The test equipment configuration is shown in Figure 2.

2.0   EQUIPMENT CALIBRATION

For the current pressure - pressure probe and real time band analyzer, one must consider at least two equipment calibration tests:

    2.1)   Intensity Calibration
    2.2)   Residual Pressure Intensity Index Measurement.

2.1 Intensity Calibration Intensity calibration was undertaken in a discrete frequency plane wave generated within a standing wave tube. The tube must have dimensions to accommodate the probe with minimal field distortion, and tube termination conditions must exist which support unidirectional net energy flow. In the present work, comparable results have been achieved between the Bruel and Kjear calibrator type 3541, and tests within the 100mm (4") tube of the standing wave apparatus, B&K type 4002.

The tube based tests were undertaken at 1kHz and with an arbitary but a high absorptive termination as shown in Figure 3. The test procedure involves measurements of the pressure maxima and minima whilst confirming the constancy of measured intensity along the tube. Application of simple standing wave theory then leads to instrument calibration.

2.2   Residual Pressure-Intensity Index The Residual Pressure-Intensity Index δ_{PI_0} is a measure of inherent probe and instrumentation channel phase mismatch applicable in finite difference probe systems and in the present work, use was made of the 30 mm (1") standing wave tube of the B&K Type 4002 and an acoustic coupler similar to the B&K type WA 0344 as shown in Figure 4. Couplers for ¼" and ½" microphone probes were manufactured in house to push fit onto the otherwise open tube end. Care should be taken to ensure symmetrical microphone placement within the coupler, and

that microphone cartridge vents receive similar field exposure. The generated sound field should also be adjusted to yield pink noise over the frequency bands of interest.

3.0 FIELD CHECK

Prior to each measurement one must perform at least two standard equipment checks, namely sound pressure level calibration with a suitable calibrator and Sound Intensity Measurement with Probe Reversal.

The probe reversal test must be undertaken at all bands of interest and serves two purposes; as a check on channel phase difference and as confirmation of intensity direction sensing. To facilitate tests independent of the sound power measurement environment, a probe reversal test apparatus was constructed as shown in Figure 5.

4. THE MEASUREMENTS

A small rectangular source of dimensions 345 x 235 x 200 mm high was placed in the centre of the hemi-anechoic chamber and a conformal surface profile at 70 cm from the source surfaces was chosen for measurement.

Sixty four points for each of the five test surfaces (total 320 points), each representing constant square measurement areas, were sensed for both pressure and intensity in the third octave bands 125 Hz to 4 kHz over the measurement surface. A measurement averaging time of 16 seconds was chosen to be in compliance with a $BT = 400$ requirement, where B is the lowest filter bandwidth and T is the averaging time.

The sound power measured is shown in Figure 6 and the results together with the measurement array could now be validated according to the requirements of the draft standard.

5. QUALIFICATION REQUIREMENTS

The ISO Draft Standard 9614 states "In order to guarantee upper limits for uncertainties of the sound power levels determined, it is necessary to check the adequacy of the instrumentation and of the chosen measurement parameters (e.g. measurement surface, distance, microphone array) in relation to the sound field/environmental condition particular to the specific measurement".

Checks involve evaluating four field indicators, F_2, F_3, F_4 and F_5 with F_2 and F_4 subsequently being employed to validate the grade of measurement by way of two criterion tests. The field indications are discussed in detail by Fahy and Hübner. The indicators for the present test at 70cm are shown in Table 1.

6.0 THE SURFACE PRESSURE-INTENSITY INDICATOR F_2 AND CRITERION 1

The indicator F_2 is prominent in the check for measurement equipment adequacy by comparing it with a dynamic capability index L_d which is a positive value.

A criterion 1 is deemed satisfied in the proposed standard if $L_d > F_2$ for the chosen measuring surface.

Table 1 displays F_2 for the present test and it is clear that Criterion 1 is satisfied for all grades of measurement. It may be noted however that F_2 assumes negative values at the 125Hz third octave band; this is thought due to standing wave effects at low frequencies despite the high absorption of the room surfaces and in their presence Criterion 1 as stated is not a qualifying parameter since any negative would satisfy.

7.0 THE EFFECT OF MEASUREMENT DISTANCE

The point to point intensity measurement procedure is time consuming by comparison with the alternative intensity based procedure of surface scanning both in actual measurement and generally in measurement assessment, so that one may question the reason for selecting the point to point technique.

One reason involves the prospect of interrogating measurements to yield diagnostic information, that is, where is the energy of a given frequency emanating, or, what contribution does a particular component appear to have. In a suitable measurement environment, at an appropriate measurement distance, one might also consider identifying the directional characteristics of the source.

To realise diagnostic capability it is desirable to be as close as practical to the source surface, (typically not closer than ten centimetres to render insignificant finite difference approximation errors). The draft standard imposes an average minimum distance requirement of 50 centimetres for sound power measurements and it is useful to test the need for this restriction in order to avoid a separate test procedure for diagnostic purposes. Accordingly two further sound power measurements employing 320 measurement points were undertaken with conformal surface profiles but at distances of 10cm and 30 cm, respectively from the source.

The sound power measured at 10, 30, and 70 cm are shown in Figure 6. Clearly agreement between each is good.

8.0 CONCLUSIONS

A facility providing good conditions for sound power measurements by the point to point sound intensity technique has been constructed, and the measurement procedure found satisfactory with respect to measurements in compliance with ISO draft Proposal 9614. However the minimum allowable surface to measurement distance of

the draft standard could be reconsidered to allow a closer probe to surface placement and the Criterion 1 should be restated to consider the prospects of negative indicator F_2.

REFERENCES

Journals

Guy, R.W., "Running a Test in an Intensity Based Measurement Facility" Canadian Acoustics, Vol. 18, No. 3, 1990, p. 31-45.

Proceedings

Hübner, G., "Sound Intensity Measurement Method - Errors in Determining the Sound Power Levels of Machines and its Correlation with Sound Field Indicators" Proceedings Internoise 87, Beijing, P.R. China, pp. 1227-1230

Books

Fahy, F.J. "Sound Intensity" Chapter 8, Pub. Elsevier Applied Science, London & New York, ISBN 1-85166-319-3, 1989.

Standards

International Standard Organisation (ISO), Draft Standard 9614 "Determination of the Sound Power Levels of Noise Sources Using Sound Intensity Measurements at Discrete Points", ISO/DIS 9614-1, 1989.

FREQ. Hz	Ld, dB	F_2	F_3	F_4	N PRECISION	N ENGINEERING
125	1.9	-0.09	-0.09	0.36	20	20
160	1.3	0.62	0.62	0.40	20	20
200	2.1	1.07	1.07	0.39	20	20
250	3.4	0.83	0.83	0.45	20	20
315	3.9	0.10	0.10	0.66	20	20
400	5.6	0.56	0.56	0.85	21	20
500	10.6	1.03	1.03	1.32	49	26
630	8.2	1.03	1.03	1.33	50	27
800	8.7	0.18	0.18	1.57	222	69
1000	9.7	0.83	0.83	1.44	187	59
1250	8.0	0.72	0.72	1.05	99	31
1600	8.9	1.18	1.18 *	0.83	63	20
2000	9.2	1.54	1.54	1.23	136	43
2500	10.6	1.31	1.31	1.19	113	35
3150	11.5	1.40	1.40	1.14	118	37
4000	3.78	1.84	1.84	1.02	94	30

TABLE 1: ISO Indicators F_2, F_3 and F_4, and Required Measurement Points for Given Classification at 70 cm Measuring Distance.
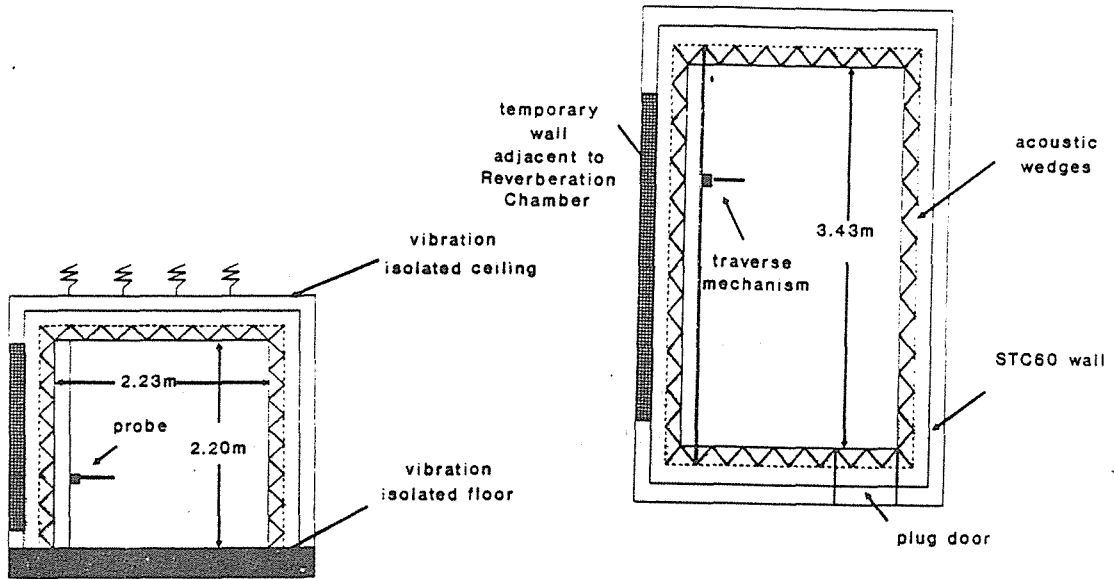
Figure 1: Configuration of the Hemi-anechoic Chamber
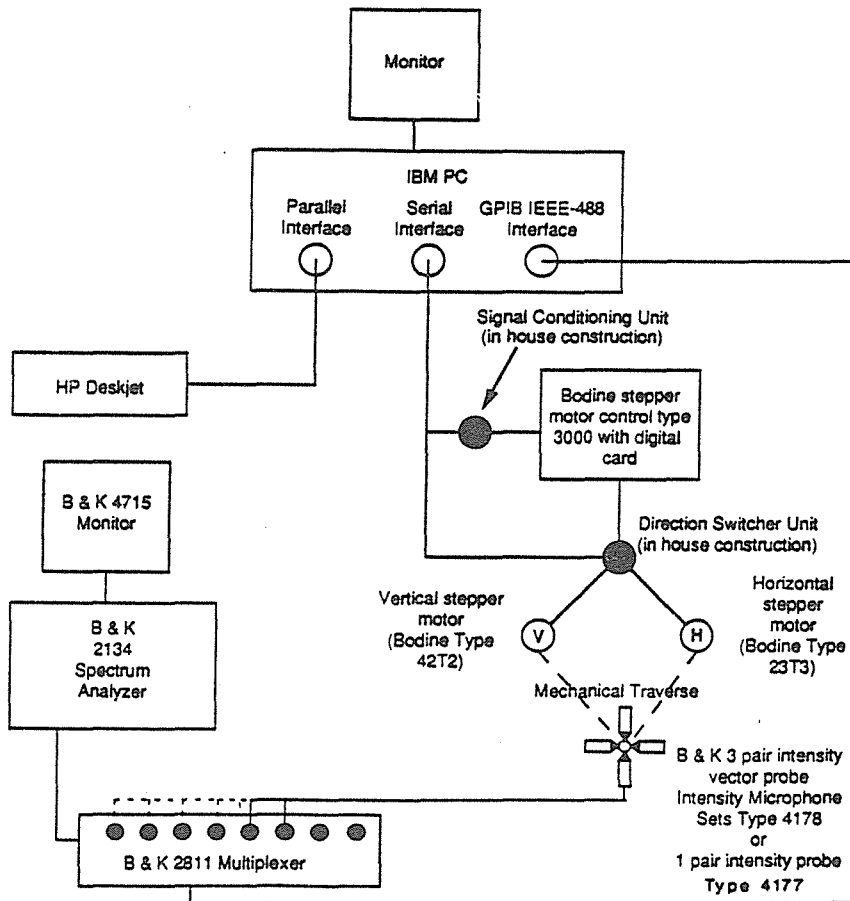
Figure 2: Configuration of Lab Equipment

restraining
mesh

High absorbent
termination

centre mounted
intensity probe

100mm diameter
tube

uncapped
end

NOISE
SOURCE

push rod

support framework
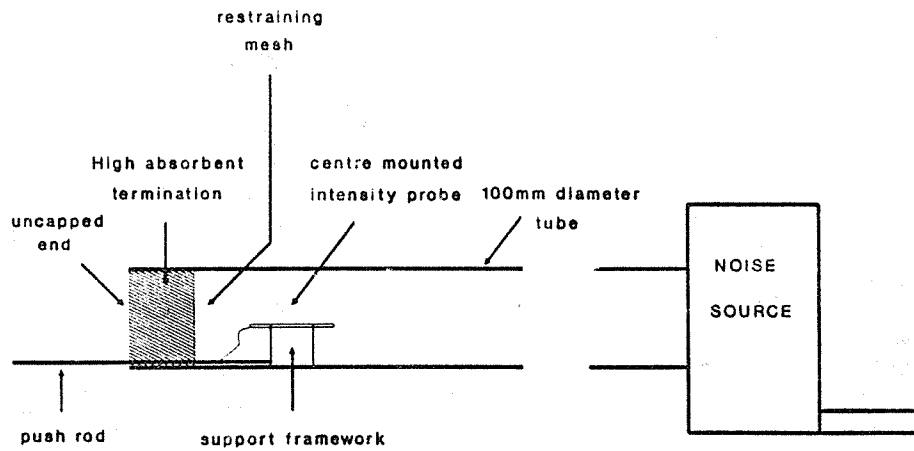
Figure 3: Intensity Calibration within a Standing Wave Tube

intensity microphone pair

Pink Noise

termination cap

30mm tube of
standing wave apparatus
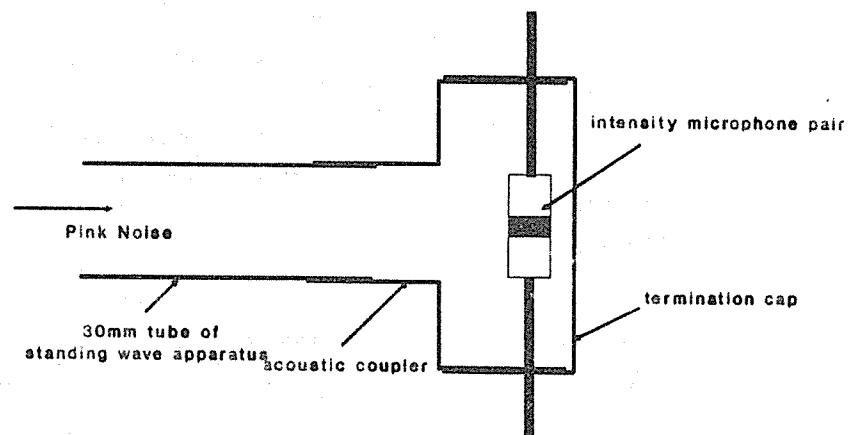
acoustic coupler

Figure 4 : Acoustic Coupler Arrangement
for Pressure-intensity Index

542
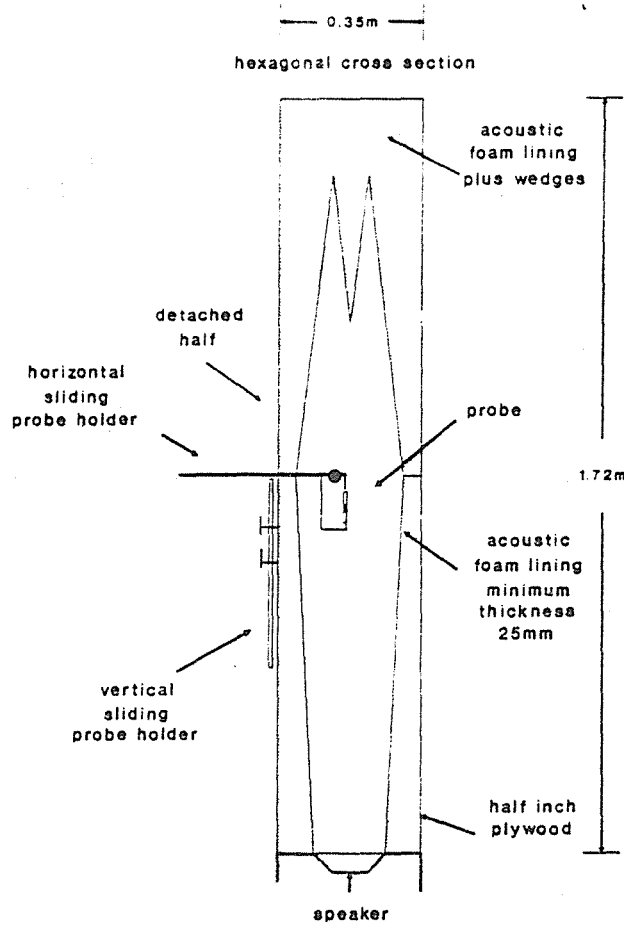
Figure 5: Probe Reversal Test Apparatus

SWL at 10cm   SWL at 30cm   SWL at 70cm
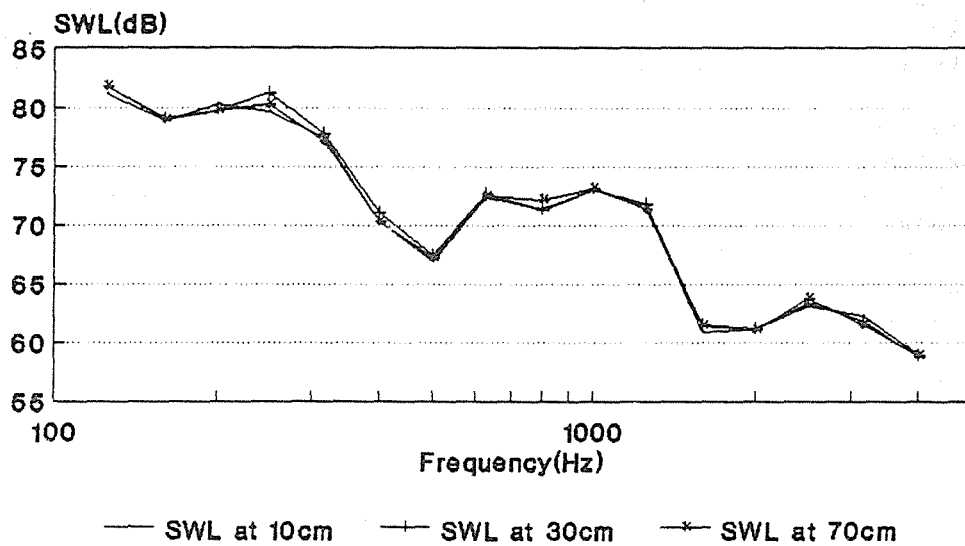
Figure 6: Sound Power Measurement of a
Rectangular Source. Measurement Distance
70cm, 30cm and 10cm.

SOUND FIELD DESCRIPTION BASED ON COMPLEX INTENSITY

Mingzhang Ren
The Acoustics Laboratory, Technical University of Denmark, Building 352,
DK-2800 Lyngby, Denmark; on leave from Department of Mechanical
Engineering, Xi'an Jiaotong University, People's Republic of China

Finn Jacobsen
The Acoustics Laboratory, Technical University of Denmark, Building 352,
DK-2800 Lyngby, Denmark

Kevin Bernard Ginn
Brüel & Kjær, Nærum Hovedgade 18, DK-2850 Nærum, Denmark

ABSTRACT

The fundamental application of the sound intensity technique is the
determination of the sound power of a source in the presence of other
sources. However, with a modern intensity analyser one can determine not
only the usual active intensity (i.e. the real part of the complex
intensity), but also the reactive intensity (i.e. the imaginary part).

This paper examines and discusses the usefulness of the two components of
the complex intensity with particular regard to source identification.
From a theoretical and experimental study of the interference of two
monopoles it is concluded that at low frequencies the reactive intensity
near a source is less affected by the presence of a neighbouring coherent
source, and thus easier to interpret, than the active intensity. The
reverse is the case at high frequencies. It is also observed that the
reactive intensity decreases more rapidly with the distance to the source
than any other energy-related quantity.

Together these observations lead to the conclusion that the reactive
intensity is useful for localising and identifying regions of an extended
complex source that would exhibit significant sound radiation *in
isolation*. Combined with the actual radiation pattern, which can be
determined with active intensity, this leads to a sound field description
that is useful for noise control.

1.0 INTRODUCTION

The concept of complex sound intensity was introduced more than 40 years ago (Westervelt P.J.). The first descriptions of practical methods of measuring the complex intensity were published much later, though (Stanton T.K. and Beyer R.T.; Pascal J.-C. 1981; Elko G.W.), and whereas sound intensity analysers that can determine the active intensity have been on the market for more than a decade, equipment that can measure both the active and the reactive intensity directly has been commercially available only for a few years.

The usefulness of equipment for determining the active intensity, which represents the flow of sound energy, is quite obvious, and the sound intensity technique is now an important, well-established supplement to more conventional measurement techniques for sound power determination. This is reflected in the fact that an international standard on sound power determination using intensity has been issued recently (ISO 9614-1); and another standard is well under way (ISO DP 9614-2).

The utility of the reactive intensity is less obvious, although many authors maintain that this quantity provides useful information (Pascal J.-C. 1985; Mann J.A., Tichy J. and Romano A.J. ; Tichy J.; Jacobsen F.). The reactive intensity indicates the presence of a sound field where the pressure and the particle velocity are in quadrature. Several authors have suggested that the reactive intensity might be useful for identifying source distributions and for distinguishing between active and passive absorbers of sound, and have presented experimental results that hint that this is indeed the case (Mann J.A. and Tichy J.; Ginn K.B. and Hald J.), but a clear analysis of the value of the reactive intensity for this purpose has never been given.

It would seem that the *active* intensity was useful for localising regions of an extended source with particular strong radiation - and indeed it is in some circumstances, as demonstrated e.g. by a study of source identification on a diesel engine (Reinhart T.E. and Crocker M.J.). However, the sound power radiated by an individual component source is affected by the presence of neighbouring coherent component sources, and this fact can make source identification on the basis of active intensity impossible - and even meaningless: in some conditions a source may act as a sink. Of course, the active intensity indicates the actual distribution of sound radiation, but this can be extremely difficult to interpret because of the interaction of coherent component sources. Complicated near fields with local regions of negative intensity have been observed by many authors (Hansen C.H. and Bies; Pettersen O.K.Ø 1979; Kihlman T. and Tichy J.).

The purpose of this paper is to examine and discuss the usefulness of active and reactive intensity for describing and analysing sound fields with particular regard to identifying and localising sources.

2.0 COMPLEX SOUND INTENSITY

The complex sound intensity is a vector that describes the coherent relation between the sound pressure and the particle velocity in a sound field. It is usually defined in terms of the complex amplitudes of these quantities, as follows:

$$\vec{I}_c = \vec{I} + j\vec{J} = \frac{1}{2}p\vec{u}^*. \tag{1}$$

However, complex notation is valid only for pure-tone sound fields. A more general definition expresses the quantity in terms of the real measurable time signals $p(t)$ and $\vec{u}(t)$ (Jacobsen F.):

$$\vec{I}_c = \vec{I} + j\vec{J} = \overline{p(t)\vec{u}(t)} + j\overline{\hat{p}(t)\vec{u}(t)}, \tag{2}$$

where the symbol $\wedge$ denotes the Hilbert transform.

The real part of the complex intensity is the usual active intensity, which is a vector that represents the sound power flux density. The remarkable interest in the sound intensity technique over a period of more than ten years is evidently due to the fundamental relation

$$\int_S \vec{I} \cdot d\vec{S} = \int_V \nabla \cdot \vec{I} dV = P_a, \tag{3}$$

which states that the time-averaged net sound power generated within a given volume equals the integral over the enclosing surface of the normal component of the active intensity.

The imaginary part of the complex intensity, the reactive intensity, represents coherent but non-propagating, oscillatory sound energy flux. The reactive intensity points out of a source (Mann A.J. and Tichy J.). It is proportional to the gradient of the mean square pressure (Pascal J.-C. and Carles C.),

$$\vec{J} = -\nabla\overline{p^2(t)} / (2\rho ck), \tag{4}$$

from which it can be deduced that surfaces of equal sound pressure are orthogonal to the trajectories of the reactive intensity (Mann J.A., Tichy J. and Romano A.J.). The divergence of the reactive intensity is proportional to the difference between potential and kinetic energy density (Westervelt P.J.; Elko G.W.; Pascal J.-C. 1985),

$$\nabla \cdot \vec{J} = 2\omega (w_{pot} - w_{kin}), \tag{5}$$

which leads to the interesting relation

$$\int_S \vec{J} \cdot d\vec{S} = \int_V \nabla \cdot \vec{J} dV = 2\omega \int_V (w_{pot} - w_{kin}) dV = 2\omega (E_{pot} - E_{kin}), \tag{6}$$

which is valid for a surface without sources in it. It is characteristic of the acoustic near field of a source that the kinetic energy density exceeds the potential energy density. From equation (6) it may be concluded that the integral of the normal component of the reactive intensity over the surface of a source is proportional to the excess kinetic energy associated with the near field of the source.

3.0 INTERFERENCE OF TWO POINT SOURCES

Since the main problem in interpreting near field sound intensity data is due to interference effects, it would seem that a reasonable starting point was to examine how the complex intensity near a monopole source is affected by the presence of another monopole. (Many authors have in fact studied interference effects produced by point sources (Pettersen O.K.Ø.

1981; Krishnappa G.; Elko G.W.; Prasad M.G. and Ham S.Y.; Fahy F.J.), but most of these studies had a slightly different purpose.)

3.1 Theoretical Model. The two harmonic monopoles shown in Figure 1 produce the sound pressure

$$p = j\rho\omega\frac{Q_1 e^{-jkr_1}}{4\pi r_1} + j\rho\omega\frac{Q_2 e^{-jkr_2}}{4\pi r_2}e^{j\phi} \tag{7}$$

at the position P. From this expression the particle velocity, the potential and kinetic energy density, and the active and reactive intensity can be determined through simple but tedious calculations (Ren M.). The results show that the reactive intensity decreases more rapidly with the distance to the combined source than any other energy-related quantity. Finally one may normalise the two components of the complex intensity in the x-direction with the corresponding

Figure 1. The model of two monopoles.

components as they would be in the absence of the second source (I_0, J_0). The result is the two expressions

$$\frac{I_x}{I_0} = 1+q^2(\frac{r_1}{r_2})^3+q\frac{r_1}{r_2}(1+\frac{r_1}{r_2})\cos[k(r_2-r_1)-\phi]$$
$$+ \frac{q}{kr_2}(1-(\frac{r_1}{r_2})^2)\sin[k(r_2-r_1)-\phi] \tag{8}$$

and

$$\frac{J_x}{J_0} = 1+q^2(\frac{r_1}{r_2})^4+q\frac{r_1}{r_2}(1+(\frac{r_1}{r_2})^2)\cos[k(r_2-r_1)-\phi]$$
$$- qk(r_2-r_1)(\frac{r_1}{r_2})^2\sin[k(r_2-r_1)-\phi], \tag{9}$$

where the parameter $q=Q_2/Q_1$ has been introduced. (Similar expressions were derived in (Prasad M.G. and Ham S.Y.)).

Equations (8) and (9) express how the active and reactive intensity components near a monopole are affected by another coherent monopole. It is apparent - and hardly surprising - that the effect of the second source depends on its relative strength, on how far it is from the observation point, and on the phase angle between the two sources. It can also be seen that negative active and reactive intensity can occur; this is well known (Pettersen O.K.Ø. 1981; Elko G.W.). However, the last terms of both expressions are interesting: they reveal that the influence of the disturbing source on the active intensity is most significant at low frequencies and decreases systematically with the frequency, whereas the influence on the reactive intensity increases with the frequency. This explains why it has been observed that reactive intensity maps of near fields can be easier to interpret than active intensity maps at low frequencies.
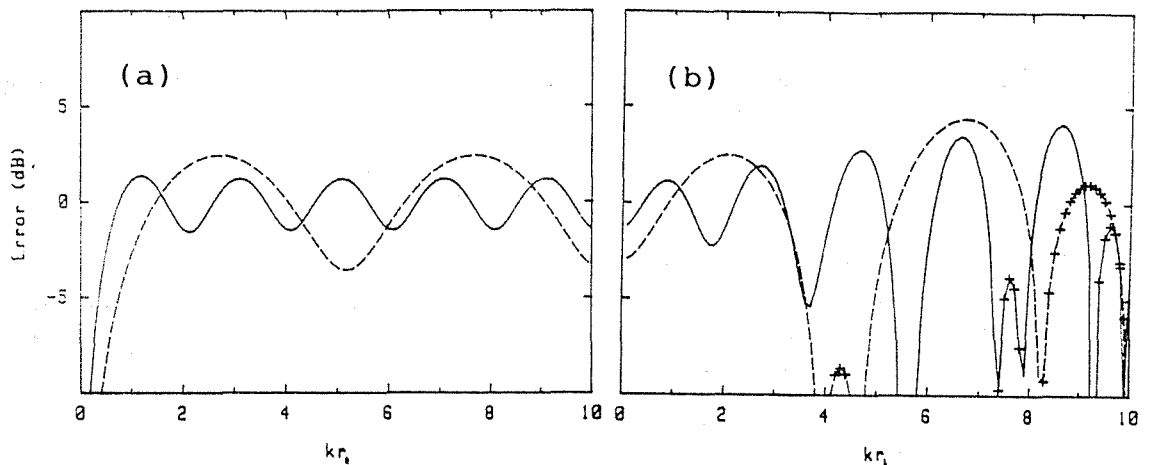
Figure 2. Effect of interfering monopole on (a) active intensity and (b) reactive intensity for q=1 and φ=π. ———, r_1/h=0.25; ----, r_1/h=0.5. *Crosses indicate negative values.*

In Figures 2 and 3 are shown examples of how I_x/I_0 and J_x/I_0 vary with frequency; further examples can be found in (Ren M.). Although it is more or less obscured by alternating constructive and destructive interference, the tendency mentioned above is apparent.
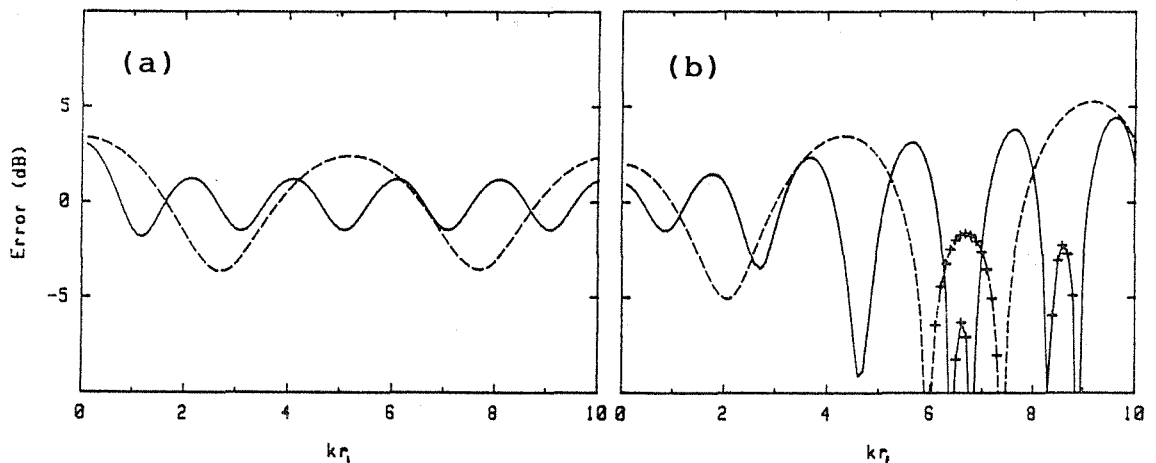
Figure 3. Effect of interfering monopole on (a) active intensity and (b) reactive intensity for q=1 and φ=0. ———, r_1/h=0.25; ----, r_1/h=0.5. *Crosses indicate negative values.*

3.2 Experimental Results.

A few experiments with two small, enclosed loudspeakers mounted in a baffle have been carried out. The experimental arrangement is sketched in Figure 4. The loudspeakers were driven with signals from a generator that can produce two pure-tone signals with variable phase difference, Hewlett Packard 8904A. The active and reactive intensity components were determined with an intensity probe, Brüel & Kjær 3545, combined with a real-time analyser, Brüel & Kjær 2133.

r=10cm. h=25cm (r/h=0.4)
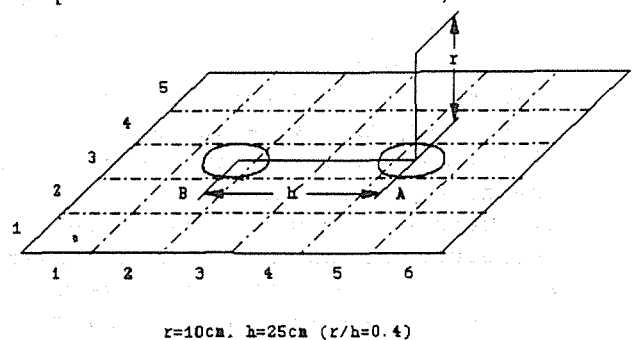
Figure 4. Two loudspeakers mounted in a baffle.

Figures 5 and 6 show some of the results of mapping the active and reactive intensity in a plane over the baffle. At this low frequency, 200 Hz, the reactive intensity assumes higher values than the active intensity, and identification of the two loudspeakers on the basis of the reactive intensity is indeed much easier than identification on the basis of the active intensity.

(a)   (b)
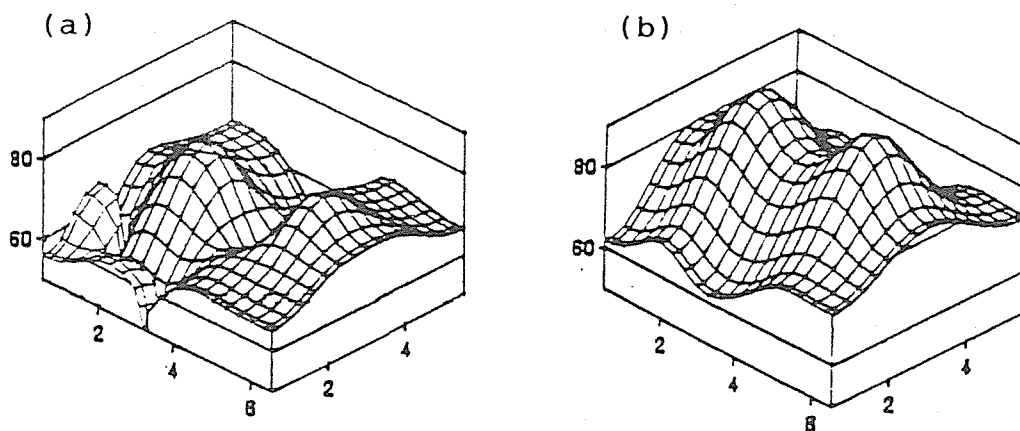
Figure 5. Active (a) and reactive (b) intensity distribution in a plane over the baffle with the two loudspeakers driven with 200 Hz in opposite phase and with equal strengths. The thin lines indicate a region with negative intensity.

(a)   (b)
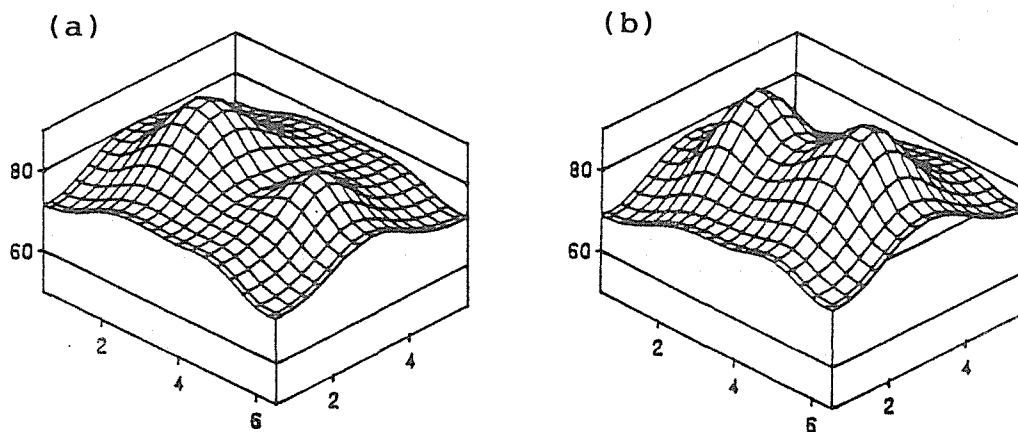
Figure 6. Active (a) and reactive (b) intensity distribution in a plane over the baffle with the two loudspeakers driven with 200 Hz in quadrature; q=0.5.

4.0 DISCUSSION

Identification and location of individual incoherent component sources on the basis of active intensity are, at least in principle, straightforward. By contrast, the very idea of localising neighbouring individual, strongly coupled *coherent* component sources is dubious or even meaningless, since it suggests that the local radiation is an attribute of a local source. This is not the case; the local radiation can be significantly altered, and the total radiation can be much stronger or much weaker than the sum of the individual radiations as they would be in isolation. In this case there is only one "source", the near

field of which is very complicated, and it is more or less meaningless to try to localise the individual component "sources" with active intensity. It is even less possible to deduce how one could reduce the total sound radiation from the near field distribution of active intensity, as pointed out by several authors (Fahy F.J., Ffowcs Williams J.E.). This does not matter, of course, if one is concerned with the actual radiation pattern and has no intention of modifying it. However, it may be useful in connection with noise control to know how each of several components of a complex source would radiate in the absence of the other components. The observations made in the preceding section suggest that the reactive intensity, at least at low frequencies, offers indications of "potential sources", that is, regions that would radiate if they were isolated. Unfortunately, there is no general relation between the reactive intensity and the strength of a source, though.

5.0 CONCLUSIONS

The usefulness of the two components of the complex intensity has been examined and discussed with particular regard to identifying and localising sources. The distribution of the active intensity near a large complex source demonstrates the radiation pattern. It also indicates the positions and strengths of the individual component sources that make up the complex source provided that these components are independent. If this is not the case, then the reactive intensity distribution offers valuable clues to how each of the components would radiate in isolation. This information may be useful in noise control.

REFERENCES

Elko G.W., _Frequency Domain Estimation of the Complex Acoustic Intensity and Acoustic Energy Density_, Ph.D. Thesis, Pennsylvania State University, 1984.

Fahy F.J., _Sound Intensity_, Elsevier, London, 1989, Sections 4.7, 7.2, 7.4 and 8.4.

Ffowcs Williams J.E., Letter to the Editor on M.Heckl's sixtieth birthday, _Acustica 72_, 79 (1990).

Ginn K.B. and Hald J., STSF - Practical Instrumentation and Applications, _Brüel & Kjær Technical Review 2_, 1-27 (1989).

Hansen C.H. and Bies D.A., Near Field Determination of the Complex Radiation Efficiency and Acoustic Intensity Distribution for a Resonantly Vibrating Surface, _Journal of Sound and Vibration 62_, 93-110 (1979).

Jacobsen F., A Note on Instantaneous and Time-Averaged Active and Reactive Sound Intensity, _Journal of Sound and Vibration 147_, 489-496 (1991).

Kihlman T. and Tichy J., Studies of Sound Intensity Measurements on a Steel Panel, _Proceedings of Inter-Noise 87_, 1231-1234 (1987).

Krishnappa G., Acoustic Intensity in the Nearfield of Two Interfering

Monopoles, _Journal of the Acoustical Society of America 74_, 1291-1294 (1983).

Mann J.A., Tichy J. and Romano A.J., Instantaneous and Time-Averaged Energy Transfer in Acoustic Fields, _Journal of the Acoustical Society of America 82,_ 17-30 (1987).

Mann J.A. and Tichy J., Extended Intensity Measurement Technique for Sound Field Identification in the Noise Source Nearfield, _Proceedings of Inter-Noise 88_, 105-110 (1988).

Pascal J.-C., Mesure de l'intensité active et réactive dans différents champs acoustiques, _Proceedings of International Congress on Recent Developments in Acoustic Intensity Measurements_, 11-19 (1981).

Pascal J.-C., Structure and Patterns of Acoustic Intensity Fields, _Proceedings of 2nd International Congress on Acoustic Intensity_, 97-104 (1985).

Pascal J.-C. and Carles C., Systematic Measurement Errors with Two Microphone Sound Intensity Meters, _Journal of Sound and Vibration 83,_ 53-65 (1980).

Pettersen O.K.Ø., A Procedure for Determining the Sound Intensity Distribution Close to a Vibrating Surface, _Journal of Sound and Vibration 66,_ 626-629 (1979).

Pettersen O.K.Ø., Sound Intensity Measurements for Describing Acoustic Power Flow, _Applied Acoustics 14,_ 387-397 (1981).

Prasad M.G. and Ham S.Y., Interference of the Acoustic Intensity and Pressure Fields of a Primary Source Due to a Secondary Source, _Proceedings of 2nd International Congress on Acoustic Intensity_, 105-112 (1985).

Reinhart T.E. and Crocker M.J., Source Identification of a Diesel Engine Using Acoustic Intensity Measurements, _Noise Control Engineering Journal 18_, 84-92 (1982).

Ren M., _Complex Intensity and Near Field Description_, The Acoustics Laboratory, Technical University of Denmark, Report No. 46 (1991).

Stanton T.K. and Beyer R.T., Complex Wattmeter Measurements in a Reactive Acoustic Field, _Journal of the Acoustical Society of America 65_, 249-252 (1979).

Tichy J., Noise Control Applications of Sound Intensity, _Proceedings of Inter-Noise 89,_ 45-68 (1989).

Westervelt P.J., Acoustical Impedance in Terms of Energy Functions, _Journal of Acoustical Society of America 23_, 347-348 (1951).

ISO _International Standard_ 9614-1 Acoustics - Determination of Sound Power Levels of Noise Sources Using Sound Intensity - Part 1: Measurement at Descrete Points (1990).

ISO Draft Proposal 9614-2 Acoustics - Determination of Sound Power Levels of Noise Sources Using Sound Intensity - Part 2: Measurement by Scanning (1991).

SOUND SOURCE IDENTIFICATION USING COMPLEX SOUND INTENSITY

Tsuyoshi Usagawa
Faculty of Engineering, Kumamoto University,
2-39-1 Kurokami, Kumamoto 860, JAPAN
Phone : +81-96-344-2111 (Ext.3622), Fax : +81-96-345-1553

Masanao Ebata
Faculty of Engineering, Kumamoto University,
2-39-1 Kurokami, Kumamoto 860, JAPAN
Phone : +81-96-344-2111 (Ext.3623), Fax : +81-96-345-1553

ABSTRACT

The identification of noise sources is important for
effective noise control. Especially, the identification
and control of noise source itself are very important for
an small noisy equipment because the control of noise and
vibration in the propagation path is usually difficult. In
such an occasion, the identification of noise sources is
required. When we analyze a small equipment, sound
intensity measurement provides more information than
conventional pressure measurement because the sound
intensity is a vector quantity of the acoustic energy
flow. This paper presents a method to identify multiple
point sources using complex sound intensity, and discusses
the performance of the proposed method through simulation.
The proposed method estimates sound sources using the
least square error criterion of estimated intensity
vectors. The computer simulations are carried under four
cases in which two or three point sources radiate sound.
The estimation error is depend on the combination of
sources, relative phase, relative volume velocity and
relative position of each other. In the case of three
point sources which are 60mm apart from each other, the
proposed method can separate point sources when relative
phases are known.

1.0 INTRODUCTION

Living and office equipments are going more quiet year by year, an equipment which had never been considered as noisy equipment comes to a serious noise source. An good example may be a refrigerator. Even it is one of the most quiet equipment in our living room, noise control of a refrigerator is required and an active control system is already announced (Saruta S. et al.). An active control system is very attractive method to control noise. However, before controlling, we need to identify the noise sources and study their characteristics first. Also the control in propagation path is more expensive to control individual noise source itself in some occasion. Considering from these standpoints, an identification of noise sources is important to realize an efficient noise control.

Usually, the source identification is based either on the cross-spectral technique or the method using the directional microphone or multiple ones. However, the direct utilization of the cross-spectral technique is not adequate when an individual source cannot be measured separately. Also the sufficient accuracy in the separation of noise sources is not provided using the analysis based on a directional microphone when the distance between noise sources is small compared with the wave length of sound. On the other hand, sound intensity measurement offers the information about energy flow of sound as vector quantity.

In this paper, the method to estimate characteristics of multiple noise sources is proposed using complex sound intensity. The proposed method is an expansion of previously proposed method which is utilized only active intensity (Usagawa, et al.). The proposed method tries to estimate position, magnitude and relative phase of volume velocity for each noise source on the assumption that each noise source is a point source. Basic idea for estimation is to reduce the mean square error of estimated complex intensity from observed complex intensity.

2.0 METHOD OF SOURCE ESTIMATION

2.1 Complex Sound Intensity
The active intensity vector I is defined as the time averaged product of pressure p and particle velocity vector **v** as follows (Tichy, Takahashi),

$$I = \overline{p\, \mathbf{v}} \ . \tag{1}$$

When we measure the sound field where the complex effective values of pressure and particle velocity are given as follows,

$$\begin{aligned} P &= p_0 \cdot \exp(j\phi_1), \\ V &= v_0 \cdot \exp(j\phi_2), \end{aligned} \tag{2}$$

the active intensity vector is given as,

$$I = \text{Re}[\ P \cdot V^* \ ].\tag{3}$$

where $*$ represents complex conjugate.
The reactive intensity vector is given as a produce of pressure and 90° phase-shifted particle velocity (Takahashi), so that the reactive intensity vector J is defined as

$$J = \text{Im}[\ P \cdot V^* \ ].\tag{4}$$

Unlike the active intensity vector, the sign of vector in the reactive intensity has no meaning. The complex intensity vector Π is given as a complex representation of active and reactive intensity as follows,

$$\Pi = I + jJ = P \cdot V^*.\tag{5}$$

2.2 Observed Complex Intensity in Multiple Sources Field

When a single point source is set in free field, the complex effective pressure and particle velocity vector are represented as follows,

$$P = j\omega\rho \cdot \frac{Q}{4\pi\ r} \cdot \exp(-jkr),\tag{6}$$

$$V_r = \frac{1 + jkr}{4\pi\ r^2} \cdot Q \cdot \exp(-jkr),$$

where ρ is the density of air, Q is the volume velocity of point source which is set at the origin of coordinate. V_r is the vector whose direction is the perpendicular to the surface of spherical wave front. From Eq.(6), the complex intensity vector is given as Eq.(7).

$$\Pi = P \cdot V^* = \frac{\omega\rho\ Q^2}{16\pi^2\ r^3} \cdot (kr + j)\tag{7}$$

Let assume that N point sources are in a free field as shown in Fig.1. $S_i = (x_i, y_i, z_i)$ represents the position of i-th source, Q_i is the absolute volume velocity and ϕ_i is the relative phase of volume velocity where $\phi_1 = 0$. The complex effective pressure and volume velocity vector for i-th source can be written as follows,

Observation Point M

Source #1
$(\ S_1,\ Q_1,\ \phi_1 = 0\ )$

Source #2
$(\ S_2,\ Q_2,\ \phi_2\ )$

z

Source #N
$(\ S_N,\ Q_N,\ \phi_N\ )$

o → y

x
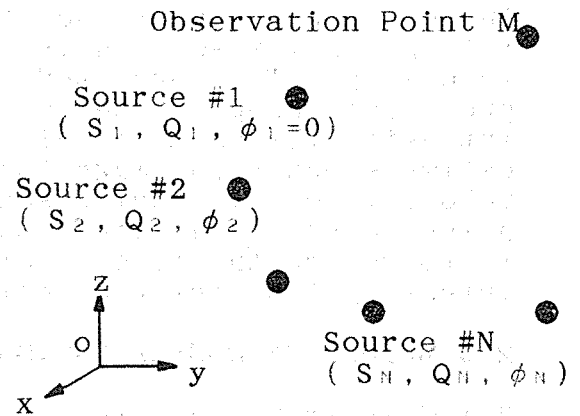
Fig.1 Model of N sources

$$P_i = j\omega\rho \cdot \frac{Q_i}{4\pi\ |S_i - M|} \cdot \exp(j(-k|S_i - M| + \phi_i))\tag{8}$$

$$V_i = \frac{1 + jk|S_i - M|}{4\pi\ |S_i - M|^2} \cdot \exp(j(-k|S_i - M| + \phi_i)) \cdot \frac{S_i - M}{|S_i - M|}.$$

So that the observed complex intensity is described as Eq.(9).

$$\Pi = \sum_{i=1}^{N} P_i \times \sum_{i=1}^{N} V_i\tag{9}$$

2.3 Estimation of multiple point sources ·

The error criterion for estimation is given as the following value E,

$$E = \sum_{i=1}^{N} | \Pi_i - \Phi |^2 \qquad (10)$$

where Π_i is the set of estimated complex intensity vectors while Φ is measured one. Although the number of point source, N, is also the big problem, we focus on the possibility of the source estimation of multiple sources so that we assume the number of sources is is treated separately.

The gradient of E is calculated using the partial differentiation of it when each of parameters are slightly changed. The parameter which gives steepest gradient will be changed as a specified step to reduce the value of E. The modification of each parameter is iterated until E becomes sufficiently small. Figure 2 shows the procedure of the proposed method.
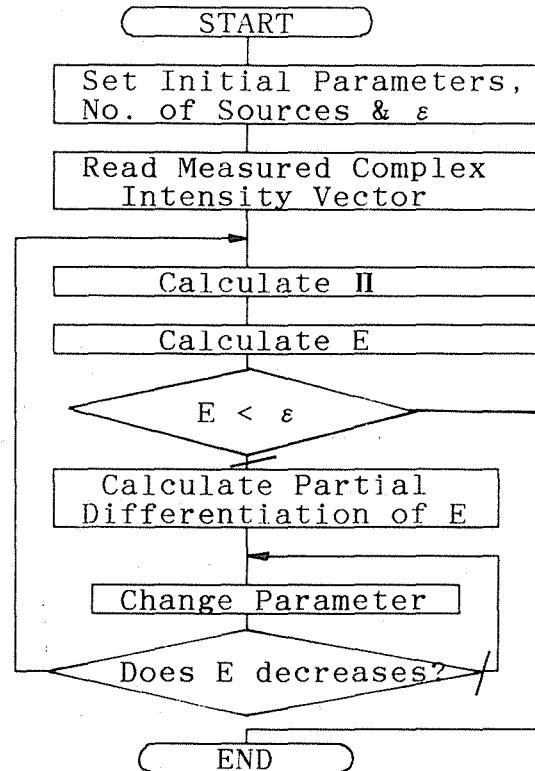
Fig.2 Flow of the proposed method.

3.0 MODEL EXPERIMENT

3.1 Condition of simulation

We simulate four cases. Conditions of sources are shown in Table.1. The complex sound intensity vectors are measured at 91 positions (7 X 13) on a plane whose dimension is 120mm X 240 mm. The intensity vectors are measured in each 20mm step. The origin of coordinate is one of noise source, and x- and y-axes are along with edges of plane. The measuring plane is rectangular shape whose opposite corners are (-60mm, -60mm, 80mm) and (60mm, 180mm, 80mm).

Basically the proposed method could estimate all of five parameters for each source; three dimensional coordinate, magnitude and relative phase of volume velocity. However, when we try to estimate all of five parameters, the proposed algorithm is not stable and sometimes not converged. So that we need to take care of phase as separate manner; at first, estimate other four parameters for each noise sources for certain phase condition, then change phase conditions and the final estimation is obtained as the set of parameters which gives minimum value of error criterion. In this paper, all simulations are done with a correct relative phase.

Table.1 Conditions of Simulation

No	Source ID	Position (mm)	Volume Velocity	Relative Phase
1	S1 S2	(0, 0, 0) (120, 0, 0)	1 : 1	0° :180°
2	S1 S2	(0, 0, 0) (120, 0, 0)	1 : 1	0° :90°
3	S1 S2	(0, 0, 0) (120, 0, 0)	2 : 1	0° :0°
4	S1 S2 S3	(0, 0, 0) (60, 0, 0) (120, 0, 0)	1:1:1	0° :180° :0°

Table.2 Results of Simulations

No	Error of Estimated Parameters (x, y, z) [mm] : ev [%]		
	S1	S2	S3
1	(1, 0, 2): 0	(2, 0, 2): 0	---
2	(1, 0,10):10	(2, 0,11):15	---
3	(4, 0, 7):15	(13, 0, 8):20	---
4	(11, 0, 4):25	(2, 0,16):65	(25, 0, 9):45

$ev = |V_{Estimated} - V_{True}|/V_{True}$: Volume Velocity

Initial positions of sources are set to S1 (-40mm, -40mm, -20mm) and S2 (160mm, 40mm, -20mm) for two sources condition and S1 and S3 for three sources condition are set to the same of S1 and S2 for two source condition, respectively, and S2 is set at (20mm, 40mm, -20mm).

3.2 Results of simulation

Table 2 shows the results of source estimation. Figure 3 to 6 show the results of source estimation in x-y plane with mesh representations for active and reactive sound intensity for the case 1 to 4, respectively.

Through case 1 to case 3, two point sources are located at the same depth with 120 mm separation. In case 1, the volume velocity is the same magnitude but out of phase. In case 2, the condition is the same as case 1 except that the relative phase of S2 is +90°. From these two results as shown in Fig.3 and Fig.4, the accuracy of estimated x and y positions is sufficient to identify and separate these noise sources. On the other hand, the error of estimation in z position is larger than one for x and y position and it has correlation with error in volume

(a) Active Intensity
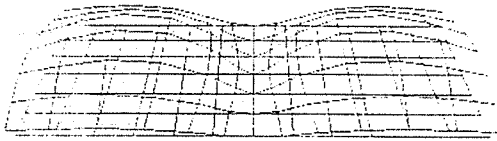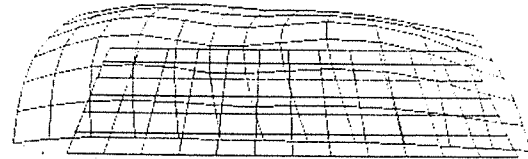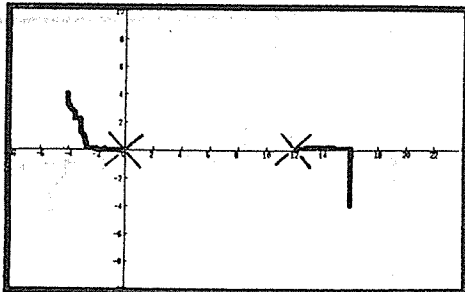
(a) Active Intensity

(b) Reactive Intensity

(b) Reactive Intensity
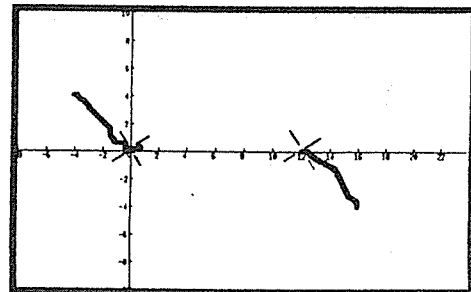
(c) Trajectory of Source
Estimation (x-y plane)
X : Position of Source

Fig.3 Result of Simulation
(Case 1 : Two anti-phase
sources with the same
magnitude of volume
velocity)

(c) Trajectory of Source
Estimation (x-y plane)
X : Position of Source

Fig.4 Result of Simulation
(Case 2 : Two 90° phase
shifted sources with
the same magnitude of
volume velocity)

velocity. In case 3, whose result is shown in Fig.5, the ratio of volume velocity is set as 2 : 1 with in-phase condition. Like as case 1 and 2, the error of z position is larger than one of x and y position and also the estimation of x position for the source S2, which has smaller volume velocity, is larger than one for S1.

In case 4, three point sources are set in a line with 60 mm apart from each other. The middle source has opposite phase to both side sources and volume velocity for all of three sources is the same. The result is shown in Fig.6. Although the error in volume velocity estimation is larger than one in case 1 through 3, the estimation error of position is almost the same as one for the case of two sources.

In all cases, the convergence of the estimation in y position is fastest in all parameters. This evidence seems that the effect of cross term of observed complex intensity vectors along y axis is smaller than ones along x and z axes. This is due to the arrangement of point sources; in all cases, two or three point sources are set in a line along x axis. In x- and z-axis components are
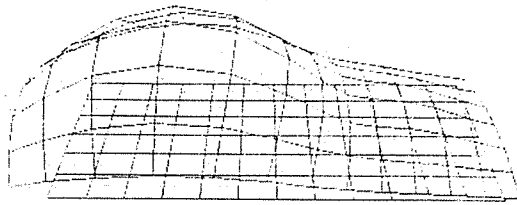
(a) Active Intensity

(a) Active Intensity

(b) Reactive Intensity

(b) Reactive Intensity
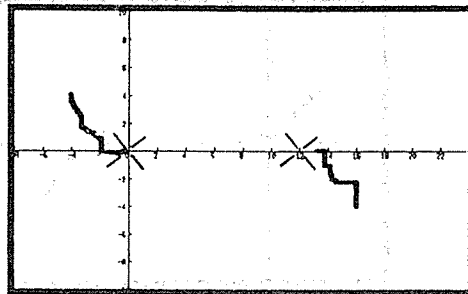
(c) Trajectory of Source
    Estimation (x-y plane)
    X : Position of Source

Fig.5 Result of Simulation
(Case 3 : Two in-phase
sources wiih different
[2 : 1] magnitude of
volume velocity)
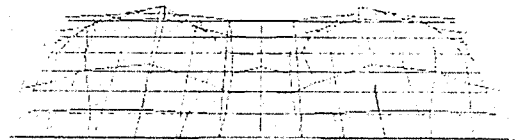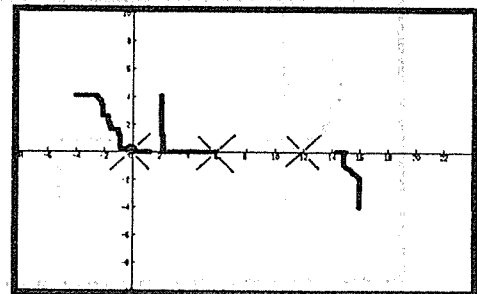
(c) Trajectory of Source
    Estimation (x-y plane)
    X : Position of Source

Fig.6 Result of Simulation
(Case 4 : Three sources
with same magnitude
of volume velocity and
center source is anti
phase)

more complex than y-axis one because of the effect of cross terms of observed complex intensity vectors.

4.0 CONCLUSION

Using the complex sound intensity in a sound field composed of multiple point sources, we proposed the method to estimate each sound source simultaneously. The performance of the proposed method is discussed by computer simulation. The results shows the possibility to identify the multiple sources even if they are located within 60 mm in the distance. Because the proposed method currently requires a priori knowledge about relative phase between sources, we need to modify the proposed method to utilize for practical usage.

REFERENCES
Saruta S., Tamura H., Nakanishi K., Sekiguchi Y., Suzuki S., Nagayasu K., Refrigerator Equipped with Active Noise Control System, Proc. Int. Sympo. on Active Control of

Sound and Vibration, 509-512, (1991)

Takahashi H., Master Thesis, Tohoku University, (1987) (in Japanese)

Tichy T., Sound Radiation and Sound Field Studies Using Sound Intensity Technique, Proc. of Sympo. on Acoustic Intensity, 70-86, (1987)

Usagawa T. and Ebata M., Identification of Multiple Sound Sources using Sound Intensity, Proc. IEEE ASSP Workshop of Digital Audio and Signal Processing (1989)

INTRODUCING TERTIARY STUDENTS TO ACOUSTICS

Ken Cook
Department of Applied Physics
Royal Melbourne Institute of Technology
GPO Box 2476V, Melbourne VIC 3001
AUSTRALIA

ABSTRACT

By way of introducing students to acoustics the Department of Applied Physics of Royal Melbourne Institute of Technology has in its degree course an element of acoustics in the second and third years. This has as a basis subjects in experimental techniques. Not only do the students receive training in handling equipment but they are made aware of standardised measurement techniques for dealing with problems faced by industry and the community generally. They are introduced to various concepts in acoustics. The facilities they use comprise transmission rooms and a reverberation room, impedance tube and equipment suitable for collection and analysis of data both in the laboratory and field. The application to real measurements is real since the facilities used have been certified by National Association for Testing Authorities, Australia (NATA). An introduction to acoustics is also provided to students studying other courses at the Institute.

1.0   INTRODUCTION

When a potential employer involved in the application of acoustics is seeking a graduate it is necessary for him to be aware of any undergraduate activity in the field of acoustics. It is therefore the purpose of this paper to bring to the notice of delegates/employers some of the details of the education provided in acoustics by the Department of Applied Physics, Royal Melbourne Institute of Technology. From this provision, previous graduates have found satisfactory, rewarding employment in industry and government establishments, and feedback has confirmed that the exposure to acoustics in the Applied Physics course has brought forward some expertise from the graduate.

2.0   COURSE DETAILS

2.1   Structure of undergraduate course

The course leading to the Degree of Bachelor of Applied Science (Physics) is of three years duration, and the current intake is 50. Experimental techniques are emphasised in four major streams, one of which is in applied acoustics, and takes place in the second and third years of the course.

In addition to laboratory subjects an elective subject of 13 hours duration is provided in building acoustics.

3.0   ACOUSTIC CONTENT OF B.APP.SC. COURSE

3.1   Second Year

In the second year of the course students spend 30 hours, over six weeks in the acoustics laboratory. Working in pairs, five exercises are carried out, selected from determination of absorption coefficient using the reverberation room or the impedance tube, audio measurements with amplifier and loudspeakers, vibration measurements, sound insulation and field measurements with subsequent laboratory analysis.

In general the exercises are based on current measurement standards to which the student is expected to refer and make comments. Use is made of the facilities and equipment which is under certification by the National Association of Testing Authorities, Australia (N.A.T.A.), so the student is made aware that they are working with refined equipment and facilities. The student is required individually to maintain a workbook for observations, and is required to submit for assessment a full report on three of the five exercises. During the final session each student delivers a 15-minute dissertation on one exercise with respect to the results obtained and the practical application of such results.

An elective subject in building acoustics is offered to second year students over 13 one-hour lectures. The topics covered are sound fields in enclosures, sound power, sound absorption, sound transmission and single-number ratings of transmission losses, subjective acoustics, the interpretation of measurement standards and the requirements of the National Building Code.

3.2   Third Year

In the third year of course a student may elect either to carry out a project for a total of 36 hours in the laboratory or a more advanced project for a total of 72 laboratory hours. Such are individual projects arising from

topics selected by staff, from queries raised either by Standards Association (since a member of staff is a member of the Acoustics nd Vibration Board and member of two standards sub-committees), practical problems raised by a section of the institute or may be a project of special interest to the student. Proper preparation is expected from the student by a literature search.

Even though a member of staff is available for assistance a student is encouraged to progress individually and independently. A detailed report is submitted on the project. A dissertation is given on the aim and extent of the project, the results obtained and recommendations on the applications of such findings. Examples of such projects include:

Noise reduction of a chainsaw
Low frequency sound absorption by audiences
Extent of the direct sound field in a reverberation room
Sound transmission loss by a transient pulse method
Acoustic foam performance by the optical interference technique
Extention of the frequency range of a loudspeaker
Rapid impedance tube measurements on perforated absorbers
Acoustic properties of brown coal
The optimisation of a sound absorbing system by impedance tube.
Measurement of noise in public telephone booths
Noise control of a household washing machine
Noise control measures at a rehabilitation centre
Vibration measures and control of noise from optical bench
The acoustic conditions of a reading room at State Library
Noise control of commercial electric hand-drier
Attenuation of structure-borne noise
Miniature reverberation room
Single-number rating of field transmission loss
Pulse mode modulation for sound recording

On occasions a project may arise as a side-study when an acoustic test is being conducted for a client from industry. This enables the student to see at first hand the part played by acoustics in a real-life situation.

A subject in the third year is the Industrial Elective where the student works in industry, a government laboratory or consultant (acoustic or other) for a total period of 21 days. Some of the destinations made available are in the field of acoustics. On the completion of this subject a written report is submitted both by the student and by the host organisation.

4.0   EXPERIENCE FOR PHYSICS STUDENTS

4.1   Benefits of laboratory techniques

By participation in the laboratory subjects offered over the two-year period the student will:

I.   Receive an introduction to the concepts of acoustics

II.   Become accustomed to using acoustic equipment to carry out specific measurements in a variety of fields

III.   Be familiar with measurement standards and their use to determine some acoustic properties of materials, structures, to feel confident in

estimating the reliability of measurement and accordingly the expression of answers to a desired confidence interval.

IV.   Be able to investigate environmental and industrial acoustic problems and means of their solution.

V.   Develop skills in communication by way of the preparation of a written report on the extent of a project and the likely applications of the results.

VI.   Cultivate acceptable, readable habits in recording the work carried out during experimental work.

VII.   Possess the ability to verbally present the results and application of an investigation in a concise manner.

VIII. Be given opportunities to attend technical meetings convened by the Australian Acoustical Society, with the chance to meet people actively involved in practical acoustics.

4.2   Benefits of industrial elective

By having been exposed to the outside world for a reasonable period the benefits have been:

I.   The student has been able to see how problems in industry are solved in the most practical way

II.   If there has been a likely interest in the type of work carried out by the host organization the student is fortunate to be able to do a "trial run" to confirm that desire or otherwise.

III   In the event the host organization has been seeking an employee they have the opportunity to have the student on trial - in more than one instance, as a result of this subject the student has been offered employment on graduation. Such examples have been working with an acoustic consultant, with Environment Protection Authority, to become a project manager for a firm producing acoustic enclosures and audiometric rooms.

Apart from the student point of view the host organization, having made the casual vacancy available, is in a position to assess the success of the Department of Applied Physics' intention to introduce tertiary students to acoustics.

5.0   POSTGRADUATE OPPORTUNITIES

It is possible for a graduate to undertake research in acoustics leading to the Degree of Master of Applied Science (Physics). The time taken for such a programme is either 2 years full time or 4 years part time. To date some three people have undertaken such research and have subsequently entered industry. Research is currently being undertaken into the acoustic absorption performance of materials in a high-pressure environment, up to 50 atmospheres. A paper on the progress of this work will be presented at Internoise 91.

It is also possible to carry out undergraduate research leading to Doctor of Philosophy, though to date there has been no candidate.

6.0   OTHER EDUCATION OFFERED IN ACOUSTICS

6.1   Students in other departments

On knowledge of the expertise available Applied Physics has been approached by other departments in the Institute to provide introductory courses in acoustics. As a result the following short courses are currently being offered:

I.   To first year students in Construction Economics and Building - the part played by acoustics in sound absorbing and sound insulating applications, importance of subjective acoustics and hearing protection.

II.   To second year students in Architecture - sound in enclosures, sound absorption and insulation

III. To third year students in Interior Design - similar course to that for architecture students. Their subsequent project in a home subject is to give consideration to acoustic comfort.

6.2   Short courses offered externally

More than one single-day course has been provided for those in industry involved with the production, distribution and retailing of acoustic materials. Even though several were not tertiary in standard the course was offered following several requests from industry. By necessity the course was restricted to sound absorption and sound insulation.

Following a request from a large governmental institution a lecture course of 24 hours has been provided to a group of people, principally engineers. The field of study was concerned with the attenuation of sound from a noise-producing plant, currently under threat of closure due to noise intruding in residential premises.

7.   CONCLUSION

It has been illustrated that the Department of Applied Physics is and has been endeavouring to introduce tertiary students to acoustics, especially in the experimental and practical field. Through experimental work, opportunities have been created to ensure that the student is aware of the methodology used in the outside world and this is enhanced by having the student spend a period with people in industry concerned with acoustics. The department welcomes the interest and attention by industry to make employment opportunities for its graduates.

References

RMIT Faculty of Applied Science Handbook 1991: Undergraduate and postgraduate programmes.

EXERCISES FOR UNDERGRADUATE STUDENTS
ON
THE USE OF SOUND LEVEL METERS

Warren C Middleton

Centre for Medical and Health Physics
Queensland University of Technology, Brisbane

ABSTRACT

Three sets of introductory experiments have been developed to facilitate understanding of

(1)   the design and use of the sound level meter,

(2)   the emission and propagation of sound in open space, and

(3)   sound in enclosed spaces.

This paper describes experiments and exercises on microphone sensitivity, amplifier gain control, frequency weighting, one and one-third octave filters, time weighting, integrating circuits, the divergence of sound, the addition of decibels, the effect of wind, the effect of atmospheric absorption, standing wave patterns and spatial averaging.

These experiments have been successfully trialled with undergraduate students in Engineering, Science, the Built Environment, Environmental Health and Occupational Hygiene at an Australian University of Technology.

1.0 INTRODUCTION

Though classical acoustics had its birthplace in ancient Greece and Rome, it is only in recent decades that the science of acoustics has come into prominence. In fact, it was only in the 1970's that international standards began to recognise the need for standardisation of quantities and units of acoustics (ISO 31:1978). Despite this advance several years ago, international standards (ISO 31, Part 0 : 1981) and national standards (AS 2900.0 : 1986) do not recognise the need for an acoustic quantity as a fundamental quantity though the need for a photometric fundamental quantity has long been recognised.

There has been a great emergence in recent times of community relevance as regards noise with the advent of numerous standards, codes of practice and pieces of legislation dealing with the problems associated with environmental noise, occupational noise and architectural and building acoustics.

Despite this emergence, there is little available in the way of laboratory and/or field manuals on training exercises in acoustics or little published involving worked problems. Reasons for this may be that there is rather a restricted market and that there is some difficulty normally encountered with some of the idiosyncrasies of acoustics.

With a view to meeting the needs of a variety of undergraduate students in Engineering, Science, the Built Environment, Environmental Health and Occupational Hygiene, a series of exercises have been developed at the School of Physics, Queensland University of Technology.

2.0 DESCRIPTION OF THE EXERCISES

2.1. Exercises on the Design and Use of the Sound Level Meter

Laboratory manuals describe instrument controls and procedures for the operation and calibration of the instrument but do not generally provide learning exercises on the principles involved in the design of the instrument.

These exercises are designed to provide such learning experiences. They relate to six components or functions of sound level meters; they include use of both integrating and non-integrating meter types and involve both analogue and digital readouts. They are described briefly below.

(a)   Microphone Sensitivity

The aim of this exercise is to give some appreciation of a microphone as a pressure transducer and some knowledge of the quantities used to describe its sensitivity.

It involves calculations only for the situation of a calibrator producing a known pressure input p_{in} for a microphone for which the output voltage v_{out} is given. The calculations include the determination of

(i)   the microphone sensitivity M_c in $V\ Pa^{-1}$ from the equation

$$M_c = \frac{V_{out}}{P_{in}},$$

(ii)   the microphone response level n in dB re 1 V Pa^{-1} from the equation

$$n = 20\ \log_{10} \frac{M_c}{M_{c\ ref}},\ \text{and}$$

(iii)   the K-factor of the microphone as the amount by which its response level differs from the value of -26 dB re 1 V Pa^{-1}.

(b)   Amplifier Gain Control and Calibration of Sound Level Meter

The aims of the exercise are

(i)   to show how a sound calibrator may be used to set the fine gain
           control of the amplifier to the appropriate level for the sound
           level meter to be in calibration,

(ii)   to show how the amplifier output voltage varies when the gain
           control setting is varied, and

(iii)   to show what happens to the voltage signal when the gain is
           increased too much and the readings have to be disregarded.

The equipment needed is simply the sound level meter, the calibrator, the
output lead for the meter, a cathode ray oscilloscope and an adjusting
screwdriver. One or more meter types can be used. An intrinsic learning
experience involves the different methods of reading the sound pressure
level for analog and digital instruments.

Calculations include determinations of the voltage level for each gain
control setting and comparisons of the change in output voltage level
with the change in gain setting.

(c)   Frequency Weighting

The aim of this exercise is to show how the A-weighted and the C-weighted
sound pressure levels depend upon the frequency content of the sound
being measured.

By measuring the A-weighted and C-weighted sound pressure levels of two
sound sources of different frequencies, students can determine the
difference between A-weighted and C-weighted sound pressure levels at
these two frequencies.

This difference can then be compared with that given in graphs or tables
for A- and C-weighting networks.

The learning experience is quite dramatic if the sound sources are, for
example, a calibrator at 1 kHz and a pistonphone at 250 Hz. An important
side issue is the need to use C- or linear weighting when calibrating a
sound level meter at a frequency of 250 Hz.

(d)   Time Weighting

The aim of this exercise is to show how the measured sound level can
depend, for certain noise types, upon the response time of the rectifier
circuit of the indicating meter.

Two types of noise are used :

(i)   a steady-level noise such as from an electric drill (possibly
           pre-recorded), and

(ii)   an impulsive noise from the dropping of the ball bearing onto a
           metal plate from a height of say 20 cm.

'Slow', 'Fast', 'Impulse' and 'Peak' rectifier response times may be used
depending on the sound level meter being used.

Comparisons are made between the readouts for these different response
times for both the steady-state noise and the impulsive noise and the
results are explained in terms of graphs showing the rectifier responses
when set to the different time weightings.

Apart from the learning experience regarding the difference between steady-state and impulsive noise and the different levels given for impulsive noise on 'S', 'F' and 'I', there is the demonstration, in the case of a steady noise source, of the amplification built into the 'P' time weighting.

(e)   Frequency Analysis

The aim of this exercise is to perform a frequency analysis of the steady-state noise from an electric drill at one-octave intervals with filters of one-octave bandwidth, and then, from the octave band levels so obtained, to determine the noise rating number (NRN) and to compute the A-weighted and C-weighted sound pressure levels and finally to compare these values with values measured at the same time as the octave band levels.

The exercise could be extended to include the use of one-third octave band filters at one-third octave steps to show the equivalence between a one-octave filter and the appropriate three one-third octave filters. Various other exercises on acoustic filtering could be incorporated.

(f)   Displayed Parameter

The aim of this exercise is to give an appreciation of 'equivalent level L_{eq}' and 'sound exposure level SEL' and the relationships between them. One or two meters may be used to determine the L_{Aeq} and the SEL_A values of a steady state noise for times T of 30, 60 and 120 seconds respectively and the relationship $SEL = L_{eq} + 10\log \frac{T^x}{T_o}$ where $T_o = 1$ second may be tested.

Students would observe the L_{Aeq} value remaining constant while the SEL_A value would increase by 3 dB(A) for each doubling of time.

Time varying noise could be included to give further learning experiences.

2.2.   Exercises on the Measurement of Sound in Free Fields

Traditionally, exercises in this area relate to the presence of reflecting bodies and the need to have sound level meters held well out from the human body.

The set of exercises described below is designed to demonstrate some aspects of sound propagation in approximately non-reflecting fields.

(a)   Divergence of Sound from a Small Source

This exercise is designed to compare the divergence, in an open space outside, of the sound from the loudspeaker of the cassette player with the divergence, in a free field, of sound from a uniform point source.

A-weighted sound pressure levels L_A due to the source are measured at increasing distances from the source and a background level is then obtained.

L_A values, corrected for background, may then be plotted as a function of distance and the consequent relationship compared with the traditional drop-off of 6 dB per doubling of distance for a uniform point source. Inferences can be made regarding the nature of the source.

(b)   Superposition of Sound Waves and the Addition of Decibels

The aim of this exercise is to show the way in which decibel values are 'added'.

To minimise complications due to standing waves, the exercise is conducted using a specially constructed absorption chamber, inside which the sound field is somewhat similar to what it would be in a free field.

Of the two speakers used inside the chamber, one is maintained at a fixed level while the other speaker's level is incremented in steps of 2 dB(A). A-weighted sound pressure levels due to each speaker separately and then due to both speakers together are measured. Levels due to the two speakers are predicted from the measured values of the separate levels by 'decibel addition' and these values compared with the measured values of the combined levels.

The decibel addition may be conducted using the formula

$$L_n = 10 \log_{10} \sum_{i=1}^{i=n} 10^{0.1L_i}$$

or from a graph or nomogram.

Exercises could be included on 'decibel subtraction'.

(c)   Effect of Wind and the Use of a Windscreen

This experiment demonstrates the effect of wind and the way in which a microphone windscreen reduces these effects. It is performed, however, indoors not outdoors.

In a place where the background noise level is low, the A-weighted and the C-weighted sound pressure levels are measured of

(i)   the background only,

(ii)   the background while someone is blowing on the microphone, taking care not to put any moisture on the microphone, and

(iii)   the background under conditions (ii) above but with a windscreen on the microphone.

Inferences may be made regarding the frequency content of the background noise, the frequency content of wind, which readings would be most wind-affected (A-weighted or C-weighted) and the effectiveness of a windscreen in reducing the effects of wind and whether or not the windscreen reduces noise levels generally.

(d)   Effect of Atmospheric Absorption

This exercise is intended to demonstrate that the atmosphere attenuates the higher frequencies of sound much more than the lower frequencies.

Traffic noise from a freeway is observed from two positions:

(i)   close to the freeway (say within 30 m), and
(ii)   further from the freeway (say 600 m away),

preferably within the space of a few minutes and at a time when dense traffic is flowing continuously, and ideally just after it has been raining.

The character of the noise at each location is observed and the difference in character is explained in terms of absorption data for sound propagation in air contained in handbooks (Harris 1981).

2.3   Exercises on the Measurement of Sound in Enclosures

(a)   Standing Wave Pattern in a Room

A signal generator is used to drive a loudspeaker at frequencies in turn of 500, 1000 and 4000 Hz. The speaker is faced into the corner of a room. At each frequency the ear is used to locate positions of maximum and minium sound pressure level and estimates are made of the distances between nodes or antinodes in both vertical and horizontal directions.

A sound level meter may be used to obtain an estimate of the variation in sound pressure level from node to antinode within the standing wave.

The extension of this exercise to the case of random noise (rather than pure tone) demonstrates why standing waves are not always aurally or instrumentally detectable.

(b)   Spatial Averaging

The aim of this exercise is to show when spatial averaging rather than arithmetic averaging should be used.

Two sets of L_A values are used for averaging, one set differing by much less than 5 dB(A) and the other set differing by much more than 5 dB(A).

Both sets are averaged arithmetically and spatially, in the latter case using the formula

$$ \overline{L} = 10 \log_{10} \frac{1}{n} \sum_{i=1}^{i=n} 10^{0.1L_i} $$

for the spatial average $\overline{L}$.

The averages are compared for the two sets of levels.

An extra challenge may be provided by asking under what conditions the spatial average of a set of sound levels L_i would be equal to the temporal average or equivalent level of the same set of levels.

3.   INFORMATION AND INSTRUCTIONS FOR THE SET OF EXERCISES

3.1.   Layout of the Notes

The information and instructions are contained in a thirty-one page document with headings - Introduction, Summary, Aim, Theory, Equipment, Experiments and Appendices.

A brief description is given of the contents of several of these sections.

3.2.   Theory

Topics include

(a)   Nature and Characteristics of Noise,

(b)   Sound Propagation and Sound Fields,

(c)   Response of the Human Ear to Sound (including frequency and intensity limits and decibel scales),

(d)   Instruments Used to Measure Sound - Both Integrating and Non-Integrating (including microphone, amplifier, filter networks, rms detector and response times and external filters), and

(e)   Measures of Noise (including percentile levels, equivalent level and sound exposure level).

3.3   Equipment

Reference is made to the particular instruments used in the set of exercises, to their setting up, calibration and use. Reference is also made to the sound sources (including calibrators) which are used as well as to any other equipment.

3.4   Instructions

General instructions, which indicate that no error analysis is necessary, are followed by detailed instructions on each exercise. It is considered that any treatment of accuracy confuses the basic issue of imparting understanding and developing skills in the basics of noise measurement.

The instructions for each exercise include pre-designed tabulations for data entry as required. An example is given below in Table 1.

Table 1   **A-weighted and C-Weighted Sound Pressure Levels of Sound Sources of Different Frequencies**

Sound Source	A-Weighted Sound Pressure Level L_A dB(A)	C-Weighted Sound Pressure Level L_C dB(C)
Brüel and Kjaer Calibrator Type 4230 (1 kHz)		
Brüel and Kjaer Pistonphone Type 4220 (250 Hz)		

3.5   APPENDICES

These include information on

(a)   A- and C-Weighting Characteristics,
(b)   One-Octave and One-Third Octave Band Filters,
(c)   Noise Rating Curves, and
(d)   Decibel Scales and the Addition and Subtraction of Decibels.

4.0   ORGANISATION AND PERFORMANCE OF EXERCISES

The set of exercises provide a versatile set of practical learning experiences which can be organised to cater for

(a)   the limitations of time, space and equipment which may apply,

(b)   the course/subject/syllabus constraints,

(c)   the educational attitudes and objectives of the teaching staff involved, and

(d)   individual or group learning techniques.

Special requirements which need consideration are obviously sound insulation, open space with low steady background and an absorption box.

5.0 DISCUSSION

Once the organisational challenges are met, the set of exercises has a tendency to release spontaneous perception in the minds of those performing the exercises. They have a reputation for generating amongst students considerable understanding of some of the difficult principles and practices of noise measurement.

The greatest learning developments are achieved in those groups of students for whom noise assessment is known to be an essential part of their professional practice. Amongst such students are those training as Health Surveyors and Occupational Hygienists.

The greatest gains amongst such students are made when the exercises are performed towards the end of their undergraduate training when their motivation is strong and their professional attitudes more highly developed.

The learning acquired through the intelligent performance of the set of exercises provides an excellent base for further development through specialised training experiments, projects and research in areas such as environmental noise, occupational noise and architectural and building acoustics (including engineering noise reduction).

6.0 REFERENCES

Australian Standards Association, AS 2900.0 Quantities, Units and Symbols, Part 0 - General Principles Concerning Quantities, Units and Symbols, 1986.

Australian Standards Association AS 2900.7 Quantities Units and Symbols, Part 7 - Quantities and Units of Acoustics, 1986.

Harris, C.M. (Ed), Handbook of Noise Control, 2nd Edition, McGraw-Hill, New York, 1979, 3-10.

International Organisation for Standardisation, ISO 31, Part 0 : General Principles Concerning Quantities, Units and Symbols, 1981.

International Organisation for Standardisation, ISO 31, Part 7; Quantities and Units of Acoustics, 1978.

ACOUSTICS INSTRUCTION FOR ARCHITECTS AND BUILDERS OF THE FUTURE

Ray Wilson
School of Architecture and Building
Deakin University Geelong, Victoria, Australia.

ABSTRACT

At Deakin University's School of Architecture and Building, students in Building Science Acoustics attend lectures on a weekly basis, and will soon be seeing regular videotapes of site visits, practical demonstrations and experiments. Many of the video images are generated on computer, and most importantly many of the video images are captured and stored on computer. The success in using video as an aid to teaching is only significant when used in conjunction with a Computer Assisted Learning program. Typically the students will watch a video in a class situation and a discussion will follow. Sections of the video are captured and combined with computer-based audio, graphics, animation, and question/answer prompting. Each student is required to arrange a time when he or she can sit at a CAL equipped computer in the school's Design Computing Centre.

Although genuine demonstrations and site visits are not easily replaced, 'multimedia' is a great improvement on lectures only.

1.0 INTRODUCTION

For many years now, university lecturers and school teachers have relied on traditional methods of teaching to convey the principles and concepts of the sciences. With ever increasing class sizes, resources are stretched to the limit. Practical exercises are becoming more impractical. This paper describes how multimedia is being used as an aid in the teaching of acoustics at Deakin University.

2.0 WHY USE MULTIMEDIA TO TEACH?

2.1 Teaching Acoustics to Architecture Students.

In 1988 the acoustics class at Deakin University consisted of sixty-five level two Architecture students. During that year students attended a series of lectures as well as toured the Victorian Arts Centre, the National Tennis Centre, and the Melbourne Sports and Entertainment Centre. Each student also took part in five acoustics practical experiments including the measurement of reverberation time and the related calculation of sound absorption coefficients of particular materials, the recording of personal audiometric data, and a variety of sound measurement and frequency analysis experiments. The supervisory role in these sessions involved two members of staff a total of four full days.

2.2 Class Sizes Increase; Practical Work Becomes Impractical.

In 1989 Deakin University commenced its new Bachelor of Building Degree Program. It was decided that all level one building students should study acoustics with the architecture students. This combined with the already large contingent of architecture students studying acoustics resulted in a class size in excess of one hundred and thirty. There was little chance that the practical experiments which had been conducted in previous years could be conducted in 1989. Even the site visits were restricted to the Tennis Centre and Entertainment Centre.

2.3 What Made Me Think of Multimedia?

Halfway through 1989, I was approached by a firm of hardware/software developers to join their team of researchers on a full time basis whilst lecturing at Deakin part time. I came into contact with IBM PC multimedia products for the first time. After a few months I left this company and soon agreed to work full time at Deakin. Since discovering the power of multimedia my mind had been wild with excitement at the prospect of applying it to the teaching of acoustics. I had admitted to myself that the simulation of practical demonstrations was better than none at all. As my role at Deakin also included the management of the School's new Design Computing Centre, I had control over the perfect multimedia 'playback' facilities.

3.0 WHICH HARDWARE AND SOFTWARE SHOULD I USE?

3.1 What Facilities for Replay are Available?

The Design Computing Centre included seven colour Macintosh II computers and twelve colour IBM PC clones. Each was configured for Computer Aided Design and was quite capable of replaying most multimedia applications. As a lecturer in Computer Aided Design (CAD) on both IBM and Mac platforms, I felt no bias towards one or the other when I first began investigating prospective multimedia hardware and software. Deakin and I arranged an agreement whereby I would establish the 'Design Computing Research Centre' and utilise my personal equipment, this in turn would be supplemented with Deakin owned equipment from funds which I had generated through externally advertised CAD Training Courses. My contribution included a colour Macintosh II and an IBM PC-AT clone.

After several weeks considering the options, I decided that the Macintosh was the most appropriate platform for my situation. During the latter months of 1989, I concluded that it had superior colour graphics on a standard machine (Mac IIcx), stereo sound output, and easy to use/learn mouse driven interface. My research also showed that multimedia hardware and software choices for the Mac were also more abundant. The most dominant negative in choosing the Mac was simply expense. In general, it was safe to assume that the Macintosh and all related multimedia hardware and software would be very expensive. I elected to live with this and proceeded to establish my Macintosh Multimedia Development Workstation.

3.2 Audio and Video Digitising.
The extra hardware components to be chosen for my workstation were based mostly on versatility and cost factors. I wanted to replay sound on seven different Macintosh's without the expense of additional audio cards for each, so I looked for sound digitisers capable of this and found only the MacRecorder. It is a touch crude and relatively inexpensive, but adequate for the type of work I have done so far. I hope to obtain a higher quality audio digitising card before proceeding too far into this project.

Making a choice of Video Digitising hardware was quite complex. I wanted a card that could digitise (capture) SVHS Video with maximum colours and resolution. It also was required to record computer images to SVHS Video tape. Ideally it would double as a good quality 24-bit graphics card for use in CAD applications. It would also be used to 'Chroma Key' computer generated images into video photography for recording to SVHS tape. I purchased a NuVista 4M Videographics card at a cost of around $10000.Following is a diagrammatic summary of the equipment used:
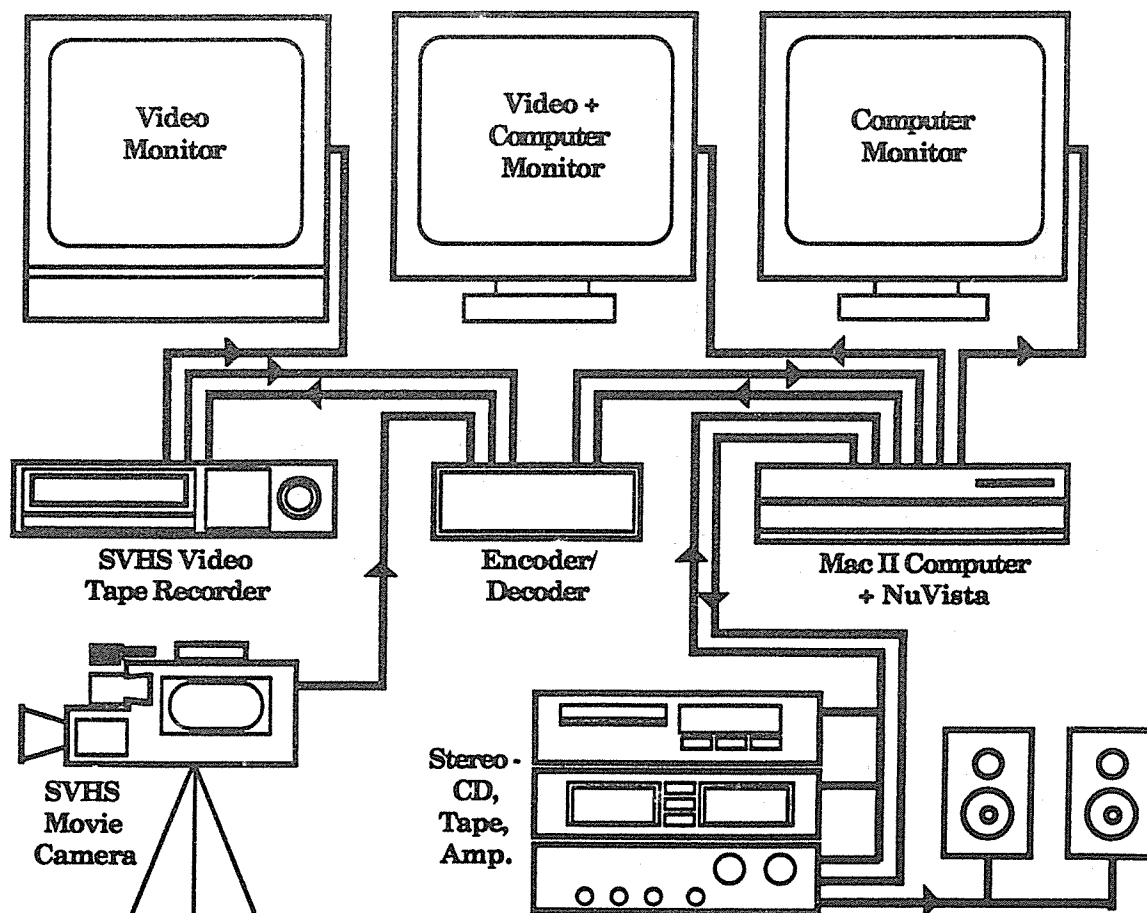
3.3 Software Choices.

Having already established that the replay machines are colour Macs, Hypercard was ruled out as unsuitable as it was only black and white. My next choice was a colour equivalent to Hypercard. There were two; Supercard and Plus. Based on reviews and advise from several consultants, I went with Plus, but found it to be very limited in the area of animation. I soon discovered MacroMind Director. This was a package based on animation (Video Works), and the new addition of an interactive component made it perfect for the work I was involved in.

Hypercard, Plus and Supercard, are all very similar in structure. Each uses a database containing graphic displays of data in a card like format. Quite complex card arrangements are possible. Each card has an address and can be called up for display using mouse driven buttons. Cards can contain a variety of text and graphics. In the early months of 1990, none of these packages had good animation. They achieved animation by flipping between cards very quickly. This proved unsuitable. Once I had seen MacroMind Director I felt it was exactly what I needed. It had excellent animation, graphics, and text, and handled interaction very well.

MMDirector software is not card based. Instead it uses a stage with castmembers, and allows digitised audio and video to be included in 'performances' easily. Castmembers can in fact be graphics, text, audio and video captures, and all are easily controlled by the program 'developer' (perhaps the 'program director' sounds more appropriate!) by inserting them into the 'score'. The 'score' controls when 'castmembers' will appear on 'stage'! MMDirector also includes a built-in paint package, which is capable of most simple editing functions.

4.0 USING MACROMIND DIRECTOR

I have been working with MMDirector for nearly two years now, and haven't yet mastered the more complex avenues available to me. It may not rate as an easy package to master, but it certainly is very easy to get started, and like many detailed software packages, the mastering only comes from regular and imaginative use. As a user/lecturer in CAD, I know quite well that the more complex a software product the longer and harder it is to master. I feel that the key to using MMDirector successfully is to fully utilise the simpler concepts, then venture into the depths of the product.

5.0 THREE ACOUSTICS DEMONSTRATIONS USING MMDIRECTOR

I have three acoustics examples which are quite different in their approach to the use of MMDirector. The first is a simple example explaining the concept of sound shadow. The student opens the file and it commences running without further prompting. It will keep repeating until the student stops it with the appropriate key sequence. This demonstration includes animated graphics with synchronised sound and text boxes explaining the various images.

A diagrammatic illustration using colour, animation, and related audio, assists in explaining a concept which may otherwise be quite difficult to convey.

The second demonstration requires the student to click on screen buttons to move on to the next part of the lesson. This assists in allowing students to work at their own pace. A combination of graphics, text and audio are utilised to clarify the differences

between Pink and White Noise. This has proved a most useful exercise as definitions are displayed simultaneously with the replay of each audio track. The related graphics are very simple, but also reinforce the students understanding.

Once again the combination of animated colour illustrations with related audio has greater impact than more traditional alternatives.

The third package is a simple sound level meter simulation. This involves the on-site video/audio recording of several sound sources. A single video image of each is captured and digitised, and the audio for each is digitised also. These are used to give some realism to the exercise. The simulation is one where the student reads through a set of screen based instructions on how to use the sound level meter, then interacts with the computer to change the settings on the image of a dBA sound level meter. By adjusting the settings on the meter correctly, a positive reading is possible, and the sound source appears to be measurable. i.e. the needle on the meter is animated to simulate the correct sound pressure level. Until the meter settings are correct, a dBA reading is not possible.

The sound level meter demonstration can be broken down into several specific areas. The exercise commences with a number of instruction screens. Once each of these is read, the student 'clicks' on the mouse to continue. The student soon comes to a menu screen where a choice of sound source is made. If the student selects the source labelled 'Circular Saw' MMDirector moves along to the section of the score which relates to the Circular Saw. The first image which appears is a close up of the saw and a graphic overlay of its frequency spectrum. A realistic sound sample is also played at this point, once again adding realism. Next the student is confronted with a reduced image of the source, and an animated image of a simple sound level meter. MMDirector allows these images to be replayed continuously until the student interacts in such a way as to prompt a change. The image of the meter has two buttons on it, which will react to a mouse click. Eventually the student adjusts the settings correctly using these two buttons, and the animated needle rises on the scale to show a positive reading. This has been achieved by creating several different animations of the needle. One for a less than zero reading, one for an excessively large reading, and of course the correct reading.

Assuming the student has no prior knowledge of sound level measuring devices, this exercise is an excellent introduction to measuring sound pressure levels in dBA, without the risks associated with handing over a sound level meter to them for the first time.

6.0 CONCLUSION - THE FUTURE
The above examples of multimedia are only a tiny sample of the potential development which I hope to achieve. With appropriate support from Deakin University, I expect to be developing more MMDirector packages for use in the teaching of acoustics, but more importantly I will be producing video tapes which will have associated Multimedia 'Mac' lessons and knowledge tests. Eventually each student will be able to view the video tape either at home or in the University Library, then sit at a computer for the appropriate reinforcement. I anticipate that the computer will be used to quiz the students on their understanding of acoustics concepts and perhaps limit their progress in stages. i.e. require that they pass one stage before proceeding to the next. More time, and continuing financial support will be required to ensure further progress is assured.

THE 24 HOUR CAR WASH - NOISE AND TOWN PLANNING ASPECTS

David Borgeaud and Frits Kamst
WBM Consulting Engineers, Brisbane, Australia

ABSTRACT

In recent times there has been a re-emergence of the automatic car wash. To guard against complaints, Councils now require the submission of an acoustical report assessing the impact of such facilities as part of the town planning requirements. The need to address the acoustic issue is mainly the result of the deregulation in the service station industry allowing owners to operate for up to 24 hours per day.

This paper presents the results of three case studies including "wet" and "dry" car washes, and highlights the conflicts between town planning/operator requirements and acoustic requirements for the car wash. It is concluded that "wet" car washes (which are considerably quieter than "dry" car washes) are more likely to be able to meet 24 hour noise level criteria. Usual treatments such as barriers and buffer distances are often not sufficient and sound reducing devices may need to be incorporated into the car wash design in order for the 24 hour car wash to co-exist with nearby neighbours.

1.0   INTRODUCTION

The demand for car washes by motorists has increased significantly in recent times, and in order to cope with the demand, the major oil companies are erecting car washes on service station sites. While in the past a car wash would normally include blowers to dry the car after the wash, the trend currently is to install a car wash which does not have blowers, so that a car drives away "wet".

One of the reasons for this trend is the environmental awareness of residents and Local Councils, since blowers are a significant source of noise. While this development is a healthy one, other developments, and in particular the 24 hour car wash, have led to complaints by nearby residents and refusal by Councils to allow the installation of some car washes. The main concern for Councils is the possibility that the car wash noise may disturb nearby residents, particularly during the late night/early morning time period when ambient levels are lowest.

This paper provides a review of the issues which need to be addressed to ensure that the 24 hour car wash and the nearby residents can co-exist.

2.0   DESCRIPTION OF CAR WASH NOISE SOURCES

The modern car wash comprises several rotating nylon brushes, high pressure water sprays, pneumatic or hydraulic systems to move the brush assembly, and in some cases, blowers (large fans) to dry the vehicle. This equipment is housed in a "single carport" sized building, typically constructed with a metal deck roof, and side walls of brick to sill height and glass up to roof height. The entry and exit end of the building are typically open. Auxiliary pump and compressor equipment is normally housed in either an enclosure near the car wash, or inside the service station building.

For car washes without blowers, the predominant noise occurs when the brushes "slap" against the larger panels (e.g. roof, bonnet, boot) of the vehicles. Noise levels outside the car wash enclosure are highest near the entrance and exit of the car wash and considerably lower along the sides of the car wash due to shielding provided by the enclosed sides. The car wash noise is quite unobtrusive as it is broadband (brush and water spray noise) with occasional other noises due to valves releasing air or the brush assembly reaching the end of its travel. Noise from the auxiliary equipment is not usually audible when it has been installed in a typical brick enclosure.

For car washes with blowers, the fan noise is dominant over the brush and water spray noises. Typical noise levels for "wet" and "dry" car washes investigated by the authors are presented in Table 1.

TABLE 1 TYPICAL CAR WASH NOISE LEVELS @ 30M

CAR WASH DESCRIPTION	ENTRANCE SIDE		EXIT SIDE	
	L_1	L_{10}	L_1	L_{10}
"Wet" - No Blowers	58	55	57	54
"Dry" - With Blowers	--	--	72	71

3.0 CASE STUDIES

Three case studies have been selected from the car washes investigated in southeast Queensland. Table 2 summarises the site specific data for each case.

TABLE 2 CASE STUDY TECHNICAL DATA

CASE	CAR WASH TYPE	L_{10} @ RESIDENCE dB(A)	RANGE OF L_{90}		DISTANCE		EXTRA ATTENUATION REQUIRED TO MEET $L_{10} = L_{90}$ + 5 CRITERION
			TIME	L_{90}	HOUSE TO Car wash	HOUSE TO MAJOR ROAD	
1	No Blowers	43 - 45	Day Evening Night	52 52 50	75m	10m	0
2	No Blowers	52	Day Evening Night	54 52 36	38m	65m	11 dB(A)
3	With Blowers	60	Day	52	15m	50m	8 dB(A)*

Notes L_{10} is the noise level exceeded 10 percent of the sample time.
L_{90} is the noise level exceeded 90 percent of the sample time.
* Includes a 5 dB(A) penality due to tonality

Case 1   The nearest houses to the service station and car wash were located on the opposite side of a major 4 lane road and hence ambient levels at the houses of interest remained high (50 dB(A)) even on Sunday. A directivity factor of -3 to -5 dB(A) was applied to the predicted L_{10} noise level as the nearest house would have no direct line of sight to the entrance or exit of the proposed car wash. Due to the distance, directivity and high ambient levels associated with this location, the predicted car wash noise would readily meet the noise level criterion. Figure 1 shows the locality plan for this case study.

Case 2   The nearest houses to the proposed car wash were well removed (30 - 100m) from the major traffic route. The residence most likely to be affected was only 38m from the exit of the proposed car wash, had direct line of sight to the exit, and was 65m from the major road. Consequently, car wash L_{10} noise levels would be reasonably high and the background L_{90} level was quite low at night at this house. Several combinations of barrier walls and changes in the orientation and location of the car wash were considered to try to reduce the car wash noise to meet the noise

level criterion. However, engineering, town planning and client requirements made it difficult to achieve a viable solution. As a result it was recommended that the car wash operations be limited to 6am - 12 midnight. Figure 2 shows the locality plan for this case study.

Case 3   For this case the operation of an existing car wash with blowers resulted in excessive noise at a nearby residence. An L_{10} of 60 dB(A) was measured with the car wash operating, while the L_{90} levels were measured at 52 dB(A). Because of the tonality of the blower fans a 5 dB(A) penalty was added to the L_{10} of 60, making it effectively 65 dB(A), so that the reduction required to meet the L_{90} + 5 criterion was 8 dB(A). This car wash was only operated during the day time because of the noise levels generated.

Table 1 indicates that the differences in L_{10} noise levels between "wet" and "dry" car washes are of the order of 17 dB(A).

It can be seen from the above case studies that the car washes which are most likely to be able to meet 24 hour noise criteria are "wet" car washes where the "car wash to the nearest house" distance is greater than the "major road to the nearest house" distance. This occurred for Case 1 where the proposed car wash was to be located at the rear of the service station, behind which was the car park for a major shopping centre. Service stations built on rezoned residential blocks, where houses abut the station's side and/or rear boundaries are unlikely to be able to operate a 24 hour car wash due to lower ambient levels and smaller buffer distances which exist between the car wash and nearby houses.

4.0   CRITERIA FOR CAR WASH NOISE

In the absence of Queensland guidelines, AS1055.2 - 1989 has been used to establish an annoyance criterion. Appendix A of this document states in essence that where the L_{10} of the total ambient sound including the noise being investigated exceeds the L_{90} of the total ambient sound in the absence of the noise being investigated, the noise is likely to be discernible, but that differences of 5 dB or less may be of marginal significance with respect to annoyance. Adjustments for tonal and impulsive characteristics of the source noise can be made.

The annoyance criterion is applicable for the full 24 hour period, and due to the broadband nature of the wet car wash noise (neither impulsive nor tonal) no adjustments are made. Noise from car washes with blowers on the other hand can be quite tonal and so an adjustment of +5 dB(A) is added to the L_{10} level.

Due to the late night operation of 24 hour car wash facilities, consideration could be given to the use of a sleep arousal criterion. One such criterion (SPCC document) states that to protect people from sleep arousal, the L_1 of the noise source should not exceed the L_{90} by made than 15 dB(A).

The sleep criterion is considered appropriate for the night-time

period 10pm - 7am.   In cases where the annoyance criterion is marginally exceeded during the night time period (but is met from 7am - 10pm) and the sleep criterion is met, then consideration could be given to recommending that the car wash be allowed to operate during the full 24 hour period.   It should be noted however that as the car wash L_1 is only 3 dB(A) greater than the L_{10}, the annoyance criterion is some 7 dB(A) more stringent than the sleep arousal criterion.

5.0   REMEDIAL MEASURES

Several remedial measures can be taken to control the impact of car wash noise on nearby residents:

Buffer distance	--	By good site selection it should be possible in many cases to provide sufficient buffer distances to enable the criteria to be met.
Acoustic Barriers	-	The ability of acoustic barriers to reduce car wash noise depends on the local topography and whether the nearby houses are highset or lowset. In addition to the purpose built barrier (timber or concrete block fence) the service station building can be located in such a way to form an effective barrier.
Time Restrictions	-	In many cases where the car wash position on the site is "fixed" by other constraints buffer distances and barriers may not provide a solution. In such cases, the hours of operation of the car wash should be restricted to avoid the quieter evening/night periods. Sufficient monitoring should be undertaken to determine suitable time limits.

In addition to the above remedial measures which seek to reduce the receptor noise level at nearby residences, consideration should be given in some cases to reducing the noise at its source.

"Wet" Car washes	-	Automatic doors could be installed to the entrance and/or exit of the car wash. The doors would be triggered to open and close prior to commencement and after conclusion of the wash cycle. In many cases this would yield a very useful 10 dB(A) of attenuation, particularly as the sides and roof of the car washes are usually enclosed.
"Dry" Car washes	-	The blower fans can usually be treated on the suction side with acoustic attenuators, however the discharge side of the fan is usually not as easily

treated. Automatic doors would again be useful in reducing the brush, water and blower noise radiating out through the entrance and exit of the car wash.

6.0 TOWN PLANNING/OPERATOR REQUIREMENTS

There are several requirements that are placed on car washes by both councils and the companies operating the service stations. Some of these requirements are beneficial from an acoustic view-point, while others may conflict with possible acoustic treatments as shown in Table 3.

TABLE 3   COMPARISON OF TOWN PLANNING AND OPERATOR REQUIREMENTS
WITH ACOUSTIC REQUIREMENTS

TOWN PLANNING/OPERATOR REQUIREMENT	ACOUSTIC REQUIREMENT
1. Service station operators require the car wash to operate the same hours (usually 24 hours) to provide a "we never close" service to customers and to maximise financial return on their investment.	Time restrictions on car wash operating hours are sometimes necessary.
2. The car wash must be visible from the major road which the 24 hour service station services.	This precludes the use of acoustic barriers in certain locations as they would tend to hide the car wash.
3. Access to the car wash must be obvious to the driver, should flow with the general direction of traffic flow through the station and must allow a minimum queueing distance for 5 vehicles.	These requirements tend to "lock" the car wash into a particular position on site which may not allow repositioning to get a larger buffer distance to nearby houses.
4. Various councils require certain setbacks for the car wash relative to property boundaries.	
5. Councils often require a 2m high fence be erected on the boundary of the service station site.	This can often be constructed as an acoustic barrier (i.e. overlapping timber paling fence or concrete block wall) to provide some barrier attenuation.
6. Most 24 hour service stations with car washes are located along major roads in order to maximum exposure.	This is beneficial as road traffic noise tends to mask the car wash noise levels at the nearby residences.

583

7.0   CONCLUSIONS

Based on the authors' experience with car washes the following conclusions can be drawn.

(1)   "Dry" car washes (with blower fans) typically cause noise levels 17 dB(A) higher than "wet" car washes. As a consequence "wet" car washes are more likely to be able to meet noise level criteria allowing them to operate 24 hours per day.

(2)   Sites for service stations with a proposed 24 hour car wash facility should not abut residential properties as the car wash noise is unlikely to meet the 24 hour noise level criteria.

(3)   The "car wash to nearest houses" distance should be greater than the "major road to nearest houses" distance so that car wash noise (reduced due to distance) can be masked by ambient noise levels at the nearby houses.

(4)   Car wash manufacturers may need to consider the incorporation of sound reducing devices into their design. One useful possibility would be the option of a car wash with automatic entrance and exit doors which would be open for the car to enter and depart, but would remain closed for the duration of the wash/dry cycles.

(5)   Although remedial measures (e.g. barriers, buffer distances, fitting doors to the car wash) all help to reduce the car wash noise, in many cases the late night/early morning noise level criterion may not be able to be met. In such cases time limits must be set on the operating hours of the car wash. This is not always as drastic a measure as it may at first appear since few people use car washes in the late night periods, so that the loss of revenue to the operator should be quite low.

8.0   REFERENCES

Standards Association of Australia. Acoustic - Description and Measurement of Environmental Noise, Part 2 - Application to Specific Situations: AS1055.2 - 1989.

State Pollution Control Commission. Environmental Noise Control Manual, Part C - Noise Quality Objectives, Chapter 19: D - West Government Printer, N.S.W., 1988.

00012891

MAJOR FREEWAY
(APPROX 250 m FROM HOUSES)

LARGE SHOPPING
CENTRE   CAR PARK

PROPOSED CAR WASH

EXISTING
24 HR
SERVICE
STATION

COMMERCIAL

EXISTING 24HR
SERVICE STATION

MINOR ROAD

MAJOR   75 m   R O A D

10m TO KERB OF MAJOR RD.

LOCAL STREET

HOME   HOME

COMMERCIAL   RESIDENTIAL
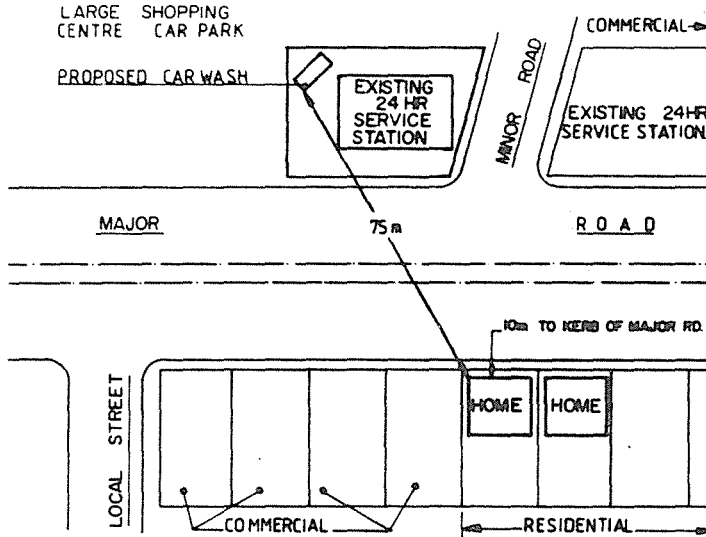
Fig. I   LOCALITY PLAN SHOWING PROPOSED
CARWASH FACILITY WHICH COULD OPERATE
24 HOURS. (Note the close proximity of the
houses to the major road)

TO LARGE SHOPPING
CENTRE

COMMERCIAL

MINOR   ROAD

RESIDENTIAL

PROPOSED
CARWASH

EXISTING
24 HR
SERVICE
STATION

MAJOR ROAD

COMMERCIAL

LOCAL   STREET

MINOR ROAD

LOCAL   STREET

38m

65m

RESIDENTIAL

HOME   HOME

RESIDENTIAL

RESIDENTIAL
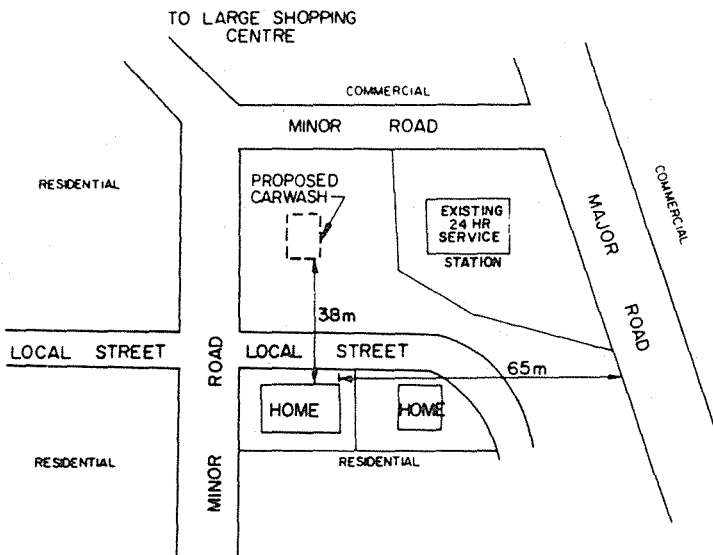
Fig. 2   LOCALITY PLAN SHOWING PROPOSED
CARWASH FACILITY WHICH COULD NOT
OPERATE 24 HOURS. (Note the large
distance from the houses to the major
road)

585

CRITERIA FOR THE CONTROL OF NIGHT-TIME ROAD TRAFFIC NOISE: DIRECTIONS FROM THE CURRENT RESEARCH LITERATURE.

A.L. Brown
School of Australian Environmental Studies
Griffith University
NATHAN QLD 4111

S. Rutherford
School of Australian Environmental Studies
Griffith University
NATHAN QLD 4111

ABSTRACT:

There is considerable concern amongst authorities responsible for regulating road traffic noise that the scale currently used to describe road traffic noise in Australia - $L_{A10,18h}$ - does not adequately predict human response to noise during the night-time hours. This paper selectively reviews the current research literature on effects of road traffic noise on sleep to look for guidance as to appropriate night-time noise scales. The research literature shows that as yet there is no simple answer as to which scale, or level on that scale, would be an appropriate criterion. L_{Aeq} for the night-time hours can predict sleep disturbance, but only where the traffic noise conditions are "continuous". Where "noise events" are discernible in the traffic stream, and it is probable that many, if not most night-time noise situations of interest would fall into this category, a sleep disturbance criterion will have to take peak noise level and/or number of noise events into account.

1.0 INTRODUCTION

The need for a night-time road traffic noise criterion stems from a general concern that the $L_{A10,18h}$ (0600h-2400h) scale currently used to describe road traffic noise in Australia does not adequately predict human response to noise during the night-time hours.

This paper reviews selected current research literature on the effects of road traffic noise on sleep particularly with respect to guidance as to appropriate control criteria for its control.

However, as will be seen below, there is by no means a simple answer as to which noise scale, and which level on that scale, is appropriate as a criterion to minimise human reaction to night-time noise.

2.0 REVIEW BY VALLET (1987)

Vallet (1987) extensively reviewed night-time effects of noise and appropriate night-time noise scales and concluded that:

> The test results as a whole confirm the common observation that people sleep badly in the presence of noise and it is, therefore, necessary to consider the possibilities of establishing noise indices which can be used to determine criteria for the protection of sleep.

Vallet notes that while the need has been demonstrated, few countries have implemented indices concerned *solely* with evening or night noise to date, though various international organizations have recommended such levels. *For example, WHO (1980) has recommended* night-time L_{Aeq} levels as low as 35 dB to protect sleep though Vallet notes that several researchers regard these levels as unduly restrictive.

Vallet points out the limitation in the use of a single L_{Aeq} value to establish noise limits to prevent sleep disturbance. Sleep disturbance will only be minimized by an L_{Aeq} criterion in noise situations where noise events in the noise stimulus are absent. However, for most road traffic noise situations at night, the noise stimulus contains isolated noise occurrences (noise events) such as where truck peaks are heard against a lowered background on a major roadway, or car peaks are heard against an even lower background on a minor roadway. Where noise events occur, *peak noise level* limits rather than L_{Aeq} is required to minimize sleep disturbance. Further, as Vallet notes:

> ... for traffic noise exposure in quiet conditions the average peak noise level causing (a sleep) effect may vary from 42-44 dB(A) while that causing the same effect in a noisy situation (would have to be) from 50 to 53 dB(A).

This indicates that the *emergence* of a noise event from its background is a determinant of sleep disturbance, not simply the peak level of the noise event.

Based on his review, Vallet suggests that the *internal* criteria to minimize sleep disturbance should consist of a Peak Noise Level of 50 dB(A), jointly with an L_{Aeq} of 35 dB.

Vallet also emphasizes that these suggested criteria are for *continuous road traffic noise* (low variance in the noise level distribution) but he does not suggest appropriate noise criteria for road traffic noise which is characterised by a lower background with intermittent noise events. However, based on evidence he presents, the Peak Noise Level should be lower than 50 dB(A) (42 to 44 dB?) in these noise environments.

3.0 STUDIES BY EBERHARDT (1988) AND EBERHARDT *ET AL* (1987)

These authors reported a series of laboratory and field studies on sleep disturbance by road traffic noise which tended to support the conclusions of Vallet's review. The study used healthy young adults and responses to noise were measured by arousal reactions, body movements, sleep stage disturbance and estimates of sleep quality and mood.

The different noise stimuli used in the experiments (all levels were *internal*) allowed examination of the effects of noise events on sleep, the effects of continuous traffic noise on sleep, and the effects of noise events emerging from continuous traffic noise.

The studies found that, where traffic noise had low variability. (Eberhardt refers to this as "continuous traffic noise") the critical level at which sleep was found to be disturbed lay somewhere between an L_{Aeq} of 35 dB and 45 dB.

However, where there were obvious peaks of noise (noise events of truck passages) the simple L_{Aeq} descriptor was found to be inadequate by itself as a predictor of effects on sleep. This was based on two findings. Firstly, with intermittent noise levels (truck passes of 45dB(A) with an L_{Aeq} of 29dB) sleep was disturbed but, for continuous traffic noise with L_{Aeq} of 36dB, no detrimental effect was found. Sleep disturbance increased when truck peak levels were raised to 55dB(A) even though overall L_{Aeq} for this experiment was 36dB. Secondly, when the 55dB(A) peak level experiment was repeated but with the peaks emerging from a continuous traffic noise (total L_{Aeq} now 46 dB) sleep disturbance still occurred, but not to the extent which occurred when the 55 dB(A) peaks were heard in quiet.

Eberhardt concluded that L_{Aeq} alone could not adequately characterize all types of noise dose relevant to sleep disturbances as arousal reactions were induced by intermittent traffic noise. This supports the concept that the emergence from background rather than absolute noise level may determine the reaction probability.

Based on his findings, Eberhardt recommended a night-time L_{Aeq} of between 36 and 45 dB. He indicated that this must be supplemented in situations in which noise events are part of the traffic noise stimulus with a measure that takes the noise peaks during the night into account. He suggested that these could be measured as L_{A01} or L_{Apmax}.

Eberhardt (1988) also noted from one of his experiments that habituation to sleep disturbance did not appear even after several years of exposure.

3.0 STUDY BY VALLET, GAGNEUX, BLANCHET, FAVRE AND LABIALE (1983)

This study is particularly interesting in that it used subjects *in situ* in their dwellings as compared to the artificial sleeping environment of laboratory studies. Homes used in the study were all located near motorways and subjects had lived in them for at least four years. Subjects sleep was monitored under the prevailing noise conditions and again when these levels had been reduced by relocation of the sleepers within the dwelling or by facade insulation. The study findings were that:

- even after four years of exposure to a noisy environment, transfer of subjects to a quieter environment within their own homes resulted in better sleep for most people.

- a night-time L_{Aeq} could be used to account for human sleep response to noise, and the authors suggested a level of 37 dB *internal* as the appropriate threshold level.

- peak levels were as significant as the L_{Aeq} in their effect on sleep. The authors showed that 80% of transient effects and changes in sleep state, and 87% of awakenings, could be avoided if *internal* peak noise levels did not exceed 40 dB(A) and about two-thirds of these could be avoided if the peak levels did not exceed 45 dB(A). They suggested the latter as a criterion level.

While this study recommended that L_{Aeq} was an adequate night-time noise criterion, this needs to be tempered by two facts. Firstly, the conclusion appears to have been based more on the arguments that L_{Aeq} was easy to predict and that it conformed to current French regulations, than on the data that the authors presented. In fact, their data showed that measures which included variability (the standard deviation of the noise level distribution in particular) were better correlated with sleep responses than was L_{Aeq}, and the peak level L_{A01} was equally correlated with sleep responses as was the L_{Aeq}.

They also pointed out that different night-time criterion measures would have to be used where traffic flows were low and that peak levels of noise, and the emergence of the peak above the continuous levels, would have to be considered for such conditions.

4.0 STUDIES BY OHRSTROM *ET AL* (1988) AND OHRSTROM AND RYLANDER (1990).

These papers introduced a further element into the choice of a night-time noise criterion. The authors suggested that the number of noise events at night is a critical determinant of night-time reaction, and that to protect people from sleep disturbance it is necessary to consider the number of vehicle passages.

An overview paper by Ohrstrom *et al* (1988) discussed three one-week laboratory experiments in which the noise exposure was either single noise events or continuous road traffic noise and human response was

589

measured by body movements, subjective sleep quality, mood and subject performance. Ohrstrom reported that:

intermittent noise caused stronger effects than continuous noise at the same Leq level,

sleep quality was significantly related to peak noise level.

In particular, sleep was affected by intermittent noise events with a peak internal noise level of 60 dB(A) even though the overall L_{Aeq} was only 35dB.

Results also showed that up to 8 noise events of peak level 60 dB(A) per night did not have a significant effect on sleep quality, but 16 noise events and above per night caused a significant decrease in sleep quality.

The laboratory study by Ohrstrom and Rylander (1990), was aimed at further examining the importance of number of noise events and the findings were:

The use of an $L_{Aeq,24h}$ as a noise criterion is insufficient to protect people from sleep disturbance effects of traffic noise.

Noise event levels of 50 dB(A) peak do not negatively influence sleep until a critical number of noise events of this level occur at somewhere between 16 and 64 events per night.

Noise event levels of 60 dB(A) peak do not negatively influence sleep until a critical number of noise events of this level occur at somewhere between 4 and 16 events per night.

Acoustic conditions in this study corresponded to the situation where noise events emerged from a lowered background.

The authors concluded that both maximum noise levels and number of noise events are important to sleep disturbance.

5.0 STUDY BY LABIALE (1983)

While the paper is not specifically related to night-time noise, it is relevant because of the noise event nature of night-time traffic flow. Labiale examined the relationship between annoyance and level of road noise (background noise and emergence of truck passages) in a laboratory study. He found that:

For peak truck noise levels up to 12 dB(A) emerging from the background noise (overall L_{eq} levels of 60 dB(A)) the number of truck peaks had only slight effect on annoyance and the overall L_{eq} remained adequate as a predictive index of annoyance (though L_{01}, L_{05} and L_{10} were equally good as predictors). Annoyance increased strongly from three to 15 truck passages and then more slowly between 15 and 30 passages;

For peak truck noise levels of 16 dB(A) or more emerging from the background noise (overall L_{Aeq} of 50 dB and 55 dB) the annoyance was a function of the number of truck passages (N), and a composite acoustic index (a.L_{eq}+b.Log N) was suggested as

a predictor (though several other composite scales including $a.L_{01}+b.L_{10}$ or $a.L_{eq}+b.N$ were equally good predictors).

Labiale was careful to point out that his study involved stimuli over a limited range and needed to be extended to a much wider range. However, he concluded that a composite index which integrated a number of noise events could prove useful for improved predictions of annoyance, especially at night when the index L_{eq} alone is not entirely satisfactory.

Composite indices did not appear as useful predictors of response in most of the other studies examined and, even in Labiale's study, alternative indices could equally account for human response.

6.0   STUDY BY GRIEFAN (1986)

Griefahn's (1986) laboratory sleep study subjected young adults to four intensities of sound: 59.4 - 63.5 dB, 51.0 - 56.5 dB, 44.5 - 50.5 dB and 37.0 - 44.0 dB and measured their responses by EEG, questionnaires and reaction time tests. The sound intensities given above were *internal* L_{Aeq} and, while it is not stated, presumably were the ranges of the $L_{Aeq,1h}$ during the hours of the experiment.

Results showed a strong correlation between L_{Aeq} and assessment of sleep quality. Griefahn identified that L_{Aeq} was a suitable predictor of sleep disturbances, *but only* if maximum levels were less than 8-10dB(A) above the L_{Aeq} - that is, the noise must have low variability. Where variability in the noise signal is high, the number of noise events and/or maximum levels also needed to be considered.

In summary, Griefahn recommended an *internal* $L_{Aeq,1h}$ of 40 dB during the night to protect sleep, but suggested that this was valid only for noise from high density traffic flows. She noted that the validity of this level would have to be investigated where there was high variability in the traffic noise distribution, namely for lower traffic densities and where there were many trucks in the night-time traffic stream.

7.0   OTHER STUDIES

Several other papers reviewed mentioned the importance of peak levels and/or number of noisy events. In Vernet's (1983) field study, which involved comparing the annoyance between road traffic noise and train noise annoyance during sleep hours, it was found that in quiet places emergence was an important factor of disturbance while in noisy areas noise duration as well as peak level act with interaction to cause sleep disturbance. A field study by Tulen *et al* (1986), focussing on the effects of sound insulation on the peak characteristics of traffic noise, identified that the transient and peaky characteristics of traffic were found to result in 'non-adaptive physiological responses during sleep'. A laboratory study carried out by Rasmussen (1979) was aimed at investigating the relationship between road traffic noise and annoyance with attention paid to the number of noise events. Annoyance and noise level measured as L_{Aeq} and L_{np} were found to be highly correlated with sleep effects and it was concluded that L_{Aeq} gave a reasonable estimate of subjective annoyance but could be improved.

591

8.0   CONCLUSIONS

The first conclusion from this review must be that the necessary
definitive research to provide answers to the question of appropriate
night-time road traffic noise criteria is not yet available.
However, there is a sufficient body of evidence in the literature to
confirm that current 24hour or 18hour road traffic noise scales are
insufficient to protect against sleep disturbance and new criteria
are warranted.

The second conclusion is that appropriate night-time road traffic
noise criteria depend on traffic conditions.

For traffic noise conditions which can be defined as "continuous" it
can be concluded that the use of an L_{Aeq} scale measured over some
period of the night finds support as a predictor of sleep
disturbance. There is no clear guidance as to which period should be
used to define "night" but the choice of 2200 h to 0600 h seems
reasonable and is not contra-indicated by any of the studies. There
remains some debate as to the level on this scale required to prevent
sleep disturbance, but the various studies point to an appropriate
level of 35 to 40 dB.

However, for traffic noise conditions which cannot be defined as
continuous, and it is probable that many if not most night-time noise
situations of interest would fall into this category, the L_{Aeq} *itself*
is an inappropriate criterion by which to prevent sleep disturbance.
In these conditions, the criterion should be the maximum peak level
of individual noise events or, more appropriately, the number of such
noise peaks exceeding a particular level. Peak noise levels of 45
dB(A) have been suggested but others suggest that peak levels of 60
dB(A) should not occur more than 16 times in a night, or peak levels
of 50 dB(A) more than somewhere between 16 and 64 times in a night.
The current literature does not resolve these differences.

A complicating, and unresolved factor in setting a limit on peak
levels, is that it is not so much the peak level *per se* which results
in sleep disturbance, but the *emergence* of the peak above the
background.   This means that, for a given pattern of noise events,
elevating the background reduces the probability of sleep
disturbance. Continuing to elevate the background further would, of
course, eventually result in the traffic noise condition changing
from "noise events" to "continuous".

Where is the divide between the continuous and noise event traffic
noise conditions? Several authors have suggested that this occurs
when the peak levels of individual vehicles exceed the L_{Aeq} by some 8
to 12 dB though alternative definition of these same conditions is
possible, say based on the standard deviation of the traffic noise
distribution.   This would be a fruitful area for some simple
modelling to determine the combination of traffic and propagation
distance conditions responsible for generating the two conditions.

REFERENCES

Eberhardt, J.L. (1988), The influence of road traffic noise on sleep, Journal of Sound and Vibration, 127(3), pp449-455.

Eberhardt, J.L., Strale, L.O. and Berlin, M.H. (1987), The influence of continuous and intermittent traffic noise on sleep, Journal of Sound and Vibration, 116(3), pp445-464.

Griefahn, B. (1986), A Critical Load for nocturnal High-density Road Traffic Noise, American Journal of Industrial Medicine, 9:261-269.

Labiale, G. (1983), Laboratory study of the influence of noise level and vehicle number on annoyance, Journal of Sound and Vibration, 90(3), pp361-371.

Ohrstrom, E. and Rylander, R. (1990), Sleep disturbance by Road Traffic Noise - A laboratory study on number of noise events, Journal of Sound and Vibration, 143(1), pp93-101.

Ohrstrom, E., Rylander, R. and Bjorkman, M. (1988), Effects of night time road traffic noise - an overview of laboratory and field studies on noise dose and subjective noise sensitivity, Journal of Sound and Vibration, 127(3), pp441-448.

Rasmussen, K.B. (1979), Annoyance from Simulated Road Traffic Noise, Journal of Sound and Vibration, 65(2), pp203-214.

Tulen, J.H.M., Kumar, A. and Jurriens, A.A., (1986), Psychophysiological Acoustics of indoor sound due to traffic noise during sleep, Journal of Sound and Vibration, 110(1), pp129-141.

Vallet, M., Gagneaux, J.M., Blanchet, V., Faure, B. and Labiale, G. (1983), Long term sleep disturbance due to traffic noise, Journal of Sound and Vibration, 90(2), pp173-191.

Vallet, M. (1987),Sleep Disturbance in 'Transportation Noise Reference Book', edited by Paul Nelson, Butterworths, Sydney.

Vernet, M. (1983), Comparison between train noise and road noise annoyance during sleep, Journal of Sound and Vibration, 87(2), pp331-335.

WHO (1980). Environmental Health Criteria 12 - Noise. WHO, Geneva.

UTILISING THE SOUND OF WATER STRUCTURES IN THE BUILT
ENVIRONMENT

L. Brown and S. Rutherford
School of Australian Environmental Studies,
Griffith University,
Brisbane.

ABSTRACT

Water structures such as fountains, artificial waterfalls or streams
are common civic design features of squares, gardens and building
plaza in cities. Their function is aesthetic, but they also provide
focal points for meeting places and relaxation. Water structures
achieve these functions through their visual quality and through the
attractiveness of the space in which they are located. However, they
contribute not only to the visual environment, but also to the
acoustic environment. The sound of falling, tumbling or splashing
water is inherently attractive to humans. Further, those sounds can
effectively mask the all pervading traffic and other noise sources
which currently dominate central city areas, significantly enhancing
the quality of their immediate environment to serve as meeting and
relaxation places. By taking examples of artificial water structures
and applying simple propagation models to their source sound levels
it is possible to identify the degree and areal extent of masking of
less desirable city noises for different settings in the city. This
provides a tool for designers of water structures to confidently
incorporate acoustical characteristics amongst the other design
requirements.

1.0 INTRODUCTION

Throughout history, water structures such as fountains and artificial waterfalls have been used for their aesthetic contribution to the urban environment. To a large extent it is the visual effects of waterfalls that make them so popular but they also stimulate other senses.

The sound that water makes in its motion is important in the parks, gardens and meeting places of the inner city. Firstly, the sound of water tumbling or splashing would be almost universally regarded as a pleasant sensation providing a relaxing atmosphere. Secondly, it has the potential to mask unwanted sounds. The sounds which currently dominate most central business districts - road traffic, construction, aircraft, trains, amplified music and ventilation systems, are rarely pleasant. Nearly two decades ago Perkins (1973) noted that,

> ....waterfalls are not just visual delights - the sound of splashing, gurgling and bubbling is important especially when you can't hear the traffic.

While the design of any particular water structure will always be determined by criteria such as setting, available space, visual appeal, intended use of the surrounding space and energy requirements, if a fountain or waterfall can also mask the unwanted noises in its immediate environs then it will be even more valuable, providing a pleasant acoustic island in the middle of a city's noises. It is suggested however that if this has been achieved in the design of water structures in the past it is likely to have been largely fortuitous. An acoustic criterion would rarely, if ever, have been included as a parameter in fountain design and this failure can be attributed firstly to oversight and secondly to a lack of knowledge of how to predict and plan the effectiveness of any acoustic masking.

The purpose of this paper is to redress these matters. Firstly it attempts to generate awareness of the potential and value of the masking of unwanted central city noises by water structures. Secondly, by taking particular examples of artificial water structures it shows how it can be possible to provide initial estimates of the area over which masking can be expected to be effective. Landscape architects and other urban designers are not trained in acoustics and the simple approach taken in this paper considers their needs.

2.0 A TYPOLOGY OF WATER STRUCTURES

The design of water structures is infinitely variable, but Dewar (1990) has identified three major categories of structure - still water structures, moving water structures, and fountains. Moving water and fountain structures have the potential to produce sound and two of the examples discussed in this paper: a jet and basin fountain and a naturalised waterfall, represent these categories.

Jet and Basin Type Fountain

The jet and basin type of fountain consists of single or multiple nozzles through which water is pumped into the air and the falling water collected in a basin. The major sources of the sounds produced by the jet and basin fountain are the hissing of the geysers and the splashing and bubbling of the water falling into the basin. Design variables which affect the sound levels generated include the type of nozzle or jet, the water flow rate, the height of the geysers and their fall, the number and positions of geysers, the type of surface on to which the water falls(for example rocks or still water) and the depth of the collecting pool.

Naturalised Waterfall

This structure simulates a natural waterfall, often incorporating features such as boulders, pools and vegetation. The sources of the sounds created by this type of water structure are the turbulence of the water falling over the boulders and splashing into a pool of water at the foot of the waterfall. The spray created during this process may also create some sound as it impacts on vegetation and rocks. The acoustical characteristics of waterfalls will depend on the height of fall, the surface of the boulders, the volume and velocity of flow, and the characteristics of the collection pool such as depth of water and presence of hard surfaces.

In addition to water related sound, noise of the pump and motor system required to recycle water can contribute to water structure noise levels. As the pump and motor sound levels can be adequately quietened by separation or enclosure, these sources of sound are not considered further.

3.0 EXAMPLES OF SOUND LEVELS GENERATED BY WATER STRUCTURES

To assess the areal extent of masking of city noises by water structures, it is useful to know the levels of sound that can be expected from some existing water structure installations. Two examples selected from water structures installed in parks and other open spaces in the Central Business District of Brisbane are discussed below. These sound levels can of course be varied by altering the many design parameters, flow rate and height of fall in particular, but it is not the purpose of this paper to attempt to relate sound levels generated to these parameters.

3.1 Example One

Example One was a small jet and basin fountain set in a park adjacent to a busy roadway. The fountain was located close to the roadway and reflects the geometric design of the surrounding buildings and road networks. It is intended as a visual feature for people using the park and the adjacent footpath. Because of its location, road traffic noise dominates the site and reduces the park's utility as a pleasant and relaxing environment.

The fountain consisted of three large geysers and four smaller geysers distributed over a concrete basin (approximately 18 metres by 7 metres). The basin had a water depth of approximately 0.15 metres and water from the geysers fell directly on a still water surface. The larger jets reached heights of 2 metres with the smaller sprays

reaching heights of up to 1 metre. The overall flow rate was approximately 20 litres/second.

The steady sound levels generated by the fountain were between 73 and 79 dB(A) at the edges of the fountain depending on which point on its perimeter the levels were measured. Water sounds masked other city sounds immediately adjacent to the fountain, though because of proximity to the roadway, vehicle peaks could still be detected. Traffic noise began to mask the fountain sounds as distance from the fountain increased and at levels of 60 to 64 dB(A) at some 20 metres from the fountain, the fountain sounds were almost continually masked by traffic noise.

Even though fountains of this type should be regarded as a distributed point acoustic source (eg. Eargle, 1990), or an areal acoustic source, for simplicity they can be represented as a point source. The simplification allows ready estimation of the pattern of water structure sound levels over the surrounding areas.

$$Lp_2 = Lp_1 - 20 \log r_2/r_1$$
where Lp_1 = measured level at close distance to the fountain r_1
Lp_2 = estimated level at greater distance from the fountain r_2

Field measurements confirmed that the assumption of a point source was satisfactory.

The pattern of water structure sounds for the fountain is shown in Figure 1. Broken lines indicate where measured levels near the fountain were higher than modelled levels because of the inappropriateness of the point source assumption close to the source.

3.2 Example Two

Example Two was a naturalised waterfall situated in an inner city park bounded by heavily trafficked streets. The park in which the waterfall was located has been designed as a "natural" enclave offering an escape from its built surroundings. The design maximises this effect by the use of rock walls to enclose the space near the waterfall. Boulders and natural vegetation created a waterfall approximately 6 metres high and 11 metres wide at the crest, with the flow falling onto boulders in a large pool. The effect is enhanced by the high flow rate - approximately 125 litres/sec.

At the base of the waterfall, sound levels were a steady 79dB(A). Despite its location near busy roadways, the waterfall sounds masked all other noises in the vicinity of the water structure and for some distance from it. As for the fountain, this water structure may also be described as a point acoustic source and modelled as shown in Figure One. Again field measurements confirmed that the assumption of a point source was adequate, except close to the source where the point source assumption broke down.

597

Legend
≋ Water sound source
— Modelled sound level (dB(A))

- - - Modelled sound level where measured sound levels were higher than modelled levels (dB(A))

0 5 10 15 20 25
Metres
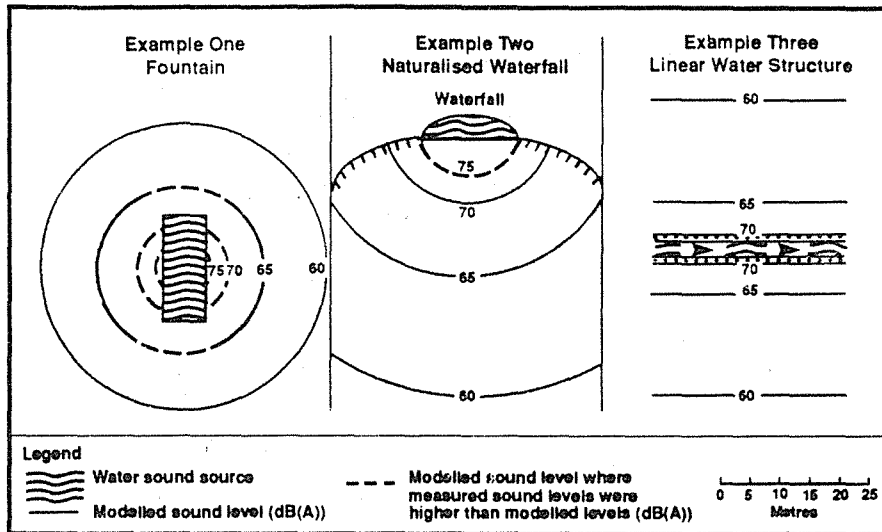
Figure 1 - Areal extent of acoustic influence of water structures

3.3 Example Three

Example Three illustrates how similar modelling can be carried out if the water structure consists of a long line of fountains or water flowing down a stepped channel.

The sound levels generated by a linear water structure could be modelled assuming a line source of sound.

$$Lp_2 = Lp_1 - 10 \log r_2/r_1$$

where Lp_1 = measured level at close distance r_1 to the source,
Lp_2 = estimated level at greater distance from the source, r_2.

Example Three is hypothetical, and a level of 75 dB(A) at the edge of the source has been assumed for illustrative purposes(Figure 1).

Provided that some estimate of water generated sound levels close to the water structure is available - and our limited observations suggest that levels of 75 to 80 dB(A) at the perimeter of structure are typical - then the examples above give a designer simple tools by which the areal extent of water structure generated noise can be estimated. More complex structures, for example streams flowing out from a fountain, could be modelled by a combination of point and line sources.

4.0 OVER WHAT AREA CAN ONE EXPECT CITY NOISES TO BE MASKED BY THE SOUND OF WATER STRUCTURES?

Masking is often referred to in a negative framework. However, as in the case of masking unwanted office noises by ventilation sounds, the masking of city noise by water structure sounds is a desirable masking effect. The extent of masking clearly depends on the city noise environment in which water structures are located.

Figure 2 shows the frequency spectra of water structures and two types of city noise. As the frequencies for the water structure and city noises are somewhat similar and relatively broad band, it can be assumed, to a first approximation, that component city noises will be masked by water structure sounds in the manner that discrete tones are masked by broad band sound (Jones and Chapman, 1984).
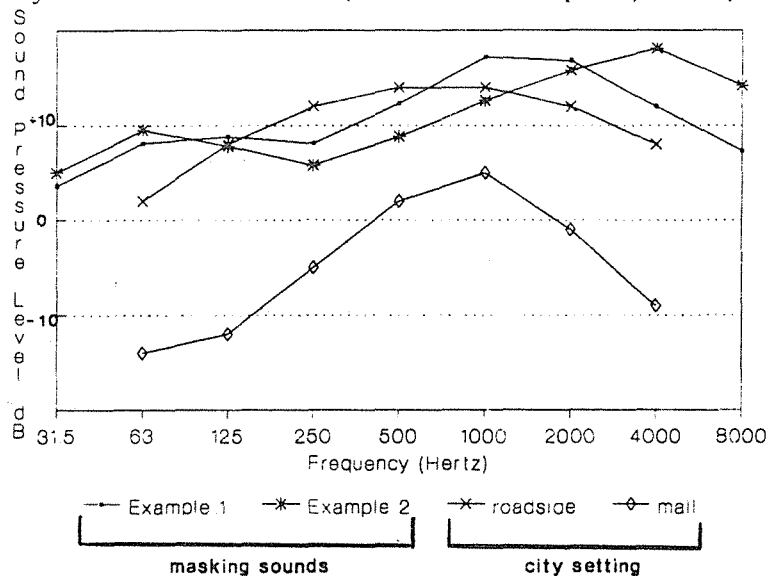
Figure 2 - Relative frequency spectra of water structure sounds and of city noises (arbitrary reference levels).

The extent of masking will depend predominantly on the relative levels of masked and masking sounds. Water structure sounds can totally mask city noises where the former is some 8 to 10 dB above the latter (considerably less at lower frequencies). However, even at lesser differentials between city and water structure sound levels, and to an extent even where city levels are 10 dB or so above water structure levels, partial masking occurs. Partial masking reduces the loudness of the city noises without masking them completely (Zwicker, E. and Fastl, H., 1990). As one approaches a water structure there will be a continuous reduction in the loudness of city noise until, close to the structure, city noises will be dominated by water structure noise.

For simplicity, two typical settings for water structures are considered in this paper. The first are squares, gardens, or malls located in positions somewhat sheltered from direct exposure to traffic on the street systems. In these noise environments there is a noticeable absence of well defined peaks. The second are areas near footpaths, or in parks or building plaza located adjacent to roadways and characterised by continuous traffic noise with intrusive peaks of individual passing vehicles.

A small section of level recording for each of the two settings is shown in Figure 3, and Table 1 summarises their characteristic levels in the setting.

a. Roadway setting   b. Mall setting
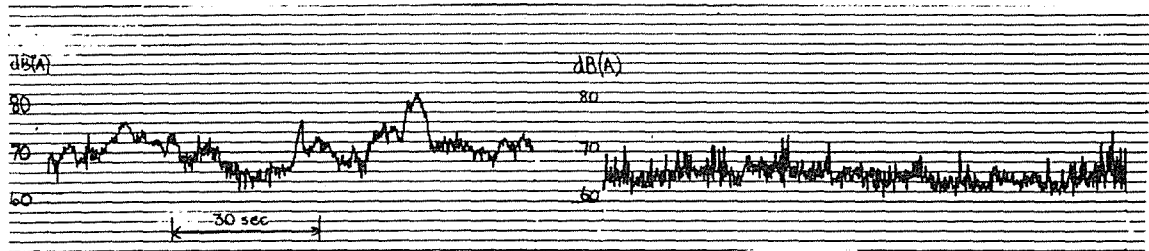
Figure 3 - Sound pressure levels for two types of city noise

TABLE 1 - CHARACTERISTIC CITY NOISE LEVELS

	CHARACTERISTIC LEVELS OF THE CITY NOISES($dB(A)$) WHICH WOULD DESIRABLY BE MASKED BY WATER SOUNDS	
	ROADSIDE SETTING	MALL SETTING
Peaks(L_{01})	80 (vehicle passby)	70 (voices,footsteps)
Median Level(L_{50})	70	65
Background Level (L_{90})	67 (bulk traffic flow)	64 (ventilation,people)

From Table 1, the degree of masking of city noises that can be achieved at different levels of water structure sound for the two chosen settings can be ascertained.

Water Structure
Sound Level(dB(A))   Degree of Masking of City Noise

60   - reduce loudness of background mall noise but no masking of roadside noise

65   - reduce loudness of most mall noise
            - reduce loudness of roadside background, but no effects on peaks

70   - reduce loudness of all mall noise
            - reduce loudness of background roadside noise and some reduction in peak loudness

75   - totally mask most mall noise
            - totally mask all background roadside sounds and reduce loudness of peaks

80   - totally mask all mall noise.
            Mask most roadside noises and reduce loudness of vehicle peaks.

600

Applying this information to the levels shown in Figure 1 would allow a designer to predict the areal extent of masking of city noises by the water structure examples selected in this study. For example, if the naturalised waterfall was located in a mall, most mall noises would be reduced in loudness up to 25 m from the waterfall.

6.0 CONCLUSION

Common features of our central city areas are artificial water structures. Their visual qualities have always been important however their potential auditory advantages of masking other, less pleasant, sounds heard in the central city have often been ignored. Achievable levels for water structure sounds have been indicated, using estimates of near-source water structure sound levels, and simple propagation models. In this way it is possible to identify the degree and areal extent of masking of less desirable city noises for different settings in the city and designers of water structures can confidently incorporate acoustical characteristics amongst the other design requirements. In practice it would be necessary to measure the acoustic environment of the setting in which the water structure was to be located as in many cases it may not conform to the two characteristic settings used in this paper.

Having recognised the potential of water structures to mask city noises, further work is to examine the design of the water structures to ascertain what features govern the sound levels produced and provide guidelines to designers as to how the acoustic levels can be modified to suit the chosen setting of the structure.

REFERENCES

Dewar, S., Water Features in Public Places - Human Responses, Q.U.T., Grad. Dip. Landscape Architecture Thesis, 1990.

Eargle, J.M., Music, Sound, and Technology, Van Nostrand Reinhold: New York, 1990. p13.

Jones, D.M., and Chapman, A.J., Noise and Society, John Wiley: Chichester, 1984. Chapter 8.

Perkins, G., The delight of a city:water, Concrete Quality, 99, p33, 1973.

Zwicker, E., and Fastl, H., Psychoacoustics: Facts and Models, Springer-Verlag: Berlin, 1990. p.191.

THE USE OF TWO MODELLING TECHNIQUES FOR PROPAGATION OF NOISE INTO THE COMMUNITY

Russell Brown
Vipac Engineers & Scientists Ltd
81 Newmarket Road
Windsor   Qld   4030
Australia

ABSTRACT

Various environmental noise prediction software packages have been developed by individuals, organizations and companies in recent years. Often the prime goals of each have been to enable calculations of the level of environmental noise to be conducted more quickly and more accurately than previously was possible using conventional "long hand" methods.

In this paper a series of case histories has been used to contrast a proprietary software package with a spreadsheet program to predict environmental noise levels. Various features of each of the calculation methods are examined. In addition to the accuracy of prediction, the features which are addressed include the extent to which the programs can be modified to suit user requirements, the attenuation features incorporated in the methods, the time required to set up, the area of the community that can be assessed, the nature of the output and user error.

1.0 INTRODUCTION

Environmental noise programs which have been developed by individuals, organizations and companies in Australia have ranged from simple single source - receiver models to those capable of plotting noise contours for 100 or more individual sources over any community of interest under any specified meteorological conditions.

This paper contrasts the use of two quite different environmental noise prediction methods. Each is PC-based, but while one contains a suite of powerful programs which can present an output directly as noise contours, the other uses a simple spreadsheet format to calculate noise levels at selected receiver locations. An assessment of other software packages is not part of the scope of this paper. Instead, the focus is on various practical features of these two methods. Further work to more fully quantify the significance of some features as well as others not addressed in this review is ongoing.

2.0 MODELLING TECHNIQUES

2.1 Environmental Noise Model. The Environmental Noise Model (ENM) is a package of programs which can calculate noise levels throughout a community area due to the operation of up to 100 sources (Tonin, 1985). The programs allow the user to input sound power data, 3-D source co-ordinates and directivity information for point, line and plane sources. In general, the algorithms are based on the CONCAWE (Oil Companies' International Study Group for Conservation of Clean Air and Water) model and Australian Standard AS1217 together with data and equations developed by various researchers (eg Parkin and Scholes, Piercy, and De Jong.) The algorithms take account of attenuation due to distance and ground type as well as directivity, barrier, wind and temperature effects.

A CAD program for digitizing of maps and interface with AutoCAD for outputting of noise contour plots are included in ENM.

2.2 Spreadsheet Method. The particular spreadsheet program that is the subject of this paper was developed by the author and others solely for their own use. (Note: Its format and scope are quite comparable to those which have been developed by many others. As a result, the review of features of this program may be considered to be generally applicable to spreadsheet programs as a whole). It uses standard acoustical theory and various empirical data in a proprietary spreadsheet format. Sound power levels and dimensions for each source are input together with source and receiver coordinates and direction cosines. Barrier attenuations are entered from another spreadsheet program. Currently, wind and temperature effects are not fully quantified. Noise contours can not be plotted directly.

3.0 CASE STUDIES

Six case studies are used to exemplify the differences in various features of the two methods. Each of these case studies has been conducted in the past two years.

A brief description of each case study is provided below.

Case Study 1: The ENM model was used to predict the level of noise expected to be emitted from a large mineral processing complex into a nearby community occupying an area of some 200 hectares. The nearest residential premises were 1000 metres (approx) from the plant. On most occasions 18 noise sources were modelled at any one time. Noise contours were plotted.

Case Study 2: Noise from earthmoving operations was modelled using ENM. The community immediately adjacent to these operations extended from 300 metres up to 2.5 kilometres from the noise sources. Noise contours were plotted, but only 3 or 4 noise sources were modelled at any one time.

Case Study 3: A range of noise sources was modelled using ENM to determine the extent of noise emission to a community area located 2 kilometres (approx.) from the centre of operations. The noise sources consisted of electric motors, gearboxes and diesel engines which were collected into groups as well as conveyors and pile drivers which were treated as individual sources. In general 3 or 4 noise sources were considered at any one time.

Case Study 4: The spreadsheet program was used to predict the level of noise to be emitted from a small plant processing natural materials. The nearest residence was 600 metres (approx.) from the plant. A total of 13 noise sources was modelled using this method. Two of the major sources were further sub-divided into 5 or 6 parts; each of which was treated as a separate source to assess the effectiveness of noise control treatment options.

Case Study 5: The propagation of noise from automobiles and items of fixed mechanical plant was modelled for 3 residences using the spreadsheet program. The nearest residence was 10 metres from the boundary of the property on which the noise sources were sited. A total of 28 noise sources was modelled at any one time.

Case Study 6: Noise emitted by earthmoving plant and fixed mechanical plant at six different sites was modelled using the spreadsheet program. In general, the nearest residential areas were 150-500 metres from the site. The noise sources were usually housed within a partly open building. As a result the noise was considered to be transmitted through the elements of the building facade and the open areas; each acting as an individual noise source.

4.0 COMPARISON OF METHODS

A comparison of these two methods is provided below. This comparison has been made on seven bases, viz -

. Flexibility   . Output
. Attenuation Features   . User Error
. Set up Time   . Accuracy of Prediction
. Community Area

Note: It is recognised that this list is not exhaustive. These features have been selected to highlight some of the major differences between the two methods by reference to the case studies only. This process of evaluation (especially the effect of ground attenuation and the accuracy of prediction) will be ongoing.

4.1 Flexibility. Both prediction methods are protected and allow the user to access only specific parts of the programs. The general purpose of the protection is to prevent tampering with the calculation algorithms as well as to "steer" the user to the data input sections. The protection on the spreadsheet program, however, can be disabled quite easily. With the protection inoperative the user is free to make modifications to the program as he/she sees fit. (The introduction of user-specific elements into the program architecture, however, can produce errors in the output data. See 4.5 below.) The spreadsheet method is considerably more flexible than the proprietary suite of programs as a result.

In addition the spreadsheet program is set up in modules; each of which can be added and subtracted easily from the basic program without loss of function. The modules allow calculation of various procedures including sound power levels from sound pressure level data, transmission of sound into and out of buildings/enclosures and sound levels from individual sources within large spaces. The number of sources and receiver locations can be expanded to suit the user's requirements: the limit being the amount of memory available in the machine being used. Some of these calculation procedures are available on the ENM model. In the spreadsheet program each of these procedures can be modified by the user to suit his particular needs and circumstances.

This flexibility is particularly useful when optimisation of noise control treatments is being undertaken. In Case Studies 4 and 6, various options for building facade constructions and sizes and locations of openings in the buildings were assessed iteratively. The sound transmission loss (STL) data for these assessments were obtained from many sources and by calculation. Where this optimisation has been required in Case Studies 1-3, the calculations generally have been performed external to the ENM model.

4.2 Attenuation Features. Currently the spreadsheet program can calculate the attenuation provided by only simple barriers. The ENM suite of programs can calculate the attenuation which results from "hilly" topography. This can not be done by the spreadsheet program.

Attenuation by atmospheric absorption and source directivities are each treated in a similar manner by each model. Wind and temperature effects and ground effects are currently addressed by the spreadsheet program in only relatively simplistic terms. These matters, however, are dealt with in far greater depth by ENM.

The combined effect of these matters is considered to be a significant limitation of the current spreadsheet program. Because the attenuation due to wind effects and ground effects tends to increase with distance, however, a limit must be placed on the distance of propagation for which the model may be used and/or the model may need to be validated for each site.

For example, ground attenuation effects for each of Case Studies 4 and 5 were ascertained from actual measured noise levels on the sites being studied. The propagation of noise levels from the noise sources has been conducted only over distances and type of terrain for which the model has been considered to be validated.

4.3 Set Up Time. In general the greater complexity of ENM requires a longer set up time than that necessary for the spreadsheet program. In addition, first time users may need to spend a significant amount of time learning to drive the ENM suite of programs. The spreadsheet program, in its protected format, may be used with success almost immediately so long as the limitations of the program are understood.

The spreadsheet model used for Case Study 5 was set up in a matter of minutes once the source sound power levels were developed and the coordinate system established. The spreadsheet model for Case Study 6 was applied successfully by three different users during various stages of the work that was conducted.

4.4 Community Area. ENM can accept numbers as large as 32000 (i.e. 2^{15}) only. The dimensional constraints of ENM are set accordingly. Most usually, however, the constraints on area or distance would be placed by the user who would define the area and/or the maximum distance on the basis of the total sound power of the source/s, the relative proximity of the community areas under assessment and the effort required to construct the model. (ie. In general the amount of topographical data that is required to be entered increases with the square of the distance from the noise source/s.)

In Case Study 1 the residential community was located totally within a band lying 1-5 kilometres from the centre of the complex. In Case Study 2 the residential community extended for tens of kilometres in most directions from the centre of the noise-producing operations. As a result, preliminary calculations were conducted to set the radial distance for the practical limit of the area of impact. This distance was 2.5 kilometres.

By contrast, in Case Studies 4-6, the community points of interest that were assessed using the spreadsheet program were located in relatively close proximity to the source/s (eg. 10-600 metres away). Until further work is conducted on the spreadsheet program to incorporate ground effects and a more sophisticated barrier calculation procedure, it is likely that the limit on the distance over which environmental noise propagation can be conducted will be in the order of 500 metres.

4.5 **Output**. The ENM program can present environmental noise levels in terms of single point calculations and noise contours. Furthermore, the single point calculation output includes overall noise levels as well as spectra. The spreadsheet program is currently limited to providing an output in terms of single point values only, but these are automatically presented as overall noise levels as well as spectra. The flexibility of the spreadsheet package, however, allows the user to add background noise levels and/or noise produced by other pre-existing noise sources to the calculated environmental noise levels.

The user of the spreadsheet program can also conduct calculations to determine the expected magnitude of any penalty/s that may need to be added to the predicted noise level to account for annoying characteristics of the noise from the source/s under consideration (eg. penalties for tonality and impulsiveness as described by AS 1055 - 1989). This facility is particularly useful when the setting of these penalties is by means of comparison of the output spectrum against the already existing background noise level.

At present this facility is not available in ENM. In fact ENM predicts only component noise levels, ie. those which result from the source/s under consideration only. There is no facility to add the contribution from background noise or other pre-existing noise sources so that noise contours would reflect the noise levels which would be expected to be measured. Nor does ENM allow the emitted noise level to be compared against the background noise level to determine the magnitude of any penalties which may apply. As a result the ENM output may include noise contours which are lower than the already existing background noise level and these contours may still require manual adjustment to account for annoying characteristics of the emitted noise if the application of penalties for such characteristics is prescribed.

For example, it was necessary to make adjustments to the output noise contours that were plotted by ENM in Case Studies 1 and 2 to account for the prescribed penalties for tonality of the emitted noise levels. In addition, for these case studies the background noise levels varied from one locality to another. Extensive manual adjustment of the plotted contours was undertaken using AutoCAD so that the final noise contours included the contribution from the existing background noise levels.

4.6 User Error. As discussed above (refer 4.1), the flexibility inherent in the spreadsheet program may also give rise to user-induced errors. These errors may result easily if calculation algorithms are tampered with or calculation boundary limits are exceeded or ignored. Any users need to be aware of the potential for generation of errors and to incorporate their own means of validating any modifications to the program architecture which are introduced to tailor the spreadsheet program to their particular needs at the time. In any event, the user would be advised to always view the output from any program with a degree of scepticism until he/she is convinced that the results broadly agree with those that could be determined from other means (eg from basic acoustic theory or even intuitive expectations).

4.7 Accuracy of Prediction. A detailed determination of the accuracy of the ENM model was conducted in Case Study 1. A comparison of noise levels predicted by the spreadsheet program and the actual noise levels was conducted in Case Study 4.

In Case Study 1 a total of 287 noise level measurements was made at 95 measurement locations throughout the community. Atmospheric conditions (wind speed, wind direction, temperature and relative humidity) and identifiable noise sources were also logged. The measured noise levels were filtered to establish a set of data which contained noise measurements for which the major contributor was the smelter only. Care was taken to ensure that the locations of the measurements were distributed well throughout the community. The ENM model was used to predict the noise levels that would be expected at the same community locations and under the same atmospheric conditions as those at the time of measurement of the actual noise levels. The results were used to establish an accuracy of prediction of noise levels for this site using the ENM model.

The accuracy of prediction was determined to be such that 74% of all predicted values fell within ± 3 dBA of the measured value and 90% of all predicted values fell within ± 4.9 dBA of the measured value (Moller and Brown, 1991).

The opportunity to conduct a similarly extensive examination of the accuracy of prediction of the spreadsheet program has not yet arisen.

In Case Study 4, however, it was determined that the spreadsheet was able to predict noise levels to within 1 dBA of the measured value under calm conditions over a distance of 600 metres. The closeness of the predicted and measured values was considered to be primarily the result of the validation work carried out at distances of 100-200 metres from the noise sources which allowed the site-specific ground effects to be established. More work needs to be done to determine the accuracy of prediction of this model under a wide range of site conditions.

5.0 CONCLUSIONS

Although the process of evaluation of these two methods is ongoing, it may be concluded that each has its advantages. The ENM method is most useful when assessing the impact of noise emission from a large number of sources to a large community area. The spreadsheet method will be of interest to users who require to calculate environmental noise levels at only a small number of community points in close proximity to the noise sources. The usefulness of the spreadsheet method will be enhanced if the terrain is relatively flat, the user wishes to add additional calculation procedures or the contribution of the background noise level and/or any prescribed penalties must be taken into account.

At one site an extensive assessment of the accuracy of prediction of the ENM method has been made. It was determined that at this site 74% of all predicted values fell within ± 3 dBA of the measured value and 90% of all predicted values fell within ± 4.9 dBA of the measured value.

REFERENCES

Australian Standard AS 1055-1989, Acoustics - Description and Measurement of Environmental Noise, Standards Association of Australia, (1989).

Moller I., Brown A.R., Application of the Predictive Noise Model ENM at Boyne Smelters, Proc. Inter-noise 91, Sydney, (1991).

Tonin R., Estimating Noise Levels from Petrochemical Plants, Mines and Industrial Complexes, Acoustics Australia, 13 (2), 59-67, (1985).

NOISE CONTROL DISTRICTS TO DEAL WITH URBAN POLLUTION

Hu Hui
Environmental Protection Bureau of Loudi
Prefecture
Hunan, P.R. China

ABSTRACT

It is planned that in urban areas control districts must be set up to deal with the problem of noise pollution in order to meet the environmental noise standards. It is one of the measures some cities and provinces in China have adopted and put into practice to deal with noise pollution comprehensively. Concrete methods to set up noise control districts were worked out in Hunan Province in 1988 and specific standards for urban noise control districts were set. They are being adopted all over the province in order to meet the standards. The control of noise pollution will be taken into account in the evaluation of the comprehensive protection of the urban environment. After the functional division of noise control districts in cities and county seats according to "CB3096-82 Standard of Environmental Noise of Urban Area" suitable for China, the comprehensive control over the noise resulting from industry, traffic, the construction of buildings and people's social activities must be exercised and the noise control districts must be managed one by one in turn so that the noise from the boundaries of enterprises and institutions may meet the standards and requirements set in the noise control districts. The beginning noise control area must cover at least one square kilometre and then expand according to the standards and requirements. Now the noise control districts in the cities of Hunan have covered ¼ of all the urban areas. It has been proven that it plays so important a role to set up noise control districts that the environment of the 100,000,000 Chinese people, who live in the urban environment beyond the limit of the noise pollution can be improved.

1.0 Noise pollution is a serious problem of urban environment. Pollution in big and medium-sized cities in China has remained in a high grade since a long time ago. Traffic noise has affected small towns as well as big and medium-sized cities. Noise pollution resulting from industry, construction and daily life are very serious. The urban inhabitants complain more and more about the pollution which does great harm to their life.

The lawsuits concerning noise pollution account for more than 30% of all the lawsuits concerning environmental problems. Some provinces have begun to lay down plans to deal with noise pollution in urban areas comprehensively and set up noise control districts. It demands that cities and towns should be divided into some suitable areas according to GB3096-82 "Standard of Environmental Noise of Urban Areas". Hunan Province has worked out concrete plans to strengthen the management of noise control districts. The plan is included in the evaluation category of comprehensive improvement of the urban environment all over the province and has become a more important part in the construction of cities. People attach great importance to it.

2.0 THE BASIC STANDARD OF NOISE CONTROL DISTRICTS.

2.1 The basic standard of noise control districts which Hunan Province sets is, first of all, the requirements of the practising plan, the maps of the geographic position, the arrangement map of monitoring and measuring stations and the data obtained through measuring and monitoring. The place at the very beginning should be more than one square kilometre in area and above all the residential area should cover more space than the industrial area. It also demands complete, reliable data and complete and detailed information.

2.2 If there exists noise resulting from air motive power, the release of exhaust, vibration etc in enterprises and institutions, the effective measures to control noise and decrease vibration should be put into practice to ensure that 90% of the noise pollution sources reaches the environmental noise standard and that other noise pollution sources don't reach more than five decibels.

2.3 The traffic noise should be controlled. It's planned that more than 70% areas of the main roads should reach the environmental noise standard.

2.4 The noise resulting from construction sites should reach the noise standard for the areas around the construction sites. If it can not reach the standard because of objective reasons, contemporary measures should be taken to protect noise from disturbing people by local environmental protection departments.

2.5 The residential areas' noise can be measured by the noise measurement stations dotting regularly in the areas.

The total number of the stations should be more than one hundred. The distance among the stations must cover 150m². It's necessary to monitor round the clock. More than 80% measurement stations in day time and 85% stations at night should reach the environmental noise standard laid down for the districts. The noise pollution in residential areas should not reach more than 5 dbs except industrial areas.

3.0 THE PLAN OF ESTABLISHING NOISE CONTROL DISTRICTS.

3.1 Hunan Province has established noise control districts and laid down the standard of noise monitoring instruments, measurement conditions, measurement methods and data handling. The noise measurement instruments are mainly sound-grading meters or noise monitoring devices. The noise measurement instruments must be recommended by the Chinese environmental protection departments concerned. Their acoustic and electrical properties should meet the requirements of Type 1 or Type 2 set in "The Properties of Sound-grading Meters and Their Testing Methods" GB3785-83. Acoustic and condenser transmitters must be attached to it. The instruments and devices must be checked carefully according to the standards set by the state. And the results of the checks must be reported to the provincial environmental protection administration department. The voltage of the battery must be stable while measuring. The sensitivity of the whole instrument must be good and its fluctuation must be less than 0.5 db(A) and the interference of the sound area must be reduced. The sensors must be placed 1.2m above the ground and point to the main source of the noise. The meteorology requires no rain or snow while measuring. The speed of the wind should be less than 5 m/s. The temperature in the surrounding area should be above 0°c. The humidity should not be more than 90%.

200 data are to be obtained by using the sound-grading meters and the noise monitoring and measuring devices should be used for 20 minutes continuously. The way to deal with the data is to put the 200 data in good order from the small ones to big ones. The 20th datum is LIO. The 100th is L50, the 180th is L90. Equivalent sound grade can be calculated according to the following formula. "Li" stands for Sound Grade A when you read for the "i" time. "N" stands for the total amount of the sampling.

$$Leq = 10 \ Lg \ (\frac{1}{N} \sum_{i=1}^{N} 10^{0.1 \ Li})$$

3.2 The evaluation of the noise pollution in cities and towns is an important step to establish noise control districts. The area includes all the established districts in the urban area. First it's necessary to divide the city into square meshes. The size of each square mesh is 500m X 500m or 250m X 250m. All square meshes are equal in area. The measuring stations are to be set up in the centre of the meshes. If the centre of the mesh is not suitable for the station, the station can be moved to a place where it's convenient to measure but the spot for the station must be closest to the centre and must be noted in the record of the measurement. If the area of the enterprise in the mesh covers more than half of the area of the mesh, no station there. Some open areas such as farming fields, patches of vegetable plots, rivers, lakes, and deserted building ground may not be monitored or the result of monitoring is kept only as reference materials. The results of monitoring can be shown in the following form.

Station No	Station Location	Statistical Sound Grade			Standard Deviation	Lmin ~ Lmax	remarks
		L10	L50	L90			
I . . . . . . N							

The arithmetic mean of equivalent sound grade in some specific areas can be calculated as required in the following formula. The plan to establish noise control districts can be based on the result. "i" stands for the number of a specific station. "N" stands for the total number of the stations.

$$Leq = \frac{1}{N} \sum_{i=1}^{N} Leq_i.$$

3.3 The general survey of fixed noise sources and traffic noise in urban areas.

It is required to know clearly the situation of enterprises' fixed noise source in setting up noise control districts, esp, the name of the source of the noise and the unit it belongs to, the type, the size, the number, the intensity of the noise and environmental noise. In order to survey the traffic noise, the transportation road must be divided into some sections. The measuring station can be set up on the pavement along every section. The noise may be measured from 8:00 to 12:00 a.m. and from 14:00 to 18:00 p.m. The average value can be regarded as the result. In the meantime the number of vehicles must be recorded while measuring. The length of the section and the average value make the average value of the traffic noise. It may be calculated in the following formula. "Li" stands for the length of the section, "n" stands for the total number of sections.

$$Leq = (\sum_{i=1}^{n} Leq_i li / (\sum_{i=1}^{n} li)$$

3.4 Make plans to establish noise control districts. After investigating the situation of the urban environmental noise and the situation of noise source according to concrete rules which Hunan province makes in establishing noise control districts, cities and towns are to be divided into residential, cultural, educational, industrial and commercial districts. Then, according to the general plan and to the economic and technological conditions in the province, we must gradually expand the noise control districts. When the districts reach the standards and meet the requirements, the environmental protection department concerned will check and issue qualification certificates.

4.0 THE MANAGEMENT OF NOISE CONTROL DISTRICTS BEFORE AND AFTER THEY ARE SET UP.

4.1 It's an important task to deal with urban noise pollution comprehensively to exercise noise control effectively. Hunan province made plans with rewards and punishments to strengthen the management. It is required that the cities' noise sources should take measures to decrease the noise and reduce vibration and exercise noise control according to the principle that whoever releases noise must control it. In the designated period of time, they must reach "the standard of urban environmental noise" and meet the requirements of the noise control districts.

4.2 Industrial noise control

It is required that industrial producers choose low noise equipment and set up noise control districts. The newly set-up enterprises must choose the place very carefully and use the terrain to avoid or decrease noise pollution. The noise prevention equipment will be designed, made and used together with other facilities for production. The noise pollution which is beyond the standard and disturbs people's life and work so much that it makes the plant unable to reach the standard should be managed by the environmental department regularly. If it does not reach the standard in a certain period of time, its time for operation must be limited and approved by the government or it can be ordered to stop production or move away.

4.3 Traffic noise control

In order to control the noise which is caused by all kinds of vehicles, firstly, the motor vehicles should be in good conditions. The silencer should be fixed in the motor vehicles to make it meet the noise standard which motor vehicles should reach. Secondly, motor vehicles must use low-sound trumpets. The sections or districts must be designated to forbid trumpet to release noise according to the requirements of the noise control district. Thirdly, if air planes and motor ships want to go to urban areas, they have to accord with corresponding noise standards. The planes are forbidden to fly low-altitude in urban areas. Loud noise motor vehicles are forbidden to go into noise control districts and trains into the urban areas are forbidden to use steam whistles.

4.4 Social life and construction noise control

The machines which produce noise through vibration in noise control districts must take effective measures to decrease the noise and vibration. Pile drivers, ramming machines, mixers, bulldozers, ditchers, oscillators, electric saws and other machines which produce noise pollution are forbidden to use in residential areas at night. Meanwhile, stipulations are laid down concerning the social life's noise. Broadcasting

trumpets and other sound equipment must accord with the country's noise control standard. If not permitted, loud-sound trumpets are forbidden to use. Firecrackers are forbidden to set off in theatres, gardens, ports and other institutions. Some loud sound tools, such as electric drills, saws and diggers and forbidden to use at night in order to meet the requirements of the noise control districts.

5.0 The quantity evaluation of comprehensive management of urban environment in Hunan reflects the achievements of municipality authorities and administrators. The establishment of noise control districts accounts for 10% marks in the 100% quantity evaluation system. The final marks depend on the percentage of the noise control districts in the whole area and on the coverage of the population in the noise control districts. Thanks to the leaders' responsibility system and clear objectives of their practical plans, the noise control project has aroused the whole society's interest. Some departments concerned, such as environmental departments, public security departments and urban management departments have had a good cooperation in the project. The project in Hunan has achieved rapid, visible and very satisfactory results despite little investment. Apart from this, now the established control districts cover one-fourth of the total provincial urban areas. It is proved that the plan is a complete, scientific one which deserves extensive expansion in the international community.

BUFFER ZONES - ENVIRONMENTAL PLANNING FOR INDUSTRIAL NOISE CONTROL

Douglas Nicolaisen
State Pollution Control Commission - New South Wales
Member Australian Acoustical Society
Clean Air Society of Australia and New Zealand
Australian Water and Wastewater Association

ABSTRACT

The need for, and increasing difficulty in implementing, practical control over offensive noise emissions from extractive industries has been clearly demonstrated in all areas where urban expansion is creeping closer to established quarries and land identified for future extractive activity.

Changes to environmental legislation controlling noise, and the ever increasing expectations of the public that intrusive noises should not enter their houses, hospitals schools and other sensitive locations, has placed a significant demand on regulatory authorities to exercise control, and on local government to provide an adequate buffer zone around such developments.

These buffer zones have been shown to be effective in providing distance attenuation to supplement on-site noise reduction works. However, the vexed question of who should own the buffer zones has raised concerns at the cost effectiveness of "sterilising land", particularly in hard economic times, and when the industry was there first. Identification of compatible land uses is therefore an essential part of the successful application of buffer zones.

1.0 INTRODUCTION

In New South Wales it is the responsibility of the State Pollution Control Commission, and local councils, to implement the environmental protection legislation. This task can often be made extraordinarily difficult by well meant, but nonetheless ill-advised planning decisions which group essentially incompatible land uses together in the same locality. Regulatory authorities can achieve some measure of control through statutory instruments served under the appropriate legislation, and this is generally the only available option in existing situations. Where new areas are to be developed however, potential exists for innovative and thoughtful co-operation between the Regulatory Authority and the Planning Authority, to overcome the identified problems and find the workable compromise that will essentially satisfy all interested parties.

The mechanism for achieving this end needs to be established by the Planning Authority, whose legislative power provides a legal framework in which planning restrictions can be placed, in order to achieve a desired level of environmental control. However, the Regulatory Authority, whose legislation provides the means by which technical and physical controls can be put in place, can provide the practical justification for the Planning Authority establishing the desired planning controls. Once determined, these controls can be included in local and regional environmental plans, and development consent conditions. The present system does not allow either Authority to adequately achieve the whole aim of having appropriate, justified controls in place without the support of the other.

There is a practical limit to the engineering based pollution controls which can be applied to any industry without its viability being jeopardised. This is a particularly pertinent consideration where quarrying or other extractive industries seek to operate, and this paper will concentrate on that industry group. For example, where residential development is permitted to encroach close to an industry that uses explosive blasting as an integral part of its operations, the extreme control measures, or curtailment of operations, that would need to be required by a regulatory authority in order to achieve a normal definition of a reasonable residential environment, could well force a shut-down of that industry in that area. The particular company may have made the substantial investment needed to set up its operations, at a time when adjoining land zoning was entirely compatible and residential development was not being considered.

Land-use conflicts commonly arise when planning authorities alter zoning to allow residential development on formerly rural-zoned land. This is a common process, especially in

areas of the state where pressures to open more and more areas of land to residential development are mounting. However, in circumstances where the land proposed to be rezoned adjoins an operating quarry, the rezoning needs to be managed so that land-uses which are not especially sensitive to noise and dust impacts, are interposed between the quarry and sensitive potential land-uses. Subdivision of rural land for residential purposes close to quarries may appear to be an attractive proposition to developers, but, any advantages to the developer should be weighed against the long term employment and economic benefits offered by any industry whose viability would be threatened thereby.

A somewhat similar situation exists where long standing rural zoned land, with existing residences and the authority to build more on the basis of the property's existing use rights under the planning legislation, is identified as containing an extractable hard rock resource of Regional, or even State significance. These are classic situations where the planning / operational buffer concept must be built into the development process of the quarry on the one hand, and the redevelopment of the rezoned land for residential purposes on the other.

2.0 BUFFER ZONES

A buffer zone is an area of land around a quarry, in which particular planning controls have been implemented to restrict or control development. This would only allow land uses which are compatible with the quarrying to be approved and developed in the core area, thereby minimising potential conflict with the surrounding community, and ensure the community benefits from the development of the resource.

The purpose of the buffer zone is to provide space in which the environmental impacts of an approved quarrying operation on the surrounding community, can be minimised or even removed. It also provides the means whereby the visual amenity of the area can be retained and enhanced, and helps to protect a valuable extractive resource from sterilisation as a consequence of ad hoc planning decisions.

The overall interests of the community are best served by the implementation of a dual planning control approach. This is achieved by splitting the buffer zone into two components and establishing an operational buffer zone, which should be under the direct control of the company having approval to operate the quarry, and a planning buffer zone, over which the local council will need to exercise some control, to protect future and as yet unapproved development of an identified and valuable mineral reserve.

2.1 Operational Buffer Zones   The operational buffer zone
in this situation is defined as the area around a proposed
development (which is the subject of a specific development
application) where environmental amenity is likely to be
significantly affected by the industry operations, in spite
of the pollution control measures adopted being the best
available.

The operational buffer zone should be in the order of 1000
metres radius from the boundary of the identified and
approved extractable resource.   Although at first glance
this approach may appear to sterilise tracts of land, it
allows the company and the community to adequately plan for
the future development of the region, without conflicting
with the development of the resource. Designating the land
as an operational buffer zone does not however, prevent it
being used for a range of uses which are compatible with
the quarrying.   Such use however would need to be under the
control, or with the approval of the quarry owner who, as
stated above, would be expected to own that land.

The zone will be delineated by a contour line around the
operation at a nominal 1000 metres or, if it has been
established by measurement of existing similar operations,
and modified by computer modelling using real parameters of
specific site meteorological conditions, at the calculated
limit of unacceptable impact for the most critical
pollution parameter.   This is usually blasting air
overpressure, or possibly ground vibrations, in the case of
quarrying, however dust pollution may also need to be
considered.

This concept was incorporated by the Mt Misery / Hurdle
Ridge Working Party when it met at Moss Vale, New South
Wales, and reported that an operating buffer zone was
appropriate to be under the control of the quarry operator,
to ensure a reasonable level of security for the quarry
company, which would invest large capital sums in order to
prove a recoverable resource and establish itself to
operate with all the appropriate approvals.

2.2 Planning Buffer Zones   The planning buffer zone is
defined as the principal area of concern surrounding and
enclosing the defined extractable resource. It can be used
to protect the recoverable sections of a known valuable
mineral deposit for which development applications can be
expected to be lodged in years to come. It will secure the
future operational buffer zones and would be derived where
possible, by actual measurement and assessment of a
particular site.
In the absence of measurements, a nominal distance of 1000
metres around an extractable deposit, modified by allotment
boundaries, should be reserved as the initial planning
buffer.   This area may subsequently be varied as more
definitive information becomes available. When the site is
being considered for approval to extract, the Operational
Buffer Zone would need to be identified and established for

each phase of the extraction.

The planning authority, in consultation with industry, Department of Mineral Resources, Department of Planning and the State Pollution Control Commission, should then apply planning controls that will exclude any incompatible land usage, for the time periods when they would adversely effect the viability of the quarry.

The planning buffer zone will also provide a safety cushion for the operation against potential demands by the community, for environmental goals beyond those achievable by point source control, even with using the best available technology. It will also help to restrict the level of environmental expenditure required of the developer or operating company, to that required to maintain the generally acceptable community standards reflected through the current environmental protection legislation.

The distance of 1000 metres for the combined buffer zone was determined initially, from the practical experience of both the Commission and the NSW Quarrymasters Association, as being the minimum distance required to allow blasting activities to be carried out in a quarry, without exceeding the Commission's environmental criteria for noise at the boundary. More recent work done on the Railway Commissioner's quarry at Bombo New South Wales, has shown that with air overblast, 900 metres has been found to be the practical minimum distance at which the Commision's limit of 115dB(Lin) criterion can be met. 1000 metres is being found to be the distance at which the Commission's day time noise limit of 45 dB(A) is most likely to be met, subject to site specific considerations.

The Planning Buffer Zone does not need to be in the ownership of the quarry operator and can be used for the conduct of any one of a range of industries or activities that are compatible with the central activity. This could mean ownership by individuals, companies or even the local council, if that were seen to be appropriate. The key aspect is that irrespective of the ownership, the land in question would be under the control of planning decisions put in place by the local council, and where possible the Department of Planning, which excluded any activity in the area likely to threaten the ongoing viability of the quarry.

3.0 GREEN-FIELD SITUATION (NO EXISTING QUARRY)

Normally it will be the responsibility of a quarry operator to obtain ownership or control of land within the defined operational buffer zone of a proposed new quarry. There is ample precedent for this concept in decisions of the New South Wales Department of Planning where, in granting Development Consent to hard rock quarries, it has

reinforced the wishes of the community and the recommendations of the Commissions of Inquiry which, after hearing submissions from all interested parties, recommended that the proponent should hold proprietorship over the land within the operational buffer zone. The identification of this land is recommended to be on the basis of a common sense appraisal of the existing allotment boundaries. It is not intended that a pedantic adherence to a drafted contour line be the criterion for identifying the land over which the proponent would be required to gain control. Moreover, it needs to be understood that gaining such control may not always be economically achievable, or even possible, if land owners did not wish to sell.

In such cases, where the planning authority, properly advised, considers that controlled exploitation of a defined recoverable resource is overall, in the community interest, it may implement planning controls over land within the operational buffer for which the proponent is unable to secure tenure. This could well restrict the ability of a landowner to fully exploit their ability to erect new dwellings, or pursue other developments that were seen as entitlements on the land, under planning approvals in existence before the identification of the resource.

Such new structures or development would now need to be restricted to something compatible with the new quarry development. The entitlements could well return as the resource was quarried and the operational buffer zone moved in sympathy with the extraction, beyond the limit of effect for a given parcel of land. Compensation in terms of double glazing of windows and / or acoustic treatment of some walls or rooms of impacted dwellings has been mooted. Each site would need specific consideration however, as a common guideline for such cases could be extremely difficult to produce.

The criteria for noise acceptability are the Commission's guidelines which apply to sensitive incompatible land usages such as residences, schools, offices, hospitals and nursing homes. Land uses which may be compatible within an operational buffer zone, subject to assessment for individual situations include: advertising structures, forestry, agriculture, plant nurseries, recreational and sporting facilities, some classes of industry and communication facilities.

4.0 EXISTING QUARRY SITUATION

4.1 No Current Land Use Conflict   Where there is no existing incompatible land use (eg houses) inside the defined operational buffer zone, the greenfield situation applies, ie, the quarry company should obtain control of the land if possible, and the planning authority devises the planning buffer zone required around the entire

extractable resource in consultation with all relevant parties. Once again the planning authority may assist orderly and cost-effective development by also implementing planning controls within the operational buffer if quarry ownership was not possible, and the social worth of the resource warrants such protection.

4.2 Current Land Use Conflict There are often acute conflicts where, as a result of unfortunate planning decisions, incompatible land uses are already established within an existing quarry's buffer zone. In practice, a practical compromise is often reached whereby residents accept a degree of lost environmental amenity and the quarry operator accepts ongoing cost penalties arising from special noise restrictions.

Experience has shown mutually painful but viable co-existence is usually possible more than 500 metres from a quarry boundary. The planning authority should assist in redressing the situation by refusing further incompatible development and preventing continuation of existing situations beyond the tenure of the existing owner, within 500 metres of the boundary of the approved, recoverable resource. The quarry meanwhile, should attempt to progressively gain control of the operational buffer zone if mid to long term operation is planned. The question of compensation for significantly effected residents has also been mooted, but would need to be a site specific consideration.

5.0 CONCLUSION

The concept of setting and protecting defined buffer zones is at this stage foreign to the basic concepts of a number of people and organisations, especially those interested in making profit from land development or resource exploitation. For too many years the processes of planning, development and environmental protection have been allowed to proceed without proper direction or guidance, and without the realisation that they are inextricably entwined. The time is now right for this imbalance to be corrected and for joint consultation between Planning and Environmental Regulating Authorities to develop and implement, the simple and effective controls of well defined operational and planning buffer zones. Additionally, firm guidelines which detail the responsibility for ownership or control of the defined areas, and the methodology recommended to be followed to determine their practical boundaries respectively, need to be established.

The precedents set by the decisions and recommendations of recent Commissions of Inquiry and Government/Industry Working Parties in New South Wales, has clearly established the expectation that the proponent company's ownership, or

at least proprietorship, over the affected lands forming the operational buffer of any quarry, will generally be seen as mandatory. There is also a strong public perception that this type of control is required and welcomed. It should therefore be understood, that any additional cost penalties incurred by the quarrying industry in dealing with environmental control, or with the creation or maintenance of an operational buffer zone, inevitably will flow through the building and road construction industries to the general community, directly as increased housing costs and indirectly through increased rates and taxes.

With the local councils taking the initiative, in setting the necessary planning controls in place to identify and secure the planning buffer zones, compatible industries or recreational pursuits can be located in the planning buffer zone. This will overcome community problems in providing space for activities which have traditionally been difficult to locate without resistance from adjacent landowners. This will secure the future exploitation of the identified recoverable quarry resource, without development pressures or conflicts which could be likely to unnecessarily raise the operating costs of the quarry. A cost-benefit analysis of competing land-use options should be carried out where such conflicts of interest are likely to arise, or have been identified. The question of resource and infrastructure development for raw materials of Regional and State significance may need to be dealt with at State Government level.

It remains now only to provide a sensible documented approach to its implementation, through all stages of the planning and approvals processes, whenever a quarry is proposed. In this way, there should be no reason why any development, having passed through the prescribed planning process and been found to be of benefit and social worth to the community, should have its viability threatened inside its approved life span.

REFERENCES

Manuals

State Pollition Control Commission. Environmental Noise Control Manual.

Reports

Dept. of Environment and Planning NSW. Report of the MOUNT MISERY/HURDLE RIDGE WORKING PARTY." Chapters 6,7 and 8. (July 1987).

Dept. of Planning NSW. Draft Working Party Report Blue Metal Quarrying in the Shellharbour and Kiama Municipalities. pp 20-23. (August 1991)

THE PRESCRIPTION OF ACCEPTABLE NOISE LEVELS

Warren D Renew
Division of Environment, Brisbane

David C Spooner
Division of Environment, Brisbane

ABSTRACT

Community noise is one of the major environmental problems faced by people in industrialised and developing societies. In order to control community noise levels a regulatory authority needs an effective procedure for setting acceptable noise levels. However, there is little consensus in Australia and abroad on the most appropriate way to prescribe these levels. In this paper the authors briefly review efforts to introduce noise rating procedures for controlling noise from commercial and industrial premises. A summary is made of criteria proposed to limit the level of noise annoyance. Relevant Australian noise control legislation is examined and the lack of uniformity in noise control policies is discussed.

1.0 INTRODUCTION

BS 4142 (British Standards Institution) and later ISO R 1996 (International Standards Organisation) were introduced to guide control authorities in assessing noise affecting residential premises. Both of these standards specified methods in which a rating noise level was compared with a noise criterion to decide on the acceptability of a particular noise. The rating noise level was obtained from the measured noise level by making corrections for tonality, impulsivity and duration. The noise criterion was determined from the measured background noise level, or a prescribed basic criterion to which corrections were applied for time of day and type of neighbourhood.

The likely response of the community to the noise depended upon the amount by which the rating level exceeded the noise criterion. Exceedences of up to 5 dB(A) were considered to be of marginal significance so that there was not likely to be any community reaction. Exceedences above 5 dB(A) were expected to provoke complaints. This convenient test led to the "background + 5 dB(A)" criterion for determining an acceptable noise level.

The most widely used indicator of community response to noise is annoyance, and several annoyance scales have been devised. As a result of a synthesis of survey results (Schultz), the percentage of people "highly annoyed" has become the most widely used measure of a community's response to noise. Graphs of percentage highly annoyed versus a noise metric such as L_{dn} are available for noise sources such as road traffic and aircraft.

2.0 ACCEPTABLE NOISE LEVELS

By "acceptable noise levels" the authors mean noise levels which they regard as being acceptable to the community as a whole. They acknowledge that a small proportion of the population, the "supersensitives", will not consider these levels acceptable for a variety of reasons. There is no intention to set levels at which a certain percentage of the population will be "highly annoyed" or likely to complain. Regulatory authorities know only too well that in prescribing acceptable noise levels they must be conscious of practical and financial factors as well as acoustical factors.

2.1 Commonly Accepted Noise Criteria. The US EPA (Environmental Protection Agency) in 1974 recommended a noise limit of 55 dB(A) L_{dn} for outdoor areas in residential and farming districts and other outdoor areas where people spend widely varying amounts of time. A value of 55 dB(A) $L_{eq(24)}$ was recommended for outdoor areas such as school yards and playgrounds where people spend limited amounts of time. The corresponding indoor limits were 45 dB(A).

In 1980 the recommendation was made (World Health Organisation) that an outdoor daytime limit of 55 dB(A) L_{eq} was desirable to prevent any significant community annoyance, as well as an indoor limit of 45 dB(A). An outdoor night-time limit of 45 dB(A) was also recommended to minimize sleep disturbance. In the same year the OECD (Organisation for Economic Co-operation and

Development) recommended, for outdoor community noise expressed in terms of L_{eq}, that:

- values less than 55 dB(A) were desirable

- values between 55 and 65 dB(A) were undesirable, and

- values greater than 65 dB(A) were unacceptable.

These recommendations indicate that daytime and night-time average levels of 55 and 45 dB(A) L_{eq} respectively, in addition to $L_{eq(24)}$ and L_{dn} values of 55 dB(A), are generally acceptable outside residences. As such, these long-period metrics are suitable for planning purposes, particularly in connection with proposed transport routes. However, they are not so useful for purposes of regulation and enforcement because they allow periods when a noise can be highly intrusive, while the effect is averaged out over the remaining time (Hooker). It is apparent that a shorter assessment period is required, say one hour at most, and also an upper noise limit.

2.2 <u>Australian Criteria</u> . Australian policies for controlling noise from commercial and industrial premises do not include any of these criteria as specific goals. However, an analysis of the policies indicates that the upper limits for intrusive noise sources in residential areas bordering commercial or industrial areas are approximately 55 dB(A) for daytime and 45 dB(A) for night-time. It is only in residences in predominantly industrial areas or areas bordering extremely dense traffic routes that noise levels of the order of 65 and 60 dB(A) during the day and night respectively are prescribed in the policies.

It is recognised that road traffic is the dominant source of community noise. A community noise survey carried out in Brisbane in 1988 (Duhs E.) indicated that about 22% of residents interviewed claimed to be seriously affected by noise from light and heavy vehicle traffic. It is interesting to note that only about 23% of these seriously affected people had complained about the noise.

State road traffic authorities have developed or are preparing policies for gradually reducing road traffic noise levels in the community. Currently some States use a noise limit of 68 dB(A) $L_{10(18 h)}$, others 63 dB(A). Proposals are in hand to lower the limit in time to 63 dB(A), which is likely to become the environmental goal for planning purposes. It is generally considered in New South Wales that a goal of 55 dB(A) is desirable but not always practically achievable (Woodward J.).

2.3 <u>Methods for Prescribing Acceptable Noise Levels</u>. Environmental noise limits may be of the following main types:

- source limits

- emitter boundary limits

- receptor limits

Receptor or immission limits seem to be the limits most commonly used by regulatory authorities, although combinations of the above types are sometimes used.

When receptor limits are involved, the major differences between prescriptive methods derive from the procedures used to obtain the allowable noise level. One can conveniently separate these procedures into two major types:

- zoning procedures

- background exceedence procedures

2.3.1 Zoning Procedures. Values of allowable noise level are based on the type of area or neighbourhood in which the receptor is located and on the time of day during which the noise occurs. Thus higher values of noise level are allowed for industrial areas than for commercial or purely residential areas. Similarly, allowable noise levels for daytime are higher than for night-time. Zones may be prescribed in certain areas, town planning zones may be adopted, or, as is often the case, an assessment of the zones may be made by officers of the noise control agency.

A variation of this procedure is the derived zoning procedure which incorporates a systematic procedure for calculating the allowable noise level. This procedure is based on the type of neighbourhood and the time of day. The standards BS 4142 and ISO 1996 are examples of this procedure. As a further variation, the Victorian EPA procedure consists in evaluating the allowable noise level from a set of graphs, using a factor derived from the relative areas of various land use zones surrounding the receptor.

Zoning procedures have the following advantages:

- simplicity - they are easy to understand

- consistency - they yield similar levels for similar situations

A major disadvantage is that such procedures are rather inflexible, so that residents in relatively quiet districts may be obliged to suffer significant increases in noise levels.

2.3.2 Background Exceedence Procedures. The allowable level is determined from the measured value of the background noise level (or a tabulated value based on data from previous noise surveys) by adding a predetermined amount called an exceedence. The value of the exceedence is often taken as 5 dB(A), based on the "background + 5 dB(A)" criterion mentioned above.

One apparent advantage of such a procedure is its basic fairness: the same exceedence is allowed in all noise sensitive areas, so that all people are treated equally. Intrusive noise is permitted to exceed the local background level by a fixed amount. By contrast, when the zoning procedure is used, the allowable noise levels in different neighbourhoods depend upon the types of area.

A major disadvantage of this procedure is that background noise levels must be determined before allowable noise levels can be evaluated. There is thus a continual demand on the resources of the control agency to measure background noise levels for individual situations. Considerable savings in time and manpower can be made if a comprehensive noise survey is carried out and background noise levels evaluated for sub-districts in cities and towns. To date noise surveys in Australia have been limited in this respect but noise mapping of a Queensland city in terms of L_{eq} and L_{90} was carried out in 1986 (Eddington N.J.E.).

Alternatively, data from noise surveys can be used as the basis for a prediction procedure for background noise. Analysis of the 1986 Brisbane noise survey (Deutscher K.) indicated that values of background noise level could be predicted at the 95% confidence level within ± 5.5 dB(A) for the night-time, ± 1.6 dB(A) for the evening, and ± 3.6 dB(A) for the daytime periods. These results were most pleasing, given the limited number of survey sites, and indicated that further sites should be surveyed to increase the accuracy of the prediction.

When noise complaints are being investigated, the assessment is preferably, and often required to be, carried out at the time when the complainant is most annoyed. For refrigerator noise this time could be when the background noise level is lowest, usually between 1.00 am and 3.00 am in Australian cities.

The problem arises as to whether the minimum value of background noise level is a suitable value for planning and control purposes. It may be more appropriate to choose the arithmetic average of the hourly values for each period, or to allow some tolerance above and below the average. Use of the minimum value is likely to be too restrictive for industrial noise sources.

A drawback of the background exceedence procedure is that the cumulative or frequency distributions of the ambient noise and the intrusive noise are not compared. Accordingly the regulatory authority does not know what the distribution (and the value of L_{10}) of the resultant noise will be. It follows that simply comparing the L_{10} of the intrusive noise and the L_{90} of the ambient noise does not give an adequate consideration of the noise situation (Eisner M.).

"Background creep" occurs when successive industrial or commercial developments in an area are allowed to gradually raise the background noise level. Of course, increases in motor vehicle flow rates will have a corresponding effect. Use of the background exceedence procedure without restraint will result in background creep. A background noise ceiling is obviously required in the procedure for each of the standard time periods. In Australia two States have adopted such a procedure in their noise policies.

3.0 AUSTRALIAN NOISE CONTROL LEGISLATION

The Australian constitution does not give the Federal government specific powers to introduce legislation for controlling environmental noise. Accordingly, in the 1970s and in line with other countries, the State governments separately introduced environmental noise legislation in response to the growing community demand for noise control.

The majority of the States established central agencies to exercise overall responsibility for noise control. This situation differed from that in England, where local authorities were given primary responsibility, and in the USA, where overall responsibility was vested in the Environmental Protection Agency.

In Australia the six State and two Territory agencies generally control noise from non-domestic premises while local authorities and the police share the control of domestic noise. There has been a trend, as in the USA, for local authorities to be given wider responsibility for noise control. Accordingly, the central agencies are adopting more of a coordinating and advisory role and provide assistance to local authorities in resolving local noise problems (Australian Environment Council).

The Environmental Noise Control Committee which reports to the Australian and New Zealand Environment Council coordinates certain activities of the State and Territory noise control agencies. Its objective is to draw up technical bases for legislation on topics where a common approach is desirable. These topics have included: shooting ranges, blasting, competitive motor sports and labelling.

Initially the prescription of acceptable noise levels was based mainly on the methods contained in AS 1055 (Standards Association of Australia). The 1973 edition of AS 1055 was modelled on BS 4142. If the background noise level could not be measured, a table of values based on the type of neighbourhood was provided for guidance. As was the case with BS 4142, values in this table were later shown to exceed those obtained in noise surveys (Renew W.D.) and accordingly had to be used with caution.

The current edition of AS 1055 suggests the following methods for rating an intrusive noise:

- comparison of a rating level L_{Aeq} or a percentile level L_{AX}, both adjusted for tonality and impulsivity, with the noise limit set by the regulatory authority.

- comparison of the adjusted value of the average maximum noise L_{Amax} with the background noise level.

L_{Amax} is the most widely specified descriptor for intrusive noise, although there is a trend towards using L_{Aeq} for certain applications, such as helipads. L_{A10} is used by some States and is commonly regarded as an approximation to L_{Amax}.

AS 1055 defines four time periods: early morning (0600 - 0700), day (0700 - 1800), evening (1800 - 2200), and night (2200 - 0600). However, the time periods specified in the majority of State noise policies are day, evening and night. Two States have dispensed with a separate evening period. Typical measurement durations range from 5 to 30 minutes, but a representative interval is commonly selected to suit the noise being assessed.

The zoning procedure is used in three State policies, and the background exceedence procedure in the others. The acceptable noise level is variously termed: noise limit, zoning level, assigned level, permissible noise level and prescribed noise level.

There is thus a confusing variety of procedures, descriptors, measurement durations and terminology employed in Australia. In addition, there is no agreement on the number and magnitude of corrections to be made to the intrusive noise level for noise character. Table 1 below shows the maximum corrections used by the State authorities. It is apparent that the rating level for a certain intrusive noise will vary in value depending upon the State in which it is being assessed.

Except in the New South Wales policy and the draft Queensland policy, acceptable noise levels specified in the policies are measured levels. That is, they comprise component levels of noise sources superimposed on ambient levels. It is suggested that the specification of component limits is the more effective procedure: the noise maker clearly knows the limit for noise emission from the premises. An acoustical consultant can then design to meet these limits without being concerned with ambient noise levels.

Faced by the differences in setting noise limits described above, manufacturers of equipment and process plants can become justifiably confused. It is likely that the design of plants will require modification to gain compliance in different States.

Table 1. Maximum corrections for noise character in Australian State and Territory noise policies.

Type	Qld	NSW	Vic	Tas	SA	WA	ACT	NT
Tone	5	5	cal	5	5	5	5	5
Impulse	5	5	mea	5	5	10!	5	5
Modulation	-	5f	5	-	5	5	5	-
Duration	-	-	cal	-	-20	-15	-	-
Repetition	-	5*	-	-	-	-	-	-
Variability	-	-	-3	-	-	-	-	-
Policy Max.	10	10	-	-	-	15	10	-

f - frequency modulation   cal - calculated
* - night-time only   mea - measured
! - on Slow response

4.0 CONCLUSIONS

The authors have shown that noise policies in Australian States and Territories generally have noise limit criteria similar to those recommended by international organisations.

There is, however, a clear need in Australia for a rationalisation of noise policies to produce consistency in the prescription of acceptable noise levels.

The opinions expressed in this paper are those of the authors and not necessarily those of the Department of Environment and Heritage.

REFERENCES

AS 1055 - 1989, Acoustics - Description and measurement of environmental noise. Part 1: General procedures; Part 2: Application to specific situations, Standards Association of Australia, Sydney, 1989.

Australian Environment Council, Environmental Noise Control Legislation in Australia, Report No 20, Second Edition, 1986.

BS 4142:1967, Method of Rating Industrial Noise Affecting Mixed Residential and Industrial Areas, British Standards Institution, London, 1967.

Deutscher K., An Ambient Noise Level Prediction Model for Brisbane, B.U.R.P. Thesis, University of New England, Armidale, 1988.

Duhs E., Eddington N.J.E. and Renew W.D., Brisbane Noise Survey 1986 to 1988, Government Printer, Brisbane, 1989.

Eddington N.J.E. and Spalding R.J., Toowoomba noise survey - a first appraisal, Proc.Aust.Acoust.Soc., Toowoomba, 100-107, (1986).

Eisner M., Taylor E. and Burgess M., Background Noise Levels for Community Noise Assessment, Proc.Aust Acoust. Soc., Hobart, 23-30, (1987).

Hooker R.J., Developments in Noise Control,Technical Paper vol 16, no. 22, Proc.I.E.Aust.(Qld), (1975).

ISO R-1996, Assessment of Community Noise with Respect to Community Response, International Standards Organisation, Geneva, 1971.

Organisation for Economic Co-operation and Development, Conference on Noise Abatement Policies, Paris, 1980.

Renew W.D., Community Noise Surveys in Australia, Proc. 12th ICA, Paper C9-1, Toronto, (1986).

Schultz T.J., Community Noise Rating, Second Edition, Applied Science Publishers, London, 1982.

U.S. E.P.A., Report No. 550/9-74-004, Information on Levels of Environmental Noise Requisite to Protect Public Health and Welfare with an Adequate Margin of Safety, Environmental Protection Agency, Washington, D.C., 1974.

W.H.O., Environmental Health Criteria 12 - Noise, World Health Organisation, Geneva, 1980.

Woodward J., Report on a Proposed Expressway from Pennant Hills Road, Beecroft to Pittwater Road, Ryde Known as the F2 Stage 1, Commissioners of Inquiry for Environment and Planning, Sydney, 1990.

NOISE ASSOCIATED WITH THE TIMBER INDUSTRY

Cedric Roberts
Division of Environment
Department of Environment and Heritage
Brisbane, Queensland

ABSTRACT

Machinery noise emanating from joinery, woodworking and sawmill premises ranks very high in terms of source noise levels, employee exposure and the impact on residences in the area. The paper will summarise the results of various noise surveys carried out at woodworking premises both locally and overseas. Some of the principal sources and noise levels associated with such operations will be identified and various engineering and building control options considered using computer modelling.

1.0 INTRODUCTION

The harvesting, processing and manufacture of timber products involves a number of inherently noisy operations due to either sawing, planing or cutting action.

Hazards of hearing loss due to occupational noise exposure and noise nuisance at locations far removed from timber processing premises have received and are continuing to receive considerable attention from governmental agencies and the general public.

Interior sound pressure levels of many plants have been measured with regard to industry hearing conservation programs. Data has been collated from 25 noise surveys carried out overseas, in Western Australia and Queensland and includes 60 source measurements on items of equipment.

While this paper will not deal with every item of equipment used by the industry, it will present typical noise levels recorded at operator positions, representative occupational noise exposures and results of computer modelling of interior and exterior noise levels. It will present the basic engineering solutions that have been found to be most suitable in dealing with some of the major noise offenders.

2.0 SOURCE NOISE MEASUREMENTS

Noise level and noise exposure surveys were carried out on behalf of a number of companies during the period July 1971 to June 1991. The majority of the surveys carried out in Western Australia were commissioned to comply with the requirements of the Noise Abatement (Hearing Conservation in Workplaces) Regulations 1983.

Specific obligations are set out in these regulations for the occupier of a factory or premises and include:

- Measurement of noise exposure for workers
- Identification of noise hazard areas, machines and tools
- Identification of employees who are likely to be exposed to noise hazards
- Recommendation of suitable hearing protection devices

The Regulations have adopted an equivalent continuous noise level, $L_{Aeq,8h}$ of 90 dB(A) for fixed, permanently located or regularly used machinery, plant, equipment, operation or process as defining the high risk areas for steady and fluctuating noise. For areas exceeding 90 dB(A) the permissible exposure time is halved for each 3 dB(A) increase in sound energy level, hence the equivalent exposure time for a noise level of 93 dB(A) is 4 hours.

The Regulations also require noise level reduction at any area or location where a noise hazard exists. This reduction can be achieved by the use of engineering methods or administrative controls such as rostering work to reduce exposure time where practicable in the workplace. Should these methods prove impracticable, every worker exposed to a noise hazard shall be provided with suitable hearing protection.

Noise levels taken around machines were generally taken at 1 metre from the envelope of the machine and at locations likely to be occupied by the operator. A precision sound level meter, octave analyser and tape recorder were used to determine the A and C weighted noise levels and octave band frequency analysis of static equipment and for evaluating the noise in the area surrounding such items of equipment.

Average sound pressure level data for a range of woodworking equipment - saws, planers, routers and sanders - on load are presented in Table 1.

TYPE OF EQUIPMENT	A-WEIGHTED OCTAVE BAND SOUND PRESSURE LEVELS, dB AT CENTRE FREQUENCIES, Hz								OVERALL dB(A)
	63	125	250	500	1000	2000	4000	8000	
SAWS	83	82	90	87	93	97	98	98	103
PLANERS	79	88	95	94	94	97	90	86	101
ROUTERS	70	74	83	93	94	93	90	84	98
SANDERS	67	89	83	80	84	87	88	85	93

TABLE 1: SOUND PRESSURE LEVEL DATA
FOR WOODWORKING EQUIPMENT

The average spectra for a variety of saws is illustrated below.

TYPICAL SAW NOISE LEVELS
AVERAGE OCTAVE BAND SPECTRA

OCTAVE BAND MID-FREQUENCIES Hz
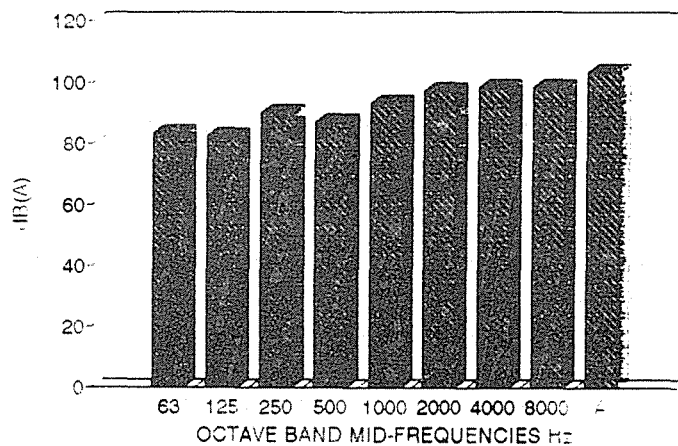
Noise dosimeters are conveniently attached to employees whose individual noise dose varies due to their mobility and variety of duties. The employees individual risk is then evaluated after the dosimeter has been worn for a sufficient time to give a representative sample of the employee's working conditions. This is normally a minimum of half a shift. The risk is expressed as the equivalent continuous noise level or mean energy level in dB(A) designated as $L_{Aeq,8h}$. This is the level of a steady state noise which at a given position and over a defined period of time, would have the same A-weighted energy content as the fluctuating noise under consideration.

The range of $L_{Aeq,8h}$ for carpenters and millwrights recorded during the surveys varied from 87.8 to 102.7 dB(A) with an average of 93 dB(A).

3.0 NOISE CONTROL

A summary of various noise control methods that have been successfully applied to woodworking machinery together with effective noise reductions achieved are outlined below:

3.1 General

Noise from circular sawing machines will depend not only on the characteristics of the material being cut but also on the rate at which it is being cut and the mechanical characteristics of the cutting saw. Noise sources may include: impact noise of the saw against the workpiece, vibration of the workpiece, aerodynamic noise from the saw blade, and also vibration of the saw blade.

Aerodynamic saw blade noise (hiss) will be considerably reduced by running at the correct blade peripheral speed. This is usually the most predominant source of saw blade noise. However, occasionally, particularly with large diameter saw blades (over 400 mm diameter), high levels of blade vibration occur which result in tonal type noise (ringing).

3.2 Damping

Two methods have proved successful in damping blades:

.   By raising the natural frequency of the blade by stiffening with a collar around the blade;

.   By adding damping pads to the surface of the disc.

The pads or stiffening rings must reach as far out towards the periphery as possible. The ideal situation is to provide stiffness and damping together.

The reduction of noise achieved at the feed end, operator position was 3 dB(A) and along the axis of the saw blade 8 to 9 dB(A). Unfortunately the use of damping pads and stiffening rings are hardly conducive to good wear and convenience.

The application of a coat of underseal to the guards and exhaust hoods of a ten blade ripsaw dampened the vibrating surfaces. The noise reduction achieved 1 m in front of the saw under idle conditions reached 5 dB(A).

3.3 Shielding

The use of shields between a noise source and an operator has proven effective when both the source and the employee are close to the shield and when the noise is predominantly high frequency. The installation of a 6 mm thick (60 x 122 cm) auto safety glass shield in a particular situation gave an overall reduction of 9 dB(A) mainly concentrated in the 2 kHz to 8 kHz octave bands. It should be noted that with multiple units close together this type of treatment would probably not be effective. A pitfall in shield design is that if room conditions are too reverberant and the ceiling is too low, the shield is bypassed.

3.4   Personnel Enclosures

A partial enclosure similar to a full height telephone booth was constructed to protect the operator from noise radiated by a radial saw in a wood working shop. The walls of the booth were sheet steel outside and 100 mm thick fibreglass plus an inner protective surface of perforated metal. It had a double glazed, safety glass observation window in one side and the opposite side was open. The noise reduction achieved varied from 12 dB at 500 Hz to 21 dB at 8 kHz.

3.5   Full Machine Enclosures

An edge planer produced a noise level at the operator position of 106 dB in the 500 Hz octave band. The noise was generated by the high speed rotary cutters planing hardwood. To confine this noise, a sound enclosure was constructed of plywood lined with 100 mm thick flexible polyurethane foam. The enclosure was sealed to the floor with mastic, the doors were weather stripped, and all controls through the enclosure walls were sealed. The feed and discharge openings were baffled with double flaps of rubber. This treatment reduced the noise level by 18 dB in the 500 Hz octave band.

4.0   INTERIOR NOISE MODELLING

Occupational noise legislation invariably requires the occupier of industrial facilities to take all practicable steps to eliminate noise hazard areas by reduction of the noise level and/or employee noise exposure. An additional benefit derived from such interior noise control is manifested in an improved noise climate experienced by the community remote from industry.

The simulation of complex noise situations in industrial facilities through computer modelling can greatly assist in achieving the optimum noise reduction by avoiding unnecessary expenditures. A computer programme has been used to predict noise levels in industrial facilities and provide valuable insight on the impact of various noise abatement strategies and plant engineering activities (ie. re-arrangement of plant layout, quietening or removing individual machines and/or increasing the sound absorption of the ceiling and walls) prior to their implementation.

The same model can also be used in the planning stages of new industrial facilities when the effect of various building materials, plant layouts, ceiling heights, machine design etc can be evaluated and noise predictions made for each operator work place.

The program calculates sound pressure levels at points around a factory floor from input data on:

.   Equipment sound pressure levels (obtained by measurement, from specifications or manufacturer's estimates) in octave band centre frequencies 125 Hz to 8 kHz with each machine running alone.

Room characteristics. The overall sound pressure level at any point is found by combining the direct and reflected sound from each machine. Reflected sound is calculated by taking a reflection off each wall, the ceiling and the floor. The sound at a receiver point is therefore compounded from six reflections from each machine.

Additional input data required is indicated in a flow diagram of the programme shown in Figure 1.
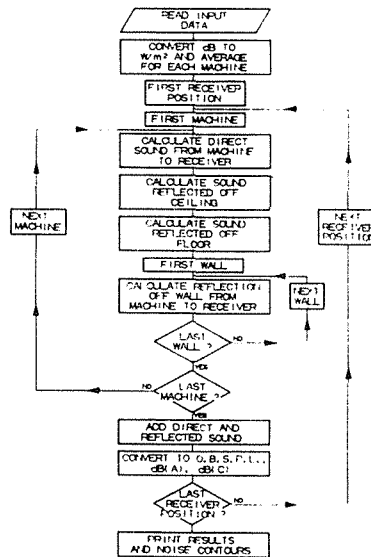
FIGURE 1: FLOW CHART OF INTERNAL NOISE MODEL

The positions of receiver points, machines and wall end points are specified as (X,Y) co-ordinates, the co-ordinate unit being 1 m. The output data given on a line printer shows the positions of the receiver points, the cumulative sound pressure level in octave bands 125 Hz to 8 kHz and the overall levels in dB(C) and dB(A) at each receiver point.

A print-out of a typical situation involving three noisy machines situated on a factory floor measuring 50 x 40 m and having a ceiling height of 4 m is given in Figure 2. The interior finish comprised a concrete floor, painted brick walls and untreated ceiling.

LOCATION OF RECEIVER POINT	OCTAVE BAND FREQUENCY	TOTAL SOUND INTENSITY	OCTAVE BAND SOUND PRESSURE LEVELS	OVERALL SOUND PRESSURE LEVELS	
CO-ORDINATES (m)	Hz	Wm^{-2}	dB	dBC	dBA
X Y Z					
5.00 10.00 1.50	125	.217E-01	103.4		
	250	.114E-01	100.6		
	500	.299E-01	104.8		
	1000	.802E-01	109.1		
	2000	.309E-02	95.0		
	4000	.703E-03	88.5		
	8000	.173E-03	82.4		
				111.7	110.1

FIGURE 2: SOUND PRESSURE LEVELS INSIDE A FACTORY

5.0 EXTERIOR NOISE MODELLING

It is sometimes necessary not only to reduce noise emission of each individual machine and equipment in the plant to ensure compliance with occupational noise regulations, but also to consider allocation of these machines within the plant area and construction of effective housing to satisfy community noise regulations.

Computer modelling allows the prediction of environmental noise levels where no direct measurements are possible at various distances from a plant for varying terrain and a range of meteorological conditions. Consideration is given to attenuation based on geometrical spreading, atmospheric absorption, ground effects, meteorological conditions and natural and man-made barriers.

These noise levels can be calculated preferably from a knowledge of the sound power levels of the noise sources or sound pressure levels measured at a reference distance in a specified direction. Reverberant sound pressure levels inside a building can also be used following interior noise modelling described in Section 4.0.

The program can predict the noise environment resulting from the operation of a number of noise sources by calculating the sound pressure level at the selected receiver position, in each octave band due to each source, making allowance for the variety of factors affecting propagation. The frequency band sound pressure levels at the receiver position for each source are converted to A-weighted values and these added logarithmically to give the overall dB(A) value. A flow diagram for the model is shown in Figure 3.
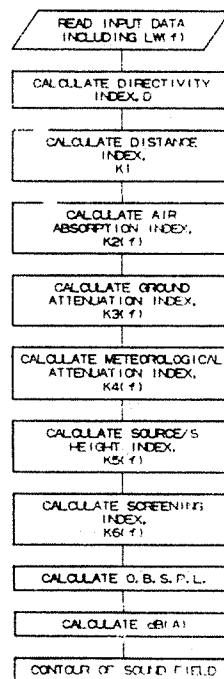
FIGURE 3: FLOW CHART OF EXTERNAL NOISE MODEL

The model has been successfully applied in determining suitable separation distances from woodworking premises in order to satisfy existing ambient noise levels and/or noise criteria prescribed in regulations.

The calculations for a joinery in terms of dB(A) at a distance of 100 m from a specific wall carried out with the help of the computer program are shown in Table 2. The dimensions of the joinery were 30 x 10 m with a ceiling height of 4 m. The building elements used in the modelling were as specified below:

Three walls of corrugated iron	total area	170 m²
One wall of concrete block	area	55 m²
Double glazed window	area	10 m²
Solid core door	area	5 m²
Roof of corrugated iron		225 m²

The reverberant level of 106 dB(A) inside the joinery was due to a thicknesser during the cutting process.

PART I.D.	DISTANCE m	AREA m²	INTERNAL NOISE LEVEL	SPL dB(A)
Wall 1	100	60	106	53
Window 2	108	10		31
Wall 2	108	50		41
Door 3	115	5		23
Wall 3	115	55		8
Wall 4	108	60		42
Roof 1	108	225		47 total 54

TABLE 2: RESULTS OF PREDICTIONS FOR JOINERY

Suitable separation distances based on an exceedance no greater than 5 dB(A) above a background noise level of 35 dB(A) with tonality present are given for different building configurations in Table 3.

BUILDING CONSTRUCTION		BUFFER DISTANCE, m
i)	Sheet metal cladding with 25% open area facing affected premises	2200 to 4000
ii)	Sheet metal cladding with 6% open area for ventilation, facing affected premises	1000 to 1800
iii)	Sheet metal cladding with all openings closed. Ventilation through treated ducting	450 to 800
iv)	200 mm dense concrete block walls, acoustic ceiling, acoustically treated ventilation system. No openings towards affected premises	30 to 60

TABLE 3: SUITABLE SEPARATION DISTANCES FOR A JOINERY

6.0 CONCLUSION

Woodworking premises usually contain many machines of greatly varying acoustical characteristics which rank very high in terms of both noise level and employee exposure. Many woodworking machinery noise problems result from the use of saw blades or cutterheads to cut or surface wood. These tools produce noise through aerodynamic disturbances and by producing structural vibration of the tool and/or workpiece.

In industrial noise control it is helpful to predict noise levels prior to machine installation as well as reductions in plant noise levels due to individual machine control. Computer simulation is helpful in predicting the reduction in noise levels resulting from noise control of particular machines.

7.0 REFERENCES

Elvhammar H., Noise Abatement in Sawmills, Sweden's New Approach to Noise Control in Industry, Inter-Noise, San Francisco 1978, 179-184.

Patrick K.L., Sawmill Noise Control, Noise-Con 81, Raleigh, North Carolina, 323-328.

Roberts C., Source of Environmental Pollution from Sawmills and Control Options, Institution of Engineers. Australia, National Engineering Conference, Hobart, April 1991, 159-162.

Roberts C., Acoustical Modelling as an Aid in Noise Planning, 7th Annual Meeting of the International Association for Impact Assessment, Griffith University, Brisbane 1988.

Roberts C., Computer Modelling for the Prediction of Internal Noise, National Conference, Australian Acoustical Society, Perth 1984, 16.1-16.5.

Journals

Roberts C., Cost-Effective Noise Control using a Computer Model, Confederation Report, June 1983, 25-27.

A Computerized Road Noise Design
and Assessment Conference Facility (RONDAC)

W.K. Szeto and Raymond Chan

Environmental Protection Department
Southorn Centre, Wan Chai, Hong Kong

ABSTRACT

The Environmental Protection Department (EPD) of the Hong
Kong Government has developed a computerized ROad Noise
Design and Assessment Conference facility (RONDAC) which
provides a conference setting for planners, architects,
designers and engineers to assess and plan against road
traffic noise impact interactively. With the aid of
RONDAC, the number of sensitive uses exposed to certain
road traffic noise levels can be effectively calculated and
displayed in a 3-D isometric image of different colour
patterns. Comparison of different road / housing scenarios
under different criteria can be interactively performed by
an individual or a conference of multi-disciplinary
professionals using the projection device. The system also
allows easy editing of road / housing schemes and
evaluation of barriers' effectiveness.

1.0 INTRODUCTION

The Hong Kong Government has set planning criteria of 70 dB(A) L10 (1 hour) and 65 dB(A) L10 (1 hour) as the maximum facade traffic noise levels for new residential premises and educational institutions respectively (Reference 1). The same criteria apply to these uses under planning as well as to new roads at the planning stage. Whilst noise abatement schemes, such as the introduction of open-textured quiet road surface (Reference 2) and the school insulation programme (Reference 3) were implemented, the key of managing the traffic exposure lies in proper planning. In order to ensure that good acoustical practice would be translated into landuse planning and building design, tools which can not only carry out accurate acoustical predictions but can also bridge the disciplines of planners, architects and engineers need to be developed. The ROad Noise Design and Assessment Conference (RONDAC) facility is such a tool.

2.0 CONCEPT & COMPONENTS OF RONDAC

2.1 Concept

Traditionally, the acoustician's contribution towards the total planning process of either a noise source (e.g. highway) or a noise receiver (e.g. a school) has been viewed as, and regrettably confined to, specialist advice which, more often than not, do not constitute a major influencing factor, either in terms of extent or in terms of getting in at the early stage of the planning process. As a result, most practical acoustical solutions could not be incorporated into a project either because it would have cost too much or it was too late.

This phenomenon survives on and is perpetuated by two facts. Fact number one is that the institutional arrangements tend to compartmentalize, separately, agencies / disciplines responsible for the planning, design and construction of noise sources and noise receivers with the pool of acoustics expertise interacting separately with these agencies at different junctures, without an integrated and wholistic approach. Figure 1 illustrates schematically this arrangement. Fact number two is that acousticians have developed prediction models which are becoming more accurate and more sophisticated but also less easily understood by others outside the acoustician compartment. In other words, there is a built-in need of communication as a result of the institutional arrangements, a need which has so far not been satisfied by the development of acoustics expertise.

Experience has shown that in real life situations, tools are necessary to, on the one hand, provide the state of the

art prediction technology whilst on the other hand, create a communication channel between all concerned agencies and disciplines. The tools must be user-friendly and designed for the purpose of communicating acoustics to the non-acousticians.
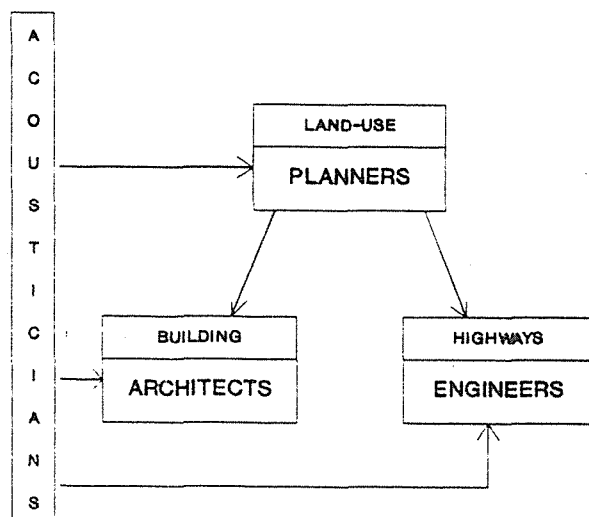
Figure 1 - Conventional institutional arrangements
          showing the acousticians' input to
          various agencies/disciplines

In Hong Kong, it has proved to be of paramount importance because of the compactness and the pace of the metropolitan developments. Conventional noise abatement measures such as low rise earth mounds are normally ineffective and the sort of measures that need to be incorporated often need to be devised in the early planning stage of a project otherwise it would not be possible to incorporate them later on. In some cases, the measures that are effective go beyond the conventional scope and boundary of the particular project under planning. Typical examples are the landuse planning involving a mass transit railway line integrating into a new town centre, and a residential development of more than ten thousand people on a podium decking over a 6800 vehicles per hour trunk road (References 1, 4 and 5).

The RONDAC, designed with the objective of effecting communications between acousticians, planners, architects, designers and engineers is intended to achieve the following :-

. an accurate and quick prediction process;

. a presentation of results in easily understandable
  parameters to non-acousticians, e.g. number of
  premises needing insulation;

. an interactive tool which would allow simple "what-if" questions raised by non-acousticians; and,

. a facility which can, if necessary, enable professionals of different disciplines to see for themselves instantly the consequences of their "what-if" questions presented in parameters of interest to them, in addition to the acoustic impact.

It is believed that the concept behind RONDAC represents a significant point sorely missing in a wholistic approach to the noise abatement design process. Whilst the individual components of RONDAC may be different as the circumstances may require, the concept and the structure of RONDAC should serve to set up the very first step of hopefully many to come, towards taking the acoustics expertise out of its own compartment in a manner subtlely influencing the decisions of non-acousticians for an ultimately better planned acoustic environment.

2.2 Components

The components of the RONDAC system are illustrated schematically in Figure 2.
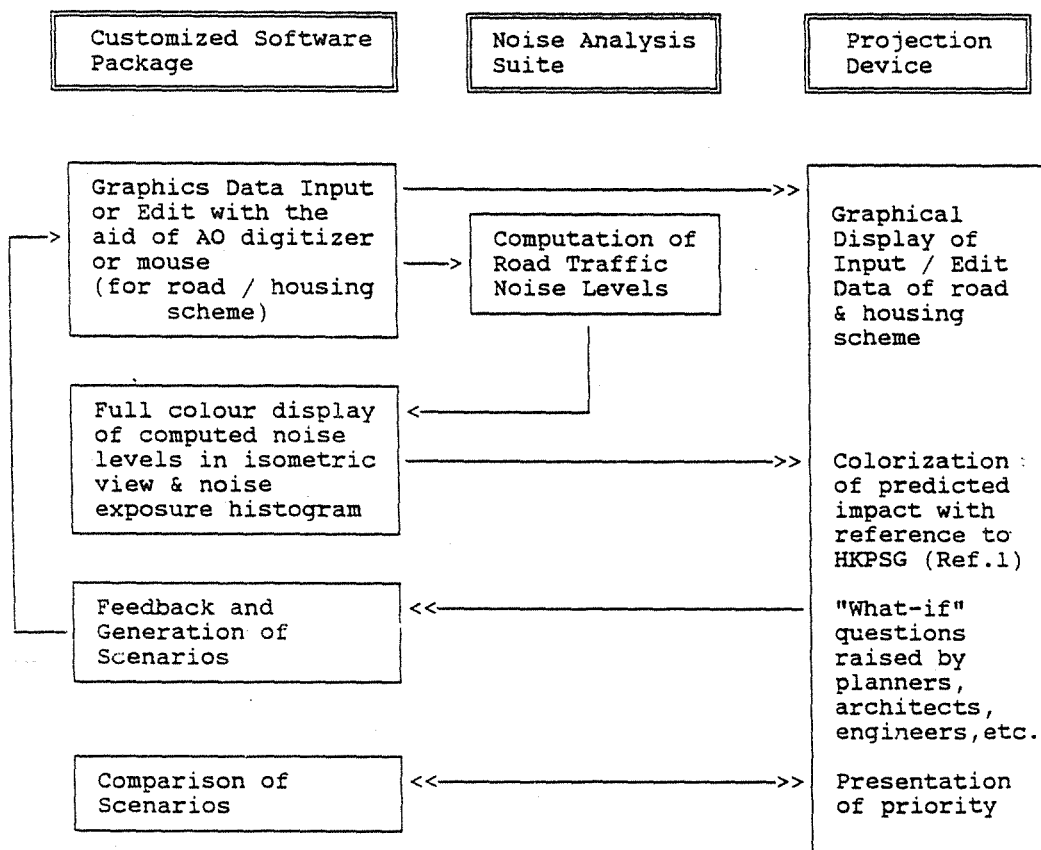
Figure 2 - Information Flow of RONDAC

3.0 CUSTOMIZED SOFTWARE GRAPHICS PACKAGE

The customized software graphics package, namely, CSPv3 is the vital part of RONDAC and was developed using AutoLISP programming language which is bundled with AutoCAD. The technical information and detailed procedures are given in References 6 to 8. As illustrated in Figure 2, the CSPv3 is to perform four main functions :-

3.1 Data Input / Edit

Both graphical data (such as road segments, buildings, etc.) and non-graphical data (traffic conditions, type of landuse, etc.) are digitized and input for subsequent program execution by a road traffic noise analysis suite.

3.2 Interpretation of Noise Level Data

After the execution of the road traffic analysis suite, the CSPv3 extracts the computed road traffic noise levels in L10 (1 hour, peak) at the specified landuse locations. Histograms showing the number of units (classrooms or residential flats) being exposed to certain road traffic noise levels are also generated. The CSPv3 assigns "red" to those histograms and buildings' facades exceeding the HKPSG criteria and "green" otherwise. This feature obviously has the advantage that the noise impact can be easily visualized by all concerned and the attention to devise a better scheme will be much more focused.

To cater for those situations where the road traffic noise analysis suite could not model accurately requiring adjustments or corrections, the CSPv3 is designed to incorporate corrections obtained by other means.

3.3 Generation of Scenarios

The CSPv3 is designed to provide the feature of easy generation of up to eight scenarios with only slight modifications on previously prepared scenario. These scenario data are stored into different sub-directories under a specified project directory for proper file management.

3.4 Scenario Comparison

The CSPv3 will at this stage rank the relative merits of all scenarios so far produced and will display the ranking results. The criteria by which ranking is carried out are incorporated in a formulae taking into account factors such as population exposure, cost and noise reduction. These factors can be pre-set at any value as the case may dictate.

4.0 CASE ILLUSTRATION

To illustrate the use of RONDAC, the following example of arriving at a proposed school development project in Hong Kong is used. Figure 3 shows the isometric views of three prepared scenarios.
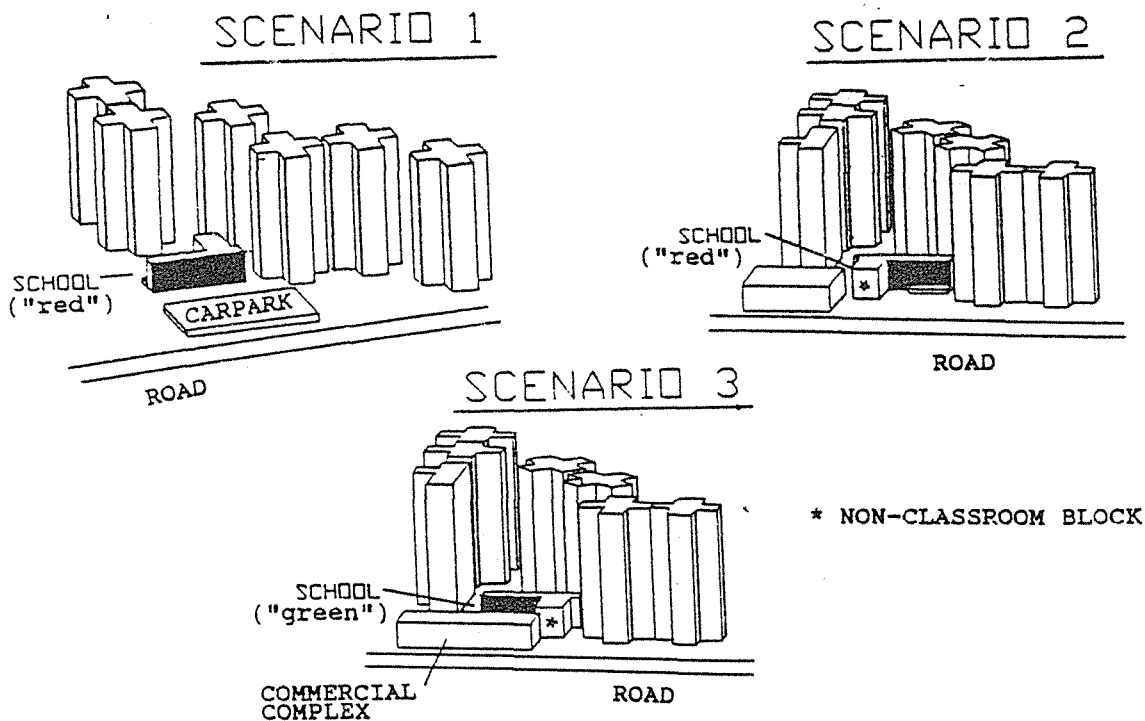
Figure 3   Isometric Views of 3 Scenarios

The proposed primary school site is adjoining and affected by a heavily trafficked trunk road carrying more than four thousand vehicles per hour having driving speed normally over 70 kilometers per hour and with heavy vehicle composition of about thirty percent. To look for possible school dispositioning alternatives by means of raising "what-if" questions and to achieve the most optimum school placement amongst them, RONDAC allows feedback from all agencies concerned in the development project for interactive creation of scenarios. In this example, three scenarios were formulated and evaluated.

Scenario one is the original layout having all classrooms directly facing the trunk road with noise levels reaching 73 dB(A) L10 (1 hour) as opposed to the recommended level

of 65 dB(A). Therefore, RONDAC shows the facade in "red" to denote that classrooms there will be exposed to levels over the pre-set criterion of 65 dB(A).

Responding to "what-if" the school building is rotated by 180 degrees to utilize the screening effect provided by its non-classroom block and "what-if" the screening effect is further enhanced by a multi-storey carpark to limit the angle of view of the road, RONDAC easily produces scenario two and carries out another road traffic noise assessment. Because of the self-protection arrangement, the facade will be exposed to a lower traffic noise level at 69 dB(A) L10 (1 hour) than that in scenario one. However, this level still exceeds the criteria and hence again, "red" is assigned by RONDAC.

The designer then further asks "what-if" the adjacent carpark is turned into a commercial complex elongated and re-positioned to maximize the screening effect, RONDAC then generates another case, scenario three. Under this situation, the traffic noise levels at the school are brought below the criteria receiving a "green" colour from RONDAC.

In this simple example, scenario number three is clearly the preferred choice as it turns "red" into "green". Further optimization based on scenario 3 is possible.

In fact, RONDAC is capable of handling more complicated projects with its substantial advantages of easy visualization, provision of feedback for accepting "what-if" questions and, therefore, better communication between acousticians and non-acousticians.

5.0 CONCLUSION

The RONDAC represents an acoustician's tool reaching out to draw the attention of his non-acoustician counterparts involved in the process of planning anything from a school to a new township. It introduces sophisticated acoustics principles and calculations in an easily understandable format which can accept "what-if" questions from these non-acousticians in an interactive process.

6.0 ACKNOWLEDGMENT

REFERENCES

1. Hong Kong Government : <u>Hong Kong Planning Standards &</u>
    <u>Guidelines - Environmental Guidelines for Planning in</u>
    <u>Hong Kong</u>, April 1991

2. CHAN, Raymond H. : "Hong Kong's Quiet Road Surface
    Programme", <u>Proceedings, International Tire/Road Noise</u>
    <u>Conference 1990</u>, Gothenburg, August 1990

3. YEUNG, K.L. : "Noise Abatement for Schools in Hong
    Kong", <u>Proceedings, Noise Con '90</u>, Austin, October 1990

4. Environmental Protection Department, Hong Kong
    Government : <u>Environment Hong Kong 1991</u>

5. Environmental Protection Department, Hong Kong
    Government : <u>Application of Screening Structures to</u>
    <u>Abate Noise from Surface Transportation</u>, 1990

6. Department of Transport : <u>Calculation of Road Traffic</u>
    <u>Noise</u>, HMSO, 1988

7. WS Atkins : <u>roadNoise version 8 - User Manual</u>, 1989

8. Swire Systems Ltd. & Environmental Protection
    Department, Hong Kong Government : <u>RONDAC - User</u>
    <u>Manual</u>, 1991

ENVIRONMENTAL NOISE ASPECTS OF THE STEEL AUTHORITY OF INDIA LIMITED'S ENVIRONMENTAL MANAGEMENT AND POLLUTION CONTROL PROJECT

Colin Tickell
BHPE-Kinhill Joint Venture
5th Floor, 6 Ganesh Chandra Avenue
Calcultta 700013
INDIA

ABSTRACT

In 1989 the Steel Authority of India Limited (SAIL) commenced a consultancy project in environmental management and pollution control. The project was funded by the World Bank and was to be for a period of two years. The consultant for the project is BHPE-Kinhill, a joint venture of two Australian engineering consultancies. The project was designed to provide the basis for environmental management and pollution control at SAIL's four integrated steel plants and their associated mines.

This paper describes the project in brief and the environmental noise aspects in particular. These included standards and specifications of instrumentation, standards for selection of environmental objective sound levels, training of SAIL engineers in noise measurement, noise source identification and noise control techniques, establishment of an environmental monitoring program and recommendations of priorities for control of major environmental noise sources.

Following completion of the project in December 1990, an implementation project for 12 months was commenced in January 1991.

1.   Introduction - The Sail Environmental Management and Pollution Control Project

The Steel Authority of India Limited (STEEL) operates five integrated iron and steel plants at different locations in India. These plants have been in operation for more than 20 years and are in various stages of modernisation. Environmental protection has gained significant importance in India in recent years due to the greater awareness among the people and also due to the importance attached by the Government of India.

Steel plants are one of the major sources of pollution and SAIL decided to take the lead in India by taking appropriate measures involving the latest technology and practices to reduce pollution and wastes.

In February, 1988, SAIL issued an international tender for consulting services for conducting a study on the "Environmental Management and Pollution Control in Steel Plants under SAIL". The study was funded by a World Bank technical assistance loan. It was proposed to be a systematic study to evaluate the levels of pollution and waste arisings in SAIL's four integrated steel plants at Bhilai, Bokaro, Durgapur and Rourkela, and their tied mines and quarries. The locations are shown in Figure 1.

Figure 1: Location of SAIL Plants and Mines in the Study
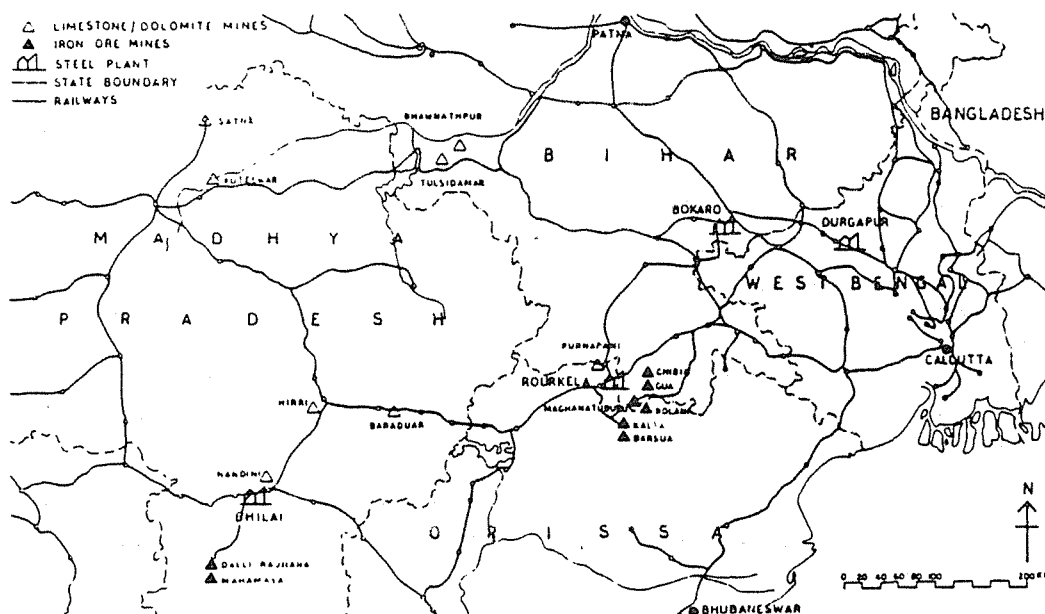
The contract was awarded to BHPE-Kinhill, a joint venture between two major Australian consulting engineering companies. Other invited tenderers were from Austria, Japan, the United Kingdom and the USA.

The general scope and purpose of the project included the following:

i.   Detailed assessment of air, water, noise pollution and solid waste generation levels in all steel plants, relative to Indian and international standards;

ii.   Assist SAIL in setting up of a comprehensive pollution monitoring network with suitable facilities and instruments;

iii.   Recommend appropriate pollution control measures (short term and long term) for phase implementation;

iv.   Assist SAIL in evolving a comprehensive long term environmental management program, including organisational arrangements for pollution control;

v.   Training of SAIL personnel in relevant aspects of pollution control, environmental management and quantified EIA/EMP techniques.

vi.   Development of retroftting methodology for pollution controls.

2. Noise Aspects of the Study

As noted above, the overall SAIL study included consideration of noise as a pollutant. As an emission to the environment, noise from steel plant activities has the potential to cause annoyance and discomfort to residents in their vicinity. There is also the potential for occupational noise induced hearing loss in the work force of the steel plants.

The noise component of the SAIL Environmental Management and Pollution Control Project can be considered as comprising three phases.

Phase 1 of the Project, which occurred during April, May and June of 1989, has involved the following three broad areas:

i.   identification of existing emissions and environmental management procedures, and commencement of training of SAIL personnel;

ii.   determination of appropriate environmental goals for emission levels and monitoring programmes; and

iii.   specification of monitoring instrumentation for procurement and recommendations for manpower and organisation for environmental management at SAIL plants.

Existing instrumentation at the plants was variable, from "antique" and uncalibrated instruments to the latest systems. Specifications were prepared for provision of an environmental noise measurement system for each plant, along with the Environmental Management Division at Calcutta, Research and Development Centre for Iron and Steel at Ranchi and two groups of mines. Uniformity between the groups was required to ensure similar reporting, management of spares and repairs, and ease of training.

Each system was to be hand held, portable and suitable for operation in the Indian climate. Performance specifications for the instruments were based on IEC and ISO standards, as well as the relevant Indian Standards.

For environmental noise measurements, the system was to give statistical sound level parameters of L_{An}% percentile sound levels, either in the field or later from downloading to a computer. Printers and tape recorders were included, along with hand-held meteorological equipment for monitoring wind speed, temperature and humidity.

The systems were also to be suitable for measurement of in-plant noise, with SPL, LEQ, and Peak display of A-weighted and Linear sound levels, one-third and one octave band filters. There were for measurement of building emission and source sound levels.

The tender was issued world-wide as a complete package, along with other packages of environmental monitoring instrumentation for air and water quality measurements. Assessment of tenders was made in November 1989, with delivery to be from May 1990.

Phase 2 of the Project involved three main areas, being:

i.　　Commissioning of monitoring instrumentation and continuation of training of SAIL environmental engineers in environmental monitoring and management;

ii.　　Detailed investigations of plant emissions to achieve sources, establishment of monitoring programmes and assessment of results; and

iii.　　Recommendations for control of emissions to achieve environmental objectives and prepare a strategy/priority rationale and timetable for control.

This occurred following receipt of the monitoring instrumentation in India, in the period May to September, 1990. Training was given in the basics of acoustics, measurement of sound levels in the plant and environmental noise, report preparation and fundamentals of noise control engineering. This training was given in two special training courses, along with on-site training at the plants during several visits. This on-site training was a valuable and necessary part of the training to give one on one interaction with the trainees. Over 20 engineers from plants, mines and other locations were trained through · this program.

The monitoring program was designed to measure the environmental noise levels in the neighbourhood of each plant, during daytime and night-time conditions, during each season of the year. Summer air temperatures in India are relatively high, which aids atmospheric absorption of sound. Thus, the need for night-time and winter month monitoring. For each plant a set number of six to 10 measurement locations were selected near the boundary or in adjacent residential areas.

The other major part of the monitoring program was in-plant noise source measurements, to produce noise contour maps of the major high noise level shops to identify major noise leakage paths.

Phase 3 of the Project is the continuation of the monitoring and environmental management activities by SAIL personnel and implementation of the recommended control measures according to the strategy determined in Phase 2. This has concentrated. mainly on simple noise control engineering activities which the plants can perform themselves, as well as on improving monitoring procedures and reporting methods.

3.　　Existing Emissions and Controls at SAIL Steel Plants

3.1　　Measurement of Sound Levels

The first measurements of sound levels reported at SAIL plants were at Bhilai in 1973/74 by the National Physical Laboratory. Since 1986 the plant Environmental Control Department at Bhilai has made measurements of sound level. Similar histories of measurements occurred at other plants, with some being done by the Environmental Control Departments, some by the Occupational Health and Safety Departments and some by external consultants.

3.2　　Major Sources

As with steel plants in general, the major sources of noise were air and steam leaks, flow noise in pipework and valves, turbine noise and impact noise. Air leaks from blast air lines from the power plants to the blast furnaces, steam line leaks from the power plants to the various users, and compressed air leaks around the plant were the major sources of noise within the plants. These were all also significant sources of energy losses, which gives added impetus to noise control.

Breakout noise from turbines and pipework was also a major source of noise in most of the utilities shops (ie: Power and Blowing stations, oxygen plants, compressor stations and various blower houses).

Impact noise from downstream processing of steel sections was a major source of both environmental and occupational noise. Rail, structural, merchant and pipe mills were all measured to have high impact sound levels. In several cases these shops were at the boundary of the plants and were potential sources of environmental noise annoyance.

Sources of environmental noise from the plants were mainly impacts in the mills noted above, power plant steam blow-offs and blast air bypass discharges. Environmental monitoring of noise levels in the neighbourhoods around the plants identified road traffic as the major source of environmental noise. However, in most cases the levels measured were below the required criteria of the Indian Central Pollution Control Board. These criteria are shown in Table 1.

Table 1: Central Pollution Control Board Sound Level Criteria

Locality type of the Receiver Area	Sound Level Criteria L_{AEq}	
	Daytime	Night-time
Silence Zone	50	45
Residential(urban)	55	45
Commercial	65	55
Industrial	75	65

By comparison, these levels are slightly above those recommended in the Indian Standard IS:4954 - 1986: Recommendations for Noise Abatement in Town Planning, by about 5 to 10 dB(A), and other similar relevant international standards. This is believed to reflect the higher general sound levels experienced in urban areas of India.

The highest sound level noise source measured was by the snort pipe discharge at a power plant, of 128 dB(A). This was an unsilenced direct discharge from a turbo-blower which would include turbine noise, flow noise and possibly organ pipe tones from the pipe. This discharge caused very high sound levels in the Power Plant, Control Room and roadway area adjacent to it. Efforts to reduce this noise were recommended be commenced as soon as possible. Typical sound levels at SAIL plants are shown in the Table 2 below.

Sound levels in steel plants in other countries, in Australia for instance, are lower in production areas because of the lack of air and steam leaks, and modern materials handling methods in downstream production areas.

Figure 2: Typical Sound Levels Measured at SAIL's Bhilai Steel Plant

Location	Sound Level dB(A) Fast	Major Source / comment
Power & Blowing Station	93 - 115 128	Steam & air leaks Snort pipe discharge
Captive Power Plant	90 - 98	Mainly steam leaks
Oxygen Plant	93 - 120	Pipe flow & turbine noise
Blast furnaces	85 - 122	Air leaks from tuyeres & stoves
Continuous Caster Pumphouse	87 - 97	Pumps & drives
Forge Shop	117 - 120	Impact noise
Rail finishing mill	89 - 115	Impact & rail/section sliding

3.3 Existing Control Measures

Installation of noise control measures at SAIL plants is a relatively recent activity. Recently constructed power plants and some mills have provided operators with quiet, air-conditioned control enclosures as part of the design.

Retrofitting of noise controls has occurred in some plants at blower stations with enclosure of turbo-blowers and lagging of blast air lines, pump houses with reverberation control and quiet control cabins in some power plants.

Recent plant initiated noise control activities have included provision of enclosures for turbo-compressors, design of silencers for boiler steam blow-off and replacement of normal air-line bypass valves with a quiet type of valve.

Noise control design activities included as part of the project include the lining of rollers in plate mills with rubber to reduce impact noise, provision of air inlet silencers on various blowers, quiet enclosures for operators in forge shops, blow-off silencers for blast-air bypass discharges, fan causing cladding, pipe breakout noise cladding and hot saw cowling noise treatment.

Research projects into a number of noise control alternatives for application in steel plants are also expected to commence in 1991.

4. Conclusion

The implementation of the Environmental Management and Pollution Control Project by the Steel Authority of India Limited has demonstrated the general intention of the Government of India to improve the environmental performance of industry. SAIL, being one of the major public sector employers and producers has set the example for other industries in India to follow in the path of environmental management.

In the area of noise monitoring and control, there is much work ahead, but with a basic team of trained engineers able to relate noise measurements to control engineering, the task has begun.

The implementation of the noise related aspects of the project will depend mainly on the attitudes of the senior management, who sanction labour and capital, and the shop floor employees who will benefit in the long run, both from reduced occupational noise exposure and reduced environmental noise emissions.

The example given by SAIL in planning for environmental management is one which is commended to all major industrial concerns, public and private sector, in all countries; especially those with large developments underway or in planning. With the correct tools and training at their disposal, which have beem provided at a very small cost in terms of annual revenue, the framework has been set for SAIL to improve its environmental performance, to the benefit of all Indians.

Acknowledgements

ECONOMIC ASSESSMENT OF LONG TERM ROAD TRAFFIC NOISE ABATEMENT POLICIES IN FRANCE

Jacques Lambert
I.n.r.e.t.s., case 24, 69375 BRON cedex, France

ABSTRACT

In the mid 1980's, 16% of the urban population were exposed to outside noise levels exceeding 65 dB(A) (Leq 8h-20h); more than 37% were exposed between 55 dB (A) and 65 dB(A). How can this unsatisfactory situation be improved, and at what cost to the community? Without ambitious policies, exposure to road traffic noise will remain globally unsatisfactory even though local improvements may be brought about by implementing measures like construction of noise barriers or re-routing of traffic. Recent research works carried out in France using cost-effectiveness analysis clearly demonstrate the interest for the long term of combining local measures on new and existing roadways (barriers, porous surfaces ...), on the traffic (speed limits, restriction of vehicles in historic centres...) and the buildings (soundproofing of the facades) with national measures, such as reducing vehicle noise emission limits. Then, in 2010, only 4% of the urban population would be exposed to noise levels exceeding 65 dB(A) and less than 30% exposed between 55 dB(A) 65 dB(A). Implementing such a programme would be costly for the whole community. However, public expenditures three times those allocated at present to fight road traffic noise could be financed by a supplementary tax on car fuel without penalizing the car owners.

1.0 INTRODUCTION

For many years, road traffic noise has been the main environmental problem facing urban populations as confirmed by surveys of environmental quality (Maurin, Lambert).

Urban density, the increased number of vehicles and traffic have created critical noise situations which the Public Authorities have been trying to remedy for the last decade.

Although exposure to high noise levels seems to have stabilized (Leq above 65 dB(A)), the number of people living in "grey areas" (i.e exposed to levels between 55 and 65 dB(A)) has probably increased, despite the tightening of noise emissions limits, the implementation of noise barriers along new highways and the partial elimination of "noise black spots" along existing roads.

The tremendous scale of the road noise problem is a major obstacle in the defining satisfactory solutions. All solutions imply considerable investments in corrective and preventive actions. Such investments cannot be envisaged without a long term action plan which the state and local authorities will have to fund.

2.0 GOALS AND METHODS

Following forecasts works on transportation noise conducted in 1987-88 by a french research team (Gerpa-Assi-Inrets), an assessment of four long term (2010) road traffic noise abatement policies has been carried out (Lambert) :

   - P_1 : a policy based on trends which only applies to previously made decisions ;

   - P_2 : a voluntarist policy designed to strengthen vehicle noise emission limits ;

   - P_3 : a voluntarist policy concerning local actions ;

   - P_4 : a voluntarist "all out" policy which is based on both types of voluntary policies stated above.

For each of these four policies, the stakes and the economic consequences have been identified. Specifically, we have examined :

   - the technical, financial, social and institutional factors which have to be taken into account for this research ;

- the advantages implied by these policies, particularly on the state of the noise environment described by the following indicators calculated using a computerized model (NOISE 2010) :

° average noise variation level ;

° urban populations exposed to noise levels exceeding a given threshold (55 dB(A), 65 dB(A) for example) ;

° variation of the aggregate noise exposure index of the $I = \sum P_i \Psi (L_i)$ type in which P_i is the population exposed to noise level L_i and $\Psi (L_i)$ a function of the exposure to noise (loudness for example).

- to throw light upon favourable factors but also the obstacles and difficulties related to their implementation.

Comparison of noise abatement policies has been carried out specifically using cost-effectiveness analysis.Effectiveness of each policy is defined in terms of the goal to be achieved which is to reduce the exposure of french urban populations to noise. The measure of effectiveness E can be analysed using the following formula :

$$E_j = I_0 - I_j = \Delta I_j$$

In which I_0 is the value of the reference situation exposure index (the trend policy for example) and I_j the value of this index after implementation of policy j ; I_j represents the noise exposure variation consequent upon implementation of policy j.

Cost-effectiveness indicator N relates to the implementation of policy j and therefore takes the following form :

$$N = \frac{E_j}{C_j} = \frac{\Delta I_j}{C_j}$$

In which C_j represents the cost of implementing policy j. N can be interpreted as the effectiveness per franc invested. Categorization of these policies is therefore possible using this cost-effectiveness indicator. In fact this statement, which compares the four possible policies, is not only based on this cost-effectiveness analysis but also on the implementation conditions of each of the policies evaluated so as to distinguish between the "gross" conclusions that the strict cost-effectiveness analysis has demonstrated.

3.0 WHAT SHOULD THE NOISE ENVIRONMENT BE IN 2010 ?

Results from simulations on the "NOISE·2010" model show that, using the hypothesis of a progress based on current trends, there will be an improvement in the situation by the year 2010, in comparison with base year 1985, particularly in areas with high noise levels. The percentage of the population exposed to over 70 dB(A) is thus divided by three and changes from 2.2 million to 720,000 inhabitants. The percentage of the population exposed to noise levels in the range 65 to 70 dB(A) is slightly reduced (by approximately 20 %) shifting from 4 million to 3.2 million inhabitants. The population living in grey areas (from 55 to 65 dB(A)) increases from 14 to 15 million inhabitants, but this is due to the fact that population moves out of black spot areas (over 65 dB(A)) towards grey areas and not due to a reduction of those populations who enjoy "acoustic comfort" (under 55 dB(A)). The population exposed to under 55 dB(A) shifts from 17 to 18.8 million inhabitants (i.e. an increase of almost 2 million inhabitants).

The results quite clearly show that there is a hierarchisation of efficiency in the policies applied between the "trend policy" ranging up to the "all out" policy with intermediate points at "low noise vehicle" policy and "local initiative" policy ; this latter is a little a more effective at every noise level than "low noise vehicle" policy. It can be observed that an "all out" voluntarist policy can shift the number of inhabitants who benefit from acoustic comfort from 17 to 25 million, (i.e. almost a 50 % increase in a quasi-constant population) ; furthermore this reduces the number of those living in grey areas (between 55 and 65 dB(A)) from 14 to 11 million (i.e. an increase of over 20%). Finally, this policy reduces extremely significantly the number of people exposed to high noise levels (i.e. between 65 and 70 dB(A)) from 4 to 1.4 million (i.e. a decrease of 65%) and to those exposed to very high noise levels (i.e. over 70 dB(A)) from 2.2 to 0.2 million (i.e. a reduction by a factor of 10) (see summary of results in table 1). This report quite clearly shows the interest of an "all out" policy which not only reduces quite significantly the population located in black spots areas and grey areas but also minimizes the number of soundproofed dwellings or dwellings which, in the hypothesis of an objective fixed at 65 dB(A) for all dwellings, will need to be treated in the future : only 638,000, i.e. 4% of all urban dwellings as opposed to 1.6 million, i.e. 10% of these dwellings, in the context of the trend policy.

This result quite clearly shows the advantageous situation induced by a differentiated policy in which the overall and general orientation has the effect of limiting the use of insulation as an action plan (which would in no sense reduce external noise levels), and favours noise reduction by actions on the sources of noise (vehicle noise levels, traffic volumes and road surfaces). It is obvious that there

is a high degree of interest in combining over the long term
actions that are undertaken on both a local level and a
national level.

Table 1 : State of the urban noise exposure in 2010

Indicators	Trend policy (P1)	Low noise vehicle policy	Local policy	All out policy
Population : < 55 dB(A) 55 - 65 dB(A) > 65 dB(A)	49.5 % 40.2 % 10.3 %	53.7 % 38.3 % 8.0 %	60.9 % 32.8 % 6.3 %	66.8 % 29.1 % 4.1 %
Average day Leq	61.5	60.6	59.7	58.6
Noise Exposure Indicator (= 100 for P1)	100	96	92	88
Dwellings exposed to Leq > 65 dB(A) - already insulated - non-insulated	613,000 950,000	510,000 700,000	413,000 560,000	378,000 260,000

4.0 WHAT INVESTMENTS ARE REQUIRED TO FIGHT NOISE?

4.1 Cost of the Policies. Investment levels required
annually to implement these policies have been evaluated and
allocated to the different types of action plans envisaged :
to vehicles, to buildings and to infrastructures
specifically (see table 2) ; and an allocation has also been
made in terms of the economic authorities concerned : i.e.
the State, the local authorities, owners and publically
owned buildings such as public housing office (see fig. 1).

The first observation is that policies based on voluntarist
actions in terms of vehicle noise levels are significantly
more costly for the community than the other policies.

Expenditure relating to the protection of buildings (both
new and existing constructions) and infrastructures (both
new and existing), of which a large part results from public
investment (84 to 88 % of expenditure), and depending on the
policy envisaged, are between 110 and 130 million US $ per
year i.e between 6 and 11 % of total expenditure.

The distribution of this expenditure among the different
economic partners concerned are primarily based on the
financing methods used for noise abatement on new roadways
and black spot elimination. These data show nevertheless

quite clearly the financial consequence of policies which follow locally-engaged actions : the share of expenditure for which local authorities are responsible significantly increases (from 42 to 67 million US $) and expenditure by the State tends to decrease (from 52 to 47 million US $).

Table 2 : Annual costs for the implementation of noise abatement policies (in million US $)

Policy Measures	Trend policy	Low noise vehicle policy	Local policy	All out policy
More stringent noise vehicle emission limits	1,000	1,800	1,000	1,800
Noise protection along new roads Leq > 65 dB(A)	8	8	5.5	5.5
Soundproofing new dwellings Leq > 65 dB(A)	4.5	3	2	1.3
Eliminating noise black spots Leq > 70 dB(A) - noise barriers - sounproofing existing dwellings	 23 77	 23 77	 16 < 77	 16 < 77
Low noise surface for the urban road network			29	29
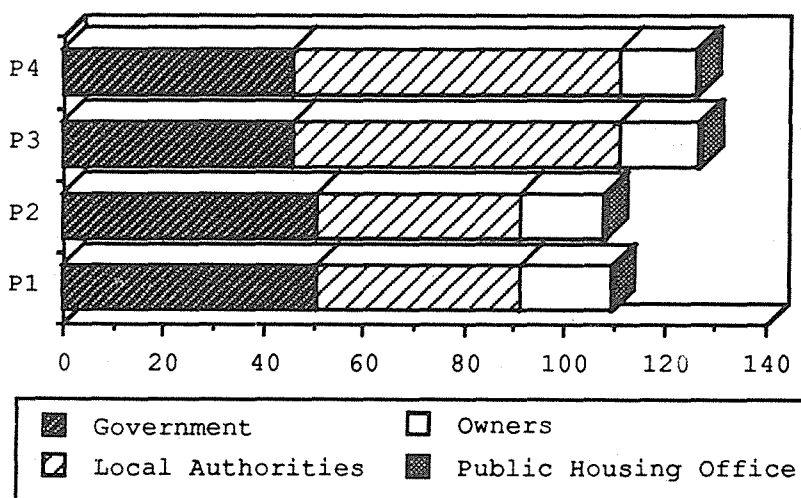
Figure 1 : Distribution of expenditure between different economic partners engaged in actions on buildings and infrastructures.

661

Comparisons between cost and effectiveness (in terms of variation of noise exposure) of the different policies suggest, and this is a new confirmation, that locally engaged actions, particularly those relating to roadways and traffic, are the least costly policy in terms of "performance levels" to improve urban noise environment conditions. This result is not surprising as a large number of the actions undertaken in the name of this policy are relatively inexpensive being part of global transportation policies with a wide range of different objectives (in particular the reduction of traffic congestion, the fight against air pollution and road safety improvement).

However, given the uncertainties and the hypotheses underlying all these estimates, this conclusion should only be considered as a decision element amongst others, in particular the conditions and difficulties in implementing noise abatement policies.

4.2 Financing of Public Noise Abatement Actions. This is probably one of the main difficulties in applying public anti-noise policies. The level of public financing which would be required annually varies, depending on the policy envisaged, from 93 to 113 million US $. It would therefore appear to be urgent to envisage additional financing means to those currently used (approximately 33 million US $ per year in the mid 80's), without which public action, notably the elimination of "noise black spots", would have to continue for several decades.

Current policies in Holland and the recommendations which resulted from the BIPE and INRETS studies carried out in 1988-1989, show that increasing taxation on vehicle fuels would be a relatively simple way of raising the money required. In the most costly hypothesis the tax would be at a rate of approximately 30 US cents per hectolitre, i.e. an annual average increased cost for a family running one car of 3.5 US $.

5.0 CONCLUSIONS AND RECOMMENDATIONS

Seven principle topics for reflection emerge from the analysis of the economic consequences and the implementation conditions of the urban noise abatement policies :

    a. Most public authorities use a "blow by blow" approach, designed to correct the most unfavourable situations ; it seems to be vital to adopt voluntarily a more global, preventive, approach. This implies clear objectives combined with coherence on both local and national levels.

    b. To ensure effective coherence, it is essential to define the task and responsibility of every territorial

echelon (national, regional and local).

    c.   Increased financial resources are required to implement an effective noise abatement policy.

    d.   Using such resources, regulations must be adopted and applied.

    e.   To arbitrate effectively, it is necessary to increase knowledge at a national level about the technical and economic aspects involved in the various actions which are the responsibility of local authorities.

    f.   It is also vital that responsibility for decisions made by local authorities be based on scientific and technical evaluations before actions are implemented ; this implies at least minimum training.

    g.   Finally, we should not forget that to be effective any action should be approved by the public. Full and clear details should be published at the same time as any decision is made.

REFERENCES

Maurin M., Lambert J., Alauzet A., Enquête nationale sur le bruit des transports en France. Rapport de recherche INRETS n° 71, 1988.

GERPA, ASSI, INRETS, Le bruit des transports terrestres en l'an 2010 - prospective et stratégies d'actions. Rapport final pour le Ministère de l'Environnement (Srétie), mars 1988.

Lambert J., Evaluation économique des politiques à long terme de lutte contre le bruit routier. Rapport final préparé par l'INRETS pour le Ministère de l'Environnement (Srétie), avril 1990.

BIPE, INRETS, Mécanismes actuels et potentiels de financement des politiques de lutte contre le bruit. Rapport final pour le Ministère de l'Environnement (Srétie), avril 1989.

ROADSIDE NOISE BARRIERS
A COMPUTERISED ACOUSTICAL COST-EFFECTIVENESS STUDY

Athol Day and Geoffrey P. Veale
Day Design Pty Ltd
Consulting Acoustical Engineers, Sydney.

ABSTRACT

The Roads & Traffic Authority of NSW (RTA) is currently spending considerable sums of money on roadside noise barriers as part of its routine noise control strategy. Day Design was commissioned by the RTA to model the Noise Reduction of various types of Roadside Noise Barriers, obtain typical installed barrier costs from suppliers and to determine a rank order of acoustical cost-effectiveness for roadside barriers in typical situations.

The six typical barriers chosen for consideration in the study are: reinforced concrete, concrete & wood wool composite, sheetmetal & mineral wool composite, glass reinforced cement & fibreglass composite, treated pine timber, ribbed sheetmetal.

The final cost effectiveness comparisons are made in terms of Dollars per linear metre of erected barrier versus Decibels of noise reduction.

INTRODUCTION

Not so many years ago, some road construction authorities said, "Our roads don't make noise. It is the cars and trucks that make the noise. If you don;t like the noise then quieten them." Legislation is now in place to limit the noise emitted by motor vehicles, but the engineering means whereby vehicle noise may be further reduced has practical limits. More and more it is realised that even with well-designed engines, exhaust silencers, tyre treads and road surfaces, road noise often exceeds acceptable environmental standards. This realisation, together with strong community reaction in some cases, has forced many road construction authorities to take positive action to reduce traffic noise by building roadside noise barriers.

The quite recent need for roadside noise barriers has brought many types of roadside noise barriers on to the market. Their physical and acoustical properties and installed costs cover a very wide range indeed. Of the six roadside barriers under consideration in this study, the barrier with the best acoustical properties is undoubtedly the GRC. However its price is the highest. The barrier with the worst acoustical properties is the treated pine timber barrier, but it has the advantage of being only a fraction of the price of the GRC. Which is the most economical in terms of decibels for dollars ? Which barrier is the most acoustically cost-effective ?

In some cases the most cost-effective roadside noise barrier is an earth berm. Its huge mass provides a greater noise reduction than any other barrier of the same height, but its cost depends on whether or not there is a nearby cutting to provide the fill. Using an earth berm can actually save money where the earth from a nearby cutting must be disposed of. However, the costs are so dependent on local conditions that we can not put a cost on them. We have therefore had to eliminate earth berms from consideration in this study.

ROADSIDE NOISE BARRIERS UNDER CONSIDERATION

Our brief was to study the acoustical cost-effectiveness of six typical roadside noise barriers, so we have selected the six commercial products which were best known at the time, three being of the Reflective and three being of the Absorptive type:

DESCRIPTION	SUPPLIER
* Abbco ribbed sheet steel	Abbco Building Products Pty Ltd
* Fanwall reinforced concrete	Reinforced Earth Pty Ltd
* RTA treated pine timber	Roads & Traffic Authority
* dB Metal steel and mineral wool	dB Metal Products Pty Ltd
* Durisol cement and wood wool	Reinforced Earth Pty Ltd
* GRC cement and fibreglass	GRC Composites

Except for the RTA timber barrier, the Sound Transmission Losses and Sound Absorption Coefficients of the above barriers were either provided by the manufacturers or established from text books. The RTA timber barrier STL was determined by field measurements above and behind a 4 metre high barrier on the F3 Freeway. Data assumed in this study is given in Figures 2 and 3.

This study is not exhaustive. We have selected what seemed at the time to be a representative sample. Other barriers may have come on the market too late to be included. However, we hope that this study will provide a rational basis for future comparisons to be made.

COST OF ROADSIDE NOISE BARRIERS

So that barrier costs can be legitimately compared, we have asked each supplier to base his prices on one kilometre of roadside barrier, erected in normal ground within 20 kilometres of their manufacturing facility, and in barrier heights of 2, 4 and 6 metres. Posts must be capable of supporting the barrier against wind velocities that may occur once in 50 years in Sydney, that is 44 metre/second. Prices in Dollars per Linear Metre are presented in Figure 7.

During the period of this study the sales allure of kilometres of roadside noise barriers and the effect of the recession have combined to make the pricing more and more competitive. Whether or not the prices used in this study are realistic for the future is a matter of conjecture. However, updating the data and making new comparisons in the future will be a simple matter.

ACOUSTICAL PERFORMANCE OF ROADSIDE NOISE BARRIERS

By acoustical performance, we mean the predicted L_{10} noise reduction at a receptor location due to the erection of a roadside barrier.

The erection of long roadside barriers of various constructions and heights and measuring their acoustic performance is a time consuming and expensive process. It was decided that a computer model could be used with sufficient

accuracy to establish the comparative acoustical performance of a range of roadside noise barriers.

If we erect a heavy reinforced concrete barrier at the roadside say 6 metres high, the Sound Transmission Loss will be much greater than the Refraction Loss over the top, so that we can with confidence use the conventional Maekawa approach to calculate the barrier noise reduction. If in the interests of saving on costs, we select lightweight materials such as timber or steel, the calculation of noise reduction is complicated by the sound energy transmitted through the barrier as well as over the top. If we then add a parallel barrier on the far side of the road we must add the reflected energy to the calculation. The problem is complicated by many other factors.

The computer program that we have written for this project to calculate the noise reduction of a barrier at a receptor location takes account of:

*   noise source heights of truck engines and vertical exhausts.
*   percentage of heavy vehicles.
*   typical traffic noise spectrum from 63 to 8000 Hz.
*   height of barriers.
*   sound refraction over the top of barriers.
*   width of the roadway.
*   distance from the barrier to the receptor location.
*   altitudes of the road and the receptor location.
*   sound reflection from roadside cuttings and parallel barriers.
*   slope of the cutting wall.
*   sound absorption of parallel barriers.
*   sound transmission loss through the roadside barrier.

We have named this program SOFTBAR because it predicts the noise reduction of Soft (absorptive) faced as well as hard (reflective) faced roadside noise barriers. Provided all barriers are assessed in the same way, the comparison in results should lead to a valid rank order of cost and acoustical effectiveness. We have taken a great deal of trouble to make the computer model accurate as possible. We have also written a program based on the widely accepted UK CORTN 1988 method of traffic noise prediction which predicts the noise reduction of simple roadside barriers. Comparing the results by both models given us confidence that SOFTBAR has the same order of accuracy as CORTN for simple reflective barriers, and a greater accuracy for dual and absorptive barriers.

Figure 4. shows how the Day Design SOFTBAR prediction compares with the CORTN prediction for the simple Case 1. Both methods agree for a concrete barrier of height in excess of three metres. The noise reduction by barriers can be influenced by the Sound Transmission Loss of the barrier material, but CORTN does not provide for any variation in STL. The Softbar program predicts a lower noise reduction for a timber barrier than for a concrete barrier because it allows for the lower Sound Transmission Loss of the timber barrier. For barrier heights of three metres or less the CORTN method tends to overestimate the noise reduction because it assumes a source height of 0.5 metre, whereas Softbar allows for the higher source height of trucks.

To confirm the noise reduction of existing barriers and further check the accuracy of the computer models, the RTA had another firm of acoustical consultants, Wilkinson Murray Griffiths, carry out noise reduction

measurements behind GRC and Treated Pine Timber barriers at the side of the
F3 Freeway north of Sydney. The measurements were of a high order of
accuracy, being subject to careful calibration procedures, and included L_1,
L_{10}, L_{44}, and L_{11} measurements in dBA and octave bands from 63 to 8000 Hz.

We did note that the GRC absorptive barrier measurements gave an average L_{11}
noise reduction approx 1.7 dBA greater than was initially predicted by the
preliminary Softbar program. We reasoned from this that the refraction of
sound waves incident on the absorptive face of the GRC Barrier was creating a
shadow zone noise reduction of approximately 2 dBA.

We are reluctant to draw this conclusion from field measurements having an
accuracy of only +/- 1.5 dBA. However, available literature on Sound
Absorptive Highway Noise Barriers also supports an excess attenuation of up
to 2 dBA for barriers with an absorptive face.

Lawther & Hayek in a study for the National Cooperative Highway Research
Program (USA) drew the conclusion that for single barriers "Generally
absorptive surfaces on barriers slightly improve barrier effectiveness ...
Barriers with absorptive surfaces were predicted to have excess attenuations
(in excess of those with hard surfaces), particularly in the barriers' deep
shadow ... At practical receiver ranges behind thin wall, the increment was
not predicted to be large (ie, somewhere in excess of 2 dB at 50 feet and
dropping towards 1 dB further out). These theoretical predictions have been
substantially qualified by the gymnasium experiment" (refer: 1.)

Rapin carried out octave band sound level measurements behind a single
barrier screening a heavy truck, with and without an absorptive facing on the
roadside of the barrier. He concluded, "This data indicates a decrease in
levels of about 1 to 4 dB when the truck is behind the absorptive wall,
compared to the reflective wall" (Refer: 2.)

Bowlby, William and Cohn using their computer model with an absorptive
barrier having a Noise Reduction Coefficient (NRC) of 0.65 estimated a
barrier noise reduction improvement of 2.1 dBA when compared with parallel
hard reflective barriers of the same height. (Refer: 3.)

In consideration of the abovementioned research by others, and the results of
L_{11} octave band sound level measurements made on this project, we have made an
adjustment to the software model that provides up to 2 dBA barrier
attenuation in excess of that calculated by the Maekawa formula for a high
NRC sound absorptive barrier such as the GRC or dB Metal barriers. Following
this modification to the Softbar program, we found that both the GRC and
timber barrier noise reduction measurements made by WMG were generally within
+/- 1 dB(A) of the Softbar computer predictions.

HORSES FOR COURSES

If noise sensitive premises are located at say 100 metres on one side of the
road only, an inexpensive timber, sheetmetal or lightweight concrete
reflective barrier would obviously be more cost effective than an expensive
sound absorptive barrier. On the other hand, if there are noise sensitive
premises within say 30 metres on both sides of the road, barriers with a high
sound absorption and a high sound transmission loss such as the more
expensive Durisol, GRC or dB Metals may well be a better selection.

In order that useful comparisons may be made in such disparate roadside configurations, we have made the acoustical cost-effectiveness comparisons for Five Configuration Cases as illustrated in Figure 1.

RANK ORDER OF ACOUSTICAL COST-EFFECTIVENESS

We have calculated the noise reduction in dBA for each of six typical construction barriers, in heights of 2, 3, 4, 5 and 6 metres. We have then taken the budget prices ($ per Linear Metre) given by the barrier suppliers and calculated the acoustical cost-effectiveness for the range of barrier heights in terms of Dollars per Decibel (dBA). The results have been graphed for each of the six roadside barrier configuration cases. We have included the Noise Reduction and Cost Effectiveness graphs for the typical dual barrier configuration Case 3 in Figures 8 and 9.

CONCLUSION

The following conclusions have been reached by considering the Cost-Effectiveness graphs for each roadside configuration case.

Case 1.   If the required noise reduction does not exceed 13 dBA, then any of the six barrier constructions will be adequate. To achieve this noise reduction, an absorptive barrier would need to be about 3.5 metre high and a reflective barrier would need to be about 4.5 metre high.

In absolute terms, a 4.5 metre high reflective barrier would cost about $350 to $500 and a 3.5 metre high absorptive barrier about $800 to $900 per linear metre. Both would achieve the same noise reduction in the Case 1 configuration. We conclude that simple reflective barriers are more cost effective than the more complex absorptive barriers for such applications.

Cases 2, 3 & 4.   These three cases are all similar, in that a parallel reflecting surface, either in the form of another barrier or a roadside cutting, increases the incident sound energy. Increasing the height of a cutting can reduce the acoustical effectiveness of a roadside noise barrier.

In such cases the absorptive barrier performs better than the reflective barrier, but the difference is not as marked as may be expected. Even for 4 to 6 metre high barriers, the difference in noise reduction between absorptive and reflective barriers is 2 to 4 dBA. In most cases increasing the height of the reflective barrier by 1.5 metre will give the same acoustical performance as the absorptive barrier. Please refer to Figure 8.

In absolute terms, a 5 metre high reflective barrier would cost about $400 to $700 and a 3.5 metre high absorptive barrier about $850 to $950 per linear metre. For such medium height barriers the reflective barrier is more cost effective.

In these configurations the limiting noise reduction for 6 metre high barriers is about 17 dBA. For such barriers the Sound Transmission Loss quality of the barrier is of great importance, and the selection is limited to either reinforced concrete or the more expensive absorptive barriers. The question of whether to use a 7 to 8 metre high reflective barrier or a 6 metre high absorptive barrier to achieve 17 dBA noise reduction is beyond the scope of this study. When barrier heights reach these levels, considerations of safety in high winds and aesthetics may well outweigh cost considerations.

CASE 5.   In this Case, at the highest receptor position 4, the nearside barrier is more or less ineffective in reducing noise. The farside barrier will reduce noise for receptor position 5, but increase the noise at position 4 due to reflection. Sound reflected from the farside barrier may well become the more dominant factor in controlling the overall noise level at the receptor location 4. An absorptive farside barrier will reflect about 2 to 3 dBA less noise than a reflective farside barrier.

In this situation sound absorptive barriers will provide the greatest noise reduction with the least barrier height for receptor positions 1 to 4, also causing the least noise increase due to reflection at position 5. Even though overall costs may be greater, an absorptive barrier would often be selected for such an application.

The aim of this study was not to stifle competition by saying this barrier is "good" and this barrier is "bad", but rather to give the Roads and Traffic Authority of NSW an objective means of comparing barriers, and determining the best application for certain types of roadside barriers. If certain barriers are identified as not being acoustically cost-effective in this study, it may be countered that appearance, longevity or other factors which are not considered by this study, may be of more importance.

ACKNOWLEDGMENT

REFERENCES

1.   Lawther & Hayek, National Highway Research Program, Report 80, pp 3-4.

2.   Rapin, J.M. "Efficacite des ecrans acoustiques vis-a-vis des poids lourds", Activities 1982: Acoustique, Centre Scientifique et Technique du Batiment, Grenoble, 1983.

3.   Bowlby, William and Cohn, "Sound Absorptive Highway Noise Barriers" Federal Highway Administration (USA) FHWA-TS-86-214, May 1986.

DAY DESIGN

ROADS & TRAFFIC AUTHORITY
ROADSIDE NOISE BARRIERS
FIVE CONFIGURATION CASES

FIGURE 1.

BARRIER

ROAD

R

25 m (4 LANES)   30 m

CASE ①

CUTTING

ROAD

R

25 m (4 LANES)   30 m

CASE ②

ROAD

R

30 m   25 m (4 LANES)   30 m

CASE ③

ROAD

R

30 m   18, 25, 32 & 39 m (2, 4, 6 & 8 Lanes)   30 m

CASE ④

④
③
②
①

ROAD

⑤

30 m   25 m (4 LANES)   30 m

CASE ⑤

FIGURE 2.

ROADSIDE NOISE BARRIERS
Sound Transmission Loss Comparison

Fanwall R.C. — Durisol — dB Metal — GRC — Abbco Steel — Timber

OCTAVE BAND CENTRE FREQUENCIES – Hz

Legend:
- —■— Fanwall RC
- —+— Durisol
- —▲— dB Metal
- —✕— G.R.C.
- —⊟— Abbco Steel
- —⊠— Timber

FIGURE 3.

ROADSIDE NOISE BARRIERS
Sound Absorption Comparison

OCTAVE BAND CENTRE FREQUENCIES – Hz

Legend:
- —■— GRC Composite
- —+— dB Metal
- —▲— Durisol

FIGURE 4.

BARRIER NOISE REDUCTION – CASE 1.
Single Barrier Comparison

FIGURE 5.

BARRIER NOISE REDUCTION – CASE 1.
Single Concrete Barrier

FIGURE 6.

BARRIER NOISE REDUCTION – CASE 1.
Single Barrier of Various Constructions

Legend:
- GRC
- dB Metal
- Durisol
- Concrete
- Abbco Steel
- Timber

X-axis: BARRIER HEIGHT – Metre
Y-axis: NOISE REDUCTION – dBA

FIGURE 7.

ROADSIDE NOISE BARRIER COSTS
Dollars per Linear Metre

ABSORPTIVE

REFLECTIVE

Legend:
- Durisol
- G.R.C.
- dB Metal
- Fanwall
- RTA Timber
- Abbco Metal

X-axis: BARRIER HEIGHT – Metre
Y-axis: COST ERECTED – $ per linear metre

FIGURE 8.

BARRIER NOISE REDUCTION – CASE 3.
Parallel Barriers Both The Same height

Legend: GRC, dB Metal, Durisol, Concrete, Abbco Steel, Timber

(Y-axis: NOISE REDUCTION – dBA; X-axis: BARRIER HEIGHT – Metre)

FIGURE 9.

BARRIER COST EFFECTIVENESS – CASE 3.
Parallel Barriers Both The Same Height

Legend: Durisol, GRC, dB Metal, Concrete, Timber, Abbco Steel

(Y-axis: DOLLARS PER dBA; X-axis: HEIGHT OF BARRIERS – Metre)

NOISE CONTROL OF A BUSINESS MACHINE:

TOWARDS MANAGING THE ACOUSTIC ENVIRONMENT

J.C.S. Lai, M.A. Burgess
Acoustics & Vibration Centre
University College, University of New South Wales
Australian Defence Force Academy
Canberra, ACT 2600, AUSTRALIA.

R.G. Tacy
Applied Risk Management Services Pty. Ltd.
10 Moore St., Canberra, ACT 2600 AUSTRALIA.

ABSTRACT

The modern office usually is equipped with a number of business machines which, while unlikely to cause hearing damage, can cause annoyance and have an adverse effect on comfort and performance. To be able to manage the acoustic environment requires good management practices, forward planning, prediction of acoustic levels generated by machines to be purchased and noise control strategies when necessary.

In this paper, the prediction and control aspects for the noise from a business machine, namely, an optical mark reader, will be discussed. The sound power level of an optical mark reader has been measured and a ranking of the various noise sources in the machine has been obtained using the sound intensity technique. By using the measured sound power data and the directivity patterns, a prediction has been made of the sound pressure level, which agrees with the measured sound pressure level to within 1 dB(A), thus supporting the prediction method used.

Based on the measured sound power and noise ranking results, a flexible acoustic cover has been constructed. The effect of the acoustic cover on the cooling requirements of the optical mark reader has also been studied. Prediction has been made of the sound pressure level for twenty optical mark readers operating in a room with a room constant at least 200 m^2. The highest sound pressure level at an operator's position has been predicted to be 78 dB(A) and can be reduced by 7-8 dB(A) with the use of acoustic covers.

1.0   INTRODUCTION

The best noise control strategy is to anticipate any potential noise problems at the planning stage and to predict the effects on the work environment so that appropriate measures can be taken before installation of machines.   The modern office is usually equipped with a number of business machines which, while unlikely to cause hearing damage, can cause annoyance. The business machine undertaken in this study is an optical mark reader (hereinafter referred to as OMR) which is controlled by a Sharp Laptop computer. The overall dimensions of an OMR are approximately 630 x 660 x 470 mm.

The objectives of this study were to predict the sound pressure level in an environment with twenty optical mark readers in operation and to make recommendations to reduce the radiated sound pressure level, if necessary.   All the measurements described in this were made at the facilities of the Acoustics and Vibration Centre, Australian Defence Force Academy.

2.0   STRATEGY ADOPTED IN THIS STUDY

In order to predict the sound pressure level due to the operation of an OMR , the sound power level of the machine and its sound radiation pattern (directivity) have to be measured. In an enclosure, the total sound pressure level L_p of a point source is related to its sound power level L_W by (see, for example, Bies & Hansen (1989))

$$L_p = L_W + 10 \log_{10} \left(\frac{Q_\theta}{4\pi r^2} + \frac{4}{R} \right) \tag{1}$$

where Q = directivity factor of the source in a particular direction θ

$\quad\quad\quad\quad = 10^{0.1 DI}$

$\quad\quad DI$ = directivity index

$\quad\quad\quad\quad = L_p - \overline{L}_p + 3$

$\quad\quad\quad\quad$ = sound pressure level (dB) at distance r and angle θ

$\quad\quad \overline{L}_p$ = space-averaged sound pressure level (dB)

$\quad\quad R$ = room constant, determined by the absorption of the room surfaces

$$= \frac{S \,\overline{\alpha}}{1 - \overline{\alpha}}$$

$\quad\quad\quad \overline{\alpha}$ = average absorption coefficient of the room surfaces

and S = total surface area (m^2)

It can be seen from equation (1) that in the near field of a point source, the sound pressure level decreases by 6 dB per doubling of the distance from the source. However, in the near field of a sound source such as the OMR, it may behave more like a line source or plane source in which case the sound pressure level in the near field will decrease only by 3 dB per doubling of the distance from the source. The method used for prediction, based on measured sound power data, will be validated by comparing the predicted sound pressure level with the measured value in a room. Based on these results, prediction for the sound pressure level in a room with 20 OMRs operating will be made for various configurations of machine layout. The noise sources in the OMR will be ranked based on the sound power data so that effective control strategies can be applied.

3.0 MEASUREMENT OF SOUND POWER LEVEL AND DIRECTIVITY PATTERNS

3.1 SOUND POWER

All sound power measurements reported here were made in an anechoic chamber built to International Standard ISO 3745 with a lower cut-off frequency of 150 Hz. In order to rank order the noise sources within the optical mark reader, measurements were made with the sound intensity technique by scanning a sound intensity probe over nine surfaces of the OMR, as shown schematically in Figure 1(a). The sound intensity probe was pointed normal to the measured surfaces which were conformal with the OMR's surfaces but at a distance of about 100 mm from each of the component surfaces. The sound intensity technique is a relatively new technique and, at present, there exists only an International Standard ISO 9614-1(1990) on the measurement of sound power by the sound intensity technique using the point-by-point method. The principle of the sound intensity technique has been described in detail by Fahy (1989). Although the measurements reported here were not made in accordance with any Standard, results obtained by Lai & Dombek (1987) using this technique indicated that they were in good agreement with those obtained using sound pressure level measurements according to International Standard ISO 3745 (1977).
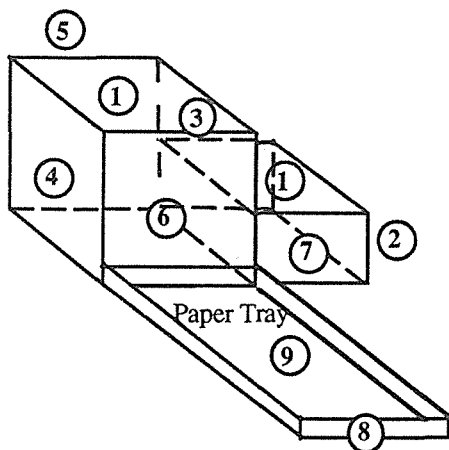
Figure 1(a) Schematic of OMR showing measured surfaces (not to scale).
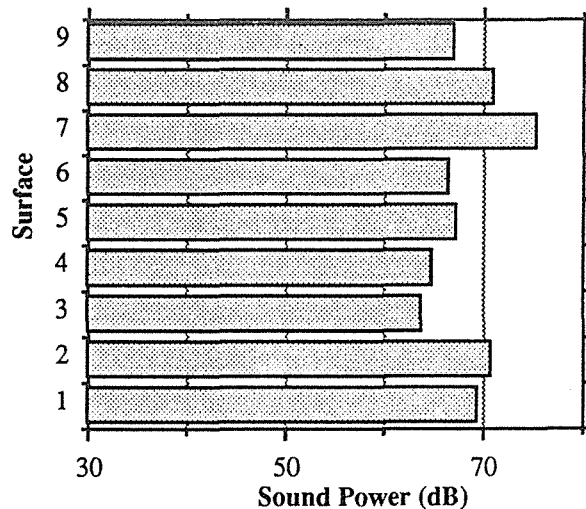
Figure 1 (b)Ranking of sound power of the measured surfaces.

The sound intensity measuring system used comprises a Bruel & Kjaer (hereafter referred to as B&K) 2032 dual channel FFT (fast Fourier transform) analyzer and a sound intensity probe made up of a pair of B&K 4181 phase-matched 1/2 inch microphones mounted in a face-to-face configuration and separated by a distance of 12 mm. Hanning window with 50% overlap and at least 128 spectra averages were used. The narrow band sound intensity data were processed and synthesized into octave bands from 125 to 4000 Hz with a Hewlett-Packard series 300 microcomputer. The microphones were calibrated with a B&K 3541 sound intensity calibrator and the calibration in sound intensity was within 0.1 dB of the value specified by the manufacturer.

The sound power has been measured for the OMR under normal paper feed operation as controlled by a Sharp Laptop computer and under continuous paper feed operation. The ranking of the 9 surfaces based on sound power under continuous paper feed operation is shown in Figure 1(b). It is interesting to note that surface 7 is most dominant based on sound power. The sound power spectra obtained under both normal and continuous paper feed operations are shown in Figure 2. It can be seen that the peak sound power

677

levels occur at about 500 Hz - 1 kHz. The overall A-weighted sound power level for the OMR is 72 dB(A) for normal paper feed operation and 76 dB(A) for continuous paper feed operation.

It has been noticed that under normal paper feed operation, the feed rate is not constant. Figure 3 shows a typical time record of the sound pressure signal between paper feeds under normal feed operation for 2 s. From these results, it has been estimated that the averaged duration for feeding a form is about 0.33 s and the averaged duration for a form to be read is about 0.6 s so that the difference between the sound power level for normal and continuous operations is about 4.5 dB(A). This value compares quite favourably with the measured difference of about 4 dB(A). It is considered that the result obtained under continuous paper feed operation is more reliable as the sound generated is constant. Consequently, most measurements were made under continuous papeer feed operation and the results extrapolated to give the values for normal paper feed operations.
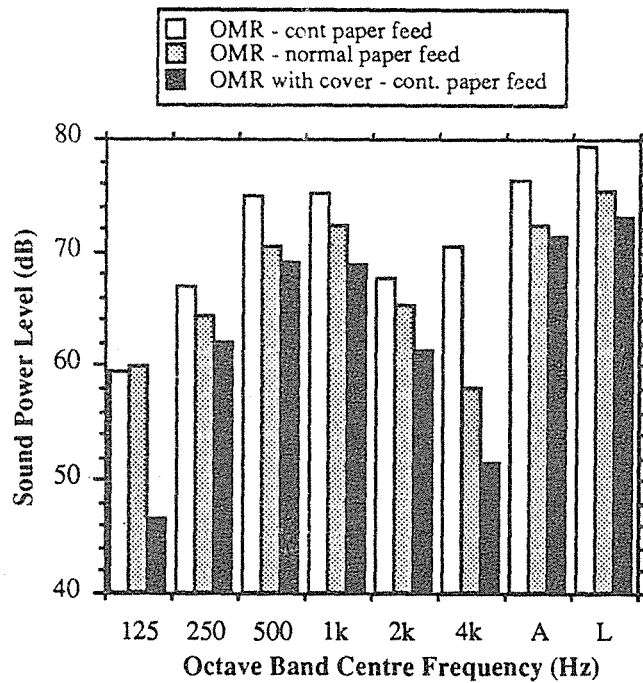
Figure 2 Measured sound power spectra of an OMR.
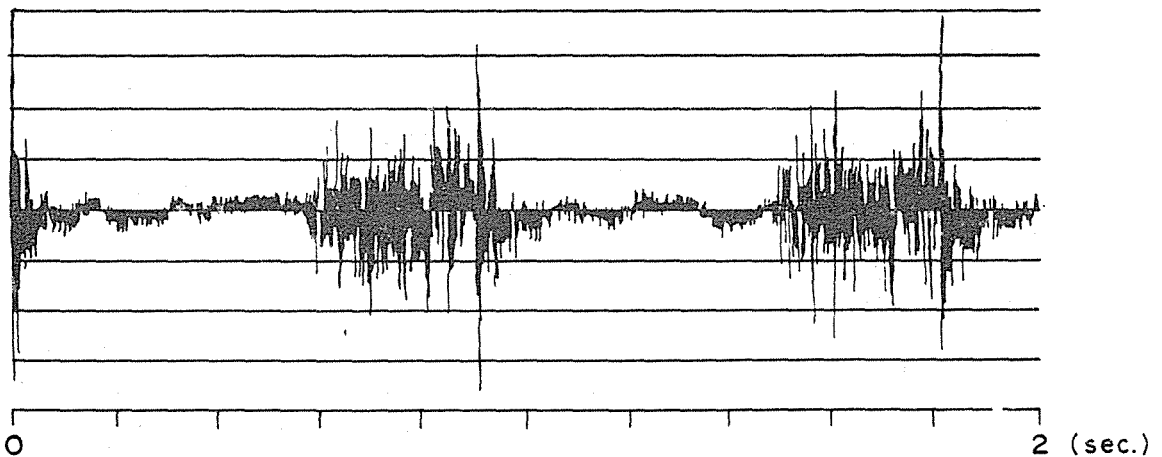
Figure 3 Time record of sound pressure signal for the paper feed, read, feed cycle.

3.2 DIRECTIVITY PATTERNS

The sound radiation (directivity) pattern of an OMR over a reflecting plane has been measured inside an anechoic chamber at 1 m from the centre of the OMR and 300 mm above the reflecting plane in 15° increments. From the directivity pattern shown in Figure 4(a), the dominant noise propagates from the front surface of the OMR and the directivity index along the 0° line is about 6 dB. These results agree with the ranking of noise sources based on sound power as shown in Figure 1(b).
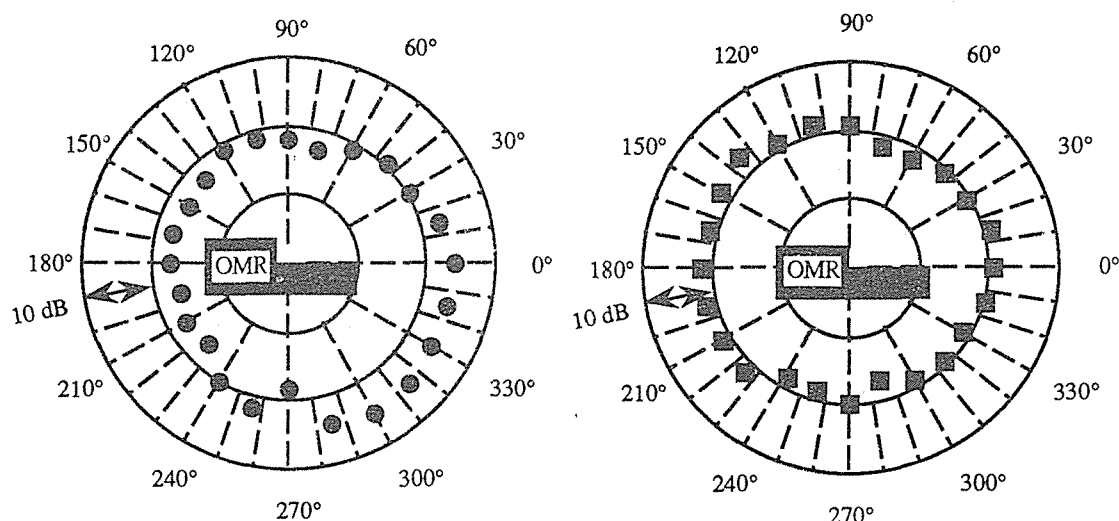
| (a) Unmodified OMR | (b) OMR fitted with an acoustic cover. |

(Concentric lines indicate sound pressure level in increments of 10 dB)

Figure 4 Directivity pattern (in a horizontal plane).

4.0 VALIDATION OF THE PREDICTION METHOD FOR THE SOUND PRESSURE LEVEL OF AN OPTICAL MARK READER IN A TYPICAL ROOM

The sound pressure level at distances 1 m, 2 m and 4 m from the centre of an OMR and along the 0° line has been measured in a room of volume 275 m^3 (referred to here as the test room). The reverberation time of the room is about 0.7 s at 500 Hz. These measurements indicate that the reduction in sound pressure level is about 4 dB per doubling of the distance from the OMR. Thus in the near field of an OMR, its behaviour is between that of a point source and a line source. For the purpose of prediction for the worst situation, it has been assumed that the OMR behaves as a line source. Prediction of the sound pressure level has been made at 1 m from the centre of the OMR (that is, about 500 mm from the paper tray) along the 0° line. The sound pressure level for this location has been measured with an B&K 2231 sound level meter. As shown in Table 1, the predicted values for all cases agree with the measured values to within 1 dB(A), thus supporting the prediction method used.

Table 1 Comparisons between measured and predicted A-weighted sound pressure levels, dB(A) at 1 m from the centre of an OMR

Without Acoustic Cover				With Acoustic Cover			
Continuous Feed		Normal Feed		Continuous Feed		Normal Feed	
Measured	Predicted	Measured	Predicted	Measured	Predicted	Measured	Predicted
75.2	74.8	69.6	69.9	66.3	66.9	63	62

Prediction has also been made for the sound pressure level at 1 m from an OMR located over a reflecting plane inside the anechoic chamber. The sound pressure levels for an OMR have been predicted to be 71.2 dB(A) and 67.3 dB(A) for continuous and normal paper feed operations respectively, which are within 1 dB of the measured values.

5.0 NOISE CONTROL STRATEGY

From Table 1, it can be deduced that in operating 20 OMRs under normal paper feed operations in a room with a room constant similar to that in the test room, the equivalent sound pressure level to which an operator would be exposed would be less than 85 dB(A) for an 8-hour period, but would be close to 80 dB(A). Although this value satisfies hearing conservation limit, it is considered to cause a fair degree of annoyance and fatigue. In order that individual comfort and performance would not be severely compromised, it was decided that the equivalent continuous sound pressure level for an 8-hour period should not exceed 70 dB(A) for any operator's position.

The noise from an OMR is basically generated by electric motors and the paper feed mechanisms. Any engineering solution would require re-design of the OMR so that a retro-fit solution was the preferred strategy. From Figure 1(b), the noise radiated from the front surface of the OMR is most dominant and it has also been noticed that a high frequency intermittent noise results from paper hitting the paper stop in the paper tray. A feasible solution to reducing the noise radiated from an OMR was to construct a flexible cover for the machine, with flaps to allow reasonably convenient access to the paper loading and unloading areas. The cover is made of a barium-loaded fabric. In order to reduce the noise resulting from paper hitting the paper stop, the paper stop has been covered with a layer of soft foam material.

The sound power spectrum of a modified OMR has been determined for continuous paper feed operation and is shown in Figure 2. The overall A-weighted sound power level for continuous paper feed operation has been found to be 71 dB(A) and that for normal paper feed operation has been estimated to be 67 dB(A), about 5 dB(A) lower than an unmodified OMR.

The directivity pattern of an OMR fitted with an acoustic cover measured at 1 m from the centre of the OMR and 300 mm above the reflecting plane in 15° increments is shown in Figure 4 (b). The directivity index along the 0° line is about 3 dB. The acoustic cover has generally rendered the noise radiation pattern less directional. The predicted and measured sound pressure levels of operating the modified OMR in the test room agree with each other to within 1 dB(A), as shown in Table 1.

In order to assess the impact of an acoustic cover on the effectiveness of cooling of an OMR, the airflow from the cooling fan was checked with an Airflow TA 300 hot-wire anemometer and the air temperature directly above the top drive motor and at the top of the electronics compartment were monitored by Technotherm type 7300 temperature probes. The acoustic cover was designed not to alter the airflow, which was confirmed by the hot-wire measurements. The temperature rise at the top of the electronics compartment for 5 hours of continuous paper feed operations is shown in Figure 5 and the steady state temperature rise has been estimated to be about 36°C by extrapolation. Under normal paper feed operations, the temperature rise would be expected to be lower. Based on an estimated maximum temperature of 70°C for the electronics compartment, the modified OMR can be operated up to a maximum ambient temperature of about 35°C, which is certainly well above the ambient temperature of an air conditioned office.
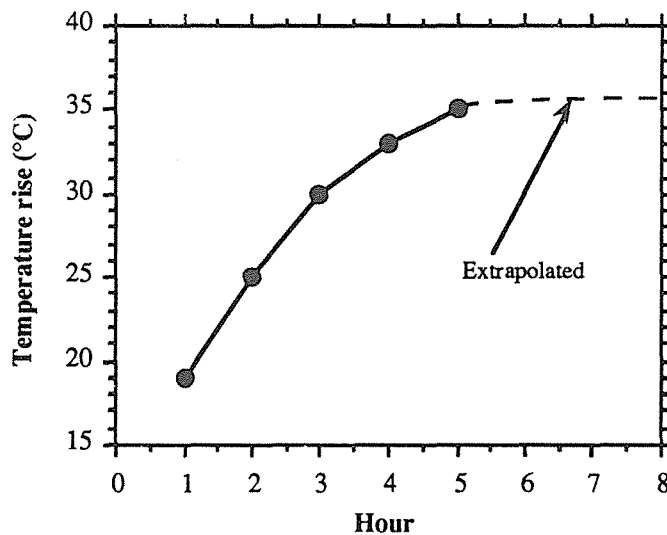
Figure 5 Temperature rise in the electronics compartment of a modified OMR.

Prediction is required for the noise exposure of an operator working in a large office (with a room constant of at least 200 m²) with 20 OMRs in operation. As the operation of a number of OMRs under normal paper feed operations is generally not synchronised, the equivalent sound power level for each OMR lies between that for normal paper feed operation and continuous paper feed operation. The equivalent sound power level of each OMR used for prediction is about 2 dB(A) higher than that for normal feed operation, that is, 74 dB(A) and 69 dB(A) for an OMR with and without an acoustic cover respectively. Various configurations of the layout of 20 OMRs have been investigated. One such configuration is shown in Figure 6 in which 20 OMRs are arranged in five modules, each module consisting of 4 OMRs. Within each module, adjacent OMRs are separated at a distance of 2 m. Four modules are placed at a distance of 5 m from the centre module and at 90° intervals. By using equation(1) and allowing for the reduction of 3 dB in sound pressure level per doubling of the distance from an OMR, the sound pressure level for the most operator's position for the layout as shown in Figure 6 has been predicted to be 70 dB(A) for OMRs fitted with acoustic covers, compared with 78 dB(A) for unmodified OMRs.
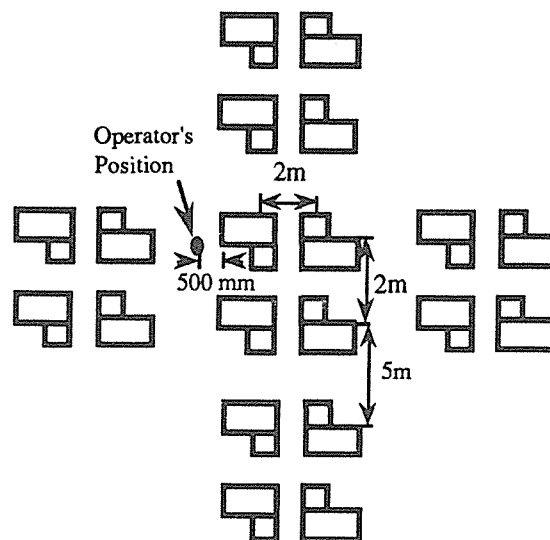
Figure 6 Schematic of layout of 20 OMRs (not to scale).

6.0 CONCLUSIONS

The assessment of the acoustic impact of business machines, which are potential noise sources, on the acoustic environment of a modern office and the development of appropriate noise control strategies are important procedures to achieve an acceptable office environment. In the present case study of an optical mark reader (OMR), the sound power level has been measured using the sound intensity technique inside an anechoic chamber under normal paper feed (controlled by a Laptop computer) and continuous paper feed operations. The major noise radiating surfaces from the OMR have been identified and recommendations have been made for the construction of an acoustic cover and a modification to the paper stop in the paper tray. The sound power level of an OMR fitted with such an acoustic cover has also been determined. The proposed acoustic cover is flexible and permits the OMR to be operated up to a maximum ambient temperature of about 35°C.

By using the measured sound power data, prediction of the sound pressure level of an OMR operating in a room with and without an acoustic cover has been made. The results agree with the measured sound pressure levels to within 1 dB(A), thus supporting the prediction method used. A layout of 20 modified OMRs for a large office has been suggested in which the sound pressure level at the most exposed operator's position has been predicted to be about 70 dB(A), compared with 78 dB(A) for unmodified OMRs in the same layout.

ACKNOWLEDGEMENT

REFERENCES

1. Bies, D.A. & Hansen, C.H. (1988) *Engineering Noise Control.* Unwin Hyman, Sydney.

2. Draft International Standard ISO 9614 Part 1 (1991) *Determination of Sound Power Levels of Noise Sources Using Sound Intensity - Measurement at Discrete Points.*

3. Fahy, F. (1989) *Sound Intensity .* Elsevier Applied Science, New York.

4. International Standard ISO 3745 (1977) *Acoustics -- Determination of Sound Power Levels of Noise Sources -- Precision Methods for Anechoic and Semi-anechoic Rooms.*

5. Lai, J.C.S. & Dombek, A. (1987) *Comparisons of Various Methods for Determination of Sound Power Levels of Noise Sources.* Acoustics in the Eighties, Australian Acoustical Society Conference, Hobart 12-13 Nov., 1987, pp. 199-208.

FLOW-NOISE OF SURFACE-WASHING NOZZLE IN THE FILTRATION-PLANT OF A WATERWORKS

Yoshiyuki MARUTA,
EBARA Research Company,Ltd., 2-1, Honfujisawa 4-chome, Fujisawa-shi,
Kanagawa 251 JAPAN

ABSTRACT

The unusual noise which happened at a filtration plant of a waterworks has been analyzed and its cause was the fluid dynamic sound from the underwater nozzles for surface-washing of a filter layer. For silencing this unusual noise, the simulation experiment about the fluid dynamic sound generated from some nozzles and orifices in water has been studied by using an air-test facility of a Quiet Flow-Noise Wind-Tunnel. The flow sound from such nozzles has a few kinds of pure-tone frequencies which are proportional to the flow velocity and these frequency components of this sound also change, with respect to the flow-passage shape of the nozzles. Finally we have explained the soundless nozzle for the surface-washing whose flow passage shape is obtained by decreasing the sectional area like a cone on the up-stream side. Then we silenced the unusual noise at the filtration plant of the waterworks.

1.0 INTRODUCTION

The unusual sound happened at a filtration plant for the waterworks when the special operation called "surface-washing" was taking place. The outline of the filtration plant is as shown in figure 1. Filter layers in the filtration plant must be washed periodically by the water-flow from nozzles connecting to the rotor-pipe and this operation is called "Surface-Washing".

The spectrum of the unusual sound was as shown in figure 2. It had been made clear by some investigations that the tone of 1150Hz is caused by the water-resonance in the rotor-pipe. However, it was not known what was the source of fluctuating pressure in the water. The problems about flow-noises radiated from the surface-washing nozzle were studied experimentally.

2.0 STUDIES ABOUT SOUND FROM SURFACE-WASHING NOZZLE

Surface-washing nozzles are attached to the rotor pipe as shown in figure 3 and they blow out a water-jet into the water field. It can be supposed that the sound generated from such nozzle is the same as the sound generated from an orifice flow. With respect to the sound
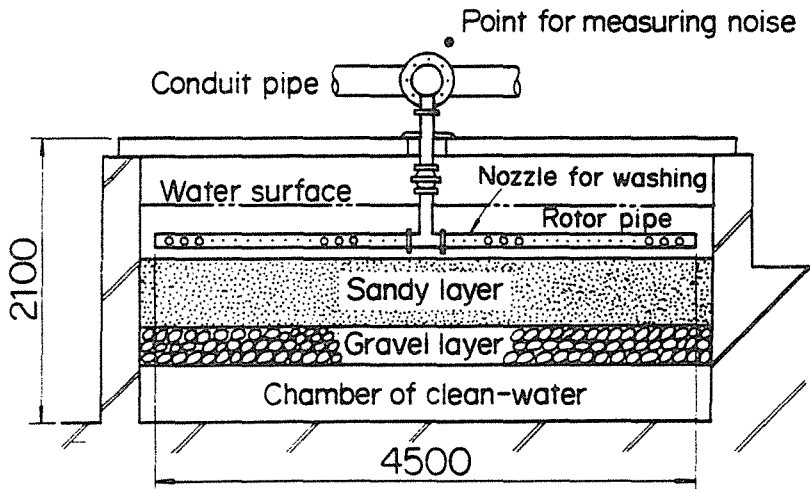
Fig.1 Outline of filteration-plant for waterworks.
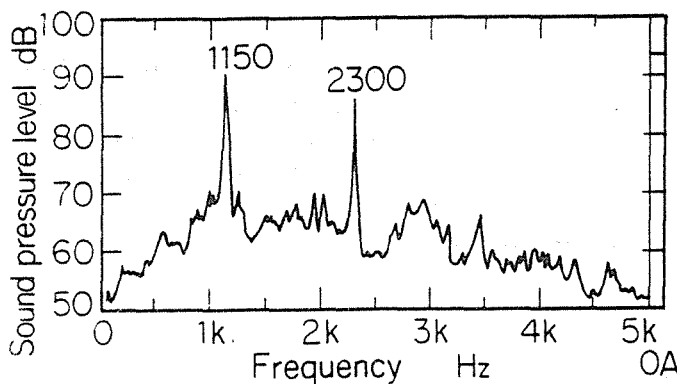
Fig.2 The unusual noise measured at the above filtration plant.
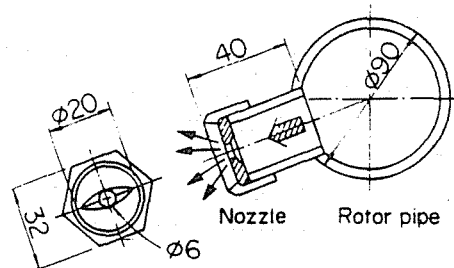
Fig.3 Detail of the surface-washing nozzle.

from orifices in the air, phenomena of generating sound are different depending on the type of orifices, thick-board or thin-plate (Anderson A.B.C.), (Tamba N., Kaji S. and Hiramoto M.) as shown in figure 4. It can also be supposed that the sound from surface-washing nozzles is induced by vortex-rings shedding from the edge of the nozzles similar to sounds from thin-plate orifice as in figure 4(b). Sounds generated from the thin-plate orifice are similar to sounds from jet-flow at the region of low Reynolds-numbers(UD/v), as in figure 4(c), where U is the flow velocity blowing out from a nozzle with diameter D and v is the coefficient of kinetic viscosity.

At the similar region of Reynolds number to a jet-flow shown in figure 4(c) (Goldstein M.E.), a model experiment using air-flows into an air field was carried out by using a "Quiet-Flow Wind-Tunnel" (Maruta Y., Ugai Y. and Suzuki S.) as shown in figure 5. This was done because it is very difficult in a model experiment to measure sounds accurately in a water field.

(c) 160 < UD/v < 1200
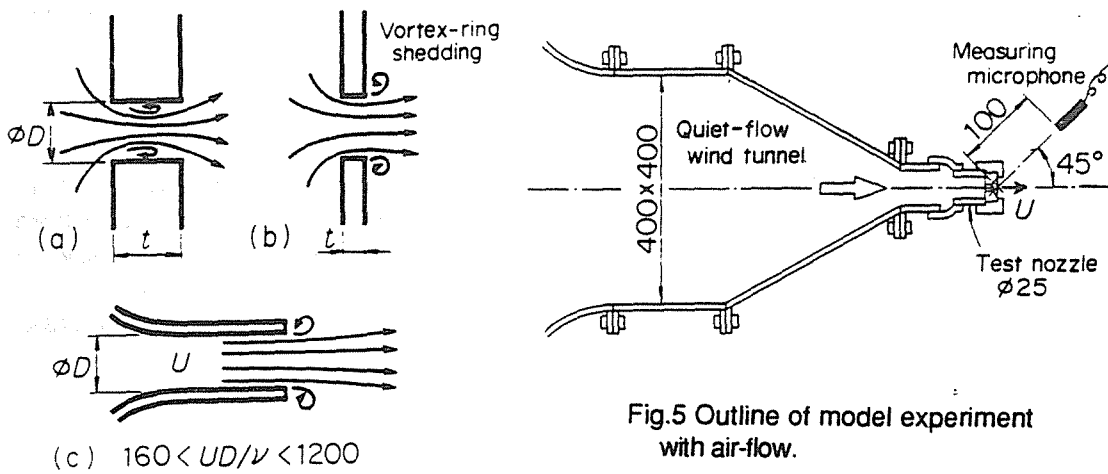
Fig.4 Flow-pattern of orifice
and jet-flow.

Fig.5 Outline of model experiment
with air-flow.
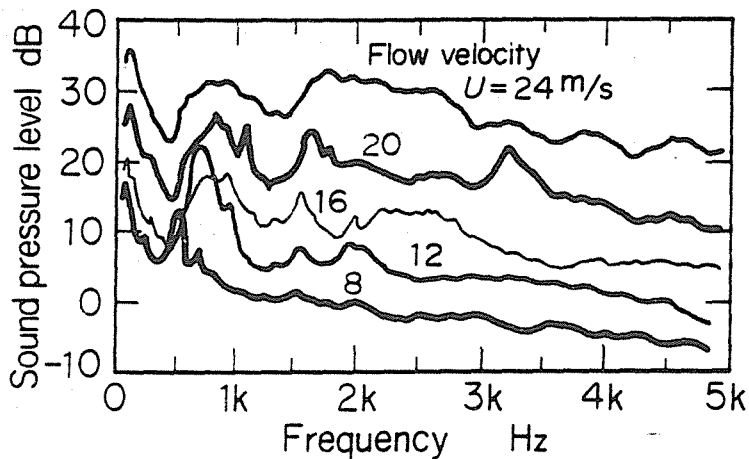
Fig.6 Noise spectra radiated from surface-washing
nozzle on model air-flow test.

The fluid-dynamic sound of the surface-washing nozzle presenting spectra as shown in figure 6 has a few peaked components at flow velocities below 20m/s and relations between the peak frequency and the flow velocity are indicated in figure 7. There are about three kinds of frequency groups which are proportional to the flow velocity as represented by solid black lines. With regard to the first group (the lowest line), the tone frequency is about 1100Hz, which is the same frequency as the unusual sound of the filtration plant, at the flow velocity of 18m/s which is the same as the operating velocity of the plant. Therefore it was recognized that the unusual sound was caused by fluid-dynamic tones from the surface-washing nozzles.

Incidentally, the dotted lateral lines in figure 7 were recognised as frequencies of an acoustic resonance with respect to only this air-flow model experiment using obtained data.

3.0 STUDY FOR THE LOW-NOISE TYPE NOZZLE

It is a simple and adaptive counter-measure for this unusual sound to only change nozzles to the low-noise type with regard to flow-sounds. The simple straight-hole nozzle similar to an orifice was tested and spectra of the sound are as shown in figure 8, for hole diameters of 10mm and 6mm. The relation between the peak frequency and the flow velocity is as shown in figure 9 and this indicates that there are four kinds of frequency groups in proportion to the flow velocity.

Experiments were carried out with the expanding hole and the taper hole,nozzles, and measured spectra are shown in figure 10. While the expanding hole nozzle generates some peak components, the taper hole nozzle does not generally generate any peaks. As shown in figure 11, the taper hole nozzle may not release the vortex-ring based on smooth flow in its hole although the expanding hole may generate vortexes and release vortex-rings.
Therefore it can be estimated that the taper hole may not have peak tones caused by vortex-ring shedding.
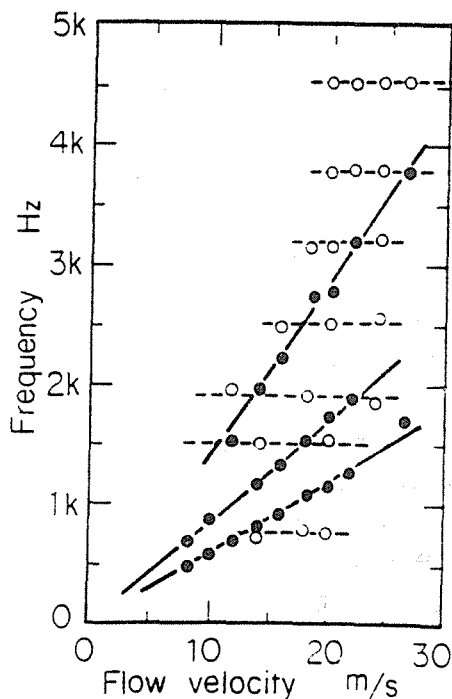
Fig.7 Relations between peak frequency and flow velocity about surface-washing nozzle. ● are remarkable peaked components.
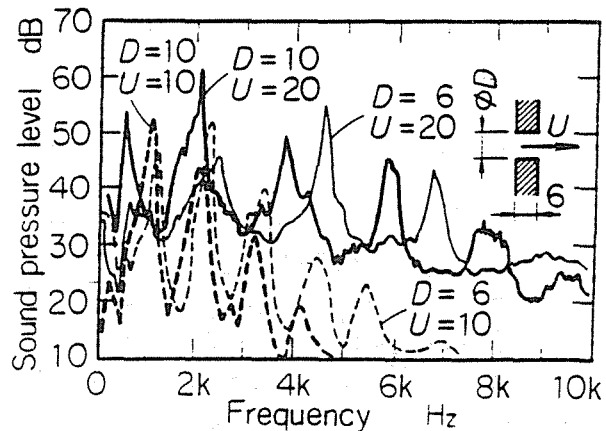
Fig.8 Flow sounds of simple straight-hole nozzle. Solid spectra are at the flow-velocity of 20m/s. Dotted spectra are at the flow-velocity of 10m/s.

4.0 IMPROVEMENT OF NOZZLE

The improvement for real surface-washing nozzles was studied with regard to the result of above experiment that sounds from the nozzle can be reduced by using a taper-hole type nozzle. The reform type was one improved directly from the customary nozzle by cutting the upstream side with a taper as shown in figure 12(b). The new type having a cone type hole on the upstream side as in figure 12(c) was selected from many kinds of nozzles on the market. Both types of nozzle were tested in the wind tunnel and spectra of both sounds were measured as shown in figure 13. The effect of the improvement was recognized for both types of nozzle. Finally, since it was easy to obtain new nozzles readily at the time, all surface-washing nozzles were exchanged for the new type in the filtration plant and the unusual sound was fully silenced.
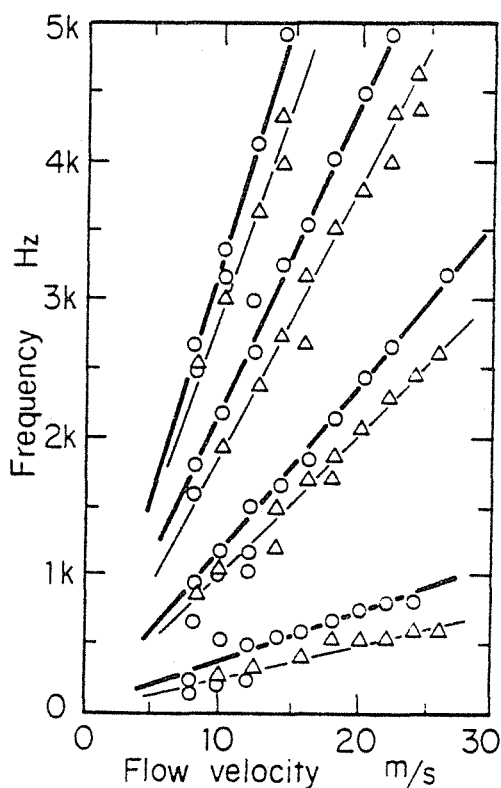
Fig.9 Relations between peak and flow velocity about straight-hole.
$\bigcirc$:D=6mm, $\triangle$:D=10mm.
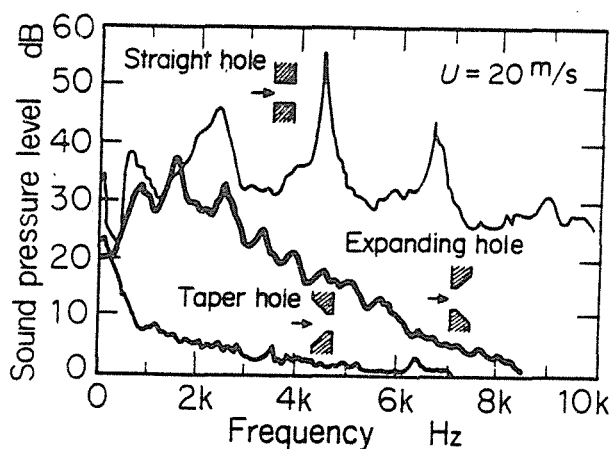
Fig.10 Spectra of flow noise from taper hole and expanding hole nozzle.

Expanding hole   Taper hole
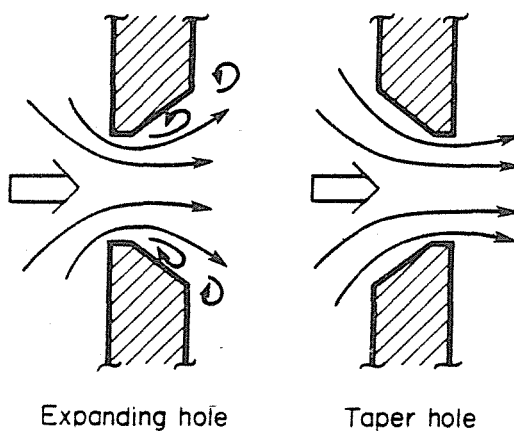
Fig.11 Flow patterns of test nozzle.

5.0 CONCLUDING REMARK

After the investigation of the unusual sound from the filtration plant in the waterworks by the model experiment using air-flow, the following conclusions can be drawn :

(i) The fluid-dynamic peak tone was the cause of the unusual sound.

(ii) Peak tones from the nozzle can be reduced by a taper hole nozzle.

(iii) The unusual sound of the filtration plant has been silenced by applying the result of model experiments in an air-field.

(iv) It is possible to simulate the flow-noise in a water field by noise from air-flows.

We have silenced the unusual noise at the filtration plant in the waterworks by applying the above conclusions.

REFERENCES

Journals

Anderson A.B.C., Journal of the Acoustical Society of America, No.24, pp.675-680(1952)

Books

Goldstein M.E., Aeroacoustics, Mc-Grawhill, pp.107-108, (1977)

Proceedings

Tamba N., Kaji S. and Hiramoto M., Proceedings of the Japan Society of Mechanical Engineers, No.810-15, pp.94-98, (1981), (in Japanease)

Maruta Y, Ugai Y. and Suzuki S., Proceedings of Inter-noise 87, pp.481-484, (1987)
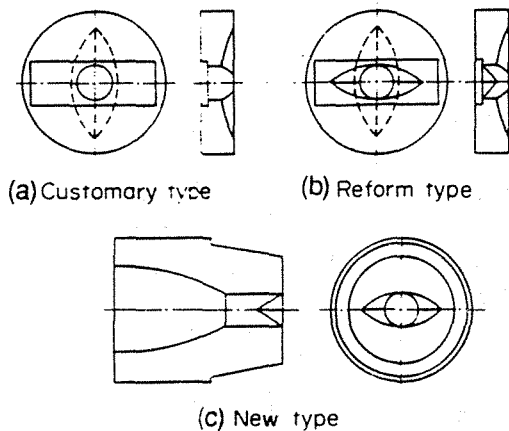
Fig.12 Improvement of
surface-washing nozzle.
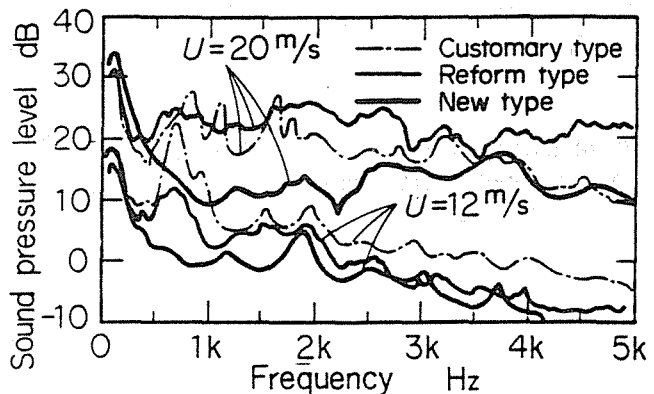
Fig.13 Sound-change of surface-washing nozzle
by improvements.

AN EXPERIMENTAL STUDY ON THE COMPOUND PSYCHOLOGICAL EFFECT OF SOUND
AND LIGHTING IN A ROOM

Hirofumi Iwashige
Faculty of Education, Hiroshima University, Higashi-Hiroshima, Japan

Mitsuo Ohta
Faculty of Engineering, Kinki University, Higashi-Hiroshima, Japan

ABSTRACT   For getting a comfortable daily life in our indoor living,
we always expend a great effort to find the skillful combination of
living environmental factors such as temperature, moisture, lighting,
sound and ventilation. If more than two different kinds of the above
environmental factors are appropriately combined, an optimum relatio-
nship between those factors might be found for a comfortable indoor
life. In this paper, the combination of three environmental factors ;
sound, lighting and temperature are first considered.   Here, the
Magunitude Estimation Method is employed to obtain some evaluation
value for many complex conditions, and our experiment is carried out
in the artificial climate chamber.   More concretely, our temperature
condition is adjusted within a range from 15°C to 30°C. Furthermore,
the illuminance condition and the sound condition are ajusted within
a range from 5 lx to 800 lx and from 50 dBA to 80 dBA.   Here, white
glow light, red light and green light are chosen as an illuminance.
Then, two kinds experiments are employed.   That is, at first, the
evaluation values for a noise level change are selected under many
conditions, and secondly the evaluation values for an illuminance
level change are selected under many conditios.   From the first
experiment, a white glow light gives some higher evaluation value of
a noise level than a green light or a red light.   Such a tendency is
seen under every temperature condition.   In the same illuminance
condition, a relatively high temperature gives more high evaluation
of a noise level than a low temperature. From the second experiment,
a high room temperature gives higher evaluation value of illuminance
more than a low temperature. And a high illuminance makes a large
difference of evaluation value.

1. INTRODUCTION

It is very important to find the compound psychological effect of heterogeneous environmental factors in the moderate range in our daily life. If more than two different kinds of the environmental factors are appropriately combined, an optimum relationship between those factors might be found for a comfortable indoor life. So, some improvement method of a living environment based on the above combination of different factors is concretely discussed from a psychological viewpoint. In experiment, more than 80 combinations of various environmental factors are used by changing noise level, illuminance condition and thermal condition. It is obvious that such a present study gives some guiding principle to make our life comfortable.
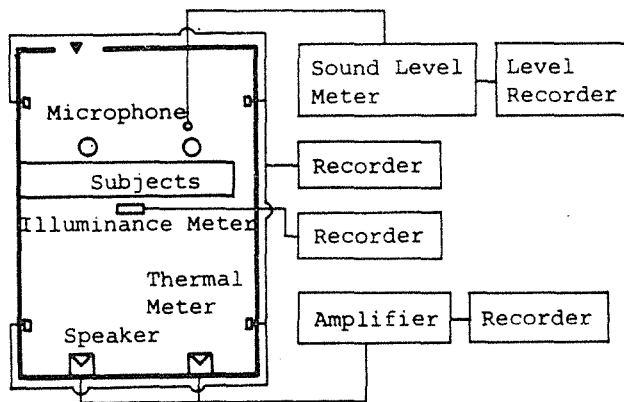
Fig.1 Blockdiagram of the artificial climate chamber, and floor plan showing the location of subjects, the noise level, the illuminance condition and thermal condition pickups.
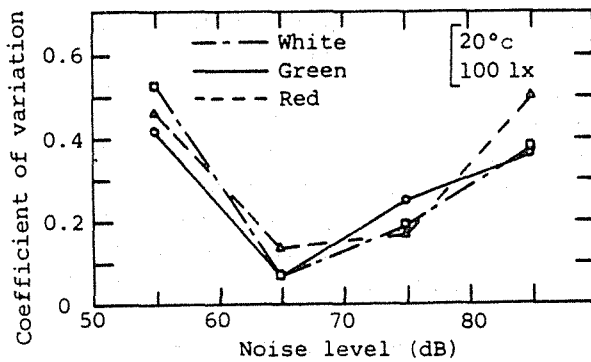
Fig.2 The coefficient of variation for evaluation values for a noise level change under three kinds of lights (white light, green light, red light) 100 lx in a room temperature 20°C (Exp.1).
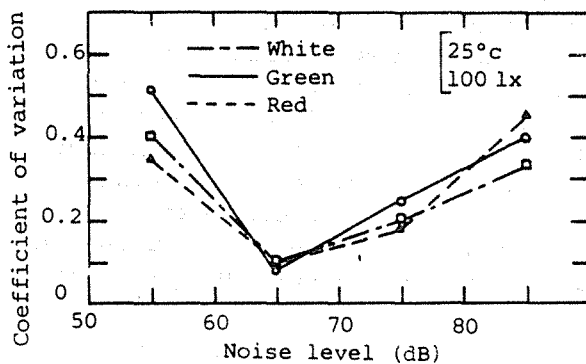
Fig.3 The coefficient of variation for evaluation values for a noise level change under three kinds of lights 100 lx in a room temperature 25°C (Exp.1).

2. EXPERIMENTAL SETTING

Two kinds of experiments are employed. In the first experiment (abbr. Exp.1), the evaluation values for noise level change are selected under many living conditions, and in the second experiment (abbr. Exp.2), the evaluation values for illuminance level change are selected under many living conditions.
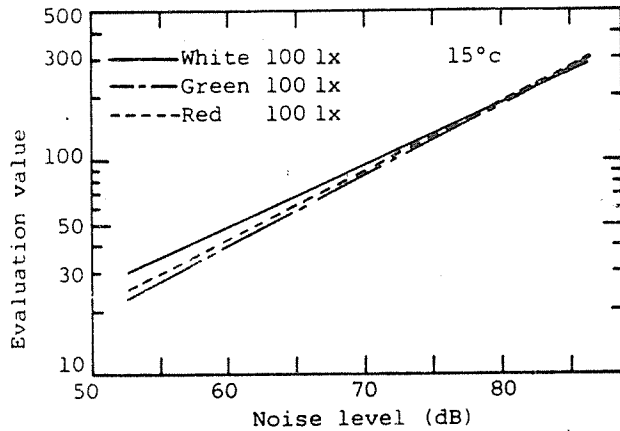
Fig.4 The evaluation values for a noise level change under three kinds of lights (white light, green light, red light) 100 lx in a room temperature 15°C (Exp.1).
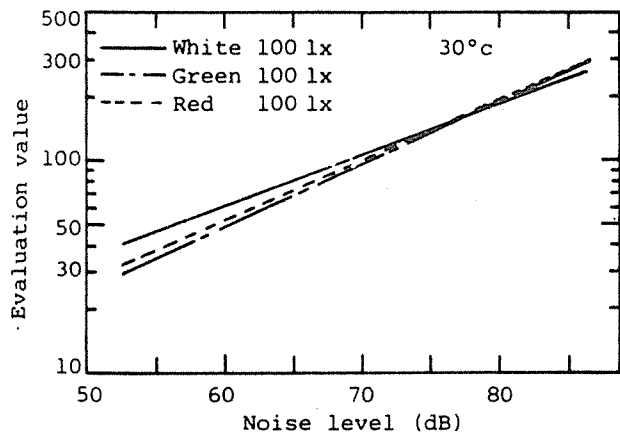
Fig.5 The evaluation values for a noise level change under three kinds of lights 100 lx in a room temperature 30°C (Exp.1).
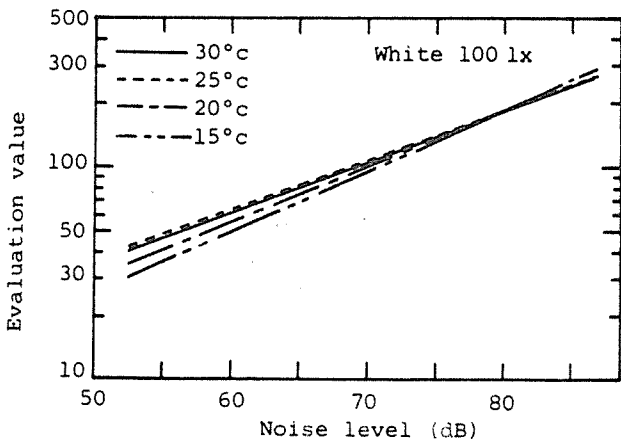
Fig.6 The evaluation values for a noise level change under four kinds of room temperature (15, 20, 25, 30°C) in a white light 100 lx (Exp.1).

An experimental chamber is made as (5.5 x 3.5 x 2.7)m^3 room. A recorded (white) noise is fed in the chamber by two loudspeakers. The room is illuminated by twelve sets of glow lamps. The illuminance of, the surface of desks are controlled by the voltage supplies. Thermal conditions are controlled by using two (heat pump type) air conditioners. The blockdiagram of the artficial climate chamber and floor plan showing the location of subjects, the noise level, the illuminance condition and thermal condition pickups are illustrated in Fig.1.

2.1 Experiment 1   Experimental conditions were determined under the actual situation appearing in our daily life. Four categories of noise level (white noise ; 55, 65, 75, 85 dB), six categories of illuminance condition (white light ; 5, 100, 400, 800 lx, red light ; 100 lx and green light ; 100 lx) and four categories of thermal condition (15, 20, 25, 30°C) were given. Subjects were healthy students (male : 10 person and female : 10 person) 19-24 years old. All of them were approved normal to a hearing test.

A Magunitude Estimation (abbr. ME) Method is employed to obtain some evaluation value for many complex living conditions. In this experiment, 65 dB noise level and 100 lx white light are fixed as a standard point (100), and every subject votes a value of noise level evaluation under relative conditions. The experiment is carried out along the order of a table of random sampling numbers.
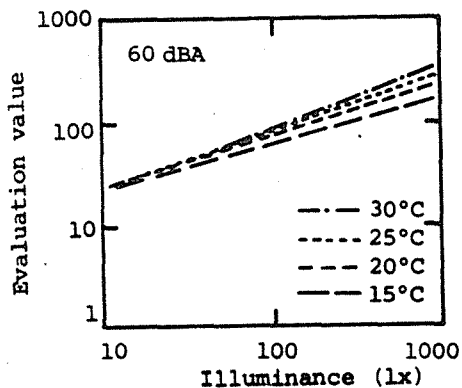
Fig.7   The evaluation values for an illuminance level change under four kinds of room temperature at a room noise level 60 dBA (Exp.2).
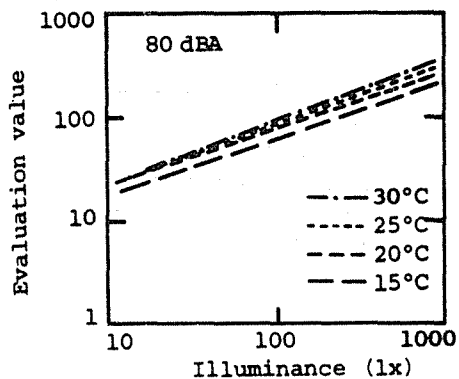
Fig.8   The evaluation values for an illuminance level change under four kinds of room temperature at a room noise level 80 dBA (Exp.2).

Four categories of noise level (white   noise   ;
50,   60,   70,   80 dBA),   five   categories   of   illuminance   condition
(white light ;   50,   100,   200,   400,   800 lx) and four categories of
thermal condition (15,   20,   25,   30°C) have been employed. All of
subjects   were healthy students (male :   10 person and female   :   15
person).   A Magunitude Estimation Method is also employed in this
experiment,   but   there is no standard in this case.   Every   subject
votes a value of illuminance evaluation under relative condituons.

3. RESULTS AND DISCUSSIONS

The results for Experiment 1   are Figs.2 - 6.   In this experiment, a
ME Method with a standard point (65 dB noise level and 100 lx white
light) is employed.   Figures 2 and 3 show the coefficient of varia-
tion for evaluation values for noise level change under three kinds
of lights (white light, green light and red light) 100 lx. Figure 2
shows the case of a room temperature 20°C,   and Fig.3 shows the case
of a room temperature 25°C. From these figures, the coefficient of
variation becomes greater far from a value at the standard point (65
dB).   And, this is obvious in the lower level from a standard point
of noise level.
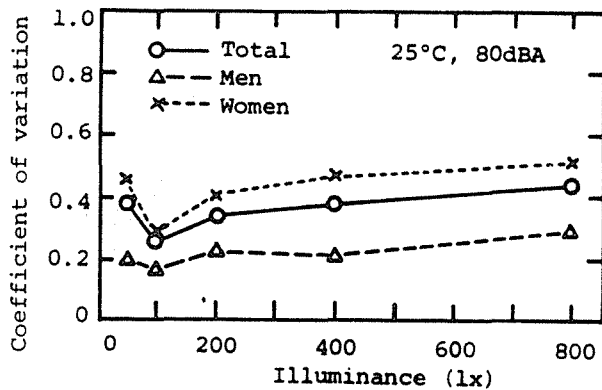
Fig.9   The coefficient
of variation for evalua-
tion values for an illu-
minance level change un-
der the subjects of men
and/or women, a noise
level 80 dBA and 25°C
room temperature (Exp.2).
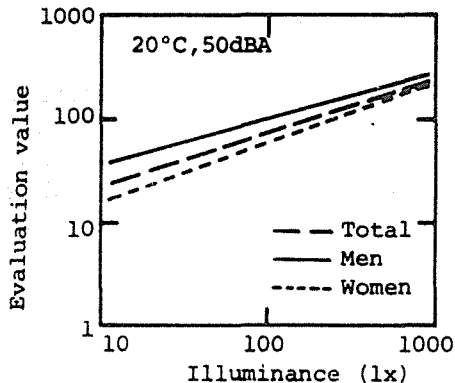
Fig.10   The evaluation
values for an illuminance
level change under the
subjects of men and/or
women, a noise level 50
dBA and a room tempera-
ture 20°C (Exp.2).

Figures 4 and 5 show the evaluation values for noise level change under three kinds of lights (white light,green light and red light) 100 lx. Figure 4 shows the case of a room temperature 15°C, and Fig.5 shows the case of a room temperature 30°C. From these two figures, in the lower part of noise level, it seems that colored lights (green light and red light) give the evaluation value smaller than that of a white light. That is, this result tells us that there is some control effect. This kind of tendency is seen under every thermal condition. Figure 6 shows the evaluation values for noise level change under four kinds of room temperatures (15, 20, 25, 30°C), in a white light 100 lx. From the above, in the same kind of illuminance, a relatively high room temperature makes the high evaluation of noise level than a low temperature.

The results for Experiment 2 are shown in Figs.7 - 14. In this experiment, a ME Method without any standard point is employed. Figs.7 and 8 show the evaluation values for an illuminance level change under four kinds of room temperatures. Figure 7 shows the case of a noise level 60 dBA, and Fig.8 shows the case of a noise level 80 dBA. From these experiments, there are some difference of evaluation value affected by a room temperature at a high illuminance. According to the law of psycho-physics $\psi = kS^{n}$, the exponent n can
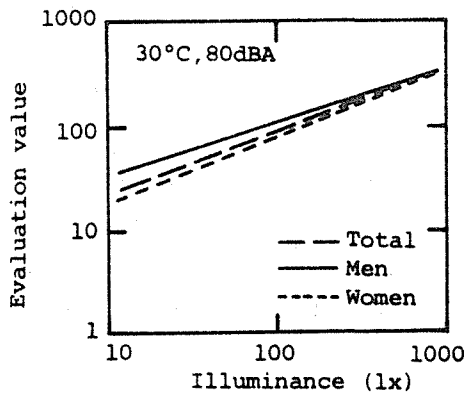
Fig.11 The evaluation values for an illuminance level change under the subjects of men and/or women, a noise level 80 dBA and a room temperature 30°C (Exp.2).
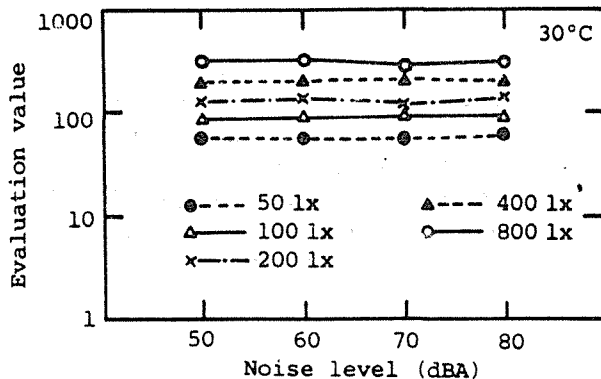
Fig.12 The evaluation values for an illuminance under a noise level change, five kinds of lights and a room temperature 30°C (Exp.2).

be found as 0.45 - 0.6 in the present experiment, and this value seems to be reasonable corresponding to Stevens' value.

Figure 9 shows the coefficient of variation for evaluation values for an illuminance level change and there is not'so big difference along the illuminance level. Figures 10 and 11 show the evaluation values for an illuminance level change based on subjects of men and/or women. Figure 10 shows the case of a noise level 50 dBA and a room temperature 20°C. Figure 11 shows the case of a noise level 80 dBA and a room temperature 30°C. From these results, there are some difference between the evaluation values of men and/or women in the lower part, but there is no difference in the higher part of an illuminance level.

Figures 13 and 14 show the evaluation values for an illuminance under the thermal condition change and five kinds of lifgts (white light ; 50, 100, 200, 400, 800 lx). Figure 13 shows the case of a noise level 60 dBA, and Fig.14 shows the case of a noise level 80 dBA. From the above, a high room temperature gives higher evaluation value of illuminance more than a lower temperature. And a high illuminance gives a large difference of the evaluation value.
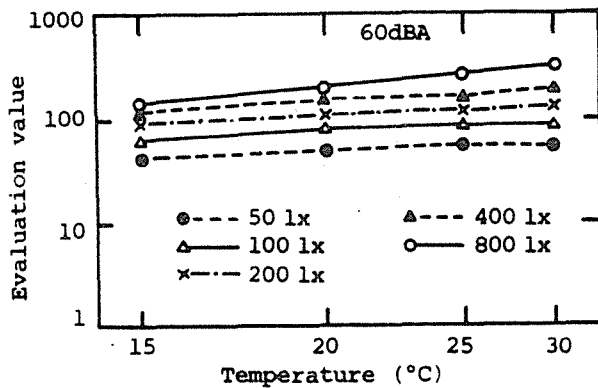
Fig.13 The evaluation values for an illuminance under a thermal condition change, five kinds of lights and a room noise level 60 dBA (Exp.2).
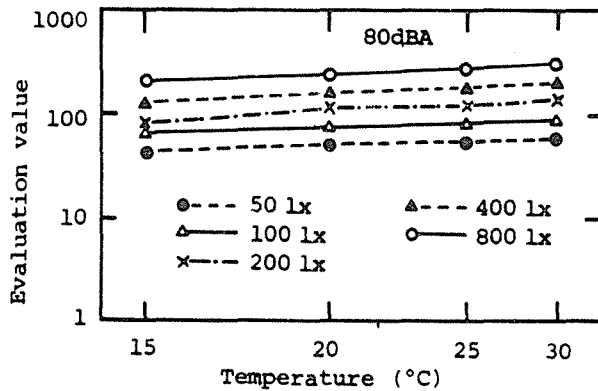
Fig.14 The evaluation values for an illuminance under a thermal condition change, five kinds of lights and a room noise level 80 dBA (Exp.2).

4. CONCLUSIONS

We always expend a great effort to find the skillful combination of living environmental factors such as temperature, moisture, lighting, sound and ventilation. If more than two different kinds of the above environmental factors are appropriately combined, an optimum relationship between those factors might be for a comfortable indoor life. In this paper, the combination of three environmental factors ; sound, lighting and temperature has been first considered. Then, two kinds of experiments have been employed. That is, at first, the evaluation values for a noise level change have been selected under many conditions, and secondly the evaluation values for an illuminance level change have been selected under many conditions. From the first experiment, a white glow light has given some higher evaluation value of a noise level than a green light or a red light. Such a tendency is seen under every temperature condition. In the same illuminance condition, a relatively high temperature gives more high evaluation of a noise level than a low temperature. From the second experiment, a high room temperature has given higher evaluation value of illuminance more than a low temperature. And a high illuminance has given a large difference of evaluation value. Thus, it is obvious that the present study gives some guiding principle to make our indoor living life comfortable.

REFERENCES
[1] S.S.Stevens, Psychophysics, (John Wily & Sons, New York, 1975).
[2] Y.Sakurai et al., "Quantification of the Synthesized Evaluation of the Combined Environment", Energy and Buildings, 14, 169 (1990).

TRENDS IN PUBLIC CONCERN ABOUT ROAD NOISE

Michel VALLET
Institut National de Recherche sur les Transports et
leur Sécurité (INRETS), 109 Av. S. Allende, 69500 F
BRON

ABSTRACT

The paper analyses the evolution of the human responses to
the traffic noise, during the period between 1965 and 1989,
according to the results from 4 major acoustical and
psychological surveys respectively carried out 1963, 1973,
1979, 1986. The relationship between the human needs,
assessed by the surveys and the regulation to protect the
environment and housing is examined : on one hand, one
observes a very good reliability of the human responses to
traffic noise across a quarter of century with a remarquable
stability of the annoyance threshold, and on the other hand
a slow but interesting change in the French regulations
about traffic noise using the Leq A 8-20 h index. The next
research on this topic shall be to control the noise
sensitivity of people living nearly arterials ways
especially during the night, like in others countries.

1 - INTRODUCTION

Environmental and protective policies concerning road usage noise are extremely costly to implement, particularly when existing "black spots" have to be corrected.

Policies are frequently based on noise thresholds determined experimentally since the beginning of the sixties.

Regulations apply to new buildings and roads; for older buildings Public Authorities undertake corrective action based on higher noise levels than those used applied for new construction work.

Considering the cost variations implied by levels different by only a few decibels, research establishments verify the pertinence of threshold values whenever possible and confirm that the thresholds proposed are stable over time.

This article reviews French researches carried out in this field between 1964 and 1986. The effects of noise on the population are classified by negative effects, direct and indirect, and positive effects such as the improvement of privacy, in dwellings and transportation, as well as the increase in activity and vigilance levels.

Directly negative effects of road noise include loss of sleep which can induce slight responses from the cardio-vascular system although not high blood pressure. It is not possible to state that road noise causes hearing impairments but it can engender anxiety states.

Noise disturbs human activities and life-styles and it can induce subjective sensations such as a feeling that the noise pollution is unpleasant, even to the point of causing psychological annoyance.

Indirect negative effects include the use of medications - particularly to combat stress - reductions in property values and reduced use of dwellings and gardens.

Many research projects devoted to the study of the impact of noise on communications have been undertaken in laboratories in which acoustic properties can be extremely closely controlled, for example by Kryter in 1985 (12).
In the same experimental conditions the effects of noise on mental activity and performance levels were studied by Moch 1987 (13) and on sleep by Vallet 1987 (14).

Some authors began by conducting surveys to isolate the various sources of noise like Morton-Williams in 1978 (15) and to determine the frequency at which inhabitants perceived noise.

Other studies seek to establish relationships between the restrictions felt by people living near roads and acoustic

energy levels - Langdon 1976 (16). New studies consider secondary acoustic factors such as the number of noises - Fields 1984 (17) or Rice 1980 (18), the period during the day in which they occur - Bullen 1982 (19) and personal or situational factors affecting annoyance such as Levy Leboyer 1988 (20).

In all these studies, scientists are seeking to determine whether thresholds exist by constructing a relationship between noise measured on the elevations of buildings and annoyance evaluated by psycho-sociological surveys using questionnaires.

The thresholds retained are the points of inflection of the response curves which are shown as clusters of values and not as a continuous graph.
Thresholds can be determined by other mathematical formulae such as the segmentation of the distribution of responses concerning annoyance. In other studies thresholds are determined as a percentage of all those stating that they are very annoyed (15% for example).

Since 1978 in France, the regulations use the Leq.index measured or calculated from 8 a,m, to 8 p,m,, which is representative of the annoyance felt during a 24 hour period ; nightime noise is not measured quite simply because, on urban freeways, there is a strong relationship between the Leq, 8 a,m, - 8 p,m, values and the noise values but the problem is very different in roads with lower traffic loads.

A threshold adopted in 1978 was 65 +/- 5dB(A); The new threshold retained is "located in a range of from 60 to 65 dB(A)", levels close to 60dB(A) were sought as far as possible for dwellings located in "calm residential areas" or in other cases if additional costs was not excessive (21).

2 - SURVEY RESULTS

2.1 - Motorway noises

The first research was published in France by Lamure and Bacelon (1) in 1964. This survey was carried out on a sample of 420 people living near motorways.

The annoyance indicator used for cross-referencing with the acoustic levels was an index related to the opening and closing of windows.

The noise indicator is the L50, i,e, the noise level reached or exceeded during 50% of the time. If traffic loads are heavy, as in this case, distribution of the measurement samples is a gaussian curve and the Leq, can be estimated from L50 (2).

Leq = L50 + 0,11 s in which s is the standard deviation of the values measured
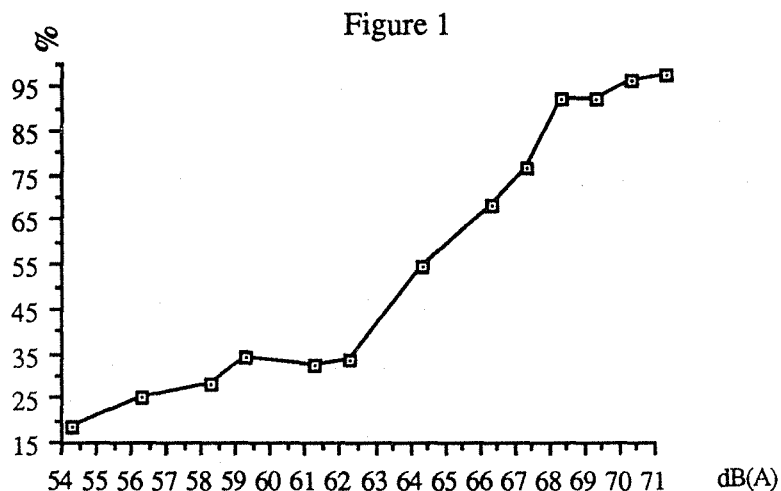
Figure 1

Figure 1 :

Are you obliged to close the windows when you invite friends
and relations ?
Question 20 in Lamure-Bacelon 1964.

The response curve as a function of noise quite clearly
shows (see Figure 1) a 62 dB(A) threshold above which
annoyance frequency increases rapidly. Using the formula
above, the Leq is thus calculated to be 63 dB(A).
This threshold virtually became officialized in the context
of the French "Acoustic Comfort Label" in 1972. Insulation
in dwellings became obligatory to obtain the Label above
L 50 = 63 dB(A) measured 2 metres in front of the
elevations.

2.2 - Noise from urban freeways

A second survey was carried out by Vallet and Maurin in 1973
(3) on a sample of 1000 people living close to urban
freeways in 10 French towns and not just in the Parisian
region unlike the study by Aubrée in 1972 (4). As an index
of annoyance the authors considered the percentage of people
who felt very annoyed and this hypothesis was used again in
1977 by Schultz in the U.S.A. when reviewing all published
studies (5).
Two acoustic indexes were retained :
- the Leq equivalent energy level during daytime and level
L1 during the evening i,e, which was reached or exceeded
during 1% of the time. The threshold proposed in the 8 a,m,
to 8 p.m, Leq is 62 dB(A) which is quite clearly
demonstrated in figure n° 2.

700

In the graph for the "quite + very annoyed" category, response rates are high at the 62 dB(A) level particularly for those people living in houses.
Because of these observations, the threshold proposed was 62 dB(A). For cost reasons, public authorities adopted a 65 dB(A) +/- 5 dB threshold. However, the upper - 70 dB(A) - threshold was very rapidly suppressed.
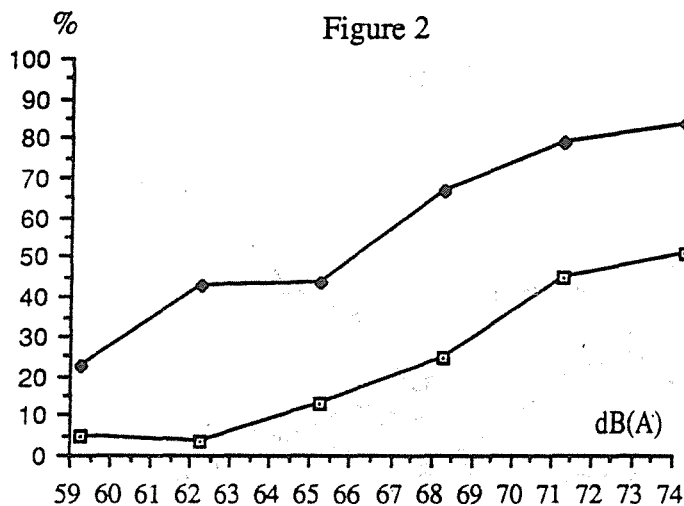
Figure 2 :
Disturbance response as a function of noise levels :
361 housewives and other people in the home

Very annoyed people   ▣
Very annoyed people + quite annoyed people   ◆

2.3 - Urban noise in large towns

A third survey was conducted by Lambert in 1979 (ref. 6) on a sample of 1500 people living in urban areas in large towns.

One of the unique features of this research was that it examined the behaviour of people exposed to noise ; the behavioural indices which were observed were, in principle, less subjective than the annoyance levels : these are the percentages of people who take sleep inducing medication or do not use their balcony or garden, who take measures to soundproof their home or who often go away for the weekend, Nevertheless, to enable comparisons with previous studies, questions on annoyance levels were asked. This survey was also characterised by a higher level of accuracy of the noise measures which were nevertheless still carried out on the front elevations of the homes. Using Favre's noise level forecasting techniques (ref. 7), acoustic levels were determined for each room within the home and weightings were applied to the measurements implemented based on values calculated as a function of annual average road traffic.

This effort to obtain accuracy and the way in which physical measurements were represented were used to obtain a correlation coefficient - 0,64 - between noise and individual responses to annoyance.

If the response rate of very annoyed people (figure 3) is considered, a 61 dB(A) threshold can be observed during the Leq 8 a,m, - 8 p,m, period and 60 dB(A) if the people who were quite annoyed and very annoyed are added together (figure 4).
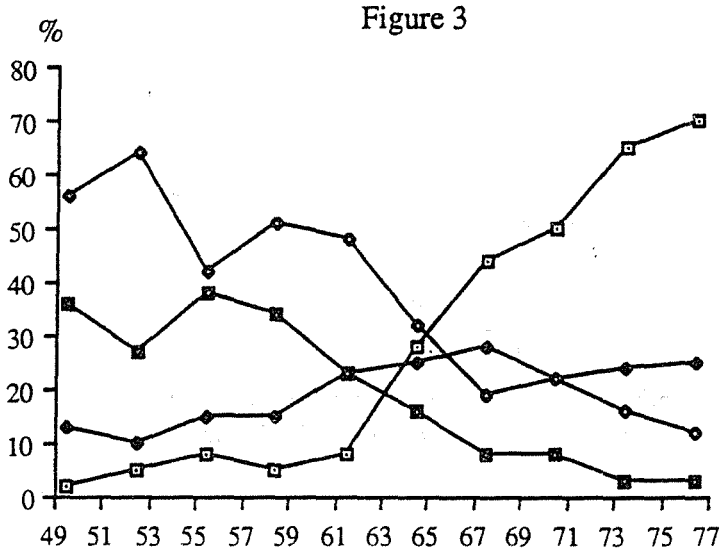
Figure 3

Figure 3 :
Noise and annoyance during daytime (from Lambert)
☐   Very annoyed   ♦   Annoyed
▣   Slightly annoyed   ◊   Not annoyed
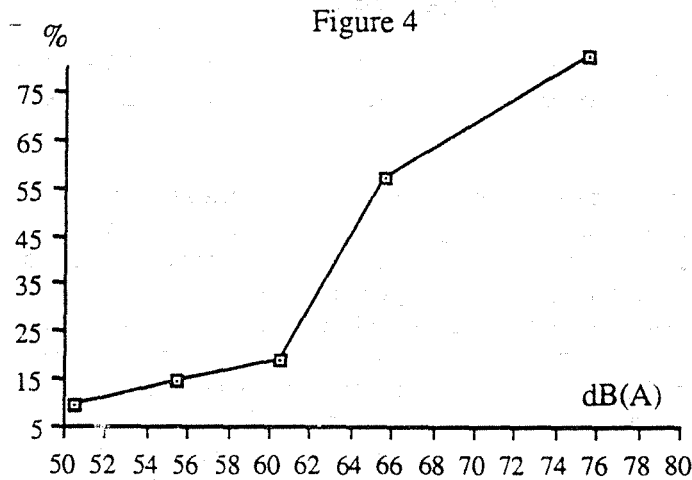
Figure 4

Figure 4 :
Daytime noise and annoyance.
Very + quite annoyed people.

702

2.4 - The French National noise survey

In 1986, Maurin and Lambert carried out a national survey on noise exposure in France (8). A sample of 2000 people were questioned in towns and communities of all sizes, from Paris to the country villages.
A major acoustic measurement campaign was implemented, which enabled the determination of relationships between annoyance and the acoustic levels measured.
The questionnaire aimed to obtain spontaneous reactions to different nuisances at home, The authors found a significant difference between people who did not mention noise and those who did.
The threshold is located between 60,2 dB(A) Leq 8 a,m, - 8 p,m, and 64,1 dB(A). Below 60 dB(A) there was no spontaneous reaction to noise as a nuisance. This survey also considered the level of annoyance expressed, presented in the following Figure 5.
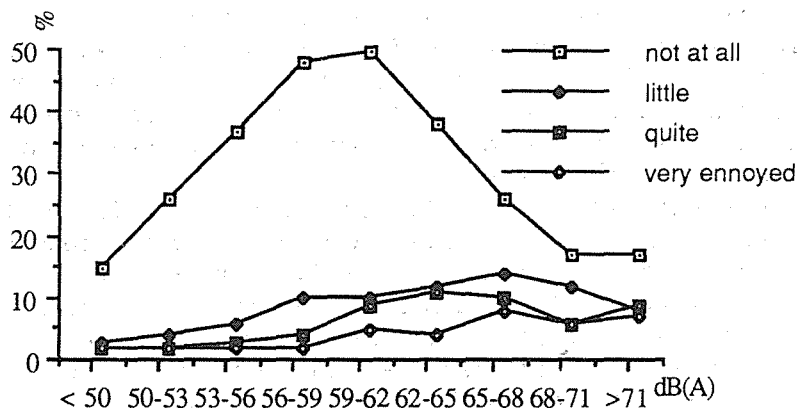
(origine : Maurin)

Figure 5
Daytime Noise VS Annoyance

As in the previous surveys, if one considers the percentage of very and quite annoyed people, a rapid acceleration in the response rate of these people at 59 dB(A) is observed, which indicates that the threshold previously determined in this survey, i,e, 60 dB(A), is identical to the survey carried out on behaviour patterns (6).

In this national study the annoyance level table was then segmented ; in this case the threshold determined is equal to 63 dB(A).
To conclude, a significant stability over time for annoyance thresholds due stemming from road noise was observed. The threshold values obtained with comparible acoustic indices are in the 60 to 63 dB(A) in daytime Leq. Given the accuracy with which annoyance was evaluated - which cannot be perfect - and the natural fluctuations of public opinion about noise, or opinions arising from informational campaigns, it

can be considered that over 25 years (i,e, from 1963 to 1988) the annoyance due to road traffic noise is stable and that the annoyance threshold is in the 60 to 62 dB(A) range in daytime Leq terms. This stability, which can be assimilated to measurement reliability, quite clearly indicates that the threshold is significantly lower than 65 dB(A) threshold currently used by the Public Authorities and that the 60 to 65 dB(A) range needs to be tightened ; this being said it is a fact that roadway and housing engineers and designers are aiming to obtain noise levels approaching 60 dB(A) whenever budgets and techniques permit.

3 - THE VALIDITY OF THE ENVIRONMENTAL QUALITY ACOUSTIC INDICATOR

We shall now examine the validity of the Leq 8 a,m, - 8 p,m, index as a meaningful indicator for a complete 24 hour period and variations in acoustic energy levels.

A close relationship between the Leq daytime and the Leq nightime values has been established on several scores of measurement points and for relatively uniform urban freeways. This relationship is often misunderstood and even contested by road construction engineers, municipal technical services and of course by residents associations living close to roads.
As long ago as 1982, Maurin (ref, 9) demonstrated that in fact differences in noise levels between daytime (Leq 8 a,m, - 8 p,m,) and nightime (Leq 12 p,m - 5 a,m,) vary from 8,2 to 13,5 dB(A) for a limited sample of measurements (i,e, obtained from 60 or so measurement points).
The differences between daytime and evening (Leq 8 p,m, - 12 p,m,) vary between 3,8 and 6,1 dB(A) and the differences in level between daytime and the early hours of the morning (5 a,m, - 8 a,m,) vary from 0,4 to 3,8 dB(A).
In those cases in which the difference in daytime (Leq 8 a,m, - 8 p,m,) and nightime (Leq 12 p,m - 5 a,m,) is low, this would correspond to roads with heavy traffic loads, Protection afforded by an acoustic threshold not to be exceeded during daytime is inadequate for the nightime period.

Lambert 1985 (10) calculated that this phenomenon also occurs when the difference is under 6 dB(A), for example in the case of Leq daytime values of from 55 to 65 dB(A). Recent work by Maurin 1988 (11) confirms that the relationship between daytime and nightime levels are far from constant.

Table 2 shows that the difference between Leq 8 a,m, - 8 p,m, values and values for the 10 p,m, - 6 a,m, period can be as much as 10 dB(A).

Leq 8 a,m,-8p,m,	Leq 8 p,m,-6 a,m.	Difference	
service roads	58,8	46,5	12,3
minor roads	63,1	52,8	10,4
arterial or trunk roads	68,6	58,3	10,3

Table 2 :
Acoustic levels measured on different types of roads.
A more detailed examination of these results, obtained from 375 acoustic measurements made during a 24 hour period throughout France, shows a rather different, more contrasted situation.

Daytime-nightime contrast is less significant when daytime noise levels increase and more significant when it affects quieter areas.
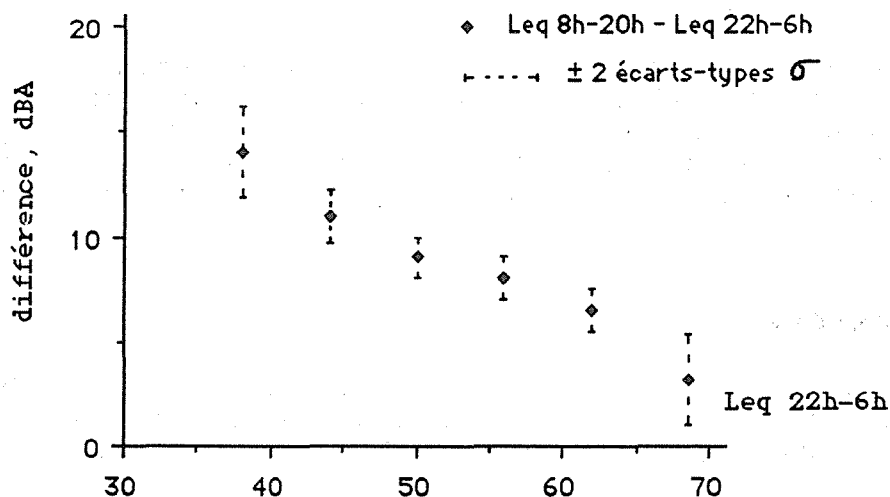
Figure 6 : (origin Maurin)
Statistical difference between Leq 8 a,m,-8 p,m,
and Leq 10 p,m,-6 a.m.

Figure 6 shows that for the 10 p,m,-6 a,m. Leq measurements below 41 dB(A) the Leq for the 8 a,m,- 8 p,m, period is higher by 12 to 16 dB(A), with a standard deviation of 1,1 dB(A).
For nightime noise levels over 65dB(A) the daytime Leq is higher by 2 to 3 dB(A) with a standard deviation of 1 dB(A). In this way we can state categorically that the differences between daytime and nightime Leq are not similar and therefore we cannot reason and work from the 8 a,m,- 8 p,m, Leq ; from this recent data the equation for the regression would be : Leq 8 a,m,-8 p,m, = 0,69 (Leq 10 p,m, -6 a,m,) + 25,8 in dB(A).

4 - CONCLUSIONS

Examination of research carried out over the last 25 years shows a remarkable stability in average levels of people's reactions to traffic noise.

The survey methods used to understand the requirements of the population are simple in design, which does not preclude a detailed investigation enabling time-space comparisons. The threshold is located between 60 and 63 dB(A) for the Leq 8 a,m,-8 p,m, acoustic indicator.

As for the indicator selected, it should be recognised that the period used for calculation and measurement does not sufficiently reflect the difference between evening and nightime.

Acoustic levels at night are not systematically related to daytime levels.

It would be interesting therefore to reexamine the question of the needs of populations during the evening and at nightime for a major part of the French road system as traffic loads on roads change with lifestyles and lifestyles have changed in a major way over the last twenty-five years.

REFERENCES

1) BACELON M., LAMURE C. La gêne due au bruit de circulation automobile, une enquête auprès des riverains d'autoroutes. Cahiers du CSTB n° 88 1967 - Paris.

2) JOSSE R., AUBREE D. Recherche d'un indice acoustique commun permettant de prévoir la gêne due aux trafics routiers et aérien. CSTB EN.SH 75.4. Rapport à l'Institut de Recherche des Transports CERNE 1975 80 p..

3) VALLET M., MAURIN M., PACHIAUDI G., FAVRE B., PAGE A.M. Annoyance from and habituation to road traffic noise from urban expressways. J of sound and vibration 1978 (60) 423-440.

4) AUBREE D., AUZOU S., RAPIN J.M. Le bruit des rues et la gêne exprimée par les riverains. Cahier du CSTB Paris 1973 n° 138.

5) SCHULTZ T.J. Synthesis of social surveys on annoyance due to noise. 9e International Congress on Acoustics 1977 - Madrid.p 10.

6) LAMBERT J., SIMONNET F., VALLET M. Patterns of behaviour in dwellings exposed to road traffic noise. J of Sound and Vibration 1984 92 (2) 159-172.

7) FAVRE B. Noise emission of road vehicles : evaluation of some simple models. *J of Sound and Vibration* 1983 91 (4) 571-582.

8) MAURIN M., LAMBERT J., ALAUZET A. Enquête nationale sur le bruit des transports en France. *Rapport INRETS n° 71* Paris 1988 - 132 p. ISSN 0768.-9756.

9) MAURIN M., in LAMURE et al. Le problème de l'indice de bruit nocturne pour les riverains de voies de circulation. *Revue d'acoustique* 1982 N°62, 180-186.

10) LAMBERT J., PLOUHINEC M. Day and Night annoyance, a comparison *Inter Noise Proceedings 1985* - Munich - pp. 941-944.

11) MAURIN M., LAMBERT J. Exposure of the French Population to Transport Noise. 1990 *Noise Control Engineering Journal*.

12) KRYTER K. *The effects of noise on man*. Académie Press N. York 1985, 685 p.

13) MOCH A. Aspects psychosociologiques des stress de l'environnement. *Thèse Paris VIII* 1987, 555 p.

14) VALLET M. Sleep Disturbance in *Reference book Transportation Noise P. NELSON* ed, Butterworths Lourdes 1987, Chapitre 5.

15) MORTON-WILLIAMS J., HEDGES B., FERNANDO E. Road Traffic and the Environment. *Social and Community Planning Research*. London 1978, 42 p.

16) LANGDON F.J. Noise nuisance caused by road traffic in residential areas Parts I, II. *J. Sound Vibration* 1976, 47, 243-282.

17) FIELDS J. The effetcs of numbers of noise events on people's reactions to noise. An analysis of existing survey data ; *J. Acousti. Soc Am* 1984 75(2) 447-467.

18) RICE C. Trade off effects of air craft noise and number of events. *Int. Congress on Noise as a Public Health Problem Proceeding ASHA* n° 10, 1980, 495-510.

19) BULLEN R., HEDE A. Time of day corrections in measure of aircraft noise exposure. *J. Acoust. Soc Am.* 1983, (73) 1620-1630.

20) LEVY-LEBOYER C. La gêne due au bruit, mesure et signification, *Ministère de l'Environnement SRETIE*, Paris 1988, 69 p.

21) Ministère de l'Equipement. Circulaire du 2 mars 1983 relative à la perception contre le bruit.

AUTHOR INDEX

WESTPRACING IV01